Fatima Zivic · Saverio Affatato
Miroslav Trajanovic · Matthias Schnabelrauch
Nenad Grujovic · Kwang Leong Choy *Editors*

Biomaterials in Clinical Practice

Advances in Clinical Research and Medical Devices

Springer

Biomaterials in Clinical Practice

Fatima Zivic · Saverio Affatato
Miroslav Trajanovic · Matthias Schnabelrauch
Nenad Grujovic · Kwang Leong Choy
Editors

Biomaterials in Clinical Practice

Advances in Clinical Research and Medical Devices

Springer

Editors
Fatima Zivic
Faculty of Engineering
University of Kragujevac
Kragujevac
Serbia

Saverio Affatato
Medical Technology Laboratory
Rizzoli Orthopaedic Institute
Bologna
Italy

Miroslav Trajanovic
Faculty of Mechanical Engineering
University of Niš
Niš
Serbia

Matthias Schnabelrauch
Biomaterials Department
INNOVENT e.V.
Jena
Germany

Nenad Grujovic
Faculty of Engineering
University of Kragujevac
Kragujevac
Serbia

Kwang Leong Choy
Institute for Materials Discovery
University College London
London
UK

ISBN 978-3-319-68024-8 ISBN 978-3-319-68025-5 (eBook)
https://doi.org/10.1007/978-3-319-68025-5

Library of Congress Control Number: 2017952922

Printed on acid-free paper

This Springer imprint is published by Springer Nature
The registered company is Springer International Publishing AG
The registered company address is: Gewerbestrasse 11, 6330 Cham, Switzerland

Preface

This book is the result of contributions from senior researchers active in the various areas of biomaterials pertaining to the current state of development in medical implants and devices. Academic researchers, as well as clinicians with extensive experience in both theoretical and practical aspects, have presented insights into the specific areas of biomaterial characterisation, development and applications. Novel biomaterials applied for medical implants and devices have boosted significant advancements not only in regenerative medicine and medical diagnostics, but also in many other health-related fields. Immense research efforts and numerous pending patents in the world all indicate the largest research field ever, if quantified by the number of people involved in the development. Beside nanotechnologies, biomaterial market represents one of the major driving forces in research today, comprising wide engaged resources. Medical implants that can fully replace organs, or tissues, or repair them, without detrimental side effects are long investigated, with ultimate goal of ideal biomaterial design. This field is especially important considering the fact that human population grows older.

Some of the largest investments ever have been recorded in case of several biotech start-ups, promising cures for incurable diseases, and significant new solutions in regenerative medicine and tissue engineering. Report on global market trends (http://www.marketsandmarkets.com) forecasts that biomaterial market will grow to USD 149.17 Billion by 2021 from USD 70.90 Billion in 2016, at a CAGR of 16.0% from 2016 to 2021. Biomaterial market is segmented by the material types (e.g. metals, ceramic, polymer, natural materials and composites) and according to the applications (e.g. orthopaedic, dental, cardiovascular, plastic surgery, wound healing, neurology, tissue engineering, ophthalmology). However, even with the undeniable proven results of different implantable devices (hip and knee prosthesis, spinal prosthetics, stenting and many other), there are still many challenges and restraints in their use. Each type of biomaterial exhibits some drawbacks, thus demanding more research efforts towards developing fully human compatible materials. Along with the growing field of nanotechnology, with many interconnections, the field of biomaterials development has drawn attention of governments, funding agencies, healthcare charities and investment bodies. This is

resulting in large available funding for research, in scope of numerous health-related national or international programs, whereas only H2020 programs have perhaps the highest dedicated funding precisely for healthcare and biomedical-related research.

The book is divided into three parts, starting from the history of biomaterials used in hip arthroplasty and their modern evolution and existing biomaterials types: metals, polymers, ceramics, up to the newly investigated structures such as biodegradable and porous metals, shape memory alloys, bioactive biomaterials and coatings and nanometals in cancer diagnosis and therapy. Part II of the book presents different methods and approaches in biomaterial properties and characterisation: chemical properties, biocompatibility, in vivo behaviour characterisation, as well as genotoxicity and mutagenicity. Different types of diagnostic techniques are also reviewed: histopathological analysis, imagining techniques and methods for physicochemical and spectroscopic characterisation. Mechanical and structural characterisation of applied biomaterials and implantable components (e.g. elements of joints) in orthopaedic surgeries, as well as manufacturability of existing biomaterials, have been reviewed. Properties of stent deployment procedures in cardiovascular surgeries, from aspects of prediction, development and deployment of stent geometries are presented by modelling approaches. Part III of the book presents clinical applications of biomaterials, together with case studies in novel advancements in dentistry, knee and hip prosthesis.

The focus of this book is to review existing biomaterials in clinical practice, from their properties to recognised issues and further development directions. Also, health-related products have incorporated many nanotechnology aspects, especially in improved medical implants or drug delivery systems. Accordingly, many unexplained phenomena are still facing the research groups, whereas existing results strongly show great future potentials. Adequate characterisation of biomaterials is of the utmost importance regarding their development. Determination of influential factors that govern in vitro simulation of biomaterial testing in order to effectively simulate in vivo conditions are still developing, especially for new material classes, such as nanomaterials, hybrid composites or bioactive materials. Material responses to different parameters, such as loading patterns, type of motion, contact velocities, as well as influence of the surrounding environment which provokes different chemical reactions, can offer valuable further directions for improvement. Many issues about their behaviour are still under debate, for both in vitro and in vivo conditions. In particular, in vivo characterisation of implanted materials needs further development in both the methodologies and instruments. Medical diagnostics will greatly benefit from high-resolution imagining techniques, which is also needed for characterisation of implanted biomaterials within the body, especially continuously during their lifetime. In vivo behaviour and responses to tissues and body fluids over time will provide valuable information for further improvement of the biomaterials and implants towards fully compatible devices, but it will also point out new directions for treatments. In vivo characterisation of the implantable devices is especially important because long-term effects still need to be studied for almost all existing biomaterials. There is still rather limited

scope of available instruments and fully reliable methods for in vivo diagnostics. In particular, high resolution in situ microscopy is expected to provide better diagnostics, and these instruments and methods belong to a cutting-edge research with extremely high cost of devices that recently have started to appear.

We believe that this book will provide young researchers and professionals with valuable insights into the state of the art in development of biomaterials in clinical practice today, from aspects of different expertise: medical, engineering, physics, chemistry and material science, to motivate them to pursue further research and practical applications. The book will provide clinicians with the review of existing solutions in specific medical areas, also from other approach beside medical, thus enabling them more profound selection of implantable solutions in clinical cases.

This work is the result of joint efforts of different academic, and research institutions participating in the large international project, WIMB Tempus, 543898-TEMPUS-1-2013-1-ES-TEMPUS-JPHES, "Development of Sustainable Interrelations between Education, Research and Innovation at WBC Universities in Nanotechnologies and Advanced Materials where Innovation Means Business", co-funded by the Tempus Programme of the European Union.

Kragujevac, Serbia — Fatima Zivic
Bologna, Italy — Saverio Affatato
Niš, Serbia — Miroslav Trajanovic
Jena, Germany — Matthias Schnabelrauch
Kragujevac, Serbia — Nenad Grujovic
London, UK — Kwang Leong Choy
April 2017

Contents

About the Editors

Fatima Zivic is assistant professor at Faculty of Engineering, University of Kragujevac, Serbia, for several courses: Biomaterials, Surface Modification Technologies, Metrology and Quality Control, Business Communication. She has actively realised research related to the novel biomaterial structures and material characterisation and the influence of nanoparticles on the directions in material developments. She has been investigated advanced novel materials for medical implants; determination of influential factors that govern in vitro simulation of biomaterial testing (mechanical and structural properties); new material structures (porous structures, composites); PMMA-based bone cement, Ti-based, Fe-based and Mg-based medical alloys, UHMWPE, medical grade AISI 316LVM stainless steel; thin coatings: Ag nanocoatings; SiC, diamond, Al2O3, Zr2O3); materials for extreme conditions (ultradense graphite); industrial biomaterials. She has published more than 50 scientific papers. She also has extensive experience in ICT area and research related to data analysis and online communication, especially aiming at start-ups and spin-offs. She regularly reviews articles for different international journals (e.g. Journal of Materials Engineering and Performance, Springer; Journal of Alloys and Compounds, Elsevier; Journal of the Mechanical Behavior of Biomedical Materials, Elsevier). Her research has been supported by H2020, FP7, TEMPUS, WUS, EAR, COST programs and Ministry of Education, Science and Technological Development of Serbia. She has extensive experience in application, realisation and administration of international projects and has participated in 19 large international projects (in management teams of more than 10 projects) and 6 national projects.

Saverio Affatato is a Medical Physicist at the Rizzoli Orthopaedic Institute (IOR) in Bologna. In this moment, he is the Head of the "Wear characterization of joint prostheses Research Unit" of the Medical Technology Laboratory at Rizzoli Orthopaedic Institute (www.ior.it/tecno). He developed new protocols for wear evaluation on hip and knee joint simulator and also particle debris characterisation. He was the Scientific and Technical Responsible of some National and European project (REPO 2000, Eureka 294, Bioker, Nanoker) where the focus

of these researches was on the development of innovative material for orthopaedics applications and their evaluation from a tribological point of view. Affatato has been actively conducting and publishing research on applying new methodologies to measure the wear from in vitro and in vivo specimens. He has been published more than 130 articles with high impact factor on international journals covering tribological aspects such us particle debris characterisation, alumina-toughness-zirconia, metal-on-metal wear behaviour, unicompartimental and bicompartimental knee prostheses, etc; moreover, he has been published three books on hip and knee characterisation and methods of measurements. He is the referee of some international and prestigious journals such us Clinical biomechanics, Acta Biomaterialia, Biomaterials, Proc. IMechE Part H: J. Engineering in Medicine, etc., and he is the taking part to the Editorial Advisory Board of some journals: Hindawi (Elsevier)-J Health Care Engineering, Lubricants-, Materials.

Miroslav Trajanovic is full professor at the Faculty of Mechanical Engineering, University of Nis, Serbia. He has more than 35 years of experience in application of ICT in mechanical engineering and medicine and more than 250 published papers. He has been the project leader of 10 national and European projects related to IT and biomedical engineering. In addition, he was participant in 14 national and 9 European (FP6, FP7, Horizon2020) projects. He is currently coordinating national project virtual human osteoarticular system and its application in preclinical and clinical practice, financed by Ministry of Education, Science and Technological Development of Serbia. He has broad expertise in modelling of the biomaterials structural design (scaffold structures, bone grafts). He is Serbian coordinator of European EURAXESS services network.

Matthias Schnabelrauch is the Head of Biomaterials Department at INNOVENT, e.V., Jena, Germany (www.innovent-jena.de). He obtained his Ph.D. in Polymer Chemistry from Friedrich-Schiller-University, Jena, and worked as a research and teaching assistant for 3 years at the same university. After postdoctoral positions at University of Zurich, ETH Zurich and the Hans-Knöll-Institute for Natural Product Research, Jena, he joined INNOVENT in 1996, where he established a new department for biomaterial research. From 2003 to date, he held various university teaching positions. His main research interests are the synthesis and characterisation of degradable biomaterials and their application in biomedicine and biotechnology. He is author or co-author of more than 150 peer-reviewed scientific papers and 50 patent applications.

Nenad Grujovic is full professor and Head of Center for Information Technologies (http://cit.fink.rs) at Faculty of Engineering, University of Kragujevac, Serbia. He was the vice-dean for scientific research (2001–2003). He teaches Rapid Prototyping, Reverse Engineering and different ICT-related academic courses, such as Software Engineering; Programming Languages; Data Bases; Project Management; Business Communication. He has research related to bioengineering, custom made medical implants, structural design of medical scaffolds and tissue engineering, especially by application of novel additive manufacturing and 3D printing, as well as advanced

modelling techniques (FEM). He leaded two clinical projects, fabrication of PMMA-based artificial sternum bone (in 2009) and Ti-reinforced PMMA artificial ribs (in 2017) by application of additive manufacturing: custom made implants used in regenerative surgery for two patients in Clinical Center Kragujevac, Serbia. He has authored over 100 peer-reviewed publications, including 5 books, related to his areas of expertise: advanced structural analysis, linear and nonlinear static and dynamic analyses of structures, heat transfer, fluid mechanics, biomechanics, coupled problems and hydroinformatics. He was visiting scientist at Harvard University, Boston, Technical University Braunschweig, National Technical University of Athens. He has extensive experience in numerous applied research projects. He coordinated more than 6 international projects and participated in 18 international and 9 national projects (H2020, FP6, TEMPUS, WUS, INTERREG, COST programs and Ministry of Education, Science and Technological Development of Serbia).

Kwang Leong Choy is the Professor of Materials Discovery at University College London and the Director of the UCL Institute for Materials Discovery (http://www.ucl.ac.uk/institute-for-materials-discovery), from 2014. She obtained her Doctor of Philosophy (D.Phil.) in Materials Science from the University of Oxford (1992) and Doctor of Science (D.Sc.) in Materials, from the University of Nottingham (2008). She has been employed at University of Oxford (1993–1994), Department of Materials, Imperial College London (1994–2002) and at Chair in Materials, Faculty of Engineering, University of Nottingham (2002–2014). She has been elected to several prestigious fellowships such as Fellow of the Royal Society of Chemistry (2010–present), European Science Foundation NANO network (2008–2014), Chartered of Science, CSi (2007–present), as well as in editorials boards (Editorial Board of Nano-Micro Letters, Journal of Nanomaterials, and Guest Editor of "Surface Engineering" and "Chemical Vapour Deposition"). She has been the Founder, Inventor and Director of Innovative Materials Processing Technologies Ltd (a spin-out company of Imperial College London). She has authored over 220 peer-reviewed publications, including 3 books and 20 patents in nanomaterials, thin films and coatings for structural, functional and biomedical applications. She has given over 100 keynote papers/invited lectures and conference session Chairman. She is leading a multidisciplinary research team ranging from material scientists, chemists, coating specialists, bioengineering, nanobiotechnology and engineers. Her team is conducting cutting-edge research and technology exploitation of high-performance, eco-friendly and cost-effective processing of new nanostructured materials, nanocomposites and superthin/thin/thick films coated products for thin film solar cells, clean energy, energy storage, electrical, opto-electronics, environment, health care and biomedical applications. She has secured and managed numerous multimillion pounds national and European flagship research programmes with extensive collaboration with academia and industry. She has also established multimillion pound state-of-the art nanomaterials, innovative thin/thick films processing and characterisation facilities.

Short History of Biomaterials Used in Hip Arthroplasty and Their Modern Evolution

Saverio Affatato, Katarina Colic, Igor Hut, D. Mirjanić, S. Pelemiš and Aleksandra Mitrovic

Abstract The hip joint is one of the largest joints in the body and is a major weight-bearing joint. The function of the hip is to withstand body weight during standing and walking; during single leg stance the hip joint must carry a load three times greater the body weight. However, Joint degeneration is the final phase of the joint cartilage destruction, leading to severe pain, loss of mobility, and sometimes even angular deformity of the limbs. The primary reasons for a large number of total hip replacements are osteoarthritis and osteoporosis of the femoral neck, which often leads to hip fractures. One of the most successful techniques to restore function of a degenerated joint is the total joint replacement. In this surgical procedure, diseased cartilage and parts of the bone are removed and replaced with an appropriate joint prosthesis. Several types of materials and techniques have been developed for this purpose: glass, polymer, metal alloy, ceramics, etc. Earliest prosthesis designs and biomaterials that have been developed to treat osteoarthritic hip degenerated joint surfaces were for the most part empirical and unsuccessful. Joint replacement heralded a revolution after the materials and replacement procedures developed by Sir John Charnley. A modern total hip prosthesis consists of a

S. Affatato (✉)
Medical Technology Laboratory, Rizzoli Orthopaedic Institute,
Via di Barbiano, 1/10, 40136 Bologna, Italy
e-mail: affatato@tecno.ior.it

K. Colic · I. Hut
Innovation Centre of Faculty of Mechanical Engineering,
University of Belgrade, Belgrade, Serbia
e-mail: kbojic@mas.bg.ac.rs

D. Mirjanić
Academy of Sciences and Arts of Republic of Srpska, Banja Luka,
Bosnia and Herzegovina

S. Pelemiš
Faculty of Technology, UES, Zvornik, Bosnia and Herzegovina

A. Mitrovic
Biomedical Engineering Department, Faculty of Mechanical Engineering,
University of Belgrade, Belgrade, Serbia

F. Zivic et al. (eds.), *Biomaterials in Clinical Practice*,
https://doi.org/10.1007/978-3-319-68025-5_1

femoral and acetabular component, where the femoral head is made of cobalt-chrome alloy, alumina or zirconium, and the stem component is now usually made of Ti- or Co-Cr-based alloy. The search for improved designs and new hip implant biomaterials with better biocompatibility and more desirable mechanical properties is still underway.

Keywords Biomaterials · Hip prosthesis · Femur · Polymer · Ceramics · Metallic biomaterials

1 Introduction

1.1 Brief Digression of Hip Anatomy

The hip is a ball-and-socket joint realized by the acetabulum (the socket) and the head of the femur (the ball). In Fig. 1 is showed this kind of articulation.

The hip joint is one of the largest joints in the body and is a major weight-bearing joint. Weight bearing stresses on the hip during walking can be 5 times a person's body weight (Dunn 1987). A healthy hip can support our weight and allow us to move without pain. Changes in the hip from disease or injury will significantly affect the gait and place abnormal stress on joints above and below the hip. The hip bears the body's weight during standing and walking and it have three different bones (Ilium, ischium, and pubis) that contribute to the formation of the coxal bone during skeletal growth. Moreover, this articulation allows large movements, i.e. flexion/extension (in the sagittal plane), abduction/adduction (in the frontal plane), and internal/external rotation.

The ilium is formed by two main parts: the body and the ala (Marieb and Hoehn 2007). The body of the ilium forms the upper part of the acetabulum while the ala is smooth and it is covered by the iliopsoas muscle whereas the external surface gives attachment to the gluteal muscles. Along its upper margin there is a longitudinal crest which has an inner and an outer lip. The ischium forms the lower and posterior part of the coxal bone. The first visible structure in the back of the ischium is the ischial spine. Under the ischial spine the lesser sciatic notch precedes the ischial tuberosity, which is a large and strong apophysis where the posterior muscles of the thigh have origin. The ischium is connected to the pubis through a lower ramus that starts from the ischial tuberosity and continues upward and medially. The pubis is connected to the ischium through the lower and upper ramus. These rami determine a hole called obturator foramen.

The acetabulum is an hemispheric cavity located at the center of the outer surface of the coxal bone. It is directed downward, lateral ward and forward (Vandenbussche et al. 2008). Its inner surface is coated by a cartilage layer except its central part which is the site of origin of the ligamentum teres. The lower part of the outer rim of the cavity is interrupted by the acetabular notch. The glenoid

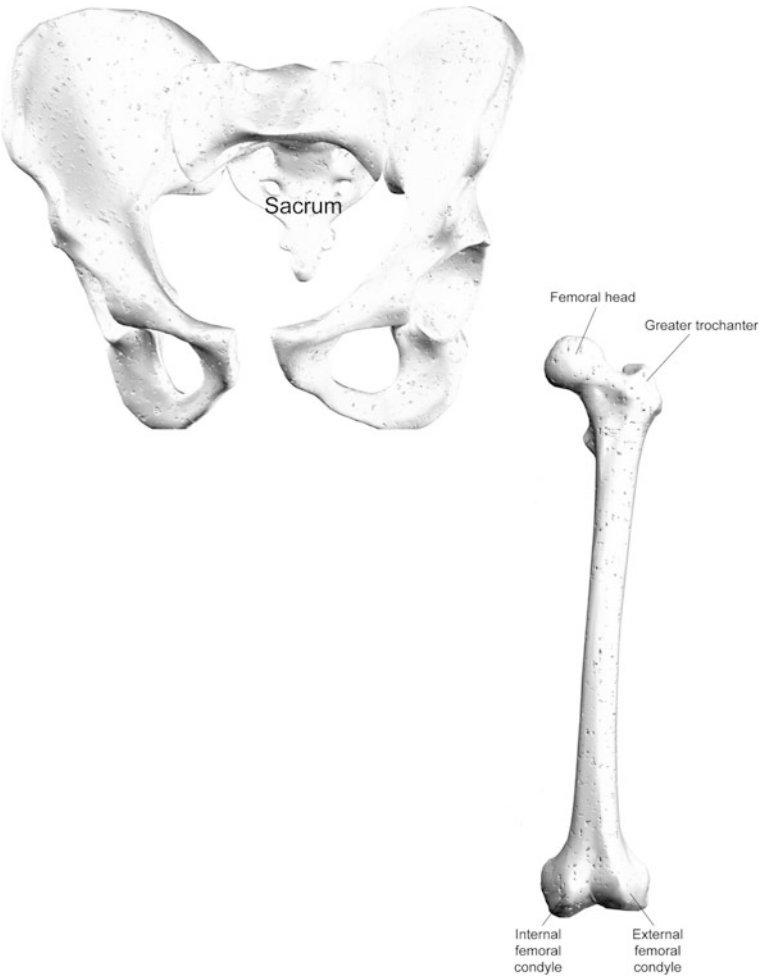

Fig. 1 The human hip joint articulation

labrum is a fibrocartilagineous structure attached to the outer rim of the acetabulum, that improves the acetabular depth. The transverse acetabular ligament is the part of the glenoid labrum contributing to close the acetabular notch. The femur is a long bone formed by a body (diaphysis) and two expanded extremities (epiphyses) (Fig. 2).

The body has a cylindrical shape and a longitudinal crest, the *linea aspera*, that divide the two rear faces. The head of the femur is hemispheric and it is almost fully covered by cartilage, with the exception of its central part, the fovea capitis, where there is the insertion of the ligamentum teres. The head of the femur is connected to the diaphysis through the neck (Gray and Bannister 1995).

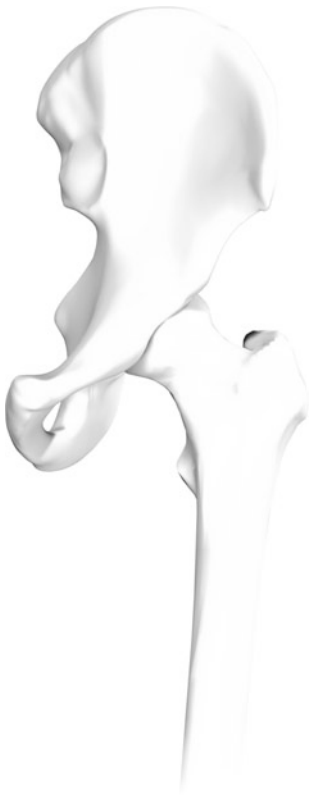

Fig. 2 Schematization of the coxal bone (together with the sacrum and the coccyx constitutes the pelvis) and the femur

The hip joint is a ball-and-socket joint that belongs to the category of diarthrodial joint. The joint present on one side the acetabulum (the socket) and on the other the head of the femur (the ball).

The articular capsule is a fibrous structure going from the origin of the glenoid labrum to the base of the femoral neck. In its front and top part it is stronger than in the bottom and rear. Do not dissociated from the articular capsule there are three ligaments of longitudinal reinforcement: the iliofemoral, the ischiofemoral, and the pubofemoral ligaments (Gray and Bannister 1995).

An additional connection between the head of the femur and the acetabulum it is guaranteed by the ligamentum teres. The functional role of the capsule, ligaments and muscles around the hip is to ensure joint stability, thus avoiding dislocation thanks to the maintenance of the bones in the right position. The smooth cartilage layer over the head of the femur and the acetabulum cushions exerts compressive forces acting on the hip joint during weight bearing. In the inner surface of the articular capsule is situated the synovial membrane, which produces the synovial fluid. The function of the synovial fluid is to lubricate the joint, ensuring a motion

without pain and with a very low friction even in the presence of great pressures (Gray and Bannister 1995).

1.2 Overview of Problems Leading to Hip Surgery

From a medical standpoint, the hip is one of the most significant joints in the body. As the hip enables articulation between the femur and the acetabulum of the pelvis, the ability to walk depends on the healthy and painless hip. The hip is troubled by two types of ailments, both very common in the elderly. Osteoarthritis is the primary reason for a large number of total hip replacements each year, and the osteoporosis of the femoral neck leads to several thousand hip fractures a year, nearly all of them requiring surgical treatment, either with implants, or metallic fixation parts (Katz 2006; Bannister 2003; Coomber et al. 2016). It is of most importance to understand forces acting on the hip joint during daily activities, especially during gait cycle, and the mechanics of the hip joint in order to solve the hip implant design problems. (Abujaber et al. 2015; Simpson et al. 2010).

Several million people fracture their hips each year, risk for women being 40%, and 13% for men (Dulić et al. 2003). Osteoporosis is the decrease of the bone mass, and fracture risk factors for osteoporosis patients of both sexes are clinically asymptotic until fracture. A large number of factors influence the risk of hip fracture, some of them being sex, age, stage of osteoporosis, body mass and height (Bottai et al. 2015; Nasiri and Luo 2016; Starup-Linde et al. 2017). Hip fracture results from acting of non-physiological forces, the main cause of the fracture being the nonelastic impact of the body on the ground. Different types and grades of hip fracture are a result of complex deformations arising from direct impact of the hip joint on the ground. Due to varied stress distribution inside the femur, a large number of different hip fracture types are possible.

The main classification of hip joint fractures is: intracapsular (occurring inside the joint capsule) and extracapsular (occurring outside the joint capsule). There are various types of hip fractures, and the fracture of the neck of the femur is the most common one, considered an intracapsular fracture.

The goals of the treatment of fracture are: swift healing, re-establishing joint function and preservation of aesthetic qualities. Generally speaking, fracture treatments can be classified as nonsurgical and surgical. The choices of the surgical treatment is established on the basis of each individual patient's clinical record, as each type and place of the fracture produce a unique problem that requires specific methods of treatment. If there is a possibility to retain the femoral head, fracture fixation method is chosen as the method of treatment in dislocated and non-dislocated femoral neck fractures (Boelch et al. 2017). This method of fixation uses screws for fastening the fracture after repositioning, and is indicated for use in patients with good bone density.

As for the intertrochanteric fractures, intramedullary nails are used as well. All internal fixation devices must conform to the defined biomaterial standards, and therefore stainless steel, cobalt-chrome alloys and titanium alloys are used.

Partial or total arthroplasty is chosen as the surgical method of treatment when it is necessary to remove the head and part of the femoral neck (Gard et al. 2000). Total hip joint prosthesis is used when the clinical record contains osteoarthrosis, rheumatoid arthritis, or several other pathological conditions. Total hip arthroplasty (THA) is a widely used strategy to restore normal hip join function, impaired through fracture or ailment (Chimento and Sculco 2001).

Joint degeneration is the final phase of the joint cartilage destruction, leading to severe pain, loss of mobility, and sometimes even angular deformity of the limbs. One of the most successful techniques to restore function of a degenerated joint is the total joint replacement. The main surgical procedure is to remove diseased cartilage and parts of the bone and insert an appropriate hip prosthesis.

Total hip replacement is an effective treatment for severe osteoarthritis (when this degenerative joint disease is mechanically initiated, which is often the case, it is more correctly termed osteoarthrosis), invalidating effects of rheumatoid arthritis, congenital deformations and some types of post-traumatic conditions (Learmonth et al. 2007). It should be noted that one of the most common indication for total joint replacement is osteoarthritis and accounts for approximately three quarters of the total (Katz 2006).

Patients with much degenerated joints greatly benefit from total hip arthroplasty, for in this way they are swiftly rid of the pain, and have their normal movement functions restored. However, total joint replacement surgical procedures have their drawbacks. Total hip arthroplasty is usually indicated in patients over 50 years of age suffering from advanced osteoarthritis, except in patients with rheumatoid arthritis, which is sometimes indicated in younger persons with rapid progressive joint destruction. The cause of this indication limitation is the longevity of the prostheses. A multicentre study of the longevity of the total joint prostheses has shown that the greatest probability for implant failure due to fracture or wear occurs around 5 to 10 years after the procedure (Archibeck et al. 2006; Schmolders et al. 2017). The designs and materials are constantly improved, but the available prostheses still have the problem with longevity (Sedmak et al. 2010).

The number of cycles of an individual prosthesis is naturally directly linked to the level of the activity of the patient. Therefore, implant failure is more common in younger, than in older patients.

2 History of Biomaterials Used in THA

Many efforts have been made to find the suitable material for hip joint: glass, polymer, metal alloy, ceramics, etc. First attempts of hip surgery found place in England between 1750 and 1820, in the effort to heal arthritis cases (Gomez and Morcuende 2005). In 1840 the idea was to think that hip joint could be replaced artificially

introducing hip arthroplasty (Pramanik et al. 2005). This technique consisted of replacing or covering the acetabular part of the femoral head. He installed a wooden block between the damaged ends of the hip joint. A large amount of wood particles released in the body fluids due to wear. Many other biological solutions were tried later on following the hip arthroplasty technique: skin, muscle tissue, pig bladder and gold foil. Several decades later, were used different material sets, such as celluloid, rubber, zinc, muscle tissue, glass, wax, silver plates and decalcified bones (Gomez and Morcuende 2005). In the effort to relieve pain and restore mechanical functionality of the patients, the hip replacement evolved to use the femoral stem technique. First attempts started in 1880, when German Professor Themistocles Glück implanted an ivory ball to the bone with nickel-plated screws with the aim to replace the damaged femoral head (Muster 1990). He discovered that human body could not accept large amounts of foreign material; later he replaced the femoral head with a mixture of powdered pumice, plaster of Paris in combination with resin. Stainless steel was later experimented by other orthopaedic surgeons (Pramanik et al. 2005).

Marius Smith-Petersen (Hernigou 2014) implanted the first glass and bakelite femoral cup, introducing mould arthroplasty. Philip Wiles (Gomez and Morcuende 2005) was the first to perform THA using a custom stainless steel implant with precisely fitted components, fixed to bone tissue with screw and bolts. Austin-Moore (Gomez and Morcuende 2005) developed a long-stemmed prosthesis based on the replacement of the femoral head and part of the femoral neck, called hemiarthroplasty. The ball, on the other side, fit into the hip acetabulum. This technique was highly successful even if loosening of the implant was the main problem (Pramanik et al. 2005). Some examples of these configurations are showed in Fig. 3.

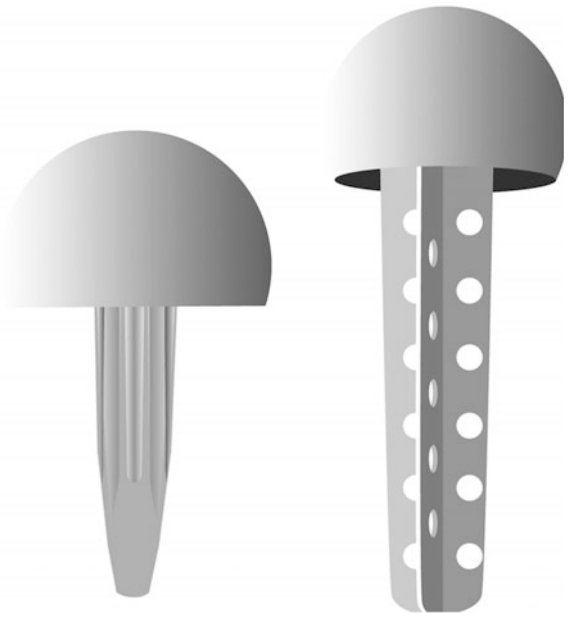

Fig. 3 Examples of total and partial hip arthroplasty

In the 1960, Dr. San Baw (Baw 1970), performed the first hip replacement on an 83 years old woman, using ivory like prosthetic material. Between the 60's and the 80's he performed over 300 ivory hip replacements describing an 88% success rate. Several approaches were made in this orthopaedic filed but was a British surgeon (Sir John Charnley) that pioneered the modern concept of total hip arthroplasty. Charnely performed its first hip implant using a combination of a femoral head (in stainless) steel coupled with acetabular cup (in Teflon -PTFE). After this failure, Charnley used, as acetabular cup, a new polymer: the *so-called* ultra-high-molecular weight- polyethylene (UHMWPE). These studies focused on the lubrication phenomena and they led to the concept of Low Friction Arthroplasty (LFA) in which the low friction depends mostly on the friction coefficient of the facing materials and only marginally on the fluid presence (McKee 1982). In Fig. 4 is showed a typical hip prosthesis.

Several variations contributed to the original design. In the 70's Cobalt-Chromium-Molybdenum (C-Cr-Mo) alloys were introduced in the low

Fig. 4 Some approaches of hip prostheses

friction arthroplasty, overcoming the first generation of metal-on-metal articulations (Ratner et al. 2004; Knight et al. 2011). In the 80's ceramic-on-ceramic bearing started with alumina and zirconia, when aseptic loosening and osteolysis emerged as major problem in metal-on-polyethylene contact.

Ceramic's hardness, scratch resistance and the inert nature of its debris made it of relevant interest for THA applications (Morrison et al. 2002). Obviously, all the materials used in the orthopaedic field must have important requirements: high strength to static and dynamic loads, high resistance to mechanical and chemical wear, biocompatibility, and fatigue resistance.

Nowadays major problem in THA is given by wear of bearings. Metal-on-polyethylene, metal-on-metal and ceramic-on ceramic are currently the bearing materials used in THA.

Recently innovative hybrid hard-on-hard bearings have been introduced in THA, coupling ceramic heads to metallic inserts (Affatato et al. 2009; Fisher et al. 2001).

The choice between these types of bearings depends on large number of factors, for example costs, age and activity of the patient, complications during surgery. Metal-on-polyethylene (M-on-PE) bearings are the most widely used in the UK today, with a rigid and remarkable follow-up control. Currently M-on-PE represents a safe, predictable and cost-effective bearing; however main concern is given by PE debris and subsequent osteolysis, leading to implant failure.

Metal-on-metal (MoM) prostheses have been taken again into consideration after the development of new design and surface finishing techniques, which allow to overtake the wear problem that in the 70's caused their fall-out. M-on-M nowadays show lower wear rate if compared to M-on-PE implants. Recent negative effects of cobalt and chromium ion release, focus the attention on these kind of materials and they are not implanted stopped in Europe even if the clinical follow-up data is insufficient to draw conclusions about the new generation M-on-M implants. Ceramic-on-ceramic (C-on-C) bearing show high level of hardness, scratch resistance, and excellent lubrication properties. In addition the inertness of wear debris makes of C-on-C bearings the best choice for young patients that need of hip joint implant. On the other side disadvantages are high costs and the need of excellent surgical insertion to prevent chipping in contact surfaces. With the introduction of ceramic-on-metal (C-on-M) it was observed a dramatic reduction of the wear rate compared to M-on-M hip prostheses; moreover, during in vitro studies it was observed a less production of smaller particle (Affatato et al. 2009; Fisher et al. 2001). In addition C-on-M bearing claim to reduce ion release and breakage of the ceramic insert rim.

2.1 The Advance in Hip Replacement Prosthesis

THA surgery is nowadays considered a safe and cost-effective surgical approach that allows to restore functionality of the hip joint and full and pain-free mobility in patients suffering from joint diseases or trauma. Ageing of the population,

decreasing of the average age of the patients undergoing first implant and limited lifetime of the prosthetic components are factors that will raise the number of people in need of this medical intervention in the next future.

The hip joint is a perfect example of congruous joint, designed for standing and walking, that allows wide variety and range of motions (Morlock et al. 2001). The particular simmetry of this joint allows for rotation about a fixed axis; infact nearly all motion between femoral head and acetabulum is rotational. The hip joint, as previously discussed, is composed by the femoral head and the three bones forming the pelvis: ilium, ischium and pubis. The femoral head, covered by cartilage, fits the acetabulum and the joint is kept lubricated with the synovial liquid (Sink et al. 2011). The human hip joint can be affected by different pathologies such as osteoarthritis, avascular necrosis, tumour, rheumatoid arthritis, femoral neck fracture, road accidents. In a THA intervention, the damaged bone and the cartilage are removed and replaced with the prosthetic components in order to restore joint functionality. The femoral head is most of times completely removed and replaced, or trimmed and covered by a metallic cap (resurfacing approach).

Artificial hip joints have evolved from their pioneering design, but, unfortunately, wear of their components remain a problem.

Some of the earliest prosthesis designs have been developed to treat degenerated joint surfaces in the case of an osteoarthritic hip. These prostheses were made from various materials, and their choice was, for the most part, empirical. There were no studies to ascertain if the material is suitable to be used in a design. Therefore, some of the implants were moderately successful, whereas other failed catastrophically.

Earliest attempts to return mobility to painful and deformed hip joints date to early 1820s and are centred on simply removing the affected femoral and acetabular bones. From 1830 to 1880 this evolved to attempts, which were quite unsuccessful, to regain joint mobility using interposition membranes between the femoral head and acetabulum, using materials such as wooden blocks and animal soft tissues (Gomez and Morcuende 2005). It was not until 1923 that Marius Smith-Petersen developed “mould”arthroplasty, which is considered the onset of modern total hip replacement (Smith-Petersen 1948; Hernigou 2014). The implant was made from glass in the shape of a hollow hemisphere, which was attached onto the femoral head, creating a new sliding surface. Although biocompatible, glass could not endure stresses during the gait cycle and failed.

The first corrosion-resistant metal that had sufficient biocompatibility, and became available in 1939, was a cobalt-based alloy named Vitallium, used by Venable, Stuck and Beach (Ratner et al. 2004). Although this new material was successful, being very hard and corrosion-resistant, the procedure of replacing the joint surface was not adequate.

Despite the excellent designs of these early long stem prostheses, they were primarily successful when they were used to replace the afflicted femoral heads, and did not perform well when acetabular reaming was necessary. Therefore, this disability started the development of total hip arthroplasty.

The first total hip arthroplasty is attributed to Philip Wiles in 1938, when he used a stainless steel ball attached to the femur and a stainless steel acetabular lining

attached by screws (Wiles 1958). The results of this design were disappointing, for these early stainless steels had low corrosion resistance in vivo and large stress concentrations on short stem prostheses.

One of the primary questions addressed by early researchers was fixation of the prosthesis component to the bone. Although Moore and Thompson's prosthesis showed excellent early results, it was not altogether successful, for cases of implant loosening were reported due to wear. Introducing an opening on the implant surface to encourage bone ingrowth did not result in sufficient biological fixation, which would stop the micro-movement of the prosthesis. To address this problem, John Charnley during the 1960s introduced poly(methyl-methacrylate) (PMMA), a cold-curing bone cement, which facilitated a safe fixation of prosthesis components (Charnley 1970).

Joint replacement heralded a revolution in treating diseased or damaged joints, bringing pain relief and restoring function. The materials and replacement procedures developed by Charnley were later used to treat other joints, such as knees, elbows and shoulders.

One of the foremost problems in the total replacement of hip and other joints is implant fixation. This problem arises because the implant is fixated onto cancellous bone, which is significantly weaker than cortical bone, and there could be insufficient trabeculae to support loads. In addition, stress concentration on the points of contact, such as the posteromedial region, and the lateral end of the femoral stem, causes resorption of already weakened bone.

In addition to providing the initial fastening of implant to bone, cement is used as a shock absorber as well, by virtue of being a highly elastic biomaterial. Bone cement also facilitates a more uniform distribution of load across the greater surface, and reduces stress concentration on the bone, which arises due to the presence of the prosthesis. This stress shielding effect causes bone resorption in the proximal region due to the reduced stress, which leads to implant loosening, or stem failure.

According to implant placement and manufacturing procedures, currently there are two types of prostheses: single-part (monolithic) or block prostheses and modular (multi-part – two or more) prostheses. Modular components are assembled during the surgical procedure, and enable implant adjustment during surgery, and subsequent revisions. Block hip prosthesis are shown on Fig. 5, whereas Fig. 6 shows femoral parts of various modular prostheses.

3 Biomaterials Used for Contemporary Types of THA

In general, total hip prosthesis consists of a femoral and acetabular component, with the femoral base divided into the head, neck and stem. In total hip prosthesis, the femoral head is most commonly made of cobalt-chrome alloy, alumina or zirconium, whereas the stem component, formerly made from 316L stainless steel, is now usually made of Ti- alloy or Co-Cr-based alloy. Sliding surfaces are often

Fig. 5 Examples of monolithic prostheses

made from cobalt-chrome alloy and ultra-high-molecular-weight polyethylene (UHMWPE), as this combination achieves low-friction sliding surfaces characteristics. In addition, polyethylene possesses moderate plasticity, allowing it to deform, and therefore create a suitable sliding surface in contact with cobalt-chrome alloy.

At present time, specific advantages of various materials are combined into modular implants. Thanks to modularization, each material can be optimized according to specific function, as shown in Table 1 (Park and Lakes 1992; Ratner et al. 2004). Material characteristics, shape and fixation method establish the stress distribution characteristics in each individual case (Ruben et al. 2012; Park 2000).

According to connection type, modular prostheses are made of high-strength Co-Cr- or Ti-based alloys, with appropriate surface finish. With modular hip prosthesis, it is possible to attach a femoral head with various neck lengths during the surgery.

Fig. 6 Examples of modular prostheses

An example of typical hip prosthesis components with titanium-based alloy stem, modular cobalt-based alloy head articulating against a UHMWPE lining, is shown in Fig. 7.

Currently, hip replacement implants are most commonly constructed from a femoral stem made from Ti or Co-Cr alloy, cemented by poly(methyl methacrylate), pressed into place, connected to a modular head made from Co-Cr alloy or ceramics, articulating against the acetabular cup lining made from UHMWPE or ceramics, cemented, screwed or pressed into place. Despite this simple archetype of hip arthroplasty, there are hundreds of variations available for use to orthopaedic surgeons, with very little in the way of absolute recommendations on which implant type, or which implant design should be considered best for defined orthopaedic afflictions (Gard et al. 2000; Ruben et al. 2012). In general, there is a wide variety of surface coarseness, coatings, geometries, material compositions, etc.

Table 1 Hip prosthesis materials

Material	Cemented hip stem	Noncemented hip stem	Femoral head	Cap/lining	Metal shell
Stainless steel	In clinical use	–	In clinical use	–	–
Co-Cr-Mo	In clinical use	In clinical use	In clinical use	In clinical use	In clinical use
CP titanium	–	–	Clinically unsuccessful	–	In clinical use
Ti-based alloys	Clinically unsuccessful	In clinical use	Clinically unsuccessful	–	In clinical use
UHMWPE	–	–	–	In clinical use	–
Ceramics	–	–	In clinical use	In clinical use	–
Zirconium	–	–	In clinical use	–	–

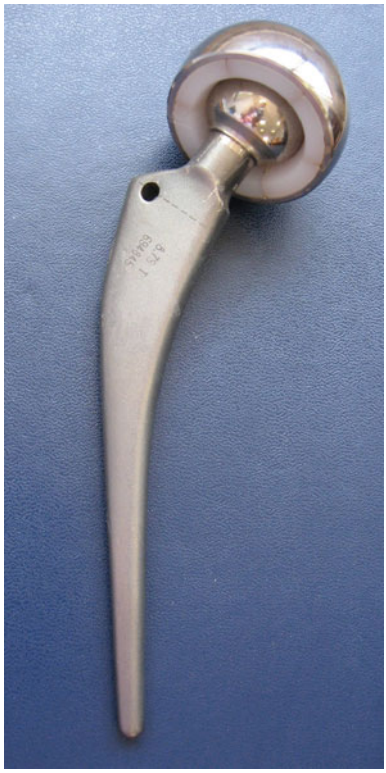

Fig. 7 Example of typical hip prosthesis components

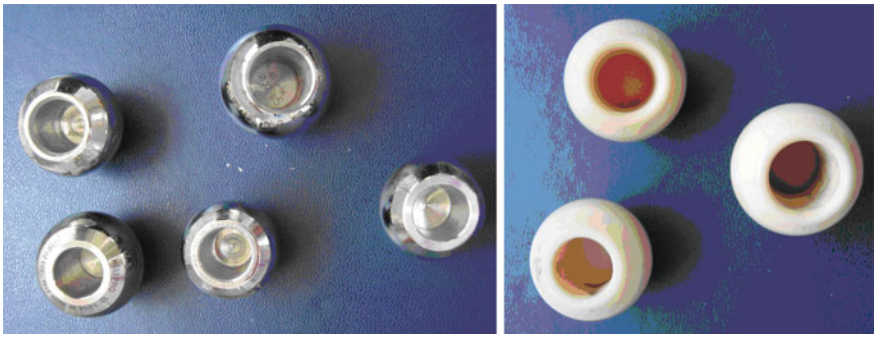

Fig. 8 Various types of metallic and ceramic sockets

It should be noted that the metallic sockets are in clinical use approximately 45 years, and alumina sockets around 35 years of clinical use so far. Figure 8 shows various types of sockets of differing diameters, made from metal or ceramics.

Polymers in orthopaedics are most commonly used for articulating sliding surfaces in joint replacement, and as a cement material between bone and implant. Polymers used for articulating surfaces must have a low coefficient of friction and low rate of wear in contact with other surface, which is usually made from metal.

Polymers used for fixation, as a structural connection between implant component and bone tissue, must have appropriate mechanical characteristics, must be able to be cast into a specific shape, and be cured in vivo.

One of the most commonly used polymers presently used in orthopaedics is a highly cross-linked UHMWPE, typically used in total hip arthroplasty as a sliding surface designed to enable sliding articulation with low friction. Polyethylene is commercially available in three types: low density, high density, and UHMWPE. Denser packing of linear chains in UHMWPE achieves better mechanical characteristics necessary for application in orthopaedics, although ductility and strength are reduced. In total hip arthroplasty, an acetabular cap made from UHMWPE typically articulates against a Co-Cr alloy femoral head (Buford and Goswami 2004).

In recent years ceramics and glass-ceramics are gaining in importance in manufacturing implants. Although they have been in use for over 25 years in Europe, only in 2003 has the FDA approved the first hip prosthesis to be made with sliding surface of type ceramic-ceramic, and be used in hip replacement procedures in the USA. The primary reason for introducing this alternative sliding surface is the superior wear resistance of ceramics in comparison to metal-metal, or metal-polymer sliding surfaces (Wang and Essner 2001). These and other improved characteristics, as the resistance to further oxidation (resulting in inertness inside the body), high strength and low friction, require using the ceramic materials with controlled, small and uniform grain size (Slonaker and Goswami 2004). Small grain size and full density are important, for they are two basic parameters controlling the mechanical characteristics of ceramics. Cavities in the ceramic body increase stress

and degrade mechanical characteristics. In ceramics, thermal contraction stresses are critical, for no plastic deformation can occur, as in the case of ductile materials.

Ceramics made from Alumina (Al_2O_3) and zirconium (ZrO_2) has been used in hip replacement since the 1970s. The first ceramic contact (alumina/alumina) was patented by Pierre Boutin in 1970. From the start, the theoretical advantage of hard/hard articular surface was low wear. Thanks to ionic bonds and chemical stability, ceramics are relatively biocompatible as well.

As the main function of long bones in the lower part of the body is load bearing, it was reasonable to expect that the initial materials for use in hip replacement would be metallic biomaterials. Stainless steel, such as 316L, and Co-Cr alloys have been chosen as appropriate materials thanks to their good corrosion resistance and reasonably long life during load-bearing application inside human body. Their characteristics, such as toughness and strength are significantly higher than those of human bone. Metals remain the central component of materials for use in contemporary total hip arthroplasty. Metals possess appropriate material characteristics, such as great strength, ductility, fracture resistance, hardness, corrosion resistance, the ability to shape, and biocompatibility, which are necessary for load-bearing applications in fracture fixations and total arthroplasty. Alloys used to manufacture implants where initially developed for aviation and maritime application, where mechanical characteristics, such as toughness and corrosion resistance, are of the highest importance. Specific differences in strength, ductility and hardness usually determine which of these three alloys will be used for certain application or implant component. All the same, high degree of strength of these alloys was instrumental in bringing them to widespread use in load-bearing implant applications.

4 Development of Modern Biomaterials Used in THA

Metallic materials have a wide range of applications in medicine, not only in orthopaedic implants, but in other areas as well. Of special importance are the reaction of the metallic surface to the biomolecules and/or the reaction to cells. Good understanding of these reactions will enable adding new functions to metallic materials having excellent mechanical properties. It is of most importance that all processes and interactions between surfaces of living tissue and biomaterials are investigated and well understood, because of their constant interaction after insertion of an implant.

New metallic biomaterials are proposed to improve implant/bone stress distribution and reduce the incidence of implant loosening and painful hip. Alloys currently used to produce implants have a relatively high module of elasticity, which limits stress distribution from implant to bone. New alloys are developed with lower module of elasticity, and greater corrosion resistance (Boudeau et al. 2012).

The search for new metallic alloys for application in hip prostheses with greater biocompatibility and better mechanical properties is still ongoing (Goi et al. 2008).

Using the Ti, Co-Cr-Mo alloys or stainless steel for specific applications effectively means that some desirable property will be traded for some other property. Some examples of this are sacrificing the chemical inertness for wear resistance, as with Ti alloys, and Co-Cr-Mo sliding surfaces of the implant, and sacrificing strength and ductility while using stainless steel instead of Ti and Co-Cr-Mo alloys for bone fixation rods.

Zirconium (Zr) and tantalum (Ta) are characterised as refractory metals for their great chemical stability (passive oxide layer). Thanks to great hardness, chemical stability and wear resistance alloys such as Oxinium will probably become popular as orthopaedic biomaterials (Good et al. 2005). Zr and Ta are very resistant to corrosion, thanks to stability to their oxide layer.

Other attempts at improving the traditional Ti-6Al-4 V alloys have been conducted in the field of improving biocompatibility and mechanical characteristics by replacing vanadium, as the relatively toxic metal, by another, less toxic metals. Properties of two Ti alloys,Ti-5Al-2.5Fe and Ti-6Al-7Nb, are shown in Table 2 (Milne et al. 2003). These alloys, while having similar characteristics as the traditional Ti-6Al-4 V, also have a greater dynamic hardness and smaller module of elasticity, and therefore have a better implant/bone stress distribution.

Often the new alloys are just a variation of already described three categories of already approved metals used for implant production. These improved alloys usually contain only a minor addition of new elements, to protect themselves from equality with existing ASTM and FDA-approved alloys, and therefore facilitate the process of regulatory approve. These new alloys, for the most part, can be classified into four categories: (1) titanium-based alloys, (2) cobalt-based alloys, (3) stainless steels, and less often approved, (4) refractory metals.

A new group of Ti alloys for application in orthopaedic components uses molybdenum in concentrations greater than 10%. The addition of Mo stabilizes the β-phase at room temperature, and therefore these alloys are called β-Ti alloys. These alloys promise a 20% lower module of elasticity, which is closer to real bone values, as well as better shaping possibilities, while retaining other mechanical

Table 2 Standardized titanium and titanium-based alloys

Alloy	Type	ASTM standard	ISO standard
Ti-3Al-2.5 V	α + β	ASTM B 348	
Ti-5Al-2.5Fe	α + β		ISO 5832-10
Ti-6Al-7Nb	α + β	ASTM F 1295	ISO 5832-11
Ti-15Mo	β	ASTM F 2066	
Ti-13Nb-13Zr	β	ASTM F 1713	
Ti-12Mo-6Zr-2Fe	β	ASTM F 1813	
Ti-45Nb	β	AMS 4982	
Ti-35Nb-7Zr-5Ta	β		
Ti-55.8Ni	Intermetal	ASTM F 2063	

characteristics typical for Ti-6Al-4 V. This low module of elasticity could lessen the incidence of stress shielding, leading to implant failure.

UHMWPE was considered for a long time to be a clinically-proven partner to metal and ceramic femoral heads. However, recently its reputation has been tarnished, because it was observed that wear-induced particles are one of the main factors of emergence of particle osteolysis (Lapcikova et al. 2009). New, highly cross-linked polyethylene has enabled greater wear resistance in laboratory testing conditions, but clinical data on wear are not available to date. In the attempts to make sliding surfaces even more resistant to abrasion, development of hard on hard sliding surfaces (such as metal, or ceramics) was soon started (Manley and Sutton 2008). In these cases both articulating surfaces are made from the same material, and are extremely resistant to wear). The amount of wear is 50–100 times lowers than in conventional polyethylene sockets.

Attempts were made to use the osteophytic surface of certain ceramics and glass-ceramics. These materials present a connection of such biological compatibility with the osteoblasts that those cells connect the bone directly to the material in a kind of direct bond. Glass-ceramics of special composition, called bioglasses, are used for implants in orthopaedics. A suggested model for the chemical bond formed between glass and bone is that glass undergoes a controlled surface degradation, producing a layer rich in SiO, Ca and P at the place of contact. Although amorphous, the layer rich in Ca and P crystallizes as a mixed hydroxy-carbonate apatite structurally integrated with collagen, which enables subsequent connection with newly formed mineralized tissues. In addition, certain, completely unrelated inorganic compounds were shown to be osteophytic. Among others, these include OHAp, a form of natural inorganic compound found inside calcified tissues, and calcite (CaCO), and its Mg analogue, dolomite. OHAp found its way to regular use in orthopaedics and stomatology. It is used as a coating for metal prostheses in orthopaedics, and in its dense, particulate form, in stomatology. Elastic properties of OHAp and glass-ceramics as coatings on metal hip prosthesis stems enable another fixation method, instead of using PMMA (Kühn 2000). In this case, the fixation is performed by direct bonding of bone to the surface of the coating.

The cement itself can create problems, like the emission of monomers, which interfere with systemic functions of the body, and lower blood pressure. A very exothermic polymerization can cause a local increase in temperature, which can lead to cellular necrosis (Hloch et al. 2014). In addition to that, the preparation of the medullar cavity, prior to applying the cement, can block the sinusoid capillaries inside the bone, leading to tissue necrosis and fat embolism.

The problems of the implant/cement bond can be ameliorated if the prosthesis is percolated with bone cement during manufacturing. Implants treated in this fashion are now commercially available. The coating not only increases the fastness of the bond, but eliminates the exposition of metal surface to the environment, decreases the quantity of bone cement needed, and therefore the quantity of heat necessary to perform the procedure, and the quantity of released monomers. This coating technique can be used for all orthopaedic implants.

Fig. 9 Example of currently used surface finishing technique for hip prostheses stems

Also, new techniques of surface finishing, such as diffusion hardening suggested for Ti-13Nb-13Zr alloy, can produce a hardened surface with wear resistance superior to Co-Cr-Mo alloy, currently having the best tribological characteristics. These surface improvements can lead to better resistance to micro-friction occurring in regions of the femoral head and neck.

A wide selection of surface finishing techniques is currently used to ameliorate short-term and long-term implant characteristics by stimulating bone in growth and improved fixation, Fig. 9. Some of those finishes are: coarse titanium surface, porous cobalt-chrome or titanium ball layer, titanium wire net, plasma-sprayed titanium, and bioactive non-metallic biomaterial coating, such as hydroxyapatite (Balac et al. 2012; Majewski and Allidi 2006). In order to improve fixation of hip prostheses osteoconductive and osteoinductive growth factors are developed to be used as osteogenic coatings of implant surface.

References

Abujaber SB et al (2015) Sit-to-stand biomechanics before and after total hip arthroplasty. J Arthroplasty 30(11):2027–2033

Affatato S et al (2009) Mixing and matching in ceramic-on-metal hip arthroplasty: an in-vitro hip simulator study. J Biomech 42(15):2439–2446

Archibeck MJ et al (2006) Cementless total hip arthroplasty in patients 50 years or younger. J Arthroplasty 21(4):476–483

Balac I et al (2012) Modeling of the matrix porosity influence on the elastic properties of particulate biocomposites. FME Trans 40(2):81–86

Bannister G (2003) Primary total hip replacement. Surgeon 1(6):332–341

Boelch SP et al (2017) Comparison of open reduction and internal fixation and primary total hip replacement for osteoporotic acetabular fractures: a retrospective clinical study. Int Orthop 41 (9):1831–1837
Bottai V et al (2015) Total hip replacement in osteoarthritis: the role of bone metabolism and its complications. Clin Cases Miner Bone Metab 12(3):247–250
Boudeau N et al (2012) Composite based on polyetheretherketone reinforced with carbon fibres, an alternative to conventional materials for femoral implant: manufacturing process and resulting structural behaviour. Mater Des 40:148–156
Buford A, Goswami T (2004) Review of wear mechanisms in hip implants: paper I—General. Mater Des 25:385–393
Charnley J (1970) Acrylic cement in orthopaedic surgery. E. S, Livingstone, Edinbourgh
Chimento GF, Sculco TP (2001) Minimally invasive total hip arthroplasty. Op Techn Orthop 11(4):270–273
Coomber R (2016) Total hip replacement for hip fracture: surgical techniques and concepts. Injury 47(10):2060–2064
Dulić B et al (2003) Prelomi kuka (in Serbian). Acta Clinica, Klinički centar Srbije, Beograd
Dunn JS (1987) Anatomy. A regional atlas of the human body. J Anat 155:214–215
Fisher J (2001) In: Toni A, Willmann G (eds), Proceedings 6th International Biolox Symposium, pp 94–98
Gard PJ, Iorio FR, Healy WL (2000) Hip replacement: choosing an implant. Op Techn Orthop 10(2):94–101
Goi KLS et al (2008) Elastic modulus of sintered porous Ti–Si–Zr, using activation by Ti–Si mechanically alloyed powder and TiH2 powder. Mater Sci Eng A 475:45–51
Gomez P, Morcuende JA (2005) Early attempts at hip arthroplasty-1700s to 1950s. Iowa Orthop J 25:25–29
Good V et al (2005) Oxidized zirconium: a potentially longer lasting hip implant. Mater Des 26(7):618–622
Gray H, Bannister LH (1995) Gray's anatomy: the anatomical basis of medicine and surgery thirty-eig., Churchill Livingstone
Hernigou P (2014) Smith-Petersen and early development of hip arthroplasty. Int Orthop 38: 193–198
Hloch S et al (2014) Thermal manifestations and nanoindentation of bone cements for orthopaedic surgery. Therm Sci 18(S1):S251–S258
Katz JN (2006) Total joint replacement in osteoarthritis. Best Pract Res Clin Rheumatol 20(1):145–153
Knight SR, Aujla R, and Biswas SP (2011) Total Hip Arthroplasty-over 100 years of operative history. Orthop Rev (Pavia) Sep 6; 3(2):e16
Kühn KD (2000) Bone cements: up-to-date comparison of physical and mechanical properties of commercial materials. Springer, New York
Lapcikova M et al (2009) Nanometer size wear debris generated from ultra high molecular weight polyethylene in vivo. Wear 266:349–355
Learmonth ID, Young C, Rorabeck C (2007) The operation of the century: total hip replacement. Lancet 370(9597):1508–1519
Majewski PJ, Allidi G (2006) Synthesis of hydroxyapatite on titanium coated with organic self-assembled monolayers. Mater Sci Eng A 420:13–20
Manley MT, Sutton K (2008) Bearings of the future for total hip arthroplasty. J Arthroplasty 23(7):47–50
Marieb EN, Hoehn K (2007) Human anatomy and physiology
McKee GK (1982) Total hip replacement—past, present and future. Biomaterials 3:130–135
Milne I, Ritchie RO, Karihaloo B (2003) Comprehensive structural integrity: bioengineering, vol 9. Elsevier Ltd, Oxford
Morlock M et al (2001) Duration and frequency of every day activities in total hip patients. J Biomech 34(7):873–881

Morrison JC et al (2002) Ceramic-on-ceramic bearings in total hip arthroplasty. Clin Orthop Relat Res 405:158–163
Muster D (1990) Themistocles Gluck, Berlin 1890: a pioneer of multidisciplinary applied research into biomaterials for endoprostheses. Bull Hist Dent 38:3–6
Nasiri M, Luo Y (2016) Study of sex differences in the association between hip fracture risk and body parameters by DXA-based biomechanical modeling. Bone 90:90–98
Park JB (2000) Hip joint prosthesis fixation-problems and possible solutions. The biomedical engineering handbook, vol 2. CRC Press LLC, Boca Raton, FL
Park JB, Lakes RS (1992) Biomaterials an introduction. Plenum Press, New York
Pramanik S, Agarwal AK, Rai KN (2005) Chronology of total hip joint replacement and materials development. Trends Biomater Artif Organs 19(1):15–26
Ratner BD et al (2004) Biomaterials science: an introduction to materials in medicine
Ruben RB, Fernandes PR, Folgado J (2012) On the optimal shape of hip implants. J Biomech 45(2):239–246
Schmolders J et al (2017) Thirteen year follow-up of a cementless femoral stem and a threaded acetabular cup in patients younger than fifty years of age. Int Orthop 41(1):39–45
Sedmak A et al (2010) Structural integrity assessment of hip implant made of cobalt-chromium multiphase alloy. Struct Integr Life 10(2):161–164
Simpson DJ et al (2010) Biomechanics in orthopaedics: considerations of the hip and knee. Surg (Oxford) 28(10):478–482
Sink EL et al (2011) Multicenter study of complications following surgical dislocation of the hip. J Bone Joint Surg Am 93:1132–1136
Slonaker M, Goswami T (2004) Review of wear mechanisms in hip implants: paper II–ceramics IG004712. Mater Des 25:395–405
Smith-Petersen MN (1948) The classic: evolution of mould arthroplasty of the hip joint. J Bone Joint Surg. 134:5–11
Starup-Linde J et al (2017) Epidemiology of Fractures in Diabetes. Calcif Tissue Int 100(2): 109–121
Vandenbussche E et al (2008) The asymmetric profile of the acetabulum. Clin Orthop Relat Res 466:417–423
Wang A, Essner A (2001) Three-body wear of UHMWPE acetabular cups by PMMA particles against CoCr, alumina and zirconia heads in a hip joint simulator. Wear 250:212–216
Wiles P (1958) The surgery of the osteoarthritic hip. Br J Surg 45:488–497

Part I
Material Classes

Progress Beyond the State-of-the-Art in the Field of Metallic Materials for Bioimplant Applications

Eva Pellicer, Martina Lorenzetti, Jordina Fornell, Maria Dolors Baró, Sasa Novak and Jordi Sort

Abstract Metallic materials have attracted the interest from a wide research community including materials scientists, materials engineers, biologists and medical doctors for their use in the biomedical area. Some alloy compositions are already in use in the market but suffer from several shortcomings. For this reason, novel, optimized, non-toxic, biocompatible compositions are being continuously devised. This chapter first reviews and discusses the advantages of bulk metallic glasses (BMGs) for orthopaedic applications, with special emphasis on their mechanical properties. Examples of newly developed permanent Ti-based and biodegradable Mg-based materials are given. In the second part of this chapter, the surface engineering methods currently available to modify the surface of Ti alloys are discussed. The outermost material layer in contact with the surrounding tissue acts as the biointerface and, hence, if appropriately designed, it can provide enhanced mechanical and corrosion resistance to the bioimplant and prevent from ions leaching. Finally, the recent progress on the formation of nanostructured titania coatings by hydrothermal treatment on the surface of Ti-based alloys is analysed.

E. Pellicer (✉) · J. Fornell · M.D. Baró · J. Sort
Departament de Física, Facultat de Ciències, Universitat Autònoma de Barcelona, 08193 Bellaterra, Spain
e-mail: Eva.Pellicer@uab.cat

M. Lorenzetti · S. Novak
Department for Nanostructured Materials, Jožef Stefan Institute, Jamova cesta 39, 1000 Ljubljana, Slovenia

S. Novak
Jožef Stefan International Postgraduate School, Jamova cesta 39, 1000 Ljubljana, Slovenia

J. Sort
Institució Catalana de Recerca i Estudis Avançats (ICREA), Passeig Lluís Companys 23, 08010 Bellaterra, Spain

F. Zivic et al. (eds.), *Biomaterials in Clinical Practice*,
https://doi.org/10.1007/978-3-319-68025-5_2

Keywords Titanium alloys · Magnesium alloys · Bioimplants · Hydrothermal treatment · Nanostructured coatings

1 Introduction

The search for materials for bioimplant applications has been a burgeoning topic for many years. Implant biomaterials can be broadly classified into metallic, ceramic, polymeric, and composite systems. Metallic formulations based on steel date back from early years of the 20th century. However, unwanted tissue reactions made surgeons to abandon these formulations till the more biocompatible 316 stainless steel (SS) emerged on 1920s. Although the medical grade 316 stainless steel has been used in orthopaedics since many decades ago, especially in U.S., most artificial joints worldwide currently consist of a metallic component (either titanium alloy or Co–Cr alloys) articulating against a polymer (typically ultrahigh molecular weight polyethylene). Ti6Al4V alloy has been long favoured as structural metallic biomaterial for the replacement of hard tissues in artificial joints. Table 1 lists some of the key properties of metallic materials used for bioimplant applications. In spite of the benefits brought by their mechanical properties, ease of fabrication and availability at low cost, the long-term corrosion and the release of toxic alloying elements in the human body is known to cause several adverse health side-effects on the long term, including cessation of bone formation/growth, synovitis and loosening of implant, neoplasm formation, and Alzheimer disease, among others.

Bulk metallic glasses (BMGs) hold a privileged position among metallic materials because of their superior physical and mechanical properties compared to crystalline counterparts. Most importantly, the chemical homogeneity of BMGs and the lack of defects like dislocations and grain boundaries make them more resistant to corrosion in body fluids. For this reason, the design of BMG compositions to be applied in the biomedical field has been the object of manifold investigations in the last decade (Schroers et al. 2009). Ti- and Zr-based BMG are the most commonly investigated alloys when it comes to permanent implant applications whereas Mg- and Ca-based BMGs have been advocated as plausible bioabsorbable implants. Zr-based BMGs have become appealing for low-friction arthroplasty applications due to their high strength, low Young's modulus and outstanding wear resistance

Table 1 Some key properties of metallic bioimplant materials used in the market

Property	Cold worked 316L SS	Ti6Al4V	Cast Co–Cr–Mo
Density (g/cm^3)	7.9	4.5	8.3
Tensile strength (MPa)	860	860	655
Yield strength (MPa)	690	795	450
Elongation (%)	12	10	8
Reduction of area (%)	50	25	8
Young's modulus (GPa)	193	115	230

(Chen et al. 2011). However, these alloys usually contain toxic elements such as Ni, Be or Al, which has hampered their penetration into the market. Yet, recent studies focusing on Zr-based BMGs containing Al and/or Ni showed no toxicity and a biocompatibility level comparable to that of commercial Ti6Al4V alloy (Huang et al. 2011; Zhu et al. 2012). Ti-based BMGs are without any doubt the most popular metallic materials when it comes to bioimplant applications. This includes artificial hip and knee joints, screws for fracture fixation, bone plates, pacemakers and cardiac valve prostheses (Morrison et al. 2007). Over the past years, there have been numerous advances in the field of Ti-based BMGs, which will be briefly reviewed in Sect. 3. Meanwhile Sect. 4 is devoted to Mg-based bioabsorbable BMGs. Section 5 provides an overview of the surface modification strategies aimed at increasing the biomechanical compatibility of metallic materials in general and Ti-based alloys in particular, with special emphasis on the hydrothermal treatment.

2 Fundamentals of BMGs

Strictly speaking, 'metallic glass' term refers to an amorphous solid formed by continuous and rapid cooling from the liquid state. At sufficiently high cooling rates, crystallization is suppressed and the atomic configuration of the liquid gets homogeneously frozen at a temperature known as the 'glass transition temperature' (T_g). BMGs exhibit a wide supercooled liquid region between T_g and the onset crystallization temperature (T_x). This enables shaping the material under a small applied pressure within this regime. Yet, the maximum size of the objects attainable by the casting method is limited by the glass forming ability (GFA). GFA is the tendency to form a glass via quenching. Different indicators of GFA for BMGs have been proposed, like the interrelationship between the reduced glass transition temperature, T_{rg} (= T_g/T_l, where T_g and T_l are the glass transition and liquidus temperatures, respectively) and the supercooled liquid range, ΔT_{xg} (Lu and Liu 2002). The rational design of alloy compositions is aimed at having a large GFA so that bulk amorphous alloys larger or equal to 1 mm in all directions can be obtained. In spite of the progress in optimizing BMG compositions, the critical diameter of the rods typically remains below 5 mm. Since BMGs do possess neither long range order nor the typical defects associated with crystalline materials, they do not deform through dislocation movement. Instead, plastic deformation in BMGs at room temperature is localized in shear bands that proceed across and over the material very rapidly, resulting in limited plasticity. The yield stress and hardness of BMGs can be twice as those of steels. Moreover, they show larger elastic strain and fracture toughness than conventional ceramics. Although BMGs suffer from limited plasticity, both fracture strength (σ_f) and Vickers microhardness (H_v) are higher than in any class of crystalline material.

Even though BMGs are amorphous in nature, some of their intriguing physical and mechanical properties stem from the local atomic structure. The local atomic structure in BMGs still remains unclear and it is in fact one of the most passionate

topics of debate. Since the pioneering works by Spaepen (1977) and Argon and Kuo (1980) in 1977 and 1980, respectively, on the "free volume" concept, different models have been put forward to explain the atomic-scale structure and defects in glassy alloys. According to the dense cluster-packing model proposed by Miracle on 2004, amorphous alloys consist of short-range order (SRO) atomic clusters (Miracle 2004). These clusters are reported to affect the atomic packing state and, in turn, the properties of BMGs (Sheng et al. 2006). Yet, the link between the SRO and the macroscopic properties of BMGs is far from being well understood and, in turn, quantified.

3 Permanent Metallic Materials. Recent Advances on Ti-Based BMGs

Since it has been long recognized that Be is highly toxic, Ti-based BMGs have been typically classified as Be-containing and Be-free alloys. They exhibit different GFA and, accordingly, distinct mechanical properties. The former alloys show higher fracture strength (σ_f exceeds 2300 MPa) but reduced plasticity (<0.5%). This poor plasticity causes catastrophic failure in load-bearing applications. Conversely, the latter display larger plastic strain but a relatively lower σ_f ($\sim$1900 MPa). However, Be-containing Ti BMGs and, in general, other compositions including Al, V, Cr, Mn, Co, Ni and/or Cu are not compatible with the human body and are thus not applicable in the biomedical field (Calin et al. 2013). Yet, the toxicity of Cu is still under debate and the literature shows conflicting results (Cortizo and Fernández Lorenzo de Mele 2004). This is because cytotoxicity is time and concentration-dependent. A great effort has been made in the recent years to produce Ti-based BMGs free from toxic and allergenic elements, showing reasonable plasticity at room temperature and Young's modulus lower than those of commercial metallic alloys currently used in the biomedical field. As a result, new body-friendly compositions have been put forward: TiZrFeSi, TiZrFeSiMoNb, TiNbZrSi (Calin et al. 2013), TiZrCuPdNb (Fornell et al. 2013), among others. Alloying Sn and/or Nb with Ti is a convenient strategy to enhance BMGs plasticity. For instance, it has been reported that the addition of 2% Sn to a Ti–Zr–Cu–Pd metallic glass increases the plasticity by about 3% while keeping both the strength and the GFA unaltered (Zhu et al. 2008). The addition of Nb is even strategically more interesting than Sn because Nb is a tougher element. Nb can increase the plasticity of BMGs through different mechanisms: (i) in situ formation of ductile body-centered cubic phase (Kühn et al. 2006), (ii) formation of quasicrystals (Qiu et al. 2005) or medium-range ordered clusters (Park et al. 2010) and (iii) nanoparticles embedded in the glassy matrix (Qin et al. 2008).

In a generic way, two main strategies have been devised in order to increase the otherwise limited plasticity of Ti-based BMGs:

Table 2 Composition of newly developed Ti-based BMGs and their mechanical properties

Alloy	State	Shape	Young's modulus (GPa)	Yield stress (GPa)	Plastic strain (%)	References
$Ti_{75}Zr_{10}Si_{15}$	Amorphous matrix + NC	Ribbon	–	2.6	–	Calin et al. (2013)
$Ti_{60}Zr_{10}Nb_{15}Si_{15}$	Amorphous	Ribbon	–	2.2	–	Calin et al. (2013)
$Ti_{40}Zr_{10}Cu_{38}Pd_{12}$	Amorphous	Rod	100 (compression)	1.90	8.7	Fornell et al. (2013)
$Ti_{38.8}Zr_{9.7}Cu_{36.9}Pd_{11.6}Nb_3$	Amorphous matrix + NC	Rod	104 (compression)	1.75	0.2	Fornell et al. (2013)
$Ti_{40}Zr_{10}Cu_{34}Pd_{14}Sn_2$	Amorphous	Rod	120 (compression)	2.00	2.4	Zhu et al. (2008)
$Ti_{45}Zr_{15}Pd_{35}Si_5$	Amorphous	Ribbon	70 (dynamic Young's modulus)	2.2	–	Oak and Inoue (2008)
$Ti_{60}Zr_{10}Ta_{15}Si_{15}$	Amorphous	Ribbon	88 (dynamic Young's modulus)	2.4 (tensile stress)	–	Oak and Inoue (2007)
$Ti_{47}Cu_{38}Zr_{7.5}Fe_{2.5}Sn_2Si_1Ag_2$	Amorphous	Rod	92 (compression)	2.01	2.5	Pang et al. (2015)

Note The yield stress (σ) for $Ti_{75}Zr_{10}Si_{15}$ and $Ti_{60}Zr_{10}Nb_{15}Si_{15}$ alloys has been calculated from Vickers microhardness (H_V) experiments using the relation $\sigma = H_V/3$

NC stands for nanocrystals

(1) Annealing treatments at temperatures between T_g and T_x can result in a certain increase of plastic strain (Qin et al. 2007).
(2) Precipitation of crystalline particles within the metallic glass matrix during casting. This can be achieved by designing suitable alloy compositions or through the mixing of a good glass-former composition with a high melting point element, which will undergo precipitation as a second phase (Ott et al. 2003). In situ formed Ti-based bimodal composites have been proposed by some authors (He et al. 2003; Zhang et al. 2007).

Young's modulus, defined as the stiffness during elastic deformation, is another clinically relevant parameter in the orthopaedics area. It indicates whether the selected material has similar elastic properties to the hard tissue that is going to replace (i.e. the bone). Bone's elastic modulus spans 15–25 GPa (Ritchie et al. 2009). To assure long life-time of the bone implant, the BMG should combine high strength and high elastic limit with relatively low Young's modulus (as close as possible to that of bone). This avoids loosening of the implant, a severe biomechanical incompatibility known as "stress shielding effect". Currently, a number of multi-component nanostructured Ti-based alloys, free from highly toxic elements have been developed, such as Ti–50Ta (Zhou and Niinomi 2008), Ti–Sn–Nb (Nouri et al. 2010), Ti–Mo–Nb (Xu et al. 2008), Ti–Mo–Zr–Fe (Naga et al. 2005), Ti–Nb–Zr–Ta (Elias et al. 2006), Ti–Fe–Sn (Han et al. 2009) and Ti–Zr–Hf–Fe (Hynowska et al. 2013). These alloys constitute the so-called second generation biomaterials (Geetha et al. 2009). Typically, they feature Young's modulus values lower than for conventional BMGs. Indeed, the values are closer to the Young's modulus of bone. However, the yield strength is usually lower than for BMGs. Table 2 lists some of the new Ti-based BMGs developed during the last decade together with some of the mechanical properties relevant to the biomedical field.

4 Biodegradable Metallic Materials. Recent Advances on Mg-Based BMGs

The interest in Mg for temporary implants dates back to the 1940s. At that time, Mg implants were tested as bone plates and screws, although were ultimately abandoned mostly due to the generation of hydrogen gas during in vivo implantation (Witte 2010). Mg shows a strange phenomenon termed as 'negative difference effect', that is, an accelerated hydrogen evolution rate with increasing anodic overpotential (Song and Atrens 1999). Besides the generation of hydrogen pockets and concomitant localized alkalinisation in the surrounding tissues, the corrosion rates of pure Mg in physiological media are exceedingly fast compared to bone healing rates. Alloying Mg with suitable elements has been demonstrated as an effective mean to (i) minimize or even block hydrogen gas release, (ii) improve the mechanical properties of the base metal and (iii) reduce the corrosion rates. Currently, two of the top Mg-based BMG families for temporary applications are

the binary Mg–Zn and the ternary Mg–Zn–Ca (Zberg et al 2009; Gu et al. 2010) alloys. For Zn percentages above 28 at.%, a dense amorphous layer enriched in Zn and O forms at the surface of the material, which, in turn, reduces the release of hydrogen down to acceptable levels. In spite of the advantages brought by the glassy nature of these alloys (and, hence, the minimized galvanic corrosion effect), their intrinsic brittleness is a primary negative concern. Although these alloys are not supposed to remain permanently inside the body, they are anyway subjected to stresses. For this reason, Mg-based BMG matrix composites with high ductility and excellent work hardening have been recently proposed in order to overcome the brittle and flaw-sensitive nature of the MgZnCa system (Gao et al. 2015). In order to further optimize the GFA, reduce the hydrogen evolution and adjust the corrosion rates, the addition of Sr to Mg–Zn–Ca BMGs has been recently proposed (Li et al. 2015). Other elements like Pd have shown to destroy the amorphous character of the system and to give rise to a fully crystalline structure. In such a case, if the alloying element content is kept at sufficiently low levels, the wear resistance can be increased without compromising the corrosion resistance (González et al. 2012).

Figure 1a displays the compressive yield stress, $\sigma_{y,C}$, against the Young's modulus, E, for different biodegradable materials. It can be seen that the Mg–Zn–Ca

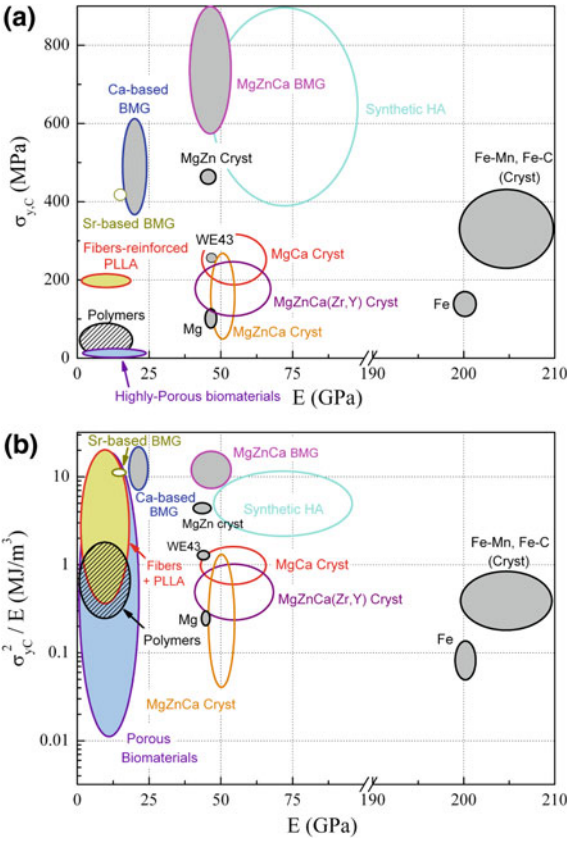

Fig. 1 **a** Compressive yield stress $\sigma_{y,C}$, against Young's modulus *E*, for different families of biodegradable implant materials, including metallic alloys (Mg-, Ca-, Sr- and Fe-based), ceramics and polymers. **b** Dependence of $\sigma^2_{y,C}$/E with E. WE43 stands for commercial Mg–Y-RE (*RE* rare-earth) alloy. PLLA, PMMA, PGA, and PCL stand for poly-L-(lactic acid), polymethylmethacrylate, poly (glycolic acid), and polycrapolactone, respectively. Adapted from Pellicer et al. (2013)

BMGs show higher compressive yield stress values compared to polymeric materials. In fact these alloys are among the hardest biodegradable materials (bear in mind that $\sigma_{y,C}$ is directly proportional to hardness). Simultaneously, they exhibit Young's modulus closer to that of cortical bone (E = 3–20 GPa).

Likewise, Fig. 1b depicts $\sigma_{y,C}^2/E$, which is proportional to the resilience, against E. The former parameter indicates the maximum energy per unit volume that can be elastically stored in the material without causing any permanent deformation. As can be seen, the MgZnCa BMGs show higher resilience than their crystalline counterparts, which is due to their rather high yield strain.

5 Surface Engineering of Ti-Based Alloys

In spite of the progress in the field of metallic biomaterials, it is rare to find a material that meets all the requirements at once. Changing the bulk by a top-down strategy is often not economically and technologically viable. If on one hand the metallurgists' strategy is based on the improvement of the bulk properties, on the other hand material chemists and biologists are more concerned about the role of the outermost atomic layers on the material surface. Due to the physico-chemical composition and the morphological characteristics, this very thin zone, referred to as "biointerface", is the most relevant for the in vivo host biological response. Surface properties are in fact responsible for the transmission of stress, adhesion, friction, abrasion, gasses and liquids permeability and compatibility within the surrounding corrosive organic environment. The exact control of the surface properties by a surface engineering approach is, thus, an essential requisite for the success or failure of the implant, based on the events occurring at the "biointerface" between the surface of the inserted material and the adjacent host tissues. Hence, among the options available for tailoring the performance of a biomaterial, the enhancement of the surface characteristics holds the key (Kurella and Dahotre 2005).

When the Ti-based alloys are employed, an amorphous layer of non-stoichiometric titanium oxide (3–7 nm thick) is naturally formed on the metallic Ti-based surfaces by passivation in air. Even though it ensures "inertness" and a good corrosion protection to the bulk implant in the physiological environment (Liu et al. 2004), at least in comparison with other metals used for implants, it becomes unstable on the long term and much less corrosion resistant. As a result, titanium, and in particular the alloying atoms, are released into the surrounding tissues. Thus, in order to minimize the adverse body reactions and improve the overall implant osseointegration, the natural titania layer is preferred to be stabilised or replaced by a more chemically stable titania coating, before being used for bio-applications.

To form a stable "protection" layer on Ti-based implants made of titania, a number of surface modification strategies have been developed, with the final goal of improving the surface properties of the load-bearing orthopaedic metallic implants, in regards to the different clinical needs and applications.

Various approaches have been used to modify the surface of Ti-based implants, either in terms of topography/roughness or chemical composition. The available methods can be distinguished in subtractive (roughing or smoothing by mechanical or chemical methods, removal of contamination and/or natural oxide layer) and additive, when an outer layer of additional material is formed (coating). The most used materials for coatings are ceramics, made of either biomimetic materials (e.g. calcium phosphates) or oxides (Ti-based, Zr-based or Si-based oxides). The achievement of a mechanically stable surface coating can be accomplished via various processes acting by chemical (e.g. etching, sol-gel deposition, etc.), electrochemical (anodic oxidation, micro-arc oxidation, etc.), physical (physical vapour deposition, thermal spray, etc.) or thermal (sintering, thermal oxidation, etc.) surface modifications (Liu et al. 2004; Pawlowski 1999; Hanawa 1999; Bosco et al. 2012; Oshida 2007). An exhaustive overview of surface modification methods for Ti-based alloys is given by Liu et al. (2004).

6 Nanostructured Coatings by Hydrothermal Treatment on Biomedical Ti-Alloys

The recent progresses in nanotechnology have been giving the boost for the production of nanostructured coatings, which have the advantage of the outstanding phenomena occurring at the nano-level and their effect on cells and biomolecules. In this sense titanium dioxide nanocrystals are known to overcome the limitations of the amorphous, non-stoichiometric titania, so that the attainment of crystalline TiO_2 coatings on Ti-based implant surfaces is desirable. Most of the available techniques (i.e. sol-gel deposition, wet chemical etching, electrochemical oxidation …) are able to produce TiO_2 coatings with controllable thickness and chemical composition, but they can lead to plastic deformation and stresses in the surface region, retain chemical residues (e.g. fluorine from the etching solution), lack in controlling the thermal and mechanical stability (e.g. adhesion to the substrate) and/or the particle morphology, especially at the nanoscale. Moreover, they usually require high temperatures to achieve crystalline products. Other general disadvantages of most of those techniques are the relative high costs and complexity of the processes (Liu et al. 2004; Riman et al. 2002).

Hydrothermal treatment (HT) responds to these technological demands. This method is simple, low-cost, relatively environmental-friendly, suitable for scaling-up and applicable even on complex shapes, therefore, very promising not only for the nanotechnology and advanced materials production, but also for the biomedical industry.

The term “hydrothermal” originates from geology, where it refers to the action of water at elevated temperatures and pressures. More recently, Byrappa and Yoshimura (2001) defined hydrothermal as “any heterogeneous (for bulk crystal growth) or homogeneous (for fine particles or nanocrystals) reaction in the presence

of aqueous solvents under high pressure and temperature conditions, in order to dissolve and recrystallize materials which are relatively insoluble under ordinary conditions".

Even though the hydrothermal method is well-known for the synthesis of very pure ceramic crystalline powders and single crystals (homogeneous nucleation), much less is known about its potential use for the growth of highly crystalline oxide films on solid substrates by heterogeneous nucleation (i.e. surface catalysed or assisted nucleation process) (Li et al. 2009; Byrappa and Yoshimura 2001).

The growth of crystals can be achieved by liquid-to-solid transformations, starting from a supersaturated solution of ions. Whichever the nucleation process is (homogeneous or heterogeneous), the driving force for the formation of nanoparticles derives from the favourable Gibb's free energy associated with the supersaturation and supercooling of the liquid phase (the free energy of the initial solution phase is greater than the sum of the free energies of the crystalline phase and the final solution phase). Four main steps are involved in the formation of a crystal, namely (Jolivet et al. 2000):

I. Formation of the zero charge precursor;
II. Achievement of supersaturation or supercooling and consequent nucleation;
III. Growth of the nuclei into single crystals of distinct phases;
IV. Aging or secondary growth.

Nucleation at surfaces (heterogeneous nucleation) plays a crucial role in the growth of crystals and thin epitaxial films. The surface tension and, consequently, the interfacial energy between a crystal nucleus and a solid substrate (solid-solid) is smaller than that of the crystal in contact with the solution (solid-liquid), because of the stronger bonds between solids instead of the bonds of solvation. This allows a more favorable nucleation at lower energies and supersaturation (De Yoreo and Vekilov 2003). Once the nucleation has occurred, the crystal growth proceeds preferentially at defects, such as steps, kinks and terraces, which act as surface active sites where the binding energy is higher (Mann 2001). Since crystals are not perfect, usually defects are created at dislocations and edges. Examples of crystal

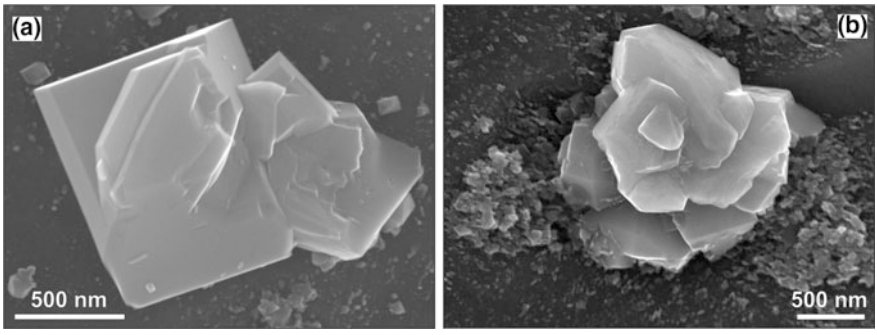

Fig. 2 Examples of hydrothermal crystal growth of TiO_2 crystals at defects after nucleation. Substrate: commercially pure titanium

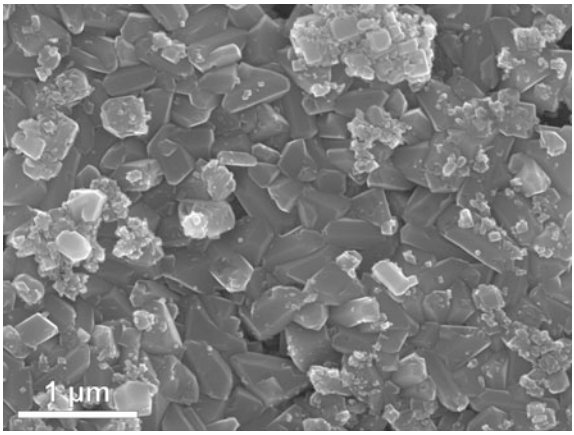

Fig. 3 Example of secondary crystal nucleation of TiO_2 crystals on a previously grown TiO_2 crystal layer. Substrate: commercially pure titanium

growth influenced by the crystal surface defects are given in Fig. 2. In addition, a secondary crystal nucleation on a formerly developed crystal layer might occur (Fig. 3).

Following Barna's theory on the structure evolution (Barna and Adamik 1995), the crystal growth stages of polycrystalline films lead to an incomplete (Fig. 4a) or complete coalescence (Fig. 4b), resulting in partial/fully densely-packed coatings.

Recently published literature showed the versatility of HT for growing dense films on different metallic substrates for biomedical uses, such as titanium (Baszkiewicz et al. 2005; Obata and Kasuga 2008; Ueda et al. 2008; Lorenzetti et al. 2014a), NiTi (Cheng et al. 2004; Wong et al. 2007), Ti6Al4V (Drnovšek et al. 2009), TiNb (Ueda et al. 2008) and Ti13Nb13Zr (Lorenzetti et al. 2014a).

The atomic structure and chemical composition of the substrate material are indeed important for the crystal nucleation and growth. The same HT procedure can produce different amount of nuclei, as well as different crystal morphologies and dimensions, by dissolving and incorporating different alloying elements from the

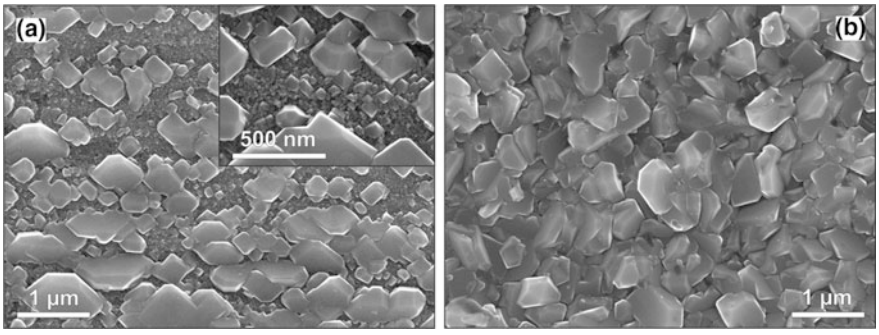

Fig. 4 Examples of TiO_2 crystal growth occurred as **a** incomplete coalescence; **b** complete coalescence. Substrate: commercially pure titanium

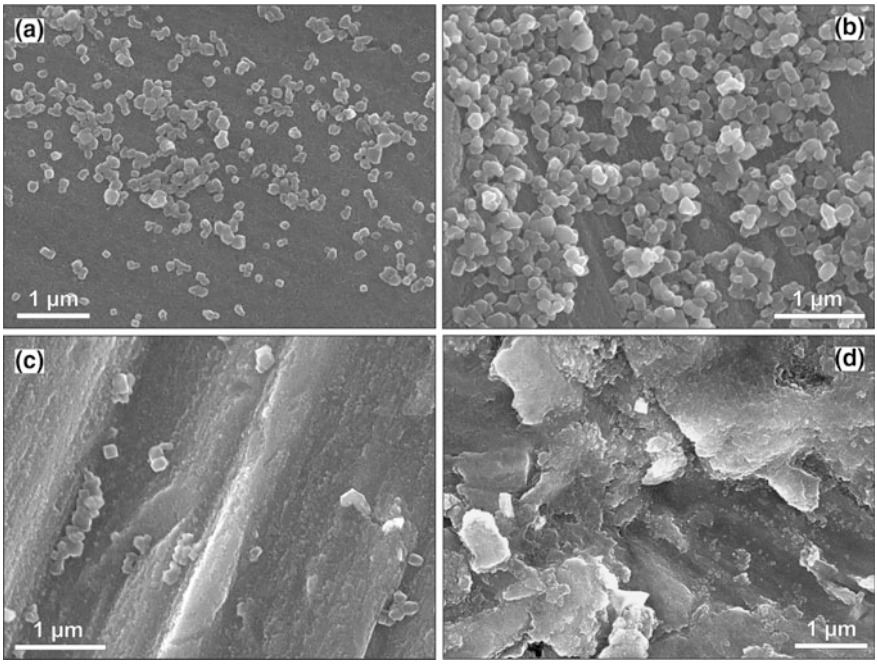

Fig. 5 Effect of the same hydrothermal treatment parameters on pre-conditioned substrates: **a** machined Ti6Al4V (30 μm width grooves); **b** machined titanium (30 μm width grooves); **c** scratched titanium with SiC paper; **d** etched titanium (HCl 37% for 1 h, NaOH 1 M for 2 h)

substrate. As an example, the presence of aluminium and vanadium on the surface of a Ti6Al4V alloy can inhibit the crystal development in respect to the solely titanium ions composing a commercially pure titanium substrate (Fig. 5a, b).

Moreover, the presence of defects or adsorbed impurities on the substrate also contributes to the clustering of nuclei (Barna and Adamik 1995). For instance, different pre-conditioning methods (polishing, machining, etching …) modify the initial substrate topography and roughness and, consequently, the occurrence of surface defects, by which the nucleation might be affected (Fig. 5b–d).

Lorenzetti et al. (2014b) observed that the grooves obtained by surface machining provided edges and surface defects which acted as active sites of higher binding energy and drove the further incorporation of ions from the solution. As a consequence, a higher amount of nuclei was formed on the machined substrate, rather than on the polished one, with a consequent growth of many more, but smaller crystals.

As it can be perceived from the examples here above, the optimization of the synthesis process is the key factor for the quality of the obtained nanostructured coating. Besides the choice of the substrate or the surface pre-conditioning, in fact, the selection of the proper solvent, the treatment temperature, the suspension pH, the Ti ions source and precursors (TiO_2 powders, Ti-alkoxides, water-soluble salts,

hydroxides, etc.) represent the main parameters for boosting the nucleation and crystal growth. The crystal development significantly relates to the autoclaving temperature (Obata and Kasuga 2008). During the HTs the temperature is raised above the water boiling point to achieve the pressure of vapour saturation, reaching the supercritical condition of 374 °C. The internal pressure is strongly influenced by the temperature and the amount of suspension in the autoclave, which can be evaluated from the Pressure-Volume-Temperature (PVT) diagram of the given solvent (Dhanaraj et al. 2010). Besides, the crystal development towards the most thermodynamically stable structure depends on the treatment time: the longer the treatment, the higher is the time for allowing the system to evolve toward the equilibrium. The selection of the abovementioned synthesis parameters tailor not only the product stoichiometry, but also the particle size and shape, and tune the crystallization with the formation of a certain polymorphic phase (Vernardou et al. 2009; Byrappa and Adschiri 2007; Lencka and Riman 2003). Figure 6 shows the faceted growth of TiO_2-anatase crystals during the aging of an anatase polycrystalline coating, hydrothermally synthesised on a Ti13Nb13Zr substrate under alkaline conditions. As the {101} crystal planes are the most thermodynamically stable in TiO_2-anatase, the faceting of crystals occurred over time.

Since TiO_2 exists in three crystalline forms (anatase, rutile, brookite), achieving a specific crystalline phase becomes essential too, especially in view of a certain application (e.g. orthopaedic metallic implants). TiO_2 single phase or multi-phase mixtures can be obtained by HT (Hanaor and Sorrell 2011). Even though the rutile-TiO_2 is the most thermodynamically stable polymorph, the production of anatase-TiO_2 for bio-applications is preferred, owing to its superior properties. In comparison to rutile and to the amorphous phases, TiO_2-anatase is better tolerated by the human body, owns higher bioactivity (i.e. it accelerates the apatite-like crystal formation during osteogenesis) (Obata et al. 2008; Uchida et al. 2003), and influences positively the cell and tissue response (Zhao et al. 2005). Accordingly, researchers have developed different hydrothermal synthesis routes aiming to obtain textured coatings on Ti-based alloys made of anatase nano-crystals with dominant

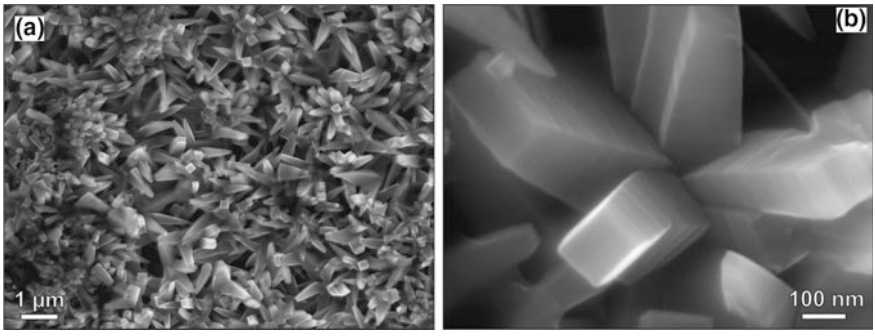

Fig. 6 Effect of aging on the crystal development of TiO_2-anatase during HT under alkaline conditions (pH = 10). Substrate: Ti13Nb13Zr alloy

{001} facets, one of the most energetically reactive planes. Barnard and Curtiss (Barnard and Curtiss 2005) predicted how to control the phase and shape transition of TiO_2 nanoparticles by surface chemistry. In particular, the degree of truncation of the typical anatase tetragonal bipyramid can be tailored as a function of hydrogenation or oxygenation of the crystal surfaces. One of the most successful methods to prepare anatase micro/nanostructures with dominant {001} facets is the hydrothermal synthesis in presence of fluorine-based capping agents. Since Yang et al. (2008) succeeded to produce anatase TiO_2 crystals with 47% of {001} facets, employing titanium tetrafluoride and hydrofluoric acid under hydrothermal conditions, lot of studies have been performed in this direction (Dozzi and Selli 2013). However, the use of highly toxic and corrosive hydrofluoridric acid and fluorine-based products should be avoided in favour of eco-friendlier fluorine-free routes. In this regard, Drnovšek et al. (2009) systematically explored the hydrothermal synthesis of nanocrystalline anatase coatings on Ti6Al4V at various pH values, with or without the addition of titania precursors, either TiO_2 powder or

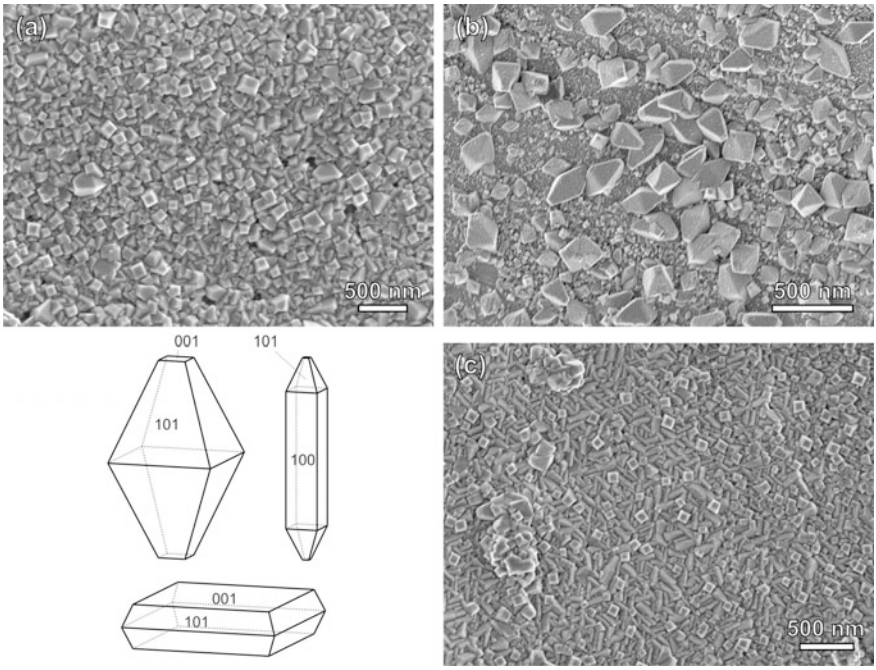

Fig. 7 Effect of the starting solution pH on the TiO_2 crystal growth: **a** pH = 5; **b** pH = 8; **c** pH = 11. The drawings represent the anatase crystal morphologies. Substrate: Ti6Al4V alloy (Drnovšek et al. 2009)

$Ti(OH)_4$. Considering the solely variation of the starting solution pH, when no titania source was included, a dense layer of anatase nanocrystals with exposed {001} and {101} facets was formed at pH = 5 (Fig. 7a), while anatase truncated bipyramids with sizes between 50 and 300 nm appeared at pH = 8 (Fig. 7b); finally, additional morphologies were observed in a very basic environment pH = 11 (Fig. 7c).

Also Obata and Kasuga's experiments (Obata and Kasuga 2008) showed the abundant crystallization of anatase on titanium surface under alkaline conditions. The authors suggested that the use of NaOH during the HT improved the formation of hydrophilic groups on the surface, important for the biocompatibility of the implant.

Another strategy to tailor the crystal morphology and changing the pH environment is to use mineralisers. Dong et al. (2010) showed that tetramethylammonium hydroxide (TMAH) can selectively adsorb on certain lattice plans during the TiO_2 crystal development by hydrogen bonds, resulting in a limited growth of the crystal planes parallel to the c-axis. This principle was employed by Lorenzetti et al. (2014b), in order to grow anatase nanocrystals in the range of 20–30 nm on titanium substrate with well-developed (001) planes. The preferential texturation of an anatase surface and the presence of bonded/adsorbed functional groups lead to unique effects, relevant for the bio-applications. For example, certain crystallographic anatase planes, such as (001) facets, are known to own a high surface energy (Lazzeri et al. 2001), responsible for the surface hydrophilicity (given by the adsorption of hydroxyl groups). As a consequence, the successful enhancement of the bioactivity and the cell response toward nanotextured HT-TiO_2-coatings was reported (Lorenzetti et al. 2015; Drnovsek et al. 2015).

As a final remark, it has to be mentioned that hydrothermal synthesis can consist of one-step treatment (crystal growth starting from the natural passivation layer), as well as of multi-steps, i.e. as a post-treatment in combination with anodization (Yamamoto et al. 2013) or micro-arc oxidation (MAO) (Zhang et al 2004). The application of a post-HT process demonstrated to improve the biological performances of the pre-deposed titania layer. Figure 8 shows the effect of the HT on the growth of crystal from pre-formed titania layers by electrophoretic oxidation at different times (Fig. 8a, b) and from a seed layer of nm-TiO_2-powder deposited by spin coating (Fig. 8c), in comparison to the same synthesis route directly applied on a naturally passivated titanium substrate (Fig. 8d).

Moreover, multi-phase systems or doped-films can be achieved by HT. Ueda et al. (2009) reported about the synthesis of bioinert ZrO_2–TiO_2 films on titanium substrates for bio-applications, by combining a chemical treatment in H_2O_2/HNO_3 solution with a subsequent hydrothermal treatment.

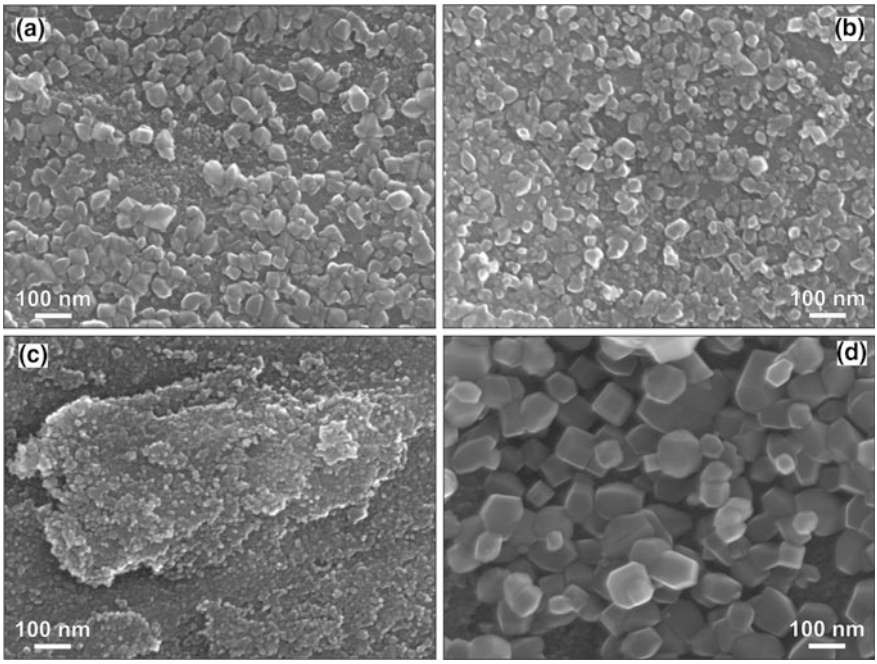

Fig. 8 Effect of the same hydrothermal treatment parameters on different pre-formed titania layers by: **a** electrophoretic oxidation (NaOH 0.5 M, 10 V, 5 min); **b** electrophoretic oxidation (NaOH 0.5 M, 10 V, 10 min); **c** spin coating (1 g TiO_2 in 100 ml EtOH, 3000 rpm, 30 s); **d** natural passivation in air. Substrate: commercially pure titanium

7 Hydrothermally-Grown Coatings Enhance the Mechanical Properties and Corrosion Resistance

When the heterogeneous nucleation of new species occurs via the existing atoms on the surface, a direct chemical bonding of the approaching atoms is formed at the interface (Benning and Waychunas 2008). Once the nucleation has started, the process allows the direct growth from the outermost atomic layer of the substrate and proceeds till the formation of well-developed crystals, as shown in Fig. 9.

Accordingly, the obtained nanostructures exhibit a high adhesion to the substrate and, if the synthesis parameters are optimal, a dense, nanostructured layer is formed on the surface. The resulting interlayer acts as a protection between the bulk (biomedical implant) and the surrounding (tissues), thanks to a reduced permeability, reactivity, and solubility of the HT oxide layer, which enhance the in vivo corrosion resistance and avoid the release of free (toxic) particles.

The high adhesion of the HT coatings was demonstrated by Drnovšek et al. (2012), who performed shear strength and scratch tests, as well as Rockwell indentation, on polycrystalline TiO_2 coatings, grown in alkaline conditions on

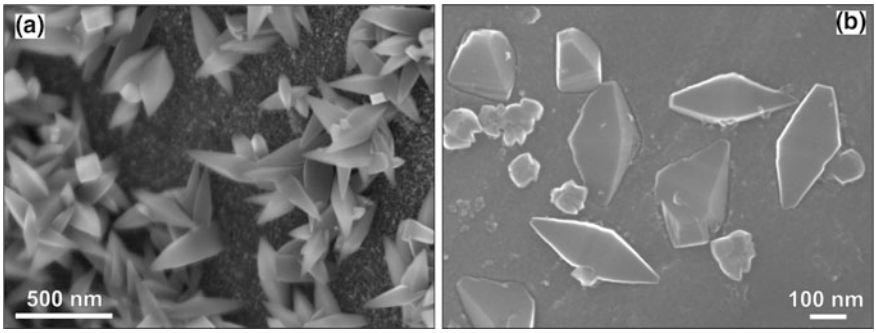

Fig. 9 Heterogeneous nucleation and growth of anatase crystals at the outermost atomic layer of **a** Ti6Al4V substrate (courtesy of Dr. Nataša Drnovšek), and **b** commercially pure titanium substrate

Ti6Al4V alloy. In addition, such dense coatings appeared to protect the substrate from ion leaching; after one month of immersion in NaCl saline solution, the quantity of released Ti, Al and V ions were far lower in comparison to the non-coated substrate. Besides, Wong et al. (2007) created a smooth and uniform oxide film, about 56 nm thick and composed of compact aggregates of 10 nm-grains, by applying the hydrothermal treatment on a NiTi alloy solely in water. Electrochemically speaking, this dense oxide layer was sufficient to improve the corrosion properties of the bulk and to reduce the surface atomic ratio Ni/Ti. However, some treatments, especially at low temperatures (120 and 150 °C), resulted in films of poor quality. Lorenzetti et al. (2014a) evaluated the electrochemical properties of hydrothermally synthesized titania coatings on commercially pure titanium and Ti13Nb13Zr alloy, in comparison with the bare substrates. It was found that the nanocrystalline anatase coatings owned a superior corrosion resistance and diminished the corrosion rate. In particular, the potentiodynamic curves showed a significant enhancement in the corrosion potentials (+0.10/+0.15 V for HT-coated Ti vs. uncoated Ti; +0.25/+0.30 V for HT-coated Ti13Nb13Zr vs. uncoated Ti13Nb13Zr) and also lower corrosion current densities in case of HT-Ti samples (Fig. 10). The behavior was interpreted in connection with other surface properties, especially the coating nano-porosity. Moreover, from the mechanical point of view, the presence of the harder ceramic anatase (compared to the Ti-based metallic alloys) generated an overall increase in the surface hardness and the Young's modulus of the coated samples.

Good corrosion resistance results were obtained also with anodized titanium surfaces, additionally hydrothermally-treated in order to grow hydroxyapatite crystals on top (Park et al. 2006). The authors stated that the thickness and stability of the titanium oxide film and the distribution of the hydroxyapatite crystals positively affected the corrosion resistance in 0.9% NaCl solution. Another study reported about the sequential deposition of multi-layered coatings on titanium by MAO, hydrothermal treatment and chitosan dip-coating application (Neupane et al.

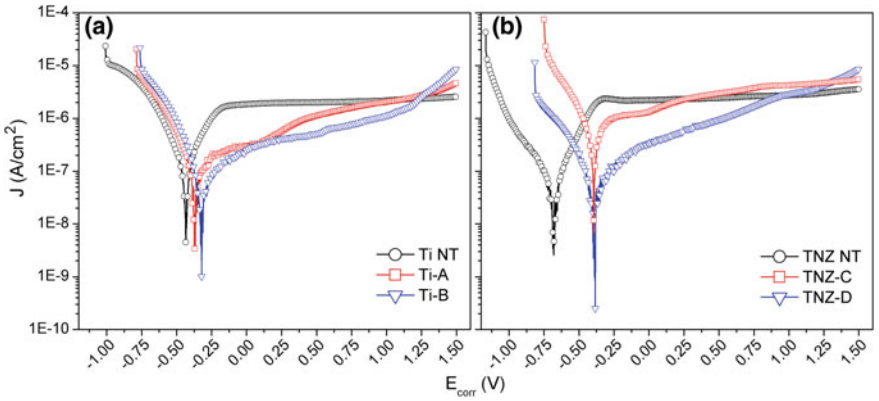

Fig. 10 Potentiodynamic polarization curves in Hank's solution at 37.5 °C of: **a** commercially pure titanium (Ti NT) and HT-titanium samples via two synthesis routes (Ti-A, Ti-B); and **b** Ti13Nb13Zr commercial alloy (TNZ NT) and HT-Ti13Nb14Zr samples via two synthesis routes (TNZ-C, TNZ-D) (Lorenzetti et al. 2014a)

2014). The HT enabled sealing the pores created by MAO, which, in return, helped to increase the corrosion resistance in saline solution. The combination of HT and chitosan coating on MAO-treated surfaces offered even a more significant increase in the corrosion resistance.

8 Conclusions

Metallic materials for bioimplant applications is a lively field of research since the last two decades. New products with controlled microstructure, suitable mechanical behavior, and free from toxic elements are being continuously developed and further tested in vitro and in vivo to assess their biocompatibility. Compared to crystalline materials, their glassy counterparts show better mechanical properties and enhanced corrosion resistance in body fluids. Ti-based BMG materials hold a privileged position among permanent implant materials within the metallic glasses community, whereas Mg-based ones are preferred for bioabsorbable uses. Various surface engineering approaches aimed at improving the osseointegration of the implant are also being tackled worldwide, especially when it comes to Ti-based alloys. The formation of bioactive nanostructured anatase titania coatings by means of low-cost and easily scalable methods like the hydrothermal treatment is shown to be extremely beneficial. Although much progress has been made since the last decade, it is expected that novel clinically relevant materials are yet to be developed.

Acknowledgements Financial support from the WIMB 543989-TEMPUS-1-2013-1-ES-TEMPUS-JPHES project from Education, Audiovisual and Culture Executive Agency (European Commission) is greatly acknowledged. E.P., J.F., M.D.B. and J.S. are also grateful to the 2014-SGR-1015 project from D.G.U. Catalunya. E.P. and J.S. acknowledge the Spanish Ministerio de Economía y Competitividad (MINECO) for the Ramon y Cajal contract (RYC-2012-10839) and the Juan de la Cierva fellowship (IJCI-2015-27030).

References

Argon AS, Kuo HY (1980) Free energy spectra for inelastic deformation of five metallic glass alloys. J Non-Cryst Solids 37:241–266

Barna PB, Adamik M (1995) Growth mechanisms of polycrystalline thin films. In: Matacotta FC, Ottaviani G (eds) Science and technology of thin films. World Scientific, Singapore, pp 1–28

Barnard AS, Curtiss LA (2005) Prediction of TiO_2 nanoparticle phase and shape transitions controlled by surface chemistry. Nano Lett 5:1261–1266

Baszkiewicz J, Krupa D, Mizera J et al (2005) Corrosion resistance of the surface layers formed on titanium by plasma electrolytic oxidation and hydrothermal treatment. Vacuum 78:143–147

Benning LG, Waychunas GA (2008) Kinetics of water-rock interaction. In: Brantley SL et al (eds). Springer, New York, pp 259–333

Bosco R, Van Den Beucken J, Leeuwenburgh S et al (2012) Surface engineering for bone implants: a trend from passive to active surfaces. Coatings 2:95–119

Byrappa K, Adschiri T (2007) Hydrothermal technology for nanotechnology. Prog Cryst Growth Charact Mater 53:117–166

Byrappa K, Yoshimura M (2001) Handbook of hydrothermal technology—A technology for crystal growth and materials processing. William Andrew Publishing/Noyes

Calin M, Gebert A, Ghinea AC et al (2013) Designing biocompatible Ti-based metallic glasses for implant applications. Mater Sci Eng C 33:875–883

Chen Q, Chan KC, Liu L (2011) Tribological characterisation of Zr-based bulk metallic glass in simulated physiological media. Phil Mag 9:3705–3715

Cheng FT, Shi P, Man HC (2004) A preliminary study of TiO_2 deposition on NiTi by a hydrothermal method. Surf Coat Technol 187:26–32

Cortizo MC, Lorenzo Fernández, de Mele M (2004) Cytoxocity of copper ions released from metal. Biol Trace Elem Res 102:129–141

De Yoreo JJ, Vekilov PG (2003) Principles of crystal nucleation and growth. Rev Mineral Geochem 54:57–93

Dhanaraj G et al (2010) Springer handbook of crystal growth, 1st ed. Springer, Berlin

Dong X, Tao J, Li Y et al (2010) Oriented single crystalline TiO_2 nano-pillar arrays directly grown on titanium substrate in tetramethylammonium hydroxide solution. Appl Surf Sci 256:2532–2538

Dozzi M, Selli E (2013) Specific facets-dominated anatase TiO_2: fluorine-mediated synthesis and photoactivity. Catalysts 3:455–485

Drnovšek N, Daneu N, Rečnik A et al (2009) Hydrothermal synthesis of a nanocrystalline anatase layer on Ti6A4V implants. Surf Coat Technol 203:1462–1468

Drnovšek N, Rade K, Milačič R et al (2012) The properties of bioactive TiO_2 coatings on Ti-based implants. Surf Coat Technol 209:177–183

Drnovsek N, Jerman UD, Romih R et al (2015) Improvement of osseointegration of Ti and Ti-alloys by hydrothermally prepared bioactive anatase coating. Int J Nano Biomater 6:18–28

Elias LM, Schneidera SG, Scheneidera S et al (2006) Microstructural and mechanical characterization of biomedical Ti–Nb–Zr(–Ta) alloys. Mater Sci Eng 432:108–112

Fornell J, Pellicer E, Van Steengerge N et al (2013) Improved plasticity and corrosion behavior in Ti–Zr–Cu–Pd metallic glass with minor additions of Nb: an alloy composition intended for biomedical applications. Mater Sci Eng A 559:159–164

Gao J, Sharp J, Guan D et al (2015) New compositional design for creating tough metallic glass composites with excellent work hardening. Acta Mater 86:208–215

Geetha M, Singh AK, Asokamani R et al (2009) Ti based biomaterials, the ultimate choice for orthopaedic implants—a review. Prog Mater Sci 54:397–425

González S, Pellicer E, Fornell J et al (2012) Improved mechanical performance and delayed corrosión phenomena in biodegradable Mg–Zn–Ca alloys through Pd-alloying. J Mech Behav Biomed Mater 6:53–62

Gu X, Zheng Y, Zhong S et al (2010) Corrosion of, and cellular responses to Mg–Zn–Ca bulk metallic glasses. Biomater 31:1093–1103

Han JH, Park DH, Bang CW et al (2009) Sn effect on microstructure and mechanical properties of ultrafine eutectic Ti–Fe–Sn alloys. J Alloy Compd 483:44–46

Hanaor DH, Sorrell C (2011) Review of the anatase to rutile phase transformation. J Mater Sci 46:855–874

Hanawa T (1999) In vivo metallic biomaterials and surface modification. Mater Sci Eng A 267:260–266

He G, Eckert J, Löser W et al (2003) Novel Ti-base nanostructure-dendrite composite with enhanced placticity. Nature Mater 2:33–37

Huang L, Cao Z, Meyer HM et al (2011) Reponses of bone-forming cells on pre-immersed Zr-based bulk metallic glasses: effects of composition and roughness. Acta Biomater 7:395–405

Hynowska A, Blanquer A, Pellicer E et al (2013) Novel Ti–Zr–Hf–Fe nanostructured alloy for biomedical applications. Materials 6:4930–4945

Jolivet JP, Henry M, Livage J (2000) Metal oxide chemistry and synthesis: from solution to solid state. Wiley, NJ

Kühn U, Mattern N, Gebert A et al (2006) Ductile Ti-based nanocrystalline matrix composites. Intermetallics 14:978–981

Kurella A, Dahotre NB (2005) Review paper: surface modification for bioimplants: the role of laser surface engineering. J Biomater Appl 20:5–50

Lazzeri M, Vittadini A, Selloni A (2001) Structure and energetics of stoichiometric TiO_2 anatase surfaces. Phys Rev B 63:155409

Lencka MM, Riman RE (2003) Crystal growth technology. In: Byrappa K, Ohachi T (eds). William Andrew Publishing, Norwich, NY, pp 271–297

Li S, Ye G, Chen G (2009) Low-temperature preparation and characterization of nanocrystalline anatase TiO_2. J Phys Chem C 113:4031–4037

Li HF, Pang SJ, Liu Y et al (2015) Biodegradable Mg–Zn–Ca–Zr bulk metallic glasses with enhanced corrosion performance for biomedical applications. Mater Des 67:9–19

Liu X, Chu PK, Ding C (2004) Surface modification of titanium, titanium alloys, and related materials for biomedical applications. Mater Sci Eng R Rep 47:49–121

Lorenzetti M, Pellicer E, Sort J et al (2014a) Improvement to the corrosion resistance of Ti-based implants using hydrothermally synthesized nanostructured anatase coatings. Materials 7:180–194

Lorenzetti M, Biglino D, Novak S et al (2014b) Photoinduced properties of nanocrystalline TiO_2-anatase coating on Ti-based bone implants. Mater Sci Eng C 37:390–398

Lorenzetti M, Dakischew O, Trinkaus K et al (2015) Enhanced osteogenesis on titanium implants by UVB photofunctionalization of hydrothermally grown TiO_2 coatings. J Biomater Appl 30:71–84

Lu ZP, Liu CT (2002) A new glass-forming ability criterion for bulk metallic glasses. Acta Mater 50:3501–3512

Mann S (2001) Biomineralization: principles and concepts in bioinorganic materials chemistry. Oxford University Press, Oxford

Miracle DB (2004) A structural model for metallic glasses. Nat Mater 3:697–702

Morrison ML, Buchanan RA, Peker A (2007) Electrochemical behavior of a Ti-based bulk metallic glass. J Non-Cryst Solids 353:2115–2124
Naga S, Banerjee R, Frasera HL (2005) Microstructural evolution and strengthening mechanisms in Ti–Nb–Zr–Ta, Ti–Mo–Zr–Fe and Ti–Mo biocompatible alloys. Mater Sci Eng 25:357–362
Neupane MP, Park IS, Lee MH (2014) Surface characterization and corrosion behavior of micro-arc oxidized Ti surface modified with hydrothermal treatment and chitosan coating. Thin Solid Films 550:268–271
Nouri A, Hodgson PD, Wen CE (2010) Effect of process control agent on the porous structure and mechanical properties of a biomedical Ti–Sn–Nb alloy produced by powder metallurgy. Acta Biomater 6:1630–1639
Oak J-J, Inoue A (2007) Attempt to develop Ti-based amorphous alloys for biomaterials. Mater Sci Eng A 449–451:220–224
Oak J-J, Inoue A (2008) Formation, mechanical properties and corrosion resistance of Ti-Pd base glassy alloys. J Non-Cryst Solids 354:1828–1832
Obata A, Kasuga T (2008) Surface modification of titanium by hydrothermal treatment. Key Eng Mater 361–363:609–612
Obata A, Zhai T, Kasuga T (2008) Apatite-forming ability on titanium surface modified by hydrothermal treatment and ultraviolet irradiation. J Mater Res 23:3169–3175
Oshida Y (2007) Bioscience and bioengineering of titanium materials. In: Oshida Y (ed). Oxford, Elsevier, pp 311–379
Ott RT, Fan C, Li J et al (2003) Structure and properties of Zr–Ta–Cu–Ni–Al bulk metallic glasses and metallic glass matrix composites. J Non-Cryst Solids 317:158–163
Pang S, Liu Y, Li H et al (2015) New Ti-based Ti–Cu–Zr–Fe–Sn–Si–Ag bulk metallic glass for biomedical applications. J Alloy Compd 625:323–327
Park I, Woo T, Lee M et al (2006) Effects of anodizing voltage on the anodized and hydrothermally treated titanium surface. Met Mater Int 12:505–511
Park JM, Na JH, Kim DH et al (2010) Medium range ordering and its effect on plasticity of Fe–Mn–B–Y–Nb bulk metallic glass. Philos Mag 90:2619–2633
Pawlowski L (1999) Thick laser coatings: a review. J Therm Spray Tech 8:279–295
Pellicer E, González S, Blanquer A et al (2013) On the biodegradability, mechanical behavior and cytocompatibility of amorphous $Mg_{72}Zn_{23}Ca_5$ and crystalline $Mg_{70}Zn_{23}Ca_5Pd_2$ alloys as temporary implant materials. J Biomed Mater Res A 101:502–5017
Qin FX, Wang XM, Inoue A (2007) Effect of annealing on microstructure and mechanical property of a Ti–Zr–Cu–Pd bulk metallic glass. Intermetallics 15:1337–1342
Qin FX, Wang XM, Inoue A (2008) Distinct plastic strain of Ni-free Ti–Zr–Cu–Pd–Nb bulk metallic glasses. Intermetallics 16:1026–1030
Qiu CL, Liu L, Sun M et al (2005) The effect of Nb addition on mechanical properties, corrosion behavior, and metal-ion release of ZrAlCuNi bulk metallic glasses in artificial body fluid. J Biomed Mater Res A 75:950–956
Riman RE, Suchanek WL, Lencka MM (2002) Hydrothermal crystallization of ceramics. Ann de Chimie Sci Matériaux 27:15–36
Ritchie RO, Buehler MJ, Hansma P (2009) Plasticity and toughness in bone. Phys Today 62:41–47
Schroers J, Kumar G, Hodges TM et al (2009) Bulk metallic glasses for biomedical applications. JOM 61:21–29
Sheng HW, Luo WK, Alamgir FM et al (2006) Atomic packing and short-to-medium-range order in metallic glasses. Nature 439:419–425
Song GL, Atrens A (1999) Corrosion mechanisms of magnesium alloys. Adv Eng Mater 1:11–33
Spaepen F (1977) A microscopic mechanism for steady state inhomogeneous flow in metallic glasses. Acta Mater 23:407–415
Uchida M, Kim H-M, Kokubo T et al (2003) Structural dependence of apatite formation on titania gels in a simulated body fluid. J Biomed Mater Res Part A 64A:164–170
Ueda M, Uchibayashi Y, Otsuka-Yao-Matsuo S et al (2008) Hydrothermal synthesis of anatase-type TiO_2 films on Ti and Ti–Nb substrates. J Alloys Compd 459:369–376

Ueda M, Sasaki Y, Ikeda M et al (2009) Chemical-hydrothermal synthesis of bioinert ZrO_2–TiO_2 film on Ti substrates. Mater Trans 50:2104–2107

Vernardou D, Vlachou K, Spanakis E et al (2009) Influence of solution chemistry on the properties of hydrothermally grown TiO_2 for advanced applications. Catal Today 144:172–176

Witte F (2010) The history of biodegradable magnesium implants: A review. Acta Biomater 6:1680–1692

Wong MH, Cheng FT, Man HC (2007) In situ hydrothermal synthesis of oxide film on NiTi for improving corrosion resistance in Hanks' solution. Scr Mater 56:205–208

Xu LJ, Chen YY, Liu ZG et al (2008) The microstructure and properties of Ti–Mo–Nb alloys for biomedical application. J Alloy Compd 453:320–324

Yamamoto D, Arii K, Kuroda K et al (2013) Osteoconductivity of superhydrophilic anodized TiO_2 coatings on Ti treated with hydrothermal processes. J Biomater Nanobiotechnol 4:45–52

Yang HG, Sun CH, Qiao SZ et al (2008) Anatase TiO_2 single crystals with a large percentage of reactive facets. Nature 453:638–641

Zberg B, Uggowitzer PJ, Löffler JF (2009) MgZnCa glasses without clinically observable hydrogen evolution for biodegradable implants. Nature Mater 8:887–891

Zhang YM, Bataillon-Linez P, Huang P et al (2004) Surface analyses of micro-arc oxidized and hydrothermally treated titanium and effect on osteoblast behavior. J Biomed Mater Res 68A:383–391

Zhang LC, Das J, Lu HB et al (2007) High strength Ti–Fe–Sn ultrafine composites with large plasticity. Scr Mater 57:101–104

Zhao L, Chang J, Zhai W (2005) Effect of crystallographic phases of TiO_2 on hepatocyte attachment, proliferation and morphology. J Biomater Appl 19:237–252

Zhou YL, Niinomi M (2008) Microstructures and mechanical properties of Ti-50 mass % Ta alloy for biomedical application. J Alloy Compd 466:535–542

Zhu S, Xie G, Qin F et al (2012) Ni- and Be-free Zr-based bulk metallic glasses with high glass-forming ability and unusual plasticity. J Mech Behav Biomed Mater 13:166–173

Zhu SL, Wang XM, Inoue A (2008) Glass-forming ability and mechanical properties of Ti-based bulk glassy alloys with large diameters up to 1 cm. Intermetallics 16:1031–1035

Review of Existing Biomaterials—Method of Material Selection for Specific Applications in Orthopedics

Dragan Adamovic, Branko Ristic and Fatima Zivic

Abstract Biomaterials have emerged as a very important material class for wide application in medicine. Intensive research during the last decade strongly indicates that many health-related problems can be efficiently overcome with these new materials. Quality of life has been significantly increased for patients who need reconstructive surgeries, especially in comparison with old solutions. This paper reviews biomaterials in orthopedics that are used either as a support or substitute for bone tissues, from the aspect of their properties and state-of-the-art results in real clinical cases. Limitations and further directions of research are presented. Metal, ceramic and polymer materials, as well as new composites and new material structures, are reviewed, such as biodegradable porous materials and scaffolds. Nowadays, optimal selection of materials is one of the challenges imposed by the presence of many novel materials that can be used in specific applications. A general method of material selection is presented related to the hip stem and permanent metal biomaterials.

Keywords Biomaterials · Metals · Polymers · Ceramics · Composite · Metal foam · Biodegradable materials · Smart materials · Scaffolds · Materials selection

D. Adamovic · F. Zivic (✉)
Faculty of Engineering, University of Kragujevac, S.Janjic 6,
34000 Kragujevac, Serbia
e-mail: zivic@kg.ac.rs

D. Adamovic
e-mail: adam@kg.ac.rs

B. Ristic
Faculty of Medical Sciences, University of Kragujevac, Kragujevac, Serbia
e-mail: branko.ristic@gmail.com

F. Zivic et al. (eds.), *Biomaterials in Clinical Practice*,
https://doi.org/10.1007/978-3-319-68025-5_3

1 Introduction

Biocompatible materials refer to those materials that are in direct contact with cells, tissues and bodily fluids in the human body. They are commonly used as tissue replacements or to repair structural components within the body. Hence, they compensate for defects caused by aging, illness or accident (Park and Bronzino 2003). The study of medical implants made from advanced materials is a very important field in both the academic and commercial sense. Development of advanced biomaterials presents a complex combination of material science and the biology of cells. In order to achieve progress, there is an essential need for the collaboration of experts in different fields, such as metallurgy, rheumatology, orthopedics, chemistry, the engineering sciences, pharmacology, and others (Ong et al. 2014).

The biomaterials in use can belong to several material classes, such as metals, ceramics, polymers, and composites, or their combinations. Medical implants must fulfill very demanding requirements from the aspect of tissues (Ratner et al. 2012; Shi 2006; Migonney 2014). Their mechanical properties must be similar to those in autogenous tissue, without any harmful effects (Bronzino 2000; Park and Lakes 2007). Selection of suitable materials used for the manufacturing of medical implants is conditioned by numerous properties, such as biocompatibility, bioadhesion, biofunctionallity, resistance to corrosion, etc. In order to understand the behavior of a biomaterial within a body, it is important to have adequate medical data on genotoxicity, carcinogenicity, cytotoxicity, irritation and sensitivity to agents, sterilization, etc. This chapter is focused on the state of knowledge of existing biomaterials, as well as on their further development and perspectives.

2 Materials in Orthopedics

Materials used in orthopedics must comply with several basic requirements, as follows (Park and Lakes 2007; Ratner et al. 2012; Shi 2006):

- *Biocompatibility*: This is one of the most important properties referring to the strong affinity of a host's cells for the implant's surface. A Large number of engineering materials with superior mechanical or other properties cannot be used due to their lack of biocompatibility with human tissue, which would cause their rejection by the body.
- *Nontoxicity*: It is important that the material does not have toxic effects due to the release of ions or other harmful products that have the ability to cause cancer, deformities, allergies, necrosis, calcification and inflammation processes.
- *Corrosion resistance*: This property is closely related to biocompatibility and toxicity, and it determines the implant's life. In the case of permanent implants, it should be very high.

- *Durability*: High fatigue strength, but also low release of particles, especially in the case of present wear and corrosion, is important in preventing failures and fractures.
- *Strength and ductility*: Due to the limited space, researchers have to look for medical implants with lower dimensions that simultaneously have relatively high strength and ductility.
- *Low Young's module of elasticity*: The elastic module of materials used for orthopedic implants is usually 5–10 times higher compared to that of the human bone. This commonly leads to stress shielding, or more loading of the implant than the bone, causing the bone cells' death over time.

Usually, these materials belong to alloys suitable for precise vacuum casting, forging and work hardening with necessary mechanical finishing processes, in order to increase their endurance limit prior to fatigue fracture (Wong and Bronzino 2007; Niinomi et al. 2015a, b).

2.1 Metal Materials

Metals have been used in this capacity for more than one hundred years, due to their excellent mechanical properties. The first metal alloy used for a medical implant was vanadium steel, which was designed for both the coatings in the case of a bone fracture and the screws. Alloys for medical implants have been produced by using alloying elements such as: iron (Fe), chromium (Cr), cobalt (Co), nickel (Ni), titanium (Ti), tantalum (Ta), niobium (Nb), molybdenum (Mo) and tungsten (W) (Yaszemski et al. 2004). Some of these elements occur in their pure form as ingredients in the blood (Fe), or in the synthesis of vitamin B12 (Co), but in larger amounts, they cannot perform well, due to the host's response. Low corrosion resistance in vivo means that these metals are not highly biocompatible with host tissue. The results of corrosion very often are material decomposition, in combination with usually toxic oxidation products that significantly reduce fatigue strength (Niinomi et al. 2015a, b). But application of certain metal materials depends on the end product, and its specific demands. Nowadays, the most common metal biomaterials are: stainless steel (austenitic and precipitation hardening steel), cobalt-based superalloys (Co–Cr), titanium and its alloys, tantalum, magnesium and composites that are emerging but are still rarely used (Teoh 2004).

Metal biomaterials are used to support or replace certain components of the human skeleton. Medical implants may be produced out of only one type of metal, or out of combinations of different metals, or combinations of metals and polymers and/or ceramics. The lion's share of metal implants is produced for artificial joints (hip, knee, foot article, shoulder, elbow, wrist, various plates and screws for setting bones, fixation devices) (Yaszemski et al. 2004; Nasab et al. 2010). High resistance to mechanical loading, fatigue and fracture is one of the most significant advantages over polymers and ceramics (An et al. 2000). The metal materials most often used

are: stainless steel 316L, cobalt-based alloy CoCrMo, commercially pure titanium and titanium alloy Ti-6Al-4V (Bronzino 2000; Migonney 2014; Park and Lakes 2007; Ratner et al. 2012). All of these materials were initially developed for industrial purposes, and only later applied as biomaterials, due to their excellent mechanical properties, high corrosion resistance, biocompatibility and insolubility in body fluids. All these metals can be easily processed with both conventional (turning, milling, drilling, grinding, forging, pressing, etc.) and unconventional methods (sintering, laser cutting, net-shape technology) (Chu and Lui 2008; Helmus 2002). The mechanical and physical properties of several common metal biomaterials are given in Table 1.

The four typical classes of metal biomaterial are stainless steel, titanium and its alloys, cobalt superalloys and other metal materials. An overview of these biomaterials and their application in regard to medical devices is given in Table 2.

Table 1 Mechanical and physical properties of several metal biomaterials

Material	Density, g/cm^3	Young's modulus, GPa	Yield strength, MPa	Tensile strength, MPa	Fatigue limit, MPa
Stainless steel	8.0	200	190–620	480–950	240–820
CoCr alloys	8.5	210–250	450–1600	650–1800	200–950
Ti-6Al-4V	4.4	90–115	580–950	600–1100	620
Cortical bone	2.0	7–30	30–70	50–150	

Table 2 Application of metal materials in orthopedics

Metal	Application area
Stainless steel Austenitic—AISI 316, 316L, 316LVM, 316Ti, 317, 321 Precipitation hardening steel—AISI 630 (17-4PH)	Artificial joints, fracture fixation devices
Titanium and its alloys Ti Ti-6Al-4V Ti-6Al-7Nb	Artificial joints
Cobalt-based superalloys Co–Cr Co–Cr–Mo	Artificial joints, fracture fixation devices
Other metals Magnesium Tantalum (trabecular metal) Niobium	Artificial joints

2.1.1 Stainless Steel

There are numerous alloys that belong to the stainless steel group, but only austenitic and precipitation hardened steel are used as orthopedic biomaterials (Table 2) (Teoh 2004). Pure iron, carbon steel alloys and other types of steel are not suitable, mainly due to low corrosion resistance in solutions containing oxygen (Ratner et al. 2012). And regardless of their high corrosion resistance, austenitic Cr–Ni–Fe steel alloys are affected by fretting corrosion, intergranular corrosion, galvanic corrosion and pitting, all of which cause the release of metal ions detrimental to tissue and also reduce the mechanical strength of the alloy (Vişan and Popescu 2011). A certain amount of chromium in stainless steel alloys is responsible for producing self-healing oxide layers, which, due to its resistance to perforation and high electrical resistance, provides excellent corrosion prevention. Molybdenum provides high pitting resistance, while magnesium and silicon improve machinability. The presence of carbon has to be under strict control due to its side effects. Carbon has a high affinity for creating carbides with alloying elements (especially chromium carbide), and its content must be kept under 0.03%. In addition, chromium produces zones with reduced corrosion resistance, and due to the affinity of carbides for forming along crystal boundaries, intergranular corrosion is promoted and certain mechanical properties are decreased (Bombac et al. 2007; Rakovic and Uskokovic 2010). Austenitic steel, mainly the AISI 316 and AISI 316L classes, has been used for medical implants. In austenitic stainless steel AISI 316L, 'L' indicates low carbon content ($C \leq 0.030\%$). This class of stainless steel is non-magnetic, and has higher corrosion resistance than all other steel alloys. These austenitic steel alloys cannot be case-hardened under high temperatures, and mechanical reinforcement is achieved using cold deformation methods (Hryniewicz et al. 2009). The development of corrosion-resistant and precipitation-hardened steel alloys has enabled high yield strength while preserving high corrosion resistance. Regardless of the low mass fraction of carbon and its highly alloyed structure, significant reinforcement is achieved using precipitation hardening of intermetallic joints. Depending on the microstructure before precipitation hardening treatment, the following classification is made: martensitic, austenitic or semi-austenitic PH steel alloys (Pilliar 2009).

Biomedical steel SAE 17-4 PH is classified as martensitic PH steel, with low carbon content ($\sim 0.05\%$) and high percentages of chromium (14–17%) and nickel (4–6%), with the possible addition of copper ($\sim 3\%$) and niobium (<0.4%). In order to achieve high yield and tensile strengths, martensitic PH-steel alloys are first annealed at 1050 °C, then case-hardened in oil or open air, and finally subjected to accelerated aging at 400–600 °C. The annealing process makes austenite homogenized, and after case-hardening, it turns into martensite. Although $Ms \approx 100$ °C, 90–95% of austenite transforms into martensite even at room temperature, while residual austenite transforms during aging. A martensitic microstructure is achieved directly, making the case-hardened microstructure immediately ready for accelerated aging. This is very significant, because copper only precipitates in martensitic form (Bombac et al. 2007). Due to the high content of chromium, a protective oxide

layer appears on the surface of stainless steel. It is also known as a passive layer that protects the substrate from corrosion. If any mechanical defects appear on this layer, it can rapidly regenerate (Davis 2012). Crevice corrosion may occur in medical implants made from stainless steel. If two parts of such an implant are set next to each other (e.g., plate-screw), it will most likely cause local corrosion due to oxygen concentration, which has negative effects on the passive chromium-oxide layer (Geetha et al. 2010). This phenomenon is not expected in one-piece implants (Rakovic and Uskokovic 2010). Surface modification methods such as anodizing and passivation are usually applied for improvement of corrosion resistance and fatigue strength (Hryniewicz et al. 2009). Fatigue fracture may occur in almost every metal that is exposed to variable loading, as in the case of the femoral component of a hip joint prosthesis. Fatigue fracture begins at irregularities in the crystal lattice or other defects originating from processing, leading to cracking of the metal structure. Crack propagation continues with each load cycling change until it reaches critical value, causing catastrophic fracture (Teoh 2000). In order to avoid inclusions in the material that are responsible for defects in the crystal lattice or crack initiation, stainless steel AISI 316LVM is melted in a vacuum environment.

Regardless of their good properties for orthopedic applications, metal implants have some major disadvantages, such as: stiffness mismatch between the implant and bone, which may cause stress shielding, the high specific weight of metals, and the inability to absorb X-rays (Disegi and Eschbach 2000). Accordingly, further improvement of metal implants is necessary. During the 19th century, steel alloys begin to be applied in medicine for fixation plates and screws for fractured bone. As opposed to the metal wires that were used earlier for bone fixation, the introduction of steel alloys into orthopedic surgery was a significant advancement in this area (Rodríguez et al. 2004).

Nowadays, stainless steel has been used for producing components for joint prostheses (total hip, knee, shoulder and elbow), parts for fracture fixation, such as plates, screws, and external fixtures, and parts for fixing the spine (Parida et al. 2012). Important research is aimed at finding suitable regimes of material fabrication in order to improve their properties (Fragassa et al. 2016). The mechanical and physical properties and chemical compositions of stainless steel alloys usually applied for use in medical implants are given in Table 3. The first three steels listed are austenitic steels and the other two are reinforced through precipitation.

2.1.2 Cobalt Superalloys

Superalloys, or high performance alloys, are designed to have superior properties in comparison to regular alloys, such as corrosion resistance, resistance to oxidation, excellent mechanical strength, fatigue-related properties, toughness, machinability (metal forming–forging) and others, due to the combination of alloying elements (Wnek and Bowlin 2008). Cobalt superalloys are non-magnetic, with good corrosion resistance and high-temperature strength. Most of these properties are due to

Table 3 Characteristics of stainless steel alloys used for medical implants

Type of material Standard–chemical composition	Tensile strength Rm, MPa	Fatigue strength Rds, MPa	Modulus of elasticity E, GPa	Toughness KIC, $MPam^{1/2}$	Density ρ, g/cm^3
AISI 316L (EN X2 CrNiMo 17 13 2) Fe/<0.03C/16–18.5Cr/10–14Ni/2–3Mo/<2Mn/<1Si/<0.045P/<0.03S	550	270	198	195	7.87
AISI 317 (EN X2 CrNiMo 18 12 3) Fe/<0.08C/17.5–20Cr/11–15Ni/3–4Mo/<2Mn/<1Si/<0.045P/<0.03S	570	290	193	170	7.97
AISI 321 (EN X10 CrNiTi 18 10) Fe/<0.08C/17–19Cr/9–12Ni/<2Mn/<1Si/0.3–0.7Ti/<0.045P/<0.03S	600	265	197	180	7.95
SAE A 286 (DIN X4 NiCrTi 25 15) 54Fe/26Ni/15Cr/2Ti/1.3Mo/1.3Mn/0.5Si/0.2Al/0.05C	1100	370	201	55	7.92
SAE 17-4 PH (EN X5 CrNiCuNb 17 4) Fe/<0.07C/15.5–17.5Cr/3–5Ni/3–5Cu/.15–0.45Nb + Ta/<1Mn/<1Si/<0.04P/<0.03S	1300	450	202	50	7.82

the nature of the cobalt crystal structure and the formation of extremely hard carbides, while the significant chromium content provides high corrosion resistance (Odahara et al. 2008). Its good biocompatibility is related to high corrosion resistance, and the presence of the passive oxide layer (Cr_2O_3), spontaneously formed on the surface, similar to the case of stainless steel (Bombac et al. 2007). Research and development of cobalt alloys started in the early 20th century, when the first cobalt superalloy Co–Cr–Mo (ASTM F75) was patented. This alloy, also known as 'Vitalium denture,' was initially designed for dentistry. However, further development and modifications made it suitable for forging and precision casting processes. Hence, cobalt alloys found further application in the production of highly thermo-resistant parts, turbo compressors for jet engines and turbines, as well as for implants with complex configurations (Ratner et al. 2012). Parts with complex geometries have been fabricated using dental precision casting methods, while in the case of implants, casting has to be performed in a vacuum. The most adequate alloys for the casting process belong to the class Co–Cr–Mo (ASTM F-75) (Wise 2000). By using the HIP (High Isostatic Pressure) process, Co–Cr–Mo alloys can be fabricated with a significant reduction in microporosity, high homogeneity of the crystal structure with small grains, and excellent mechanical properties (Pilliar 2009). Co–Cr–Ni–Mo (ASTM F562) alloys can be processed using warm hot forging or cold drawing. Alloy forging provides structure and properties similar to those achieved in the HIP process. Superior mechanical characteristics make them appropriate for both the femoral component of the hip joint and the knee (Fig. 1) and the elements of internal fixation (plates, screws, pins). Forging can also be used in cases of Co–Cr–W–Ni (ASTM F90) and Co–Ni–Cr–Mo–W–Fe (ASTM F563) alloys, but their application in medical implants is much rarer (Bombac et al. 2007). The chemical compositions of standard Co–Cr-based alloys are given in Table 4.

Two of the basic elements of Co–Cr alloys are Co and Cr, with more than 60% of Co. Molybdenum is added in order to obtain a fine-grain structure that increases strength under casting and forging. The addition of chrome increases corrosion resistance and the overall strengthening of the alloy (Odahara et al. 2008).

Fig. 1 Components of artificial hips and knees made from the Co–Cr superalloy (Zimmer Biomet). Reprinted by permission of Zimmer Biomet. "Other than providing permission to use the Zimmer Biomet picture(s), this publication is not financially supported by Zimmer Biomet. Zimmer Biomet is the owner of the copyrights and all other intellectual property rights in relation to the picture(s) used"

Table 4 Chemical compositions of Co–Cr-based alloys

Element	CoCrMo (ASTM F75) min.–max. %	CoCrWNi (ASTM F90) min.–max. %	CoNiCrMo (ASTM F562) min.–max. %	CoNiCrMoWFe (ASTM F563) min.–max. %
Cr	27.0–30.0	19.0–21.0	19.0–21.0	18.0–22.0
Mo	5.0–7.0	–	9.5–10.5	3.0–4.0
Ni	<0.5	9.0–11.0	33.0–37.0	15.0–25.0
Fe	<0.75	<3.0	<1.0	4.0–6.0
C	<0.35	0.05–0.15	<0.02	<0.05
Si	<1.00	<0.4	<0.15	<0.50
Mn	<1.00	1–2.00	<0.15	<1.0
W	<0.2	14.0–16.0	–	3.0–4.0
P	<0.02	<0.04	<0.015	–
S	<0.01	<0.03	<0.010	<0.01
Ti	<0.1	–	<1.0	0.5–3.5
Co	Ostalo	Ostalo	Ostalo	Ostalo

CoNiCrMo (F562) contains approximately the same amount of both Co and Ni, around 35% of each element. It is highly corrosion-resistant in salt water under load-bearing conditions. Cold forming processes can significantly increase the strength of alloys, but this process is not suitable for production of large-size implants such as hip and other large joint implants, for which hot forming is used. Nickel enhances resistance to the fracture that occurs due to stress corrosion in water solutions. However, a greater amount of nickel promotes an allergic reaction (Bronzino 2000).

The wear properties of the wrought CoNiCrMo alloy are similar to those of the cast CoCrMo alloy. However, due to the poor friction properties, for almost all metal contacts, it is not recommended for prosthesis joints. The excellent fatigue and tensile strength of the forged CoNiCrMo alloy make it suitable for static, non-moving implants, such as hip stems. This is important, because it is rather difficult to remove damaged metal parts deeply implanted into the femoral tunnel (Rakovic and Uskokovic 2010). The mechanical properties of CoCr alloys are presented in Table 5. The CoNiCrMo (F562) alloy has very high tensile properties and is one of the strongest available alloys aimed for use in implants. As in the case of other alloys, an increase in strength leads to a decrease in ductility.

2.1.3 Titanium and Its Alloys

Titanium is extremely reactive to oxygen, and is usually found in nature as a stable oxide. This is perhaps the main reason that the use of titanium only began during the fourth decade of the past century. Although titanium came into use in medicine much later than other metals, its unique properties rapidly increased its application: relatively high specific hardness, low density (4.5 g/cm^3), low elastic modulus, high

Table 5 Mechanical properties of CoCr-based alloys

Properties	Cast alloy and annealed CoCrMo (F75)	Forged alloy CoCrWNi (F90)	CoNiCrMo (F562)	
			Annealed	Cold forming and aging
Tensile strength Rm (MPa)	655	860	790–810	>2000
Yield strength Rp (MPa)	450–520	310	280–320	1185–1950
Elongation A (%)	10–15	10	45–55	8–12
Reduction in area Z (%)	5–10	–	≈65	30–40
Fatigue strength R_D (MPa)	250–310	–	320–360	400–410

Fig. 2 The application of titanium alloys in orthopedics (Zimmer Biomet). Reprinted by permission of Zimmer Biomet. "Other than providing permission to use the Zimmer Biomet picture(s), this publication is not financially supported by Zimmer Biomet. Zimmer Biomet is the owner of the copyrights and all other intellectual property rights in relation to the picture(s) used"

biocompatibility and an extremely low level of toxicity. Its use is very wide, regardless of its poor tribological properties, especially compared to stainless steel and Co–Cr alloys. At room temperature, the rapid reaction of titanium to oxygen forms a very stable protective passive oxide film of Tio_2 (Geetha et al. 2009). Out of all Ti-based alloys, commercially pure (CP) titanium and Ti-6Al-4V alloy are the ones most used in medicine (Freese et al. 2001; Long and Rack 1998). Several commercial products are shown in Fig. 2. Titanium and its alloys also exhibit good osseointegration, which is especially important for orthopedic implants. All alloys are nonmagnetic, and diagnostic tools such as magnetic resonance can be safely used (Niinomi 1998). Osseointegration enables the use of cementless prostheses and rough bioactive surfaces (Rautray et al. 2011; Seifalian et al. 2014).

CP titanium is distinguished by a single-phase α microstructure. It may contain extremely low quantities of iron, nitrogen and oxygen, while the total quantity of other elements is always lower than 0.7%. Because of the slight but strictly defined differences in its composition, CP titanium is produced in four basic compositions, denoted by CP1–CP4. With each increase in number, the tensile strength value also increases. CP titanium has high corrosion resistance. α titanium alloys are characterized by a better resistance to higher temperatures and better welding capacity compared to β alloys, but they are also characterized by a lower hardness and the ability to be modelled (Geetha et al. 2009). CP titanium is mainly used for dental implants, but it also has application in orthopedics, serving as porous sintered wires placed on the surface of titanium alloys (Li et al. 2014a, b).

Different combinations of alloying elements result in a wide range of properties for TiAIV alloys, such as (Rakovic and Uskokovic 2010):

- Aluminum tends to stabilize the α-phase, that is, to increase the temperature of the α → β phase transition, and it leads to excellent hardness properties and resistance to oxidization under high temperatures (300–600 °C). The α-phase has a single-phase microstructure that is positive for welding, but not for thermal treatment.
- Vanadium stabilizes the β-phase by lowering the temperature of the α → β phase transition. Precise addition of β stabilizers can increase the hardness of the β-phase below the temperature of the phase transition, which results in the creation of a two-phase system. After the thermal treatment, precipitates of the β-phase appear at the solid solution temperature. The aging cycle causes precipitation of certain fine β grains from metastable β grains, thus increasing the share of the α structure, which is harder than the annealed α-β structure. A higher percentage of β stabilizing elements (e.g. 13% V in Ti13V11Cr3Al alloy) enables strengthening by thermal treatment.

Titanium and titanium alloys, especially α + β alloys such as Ti-6Al-4V (ASTM F 1472), are considered to be the most suitable biocompatible metal materials, due to the excellent combination of their mechanical properties, corrosion resistance and biocompatibility (Oldani and Dominguez 2012). However, the value of their elastic module is still considerably higher than the values of the elastic module of a human bone, and the most important direction the research has taken is towards low values of elastic module (Geetha et al. 2009). Also, research results have shown that vanadium is highly toxic. It has also been studied as to how to replace vanadium and aluminum with niobium, tantalum and zirconium, to prevent the known side effects of commercial Ti-6Al-4V alloys (Zhou et al. 2007; Long and Rack 1998).

During the first decade of the 21st century, two new generations of titanium–aluminium alloys were developed, specifically designed for orthopedics. The first generation Ti-6Al-7Nb and Ti-5Al-2.5Fe alloys have similar properties to the Ti-6Al-4V alloy, but exclude vanadium because of its potential cytotoxicity. The lowering of the elastic module was achieved with the second generation, including the Ti-12Mo-6Zr-2Fe, Ti-15Mo-5Zr-3Al, Ti-15Zr-4Nb-2Ta-0.2Pd,

Ti-15Sn-4Nb-2Ta-0.2Pd, and Ti-13Nb-13Zr alloys (Niinomi 2003; Mohammed et al. 2014). One of the recent new alloys developed with extraordinary properties is the Ti-13Nb-13Zr alloy. It is a β type alloy with low values of its elastic module and significantly improved hardness (Mohammed et al. 2014). The relatively low hardness of titanium alloys, however, results in low wear resistance (Zivic et al. 2011). One way to overcome this issue is surface treatments, such as ionic implementation (Fellah et al. 2014; de Viteri and Fuentes 2013; Lui et al. 2004; Kustas and Misra 1992; Rautray et al. 2011). Stimulation of osseointegration increases the implant's life, and use of a cemented prosthesis has decreased while rough bioactive surfaces are in greater application (Seifalian et al. 2014; Tapash et al. 2011). Important studies are being conducted related to simulation, and thus prediction, of the material's behavior within the body, which also depends on the fabrication technology used for the implant (Sljivic et al. 2016). The mechanical properties of several already applied alloys are given in Table 6.

2.2 Polymers

Polymers consist of many small units—chains, which are covalently bonded, and created via processes of polymerization and polycondensation. They consist of long flexible macromolecules that change their shape constantly. From the macromolecular aspect, polymers can be differently shaped to be: linear, branched, networked, or reticulated, each of which provide different properties of the end product. The structure of the main chain determines the polymer's properties.

Table 6 Mechanical properties of titanium alloys for biomedical applications

Legura	Type of alloy	Elastic modulus, GPa	Yield strength, MPa	Tensile strength, MPa	Elongation, %	Reduction in area, %
CP Ti grade 1	α	≈103	170	240	24	30
CP Ti grade 2	α	≈103	275	345	20	30
CP Ti grade 3	α	≈103	380	450	18	30
CP Ti grade 4	α	≈103	485	550	15	25
Ti-6Al-4V (annealed)	α + β	115	840–870	895–950	10–15	20–25
Ti-6Al-7Nb	α + β	105	780–820	850–950	8–12	25–45
Ti-5Al-2.5Fe	α + β	112	800–840	920–1000	5–7	30–35
Ti-13Nb-13Zr (aged)	β	80–85	860–910	970–1050	10–15	25–50
Ti-12Mo-6Zr-2Fe (annealed)	β	75–85	980–1050	1050–1100	18–22	64–73
Ti-15Mo-5Zr-3Al (aged)	β	80–85	840–1060	8502–1100	17–25	55–70

Monomers are held together by covalent bonds, and chains can be joined together by different forces such as: Van der Waals, hydrogen bonds, and hydrophobic or hydrophilic interactions. Copolymers are predominantly amorphous, due to their irregular arrangements within the molecule or at the micro level.

There are different classifications of polymer. According to their origin, they can be natural polymers, synthetic organic polymers, inorganic synthetic polymers and semi-organic synthetic polymers. According to their mechanical and thermal properties, they can be: thermoplastics, thermosetting polymers or elastomers. **Thermoplastics** consist of long chains made by linking small molecules or monomers, and they behave in a typically plastic way. They become softer and plastic with warming, and can be easily processed. At higher temperatures, they become liquid, with high viscosity. Thermoplastics melt, but due to their amorphous structure, they do not have a specific melting point. When cooled down, they harden and preserve their given shape. Thermoplastics are easily recycled. **Thermosetting polymers** (duroplast) consist of long chains of molecules strongly and transversely linked to one another in a 3D net structure. These polymers are stronger, but more brittle than thermoplastics. They do not become softer at higher temperatures. After hardening, this type of hard plastic can either be dissembled or melted, but it can also be melted down at higher temperatures with the addition of certain chemicals. Hard plastics cannot be easily recycled. The structure of **elastomers** (including rubbers), which is somewhere in between the two previous polymer structures, can have some transverse links. Elastomers have the ability of high elastic deformation without permanent shape change. It is important to emphasize that there is no clear distinction between these three categories of polymer. The amount and strength of linking determine the specific properties. Polymers are rarely used in their original chemical composition. Various additives are used to enhance some specific property and to obtain technically applicable polymer-based material.

When compared to traditional materials, their positive properties are: low density, good chemical resistance, low coefficient of friction and high wear resistance, low electrical conductivity (insulators), low thermal conductivity, good vibration damping, facility for painting, good manufacturability and feasible production. They also have several drawbacks, such as a high dependence on external conditions (temperature, load), low resistance to high temperatures, large thermal deformations, low surface hardness (low hardness in general), low strength and low elasticity module in most cases, and costly production for small batches (Bronzino 2000).

Numerous polymer-based materials have been studied and applied in medicine. The main reason for this is their biocompatibility and the rather large number of polymer materials whose biodegradability produces degradation products that are not toxic (Labarre and Carreno 2002). The polymer's properties are influenced by many factors, such as the structures of main and side groups, the chain structure (dependent on the choice of solvent used in polymer synthesis, drying dynamics, etc.) and the molar mass (dependent on the recrystallization of monomers, concentration of initiators, the vacuum level in the process of drying the polymer, etc.).

Table 7 Application areas of polymer materials in orthopedics

Polymer	Application area
Silicone	Finger joints
Polyester	Fixing breaks
Polyethylene (PE)	Parts of knee, hip implants, artificial ligaments and tendons
Poly(methyl methacrylate (PMMA)	Bone cement
Polyether ether ketone (PEEK)	Finger joints, parts of hip prosthesis, spinal implants and screws

Polymers can demonstrate viscoelastic properties similar to those in a natural bone (Marconi and Piozzi 2002). Application areas of the main polymer materials in orthopedics are given in Table 7.

Polymer implants and their parts are rather reliable. Careful selection of compositions, along with intensive clinical testing, provides functionality and endurance. However, even for highly reliable implant components, it is impossible to predict their behavior over longer periods (He and Benson 2014). There is no such polymer that is completely inert to chemical processes in the body, and these external factors eventually determine the functional duration of the implant. The best example is gamma radiation for the sterilization of polymer joint components. During this process, free radicals are created that produce rather harmful effects in contact with oxygen. Oxidation or the breaking of polymer chains might develop over months or sometimes years, leading to a loss of efficiency. Sterilization of polymers can be a rather complex process, and heating with dry steam, radiation and ethylene oxide are commonly applied. For example, sterilization of polyethylene at high temperatures is not allowed, because it leads to deformation and changes in mechanical characteristics. It is usually done by using irradiation and ethylene oxide instead.

Despite the fact that hundreds of polymers can be used as biomaterials, only 10–20 of them are particularly well suited for medical application. Application of polymers in orthopedics is related to fixation elements or those subjected to variable loads or wear-resistant parts (e.g., joints). The most commonly used polymers in orthopedics are: ultra-high-molecular-weight polyethylene (UHMWPE), polymethyl methacrylate (PMMA), and Polyether ether ketone (PEEK) (He and Benson 2011). A few examples of polymer orthopedic implants are given in Fig. 3.

Polyethylene homopolymer (PE) is made through the polymerization of monomer ethene ('ethylene'). Formed PE has a crystal structure. There are several variations, such as (Kutz 2009):

1. high density polyethylene (HDPE),
2. low density polyethylene (LDPE),
3. linear low density polyethylene (LLDPE),
4. very low density polyethylene (VLDPE),

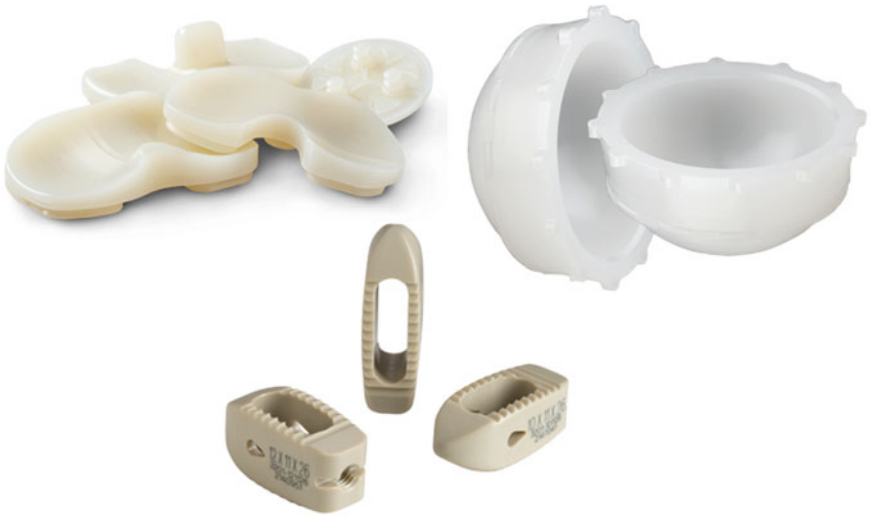

Fig. 3 Examples of the use of polymeric materials in orthopedics (Zimmer Biomet). Reprinted by permission of Zimmer Biomet. "Other than providing permission to use the Zimmer Biomet picture(s), this publication is not financially supported by Zimmer Biomet. Zimmer Biomet is the owner of the copyrights and all other intellectual property rights in relation to the picture(s) used"

5. ultra-high molecular weight polyethylene (UHMWPE).

HDPE is polymerized at low temperatures (60–80 °C) and under low pressure (up to 10 kg/cm^2) through the use of a metal catalyst. Highly crystallized, linear polymer with variable weight from 0.94 to 0.965 g/cm^3 is used as a biomaterial. LDPE is made at high temperatures (150–300 °C) and pressure (1000–3000 kg/cm^2) and through the use of an initiator of free radicals. Highly networked polymer with a lower crystallized structure varying from 0.915 to 0.935 g/cm^3 is used as a biomaterial. LLDPE (density: 0.91–0.94 g/cm^3) and VLDPE (density: 0.88–0.89 g/cm^3) are linear polymers, polymerized under low pressure and temperature through the use of metal catalysts with co-monomers in order to get the desired physical properties and density span. HDPE is used for pharmaceutical vials and capsules. LDPE found its use in flexible containers, disposable laminated foil (or co-extruded with paper), and packing. LLDPE is frequently used to make small bags and cases due to its sticking resistance, and VLDPE is used for extruded pipes.

UHMWPE is linear polyethylene of molecular mass between 2 and 6 million g/moll. High toughness, a low coefficient of friction, high fatigue strength, hardness and low density make it a good choice for contact surfaces in artificial joints (Wang and Ge 2007). One of its disadvantages can be the long-lasting presence of radicals made by ionizing radiation during the sterilization process. These radicals can react with oxygen and also with wear debris particles, and might cause harmful effects,

such as sieve lesions, osteolysis, bone resorption and unsuccessful implanting. In order to prevent these, different additives and antioxidants are being studied.

Polyether ether ketone (PEEK) is a polyaromatic polycrystalline thermoplastic (30–35% is of crystal structure) with a melting point at 343 °C, and a glassy temperature of 145 °C. It can be easily processed in a melted state by injection or extrusion via traditional processing techniques. PEEK is highly firm, non-hygroscopic and resistant to ionizing radiation. This polymer can be repeatedly sterilized via traditional techniques (e.g., steam, radiation) without significant deterioration of its characteristics (Kurtz 2012). Its use is mainly for spinal implants, with many successful clinical trials having taken place. Additionally, it is studied as the polymer matrix for polymer-polymer or polymer-metal composites. Frequently used reinforcements are: carbon fibers (CRF) and hydroxyapatite (HAp), which can be easily adapted (e.g., fiber length) to have significant influence on physical and mechanical properties. By adding biologically active materials, such as hydroxyapatite and bioactive glass, ether as a reinforcement or surface film, surface properties and biocompatibility can be tailored (Kurtz and Devine 2007). One of the excellent properties of the PEEK is its low density, similar to that of a bone, thus preventing shielding of the bone and osteoporotic changes. A significant advantage when compared to metals is the elimination of imaging artifacts and the absence of allergic reactions to metal ions. From the aspects of diagnostic techniques and imaging, PEEK is transparent for X-rays (CT cannot be used), and it is non-magnetic (MRI can be used). The total content of metal ions is very low, due to the high strength of the PEEK polymer, and accordingly, there is no danger of allergic reactions, such as in the case of nickel or other metal ions. Surface modification technologies can be performed far more easily than in the case of metal surfaces (Roeder and Conrad 2012). Suitable processing and joining technologies offer additional benefits for implant design. Comparison of the basic properties of UHMWPE, PMMA, and PEEK polymers is given in Table 8.

Poly(methyl methacrylate) (PMMA) is an amorphous polymer, chemically resistant to light, acids and bases (Polyn 2008). It is well suited for processing and has good stability of shape. Its mechanical properties primarily depend on molar mass and the amount of softener constituent (Ginebra et al. 2002). The presence of the polar ester groups increases intermolecular forces, which enhance strength and

Table 8 Typical properties of UHMWPE, PEEK and PMMA polymers

	UHMWPE	PEEK	PMMA
Polymer type	Semi-crystalline	Semi-crystalline	Amorphous
Degree of crystallinity, %	48–60	30–35	Noncrystalline
Molecular weight, 10^6 g/mol	2–6	0.08–0.12	0.1–0.8
Poisson ratio	0.43	0.39–0.41	0.38–0.40
Specific gravity, kg/m^3	930–950	1300–1320	1170–11200
Flexural modulus, GPa	0.89–0.96	3.76–3.95	2.23–3.16
Tensile strength, MPa	38–48	70–103	48–72
Tensile elongation, %	350–525	30–150	2–5.5

surface hardness (Robinson et al. 1981). These qualities make it similar in behavior to glass, and accordingly, it is called "organic glass." However, PMMA is brittle, inflammable, has a large amount of residual monomers depending on the polymerization type, and greatly influences the quality of the end product (Lewis 1997). Slow cooling during fabrication of PMMA is necessary to avoid the creation of residual stresses within the material (Stanczyk and Rietbergen 2004; Lesson and Lippitt 1993). From the commercial point of view, PMMA is one of the most important biomaterials, with diverse applications. Pure PMMA is used for fabrication of intraocular lenses and glass lenses, due to its high transparency (Bombac et al. 2007).

Perhaps the most important application is its use as the bone cement basis for the fixation of joint implants, enabling implant stability and functionality. It hardens very quickly and enables patients to start using their joints almost immediately after surgery. For implants that are supported only by bones, this process can usually take up to 12 weeks. PMMA bone cement serves as the shock and load absorber, and the media to transfer the load from the implant to the bone. However, joint implants that use cement for fixation exhibit some drawbacks, such as the possibility of developing avascular necrosis due to the high temperature of PMMA polymerization (Webb and Spencer 2007; Lu et al. 2002). Another issue with PMMA is its high cost, especially compared to other polymers. Also, processing of the two phases into hard cement has significant influence on its mechanical properties after implantation, and various methods have been studied to provide good mechanical behavior of the PMMA used for the fixation of implants (Zivic et al. 2012, 2013).

Sterilization of biomedical polymers is very important in relation to their properties, because polymers have lower thermal and chemical stability than other materials, such as ceramics and metals. It is more difficult to sterilize them with conventional techniques. It is not simple to sterilize polyethylene parts. High temperatures are not allowed because deformation will occur and mechanical properties will change. A common practice is heating in dry vapor, gamma radiation and ethylene oxide gas. Biodegradable polymers that are hydrolytically unstable can degrade due to humidity in storage, during processing or after fabrication. In order to minimize the possible effects of humidity, polymers are usually kept in a freezer. Biodegradable polymers can be sterilized with gamma rays, an electron beam or ethylene oxide gas (Bernkopf 2007).

2.3 Ceramics

Ceramics contain metallic and non-metallic elements, bonded to each other by ionic and covalent bonds, forming complex compounds and solid solutions (Si02, ZrO2, Al203, BaTi03, WC, TiC, SiC). They can have crystalline and amorphous structures. The amorphous structure is related to glasses, and the polycrystalline to ceramics made by sintering, wherein ceramics with high density can be made at

high temperature and pressure (Heimann 2002). They are hard, brittle, solid, hard to melt, wear-resistant and-corrosion resistant, with very low thermal and electric conductivity (Sáenz et al. 1999). Ionic and covalent chemical bonds prevent the movement of dislocations under the influence of deformation, thus making ceramics very brittle. Toughness might be increased if they are produced through the sintering of high purity fine powder, which lowers the possibility of pores and voids as crack initiators. There are other ways of increasing toughness, such as surrounding brittle ceramic particles with a ductile material (as in the case of cermet), or by deliberately forming microcracks to prevent larger ones. Ceramic biomaterials (bioceramics) are not as widely applied compared to metal and polymer biomaterials, but they are unsurpassed in their specific end application products. They are used in orthopedics for different scaffolds and as bone substitutes (Hamadouche and Sedel 2000). Bioceramics are also used for implant coatings to provide biocompatibility (Ratner et al. 2012). Applications of the most common forms of bioceramic are given in Table 9.

Oxide ceramics are used because they are chemically inert in physiological fluids, while surface-active ceramics have mild reactivity, which is used for tissue bonding. The basic disadvantage of bioceramics is their low resistance to fracture, which imposes limitations, especially under conditions of dynamic stress and strain (Ben-Nissan and Pezzotti 2002). The main advantage of bioceramics is related to their excellent biocompatibility with elements that are usually found in physiological fluids (Ca, K, Mg, Na). Other possible elements found in bioceramics have some toxicity (Zr, Ti), but it can be easily regulated by the body (Billote 2006).

Bioactive ceramics promote specific tissue response to the implant surface to enhance bonding between them. They assist bone ingrowth into the rough porous implant surface. Bioactive ceramics include bioactive glass, bioactive glass-ceramic and thick calcium-phosphate ceramic, such as synthetic hydroxyapatite (HAp) (Heness and Ben-Nissan 2004). All bioactive ceramics create an apatite layer on the implant's surface within the body environment, very similar to bone tissue, thus creating efficient bonding with the living tissue (Kim 2003). Bioceramics can be classified into four types based on how they create bonding with the tissue (Rakovic and Uskokovic 2010):

- Inert (Al_2O_3, ZrO_2),
- Porous (hydroxyapatite (HAp, HAp coating),
- Bioactive (bioactive glass, bioactive glass-ceramics),
- Degradable (calcium-phosphate).

Table 9 Application of ceramic materials in orthopedics

Ceramics	Fields of use
Aluminium oxide—Al_2O_3	Parts of a hip implant
Zirconium dioxide—ZrO_2	Parts of a hip implant
Calcium phosphate	Additive for healing bones, surface coating for artificial hips
Carbon	Coating for orthopedic implants

Inert implants do not form bonding with the bone. They create fibrous layers in between that serve as the strong mechanical bonding to prevent implant dislocation during functioning. In the case of higher loads, it might lead to implant rejection, even with formation of thicker layers. If the implant were to be exposed to a bigger load that would lead to interface changes, the thickness of the fiber layer would be increased and the implant would quickly be rejected (Hench 1991). Porous implants create bonds through tissue ingrowth into the pores and voids. Porous ceramics and HAp coating provide strong bonds between the implant and the surrounding tissue through biological fixation. The bond created in this way can endure far greater mechanical loads than in the case of morphologic fixation created by the inert bioceramics. Bioactive implants enhance active chemical reactions with tissue (surface functionalization). Resorbable implants gradually disappear over time, and are simultaneously replaced by newly formed tissue.

Bioceramics based on calcium-phosphate are very significant, because their inorganic components have properties similar to those of mineral components of the bone, which has led to their wide used in bone tissue repair (Dorozhkin 2010). They are non-toxic, but also behave in ways similar to natural processes, integrating with the tissue through a process much like natural bone regeneration. The main disadvantage of calcium-phosphate-based materials is their rather poor mechanical characteristics (Rakovic and Uskokovic 2010).

Calcium-hydroxyapatite (HAp) is the most important salt made of calcium and phosphorus. Synthetic hydroxyapatite ($Ca_5(PO_4)_3OH$) belongs to a group of bioceramics that is made through a form of synthesis that mimics the natural biological synthesis process. This bioceramic is chemically and morphologically very similar to the mineral component of bone and cartilage tissue. Bone tissue is made of organic (mainly collagen protein) and inorganic parts (mainly apatite). The inorganic part is natural material that makes up 70% of bone tissue and consists of calcium-phosphate, calcium-carbonate, calcium-fluoride, calcium-hydroxyapatite, calcium-hydroxide and citrate. Such bone tissue structure is naturally made order to enable adequate support and mechanical function of the bone (Yoshikawa et al. 2009). The specific density of hydroxyapatite in bone tissue is 3.16 g/cm^3 and hardens at 5 on the Mohs scale of hardness. Synthetic hydroxyapatite has excellent biocompatibility, bioactivity, and non-toxicity, and exhibits mechanical properties similar to those of natural hydroxyapatite. Nowadays, it is intensively used in orthopedics, for bone tissue reparation and reconstruction. Some physical and mechanical characteristics of HAp are given in Table 10.

Table 10 Physical and mechanical properties of the synthetic calcium phosphates (HAp)

Properties	Values
Elastic modulus (GPa)	70–120
Tensile strength (Mpa)	40–200
Compressive strength (MPa)	100–900
Bending strength (MPa)	20–80
Hardness	500–800 HV
Poisson's ratio	0.27
Density (g/cm^3)	3.05–3.15

However, the most frequent use of HAp is for the coating of metal surfaces (e.g., titanium, steel), and in that case, the only 'visible' layer of the tissue is the apatite-based material, which is not perceived as a foreign body by the tissue. Hydroxyapatite is also used for the substitution of bone parts (surgically removed due to some defects, or trauma), applied in powder form or as a porous block. This use is significant in cases in which it is necessary to remove a bigger part of the bone tissue (e.g., bone tumor). Hydroxyapatite can fill bone defects, react with the surrounding tissue and integrate itself into it after some time, and, especially important, stimulate natural regeneration of bone tissue. Hydroxyapatite produced through the sintering process at high temperature has weak reabsorption and can stay in the implantation site for years, even decades, which can potentially slow the bone remodeling process. However, in certain cases, this behavior might be desirable. With younger patients or children, resorbable implants are desirable, because material becomes bone tissue over time. Behavior of the low density HAp with high connected porosity is different from that of the high density HAp. Porous biocompatible structures enable bone ingrowth that supports mechanical stability and reparation.

Calcium-phosphate cements are usually delivered in the form of granules, 0.5–2.0 mm in diameter, which are mixed with blood before implantation. In this way, easier bone growth between granules is enabled. Unlike granules, calcium-phosphates in the form of a block have higher mechanical strength, but it is impossible to form it exactly to the shape of the bone defect. When this block has an open porous structure, to enable faster bone ingrowth, its mechanical properties are not so good, and it is mainly used for substitution of bone defects at sites not exposed to higher loads (Thamaraiselvi and Trends 2004). In order to better and more easily adapt to irregularly-shaped bone defects, self-setting calcium-phosphate cements are made. These cements are prepared in the form of a paste, by mixing a powder and liquid salt solution, and then easily injecting it into the bone defect site, where it hardens. Bone cement properties can be improved by adding glass, polymer or metal particles.

Some glasses can bond to the bone tissue; these are known as bioactive glasses. The major components of bioactive glasses and glass-ceramics, made by traditional melting at high temperatures, casting and sintering, are SiO_2, Na_2O, CaO and P_2O_5 (Carter and Norton 2007). In comparison with HAp, bioactive glasses have higher mechanical strength and the ability to create strong chemical bonds with bone tissue. An additional advantage of bioactive glasses over bioactive ceramic and glass-ceramic is the ability to easily control the chemical structure and speed of bonding—custom glass compositions can be easily created. Bioactive glasses with SiO_2 demonstrate slow and incomplete reabsorption, and glasses containing oxides of calcium and phosphor enable controlled ion release (Rakovic and Uskokovic 2010). In contact with bodily fluids, bioglasses based on SiO_2 form a layer of carbonate hydroxyapatite with a silica gel layer, whereas glasses with controlled ion release are completely soluble in water, thus creating an acidic environment. Glasses with controlled ion release are biocompatible and enable faster tissue ingrowth. Blocks made of bioactive glass are too brittle to be used for reparation of

bones exposed to load. The main use of bioactive glass is for bone grafting in dentistry, and glass-ceramics in orthopedics (Rakovic and Uskokovic 2010).

Specific thermal regimes during glass production can turn the glass into glass-ceramic that contains crystal phases with controlled size and structure. Glass-ceramic has much better properties than either glass or ceramic. Glass-ceramic can be easily mechanically cut into various forms. Its physical properties are: density 3.07 g/cm^3, bend strength 215 MPa, compression strength 1080 MPa, Young's module 118 GPa and hardness 680 HV. The bend strength of glass-ceramics is almost twice as high as in the case of thick sintered HAp (115 MPa) and considerably higher than human cortical bone. When glass-ceramic is loaded within a normal physiological environment, it exhibits a decrease in fatigue strength due to stress corrosion and the occurrence of micro-cracks (Krajewski and Ravaglioli 2002). Upon implantation, either within the bone or in contact with bodily fluids, it forms a thin apatite layer, as in the case of bioactive glasses.

A thin layer of apatite is formed on the surface of the glass-ceramic after its insertion into the bone defect site and its connection with the surrounding tissue. The same type of apatite is formed after contact with bodily fluids. The composition and structure are similar to the apatite of natural bone, due to which cells rapidly proliferate on its surface. This is the reason why fibrous tissue usually present around foreign material in the body does not form on the apatite surface, enabling direct growth of the bone tissue on its surface.

Alumina (Al_2O_3) bioceramic has high density and purity (>99.6%), good biocompatibility, thermodynamic stability, chemical inertness, high mechanical strength and excellent resistance to corrosion and wear. Very fine grains of polycrystalline Al_2O_3 structure are produced by pressing and sintering at temperatures of 1600 and 1800 °C, depending on the properties of the starting material (bauxite or natural corundum). The characteristics of alumina largely depend on the carefully chosen raw materials and the production process. By adding a small amount of MgO or CaO (<0.5%), a fine-grained structure and very high density of sintered material can be obtained. The lower strength is compensated for by adding small amounts of Cr_2O_3. On the other side, SiO_2 and alkali oxides result in larger grain sizes, and their content is thus kept as low as possible (<0.1%). The strength of alumina depends on the grain size and porosity. In general, smaller grains and lower porosity mean higher strength (Rahman et al. 2013; Park and Lakes 2007). Al_2O_3 has very high hardness (over 2000 HV), accompanied by low friction and wear. The surface of this ceramic has a hydrophilic layer that influences low wear. However, Al_2O_3 is a very brittle material, and cracks are easily branched once they are formed, especially if grain and porosity are higher. Surface defects, such as scratches, dents or a rough surface with imperfections, would also influence crack development, and very fine surface roughness is one way to prevent it. The process of hot isostatic sintering additionally enhances resistance to crack development, due to lowering of residual stresses and bringing density closer to the theoretical. The newest generation of ceramics is produced by adding zirconia (ZrO_2) into alumina, thus further enhancing its properties (Piconi et al. 2003). Because of the very good

tribological properties, especially when in contact with UHMWPE, alumina is very frequently used for heads and acetabular cups, in total hip replacements. The strength, fatigue resistance and ductility of Al_2O_3 are material properties dependent on the grain size and degree of sintering, as well as the purity of the initial material. Even though alumina has excellent compressive strength, hardness and wear resistance, it has moderate bending strength and ductility. The properties of alumina and zirconia are given in Table 11.

Ceramics based on zirconium-oxide (ZrO_2, zirconia) are extremely inert in a physiological environment. If compared to alumina, this ceramic is resistant to cracking and has higher bend strength. Zirconium has three different shapes of crystalline structure: monoclinic, tetragonal, and cubic. It exhibits martensitic transformation from monoclinic into tetragonal, and vice versa, during which its volume might change from 3 to 5%, which could lead to cracking. In order to avoid this transformation, a complete or partial stabilization by yttrium oxide (Y_2O_3) or magnesium oxide (MgO) and adequate additional thermal treatment is performed to obtain a complete tetragonal microstructure with very small grains of 0.2–0.5 μm (Piconi and Maccauro 1999). Accordingly, bioceramics based on the use of zirconium-oxide can be classified as follows:

- tetragonal ceramics based on zirconium-oxide completely stabilized by yttrium oxide and
- ceramics based on zirconium-oxide partially stabilized by magnesium oxide.

It is important to make a balance between density and grain size (Manicone et al. 2007). The properties of zirconium-oxide are given in Table 11. This type of ceramic is convenient for wear-resistant surfaces in total hip replacements (heads and acetabular cups). Even with all its good qualities, there are some possible

Table 11 Comparison of Properties of Alumina and Zirconia

Property	Alumina	Zirconia
Chemical composition	Al_2O_3 + Other	ZrO_2 + Y_2O_3 + Other
Purity (%)	99.8–100	95–97
Density (kg/m^3)	3930–3980	5.85–5.9
Porosity (%)	<0.1	<0.1
Bending strength (MPa)	540–560	850–910
Compressive strength (MPa)	4400–4600	1900–2000
Young's modulus (GPa)	380–400	205–212
Poisson's ratio	0.22–0.24	0.24–0.26
Fracture toughness (MPam$^{1/2}$)	1.52–1.53	9–10.5
Thermal expansion coefficient (q10^{-6}/K)	6.2–6.4	10.5–11.5
Thermal conductivity (W/m/K)	27–29	1.6–1.8
Hardness vickers	1960–2300	1200–1250
Grain size (μm)	3–6	≈0.6

Fig. 4 Heads and acetabular cup made of ceramics (Zimmer Biomet). Reprinted by permission of Zimmer Biomet. "Other than providing permission to use the Zimmer Biomet picture(s), this publication is not financially supported by Zimmer Biomet. Zimmer Biomet is the owner of the copyrights and all other intellectual property rights in relation to the picture(s) used"

issues, mainly related to the changes in mechanical properties over time during its use and the potential radioactivity of the material, but these long-term effects still need to be studied (Afzal 2014). The traditional sterilization process is not recommended because of a possible phase transformation during hydrothermal steam treatment. Sterilization is usually done by gamma rays. Ionizing radiation might cause color changes, but that can be reversed by heating and exposing it to intensive light. Due to its high bending strength and toughness, it can be used for hip endoprosthesis heads of smaller diameter (∅22 and ∅26 mm). It is usually paired with UHMWPE, and the wear factor with ZrO_2 ceramics is 40–60% lower than against Al_2O_3 ceramics or 10–20% than with metal heads. Heads and acetabular cups of hip prostheses are shown in Fig. 4.

Hybrid ceramics Al_2O_3-ZrO_2, produced by adding up to 25% ZrO_2 into an Al_2O_3 matrix, have significantly higher toughness. Thus, they overcome the disadvantages of alumina (low strength) and zirconia (aging effects). One of the typical representatives of this type of ceramic is commercial BIOLOX delta Zimmer Biomet ceramics with the following composition: 82% of alumina (Al_2O_3), 17% of zirconium-oxide (ZrO_2) and small additions of other oxides (e.g., CrO_2, Y_2O_3 and SrO). An alumina matrix with very fine grains contributes to wear resistance, and zirconia enhances its mechanical properties. Very fine grains of ZrO_2 are located between larger grains of Al_2O_3, thus preventing the initiation and development of cracks (Aza et al. 2005). The resulting material is a high performance ceramic with excellent biocompatibility, low wear, high hardness, excellent chemical and hydrothermal stability and better mechanical properties, especially strength. It is used for hip prostheses (heads and acetabular cups). The structure of the Al_2O_3-ZrO_2 hybrid ceramic is shown in Fig. 5a, and the mechanism of crack arresting in Fig. 5b. Recent research has been related to the effects of the addition of transition metals (TiN, ZrN, TiAlN, NbN, TaN, VN) for enhancing wear and corrosion resistance to prolong durability of the prosthesis (Chevalier and Gremillard 2008).

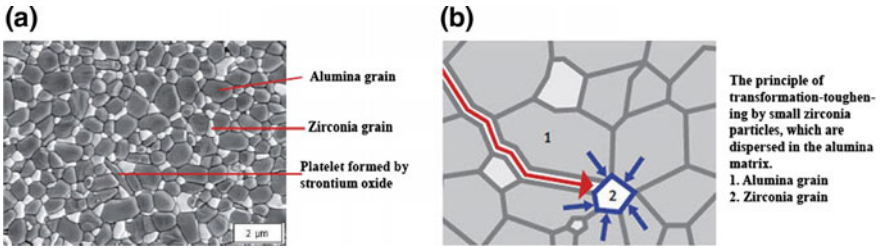

Fig. 5 **a** Structure of hybrid ceramics Al_2O_3-ZrO_2, and **b** mechanism for stopping movement of cracks through the material (Zimmer Biomet). Reprinted by permission of Zimmer Biomet. "Other than providing permission to use the Zimmer Biomet picture(s), this publication is not financially supported by Zimmer Biomet. Zimmer Biomet is the owner of the copyrights and all other intellectual property rights in relation to the picture(s) used"

2.4 Composite Materials

Composite materials are made by combining two or more materials of different properties in order to get a material with properties different from those of the constituent materials themselves. The composite is made of a continuous phase (matrix) and a discontinuous phase (reinforcements) within the matrix. The matrix protects the reinforcements from external influences. The motive for composite development initially was to develop materials with high strength and stiffness that simultaneously had a decrease in weight. Zones within the composite can be designed to follow specific loads foreseen to act upon those specific zones. In general, all combinations of traditional material are possible, but not all of them are possible in practice, or are at least very hard to achieve due to various issues (e.g., metal-polymer). The most common composites nowadays are: metal-metal, metal-ceramic, ceramic-polymer, ceramic-ceramic, polymer-polymer, and polymer-ceramic (Iftekhar 2009). Composites can be classified as particulate, fiber or layered, based on their structure. Particulate composites are used in engineering for high speed tools, and fiber composites are mainly used as exquisite construction materials.

The production technology has a profound effect on the composite structure and further properties. For example, if all the fibers and grain fillers are oriented in one direction, anisotropic composites are made. Spherical particles randomly packed into a matrix result in isotropic composites. The most commonly used composites have orthotropic characteristics, with properties depending on the three orthogonal directions (Iftekhar 2009). In general, the matrix has higher plastic toughness, whereas particles, fibers and layers are of higher density. This way, a material with an exquisite combination of hardness, strength, plasticity and toughness is made. The matrix prevents movement of dislocations or cracks from the harder material through the tougher matrix (depending on the composite structure) (Bronzino 2000; Iftekhar 2009). Common reinforcements for composite biomaterials are carbon,

polymer, ceramic and glass fibers, as well as particles. Depending on their use, reinforcements might be permanent or degradable.

In biomaterial development, composite materials can overcome issues related to traditional material classes (metals, polymers, ceramics). Metals are stiff and corrosive; polymers are too flexible and have poor mechanical properties; and ceramics are brittle. Composites can provide combinations of properties for optimal design according to specific organs. Some of their advantages over traditional materials are: the possibility of making very complex shapes, low cost production, the possibility of connecting elements during production, dimensional stability under extreme conditions, and corrosion resistance (Iftekhar 2009; Peters 1998).

Composites with a polymer matrix (polyethylene (PE), polyurethane (PUR), poly(ether-ether-ketone) (PEEK), polysulfone (PSU)), a metal matrix (stainless steel, cobalt-chrome and titan compound) and a ceramic matrix (based on Al_2O_3, ZrO_2 or HAp) are used as biomaterials. Surface compatibility is very important, and includes the chemical, physical (morphologic) and biologic matching of the implant and the host tissue, whereas structural compatibility means good adjustment of the implant to the mechanical behavior of the host tissue (stiffness, strength and load bearing and load transfer to the tissue). By changing the amount and reinforcements, implant properties can be significantly improved so as to adequately respond to the mechanical and physiological requirements of the host tissue (Ramakrishna et al. 2001a, b). Polymer composites are suitable for CT or MRI diagnostics, unlike metal or ceramic ones. Polymer composites have a wide application: artificial joints, bone fixtures, bone replacement and restoration in dentistry, instruments for straightening and stabilizing spine deformation, vascular transplantations, hernia implants, prosthesis of tendons and ligaments, artificial skin, prosthesis for the replacement and repair of cartilage, artificial extremities, etc. (Green 2012). A particularly interesting type of composite is that with HAp, because hydroxyapatite ceramic is the only material that can form a direct bond with living bone tissue. Reinforcements for composite biomaterials are: particles and fibers of carbon, polymers, ceramic and glass. They can be inert or absorbable, depending on the final application. Carbon fibers are light (density of 1.7–2.1 g/cm^3), flexible and have high strength (up to 4.5 GPa) and high elastic modulus (up to 900 GPa). They are used for composites, in applications that demand low weight and strong mechanical properties. Their drawback is low shearing strength and the fact that they might be brittle. They are made through pyrolysis, usually up to 1000 °C in an inert environment (carbonization process), out of different organic compounds (tar pitch). Carbon fibers embedded in PEEK, UHMWPE or an epoxy matrix can be used for joint implants, but they are still not widely used in practice (Zhao et al. 2003).

Polymer fibers are not comparable to carbon fibers as regards aspects of strength and stiffness, with the exceptions of aramid and UHMWPE (Migliaresi and Pegoretti 2002). Aramid fiber is made of synthetic linear macromolecules consisting of aromatic groups connected by amide and imide bonds. Aramid is a generic name for aromatic polyamide fibers. Aramid fibers are relatively light (density = 1.44 g/cm^3), stiff (modulus is up to 190 GPa) and strong (tensile

strength is about 3.6 GPa). They are resistant to abrasive wear. These fibers are less stiff and strong than carbon, but since they are lighter, they have comparable specific weight. A related issue in biomedical applications is that they are hygroscopic, and their compressive strength is significantly lower than their tensile strength (about 8 times). These fibers are used as reinforcements when high tensile strength, stiffness and fatigue resistance are needed. In medicine, these composites are not so widely used due to their still unknown long-term biocompatibility. In orthopedics, these composites (PMMA-Kevlar) are used for plates for bone fixing and ligament prosthesis. UHMWPE fiber has the biggest specific strength when compared to all currently available commercial fibers. UHMWPE fibers have high elastic modulus and strength and are very light (density about 0.97 g/cm^3). They are abrasion-resistant, non-hygroscopic and have excellent biocompatibility. Low melting temperature (around 147 °C) is a limiting factor for production at high temperature. UHMWPE fibers are used for strengthening acrylic resin used to make intervertebral discs prostheses and ligaments (Kutz 2009).

Poly(ethylene terephthalate (PET) fibers are used in orthopedics for artificial tendons and ligaments and intervertebral discs, as fibers or fabrics, independently or as reinforcements in a polymer matrix. Fibers made of poly(lactic acid) (PLA), poly (glycolic acid) (PGA) and their copolymers (poly(lactic-co-glycolic acid), PLGA) are biodegradable polymer fibers. Their properties depend on hygroscopicity, molar mass, strength, etc. Fibers made of these polymers are used for reconstruction of ligaments or as scaffolds in tissue engineering. PLA and PGA are also used in combination with a PLA biodegradable matrix. Examples of this use are intramedullary biodegradable nails and plates and biodegradable scaffolds for regeneration of bones (Rakovic and Uskokovic 2010).

Ceramic reinforcements, due to being too brittle, are mainly used in the shaping of particles, and very rarely as fibers. Phosphates of calcium, aluminium, and zinc, as well as with Al_2O_3, ZrO_2, SiO_2, and $CaSO_4$, are used as reinforcements, with ceramic or polymer matrices. Ceramic-ceramic composites are mainly made with tricalcium-phosphate (TCP), or a HAp matrix. With an increase in reinforcement content, an increase in mechanical strength is achieved, but biocompatibility is lowered. These types of composite are not widely used in medicine.

Polymer-ceramic composites are the closest match to natural bone tissue according to their mechanical properties. The main issue here is polymer toxicity and aging tendency. The majority of polymers release toxic products over time in the body, and this also leads to structural changes and unknown behavior of the implant. From a structural point of view, the HAp component in the composites is similar to bone tissue, with a polymer matrix resembling a collagen component inside of which particles of crystal HAp are finely distributed. These composites can be made to be bioresorbable or non-resorbable (Chevalier and Gremillard 2008). Nonresorbable polymer-HAp composites (e.g., PE-HAp) are used for replacement of bone tissue. HAp granules or powder is mixed with high density PE. The ratio of polymer and HAp content determines the composite's mechanical characteristics. An increase in HAp leads to a higher elastic modulus and better biocompatibility. The bioresorbable polymer-HAp composite is a rather new

concept in biomaterials that change over time, from acting as a stable implant during the healing process to their gradual disappearance after the healing is over (Salernitano and Migliaresi 2003). Bioresorbable polymers used for this type of composite are: poly(lactic-co-glycolic acid) (PLGA), poly-L-lactide (PLLA), polyglycolic acid (PGA), poly-D,L-lactide (DLPLA), Poly-epsilon-caprolactone (PCL), poly (D,L-lactide-co-glycolide) (DLPLG), etc.

Glass fibers are made by having melted glass flow through small openings in a platinum tool, from two types of glass: E-glass (52–56% SiO_2, 12–16% Al_2O_3, 16–25% CaO, 8–13% B_2O_3) and S-glass (65% SiO_2, 25% Al_2O_3, 10% MgO). E-glass has good tensile strength and elastic modulus. S-glass has a higher value of specific strength and stiffness, but it is more expensive. In general, glass fibers belong to the low cost materials. Commercial composite materials strengthened with glass fibers have enhanced properties such as: high specific strength, good dimensional stability, good stability in temperature changes, humidity and corrosion resistance, with a low cost of production. However, their application in medicine is not wide, except for several studies with hip prostheses, made of poly (ether-imide) (PEI) and hybrid reinforcements made of glass and carbon fibers, or isoelastic intramedullary nails made of PEEK polymer (matrix) and glass fibers (reinforcement) (Pirhonen 2006). Besides glass fiber composites, biomaterials with bioactive glass reinforcement and a ceramic matrix are currently used for the replacement of tiny bones of the middle ear. Ceramic components are mainly: calcium-phosphate (CP), biphasic calcium phosphate (BCP) or hydroxyapatite (HAp). This type of composite has higher biocompatibility and bioactivity, resulting in a strong implant-tissue bond (Chen et al. 2012).

Even though composite materials with a ceramic or metal matrix are very important in technology, they have very few applications in medicine, calcium-phosphate bone cement being the most important (Ramakrishna et al. 2001a, b). The majority of biomedical composites have a polymer matrix, mainly thermoplastic. The common materials for a biomedical composite matrix are: PEEK, UHMWPE, PTFE and PMMA (Steinberg et al. 2013) and can be reinforced by fibers of carbon, polyethylene, or glass and ceramic particles. They are used for components of joint prosthesis (hip, knee, shoulder), bone fixation plates, etc. Composite materials with an epoxy are rarely used, due to the release of toxic monomers.

The biomimetic approach in material design has produced composite materials that mimic bone structure, mainly related to ceramic-polymer composites in which the ceramic part is tricalcium phosphate (TCP) or hydroxyapatite (HAp). The natural polymer used in such composites is collagen type 1, because it is the essential ingredient in human bone tissue, thus enabling better connection of the implant to a tissue (Brkic 2013). One novel area of research is related to hybrid composites, such as polymer composites reinforced with natural fibers (Zivkovic et al. 2017; Hyseni et al. 2013).

Bioresorbable synthetic polymers based on PLA, PGA and PLGA are the most widely used materials in medicine, because the final products of their degradability are non-toxic and do not impede the metabolism of the surrounding tissue. These

polymers enable good surface adhesion of osteoblasts and the adhesion of proteins and growth factors responsible for reparation of bone tissue. However, the most common reason for using this class of composite matrix was to achieve total implant dissolution. Their reinforcement with some particles or fibers is important, since they do not have adequate strength, a typical example being fixture plates in orthopedics.

2.4.1 Practical Examples of Commercially Applied Composite Materials

PMMA bone cement is used in trauma defects, vertebroplasty (fixing vertebrae) and kyphoplasty (fixing vertebrae with the possibility of restoring their height), and for repairing fractures due to osteoporotic changes. In prosthetics, the cement's function is to distribute body weight in such a manner that the reconstructed zone is not overly loaded. However, a related issue is the stress shielding effect on the adjoining bone zones. An increase in the biocompatibility and bioactivity of PMMA cement is achieved by adding an optimal amount of ceramic particles (bioactive glass or hydroxyapatite). But the optimal content of these particles continues to be studied, because it can provoke unwanted worsening of mechanical properties owing to the weak adhesion, when particles start to behave like voids and crack initiators.

Acrylic bone cement reinforced with bioceramics is synthesized by mixing polymer PMMA, monomer MMA, benzoyl peroxide as a free radicle initiator and tetragonal ZrO_2 synthesized through he sol-gel procedure as a bioceramic part. These are used in dental implants, maxillofacial surgery (surgery of face, mouth and jaw), for prostheses and fixing artificial extremities. This cement is used as the mechanical bond between metal prostheses and bones. The main disadvantages of acrylic cement are incompatibility between bone and cement, shrinking of cement after polymerization with the possibility of producing cracks, and limited mechanical properties. In order to overcome these issues, different reinforcements, such as carbon fibers, HAp particles or fibers, PMMA fibers, fibers of stainless steel, and titanium fibers, are being studied.

Composite biomaterials are also made as injectable fillers, gel, paste or cement. These can be injected into a living tissue, where they harden and take on the 3D shape of the zone that needs repairing. An injectable composite might have a different purpose. It is used for fixation of different kinds of prosthesis in orthopedics, but also for filling out the holes in soft and hard tissues. There is a wide range of different classifications and types. Different properties can be obtained depending on the compositions. HAp and high density polyethylene (HDPE) make bioinert injectable composites, and polylactides (PLA) result in bioactive ones (Davis and Leach 2008). One special group of injectable composite materials consists of those made of calcium-phosphate (CP). They have minimal inflammatory response in the organism and excellent osteoinductivity, as well as mechanical

properties. The size of the composite particles has a major influence on the final properties (Ignjatovic and Uskokovic 2008).

Different bone fixtures (e.g., plates, screws) have been in common use for years in orthopedics and trauma, usually made of stainless steel, Cr–Co alloys and titanium alloys. Nowadays, PEEK reinforced with carbon fibers are studied and applied, commonly in the form of a braid.

3 Advanced Material Structures

3.1 Porous Metals—Metal Foams

Nature creates honeycombed material structures, such as in a tree, stone, bone, coral, etc., whose properties are optimally adjusted to the surrounding conditions. Metal foams are such artificial structures for technical applications. Metal foams have high porosity of 40–90% and can be made with an open or closed cell type. Production process regimes and parameters can tailor the final properties (Ashby et al. 2000; Kennedy 2012). Metal foams are a rather new class of metal material, currently emerging in the practice of engineering. Even though the initial patents are almost 50 years old, intensive research of metal foams for industrial use started about 20 years ago. Their basic properties are: low density (mass), relatively high stiffness (especially with sandwich designs), good insulation properties (sound, warmth), non-flammability and excellent absorption of impact energy (Ashby and Tianjian 2003). These porous metals, by their shape, resemble spongy bones with high surface friction properties and relatively low elastic modulus. The main way to produce metal foam is through powder metallurgy or dissolution. The foaming of the material is always conducted in a liquid phase so that the powder is also in a state of dissolution. External gas is necessary to produce pores inside the structure. It can be added externally or via a spraying agent to accelerate foaming during dissolution. The foam produced can be immediate or delayed (Ryan et al. 2006). The main classification of metal foams is between those with open and those with closed cells. Foams with closed cells have every cell completely closed by thin walls or membranes, completely separated from the adjacent cell, while in open cells, all the cells are interconnected, enabling tissue to infiltrate into the foam and strengthen in that position (Miao and Sun 2010).

Regarding implant applications, there are three types of porous implant:

- partially or completely porous with a coated solid base,
- totally porous materials,
- porous metal segments added to a solid metal part.

The materials used for the production of metal foams are: Co–Cr alloys, stainless steel, titanium and its alloys, tantalum and magnesium (Murr et al. 2010). The traditional medical grade stainless steel alloys are AISI 316L and AISI 304 alloys

with an austenitic structure. These steel alloys have an increased content of Ni in order to maintain their austenitic structure, and they are not convenient for metal foams, because of their release of Ni (Bakan and Korkmaz 2015). Steel type 17-4 PH reinforced by precipitation has a relatively lower content of Ni than austenitic stainless steel, and it is considerably better for porous structures. Also, 17-4 PH stainless steel has better mechanical properties, which can be enhanced by aging: a combination of strength, simple thermal processing (aging), and good corrosion resistance. This steel foam can provide low density and mechanical support for tissue ingrowth (Mutlu and Oktay 2013).

Porous surfaces made of Co–Cr alloy exhibit inertness, biocompatibility and mechanical durability. Macro and micro porous surfaces are formed on the implant's surface through the deposition of pearls of Co–Cr alloy, as with acetabular cups and femoral heads in total hip replacement, or components of total knee replacements (Matassi et al. 2013).

Such coatings can also be made of titanium alloys through the plasma-spraying method, usually with a porosity of 60–80% and a pore size of 100–600 μm; these can also be used in bulk shape. These porous materials resemble spongious bone with high surface friction and relatively low elasticity modulus, and thus provide such a surface as to enable a long-term connection with the implant due to ingrowth of the bone tissue into the pores. In general, Ti alloy foams are commonly used in hip, knee and shoulder joint prostheses (Rivard et al. 2014; Li et al. 2014a, b).

One specific type of porous material is "trabecular metal," developed by Zimmer Biomet (Fig. 6), with a structure similar to that of spongy (trabecular) bone. The cellular structure of this material is closer to the physical and mechanical properties of the bone than that of any other synthetic material. The unique, trabecular configuration and crystal microstructure both enhance rapid direct infiltration of bone tissue into the implant (Eid 2013). Tantalum used for making trabecular metal has mechanical strength and resistance to corrosion, along with exquisite

Fig. 6 Trabecular metal of monoblock tibial components (Zimmer Biomet). Reprinted by permission of Zimmer Biomet. "Other than providing permission to use the Zimmer Biomet picture(s), this publication is not financially supported by Zimmer Biomet. Zimmer Biomet is the owner of the copyrights and all other intellectual property rights in relation to the picture(s) used"

biocompatibility, and as such, it has successfully been used in surgery for more than 50 years (plates for cranioplasty in neurosurgery or parts for cardio pacemakers) (Levinea et al. 2006).

Magnesium-based alloys are prospective biomaterials for bone replacements, due to their low ionizing energy, suitable strength, good biocompatibility and biological degradability, especially in porous forms (Mediaswanti et al. 2013). They might be used as light, degradable, load-bearing orthopedic implants, which remain for a period of 12–18 weeks, to support the bone tissue as it grows into the pores and heals. However, the issue of rapid corrosion in bodily fluids is still under investigation, so that the implant's durability may be prolonged to the necessary time frame. The corrosion rate of Mg-based alloys can be controlled in several ways (alloying elements, or coatings), but this is still under investigation, with no final solutions having been achieved thus far (Osorio-Hernández et al. 2014).

3.2 Biodegradable Materials

3.2.1 Biodegradable Polymers

Over the last several decades, bioresorbable (biodegradable) polymers have been frequently studied and used in different medical areas: controlled drug release, as scaffolds in tissue engineering, for fixing bone fractures (screws and plates), as membranes, surgical sutures, etc. (Santos 2010). The biodegradation mechanism is complex, with many simultaneous phases developing, including both traditional and enzymatic hydrolysis. The mechanical properties deteriorate during biodegradation, and it is assumed that this begins within the amorphous material zones. The most frequently used biodegradable polymers include polylactides, and polyglycolides, as well as their copolymers, apertures, etc. (Ghanbarzadeh and Almasi 2013; Gunatillake and Adhikari 2003). Table 12 shows the physical, mechanical, and degradation properties of selected biodegradable polymers.

When a bioresorbable polymer is implanted into a body, its degradation starts in accordance with the structure and properties of the polymer. There are various factors affecting degradation: type of chemical bonds in the polymer, permeability of water, porosity, molar mass, chemical structure, released surface energy, dimensions and shape of polymeric implant, pH, shape of crystallite, amorphous/crystal relation, etc. (Park et al. 2007). The degradation rate and mechanisms both depend on the types of hydrophilic group inside and at the ends of the chains, the reactivity of the hydrolytic groups, the amorphous and crystalline regions, and the porosity and molar mass of the polymers. Generally, degradation begins when the liquid penetrates the polymer's structure, first towards the amorphous regions of the polymer where the chemical bonds are breaking and disintegration of the chains occurs. The nature of the phenomenon indicates a decrease in the molar mass, accompanied by physical changes. Different influences govern the process, depending on the material type. For example, if the polymer is

Table 12 Physical, mechanical, and degradation properties of selected biodegradable polymers

Polymer	Melting point (°C)	Glass transition temperature (°C)	Tensile or flexural modulus (GPa)	Elongation (%)	Time to complete resorption (months)
PGA—poly(glycolide)	222–231	34–43	6.1–7.2	4.6–18.9	6–12
LPLA—poly(L-lactide)	172–180	60–65	2.7	5–10	>24
DLPLA—poly(DL-lactide)	Amorphous	55–60	1.9	3–10	12–16
PCL—poly (ε-caprolactone)	58–63	−65 to −60	0.4	300–500	>24
PDO—poly(dioxanone)	–	−10 to 0	1.5	–	6–12
PGA-TMC—poly (glycolide-co-trimethylene carbonate)	–	–	2.4	–	6–12
85/15 DLPLG—poly(DL-lactide-co-glycolide)	Amorphous	50–55	2.0	3–10	5–6
50/50 DLPLG	Amorphous	45–50	2.0	3–10	1–2

hydrophobic, the chemical bonds at the surface of the polymer are very favorable for the hydrolysis process or bioerosion (Bohner 2010).

Biodegradable polymers are biocompatible; generally, they do not lead to an inflammatory response, and via hydrolysis and possible enzyme reactions, they degrade in vivo into products that are removed from the body through regular metabolic processes. In general, the degradation rate can be tailored through the different content of their two monomer components during hardening, and this can be applied in orthopedics to obtain material adapted to the specific bone. However, due to their poor mechanical properties, polymers are not used for load-bearing implants, and are mainly recommended only in specific situations, such as fixation of the joints of elbows and knees (Avérous and Pollet 2012).

Biodegradable polymers can be natural or synthetic. Basically, synthetic polymers have an advantage over natural ones, because they can be shaped into wider forms with predictable and reproducible properties (Tian et al. 2012). There are many reasons why it is important for the material to be degradable, but one of the main reasons is the possibility of making an implant that does not require further surgery for its removal. Permanent implants such as bone fixtures are commonly removed after the healing is finished, requiring surgery that is painful, and the bone shows a tendency to break again afterwards, due to the shielding effects of permanent implants, which makes the surrounding bone tissue weaker than that of healthy ones. Contrastingly, implants made of biodegradable materials gradually transfer the load to the bone via the degradation process (Middleton and Tipton 2000).

The basic criteria for the selection of biodegradable polymers are their mechanical properties, degradation time, in vivo properties, etc. The ideal polymer implant has sufficient mechanical properties to support the tissue throughout the

healing process; it does not lead to inflammation or toxic effects; degradation products can be eliminated from the tissue through natural metabolism and by leaving no particles behind; it is easy to use and sterilize (Middleton and Tipton 2000). The factors that determine the mechanical properties are the synthesis conditions, the types of monomer and initiator, and the presence of additives. These factors influence polymeric hydrophilicity, crystallinity, melting and gazing point, the reaction of side chains, and others that further define the final in vivo properties. Biodegradation is based on unstable polymer bonds with respect to hydrolysis. Chemical compounds with such properties are esters, anhydrides, orthoesters and amides. The most commonly used are polyesters that can be homopolymers made of one type of monomer or copolymers made of a different kind of monomer, such as lactide or glycolide. Copolymers of trimethylene carbonate, ε-caprolactone, and polydioxanone are also frequently used (Fambri et al. 2002).

Polyglycolide acid (PGA) is the simplest linear aliphatic polyester, and it is most commonly made through polymerization of a ring-opening cyclic diester of glycolic acid, glycolide. The monomer of glycolide is synthesized through the dimerization of glycolic acid, and polymerization leads to materials of high molar mass with approximately 1–3% of non-reacted monomer remaining. PGA is a strong, tough, crystallized polymer with a melting temperature of 225–225 °C and a glass transition temperature of 35–40 °C. Unlike other similar polyesters (e.g., PLA), PGA does not dissolve in most traditionally-used solvents because of its high level of crystallinity. PGA has a very good affinity to form fibers. PGA was used commercially for the first time in the 1970s as the first synthetic biodegradable suture. PGA sutures have high strength and stiffness. They can also be copolymerized with other monomers. Surgical suture materials made of PGA lose 50% of their strength after two weeks and 100% after four weeks, and they are completely resorbed within a period of four to six months. The low solubility and high melting point of PGA limit its use in drug delivery, because it cannot be used in the form of films, sticks, capsules or microspheres (Ulery et al. 2011).

Polylactic acid (PLA) is an aliphatic polyester made through the polymerization of polylactic acid. Polymers based on lactic acid have had major importance in medicine, because this polyester is degraded in the body via simple hydrolysis into the ester base and a neutral component. The product of degradation is excreted through the kidneys or it is biochemically eliminated as CO_2 and H_2O (Middleton and Tipton 2000). PLA has many possible applications, such as: internal sutures, elements of prosthesis, scaffolds, heart valves, bone screws, needles and carriers for the temporary internal fixation of fractures or controlled drug delivery. Exquisite properties such as easy processability, high biocompatibility and controlled biodegradability make this polymer one of the most widely applied materials today.

PLA can be tailored to have widely different physical and chemical properties due to the presence of the methyl group in alpha carbon. Possible isomers are L, D, and DL. Poly(L-lactic acid) (PLLA), poly(D-lactic acid) PDLA and poly(DL-lactic acid) (PDLLA) are synthesized from the L(−), D(+) and DL-monomers of lactic acid, respectively (Avérous and Pollet 2012). By varying of the molar mass and composition of copolymers, a wide span of degradation rate can be achieved, as

well as physical and mechanical properties. There is no linear dependence between a copolymer's composition and its mechanical and degradable properties. Numerous studies have shown that PLA is completely resorbable and that it provokes almost no negative tissue responses, either in bulk or degradation products. Biodegradability is developed by hydrolysis at temperatures up to 50 °C (e.g., in composites) within a period of from several months to two years. Hydrolytic degradation of PLA produces monomers of lactic acid, which are compatible for metabolism via tricarboxylic acid and eliminated as CO_2 through the respiratory system. Various aliphatic polyesters have these properties, but PLA has proven to be the most efficient class of biodegradable polyester.

Lactic acids are easily produced via biotechnological processes through the use of low cost materials. It is produced from sugar (dextrose, glucose and sucrose), sugar beet, molasses or the starch of produced corn, wheat or rice. Polymers for PLA production should have adequate thermal stability to protect it from degradation and to maintain molar mass and properties. Degradation of PLA depends on molar mass, temperature, impurities, the concentration of catalysts, etc. PLA used in orthopedics and oral surgery must have a high molar mass to achieve high mechanical strength. But in PLA used as drug delivery carriers, low molar mass is necessary to obtain a shorter period of time for polymer degradation in order to achieve an efficient, controlled release of the active substances (Naira and Laurencin 2007).

Poly(lactic-co-glycolic acid) (PLGA) is a copolymer glycolide with L-lactyde or DL-lactyde, developed for drug delivery systems. Due to its commercial availability, reasonable cost, biocompatibility and products of hydrolytic degradation, which are resorbable and not harmful, PLGA is also often used as the basis for the material matrix in drug delivery systems. Copolymerization of glycolide and lactide produces a polymer with characteristics presenting a combination of PGA and PLA (PLLA and PDLLA) properties. PLGA is less brittle than its original components, since crystallinity is lowered by increasing the content of any other homopolymer (Naira and Laurencin 2007). PLGA with 25–70% of PGA is amorphous and has adequate properties for controlled drug delivery. By increasing the number of PGA units in a polymer, its hydrophilicity also increases. The degradation period of PLGA is up to two months.

Unlike PLA and PGA, which are homomers, PLGA is a heteromer, and it has quite different characteristics. Some of the differences are related to crystallinity, solvability, temperature of phase change (glass transition temperature), degradation and use. Namely, all PLGA polymers have very low crystallinity. The glass transition temperature is around 45–55 °C, and they react in many solvents, such as acetone, ethyl-acetate, tetrahydrofuran and chlorinated organic solvent (Ulery et al. 2011). The isomer type of lactide acid, which is in the structure of PLGA, might sometimes be indicated in the name of this polymer. If PLGA is built of both isomers, it will carry the name poly(D,L-lactide-co-glycolide) (DLPLG), while the presence of only one isomer in this polymer will be indicated as poly(L-lactide-co-glycolide) (LPLG) or poly(D-lactide-co-glycolide) (DPLG). Accordingly, DLPLG, DPLG and LPLG belong to the PLGA group of polymers, which is the common way that they are

denoted. During polymerization, successfully bonded monomeric units are bonded by an ester link, resulting in linear aliphatic polyester.

PLGA degradation is realized through hydrolysis, and the degradation products are suitable acids (lactic and glycolic) that are also natural products of human metabolism and could be included in natural metabolic processes, thus enabling their easy disposal out of the body. This characteristic makes it suitable for "in vivo" applications. The degradation of PLGA changes depending on the composition of the monomers. With monomers of composition of 50:50 degradation, kinetic is the fastest, and the rate is decreased by increasing the amount of glycolic and lactic monomers (Ulery et al. 2011). Biodegradable polymers that are hydrolytically unstable might be degraded due to the presence of moisture in storage, during or after production of the material. In order to minimize this, polymers are usually kept in a refrigerator. Biodegradable polymers can be sterilized by gamma rays or an electronic beam, or they can be exposed to ethylene oxide (EtO) (Bernkopf 2007).

3.2.2 Biodegradable Metals

The traditional approach to metal biomaterials imposed a strict rule of high anticorrosion properties in bodily fluids. Recently, new classes of biodegradable metal have been developed precisely through the use of corrosive material properties. Biodegradable metals are expected to corrode gradually in vivo, with an appropriate host response to the corrosion products, and then, to disappear completely after assisting in the tissue healing process. Accordingly, the main component of biodegradable metal alloys should be elements metabolized by the body that exhibit suitable degradation phases within the bodily fluids (Hermawan 2012). New implant materials based on biodegradable metals, such as magnesium (Mg) and iron (Fe), have been studied for gradual disappearance within a controlled time frame. This is mainly associated with bone tissue replacements, used to provide mechanical support through the healing process due to their significantly superior mechanical properties in comparison with polymers. It is especially important for children and young patients who would be saved from repeated surgeries to remove implants such as bone fixtures. Also, besides bone replacements, biodegradable metals represent prospective materials for biomedical application related to blood vessels, such as different types of stent (Li et al. 2014a, b).

Mg-based (pure Mg, Mg–Ca alloys, Mg–Zn alloys) and Fe-based (pure Fe, Fe–Mn alloys) materials are two basic types of biodegradable metal. Both Mg and Fe are present within the human body and both are essential for human metabolism. Corrosion products are non-toxic and can be easily eliminated. Several studies have indicated that Mg can have a stimulating effect on bone growth (Brar et al. 2009; Gu and Zheng 2010). A comparison of their properties with medical grade stainless steel is given in Table 13.

However, even with all the positive properties, the degradation rate for both of them is not yet adequate. The degradation rate needs to be further reduced for

Table 13 Comparative mechanical properties of biodegradable metals Fe, Mg and stainless steel

Metals	Main alloying composition, wt%	Density, g/cm^3	Young's modulus, GPa	Yield strength, MPa	Ultimate tensile strength, MPa	Elongation, %
Stanless steel: 316L type (annealed) (ASTM, 2003)	Fe; 16–18.5Cr; 10–14Ni; 2–3Mo; <2Mn; <1Si; <0.003C	8.0	193	190	490	40
Degradable metals: pure iron (annealed-550°)	99.8 Fe	7.87	210	120–150	180–210	22–28
Degradable metals: Magnesium (annealed) (ASM 2005)	99.98 Mg	1.74	45	80	150	3

Mg-based alloys and increased for Fe-based alloys so as to fit into the projected healing time, depending on the type of implant. The ideal degradation rate would be somewhere in between pure magnesium and iron (Zheng et al. 2014). Naturally, the first attempts to design a new biodegradable alloy with a controlled corrosion rate were tried through alloying element variations. Selection of alloying elements in order to change the corrosion rate has been attempted according to their standard electrode potential. The following elements have a standard electrode potential between Fe and Mg: Ga, Ta, Cr, Zn, Nb, V, Mn, Zr, Ti, Al and Be. Among these, some are not suitable for biomedical applications due to their toxicity, such as: Ga, V, Al, Cr. Others (Ta, Nb, Ti, Zr) are corrosion-resistant and considered bioinert, due to the formation of the thin passive layer on their surfaces. This leaves Zn and Mn as widely investigated elements for Fe- and Mg-based biodegradable materials. The order of corrosion rate is (from highest to lowest): Mg > Fe > Zn > Mn. Corrosion and degradation rates can be influenced by the selection of alloying elements, but it can also be adjusted through the microstructure, production technologies, or surface treatments (Cheng et al. 2013). This area is one of the novel research fields in bioengineering.

3.3 Scaffolds

Scaffolds are essential in bone tissue regeneration. Scaffolds are carriers that serve as a basis for cellular interactions and the formation of the bone's extracellular matrix with the purpose of securing structural support for the newly-formed tissue.

One of the most common methods used in tissue engineering includes the isolation of specific cells from patients using a biopsy and their culturing on a three-dimensional scaffold in a controlled environment. After that, the formed scaffold is implanted into the desired site within the body to grow the new tissue inside the scaffold, which is degraded after a specific amount of time. A different, alternative approach includes the direct implantation of a scaffold in vivo in order to stimulate direct tissue formation in situ. The advantage of the latter approach lies in the decreased number of necessary operations, which shortens the time required for the patient's recovery. Scaffolding materials used for bone regeneration must meet certain requirements, including mechanical properties similar to the tissue in the implantation zone, besides the obligatory biocompatibility and biodegradability, which corresponds to the remodeling time.

The main purpose of a scaffold is to form a new tissue within it, along with the process of its substitution by the surrounding living tissue. Scaffolds may also serve as cytokine carriers, such as bone morphogenetic proteins, insulin-like growth factors and transformational growth factors, which change renewed precursor cells from the host tissue into cells that create the bone matrix, thus securing osteoinductivity (Spector 2006). The process of osteogenesis is initiated before implantation by embedding the cells into the scaffold, which will form new ossification centers, such as osteoblastic and mesenchymal cells that possess the potential to memorize the origin. Genetically transformed cells that exhibit osteoconstructive properties may also be used for this purpose. The combination of scaffolds, cytokines and cells with the purpose of creating an ex vivo tissue construction presents the hypothesis that should secure a more effective bone regeneration under in vivo conditions, compared to the biomaterial matrix itself. Additionally, the improved tissue growth, similar to the bone tissue growth under in vitro conditions, offers new possibility for monitoring the disease's progression.

Scaffolds, whose role is to improve the osteogenesis process, should have a morphology that is similar to the morphology of the bone, so that integration with the surrounding tissue can be optimized. The complexity of the structure and the differences among the properties of the bone tissue (for instance, porosity, the size of the pores and the cellular type), as well as the differences related to the aging process, the nutrition, the activity (mechanical load) and the health condition of every individual, represent a major challenge in the production of scaffolds and the engineering of bone tissue. Scaffold properties mainly depend on the nature of the material and the fabrication process. The advantages and disadvantages of the materials used for scaffold fabrication (metals and their alloys, ceramics, glass, chemically synthesized polymers, natural polymers, and their composites) are the focus of the research conducted by many scientists (Barrere et al. 2008). The properties and requirements of the scaffolding materials in the engineering of bone tissues can be related to different aspects, such as: the degradation process, mechanical characteristics, delivery of the cytokines, or proliferation of the scaffold by various cell cultures (Mallick et al. 2015).

Porosity is one of the major requirements, because the presence of pores is a necessary condition for enabling cell proliferation (osteoblastic and mesenchymal

cells for bone tissue) and new tissue growth, as well as vascularization. Additionally, the porous surface enhances the mechanical attachment between the implanted biomaterial and the surrounding (living) tissue, thus securing mechanical stability in critical zones. The most commonly used technologies for fabrication of porosity within biomaterials include salt secretion, gas formation, phase separation, freeze-drying and sintering, depending on the material of the scaffold. It is elaborated that the smallest pore size for enabling regeneration of the mineralized bone is around 100 μm, while larger pores (100–200 μm) exhibit considerable bone ingrowth, and smaller pores (75–100 μm) result in the ingrowth of the non-mineralized osteoid tissue. Smaller pores (10–44 and 44–75 μm) only enable the penetration of the fibrous tissue. These results are in accordance with the functional unit of a compact bone—a normal Haversian system with a diameter of approximately 100–200 μm.

The most commonly used materials for scaffolds are natural or artificial polymers, such as: polysaccharides, poly(a-hydroxy esters), hydrogels and thermoplastic elastomers. The second important group is bioactive ceramics, such as: calcium phosphate and bioactive glass or glass-ceramics. The third group includes metallic biodegradable materials, such as Mg and Fe, but this is still in early development. At the moment, significant attention is being given to the development of composites based on polymers and ceramics aimed at improving mechanical properties and interactions with the surrounding tissue. Also, a lot of effort is being put into the development of scaffolds with the capability for controlled drug release. These scaffolds may release growth factors or antibiotics locally, and thus improve bone healing in the area of the defect, as well as facilitate faster wound healing (Schieker et al. 2006). Scaffolding materials must address numerous demands, starting with the biological requirements of biocompatibility, low cytotoxicity and minimal provocation of inflammatory processes (O'Brien 2011). Also, different physico-chemical requirements are imposed, such as: a high specific surface for the adhesion of cells; adequate mechanical properties, porosity, size and shape of the pores, etc. (Bose et al. 2012).

There are two types of biodegradable polymer used for scaffolds: natural and synthetic ones. The natural materials include polysaccharides (starch, alginate, chitin/chitosan, hyaluronic acid derivatives) and proteins (soy, collagen, fibrin gel, silk), and various types of biofibers, such as the natural fibers of lignocellulose, used as strengthening materials. Synthetic polymers can be obtained under controlled conditions, which enable predictable and reproducible mechanical and physical properties, such as hardness, the elastic modulus and the degradation rate. Another advantage is the control of impurities in the material. Also, the possible risk of toxicity, immunoresponse and infection are considerably decreased in pure polymers, which are built from monomeric units with a simpler structure. The most commonly used biodegradable synthetic polymers for the fabrication of scaffolds are: bulk-eroding polymers—PGA, PLGA, PLLA, PDLLA, PPF, PCL, LPLA, DLPLG and surface-eroding polymers—polyanhydrides, polyorthoesters and polyphosphazenes (Shoichet 2010; Dhandayuthapani et al. 2011).

The ceramic scaffolds used with the aim of improving the process of osteogenesis are mostly based on hydroxyapatite, the basic building block of bone tissue. Other types of ceramic include porous calcium-metaphosphate ([Ca(PO3)2]n) ceramics, natural corals, porous biphasic ceramics (hydroxyapatite/calcium phosphate), etc. The most commonly used fabrication technology is based on the high-temperature sintering of ceramic compacts. In general, ceramic biomaterials exhibit the ability to form carbonate hydroxyapatite on the surface, similar to that which exists in bones, thus improving osseointegration. Also, it has been proven that these materials exhibit the ability to bind concentrated cytokines in the same way that a natural bone does. Brittleness and slow degradation are the main disadvantages of these materials (Hutmacher et al. 2007).

Porous spongy scaffolds based on biodegradable glass may also be used. The macroporous structure of such spongy scaffolds is very similar to the structure of the spongious bone with an open porosity. Bioactive glass fabricated through the sol-gel technique has a nanoporosity that controls the degradation rate, which makes it similar to the microstructure of the cancellous bone. Scaffolds based on bioactive glass, with optimized nanoporosity, are pressure-resistant, but they have low ductility. The ideal scaffold should have all the glass properties and increased ductility. Such materials can only be obtained by using nanocomposite materials (Ducheyne and Qui 1999). The distinctive properties of metal materials are hardness and ductility, the main factors that make them attractive for hard tissue scaffolds. Mg- and Fe-based alloys, such as Mg-RE (rare earth), Mg–Ca, pure Fe and Fe–Mn, have found an application in scaffolds for hard tissues (Alvarez and Nakajima 2009; Yusop et al. 2012).

The development of composite scaffolding materials has begun in recent years. Composites enable the advantages of polymers, and by including a controlled amount of a bioactive ceramic phase, it is possible to increase mechanical hardness (Antonio et al. 2010). At the same time, poor bioactivity of most polymers can be neutralized by including bioactive compounds or by applying bioactive coatings based on the polymer. The degree of bioactivity can be controlled by the volume of the fraction, the size, shape and the distribution of the inclusions. The addition of a bioactive phase into a bioresorbable polymer may even lead to a change in the degradation of the polymer. Inclusions of bioactive glass modify the surface and volume properties of composite scaffolds by increasing hydrophilic ability and absorption of a polymer matrix, thus changing the speed of degradation. Ideally, the kinetics of degradation and the resorption of composite scaffolds should be such that cells can proliferate and secrete an extracellular matrix, while the scaffold gradually disappears, leaving space for the new cells to spread and tissue to grow. It is necessary to keep the 3D scaffold structure until the newly formed tissue obtains sufficient mechanical properties to exist independently (Wang 2006).

3.4 Smart Biomaterials

The term "smart" refers to those materials that have a certain response to their surrounding conditions or external inputs, in general (temperature, mechanical strain, chemical action, electric or magnetic field, light, and so on), and thus change their microstructure and properties (Schwartz 2002).

Ferroelectric (FE) and ferromagnetic (FM) materials, together with Shape Memory Alloys (SMA), exhibit phase transformations under low temperatures related to the changes in volume and shape. Deformation is initiated but also limited by the distortion of the crystal structure during the decrease in volume within the magnetic field (FM materials), or the decrease in volume within the electric field (FE materials) or by the crystallographic shear (SMA). These effects limit the level of shape changes (Harvey 2006). The development of SMA started with alloys such as Ni–Ti, and ternary alloys based on Cu were later discovered: Cu–Al–Ni, Cu–Zn–Al and Cu–Al–Be, and several iron-based alloys. Their important physical and mechanical properties are given in Table 14.

The behavior of SMA is defined by three possible shape memory effects (Machado and Savi 2003; Jani et al. 2014):

- a one-way effect (pseudoplasticity), in which apparent relatively large plastic deformation occurs under loading. Since the deformation is the effect of the martensite structure, further heating initiates a reversal of the change and the deformation disappears;
- a two-way effect, in which the deformation is a consequence of a change in temperature, but the alloy must be "trained" prior to that;
- pseudoelasticity, in which the material, under the constant loading, is significantly deformed due to the influence of the structural transformation initiated by said loading. The deformation completely disappears after unloading.

The application of biomedical smart materials can be divided into three categories (Machado and Savi 2003; Jani et al. 2014):

Table 14 Physical and mechanical properties of metal shape memory alloys

Properties	NiTi	CuAlNi	CuZnAl
Melting temperature, °C	1240–1310	1000–1050	950–1020
Density, g/cm^3	6.45	7.12	7.64
Young's modulus, GPa	28–40	70–100	80–100
Yield strength, MPa	70–140	130	80
Tensile strength, MPa	754–960	500–800	600
Poisson's ratio	0.33		
Transformation-temperature range, °C	−50 to 110	−140 to 100	−180 to 200
Corrosion resistance	Excellent	Average	Good
Biocompatibility	Excellent	Poor	Poor

- implants and stents, such as bones, plates and needles, for which suitable biocompatibility is necessary, because they are implanted into the body for a longer period of time.
- surgical and dental instruments, such as orthodontic fixtures and biopsy clamps —they need to have excellent mechanical properties along with biocompatibility.
- devices and instruments for medical examinations (e.g., ultrasound).

Among smart materials, *Ti-Ni smart alloys* that memorize shape have been the most studied and used in biomedical applications, for both implants and instruments, mainly because of their good biocompatibility and mechanical properties. The most famous NiTi-alloy (or TiNi) is *Nitinol* (approximately the same percentage of Ti and Ni); it is single-phase, and has a direct conversion of heat to mechanical energy, low material fatigue and low increase in bending flexibility due to temperature increase. The shape memory effect is generally related to the transformation of the martensite phase, which is thermoelastic. It is still necessary to completely understand the mechanical and thermal behavior related to the transformation of the martensite phase in order to develop better implants (Jani et al. 2014).

Biocompatibility is the most significant property. Others include super-elasticity, shape memory, hysteresis and high fatigue strength. For the NiTi alloy, it is known that titanium is biocompatible, with long-lasting corrosion resistance. Unlike Ti, Ni ions are released from the implant's surface and can cause allergic and inflammatory reactions above a certain concentration. It is established that NiTi alloys have exceptional corrosion resistance due to the formation of a passive TiO_2 oxide surface film. This oxide film increases the stability of the surface layer by protecting the harder material from corrosion, and it creates a physical and chemical barrier to further oxidization of Ni and diffusion of Ni ions. The formed oxide film, however, can be damaged due to wear, corrosion or fatigue when repassivation occurs, during which the damaged film is regenerated. The integrity of the protective titanium oxide film is affected by surface roughness, inhomogeneities, wear products, porosity, and geometry. Different surface modifications can decrease the amount of Ni ions released down to a negligible amount (Machado and Savi 2003).

Nitinol has excellent ductility and can be produced in the shape of wires, straps, pipes, sheets, or bars, thus providing a wide range of possibilities for application in medicine (Schuessler and Piper 2004). It is suitable for invasive surgical methods, but also for treatment of the younger population, especially children with inherent diseases.

In general, SMA implants surpass conventional orthopedic implants and are well suited for the fixation of different fractures. Their first application was for plates and fixtures to connect broken bone fragments. Nowadays, that application is even wider, moving into other areas as well. Bones and Nitinol have similar stress-strain behavior, thus making Nitinol almost the ideal material for bone plates and fixtures, intramedullary nails, bars for spinal corrections and other implants for treatment of

fractures (Schwartz 2002; Machado and Savi 2003; Bahraminasab and Sahari 2013; Pelton et al. 1999).

Besides metal SMAs, networks of shape memory polymers (SMP), in which the shape memory effect is realized through the formation of an extended network of molecular chains, are being increasingly studied today. Their most common application is in drug delivery, but also in surgical sutures and stents. For example, ethylene-vinyl acetate (EVA) is a copolymer of ethylene and vinyl acetate, which is soft and flexible. It is an ideal material for slow drug release over time. Polylactide (PLA) is one of the most popular biodegradable polymers in biomedicine today. EVA and PLA can exhibit an excellent memory effect. The application of such biodegradable shape memory polymers can eliminate the need for additional surgery to remove the implant after the healing is finished (Ratner et al. 2012; Jaros et al. 2010; Furth et al. 2007).

4 Case Study of Material Selection for the Femoral Component of an Artificial Hip Prosthesis

In the field of orthopedics, which deals with skeletal disorders, such as injuries or diseases in bones, joints and the spinal system, metals (titanium alloys, stainless steel alloys and cobalt-based superalloys), ceramics, polymers and composite materials have a wide application in the stabilization of injuries of supporting tissues or as a substitute for bone tissue. Implants, which are often used in orthopedic surgery, include joint prostheses (total prostheses of hip, knee, shoulder and elbow), components for the fixation of fractures (plates, screws, fixtures) and components for the fixation of the spinal column (Yaszemski et al. 2004). While the implantation of implants is relatively simple from a mechanical point of view, biocompatibility can be an issue, since implants can provoke unwanted tissue responses. The designs of joint prostheses and their materials have been considerably improved within the last decade, but there are still some unresolved issues, especially related to the life of the implant, and research in this area is extremely important. For example, in the case of a total hip prosthesis, several materials are usually used for its fabrication (metals, ceramics, polymers) in order to obtain optimal characteristics and a long life cycle.

The material selection for the femoral hip stem (Fig. 7) is analyzed here, to show that a number of different materials can be considered, with higher or lower life cycles and costs. The hip joint ("plain bearing") is not analyzed here, because it is mostly made of polyethylene of high density (UHMWPE) or ceramics to obtain the lowest possible friction coefficient.

For proper material selection, it is necessary to know the bone structure and properties. Bone is a living tissue comprised of inorganic matter, which contains crystals that make the bone fragile, and organic, gelatinous matter, which makes the bone ductile enough. If compared to metals and composites, the mechanical

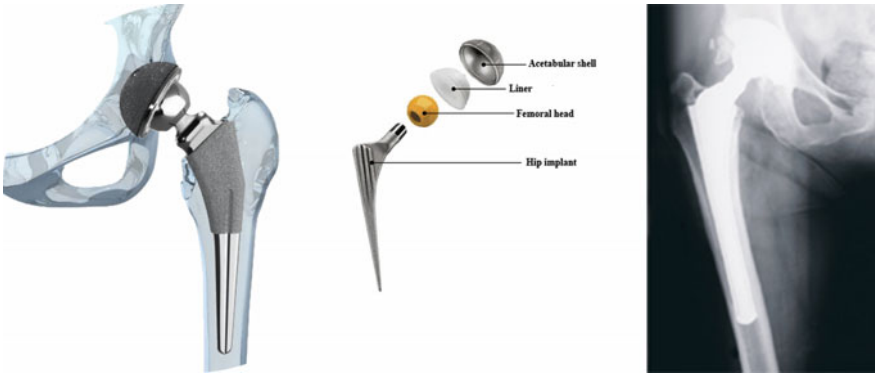

Fig. 7 Components of an artificial hip prosthesis made from different materials and an RTG scan of the implanted prosthesis (Zimmer Biomet). Reprinted by permission of Zimmer Biomet. "Other than providing permission to use the Zimmer Biomet picture(s), this publication is not financially supported by Zimmer Biomet. Zimmer Biomet is the owner of the copyrights and all other intellectual property rights in relation to the picture(s) used"

properties of bone are significantly lower. But a healthy bone can heal itself and has an excellent resistance to external variable loads. This is the main reason why prosthesis material should have stronger mechanical resistance, since its life is unquestionably limited, without the possibility of regenerating in the case of traditional materials (Sinha 2002). For this very short general analysis, the stress and strains from external loads (during sitting or walking) are not defined.

4.1 Analysis of the Material Requirements in Case of a Hip Prosthesis

The basic material requirements in the case of a hip prosthesis are (Teoh 2004; Farag 1989; Adamovic et al. 2009; Ristic et al. 2010; Bahraminasab and Jahan 2011):

1. *Tissue acceptance (TA)* is a very basic requirement, related to the risk of implant rejection. The grades of the material vary from 1, being the worst, to 10, being the best. The acceptable limit is 7.
2. *Corrosion resistance (CR)* is a very important requirement, since bodily fluids are saline water solutions, making for a very aggressive environment for the implant material. Corrosion is detrimental, because it can lead to fracture, especially for varying load. Grades vary from 1 to 10, and the materials with a grad >7 are suitable.
3. *Fracture toughness (KIC)*
   Numerical analysis of implant components has long been based on the yield stress and safety coefficient. And even with lower stresses during functioning

than those allowed, fractures occurred suddenly in some cases. Fracture appears due to the development of initial cracks at sites of inclusion and other discontinuities, and metals with high yield stress and high strength are especially sensitive. Consequently, the critical stress intensity factor was introduced as an important parameter for this material class, which refers to the resistance of material to crack development. The acceptable lower limit is K_{Ic} = 40 MPam$^{1/2}$

4. *Tensile strength (Rm)*
   Based on the load analysis, the material tensile strength should be Rm > 95 MPa.
5. *Fatigue Strength (Rd)*
   Loading frequency is in the range of 1–2.5 × 10^6 cycles per year, depending on the physical activity of the person. The loading of the hip is around 2.5–3 times that of the body weight, and calculations indicate variable loading around 3.1 MPa. With the ratio of Rd/Rm = 0.35, the lower limit of fatigue strength is Rd = 33 MPa.
6. *Wear resistance* (*WR*)
   In order for the implant to have a longer life, the best possible wear resistance is required, especially resistance to adhesive and abrasive wear, and materials with a grade >7 are acceptable.
7. *Elastic modulus* (*E*)
   Compatibility of elastic modulus between the implant and bone tissue is required and desired, in order to prevent stress shielding and gradual separation of the prosthesis from the bone due to a mismatch of these values. Unfortunately, the elastic modulus of all substituting materials so far has proven higher than the elastic modulus of bone. Ongoing research is aimed at obtaining strong materials with elastic modulus around 17 kN/mm^2.
8. *Density* (*R*)
   Implant and bone should have a similar density, which is also the subject of research nowadays. The ideal value is around 1.8 g/cm^3.
9. *Costs* (*C*)
   In general, cost includes material price, and costs of production and final treatment. Serial production does not yet exist, and costs of production and final treatment are more significant in total costs. Usually, the upper limit of this property is related to application of the most expensive materials, which is 60 GBP/kg.

In practice, the most widely applied materials for fabrication of hip prostheses are stainless steel alloys, Ti alloys and Co–Cr-based alloys.

Quantitative comparison of material properties has been carried out by using the limit values method, according to the values of M indicators for each material (Farag 1989; Filetin 2000; Adamovic et al. 2009; Ristic et al. 2010), as per the following equation:

$$M = \left[\sum_{i=1}^{n_l} B_i \frac{Y_i}{X_i}\right]_l + \left[\sum_{j=1}^{n_u} B_j \frac{Y_j}{X_j}\right]_u + \left[\sum_{k=1}^{n_a} B_k \left|\left(\frac{Y_k}{X_k}\right) - 1\right|\right]_a \rightarrow \min$$

where l, u and a refer to the lower, upper and optimal values of the considered property, respectively:

n_l, n_u, n_a refer to the number of lower, upper and optimal values;
B_i, B_j, B_k are importance factors for the lower, upper and optimal values;
X_i, X_j, X_k are the specific lower, upper and optimal values;
Y_i, Y_j, Y_k are the determined lower, upper and optimal limits.

The concept of this method is the mapping of the requirements towards the limit values of t he material properties, defined as:

1. lower limit values of the properties;
2. upper limit values of the properties;
3. optimal values of the properties.

Whether a certain property will be defined as lower or upper limit (minimum or maximum) depends on the application. For example, if resistant and light material is required, the lower limit is set for the hardness and the upper limit for the density. In this way, all unsuitable materials are eliminated from selection if any of the observed properties is outside of the setup limits. In general, this method of limit values is usually used for optimization of the selection process for materials and production technologies with a rather high number of possible options (Adamovic et al. 2009; Ristic et al. 2010; Filetin 2000; Black and Hastings 1998; Geetha et al. 2009; Ashby and Cebon 2005; Kutz 2002). Without going into detail, and just for the sake of the overview of this selection process, one practical case of calculated and empirically obtained values is presented in Table 15 (optimal values of properties and importance factors) and Table 16 (real properties of several candidate materials and the corresponding evaluation-grading).

Table 15 Required property limits and importance factors in the case of metal hip implant material

Property	Limit	Importance factor
Tissue acceptance (TA)	Lower Yi = 7	0.2222
Corrosion resistance (CR)	Lower Yi = 7	0.1944
Fracture toughness (KIC)	Lower Yi = 40 $MPam^{1/2}$	0.0833
Fatigue strength (Rd)	Lower Yi = 33.25 MPa	0.1389
Tensile strength (Rm)	Lower Yi = 95 MPa	0.0833
Wear resistance (WR)	Lower Yi = 7	0.0833
Elastic modulus (E)	Aimed Yk = 17 MPa	0.0833
Density (R)	Aimed Yk = 2100 kg/m^3	0.0556
Costs (C)	Upper Yj = 60 GBP/kg	0.0556

Table 16 Several candidate materials and their properties in the case of a hip prosthesis and their gradings in comparison to bone tissue

Type of material Standard–chemical composition	TA	CR	Rm, MPa	Rd, MPa	E, GPa	KIC, $MPam^{1/2}$	WR	R, g/cm^3	C, GBP/kg	M	Grade
AISI 316L (EN X2 CrNiMo 17 13 2) Fe/<0.03C/16–18.5Cr/10–14Ni/2–3Mo/<2Mn/<1Si/<0.045P/<0.03S	8	7	550	270	198	195	8	7.87	2.8	0.617	**5**
AISI 317 (EN X2 CrNiMo 18 12 3) Fe/<0.08C/17.5–20Cr/11–15Ni/3–4Mo/<2Mn/<1Si/<0.045P/<0.03S	8	7	570	290	193	170	8.5	7.97	3.2	0.633	**8**
AISI 321 (EN X10 CrNiTi 18 10) Fe/<0.08C/17–19Cr/9–12Ni/<2Mn/<1Si/0.3–0.7Ti/<0.045P/<0.03S	8	7	600	265	197	180	8	7.95	2.4	0.632	**7**
SAE A 286 (DIN X4 NiCrTi 25 15) 54Fe/26Ni/15Cr/2Ti/1.3Mo/1.3Mn/0.5Si/0.2Al/0.05C	8	8	1100	370	201	55	9	7.92	2.3	0.631	**6**
SAE 17-4 PH (EN X5 CrNiCuNb 17 4) Fe/<0.07C/15.5–17.5Cr/3–5Ni/3–5Cu/.15–0.45Nb + Ta/<1Mn/<1Si/<0.04P/<0.03S	8	8	1300	450	202	50	9	7.82	2.3	0.633	**9**
Co–Cr–Mo (ISO 5832/4) cast 45–65Co/20–30Cr + other elem., e.g. Fe,Mn,Nb,Ni,Ta,W	9	9	700	350	225	135	10	8.6	22	0.572	**2**
Co–Cr–Ni–W forged 40–70Co/19–32Cr + other elem, e.g. Fe,Mn,Nb,Ta,W	9	9	1070	490	230	135	10	8.6	35	0.577	**3**
Unalloyed Ti—forged 99Ti + other elem.	10	10	620	380	112	50	7	4.53	20	0.590	**4**
Ti6Al4V 90Ti/6Al/4V	10	10	1020	625	114	90	7.5	4.42	20	0.544	**1**
Epoxy resin + 70% Carbon fiber	7	7	580	170	46	45	7	1.55	60	0.736	**10**
Bone	–	–	130	–	17	12	–	1.8	–	–	–

Based on the values of the M indicator in Table 16, titanium alloy has a slight advantage over cast and forged cobalt alloys and unalloyed titanium. Among steel alloys, the best candidates are austenitic AISI 316L stainless steel and SAE A286 steel. If corrosion resistance was given a lower importance, and costs a higher importance, then common austenitic stainless steel alloys would be recommended.

Acknowledgements This work has been supported by research grants from the Ministry of Science and Technological Development, Serbia, project no. TR 32036 and TR 35021, for a period 2011–2017.

References

Afzal A (2014) Implantable zirconia bioceramics for bone repair and replacement: a chronological review. Mater Express 4(1):1–12

Adamovic D et al (2009) A choice of materials for implants. In: Proceedings of the 33rd international conference on mechanical production in serbia (in Serbian), Belgrade, June 2009. Faculty of Mechanical Engineering Belgrade, Belgrade, pp 51–60

Alvarez K, Nakajima H (2009) Metallic scaffolds for bone regeneration. Materials 2(3):790–832

An YH, Draughn RA (eds) (2000) Mechanical testing of bone and the bone-implant interface. CRC Press, New York

Antonio G, Roberto DS, Luigi A (2010) Polymer-based composite scaffolds for tissue engineering. J Appl Biomater Biomech 8(2):57–67

Ashby MF, Cebon D (2005) Materials selection in mechanical design, 3rd edn. Butterworth-Heinemann, London

Ashby MF, Tianjian LU (2003) Metal foams: A survey. Sci Chin 46(6):521–532

Ashby MF, Evans AG, Fleck NA (2000) Metal foams: a design guide. Butterworth-Heinemann, London

Avérous L, Pollet E (2012) Biodegradable polymers (chapter 2). In: Avérous L, Pollet E (eds) Environmental silicate nano-biocomposites. Springer-Verlag, London, London, pp 13–39

Aza PN, Aza AH, Aza S (2005) Crystalline bioceramic materials. Bol Soc Esp Ceram Vidrio 44 (3):135–145

Bahraminasab M, Jahan A (2011) Material selection for femoral component of total knee replacement using comprehensive VIKOR. Mater Des 32(8–9):4471–4477

Bahraminasab M, Sahari BB (2013) Shape memory alloys, promising materials in orthopedic applications (chapter 10). In: Fernandes FMB (ed) Shape memory alloys—processing, characterization and applications. InTech, Rijeka, pp 261–278

Bakan HI, Korkmaz K (2015) Synthesis and properties of metal matrix composite foams based on austenitic stainless steels–titanium carbonitrides. Mater Des 83:154–158

Barrere F, Mahmood TA, Groot K et al (2008) Advanced biomaterials for skeletal tissue regeneration: instructive and smart functions. Mater Sci Eng 59:38–71

Ben-Nissan B, Pezzotti G (2002) Bioceramics processing routes and mechanical evaluation—review. J Ceram Soc Jpn 110:601–608

Bernkopf M (2007) Sterilisation of bioresorbable polymer implants medical device technology. PubMed 18(3):26–28

Billote WG (2006) Ceramic biomaterials. In: Bronzino JD, Peterson DR (eds) Biomedical Engineering Fundamentals. CRC Press, Boca Raton

Black J, Hastings G (eds) (1998) Handbook of biomaterial properties. CHAPMAN & HAIL, London

Bohner M (2010) Resorbable biomaterials as bone graft substitutes. Mater Today 13(1–2):24–30

Bombac D, Brojan M, Fajfar P et al (2007) Review of materials in medical applications. RMZ. Mater Geoenvironment 54(4):471–499
Bose S, Roy M, Bandyopadhyay A (2012) Recent advances in bone tissue engineering scaffolds. Trends Biotechnol 30(10):546–554
Brar HS, Platt MO, Sarntinoranont M et al (2009) Magnesium as a biodegradable and bioabsorbable material for medical implants. JOM 61(9):31–34
Brkic S (2013) The application of polymer composites in surgery. Polymers 34:1 (in Croatian)
Bronzino J (ed) (2000) The biomedical engineering handbook. Boca Raton, Florida
Carter CB, Norton MG (2007) Ceramic materials science and engineering. Springer Science-Business Media, New York
Chen Q, Zhu C, Thouas GA (2012) Progress and challenges in biomaterials used for bone tissue engineering: bioactive glasses and elastomeric composites. Prog Biomater 1(2):1–22
Cheng J, Liu B, Wu YH et al (2013) Comparative in vitro study on pure metals (Fe, Mn, Mg, Zn and W) as biodegradable metals. J Mater Sci Technol 29(7):619–627
Chevalier J, Gremillard L (2008) Ceramics for medical applications: a picture for the next 20 years. J Eur Ceram Soc 29(7):1245–1255
Chu PK, Liu X (eds) (2008) Biomaterials fabrication and processing handbook. CRC PRESS, Taylor & Francis Group, New York
Davis JR (ed) (2012) Handbook of materials for medical devices. ASM International, Ohio
Davis HE, Leach JK (2008) Hybrid and composite biomaterials in tissue engineering (chapter 10). In: Ashammakhi N (ed) Topics in multifunctional biomaterials and devices, ebook. Tampere University of Technology, Tampere, pp 1–25
de Viteri VS, Fuentes E (2013) Titanium and titanium alloys as biomaterials (chapter 5). In: Gegner J (ed) Tribology—fundamentals and advancements. InTech, Rijeka, p 1
Dhandayuthapani B, Yoshida Y, Maekawa T et al (2011) Polymeric scaffolds in tissue engineering application: a review. Int J Polym Sci 290602:1–19
Disegi JA, Eschbach L (2000) Stainless steel in bone surgery. Injury 31(4):D2–D6
Dorozhkin SV (2010) Calcium orthophosphates as bioceramics: state of the art—review. J Funct Biomater 1:22–107
Ducheyne P, Qiu Q (1999) Bioactive ceramics: the efect of surface reactivity on bone formation and bone cell function. Biomaterials 20(23–24):2287–2303
Eid Y (2013) The myths of trabecular metal: 'The next best thing to bone'. Egypt Orthoped J 48 (4):327–329
Fambri L, Migliaresi C, Kesenci K et al (2002) Biodegradable polymers (chapter 4). In: Barbucci R (ed) Integrated biomaterials science. Kluwer Academic/Plenum Publishers, New York, pp 119–170
Farag MM (1989) Selection of materials and manufacturing processes for engineering design. Prentice Hall, London
Fellah M, Assala O, Labaïz M et al (2014) Friction and wear behavior of Ti-6Al-7Nb biomaterial alloy. J Biomater Nanobiotechnol 4:374–384
Filetin T (2000) Materials selection for the construction. Faculty of Mechanical Engineering and Naval Arehitecture, Zagreb (in Croatian)
Fragassa C, Radovic N, Pavlovic A et al (2016) Comparison of mechanical properties in compacted and spheroidal graphite irons. Tribol Ind 38(1):49–59
Freese H, Volas MG, Wood JR (2001) Metallurgy and fabrication; surface and technological properties (chapter 2). In: Brunette DM, Tengvall P, Textor M et al (eds) Titanium in medicine. Springer, Berlin, pp 25–51
Furth ME, Atala A, Van Dyke ME (2007) Smart biomaterials design for tissue engineering and regenerative medicine. Biomaterials 28(34):5068–5073
Geetha M, Singh AK, Asokamani R et al (2009) Ti based biomaterials, the ultimate choice for orthopaedic implants—a review. Prog Mater Sci 54(3):397–425
Geetha M, Durgalakshmi D, Asokamani R (2010) Biomedical implants: corrosion and its prevention. Recent patents on corrosion science, vol 2. pp 40–54

Ghanbarzadeh B, Almasi H (2013) Biodegradable polymers (chapter 6). In: Chamy R (ed) Biodegradation—life of science. InTech, Rijeka, pp 141–185
Ginebra MP, Gil F, Planell J (2002) Acrylic bone cements (chapter 20). In: Barbucci R (ed) Integrated biomaterials science. Kluwer Academic/Plenum Publishers, New York, pp 569–584
Green S (2012) Compounds and composite materials (chapter 3). In: Kurtz S (ed) PEEK biomaterials handbook. William Andrew Publishing, London, pp 23–49
Gu X, Zheng Y (2010) A review on magnesium alloys as biodegradable materials. Front Mater Sci Chin 4(2):111–115
Gunatillake PA, Adhikari R (2003) Biodegradable synthetic polymers for tissue engineering. Eur Calls Mater 5:1–16
Hamadouche M, Sedel L (2000) Ceramics in orthopaedics—review. J Bone Joint Surg 82 (8):1095–1099
Harvey JA (2006) Smart materials (chapter 11). In: Kutz M (ed) Mechanical engineers' handbook: materials and mechanical design. Wiley, Hoboken, pp 418–432
He W, Benson R (2011) Polymeric biomaterials (chapter 4). In: Kutz M (ed) Applied plastics engineering handbook—processing and materials. Elsevier, London, pp 143–193
He W, Benson R (2014) Polymeric biomaterials (chapter 4). In: Modjarrad K, Ebnesajjad S (eds) Handbook of polymer applications in medicine and medical devices. Elsevier, London, pp 55–69
Heimann RB (2002) Materials science of crystalline bioceramics: a review of basic properties and applications. CMU J 1(1):23–46
Helmus MN (2002) Biomaterials in the design and reliability of medical devices. Springer, Washington
Hench LL (1991) Bioceramics: from concept to clinic. J Am Ceram Soc 74(7):1487–1510
Heness G, Ben-Nissan B (2004) Innovative bioceramics. Mater Forum 27:104–114
Hermawan H (2012) Biodegradable metals. Springer, Heidelberg, New York
Hryniewicz T, Rokosz K, Filippi M (2009) Biomaterial studies on AISI 316L stainless steel after magnetoelectropolishing. Materials 2(1):129–145
Hutmacher DW, Schantz JT, Lam CXH et al (2007) State of the art and future directions of scaffold-based bone engineering from a biomaterials perspective. J Tissue Eng Regenerative Med 1(4):245–260
Hyseni A, De Paola S, Minak G et al (2013) Mechanical characterization of ecocomposites. In: Proceedings of 30th Danubia Adria symposium, symposium on advances in experimental mechanics, DAS 30, Code 125164:175–176. Primošten, Croatia, 25–28 Sept 2013
Iftekhar A (2009) Biomedical composites (chapter 14). In: Kurtz M (ed) Biomedical engineering and design handbook, vol 1. McGraw-Hill Professional, New York
Ignjatovic N, Uskokovic D (2008) Biodegradable composites based on nanocrystalline calcium phosphate and bioresorbable polymers. Adv Appl Ceram 107(3):142–147
Jani JM, Leary M, Subic A et al (2014) A review of shape memory alloy research, applications and opportunities. Mater Des 56:1078–1113
Jaros A, Smola A, Kasperczyk J et al (2010) Biodegradable shape memory polymers for medical purposes. CHEMIK 64(2):87–96
Kennedy A (2012) Porous metals and metal foams made from powders (chapter 2). In: Kondoh K (ed) Powder metallurgy. InTech, Rijeka, pp 31–46
Kim HM (2003) Ceramic bioactivity and related biomimetic strategy. Curr Opin Solid State Mater Sci 7(4–5):289–299
Krajewski A, Ravaglioli A (2002) Bioceramics and biological glasses (chapter 5). In: Barbucci R (ed) Integrated biomaterials science. Kluwer Academic/Plenum Publishers, New York, pp 189–252
Kurtz S (ed) (2012) PEEK biomaterials handbook. Elsevier, Amsterdam
Kurtz S, Devine JN (2007) PEEK Biomaterials in trauma, orthopedic, and spinal implants. Biomaterials 28(32):4845–4869

Kustas FM, Misra MS (1992) Friction and wear of titanium alloys (chapter 18). In: Henry SD (eds) Friction, lubrication and wear technology. ASM International, pp 1585–1598
Kutz M (ed) (2002) Handbook of materials selection. Wiley, New York
Kutz M (ed) (2009) UHMWPE biomaterials handbook. Elsevier, London
Labarre D, Carreno M (2002) Inflammatory response to polymeric materials (chapter 25). In: Barbucci R (ed) Integrated biomaterials science. Kluwer Academic/Plenum Publishers, New York, pp 691–734
Leeson MC, Lippitt SB (1993) Thermal aspects of the use of polymethylmethacrylate in large metaphyseal defects in bone. A clinical review and laboratory study 295:239–245
Levinea BR, Sporera S, Poggieb RA et al (2006) Experimental and clinical performance of porous tantalum in orthopedic surgery. Biomaterials 27(27):4671–4681
Lewis G (1997) Properties of acrylic bone cement: state of the art review. J Biomed Mater 38 (2):155–182
Li H, Zheng Y, Qin L (2014a) Progress of biodegradable metals. Prog Nat Sci Mater Int 24 (5):414–422
Li Y, Yang C, Zhao H, Qu S et al (2014b) New developments of Ti-based alloys for biomedical applications—review. Materials 7(3):1709–1800
Liu X, Chu PK, Ding C (2004) Surface modification of titanium, titanium alloys, and related materials for biomedical applications. Mater Sci Eng 47(3–4):49–121
Long M, Rack HJ (1998) Titanium alloys in total joint replacement a materials science perspective —review. Biomaterials 19(18):1621–1639
Lu JX, Huang ZW, Tropiano P (2002) Human bio-logical reactions at the interface between bone tissue and polymethylmethacrylate cement. J Mater Sci 13(8):803–809
Machado L, Savi M (2003) Medical applications of shape memory alloys. Braz J Med Biol Res 36 (6):683–691
Mallick S, Tripathi S, Srivastava P (2015) Advancement in scaffolds for bone tissue engineering: a review. IOSR J Pharm Biol Sci 10(1):37–54
Manicone PF, Iommetti PR, Raffaelli L (2007) An overview of zirconia ceramics: basic properties and clinical applications—review. J Dent 35(11):819–826
Marconi W, Piozzi A (2002) Structure and properties of polymeric materials (chapter 2). In: Barbucci R (ed) Integrated biomaterials science. Kluwer Academic/Plenum Publishers, New York, pp 25–68
Matassi F, Botti A, Sirleo L et al (2013) Porous metal for orthopedics implants. Clin Cases Min Bone Metab 10(2):111–115
Mediaswanti K, Wen C, Ivanova EP (2013) A review on bioactive porous metallic biomaterials. J Biomimetics Biomater Tissue Eng 18:1–8
Miao X, Sun D (2010) Graded/gradient porous biomaterials—review. Materials 3(1):26–47
Middleton JC, Tipton AJ (2000) Synthetic biodegradable polymers as orthopedic devices. Biomaterials 21(23):2335–2346
Migliaresi C, Pegoretti A (2002) Fundamentals of polymeric composite materials (chapter 3). In: Barbucci R (ed) Integrated biomaterials science. Kluwer Academic/Plenum Publishers, New York, pp 69–114
Migonney V (ed) (2014) Biomaterials. Wiley-ISTE, New York
Mohammed MT, Khan ZA, Siddiquee AN (2014) Beta titanium alloys: the lowest elastic modulus for biomedical applications: a review. Int J Chem Nucl Mater Metall Eng 8(8):772–777
Murr LE, Gaytan SM, Medina F et al (2010) Next-generation biomedical implants using additive manufacturing of complex, cellular and functional mesh arrays. Philos Trans R Soc 368 (1917):1999–2032
Mutlu I, Oktay E (2013) Characterization of 17-4 PH stainless steel foam for biomedical applications in simulated body fluid and artificial saliva environments. Mater Sci Eng 33 (3):1125–1131
Naira LS, Laurencin CT (2007) Biodegradable polymers as biomaterials. Polym Biomed Appl 32 (8–9):762–798

Nasab MB, Hassan MR, Sahari BB (2010) Metallic biomaterials of knee and hip—a review. Trends Biomater Artif Organs 24(2):69–82
Niinomi M (1998) Mechanical properties of biomedical titanium alloys. Mater Sci Eng 243 (1–2):231–236
Niinomi M (2003) Recent research and development in titanium alloys for biomedical applications and healthcare goods—review. Sci Technol Adv Mater 4(5):445–454
Niinomi M, Narushima T, Nakai M (eds) (2015a) Advances in metallic biomaterials processing and applications. Springer, Berlin
Niinomi M, Narushima T, Nakai M (2015b) Advances in metallic biomaterials tissues. Springer, Berlin
O'Brien FJ (2011) Biomaterials & scaffolds for tissue engineering. Mater Today 14(3):88–95
Odahara T, Matsumoto H, Chiba A (2008) Mechanical properties of biomedical Co-33Cr-5Mo-0.3 N alloy at elevated temperatures. Mater Trans 49(9):1963–1969
Oldani C, Dominguez A (2012) Titanium as a biomaterial for implants (chapter 9). In: Fokter S (ed) Recent advances in arthroplasty. InTech, Rijeka, pp 149–162
Ong K, Lovald S, Black J (2014) Orthopaedic biomaterials in research and practice. Florida, Boca Raton
Osorio-Hernández JO, Suarez MA, Goodall R et al (2014) Manufacturing of open-cell Mg foams by replication process and mechanical properties. Mater Des 64:136–141
Parida P, Behera A, Mishra SC (2012) Classification of biomaterials used in medicine. Int J Adv Appl Sci 1(3):31–35
Park JB, Bronzino JD (eds) (2003) Biomaterials: principles and applications. Florida, Boca Raton
Park JB, Lakes RS (2007) Biomaterials—an introduction. Springer Science+Business Media, New York
Park H, Temenoff JS, Mikos AG (2007) Biodegradable orthopedic implants (chapter 4). In: Felix B, Farach-Carson F, Mikos AG (eds) Engineering of functional skeletal tissues. Springer, London, pp 55–68
Pelton AR, Stöckel D, Duerig TW (1999) Medical uses of nitinol. Proc Int Symp Shape Mem Mater Held Kanazawa 327–328:63–70
Peters ST (1998) Handbook of composites. Chapman & Hall, London
Piconi C, Maccauro G (1999) Zirconia as a ceramic biomaterial—review. Biomaterials 20(1):1–25
Piconi C, Maccauro G, Muratori F et al (2003) Alumina and zirconia ceramics in joint replacements—review. J Appl Biomater Biomech 1:19–32
Pilliar RM (2009) Metallic biomaterials In: Narayan R (ed) Biomedical materials. Springer Science +Business Media, LLC. doi:10.1007/978-0-387-84872-3-2
Pirhonen E (2006) Fibres and composites for potential biomaterials applications. Dissertation, Tampere University of Technology
Polyn LV (2008) Bone cement: chemical composition and chemistry (chapter 2). In: Sanjukta D (ed) Orthopaedic bone cements. Woodhead Publishing, Boca Raton, pp 183–200
Rahman HSA, Choudhury D, Osman NAA et al (2013) In vivo and in vitro outcomes of alumina, zirconia and their composited ceramic-on-ceramic hip joints. J Ceram Soc Jpn 121(4):382–387
Rakovic D, Uskokovic D (eds) (2010) Biomaterials. Institute of Technical Sciences of the Serbian Academy of Arts and Sciences, Belgrade
Ramakrishna S, Mayer J, Wintermantel E, Leong KW (2001) Biomedical applications of polymer-composite materials: review. Compos Sci Technol 61(9):1189–1224
Ratner BD, Hoffman SA, Schoen JF et al (2012) Biomaterials science: an introduction to materials in medicine, 3rd edn. Elsevier Academic Press, London
Rautray TR, Narayanan R, Kim K (2011) Ion implantation of titanium based biomaterials. Prog Mater Sci 56(8):1137–1177
Ristic B, Popovic Z, Adamovic D et al (2010) Selection of biomaterials in orthopedic surgery. Vojnosanit Pregl 67(10):847–855
Rivard J, Brailovski V, Dubinskiy S et al (2014) Fabrication, morphology and mechanical properties of Ti and metastable Ti-based alloy foams for biomedical applications. Mater Sci Eng 45:421–433

Robinson RP, Wright TM, Burstein AH (1981) Mechanical properties of poly (methyl methacrylate) bone cements. J Biomed Mater Res 15(2):203–208
Rodríguez B, Romero A, Soto O et al (2004) Biomaterials for orthopedics. Appl Eng Mech Med 1:1–25
Roeder RK, Conrad TL (2012) Bioactive polyaryletherketone composites (chapter 7). In: Kurtz S (ed) PEEK biomaterials handbook. Elsevier, Amsterdam, pp 163–179
Ryan G, Pandit A, Panagiotis Apatsidis D (2006) Fabrication methods of porous metals for use in orthopaedic applications—review. Biomaterials 27(13):2651–2670
Sáenz A, Rivera-Muñoz E, Brostow W et al (1999) Ceramic biomaterials: an introductory overview. J Mater Educ 21(5–6):297–306
Salernitano E, Migliaresi C (2003) Composite materials for biomedical applications: a review. J Appl Biomater Biomech 1:3–18
Santos AR (2010) Bioresorbable polymers for tissue engineering (chapter 11). In: Eberli D (ed) Tissue engineering. InTech, Rijeka, pp 225–246
Schieker M, Seitz H, Drosse I et al (2006) Biomaterials as scaffold for bone tissue engineering. Eur J Trauma 32(2):114–124
Schuessler A, Piper A (2004) Boundaries for the use of Nitinol in medical applications. In: Mertmann S (ed) Proceedings of the international conference on shape memory and superelastic technologies, ASM International, Kurhaus Baden-Baden, 3–7 Oct 2004, pp 563–571
Schwartz M (ed) (2002) Encyclopedia of smart materials. Wiley, New York
Seifalian A, Mel A, Kalaskar DM (2014) Nanomedicine. One Central Press, London, pp 112–130
Shi D (ed) (2006) Introduction to biomaterials. Tsinghua University Press Beijing and World Scientific Publishing Singapore, Beijing
Shoichet M (2010) Polymer scaffolds for biomaterials applications. Macromolecules 43(2): 581–591
Sinha RK (ed) (2002) Hip replacement—current trends and controversies. Marcel Dekker, New York
Sljivic M, Stanojevic M, Durdevic D et al (2016) Implemenation of FEM and rapid prototyping in maxillofacial surgery. FME Trans 44(4):422–429
Spector M (2006) Biomaterials-based tissue engineering and regenerative medicine solutions to musculoskeletal problems. Swiss Med Wkly 136:293–301
Stanczyk M, Rietbergen B (2004) Thermal analysis of bone cement polymerisation at the cement–bone interface. J Biomech 37(12):1803–1810
Steinberg EL, Rath E, Shlaifer A et al (2013) Carbon fiber reinforced PEEK optima—a composite material biomechanical properties and wear/debris characteristics of CF-PEEK composites for orthopedic trauma implants. J Mech Behav Biomed Mater 17:221–228
Tapash RR, Narayanan R, Kim KH (2011) Ion implantation of titanium based biomaterials. Prog Mater Sci 56:1137–1177
Teoh SH (2000) Fatigue of biomaterials: a review. Int J Fatigue 22(10):825–837
Teoh SH (2004) Engineering materials for biomedical applications. World Scientific Publishing Co. Pte. Ltd., Singapore
Thamaraiselvi TV, Trends R (2004) Biological evaluation of bioceramic materials—a review. Biomater Artif Cells Artif Organs 18(1):9–17
Tian H, Tang Z, Zhuang X et al (2012) Biodegradable synthetic polymers: preparation, functionalization and biomedical application. Prog Polym Sci 37(2):237–280
Ulery BD, Nair LS, Laurencin CT (2011) Biomedical applications of biodegradable polymers. Polym Phys 49(12):832–864
Vişan S, Popescu RF (2011) Biomaterials. The behavior of stainless steel as a biomaterial. Economia Seria Manag 14(1):177–183
Wang M (2006) Composite scaffolds for bone tissue engineering. Am J Biochem Biotechnol 2 (2):80–84
Wang S, Ge S (2007) The mechanical property and tribological behavior of UHMWPE: effect of molding pressure. Wear 263(7–12):949–956

Webb JCJ, Spencer RF (2007) The role of polymethylmethacrylate bone cement in modern orthopaedic surgery. J Bone Joint 89(7):851–857

Wise DL (ed) (2000) Biomaterials and bioengineering handbook. CRC PRESS, Taylor & Francis Group, New York

Wnek GE, Bowlin GI (eds) (2008) Encyclopedia of biomaterials and biomedical engineering. Informa Healthcare, New York

Wong J, Bronzino J (eds) (2007) Biomaterials. CRC PRESS Taylor & Francis Group, New York

Yaszemski M, Trantolo D, Lewandrowski K et al (eds) (2004) Biomaterials in orthopedics. CRC PRESS Taylor & Francis Group, New York

Yoshikawa H, Tamai N, Murase T (2009) Interconnected porous hydroxyapatite ceramics for bone tissue engineering—review. J R Soc Interface 6:341–348

Yusop AH, Bakir AA, Shaharom NA et al (2012) Porous biodegradable metals for hard tissue scaffolds: a review. Int J Biomater 2012:1–10

Zhao J, Fu T, Han Y et al (2003) Reinforcing hydroxyapatite/thermosetting epoxy composite with 3-D carbon fiber fabric through RTM processing. Mater Lett 58(1–2):163–168

Zheng YF, Gu XN, Witte F (2014) Biodegradable metals. Mater Sci Eng R 77:1–34

Zhou Y, Niinomi M, Akahori T et al (2007) Comparison of various properties between titanium-tantalum alloy and pure titanium for biomedical applications. Mater Trans 48(3): 380–384

Zivic F, Babic M, Mitrovic S et al (2011) Continuous control as alternative route for wear monitoring by measuring penetration depth during linear reciprocating sliding of Ti6Al4V alloy. J Alloy Compd 509:5748–5754

Zivic F, Babic M, Grujovic N et al (2012) Effect of vacuum-treatment on deformation properties of PMMA bone cement. J Mech Behav Biomed Mater 5:129–138

Zivic F, Babic M, Grujovic N et al (2013) Influence of loose PMMA bone cement particles on the corrosion assisted wear of the orthopaedic AISI 316LVM stainless steel during reciprocating sliding. Wear 300:65–77

Zivkovic I, Fragassa C, Pavlovic A et al (2017) Influence of moisture absorption on the impact properties of flax, basalt and hybrid flax/basalt fiber reinforced green composites. Compos B Eng 111:148–164

Polymeric Biomaterials in Clinical Practice

Željka Marjanović-Balaban and Dijana Jelić

Abstract Biomedical implants improve and enhance human lives, and millions of people have experienced the benefits of incorporation of implants in the human body. Up until today, the list of biomaterial applications has included smart delivery systems for drugs, tissue cultures, engineered tissues, and hybrid organs. Because of the continuous and ever-expanding practical needs of medicine and health care practice, there are currently thousands of medical devices, diagnostic products, and disposables on the market. Polymeric materials such as films, fibers, and rods have a wide variety of applications for implantation, since they have some unique properties and can be easily fabricated. They are noncancerous, nontoxic and nonallergic. Polymeric materials possess good strength, elasticity and durability. These materials have been widely used as dental materials, drug delivery systems, prosthetic materials, tissue-engineered products, etc. Undoubtedly, biomaterials have had a major impact on the practice of contemporary medicine and patient care in both saving and improving the quality of lives of humans and animals, and with the high-tech revolution, tremendous further goals will continue to be achieved in this field.

Keywords Polymeric biomaterials · Biocompatible · Implant materials · Drug delivery · 3D implants

Ž. Marjanović-Balaban (✉)
Faculty of Forestry, University of Banja Luka,
Banja Luka, Bosnia and Herzegovina
e-mail: zeljka.marjanovic@sfbl.org

D. Jelić
Faculty of Medicine, Pharmacy Department,
University of Banja Luka, Banja Luka, Bosnia and Herzegovina

F. Zivic et al. (eds.), *Biomaterials in Clinical Practice*,
https://doi.org/10.1007/978-3-319-68025-5_4

1 Polymeric Biomaterials—Basis of Structure

Biomaterials are materials that interact with biological systems and are applied in contact with cells, tissues or human liquids. A comprehensive definition of a biomaterial says that a biomaterial is "any substance (other than a drug) or mixture of substances, synthetic or natural, which can be used for any period of time, as an entity or as a part of a system which treats, heals or replaces any human organ, tissue, or function of the body." Today, biomaterial usage is enormous, from medical implants to the controlled delivery of pharmaceuticals to the engineering of functional tissues. Keeping such diversity of application in mind, the field of biomaterials requires material scientists and engineers to be very familiar with cellular, biochemical, molecular and genetic issues, and to work very efficiently with representatives of different branches of science, including molecular biologists, biochemists, polymer chemists, geneticists, physicians and surgeons. It is very important to emphasize that materials that are used as biomaterials ought to fulfill certain special criteria and should be distinguished from other classes of materials as a result. The most important and precious feature of any biomaterial is biocompatibility. There are many materials that are, from the engineering point of view, very desirable, but human tissue simply rejects them. Biomaterials must be of medical grade. The immune system of the patient must accept the biomaterial and must not attack it. Furthermore, non-toxicity, corrosion resistance, durability, toughness, and a low modulus of elasticity are some of the other characteristics that a good biomaterial should possess. Synthetic materials currently used for biomedical applications include metals and their alloys, polymers, ceramics and glass biomaterials. Because the structures of these materials differ, they have different properties, and therefore different uses in the human body. For example, metallic biomaterials are used for hip and knee prostheses, heart valves, and pacemaker leads; polymeric biomaterials can be used as cardiovascular implants, mechanisms for drug release and delivery or orthopedic implants; ceramics can be used as hip implants, dental implants, middle ear implants, etc.

Among these biomaterials, polymers are the most widely used for biomedical applications, and these are what will be reviewed here. Polymeric biomaterials are used for their flexibility and biocompatibility, and most especially for their mechanical, chemical, thermal and electrical characteristics.

The word 'polymer' means '*many parts*,' and a polymer represents one large molecule consisting of thousands of atoms bonded together in a repeating pattern. Those small repeating units are called monomers (often called "*mers*"). Monomers are classified into the olefinic and the functional. The former possess a double bond and the latter contain some form of reactive functional group. An organic molecule that contains more then 200 monomers is a polymer. Polymers are formed through a polymerization reaction, by one of two different paths: condensation or addition. Addition polymerization is also called chain-growth reaction. Whether they interact through condensation or a chain growth polymerization reaction depends on their structure. If a monomer contains a double bond of σ (sigma) and π (pi) between a

pair of electrons, chain growth polymerization will be applied, while on the other hand, if a functional group such as hydroxyl, carboxyl or amines are present, they can interact via condensation.

Condensation polymerization occurs when two monomers are bonded together to form a repeating unit over and over and a small molecules such as water are removed. [AU: I had trouble figuring this last part out, but this interpretation matched up with the research I did.]

$$\underset{(\text{amine})}{\text{R-NH}_2} + \underset{(\text{carboxylicacid})}{\text{R}'\text{COOH}} \leftrightarrow \underset{(\text{amide})}{\text{R}'\text{CONHR}} + \underset{(\text{condensationmolecule})}{\text{H}_2\text{O}}$$

Typical condensation polymers are: polyester, polyamide, polyuria, cellulose, polyurethane, etc. In chain growth reaction, monomers create a very reactive free radical or molecule with an unpaired electron, which reacts with another monomer so that the polymer chain continues to grow longer. Monomers suitable for additional polymerization are acrylonitrile, methyacrylate, styrene, and vinyl chloride (Fig. 1).

A polymer can be in the form of a linear, branched or cross-linked chain. Chains of atoms are bonded with strong covalent bonds, while interaction between macromolecules is exercised via hydrogen and weak VDW (Van der Waals) bonds, unless macromolecules are cross-linked. It is interesting to note that polymers have extremely high molecular weight, and therefore thermodynamics allows for the existence of polymers only as a liquid or solid material. Furthermore, a polymer's molecular weight can be adjusted depending on its application, unlike other materials such as metals and ceramics (Fig. 2).

The properties of polymers, such as the thermal, mechanical and physical, depend on their structure and bonding, the identity of side groups, the chain length and the degree of cross-linking. Polymers are generally cheap materials, since polymers originate from oil.

Polymeric materials can be classified in a variety of ways. Their classification in regard to physical properties and chemical composition is very useful. Polymeric materials are solids, and upon heating, polymer molecules can start to flow. Solid

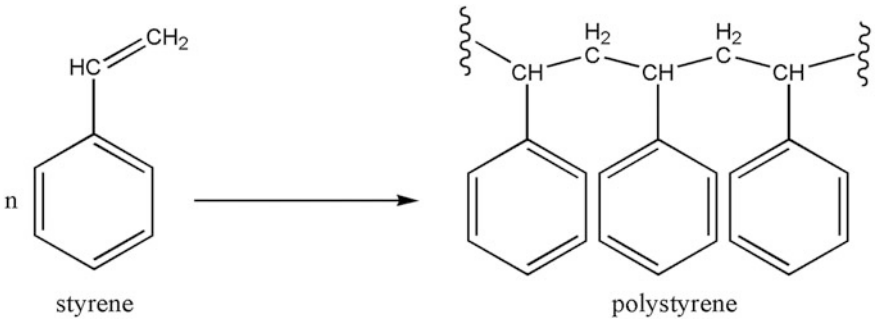

Fig. 1 Addition polymerization

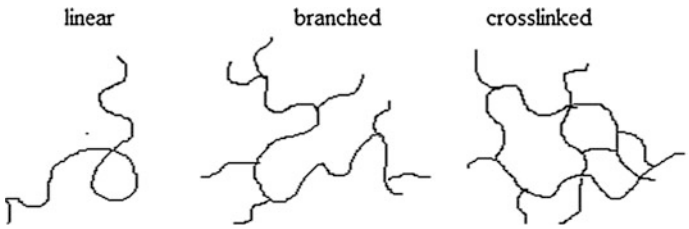

Fig. 2 Topology of polymers

turns to liquid. With the temperature rising above the melting temperature T*m*, polymer crystal cells start to melt; but upon rapid cooling of the polymer, an amorphous structure is created. The amorphous structure is also called a glassy, no crystalline state. A very important feature of the polymer is the glass transition temperature, T*g*. At temperatures below T*g*, polymers are hard and glass-like, and above T*g*, polymers have the ability to flow. T*m* and T*g* can be detected by DCS (differential scanning calorimetry), a feature that reflects the existence of a crystalline and amorphous region in the polymer's structure.

Based on their physical properties, there are four groups of polymers: *thermoplastic (TP)*, *thermosetting plastic* (TSP), *plastic* (P) and *elastomer (EL)*. Polymers with a linear or branched structure are mostly thermoplastics, and they can be shaped more than once, while cross-linked polymers behave like thermosetting plastics. Unlike TP, which are a good replacement for blood vessels, TSP material can be formed just once. Thermosetting plastic is used for dental implants, while elastomers are mostly used as catheters, pacemakers and for covering leads on implanted electronics. Plastic polymers can be formed into various forms and shapes.

Polymeric materials can also be classified based on their origin (natural, synthetic polymers and bio-inspired polymers). But the more general classifications with regard to biomaterials are synthetic and natural/semisynthetic polymers or degradable and non-degradable polymers.

Proteins and nucleic acids are well known supporters of life, and these natural polymers retain and structure water (Hossein et al. 2011). Even though they are natural, these polymers also have some disadvantages. The side effects of natural polymers are microbial contamination and the possibility of antigenicity. Contrastingly, synthetic polymers (polyesters, polyanhydrides, polyamides) have been the material of choice for implants because of their availability and simple production process. Some synthetic polymers do not have the ability to provoke an immune response in the body of a human or animal, which is considered to be very important for biomedical application, and therefore they have great potential to replace unhealthy or damaged cell components in many organs.

Chemical composition is very important for polymer classification, since composition is related to the polymer's activity, including the mechanism of polymer decomposition. Scientists and engineers have managed to produce more useful

materials just by manipulating a polymer's molecular structure, incorporating various fillers, additives or some reinforcements into it.

1.1 Mechanical Properties

Due to their mechanical properties (Table 1), numerous biomedical applications of polymers are possible. Changes in a polymer's composition or structure can yield increased strength, while the plasticity of the material is decreased. If a macromolecule's length is increased (molecular weight), the chains become less movable and obstruct their relative movement (Dee et al. 2002). Polymers have much lower strengths and modules than other biomaterials such as metals and ceramics, but they can be deformed to a greater extent before beginning to deteriorate. The mechanical and thermal properties of polymers depend on a number of elements, such as the composition of the backbone and side groups, the chain structure and the molecular weight of the molecules. When the applied mechanical forces cause the macromolecular chains to move smoothly with each other, the deformation of the plastic appears. Application of polymers has one limiting factor when it comes to biomedical applications in which body weight is crucial and important. The exception to this limitation is ultra-high-molecular-weight polyethylene, which is used as a bearing surface in hip and knee replacements.

1.2 Degradation

Degradation of polymers is a process related to the properties of the polymer material and its position in the body. Degradation is related to biological processes

Table 1 Mechanical properties of polymers (Kohn and Langer 1996)

Polymer	Tensile strength UTS (MPa)	Young's modulus, E (GPa)	% elongation
Poly(methyl methacrylate)(PMMA)	30	2.2	1.4
Nylon 6/6	76	2.8	90
Poly(ethylene terephthalate)	53	2.14	300
Poly(lactic acid)	28–50	1.2–3	2–6
Polypropylene	28–36	1.1–1.55	400–900
Polytetrafluoroethylene	17–28	0.5	120–350
Silicone rubber	2.8	Up to 10	160
Ultra-high-molecular-weight polyethylene (UHMWPE)	≥ 35	4–12	≥ 300

that can cause decomposition of the polymeric material. To degrade polymers, their macromolecular structures must be separated. The process can happen due to alteration of the covalent interatomic bonds in the chains or alteration of the intermolecular interactions between chains. Chemical processes such as hydrolysis and oxidation and physical and enzymatic degradation contribute to the degradation of polymers used as biomedical implants or devices. Some of the above-mentioned chemical reactions, such as oxidation and hydrolysis, can change the properties of implanted polymers. Substances such as superoxide anion (O_2^*), hydrogen peroxide (H_2O_2), and hypochlorite, which are produced from neutrophils, macrophages, and foreign body giant cells, may cause oxidation, which results in chemical changes on the surface of the polymers. Hydrolysis can be catalyzed by physiological ions, such as PO_4^{3-}, or by enzymes secreted during the wound healing process. Processes of oxidation and hydrolysis can cause the splitting of macromolecular chains, resulting in the appearance of various functional groups on the surface of the material and/or changes in surface texture.

In order to prevent unexpected degradation, some polymers are subjected to controlled degradation. These materials can be degraded into smaller pieces, as well as monomers, such as lactic acid, and can be removed from the body through normal metabolic processes. In addition, polymers may contain different kinds of (often unspecified) additive, traces of catalysts, inhibitors, and other chemical compounds essential for their synthesis. The chemicals released from polymers may induce harmful local and systemic reactions that can cause clinical complications for a host. This is the problem with materials, such as bone cement, that are polymerized in the body, and with flexible polymers, such as poly(vinyl chloride), that contain low molecular-weight compounds (plasticizers) that make them applicable. The process of degradation must be well understood in order to achieve the greatest benefit from application of polymers as biomaterials.

2 Applications of Polymers

Polymer materials are widely used for biomedical implants. Biomedical implants and devices enhance the quality of our lives by extending the functionality of essential body systems beyond their supposed lifespans. They are used as objects that provide physical support, such as knee and hip implants, and for such vital functions as synthetic blood vessels, but also as applications that enhance the functionality of actual human organs, such as pacemakers. The basic aim of all these devices is the preservation of human life and improvement of the quality of daily life. Even though natural polymers have certain advantages over synthetic ones, such as biodegradability, the use of synthetic polymers is quite common, owing to their availability and low cost of production. Some future trends in the use of polymers as biomaterials should be through creation of composites made of natural and synthetic polymers. Table 2 summarizes the common synthetic

Table 2 Synthetic polymers used as implants

FDA category	Common devices	Synthetic polymer material used
Anesthesiology	Epidural catheters	Polyethylene Polyamide Polytetrafluoroethylene
Cardiovascular	Pacemaker Left ventricular assist device Mechanical heart valves Implantable cardioverter/defibrillator Artificial blood vessels Catheters	Polypropylene Polyethylene Polyamide Polytetrafluoroethylene Polyethyleneterephthalate Polyhydroxyalkanoates Polydimethylsiloxane
Dental	Dental implants Dentures	Polymethylmethacrylate
Ear, nose, and throat	Stapes implants Cochlear implants Nasal implants for nose reconstructions	Polyethylene Polydimethysiloxane Liquid crystal polymer Silicone Parylene
Gastroenterology and urology	Penile implants Neurostimulator in sacral nerve stimulation Hernia or vaginal mesh Foley catheter Artificial urinary sphincter implant	Polyethylene Polypropylene Polyamide Polydimethysiloxane Polytetrafluoroethylene Polyhydroxyalkanoates Silicone
General and plastic surgery	Synthetic blood vessels Breast implants Cheek, jaw and chin implants Lip implant Titanium surgical implants Hip implant	Polypropylene Polyethyleneterephthalate Polytetrafluoroethylene Silicone Polydimethylsiloxane
Hematology and pathology	Central venous access device Peripherally inserted central catheter	Polyethylene Polyamide Polytetrafluoroethylene
Neurology	Neuroprosthetics Implantable pulse generator for deep brain stimulation Cognitive prostheses Catheters	Polyimides Polyamide Polyethylene Polydimethylsiloxane Parylene Liquid crystal polymers SU-8[a] Polytetrafluoroethylene Polyhydroxyalkanoates
Obstetric and gynecologic	Intrauterine device (IUD) Intravaginal rings Etonogestrel-releasing contraceptive implant Urogynecologic surgical mesh implants Fetal micro-pacemaker	Silicone Polyurethane Polypropylene

(continued)

Table 2 (continued)

FDA category	Common devices	Synthetic polymer material used
Ophthalmic	Retinal prosthesis Dexamethasone intravitreal implant Artificial intraocular lens Glaucoma valve Fluocinolone opthalmic implant Orbital implant Catheters	Polymethylmetacrylate Polytetrafluoroethylene Polyamide Polyethylene
Orthopedic	Orthopedic implants	Polyethylene Polyether ether ketone Polyhydroxyalkanoates

[a]Negative epoxy type; near UV photoresist material

polymers approved by the FDA for use as biomaterials, including their specific applications.

Polyethylene (PE), a linear thermoplastics polymer, is obtainable in three major grades: low and high density and ultrahigh molecular weight (Table 3). In fact, it is almost impossible to produce polyethylene with no crystallinity because of the small hydrogen side groups, which causes high mobility of chains. The first polyethylene was synthesized through the reaction of ethylene gas at high pressure (100–300 MPa) in the presence of a catalyst (peroxide) to initiate polymerization. This process yields the *low*-density polyethylene. By using a *Ziegler catalyst* (stereospecific), high-density polyethylene can be produced at low pressure (10 MPa). Unlike the low-density variety (LDPE), high-density polyethylene (HDPE) does not contain branches. The result is a better packing of chains, which increases density and crystallinity. The crystallinity is usually 50–70% and 70–80% for the low- and high-density polyethylenes, respectively. HDPE is a very good choice for rhinoplasty surgery (Zhou et al. 2014) on account of its good elasticity and very pronounced anti-infective properties.

Ultrahigh-molecular-weight polyethylene (UHMWPE) has been used extensively for orthopedic implant fabrications, especially for knee joints and hips. Since the folded chains are crystalline, the extent of the amorphous region is reduced, thus reducing the possibility of an environmental attack (usually oxidation). A more crystalline polyethylene also exhibits enhanced mechanical properties (greater hardness, modulus of elasticity, tensile yield strength). Moreover, it screep properties are superior (i.e., less creep), which is an important factor for designing joint implants. This material has no known effective solvent at room temperature; therefore, only high temperature and pressure sintering may be used to produce the desired products. Conventional extrusion or molding processes are difficult to employ. Recently, a crosslinked ultrahigh-molecular-weight polyethylene has been developed for use in articulating joint materials, such as the acetabular cup of a hip joint prosthesis. A particular advantage of crosslinked UHMWPE in this application is that it has a low wear rate compared to the conventional uncrosslinked material.

Table 3 Properties of polyethylene (Park and Lakes 2007)

Properties	Low density	High density	UHMWPE[a]	Enhanced UHMWPE[b]
Molecular weight (g/mol)	3–4 × 10^3	5 × 10^5	2 × 10^6	B
Density (g/cm^3)	0.90–0.92	0.92–0.96	0.93–0.94	B
Tensile strength (MPa)	7.6	23–40	27 min.	D
Elongation (%)	150	400–500	200–250	B
Modulus of elasticity (MPa)	96–260	410–1240	[c]	2200
Crystallinity (%)	50–70	70–80	[d]	E

[a]Data from ASTM F648; also. 2% deformation after 90 min recovery subjected to 7 MPa for 24 h (D621)
[b]Same as the conventional UHMWPE (ASTM, F648). Data from *A new enhanced UHMWPE for orthopaedic applications: a technical brief*, Warsaw, IN: DePuy, 1989
[c]Close to 2200 MPa
[d]Higher than high-density polyethylene
[e]Equal to or slightly higher than d

Although the crosslinking is similar to that performed for the elastomeric (rubbery) polymers used in tires, polyethylene is much stiffer than rubber. During crosslinking, the material also becomes weaker and sometimes changes color from white to brown. Crosslinking of polyethylene can be achieved through chemical reactions or by ionizing radiation. Crystallinity is decreased after crosslinking. Biocompatibility tests for nonporous (F981) and porous polyethylene (F639 and 755) are given according to ASTM standards (Park and Lakes 2007). To serve as a component of an endoprosthesis of the hip joint, the material must meet certain mechanical properties, particularly wear resistance, but also must have properties of biocompatibility. The only plastic material that is currently acceptable for the preparation of the implant is ultra high molecular weight polyethylene, UHMWPE, to DIN 58834, which is known under the trade name "chirulen" 7 (Ratner et al. 1996). Plates of different thickness are made with polyethylene granules under high pressure at the appropriate temperature, semi-finished products in the form of rods are made by cutting, and mechanical treatment is used to produce components for endoprostheses of the hip and knee. Sterilization of polyethylene parts is not simple. Sterilization at high temperatures isn't allowed, because there is a change in deformation and mechanical characteristics. The usual sterilization method is by "gamma" rays and ethylene oxide. For polymers, the method of sterilizing the biomaterial can significantly alter its properties. For example, high temperatures (121–180 °C), steam, chemicals (ethylene oxide), and radiation can compromise the shape and/or mechanical properties of polymeric materials. Riveiro et al. (2014) reported modification of UHMWPE by laser radiation that contributed to changes in surface roughness and wettability, making the bone binding to the medical implant's surface at 1 μm. Also, Cools et al. (2014), by using atmospheric pressure plasma technology, were able to modify the PE implant's surface, making it very

smooth. When creating artificial hip prostheses, high density polyethylene (UHMWPE) is mainly used for making the hip socket ("plain bearing") in order to achieve a significant reduction in friction between the sliding surfaces, but considerably more attention is paid to the use of stainless steel Ti-alloy and Co–Cr alloy (Ristic et al. 2010).

Polypropylene (PP), a thermoplastic polymer very similar to PE, is mostly used as a reinforcement for weakened tissue. PP was used in urogynecology for urinary incontinence or as a blood oxygenator membrane. The disadvantage of PP is the existence of bioincompatibility, so further research is mostly aimed at improving its biocompatibility issue via modification of the material's surface (Abednejad et al. 2013, 2014). Contemporary research on polypropylene has even considered PP as a suitable material for breast implants (Li et al. 2014). However, there is some controversy in regard to this issue, led by Zheng et al. (2007) who reported the existence of some inflammatory processes that could postpone the healing process.

Another synthetic polymer, poly(methyl methacrylate), belongs to the group of transparent thermoplastic polymers. Literature on poly(methyl methacrylate) has reported the use of PMMA as a bone cement (Parida et al. 2012), an intraocular lens (Pérez-Merino et al. 2013), in rhinoplasty (Rivkin 2014), etc. The side effect of PMMA is a lack of support for osseointegration with the other structures with which PMMA is in contact. A solution was found to promote osseointegration by inducing growth of a $Ca_3(PO_4)_2$ layer on the surface of the cement disc. 3D printing has also contributed to better PMMA features, making PMMA a choice material for certain specific biomedical applications (Espalin et al. 2010).

Silicones are characterized as inert materials with a low infection rate and various biomedical applications. Their use in nose (Dutta et al. 2013), breast (Najafi and Neishaboury 2014) and lip implant are well known. Van Ardenne et al. (2011) reported improved vocal function using titanium and silicone implants. There are two derivatives of silicone parylene and polydimethylsiloxane that are used in biomedical application. The first one, poludimethylsiloxane (PDMS), is commonly used in blood pumps, pacemakers, catheters, and esophageal replacement. The use of PDMS in implantable MEMS devices for delivery of drugs to the human eye was reported. Among parylene variants, parylene C is mostly used as packaging material in implanted neural prostheses (Hogg et al. 2013; Hassler et al. 2010).

There many other synthetic polymers in use in the scope of biomedical application. Table 4 presents the most commonly used synthetic polymers, along with their benefits and side-effects.

Many kinds of reconstructive medical implant (hip replacements, for example, or dental implants) need to integrate with the surrounding tissues to restore adequate function, without releasing harmful chemical products. Pacemakers, arterial grafts, and dialysis machines are examples of devices that include a polymeric material that is in interaction with the tissues and/or bodily fluids. The environment within the body is very active in the sense of electrical, chemical, and mechanical responses, and the interface between an implanted biomaterial and the body is the location of a variety of dynamic biochemical processes and reactions. From the first contact of biological molecules with an implant's surface to the final tissue

Table 4 Advantages and disadvantages of synthetic polymeric biomaterials (Adrian et al. 2016)

	Advantages	Disadvantages
Polyethylene	Mechanical properties modifiable via molecular weight Porous HDPE has good biocompatibility, good elasticity, and strong anti-infective properties Good chemical resistance Low melting temperature	Plastic feel to skin High friction coefficient
Polypropylene	Non-toxic High melting point Good dielectric properties	Non-degradable Questionable Biocompatibility
PMMA	Lightweight Mechanically strong Poor thermal and electrical conductivity Acceptable biocompatibility	Lack of osseointegration
Silicone	Low toxicity Chemically inert Good biocompatibility Low thermal conductivity Thermal stability High gas permeability Hydrophobic	High coefficient of friction Long term effects unknown Soft (prone to damage during implantation)
Polyurethane	High durability and toughness Good biostability and biocompatibility Low coefficient of friction Low water permeability	Degradation of the material in vivo Environmental stress cracking Metal ion oxidation
Polyamide	Long-lasting tensile strength and high elasticity Causes minimal tissue reactivity Moisture absorbent Able to prevent bacterial transmission	High fraction coefficient Moisture permeability
Polyimide	Good chemical resistance Flexible, stable over wide range of temperatures High light transmittance for a wide range of wavelengths Certain polyimides are biocompatible upon interaction with blood Good mechanical and electrical properties High tensile strength and heat resistance	High moisture absorption
Liquid Crystal Polymer	Chemically inert High mechanical strength and durability Resistant to fire and low moisture absorption Able to fabricate thin layers Flexible and easily conformable to difficult shapes	Composite film has poor adhesion to flexible substrates
Carbon Nanotube Composite	Good bonding strength with metal substrates Good mechanical and surface properties	Possible cytotoxicity Easily compressed

remodeling around an implant, understanding the temporal progression of wound healing is a vital part of understanding tissue-implant relations. The interface between a man-made, synthetic biomaterial and the body is quite complex (Fig. 3). Interfaces between the body and the biomaterial, between the body and the living cells, and between the cells and the biomaterial are crucial for successful implementation (Fig. 4).

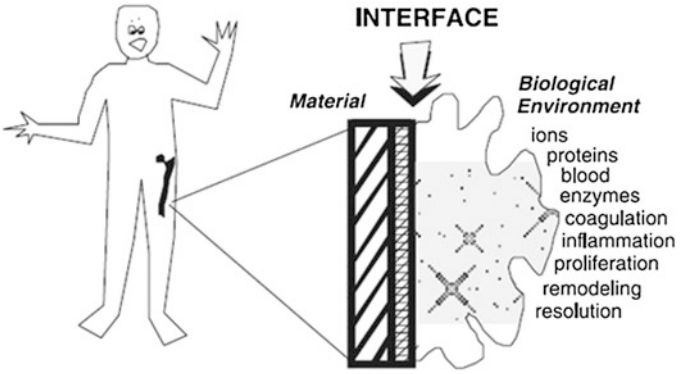

Fig. 3 The interface between a biomaterial (metallic, titanium oxide) and the body. In this figure, a hip implant is used as an example. The interface between this surface oxide and the biological environment is the location for ions, proteins, enzymes, and other biomolecules to interact with the biomaterial. Copyright with permission from reference 19

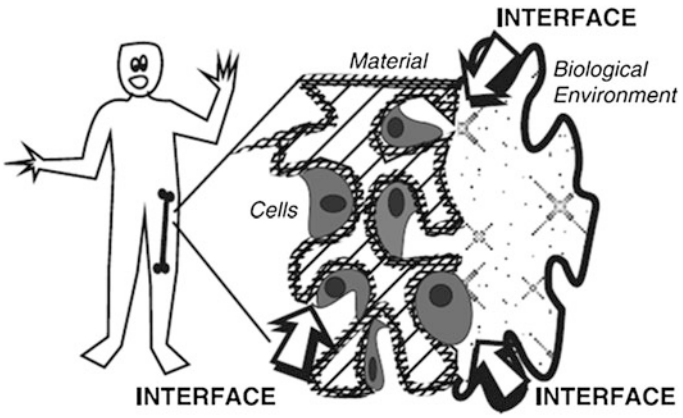

Fig. 4 The interface(s) between a tissue-engineered product and the body. In this figure, a tissue-engineered femur, consisting of living cells cultured on a biomaterial scaffold, is used as a futuristic example of a substitution for a traditional metallic hip implant (with permission of authors Dee et al. 2002). Copyright permission by reference 19

Scientists are moving frontiers in diagnosing, treating, curing, and preventing diseases at the genetic level. With this knowledge on the molecular level, there will be further need for innovative formulations and/or modifications of existing materials, and for nontraditional applications of biomaterials. This knowledge will result in tissue engineering. Promising developments include bioinspired chemical and topographic modifications of material surfaces, current-conducting polymers, and nanophase materials. In addition to new challenges and opportunities, some of the unresolved issues (primarily biocompatibility) of the past and present will also need to be addressed in the future (Dee et al. 2002; Bazaka and Jacob 2013). A large number of researchers are studying this problem (Saum et al. 2001; Thakrar 2000; Merrill et al. 1999; Joung 2013). Contemporary data on medical implants combine experience from medicine, material science and surface science. Nowadays, medical implants are high-tech products. 3D printing is an exciting and promising tool for the processing of biomaterials and can overcome most of the disadvantages of classical biomaterial production. New 3D technology produces complex biomaterial implants and devices through computer design by using specific anatomical data from patients. When producing a 3D implant, the biggest accent is on surface microstructure and macrostructure, form, shape and configuration. 3D printing will have the biggest impact on orthopedic and dental implants. Let us consider some benefits of 3D printing! 3D implants can use polymers that are chemically very close to the tissue, can be customized for each patient with their specific needs, and have very low levels of toxicity, cost and production time. By using polymers, both natural and synthetic, medical implant technology with 3D printing will rise to its next level. In the future, 3D printing can contribute to soft tissue printing, which will reduce or, dare we say, even eliminate the need for tissue and organ donors.

2.1 Polymers in Drug Delivery

Polymers are becoming very significant in pharmaceutical applications due to some of the unique properties they offer. Their physical-chemical properties, such as viscosity, molecular weight, solubility and the ability to form gel, are considered to be outstanding. Polymers are used in pharmaceuticals for the achievement of better taste, better stability, as protective agents, for controlled release and in the improvement of bioavailability (Reja et al. 2003; Taylor and Francis 2006; Ravinder and Sukhvir 2014). Their application in the field of drug delivery systems is developing very fast, and this has become one of the most attractive and most challenging of areas (Vicky 2010). Knowledge of the bulk and surface properties of polymers is very helpful for designing various drug delivery applications. The purpose of a polymer in biomedicine application is to prolong drug availability if drugs are formulated as hydrogels (Park and Webster 2005) or microparticles; to enable hydrophobic administration of a drug if it is formulated as micelles (Reja

et al. 2003); and to transport a drug to an inaccessible site if it is formulated as a gene medicine.

A drug delivery system is a system that controls the drug release rate from its formulation and/or provides delivery of a drug to a desired body location via diffusion through the matrix, biodegradation, membrane diffusion or osmosis. All the polymers that are used for drug delivery systems are classified based on their chemical nature, stability (biodegradability/non biodegradability) and solubility in water (hydrophobic and hydrophilic), and must fulfill the following requirements: chemical inertness, biocompatibility and minimum undesirable degradation byproducts, the ability not to leach, ease of fabrication and sterilization, and possession of suitable mechanical properties (Kim 2000; Uchegbu et al. 2006; Mashak and Rahimi 2009).

Polymer materials are usually combined with a drug in one of three ways: the drug is coated with a polymeric membrane (tablets, transdermal systems, osmotic pumps, film …), the drug is distributed within a polymeric material known as reservoir system (matrix system) or the drug is chemically attached to a polymeric carrier. The complex formed of a polymeric material as a carrier and a drug being carried is disintegrated at the desired/targeted place in the body.

In a membrane system, the drug is coated with a polymeric membrane (porous/nonporous), which regulates drug release over time. If a nonporous membrane is employed, a diffusion process dominates, unlike with a porous membrane, for which a diffusion process is combined with drug release through the pores. It is important to emphasize that drug release can be affected and modified through membrane thickness, pore size, pore morphology, etc.

Membranes are mostly made from biopolymers (cellulose and cellulose derivates), but can be made from synthetic ones, which can be modified with different functional groups based on the application. Enteric–coated products are the ones that pass through the stomach environment of the intestine, since the stomach represents a harsh environment for many drugs (pH below 2). Polymers that have methacrylic acid as a functional group are generally used for drug delivery as a barrier that helps by protecting the drugs from the pH of the stomach (Lee and Good 1987). This approach has found its application in taste-masking, drug stability and sustained release.

A reservoir system is a system in which the drug is concentrated within a polymer matrix. The rate of drug release depends on the diffusion of the drug, the solubility of the drug in a core and penetration of the surrounding medium through the polymeric membrane. A system in which a drug is dispersed within a polymer matrix and released by diffusion is often called a monolithic delivery system. Initial drug concentration and the length of the polymer chain are important for the rate of drug release. The process of diffusion happens through polymeric matrix pores or between polymeric chains. In monolithic matrix systems and reservoir-based systems, drugs are noncovalently bonded within the polymer matrices (Fig. 5).

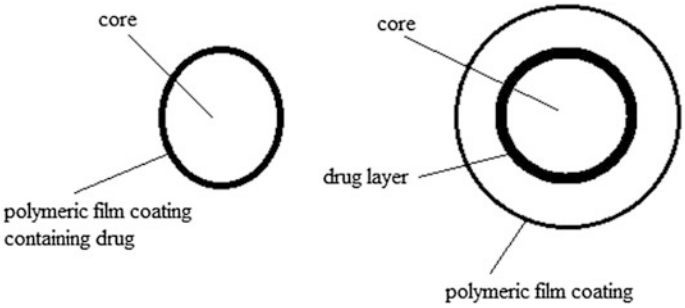

Fig. 5 Matrix system (*left*) and reservoir-based system (*right*)

The viscosity of the polymeric materials used for a matrix system is important. Polymers with a lower value of viscosity release a drug much faster than polymers with higher viscosity values (Brannon-Peppas 1997). The most widely used polymers for matrix systems are cellulose-based polymers or polyethylen oxide and polyethylen glycol. Reservoir systems have been used for taste-masking for acetaminophen and caffeine. Based on morphology, reservoir-based systems can be categorized into three classes: injectables (micro/nanospheres), implants (solid core, thin film) and hydrogels (Yang 2011). Some of the contemporary polymers that are used in the drug delivery process are as follows: poly(urethanes), poly(methacrylic acid), poly(vinyl alcohol), poly(acrylic acid), polyamide, poly(N-vinylpyrrolidone), polylactides, poly(lactide-*co*-glycolides), polyanhydrides, polyorthoesters, and silioxanes.

3 Summary

Polymeric materials have great potential in the field of biomaterials. Their applications in medicine, pharmacology, technology, agriculture, etc., are well-known, and their possibility for improvement is ongoing, since polymeric materials can undergo certain substantive modifications that can improve their properties depending on the application. The most important feature of every implant is biocompatibility with the human organism, so a combination of natural and synthetic polymers in the form of a composite can overcome a lack of biocompatibility of synthetic polymers. The 3D printing technique will provide answers for some specific demands and help in the creation of some unique implants. Another novel aspect of polymers as biomedical implants and devices would be the development of stimuli-responsive polymers and shape memory polymers, materials that will be able to deform upon receiving an external sign. For those purposes, the mechanical characteristics of polymers will be very crucial.

References

Abednejad AS, Amoabediny G, Ghaee A (2013) Surface modification of polypropylene blood oxygenator membrane by poly ethylene glycol grafting. Adv Mater Res 816:459–463
Abednejad AS, Amoabediny G, Ghaee A (2014) Surface modification of polypropylene membrane by polyethylene glycol graft polymerization. Mater Sci Eng C 42:443–450
Adrian JTT, Abhinay M, Inkyu P, Young-Jin K, Woo-Tae P, Yong-Jin Y (2016) Polymeric biomaterials for medical implants and devices. ACS Biomater Eng 2:454–472
Bazaka K, Jacob MV (2013) Implantable devices: issues and challenges. Electronics 2(1):1–34
Brannon-Peppas L (1997) Polymers in controlled drug delivery. Med Plast Biomat
Cools P, Van Vrekhem S, De Geyter N, Morent R (2014) The use of DBD plasma treatment and polymerization for the enhancement of biomedical UHMWPE. Thin Solid Films 572:251–259
Dee KC, Puleo DA, Bizios R (2002) An introduction to tissue-biomaterial interactions. Wiley, Hoboken, New Jersey
Dutta SR, Singh SP, Rathor A (2013) Research article case report: silicone implant in augmentation of saddle nose. Int J Rec Sci Res 4:1661–1662
Espalin D, Arcaute K, Rodriguez D, Medina F, Posner M, Wicker R (2010) Fused deposition modeling of patient-specific polymethylmethacrylate implants. Rapid Prototyping J 16(3):164–173
Hassler C, Von Metzen RP, Ruther P, Stieglitz T (2010) Characterisation of parylene C as an encapsulation material for imlanted neural prostheses. J Biomed Mater Res 93(1):266–274
Hogg A, Aellen T, Uhl S, Graf B, Keppner H, Tardy Y, Burger J (2013) Ultra-thin layer packaging for implantable electronic devices. J Micromech Microeng 23(7):075001
Hossein O, Park K, Sinko P (2011) Martin´s physical pharmacy and pharmaceutical sciences. In: Pharmaceutical polymers, pp 497–500
Joung YH (2013) Development of implantable medical devices: from an engineering perspective. Int Neurourol J 17(3):98–106
Kim CJ (2000) Controlled release dosage form design. Technomic, Lancaster, PA, pp 49–74
Kohn J, Langer R (1996) Bioresorbable and Bioerodible. Materials 64–73
Lee PI, Good WR (1987) Controlled-Release Technology Pharmaceutical Applications, ACS Washington DC
Li X, Kruger JA, Jor JWY, Wong V, Dietz HP, Nash MP, Nielsen PMF (2014) Characterizing the ex vivo mechanical properties ofsynthetic polypropylene surgical mesh. J Mech Behav Biomed Mater 37:48–55
Mashak A, Rahimi A (2009) Iran Polym J 18(4):279–295
Merrill EW, Harris WH, Venugopalan P, Jasty M, Bragdon CR, O'Connor DO (1999) Melt-irradiated ultra high molecular weight polyethylene prosthetic devices. United States Patent 5(879):400
Najafi M, Neishaboury M (2014) Acute immunologic reaction to silicone breast implant after mastectomy and immediate reconstruction: case report and review of the literature. Arch Breast Cancer 1(2):33–36
Parida P, Behera A, Mishra SC (2012) Classification of Biomaterials used in Medicine. Int J Adv Appl Sci. doi:10.11591/ijaas.v1i3.882
Park J, Lakes RS (2007) Biomaterials. An introduction. Springer Science + Business Media LLC, Berlin
Park GE, Webster TJ (2005) A review of nanotechnology for the development of better orthopedic implants. J Biomed Nanotechnol 1:18–29
Pérez-Merino P, Dorronsoro C, Llorente L, Dura´ NS, Jimenez-Alfaro I, Marcos S (2013) In vivo chromatic aberration in eyes´ implanted with intraocular lenses. Invest Ophthalmol Visual Sci 54(4):2654–2661
Ratner BD, Hoffman SA, Schoen JF, Lemins EJ (1996) Biomaterials science: an introduction to materials in medicine. Elsevier Academic Press, London
Ravinder K, Sukhvir H (2014) J Drug Deliv Ther 4(3):32–36

Reja M, Quadir MA, Haider SS (2003) Comparative evaluation of plastic, hzdrophobic and hzdrofillic polymers as matrices for controlled release drug delivery. J Pharm Sci 692:274–291
Ristić B, Popović Z, Adamović D, Devedžić G (2010) Selection of biomaterials in ortopedic surgery. Vojnosanit Pregl Belgrade Serbia 67(10):847–855
Riveiro A, Soto R, del Val J, Comesaña R, Boutinguiza M, Quintero F, Lusquiños F, Pou J (2014) Laser surface modification of ultrahigh-molecular-weight polyethylene (UHMWPE) for biomedical applications. Appl Surf Sci 302:236–242
Rivkin AA (2014) Prospective study of non-surgical primary rhinoplasty using a polymethylmethacrylate injectable implant. Dermatol Surg 40(3):305–313
Saum KA, Sanford WM, DiMario WG, Howard EG (2001) Process for medical implant of cross-linked ultrahigh molecular weight polyethylene having improved balance of wear properties and oxidation resistance. United States Patent 6,316,158 B1
Taylor and Francis (2006) Polym Drug Deliv 1:236
Thakrar AR (2000) Medical devices made from improved polymer blends. United States Patent 6,093,463
Uchegbu IF, Schätzlein AG (2006) Polymers in drug delivery. CRC, New York
Van Ardenne N, Vanderwegen J, Van Nuffelen G, De Bodt M, Van de Heyning P (2011) Medialization thyroplasty: vocal outcome of silicone and titanium implant. Eur Arch Oto-RhinoLaryngology 268(1):101–107
Vicky V (2010) Introduction to polymeric drug delivery. Int J Med Update 5(2):1–2
Yang WW, Pierstorff E (2011) J Lab Autom 17(1):50–58
Zheng F, Xu L, Verbiest L, Verbeken E, De Ridder D, Deprest J (2007) Cytokine production following experimental implantation of xenogenic dermal collagen and polypropylene grafts in mice. Neurourol Urodyn 26(2):280–289
Zhou J, Huang X, Zheng D, Li H, Herrler T, Li Q (2014) Oriental nose elongation using an L-shaped polyethylene sheet implant for combined septal spreading and extension. Aesthetic Plastic Surg 38(2):295–302

Polymeric Biomaterials Based on Polylactide, Chitosan and Hydrogels in Medicine

Aleksandra Mitrovic, Jelena Muncan, Igor Hut, Svetlana Pelemis, Katarina Colic and Lidija Matija

Abstract Polymeric biomaterials represent large and very adaptable class of biomaterials, which makes them very suitable for diversity of biomedical applications. Polymers can be synthesized to have a variety of structures and suitable chemical, physical, biomimetic and surface properties. An overabundance of polymeric biomaterials with different compositions and physicochemical properties have already been developed and investigated; however, there are still many active studies about these materials. This chapter ensures a structural review of biodegradable polymers and discusses their physicochemical characteristics, structure property, applications and limitations in medicine. It is the authors' intent to provide an insight over the available synthetic and natural polymer classes. Some types of polymer materials are less discussed than the other more relevant. A biocompatible, degradable polymer, polylactic acid is very popular so called green 'eco-friendly' material with a most promising development prospect. Besides biocompatibility and biodegradability, natural polymer, chitosan, possess outstanding properties. Hydrogels are super absorbent polymeric materials with one of the main role in health care. For these biopolymers, reviews are referenced to present guidance for further reading.

Keywords Polymeric biomaterials · Polylactic acid · Chitosan · Hydrogels

A. Mitrovic (✉) · J. Muncan · I. Hut · L. Matija
Biomedical Engineering Department, Faculty of Mechanical Engineering, University of Belgrade, Kraljice Marije 16, 11120 Belgrade, Serbia
e-mail: adebeljkovic@mas.bg.ac.rs

S. Pelemis
Faculty of Technology, University of East Sarajevo, Lukavica, Bosnia and Herzegovina

K. Colic
Innovation Center of Faculty of Mechanical Engineering, University of Belgrade, Belgrade, Serbia

F. Zivic et al. (eds.), *Biomaterials in Clinical Practice*,
https://doi.org/10.1007/978-3-319-68025-5_5

1 Polymeric Biomaterials

Despite of the wide use of polymeric biomaterials in medicine, a lot of these materials have failured with functional properties to interface with biological systems. Also they have not been designed for optimized performance. New materials are developing in order to solve such problems in medicine (Peppas et al. 2006).

Biomaterials are necessary in developing the fields such as nanotechnology, tissue engineering, delivery of bioactive agents for treating, repairing, and restoring function of tissues. Biomaterials can be divided into: metals, ceramics, natural or synthetic polymers and composites (Kulshrestha and Mahapatro 2008).

Biomaterials are natural or synthetic substances which have the role to react with biological systems (Williams 2009). This type of materials must possess property of biocompatibility. That means that biomaterials can perform the biomedical task for which they were designed with an appropriate host response (Black 2006).

These materials are progressing very fast year in a year out. The vast diversity of chemical structures, with the possibility of precise control and regulation of molecular design and morphology, allows for the numerous uses of biopolymers in medical applications.

Research into design and potential applications of biocompatible, biodegradable synthetic polymeric biomaterials has led to significant advances in this field (Anderson and Shive 1997; Langer and Tirrell 2004). In biomedicine, particularly in the fields of drug delivery (Zhang et al. 1996; Siepmann and Göpferich 2001) and tissue engineering (Freed et al. 1994; Langer and Tirrell 2004), these polymeric biomaterials have found numerous applications through theoretical and experimental investigations.

Biomaterial history can separate into four eras: prehistory, the era of the surgeon hero (first generation biomaterials), designed biomaterials and engineered devices (second generation biomaterials), and the modern age (third generation biomaterials) (Hench and Polak 2002; Ratner 2004).

This chapter gives an overview those biodegradable polymers that may be helpful in the development of medical implants and tissue-engineered products. Hereinafter, chemical composition of the materials, breakdown products, mechanical properties and clinical limitations of these materials are represented.

2 Introduction

The word “biomaterials” was first introduced within the last 50 years. First types of biomaterials that was used to replace human tissue were supposed to match its physical properties with minimal toxic response in the host (Hench 1980). Nearly 40 years ago, researchers were studying phenomenon of a bioinert tissue response to materials that actively interacted with their environment. Another progress in this second generation was the development of biodegradable materials that showed

controllable chemical breakdown into non-toxic degradation products, which were either metabolized or directly eliminated. When the foreign material was finally replaced by regenerating tissues, in order to resolve the interface problem, scientists started to synthesize biodegradable polymers. At last, the regeneration site was histologically insensible from the host tissue. Resorbable polymers were used in clinical terms as sutures by 1984. Other applications in fracture fixation aids or drug delivery devices appeared quickly. There is still a high long-term prostheses failure rate and need for revision surgery despite substantial clinical success of bioinert, bioactive and resorbable implants (Ratner 2004). First and second generation of biomaterials had a weak point; unlike living tissue, artificial biomaterials do not have ability to respond to change physiological loads or biochemical stimuli. This fact restricts the lifetime of artificial body parts. To prevail these limitations, a third generation of biomaterials is being developed. This implies molecular tailoring of resorbable polymers for specific cellular responses. There was a possibility to mimic the extracellular matrix (ECM) environment and to ensure a cell-adhesive surface by immobilizing specific biomolecules, such as proteins, cell-specific adhesion peptides as well as signaling molecules onto material (Hench and Polak 2002; Drotleff et al. 2004; Lutolf and Hubbell 2005). Synthetic polymer matrices can be also assimilated to deliver drug, signaling molecules, and genetic code and thus provide versatile technologies for regenerative medicine (Saltzman and Olbricht 2002; Segura and Shea 2002; Tabata 2003).

Polymer biomaterials are of great importance in many applications of regenerative medicine, including implants, controlled drug delivery, tissue engineering scaffolds and orthopedic fixation devices (Peters et al. 2011; Hacker and Mikos 2011). Sutures, sensors and non-viral gene delivery vectors are just some of applications of these materials. Numerous, both, synthetic and natural biodegradable biomaterials have been explored and still play a critical role in clinical applications, as well in laboratory research (Lin and Anseth 2013). Many research groups have been studying a different polymeric compounds and have been testing them as degradable biomaterials. However, commercial efforts to develop these new materials for specific medical applications have been limited. Unfortunately, toxicological studies in vivo, mechanism and degradation rate, but also a physicomechanical properties have so far been published for limited number of those polymers (Zhang et al. 2013).

Biodegradable polymers are only those with therapeutically-relevant degradation rates although almost all polymers degrade at some point. Among all, synthetic biodegradable polymers are particularly interesting. Unlike natural biopolymers, synthetic polymers can be synthesized in a highly controllable conditions, with strictly defined material properties and degradability (Middleton and Tipton 2000). Deficiency of immunogenicity of these polymers also enhances their potential in clinical applications. There have been great advances in the design and applications of synthetic polymeric biodegradable materials in the past few decades (Anderson and Shive 1997; Langer and Tirrell 2004). Thermal, mechanical and photodegradation are some of degradation types of biopolymers. In a therapeutically-relevant in vivo environment, hydrolytic or enzymatic degradation are the most common

modes of degradation. Biodegradation represent degradation that involves biological processes, such as body fluids, cellular activities and enzymatic reactions. Therefore, determination of the rate of polymer degradation depends greatly on the conditions of the biological environment (Lin and Anseth 2013).

Many polymers that purport to be 'biodegradable' are actually 'hydro-biodegradable', 'bioerodible', or 'photo-biodegradable'. These different polymer classes belongs to the category of 'environmentally degradable polymers'. The 'biodegradability' of plastics is dependent not only on the material chemical structure but also on the final product constitution. Hence, biodegradable plastics can consist of natural or synthetic resins. Natural biodegradable plastics are primarily based on renewable resources. The example is starch. It can be either naturally produced or synthesized from renewable resources. For example, these are: polysaccharides (chitosan, starch, lignin, cellulose, etc.), proteins (wool, gelatin, silk, etc.), lipids (fats and oil), polyesters derived from bioderived monomers (polylactic acid) and polyesters polyhydroxyalkanoates produced by plant or microorganisms and miscellaneous polymers such as composites, natural rubbers, etc. Non-renewable synthetic biodegradable plastics are based on petroleum. Many natural biodegradable plastics are blended with synthetic polymers to produce plastics which satisfy the functional requirements (Nampoothiri et al. 2010).

Disappearance of implanted foreign materials from the body as a result of their biodegradation is one of the most important advantage of biodegradable polymers. For example, important biodegradable polymers used in biomedical applications are: poly(lactic acid) (PLA), poly(glycolic acid) (PGA), copolymers of polyglycolide, poly(e-caprolactone) (PCL), poly(3-hydroxybutyrate) (PHB), chitosan and soy protein (Edlund and Albertsson 2002; Kamath and Park 1993; Mikos et al. 1994; Park et al. 1992; Taylor et al. 1994; Tsuji and Ikada 1998; Wani et al. 1971).

Synthetic biodegradable polymers are usually based on PLA, PGA, PHB, PCL, poly(hyaluronic acid), and their copolymers, since polymers with these building blocks have admissible toxicological profiles (Juni and Nakano 1987; Anderson and Shive 1997). The main drawback of the use of aliphatic polyesters as carriers for hydrophilic drugs such as proteins is exactly their hydrophobicity (Schwendeman 2002; Jain et al. 1998). Therefore, these biodegradable aliphatic polyesters are usually modified with ethers, urethanes, amides, imides, anhydrides or other functional groups. This process offers opportunity to modify the biomechanical properties of these polymers within a broad range of desired characteristics (Vlugt-Wensink et al. 2006; Babu et al. 2006). The use of biocompatible poly (ethylene glycol) (PEG) as a hydrophilic building block in polylactide or poly (lactide-co-glycolide) polymers enhances their biocompatibility (Peters et al. 2011).

Polysaccharides are natural biodegradable hydrophilic polymers that indicate enzymatic degradation behavior. Polysaccharides have relatively good biocompatibility properties and accordingly biomedical applications. They are insoluble in common organic solvents. Saccharides and polysaccharides contain multiple hydroxyl groups. Hence, they have found utility as hydrophilic and bioactive segments in some hybrid biomaterials. Syntheses of biodegradable polymers having both aliphatic groups and hydrophilic saccharide unit in their main chains have been

reported (Choi et al. 1999; Ydens et al. 2000; Li et al. 1997; Donabedian and McCarthy 1998).

Modification of natural polymers allows them to be useful materials that are required for many functional engineering applications (Rudin and Choi 2013).

3 Poly(Lactic Acid)

Polyesters can be divided according to the monomers structure. In the case of poly (α-hydroxy acids) (PHA) each monomer carries two functionalities, a carboxylic acid and a hydroxyl group. They are located at the carbon atom next to the carboxylic acid (α-position), that form ester bonds. PHA belong to the group of linear thermoplastic elastomers which are produced by ring-opening polymerization of cyclic dimers of the building blocks. PLA, PGA and a range of their copolymers such as poly (lactic-*co*-glycolic acid), PLGA, (Fig. 1) are prominent among the biodegradable polyesters and also biodegradables polymers in general. These synthetic biodegradable materials have a lot of clinical applications. One of the first applications were in the form of resorbable sutures that were made from these materials (Cutright et al. 1971). PHA were also the basis for controlled release systems for drugs and proteins and also for orthopedic fixation devices (Juni and Nakano 1987; Brannon-Peppas 1995; Jain 2000). These polymers were used as porous scaffolds for tissue engineering (Langer and Vacanti 1993).

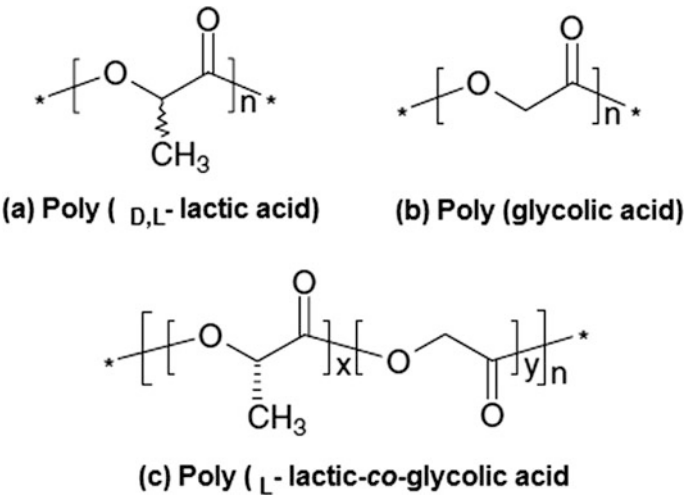

Fig. 1 **a** Poly (lactic acid) (PLA), **b** poly (glycolic acid) (PGA), and **c** range of their copolymers (poly (lactic-co-glycolic acid), PLGA)

3.1 Properties of PLA

Renewable resource generates monomers that possess better mechanical properties and easy processability by conventional methods with non-toxic degradation products. It has made them superior than the other conventional thermoplastics. Non-toxic degradation products are another important requests for any potential application. According to numerous polyesters studies so far, polylactide has proven to be the most attractive and useful class of biodegradable polyesters. This role comes due to several reasons. From a relatively inexpensive raw materials, lactic acid is obtained as the main product in a biotechnological process that usually based on the strain of a lactobacillus (Narayanan et al. 2004). PLA is thermoplastic with a high values of strength and high values of elastic modulus. It can be easily processed by conventional techniques used for thermoplastics like blow molding, injection molding, thermoforming and extrusion. PLA and its copolymers have been investigated in many biomedical studies, especially for resorbable medical implants (Hoogsteen et al. 1990; Vert et al. 1992, 1995; Mainil-Varlet et al. 1997) in the shape of plate, sheet, fiber, screw, beads for bone, rod, sponge, and tissue engineering, microsphere for drug delivery system (Duncan and Kopeček 1984), films or foils for wound treatment (Gupta and Kumar 2007).

It is generally accepted that intermediate PLGA copolymers are more unstable than either homopolymer. Many in vitro and in vivo studies showed revealed satisfying results in the field of biocompatibility of PLA, PGA and PLGA (Athanasiou et al. 1996). For that reason, PLA, PGA and PLGA copolymers belong to the group of biodegradable polymers with FDA approval for human clinical use. Accumulation of acidic degradation products that can have damaging effects on encapsulated drugs in delivery applications is one of the main problem in the case of poly(α-hydroxy esters) (Brunner et al. 1999; Lucke et al. 2002). Likewise, when released in a sudden burst upon structure breakdown it can cause late non-infectious inflammatory responses (Simon et al. 1997).

In the cases of orthopedic and oral surgeries, for production of devices of high mechanical strength such as fixation of augmentation devices, PLA of high molecular weight is utilized. When it is utilized as a carrier for drug delivery systems, such high molecular weights are not necessary. In such pharmaceuticals applications, lactide copolymers of low molecular weights are usually utilized since shorter degradation time results in better release property. PLA degrades by hydrolysis of the ester bond. Enzymes are not necessary to catalyze hydrolysis. The degradation products of PLA are non-toxic to the living organisms (Hacker and Mikos 2011), since lactic acid occurs itself in the metabolism.

Due to the chiral nature of lactic acid, several forms of poly (lactid acid) exist. Poly (L-lactic acid) (PLLA) is synthesized from dilactide in the L form. PLLA is a semicrystalline polymer with 37% of crystallinity. PLLA is characterized by a glass transition temperature between 50 and 80 °C and a melting temperature between 173 and 178 °C. The polymerization of racemic dilactide leads to poly (D, L-lactic acid) (PD,LLA), which is an amorphous polymer (Hacker and Mikos 2011).

Due to more coherent and compact structure, PLLA of same molecular weight has better mechanical properties and longer service time than PD,LLA. Since the higher degree of crystallinity is achieved by annealing, annealed PLLA has better mechanical properties than un-annealed PLLA (Perego et al. 1996). A various values of degradation rates, physical and mechanical properties can be achieved if molecular weights and composition in its copolymers are modified.

Semicrystalline PLLA is usually used in applications where high mechanical strength and toughness are required (e.g. for sutures and orthopedic devices). Amorphous PD,LLA is typically used in drug delivery applications (Hacker and Mikos 2011).

Polymer degradation occurs through rupture of the main chains or side chains of macromolecules. In nature, polymer degradation is caused by hydrolysis, thermal activation, biological activity (i.e., enzymes), oxidation, photolysis or radiolysis (Müller 2008). PLA degradation depends on a many different factors, such as molecular weight, temperature, pH, crystallinity, purity, water permeability, presence of terminal carboxyl or hydroxyl groups and additives acting catalytically (Park and Xanthos 2009).

Different techniques, i.e. optical microscopy, optical rotation (Gonzalez et al. 1999), mercury-intrusion porosimetry (Lu et al. 2000), dynamic light scattering (Zweers et al. 2004), X-ray scattering (Gonzalez et al. 1999), scanning electron microscopy (Park et al. 1995) and differential scanning calorimetry (Yoo and Smith 2004; Vey et al. 2007) are using to analyzed the physical changes as a function of the degradation of cross-linked materials. Chromatographic methods are used for release studies of drugs after simulating the appropriate degradation medium and conditions (Park et al. 1995; Pişkin et al. 1995). Drug mobility and drug-polymer interaction can be established by nuclear-magnetic resonance (NMR) spectroscopic methods (Tomić et al. 2008).

3.2 Copolymers, Blends and Composites of PLA

Since PLA has good mechanical properties, it may slowly broke down into non-toxic metabolites by bio-organisms. The degradation kinetics, initial mechanical properties and a balanced course of time between the degradation and its strength change are necessary characteristics. Also, very important factor is the environment to which it was exposed during or after their practical use as well as application of the biodegradable polymer. However, the ranges of their application are slightly limited because of crystallinity, high rigidity, difficult control of the hydrolysis rate and poor hydrophilicity. In an attempt to overcome these problems, different types of PLA blends with other biodegradable polymers have been investigated, e.g. chitosan, starch, polyethylene glycol, PLC, etc. PLA is often blended with starch to increase biodegradability and reduce costs. In PLA–starch blend, a basic parameter that determines mechanical properties of the blend is starch concentration. As starch concentration and the moisture increases, values of tensile

strength and elongation decreases. Starch is sensitive to water since it is hydrophilic polymer. PLA is hydrophobic and therefore water resistant. Novon is commercialized name for mixtures of PLA blends and starch (10–20%) (Ecostar, Germany). PLA is a brittle material with low possible elongation. Adding the starch into such a material results in even more brittle material. Also, the blend of plasticized PLA with thermoplastic starch shows a small degree of compatibility with the radically decrease in mechanical properties (Martin and Avérous 2001). The blend shows the similar behavior with hydrophobised starch (Kozlowski et al. 2007).

To improve the quality and reduce the production cost, lactic acid polymerizes with PLA blend or other monomers and polymers. A copolymer, poly (lactic-glycolic acid), has clinical application and the approval of FDA for this use. The compound so called VICRYL (Ethicon Inc.) is composed of lactic acid and glycolic acid in 2:23 ratio (Ramzi et al. 2015). Controlled drug release is the most important application of this copolymer. The ester linkages in PLA are sensitive to process of chemical hydrolysis and also enzymatic chain cleavage.

Other isomer PLA and for example polymers: poly (ethylene oxide) (Nijenhuis et al. 1996), poly (vinyl acetate) (Gajria et al. 1996), poly (ethylene glycol) (Sheth et al. 1997) can create miscible blend with one type of PLA. It is used as a matrix in biocomposites combined with natural fibers since PLA is still quite expensive. Compared to PLA, Jute-PLA composite has values of tensile strength and tensile modulus that increases with a slight reduction in the elongation at maximum stress. Poly (L-lactic acid)-poly(L-lactic acid-co-citric acid)-poly(ethylene glycol) multiblock copolymers (PLLA–PLCA–PEG) were synthesized through polycondensation reaction. Wang and coworkers were studied properties of the scaffolds such as swelling, degradation behavior, morphology and mechanical moduli (Wang et al. 2007). Results show that the mechanical flexibility improves, as the content of PLLA–PLCA–PEG copolymers in the scaffolds increases. The study indicates that the modification of PLLA scaffold with PLLA–PLCA–PEG may have application in tissue engineering.

Chitosan is considered to be one of the most promising biopolymer used in tissue engineering, wound healing, drug delivery agents, blood anticoagulants, scaffolds and burn treatment. It is known that biodegradability, biocompatibility and antibacterial are necessary properties of biopolymers. It should neither cause inflammation to human tissue nor induce antibody from the immune system (Tomihata and Ikada 1997). These properties enable this polysaccharide to be used with PLA. PLA and its copolymers have high values of initial strengths. In contrast, natural products like chitin and its derivatives like chitosan possess low mechanical strength but excellent cell adhesion (Chen et al. 1997). High crystallinity and low hydrophilicity of PLA decreases its degradation rate which results in poorer soft tissue compatibility. Melting the blend of PLA and chitosan reduces the values of tensile strength and elongation. Hence, there is an increase in the elastic modulus, without any noticeable miscibility (Correlo et al. 2005). Similar results were obtained when PLA and chitosan were blended in solution. Chloroform and acetic

acid were used as solvent (Suyatma et al. 2004). However, the miscibility and intermolecular hydrogen bonding (Chen et al. 2005) were shown when PLA and chitosan were blended by solution–precipitation method.

3.3 Application

Synthetic polymers such as polylactide, polyglycolide and their copolymers have application in tissue engineering especially in the field of construction of temporary scaffolds for the of cartilage (Ma and Langer 1999; Hutmacher 2000), bone (Winet and Bao 1998; Whang et al. 1998), tendon (Cao et al. 1994), skin (Beumer et al. 1994; Zacchi et al. 1998), liver (Kaufmann et al. 1997) and heart valve (Zund et al. 1997).

PLA has wide applications in biomedical fields, including suture, bone fixation material, drug delivery system protein encapsulation and delivery (Hu et al. 2003; Singh et al. 2001; Castelli et al. 1998; Ouchi et al. 2004; Romero-Cano and Vincent 2002; Olivier 2005), microsphere (Kim et al. 1998; Murakami et al. 2000; Matsumoto et al. 1999; Gonsalves et al. 1998; Deng et al. 2002; Pluta et al. 2002; Lacasse et al. 1998), hydrogels (Li 2003) and tissue engineering (Zhao et al. 2004; Mehta et al. 2005). Poly(esters) based on poly(lactic acid), poly(glycolic acid) and their copolymers, also poly(lactic acid-co-glycolic acid) represent the best biomaterials in terms of design and performance in drug release in a controlled manner.

PLA, PGA and their copolymers can combine with bioactive ceramics, such as Bioglass particles or hydroxyapatite. This combination of the materials stimulate bone regeneration and improve the mechanical strength of the composite material (Rezwan et al. 2006). Scientists have found that composites of polymer and Bioglass are angiogenic (e.g. they supported the growth of blood vessels). A novel approach for providing a vascular supply to implanted device has been suggested (Day et al. 2005).

3.4 PLA—Challenges

The price of PLA is definitely the major concern. Several issues are referring to the biotechnological production of lactic acid. That includes the development of high-performance lactic acid producing the microorganisms but also lowering the costs of raw materials and fermentation processes. The biotechnological processes for the production of lactic acid should be improve by making cheap raw materials competitive with the chemically derived one (John et al. 2007). One of the main challenges to widespread the use of bio-based polymers is to achieve mechanical and barrier properties comparable to conventional synthetic polymers. Of course,

biodegradability has to be maintained. Inferior moisture of bio-based polyesters, compared to those of synthetic polymers, presents limitation for effective commercialization. Therefore, it is very important that during the manufacturing, shipping, storage and end-use of polylactide products, process of moisture penetration and hydrolytic degradation is controlled (Cairncross et al. 2006). The synthesis of recyclable and degradable polymers, like PLA, that have a highly cross-linked three-dimensional network structure is crucial for supporting a green sustainable society.

4 Chitosan

Beside biocompatibility and biodegradability, chitosan is a inimitable biopolymer that shows outstanding properties. It is derived from natural polymer, chitin. The presence of primary amines along the chitosan backbone is the main factor that gives this biopolymer remarkable properties. Hence, this polysaccharide is a most desirable representative in the field of biomaterials, especially for tissue engineering (Croisier and Jérôme 2013).

Chitosan is a linear, semi-crystalline polysaccharide. It consist of (1→4)-2-acetamido-2-deoxy-β-D-glucan (*N*-acetyl D-glucosamine) and (1→4)-2-amino-2-deoxy-β-D-glucan (D-glucosamine) units. Figure 2 represents the structure of this biopolymer. Unfortunately, chitosan is not very common in the environment. Nevertheless, it is easily derived from the chitin (Fig. 3) in its reaction of partial deacetylation (Croisier and Jérôme 2013).

After cellulose, chitin is the second bountiful biopolymer (Rinaudo 2006). It is commonly found in invertebrates—as crustacean shells or insect cuticles. Chitin also exists in some mushrooms envelopes, green algae cell walls and yeasts (Rane and Hoover 1993; Aranaz et al. 2009, 2010). It is difficult to predict chitosan characteristics during its production (Croisier and Jérôme 2013).

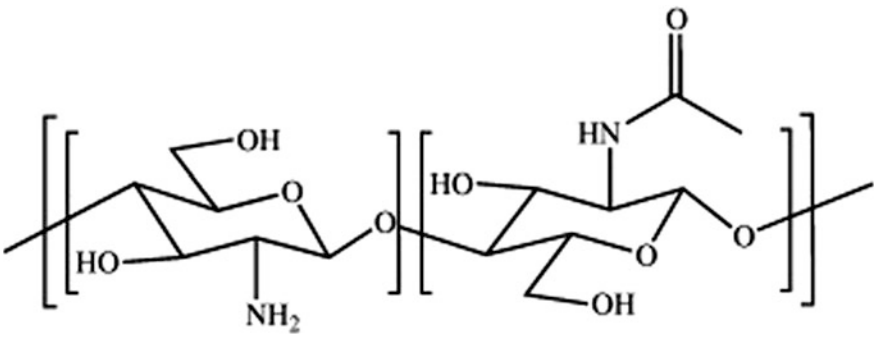

Fig. 2 Chemical structure of chitosan

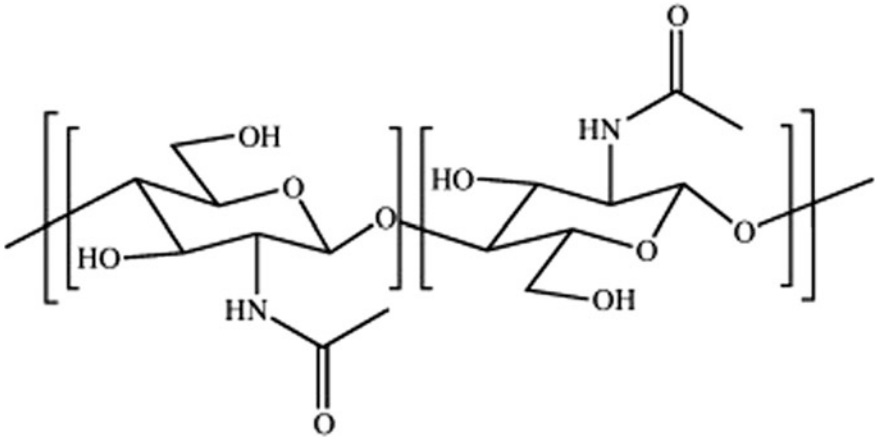

Fig. 3 Chemical structure of chitin

4.1 Properties of Chitosan

Chemical modification of chitosan produces materials with a variety of physical and mechanical properties (Muzzarelli et al. 1988; Wang et al. 1988; Laleg and Pikulik 1991). For example, chitosan films and fibers can be synthesized by cross linking. This reaction comes from techniques for altering other polysaccharides, such as treatment of amylase with epichlorohydrin (Wei et al. 1977). Like hyaluronic acid, chitosan is not antigenic and is a well-tolerated implanted material (Malette et al. 1986).

Frequently, organic and inorganic impurities are contaminating the chitosan since it is natural-based compound. Polydispersity is one of important chitosan characteristics. Producers mostly refer to samples viscosity rather than molecular mass due to this property. One of the chitosan shortcomings is poorly solubility. It is relatively soluble only in acidic medium which makes analyzes difficult to perform. Experimental technique such as UV-spectroscopy, IR-spectroscopy (Tarek et al. 2016), 1H NMR spectroscopy, pH-potentiometric titration, colloidal titration and enzymatic degradation (Croisier et al. 2013) are usually used for studying the properties of chitosan like the determination of chitosan deacetylation degree. Unlike chitin, presence of amino groups in the chitosan structure (Fig. 2) gives to this biopolymer many peculiar properties. The amino groups of the D-glucosamine residues can be protonated so diluted acidic aqueous solutions become more soluble (pH < 6) (Leedy et al. 2011). Due to its very poor solubility, chitin does not have a wider practical applications (Pavinatto et al. 2010). Chitosan with protonated amino groups becomes a polycation that can afterwards form ionic complexes with a wide diversity of natural or synthetic anionic species (Madihally and Matthew 1999). Those species are usually proteins, lipids, DNA, and some negatively charged synthetic polymers such as poly(acrylic acid) (Madihally and Matthew 1999;

Pavinatto et al. 2010; Takahashi et al. 1990; Kim et al. 2007). Chitosan presents the only positively charged, naturally occurring polysaccharide (Pavinatto et al. 2010). As a polyelectrolyte, chitosan can considerably be employed for the preparation of multilayered films, using layer-by-layer deposition technique (Decher 1997). This natural polymer can form stable covalent bondings with other species due to amino and alcohol groups along chitosan chains. Chitosan has other outstanding inherent properties such as antibacterial activity (Sudarshan et al. 1992; Ong et al. 2008), along with antifungal (Aranaz et al. 2009), mucoadhesive (Lehr et al. 1992), analgesic (Aranaz et al. 2009) and haemostatic properties (Yang et al. 2008). Also, one of the most important advantage of chitosan is that biodegrades into non-toxic residues (Bagheri-Khoulenjani et al. 2009; Vårum et al. 1997). The rate of its degradation is mostly depends on the molecular mass of chitosan, its deacetylation degree and the distribution of *N*-acetyl D-glucosamine residues (Aiba 1992; Tomihata and Ikada 1997). Degree of deacetylation of chitosan is a parameter that can easily be varied.

To some extent, it has proved biocompatibility with physiological medium (VandeVord et al. 2002; Sashiwa and Aiba 2004). Due to its remarkable properties, chitosan represents one of most promising biopolymer in the field of medicine.

Chitosan is actually degraded in vivo by several proteases and mainly through lysozyme, which acts slowly to depolymerize the polysaccharide (Aranaz et al. 2009; Dash et al. 2011; Kean and Thanou 2009). Until now, eight human chitinases have been identified. However, enzymatic activity on chitosan have found only among three of them (Pangburn et al. 1982; Funkhouser and Aronson 2007). Process of chitosan biodegradation gives non-toxic products. After this biodegradation process, these products such as oligosaccharides of variable length, might get into in metabolic pathways or be further exuded (Pangburn et al. 1982).

4.2 Application

Chitosan has application in tissue-engineering as form of membranes and matrices and also as conduits for guided nerve regeneration (Bini et al. 2005; Sundback et al. 2003; Hirano 2001). Chitosan matrix manipulation can be achieved using the inherent electrostatic properties of the molecule. Chitosan chains are extended via the electrostatic interaction between amine groups whereupon orientation occurs. This process occurs at low values of ionic strength. As ionic strength is increased and chain-chain spacing decreases the consequent enhances in the junction zone and stiffness of the matrix result in upgrowth average pore size. For applications such as encapsulation, cell culture, membrane barriers, contact lens materials and inhibitors of blood coagulation different forms of chitosan are investigated. For example, chitosan was tested and used in the form of gels, powders, films and fibers (East et al. 1991).

Croisier and Jérôme have shown the main advantages and disadvantages of the chitosan biomaterials in the field of biomedicine (Table 1). Hence, this

Table 1 Main advantages, disadvantages and applications of the chitosan biomaterials presented (Croisier and Jérôme 2013)

Biomaterial type	Hydrogels (3D)	Sponges (3D)	Films (2D)	Porous membranes (2D)
Specifications	Physically associated (reversible) Chemically cross-linked (irreversible)	Free-standing	Thin (Langmuir–Blodgett, LB) Thin (layer-by-layer, LBL)	Nanofibers
Main advantage(s)	Soft flexible non-toxic Soft flexible stable Controlled pore size	High porosity Soft	Material coating Multilayer construction	High porosity Mimic skin extracellular matrix
Main disadvantage (s)	Not stable (uncontrolled dissolution may occur) Low mechanical resistance Pore size difficult to control May be toxic Crosslinking may affect chitosan intrinsic properties	May shrivel Low porosity	Laborious for the construction of multilayers Many steps	Electrospinning (ESP) of pure chitosan difficult
Main biomedical application(s)	Tissue replacements/engineering drug/growth factor delivery	Tissue engineering (filling material)	Wound dressings skin substitutes Coatings for a variety of scaffolds wound dressings skin substitutes	Coatings for a variety of scaffolds wound dressings skin substitutes

polysaccharide is very attractive for biomedical uses, notably in tissue engineering. As it can be seen in Table 1, outstanding properties of chitosan and processed materials gives them a chance for promising future.

5 Hydrogels

Hydrogels comprise a large group of polymeric materials with the very hydrophilic three-dimensional polymer structure capable of absorbing and holding considerable quantities of water. These materials are very suitable for biological applications because of their high water content and biocompatibility. Over the last couple of decades, they have attracted a great deal of attention which galvanized significant progress in the areas of the design, synthesis and applications for biomedical purposes. Recent developments include the design and synthesis of novel hydrogels and their use in tissue engineering, drug delivery, and nanomedicine.

Hydrogels are cross-linked, three-dimensional polymer networks that can absorb large amounts of water or aqueous solutions in general. The amount of water, usually comprise at least 20% of the total hydrogel weight. If water amounts to more than 95% of the total weight, then the hydrogel is called superabsorbent (Park and Park 1996). The most important property of hydrogels as materials is that they swell in the presence of water or aqueous solutions, but collapse in the absence of it. The magnitude of swelling depends on the nature of polymer chains and the crosslinking density of polymer network. The drying of hydrogel leads to collapsing of swollen network due to the high surface tension of water. In its dried state hydrogel (or xerogel) becomes much smaller in size than the hydrogel swollen in aqueous solution. During swelling and collapsing of the hydrogel its shape can be preserved.

Novel approaches in hydrogel design have led to development of hydrogels with swelling and shrinking property engineered to be a response to a signal from the environment (Fig. 4). These hydrogels with additional functions are called "smart (or intelligent) hydrogels" (Takagi et al. 1993). The most well-known smart hydrogels are those which respond with either swelling, shrinking, bending or degradation to changes in environmental conditions. The signals from the environment which are known to cause volume change in hydrogels are: pH, temperature, electric field, ionic strength, salt type, solvent, stress, light and pressure (Park and Park 1996; de Lima et al. 2015).

In order to preserve the three-dimensional network structure of the hydrogel in their swollen state, polymer chains are usually cross-linked—chemically or physically. Depending on the type of the cross-linking used, the hydrogels can be classified into two categories based on the nature of the crosslink junctions: chemically cross-linked networks have permanent junctions, while physical networks have impermanent or transient junctions that arise from either entanglements

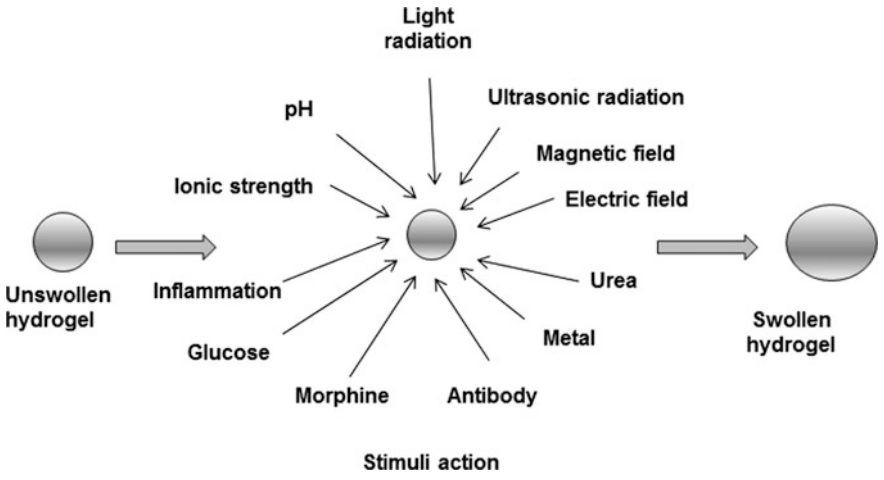

Fig. 4 Stimuli responsive swelling of hydrogels [adapted from Gupta et al. (2002)]

of polymer chains or physical interactions such as ionic interactions, hydrophobic interactions or hydrogen bonds (Jen et al. 1996).

The high water content of hydrogels makes them biocompatible with a majority of biological tissues. They are soft and adaptable, resulting in minimized damage to the surrounding tissue during and after implantation procedure (Dash et al. 2011). The mechanical properties of hydrogels strongly resemble those of the soft biological tissues, which results in successful mimicking of their functional and morphological properties (Dash et al. 2011). This is the reason why hydrogels are often utilized as biomedical scaffolds for tissue replacements, but they have numerous other biomedical applications as well, such as delivery systems for drugs and growth factors (Muzzarelli and Muzzarelli 2005; Drury and Mooney 2003; Seol et al. 2004).

Hydrogels can also be classified into two groups according to their natural or synthetic origin (Lee and Mooney 2001). Thus, they can be made of natural biopolymers, synthetic polymers or their hybrids. Hydrogels of natural origin are purified from natural sources and they may be further modified in the laboratory. Natural polymers used in hydrogel synthesis include materials such as proteins—collagen and gelatin, polysaccharides such as agarose and alginate, hyaluronic acid, fibrin and chitosan. Synthetic hydrogels are completely synthesized in the laboratory and they are traditionally made of polymers using chemical polymerization methods. Some examples of often used synthetic hydrogels include poly(hydroxyethyl methacrylate) (PHEMA), poly(ethylene glycol) (PEG)-based materials, such as polyacrylamide (PAAm), as well as PEG diacrylate (PEGDA) based gels.

In general, synthetic materials allow for more fine-tuned control over molecular weight numbers and distributions, as well as crosslinking densities, allowing for precise modulation of specific mechanical properties such as Young's module or stiffness. Natural hydrogels, on the other hand, often have an innate bioactivity that aids with cell and tissue integration and biocompatibility (Skardal 2014).

5.1 Natural Hydrogels (Biological Hydrogels)

Natural hydrogels have specific properties and can be used for various purposes depending on their origin and composition. Majority of natural polymers used for synthesis of these hydrogels are derived from numerous components of the mammalian extracellular matrix, like collagen or gelatin, hyaluronic acid and fibrin. Collagen is the main structural of connective tissues in mammals, gelatin is obtained by thermal denaturation of collagen, fibrin is fibrous, non-globular protein involved in the clotting of blood, while hyaluronic acid (hyaluronan) is carbohydrate, more specifically polysaccharide that is found in nearly all mammalian tissues and fluids. Other polysaccharides also used in natural hydrogel design are alginate and agarose, and these are derived from marine algae sources. Chitosan is another naturally occurring linear polysaccharide derived by deacetylation of chitin, which is the structural element in the exoskeleton of crustaceans and cell walls of

fungi. Chitosan can be physically associated, coordinated with metal ions or chemically cross-linked into hydrogels, giving two types of hydrogels with reversible gelation and one with irreversible (based on chemical modification) gelation (Dash et al. 2011).

The main advantages of natural hydrogels compared to synthetic ones are low toxicity and biocompatibility because the natural polymers used for their synthesis are either components of or have macromolecular properties similar to the natural extracellular matrix (Barbucci 2009).

5.2 *Synthetic Hydrogels*

Synthetic hydrogels are appealing for biomedical applications because of their one advantage comparing to natural hydrogels—their chemistry and consequently their properties that can be controlled and reproduced according to the specific requirements and needs. For example, synthetic polymers can be reproduced to have specific molecular weight, block structure, crosslinking modes and degradable linkages. All these properties in turn, determine formation dynamics of hydrogel, the crosslinking density as well as mechanical and degradation properties (Barbucci 2009).

Polymer networks can be synthesized using various chemical methods (based on heat (thermal initiated polymerization) or light e.g., photo-initiated polymerization). Design and synthesis of polymer networks can be done in a controlled manner, on the molecular-scale of the structure with specifically tailored properties such as biodegradation or mechanical strength, chemical and biological response to stimuli in order to meet specified requirements (Peppas et al. 2006).

Neutral synthetic polymers can be generated from derivatives of PHEMA, PEG, and PVA (Peppas et al. 2006). Their chemical structure is presented in Figs. 5, 6 and 7 respectively.

One of the first produced and today most widely used synthetic hydrogel is PHEMA. Since its initial discovery and production it has been modified with many natural and synthetic substances and by various methods, and has been applied mostly for the contact lenses production, wound dressings, drug delivery systems

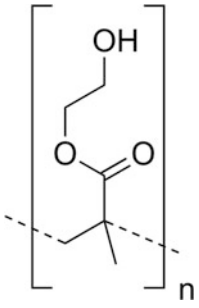

Fig. 5 Poly(hydroxyethyl methacrylate) chemical structure

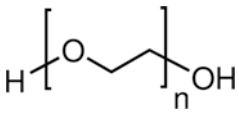

Fig. 6 Poly(ethylene glycol) (PEG) chemical structure

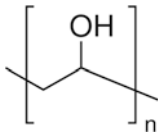

Fig. 7 Poly(vinyl alcohol) (PVA) chemical structure

and in tissue engineering (Sefton et al. 2000). The most appealing properties of PHEMA include its mechanical properties, optical transparency, and its stability in water. The properties of PHEMA depend on many things, namely: the method of synthesis, polymer content, the degree of cross-linking, temperature and final application environment. The synthesis can be carried out with simultaneous cross-linking by UV-radiation and the final products are produced as films or membranes (Gibas and Janik 2010).

In order to achieve desired properties depending on the specific purpose, various modifications have been introduced to PHEMA structure. For example, modulation of degradation properties have been achieved by synthesis of dextran-modified PHEMA gels (Meyvis et al. 2000). Also, copolymerization of HEMA monomers with other monomers, such as methyl methacrylate, can be used to control swelling properties and mechanical properties.

PEG hydrogels are one of the most well-known and studied materials for biomedical application purposes. They are very attractive from the aspect of biocompatibility because they are not toxic, do not provoke an immune response in the body, and they are chemically inert to most biomolecules such as proteins. To enhance biocompatibility of PEG hydrogels, various different forms of PEG surface modification have been used in order to create protein-resistant surface (Ratner 2004). Most common methods used for PEG surface modification include covalent bonding through silane, acrylate, and thiol linkages, adsorption, and ionic and hydrogen bonding (Ratner 2004; Whitesides et al. 2001).

PVA hydrogels are stable, and elastic gels that can be formed by the repetition of freezing-thawing process or by chemical cross-linking (Nuttelman et al. 2001; Kenawy et al. 2014). They can be formed by both physical and chemical crosslinking methods, where those versions which are physically crosslinked are biodegradable due to reversible gelation, and can therefore be used for various biomedical applications (Peppas et al. 2006). In order to be suitable for desired application PVA hydrogels must have stable 3D network which is done by cross-linking achieved by chemical or physical methods. PVA-based hydrogels have excellent mechanical properties and distinctive ability to retain water in the structure, thus ensuring a prolonged moist environment. Polyvinyl alcohol hydrogels have numerous applications such as in manufacturing of contact lenses,

reconstruction and regeneration of cartilage, artificial organs, drugs systems and wound dressings (Lee and Mooney 2001; Lee et al. 2001).

5.3 *Biohybrid Hydrogels*

Hybrid hydrogels or as they are usually known—hydrogel systems, possess components from at least two specific classes of molecules: synthetic polymers and biological macromolecules, which are interconnected covalently or non-covalently (Kopeček et al. 2001). By integrating biological entities with synthetic hydrogels, novel synergistic systems can be created.

Hydrogels have been synthesized so that they contain functional groups which promote cellular adhesion. In this scheme, the addition of such modalities can result in dramatic change of the hydrogel properties. Amino acid sequences extracted from natural proteins are the most common peptides used for modification of hydrogels. Using these approaches, PEG and other hydrogels, such as alginate have been modified for enhanced cellular adhesion (Hern and Hubbell 1998; Burdick and Anseth 2002; Burdick et al. 2004; Rowley et al. 1999).

PVA gels have also been modified to enhance cellular adhesion by incorporation of amino acid sequences for the purpose of stimulated adhesion of hepatocytes and epithelial cells (Kobayashi and Ikada 1991; Kawase et al. 1999).

In addition, the degradation properties of hydrogels can also be modified by using degradable linkers. Many synthetic gels have been modified in various ways to change their properties; one of the most common form of modification is introduction of the degradable units to make them degradable (Peppas et al. 2006). One such example is incorporation of dextran into PHEMA gels in order to make them enzymatically degradable (Meyvis et al. 2000). Another often used form of modification is the incorporation of growth factors which can be covalently bound to the hydrogels. Mann et al. (2001) have incorporated transforming growth factor beta (TGF-β) in PEG hydrogels to help control smooth muscle cell function.

Natural monomers such as peptides have been used to synthesize hydrogels with desired properties. Growth of genetic engineering resulted in approaches to synthesize artificial peptides and proteins for the specific purposed fabrication of hydrogels. However, polypeptides designed using genetic engineering show many advantages over synthetic peptides, such as environmentally controlled self-assembling properties (Tirrell 1996; Petka et al. 1998; Wang et al. 1999).

Although current methodologies to synthesize the hydrogels are expensive, it is anticipated that the recent progress in materials science will lead to enhancement of such techniques making the production of gels economically feasible (Peppas et al. 2006; Vermonden and Klumperman 2015).

5.4 Biomedical Applications of Hydrogels

The applications of hydrogels in biomedicine are diverse ranging from tissue engineering, controlled drug delivery to diagnostic devices (Baek et al. 2013; Fusco et al. 2015).

From a practical biomedical perspective, the main areas of hydrogel applications are as materials for contact lenses, wound dressings, drug delivery systems, tissue engineering, and hygiene products (Caló and Khutoryanskiy 2015).

The very first use of hydrogels in biomedical field was for contact lenses and intraocular lenses. Soft contact lenses made of hydrogels possess desirable properties such as high oxygen permeability and transparency, but protein deposits and lens spoliation still pose a significant problem in application (Myers et al. 1991). Soft intraocular lenses have advantages over rigid types because of their flexibility and softness, which allow smaller surgical incisions during inserting and thus less invasive surgery (Carlson et al. 1993).

In biomedical applications hydrogels are highly valued for many of their remarkable properties: they can provide immediate pain control effect, they are easy to handle and can be easily replaced. These materials have high transparency, they provide good barrier against bacteria, good adhesion, excellent water absorption ability and oxygen permeability; they allow easy control of drug dosage and prevention of loss of body fluids (Higa et al. 1999; Şen and Avcı 2005; Roy et al. 2010a, b, c; Saha et al. 2011). Hydrogel based wound dressings have become a very interesting field of research with the objective of development of various user-friendly medical devices.

Numerous research studies proved that a moist wound environment is best for wounds to heal properly (Winter and Scales 1963; Martineau and Shek 2006; Yang et al. 2010). Hydrogels are commonly used as wound dressing materials, since they are flexible, durable, non-antigenic, and permeable to water vapor and metabolites, while securely covering the wound to prevent bacterial infection (Corkhill et al. 1989).

Hydrogels are also used for coating of urinary catheter surface to improve its biocompatibility and provide smooth, slick surface as well as for prevention of bacterial adhesion (Nigam et al. 1988; Graiver et al. 1993).

The potential applications of hydrogels in sterilization and cervical dilatation have also been explored as dilatation of the cervical canal is necessary for the first trimester-induced abortion by suction curettage (Molin and Brundin 1992).

One of the recent, advanced applications of hydrogels is in the development of artificial muscles. Smart hydrogels which can transform electrochemical stimuli into mechanical work can be used like artificial muscles and generate functions like the human muscle tissue. Smart materials that emulate the contractions and secretions of human organs in response to changes in environmental conditions may soon find a use in medical implants, prosthetic muscles or organs, and even robotic grippers (Park and Park 1996).

Due to their unique properties, hydrogels seem especially suitable for development of controlled drug delivery systems. When the drug loaded hydrogel comes in contact with aqueous environment, water penetrates into the system and dissolves the drug. Diffusion is the underlying process by which the dissolved drug is released from the delivery system into the surrounding aqueous medium. Hydrogel materials have been used for a wide spectrum of controlled drug-delivery applications. They can be considered as intelligent carriers because release of the drug is controlled by the conditions of the environment, and with incorporation of enzymes hydrogels can be made responsive to changes in levels of various blood analytes. The same properties that make hydrogels attractive for controlled drug-delivery, can also be applied for delivery of imaging agents and targeting in controlled imaging applications (Peppas et al. 2006).

Hydrogels, especially injectable systems (Patenaude et al. 2014; Nguyen et al. 2015), are very appealing biomedical materials due to the easiness and comfort of their application, their structural similarity to extracellular matrix, and their good biocompatibility because they are directly encapsulated by cells due to high water contents. It is no longer believed in tissue engineering that the biomaterial itself has to provide mechanical properties comparable to the diseased tissue; the polymer rather has to promote remodeling of damaged sites and tissue regeneration in vivo in a way that the regenerated tissue is histologically and functionally indistinguishable from the surrounding tissue.

Hydrogels might be superior to hydrophobic polymers in that regard, as they have higher rate of degradation which solves the problem of non-functional fibrous tissue formation on the polymer–tissue interface. Also, hydrogel breakdown can be synchronized with cell proliferation and migration by using enzymatically cleavable crosslinker (Hacker and Mikos 2011).

6 Future Perspectives

In the last twenty years, many advances have been made in the fields of structured materials, intelligent materials and nanomaterials science. The variety of chemical structures, together with the precise control of the molecular architecture and morphology, explain the numerous uses of polymers in high technology and biological applications. Significant interest has been shown in the use of natural, synthetic and biohybrid hydrophilic polymers as biomaterials and as carriers for drug delivery. Hence, it is necessary to expand the studies and understanding of the fundamental phenomena and molecular mechanisms combined, and perfect the design and formation of new surfaces and interfaces to solve technology problems for high performance materials.

The need to improve patient care is always present in medical diagnostics and therapeutics; accordingly, there is a continuous effort to enhance methods, materials, and devices. The development of novel biomaterials and their application to medical problems have drastically improved the treatment of many diseases

(Langer and Peppas 2003; Langer 2000). Despite the widespread use of materials in medicine, many biomaterials still lack the desired functional properties to interface with biological systems and there are still several challenges to overcome before clinical translation (Buwalda et al. 2014). There is still much room for improvement as they are still not engineered for optimized performance. Therefore, there is an increasing need to develop new materials to inscribe such problems in medicine and biology.

This development will occur through synthesis of new polymers or by modifying natural polymers. With respect to drug delivery, the continued development of "smart" biocompatible materials that can respond to their environments will provide new and improved methods of delivering drug molecules. Finally, advancing the knowledge and the use of hydrogels and smart polymers for nanotechnology is an important area with notably potential that remains to be fully investigated. The incorporation of functional hydrogels into micro-devices and the use of micro-devices to engineer hydrogels will continue to provide new methods for fabricating improved hydrogel based systems (Peppas et al. 2006).

We must gain a much deeper insight into the biological principles to understand all of the phenomena that are involved in small cellular events. One of the examples is the transfer of genes by viruses or the process of adhesion and differentiation of cells on biocompatible surfaces. Hopefully, some of the future developments will lead to development of therapeutic solutions for various diseases, which current medicine still lacks and allow achievement of generally better worldwide healthcare. With the continuing development of new materials and novel methods of engineering mechanical, chemical and biological functionalities we can expect that in the future hydrophilic polymers will play an even greater role in biomedical applications and nanomedicine (Peppas et al. 2006; Gaharwar et al. 2014).

References

Aiba S (1992) Studies on chitosan: 4. Lysozymic hydrolysis of partially N-acetylated chitosans. Int J Biol Macromol 14(4):225–228

Anderson J, Shive M (1997) Biodegradation and biocompatibility of PLA and PLGA microspheres. Adv Drug Delivery Rev 28(1):5–24

Aranaz I, Mengibar M, Harris R et al (2009) Functional characterization of chitin and chitosan. Curr Chem Biol 3(2):203–230

Aranaz I, Harris R, Heras A (2010) Chitosan amphiphilic derivatives. Chemistry and applications. Curr Org Chem 14(3):308–330

Athanasiou K, Niederauer G, Agrawal M (1996) Sterilization, toxicity, biocompatibility and clinical applications of polylactic acid/polyglycolic acid copolymers. Biomaterials 17(2):93–102

Babu V, Sairam M, Hosamani K et al (2006) Development of 5-fluorouracil loaded poly (acrylamide-co-methylmethacrylate) novel core-shell microspheres: in vitro release studies. Int J Pharm 325(1–2):55–62

Baek K, Jeong J, Shkumatov A et al (2013) In situ self-folding assembly of a multi-walled hydrogel tube for uniaxial sustained molecular release. Adv Mater 25(39):5568–5573

Bagheri-Khoulenjani S, Taghizadeh S, Mirzadeh H (2009) An investigation on the short-term biodegradability of chitosan with various molecular weights and degrees of deacetylation. Carbohydr Polym 78(4):773–778

Barbucci R (2009) Hydrogels: biological properties and applications. Springer-Verlag Italia, Milan

Beumer G, Van Blitterswijk C, Ponec M (1994) Biocompatibility of a biodegradable matrix used as a skin substitute: an in vivo evaluation. J Biomed Mater Res 28(5):545–552

Bini T, Gao S, Wang S et al (2005) Development of fibrous biodegradable polymer conduits for guided nerve regeneration. J Mater Sci Mater Med 16(4):367–375

Black J (2006) Biological performance of materials; fundamentals of biocompatibility. CRC Press, Taylor & Francis Group, Boca Raton

Brannon-Peppas L (1995) Recent advances on the use of biodegradable microparticles and nanoparticles in controlled drug delivery. Int J Pharm 116(1):1–9

Brunner A, Mäder K, Göpferich A (1999) pH and osmotic pressure inside biodegradable microspheres during erosion1. Pharm Res 16(6):847–853

Burdick J, Anseth K (2002) Photoencapsulation of osteoblasts in injectable RGD-modified PEG hydrogels for bone tissue engineering. Biomaterials 23(22):4315–4323

Burdick J, Khademhosseini A, Langer R (2004) Fabrication of gradient hydrogels using a microfluidics/photopolymerization process. Langmuir 20(13):5153–5156

Buwalda SJ, Boere KW, Dijkstra PJ et al (2014) Hydrogels in a historical perspective: from simple networks to smart materials. J Controlled Release 190:254–273

Cairncross R, Becker J, Ramaswamy S et al (2006) Moisture sorption, transport, and hydrolytic degradation in polylactide. In: McMillan J, Adney W, Mielenz J, Klasson K (eds) Twenty-seventh symposium on biotechnology for fuels and chemicals. ABAB symposium. Humana Press, Denver, pp 774–785

Caló E, Khutoryanskiy VV (2015) Biomedical applications of hydrogels: a review of patents and commercial products. Eur Polym J 65:252–267

Cao Y, Vacanti J, Ma P et al (1994) Generation of neo-tendon using synthetic polymers seeded with tenocytes. Transplant Proc 26(6):2–3390

Carlson K, Cameron J, Lindstrom R (1993) Assessment of the blood-aqueous barrier by fluorophotometry following poly (methyl methacrylate), silicone, and hydrogel lens implantation in rabbit eyes. J Cataract Refract Surg 19(1):9–15

Castelli F, Conti B, Maccarrone D et al (1998) Comparative study of 'in vitro' release of anti-inflammatory drugs from polylactide-co-glycolide microspheres. Int J Pharm 176(1): 85–98

Chen X, McCarthy S, Gross R (1997) Synthesis and characterization of [l]-lactide−ethylene oxide multiblock copolymers. Macromolecules 30(15):4295–4301

Chen C, Dong L, Cheung M (2005) Preparation and characterization of biodegradable poly (l-lactide)/chitosan blends. Eur Polym J 41(5):958–966

Choi E-J, Kim C-H, Park J-K (1999) Synthesis and characterization of starch-g-polycaprolactone copolymer. Macromolecules 32(22):7402–7408

Corkhill P, Hamilton C, Tighe B (1989) Synthetic hydrogels VI. Hydrogel composites as wound dressings and implant materials. Biomaterials 10(1):3–10

Correlo V, Boesel L, Bhattacharya M et al (2005) Properties of melt processed chitosan and aliphatic polyester blends. Mater Sci Eng, A 403(1–2):57–68

Croisier F, Jérôme C (2013) Chitosan-based biomaterials for tissue engineering. Eur Polym J 49 (4):780–792

Cutright D, Beasley Iii J, Perez B (1971) Histologic comparison of polylactic and polyglycolic acid sutures. Oral Surg Oral Med Oral Pathol 32(1):165–173

Dash M, Chiellini F, Ottenbrite R et al (2011) Chitosan—a versatile semi-synthetic polymer in biomedical applications. Prog Polym Sci 36(8):981–1014

Day R, Maquet V, Boccaccini A et al (2005) In vitro and in vivo analysis of macroporous biodegradable poly(D,L-lactide-co-glycolide) scaffolds containing bioactive glass. J Biomed Mater Res Part B Appl Biomater 75A(4):778–787

de Lima GG, Kanwar D, Macken D et al (2015) Smart hydrogels: therapeutic advancements in hydrogel technology for smart drug delivery applications. In: Kumar V, Thakur DK (ed) Handbook of polymers for pharmaceutical technologies: bioactive and compatible synthetic/hybrid polymers, vol 4. Wiley, Hoboken, New York, pp 1–16
Decher G (1997) Fuzzy nanoassemblies: toward layered polymeric multicomposites. Science 277 (5330):1232–1237
Deng X, Liu Y, Yuan M et al (2002) Preparation and characterization of poly-DL-lactide–poly (ethylene glycol) microspheres containing λDNA. J Appl Polym Sci 86(10):2557–2566
Donabedian D, McCarthy S (1998) Acylation of pullulan by ring-opening of lactones. Macromolecules 31(4):1032–1039
Drotleff S, Lungwitz U, Breunig M et al (2004) Biomimetic polymers in pharmaceutical and biomedical sciences. Eur J Pharm Biopharm 58(2):385–407
Drury J, Mooney D (2003) Hydrogels for tissue engineering: scaffold design variables and applications. Biomaterials 24(24):4337–4351
Duncan R, Kopeček J (1984) Soluble synthetic polymers as potential drug carriers. In: Polymers in medicine. Advances in polymer science, vol 57. Springer, Berlin, pp 51–101
East G, McIntyre J, Qin Y (1991) Medical use of chitosan. In: Skjak-Brack G, Anthonsen T, Sandford P (eds) Chitin and chitosan. Elsevier, London, pp 757–764
Edlund U, Albertsson A (2002) Degradable polymer microspheres for controlled drug delivery. In: Degradable aliphatic polyesters. Advances in polymer science, vol 157. Springer, Berlin, Heidelberg, pp 67–112
Freed L, Vunjak-Novakovic G, Biron R et al (1994) Biodegradable polymer scaffolds for tissue engineering. Nat Biotech 12(7):689–693
Funkhouser J, Aronson N (2007) Chitinase family GH18: evolutionary insights from the genomic history of a diverse protein family. BMC Evol Biol 7(1):96
Fusco S, Huang H, Peyer K et al (2015) Shape-switching microrobots for medical applications: the influence of shape in drug delivery and locomotion. Appl Mat Interfac 7(12):68–6803
Gaharwar AK, Peppas NA, Khademhosseini A (2014) Nanocomposite hydrogels for biomedical applications. Biotechnol Bioeng 111(3):441–453
Gajria A, Davé V, Gross R et al (1996) Miscibility and biodegradability of blends of poly(lactic acid) and poly(vinyl acetate). Polymer J 37(3):437–444
Gibas I, Janik H (2010) Review: synthetic polymer hydrogels for biomedical applications. Chem & Chem Technol 4:297–304
Gonsalves K, Jin S, Baraton M-I (1998) Synthesis and surface characterization of functionalized polylactide copolymer microparticles. Biomaterials 19(16):1501–1505
Gonzalez M, Ruseckaite R, Cuadrado T (1999) Structural changes of polylactic-acid (PLA) microspheres under hydrolytic degradation. J Appl Polym Sci 71(8):1223–1230
Graiver D, Durall R, Okada T (1993) Surface morphology and friction coefficient of various types of Foley catheter. Biomaterials 14(6):465–469
Gupta A, Kumar V (2007) New emerging trends in synthetic biodegradable polymers—polylactide: a critique. Eur Polym J 43(10):4053–4074
Gupta P, Vermani K, Garg S (2002) Hydrogels: from controlled release to pH-responsive drug delivery. Drug Discov Today 7(10):569–579
Hacker M, Mikos A (2011) Synthetic polymers. In: Atala A, Lanza R, Thomson JA, Nerem RM (eds) Principles of regenerative medicine, 2nd edn. Academic Press, Bulrington, pp 587–622
Hench L (1980) Biomaterials. Science 208:826–831
Hench L, Polak J (2002) Third-generation biomedical materials. Science 295(5557):1014–1017
Hern D, Hubbell J (1998) Incorporation of adhesion peptides into nonadhesive hydrogels useful for tissue resurfacing. J Biomed Mater Res 39(2):266–276
Higa O, Rogero S, Machado L et al (1999) Biocompatibility study for PVP wound dressing obtained in different conditions. Radiat Phys Chem 55(5):705–707
Hirano S (2001) Wet-spinning and applications of functional fibers based on chitin and chitosan. Macromol Symp 168(1):21–30

Hoogsteen W, Postema A, Pennings A et al (1990) Crystal structure, conformation and morphology of solution-spun poly(L-lactide) fibers. Macromolecules 23(2):634–642
Hu Y, Jiang X, Ding Y et al (2003) Preparation and drug release behaviors of nimodipine-loaded poly(caprolactone)-poly(ethylene oxide)-polylactide amphiphilic copolymer nanoparticles. Biomaterials 24(13):2395–2404
Hutmacher D (2000) Scaffolds in tissue engineering bone and cartilage. Biomaterials 21 (24):2529–2543
Jain R (2000) The manufacturing techniques of various drug loaded biodegradable poly (lactide-co-glycolide) (PLGA) devices. Biomaterials 21(23):2475–2490
Jain R, Shah N, Malick A et al (1998) Controlled drug delivery by biodegradable poly(ester) devices: different preparative approaches. Drug Dev Ind Pharm 24(8):703–727
Jen A, Wake M, Mikos A (1996) Review: hydrogels for cell immobilization. Biotechnol Bioeng 50(4):357–364
John R, Nampoothiri K, Pandey A (2007) Fermentative production of lactic acid from biomass: an overview on process developments and future perspectives. Appl Microbiol Biotechnol 74 (3):524–534
Juni H, Nakano N (1987) Poly(hydroxy acids) in drug delivery. Crit Rev Ther Drug Carrier Syst 3 (3):209–232
Kamath K, Park K (1993) Biodegradable hydrogels in drug delivery. Adv Drug Delivery Rev 11 (1–2):59–84
Kaufmann P, Heimrath S, Kim B et al (1997) Highly porous polymer matrices as a three-dimensional culture system for hepatocytes. Cell Transplant 6(5):463–468
Kawase M, Miura N, Kurikawa N et al (1999) Immobilization of tripeptide growth factor glycyl-L-histidyl-L-lysine on poly(vinylalcohol)-quarternized stilbazole (PVA-SbQ) and its use as a ligand for hepatocyte attachment. Biol Pharm Bull 22(9):999–1001
Kean T, Thanou M (2009) Chitin and chitosan—sources, production and medical applications. In: Tang B-Z, Williams P (eds) Renewable resources for functional polymers and biomaterials: polysaccharides, proteins and polyesters. Kentus Books, London, pp 327–361
Kenawy ER, Kamoun EA, Eldin MSM et al (2014) Physically crosslinked poly (vinyl alcohol)-hydroxyethyl starch blend hydrogel membranes: synthesis and characterization for biomedical applications. Arab J Chem 7(3):372–380
Kim S, Shin I, Lee Y (1998) Preparation and characterization of biodegradable nanospheres composed of methoxy poly(ethylene glycol) and dl-lactide block copolymer as novel drug carriers. J Control Release 56(1–3):197–208
Kim T-H, Jiang H-L, Jere D et al (2007) Chemical modification of chitosan as a gene carrier in vitro and in vivo. Prog Polym Sci 32(7):726–753
Kobayashi H, Ikada Y (1991) Covalent immobilization of proteins on to the surface of poly (vinyl alcohol) hydrogel. Biomaterials 12(8):747–751
Kopeček J, Tang A, Wang C et al (2001) De novo design of biomedical polymers: hybrids from synthetic macromolecules and genetically engineered protein domains. Macromol Symp 174 (1):31–42
Kozlowski M, Masirek R, Piorkowska E et al (2007) Biodegradable blends of poly(L-lactide) and starch. J Appl Polym Sci 105(1):269–277
Kulshrestha A, Mahapatro A (2008) Polymers for biomedical applications. In: Kulshrestha AS, Mahapatro A (eds) Polymers for biomedical applications. ACS symposium series, vol 977. American Chemical Society, Washington, pp 1–7
Lacasse F, Hildgen P, McMullen J (1998) Surface and morphology of spray-dried pegylated PLA microspheres. Int J Pharm 174(1–2):101–109
Laleg M, Pikulik I (1991) Wet-web strength increase by chitosan. Nordic Pulp Paper Res J 6 (3):99–103
Langer R (2000) Biomaterials in drug delivery and tissue engineering: one laboratory's experience. Acc Chem Res 33(2):94–101
Langer R, Peppas N (2003) Advances in biomaterials, drug delivery, and bionanotechnology. AIChE J 49(12):2990–3006

Langer R, Tirrell D (2004) Designing materials for biology and medicine. Nature 428(6982):487–492
Langer R, Vacanti J (1993) Tissue engineering. Science 260(5110):920–926
Lee K, Mooney D (2001) Hydrogels for tissue engineering. Chem Rev 101(7):1869–1880
Lee C, Grodzinsky A, Spector M (2001) The effects of cross-linking of collagen-glycosaminoglycan scaffolds on compressive stiffness, chondrocyte-mediated contraction, proliferation and biosynthesis. Biomaterials 22(23):3145–3154
Leedy M, Martin H, Norowski P et al (2011) Use of chitosan as a bioactive implant coating for bone-implant applications. In: Jayakumar R, Prabaharan M, Muzzarelli R (eds) Chitosan for biomaterials II, vol 244. Advances in polymer science. Springer, Berlin, pp 129–165
Lehr C-M, Bouwstra J, Schacht E et al (1992) In vitro evaluation of mucoadhesive properties of chitosan and some other natural polymers. Int J Pharm 78(1–3):43–48
Li S (2003) Bioresorbable hydrogels prepared through stereocomplexation between poly (L-lactide) and poly(D-lactide) blocks attached to poly(ethylene glycol). Macromol Biosci 3 (11):657–661
Li Y, Nothnagel J, Kissel T (1997) Biodegradable brush-like graft polymers from poly(D, L-lactide) or poly(D, L-lactide-co-glycolide) and charge-modified, hydrophilic dextrans as backbone—synthesis, characterization and in vitro degradation properties. Polymer J 38 (25):6197–6206
Lin C-C, Anseth K (2013) The biodegradation of biodegradable polymeric biomaterials. In: Ratner A, Hoffman F, Schoen J, Lemons B (eds) Biomaterials science, 2nd edn. Academic Press, London, pp 716–728
Lu L, Peter S, Lyman M et al (2000) In vitro degradation of porous poly(L-lactic acid) foams. Biomaterials 21(15):1595–1605
Lucke A, Kiermaier J, Göpferich A (2002) Peptide acylation by poly(α-hydroxy esters). Pharm Res 19(2):175–181
Lutolf M, Hubbell J (2005) Synthetic biomaterials as instructive extracellular microenvironments for morphogenesis in tissue engineering. Nat Biotech 23(1):47–55
Ma P, Langer R (1999) Morphology and mechanical function of long-term in vitro engineered cartilage. J Biomed Mater Res 44(2):217–221
Madihally S, Matthew H (1999) Porous chitosan scaffolds for tissue engineering. Biomaterials 20 (12):1133–1142
Mainil-Varlet P, Rahn B, Gogolewski S (1997) Long-term in vivo degradation and bone reaction to various polylactides. 1. One–year results. Biomaterials 18(3):257–266
Malette W, Quigley M, Quigley H Jr et al (1986) Chitosan effect in vascular surgery, tissue culture and tissue regeneration. In: Muzzarelli R, Jeuniaux C, Gooday G (eds) Chitin in nature and technology, 1st edn. Plenum Press, New York, pp 435–442
Mann B, Gobin A, Tsai A et al (2001) Smooth muscle cell growth in photopolymerized hydrogels with cell adhesive and proteolytically degradable domains: synthetic ECM analogs for tissue engineering. Biomaterials 22(22):3045–3051
Martin O, Avérous L (2001) Poly(lactic acid): plasticization and properties of biodegradable multiphase systems. Polymer J 42(14):6209–6219
Martineau L, Shek P (2006) Evaluation of a bi-layer wound dressing for burn care: II. In vitro and in vivo bactericidal properties. Burns 32(2):172–179
Matsumoto J, Nakada Y, Sakurai K et al (1999) Preparation of nanoparticles consisted of poly (l-lactide)–poly(ethylene glycol)–poly(l-lactide) and their evaluation in vitro. Int J Pharm 185 (1):93–101
Mehta R, Kumar V, Bhunia H et al (2005) Synthesis of poly (lactic acid): a review. J Macromol Sci Polym Rev 45(4):325–349
Meyvis T, De Smedt S, Demeester J et al (2000) Influence of the degradation mechanism of hydrogels on their elastic and swelling properties during degradation. Macromolecules 33 (13):4717–4725
Middleton J, Tipton A (2000) Synthetic biodegradable polymers as orthopedic devices. Biomaterials 21(23):2335–2346

Mikos A, Lyman M, Freed L et al (1994) Wetting of poly(l-lactic acid) and poly (dl-lactic-co-glycolic acid) foams for tissue culture. Biomaterials 15(1):55–58
Molin A, Brundin J (1992) Cervical dilatation before first trimester elective abortion: a comparison between laminaria and a newly developed hydrogel tent, the A rod. Gynecol Obstet Invest 34 (1):12–14
Müller R-J (2008) Biodegradability of polymers: regulations and methods for testing. In: Steinbuchel A (ed) Biopolymers online, vol 10. Wiley Publishers, p 366
Murakami H, Kobayashi M, Takeuchi H et al (2000) Further application of a modified spontaneous emulsification solvent diffusion method to various types of PLGA and PLA polymers for preparation of nanoparticles. Powder Technol 107(1–2):137–143
Muzzarelli R, Muzzarelli C (2005) Chitosan chemistry: relevance to the biomedical sciences. In: Heinze T (ed) Polysaccharides I. Advances in polymer science, vol 186. Springer, Berlin, pp 151–209
Muzzarelli R, Baldassarre V, Conti F et al (1988) Biological activity of chitosan: ultrastructural study. Biomaterials 9(3):247–252
Myers R, Larsen D, Taso M et al (1991) Quantity of protein deposited on hydrogel contact lenses and its relation to visible protein deposits. Optom Vis Sci 68(10):776–782
Nampoothiri K, Nair N, John R (2010) An overview of the recent developments in polylactide (PLA) research. Bioresour Technol 101(22):8493–8501
Narayanan N, Roychoudhury P, Srivastava A (2004) L (+) lactic acid fermentation and its product polymerization. EJB Electron J Biotechnol 7(2):167–178
Nguyen QV, Park JH, Lee DS (2015) Injectable polymeric hydrogels for the delivery of therapeutic agents: a review. Eur Polymer J 72:602–619
Nigam S, Sakoda A, Wang H (1988) Bioproduct recovery from unclarified broths and homogenates using immobilized adsorbents. Biotechnol Prog 4(3):166–172
Nijenhuis A, Colstee E, Grijpma D et al (1996) High molecular weight poly(L-lactide) and poly (ethylene oxide) blends: thermal characterization and physical properties. Polymer J 37 (26):5849–5857
Nuttelman C, Mortisen D, Henry S et al (2001) Attachment of fibronectin to poly (vinyl alcohol) hydrogels promotes NIH3T3 cell adhesion, proliferation, and migration. J Biomed Mater Res 57(2):217–223
Olivier J (2005) Drug transport to brain with targeted nanoparticles. NeuroRx 2(1):108–119
Ong S-Y, Wu J, Moochhala S et al (2008) Development of a chitosan-based wound dressing with improved hemostatic and antimicrobial properties. Biomaterials 29(32):4323–4332
Ouchi T, Saito T, Kontani T et al (2004) Encapsulation and/or release behavior of bovine serum albumin within and from polylactide-grafted dextran microspheres. Macromol Biosci 4 (4):458–463
Pangburn S, Trescony P, Heller J (1982) Lysozyme degradation of partially deacetylated chitin, its films and hydrogels. Biomaterials 3(2):105–108
Park H, Park K (1996) Hydrogels in bioapplications. In: Ottenbrite R, Huang S, Kinam P (eds) Hydrogels and biodegradable polymers for bioapplications. ACS symposium series, vol 627. American Chemical Society, Washington, pp 2–10
Park K, Xanthos M (2009) A study on the degradation of polylactic acid in the presence of phosphonium ionic liquids. Polym Degrad Stab 94(5):834–844
Park T, Cohen S, Langer R (1992) Poly(L-lactic acid)/pluronic blends: characterization of phase separation behavior, degradation, and morphology and use as protein-releasing matrixes. Macromolecules 25(1):116–122
Park T, Lu W, Crotts G (1995) Importance of in vitro experimental conditions on protein release kinetics, stability and polymer degradation in protein encapsulated poly (d, l-lactic acid-co-glycolic acid) microspheres. J Control Release 33(2):211–222
Patenaude M, Smeets N, Hoare T (2014) Designing injectable, covalently cross-linked hydrogels for biomedical applications. Macromol Rapid Commun 35(6):598–617
Pavinatto F, Caseli L, Oliveira O (2010) Chitosan in nanostructured thin films. Biomacromolecules 11(8):1897–1908

Peppas N, Hilt J, Khademhosseini A et al (2006) Hydrogels in biology and medicine: from molecular principles to bionanotechnology. Adv Mater 18(11):1345–1360
Perego G, Cella G, Bastioli C (1996) Effect of molecular weight and crystallinity on poly (lactic acid) mechanical properties. J Appl Polym Sci 59(1):37–43
Peters R, Lebouille J, Plum B et al (2011) Hydrolytic degradation of poly (d, l-lactide-co-glycolide 50/50)-di-acrylate network as studied by liquid chromatography–mass spectrometry. Polym Degrad Stab 96(9):1589–1601
Petka W, Harden J, McGrath K et al (1998) Reversible hydrogels from self-assembling artificial proteins. Science 281(5375):389–392
Pişkin E, Kaitian X, Denkbaş E et al (1995) Novel PDLLA/PEG copolymer micelles as drug carriers. J Biomater Sci Polym Ed 7(4):359–373
Pluta M, Galeski A, Alexandre M et al (2002) Polylactide/montmorillonite nanocomposites and microcomposites prepared by melt blending: Structure and some physical properties. J Appl Polym Sci 86(6):1497–1506
Ramzi A, Azzam A, Nor O et al (2015) Recent applications of polylactic acid in pharmaceutical and medical industries. J Chem Pharm Res 7(12):51–63
Rane K, Hoover D (1993) Production of chitosan by fungi. Food Biotechnol 7(1):11–33
Ratner B (2004) Biomaterials science: an introduction to materials in medicine, 2nd edn. Elsevier Academic Press, Amsterdam, Boston
Rezwan K, Chen Q, Blaker J et al (2006) Biodegradable and bioactive porous polymer/inorganic composite scaffolds for bone tissue engineering. Biomaterials 27(18):3413–3431
Rinaudo M (2006) Chitin and chitosan: properties and applications. Prog Polym Sci 31(7):603–632
Romero-Cano M, Vincent B (2002) Controlled release of 4-nitroanisole from poly(lactic acid) nanoparticles. J Control Release 82(1):127–135
Rowley J, Madlambayan G, Mooney D (1999) Alginate hydrogels as synthetic extracellular matrix materials. Biomaterials 20(1):45–53
Roy N, Saha N, Humpolicek P et al (2010a) Permeability and biocompatibility of novel medicated hydrogel wound dressings. Soft Mater 8(4):338–357
Roy N, Saha N, Kitano T et al (2010b) Development and characterization of novel medicated hydrogels for wound dressing. Soft Mater 8(2):130–148
Roy N, Saha N, Kitano T et al (2010c) Novel hydrogels of PVP–CMC and their swelling effect on viscoelastic properties. J Appl Polym Sci 117(3):1703–1710
Rudin A, Choi P (2013) Biopolymers. In: Choi AR (ed) The elements of polymer science & engineering, 3rd edn. Academic Press, Boston, pp 521–535
Saha N, Saarai A, Roy N et al (2011) Polymeric biomaterial based hydrogels for biomedical applications. J Biomater Nanobiotechno 2(1):85–90
Saltzman W, Olbricht W (2002) Building drug delivery into tissue engineering design. Nat Rev Drug Discov 1(3):177–186
Sashiwa H, Aiba S-i (2004) Chemically modified chitin and chitosan as biomaterials. Prog Polym Sci 29(9):887–908
Schwendeman S (2002) Recent advances in the stabilization of proteins encapsulated in injectable PLGA delivery systems. Crit Rev Ther Drug Carrier Syst 19(1):73–98
Sefton M, May M, Lahooti S et al (2000) Making microencapsulation work: conformal coating, immobilization gels and in vivo performance. J Control Release 65(1):173–186
Segura T, Shea L (2002) Surface-tethered DNA complexes for enhanced gene delivery. Bioconjug Chem 13(3):621–629
Şen M, Avcı E (2005) Radiation synthesis of poly (N-vinyl-2-pyrrolidone)–κ-carrageenan hydrogels and their use in wound dressing applications. I. Preliminary laboratory tests. J Biomed Mater Res A 74(2):187–196
Seol Y, Lee J, Park Y et al (2004) Chitosan sponges as tissue engineering scaffolds for bone formation. Biotechnol Lett 26(12):1037–1041
Sheth M, Kumar R, Davé V et al (1997) Biodegradable polymer blends of poly(lactic acid) and poly(ethylene glycol). J Appl Polym Sci 66(8):1495–1505

Siepmann J, Göpferich A (2001) Mathematical modeling of bioerodible, polymeric drug delivery systems. Adv Drug Delivery Rev 48(2–3):229–247
Simon J, Ricci J, Di Cesare P (1997) Bioresorbable fracture fixation in orthopedics: a comprehensive review. Part II. Clinical studies. Am J Orthop 26(11):754–762
Singh M, Shirley B, Bajwa K et al (2001) Controlled release of recombinant insulin-like growth factor from a novel formulation of polylactide-co-glycolide microparticles. J Control Release 70(1–2):21–28
Skardal A (2014) Extracellular matrix-like hydrogels for applications in regenerative medicine. In: Connon C, Hamley I (eds) Hydrogels in cell-based therapies, vol 2. The Royal Society of Chemistry, Cambridge, p 250
Sudarshan N, Hoover D, Knorr D (1992) Antibacterial action of chitosan. Food Biotechnol 6 (3):257–272
Sundback C, Hadlock T, Cheney M et al (2003) Manufacture of porous polymer nerve conduits by a novel low-pressure injection molding process. Biomaterials 24(5):819–830
Suyatma N, Copinet A, Tighzert L et al (2004) Mechanical and barrier properties of biodegradable films made from chitosan and poly (lactic acid) blends. J Polym Environ 12(1):1–6
Tabata Y (2003) Tissue regeneration based on growth factor release. Tissue Eng 9(4, Supplement 1):5–15
Takagi T, Takahashi K, Aizawa M et al (eds) (1993) In: Proceedings of the first international conference on intelligent materials—ICIM, Lancaster, PA. Technomic Publishing Co., Inc., Kanagawa, Japan
Takahashi T, Takayama K, Machida Y et al (1990) Characteristics of polyion complexes of chitosan with sodium alginate and sodium polyacrylate. Int J Pharm 61(1–2):35–41
Tarek A, Bader A (2016) Preparation, characterization, and potential application of chitosan, chitosan derivatives, and chitosan metal nanoparticles in pharmaceutical drug delivery. Drug Des Devel Ther 10:483–507
Taylor M, Daniels A, Andriano K et al (1994) Six bioabsorbable polymers: in vitro acute toxicity of accumulated degradation products. J Appl Biomater 5(2):151–157
Tirrell D (1996) Putting a new spin on spider silk. Science 271(5245):39–40
Tomić K, Veeman W, Boerakker M et al (2008) Lateral and rotational mobility of some drug molecules in a poly(ethylene glycol) diacrylate hydrogel and the effect of drug-cyclodextrin complexation. J Pharm Sci 97(8):3245–3256
Tomihata K, Ikada Y (1997) In vitro and in vivo degradation of films of chitin and its deacetylated derivatives. Biomaterials 18(7):567–575
Tsuji H, Ikada Y (1998) Blends of aliphatic polyesters. II. Hydrolysis of solution-cast blends from poly(L-lactide) and poly (ε-caprolactone) in phosphate-buffered solution. J Appl Polym Sci 67 (3):405–415
VandeVord P, Matthew H, DeSilva S et al (2002) Evaluation of the biocompatibility of a chitosan scaffold in mice. J Biomed Mater Res 59(3):585–590
Vårum K, Myhr M, Hjerde R et al (1997) In vitro degradation rates of partially N-acetylated chitosans in human serum. Carbohydr Res 299(1):99–101
Vermonden T, Klumperman B (2015) The past, present and future of hydrogels. Eur Polymer J 72:341–343
Vert M, Li S, Spenlehauer G, Guerin P (1992) Bioresorbability and biocompatibility of aliphatic polyesters. J Mater Sci Mater Med 3(6):432–446
Vert M, Schwarch G, Coudane J (1995) Present and future of PLA polymers. J Macromol Sci, Pure Appl Chem 32(4):787–796
Vey E, Miller A, Claybourn M et al (2007) In vitro degradation of poly(lactic-CO_2-glycolic) acid random copolymers. Macromol Symp 251(1):81–87
Vlugt-Wensink K, Jiang X, Schotman G et al (2006) In vitro degradation behavior of microspheres based on cross-linked dextran. Biomacromol 7(11):2983–2990
Wang E, Overgaard S, Scharer J et al (1988) Occlusion immobilization of hybridoma cells in chitosan. Biotechnol Tech 2(2):133–136

Wang C, Stewart R, Kopecek J (1999) Hybrid hydrogels assembled from synthetic polymers and coiled-coil protein domains. Nature 397(6718):417–420

Wang Y, Li Y, Pei X et al (2007) Genome-shuffling improved acid tolerance and l-lactic acid volumetric productivity in *Lactobacillus rhamnosus*. J Biotechnol 129(3):510–515

Wani M, Taylor H, Wall M et al (1971) Plant antitumor agents. VI. Isolation and structure of taxol, a novel antileukemic and antitumor agent from *Taxus brevifolia*. J Am Chem Soc 93(9): 2325–2327

Wei J, Hudson S, Mayer J et al (1977) A novel method for crosslinking carbohydrates. J Polym Sci 20:2187–2193

Whang K, Tsai DC, Nam EK et al (1998) Ectopic bone formation via rhBMP-2 delivery from porous bioabsorbable polymer scaffolds. J Biomed Mater Res 42(4):491–499

Whitesides GM, Ostuni E, Takayama S et al (2001) Soft lithography in biology and biochemistry. Annu Rev Biomed Eng 3(1):335–373

Williams DF (2009) On the nature of biomaterials. Biomaterials 30(30):5897–5909

Winet H, Bao JY (1998) Fibroblast growth factor-2 alters the effect of eroding polylactide-polyglycolide on osteogenesis in the bone chamber. J Biomed Mater Res 40 (4):567–576

Winter GD, Scales JT (1963) Effect of air drying and dressings on the surface of a wound. Nature 197:91–92

Yang J, Tian F, Wang Z et al (2008) Effect of chitosan molecular weight and deacetylation degree on hemostasis. J Biomed Mater Res Part B Appl Biomater 84B(1):131–137

Yang X, Yang K, Wu S et al (2010) Cytotoxicity and wound healing properties of PVA/ws-chitosan/glycerol hydrogels made by irradiation followed by freeze–thawing. Radiat Phys Chem 79(5):606–611

Ydens I, Rutot D, Degée P et al (2000) Controlled synthesis of poly(ε-caprolactone)-grafted dextran copolymers as potential environmentally friendly surfactants. Macromolecules 33 (18):6713–6721

Yoo J, Smith L (2004) Involvment of Ca_{2+}/calmodulin-dependent protein kinase II in the spontaneous activation in rat oocytes. Reprod Fertil Dev 17(2):279–280

Zacchi V, Soranzo C, Cortivo R et al (1998) In vitro engineering of human skin-like tissue. J Biomed Mater Res 40(2):187–194

Zhang I, Shung K, Edwards D (1996) Hydrogels with enhanced mass transfer for transdermal drug delivery. J Pharm Sci 85(12):1312–1316

Zhang Z, Ortiz O, Goyal R et al (2013) Biodegradable polymers. In: Ebnesajjad S, Modjarrad K (eds) Handbook of polymer applications in medicine and medical devices. PDL handbook series. Elsevier, Oxford, p 303

Zhao Y, Wang Z, Wang J et al (2004) Direct synthesis of poly (D, L-lactic acid) by melt polycondensation and its application in drug delivery. J Appl Polym Sci 91(4):2143–2150

Zund G, Breuer C, Shinoka T et al (1997) The in vitro construction of a tissue engineered bioprosthetic heart valve. Eur J Cardiothorac Surg 11(3):493–497

Zweers M, Engbers G, Grijpma D et al (2004) In vitro degradation of nanoparticles prepared from polymers based on DL-lactide, glycolide and poly(ethylene oxide). J Control Release 100 (3):347–356

Polyethylene Based Polymer for Joint Replacement

Saverio Affatato, Sami Abdel Jaber and Paola Taddei

Abstract It is well known that the debris generated from the Ultra-High molecular weight polyethylene socket may cause adverse tissue biological reactions leading to bone loss or osteolysis. A major consequence of the debris-induced osteolysis is the loosening of the implant inside the femur or acetabular cup, which often necessitates a revision surgery. Throughout the years several materials have been used in total hip replacement surgery. In particular, metals, ceramics and polymers are used nowadays for acetabular cup components. High molecular weight polyethylene is widely used and represents the principal polymeric material used in artificial replacement of hip and knee joints. High molecular weight polyethylene is known to have superior resistance to wear compared to other polymers. Actually, in order to increase long-term performance of Ultra-High molecular weight polyethylene acetabular cups, reinforcement as carbon fibres has been added in the polymeric matrix. The leading opinion is to develop a high strength reinforced polymeric matrix such as self-reinforced Ultra-High molecular weight polyethylene. With increasing patient longevity and activity levels, a search for the ultimate polymer is important.

Keywords UHMWPE · Hip simulator · Knee simulator · Ageing · DSC

S. Affatato (✉) · S.A. Jaber
Medical Technology Laboratory, Rizzoli Orthopaedic Institute,
Via di Barbiano 1/10, 40136 Bologna, Italy
e-mail: affatato@tecno.ior.it

P. Taddei
Department of Biomedical and Neuromotor Sciences, University of Bologna,
Via Belmeloro 8/2, 40126 Bologna, Italy
e-mail: paola.taddei@unibo.it

F. Zivic et al. (eds.), *Biomaterials in Clinical Practice*,
https://doi.org/10.1007/978-3-319-68025-5_6

1 Introduction

Orthopaedic implantations are common procedures today: every year, approximately 1.4 million joint replacement procedures are performed worldwide.

Throughout the years several materials have been used in total hip replacement surgery. In particular, metals, ceramics and polymers are used nowadays for acetabular cup components. High molecular weight polyethylene (UHMWPE) is widely used and represents the principal polymeric material used in artificial replacement of hip and knee joints. UHMWPE is known to have superior resistance to wear compared to other polymers (James et al. 2009). It is made of long chains of polyethylene and each individual molecule adds strength to the whole structure through its length. Between the molecules (or chains), which all align in the same direction, a high number of weak Van der Waals bonds are established; this allows to the whole structure the capability to withstand high tensile loads.

Polyethylene can be produced through various chemical methodologies: radical polymerization, anionic addition polymerization, ion coordination polymerization or cationic addition polymerization. UHMWPE is produced as a powder by the chemical process of polymerization, which involves usually Ziegler catalysts as titanium tetrachloride (Kurtz et al. 1999; McKellop et al. 1999; Sobieraj and Rimnac 2009). The Ziegler-Natta catalyst is synthesized by treating crystalline α-$TiCl_3$ with $[AlCl(C_2H_5)_2]_2$. The alkene binds at these vacancies and converts to an alkyl ligand group.

The obtained powder must be compacted in order to obtain the final form. Compaction of the polymer powder, in order to determine the quality of the consolidation of the polyethylene, may be measured to verify that there are not variations in different manufacturing lots. After consolidation, the plastic material in powder is compressed into a solid slab of the material via ram extrusion, compression molding, or isostatic pressing. In the extrudating chamber the resin powder is heated on sintering temperature (McGloughlin and Kavanagh 2000). During the ram extrusion and slab compression moulding is not produced uniform conditions in the compacted mass. In the past, these techniques have used calcium stearate as an additive for the residual catalyst stabilization, in order to ease the material flow and to minimise corrosion of the tools. During the 1980s the influence of calcium stearate on the properties and performance of UHMWPE in total joint replacement was the aim of several studies, which showed association of this additive with fusion defects and oxidation of UHMWPE. In fact, "calcium stearate may accelerate oxidative degradation of polyethylene after γ-irradiation in air and may also cause poor consolidation of the powder" (Jacob et al. 2001; Rimnac et al. 1994; Schmidt and Hamilton 1996). In the meantime, polymerisation and processing technology evolved to the point that the additive was no longer necessary; consequently, orthopaedic manufacturers began switching to UHMWPE resins without adding calcium stearate.

In direct compression moulding, the components are formed without the need of further machining, but the technique is expensive and hence not suitable for

prototypes. The choice of the conversion method is then as important as the choice of the resin for the final properties of an UHMWPE component, because both these factors introduce some changes in the morphology of the consolidated polymer. However, there is still not a standardization on which resin and conversion method would be universally proposed as best choice for all the various orthopaedic devices. Hence, it is the orthopaedic manufacturer who determines which conversion method is the most suitable for orthopaedic applications.

Since the molecular chains of UHMWPE are not static, they can become mobile at elevated temperatures. When cooled below the melting temperature, the molecular chains have the tendency to rotate the C–C bonds creating chain folds. These folds, in their turn, enable chains to form a more ordered structure known as "crystalline lamellae". These lamellae are embedded within the amorphous (disordered) region and may communicate with surrounding lamellae. UHMWPE molecules tend to have 100,000–250,000 monomers each, while other types of polyethylene have considerably less units of monomer; for example, high-density polyethylene (HDPE) molecules generally have between 700 and 1800 monomer units per molecule. Currently, medical grade resins are described as GUR1020 and GUR1050 depending on their molecular weights: GUR1020 has an average molecular weight of 3.5 million Dalton and GUR1050 above 5 million Dalton (Li and Burstein 1994; Blunn et al. 2002). The requirements for medical grade UHMWPE powder are specified in ASTM standard F648 and ISO standard 5834-1.

Regardless of the process of compaction, UHMWPE in the manufactured component shows two different phases, crystalline and amorphous. The content and the orientation of crystalline regions within polyethylene depend on many factors such as molecular weight, processing conditions, etc. When air accesses a block of polyethylene, either by being trapped between the granules as they are compressed or by diffusion from ambient air during storage, the oxidation process may start. With oxidation of polyethylene are identified a series of chemical reactions that result in chain scission (fragmentation and shortening of the large polymer chains) and introduction of oxygen into the polymer, which is more rapid in amorphous regions, rather than in crystalline lamellae. If oxygen is present, it may react with free radicals, lowering the molecular weight of the polymer, reducing its yield strength, ultimate tensile strength, elongation to break, toughness and increasing its density.

Clinical and laboratory research revealed that sterilization methods can radically affect the in vivo performance (and life) of an UHMWPE component, especially as far as the resistance to wear is concerned (Heisel et al. 2003). Historically, polyethylene components were sterilised by ethylene oxide (EtO) gas; this technique has been abandoned turning to exposure to γ-radiation. The γ-irradiation was typically made at doses ranging from 25 to 40 KGy, with the components packaged in air (McKellop 1996; McKellop et al. 2000). However, since 1995 all the major orthopaedic manufacturers began to use γ-radiation in a reduced oxygen environment or sterilise without ionising radiation (EtO or gas plasma). The evidence that γ-sterilisation, followed by long-term shelf storage, could accelerate oxidative chain scission and degradation of the mechanical and physical properties of UHMWPE, promoted the shift in sterilisation practice (McKellop et al. 1999; Shaw 1997).

2 Improvements of Polyethylene for Joint Replacement

It is well known that the debris generated from the UHMWPE socket may cause adverse tissue biological reactions leading to bone loss or osteolysis. One of the main consequences of the debris-induced osteolysis is the loosening of the implant inside the femur or acetabular cup, which often necessitates a revision surgery. The necessity for an improvement of the UHMWPE has gained considerable interest from the scientific community. In fact, to improve the wear resistance of the polymer scientists have proposed alternate varieties of UHMWPE. In particular, the attention of the scientific community has been focused on (a) the development of methods that increase the level of cross-linking in PE and (b) the creation of a polymer composite (i.e. UHMWPE through the inclusion of carbon fibres).

The first strategy has been developed since the polymer microstructure for optimal wear resistance appeared a three-dimensional network with the polymeric chains connected by covalent bonds (Kurtz et al. 1999). With regards to the second strategy, it must be recalled that a composite material has superior mechanical properties relative to non-filled UHMWPE, including higher strength and impact strength, increased creep resistance, and improved modulus.

2.1 Cross-linked Polyethylene

This type of polyethylene, commonly shortened as XLPE, is a form of polyethylene with cross-links. Cross-linking represents the most exciting potential advantage in articular technology since in this process polyethylene molecules are bonded together to result in a stronger material, of improved wear resistance. Covalent bonds are formed between the polymeric chains and therefore chain mobility, orientation, and as a result wear, are inhibited. There are three main methods of cross-linking polyethylene, i.e. using peroxides, moisture, and irradiation.

The irradiation is the most used method to cross-link UHMWPE for medical purpose and consists in bombing the polyethylene with high-energy electrons that liberate free radicals and cause the subsequent cross-linking reaction. The irradiation procedures are similar to sterilization methods. The final product passes through a large irradiation unit until the desired level of curing is achieved. Polyethylene can be cross-linked in this way without any chemical additives, but usually accelerators or promoters are incorporated to speed up the reaction and improve cross-linking efficiency. Oxidative degradation is a reaction between oxygen and the free radicals generated during irradiation. This represents a problem for UHMWPE since leads to lowered molecular weight and reduced mechanical properties. This process is due to the oxygen trapped in the polyethylene during irradiation, or to the molecules that diffuse into the polyethylene during shelf storage and/or in vivo. In order to eliminate or minimise the oxidative degradation,

higher doses of irradiation (range 50–100 kGy) are used on the polyethylene acetabular cups. After the irradiation, the cups are heat treated to reduce any radicals that are still present in the material. Typical post/irradiation treatments are annealing heating under the melting point of UHMWPE and remelting heating above the melting point of UHMWPE. After the heat treatment the material is then sterilised, either without using irradiation (EtO or gas plasma) or by irradiating in inert atmosphere.

Cross-linking has been reported to improve the wear characteristics with respect to non-cross-linked PE in clinical studies and laboratory tests using hip joint simulators (Oonishi 1995; Kurtz et al. 1999). However, the reduction in the mechanical properties of polyethylene under certain conditions used to produce cross-linking has been a concern. This worsening is known to result from the processes used to increase the cross-link density and could affect the device performance in vivo (Muratoglu et al. 2001).

2.2 Composite Polyethylenes

The word "composite" describes the combination of two or more materials, different for composition, morphology and physical properties. Since 40 years these materials have been studied and their use in different applications has been progressively increased. Composite materials show some advantages in quality and improved properties that the single constituents cannot have. Moreover, composite materials allow a flexible design so that their properties can be tailored to specific applications (Salernitano and Migliaresi 2003). Biocompatibility is a crucial point in developing new materials; this property cannot be compromised in favour of better mechanical properties. Composite materials suitable for hip or knee joint prostheses should be provide excellent wear performance and reduced particles debris. To do this and in order to increase long-term performance of UHMWPE acetabular cups, reinforcement as carbon fibres (CF) has been added in the polymeric matrix. The leading opinion is to develop a high strength reinforced polymeric matrix such as self-reinforced UHMWPE, UHMWPE reinforced with polymethyl methacrylate (PMMA) or CF and polyether ether ketone (PEEK) reinforced with CF. The self-reinforced UHMWPE is essentially a non-oriented matrix of UHMWPE in which reinforcement has been dispersed. The resulting polymer offers an excellent biocompatibility, increased mechanical properties and the possibility to be sterilized and cross-linked exactly as the conventional UHMWPE. Clinical experience for these composite materials was not so satisfactory; this is mainly due to the poor bonding strength between CF and the UHMWPE matrix or to the poor creep resistance of this latter, which promotes debonding of the CF from the matrix under load. A CF-reinforced PEEK has been proposed as an alternative for UHMWPE and it has been studied with great interest although is not currently used in clinical practice for total hip replacement. For

CF-reinforced PEEK it is crucial to determine the optimal combination of CF type and weight and the nature of the counterface (femoral head material).

Many investigations have shown that an excellent tribological behaviour is obtained with the combination of 30 wt% pitch-based CF-reinforced PEEK composite acetabular cup in articulation with a zirconia ceramic head: this combination showed a reduction in the wear rate by almost two orders of magnitude compared to conventional UHMWPE/metal or UHMWPE/ceramic couplings on a hip joint simulator run for 10 million loading cycles (Wang et al. 1998).

The composite of UHMWPE with added particles produced great improvement in tribological characteristics and mechanical behaviour. For example, lubricant-treated UHMWPE composites showed better friction properties than pure UHMWPE. Composites are typically made from mixtures containing up to 5.0 wt% of lubricant and prepared by compression moulding. Lubricants may be different: solid as molybdenum disulphide (MoS_2), carbon black (CB), and liquid perfluoropolyether (PFPE). 3D networks formed as result of the combination between UHMWPE and the lubricants; in particular, the lubricant was homogeneously spread over the UHMWPE particles.

Reaching new forms of composite UHMWPE is a common aim for the scientific community.

Nowadays, within this class of materials we can mention UHMWPE composites reinforced with CF, PMMA, nano-sized hydroxyapatite (HA) particles; nano-Al_2O_3/UHMWPE composites; UHMWPE composites filled with wollastonite fiber or nano-powder of SiO_2 fiber. Even if many of these composites led to an improvement of some mechanical properties, there is still no consensus about the in vivo performance of these materials and deeper clinical and in vitro studies are needed.

3 Aging of Polyethylene

Despite UHMWPE improvements, the problem of oxidative degradation of UHMWPE components still remains because of γ-radiation sterilization and subsequent shelf aging in air, with consequent changes in properties such as density, molecular weight, crystallinity degree or toughness and wear resistance (Currier et al. 1997; Goldman et al. 1997; Costa et al. 1998).

The oxidation of UHMWPE consists in a complex series of cascade reactions, not fully understood. The induced degradation is detected as a "white band" mostly concentrated 1–2 mm below the surface (Bostrom et al. 1994; Sutula et al. 1995) rather than on the surface, where exposure to oxidising species should be higher.

To evaluate the long-term stability of polymers towards oxidation, many accelerated aging methods have been proposed. Actually, oxidation of UHMWPE occurs at slow rates [i.e. takes years (Kurtz et al. 1999)]; therefore, accelerated aging tests, which exacerbate the conditions responsible for degradation, have been

developed under the expectance that the wear behaviour after accelerated aging is comparable to that of naturally aged materials.

Several different aging methods have been proposed (Kurtz et al. 1999), differing each other for the testing conditions. Test temperatures range from 60 to 127 °C; test environments range from air at ambient pressure to oxygen at 102 atm of pressure; the duration of the test range from 1 to 28 days. Actually, only two methods have been standardized by the ASTM. The first method was proposed by Sun et al. (1996) and consists in the treatment of UHMWPE sample in an air furnace at 80 °C for three weeks. Sanford and Saum (1995) proposed the second method in which UHMWPE samples are treated at 70 °C in an oxygen bomb at 5 atm of pressure for two weeks.

Several studies have been aimed at evaluating if the UHMWPE samples treated according these two protocols really resemble shelf-aged and retrieved components (Kurtz et al. 1999). Sanford and Saum (1995) have reported that their method, differently from that of Sun, produces an oxidation distribution through the sample thickness similar to that of retrieved components. On the other hand, McKellop (McKellop et al. 1999) has shown that the oxidation profiles of UHMWPE components obtained by both standardized methods were comparable to those of retrieved specimens. Actually, although the orthopaedic community has widely used these to test the resistance of UHMWPE, the question remains as to whether these treatments exactly reproduce the morphology and mechanical properties of shelf-aged and retrieved UHMWPE components. At this purpose, the ASTM clearly states that both protocols have been validated on the basis of the oxidation levels observed in shelf-aged UHMWPE components packaged in air and sterilized with γ-radiation; moreover, this international organization admits that both methods may not exactly reproduce the degradation mechanisms experienced by an implant during real-time shelf ageing and implantation. However, although the poor inter-laboratory reproducibility observed especially for the method by Sanford and Saum (Kurtz et al. 2001), the above mentioned standardized methods are useful and valid tools to determine the relative stability of UHMWPE materials towards oxidation.

4 Wear Tests on Polyethylene

Wear resistance of PE depends on several factors and hence does not represent an intrinsic material property. Surface finishing, the type of counterface, the operating environment, kinematics and loading are just few of the variables that may lead to different wear behaviours of a specific material. Thus, polyethylene for orthopaedic devices should be characterized for an evaluation of its wear properties in order to prevent failures or produce improvements in the materials for artificial joints. With this in mind, several methods have been developed in order to evaluate the wear behaviour, mainly using wear screening devices and wear joint devices. Wear screening devices (Fig. 1) provide quick data on the intrinsic features of the tested materials, giving the possibility to reproduce single wear mechanisms, but they do

not allow a global analysis on a real artificial joint whose results very often dramatically differ.

For this reason wear hip (Fig. 2) and knee (Fig. 3) joint simulators are used nowadays to analyse actual joint replacement devices, giving the possibility to reproduce the dynamical and physiological conditions to which the artificial devices are subjected in vivo.

The joint simulator tests have been developed to replicate the biomechanics of the human joints, and usually tests are carried out simulating motions and loading of steady walking conditions. A wide number of analyses on various factors have been made in research: lubrication conditions, materials coupling, loads and motions into play, prosthesis design etc.

4.1 Polyethylene and Hip Wear Simulation

As discussed above, polyethylene performance may be affected by oxidation during consolidation of the resin, sterilisation of the finished specimens and post-irradiation storage. To evaluate the influence of the sterilisation method (γ-irradiation and EtO) a lot of wear tests were performed. To this purpose, Affatato and co-workers carried out an in vitro hip wear test on γ- and EtO-sterilized UHMWPE under severe simulator conditions (i.e. adding third-body particles (PMMA) to the bovine calf serum trough the test). The test ran on a hip joint

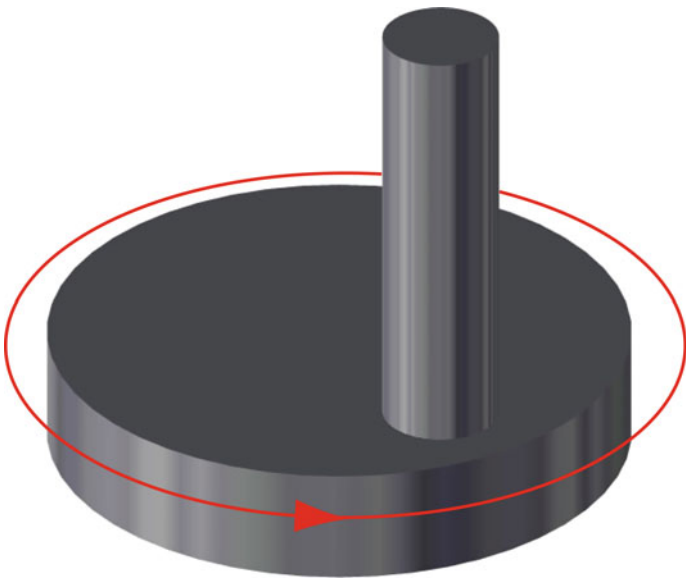

Fig. 1 Pin-on-disk device

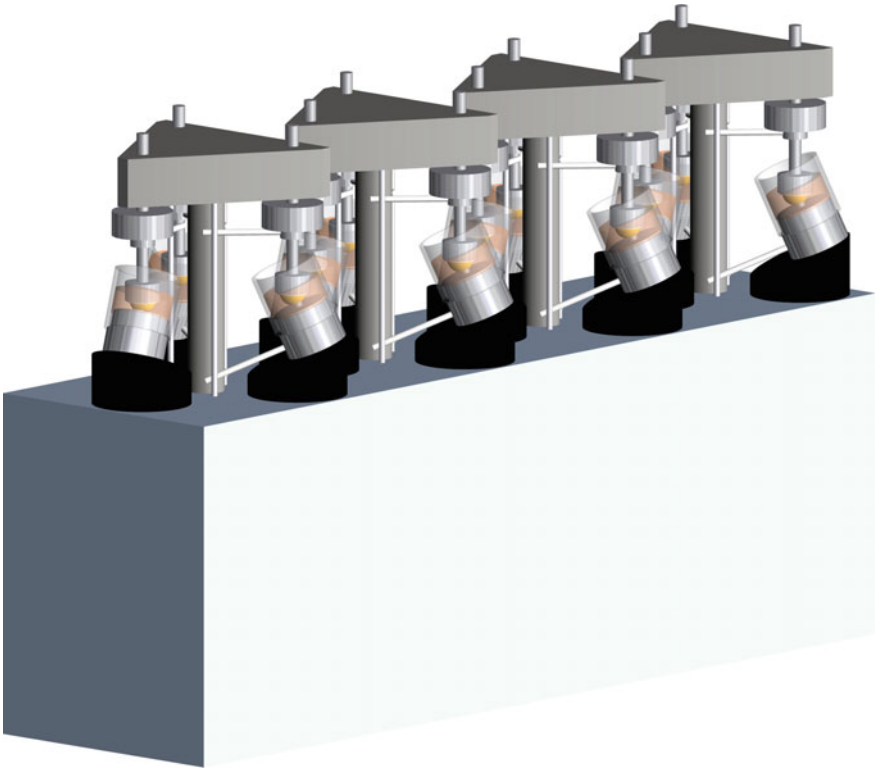

Fig. 2 Schematisation of a hip joint simulator

simulator for 2.5 million cycles. The results of this test revealed that the γ-sterilised acetabular cups exhibited a significantly lower wear rate than those EtO-sterilised.

With the improvements in PE properties, comparative studies were performed to evaluate the wear behaviour of conventional and improved XLPE. Affatato et al. (2008) tested on a hip simulator, for 5 million cycles, five different types of conventional and cross-linked polyethylenes. They compared the relative long-term wear resistance in relation to material properties (PE grade, conventional or cross-linked) and sterilisation method (EtO treatment or γ-irradiation). After 5 million cycles, these authors found significant differences ($p < 0.05$) between the wear behaviours of the acetabular cups. Weight loss was found to decrease for the XLPE with respect to the standard UHMWPE.

In recent years, cross-linked vitamin-E-stabilized polyethylene acetabular cups were compared with both commercially available conventional and custom-XLPE acetabular cups in terms of wear behaviour, in a hip joint simulator run for five millions cycles, using bovine calf serum as lubricant. The weight loss during the whole wear test was lower for XLPE than vitamin-E-stabilized XLPE ($p < 0.02$).

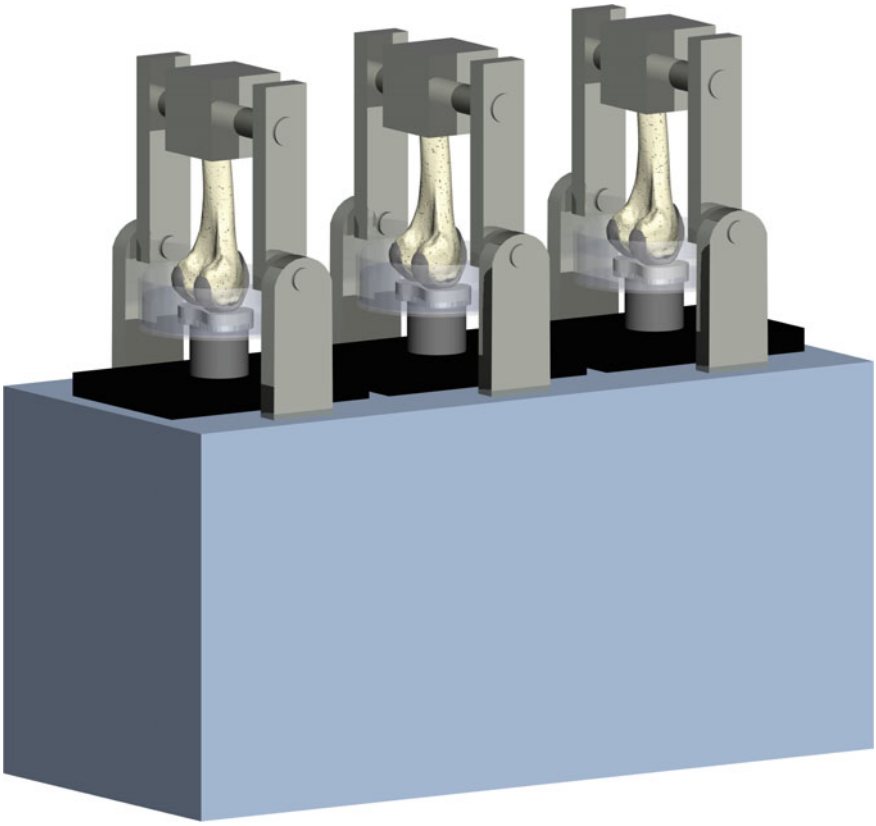

Fig. 3 Schematisation of a knee joint simulator

4.2 Polyethylene and Knee Wear Simulation

In the last few years the simulation concept moved toward the direction of the simulation of daily living activities such as stair ascent and descent, chair sitting and rising, squatting etc. In recent studies (Battaglia et al. 2014) wear tests on a knee simulator suggested a relationship between Patient's body weight and possible activation of different wear phenomena at molecular level. These authors hypothesized that stresses concentration due to smaller total knee prostheses combined to a load increase would have strong impact on the increase of the amorphous phase, with a consequently doubled wear rate.

This phenomenon was not detectable on larger prostheses, in which wider areas allowed more homogenous stresses distribution, showing no effect on wear rate by increasing loads i.e. patient weight. A study by Jaber et al. (2014) carried out wear simulation on two groups of the same total knee prosthesis, applying ISO level walking and stair climbing conditions. This study showed that higher wear rate was

accompanied by a decrease in crystallinity of the UHMWPE liners in the case of simulation with stair climbing conditions, which presented higher loads and A/P displacements. These relevant findings were also supported by digital scanning microscopy, which revealed the activation of pitting phenomena, which increases wear loss due to a more aggressive wear mechanism.

5 Molecular Characterization of PE

Several studies investigated on a molecular scale the influence of in vitro and in vivo aging and sterilization on PE properties (Costa et al. 1998; Goldman et al. 1997). IR spectroscopy represents a valid tool to analyse the surface and subsurface oxidative degradation of PE on thin sections of the material, as a function of sterilization, aging and cross-linking (Costa et al. 1998); actually, this technique is well sensitive to the oxidised species which typically form upon PE oxidation and each of them may be identified through its characteristic vibrational IR bands. The main disadvantage of this kind of measurements is their destructive character; actually, the sample needs to be cut in thin sections and thus becomes useless for subsequent tests. Figure 4 reports as an example the IR spectra of thin sections of UHMWPE and XLPE acetabular cups; Table 1 reports the assignments of the main IR bands due to oxidised species.

The oxidation of PE has been typically revealed by the presence of IR bands (see Table 1) at about 1740 cm^{-1} (esters), 1720 cm^{-1} (ketones) and 1705 cm^{-1} (carboxylic acids) observed on the surface and at various depths in the PE samples (Costa et al. 1998; Goldman et al. 1997). UHMWPE γ-sterilized in air proved to show a higher oxidation level than EtO-sterilized prostheses; moreover, oxidation was found to increase with aging. Chain-scission of γ-irradiated UHMWPE, as detected by IR analyses, results in a reduction of molecular weight and less abrasive resistance.

Taddei et al. (2006) compared the stability towards oxidation of commercial XLPE and UHMWPE acetabular cups. The two sets of control unworn samples showed different oxidation profiles and different distributions of oxidised species; unworn UHMWPE was characterized by higher contents of carbonyl species and hydrogen-bonded alcohols and lower contents of trans-vinylene species than unworn XLPE. Upon hip joint simulator testing against deliberately scratched CoCrMo femoral heads, XLPE showed less significant changes in oxidation indexes and distribution of carbonyl compounds than UHMWPE, confirming a better wear behaviour for the former under severe testing conditions.

Costa et al. (1998) detected oxidation products up to 2 mm depth in many retrieved EtO- and γ-sterilized UHMWPE prostheses. In the latter samples, the oxidation processes due to γ-irradiation were hardly distinguishable from those due to biodegradation. With regards to in vitro simulator tested EtO- and γ-sterilized UHMWPE acetabular cups, IR spectroscopy did not disclose significant amounts of oxidised products in the interior of the EtO-sterilised worn and unworn cups; the

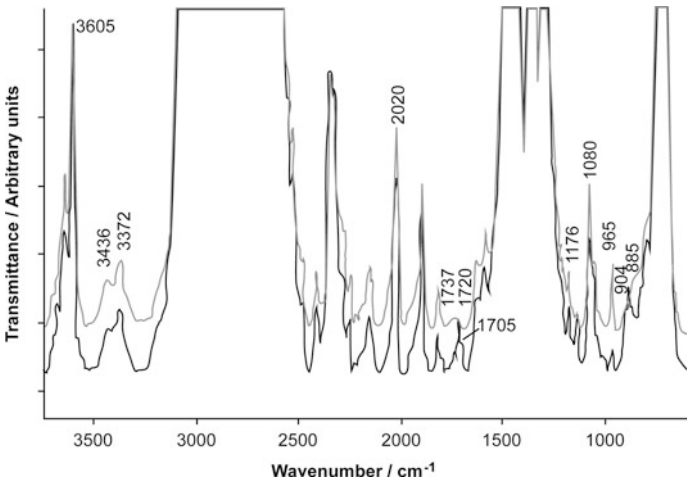

Fig. 4 IR spectra of thin sections of UHMWPE (*black*) and XLPE (*grey*) acetabular cups. The band at 2020 cm^{-1} represents the internal standard (CH_2 vibration in both crystalline and amorphous PE)

Table 1 Assignments (according to the literature) of the main IR bands due to oxidised species

Wavenumber/cm^{-1}	Assignment
3605	O–H stretching of non-hydrogen-bonded alcohols
3436	O–H stretching of hydrogen-bonded hydroperoxides
3372	O–H stretching of hydrogen-bonded alcohols
1737	C=O stretching esters
1720	C=O stretching ketones
1705	C=O stretching carboxylic acids
1176	C–O stretching of lactones and long linear esters
1080	C–O stretching of hydroperoxides
965	trans-vinylene, CH=CH
904	Vinyl, $CH=CH_2$
885	Vinylidene $C=CH_2$

γ-sterilised cups had a noticeably higher oxidation degree, especially in the worn regions and after accelerated aging.

Brach del Prever et al. (1996) characterised a tibial plateau after γ-irradiation and retrieved after in vivo service, by using an oxidation index, defined as the ratio of the IR integral absorption between 1790 and 1680 cm^{-1} to that between 2100 and 1980 cm^{-1}. Their findings evidenced a significant oxidation already in the original UHMWPE bar; the oxidation index increased in the plateau ready for implantation both because of manufacturing and sterilisation and became still higher after in vivo service, especially in the worn regions. Complementary to the IR absorption technique, Raman spectroscopy has experienced a surge in interest in the study of

PE and proved a valid method to characterise the structure and crystallinity of the polymer as well as its changes in crystallinity. Actually, it is well known that the polymer crystallinity is modified by mechanical stress, since the crystalline lamellae tend to reorganise when UHMWPE components are tested under uniaxial and multiaxial loading conditions. Consequently, a region of lamellar orientation near the articulating surface (termed plasticity-induced damage layer) has been reported to form (Edidin et al. 2002). Micro-Raman spectroscopy confirmed that this layer is thinner in XLPE than in UHMWPE.

In the light of these considerations, the availability of a tool able to monitor the crystallinity changes upon in vitro and in vivo wear appears of crucial importance. The technique mainly used to this purpose is differential scanning calorimetry (DSC); unfortunately, this technique, as well as IR spectroscopy, destructs the sample and thus does not allow its use for following tests. From this point of view, Raman spectroscopy appears particularly useful; actually, this technique allows an accurate non-destructive and in situ analysis of the sample during in vitro tests (for example between the periodical lubricant changes), without sacrificing the specimen. The optical arrangement of traditional dispersive spectrometers may be easily modified to perform Raman microscopy. More in detail, the excitation laser is focused onto the sample by the microscope's objective (Fig. 5), allowing a spatial resolution in the micron range, not only in the XY plane, but also along the Z axis. In other words confocal Raman microscopy is a useful technique for non-destructively probing depths of the sample without cross-sectioning.

The Raman spectrum of PE is well known (Fig. 6) and several studies have correlated the intensity of marker bands with the crystallinity of the polymer. In particular, the 1417 cm^{-1} band (CH_2 bending region) was assigned to the crystalline orthorhombic phase and the broad bands at about 1305 cm^{-1} (CH_2 twisting region) and 1080 cm^{-1} (CC stretching region) to the amorphous phase. Actually, several authors proposed a model which considers three different phases in PE: a crystalline orthorhombic phase [whose content is proportional to the intensity of the 1417 cm^{-1} band], a melt-like amorphous phase (with a prevailing gauche conformation of the chains), and an anisotropic disordered phase ("third phase", with a prevailing trans conformation of the chains).

On the basis of these findings, many papers have described the use of Raman microscopy to study the effects of sterilization, in vitro and in vivo wear on the morphology of UHMWPE prosthetic components and wear debris. Chenery (1997) analyzed γ-sterilized UHMWPE just after sterilization by both IR and Raman spectroscopy. Through the detection of bands attributable to epoxide, alcohol and three different peroxy-containing species, he demonstrated that the oxidation of the material proceeds via a γ-induced free radical mechanism. As above reported, this mechanism results in chain scission and a consequent increase in crystallinity was observed upon γ-irradiation

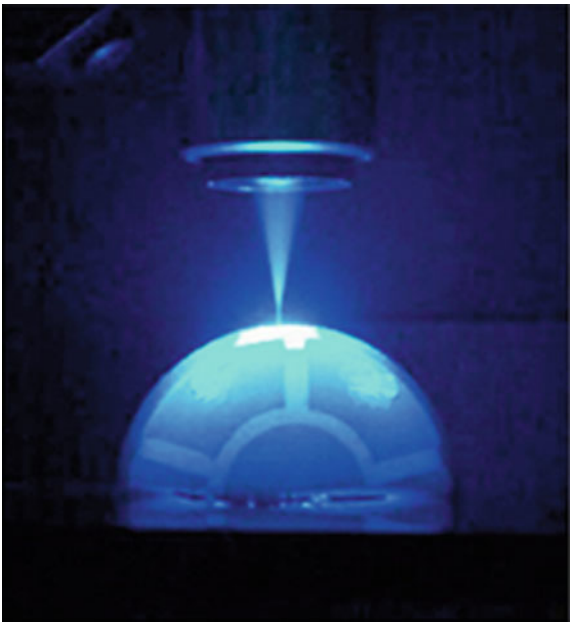

Fig. 5 An UHMWPE acetabular cup when non-destructively analysed by micro-Raman spectroscopy. The excitation laser (at 488 nm) is focused onto the sample by the microscope's objective

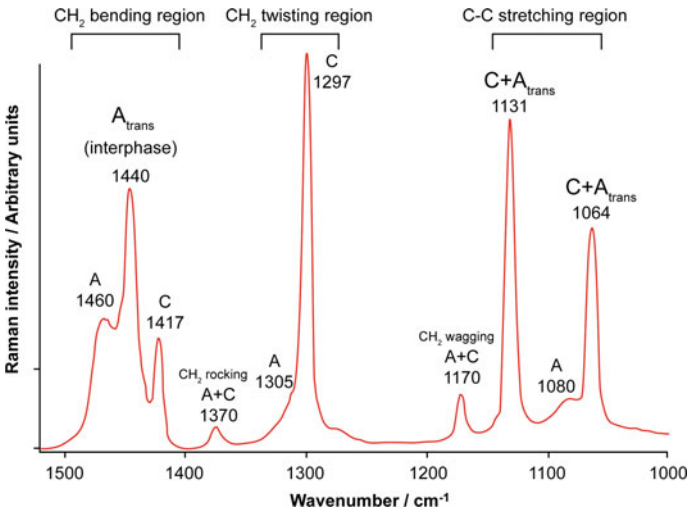

Fig. 6 Raman spectrum of PE. The bands prevalently due to orthorhombic crystalline phase (C), amorphous phase (A) and interphase are indicated. Assignments have been given according to the literature

Hahn et al. (1997) detected β-carotene by micro-Raman spectroscopy on UHMWPE wear debris isolated from revised knee replacements and hypothesized a role of this antioxidant in the mitigation of in vivo degradation of UHMWPE components. The use of micro-Raman spectroscopy allowed to ascertain that the material experience a considerable stress prior to wear debris production; actually, the crystallinity of PE in a wear particle was found to be significantly higher than that of the UHMWPE acetabular cup from which was generated. With regards to Hylamer™ acetabular cups, also a partial transformation from orthorhombic into monoclinic phase was detected in the wear debris produced during in vivo service, probably responsible for the poor clinical performance of Hylamer™ acetabular cups.

Hip joint simulator studies on γ- and EtO-sterilised UHMWPE acetabular cups showed a higher weight loss due to wear in the latter, which also underwent the most significant changes on a molecular scale, as detected by micro-Raman spectroscopy. In several studies, the wear behaviour of different PEs has been correlated to the morphology at molecular level detected by micro-Raman spectroscopy (Battaglia et al. 2014).

6 Future Directions

Even if problems of oxidative degradation and wear are still unsolved, UHMWPE remains the gold standard as a bearing surface for total arthroplasty.

The categorical factors limiting the function and longevity of total hip replacement are surgical technique, fixation of the implant, osteolysis, fatigue failure and long term skeletal remodelling. The challenge is to obtain improvement on fixation and durability, which in UHMWPE is widely influenced by oxidative degradation and wear.

Attempts to solve these problems concern new sterilization techniques and new forms of more highly cross-linked polyethylene.

Actually, carbon nanotubes (Ruan et al. 2003) or UHMWPE-PMMA composites (Zhang et al. 2003) are studied in order to improve the properties of the polyethylene. In particular, a drastically enhanced toughness in UHMWPE films, due to the addition of 1 wt% carbon nanotubes (MWCNTs), has been shown. Raman spectroscopic analyses revealed that the presence of MWCNTs in the composites could lead to a 150% increase in strain energy density accompanied with an increase of 140% in ductility and up to 25% in tensile strength in comparison with pure UHMWPE.

With increasing patient longevity and activity levels, a search for the ultimate polymer is important even if these "new age polyethylenes" offer no direct clinical evidence to demonstrate their efficacy.

These solutions have to be confirmed through clinical performance and in vitro studies in order to confirm their better performances with respect to the previous polyethylenes.

References

Affatato S et al (2008) Comparative study on the wear behaviour of different conventional and cross-linked polyethylenes for total hip replacement. Tribol Int 41:813–822

Battaglia S et al (2014) A new protocol from real joint motion data for wear simulation in total knee arthroplasty: stair climbing. Med Eng Phys 36:1605–1610

Brach del Prever et al (1996) Unacceptable biodegradation of polyethylene in vivo. Biomaterials 17(9):873–878

Blunn G, Brach del Prever EM, Costa L, Fisher J, Freeman MAR (2002) Ultra high molecular-weight polyethylene (uhmwpe) in total knee replacement: fabrication, sterilisation and wear. J Bone Joint Surg [Br] 84(B):946–949

Bostrom MP, Bennett AP, Rimnac CM, Wright TM (1994) The natural history of UHMWPE. Clin Orthop Rel Res 309:11–19

Chenery DH (1997) Detection of peroxy species in ultra-high-molecular-weight polyethylene by Raman spectroscopy. Biomaterials 18(5):415–419

Costa L, Luda MP, Trossarelli L, Brach del Prever EM, Crova M, Gallinaro P (1998) Oxidation in orthopaedic UHMWPE sterilized by gamma-radiation and ethylene oxide. Biomaterials 19:659–668

Currier BH, Currier JH, Collier JP, Mayor MB, Scott RD (1997) Shelf life and in vivo duration. Impacts on performance of tibial bearings. Clin Orthop Rel Res 342:111–122

Edidin AA, Villarraga ML, Herr MP, Muth J, Yau SS, Kurtz SM (2002) Accelerated aging studies of UHMWPE. II. Virgin UHMWPE is not immune to oxidative degradation. J Biomed Mater Res 61:323–329

Goldman M, Lee M, Gronsky R (1997) Oxidation of UHMWPE characterized by fourier transform infrared spectometry. J Biomed Mater Res 37:43–50

Hahn D et al (1997) Analysis of polyethylene wear debris using micro-Raman spectroscopy: a report on the presence of beta-carotene. J Biomed Mater Res 35:31–37

Heisel C, Silva M, Schmalzried P (2003) Bearing surface options for total hip replacement in young patients. J Bone Jt Surg Am 85:1367–1369

Jaber SA et al (2014) In vitro effects on mobile polyethylene insert under highly demanding daily activities: stair climbing. Int Orthop (SICOT). doi:10.1007/s00264-014-2622-5

Jacob RJ, Pienkowski D, Lee KY, Hamilton DM, Schroeder D, Higgins J (2001) Time and depth dependent changes in cross-linking and oxidation of shelf-aged polyethylene acetabular liners. J Biomed Mater Res 56:168–176

James SP, Oldinski RK, Zhang M, Schwartz H (2009) UHMWPE biomaterials handbook

Kurtz SM, Muratoglu OK, Evans M, Edidin AA (1999) Advances in the processing sterilization, and crosslinking of ultra-high molecular weight polyethylene for total joint arthroplasty. Biomaterials 20:1659–1688

Kurtz SM, Muratoglu OK, Buchanan F, Currier B, Gsell R, Greer K, Gualtieri G, Johnson R, Schaffner S, Sevo K, Spiegelberg S, Shen FW, Yau SS (2001) Interlaboratory reproducibility of standard accelerated aging methods for oxidation of UHMWPE. Biomaterials 22:1731–1737

Li S, Burstein AH (1994) Ultra-high molecular weight polyethylene: the material and its use in total joint implants. J Bone Joint Surg [Am] 76(A):1080–1089

McGloughlin TM, Kavanagh AG (2000) Wear of ultra-high molecular weight polyethylene (UHMWPE) in total knee prostheses: a review of key influences. Proc Inst Mech Eng [H] 214:349–359

McKellop H (1996) Does gamma irradiation speed or slow wear?. AAOS, The American Academy of Orthopaedic Surgeons, USA

McKellop HA, Shen FW, Campbell P, Ota T (1999) Effect of molecular weight, calcium stearate, and sterilization methods on the wear of uhmwpe acetabular cups in a hip joint simulator. J Orthop Res 17:329–339

Mckellop H, Shen FW, Lu B, Campbell P, Salovey R (2000) Effect of sterilization method and other modifications on the wear resistance of acetabular cups made of ultra-high molecular weight polyethylene. A hip-simulator study. J Bone Jt Surg Am 82(A):1708–1725

Muratoglu OK, Bragdon CR, O'Connor DO, Jasty M, Harris WH (2001) A novel method of cross-linking ultra-high-molecular-weight polyethylene to improve wear, reduce oxidation, and retain mechanical properties. J Artroplasty 16:149–160

Oonishi H (1995) Long term clinical results of THR: clinical results of THR of an alumina head with a cross-linked UHMWPE cup. Orthop Surg Traumatol 38(11):1255

Rimnac CM, Klein RW, Betts F, Wright TM (1994) Post-iIrradiation aging of ultra-high molecular weight polyethylene. J Bone Jt Surg Am 76(7):1052–1056

Ruan SL, Gao P, Yang XG, Yu TX (2003) Toughening high performance ultrahigh molecular weight polyethylene using multiwalled carbon nanotubes. China, Hong Kong

Salernitano E, Migliaresi C (2003) Composite materials for biomedical application: a review. J of Appl Biomater Biomech 1:3–18

Sanford WM, Saum KA (1995) Accelerated oxidative aging testing of UHMWPE. ORS 20:119

Schmidt MB, Hamilton JV (1996) Calcium stearate-free UHMWPE therefore appears to be a superior choice for use in total joint replacement applications. In: 42nd ORS. Atlanta, USA

Shaw JH (1997) The effect of gamma irradiation on ultra high molecular weight polyethylene. Medical Devices Agency

Sobieraj MC, Rimnac CM (2009) Ultra high molecular weight polyethylene: Mechanics, morphology, and clinical behavior. J Mech Behav Biomed Mater 433–443

Sun DC, Scmidig G, Stark C, Dumbleton JH (1996) A simple accelerated aging method for simulations of long-term oxidative aging ejects in UHMWPE implants. In: 42th ORS. Atlanta, USA

Sutula LC, Collier JP, Saum KA, Currier BH, Currier JH, Sandorf WM, Mayor MB, Wooding RE, Sperling DK, Williams IR, Kasprzak DJ, Surprenant VA (1995) Impact of gamma sterilization on clinical performance of polyethylene in the hip. Clin Orthop Rel Res 319:28–40

Taddei P et al (2006) Oxidation in ultrahigh molecular weight polyethylene and cross-linked polyethylene acetabular cups tested against roughened femoral heads in a hip joint simulator. Biomacromolecules 7:1912–1920

Wang A, Lin R, Polineni VK, Essner A, Stark C, Dumbleton JH (1998) Carbon fiber reinforced polyether ether ketone composite as a bearing surface for total hip replacement. Tribol Int 11:661–666

Zhang YD, Wang YL, Huang Y, Wan YZ (2003) Preparation and properties of three-dimensional braided UHMWPE fiber reinfoced PMMA composites. Hong Kong, China

Ceramics for Hip Joint Replacement

Saverio Affatato, Sami Abdel Jaber and Paola Taddei

Abstract Ceramic materials for total hip replacement (THR) were introduced more than 20 years ago to solve the critical problems of polyethylene wear. Ceramic materials present excellent biocompatibility, mechanical resistance and high wettability. The ideal joint bearing for THR should be able to tolerate high cyclic loading for several decades, without undergoing corrosion or fretting at modular metal tapers, and would possess proven biocompatibility and material stability in vivo, as well as to reduce wear rates. The search for the ideal total joint bearing has led to the development of ceramic bearings. They have shown a good response to the matter of wear, providing the lowest wear rates compared to other material couplings, and could represent an optimum solution for young and active patients who have high risk of loosening or osteolysis in the mid and long term. Bearings made of ceramics (i.e. aluminium oxide and/or zirconium oxide) have been shown to possess extremely low wear properties that make them suitable for THR. Further developments could be made in the direction of reducing the crack propagation, thus diminishing ceramic brittleness.

Keywords Ceramics · Joint replacement · Hip prosthesis · Biolox® · Fluorescence · Raman spectroscopy

Nomenclature

Al_2O_3	Aluminium oxide
ZrO_2	Zirconium oxide
Y_2O_3	Yttrium oxide
Y-TZP	Yttrium Stabilized Zirconia
ZTA	Zirconia Toughened Alumina

S. Affatato (✉) · S.A. Jaber
Medical Technology Laboratory, Rizzoli Orthopaedic Institute,
Via di Barbiano, 1/10, 40136 Bologna, Italy
e-mail: affatato@tecno.ior.it

P. Taddei
Department of Biomedical and Neuromotor Sciences,
University of Bologna, Via Belmeloro 8/2, 40126 Bologna, Italy

F. Zivic et al. (eds.), *Biomaterials in Clinical Practice*,
https://doi.org/10.1007/978-3-319-68025-5_7

ZPTA Zirconia platelet toughened alumina
Cr_2O_3 Chromium oxide
SrO Strontium oxide
THR Total hip replacement

1 Introduction

Ceramics represent a class of new engineering materials specified for wear-resistant applications under severe environments. Ceramics, in agreement with the definition given by Hsu and Shen (1996), have been called "the material of the future" since they are derived from sand (which is about 25% of the earth's crust as compared to 1% for all metals). Scientific literature has produced a large variety of definitions for the term ceramic; in the field of materials science, the term ceramic includes all non-metallic, inorganic materials and, in most cases, these materials have been treated at a high temperature at some stage during manufacture (West 1994). The term "ceramic" is derived from a Greek word (*keramos*), which includes a lot of materials like glass products, cements, plasters, porcelain and other refractory coatings for metals, etc. (Thompson and Hench 1998; Kothiyal et al. 2012).

In recent years ceramic materials earned wide diffusion and importance for their chemical and physical characteristics, and progressively attracted interest in the field of biomedicine (Cuckler et al. 1995; Toni et al. 1995). Ceramic materials for the orthopaedic field were introduced more than 30 years ago to solve some critical problems due to polyethylene wear (Willmann 1998). Ceramic materials present excellent biocompatibility, mechanical resistance and high wettability. Last but not least, ceramics show outstanding properties at high temperatures, where most metals lose their efficacy. Alumina ceramics present good thermo-mechanical and tribological properties, high hardness, wear resistance, and chemical stability (Hamadouche and Sedel 2000). Alumina is chemically stable, but is mechanically weaker than other materials; it is commonly perceived as rigid and subjected to brittle fracture.

2 Alumina for Hip Prostheses

Due to their hardness and excellent biocompatibility, ceramics are ideally suited for joint prostheses. Alumina was introduced in 1971 by Boutin for alumina-on-alumina hip couplings, with good clinical results (Boutin 1971; Boutin and Blanquaert 1981). Although alumina shows very good performances in compression, but it is more sensitive to tensile stresses (Piconi et al. 2003), its use as biomaterial is recognized for its biological safety and stability in the human body.

With the introduction of ceramics (alumina and zirconia) in the orthopaedic filed as medical devices it was observed a reduced the wear rate in the total joint replacement (Macchi and Willman 2001). Some authors suggest that the use of zirconia may improve the mechanical strength of the ball head over alumina (Cuckler et al. 1995).

2.1 1st Generation of Alumina

The initial alumina components, produced for industrial applications, was unsuited for biomedical use due to its poor microstructure with low-density and purity and the large grain size caused by long sintering times during production. Continuous efforts performed in manufacturing techniques allowed the development of the first generation of alumina ceramics for hip joints; in 1974, alumina (obtained from chemically purified and grounded corundum powders) was marketed as Biolox® (Fig. 1).

The ISO standard 6474 was introduced in 1980 to improve the alumina quality used for hip prostheses and reduce the risk of fracture. Several factors influence alumina quality, such as grain size, density and purity. The grain size of alumina influences the wear rate, which decreases with decreasing grain size (Mukhopadhyay and Yiu-Wing 1993; Affatato et al. 2012b).

2.2 2nd Generation of Alumina

In the 1990s alumina hip joints were improved with the introduction of Biolox® forte, whose mechanical characteristics were highly enhanced. In 1995, this new material was produced using an improved raw material, which had a smaller grain size, lower level of impurities and was sintered in air (Macchi and Willman 2001); its brand name is Biolox® forte and an example of this kind of materials is showed in Fig. 2.

If compared with Biolox®, Biolox forte has higher density (3.98 g/cm^3 vs. 3.96 g/cm^3) and smaller grain size (3.2 μm vs. 4.2 μm).

2.3 3rd Generation of Alumina

In order to search for new applications, an innovative ceramic has been developed by CeramTec and in 2000 was introduced in the market with the name of Biolox® delta (Fig. 3).

It is a hot isostatic pressed zirconia-toughened alumina composite material specifically engineered to obtain substantially improved mechanical properties. This

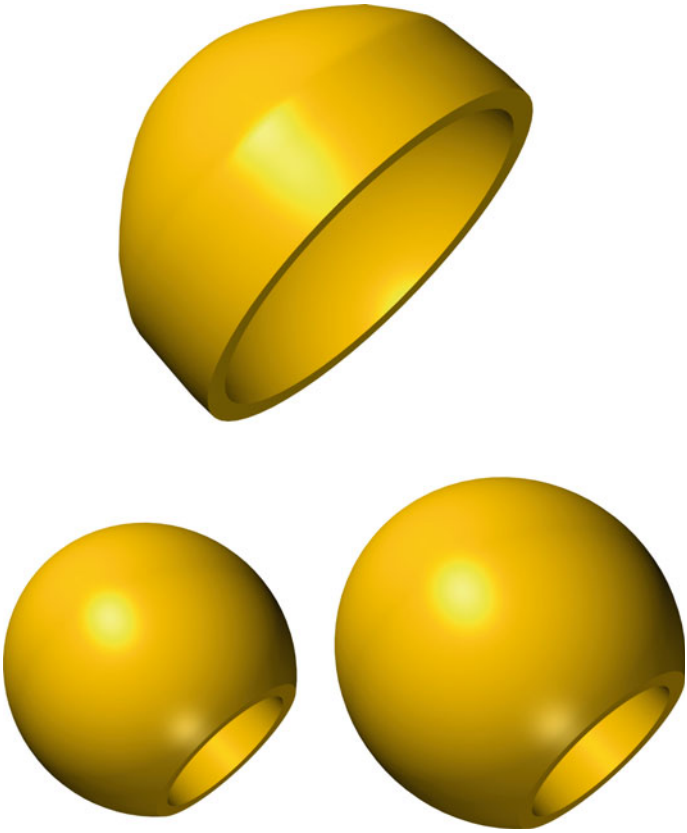

Fig. 1 The picture shows some specimens of the first generation of alumina named Biolox®. This generation was produced for industrial applications and had a poor microstructure with low density, scarce purity and large grain size

material exhibits an extremely high fracture toughness and a much higher capacity than other ceramic materials to resist the onset of cracking and to arrest the propagation of cracks (Dickinson et al. 2009; Merkert 2003). Biolox® delta is the latest commercial material for joint replacements developed by the current leader in the bioceramic product field (CeramTec AG, Germany) (Ma and Rainforth 2010); a zirconia toughened alumina based ceramic composite with several reinforcing principles that combine the best characteristics of both alumina and zirconia (the excellent strength and toughness of alumina and the higher performances of alumina in terms of wear, chemical and hydrothermal stability). To obtain these characteristics and avoid aging phenomena (as claimed by the manufacturer), nano-sized particles of yttria-stabilised tetragonal zirconia (Y-TZP) were uniformly distributed in the alumina matrix, so that the below-described phase conversion toughening mechanism is active. A small percentage of chromium oxide (Cr_2O_3) was added to counterbalance the reduction of hardness caused by the introduction

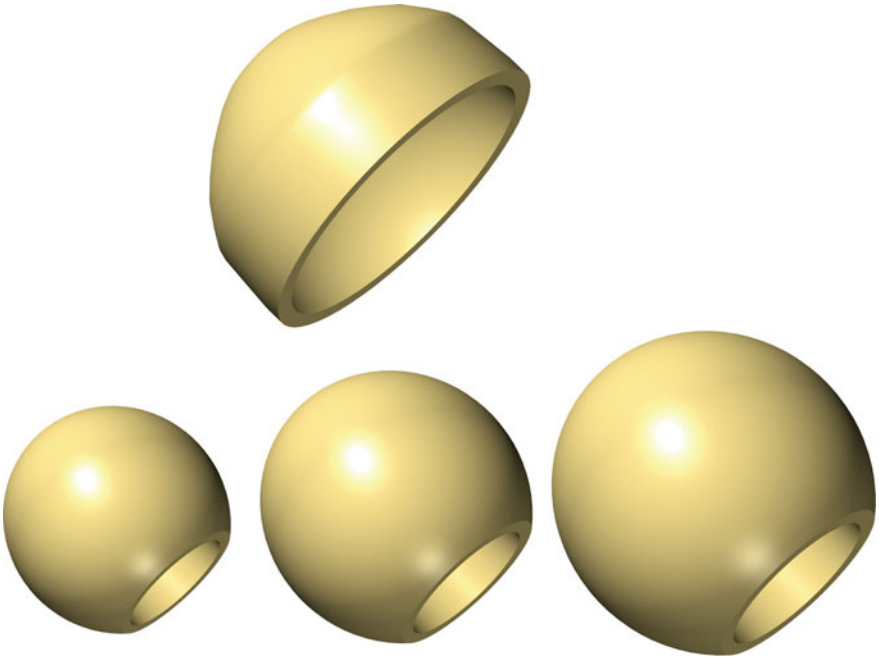

Fig. 2 The picture shows some specimens of the second generation of alumina named Biolox® Forte. This material is made of ultra-pure alumina with a small share of magnesium oxide to control grain growth and achieve maximum density

of zirconia. Finally, strontium oxide (SrO) added to the material forms strontium aluminate ($SrAl_{12}–xCr_xO_{19}$) platelets during the sintering process. Due to their size, these flat and elongated crystals prevent any cracks from advancing by dissipating crack energy. In fact, when the crack reaches one of these crystals, it needs extra energy to overtake this obstacle. This strengthening process increases the threshold of the energy that the crack needs for propagation. The final product is a mixture of roughly 75% alumina, 25% zirconia, and less than 1% chromium oxide and strontium oxide (Piconi et al. 2003; Affatato et al. 2012a).

3 Zirconia Used as Medical Device

Zirconia has become a very popular alternative to alumina because of its higher mechanical properties and higher toughness with respect to other medical grade ceramic materials (Derbyshire et al. 1994). Indeed, among all the monolithic ceramics, Y-TZP has the largest value of crack resistance.

The early developments were focused on magnesia partially stabilized zirconia (MgPSZ), in which a tetragonal phase is present in the form of small acicular

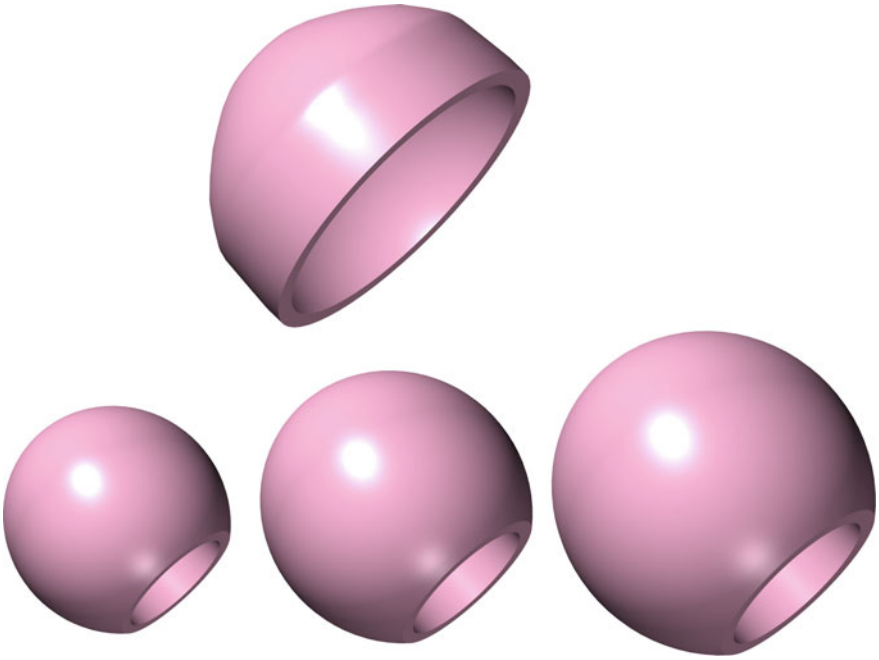

Fig. 3 The picture shows some specimens of the second generation of alumina named Biolox® Delta. The final product is a mixture of roughly 75% alumina, 24% zirconia, and 1% of mixed oxides (chromium and strontium oxide)

precipitates within large cubic grains (with a 40–50 μm diameter) forming the matrix. As this feature may negatively influence wear properties, most of the developments were focused on Y-TZP, a ceramic completely formed by submicron-sized grains, that is today the standard material for clinical applications (Kelly and Denry 2008; Willmann et al. 1996).

Y-TZP is composed by tetragonal grains less than 0.5 μm in size. The fraction of the tetragonal phase retained at room temperature depends on the size of grains, on its homogeneous distribution and on the concentration of the yttria stabilizing oxide (Piconi et al. 2003).

Mechanical properties of Y-TZP ceramics depend on the equilibrium among such microstructural parameters. The tetragonal grains can transform into monoclinic producing 3–4% volume expansion: this is the origin of the toughness of the material, and thus of its ability to dissipate fracture energy. When the pressure on the grains is released, i.e. by a crack advancing in the material, the grains near the crack tip shift into monoclinic phase. This gives origin to increased toughness, because the energy of the advancing crack is dissipated at the crack tip in two ways; the first one due to the T-M transformation, the second one due to the compression induced by volume expansion of the grains, which creates additional energy that the crack must overcome in order to advance. The existence of the metastable

tetragonal phase depends on the three factors reported above (e.g. grain size, stabilizing oxide concentration, matrix constraint). Now, it is well known that at temperatures above 100 °C in wet environments, the metastable tetragonal phase of zirconia ceramics can spontaneously transform into monoclinic.

As the transformation progresses from the surface of the material, a decrease in material density and a reduction in strength and toughness of the ceramic can be observed. The transformation can be explained by the formation of zirconium or yttrium hydroxides at grain boundaries, which scavenge yttrium ions from grains, thus changing the phase equilibrium of the material (Piconi and Maccauro 1999; Kelly and Denry 2008).

As above reported, the structure of Y-TZP at room temperature is formed by submicron sized grains. As the grains during sintering will grow, it is necessary to start from submicron grain size powders (e.g. = 0.02 μm) and to introduce some sintering aid to limit the phenomenon (Kohorst et al. 2012). A second aspect is linked to the introduction of the stabilizing oxide (yttria Y_2O_3), which is a key component in Y-TZP structure at room temperature.

As well as alumina, Y-TZP shows superior wettability properties with respect to metals, which allows fluid film formation at the interface of prosthetic joints, acting as a lubricant. In clinical practice Y-TZP ball heads were coupled only to UHMWPE sockets, but it should be noted that tests performed on Y-TZP-alumina joints gave positive results also in randomised clinical tests (Pitto et al. 2002). Many authors investigated the wear properties of the UHMWPE/zirconia coupling with mixed results. It can be observed that there is almost general agreement on the fact that UHMWPE wear against zirconia is not higher than against alumina (Affatato et al. 1999, 2001; Piconi et al. 1998). Discrepant results may be attributed to the differences in the materials used by the different laboratories, in their finishes, testing procedures, etc.

3.1 Zirconia Toughened Alumina

The introduction of zirconia up to 25% wt into an alumina matrix results in a class of ceramic materials with increased toughness, known as zirconia toughened alumina (ZTA). In these materials, developed in the second half of the 1970s, toughness (K_{IC}) up to 12 MPa $m^{-1/2}$ were achieved as well as bending strength up to 700 MPa.

The toughening of the material derives from a displacive phase transformation between the tetragonal (t) and monoclinic (m) crystal structures (Manicone et al. 2007). The *t-m* transformation can be induced by the combined action of stress and temperature, as well as other factors applied to the ceramic (Kusum and Harsimaran 2010). The resulting phase change introduces a combination of shear and volume expansion (of 7%) that, for example, can lead to the reduction of tensile stress near crack tips (Roberts et al. 2014). Due to the difference in elastic modulus between the alumina matrix and the zirconia particles, cracks will tend to move across the

less stiff zirconia particles inducing their *t-m* phase transformation, thus dissipating the crack energy.

A further dissipative effect is due to the micro-cracking of the matrix due to the expansion of the dispersed particles. The high density of the matrix and the optimisation of the microstructure of the zirconia particles, which must retain the maximum of the metastable phase and assure the transformation of the maximum volume, are the parameters that assure the better material performances. All the physical characteristics of the ceramics used as medical devices are showed in Table 1.

4 Wear Tests on Ceramic Components

The use of ceramic-on-ceramic as bearing surfaces for hip joint prostheses has been reported to produce a lower wear rate than other combinations (i.e. metal-on-polyethylene and ceramic-on-polyethylene) in total hip arthroplasty. Therefore, an increase in the life expectancy of hip implants is expected as well as an improvement of the life of patients.

The clinical success associated to the use of ceramics led to the implantation of more than 3.5 million alumina components and more than 600.000 zirconia femoral heads worldwide since 1990 (Chevalier et al. 2011). Ceramics components used in the orthopaedic field have to be characterized for an evaluation of their wear properties in order to prevent failures or produce improvements in the materials for artificial joints. At this regard, some wear tests have been performed. Affatato et al.

Table 1 Chemical composition and physical properties of alumina and zirconia ceramics used in orthopaedics

Chemical/physical characteristics	Alumina (99.95% Al_2O_3)	Y-TZP (ZrO_2 + 3% Y_2O_3)	ZTA (Al_2O_3 + ZrO_2 + Y_2O_3)	ZPTA (Al_2O_3 + ZrO_{2+} Y_2O_3 + Cr_2O_{3+} SrO)
Density [g/cm_3]	3.98	6.08	5.00	4.36
Aveage grain size [μm]	≤ 1.8	0.3–0.5	–	–
Bending strength [MPa]	>550	1200	900	1150
Compression strength [MPa]	5000	2200	2900	4700
Young modulus [MPa]	380	200	285	350
Fracture toughness [$M_{pam}^{4/2}$]	4–5	9	6.9	8.5
Microhardness [HV]	2200	1000–1300	1500	1975

(2009) carried out a wear test which compared the wear behaviour of different sizes of ceramic components. Two different batches of alumina Biolox® forte (28-mm vs. 36-mm) were tested on a hip simulator under bovine calf serum for five million cycles. These authors found that the 36-mm Biolox® forte size showed less weight loss than the 28-mm Biolox® forte size.

Ceramic hip components are commonly perceived as rigid and subjected to brittle fracture. The addition of zirconia into an alumina matrix (ZTA) has been reported to result in an enhancement of flexural strength, fracture toughness, and fatigue resistance (Affatato et al. 2006). Combining alumina and zirconia in different percentages resulted as a good solution to obtain a new material with better mechanical and tribological properties than the pure ceramic components. In this experiment, Affatato et al. tested (Affatato et al. 2006) different ceramic configurations, i.e. pure alumina versus alumina composite. The test ran for 7 million cycles under bovine calf serum as lubricant. The wear rate was lower for the pure alumina than for the alumina composites. However, no statistically significant differences were observed between the wear behaviours of these cups at a 95% level of confidence.

5 Molecular Characterization of Ceramic Materials

In the late 1970s, Grabner (1978) proposed a piezospectroscopic technique, which has been widely applied to characterise the residual stress state in alumina and alumina-zirconia composites (Krishnan et al. 2003; Garcia et al. 2002; Ma and Clarke 1994; Sergo et al. 1998). This method is based on the frequency shift experienced by a spectroscopic band of a solid upon an applied strain or stress. Although the spectral band may be generated by a variety of transitions (Raman scattering, absorption or luminescence), many studies on alumina and alumina-zirconia composites have focused on the stronger R_1 and R_2 fluorescence bands (Fig. 4).

The fluorescence, which derives from the red photoluminescence of ruby, is due to the presence of Cr^{3+} ions which substitute, as natural impurity, the Al^{3+} ions in the Al_2O_3 lattice. When the part of the lattice surrounding the Cr^{3+} ion is distorted due to an applied stress, the crystal field potential at the Cr^{3+} ion is altered, and thus also the energies of the electronic transitions of the Cr^{3+} ion are altered, giving information (through the wavenumber position and full-width at half maximum (FWHM) of the R_1 and R_2 bands) on the residual stress state of the sample.

In a previous study (Taddei et al. 2006a), fluorescence measurements have been used to clarify the role played by the implant position on wear; to this purpose, commercial alumina couplings have been tested in a hip joint simulator under three different angles of cup inclination (23°, 45°, 63°) with respect to a horizontal plane. The increase in the FWHM of the R_2 band was interpreted by considering that an angle of 63° represents a more severe mechanical condition for the prosthetic

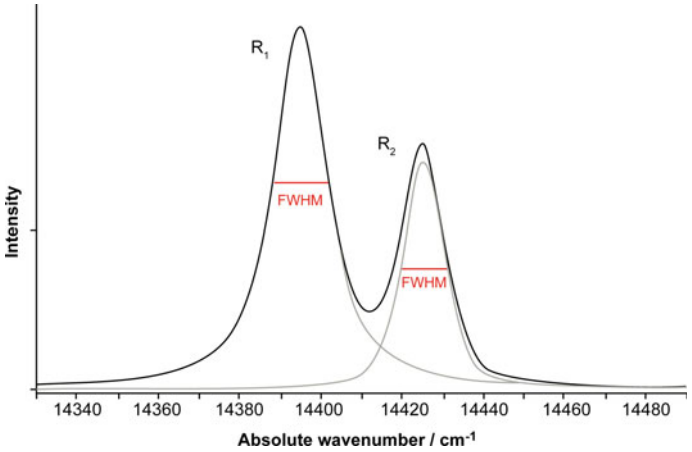

Fig. 4 R_1 and R_2 fluorescence bands of alumina. The choice of these spectral signals is due to the higher sensitivity obtainable for the residual stress measurements due to the strong fluorescence intensity. FWHM = full-width at half maximum

component, with a consequently higher probability of fracture and/or damage potentially conducive to massive wear.

Also the fluorescence intensity provides important information. Actually, a high fluorescence is indicative of a compact and dense material with few pores; in fact, pores behave as scattering centres of the incident laser beam and are responsible for lower fluorescence intensity. On the other hand, in a material with low porosity the volumetric concentration of the Cr^{3+} ions is higher and thus the fluorescence intensity as well. The better surface finishing of Biolox® forte has been demonstrated also by photoluminescence measurements (Taddei et al. 2006b, 2012; Chevalier et al. 2011; Affatato et al. 2012a). This result may be related to its better wear behaviour; in other words, fluorescence measurements demonstrated that an improved sample finishing resulted in a better wear behaviour (Taddei et al. 2006b; Chevalier et al. 2011).

The trend of the fluorescence FWHM and intensity provides information of the wear mechanism of ceramic materials. In a recent paper (Affatato et al. 2012a, b) we analysed three generations of ceramic hip retrievals (i.e. Biolox®, Biolox® forte and Biolox® delta). Upon wear, the intensity and the FWHM of the R_1 and R_2 bands changed in different ways in the three sets of retrievals, suggesting different wear mechanisms. The increase in the fluorescence intensity observed in the Biolox® and Biolox® forte retrievals suggests that the friction generated at the articulating surface caused a significant polishing effect. This phenomenon improved the quality of the surface, thus increasing fluorescence; on the contrary, no significant changes in the fluorescence intensity upon wear were observed in Biolox® delta retrievals, suggesting a negligible change in the surface finishing. Also the FWHM of the R_1 and R_2 bands showed a different trend in the three sets of retrievals upon wear: a significant increase in this parameter was observed for both Biolox® forte and delta,

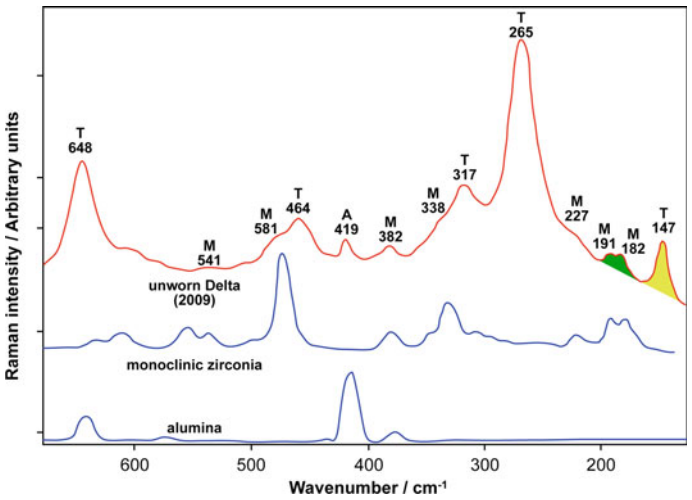

Fig. 5 Raman spectra of an unworn Biolox® delta component dated back to 2009, monoclinic zirconia and alumina. The bands assignable to tetragonal zirconia (T), monoclinic zirconia (M) and alumina (A) are indicated. The band areas utilised according to the method by Katagiri et al. to determine the monoclinic content are indicated

suggesting a wider range of residual stress values (Garcia et al. 2002). On the contrary, in the worn area of the Biolox® components both R_1 and R_2 bands sharpened upon wear, probably due to micro-cracking. Actually, micro-cracks are known to reduce the width of the Gaussian residual stress distribution (Ortiz and Suresh 1993).

With regards to Biolox® delta retrievals, micro-Raman spectroscopy was used to investigate the extent of tetragonal-to-monoclinic zirconia transformation, since tetragonal and monoclinic zirconia are easily distinguishable through marker bands characteristic of each form (Pezzotti et al. 2008). The main bands characteristic of the tetragonal phase can be identified at 147, 265, 317 and 464 cm^{-1}, while the marker bands of the monoclinic phase are located at 182, 191, 338, 382 and 481 cm^{-1} (Fig. 5).

Quantitative methods have been developed to determine from the Raman spectrum the amount of the monoclinic phase (Muñoz Tabares and Anglada 2010; Elshazly and Ali 2008).

The equation proposed by Katagiri et al. (1988) to evaluate the monoclinic content as volume fraction (V_m) appeared preferable:

$$V_m = \frac{I_m^{182} + I_m^{191}}{2.2 \times I_t^{147} + I_m^{182} + I_m^{191}}$$

where $I_m^{182} + I_m^{191}$ and I_t^{147} were the areas of the monoclinic doublet at 182 and 191 cm^{-1} and the tetragonal band at 147 cm^{-1}, respectively.

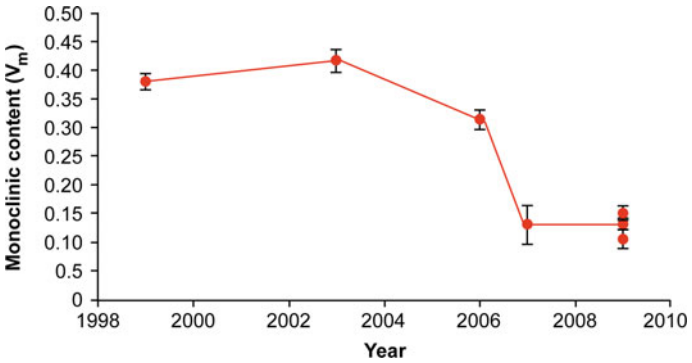

Fig. 6 Trend of the monoclinic content (V_m) in the period between 1999 and 2009

Raman spectroscopy, coupled to the method by Katagiri et al., was used to characterise new and retrieved Biolox® *delta* femoral heads (Affatato et al. 2012a; Taddei et al. 2012). Raman measurements on new and retrieved Biolox® *delta* femoral heads showed that a detectable amount of monoclinic zirconia was present in the as-received components and tended to increase upon wear (Affatato et al. 2012a; Taddei et al. 2012). In our new component, presumably dated back to 2009, the monoclinic content was about 10 vol%, i.e. lower than that reported by Pezzotti et al. in 2008 (about 20 vol%). This result would indicate an improvement of the material since its introduction in the market. Our Raman measurements confirmed this hypothesis (Fig. 6): a progressive improvement of the material properties (i.e. a progressive decrease in the monoclinic content) has occurred in the period between 1999 and 2009.

Raman spectroscopy showed that wear was the main cause of the in vivo tetragonal-to-monoclinic zirconia transformation. Our findings validated the in vitro accelerated ageing protocols proposed in the literature to simulate the effects of the in vivo wear, because the mechanism operating in vivo was found to be the same active in vitro. The in vitro fracture of a new femoral head appeared to be an extreme wear condition that determined the most significant changes in the residual stress state and monoclinic content both in the section of the fragments and on their surface. The micro-Raman mapping of the fractured articulating surface showed that the tetragonal-to-monoclinic transformation involved a region much more extended than as reported in the literature (Taddei et al. 2012).

6 Conclusions

Ceramic materials have been widely studied in the last few years and they show very interesting properties, which have been used to face several problems in the orthopaedic field. Excellent biocompatibility and outstanding tribological properties

made them the new solution for bearing materials in THR. Several improvements in the manufacturing process have been made in order to produce reliable materials. They have shown a good response to the matter of wear, providing the lowest wear rates compared to other material couplings, and could represent an optimum solution for young and active patients who have high risk of loosening or osteolysis in the mid and long term. Further developments could be made in the direction of reducing the crack propagation, thus diminishing ceramic brittleness.

In addition future trends are represented by the second generation of biomaterials, i.e. bioactive materials with the ability to interact with biological environment. Current applications are used to enhance biological response at the interface between implant and surrounding bone tissue. Ceramic coatings provide an alternative to biological fixation.

Acknowledgements The author's wish to thank Luigi Lena (Rizzoli Orthopaedic Institute) for his help for drawing these original figures.

References

Affatato S et al (2006) Advanced nanocomposite materials for orthopaedic applications. I. A long-term in vitro wear study of zirconia-toughened alumina. J Biomed Mat Res—Part B Appl Biomat 78:76–82

Affatato S et al (1999) Mixed oxides prosthetic ceramic ball heads. Part 2: effect of the ZrO_2 fraction on the wear of ceramic on ceramic joints. Biomaterials 20:971–975

Affatato S et al (2001) Mixed oxides prosthetic ceramic ball heads. Part 3: effect of the ZrO_2 fraction on the wear of ceramic on ceramic hip joint prostheses. A long-term in vitro study. Biomaterials 22:717–723

Affatato S et al (2009) Mixing and matching in ceramic-on-metal hip arthroplasty: an in-vitro hip simulator study. J Biomech 42(15):2439–2446

Affatato S, Modena E et al (2012a) Retrieval analysis of three generations of Biolox® femoral heads: spectroscopic and SEM characterization. J Mech Behav Biomed Mater 13:118–128

Affatato S, Taddei P et al (2012b) Severe damage of alumina-on-alumina hip implants: wear assessments at a microscopic level. J Eur Ceram Soc 32:3647–3657

Boutin P (1971) Alumina and its use in surgery of the hip. (Experimental study). Presse Med 79 (14):639–640

Boutin P, Blanquaert D (1981) A study of the mechanical properties of alumina-on-alumina total hip prosthesis. Revue de chirurgie orthopédique et réparatrice de l'appareil moteur 67:279–287

Chevalier J et al (2011) Reliability assessment in advanced nanocomposite materials for orthopaedic applications. J Mech Behav Biomed Mater 4(3):303–314

Cuckler JM, Bearcroft J, Asgian CM (1995) Femoral head technologies to reduce polyethylene wear in total hip arthroplasty. Clin Orthop Relat Res 317(317):57–63

Derbyshire B et al (1994) Comparative study of the wear of UHMWPE with zirconia ceramic and stainless steel femoral heads in artificial hip joints. Med Eng Phys 16:229–236

Dickinson A et al (2009) Development of a ceramic acetabular cup design for improved in vivo stability and integrity. In *BIOLOX Symposium*. p 227

Elshazly ES, Ali ME (2008) Alumina effect on the phase transformation of 3Y-TZP ceramics. J Mater Sci Technol 24:873–877

Garcia MA, Paje SE, Llopis J (2002) Relationship between mechanical grinding and photoluminescence of zirconia-toughened-alumina ceramics. Mater Sci Eng, A 325:302–306

Grabner L (1978) Spectroscopic technique for the measurement of residual stress in sintered Al_2O_3. J Appl Phys 49:580–583
Hamadouche M, Sedel L (2000) Ceramics in orthopaedics. J Bone Joint Surg. Br Vol 82:1095–1099
Hsu Sm, Shen MC (1996) Ceramic wear maps. Wear 200:154–175
Katagiri G et al (1988) Science and technology of zirconia III, Volume 2. In: S Somiya, N Yamamoto, H Yanagida (eds) American Ceramic Society
Kelly JR, Denry I (2008) Stabilized zirconia as a structural ceramic: An overview. Dent Mater 24:289–298
Kohorst P et al (2012) Low-temperature degradation of different zirconia ceramics for dental applications. Acta Biomater 8:1213–1220
Kothiyal GP, Ananthanarayanan A, Dey GK (2012) Glass and glass-ceramics. In: Functional Materials, pp 323–386
Krishnan R et al (2003) Raman spectroscopic and photoluminescence investigations on laser surface modified a-Al2O3 coatings. Scripta Mater 48:1099–1104
Kusum D, Harsimaran K (2010) A review of zirconia. BFUDJ 1
Ma L, Rainforth WMÃ (2010) Tribology International A study of Biolox s delta subject to water lubricated reciprocating wear. Tribol Int 43:1872–1881
Ma Q, Clarke DR (1994) Piezospectroscopic determination of residual stresses in polycrystalline alumina. J Am Ceram Soc 77:298–302
Macchi F, Willman G (2001) Allumina biolox forte: evoluzione, stato dell'arte e affidabilità, 15, pp 99–106
Manicone PF, Iommetti PR, Raffaelli L (2007) An overview of zirconia ceramics: Basic properties and clinical applications. J Dent 35:819–826
Merkert P (2003) Next generation ceramic bearings. In: Bioceramics in Joint Arthroplasty. pp 123–125
Mukhopadhyay AK, Yiu-Wing M (1993) Grain size effect on abrasive wear mechanisms in alumina ceramics. Wear 162–164:258–268
Muñoz Tabares JA, Anglada MJ (2010) Quantitative analysis of monoclinic phase in 3Y-TZP by raman spectroscopy. J Am Ceram Soc 93:1790–1795
Ortiz M, Suresh S (1993) Statistical properties of residual stresses and intergranular fracture in ceramic materials. J Appl Mech 60:77–84
Pezzotti G et al (2008) Raman spectroscopic analysis of advanced ceramic composite for hip prosthesis. J Am Ceram Soc 91:1199–1206
Piconi C et al (2003) Alumina and zirconia ceramics in joint replacements. J Appl Biomat Biomech 1:19–32
Piconi C et al (1998) Y-TZP ceramics for artificial joint replacements. Biomaterials 19(16):1489–1494
Piconi C, Maccauro G (1999) Zirconia as a ceramic biomaterial. Biomaterials 20:1–25
Pitto RP, Blanquaert D, Hohmann D (2002) Alternative bearing surfaces in total hip arthroplasty: zirconia-alumina pairing. Contribution or caveat? Acta Orthop Belg 68:242–250
Roberts O et al (2014) A study of phase transformation at the surface of a zirconia ceramic, II (April), pp 0–4
Sergo V et al (1998) Grain size influence on residual stresses in alumina/zirconia composites. Acta Mater 46:1701–1710
Taddei P, Affatato S, Fagnano C et al (2006a) Photoluminescence investigations on alumina ceramic bearing couples tested under different angles of inclination in a hip joint simulator. J Mat Sci 41:399–407
Taddei P et al (2012) Raman and fluorescence investigations on retrieved Biolox® delta femoral heads. J Raman Spectrosc 43(12):1868–1876
Taddei P, Affatato S, Torrecillas R et al (2006b) Wear behaviour, fluorescence and SEM investigations on nanocomposite zirconia-toughened alumina. J Mat Sci 41(16):5310–5316
Thompson ID, Hench LL (1998) Mechanical properties of bioactive glasses, glass-ceramics and composites. Proc Inst Mech Eng. Part H, J Eng Med 212:127–136

Toni A et al (1995) The use of ceramic in prosthetic hip surgery. The state of the art. Chir Organi Mov 80:13–25
West G (1994) Modern ceramic engineering: properties, processing and use in design. Comp Manuf 5:58–59
Willmann G (1998) Ceramics for total hip replacement - what a surgeon should know. Orthopedics 21(2):173–177
Willmann G, Fruh HJ, Pfaff HG (1996) Wear characteristics of sliding pairs of zirconia (Y-TZP) for hip endoprostheses. Biomaterials 17(22):2157–2162

Metallic Biomaterials

Goran Radenković and Dušan Petković

Abstract The development of science and technology contributes to an increased number of available materials. Biomaterials are considered a special class of materials, which is intensively studied by scientists, doctors, surgeons and engineers all over the world. Biomaterials are used for the production of implants with the aim of compensating or replacing diseased damaged living tissues or organs. Metallic biomaterials make a significant group of biomaterials mostly used for orthopaedic and dental applications due to a superior combination of high mechanical strength and fracture toughness. Metal alloys have played a predominant role as structural biomaterials in reconstructive surgery, especially orthopaedics, with more recent uses in non-osseous tissues, such as blood vessels. These biomaterials can be classified in five groups depending on their basic metal. Metallic biomaterials include stainless steels, titanium-based alloys, cobalt-based alloys, Ni–Ti alloys, and magnesium alloys. This study provides an overview of the most important alloys within the above classes, applications, advantages and shortcomings. Special requirements such as biocompatibility, corrosion and wear resistance, and mechanical properties are also analyzed. In addition, the most significant challenges for metallic biomaterials are summarized, with the emphasis on the most promising approaches and strategies.

Keywords Stainless steel · Titanium alloys · Cobalt alloys · Nickel–Titanium alloys · Magnesium alloys

G. Radenković (✉) · D. Petković
Faculty of Mechanical Engineering,
University of Niš, A. Medvedeva 14, 18000 Niš, Serbia
e-mail: rgoran@masfak.ni.ac.rs

F. Zivic et al. (eds.), *Biomaterials in Clinical Practice*,
https://doi.org/10.1007/978-3-319-68025-5_8

1 Introduction

The evolution of human civilization has undoubtedly caused the development of biomaterials, involving different materials, with a simple aim to extend and improve the quality of human life. More than 1000 years ago, gold and iron were used for dental applications, while silver in different forms was used as an antimicrobial agent to prevent infection. Different types of surgical procedures could also be found during early stages of civilization. However, probably the most significant developments took place in the field of biomaterials in the 20th century (Bose and Bandyopadhyay 2013). Since the early 1900s, metal plates have been used to stabilize long bone fractures with the aim of faster and more functional healing. Due to joint replacements and different cardiovascular devices, the quality of life for millions of people has been improved. In this century, tissue engineering and organ regeneration are the main scientific topics in the field of biomaterial research. Moreover, it is also important to carry out testing the following appropriate standards to get a regulatory approval in order to commercialize biomedical devices.

Civilization development and application of modern healing procedures and methods have significantly influenced a better and longer life of people. Furthermore, the life expectancy of the world as a whole is rising while the fertility rate is declining, creating a challenge in health care for the aging population (Gavrilov and Heuveline 2003). The United States alone will have 20% of the population over the age of 65 years by 2050, Europe will see rates close to 30% while Japan will arise to almost 40%, as shown in Table 1 (Romero 2013). Additionally, apart from old people, young and dynamic people, such as sports persons and people injured in accidents often need some kind of implants due to fractures or losing some part of the body. Because of that, one can expect an increase in the demand for various medical interventions and biomedical implants.

Biomaterials are a special class of materials which are used to construct artificial organs, rehabilitation devices, or implants to replace natural body tissues. Biomaterials have been of significant interest as they are extensively used to fix and replace decayed or damaged parts of the human systems such as bones, joints, teeth, heart valves, arteries, eyes and skin. The main function of biomaterials is to interact with biological systems, but they may also be used for drug delivery. The research in this field initially started by testing biomaterials on animals and their acceptability by the human body system was indirectly established.

Biomaterials have been defined as any substance (other than a drug) or a combination of substances, synthetic or natural in origin, which can be used for any

Table 1 Percentage of population over 65 years old

Region	1950	2000	2050
World	5.2	6.8	16.2
USA	8.3	12.4	21.6
Europe	8.2	14.8	27.4
Japan	4.9	17.2	37.8

period of time, as a whole or as a part of a system which treats, augments, or replaces any tissue, organ, or function of the body that has been lost through trauma, disease or injury (Boretos and Eden 1984). Additionally, the term "biomedical materials" is mostly used with the meaning of components of any biomedical devices applied with or without direct contacts with living tissue. On the other hand, the term "biomaterials" is used for biomaterials that are in direct contact with living tissues (Chen and Thouas 2015). Accordingly, biomaterials represent implanted biomedical materials. The single most important factor that distinguishes a biomaterial from any other material is its ability to exist in contact with tissues of the human body without causing an unacceptable degree of harm to that body, i.e. a biomaterial has to be biocompatible.

Depending on the crystal structure, chemical composition, bonding, and macrostructures, biomaterials are divided into several groups. Biomaterials can be natural or synthetic, whereas based on their macrostructures biomaterials can be distinguished as dense or porous. They can be generally grouped in four major categories such as metals, polymers, ceramics, and composites. The scope of this chapter is focused only on metallic biomaterials, their properties and applications.

Biomaterials should have specific physical, mechanical, chemical, and biological properties (Bose and Bandyopadhyay 2013). Microstructures, phases, density and porosity are physical properties. Strength, stiffness, hardness and toughness of the materials along with different failure mechanisms are mechanical properties. Chemical properties mean chemistry of the materials such as composition, bonding and atomic structures. Biological properties describe materials' behavior in a biological environment. It is important to mention that biological properties depend on the biological environment, so that "in vitro" ones are measured in the created biological environment, while "in vivo" are measured inside an animal or a human body. Surface properties define the outer layer where all bonds are not satisfied and therefore surface properties are often quite different from the bulk properties of materials. All these material properties are linked with chemistry, structure and processing of materials. For example, carbon is a material with very different properties depending on its bonding and structure. Graphite is formed when carbon has a hexagonal close-packed structure with covalent bonding. On the other hand, in diamond, the atoms are very closely packed and covalently bonded providing very strong and rigid structure.

Taking into account the desires, needs, and capabilities, it can be highlighted that the selection of the most suitable materials for different biomedical devices is a complex process. It depends on many factors such as mechanical loading requirements, chemical and structural properties, biological properties, and so on. Biological requirements should be met for each application, and materials should be capable of fulfilling the majority of needs. Human biology is a system composed of many complex and intricate processes and interactions between synthetic materials and the human body. Figure 1 illustrates the general application of biomaterials (Bose and Bandyopadhyay 2013).

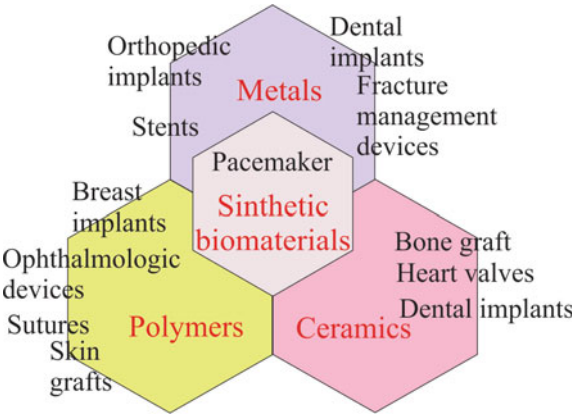

Fig. 1 Application areas of biomaterials

2 Basic Properties of the Metal Materials Used in Medicine

According to the basic definition, materials that are bonded via metallic bonds are called metals. Due to plenty of free electrons in metallic bonds, metals are thermally and electrically conductive, and show plasticity in terms of their mechanical properties. In general, the main advantage of metallic biomaterials lies in very high strength. Besides their high strength, stiffness and toughness, metallic materials can be processed reliably due to thousands of years of experience. Metals are more suitable for load-bearing applications compared with ceramics or polymeric materials due to their combination of high mechanical strength and fracture toughness; as biomaterials they are mostly used for orthopaedic and dental applications.

Metallic materials have been indispensable in orthopaedic surgery, playing a major role in most orthopaedic devices, including temporary (bone plates, screws and pins) and permanent implants (total joint and knee replacements). When it comes to temporary devices, the time period for bone healing, over which the host (body) is exposed to the bone screw/plate is in the range from 3 to 12 months (Enderle et al. 2005). Most of implanted biomaterials are orthopaedic prostheses and devices with the cost of about $10 billion (Holzapfel et al. 2013). Table 2 provides a list of applications of metallic materials in the body. Moreover, Table 2 also gives estimates of the numbers of medical devices containing metallic biomaterials that are implanted in humans each year (Ratner et al. 2012).

Metallic biomaterial implants can be divided into two groups, i.e. prosthesis and bone healing fixation equipment, based on the duration of their functionality in the body. Prostheses are designed for long-term applications in the body of a patient while the fixation is only used for keeping the bone in shape for a temporary period of bone reconstruction; after the healing period has been completed the fixation equipment is removed from the human body (Petković et al. 2012).

Table 2 Applications of metallic materials in medicine with the estimation of the number of users

Application	Biomaterials used	Number (World market in US$)
Skeletal system		
Joint replacements (hip, knee, shoulder)	Titanium, stainless steel, polyethylene	2,500,000
Bone fixation plates and screws	Metals, poly-lactic acid (PLA)	1,500,000
Dental implant-tooth fixation	Titanium	(4 billions $)
Cardiovascular system		
Heart valve	Dacron, carbon, metal, treated natural tissue	400,000
Pacemaker	Titanium, polyurethane	600,000
Implantable defibrillator	Titanium, polyurethane	300,000
Stent	Stainless steel, other metals, PLA	1,500,000
Organs		
Heart assist device	Polyurethane, titanium, stainless steel	4,000
Other		
Cochlear prosthesis	Platinum, platinum-iridium, silicone	250,000 total users

This kind of biomaterial has also found wide applications in dental and orthodontic practice for tooth fillings, roots, and dentures. Metals are used in dentistry due to their strength and durability. They are also used for vascular stents and tissue engineering and regeneration. However, metals lack proper appearance, chemical durability and biocompatibility. Regardless of a large number of available metals and metallic alloys and their ability to be processed, only a few are biocompatible and capable of long-term application as implant material. Figure 2 shows some medical devices made of metallic biomaterials.

Metallic biomaterials can be classified on the basis of the major alloying element as follows: stainless steels, titanium-based alloys, cobalt-based alloys, and magnesium alloys. However, the classification based on their properties and applications is somewhat different, as given in Table 3.

The design and selection of the most suitable biomaterial depends on its specific medical application. Implants and prosthetic devices need to fulfill several serious requirements so that they can be successful in service over a long-term usage in the body without rejection and minimal failure. Metal implants should possess the desired properties in order to serve safely and appropriately for a long period of time. Some of the requirements are listed below (Chen and Thouas 2015):

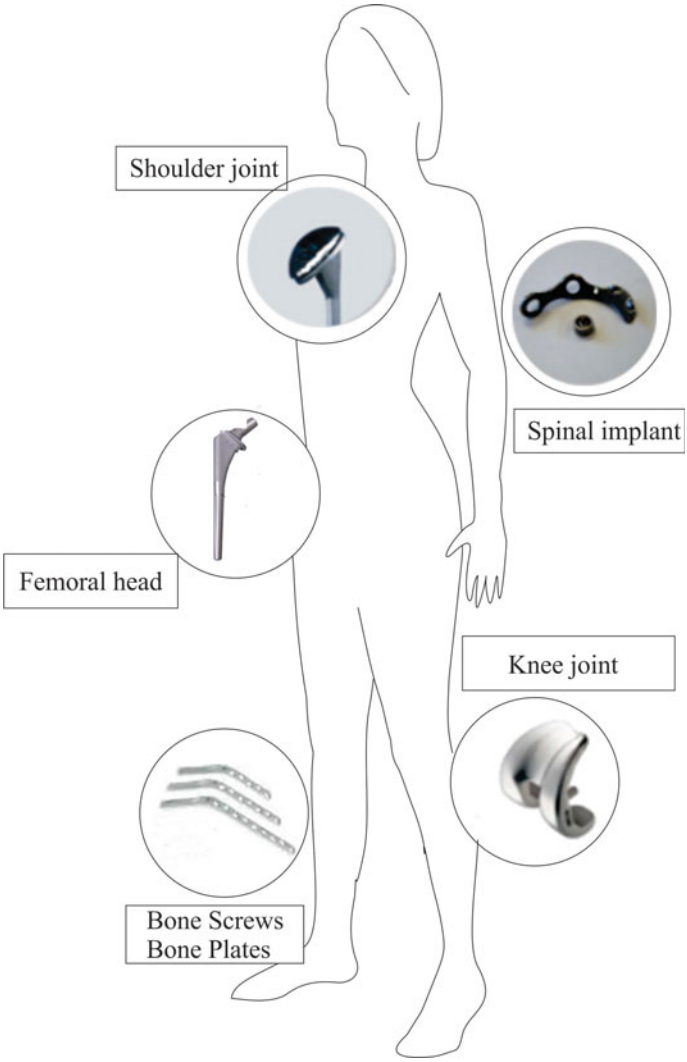

Fig. 2 Medical implants made of metallic materials

(1) Excellent biocompatibility,
(2) Suitable mechanical properties,
(3) High corrosion resistance,
(4) High wear resistance,
(5) Osseo-integration (in the case of bone prosthetics).

All aforesaid requirements have to be considered in the design of medical devices.

Table 3 Five categories of metallic biomaterials and their applications

Class	Application
Stainless steel	Temporary devices (fracture plates, screws, nails)
	Total hip prosthesis
Titanium alloys	Total hip and knee prosthesis
	Other permanent devices (screws and nails, pacemakers)
Co–Cr alloys	Total joint replacements (wrought alloys)
	Dentistry castings
Ni–Ti alloys	Orthodontic dental arch wires Vascular stents Vena cava filter Intracranial aneurysm clips Catheter guide wires Orthopaedic staples
Mg-based alloys	Biodegradable orthopaedic implants

2.1 Biocompatibility

Since a biomaterial replaces a lost or treats ill organ/organ system, an intimate contact with the living tissue is inevitable. In order to define biomaterials–tissue responses, four different types of biomaterials can be distinguished, i.e. toxic, bioinert, bioactive, and bioresorbable. Toxic materials cause death to the surrounding tissue. Biomaterials that are nontoxic but biologically inactive represent a group of bioinert materials such as metals. Loosening and failure of the bioinert materials is caused by fibrous tissue encapsulation. A bioactive material coating on a metallic implant may prevent fibrous tissue encapsulation. If a biomaterial is nontoxic and biologically active then it is classified as bioactive. Bioactive materials form an interfacial bond between host tissue and themselves. Some of bioactive materials are bioactive glasses, certain polymers and most calcium phosphate ceramics. Bioresorbable biomaterials are nontoxic in vivo soluble materials such as calcium sulfate and tricalcium phosphate.

The attempt to define a perfect biomaterial as the ideal replacement for a living body is still not convincing. The success of a biomaterial implantation depends largely on its biocompatibility. According to Williams, the term biocompatibility includes all aspects of bio-device function and interaction of cells and tissues with the implanted biomaterials (Williams 1987). It means that there is no cell death, chronic inflammation or other impairment of cellular/tissue functions. Biocompatibility requirements are complex, strict and vary with specific medical applications. The metallic implants are expected to be made of nontoxic elements and therefore cause no measurable inflammatory or allergic reactions in the human body.

One widely accepted definition of biocompatibility is the ability of a material to elicit an appropriate biological response in a given application (Williams 1987). In other words, this definition implies an interaction between the host, material, and

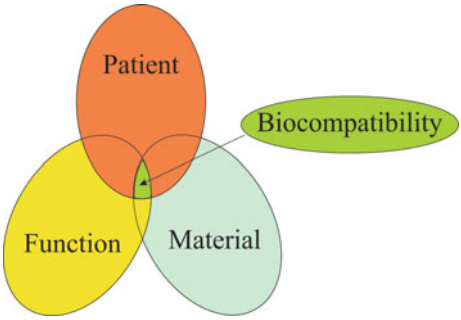

Fig. 3 Biocompatibility exists only when all 3 factors are considered, and it can change if any of these factors changes

expected function of the material as schematically shown in Fig. 3. All 3 factors must be in harmony before the material can be considered biocompatible (Wataha 2001).

Metals have been used in various forms as implants. Most metals used for manufacturing implants (e.g., Fe, Cr, Co, Ni, Ti, Ta, Mo, and W) can be tolerated by the body in very small amounts. Some of them are essential in cell functions as trace elements (micronutrients) in naturally occurring forms such as iron, cobalt, cuprum, manganese, zinc and selenium. However, some of these elements become toxic at levels higher than required (Park and Lakes 2007). Consequently, there are a lot people who suffer from metal allergies due to higher levels of metals in the body. Table 4 shows the percentages of the population who suffer from metal allergies (Niinomi 1999).

Ideally, nontoxic elements should be selected as alloying elements in developing a biomedical alloy. In reality no metals are completely inert or nontoxic. Hence metal implants require the alloys with elements which are more acceptable in terms of toxicity, or in the case of reactive alloys, the use of highly corrosion-resistant elements such as titanium. However, the complete elimination of toxic elements from all metallic biomaterials has been an everlasting goal.

The traditional paradigm for biocompatibility assessment of new materials is graphically presented in Fig. 4.

The first test of a new material is the in vitro test—the bottom of the pyramid. Only materials that 'pass' the in vitro tests move forward for further testing. The second phase is the in vivo animal tests. Some materials will also be screened out by animal tests, and relatively few will reach the state of clinical tests. The third phase is the clinical tests and only materials that 'pass' clinical tests can be introduced for clinical use. The paradigm was established in order to efficiently evaluate a large number of new biomaterials while maintaining economic and ethical feasibility (Wataha 2012).

Table 4 Metal sensitivity of population

Population	(%)
General population	10
Patients with stable total joints	25
Patients with loose total joints	60

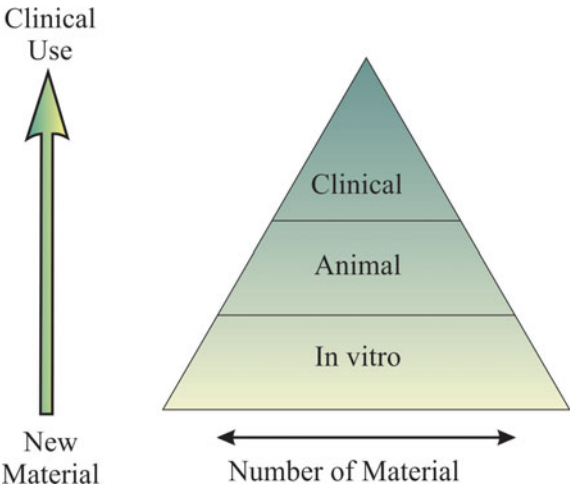

Fig. 4 The traditional paradigm for biocompatibility assessment of new materials

Osseo-integration is a fundamental requirement in orthopaedics, a term that describes the process of new bone formation and bone healing (Nasab et al. 2010). The inability of an implant surface to bond to adjacent bone and other tissues due to micro motions will cause the formation of fibrous tissue around the implant, which causes loosening of the prosthesis. Consequently, the implants should have suitable surface properties in order to integrate well with the surrounding bone. Surface chemistry, surface roughness and surface topography are all factors that need to be considered for good osseo-integration (Parsapour et al. 2012).

2.2 Corrosion Resistance

Medical devices and prostheses should remain intact for a longer period and should not fail while the person is alive. Therefore, a minimum service period from 15 to 20 years in older patients and more than 20 years for younger patients is desired. The success of an implanted biomaterial depends on four factors, i.e. the biomaterial properties (mechanical, chemical and tribological), biocompatibility of the implant, the health condition of the recipient, and the competency of the surgeon. The currently used materials usually fail within a period of about 12–15 years, which leads to revision surgery in order to regain the functionality of the system (Manivasagam et al. 2010). The reasons for their failure can be classified as mechanical, chemical, tribological, surgical, manufacturing and biocompatibility issues. Apart from all these issues, the implant failure due to corrosion is dominant and represents one of the challenging problems.

Corrosion is a destruction of materials caused by chemical or electrochemical action of the surrounding environment. Corrosion is affected by several factors such as electrochemical, metallurgical, physicochemical, and thermodynamic (Fontana

and Greene 1978). Blood with other constituents and body fluids creates corrosion environments for implants. The majority of human body fluids, under normal conditions, contain around 0.9% saline (predominantly NaCl) and other trace ions with certain small amount of soluble proteins and amino acids. The pH value of these fluids is nearly neutral—7.2–7.4. However, the pH value of a body fluid may fall to 3–4 due to inflammatory cell secretions caused by surgery or injury (Sumita et al. 2003).

Any metal material is not resistant to corrosion and/or ionization within living tissues. Since the corrosion process is unavoidable, it has been accepted that the tolerable corrosion rate for metallic implant systems should be about 2.5×10^{-4} mm/year (Mohanty et al. 2003). The most common forms of corrosion include uniform corrosion, and localized corrosion such as galvanic, pitting, stress corrosion cracking, and fatigue corrosion. It is important to highlight that localized corrosion is more dangerous because it is more difficult to predict than uniform corrosion (Virtanen et al. 2008).

Corrosion of implants has double consequences: first—weakening and premature failure of the implants and second—release of corrosion products from the implant leading to the tissue reaction. Upon a prolonged contact with human tissue (elevated temperature and saline conditions), surface corrosion phenomena take place resulting in a high rate of locally systemically released corrosion products (Krischak et al. 2004). The release of metal ions in large amounts may cause some harmful effects (Hanawa 2004). Accordingly, the biocompatibility of a metallic biomaterial is directly determined by its corrosion resistance and the biological effects of released metal ions.

When it comes to orthopaedic implants there are temporary and permanent implants. Temporary ones include plates, screws, and nails while permanent ones include replaces for hip, knee, spin, shoulder, toe, finger and so on. Temporary implants suffer from pitting corrosion, crevice corrosion at shielded sites as well as beneath the heads of fixing screws (Yu et al. 1993). It was shown that pitting and crevice corrosion attack causes more than 90% failures of implants (Antunes and de Oliveira 2012). The problem of corrosion attacks and leaching of metallic ions from implants can be alleviated either by bulk alloying or modifying the surface (Mudali et al. 2003). In some cases though the material will not fail directly due to corrosion, it is found to fail due to accelerated processes such as wear and fretting leading to tribo-corrosion. In the presence of wear the corrosion process is accelerated, which is often encountered in biomedical implants. ASTM standards are established procedures for testing corrosion resistance of biomaterials under different conditions. Commonly used standards for testing different corrosion processes are given in Table 5.

Metallic biomaterials form a stable oxide layer (passive film) on their surface in the reaction with environments. The passive film, which forms on the metal surface, plays an important role both in corrosion stability and biocompatibility (Milosev and Strehblow 2000). This film is typically a few nanometers thick, thus, it acts as a highly protective surface barrier between the bulk metal and the aggressive biological environment (Schmuki 2002). Protective quality of the passive film is

Table 5 Standards for testing corrosion resistance of biomaterials

ASTM Standards	Specifications
ASTM G61-86 (2014)	Standard test method for conducting cyclic potentiodynamic polarization measurements for localized corrosion susceptibility of iron-, nickel- or cobalt-based alloys
ASTM G5-14 (2014)	Standard reference test method for making potentiodynamic anodic polarization measurements
STM G71-81 (2014)	Standard guide for conducting and evaluating galvanic corrosion tests in electrolytes
ASTM F746-04 (2014)	Standard test method for pitting or crevice corrosion of metallic surgical implant materials
ASTM F2129-08 (2008)	Standard test method for conducting cyclic potentiodynamic polarization measurements to determine the corrosion susceptibility of small implant devices

kinetically determined by the ion transfer through the film as well as by its dissolution stability (Schultze and Lohrengel 2000) (Fig. 5). An increased content of elements that form the most stable oxides in the passive film results in an increased resistance of the metallic biomaterial to corrosion. On the other hand, the presence of some nonmetallic inclusions on the material's surface represents a major problem due to their negative role in pitting corrosion (Shih et al. 2004; Li and Bell 2004).

After the film has deteriorated, the process of its regeneration starts spontaneously. The regeneration time of the passive film after disruption can vary depending on the environmental conditions, which cause metal ions release from the surface. Crucial factors for the reformation of the oxide layer and the time taken for the same are interactions between the biomaterial and the physiological

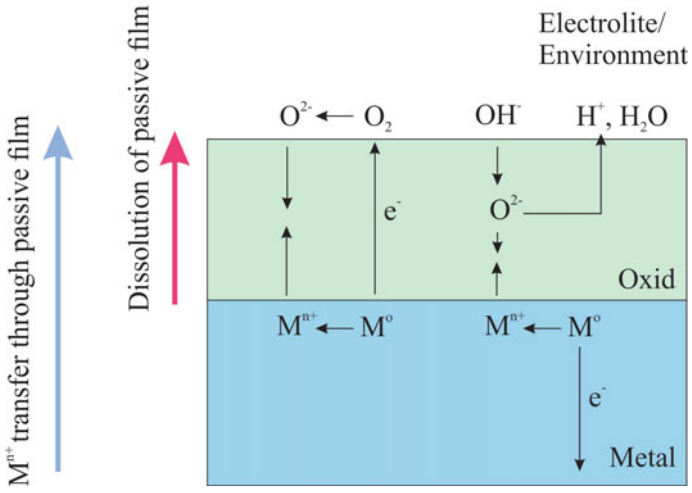

Fig. 5 Oxide film on a metal surface

medium. The regeneration time of the film is different for various materials. Sumita et al. determined the duration of the regeneration time taken to form surface oxide films for various metallic biomaterial alloys (Sumita et al. 2003). He found that the regeneration time in stainless steel AISI 316L is around four times longer than in Ti–6Al–4V alloy. A slightly longer regeneration time was also specified for Co–28Cr–6Mo alloy in comparison with Ti–6Al–4V alloy.

It is a well-known fact that the success of a biomaterial depends on the reactions between the metal surface and human tissues soon after implantation (Manivasagam et al. 2010). That way biocompatibility is basically determined by the reactions which occur at the initial stages after implantation.

Environmental conditions such as the composition of the electrolyte, the redox conditions, the exposure time and temperature determine the nature and stability of the passive film on a biomedical metal. Depending on the type of the oxide formed, the passive film may remain stable and sustain passivity upon exposure to the biological environment. Localized breakdown of the passive film occurs under certain conditions, leading to material dissolution at the site of the breakdown. Various inhomogeneities in the material, or in the surrounding environment, are ideal sites for the initiation of localized corrosion. Even though most of the surface is still covered by the undamaged passive film, the corrosion rate at locally activated sites can reach very high values. The results of surface oxide layer analysis on various metallic biomaterials are given in Table 6 (Manivasagam et al. 2010).

The surface present on a metallic material plays a very important role, not only for corrosion resistance but also for tissue compatibility. Hence the analysis of surface characteristics of a metal biomaterial is important due to the issues of corrosion and tissue compatibility (Kasemo and Lausmaa 1986). Bearing in mind the importance of the metallic biomaterials surface, the possible improvements of the surface in terms of both corrosion properties and body tissue compatibility include: (1) the technique to improve the quality of the protective passive film (passivation) and (2) the technique to coat the surface in order to improve surface properties compared with the bulk metallic biomaterials.

2.3 Mechanical Properties

Apart from biocompatibility, mechanical properties are often very important for biomaterials used in most medical devices and implants. Metallic biomaterials are widely used for repairing broken or cracked bones. The main reason is their ability to appropriately carry loads applied to the bones. Generally, mechanical properties of materials determine a material's behavior when subjected to mechanical load. The ability of a material to withstand the applied load without any permanent deformation is expressed in two ways, i.e. strength and hardness. Strength is defined in many ways as per the design requirements, while the hardness may be defined as resistance to indentation or scratch. Material deformation caused by the action of a force can be permanent or temporary. Permanent deformation is

Table 6 Oxide layer on metallic biomaterials

Metallic biomaterial	Surface oxides	Surface analysis
Titanium and titanium alloys		
Titanium	Ti^{0+}, Ti^{2+}, Ti^{3+}, Ti^{4+}	• Ti^{2+} oxide thermodynamically less favorable than Ti^{3+} formation at the surface • Ti^{2+} and Ti^{3+} in the uppermost part of the surface film • Ti^{4+} observed on the surface outer most layer
Ti–6Al–4V	TiO_2	Small amount of Al_2O_3, hydroxyl groups, alloying element and bound. V was not detected
Ni–Ti	TiO_2 based oxide	Minimal amounts of Ni in both oxide and metal states
Ti–56Ni	TiO_2	Very low concentration of NiO, hydroxyl groups, metallic nickel, and bound water was detected on the surface
Ti–Zr	Ti and Zr oxides	Uniform distribution of Ti and Zr along the depth direction. The thickness of the oxide film increases with an increase in the zirconium content
Stainless steels		
Austenitic stainless steel	Fe and Cr	Only a very small amount of Mo was observed on the surface and Ni was absent when tested in both air and chloride solutions
AISI 316L	Oxide of Fe, Cr, Ni, Mo and Mn (thickness about 3.6 nm)	The surface film contains a large amount of OH–, that is, the oxide is hydrated or oxyhydrated. Fe is enriched in the surface oxide film. Ni, Mo and Mn are enriched in the layer just under the surface oxide film
Co–Cr–Mo alloy		
Co–36.7Cr–4.6Mo	Oxides of Co and Cr without Mo (thickness 2.5 nm)	Surface contains a large amount of OH^-, that is, the oxide is hydrated or oxyhydrated. Cr and Mo are distributed more at the inner layer of the film

irreversible, i.e. stays even after the removal of the applied forces, while the temporary deformation disappears after the removal of the applied forces. Temporary deformation is called elastic deformation, while the permanent deformation is called plastic deformation.

When a material is subjected to certain forces, at first an elastic deformation occurs followed by a plastic deformation. The extent of these elastic and plastic deformations will primarily depend on the kind of material and rate of load application. The change from the elastic state to the plastic state is characterized by the yield stress of the material.

When it comes to hard tissue replacements, mechanical properties are a priority. For example, the femoral part of a total hip prosthesis must bear static and cyclic loads which occur due to the body weight and muscle forces, and it must not fail during the lifetime of the implant. A case of the premature fractured femoral part of a hip implant made of stainless steel is shown in Fig. 6. It is evident the fracture appeared at the point with the highest internal stress due to the dynamic bending load.

It is desirable that mechanical properties of biomaterials are similar with the replaced tissues. Thus a femoral stem should have the stiffness of a femur, otherwise the cells in the adjacent bone tissue would be shielded from mechanical load leading to the implant failure via osteolysis, bone resorption, and loosening of the stem in the femur (Sumner et al. 1998). That way, in almost all orthopaedic devices, the optimum device performance depends on the optimum mechanical properties, which include a design compromise. Also mechanical properties of biomaterials

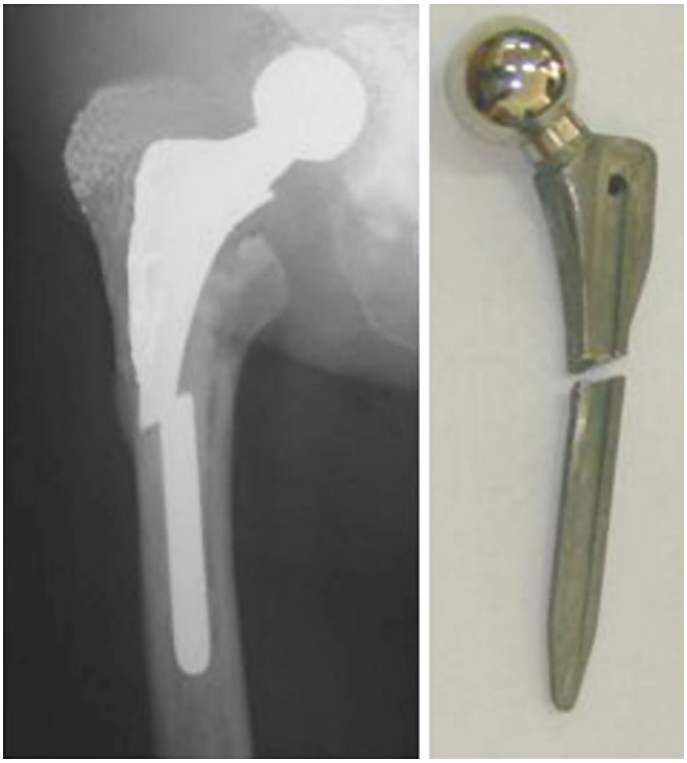

(a) Radiographs of the broken hip

(b) Broken hip implant after surgery

Fig. 6 Fractured femoral part of the hip prosthesis

may vary in space and time. For example, sutures and fixation screws that are used for arthroscopic reconstruction of a torn anterior ligament, may have such mechanical properties which intentionally degrade over a desirable time scale after implantation (Middleton and Tipton 2000).

Metallic biomaterials have to be satisfactorily strong and tough in order to replace bone. The fundamental mechanical properties of metallic biomaterials include Young's modulus of elasticity, yield tensile strength, ultimate tensile strength and toughness. Quantitative values of mechanical properties are determined on the basis of the testing results and calculated by using a corresponding equation. A summary of these mechanical properties for five groups of metallic biomaterials is given in Table 7, based on authors' experience and available data. Mechanical properties such as ultimate strength, yield strength, fatigue strength, elasticity, fracture toughness, ductility, hardness and wear resistance depend on the material structure. Therefore, the range of these properties is due to their dependence on the material microstructure that, in turn, is a function of the processing method as well as post-processing treatments (Pillar 2009).

It is obvious that stainless steel, cobalt-based alloys and titanium-based alloys have much higher Young's modulus (>100 GPa) in comparison with bone (10–30 GPa). Nevertheless, they are still popular primarily due to their ability to bear loads and undergo significant plastic deformation before failure, as indicated by their respective ultimate tensile strength and fracture toughness. It is also important to have an orthopaedic biomaterial with elasticity modulus closer to that of bones in order to avoid atrophy around the implant site ("stress shielding effect"). Working conditions, especially mechanical, within the human body are very complex. Human beings commonly make several thousand steps a day with the frequency of 1 Hz, assuming the average is around 2000 steps. Therefore, the total calculation of the number of steps over 20 years is as follows: 2000 steps × 365

Table 7 Mechanical properties of metallic implant materials and cortical bone

Material	Young's modulus of elasticity (GPa)	Yield tensile strength (MPa)	Ultimate tensile strength (MPa)	Elongation (%)	Fracture toughness (MPa $m^{1/2}$)	Hardness, (HV)
Stainless steel alloys	200–205	170–690	540–1000	12–40	~100	130–180
CP Ti	100–115	170–480	240–550	15–24	~80	120–200
Ti-based	100–110	585–1050	690–1150	10–15	~80	~300
Co-based	210–240	450–1500	655–1900	5–30	~100	300–400
Ni–Ti alloys	30–50	70–140	895–1350	~9	30–60	
Mg	40–45	–	100–250	15–40		
Cortical bone	10–30	–	100–300	1–2	2–12	–

Table 8 Typical fatigue mechanical working conditions of some implants

Implant	Frequency of load (Hz)	Strength	Expected total number of loading for 20 years
Joints	1	Compression ~50 MPa Bending ~200 MPa	10^7
Pacemaker	1	Not available	10^9
Tooth fillings	1	Not available	10^7

day $\times$ 20 years $\approx 10^7$ steps (cycles). Because of such cyclic loading, various bone implants (hip and knee joints, spinal fixations, nails, plates and wires) suffer from fatigue. Thus, the loading stress level of an artificial hip joint is several times higher than that of the patient body weight. Cyclic stress also occurs in dental implants due to chewing as well as in cardiovascular implants as response to myocardial activity. Typical fatigue mechanical working conditions of some implants are summarized in Table 8.

Generally, a material can fracture far below its ultimate tensile strength or even below its yield strength when it is subjected to cyclic loading. The reason for that lies in the fact that variable internal stresses may lead to the initiation and growth of a crack. When the crack reaches a critical size, material fracture is unavoidable. Fatigue can also be complicated by a simultaneous corrosion action. When fatigue occurs along with corrosion, the phenomenon is known as corrosion fatigue.

ASTM standards have established procedures for fatigue testing of metal biomaterials. Some of those are: F1440-92 and E602 (fatigue testing of metallic implants), F1801-97 (compression fatigue), F1612-95 (Stem of total hip replacement), F1717-96 (Spinal device), F1539-95 (Staple).

2.4 Wear

Wear is often reposted as a major cause of implants' failure. Additionally, it has been proved that wear accelerates the corrosion of the biomedical devices and implants (Zivic et al. 2013). Wear can be defined as damage to a solid surface that generally involves progressive loss of material and is due to relative motion between that surface and a contacting substance or substances (Blau 1992). It is an inevitable problem in any joint replacements no matter what materials are used. Material selection for joints primarily depends on the type of joint. In the human body there are several types of mobile joints between long bones (knee, hip, shoulder, ankle and elbow). Joints such as jaw, wrist and scull are classified as more static ones (Chen and Thouas 2015). Depending on how closely the opposed bones fit together, mobile joints are divided into two groups, i.e. congruent (hip and

Table 9 Ranking of pairs of materials for congruent joints in terms of wear resistance

Ball and socket	Wear resistance
Ceramic-on-Ceramic ($Al2O_3$ or ZrO_2)	Superior
Co-CrMo-on-Co-Cr-Mo	Excellent
Al2O3-on-Co-Cr-Mo	Excellent
Al2O3 on UHMWPE[a]	Excellent
Co-Cr-Mo on UHMWPE	Good
Ti6Al4V on UHMWPE	Good
Metal on metal (stainless steels or titanium alloys)	Poor

[a]UHMWPE—ultra-high molecular weight polyethylene

shoulder) and incongruent (knee and ankle). In congruent joints stress is distributed evenly due to a ball-shaped head that fits closely into a cup-like socket. The most suitable materials for such mechanical stress state are biomaterials with high strength and hardness, even including brittle ceramic materials. Table 9 shows the ranking of articulating materials for ball-and-socket joints depending on wear resistance (Chen and Thouas 2015).

When it comes to incongruent joints, mechanical stress is heterogeneously distributed (concentrated) due to the contact of two incongruent hard surfaces, which is compensated by the presence of thick cartilage layers and synovial fluid. Brittle ceramic materials are not suitable for such a stress state and therefore some metallic and hard polymeric materials are preferred.

A high friction coefficient (low wear resistance) of a joint system leads to the loosening of the implant. The so-called "aseptic loosening" is a frequent incident caused by wear, which occurs in any material when micro-particles are generated at the bearing couples of a joint replacement (Schweizer et al. 2003).

Most common metallic biomaterials, their properties and applications have been considered in the previous five chapters. There is no doubt that an ideal (metallic) biomaterial as a replacement for the living tissue does not exist. In other words, each of the aforementioned metal alloys has both advantages and certain drawbacks, particularly in terms of biocompatibility. A high degree of biocompatibility of these alloys is due to the formation of a surface oxide layer consisting of Cr or Ti oxides (depending on the chemical composition). This oxide layer, commonly named the passive film, is a specific kinetic barrier between the bulk metal and the surrounding living tissue which physically prevents corrosion reactions. Hence the surface of biomaterials is very important due to its reaction with host tissue which is mostly crucial for successful implantation. Ti alloys have proved to be the best ones regarding biocompatibility, but are far from ideal.

Despite the formation of the passive film on the metal surface, clinical research has proved that a certain amount of metal ions is released from the surface of metal biomaterials. In order to limit further oxidation, initially formed passive films must have desired characteristics such as non-porous, high abrasion resistance and atomic structure that will limit the migration of ions across the metal oxide—solution interface (Manivasagam et al. 2010). However, the native oxide layers are

not bioinert and bioactive enough to totally prevent the corrosion reaction and form a direct bonding with bone. As a consequence it might lead to a long-term failure after implantation. Therefore, scientists and engineers attempt continuously to improve surface properties of metallic biomaterials in order to reduce the number of implants' failures due to poor cell adhesion, corrosion and wear resistance. Hence surface modification can be a key technology to enhance the in vivo performance of biomaterials. Proper surface modification techniques not only retain the desired bulk attributes of biomedical materials, but also improve specific surface properties required by different clinical applications (Petković et al. 2013). The main task of surface engineering is to adapt the implant surface so as to avoid the negative effects of biomaterials on the surrounding tissue as well as to enhance the interplay between the body tissue and the implanted material. There are numerous techniques to improve the biocompatibility of metal biomaterials such as mechanical, chemical, electrochemical, heat treatment and coating. Consequently, different surface treatments and coatings have been carried out on metallic biomaterials in order to improve biocompatibility and corrosion and wear resistance.

Surface engineering methods of metallic biomaterials were extensively reviewed by Kurella and Dahotre (2005) and Bauer et al. (2013). In order to improve surface-based properties of biomedical metals, various methods have been employed. These methods include blasting, passivation, anodization, nitriding, plasma treatment, laser alloying, and Physical vapor deposition (PVD) or Chemical vapor deposition coating. Blasting is a use of abrasive particles such as hard ceramics against another metallic material under high pressure in order to improve surface biocompatibility (Piattelli et al. 2002). Nitric acid has been used as one of the most popular chemical passivating reagents for surface treatment of Ti alloys and AISI 316 L stainless steel. The determination of the effects of nitric acid concentration, temperature and passivation period on the corrosion resistance of the AISI 316L stainless steel and beneficial effects were also reported (Petković and Radenković 2013). Additionally, a simple cyclic linear potentiodynamic polarization technique was used as a method of improving corrosion properties a biomedical-grade AISI 316LVM stainless steel surface in phosphate buffer (Bou-Saleh et al. 2007). Due to Ti alloys inferior tribological properties (low wear resistance, higher coefficient of friction, and lower hardness), the process of laser nitriding has emerged as a unique method for tailoring the surface microstructures and composition of titanium for enhanced tribological characteristics of titanium and its alloys (Dahotre et al. 2013).

Coating is one of the ways for improving surface properties without compromising the basic bulk mechanical properties (Frutos and Gonzalez-Carrasco 2013). Methods such as physical vapor deposition coating (TiN, TiC) have been examined for improving wear and corrosion resistance (Long and Rack 1998). Further, plasma spraying is the most commonly used coating technique for calcium phosphates, and it presents a coating which can combine surface topography with chemical effects (Geesink 2002). The sol–gel technique aims also to deposit hydroxyapatite and calcium phosphate coatings on medical devices (Kim et al.

2005). PVD techniques such as ion plating, magnetron sputtering and ion beam dynamic mixing, have been introduced to deposit thin calcium phosphate coatings onto metallic implants. The frequent initial amorphous nature of these coatings can be easily improved by a rapid heat treatment (Bauer et al. 2013).

3 Metal Materials in Current Biomedical Applications

3.1 Stainless Steel

Stainless steel is an alloy of iron with a minimum of 10.5% chromium and varying amounts of other alloying elements such as nickel, molybdenum, carbon, manganese, silicon, nitrogen and so on. Based on the chemical composition, stainless steels can be classified in two groups: chromium and chromium–nickel types. Additionally, they can also be classified in terms of microstructure as martensitic, ferritic, austenitic, precipitation-hardened stainless steels and duplex stainless steels (Davis 2003). Apart from the duplex stainless steel, each of the other three groups has applications in medical devices. Martensitic stainless steels have an excellent hardness (up to 97 HRB) which makes them ideal for dental and surgical instruments. Ferrite stainless steels are commonly used for manufacturing medical devices. On the other hand, austenitic stainless steels can be used for manufacturing various non-implantable devices where moderate strength and good corrosion resistance are needed. These applications often require a material that is easily formed into complex shapes. However, only austenitic stainless steels are used for implants (Chen and Thouas 2015).

Stainless steels were the first metals to be used in orthopaedics in 1926. However, it was not until 1943, when AISI 304 (using the American iron and steel industry nomenclature) was recommended as a standard material for implants (Hallab and Jacobs 2013). The austenitic type of stainless steel AISI 316L is a low carbon version of the AISI 316 stainless steel used extensively in many purposes due to its very good corrosion resistance, smoothness, biocompatibility and clean ability after the electropolishing treatment (Petković et al. 2013). The carbon content must be kept at a low level to prevent carbide (chromium–carbon) accumulation at the grain boundaries. In order to ensure a low content of non-metallic inclusion, vacuum melting is required. Non-metallic inclusions are undesirable since they act as stress concentrators reducing mechanical properties (especially fatigue strength) of components and aggravating the fabrication of the components to the final shape. After final shaping, medical devices and implants are usually ground and polished in order to accomplish the desired surface roughness, followed by the passivation treatment (commonly by exposure to a 40% HNO_3 solution or thermal oxidation treatment—ASTM F 86). Thus designed form of stainless steel, most commonly used in orthopaedic practice, is marked as AISI 316LVM (American Society for Testing and Materials F138, ASTM F138; others include F139, F899, F1586, F621, …).

Stainless steel AISI 316LVM is a molybdenum alloyed vacuum melted stainless steel for the production of both temporary and permanent implants. Such a stainless steel has better corrosion resistance due to its purer structure and higher price than AISI 316L. AISI 316L stainless steel is a desirable surgical-implant material due to its reasonable biocompatibility, tensile strength, corrosion resistance, fatigue resistance for load-bearing applications. Compositions of AISI 316L (ASMT F138) stainless steel and its variants are listed in Table 10.

In comparison with AISI 316L, other stainless steel grades are used in a significantly lesser amount for surgical implants. Austenitic stainless steels AISI 304 and AISI 316 (with C content up to 0.08%) in wire form are applied in surgical sutures and microvascular clips. Martensitic stainless steels (type AISI 420 and AISI 431) and precipitation hardened stainless steels (17-7 PH) can be also used for neurosurgical and microvascular clips. Vascular stents, conducting lead wires, electrodes and pulse generator housings of cardiac pacing systems are often made of austenitic stainless steels (AISI 304, AISI 316, AISI 316L alloys).

Although AISI 316L stainless steel has relatively good biocompatibility, it is not on a satisfactory level compared with Co–Cr–Mo and titanium alloys. The wear resistance of AISI 316L austenitic stainless steel is also relatively poor, and wear debris leading to allergic reaction in the surrounding tissue is another reason to restrict their application in permanent implants. Today, AISI 316L stainless steels are widely used in a variety of surgical instruments and short-term implant devices due to cost savings.

It is a cost-effective orthopaedic biomaterial which is used for internal bone fixation devices due to its good mechanical strength and bending and shaping possibility in situ. Examples of stainless steel applications include bone plates and screws, femoral fixation devices, intramedullary nails and pins, aneurysm clips, joints for ankles, elbows, fingers, knees, hips, shoulders and wrists (Cieślik et al. 2009), Fig. 7.

Most mechanical properties such as yield strength, fatigue strength, ultimate tensile strength, and elongation vary with both alloy type (chemistry) and processing (microstructure). The Young's modulus of elasticity is an exception; namely, it is pretty insensitive in regard to chemistry and microstructure within stainless steel alloys. These devices and implants are fabricated by forging and machining. Mechanical properties of AISI 316L that depend on the work condition (microstructure) are given in Table 11.

However, major disadvantages of this material are well documented. During the long-term contact of the human tissue with the metal surface corrosion takes place releasing corrosion products into the surrounding tissues. The main lack of the AISI 316L stainless steel lies in the release of certain metal ions that may lead to some serious diseases (Hanawa 2004). The ions released are mostly those of iron, nickel and chromium. Nickel particularly provokes strong immunological reactions such as hypersensitivity, asthma, contact dermatitis and moderate cytotoxicity (Oh and Kim 2005). Therefore, a tendency to replace nickel with a more biocompatible elements is justified. Nitrogen is often used to substitute nickel as an austenitic structure stabilizer and consequently enhance both the mechanical strength and the

Table 10 Compositions (wt%) of AISI 316L stainless steel (ASTM F138) and variants

ASTM code/UNS No of stainless steels	Cr	Ni	Mo	Mn	Si	Cu	N	C	P	S	Fe
F138/S31673	17.0–19.0	13.0–15.0	2.25–3.00	2.00	0.75	0.50	0.10	0.03	0.025	0.01	Balance
F1314/S20910	20.5–23.5	11.5–13.5	4.00–6.00	2.0–3.0	0.75	0.50	0.2–0.4	0.03	0.025	0.01	
F1586/S31675 (Orthinox)	19.5–22.0	9.0–11.0	2.00–4.25	2.0–3.0	0.75	0.25	0.25–0.50	0.08	0.025	0.01	
2229/S29108	19.0–23.0	0.10	21.0–24.0	0.5–1.5	0.75	0.25	>0.90	0.08	0.03	0.01	

Fig. 7 Biomedical devices and implants made of stainless steel

Table 11 Mechanical requirements for AISI 316L (ASTM F138) and variants in bar or wire

Steels	Condition	Minimal ultimate tensile strength (MPa)	Minimal yield stress (0.2%) (MPa)	Minimal elongation in 4D (%)
F138	Annealed	500	200	39
	Cold worked	860	690	12
	Extra hard	1350	–	–
F1314	Annealed	690	380	35
	Cold worked	1035	862	12
F1586	Annealed	740	430	35
	Cold worked	1000	700	20
	Hard	1100	1000	10
F2229	Annealed	931	586	52
	Cold worked 10%	1062	786	37
	Cold worked 20%	1262	952	25
	Cold worked 30%	1496	1227	19
	Cold worked 40%	1731	1551	12

resistance to pitting and crevice corrosion. In 1998, ASTM 1586 (Orthinox) came into use as a stem material in total hip replacement (Rokkum et al. 1995). Chen and Thouas (Chen and Thouas 2015) have noticed that nowadays stems made of Orthinox stainless steel occupy 70% of the market for total hip replacements in the United Kingdom. Additionally, nickel-free austenitic steels with high nitrogen concentration (ASTM F2229) have also been developed for medical use.

Although the mechanical properties and biocompatibility of stainless steels are generally less desirable than those of the other implant alloys, stainless steels have greater ductility, indicated quantitatively by a three-fold greater "percentage of elongation at fracture" when compared to other metallic biomaterials. This fact has allowed it to remain popular as a material for temporary orthopaedic implants such as bone screws, plates and implanted medical devices, cable fixation components in total knee arthroplasty, and a low cost alternative to titanium and cobalt alloys. Moreover, Orthinox—high-nitrogen stainless steel is a quite common material in manufacturing femoral components for total hip prostheses (Chen and Thouas 2015).

3.2 Titanium Alloys

Titanium is an extremely reactive element, which as a stable oxide exists in the earth's crust. For this reason, titanium was first used commercially in the United States at the end of the 1940s. Titanium is a low density element (the density of 4.5 g/cm^3 is approximately 60% of the density of iron and nearly half of the density of cobalt) that can be strengthened considerably by alloying and deformation processing. It is a transition metal with an incomplete shell in its electronic structure, which enables it to form solid solutions with most substitutional elements having a size factor within ±20%. In its elemental form pure titanium has a high melting point of 1678 °C, exhibiting a hexagonal close-packed structure (α phase) (Long and Rack 1998). Its allotropic transformation starts at approximately 885 °C, changing from a hexagonal close-packed crystal structure (α phase) to a body-centered cubic structure (β phase) (Collings 1984). Titanium alloys may be classified as either α, near α, α + β, metastable β or stable β depending on their room temperature microstructure (Polmear 1981). In this regard alloying elements for titanium fall into three categories: α-stabilizers (Al, O, N, C, B), β-stabilizers (H (eutectoid), Mo, V, Nb, Fe, Cr, Si, Ni, Co, Mn, W), and neutral (Zr, Hf, Sn) (Lütjering and Williams 2003). α and near α titanium alloys exhibit superior corrosion resistance with their utility as biomedical materials being principally limited by their low ambient temperature strength. In contrast, α + β alloys exhibit higher strength due to the presence of both α and β phases. Contrary to stainless steels and Co-based alloys for which the main purpose of alloying is to enhance corrosion resistance, the basic aim in the design of titanium alloys is the improvement of mechanical properties; titanium's main advantage is an excellent corrosion resistance by itself. The properties of titanium alloys depend on the composition, the

relative proportions of the α/β phases, and an alloy's prior thermal treatment and thermo-mechanical processing conditions. β alloys (metastable or stable) are titanium alloys with high strength, good formability and high hardenability. β alloys also offer the unique possibility of combined low elastic modulus and superior corrosion resistance (Long and Rack 1998).

α—common titanium alloys phase occurs in microstructure at low temperatures, below 800 °C. Since α solid solution is prevailing (at least 95% mass), the properties of these alloys cannot be significantly altered by heat treatment. Strengthening of α titanium alloys can be achieved by cold working, combining cold working and annealing in order to control the α grain size, or by solid solution (Cvijović-Alagić and Rakin 2008). Commercially pure (CP) titanium has only α single phase microstructure. CP titanium can contain very small amounts of iron, nitrogen and oxygen, while the total amount of other elements must be lower than 0.7%. Because of slight, but strictly defined differences in composition, there are four CP titanium grades marked with numbers from 1 to 4, as given in Table 12.

β titanium alloys are often described as second generation titanium biomaterials. One of the reasons for their development is a high elasticity modulus of the implant. In β alloys, the β phase can be completely retained at room temperature upon sufficiently fast cooling, following solution treatment. These alloys have excellent forgeability, good cold formability, and high hardenability as well as elasticity modulus closer to that of bone (Table 13), (Davis 2003).

Two-phase α + β titanium alloys are obtained by alloying titanium with α and β solid solution forming elements. Significant improvement of α + β titanium alloy strength, with a relatively minor drop in plasticity, can be achieved by heat treatment, while the weldability of these alloys is limited. The microstructure in the final products is mainly determined by alloy composition, solution-treating temperature, cooling rate and section size. Microstructure can also be significantly varied by the subsequent aging treatment conditions, normally at 480–650 °C, to precipitate α and produce a fine mixture of α and β microstructure. Solution treatment and aging can enhance the strength of α + β alloys by 30–50%, while their elasticity modulus remains at a similar level. Long-term research has resulted in the development of two-phase α + β alloys with a dispersed β phase in the α phase, contributing to excellent characteristics of each of the two phases.

Table 12 Chemical composition of CP Ti (ASTM F 67) and Ti–6Al–4V alloy (ASTM F 136) (wt%)

Materials		N	C	H	Fe	O	Ti
		Maximal values					
CP Ti	ASTM grade 1	0.03	0.08	0.0150	0.20	0.18	Balance
	ASTM grade 2	0.03	0.08	0.0150	0.30	0.25	Balance
	ASTM grade 3	0.05	0.08	0.0150	0.30	0.35	Balance
	ASTM grade 4	0.05	0.08	0.0150	0.50	0.40	Balance
Ti–6Al–4V		0.05	0.08	0.0125	0.25	0.13	Balance

Table 13 Basic mechanical properties of titanium and titanium alloys developed for orthopaedic implants

Materials	Young's modulus (GPa)	0.2% yield stress (MPa)	Ultimate tensile strength (MPa)	Elongation (%)
α microstructure				
ASTM grade 1	115	170	240	24
ASTM grade 3	115	380	450	18
ASTM grade 4	115	480	550	15
α + β microstructure				
Ti–6Al–4V	110	860	930	10–15
Ti–6Al–7Nb	105	795	860	10
Ti–5Al–2.5Fe	110	820	900	6
Ti–3Al–2.5V	100	585	690	15
β microstructure				
Ti–13Nb–13Zr	79–84	840–910	970–1040	10–16
Ti–12Mo–6Zr–2Fe (TMZF)	74–85	1000–1060	1060–1100	18–22
Ti–15Mo	78	655	800	22
Ti–15Mo–5Zr–3Al	75–88	870–970	880–980	17–20
Ti–15Mo–2.8Nb–0.2Si–0.26O (21SRx)	83	950–990	980–1000	16–18
Ti–16Nb–10Hf	81	730–740	850	10
Ti–(10–80)Nb	65–93	760–930	900–1030	
Ti–35.5Nb–7.3Zr–5.7Ta (TNZT)	55–66	800	830	20
Ti–(70–80)Ta	80–100	350–600	600–650	10–25
Ti–Ta–Nb/Nb/Sn	40–100	400–900	700–1000	17–26
Ti–Zr–Nb–Ta	46–58	–	650–1000	5–15
Stainless steels and Co-alloys				
AISI 316L	200	200–700	500–1350	10–40
Co-alloys	240	500–1500	900–1800	10–50

Titanium is not found in the human body and it is non-toxic even in large doses. Its implants are not rejected by the body, and generally make good physical connections with the host bone (Yaghoubi et al. 2000). The α + β alloy Ti–6Al–4V is the most widely used titanium alloy (approximately 45% of total titanium production), while unalloyed grades comprise approximately 30% of production, and all other alloys combined form the remaining 25% (Chen and Thouas 2015).

Commercially pure titanium (CP Ti), Ti–6Al–4V and its Extra-Low Interstitial (ELI) variant (Ti–6Al–4V ELI) are the most common titanium base implant biomaterials, whose chemical composition is given in Table 12 (Munoz and Costa 2012) and appearance in Figs. 8 and 9. These materials are classified as biologically inert biomaterials so that they remain essentially unchanged when implanted into

Fig. 8 Biomedical devices and implants made of CP titanium

Fig. 9 Biomedical devices and implants made of titanium alloys

human bodies. The human body is able to recognize these actions and they are tolerated well by the human tissues. These metals do not induce allergic reactions such as has been observed with some stainless steels, which have induced nickel hypersensitivity in the surrounding tissues (Oldani and Dominguez 2012).

Table 14 lists the standards for titanium and titanium alloys used for medical implants (Davis 2003). It can be seen that Ti–6Al–4V and Ti–6Al–4V ELI are currently standardized and most widely applied titanium alloys. Ti–6Al–7Nb and Ti–5Al–2.5Fe are metallurgical similar to Ti6Al–4V, except for the absence of vanadium, which has been reported to be toxic.

Compared with stainless steels and cobalt alloys, titanium alloys have proven to be superior in terms of biocompatibility because of their excellent corrosion resistance (Chen and Thouas 2015). CP Ti has a very good biocompatibility due to the formation of an oxide film (TiO_2) over its surface. This oxide is a strong and stable layer that grows spontaneously in contact with air and prevents the diffusion of the oxygen from the environment providing corrosion resistance. It is a biomaterial with a high superficial energy, and after implantation it provides a favorable body reaction that leads to direct apposition of minerals on the bone-titanium interface and titanium osseointegration (Acero et al. 1999). Mechanical properties of titanium alloys are affected by their chemical compositions, as shown in Table 13. In CP titanium (98.9–99.6% Ti), which is essentially all titanium with relatively low strength and high ductility, ultimate tensile strength and yield strength vary from 240 to 550 MPa, and from 170 to 480 MPa, respectively, as a result of variations in the interstitial and impurity levels. Oxygen and iron are the primary variants in the CP Ti grades, with strength increasing as their content increases.

Besides biocompatibility, a major advantage of titanium alloys, compared with other metallic biomaterials, is its extraordinary specific strength (strength/density ratio). Compared with stainless steels and cobalt–chromium alloys, titanium is superior in specific strength but inferior in tribological properties. However,

Table 14 ASTM/UN standards for titanium and titanium alloys used for medical implants

Category	ASTM	UNS no.	Materials
α microstructure	F67	R50250	CP-Ti grade 1
		R50400	CP-Ti grade 2
		R50550	CP-Ti grade 3
		R50700	CP-Ti grade 4
α + β microstructure	F136	R56401	Ti–6Al–4V ELI (currently standardized)
	F1472	R56400	Ti–6Al–4V (currently standardized)
	F1295	R56700	Ti–6Al–7Nb (not currently standardized)
	F2146	R56320	Ti–3Al–2.5 V (not currently standardized)
β microstructure	F1713		Ti–13Nb–13Zr
	F1813	R58120	Ti–12Mo–6Zr–2Fe
	F2066	R58150	Ti–15Mo

high-strength alloys have a high sensitivity to stress concentration. Sensitivity to stress concentration can be defined as a measure of a material's ability to plastically deform locally at regions of high stress, otherwise an occurrence of crack and fracture can be initiated (Cvijović-Alagić and Rakin 2008). Therefore, a mechanically reliable titanium implant alloy has yet to become a reality. In addition, poor wear resistance stands out as the main drawback of titanium alloys, which can be improved by applying any surface modification techniques such as passivation and coating.

Examples of biomedical applications for CP-Ti grades include pacemaker cases, housings for ventricular-assist devices and implantable infusion drug pumps, dental implants, maxillofacial and craniofacial implants, and screws and staples for spinal surgery. As shown in Table 14, there are four ASTM standardized $\alpha + \beta$ alloys currently used for medical devices. Ti–6Al–4V and Ti–6Al– 4V ELI are the most commonly employed alloys. The applications of Ti–6Al–4V include dental implants and parts for orthodontic surgery; replacement parts for hip, knee, shoulder, spine, elbow and wrist joints; bone fixation devices such as nails, screws and nuts; housing parts for pacemakers and artificial heart valves; surgical instruments and components in high-speed blood centrifuges. However, both Al and V released from Ti–6Al–4V alloy are found to be linked to long-term health problems, such as Alzheimer's disease, other neuropathies and osteomalacia (Nag et al. 2005).

3.3 Cobalt-Based Alloys

The cobalt–molybdenum superalloy, called stellite, was first developed by Haynes for use in aircraft engines (Sumita et al. 2003). Co-based alloys were first used in medical implants in the 1930s. One of the first Co–Cr–Mo alloy, vitallium, was used as a cast dental alloy in the 1940s. To date, several cobalt based alloys with diverse chemical compositions and manufacturing have been developed, as summarized in Tables 15 and 16 (Davis 2003).

Cobalt–chromium based alloys are superior to stainless steels in corrosion resistance, which is related to their chemical composition. The high chromium content leads to spontaneous formation of a passive oxide (Cr_2O_3) layer within the human body environment. The roles of Cr and other alloying elements are summarized in Table 17. Namely, Cr, Mo and Ni are responsible for corrosion resistance, very much like their roles in stainless steels. Tungsten adds to an increased solid-solution strengthening and to the control of the distribution and size of carbides. However, the addition of tungsten reduces the corrosion resistance and corrosion fatigue strength of these alloys. Therefore, Co–20Cr–15W–10Ni and Co–Ni–Cr–Mo–W–Fe alloys are restricted to temporary implants, such as bone plates and wire, due to both unsatisfactory corrosion resistance and a high amount of toxic nickel release when used for permanent implantation (Chen and Thouas 2015). Cobalt alloys were initially used as cast components, whereas the wrought alloys came into use later.

Table 15 Compositions (in wt%) of cobalt-based alloys used for orthopaedic implant fabrication

ASTM	Cr	Mo	Ni	Fe	C	Si	Mn	W	P	S	Other
F75	27–30	5–7	1.0	0.75	0.35 max	1.0	1.0	0.2	0.02	0.01	0.25N; 0.3Al; 0.01B
F799 (low-C)	26–30	5–7	1.0	0.75	0.05	1.0	1.0	–	–	–	0.25N
F799 (high-C)	26–30	5–7	1.0	0.75	0.25	1.0	1.0	–	–	–	0.25N
F563	18–22	3–4	15–25	4–6	0.05	0.5	1.0	3–4	–	0.01	0.50–3.50Ti
F562 (MP35 N)	19–21	9–10.5	33–37	1.0	0.025 max	0.15	0.15	–	0.015	0.01	1.0Ti
F90	19–21	–	9–11	3.0	0.05–0.15	0.40	1.0–2.0	14–16	0.04	0.03	–
F1058 (Elgiloy)	19–21	6–8	14–16	Bal	0.15	1.2	1.0–2.0	–	0.015	0.015	0.10Be; 39.0–41.0Co

Table 16 Co-Cr alloys used in surgical implants

ASTM standard	Nominal compositions	Cast/wrought status	Medical application
F75-98	Co–28Cr–6Mo	Cast	Permanent implant
F90-97	Co–20Cr–15W–10Ni	Wrought	Temporary implant
F562-95	Co–35Ni–20Cr–10Mo	Wrought	Permanent implant
F563-95	Co–Ni–Cr–Mo–W–Fe	Wrought	Temporary implant
F799-99	Co–28Cr–6Mo	Forged	Permanent implant
F961-96	Co–35Ni–20Cr–10Mo	Forged	Permanent implant
F1058-97	Co–Cr–Ni–Mo–Fe	Wrought	Permanent implant
F1537-94	Co–28Cr–6Mo	Wrought	Permanent implant

Table 17 The roles of alloying elements

Elements	On corrosion resistance	On microstructure	On mechanical properties
Cr	Increase corrosion resistance	Form $Cr_{23}C_6$	Enhance wear resistance
Mo	Increase corrosion resistance	Refine grain size	Enhance solid-solution strengthening
Ni	Increase corrosion resistance		Enhance solid-solution strengthening; Increase castability
W	Decrease corrosion resistance	Reduce shrinkage cavity, gas blow hole and grain boundary segregation	Enhance solid-solution strengthening; Decrease corrosion fatigue strength
C	Decrease corrosion resistance	Form $Cr_{23}C_6$	Increase castability; Enhance wear resistance

Cobalt is an essential trace element found principally in the maturation of human red blood cells (Kennedy et al. 1995). This essential trace element can also cause serious adverse health effects at high exposure levels, such as the beer drinker's cardiomyopathy (Barceloux 1999) and contact dermatitis (Basketter et al. 2003). Cobalt toxicity has also been reported to contribute to the pathology of systemic and neurological symptoms in some patients with metal-on-metal hip prostheses after 4–5 years of implantation (Mao et al. 2011). In regard to metallic implants, no data are reported on systemic toxicity of molybdenum (Chen and Thouas 2015). The toxicity of tungsten is very low; however, implantable materials made from this metal degrade very rapidly in the body, and remain in the serum, probably as tungsten particles (Peuster et al. 2002). Generally, in vitro evaluation showed that the Co–Cr–Mo alloy is much less toxic than pure cobalt or nickel due to its excellent corrosion resistance (Evans and Thomas 1986). While the excellent

corrosion resistance of Co–Cr-based alloys is primarily imparted by alloying chromium, their superior mechanical properties over stainless steels are due to the crystallographic nature of the base element cobalt.

The elastic modulus of pure cobalt is about 210 GPa in tension and about 180 GPa in compression, which is similar to those of iron and nickel. The superior wear and fatigue resistances of cobalt alloys in comparison with iron alloys is due to their two closely packed structures, i.e. hexagonal closely packed and face-center cubic crystal structure. The cast alloys are superior to non-cast alloys in wear resistance, pitting resistance and crevice corrosion resistance, while the cast alloys are inferior to wrought or forged alloys in terms of fatigue strength and fracture toughness (Chen and Thouas 2015).

The type of manufacturing of cobalt alloys has a significant influence on their mechanical properties. Generally, wrought/forged Co–Cr-based alloys have higher strength values than their cast counterparts. The primary strengthening mechanism in wrought cobalt alloys is the solid-state phase transformation of part of the matrix from a face-center cubic to a hexagonal closely packed structure by cold working. Mechanical properties of cast and wrought cobalt-based alloys are summarized in Table 18, showing that the majority of cobalt alloys have yield strengths higher of 500 MPa (Davis 2003). Therefore, this property is in excess of the above biological values, pointing out to be safe for implant applications in the leg and arm. However, cobalt–chromium alloys are very difficult to machine. Hence, the preferred machining method of cobalt-base alloy implants is a function of the trade-off between cost and properties. In that sense, where the properties of casting are sufficient, this method will have priority; contrarily, in cases where maximum strength is required, hot pressing or forging will be the preferred method.

Table 18 Mechanical properties of cast and wrought cobalt-based alloys

Alloys	Modulus of elasticity (GPa)	Ultimate tensile strength (MPa)	0.2% yield stress (MPa)	Elongation (%)
F75/Cast, annealed	210	650–890	450–520	11–17
F75/P/M HIP	250	1280	840	
F799/Forged	210	1400–1590	900–1030	28
F90/Annealed	210	950–1220	450–650	
F90/44% cold worked	210	1900	1610	
F562/Forged	230	1210	960–1000	
F562/cold worked, aged	230	1800	1500	8
F563/annealed	230	600	280	50
F563/cold worked	230	1000–1310	830–1170	12–18
F563/cold worked, aged	230	1590	1310	
F1058 wire	230	1860–2280	1240–1450	

ASTM F75, F799, F90, and F562 are the most widely used cobalt alloys for implant applications. ASTM F75 is a cast Co–Cr–Mo alloy, which has extraordinary wear resistance and excellent corrosion resistance. Total artificial hip joints made from this alloy are even more viable, due to its excellent tribological properties against plastic sockets, i.e. in a metal-on-plastic joint. As its main drawback one can mention relatively low strength determined by the extremely large grain size structure. ASTM F799 is a wrought version of the F75 alloy, mechanically processed by hot forging rough billets to make the final shape. The carbon content of a wrought alloy must be sufficiently low in order to have a good ability for forging. Although the low carbon content compromises wear resistance of wrought alloys, they are superior in fatigue strength imparted by the wrought microstructure. The strength of F799 alloy is approximately twice that of the cast F75. Modern Metal-on-Metal joint prostheses are almost always made from the F799 alloy. ASTM F90 is a wrought Co–Cr–W–Ni alloy. Tungsten and nickel are added to improve machinability and fabrication characteristics (Ratner et al. 2012). In the annealed state, the mechanical properties of F90 are similar to those of the cast F75, but when cold worked to 44%, the properties can be improved to be more than double. ASTM F562 is a wrought Co–Ni–Cr–Mo alloy. The microstructure of the worked F562 is the hexagonal closely packed structure solid-state phase formed from the face-center cubic matrix by cold working. Subsequent age hardening in the 425–650 °C range acts to further strengthen these two phases through the precipitation of carbides, primarily $Cr_{23}C_6$ (Chen and Thouas 2015). It is important to mention that the cold worked and aged F562 can exceed tensile strength levels in excess of 1795 MPa, which is the highest strength of any of the surgical implant alloys, while its elongation is in excess of 8%.

Co-based surgical implant alloys are used to fabricate a variety of implant parts and devices. The superior fatigue resistance of Co–Cr–Mo alloys makes them an ideal choice of materials for total joint replacements. Currently around 20% of total hip replacements have stems and/or the hard-on-hard bearing systems made of wrought Co–Cr–Mo alloys. As for total knee and ankle replacements, the prostheses are almost exclusively made of Co–Cr–Mo alloys with UHMWPE as a lining. The use of wrought, cobalt-based alloys for fix bone fractures such as bone screws, staples, plates, support structures for heart valves, and dental implants is not as yet commonplace, probably as a result of its increased cost compared with that of stainless steel. Wrought Co–Cr–Mo alloys are expensive, which limits their share on the medical market, compared with stainless steels.

Other issues associated with cobalt-based alloys include stress shielding effects and metal toxicity. Cobalt alloys have a high Young's modulus (220–230 GPa), which is much higher than that of cortical bone (20–30 GPa), resulting in uneven energy distribution from propagating shock waves during walking and load bearing. On the other hand, cobalt based alloys are generally superior to stainless steels in terms of resistance to corrosion, fatigue and wear. Although imperfect, wrought Co–Cr–Mo alloys remain the most popular metallic implant materials for joint bearing systems, improving the life quality of thousands of people worldwide (Chen and Thouas 2015).

3.4 Ni–Ti Shape Memory Alloys

Ni–Ti shape memory alloys are a group of materials named smart functional materials. On the other hand, due to the two-element based composition these alloys became known as Nitinol—an acronym for the elements from which the material was composed (*ni* for nickel, *ti* for titanium and *nol* from the Naval Ordnance Laboratory) (Thompson 2000). The crystal structure of an Ni–Ti alloy at high temperature ranges (100 °C) is a stable, body centered cubic lattice which is referred to as the austenite phase. Nitinol has the particular characteristic that when it is cooled through a critical transformation temperature range, the alloy shows dramatic changes in its modulus of elasticity (stiffness), yield strength and electric resistivity as a result of changes in electron bonding. By reducing or cooling the temperature through this range, there is a change in the crystal structure which is known as the martensitic transformation. The phenomenon causes a change in the physical properties of the alloy and gives rise to the shape memory characteristic (Wang et al. 1972).

The outstanding properties exhibited by these alloys are the thermal shape memory effect (the alloy recovers its programmed shape after heating above a specific temperature) and superelastic (rubber-like) behavior (the alloy recovers its original shape after deformation to tensile strains as high as 8%) (Es-Souni et al. 2005). These properties are both based on a thermoelastic, reversible martensitic transformation (Saburi 1998). The Ni–Ti shape memory alloys usually consist of binary alloys with Ni and Ti concentrations near an equiatomic composition. Other alloying elements like Fe, Cu and Nb may be added in order to influence the transformation hysteresis behavior as well as the transformation temperatures and mechanical properties, especially fatigue properties (Saburi 1998, Gil and Planell 1999). Their microstructures are generally processed using complex thermo-mechanical treatments in order to obtain suitable properties such as thermal shape memory, superelasticity, and all-round memory effect.

The first research, which dealt with the potential of Ni–Ti as an implant material, was done in 1968 and it revealed that Ni–Ti showed excellent corrosion resistance in sea water (Michiardi et al. 2008). The use of Ni–Ti for medical applications was first reported in 1973 (Cutright et al. 1973), while the clinical trials in orthopaedics were done in the 1980s (Matsumoto et al. 1993). These alloys are now being used in many biomedical applications such as orthodontic arch wires, stents, filters, guide wires, catheter tubes, Ni–Ti osteosynthesis plates and staples, and face and jaw surgical implants.

Ni–Ti is one of the most innovative concepts introduced in the field of metallic biomaterials, but its biocompatibility remains controversial. Although the exact concentrations of metallic compounds released from the implanted material due to the complicated local conditions are still unknown, the high nickel content of Ni–Ti (50 at.%) is of concern, as deleterious amounts of nickel may be released. The overall inflammatory response and capsule thickness around these alloys are similar to those observed for stainless steels and Ti alloys. So far, there have been no

reports of tissue necrosis, granulomas, and signs of tissue dystrophy or calcification in vivo. In neural and perineural tissue, Ni–Ti implants are also reported to be non-toxic and non-irritant (Ryhanen 1999). The surface properties are largely defined by the fact that Ti is more readily oxidized than Ni. Generally, Ni–Ti devices often exhibit an outermost protective Ti-based oxide layer which confers corrosion resistance to this material, and acts as an effective barrier to Ni ion diffusion/release. From a biological point of view, it is the state of the material's surface (the extent to which it hinders ion leaching processes) that influences the biocompatibility of these materials (Pillar 2009). To minimize ion release from Ni–Ti implants, especially in stents that have high surface area and are in a dynamic flow, polymer coatings have been applied.

Mechanical properties of Ni–Ti alloys are specific and depend on the microstructure. For instance, Young's modulus of an Ni–Ti alloy is in the range of 30–80 GPa (Petrini and Migliavacca 2011), which is the closest to that of the human cortical bone, even closer than β Ti alloys (Table 13). A relatively low level of Young's modulus in Ni–Ti alloys does not affect their yield strength and ultimate tensile strength, which are in the range of the AISI 316L stainless steels (Table 19). The most attractive mechanical property of Ni–Ti is its large elastic strain of around 10%, which is higher than any traditional alloys. Mechanical properties, especially fatigue properties, of Ni–Ti alloys sensitively depend on the deformation temperatures, whether in austenite or martensite phase. The fatigue strength of austenitic Ni–Ti alloys is, in general, higher than that of martensitic alloys and the fatigue strength of austenitic Ni–Ti alloys is higher at elevated temperatures. At both room and body temperature, the fatigue strength of austenitic Ni–Ti alloys is typically around 400 MPa (Chen and Thouas 2015).

The generic term 55-Nitinol (56% (wt) nickel and 44% (wt) titanium, although in some Ni–Ti alloys, a small percentage (<2% wt) of nickel can be substituted by cobalt) is the most common form of these alloys. Besides it, the second group of Nitinol alloys are referred to as 60-Nitinol, which contain nickel of 60% (wt). The shape memory effect of this alloy is lower, although its ability to be heat-treated

Table 19 Comparison of the mechanical properties of Ni–Ti, AISI 316L stainless steel and cortical bone

Alloys	Modulus of elasticity (GPa)	0.2% yield stress (MPa)	Maximal elastic strain (%)	Ultimate tensile strength (MPa)	Elongation (%)	Fracture toughness (MPa $m^{1/2}$)
AISI 316L	200	200–700	~0.20	500–850	10–40	~100
Ni–Ti (martensite)	50–80	200–700	~10	900–1355	14.3	30–60
Ni–Ti (austenite)	30–40	70–140	10	–	–	–
Cortical bone	7–30	–	–	50–150	–	2–12

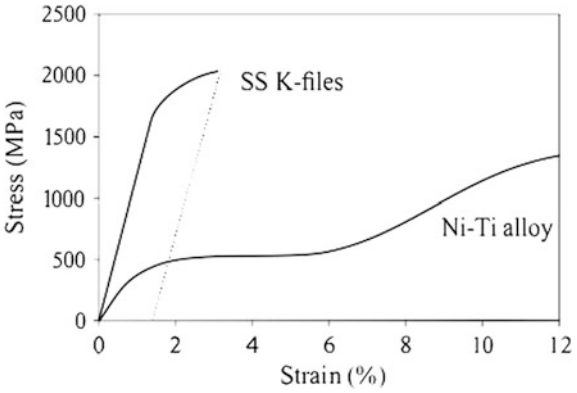

Fig. 10 Stress–strain curve for stainless steel and nickel–titanium alloy

increases. Both 55 and 60-Nitinols are more resilient, tougher and have a lower modulus of elasticity than other alloys such as stainless steel (Fig. 10), Ni–Cr or Co–Cr (Thompson 2000).

The trends in modern medicine are to use less invasive surgery methods which are performed through small, leak-tight portals into the body, called trocars. Medical devices made from shape memory alloys use a different physical approach and can pull together, dilate, constrict, or push apart. Such devices have made difficult or problematic tasks in surgery quite feasible. Therefore, unique properties of these alloys are utilized in a wide range of medical applications. Some of the devices used in various medical applications are illustrated in Fig. 11.

Stents are most rapidly growing cardiovascular cylindrical mesh tubes made of shape memory alloys. They are inserted into blood vessels to maintain the inner diameter of a blood vessel. The product has been developed in response to limitations of balloon angioplasty, which resulted in repeated blockages of the vessel in the same area. Ni–Ti alloys have also become the material of choice for superelastic self-expanding stents which are used for a treatment of the superficial artery disease. The Simon Inferior Vena Cava (IVC) filter was the first shape memory alloy cardiovascular device (Simon et al. 1977). It is used for blood vessel interruption for preventing pulmonary embolism via placement in the vena cava. The Simon filter filters clots that travel inside the bloodstream. The device is made of Ni–Ti wire curved similarly to an umbrella, which traps the clots that are better dissolved in time by the bloodstream. Additionally, self-expandable stents are applied for gastrointestinal, urological and pulmonary stenoses treatment. Wires made of nitinol are often used in orthodontics. Apart from the above, nitinol has also been proposed in orthopaedics for manufacturing fixation devices, spinal rods for treatment of scoliosis, cages for use during spinal fusion and even self-locking joint replacement components (Pillar 2009).

Despite the most exciting and successful applications of Ni–Ti as stents in the treatment of the occlusion of various vessels and ducts in the body, there are concerns over the systemic toxicity associated with the release of pure Ni over a long-term implantation period, especially from a bone implant. The reports of the

Fig. 11 Application of nitinol medical devices

investigation into the biocompatibility of Ni–Ti alloys have been controversial, especially those on orthopaedic implant trials. So far, many researchers believe that Ni–Ti alloys have excellent corrosion resistance and biocompatibility, while on the other hand, there are serious concerns over the long-term systemic toxicity of nickel ion release. The development of new nickel-free shape memory alloys may offer new opportunities to obviate these concerns (Chen and Thouas 2015).

3.5 Mg Alloys

The development of biomaterials for medical and dental applications has evolved through three generations: inert, bioactive and biodegradable materials. Each of them has had a period of evolution with overlapping. Nowadays the third generation of biomaterials, the logical extension of the rapidly progressing state of the art, has the goal of supporting and stimulating the regeneration of functional tissue (Ratner et al. 2012). With advances in tissue engineering and regenerative medicine, it seems that a true replacement of a biomaterial by the living tissue will be possible. Biomaterials have to act as a temporary structure, which enables them to degrade and allow the native tissue to integrate with the implant and eventually replace it.

Apart from degradable bioglass and degradable polymers, magnesium alloys fall into the third category of implant biomaterials. The potential application of this alloy system for orthopaedic implant materials is based on the potential benefits of these alloys such as benign macro-element in the body, similar density and Young's modulus to those of bone, and controllable corrosion rates (Chen and Thouas 2015). Therefore, magnesium alloys are possible candidates for the use in both cardiovascular intervention and bone repairing.

There have been a number of alloying elements used in magnesium-based materials in an attempt to control their corrosion properties and feasibility as implants. Elements such as Mn, Cu, Al, Ca, Zr, Gd, and Zn have all been explored (Petrie et al. 1998). Meanwhile, the solubility of alloying elements in crystalline Mg is limited, and thus corrosion rates can only be altered within a limited range. Additionally, Hydrogen evolution remains a problem during the degradation of crystalline Mg alloys (Witte et al. 2005).

As a trace element, magnesium is needed for more than 300 biochemical reactions in the body. At the biochemical level, magnesium is involved in energy metabolism and protein synthesis, maintains normal muscle and nerve function, supports a healthy immune system and keeps bones strong. Magnesium also helps regulate blood sugar levels and promotes normal blood pressure, playing important roles in preventing and managing disorders such as hypertension, cardiovascular disease and diabetes (Torshin and Gromova 2009).

Magnesium alloys have ultimate tensile strength and elongation in the range of 90–280 MPa and 3–20%, respectively (Table 20). The rapid reduction in strength due to degradation is in principle not an issue to tissue engineering applications, as the degradable implant is expected to provide temporary support rather than a permanent substitute for bone (Chen and Thouas 2015). The mechanical properties of a magnesium alloy can be tuned by the alloying and processing history. The addition of Al, Ag, In, Si, Sn, Zn, and Zr can improve both strength and elongation (Gu et al. 2009), while hot rolling and extruding can further improve strength. At

Table 20 Mechanical properties of Mg–Zn- and Mg–Ca-based alloys

Alloys	Elongation (%)	Modulus of elasticity (GPa)	Ultimate tensile strength (MPa)	0.2% yield stress (MPa)
Mg-cast	13	41	87	21
AZ91D-die cast	3	45	230	150
AZ31-extruded	7	45	235	125
LAE442	18	–	247	148
AE43-extruded T5	10	44	280	195
AM60B-die-cast	6–8	45	220	–
Mg–Zn–Mn extruded	22	–	180	246
Mg–1Ca-extruded	11	–	240	135

the same time, it should be taken into account that these processes can deteriorate both ductility and biocompatibility of alloys (Li et al. 2008).

In short, Mg alloys are mechanically compatible with bone and have suitable biodegradability. Therefore, their development as degradable biomaterials has been directed to tissue engineering applications. A number of issues must be addressed prior to any clinical applications, among which hydrogen bubble generation and infection are the most challenging ones. Caution is advised also for the toxicity of any alloying elements used in new alloy compositions.

4 Summary and Looking to the Future

Despite the increasing use of metallic biomaterials, the knowledge of the effects and consequences of their installation into the human body points to significant deficiencies. Insufficient biocompatibility and resistance to abrasion, high modulus of elasticity, and high density stand out as the main shortcomings. However, each class of biomaterials such as stainless steels, Ti alloys, Co–Cr alloys, and Ni–Ti alloys does not suffer simultaneously from all deficiencies. Therefore, regardless of their imperfections, these implant materials remain dominant in orthopaedic surgery.

Here considered metallic biomaterials have conventional polycrystalline structures. Components for medical devices and implants are manufactured by standard manufacturing processes such as forging, casting, milling, machining and honing. Specifically, they can be manufactured by metal powder compaction and sintering, which includes the contemporary approach of metal injection molding in order to form near net-shape parts, hot isostatic pressing and so on. Improved mechanical properties can be achieved by using processes such as grain refinement, strain hardening, alloy additions, precipitation hardening and development of multi-phase structures. Wear resistance of these materials can be achieved by surface modification through ion implantation or by formation of hard non-metallic layers. Corrosion resistance can be enhanced by stabilization of passive metal oxide layers or by coating with a corrosion resistant layer. The much greater hardness and improved corrosion resistance of the nano-crystalline metals suggest their potential as surface coatings.

Although metallic biomaterials exhibit significantly greater strength and toughness than bone in the laboratory, it has been reported that their service longevity is 20–25 years, which in most cases is much shorter than the life expectancy of the patient. The failure of these implants occurs most often within the service period of 15–20 years. Such results are attributed to a very high modulus of elasticity of the bulk materials in comparison with bone, which significantly reduces the fatigue strength due to stress-shielding effects. In this regard, the development of β Ti alloys, with the modulus of elasticity most similar to that of bones and improved wear and fatigue properties, is the subject matter of future research. In addition, one of the most promising strategies to achieve a synthetic permanent

substitute that has an elasticity modulus of bone is the use of a porous metallic implant. Finally, one of the future challenges which may enable long-term success of metallic implants is the development of biodegradable metallic materials, such as magnesium alloys and metal ceramics.

References

Acero J, Calderón J, Salmeron J et al (1999) The behaviour of titanium as a biomaterial: microscopy study of plates and surrounding tissues in facial osteosynthesis. J Cranio-maxillofac Surg 27(2):117–123

Antunes RA, de Oliveira MCL (2012) Corrosion fatigue of biomedical metallic alloys: mechanisms and mitigation. Acta Biomater 8:937–962

Barceloux DG (1999) Cobalt. J Toxicol Clin Toxicol 37:201–216

Basketter DA, Angelini G, Ingber A et al (2003) Nickel, chromium and cobalt in consumer products, revisiting safe levels in the new millennium. Contact Dermatitis 49:1–7

Bauer S, Schmuki P, Mark KVD et al (2013) Engineering biocompatible implant surfaces Part I: materials and surfaces. Prog Mater Sci 58:261–326

Blau PJ (ed) (1992) ASM handbook volume 18: friction, lubrication, and wear technology. ASM International, USA

Boretos JW, Eden M (1984) Contemporary biomaterials, material and host response, clinical applications, new technology and legal aspects. Noyes Publications, Park Ridge

Bose S, Bandyopadhyay A (2013) Introduction to biomaterials. In: Bandyopadhyay A, Bose S (eds) Characterization of biomaterials, 1st edn. Elsevier, The Netherlands, pp 1–9

Bou-Saleh Z, Shahryari A, Omanovic S (2007) Enhancement of corrosion resistance of a biomedical grade 316LVM stainless steel by potentiodynamic cyclic polarization. Thin Solid Films 515:4727–4737

Chen Q, Thouas GA (2015) Metallic implant biomaterials. Mater Sci Eng R 87:1–57

Cieślik M et al (2009) Metal release and formation of surface precipitate at SS grade 316 and hanks solution interface—inflammatory response and surface finishing effects. Corr Sci 51:1157–1162

Collings EW (1984) The physical metallurgy of titanium alloys. American Society for Metals, Metals Park, Cleveland, OH

Cutright DE, Bhaskar SN, Perez B et al (1973) Tissue reaction to nitinol wire alloy. Oral Surg Oral Med Oral Pathol Oral Radiol Endod 35:578–584

Cvijović-Alagić I, Rakin M (2008) Integrity of biomedical implants of titanium alloys (First part). Struct Integrity Life 8(1):31–40

Dahotre SN, Vora HD, Pavani K et al (2013) An integrated experimental and computational approach to laser surface nitriding of Ti–6Al–4V. Appl Surf Sci 271:141–148

Davis JR (ed) (2003) Handbook of materials for medical devices. ASM International, Materials Park, Ohio

Enderle JD, Bronzino JD, Blanchard SM (2005) Introduction to biomedical engineering, Second edition. Elsevier Academic Press, The Netherlands

Es-Souni M, Es-Souni M, Fischer-Brandies H (2005) Assessing the biocompatibility of Ni-Ti shape memory alloys used for medical applications. Anal Bioanal Chem 381:557–567

Evans EJ, Thomas IT (1986) The in vitro toxicity of cobalt-chrome-molybdenum alloy and its constituent metals. Biomaterials 7:25–29

Fontana MG, Greene ND (1978) Corrosion engineering, materials science and engineering series, second edition. McGraw-Hill, USA

Frutos E, Gonzalez-Carrasco JL (2013) A method to assess the fracture toughness of intermetallic coatings by ultra microindentation techniques: applicability to coated medical stainless steel. Acta Mater 61:1886–1894

Gavrilov LA, Heuveline P (2003) Aging of population. In: Demeny P, McNicoll G (eds) The encyclopedia of population. Macmillan Reference, New York, pp 32–37

Geesink RG (2002) Osteoconductive coatings for total joint arthroplasty. Clin Orthop Relat Res 395:53–65

Gil FJ, Planell JA (1999) Effect of copper addition on the superelastic behavior of Ni-Ti shape memory alloys for orthodontic applications. J Biomed Mater Res 48(5):682–688

Gu X, Zheng Y, Cheng Y et al (2009) In vitro corrosion and biocompatibility of binary magnesium alloys. Biomaterials 30:484–498

Hallab NJ, Jacobs JJ (2013) Orthopedic applications. In: Ratner BD et al (eds) Biomaterials science—an introduction to materials in medicine, 3rd edn. Elsevier, Waltham, pp 841–882

Hanawa T (2004) Metal ion release from metal implants. Mater Sci Eng C 24:745–752

Holzapfel BM, Reichert JC, Schantz JT et al (2013) How smart do biomaterials need to be? A translational science and clinical point of view. Adv Drug Deliv Rev 65:581–603

Kasemo B, Lausmaa J (1986) Surface science aspects on inorganic biomaterials. CRC Crit Rev Biocompat 2:335–330

Kennedy DG, Young PB, Kennedy S et al (1995) Cobalt-vitamin B12 deficiency and the activity of methylmalonyl CoA mutase and methionine synthase in cattle. Int J Vitam Nutr Res 65:241–247

Kim HW, Kim HE, Salih V et al (2005) Sol–gel-modified titanium with hydroxyapatite thin films and effect on osteoblast-like cell responses. J Biomed Mater Res Part A 74A:294–305

Krischak GD, Gebhard F, Mohr W et al (2004) Difference in metallic wear distribution released from commercially pure titanium compared with stainless steel plates. Arch Orthop Trauma Surg 124:104–113

Kurella A, Dahotre NB (2005) Surface modification for bioimplants: the role of laser surface engineering. J Biomater Appl 20:5–50

Li CX, Bell T (2004) Corrosion properties of active screen plasma nitrided 316 austenitic stainless steel. Corr Sci 46:1527–1547

Li Z, Gu X, Lou S et al (2008) The development of binary Mg–Ca alloys for use as biodegradable materials within bone. Biomaterials 29:1329–1344

Long M, Rack HJ (1998) Titanium alloys in total joint replacement—a materials science perspective. Biomaterials 19:1621–1639

Lütjering G, Williams JC (2003) Titanium. Springer, New York

Manivasagam G, Dhinasekaran D, Rajamanickam A (2010) Biomedical implants: corrosion and its prevention—a review. Recent Pat Corros Sci 2:40–54

Mao X, Wong AA, Crawford RW (2011) Cobalt toxicity-an emerging clinical problem in patients with metal-on-metal hip prostheses. Med J Aust 194:649–651

Matsumoto K, Tajima N, Kuwahara S (1993) Correction of scoliosis with shape-memory alloy. Nippon Seikeigeka Gakkai Zasshi 67:267–274

Michiardi A, Engel E, Aparicio C et al (2008) Oxidized NiTi surfaces enhance differentiation of osteoblast-like cells. J Biomed Mater Res A 85A:108–114

Middleton JC, Tipton AJ (2000) Synthetic biodegradable polymers as orthopedic devices. Biomaterials 21:2335–2346

Milosev I, Strehblow HH (2000) The behavior of stainless steels in physiological solution containing complexing agent studied by X-ray photoelectron spectroscopy. J Biomed Mater Res 52:404–412

Mohanty M, Baby S, Menon KV (2003) Spinal fixation device: a 6-year postimplantation study. J Biomater Appl 18:109–121

Mudali KU, Sridhar TM, Raj B (2003) Corrosion of bioimplants. Sadhama 28(3–4):601–637

Munoz A, Costa M (2012) Elucidating the mechanisms of nickel compound uptake: a review of particulate and nano-nickel endocytosis and toxicity. Appl Pharmacol 260:1–16

Nag S, Banerjee R, Fraser HL (2005) Microstructural evolution and strengthening mechanisms in Ti–Nb–Zr–Ta, Ti–Mo–Zr–Fe and Ti–15Mo biocompatible alloys. Mater Sci Eng C 25: 357–362

Nasab MB, Hassan MR, Sahari BB (2010) Metallic biomaterials of knee and hip—a review. Trends Biomater Artif Organs 24(2):69–82

Niinomi M (1999) Recent research and development on titanium for biomedical applications in Japan. JOM 51:32–34

Oh KT, Kim KN (2005) Ion release and cytotoxicity of stainless steel wires. Eur J Orthod 27: 533–540

Oldani C, Dominguez A (2012) Titanium as a biomaterial for implants. In: Fokter S (ed) Recent advances in arthroplasty, InTech, Croatia

Park JB, Lakes RS (2007) Biomaterials. Springer, Berlin

Parsapour A, Khorasani SN, Fathi MH (2012) Effect of surface treatment and metallic coating on corrosion behavior and biocompatibility of surgical 316L stainless steel implant. J Mater Sci Technol 28:125–131

Petković D, Radenković D (2013) Effect of stainless steel passivation on resistance to pitting corrosion in Hank's solution. In: Abstracts of the 2nd international conference mechanical engineering in XXI century, University of Niš, Faculty of Mechanical Engineering in Niš, Niš, 20–21 June 2013

Petković D, Radenković G, Mitković M (2012) Fractographic investigation of failure in stainless steel orthopedic plates. Facta Univ Ser Mech Eng 10(1):7–14

Petković D, Živić F, Radenković G et al (2013) Coating: a way to improve biomedical properties of AISI 316L stainless steel. In: Abstracts of 35th international conference on production engineering, Faculty of Mechanical and Civil Engineering in Kraljevo, Kraljevo, 25–28 Sept 2013

Petrie RS, Hanssen AD, Osmon DR et al (1998) Metal-backed patellar component failure in total knee arthroplasty: a possible risk for late infection. Am J Orthop 27:172–176

Petrini L, Migliavacca F (2011) Biomedical applications of shape memory alloys. J Metall. doi:10.1155/2011.501483

Peuster M, Fink C, von Schnakenburg C et al (2002) Dissolution of tungsten coil not produce systemic toxicity but leads to elevated level of tungsten in the serum and recanalization of the previously occluded vessel. Cardiol Young 12:229–235

Piattelli M, Scarano A, Paolantonio M et al (2002) Bone response to machined and resorbable blast material titanium implants: an experimental study in rabbits. J Oral Implantol 28:2–8

Pillar RM (2009) Metallic biomaterials. In: Narayan R (ed) Biomedical materials, Springer, Berlin

Polmear JJ (1981) Light alloys. Edward Arnold Publications, London

Ratner BD, Hoffman AS, Schoen FJ et al (2012) Biomaterials science—an introduction to materials in medicine. Elsevier Academic Press, The Netherlands

Rokkum M, Bye K, Hetland KR et al (1995) Stem fracture with the exeter prosthesis. 3 of 27 hips followed for 10 years. Acta Orthop Scand 66:435–439

Romero E (2013) Powering biomedical devices. Elsevier, The Netherlands

Ryhanen J (1999) Biocompatibility evaluation of nickel–titanium shape memory metal alloy. Dissertation, Oulu University

Saburi T (1998) Ti-Ni shape memory alloys. In: Otsuka K, Waymann CM (eds) Shape memory materials. Cambridge University Press, NY, pp 49–96

Schmuki P (2002) From bacon to barriers: a review on the passivity of metals and alloys. J Solid State Electrochem 6:145–164

Schultze JW, Lohrengel MM (2000) Stability, reactivity and breakdown of passive films. Problems of recent and future research. Electrochim Acta 45:2499–2513

Schweizer A, Riede U, Maurer TB et al (2003) Ten-year follow-up of primary straight-stem prosthesis (MEM) made of titanium or cobalt chromium alloy. Arch Orthop Trauma Surg 123:353–356

Shih CC, Shih CM, Su YY (2004) Effect of surface oxide properties on corrosion resistance of 316L stainless steel for biomedical applications. Corr Sci 46:427–441

Simon M, Kaplow R, Salzman E et al (1977) A vena cava filter using thermal shape memory alloy: experimental aspects. Radiology 125:87–94
Sumita M, Hanawa T, Ohnishi I et al (2003) Failure processes in biometallic materials. In: Milne I, Ritchie RO, Karihaloo B (eds) Bioengineering. Elsevier Science Ltd., London, pp 131–167
Sumner DR, Turner TM, Igloria R et al (1998) Functional adaptation and ingrowth of bone vary as a function of hip implant stiffness. J Biomech 31:909–917
Thompson SA (2000) An overview of nickel–titanium alloys used in dentistry-review. Int Endod J 33:297–310
Torshin IY, Gromova OA (2009) Magnesium and pyridoxine: fundamental studies and clinical practice. Nova Science Publishers Inc, New York
Virtanen S, Milošev I, Gomez-Barrena E et al (2008) Special modes of corrosion under physiological and simulated physiological conditions. Acta Biomater 4:468–476
Wang FE, Pickart SJ, Alperin HA (1972) Mechanism of the TiNi martensitic transformation and the crystal structures of TiNi-II and TiNi-III phases. J Appl Phys 43:97–112
Wataha JC (2001) Principles of biocompatibility for dental practitioners. J Prosthet Dent 86:203–209
Wataha JC (2012) Predicting clinical biological responses to dental materials. Dent Mater 28:23–40
Williams DF (1987) Consensus and definitions in biomaterials. In: de Potter C, de Lange K, de Groot K et al (eds) Advances in biomaterials. Elsevier, Amsterdam, pp 11–16
Witte F, Kaese V, Haferkamp H et al (2005) In vivo corrosion of four magnesium alloys and the associated bone response. Biomaterials 26:3557–3563
Yaghoubi S, Schwietert CW, McCue JP (2000) Biological roles of titanium. Biol Trace Elem Res 78:205–217
Yu J, Zhao ZJ, Li LX (1993) Corrosion fatigue resistances of surgical implant SSs and titanium alloy. Corr Sci 35:587–597
Zivic F, Babic M, Grujovic N et al (2013) Influence of loose PMMA bone cement particles on the corrosion assisted wear of the orthopedic AISI 316LVM stainless steel during reciprocating sliding. Wear 300:65–77

Biodegradable Metals as Biomaterials for Clinical Practice: Iron-Based Materials

Fatima Zivic, Nenad Grujovic, Eva Pellicer, Jordi Sort, Slobodan Mitrovic, Dragan Adamovic and Maja Vulovic

Abstract This review presents the state-of-the-art in the development of iron-based degradable medical implants. Basic properties demanded by the new concept of degradable implants are elaborated, along with the work devoted to understand the underlying mechanism and to improve the properties towards best fitted to the natural tissue. Three application areas are considered: vascular stents, orthopedic implants and tissue engineering scaffolds. Each of these has its own specific demands imposed upon the artificial substitution materials. Biocompatibility is an essential feature that each medical implant must have, but different aspects can be considered depending on the end application. Furthermore, adequate mechanical properties and various characteristics related to the fabrication and in vitro and

F. Zivic (✉) · N. Grujovic · S. Mitrovic · D. Adamovic
Faculty of Engineering, University of Kragujevac, S.Janjic 6,
34000 Kragujevac, Serbia
e-mail: zivic@kg.ac.rs

N. Grujovic
e-mail: gruja@kg.ac.rs

S. Mitrovic
e-mail: boban@kg.ac.rs

D. Adamovic
e-mail: adam@kg.ac.rs

E. Pellicer · J. Sort
Departament de Fisica, Facultat de Ciencies,
Universitat Autonoma de Barcelona, 08193 Bellaterra, Spain
e-mail: Eva.Pellicer@uab.cat

J. Sort
Institucio Catalana de Recerca i Estudis Avancats (ICREA),
Passeig Lluís Companys 23, 08010 Barcelona, Spain
e-mail: Jordi.Sort@uab.cat

M. Vulovic
Faculty of Medical Sciences, University of Kragujevac, Kragujevac, Serbia
e-mail: maja@medf.kg.ac.rs

F. Zivic et al. (eds.), *Biomaterials in Clinical Practice*,
https://doi.org/10.1007/978-3-319-68025-5_9

in vivo testing are presented for pure iron, alloys and composites, as well as joint structures. Corrosion control is a foundation in the development of these materials development and different aspects are also given. Iron-based materials need increased degradation rate because they are still more similar to the permanent implants, due to the slow corrosion process and various methods to overcome this issue have been tried. Porosity and its relation to material structures, mechanical properties, degradation behaviour, magnetic properties, and fabrication technologies, as well as methods of numerical simulations as a supporting tool have been elaborated. Porous structures represent one way to enhance corrosion, while maintaining intact other necessary properties of the biomaterial. Economic impact of the biomaterials sector in general is significant and justifies large investments in research. Iron-based materials for degradable implants are not in clinical practice yet, but the research results achieved so far promise the future applications.

Keywords Biodegradable metals · Iron · Alloys · Composites · Economic impact

1 Introduction

Recent development of different novel tools, technologies and methodologies, both theoretical and experimental setups, enabled great advancements in the area of new materials and medical devices. The determinant from aspect of practical application of newly developed materials, independently of their superb properties is their production price, closely connected with the available production technologies. Economic feasibility of new materials and consequently new medical devices is also closely related to the availability of constituting raw materials. Some excellent materials are yet out of practical applications precisely due to the enormously high price either because of lack of production technologies for large series or very high price of raw materials.

Several material classes are traditionally used for medical implants, such as metals, polymers and ceramics, but number of new hybrid materials, alloys, composites and nanomaterials are fast emerging offering completely novel behaviour with better fitted properties. Metallic biomaterials can be considered as the oldest used materials to make implants, such as orthopedic wires, hip or knee prosthesis, coronary stents, and other. Even in case of these traditional materials, such as medical grade stainless steel that has been used for years, some issues still exist and need further improvement. The ideal artificial medical material, which could replace human tissue without any side effects, does not exist and is a goal of all related investigations. Even more questions are raised for completely novel materials discovered in recent years, which usually needs profound understanding of number of exhibited properties. The significantly better behaviour of these new material classes proved in lab conditions motivates researchers to pursue explanations and their further development.

The extent and dynamics of the biomaterials market today completely justifies investments into these areas, and associated research activities, due to several reasons. Human population has significantly prolonged life cycle compared to the earlier historic periods. Old age is commonly associated with health problems and variety of them can be solved through use of medical implants (e.g. coronary stents, hip arthroplasty, etc.). On the other hand, many medical statistics show the significant increase of similar problems in younger population, mainly associated with the modern way of life. At first, it might seem that solutions used for elderly population can also be used for young people, but that usually results in a series of new problems precisely because of the patient age. For instance, first hip replacements were made for rather old people, meaning that the implants were not designed to last over the time period of 50 years or more, but for much less time. The extremely long implant life in such cases was not one of the priority criteria imposed during the design process. But for young patients, this is one of the most important design criteria for both the material used and the implant shape and size. Treatments of the younger population indicated that side effects of artificial implants can be totally avoided only by completely removing the implant after the healing is done. This is usually done by revision surgeries, such as removing steel bars which hold bones long enough for them to remodel and heal. A medical implant is usually needed for a certain period of time to allow and help the surrounding tissue to heal and after this time the permanent implant just becomes foreign object. This is true even in case of arterial stents, because during 6–12 months period the artery tissue "learn to be wide open to allow blood flow" and after that stent is not needed. And the patient must take different drugs to prevent side effects (e.g. implant rejection by the tissue) during the whole time of the implant presence in the body, thus causing other serious drugs related side effects. It was natural to investigate possibilities to discover such implant materials which would allow the implant to stay in the body for a certain pre-determined period of time, performing their function and afterwards to degrade and vanish from the body without leaving a trace of foreign material. This opened up important new avenues of research aiming at new material classes which would enable fabrication of degradable medical implants. Traditionally, design and development of new materials are associated with numerous trials and errors in the lab, being costly procedure from both aspects of time and investments. Many research results indicated that degradable metal materials would be the best candidates, but the science has yet to offer the solutions here.

The first metallic biomaterials used in clinical practice were permanent implants. Two key properties in their design were structural function and resistance to corrosion (inertness), because corrosion of metal materials was associated with numerous detrimental consequences for the surrounding tissue. The last decade however revealed results which enabled to observe corrosion as favorable process if implant material is adequately designed. This, in return, directed research and development of implants towards biodegradable ones, which promise significantly better suited coronary stents or orthopedic wires for example. Perhaps, the start of this new exciting area of medical devices was initiated by the development of tissue

engineering field with many new obligatory demands on materials used there. Biodegradability becomes the very important property of the medical implants and promises high advancements in the regenerative medicine. This is especially important for metallic biomaterials which traditionally have been observed as the best candidates for implants due to their strength and good mechanical properties that can be tuned in different ways. Degradable biomaterials should actively interact with the tissue and promote healing, instead of passively replacing the missing tissue (permanent bone substitutes) or support the vessel (permanent coronary stents). The essence of the biodegradable medical implant concept lies in the fact that in many cases (e.g. stents), the implant is needed in the body only during the healing process, to provide, for instance, necessary mechanical strength and support to the live tissue. After the healing process is finished, ideally, it should gradually disappear and leave no harmful elements behind. Very important property also wanted of the engineered tissue is to have a healing function, such as drug delivery systems designed precisely for targeted delivery of the drug to some specific site within the human body.

Good definition of biodegradable metals is given by Zheng et al. (2014): "Metals expected to corrode gradually in vivo, with an appropriate host response elicited by released corrosion products, then dissolve completely upon fulfilling the mission to assist with tissue healing with no implant residues". It is obvious that elements that constitute the whole metallic material (alloying elements or composite elements) must be of such characteristics that would not have harmful effects on the living tissue during the degradation process. There are many influential factors if synergetic effects of the material development process and later degradation are taken into account and need multidisciplinary approach to both research and practical clinical application. High quality and well structured multidisciplinary teams from aspects of all necessary knowledge and skills, gathering engineers, medical doctors, physicists, chemists, biologist and other professionals, are of the utmost importance in order to comprehensively observe all material properties and responses.

1.1 Application Areas of Degradable Implants

There are many possible fields of application for biodegradable materials in medicine. Three areas can be distinguished according to existing research results that indicate the most probable real advancements in clinical applications within relatively recent future: bone implants, coronary stents and tissue engineering scaffolds. Coronary stents and bone fixtures alone represent millions of surgeries per year, in Europe only. Currently, permanent bone fixtures are removed after the healing is done, resulting in another painful surgery for the patient with all possible associated risks. Degradable implants would prevent this. Several good review articles can be found in the literature with a focus on metallic medical materials (Chen and Thouas 2015; Niinomi et al. 2012; Hermawan et al. 2011) and degradable metallic medical materials (Li et al. 2014; Henderson et al. 2014; Walker et al. 2014; Chen et al. 2014;

Purnama et al. 2013; Li and Zheng 2013; Alexy and Levi 2013; Tan et al. 2013; Hermawan 2012; Yusop et al. 2012; Persaud-Sharma and McGoron 2012; Moravej and Mantovani 2011; Hermawan et al. 2008a, 2010a, b; Purnama et al. 2010; Zberg et al. 2009; Witte et al. 2008). Based only on the quantity of review papers, importance of this field is obvious. Several practical applications have already used some of the biodegradable materials in clinical practice, even if it is still in the beginning phase, such as degradable coronary stents or degradable bone fixation.

Used in coronary interventions, a stent is a small mesh tube, placed inside a blood vessel to act as a scaffold (Fig. 1). The stent pushes against the walls of the vessel to provide normal blood flow and prevents the closing, narrowing or blockage of the vessel by mechanically supporting it. There are several reasons that can lead to the narrowing or blockage of the coronary vessels, but all of them can be healed by forcefully making the vessel opened for the blood to flow though it, for the certain period of time, during which the vessel walls 'learn' to have that shape and position. For the most vessel types, approximate period when this healing process can be satisfactory achieved is a period of 6–12 months and afterwards the stent has no beneficial influence (Moravej and Mantovani 2011). Accordingly, the period of 12–24 months is recognised as probable optimal time during which the stent presence is needed within the vessel (Reindl et al. 2014; Henderson et al. 2014; Hermawan 2012; Serruys et al. 2006; Schomig et al. 1994). Coronary stenting is one of the commonly known procedure, widely used and millions of different stents are daily implanted all over the world. Current technology uses permanent metallic stents made of several metal types (mainly medical grade stainless steel and nitinol). Degradable stents are just in a beginning phase of their application with only limited number of clinical trials still ongoing and only a few

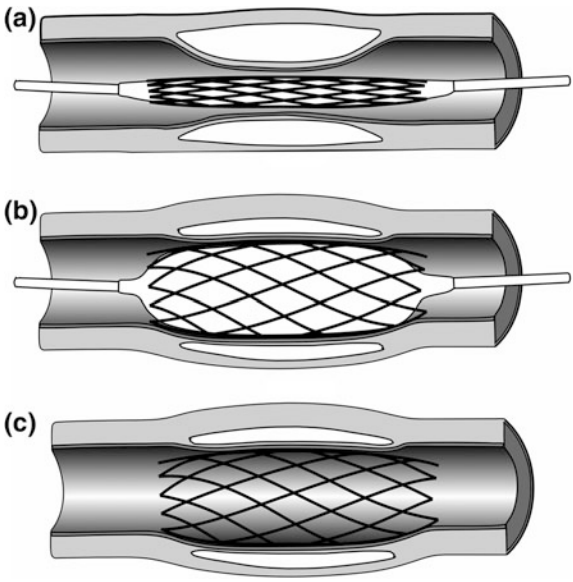

Fig. 1 Schematic representation of stent applications

commercially available types. Permanent metallic stents are related to different recognised problems, such as possible harmful effects on the live tissue, release of the toxic elements into the body, unwanted mechanical stress, restenosis and other. Literature data indicate that even up to 44% of patients can suffer from restenosis (narrowing of the coronary vessel due to adverse immune reaction of the organism to the wall damage that can occur during the stenting procedure) and accordingly need further medical procedures (Blackhear et al. 1987; Farooq et al. 2011). Permanent metallic stents are also related to other problems such as very late stent thrombosis as a consequence of incomplete healing process of the tissue around the stent, especially in case of drug eluting stents (Brodie et al. 2011). Studies related to the cell viability of novel materials can be focused on the control of cell proliferation for vascular smooth muscle cells or platelet adhesion in case of stent materials as beneficial for prevention of the restenosis phenomena. Several review articles can be found related to the state-of-the-art in development of biodegradable stents as one highly important area of application (Alexy and Levi 2013; Moravej and Mantovani 2011; Hermawan et al. 2010a, b).

Orthopedic implants, such as plates, screws, wires, sutures or various fixation devices, as shown in Fig. 2, are used in case of traumatic injuries, until the fractured bone is healed. Some statistics point to approximately 2 Mil surgeries annually, in Europe only. In case when permanent implants are used, they often need to be surgically removed after the bone regeneration, which is a painful and costly operation. For the bone replacements, optimal period to complete the healing of the bone, or the remodeling process around a fracture is within a timeframe of 2–8 months during which the mechanical support to the bone is needed (Kini and Nandeesh 2012). After that period, the implant has no structural function and needs to be removed. Biodegradable orthopedic implants must possess adequate mechanical strength to support the bone during the healing process, but the material

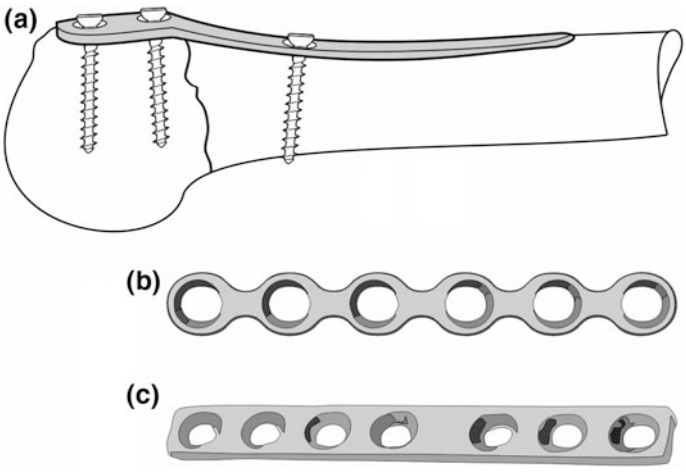

Fig. 2 Schematic representation of different bone fixation

should ideally have elasticity modulus close to that of the bone in order to distribute the external stress evenly. During degradation, implant will gradually lose its strength and loads will be gradually redistributed to the bone until the implant disappears completely. Bone scaffolds have been a subject of research for a long time, but ideal solution is still missing. Ryan et al. (2006) presented a good review of technologies used for fabrication of porous orthopaedic scaffolds made of metals. Metals are superior candidates for orthopedic scaffolds because they have all necessary properties as compared to ceramics (which have issues related to brittleness) or polymers (that cannot satisfy mechanical strength). Yusop et al. (2012) presented a review of existing metals which can be used for biodegradable orthopedic tissue scaffolds. Good review articles in this area are also presented by Walker et al. (2014) and Tan et al. (2013).

The first activities in tissue engineering field which perhaps initiated the novel field of degradable materials for medical purposes, started back in 80s and had no clear defined concept except the focus to grow tissue or whole organs directly from one cell taken from actual person (Peck et al. 2011). The research related to different artificial scaffolds for cell growing has since gained significant attention since then and accordingly introduced issues related to cell reactions and in vivo behaviour of scaffold materials, primarily associated with implant infections due to some incompatibility of the scaffold material. Polymers were the first selection for scaffolds fabrication, but series of new materials are also investigated nowadays. In general, tissue engineering starts with fabrication of scaffolds where cells are seeded and grown. One simple tissue scaffold is shown in Fig. 3. Scaffolds are 3D structures optimised for better cell adhesion and viability and accordingly they tend to mimic natural tissue, preferably extracellular matrix structure. Thus, the foundation of tissue engineering area is the design of 3D scaffolds as highly complex structures from aspects of appropriate pore size and shapes, interconnections, porosity levels, etc. Porosity is one of the most important properties, and there are some recommendations regarding pore sizes and other properties of porous structure. For cell

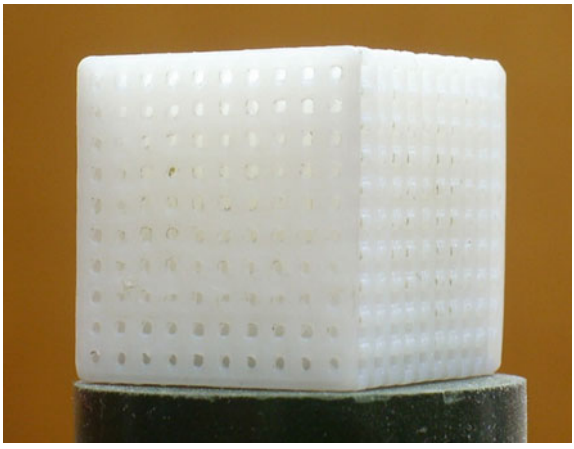

Fig. 3 Simple geometry of the polymer scaffold made for cell seeding

ingrowth and viability, interconnected network of pores, with pore sizes of 50–1000 μm is recommended (Butscher et al. 2011).

Traditional fabrication technologies generally lack tools and methods and especially materials for production of such structures are still under investigations. So another issue imposed by the demand for porous structures is its fabrication technology. Namely, traditional technologies are hard to use for production of porous scaffolds, due to the fact that it is mainly the question of nano and micro level porosity and characteristics. One promising direction is the utilization of new 3D printing technologies which starts from powder material forms, enabling almost unlimited variety of geometries and shapes of 3D pores. However, the price of the technology is still too high, but maybe the most significant issue is related to the limited accuracy of fabricated parts and most of all lack of proper materials. One distinct advantage of 3D printing is the possibility to form vast number of material combinations leading to the completely new composites, or functionally graded materials with predefined properties that change over the bulk. Such structures would properly mimic natural tissues and this direction of research is currently gaining high interest. The size of particles in a powder is also under debate from different aspects of final material properties. It is assumed that high resolution could be achieved by using fine powders, with high flowability, to form fine layers, but this is very difficult to obtain with polymer materials which are highly ductile and deformable. Metal materials are more suitable from this aspect, but they have other drawbacks associated with the use of this technology.

Porous bone tissue scaffolds are advantageous because they enable cell proliferation thus promoting new tissue formation, deposition and migration of extracellular matrix to enable adhesion of cells, communication between cells and differentiation. Another significant advantage is the possibility of fluids flow through the porous structure. It is well documented that porous materials enable better ingrowth of bone cells and blood vessels. One research direction in bone grafts is focused on simultaneous progressive osseointegration and gradual degradation of the implant what would enable optimal adaptation to the corresponding strength state at any time.

1.2 Basic Properties

There are several properties that the biomaterial should fulfill to be a good candidate for the medical implant (Hermawan 2012; Hermawan et al. 2011). The basic condition is that it must be biocompatible and non-toxic. But other properties are significant as well, depending on the specific application case, such as mechanical strength, ductility, resistance to fatigue damage, ability to resist cracking, low cost production, etc. For example, in case of bone implants, large difference between the values of Young's modulus of the material used for bone substitute (e.g. AISI 316L stainless steel) and the bone itself provokes important problems in structural functioning over longer time. Ideally, the Young's modulus of the implant material

should not exceed the bone stiffness, which currently is way below modulus of traditionally used materials. There are many properties that need to be considered for the development and design of a new material. The design process sometimes must consider opposing requirements and optimal balance is very important and very hard to achieve. Currently, since the degradable materials are still in its beginning, the approach is to focus on one property (e.g. corrosion rate) and to find its balance with one or two other required properties (e.g. biocompatibility and strength).

Experimental laboratory testing and in vitro studies together with numerical modeling and simulations both provide valuable insights, but the final testing is always in vivo, first within animal studies, followed by clinical trials on humans. Altogether, it is a very long (usually not less than 10 years) and very costly process. In vivo testing is the most sensitive area of investigations and there are many unresolved approaches there (Bartosch et al. 2014; Kirkland et al. 2012). The majority of commonly accepted investigation methods used in lab tests cannot be used in vivo, such as all of the methods which involve destruction of the sample in anyway. Medical imagining is by far the most commonly used techniques for in vivo tests and it is fair to expect that new materials will bring advancements in this area also. Numerous different in vitro experiments can be found throughout the literature as necessary to evaluate proposed materials. However, all in vitro tests provide more or less satisfying results and can never be taken as completely reliable from aspects of in vivo testing. In vitro testing is necessary as a preliminary study which points out to different issues, some of which can be recognised and solved before in vivo approach. Clinical studies that involve either animal study or clinical trials on humans are realised only when all comprehensive in vitro testing indicate that there will be no apparent problems in vivo. And even then, clinical trials very often result in complete dismissal of the developed material, or in less severe cases, its further modifications and repetition of the in vitro testing. Screening technologies and models have been investigated and developed to lower the utilization of animal models as pre-clinical trials (Higuera et al 2013).

Medical diagnostics and monitoring of the implant after performed surgery, as the next step, is of the utmost importance for the post-operative period. Accordingly, materials used for fabrication of implants must be also compatible with existing medical instruments for imagining or diagnostics in general and possible contraindications with magnetic resonance imagining (MRI) is one of the usual tests (Dill 2008). This is especially important to consider for metals. Generally, non-invasive technologies such as MRI or computed tomography (CT) are safe to use with permanent metallic stents but there are different recommendations to use it only after the certain amount of time passed after the stenting procedure (e.g. 3 weeks) to avoid a risk of dislodging, rotating or otherwise moving of a stent under the influence of the magnetic field (MRI). For example, the main issue related to the use of MRI with metallic implants is their ferromagnetic properties. Ferromagnetic metals will move under the influence of the strong magnetic fields, towards or against the field. Accordingly, metallic implants are made of metal materials which are either weak ferromagnetic or non-ferromagnetic,

but certain influence of the applied magnetic field when subjected to MRI scanning is always evident and there are several studies of such effects (Dill 2008). MRI produces three types of mechanisms that may provoke unwanted effects on ferromagnetic stents: strong static magnetic fields; pulsed gradient magnetic fields and pulsed radiofrequency fields (Dill 2008). Strong static magnetic field attracts ferromagnetic objects thus producing object motion and might influence the function. Neuromuscular stimulation may occur as a consequence of the pulsed gradient magnetic field which produces electrical current in conductive devices. Radiofrequency energy increases the heat locally in metallic devices and can induce electrical current. Also, the combination of MRI contrasting agents with certain medical conditions can represent risk factors.

Until recently, degradable materials were mainly considered to be biodegradable polymers. However, one of the major concerns regarding the use of biodegradable polymers as scaffolds is their poor mechanical properties, especially in the case of hard tissue applications such as bone, where adequate strength is necessary. The natural following was to consider metals as degradable biomaterials, due to their high mechanical strength, as desired in bone fixation screws/pins and for coronary stents. Corrosion resistance was one of the first and foremost demands imposed upon permanent metallic implants. But with the appearance of degradable metal materials concept, corrosion becomes the mean to control the degradation rate. In other words, it can be said that the possibility to control the corrosion rate enables development of biodegradable metallic materials. However, even with the fact that certain level of control over the material degradation has been achieved, there is no complete and final solution. Understanding of underlying corrosion mechanisms are still under investigations for the majority of possible materials that can be used for biodegradable implants. Thus, research aimed at establishing the exact mechanisms to control the rate of degradation in metallic biomaterials within a human body has been the subject of many studies.

One of the reasons that metallic biomaterials have started to be of interest as degradable materials instead of polymers is their far better mechanical properties such as strength, density or resistance to fatigue damage. As previously mentioned, they need to be completely biocompatible, non-magnetic and with satisfying high density to be suitable for MRI and visible under X-rays. Orthopedic implants are subjected to high dynamic loadings and materials should exhibit good combination of strength and ductility in order to maintain structural functionality over longer time. Polymers lack these properties in comparison to metals. Furthermore, specific area of application requires additional specific properties. For instance, cardiovascular and orthopedic implants have significantly different material requirements, from aspects of loadings, shape, size, plasticity, environment and many other influential factors. For example, osseointegration benefits from the controlled surface porosity of determined shape and size are proven in case of bone tissue scaffolds. Good ductility enables thinner stent struts and enables proper expansion, but stiffness is also significant for dilatation (Hermawan 2012; Hort et al. 2014). Resistance to fracture and wear resistance both are very important material properties for orthopedic implants, such as hip or knee joints. One recognised problem

for the metal bone implants is stress shielding occurring due to the difference between elastic modulus of the bone and the metallic implant material. The living bone tissue is reinforced by the implant and loading is redistributed to the material of implant, due to significantly higher elastic modulus of the metal in comparison to that of the bone. This effect is known as the stress shielding and has very detrimental influence on the bone, causing deterioration of the unloaded bone cells and bone loss. With time, even the complete failure of implant can occur, leading to urgent revision surgeries. Elastic modulus of some commonly used metal materials for permanent implants are: CoCr alloy—240 GPa; medical grade 316L stainless steel—210 GPa; Ti6Al4V—112 GPa; NiTi—48 GPa (Geetha et al. 2009). These are all significantly higher than that of the elastic modulus of the bone (30 GPa). Accordingly, development of new metal alloys is aimed at low values of elastic modulus, close to that of the bone. Very good approach to this issue is porous material structure that can produce decrease of elastic modulus for materials with otherwise higher modulus for high-density structures. However, there is a need to comprehensively investigate the influence of the porous structures on material fatigue properties during functional time (Ryan et al. 2006).

1.3 Production Technologies

Production technologies should be economically feasible and this opened up yet another novel area of research activities in order to adjust and use traditional technologies to produce new materials with custom designed structure properties, which very often consider aspects of novel nano- and micro-level behaviour, the pre-designed phase distributions, heat and pressure regimes, post-processing and many other. The recognised issue with new materials is small production batches that is usually required, which in turn makes the manufacturers hesitate to engage in such production, especially in case of metal alloys, since the large production series produce larger profit and lower risks. This serious limitation is imposed also by the industrial systems used for metal alloys production. Namely, traditional manufacturing in this field uses very large, heavy and costly furnaces, presses, melting and processing systems, etc., from both aspects of starting the production and keeping it. Adjustments and changes of such large production facilities to the new material processing, need serious justification of costs and manufacturers are very reluctant to try new materials which are not yet proven to be economically justified. Accordingly, many research groups around the world are beginning to setup and use small foundries, heat and pressure processing units or powder metallurgy systems and coating systems, in order to form flexible production lines for small batches. These represent the foundation for development of new materials by using traditional production technologies such as alloying, casting, powder metallurgy, traditional coating technologies (e.g. PVD, CVD). But, in any concept, establishing even small production facilities is very costly from both aspects of time and resources. Beside traditional ones, some new production technologies have

emerged in recent decade, especially supported by improved computer technologies and automated control systems. They are still not cost-efficient for a mass production but offer great variety of different approaches in material designing and they are better suitable for small material batches. Previously mentioned 3D printing is one such technology which is proved to enable freedom and custom design of porous structures, with defined pore size, distribution and wide application of materials (Butscher et al. 2011). Fabrication of the implant itself, not just production of the material is also area of current research, in order to provide optimal parameters from aspect of final function. For example, method and parameters of stent production has the influence on its properties (Hermawan and Mantovani 2013).

Additional complexity for material production routes is the incorporation of porous structures since it imposes further limitations on the available technologies. Several technologies can be used, such as plasma spraying, sintering of metal powders, space holder method, replication method, infiltration casting, combustion synthesis, additive manufacturing, chemical vapour deposition (CVD) on replica forms substrate, vacuum suction casting, but these are all under investigations from various aspects of final material properties, because applied technology has profound effect on it (Ryan et al. 2006; Hermawan 2012; Wegener et al. 2011; Trinidad et al. 2014; Chou et al. 2013; Wang et al. 2013; Butscher et al. 2011). It is well documented that the production technology determines various characteristics of the material structure and numerous studies has been devoted to find optimal technology and production parameters for fabrication of degradable metal materials, ranging from traditional ones like casting to novel techniques (Fang et al. 2013; Chou et al. 2013; Hermawan and Mantovani 2013; Moravej et al. 2010a; Ryan et al. 2006; Schaffer et al. 2012; Butscher et al. 2011, 2012; Schinhammer et al. 2010; Hermawan et al. 2008b; Murakami et al. 2007; Crane et al. 2006; Hutmacher et al. 2004).

1.4 Biodegradable Metal Materials

Generally, existing metallic biodegradable materials can be classified as: (1) pure metals, (2) alloys, and (3) composites. Significant research activities have also been addressing coatings on each of these material types and their functionalisation. Especially, metal-polymer composites are subject of research promising advancements in this area, by combining mechanical strength of metals and biocompatibility and biofunctionality of polymers to provide optimal implant performance.

During the last decade, two classes of metallic materials have been recognised as suitable candidates for biodegradable implants: iron (Fe) based and magnesium (Mg) based materials. In comparison to Mg-based alloys, which have an issue of too fast degradation rate, Fe-based alloys exhibit exceedingly slow degradation time, close to the behaviour of permanent implants. Another important property which determined the selection of Fe-based compositions is their antiferromagnetic

properties. It might seem odd that iron is non-magnetic since it is a widely known magnetic material. However, iron is interesting material due to its known polymorphism, meaning that its magnetic characteristics are determined by the presence of different iron phases that can form either magnetic or non-magnetic iron-based material when alloyed with suitable elements.

Magnesium based materials were first considered, starting with bone fixations and then magnesium based stents (Witte et al. 2008). A few years ago, the international company Biotronik offered the first commercially available degradable stent made of Mg alloy on the market. That was a result of comprehensive investigations of several research groups (Erbel et al. 2007; Waksman et al. 2009; Schinhammer et al. 2010; Hänzi et al. 2010; Geis-Gerstorfer et al. 2011; Niinomi et al. 2012; Kirkland et al. 2012; Bartosch et al. 2014; Willbold et al. 2015). Magnesium is already one of the essential elements of the human body and even its excess is not harmful. Magnesium cations are one of the most common cations in the human body and necessary cofactor in over 300 enzyme reactions. They have multiple roles in the body. It is essential for the process of cell breathing, synthesis of nucleic acids, metabolism of numerous hormones and neurotransmitters, activity of Na-K-ATPase and other. The body contains around 22–26 mg of Mg and 50–60% is in the bones. Mg is primarily absorbed by the distal jejunum and ileum and the most responsible to maintain the homeostasis are the kidneys. Around 20% of Mg is connected to the plasma proteins and around 65% is in ionized form. Daily dosage is around 4.5 mg/kg (Swaminathan 2003).

Alloys based on Mg rapidly dissolve in corrosive environment and this was the foundation of its use as degradable implant material. However, the degradation speed is too high, apart from a few more drawbacks of its use, such as the associated hydrogen gas evolution during degradation which is very problematic. Nevertheless, magnesium alloys are good materials for fabrication of degradable medical implants and large research activities are undertaken to overcome recognised issues in its functioning or production. Different combinations of elements have been investigated for alloy production, as well as production methods to avoid extremely dangerous flammability. Aluminium (Al) and rare earth (RE) elements are added to increase alloy strength and improve corrosion resistance, thus prolonging the degradation time. And it is known that Al is toxic for cells and RE elements are extremely costly. Addition of Ca and Zn has been tried to increase strength, ductility (elongation to fracture as very important for stents), and hardness. Also, coating of the alloy has been applied to slow the corrosion on one side and on the other side it has been used in drug eluting stents (DES) for drug delivery (Hornberger et al. 2012). Polylactide (PLA) based coatings prevented biomaterial-associated infections. Mg alloys with Hydroxyapatite (HAp)-doped PLA porous film coating exhibited suitable corrosion rates and biologically safe implants. Composite coatings on Mg alloy, such as chitosan (CHI) and poly (styrene sulfonate) (PSS) polyelectrolyte multilayer showed better corrosion resistance. A very good review articles related to the state-of-the-art in the development

of Mg-based materials is presented by Li and Zheng (2013), Neacsu et al. (2015) and Sanchez et al. (2015).

As previously stated, there are a few significant drawbacks associated with Mg-based materials, especially related to the alloy price and highly demanding production technologies. Materials with iron matrix were in some way a natural follow-up, and during the last several years Fe-based materials got very serious attention. Perhaps the most important advantages of iron based materials are their high mechanical strength and low cost, as well as wide availability of constituting alloy additions, especially compared to rare earth elements in Mg-based materials. Permanent stainless steel stents are already in practice for years, with well known behaviour. Ductility is higher than of Mg-based materials, which is especially important in case of stenting procedures, allowing thinner struts.

2 Iron and Iron-Based Materials for Biodegradable Implants

Pure iron and iron-based materials has recently started to be extensively studied as potential suitable materials for degradable implants, especially for cardiovascular stents (Hermawan et al. 2008a, b, 2010a, b; Alexy and Levi 2013). The mechanical properties of iron can be compared to those of 316L stainless steel, which is a standard material for permanent stents or hip implants, designed to be highly corrosion-resistant material (Zivic et al. 2013). Iron has high strength and high elastic modulus, but also high ductility which is important for plastic deformation during the stenting procedure. Pure iron and iron oxides show no toxicity or immunogenicity in vivo and even its nanoparticles are biocompatible as per several studies (Moravej and Mantovani 2011; Ling and Hyeon 2013; Peuster et al. 2001, 2006; Waksman et al. 2008). Investigations related to different aspects of biocompatibility are preceding all other studies and they showed that iron-based materials can be used (Ulum et al. 2014a, b, c; Huang et al. 2014; Ling and Hyeon 2013; Wegener et al. 2011; Glorius et al. 2011; Purnama et al. 2010; Liu and Zheng 2011; Peuster et al. 2006).

Another significant advantage of Fe-based alloys is their cost-efficiency and widely available production technologies, as well as companies all over Europe that deals with production of iron alloys, especially if compared to Mg alloys whose production is mostly based in China and the USA. Also, elements in Fe-based alloys which currently promise to provide desired material characteristics are widely available elements, not like rare and costly RE elements in Mg alloys that are influencing their very high price. Also, degradation of Fe alloys does not produce hydrogen as in case of Mg alloy degradation. However, even with very promising results so far, iron alloys has not been yet developed to efficiently serve as a material for degradable implants, due to slow corrosion rate, making these materials still very similar to permanent implants. But this is new area of research

and many results are yet to be seen, starting from variation of alloying elements, composites, coatings, or heat regimes modifications, etc.

2.1 Iron Properties

Iron is the fourth common chemical element of the Earth crust (around 5%), with a symbol Fe. It has atomic number 26, atomic weight of 55.847 and belongs to the group 8 of the periodic table. Iron can exhibit various oxidation states (−2 to +6), although +2 and +3 are the most common ones. The number of electrons in the two outer shells can be 2, 8 and 14. Iron has been used for making of tools even in antique times. Elemental or pure iron can exist in nature only in meteoroids or low oxygen environment, because it oxidizes very rapidly forming outer passive layer. Melting temperature of iron is 1538 °C, boiling temperature 3070 °C and density 7.874 g/cm^3. Young's modulus at room temperature is 200.4 GPa and shear modulus 78 GPa. In engineering, the term "iron" (Fe) often refers to the alloying of Fe with addition of carbon (C), whereas it forms steel (between 0.002 and 2.1% of carbon addition). There are two types of iron in use, depending on its purity: chemically pure iron (99.999% Fe) and technically pure iron (99.8–99.9% Fe with impurities made of small amounts of C, Mn, Si, S i P). The majority of Fe alloys are produced by casting. Today, iron-based alloys account for 95% of the total world production of metal alloys. Such high production and use is enabled by the large quantities of iron ores, easy to exploit, rather low cost processing and large variety of metal alloy properties which can be obtained.

Iron can exhibit several different crystal structures, due to its polymorphism and basic ones are shown in Fig. 4. Depending on the temperature and pressure regimes, iron can have different crystalline modifications: δ-iron allotrope, body-centered (bcc) crystal structure; γ modification, face-centered cubic (fcc) structure (austenite); α allotrope, bcc structure (ferrite). Under higher pressures (10 GPa), iron can have hexagonal close-packed (hcp) crystal structure, or ε allotrope and some new modifications seems to be possible at very high pressures and temperatures, such as β-iron with double hcp structure; ε martensite or others, what will be discussed later in the text. Very general phase diagram of the pure iron

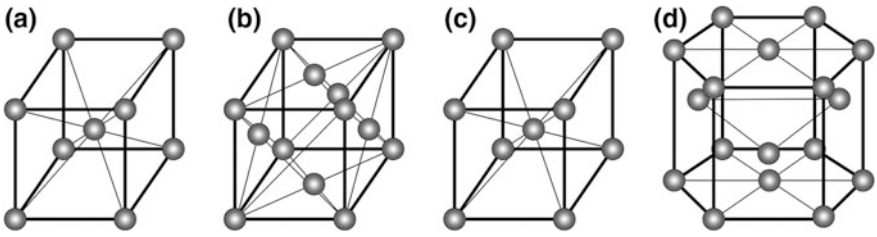

Fig. 4 Allotropes of iron **a** alpha (α) iron, **b** delta (δ) iron, **c** gamma (γ) iron and **d** hcp iron

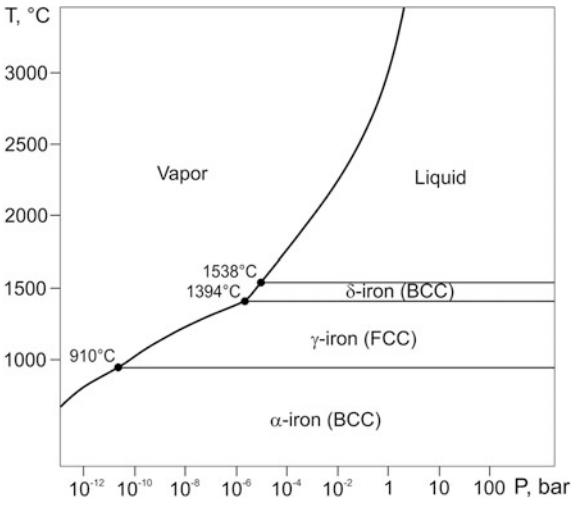

Fig. 5 Phase diagram of the pure iron under low pressure

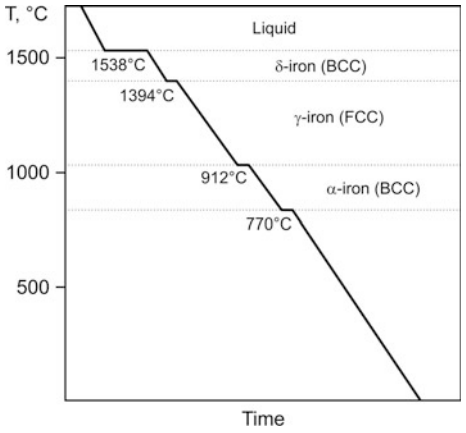

Fig. 6 Cooling curve of the pure iron

under low pressure is shown in Fig. 5 with regions with specific crystal structures. It can be seen from Fig. 6, that upon cooling from the molten state, iron exhibits δ (bcc) structure, then changes into γ (fcc) structure and α (bcc) allotrope. Changes from α to γ decreases material volume and vice versa, because γ-iron is denser than α-iron since more atoms are packed closer to each other in the γ-crystal lattice than in α-lattice. Unit element of γ-lattice has 4 atoms and α-lattice has 2 atoms. These volume changes are small, not more than 1%. Important iron property is the Curie point (770 °C temperature) below which iron becomes magnetic. However, this is traditional knowledge about iron and several new discoveries opened up the research directions towards non-magnetic iron for degradable material applications, probably mainly due to new crystal modifications.

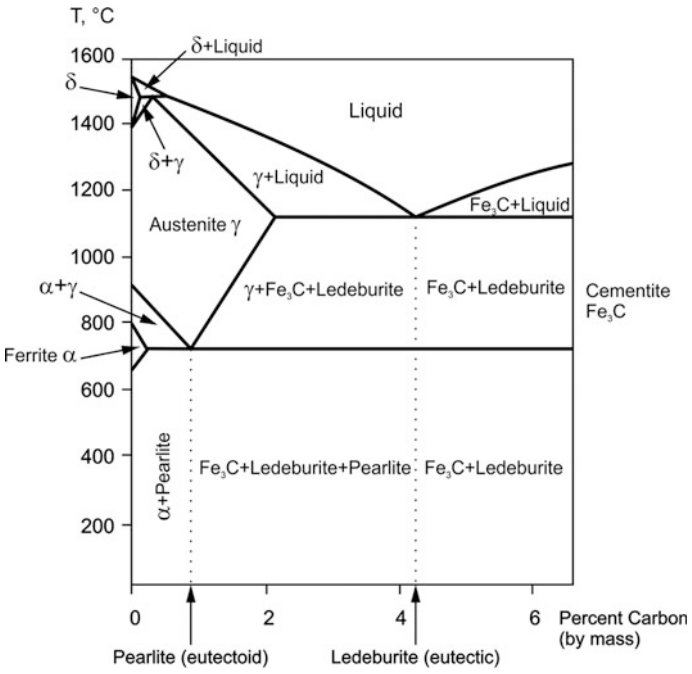

Fig. 7 Phase diagram of iron-carbon system

With all the complexity of pure iron system, addition of other elements makes the material even more complex but on the other hand such complexity opens up possibilities to tailor material properties. Standard phase diagram of the Fe–C binary alloy system is given in Fig. 7. There are numerous Fe alloys for many different applications, where material properties can be adjusted by addition of many other elements (C, Si, Mn, S, P, Cr, Ti, Mo, Ni, Ta, V, Co, Ni, W, etc.). Left in humid air, iron alloys are highly susceptible to oxidation and corrosion development and they do not form outer passive layer to protect them from corrosion development up to catastrophic levels, except for those alloys made to be corrosion resistant (with addition of Ni, Cr, etc. or stainless steels). Carbon is however the constant element in Fe-based alloys and depending on the C content, they can be divided into 3 groups: (1) wrought iron (pure iron with very low C content or other elements originating from iron ore), (2) steel (usually C content is below 2%) and (3) pig iron and cast iron (C content above 2%, usually up to 4%).

2.2 Iron Biochemistry

Iron is necessary for humans because it is used in production of new red blood cells and is one of the essential constituents of the human metabolism and in many vital substances within a body. Iron is the most common oligoelement in the human body and can appear in two valence oxidized states: divalent (ferrous), Fe^{2+} and trivalent (ferric), Fe^{3+} state. Most proteins which have iron contain ferric ions. Iron is essential element for production of blood because it is necessary for production of haemoglobin and myoglobin, as well as for number of enzymes which participates in different vital cell processes (e.g. oxidase, catalase, peroxidase, cytochromes, aconitase, ribonucleotide reductase and nitric oxide synthases). Usual daily intake of iron is 10–20 mg, but less than 10% is absorbed. There are two ways of iron absorption from food. Heme group of haemoglobin and myoglobin is released from the protein complex during food digestion. Absorption mechanism of the heme iron groups are yet not understood well enough, but it is known that it goes into enterocytes as the intact metalloporphyrin, by the endocytosis mechanism, after which the porphyrin ring is opened by enzymatic process and iron ions are released. It is also confirmed that the intake of divalent and trivalent iron goes via two separate ways. Transport of divalent iron is mediated by the Nramp2 molecule (DMT-1 protein), which serves as the carrier of divalent metals, also called carrier of divalent cations (DMT-1, divalent metal transporter; DCT-1, divalent cation transporter) and its function is to transport the iron from the luminal mucin to the enterocytes. Membrane complex of molecules, called paraferritin, is responsible for the transport of trivalent iron ions. Simultaneously with absorption from the luminal mucin, enterocytes take the iron also by the endocytosis of the transferrin iron—complex, transferrin receptor. Recently discovered molecule, ferroportin, is responsible for the iron transport from the enterocytes to the plasma. Transport of iron to the tissue is regulated by the transferrin, serum glycoprotein with molecular mass of 80 kDa (kilodaltons). Since the iron excretion is rather fixed, body regulates its level by changing the quantity of absorbed iron, by the "mucose intelligence" mechanism. These mechanisms refer to the increased intake of Fe in case of its deficiency, or often lower absorption in case of iron overload. Absorption level of iron by the body is conditioned by many factors, one of which is the Fe amount in intestinal mucose. Some studies indicate that there is a physiological mechanism in mucose cell for capturing the iron, what prevents its further absorption when there is an overload. If the iron depot is not full, or has very low level of iron, then Fe goes directly from intestinal lumen through the cell into the plasma or blood. Adult human body contains 3–5 g of iron, whereas around two thirds are built in the haemoglobin of adult erythrocytes and their precursors. The majority of the remaining iron amounts are in hepatocytes where it is stored and in reticuloendothelial macrophages (Gkouvatsos et al. 2012).

2.3 Development of Biodegradable Medical Implants Made of Iron Based Materials

The first iron biodegradable stent was made of pure iron (Fe > 99.8%) in 2001 and implanted into the rabbits, showing no inflammation or other harmful effects (Peuster et al. 2001). But pure iron also had too low biodegradation rate thus being similar to permanent steel stents. Several other studies were performed after that, but first investigations related to suitable compositions of Fe-based alloys for biodegradable stents were done by research groups of Hendra Hermawan and Diego Mantovani and they continued comprehensive studies on different aspects of fabrication, alloying elements, biocompatibility influences, ferromagnetism etc., with more than 50 publications in high ranked journals (Hermawan et al. 2007, 2008a, b, 2010a, b; Purnama et al. 2010, 2013; Yusop et al. 2012; Hermawan and Mantovani 2013; Mouzou et al. 2014; Ulum et al 2014a, b; Yusop et al. 2015). They studied influences of several alloying elements, as well as the variation of weight percentage and marked Fe-35Mn alloy as the most promising candidate to increase the biodegradation rate with good mechanical properties and MRI compatibility (Hermawan et al. 2010a, b). A very recent study showed that FeMn alloys with lower Mn content (0.5; 2.7 and 6.9 wt%) exhibited no corrosion evidence even after 9 months of animal implantation (Drynda et al. 2015). They proposed that FeMn phosphate layers were responsible acting as the protective layers against corrosion and some novel strategies to dissolve them would perhaps be the solution. Purnama et al. (2013) investigated the influence of Mn on cell response, as a potentially toxic element in Fe–35Mn alloy. Fe–Mn alloy is non-ferromagnetic for certain compositions and has low inhibition to fibroblast cells, indicating that the alloy is biocompatible (Hermawan et al. 2010b). Moreover, manganese (Mn) chemical element is also one of the essential elements in the human body (Hermawan et al. 2010a; Keen et al. 2000). Different standard iron alloys with better mechanical properties than pure iron have also been tested for degradation behaviour, but these usually showed lower corrosion rate than pure iron. For instance, Fe–20Mn–1.2C alloy with high deformation properties, as well as high tensile and yield strength would be a good candidate but it exhibited lower corrosion rate than pure iron (Mouzou et al. 2014). During the last years, several research groups have also published their results related to Fe-based alloys aimed at biodegradable stents. Liu and Zheng (2011) studied the effects of different alloying elements on biodegradability and in vitro biocompatibility of pure iron, such as Mn, Co, Al, W, Sn, B, C and S. Schinhammer et al. (2010) investigated Fe–Mn–Pd alloys and Liu et al. (2010) studied Fe–30Mn–6Si shape memory alloy. In general, they all confirmed Fe–Mn alloy with 30–35wt% of Mn as the best candidate.

From aspects of orthopedic applications, Yusop et al. (2012) presented state-of-the-art materials and Fe foam and Fe-phosphorous alloys are a few Fe-based materials mentioned in this review because this area of research is at its very beginning and there are not many published results yet. Research groups of Dr Bernd Wegener and Dr Peter Quadbeck has been investigating powder metallurgy

and 3D printing for production of Fe-based dense materials and foams as biodegradable bone substitutes (Quadbeck et al. 2011; Wegener et al. 2011; Farack et al. 2011).

Wegener et al. (2011) studied microstructure, degradation rate and the influence of alloying elements on the cytotoxicity and bone regeneration for several Fe-based alloys produced by powder metallurgy as open cell structures aimed at porous degradable bone implants (Fe–C, Fe–0.6P, Fe–1.6P, Fe–B and Fe–Ag). The main purpose of alloying elements was to obtain better mechanical properties of the iron alloys. Microstructure is greatly influenced by the phosphorous addition since it decreases the temperature above which the material is completely liquid. Diffusion of phosphorous in iron is beneficial for rapid densification and increase of the sintering density (reducing microporosity), as well as the material strength (Wegener et al. 2011). They also showed that phosphorous did not have harmful effects on corrosion rate or cell proliferation, while mechanical properties were significantly better, especially increase of the strength. They tried addition of silver particles aiming to increase corrosion rate but did not get any better result, explained by the small percentage of silver. Also, silver has antibacterial properties. But different silver quantities used in their alloys showed cytotoxicity to normal cells and they concluded that it should not be used as an alloying element in this material. Also, carbon has been shown to produce slight corrosion increase. Different tests related to corrosion resistance of Fe–Mn alloys with various weight percentage of Mn element indicated that corrosion is enhanced by active Cl^- ions in the surrounding solution what can be expected. It is also shown that Mn oxides which are produced during passivation of the alloy surface promote corrosion, while Fe oxides form passivation film reducing corrosion (Zhang et al. 2004; Heiden et al. 2015a).

2.3.1 Alloying Elements

Alloying elements are very influential to the corrosion rate and underlining mechanisms and they are the first instance in modification of material behavior from different aspects since they basically influence all properties. Schinhammer et al. (2010) investigated Mn and Pd as alloying elements and showed that both of them are favorable for degradable Fe-based alloys. Manganese dissolves in iron and directly causes a decrease of the electrode potential by increasing susceptibility of Fe matrix to corrosion, while addition of palladium results in forming of homogenously distributed small noble intermetallics (<10 nm in size) to serve as cathodic sites and promote microgalvanic corrosion. Small noble intermetallics (Fe, Mn)Pd had very low diffusion coefficient at observed temperatures of applied heat treatments, thus making these fine precipitates (Schinhammer et al. 2010). They proposed Fe–Mn–Pd alloys as good candidates for stent applications because they achieved better corrosion rate of one order of that for pure iron, with good mechanical properties (strength and ductility). They also showed that mechanical properties can be further adjusted by the heat treatments, which can influence the

microstructure. Schinhammer et al. (2010) proposed the weight percentage of Mn below 30%, in line with 35% of Mn proposed by Hermawan research group also (Hermawan et al. 2010a, b), according to the defined phase diagrams of binary Fe–Mn alloy. They used aging and annealing with different time and temperature parameters and obtained significantly different microstructures of Fe–Mn–Pd alloys (Schinhammer et al. 2010; Moszner et al. 2011). Different phases existing within the microstructure define further behaviour from aspects of ferromagnetism and corrosion. Schinhammer et al. (2010) obtained different microstructural domains, depending on the heat treatment, such as: metastable ferromagnetic α′ martensite, paramagnetic austenite and ε martensite. For example, iron structure of α′ martensite has body-centered tetragonal (bct) structure, ε martensite has hexagonal close-packed (hcp) structure, while the gamma (γ) phase, or austenite consists of face-centered cubic (fcc) structure and alpha (α) phase, or ferrite is with body-centered cubic (bcc) structure. Different phases and crystal lattice structures influence different material properties, such as magnetic properties, elongation, yield strength and tensile strength, macro- and micro-hardness and crack susceptibility in localized domains, as well as crack development models, as a foundation of corrosion mechanism. γ-Fe and ε-Fe phases are considered to be non-magnetic (Hermawan et al. 2010a).

One of the goals for stent application is to obtain the material with high strength and high ductility. Addition of Pd along with Mn in iron (e.g. the alloy Fe–10Mn–1Pd), resulted in rather high yield strength and tensile strength (approximately 900 and 1550 MPa, respectively), together with satisfactory elongation to fracture (above 7%) and uniform elongation (above 6.5%) (Schinhammer et al. 2010). On the other hand, the presence of the ferromagnetic α′ martensite makes this Fe–Mn–Pd alloy still unsuitable for certain applications and needs further improvements and authors propose variations of Mn content and parameters of the applied heat treatments. Increase of Mn content resulted in lowering of the ferromagnetic phase and above 18 wt% Mn it should not be used. But it was obvious from several experimental tests that small amounts of added Pd (1 wt% or approximate 0.5 at.%) into Fe–Mn alloy resulted in significant strengthening of the material (Schinhammer et al. 2010; Moszner et al. 2011). Wu et al. (2011) investigated the influence of the heat treatments during fabrication of stainless steel for orthopedic applications. They found out that in the case of steel, fine κ-phase within a microstructure had a significant role in higher strength of the alloy, because coarse κ-phase produced lowering of the strength.

Temperature regimes of heat treatments determine the final state of Pd in the Fe–Mn–Pd alloy, where precipitation is favorable from aspect of corrosion enhancement. Namely, recrystallization or precipitation of Pd can be obtained depending on the applied processing temperature (Moszner et al. 2011; Schinhammer et al. 2012). They identified two mechanisms which prevent recrystallization: (1) Zener pinning and (2) reduced dislocation mobility. Zener pinning occurs due to the influence of dispersion of fine Pd precipitates on the grain boundaries of the matrix thus preventing recrystallization. These accumulated particles also prevent the motion of grain boundaries. Recrystallization is not

favorable process because it reduces the number of dislocation density which is very important as precipitation sites for fine Pd particles. Solute Pd atoms create solute drag by the following mechanism: solute atoms segregate on the grain boundaries, leading to the decrease of the grain boundary energy, by reducing the disorder and internal energy of the boundaries. This in return, makes the boundaries with less energy to move away, thus decreasing their mobility compared to the pure material. Several authors proposed control of this precipitation process as a mean to control degradation (Moszner et al. 2011; Schinhammer et al. 2012).

Schinhammer et al. (2013a) also investigated degradation of these new alloys, austenitic Fe–Mn–C–Pd alloy, as compared to martensitic Fe–Mn–Pd alloy (Fe–21Mn–0.7C and Fe–21Mn–0.7C–1Pd in wt%), by using immersion testing and electrochemical measurements and both techniques showed that these alloys have higher degradation rate than pure iron. Electrochemical impedance spectroscopy (EIS) here also proved to be sensitive enough to observe changes in degradation rate because polarization resistance was fully correlated to corrosion tendency. But this method also provided insights into the degradation products. Schinhammer et al. (2013a) reported that degradation rate decreases over time, due to deposited layers of degradation products on the alloy surface. Immersion tests (28 days) showed that degradation of the alloy is not prevented completely by the forming of these deposits, that is, it is not stopped, but the initially high rate of degradation abruptly decreases during the period of approximately 2–7 days, after which it has slight further decrease but it can be observed as rather constant for a period of approximately 14–28 days. They tried different setups for in vitro testing, to simulate in vivo conditions and concluded that in order to properly evaluate corrosion mechanisms some flow of the fluid that surround the material, should be applied since it exhibited the important influence. Namely, corrosion was enhanced for the setup with fluid flow compared to static immersion tests. This was attributed to the fact that surrounding fluid takes away corrosion degradation product, to some extent, from the material surface, thus preventing its deposition and protective influence. They also investigated and found satisfying cytocompatibility of these alloys (Schinhammer et al. 2013b). They also studied the influence of these alloying elements (Fe, Mn, Pd) on the cell viability and metabolism and showed that Mn has limited cytocompatibility. But they also showed that pH value of surrounding environment has a detrimental role in cell responses to these elements, due to promotion of different chemical reactions of those elements depending on the solution pH (Schinhammer et al. 2013b).

The latest patent, in 2014, filed by Biotronik Ag, Germany proposed the following composition for the biodegradable iron stent, aimed for vascular stents: 88–99.8% iron, 0.1–7% chromium, 0–3.5% nickel, and less than 5% other metals (Mn, Co, Cu, Cd, Sn/Pb, Th, Zr, Ag, Au, Pd, Pt, Rh, Si, Ca, Li, Al, Zn, S), and, optionally, up to 7% carbon, as given in patent description: “Metallic implant which is degradable in vivo”, US 8771751 B2. They claim that satisfactory complete degradation time of iron alloy is achieved, while the device completely supports the vessel through healing process. They also divide it into four types of materials in relation to complete degradation time depending on the device thickness, as:

(1) 5 days to 6 months; (2) 2–8 weeks; (3) 6 months to 10 years and (4) 1–5 years. However, no detailed study of any kind can be found in the literature related to this patent claims.

Different alloying elements and their influence on corrosion resistance, and accordingly, on the degradation behavior has been studied by different authors. Zhang et al. (2004) investigated electrochemical properties of Fe–Mn–Al alloys and showed that Al, Cr and Fe form oxides on the material surface, thus decreasing corrosion or degradation, when in environment which promote oxides and hydroxides formation, while Mn oxides has opposite effect—promote corrosion by preventing passivation. Also, the exact composition, formation, cracking and degradation of possible corrosion protective films on the surface of these new alloys, especially in vivo is still under investigations. This research was not focused on biomedical applications, but findings are important. Another study related to the influence of alloying elements on pure iron, to form binary Fe–X alloys, was conducted by Liu and Zheng (2011). They tried common elements used for alloying of pure iron in industry (C, Mn, Si, P, S, B, Cr, Ni, Pb, Mo, Al, Ti, Cu, Co, V and W), with a special focus to those elements proven to increase iron corrosion, such as: Cr, Ni, Mo, Cu, Ti, V and Si. They investigated mechanical and electrochemical properties and cytocompatibility (cell toxicity and adhesion). For all combinations, mechanical properties were improved, but only in case of Fe–Mn alloy, corrosion rate was increased compared to pure iron, as shown by other previously listed research. But they also recommended further research with Co, W, C and S as alloying elements with higher content in multi-component alloys, because it seems they significantly improved mechanical properties, especially ultimate strength and elongation were higher and those alloys also showed good biocompatibility, even with the fact that they did not increase corrosion rate of the material. Yield strength was also higher for Co, W, C and S binary Fe–X alloys, what is important property at the time of the stenting procedure, or setup of the stent to the initial position to avoid breakage of thin struts, because the procedure involves dilatation of stent.

Microstructural properties such as dislocation of grain boundaries behavior are significant for degradation. Several authors studied those phenomena in iron alloys, but there are also numerous papers related to physics of grain boundaries in iron or iron alloys, majority of which are not focused on degradable iron stents but those findings can provide important insights into further development of iron materials specifically aimed for medical implants. For example, Fe^{3+} ions are present in the human organism and as such they represent influential factor on the implant material behavior. There is the difference between pure Fe and Fe–1.4Mn related to the nature of dislocation when irradiated with Fe^{3+} ions (Yabuuchi et al. 2013). Their results indicated that, as the consequence of this irradiation, inhomogeneous dislocation loops formed mainly around residual dislocation in pure Fe and their mobility was focused to those areas, while in case of Fe–1.4Mn alloy, homogenous numerous dislocation loops formed throughout the whole material matrix and they were less mobile (Yabuuchi et al. 2013). This difference is attributed to the influence of Mn as alloying element, which suppressed mobility of dislocations. Material defects such as dislocations and voids are initiation sites for the

development of corrosion mechanisms and research related to the interactions of alloying elements with Fe matrix and with defects should indirectly point to the underlining corrosion mechanisms. Also, the presence of numerous dislocation loops in Fe–Mn binary alloy resulted in significant hardening of this alloy compared to pure iron (Yabuuchi et al. 2013).

Alloying elements in iron alloys can have yet another influence related to the effect of segregation to grain boundaries of the matrix, as well as influencing the concentration of other alloying element. Grain boundary segregation refers to the process of increasing the concentration of one element (segregant) at the grain boundaries or dislocation sites. For example, Mn segregates on the grain boundaries and its presence in alloy is favorable for shifting the equilibrium to the segregation of P element as well. Mn further promotes carbide forming, decrease dissolved C concentration, by decreasing its solubility and activity and Mn presence is also favorable for temper embrittlement, due to Mn segregation and possibility to provoke intergranular fracture (Yang et al. 2001; Grabke et al. 1987). Alloying elements can add significant property, such as shape memory feature in case of Si element addition to form Fe30Mn6Si alloy (Liu et al. 2010). Liu et al. (2010) investigated the influence of Si addition to Fe–Mn alloy from aspects of microstructure, corrosion behaviour cytotoxicity and hemolysis (damage of red blood cells). They obtained increased corrosion rate with no harmful effects on cells, as well as possibility for shape memory effect, making this material also the promising candidate for stent applications.

2.3.2 Composites

Extensive work has been devoted to the development of various Fe-based composites, such as Fe–Pd and Fe–Pt composites (Huang et al. 2014), metal foam—bone cement composites (Glorius et al. 2011), and iron-bioceramic composites (Ulum et al. 2014a, b). Huang et al. (2014) used spark plasma sintering to produce Fe-5 wt%Pd and Fe-5 wt%Pt composites and obtained smaller size grains compared to as-cast pure iron microstructure and better mechanical characteristics. Both Pd and Pt elements increased corrosion rate by approximately 2.73 times in comparison with pure iron, especially Pt addition enhanced corrosion. Hemolysis was lower than tolerated level of 5% for both composites. Another research group investigated the effects of adding bioactive bioceramics to pure iron as a mean to increase and control the corrosion rate (Ulum et al. 2014a, b, c). They fabricated three types of iron-bioceramic composites by using each of the following bioceramics mixed with iron powder and followed by sintering: hydroxyapatite (HA), tricalcium phosphate (TCP) and biphasic calcium phosphate (BCP), and obtained slight increase of corrosion rate but they nevertheless concluded that these materials are possible good candidates for degradable implants due to good viability and enhanced proliferation of cells. Another ceramic tested as possible component for iron-ceramic composites was iron-beta-tricalcium phosphate composites, Fe/ß-TCP,

fabricated by powder injection molding (PIM) with different amounts of ß-TCP (0–50 vol.%) and investigated as candidates for bone scaffolds (Reindl et al. 2014). Samples with 40 vol.% ß-TCP exhibited rate of degradation 28% higher than in case of pure iron. At the same time, Fe-40% ß-TCP kept compressive yield strength at nearly the same level, while pure iron exhibited strength decrease for almost 50% under the same immersion conditions. The conclusion of this research is that good calcium phosphate solubility is the main reason for such behaviour and it should be further studied as a way to achieve desired degradation time of the material for bone substitutes. Fe-40% ß-TCP composite achieved degradation rate of 196 μm/year in in vitro conditions, which is a satisfying timeframe as recommended by Reindl et al. (2014) for the bone remodeling process. Another study of this research group indicated that Fe-5 wt% HA composite also has very good osseointegration properties, also proved by Ulum et al. (2014c).

Gold (Au) and silver (Ag) were also studied as addition to pure iron to form the iron-based composites Fe–Au and Fe–Ag (Huang et al. 2015). Corrosion test showed increased rates in comparison to pure iron, while all other important properties were satisfying, such as hemolysis, cytotoxicity and mechanical properties which was improved. They used powder metallurgy for fabrication of samples with different amount of Au and Ag in Fe: 2, 5 and 10 wt%. The most satisfying results were obtained with 5 wt% addition of Ag or Au.

Cheng et al. (2014) investigated Fe–Fe_2O_3 composites, by varying weight percents of Fe_2O_3 addition (2, 5, 10 and 50 wt%) and by using powder metallurgy production route and obtained increased corrosion rate in comparison to the pure iron. They showed that composite microstructure exhibited more grain boundaries indicating more sites for corrosion attacks. The final composite structure consisted of α-Fe and FeO instead of Fe_2O_3. The best composite option from aspects of corrosion rate was Fe–5Fe_2O_3. Cytotoxicity was not observed and hemocompatibility was good, with better ultimate compressive strength and yield strength than pure Fe (Cheng et al. 2014).

Two composites of pure iron and tungsten (W) and carbon nanotubes (CNT), produced by powder metallurgy (spark plasma sintering) were investigated in order to increase degradation rate (Cheng and Zheng 2013). Different amounts of addition elements were tested: 2 and 5 wt% of W and 0.5 and 1 wt% of CNT. All samples exhibited high density. It was shown that both elements decreased grain size of the iron in comparison with pure iron samples. According to electrochemical measurements, both second phases produced faster degradation of the composites, whereas the addition of CNT was more beneficial, but immersion tests indicated no significant difference from pure iron. As expected, both additions produced increase of compressive strength, especially in case of CNT. Biocompatibility properties were good, even in case of CNT addition. Dominant corrosion mechanism for both composites was explained by the galvanic corrosion occurring between the iron matrix and W or CNT, rather than the galvanic corrosion between grain boundaries and iron matrix. They also confirmed that smaller grain size of pure iron is beneficial for faster degradation, what is shown in other research results as well (Moravej et al. 2010a, b).

Apart from testing of different combinations of constituting elements in iron alloys/composites, the processing parameters during material production also have large influence on the final material properties. Schaffer et al. (2012) showed that cold drawing can be used to produce fine microstructure of iron-based wires and along with the proposed stent design made of braided wires, some novel composites can be considered as good material candidates for resorbable endovascular stents. They developed custom fabrication process, by using wire-drawing of pure Fe, Fe35Mn alloy, and two composites. Two composite structures were made by filling the core of pure iron wire and Fe35Mn alloy wire (12.7 mm rods and 7 mm hollow rod cores) with magnesium or ZM21 magnesium alloy, followed by cold drawing of such composite wires to the final diameter of 127 μm (Schaffer et al. 2012). This produced iron-magnesium drawn-filled tube (DFT) composite and Fe35Mn–magnesium DFT composite. Also, pure iron wires were fabricated with different cold work levels (50, 90 and 99% reduction of wire area), resulting in fiber texture and introducing axial strain. Fe35Mn–25 Mg wires showed excellent toughness and similar fatigue strength as cold-drawn 316 stainless steel. However, fatigue life significantly decreased in saline environment.

2.3.3 Porosity

Significant direction of research on the increase and control of corrosion rate is the introduction of controlled porosity, by fabrication of porous metals or metal foams (Ryan et al. 2006). Metal foams are the wide topic of investigations today and many results associated with different aspects of the material development could potentially be used to develop iron-based metal foams. Porous structure has lower Young's modulus than the dense one, and surface area is significantly increased, meaning significant promotion of the corrosion process related mainly to the material surface. For bone tissue engineered scaffolds, porosity enables another very important feature—the possibility of surrounding cells to proliferate through the pores and around the metal matrix, thus making the excellent fixation of the implant. Another significant advantage of porous structures is the closer matching of the stiffness with that of the natural bone structure. On the contrary, in case of stent applications, cell proliferation and migration of smooth muscle cells is observed as negative since it is one of the risk factors of in-stent restenosis. Accordingly, porous structures are not considered for stent applications.

Porosity of pure iron and iron based alloys with open cell structure, aimed at bone scaffolds has been subject of study for many years of the research group of Dr. Peter Quadbeck, from different aspects such as optimization of the production and processing parameters, size, distribution and interconnection of pores, influence of the micro to macro level of porosity, uniformity, as well as different constituting material elements (alloys, composites or pure iron) and influence on the biocompatibility and mechanical properties (Quadbeck et al. 2010; Stephani et al. 2010; Glorius et al. 2011; Wegener et al. 2011). Their research is mainly aimed at bone substitutes. They investigated the possibilities to make porous Fe-based alloys with

alloying elements recognised as suitable for degradable medical materials: C, P, B, Si, Ag, by using powder metallurgy and variation of alloying elements amounts (Quadbeck et al. 2010). Along with research aimed at obtaining the optimal material microstructure related to increase of the corrosion rate, while preserving or improving necessary mechanical properties, series of animal probes have been conducted in order to investigate different biocompatibility properties (Wegener et al. 2011).

Quadbeck et al. (2010) recommended phosphorous as one good possible alloying element for porous iron structure, as observed in Fe0.6P alloy, due to its beneficial influence on improvement of the mechanical strength (compressive and yield strength). Additionally, they proved that phosphorous did not decreased corrosion rate of Fe0.6P alloy in comparison with pure iron metal foam, as expected since P usually has that influence which of course is not wanted in this case. This research group also investigated powder metallurgy to obtain iron foam of predetermined shape and size of porosity (Stephani et al. 2010) and then introduced coating to the porous structure in the form of degradable bone cement, brushite ($CaHPO_4 \cdot 2H_2O$), in order to minimize initial corrosion. Unlike desired enhanced corrosion over time, initially high corrosion, right after the implantation is not good because it can provoke unwanted infections by sudden increased release of iron ions during this initial period. They also obtained promising results for completely filled porous pure iron samples with mineral bone cement, magnesium calcium phosphate cement (MgCPC) to obtain composite structure for bone tissue scaffolds. These composites showed excellent biocompatibility. Bone cement is very suitable material for incorporation of various particles due to its porous nature that can be adjusted by changes of the processing parameters (Zivic et al. 2012).

One of the proposed ways to control the degradation of porous iron is to infiltrate the iron with poly(L-lactic-co-glycolic acid)—PLGA (Yusop et al. 2015). This research showed that PLGA dominated degradation process, while preserving mechanical strength of the iron-based material. The authors elaborated that PLGA hydrolysis oppose the formation of passive layers made of iron oxides and phosphate on the surface of the iron alloy implant. Once formed, such passive layers significantly decrease further degradation. PLGA hydrolysis produces local acidity in vicinity of the surface, thus dissolving these passive layers and provoking further iron degradation and the complete PLGA degradation takes approximately 1–2 months. This is the main reason of good results obtained by filling the porous iron with PLGA, thus fabricating composite structure that promise successful degradation control of the material. The iron-PLGA composite showed increased mechanical strength in comparison with porous iron, faster degradation and cell viability was not affected by the rapid PLGA degradation process (Yusop et al. 2015).

Traditionally, for a long time now, coatings and thin films are well recognised way to control and tailor surface characteristics of bulk/porous materials and are also widely applied as means to control the cell adhesion, or bone ingrowth for tissue engineered scaffolds or medical implants and for the controlled drug delivery systems. However, only a few existing studies are related to the coating of iron or

iron-based alloys for degradable implants. There were some attempts to increase Fe corrosion rate by applying coatings or thin films on pure iron (Cheng et al. 2015; Wu et al. 2013; Zhu et al. 2009). Cheng et al. (2015) investigated micro-patterned gold disc films deposited by sputtering and they obtained 4 times increase of the corrosion rate, as well as 3 times deeper corrosion affect on pure iron. Investigations related to deposition of thin Fe–O films, expectedly showed that it improved corrosion resistance, rather than increase corrosion rate (Zhu et al. 2009). But the focus of their study was to prevent premature degradation of pure iron stents during the initial postoperative period. Investigation of degradation behavior of bone scaffolds made of Fe-based foams with different coatings (hydroxyapatite and other calcium phosphates) showed that coatings can be used for controlling the corrosion rate (Farack et al. 2011). But further studies will show if and how these combinations can be used for bone substitutes. PLGA coating was deposited on the pure iron aimed for stents, in order to investigate the possibility to utilize the effect of externally introduced hydrogen evolution, on corrosion behaviour (Wu et al. 2013). They obtained increased corrosion rate and attributed it to the increased release of H^+ from PLGA. One of the recent works showed that iron coatings of bioceramic HAp or HAp with addition of Mn could improve biocompatibility and also influence the corrosion behaviour (Orinakova et al. 2015).

There are also interesting attempts to make joint structure, wherein the whole implant consists of one part made of non-degradable materials and the other part of degradable material. Nasution et al. (2015) investigated such combination of 316L stainless steel joined by friction welding with degradable pure iron, aimed at bone implants such as rods for fractured bones.

2.3.4 Production Technologies

Microstructural modifications, different fabrication and processing techniques effects originating from the material or product fabrication have been investigated, such as heat treatments, combination of processing techniques, modifications of existing traditional powder metallurgy routes and other. It is well known that different processing parameters (e.g. temperature or time regimes, pressure or environment, etc.) during manufacturing of the material, can produce ductile or brittle structure, coarse or fine grain structure, different microstructure or type of crystal lattice and/or crystal orientations, dislocation densities or porosity. Small variations in processing parameters can produce significant changes in material structure leading to completely different material behaviour. For example, one type of crystal lattice results in magnetic properties and other in anti-ferromagnetic ones. Grain size with alloy/composite microstructure is well recognised as the very important parameter related to the mechanical properties, especially strength, as well as the corrosion behaviour of the material. Usually, nano and micro sizes of the grains are associated with higher strength and higher corrosion rate, due to the larger amount of grain boundaries recognised as sites for initiation and development of corrosion chemistry. On the other side, higher strength and hardness are often related to the

decrease of ductility up to the making the material brittle, which is not suited for some applications, such as stents where appropriate ductility is very important.

There are several production technologies that can be efficiently used for fabrication of iron-based materials and further implants, but all of them are still under investigations to some extent in order to result in desired final properties (Francis et al. 2015). The main focus of investigations related to the production routes are related to the increase of corrosion rate, while providing sufficient mechanical support and biocompatibility. Standard process of making an alloy is casting and it is usually the reference sample for studies (Liu and Zheng 2011). Furnace melting of alloying elements in different percentages, under different environment and pressure, is followed by cooling in some type of moulds and alloy is casted into ingots. Ingot needs further processing, such as hot forging or cutting, since they are usually of large sizes (e.g. 25 kg), and after that yet additional treatments are also done (e.g. solution treatments, cold/hot rolling, annealing, or surface treatments—polishing, etc.) and each of these influences the microstructure and material characteristics. Even the final processing to the desired product, such as laser cutting, as a standard route for fabrication of stents from tubes, has different influences on the material properties (Hermawan and Mantovani 2013). For instance, some recent works indicated that effect of the cold work during the stenting procedure also has the influence on the behaviour of the material and that degradation behaviour of FeMn alloy was different when in the form of the stent than the one observed for the flat samples (Sing et al. 2015).

Schinhammer et al. (2010) tried different heat treatments to see their effects on the material microstructure and electrochemical and mechanical behaviour. They showed that appropriately selected heat treatment can produce desired combinations of strength and ductility, and adjust phase content within the alloy. Schaffer et al. (2012) studied the use of cold drawing technology for composite wires manufacturing and microstructural modifications beneficial for corrosion rate increase. They showed that fine microstructure can be obtained by cold-drawing producing high strength and enhanced elasticity of composite wires for four different composite structures comprising Fe, Mn, Mg, and Zn in different amounts. Another approach to increase corrosion by using processing technologies is shown by Feng et al. (2013). They used vacuum plasma nitriding of pure iron tubes aimed for stent production, in order to incorporate fine particles of nitrogen into the diffusion layers of iron. Fine particles of nitrogen together with iron promoted micro galvanic corrosion.

Hot or cold plastic deformation has a significant influence on the final material microstructure, namely on grain size, dislocation density and crystal orientations and it is assumed that degradation properties can be consequently adjusted by utilizing these technologies. Nie et al. (2010) used severe plastic deformation to produce nanocrystalline pure iron, namely equal channel angular pressure (ECAP) method and obtained increased corrosion resistance. However, very recent work of Obayi et al. (2015) showed no significant difference between as-rolled sheet of ingot iron and cold-rolled sheets followed by annealing, except for some slight increase of corrosion rate in case of cross rolled samples with higher annealing

temperature (900 °C). But it also indicated that thermo-mechanical processing can adjust final corrosion properties of iron.

Suitable technology for production of Fe-based films is electroforming (Moravej et al. 2010a, b). Electroforming uses moulds or patterns upon which the metal is deposited and after its separation from the mould, elements of predefined size and shape can be obtained. Also, electroforming produces the very fine polycrystalline microstructure with small grains—smaller than with other available production technologies. Iron is one of the metals very suitable for this technology. Moravej et al. (2010a, b, 2011) investigated electroforming as means to modify corrosion rate of iron, due to decrease of the grain sizes and they obtained good results. They obtained material with fine grains, good mechanical properties and biocompatibility and achieved increased corrosion in comparison with cast iron, from 0.14 to 0.25 mm/year degradation.

Powder metallurgy is the powerful technology for controlling material properties, especially because it can produce very pure materials almost without inclusions and impurities except those predefined by the material design. Fabrication of dense and porous iron alloys, by powder metallurgy, aimed at biodegradable orthopedic implants, has been studied from various aspects and showed promising possibilities to tailor corrosion properties, while maintaining other necessary properties. Hermawan et al. (2008b, 2010a, b) obtained corrosion rate of 0.52 mm/year for Fe–Mn alloys, fabricated by powder sintering, aimed for stents. Huang et al. (2014) used plasma sintering for production of iron composites with Pd and Pt and obtained smaller grains and increased corrosion than as cast pure iron. But perhaps the most promising production route is related to the fabrication of porous structures by using powder metallurgy, for bone implants (Quadbeck et al. 2010); Wegener et al. 2011). They fabricated different iron based alloys, with various additions of C, P, B, Si, Ag, in order to preserve mechanical properties and influence corrosion. Their open cell porous material structures exhibited approximate 10 MPa compressive strength and increased corrosion rate for phosphorous (P) addition, as suitable for bone scaffolds. Čapek and Vojtěch (2014) obtained 34–51 vol.% of pure iron porosity by using powder metallurgy with space holder method, with ammonium bicarbonate powder as spacer material. Orinak et al. (2014) used powder metallurgy route with replication method to produce open cell porous iron, and two composites, containing 0.5 wt% of Mg and CNT particles, aimed for bone implants. Apart from powder metallurgy studied in details by Quadbeck et al. (2010), porous iron structure can be efficiently produced by introduction of nitrogen under high pressure into the iron melt, during casting (Hyun et al. 2004). Some novel biomimetic approaches has been tried also, such as using wood template to make hierarchical porous iron oxide (Liu et al. 2005; Bantsis et al. 2012).

Recent works have started to study fabrication technologies of porous structures as combination of powder metallurgy concepts and novel additive manufacturing (AM), rapid prototyping or 3D printing technologies (Andani et al. 2014; Chou et al. 2013; Yusop et al. 2012; Hutmacher et al. 2004; Ryan et al. 2006, 2008). These technologies can fabricate predefined shapes and geometries with numerous

combinations and this is very important advantage as compared to traditional production of porous structures. However, 3D printing has not been well understood from aspects of different influences such as particle size, flowability, wettability and roughness on the final material properties (Butscher et al. 2011, 2012). Also, materials that can be used in these technologies are still limited to manufacturers' offer, mainly comprising commercial low cost plastics, a few standard ceramics and very few metals (e.g. Ti alloys). Accordingly, custom made materials are investigated but the versatility of complex porous structures that can be made and the possibility of endless combinations in shapes and geometries justify this direction of research, also for iron based scaffolds (Chou et al. 2013). Very important is also the possibility of tailored geometries which, in return, can provide desired stiffness to the scaffold, in order to match to the adjacent tissue.

Additive manufacturing uses layer-by-layer fabrication of the solid part, making it suitable for custom design of shape and size of porous structures, rendering an especially favorable technology for investigation of tissue engineering scaffolds, both materials and structures (Hutmacher et al. 2004). These technologies reduced the time of fabrication of elements for the post-processing part of activities which cannot be avoided with traditional production technologies and this is especially important for custom made complex shapes where post-processing is often impossible. Direct metal manufacturing additive technologies such as selective laser melting (SLM) has been used for fabrication of different elements, but until very recent time it has not been used for degradable iron materials. In SLM, metal powder is prepared and mixed with alloying elements and then locally melted, within very small physical zones, by using laser beam, what should lead to rather uniform bulk structure. Niendorf et al. (2015) investigated SLM technology for fabrication of Fe–22Mn–0.6C alloy with silver (Ag) as additional alloying element in different weight percentages. They concluded that AM technologies can efficiently serve as the enabling technology to add alloying elements which are otherwise hard to mix with iron, such as Ag. Niendorf et al. (2015) added silver in several weight percentages (1, 2 and 5 wt% Ag), by mixing it into the powder of high-manganese TWIP steel (22 wt% Mn and 0.6 wt% C), in order to influence the electrochemical properties of the alloy. TWIP steels are well known for their excellent combination of strength and ductility. Particles of silver uniformly distributed within the material served as cathodic sites which promoted micro-galvanic corrosion and they obtained increase of degradation rate (2.3 mg/cm^2 per day, for 5 wt% Ag addition), while simultaneously not affecting the mechanical properties. But, even with no effect shown in this study, silver particles should be seen as possible stress initiation sites due to their inability to be dissolved in iron. Mean particle size for SLM processing was around 40 μm. However, they did not investigate biocompatibility properties of this new material and it is yet to be shown how the silver release during degradation affects the cells.

Among all existing additive manufacturing technologies, 3D printing currently represents the most cost-efficient technology, due to the wide availability of devices and drastic decrease of machine prices if compared to just a few years ago. Nowadays, focus is on novel materials to use it with 3D printing. 3D printing of

Fe–30Mn powder into the compact alloy has been tried by Chou et al. (2013). They showed that this alloy has a potential to serve as a biodegradable bone scaffold material, for craniofacial applications. Also, 3D printing can be used to produce moulds made of material that can be efficiently removed in the further processing of the materials, leaving uniform porous metal structure with predefined pore sizes and distribution (Ryan et al. 2008; Melican et al. 2001; Curodeau et al. 2000). Curodeau et al. (2000) and Melican et al. (2001) used ceramic powder with appropriate binder (alumina with silica binder) to produce ceramic moulds with controlled surface porosity, aimed for fabrication of metal implant (Co–Cr alloy) with predefined porosity (around 38% of porosity and 271 μm size of the pores). 3D printing was used here to generate the mould for metal casting and at the same time to provide controlled texturing of the implant surface, otherwise very complex and costly processing for metal alloys. Approximate resolution of 3D printing was down to 175 m and this technology can produce pores in the range of 200–1000 m. Also, additive manufacturing has been investigated for fabrication of scaffolds incorporating nanoparticles of some tailored property, such as nanocomposites magnetic scaffolds comprising FeHA (iron-doped hydroxyapatite) nanoparticles (Russo et al. 2013).

2.3.5 Biocompatibility Properties

The basic precondition and the first obligatory property of any material used for medical devices in general is good biocompatibility. Biocompatibility can refer to wide list of material properties depending on the application, but essentially good biocompatibility means that the material is compatible with the surrounding living tissue and makes no harmful effects on it. There is no simple way to test the biocompatibility, since it comprises not only the material property but also the responses of the living tissue in contact, whereas the immune system responses together with the influence on cells genetic behaviour makes it even more complicated for comprehensive investigations. Test methods to determine immediate toxic effect of some material on the surrounding cells are well established, but the influence of the artificial material on the host response from aspects of genetic and immune effects within the longer time is very complex and not so straightforward. Also, in vitro methods to test cytotoxicity of novel degradable metal materials are still under development, from aspects of reliable ways of contacts between metal particles and cells, environment influence, flow or diffusion, immersion media, cell types and control assay types and other influential factors. Another issue surrounding the development of materials for medical implants is the common existing difference between in vitro and in vivo tests, resulting in necessity to test all material candidates under in vivo conditions. In case of degradable metal materials, for both alloys and composites, porosity as imminent property introduces yet another issue related to biocompatibility studies. Degradation involves dynamic changes of present elements in contact with living tissue, from different aspects, such as size of particles, chemical composition, particles flow, etc. If only size of foreign particles in contact

with cells is observed, it is clear that nanoparticles has completely different (and yet largely unknown) effect on cells in comparison to macro-size particles. At present time, it is difficult to find data even on simple cytotoxicity study of degradable metals for cardiovascular or osteosynthesis applications. Existing data and research papers focused on these novel materials are very limited and further studies are of the utmost importance. If one bears in mind that new classes of materials have been developed as a combinations of two or more materials, such as in case of previously listed alloys, composites or coatings applied on the surface of alloys/composites, it is clear that biocompatibility studies here usually are not related only to one material at the time, what makes it even more complex.

Starting from the Fe–35Mn alloy, in vitro tests of cell viability showed no significant toxic effects and low inhibition on metabolic activity, mainly originating from Mn (Hermawan et al. 2010b). Following the procedure established by Hänzi et al. (2010) for Mg-based degradable alloys, Schinhammer et al. (2013b) performed in vitro cytotoxicity tests of two biodegradable Fe-based alloys: Fe–21Mn–0.7C and Fe–21Mn–0.7C–1Pd (in wt%). They found somewhat limited cytocompatibility of Mn, which is in accordance with Hermawan et al. (2010b), and also concluded that pH value of the solution has significant influence on the results. Also, Hermawan et al. (2010b) demonstrated that pure Mn has more detrimental effect on cells' metabolic activity than Mn as alloying element within Fe–Mn alloy powder.

Although iron is a constituent element of the human body, it can also produce negative effects on cells, depending on its form. In the study by Zhang et al. (2010), in vitro testing of the pure iron showed satisfying hemolysis, very good adhesion of platelets and anti-clotting properties, but the fabrication technology or microstructural properties were not presented. They tested hemolysis (destruction of red blood cells), dynamic clotting time, prothrombin and plasma recalcification time and platelet adhesion, by using animal healthy blood. However, ions of iron exhibited cell toxicity when ions concentration was above some critical level, what was expected (Zhang et al. 2010). Cell viability studies realised by Moravej et al. (2010b) showed that small grains of electroformed pure iron did not influence inhibition of cells activity, but nevertheless inhibited cell proliferation, thus being very good for stent applications. Prevention of cell proliferation is important for stent materials because it is one of the mechanisms to prevent in-stent restenosis, being one of the serious complications in post-surgical period. It should be noted that negative effects of cell proliferation on in-stent restenosis is related to the vascular smooth muscle cells, while enhanced endothelialization is beneficial and related to the fibroblast cells proliferation. It is obvious that biocompatibility should consider different complex biological and biochemical relations. Another study by Nie et al. (2010) was realised with nanocrystalline pure iron and showed that grain size has influence on the biocompatibility. Nanocrystalline iron enhanced cells proliferation for fibroblast cells and promoted formation of endothelial cells, both of these cell activities being beneficial for stent applications. At the same time they obtained suppression of platelet adhesion and inhibited vascular smooth muscle cells viability. This was excellent combination for stent applications, from aspect of

in-restenosis prevention. Another term used in investigations of biocompatibility is "hemocompatibility", whereas it might comprise adhesion of platelets, hemolysis, platelet activation, fibrin formation, contact activation etc. It is important to investigate specific biocompatibility aspects which are important for specific end application. For example, Zhu et al. (2009), tested Fe–O coating on pure iron for adhesion of platelets, thrombin and prothrombin times, in order to evaluate novel thin coatings for stent applications from aspects of cell adhesion and proliferation.

Liu and Zheng (2011) investigated the effects of different alloying elements of iron (Mn, Al, Co, W, B, S, C and Sn) on biocompatibility, under in vitro conditions. Their results showed that same element can be detrimental on one type of cells and beneficial for other ones. Cell viability for all these alloying elements was lower for L929 cell line (murine fibroblast cells), and higher for ECV304 cell line (human umbilical vein endothelial cells, HUVECs), excluding Mn element (Liu and Zheng 2011). All alloying elements in these tests had neutral effect on cell viability of vascular smooth muscle cells. They also tested those binary Fe alloys on hemolysis, by using healthy human blood and thrombogenicity (tendency to produce thrombus), by observing platelet adhesion on the surface of samples via SEM microscopy, with satisfying results for all elements. Hemolysis under 5% is considered as tolerable level for application of the material as foreign body. They excluded some elements and recommended C, Co, W, and S as iron alloying elements, based on the obtained mechanical properties since corrosion rate was not significantly changed in any combination of elements (Liu and Zheng 2011).

As mentioned previously, another important issue related to the biocompatibility properties is the effect of the degradation products on the surrounding cells, or their interactions. Namely, dynamic changes of different material properties, very complex and still largely unknown, from many aspects such as compositions or concentrations of degradation products, uniformity or aggregation on specific sites and their evolution over time, and underlining and governing corrosion mechanisms, clearly result in complex interactions between cells and these particles. It is probable that not only particle size degradation products appear, but also larger detached pieces of implant material. Mueller et al. (2006) investigated these interactions in the case of pure iron degradable stent in contact with smooth muscle cells. The main byproducts of iron degradation due to corrosion were iron ions. As confirmed by Zhang et al. (2010), iron ions are harmful for cells, above some critical level. Investigations by Mueller et al. (2006) reached similar conclusions. They showed that cell growth was decreased in the presence of iron ions and they also influenced lowering of mRNA necessary for cell proliferation. Accordingly, it can be supposed that cell proliferation is decreased in the presence of iron ions, but this cannot be definitive conclusion, based only on two studies in rather limited setup conditions.

Final testing of all medical devices and especially implants that goes into the body are in vivo tests. They definitely show the suitability of the material, based on many different tissue responses properties, such as appearance of increased or prolonged tissue inflammation after implantation, stent restenosis, or other. In vivo tests with stents made of pure iron showed excellent results with no evident toxic effects of any serious type (Peuster et al. 2001, 2006; Waksman et al. 2008). The

majority of proposed material solutions for iron-based degradable implants were still not tested in vivo because they also lack comprehensive in vitro studies as a necessary precondition to in vivo analysis. But even in vivo tests are subject to different approaches, because there is no generally accepted method and can show ambiguity, especially if long term consequences are considered as genetic responses or other issues that are not addressed yet (Bartosch et al. 2014).

2.3.6 Magnetic Properties

Magnetic properties of iron-based materials for implants are very important because they define the ability of the material to undergo medical diagnostic tools, such as MRI (Magnetic Resonance Imaging), X-ray scans, computed tomography (CT) imaging or other. Ferromagnetic materials can provoke serious harmful consequences, such as physically dislocating themselves, under the influence of the external magnetic or electric field (e.g. originating from MRI). Thus ferromagnetic alloys are not suitable for medical implants. In general, MRI compatible materials need to be antiferromagnetic, paramagnetic or diamagnetic. In the case of iron, these are usually related to austenite structure or gamma-phase iron, γ-Fe, with fcc (face centered cubic) crystal structure, being the non-magnetic allotrope of iron. As elaborated in previous part of this chapter, different phases can co-exist together in one alloy system, and their presence and content may depend on the content of alloying elements (e.g. Mn) or temperature regime (or pressure). The differences between specific iron phases can be very small and phase diagrams of different binary Fe–Mn or tertiary Fe–Mn–C alloys which have been studied are used as valuable information on Fe-based material compositions (Djurovic et al. 2011; Pepperhoff and Acet 2001; Huang 1989; Lee and Lee 1989; Huang 1987). Transition between structural states occurs rapidly at the phase boundaries, complemented by the abrupt changes also in magnetic properties. Accordingly, both structural phase diagrams and magnetic domains should be taken into account since they exhibit strong interrelations. One existing paradigm is that iron magnetism is usually perceived as well understood, whereas the appearance of these novel materials clearly showed that magnetism of iron still needs clarifications. Many aspects of iron magnetic properties are still under debate or remain unknown, especially phase transformations that governs the magnetic state of the final structure (Pepperhoff and Acet 2001).

Previously described Fe–35Mn alloy has been tested for magnetic properties and it is antiferromagnetic, even after plastic deformation (Hermawan et al. 2008b, 2010a). Phase transformation can occur due to thermomechanical processing (e.g. sintering, cold rolling, etc.) as shown by Hermawan et al. (2010a). Very detailed phase diagram of the binary Fe–Mn alloy is given in Kubaschewski (1982). This implies that finally obtained material structure should be tested on magnetic properties as well, since different iron phases result in different magnetic properties, from ferromagnetic to antiferromagnetic ones. They also proved that Mn content greatly affects these transformations, as well as presence of porosity, with lower

sensitivity to these changes along the increase of Mn content. This is in accordance with Ishikawa and Endoh (1968) who investigated magnetic properties of γ-FeMn alloys and concluded that Mn concentration has significant influence because its increase further increases the Néel temperature, or antiferromagnetic ordering temperature, T_N. Their recommendation is to avoid severe local deformation (e.g. repeated cold rolling), or processing that might produce dual phases on specific material sites, especially for stent applications (Hermawan et al. 2010a). The elevated pressure results in lowering of the temperature of the γ-α equilibrium, and accordingly the line of structural α-γ transition will intersect with magnetic α-phase transformation (Blank and Estrin 2014). Also, alloying elements influence the increase or decrease of the phase transformation pressure, whereas Mn decreases this pressure (Blank and Estrin 2014). Another important conclusion from this study is that Fe–Mn alloys containing γ-Fe were more ductile than alloys with presence of both γ-Fe and ε-Fe phases, even though they exhibited higher strength (Hermawan et al. 2010a). It is known from earlier studies that ε-Fe exhibits the highest density if compared to other possible iron phases (Rabinkin 1979). Another study showed that small addition of C to Fe–Mn alloy, can direct formation of mainly austenite phase in the Fe–Mn–C alloy, even with lower Mn content (Harjanto et al. 2013). Transformations from magnetic to non-magnetic phases under any external factors that can induce such changes (pressure or temperature) further provoke changes of the material grain structure and in case of Fe–Mn alloy structure with mixed domains (e.g. paramagnetic and antiferromagnetic) this means very complex behavior which needs further study. For instance, Bogachev et al. (1975) stated that when Fe–Mn alloy exhibits mixed domains (e.g. due to phase transitions), antiferromagnetic domains prevents motion of dislocations thus producing strengthening of the alloy. Gorkunov et al. (2008) investigated deformation stability of the metastable Fe–20Mn steel with two phases: 40% γ + 60% ε structure and sensitive to deformation. They studied the critical level of applied load and different stress states (by applying tension and torsion) which provokes changes of magnetic properties. They correlated the level of shear deformation with changes in magnetic properties during loading and also transitions between phases due to applied deformation. These tests clearly showed that Fe–Mn alloys can change their magnetic properties if subjected to the critical elastoplastic deformation, which, on the other hand, is strongly influenced by the phase distribution, as well as Mn content.

Perhaps the magnetic properties of iron-based degradable materials aimed for stents, or orthopedic solutions are the least investigated of all important properties that these materials should have. Apart from the two previously mentioned studies by Hermawan et al. (2010a) and Harjanto et al. (2013), there are no similar research studies in the literature devoted to newly developed iron-based materials and this aspect of biodegradable materials still needs further attention. However, other studies on magnetic properties might be used as well to point out directions of research. For instance, Long et al. (2008) studied magnetic and structural properties of Fe–Zr nanocrystalline alloy and investigations such as this one, even though they

are not precisely aimed at biodegradable medical materials, might provide insights into fundamental mechanisms underlining the material performance. They produced two alloys, by using powder metallurgy (arc melting): $Fe_{80}Zr_6Si_{14}$ and $Fe_{79}Zr_6Si_{14}Cu_1$ alloys, whereas Cu addition was observed to serve as a nucleation agent during the primary crystallization of DO_3 type structure of Fe_3Si nanocrystals, resulting in a homogenous structure and fine grains (Long et al. 2008). The conclusion of this study is that Cu can effectively serve to control the grain size and homogenous distribution of alloying elements within the nanocrystalline alloys. Another focus of this study was the influence of the grain size and structure type distribution on the low coercivity of this alloy, that is, a resistance of the ferromagnetic material to become demagnetized.

Additionally, the study of magnetic properties can be focused on solutions for drug delivery systems in materials which exhibit magnetic properties, such as bioglass composite made of iron oxide and chitosan-gelatin, with soft magnetic properties for drug delivery systems (Jayalekshmi et al. 2013) or nanocontainers made of biodegradable polymer shell with high content of super-paramagnetic Fe–Mn–O nanoparticles for applications in drug delivery or MRI contrast agents (Bannwarth et al. 2014). Magnetic properties of iron nanoparticles can also be used in bone tissue scaffolds to promote bone regeneration and preliminary studies showed significant possibilities (De Santis et al. 2015; Russo et al. 2013; Tampieri et al. 2012).

2.3.7 Research Direction—Material Degradation

Generally, three main research directions can be distinguished today, as related to Fe-based degradable materials: (1) To control and increase the corrosion rate to be able to consider these materials as biodegradable; (2) To improve mechanical properties according to end applications; for example bone scaffolds require high strength, good ductility in some cases (e.g. stent application) and lower Young's modulus closer to that of the bone; (3) To obtain good biocompatibility for alloys and composites even for those containing possible harmful elements, especially during degradation. Generally, the latter two demands have been already considered for many other biomaterials in use, whereas controlled corrosion is rather newly introduced demand for biodegradable materials. Consequently, the majority of research activities aimed at development of degradable materials are first and foremost related to the understanding and thus controlling of the corrosion processes, since governing mechanisms underlining the process is currently lacking in general. Additionally, it is the fact that until the appearing of the degradable material concept, the main focus of the corrosion research was how to prevent it, that is, how to make corrosion resistant metals. Hence, there are almost none or very limited results related to the behaviour of metal materials during development of the corrosion process over longer time. Three articles which present more detailed explanation of degradation mechanisms of iron-based alloys are those by Schinhammer et al. (2013a), Fagali et al. (2015) and Zhen et al. (2013).

Material degradation introduces very complex dynamic processes from aspects of changes in mechanical and structural properties, material morphology, chemical compositions and biochemical reactions, leakage of elements of the nano/micro sizes into the surrounding tissue that might change from non-toxic to toxic, and many other still unexplained phenomena. Young's modulus would decrease during the transformation from dense to porous material, simultaneously accompanied with the significant increase of the surface area, what theoretically should promote faster corrosion. Also, introduction of porosity inevitable leads to increase of material brittleness. Additionally, changes of external factors such as fluctuation of body fluids chemistry or thermal properties, also influence material changes. On the other hand, degradation and porosity will lower the Young's modulus from relatively high (close to 200 GPa for Fe-based alloys) to eventually approaching that of a bone (30 GPa) what should be beneficial from aspects of biomechanical compatibility between the bone and the implant, but temporary nature of such changes should be also considered. Cell adhesion is also influenced by the rate of porosity generation. Another important research focus is possible interrelations between the governing corrosion mechanisms and other external factors and synergetic influence on material properties. Further studies of mechanical properties during degradation of solid and porous alloys and composites are needed because it is expected that they will also help to provide the answers related to the underlining corrosion mechanisms. Furthermore, it is necessary to predict evolution of properties as the alloy becomes progressively dissolved, what is currently impossible. In terms of magnetic properties, for example, $Fe_{50}Mn_{50}$ is indeed antiferromagnetic but if the alloy becomes non-stoichiometric, it might become ferromagnetic. Accordingly, it is interesting to study if the starting material becomes magnetic as it is being dissolved. It is very important for all metal-based implants to be antiferromagnetic.

Many unresolved questions exists related to the corrosion behaviour, starting from governing corrosion mechanisms, ways in which they could be provoked or mitigated, different synergetic effects such as the influence of produced nano and micro particles within the environment during degradation, and changes they initiate in the material structure or surrounding tissue, interplay between scales of occurring phenomena (e.g. connection between micro/nano and macro mechanical properties), or stability and transitions between alloy phases under temperature/pressure changes, but also under the influence of particles occurring during degradation and their effects, tissue immune response, especially to polymers and many other. For instance, in case of stent application, any particle debris generated by degradation or by natural body processes, such as blood flow or pressure exerted by the blood vessel, can provoke harmful consequences. Such particles detached from the implant can initiate thrombogenesis but the exact reasons for the occurrence of this phenomenon are not well understood. Nano/micro-scale fatigue, friction and wear investigations, along with tribo-corrosion studies should be conducted related to initiation of cracks and their development on both nano and micro levels, influence of roughness changes during self-expanding stent procedures, etc.

Generally, according to the ASM standard, corrosion can be divided into two large groups: uniform and localized, whereas localized corrosion can be observed as macroscopic or microscopic phenomenon. Macroscopic corrosion can occur in several forms: galvanic, erosion-corrosion, crevice, pitting, exfoliation and dealloying, whereas microscopic forms of corrosion can be: intergranular, stress-corrosion cracking and corrosion fatigue (Davis 2000). Very often, several types of corrosion occur simultaneously and it is very difficult to determine exact type and governing mechanisms at micro scale level, especially with many unknown properties in case of new materials. Profound understanding of the underlining behaviour is necessary to gain control over the corrosion process, either to speed it up or to slow it down. Published results indicate that the mechanisms affecting the corrosion behaviour of Mg-based stents in service conditions can be: internal galvanic corrosion; localized corrosion (pitting and filiform); stress corrosion cracking (SCC) and fatigue corrosion.

Another question related to the corrosion testing of novel biomaterials is the applied methodology. Namely, there are numerous methods to test corrosion, from in vitro static immersion test, dynamic electrochemical measurements up to a dynamic in vivo monitoring, which is still under debates from many aspects. Perfectly suitable in vitro test does not exist for many novel materials, as it is the case also for the evaluation methodology of the degradation rate. Zhen et al. (2013) presented a very good review of existing technologies and their suitability for corrosion testing and degradation rate evaluation of Fe-based and Mg-based degradable materials. Pierson et al. (2012) proposed a simple rapid in vivo evaluation of corrosion behaviour for degradable iron- or magnesium-based materials. They implanted iron and magnesium wires, instead of the final stent product, into the abdominal aorta of the rat, in two ways: one tightly embedded in the extracellular matrix and the other loosely put in the aorta with only slight contact with the aorta wall and monitored them for 9 months in total. This in vivo study also pointed out the importance of the immediate live environment on corrosion behaviour because they obtained different results for the matrix contact and for the blood flow contact within aorta. They showed that iron corrosion products were retained in the tissue in some cases which may provoke undesired function of the cells.

Quadbeck et al. (2014) analysed different iron alloying elements (Ag, Mn, S, W, Si) and the microstructural influences (e.g. spot like or continuous silver phases) in order to study the ways to initiate and control certain types of corrosion (galvanic, surface corrosion, pitting or intergranular corrosion). Surface corrosion is desirable mechanism for uniform implant degradation process, but synergetic contribution of each of other corrosion types need to be further studied as means to control corrosion rate of iron alloys (Quadbeck et al. 2014). They concluded that continuous silver phases in Fe0.6P31Ag foam and also small amounts of silicon or tungsten are favorable to increase corrosion rate of pure iron. They proposed systematic activation of specific types of corrosion as a method to control corrosion rate of iron alloys (Quadbeck et al. 2014). Mouzou et al. (2014) compared in vitro degradation of pure Fe and Fe–20Mn–1.2C alloy. The protective $MnCO_3$ deposit on the surface of Fe–20Mn–1.2C alloy resulted in lower degradation rate in modified Hanks'

solution due to insoluble adhesive layer. They also indicated that CO_2 rich atmosphere, HCO_3^-, CO_3^{2-}, Cl^-, Ca^{2+} and phosphate ions are important for corrosion process (Mouzou et al. 2014).

Corrosion process of iron and iron based materials within the body fluids releases Fe ions which may produce harmful effects on the surrounding cells and tissue. Two types of Fe ions are recognised in this process: Fe^{2+} and Fe^{3+} ions. Fagali et al. (2014, 2015) evaluated the influence of these Fe ions and pH variations on CHO–K1 cells during degradation, elaborating that oxidative stress and inflammation may occur. They also reported that Fe^{3+} ions had more harmful effect than pH variation or Fe^{2+} ions. Another study also showed that iron ions are toxic for cells above certain level of concentration (Zhang et al. 2010). However, underlining mechanisms are still not understood well and this study indicated that many different variables are important (pH, ions concentrations, other precipitates).

Literature data related to corrosion are even more missing for novel composites. As mentioned earlier, Cheng and Zheng (2013) studied corrosion mechanisms of two iron composites (Fe-W and Fe-CNT) and they proposed galvanic corrosion between the iron matrix and W or CNT, rather than the galvanic corrosion between grain boundaries and iron matrix. Orinak et al. (2014) obtained significant increase of corrosion rate for Fe–Mg material, namely two times faster than iron. CNT addition slowed degradation. But they obtained high cytotoxicity for all samples, emphasizing that they conducted only static tests that exhibited high accumulation of corrosion products, which might be the cause of such behaviour. It is well known that thin surface oxide layer is formed on the surface of the iron-based materials and this layer essentially influences further corrosion behaviour. Different factors influence the formation and destruction of this oxide layer, such as basic material composition, microstructure, manufacturing processing, but also those originating from surrounding environment (e.g. presence of calcium or aggressive Cl ions, fluctuations in temperature or pH factor, etc.). Different authors proved rapid formation of such layer and in some occurrences it inhibits development of corrosion processes, while in other cases it promotes the degradation (Heiden et al. 2015a; Wu et al. 2013; Zhang et al. 2004). Very detailed discussion on formation and behaviour of such passive layers, in case of several alloying elements, are given in Zhang et al. (2004). Ulum et al. (2014a) investigated novel iron-bioceramic composites and proved deposition of calcium and phosphorous which inhibits degradation, as shown also by Wu et al. (2013) who proposed deposition of PLGA coating to overcome this inhibition. Degradation of PLGA coating results in abundant amounts of H+ release which stimulates the iron corrosion and additionally, PLGA coating prevented formation of the passivation layer comprising Ca/P.

Very important factor that should be encountered is the final shape of the biomaterial, and accordingly production technology involved. Namely, in vitro corrosion tests of iron-based flat samples showed the difference in comparison with tests realised with the same material in the shape of stents. Sing et al. (2015) showed that curvatures of the stent represented the site of enhanced corrosion process, and that the fabrication induced deformation of the material has effect on

the degradation. They investigated Fe35Mn alloy as the stent material and the in vitro corrosion process occurring within the short timeframe immediately after the stenting procedure is done. Visible stent degradation was achieved after 1 h time. It is assumed that corrosion starts as soon as the implant surface is in contact with the surrounding fluid, due to the existence of micro-galvanic sites on the material surface. They also elaborated that Mn content on the surface of the deformed stent is significantly lowered to around 2 wt% in contrast to the 35 wt% within the bulk material, due to the stent fabrication and evaporation of Mn, leading to the material corrosion behaviour very similar to that of the pure Fe within the first period of stent implantation. The fabrication process and cold forming resulted in increased roughness which in return should favour degradation.

It was also shown that material structure with smaller grains are supporting enhanced degradation (Cheng and Zheng 2013; Moravej and Mantovani 2011; Moravej et al. 2010a, b, 2011). However, nanocrystals microstructure of pure iron exhibited highly increased corrosion resistance (Nie et al. 2010) and it might seem that only certain grain size ranges favour corrosion, while other inhibits it. Also, study by Moravej et al. (2011) showed that electrodeposition current can influence the final microstructures and hence the corrosion behaviour. Severe plastic deformation and post-fabrication heat treatments of FeMn alloys can (but not always) promote faster degradation and this was shown by Heiden et al. (2015b). They showed that deformation strain induced in some way by the processing technology influences increase of the degradation rate but only up to certain level, after which it showed no influence. Their conclusion, based on comprehensive testing, is that there is a connection between grain size and induced deformation strain, both further influencing corrosion behaviour, but it is still unknown precisely how.

In vitro tests with FeMn alloy with different amounts of Mn content were done with flat samples to simulate their degradation behaviour under conditions of the blood flow, in the flowing Henk's solution. These showed that degradation products were mainly metal hydroxides and layers of calcium and phosphorous (Hermawan et al. 2010b). The corrosion was distributed over the whole surface of the sample, with pits forming in some zones. Degradation surface layers exhibited lower concentration of manganese, with extensive presence of oxygen (around 26 wt%), and small amounts of chlorine (3.5 wt%), calcium (2 wt%) and phosphorous (2.1 wt%), as well as slight amounts of sulphur (0.7 wt%). The agglomeration of calcium and phosphorous can be noticed along the degradation layer, with increased concentrations in some sites, also shown by Ulum et al. (2014a).

The formation of degradation layers on the surface of the iron-based materials decrease corrosion at least from initially extensive to the slower one and this is recognised as perhaps the main issue in making the degradation rate faster. In the literature, only approximative values of degradation rate of different iron-based materials can be found, depending on the different testing methods, applied test environments, time periods of observation (e.g. initial corrosion vs. corrosion after longer time—months) and material combinations, as well as fabrication and preparation of samples. Accordingly, degradation rate of pure Fe can be evaluated around 0.22 mg/cm^2 per day or 0.1 mm/year (Schinhammer et al. 2013a), whereas

different resources state it in the range of 0.14–0.23 mm/year. Pure iron film fabricated by electroforming exhibited corrosion rates in a range 0.4–1.2 mm/year, depending on the applied current and this was well increased in comparison with cast iron with 0.14–0.25 mm/year (Moravej et al. 2010a, b, 2011). This increase was explained by fine grains obtained by the electroforming. These authors even obtained 1.7 mm/year corrosion rate when samples were annealed after electroforming. However, larger rates were obtained in tests with potentiodynamic polarization and quite lower rates were exhibited in static immersion tests for 'better' samples where annealing was done after the electrodeposition (0.23–0.28 mm/year). Addition of Mn produces increase of degradation rates ranging from 0.13 mm/year up to 0.52 mm/year for Fe25Mn and 0.44 mm/year for Fe35Mn (Hermawan et al. 2010b; Moravej and Mantovani 2011; Schinhammer et al. 2013a). Reindl et al. (2014) obtained degradation rate of 0.19 mm/year for Fe-TCP composite and evaluated it as good for orthopedic applications. Addition of silver to TWIP steel resulted in corrosion rate of 2.3 mg/cm^2 per day, and this was explained by its micro-galvanic influence (Niendorf et al. 2015).

It can be seen that different corrosion rates can be found throughout the literature, but they are all related to in vitro tests of flat samples under different test conditions and test methods. These data also showed the complexity of corrosion testing and impossibility to generalize current data related to corrosion behaviour. It is obvious that corrosion rate can be significantly influenced by the material, but also by applied test methodology. Corrosion rates related to in vivo tests are lacking and those are the most relevant data.

2.3.8 Modeling and Simulation

Development of computer science and numerical modeling enabled significant support in the development of new materials through different modeling and simulation methods, what ideally should lower the number of costly physical trials and errors in a lab. On one side, virtual modeling and simulation is used to support experimental investigations—develop theoretical curves and models describing experimental setups. This on the other side should enable prediction of properties beyond experimental conditions, aiming towards final goal—prediction of material properties in vivo. For degradable materials, and especially metal materials, it is obvious that with a lack of profound knowledge in many aspects, correct models are very hard to develop. Predictive models of iron-based bulk or porous metal behaviour during its functioning would be very useful and this is rather novel area of research, especially in corrosion science. It is very hard to propose a model for something that is not yet quite well perceived or understood as a phenomenon, such is the case of new degradable metal materials. Many material characteristics are still unknown and it might seem that introduction of modeling and simulation techniques would only increase the complexity, but in reality application of modeling theories can be a very powerful tool as additional means of research. For instance, continuum damage mechanics can offer already developed models that can be used

in early prediction of material fatigue behavior or crack initiation, as useful for degradation process of the implant. Apart from experimental testing, numerical modeling of corrosion process can assist in evaluation and selection of implant geometries, prediction of implant life or mechanical integrity, as well as to provide additional insights into the observed processes. There are numerous approaches that can be applied, but only limited number of existing models can be found in the literature related to the corrosion of degradable metals. Models related to the corrosion behaviour of steels could be used as well, although there are not many fully developed models for steel corrosion also. Biomedical steel alloys are designed to be highly corrosion-resistant and they usually are not significantly influenced by corrosion processes, even though they can exhibit some forms such as stress corrosion cracking (Zivic et al. 2013).

The very few models developed specifically for degradable metals applied for stents are done by research group from Ireland (Grogan et al. 2011, 2014), based on the previous work of Gastaldia et al. (2011). They developed numerical model for prediction of mechanical properties as influenced by the corrosion, thus observing the effect of the corrosion process on the integrity of the deployed stent. Gastaldia et al. (2011) used continuum damage mechanics to model damage provoked by corrosion, assuming presence of two simultaneous corrosion types: stress corrosion cracking and uniform microgalvanic corrosion, what could be taken as the two most important phenomena related to the functioning of degradable stents. Pitting would be advantageous to be additionally included in the model which they claim would not be so difficult to add. Their model was related to magnesium stents and fitted to the static immersion experimental corrosion testing. The models of loaded stent corrosion indicated that the corrosion starts at sites with maximum stress in a form of concentrated pitting but over the time uniform corrosion becomes dominant mechanism (Gastaldia et al. 2011). The more recent work of Grogan et al. (2011, 2014) observed foils of materials and investigated models related to the corrosion behavior itself and also the resulting influence of the loading on the corrosion process. They started with a simple geometries related to foil behavior and further developed corrosion model for stents made of degradable metals. Their model anticipated corrosion as the result of the electrochemical reactions at the surface and transportation of ions away from the surface and into the bulk, in case of pure magnesium without any defects of impurities. Other authors investigated phenomenon related to the steel behaviour in corrosive environment under external strain and stress fields and relations with stress corrosion, and such results can be used as additional source of information for study of the degradable iron from aspects of corrosion, such as modeling of stress corrosion cracking (Costa-Mattos et al. 2008).

Complex nature of combined effect of mechanical stress and corrosion leads to even more complex modelling of such a material behavior. As described by Costa-Mattos et al. (2008), simulation in macroscopic scale model that accounts for stress corrosion cracking can be based on a very simple model with assumption of slow strain rate and constant load corrosion. First, geometric simplicity of a model is due to one-dimensional geometric modelling of a constant load and slow strain

rate via basic experimental material testing widely used in stress corrosion cracking research. The continuum damage mechanics framework is the background for the material model that relays on standard viscoplastic mathematical nonlinear description extended with terms related to the damage simultaneously induced by mechanical deformation and corrosion. This extension is represented by macroscopic scalar variable D which can take value from 0 to 1 as the multiplayer that scales undamaged material to damaged material stress. The model shows reasonable accuracy for the simple tensile uniaxial loading experiment with a bar, but only if environment pH is not very low.

Starting from the magnesium alloy as the material for absorbable metal stent, Grogan et al. (2014) have developed physical model that uses the adaptive FEM meshing (ALE formulation) to model the diffusion based corrosion at 3D stent structure. Authors simulate moving corrosion surfaces due to stent mass loss, assuming that the mass is conserved in the solid, meaning that the solution of corrosive environment is modelled together with the stent. This way, the interrelated processes of stent corrosion and corrosion products behaviour are simultaneously analyzed, by this complex yet efficient algorithm. Implementation of this model was realized by coding user subroutines in the commercial FEM code Abaqus Standard implicit solver.

The continuum damage mechanics approach represents the reduction of macroscopic mechanical material properties (stress, stiffness, etc.) due to material discontinuities. Degradation process such as corrosion, is modelled as damage developing from material virgin state to disintegrated state, and represented by D taking values from 0 to 1. In Gastaldia et al. (2011), corrosion damage is assumed as the superposition of uniform microgalvanic corrosion damage D_u and stress corrosion damage D_{sc}. Presented concept is very clear and relatively simple, and it is arranged for the implementation through user subroutines in explicit FEM code Abaqus Explicit. Special attention is given to evaluation of the corrosion surface whereas the criteria and algorithm for the removal of "dead" elements (D close to 1) from FEM mesh is explained. Various alloys are analyzed in realistic 3D stent structure accounting for interaction with the arterial vessel through combined effects of aggressive environment and mechanical loading. Similar model and algorithm has been developed by Grogan et al. (2011), providing modelling of a pitting corrosion. The idea behind capturing the effects of heterogeneous pitting corrosion is the introduction of an element-specific parameter generated using Weibull distribution random number generator. The implementation is also based on Abaqus explicit code. Very complex modelling of real stent application, including stent, balloon and artery is described. Since complicated procedures are used, such as the contact algorithm to model contacts between substructures in the model, even high-performance computer required many CPU hours for calculation.

Kashef et al. (2013) simulated fracture response and observed crack-resistance curves (R-curves) obtained by developed models and experiment, in open cell and closed cell steel foam structures. They showed that material microstructure has great influence on crack initiation and propagation rate, what can be expected. They also reported that crack propagation mechanism is less significant for foam

structures than dense material, because of the thin struts bridging the cracks and closing it. On the other hand, their models predicted failure according to standard R-curves, validated by experimental tests (Kashef et al. 2013).

Schinhammer et al. (2010) proposed a design strategy for biodegradable Fe-based alloys, by using standard approach in design of alloy phases: (1) elements soluble in iron that enhance corrosion and (2) noble elements forming intermetallic phases aiming to form initiation sites for microgalvanic corrosion. Such approach can be used in a large variety of elements and is a very time consuming process for experimental investigations. Thus, application of models and simulation techniques would be of great support. It seems that specific modeling field such as ab initio calculations, based on the use of thermodynamic theories, could serve well for the development of new alloy systems, by prediction of temperature and pressure ranges during the production of alloys which are related to certain wanted material structure or energy levels. Namely, phase diagrams for many new materials are not determined at all, or just portions are known and crystal structures related to its specific zones are determinant for the material behaviour and are tightly connected to its many basic properties, such as magnetic features, ductility, mechanical strength, deformation or elasticity properties etc.

Ab initio calculations and the first principles modeling can provide the insights into the relations between material structure and final properties, from nano and micro, up to the macro behaviour. This, in return, enables prediction of better structures and compositions, from aspect of some specific wanted final material property. Calculations that start directly from laws of physics and chemistry and are not based on assumptions or fitting parameters, are defined as ab initio calculations or calculations based on the first principles. For example, quantum mechanics laws taken into ab initio calculations, without taking any fitting parameters, can provide insights into energy levels of atoms and further connect it with larger scale material behaviour. For iron based materials, calculations based on density functional theory (DFT) have been used to derive enthalpy—composition phase diagram of the Fe–Mn alloy system to point out areas of magnetic behaviour (Lintzen et al. 2013). It is well known that this alloy can exhibit different magnetic properties depending on the retained crystal structure (bcc, hcp, fcc) and alloy phase, as previously elaborated and this type of phase diagrams are very important for the determination of optimal compositions. This kind of modeling can also indicate unstable regions which should be avoided for the final alloy structure, since these produce material zones with unpredictable behaviour even from aspects of basic properties, and especially considering many variables of external factors. Thermodynamic evolution of different binary or multi-component alloys has been an important topic for some years and one of the reasons is that it can predict phase stability. Rather well established method is the calculation of phase diagrams or CALPHAD modeling, very often used as a support to experimental data. Theoretical thermodynamic parameters that describe phases of the binary Fe–Zn system which are well fitted with experimentally obtained data enabled further prediction of the alloy behavior as given in Sua et al. (2001).

In 2012, Chookajorn et al. (2012) published an article in the Science journal showing a way to make a map of a given element's stability at a certain temperature, using a mathematical model. They developed a theoretical model that enables design of stable nanostructured alloy. The model generates the map of stable regions, and the work is based on the thermodynamics. The metallurgists can use this model to determine which constituents (elements) can be added to the base metal and obtain stable structures at high temperatures. They validated the model for Ti alloys.

There are number of modelling approaches in existing literature related to specific properties of alloys and composites. Linearized Augmented Plane Wave (LAPW) density functional theory for crystalline structures has been used for wide number of compositions to predict the electronic structure and the total energy curves (structures pertaining to the optimal energy levels, equilibrium states from aspects of lattice properties, or bulk modulus). Classical molecular dynamics has been applied for thermodynamic properties and diffusion. Different modeling approaches, discrete (Dissipative Particle Dynamics) and continuum (Finite Element Method), have been used to investigate micro/nanoscale defects within structures. However, all of these models are developed with specific focus and usually cannot consider all necessary properties of the real application case of the material.

Regarding degradable medical materials prediction of the porous "time-dependent" properties is still out of reach and represents one challenging task, especially considering corrosion which is not well understood even in case of traditional materials. One promising direction is the linking between existing and developed electronic, atomistic, mesoscopic models and continuum scale models or coupling of different wanted properties in some synergetic way. That would result in one comprehensive supportive tool that could be used in the development of new materials for different purposes.

3 Economic Impact of Biodegradable Metallic Implants

As already mentioned, modern society is facing the various issues related to the prolonged age of the population and the prime concern is the quality of life for elderly people, unavoidably connected to the prevention of diseases and adequate suitable treatments. Especially important are different medical implants, such as the bone implants for regenerative surgeries, or vascular implants for different arterial treatments (e.g. coronary stents) where degradable metallic materials would greatly enhance quality of service from many aspects. Prolonged implant function or life, more fitted to the natural tissue in contact and lighter, but at the same time, stronger materials that can endure long standing loads will enable patients to have a life very similarly as if they still have the natural tissue (e.g. artificial hip implants). Tissue engineering as the new promising area will complement the already acquired knowledge and is expected to provide a breakthrough in regenerative medicine, as

well as in many other areas such as stem cell therapy, drug delivery or targeted drug delivery systems.

The importance of this field is emphasized by the many established official programs in Europe and all over the world, such as the European Innovation Partnership on Active and Healthy Ageing, with a goal to increase healthy life in EU by 2020. Research areas related to health, material science and medical devices account for a significant share of every funding in EU, USA, Japan, China, and all over the world. Based on many commercial and market analysis, development of new materials and subsequently new or better medical devices is evaluated as one of the highly profitable field and accordingly the new significant investments followed by both the large companies and governmental funding agencies. Medical devices market has one of the largest shares within the healthcare sector. For example, market report by Visiongain UK company showed that medical devices market was valued at US$266 billion in 2011. Another global market analysis (MarketsandMarkets) estimated that for 10 largest medical devices sectors, market was worth US$164 billion in 2010 and their prognosis then for 2015 was US$228 billion market value. They comprised ten major sectors starting with cardiovascular devices, orthopedic devices, and diagnostic imaging devices as the largest sectors together and then adding: minimally invasive devices; diabetes devices; anesthesia and respiratory care devices; dialysis products; ophthalmology devices; patient monitoring devices; point-of-care diagnostic devices (MarketsandMarkets).

Within the medical devices sector, global biomaterials market was worth US $8.5 billion in 2008 and US$44.0 billion in 2012, mainly due to the constant demands for new materials. Even superficial evaluation of the published news on novel materials and new medical devices evidently show that this sector exhibits very rapid growth and that manufacturers are racing for patents and commercialization of new products. In a world, Europe represents the 2nd largest sector within global biomaterials market with 33% shares, with USA being the world largest market (50%) and Japan related to around 10% share. And among EU countries, Germany and France lead with around 20% participation, UK $\sim$10% and Netherlands $\sim$5–10%. The biomaterial market is expected to have around 15% compound annual growth rate (CAGR) in the next years, meaning to reach US $88.4 billion by 2017.

Biomaterials market can be broadly divided according to: (1) the type of material (polymers, metals, ceramics, composites, natural biomaterials) or (2) the application field (cardiovascular, orthopedic, dental, ophthalmology, plastic surgery, wound healing, tissue engineering, neurology, drug delivery system, and other). The two largest sectors of the global biomaterial market are cardiovascular (around 34.5%) and orthopedic biomaterials. Distribution of orthopedic sectors in USA indicates that resorbable products accounts for 7%, whereas hip implants (18%) and knee implants (11%) are the largest sectors in orthopedics, according to Driscoll (2009). Some predictions additionally point out plastic surgery and wound healing to be among the most propelling areas for growth. And the most pronounced growth rate has been related to the biodegradable polymers (predicted at 22.1% in a period

Table 1 Selected medical devices in numbers per year in a world

Number of medical devices worldwide per year (millions)	
Cardiovascular stents	>2
Heart valves	0.2
Vascular grafts	0.4
Bone grafts	2.2
Hip and knee prosthesis	1
Dental implants	0.5
Catheters	300

Adapted from Ratner (2004)

2012–2017). Very rough evaluation of general number of implants used each year according to sectors is given in Table 1.

It can be clearly seen that any improvement in these fields influence significant number of patients, thus completely justifying high investments. Venture capital funding of the private biotech companies and even in startup biotech companies has enormously increased in the recent years. Last year, the largest ever recorded sum in the history of investments in the early stage medical devices company was around US$2 billion (Peatman 2015). It is obvious that great things for the wellbeing of the humankind are expected from the research dedicated to the development of specific biomaterials.

4 Conclusions

Biodegradable materials constitute one of the new directions of research aiming at better suited medical implants which will stay in the body until the healing process is finished and then gradually vanish. The basic condition is biocompatibility, especially to maintain it during degradation, along with adequate mechanical strength, ductility, fatigue resistance, magnetic properties and other characteristics, depending on the specific application. Several material classes have been considered for this purpose, starting from polymers with significant research activities so far. However, polymers generally lack mechanical strength while metals are better for many applications. Consequently, metallic materials started to be considered for biodegradable implants. Magnesium and iron have been recognised as promising candidates in relation to degradable stents, bone grafts and tissue engineering. Pure metals, alloys, and composites based on Fe and Mg are investigated from different aspects, in order to make them suitable for clinical applications as degradable implants. Important focus in this area is to control corrosion and thus provide predictable and controlled way of degradation. During the last decade, comprehensive investigations have started from testing of basic properties (material structures, alloying elements, composite or joint structures), biocompatibility,

mechanical properties, magnetic behaviour, fabrication technologies for both the material and the implant itself, up to the different corrosion related investigations, in order to find optimally suited material.

Magnesium based materials were first considered and resulted in a few patented coronary stent solutions. Iron has started to be investigated later because of the several drawbacks of Mg-based materials. Recognised advantages of Fe-based materials are: low cost, wide availability of alloying elements and the widest possible presence of the production plants for iron processing throughout the world. Some estimates state that 95% of all metal alloys production in the world is related to iron. Degradation of iron does not produce hydrogen such as in case of Mg. However, the degradation rates of iron-based alloys or composites are still too low to be considered for clinical trials. The first iron biodegradable stent was made of pure iron (Fe > 99.8%) in 2001, and acted more like permanent stainless steel stent, but showed very good biocompatibility. Wide research activities are devoted to the development of Fe-based degradable implants, in order to adjust corrosion rate. Several alloying elements (P, Pd, Ag, Zn) have been suggested, depending on the end application. Fe–35Mn alloy has been denoted as the best candidate. Also, a few composites showed promising results (e.g. Fe-40% ß-TCP). Porous structures are also recognised as suitable from several aspects, such as enhanced corrosion rate, lower Young's modulus, or the possibility to infiltrate them with polymers to control corrosion rates (e.g. PLGA). The use of porous structures in combination with degradability imposed quite new area of research: material behaviour during degradation and prediction of properties over time. Also, different processing techniques (e.g. hot or cold plastic deformation) and heat treatments showed that both the material structures and corrosion rate can be adjusted in such way. Different fabrication technologies have been tried, for both dense and porous structures of these new Fe-based materials. Electroforming proved to be very good technology for Fe-based films, resulting in fine grains and good biocompatibility in stent application, especially suited for the in-restenosis prevention. Powder metallurgy is powerful in providing varieties of end properties, as well as producing different porous Fe-based structures. But the latest direction is combination of powder metallurgy concepts with novel 3D printing technologies, which can provide endless combinations of properties related to the porous structure (shape and size of the pores), thus enabling completely custom-made design of the materials and structures. Also, numerical modeling should soon provide valuable tools, as a support in development of new materials.

Understanding the complex, "time-dependent" properties of the porous structures during the degradation is a challenging task, especially for in vivo conditions and represents one of the important goals of all research related to degradable materials. Economic impact of these new materials is enormous and all market analyses indicate the constant growth of this sector, thus justifying large investments. But, it is not the economic effects that solely propel the investigations. Better medical implants have profound effects on the humankind because the amount of such treatments is routine and everyday reality in every hospital today. Improved implants represent quality of life for a millions of patients.

Acknowledgements This work has been partially funded by the 2014-SGR-1015 project from the Generalitat de Catalunya, and the MAT2014-57960-C3-1-R (co-financed by the Fondo Europeo de Desarrollo Regional, FEDER) and SELECTA H2020-MSCA-ITN-2014 no. 642642 project and part of the project III41017—(Virtual Human Osteoarticular System and its Application in Preclinical and Clinical Practice which is sponsored by the Ministry of Education, Science and Technological Development of the Republic of Serbia for the period of 2011–2016.

References

Alexy RD, Levi DS (2013) Materials and manufacturing technologies available for production of a pediatric bioabsorbable stent. Biomed Res Int 2013:137985. doi:10.1155/2013/137985 Epub 2013

Andani MT, Moghaddam NS, Haberland C et al (2014) Metals for bone implants. Part 1. Powder metallurgy and implant rendering. Acta Biomater 10:4058–4070

Bannwarth MB, Ebert S, Lauck M et al (2014) Tailor-made nanocontainers for combined magnetic-field-induced release and MRI. Macromol Biosci 14:1205–1214

Bantsis G, Betsiou M, Bourliva A et al (2012) Synthesis of porous iron oxide ceramics using greek wooden templates and mill scale waste for EMI applications. Ceram Int 38:721–729

Bartosch M, Peters H, H-Ici DO et al (2014) Different approaches for in vivo testing of absorbable metals in blood vessels. In: Abstract book of the 6th symposium on biodegradable metals, Maratea, Italy, 24–29 Aug 2014

Blackhear JL, O'Callaghan WG, Califf RM (1987) Medical approaches to prevention of restenosis after coronary angioplasty. J Am Coll Cardiol 9:834–848

Blank VD, Estrin EI (2014) Chapter 5: phase transformations in iron and its alloys at high pressure. In: Phase transitions in solids under high pressure. CRC Press, Taylor & Francis Group, Boca Raton, pp 166–190

Bogachev IN, Zvigintseva GY, Chumakova LD (1975) Influence of the magnetic transformation of austenite on the fine structure of iron-manganese alloys. Phys Met Metallogr 39:96–101

Brodie B, Pokharel Y, Fleishman N et al (2011) Very late stent thrombosis after primary percutaneous coronary intervention with bare-metal and drug-eluting stents for st-segment elevation myocardial infarction. J Am Coll Cardiol Intv 4(1):30–38

Butscher A, Bohner M, Hofmann S et al (2011) Structural and material approaches to bone tissue engineering in powder-based three-dimensional printing. Acta Biomater 7:907–920

Butscher A, Bohner M, Roth C et al (2012) Printability of calcium phosphate powders for three-dimensional printing of tissue engineering scaffolds. Acta Biomater 8:373–385

Čapek J, Vojtěch D (2014) Microstructural and mechanical characteristics of porous iron prepared by powder metallurgy. Mater Sci Eng C 43:494–501

Chen Q, Thouas GA (2015) Metallic implant biomaterials. Mater Sci Eng R Rep 87:1–57

Chen Y, Xu Z, Smith C et al (2014) Recent advances on the development of magnesium alloys for biodegradable implants. Acta Biomater 10:4561–4573

Cheng J, Zheng YF (2013) In vitro study on newly designed biodegradable Fe-X composites (X = W, CNT) prepared by spark plasma sintering. J Biomed Mater Res Part B 101B:485–497

Cheng J, Huang T, Zheng YF (2014) Microstructure, mechanical property, biodegradation behavior, and biocompatibility of biodegradable Fe–Fe_2O_3 composites. J Biomed Mater Res A 102:2277–2287

Cheng J, Huang T, Zheng YF (2015) Relatively uniform and accelerated degradation of pure iron coated with micro-patterned Au disc arrays. Mater Sci Eng C 48:679–687

Chookajorn T, Murdoch HA, Schuh CA (2012) Design of stable nanocrystalline alloys. Science 337:951–954

Chou D, Wells D, Hong D et al (2013) Novel processing of iron-manganese alloy-based biomaterials by inkjet 3-D printing. Acta Biomater 9:8593–8603

Costa-Mattos HS, Bastos IN, Gomes JACP (2008) A simple model for slow strain rate and constant load corrosion tests of austenitic stainless steel in acid aqueous solution containing sodium chloride. Corros Sci 50:2858–2866

Crane NB, Wilkes J, Sachs E et al (2006) Improving accuracy of powder-based SFF processes by metal deposition from a nanoparticle dispersion. Rapid Prototyping J 12:266–274

Curodeau A, Sachs E, Caldarise S (2000) Design and fabrication of cast orthopedic implants with freeform surface textures from 3-D printed ceramic shell. J Biomed Mater Res 53:525–535

Davis JR (ed) (2000) Corrosion: understanding the basics. ASM International, Materials Park, Ohio, USA, pp 1–20

De Santis R, Russo A, Gloria A et al (2015) Towards the design of 3D fiber-deposited poly (ε-caprolactone)/iron-doped hydroxyapatite nanocomposite magnetic scaffolds for bone regeneration. J Biomed Nanotechnol 11:1236–1246

Dill T (2008) Contraindications to magnetic resonance imaging. Heart 94:943–948

Djurovic D, Hallstedt B, von Appenb J et al (2011) Thermodynamic assessment of the Fe–Mn–C system. Calphad 35:479–491

Driscoll P (2009) http://mediligence.com/blog/2009/01/30/orthopedic-biomaterials-market-growth-strongest-in-us/

Drynda A, Hassel T, Bach FW et al (2015) In vitro and in vivo corrosion properties of new iron–manganese alloys designed for cardiovascular applications. J Biomed Mater Res Part B 103B:649–660

Erbel R, Di Mario C, Bartunek J et al (2007) Temporary scaffolding of coronary arteries with bioabsorbable magnesium stents: a prospective, non-randomised multicentre trial, PROGRESS-AMS (clinical performance and angiographic results of coronary stenting with absorbable metal stents). Lancet 369(9576):1869–1875

Fagali NS, Grillo CA, Puntarulo S et al (2014) Evaluation of cell damage produced by Fe ions released as degradation products of biomaterials. Influence of pH changes. In: Abstract book of the 6th symposium on biodegradable metals, Maratea, Italy, 24–29 Aug 2014

Fagali NS, Grillo CA, Puntarulo S et al (2015) Cytotoxicity of corrosion products of degradable Fe-based stents: relevance of pH and insoluble products. Colloids Surf B 128:480–488

Fang G, Ai W, Leeflang S et al (2013) Multipass cold drawing of magnesium alloy minitubes for biodegradable vascular stents. Mater Sci Eng C 33:3481–3488

Farack J, Wolf-Brandstetter C, Glorius S et al (2011) The effect of perfusion culture on proliferation and differentiation of human mesenchymal stem cells on biocorrodible bone replacement material. Mater Sci Eng B 176:1767–1772

Farooq V, Gogas BD, Serruys PW (2011) Restenosis. Delineating the numerous causes of drug-eluting stent restenosis, contemporary reviews in interventional cardiology. Circulation 4:195–205

Feng Q, Zhang D, Xin C et al (2013) Characterization and in vivo evaluation of a bio-corrodible nitrided iron stent. J Mater Sci Mater Med 24:713–724

Francis A, Yang Y, Virtanen S et al (2015) Iron and iron-based alloys for temporary cardiovascular applications. J Mater Sci Mater Med 26:138

Gastaldia D, Sassia V, Petrinia L et al (2011) Continuum damage model for bioresorbable magnesium alloy devices—application to coronary stents. J Mech Behav Biomed Mater 4: 352–365

Geetha M, Singh AK, Asokamani R, Gogia AK (2009) Ti based biomaterials, the ultimate choice for orthopaedic implants—a review. Prog Mater Sci 54:397–425

Geis-Gerstorfer J, Schille Ch, Schweizer E et al (2011) Blood triggered corrosion of magnesium alloys. Mater Sci Eng B 176(20):1761–1766

Gkouvatsos K, Papanikolaou G, Pantopoulos K (2012) Regulation of iron transport and the role of transferrin. Biochim Biophys Acta 1820:188–202

Glorius S, Nies B, Farack J et al (2011) Metal foam—bone cement composites mechanical and biological properties and perspectives for bone implant design. Adv Eng Mater 13:1019–1023

Gorkunov ES, Gladkovskii SV, Zadvorkin SM et al (2008) Evolution of magnetic properties of Fe–Mn and Fe–Mn–Cr steels with different stability of austenite during plastic deformation. Phys Metals Metallography 105(4):343–350
Grabke HJ, Hennesen K, Möller R et al (1987) Effects of manganese on the grain boundary segregation, bulk and grain boundary diffusivity of P in ferrite. Scr Metall 21:1529–1534
Grogan JA, O'Brien BJ, Leen SB et al (2011) A corrosion model for bioabsorbable metallic stents. Acta Biomater 7:3523–3533
Grogan JA, Leen SB, McHugh PE (2014) A physical corrosion model for bioabsorbable metal stents. Acta Biomater 10:2313–2322
Hänzi AC, Gerber I, Schinhammer M et al (2010) On the in vitro and in vivo degradation performance and biological response of new biodegradable Mg–Y–Zn alloys. Acta Biomater 6:1824–1833
Harjanto S, Pratesa Y, Prasetyo Y et al (2013) Properties of Fe-Mn-C alloy as degradable biomaterials candidate for coronary stent. Adv Mater Res 789:210–214
Heiden M, Walker E, Nauman E et al (2015a) Evolution of novel bioresorbable iron–manganese implant surfaces and their degradation behaviors in vitro. J Biomed Mater Res Part A 103A:185–193
Heiden M, Kustas A, Chaput K et al (2015b) Effect of microstructure and strain on the degradation behavior of novel bioresorbable iron–manganese alloy implants. J Biomed Mater Res Part A 103A:738–745
Henderson SE, Verdelis K, Maiti S et al (2014) Magnesium alloys as a biomaterial for degradable craniofacial screws. Acta Biomater 10:2323–2332
Hermawan H (2012) Biodegradable metals, from concept to applications. Springer briefs in materials. Springer, Heidelberg
Hermawan H, Mantovani D (2013) Process of prototyping coronary stents from biodegradable Fe–Mn alloys. Acta Biomater 9:8585–8592
Hermawan H, Dube D, Mantovani D (2007) Development of degradable Fe-35Mn alloy for biomedical application. Adv Mater Res 15:107–112
Hermawan H, Dube D, Mantovani D (2008a) Degradable metallic biomaterials: design and development of Fe–Mn alloys for stents. J Biomed Mater Res A 93(1):1–11
Hermawan H, Alamdari H, Mantovani D et al (2008b) Iron-manganese: new class of metallic degradable biomaterials prepared by powder metallurgy. Powder Metall 51(1):38–45
Hermawan H, Dube D, Mantovani D (2010a) Degradable metallic biomaterials: design and development of Fe-Mn alloys for stents. J Biomed Mater Res A 93:1–11
Hermawan H, Purnama A, Dube D, Couet J, Mantovani D (2010b) Fe–Mn alloys for metallic biodegradable stents: degradation and cell viability studies. Acta Biomater 6:1852–1860
Hermawan H, Ramdan D, Djuansjah JRP (2011) Metals for biomedical applications. In: Fazel R (ed) Biomedical engineering—from theory to applications, InTech, www.intechopen.com. pp 1–20
Higuera GA, Hendriks JAA, van Dalum J et al (2013) In vivo screening of extracellular matrix components produced under multiple experimental conditions implanted in one animal. Integr Biol (Camb) 5:889–898
Hornberger H, Virtanen S, Boccaccini AR (2012) Biomedical coatings on magnesium alloys—a review. Acta Biomater 8(7):2442–2455
Hort N, Wiese B, Wolff M et al (2014) Stiffness of metals, alloys and components. In: Abstract book of the 6th symposium on biodegradable metals, Maratea, Italy, 24–29 Aug 2014
Huang W (1987) An assessment of the Fe-Mn system. Calphad 2:183–186
Huang W (1989) An assessment of the Fe-Mn system. Calphad 13:243–252
Huang T, Cheng J, Zheng YF (2014) In vitro degradation and biocompatibility of Fe–Pd and Fe–Pt composites fabricated by spark plasma sintering. Mater Sci Eng C 35:43–53
Huang T, Cheng J, Bian D et al (2015) Fe–Au and Fe–Ag composites as candidates for biodegradable stent materials. J Biomed Mater Res B Appl Biomater. doi:10.1002/jbm.b.33389
Hutmacher DW, Sittinger M, Risbud MV (2004) Scaffold-based tissue engineering: rationale for computer-aided design and solid free-form fabrication systems. Trends Biotechnol 22:354–362

Hyun S-K, Ikeda T, Nakajima H (2004) Fabrication of lotus-type porous iron and its mechanical properties. Sci Technol Adv Mater 5:201–205
Ishikawa Y, Endoh Y (1968) Antiferromagnetism of γ-FeMn alloys. J Appl Phys 39:1318–1319
Jayalekshmi AC, Victor SP, Sharma CP (2013) Magnetic and degradable polymer/bioactive glass composite nanoparticles for biomedical applications. Colloids Surf B 101:196–204
Kashef S, Asgari A, Hilditch TB et al (2013) Fracture mechanics of stainless steel foams. Mater Sci Eng A 578:115–124
Keen CL, Ensunsa JL, Clegg MS (2000) Manganese metabolism in animals and humans including the toxicity of manganese. In: Siegel A, Siegel H (eds) Manganese and its role in biological proceses. Marcel Dekker, New York, pp 89–121
Kini U, Nandeesh BN (2012) Physiology of bone formation, remodeling, and metabolism. In: Fogelman I et al (eds) Radionuclide and hybrid bone imaging. Springer, Berlin, p 43
Kirkland NT, Birbilis N, Staiger MP (2012) Assessing the corrosion of biodegradable magnesium implants: a critical review of current methodologies and their limitations. Acta Biomater 8:925–936
Kubaschewski O (1982) Iron—binary phase diagrams. Springer, Berlin, pp 61–63
Lee BJ, Lee DN (1989) A thermodynamic study on the Mn-C and Fe-Mn systems. Calphad 4: 345–354
Li N, Zheng Y (2013) Novel magnesium alloys developed for biomedical application: a review. J Mater Sci Technol 29(6):489–502
Li H, Zheng Y, Qin L (2014) Progress of biodegradable metals. Prog Nat Sci Mater Int 24:414–422
Ling D, Hyeon T (2013) Chemical design of biocompatible iron oxide nanoparticles for medical applications. Small 9:1450–1466
Lintzen S, von Appen J, Hallstedt B et al (2013) The Fe–Mn enthalpy phase diagram from first principles. J Alloy Compd 577:370–375
Liu B, Zheng Y (2011) Effects of alloying elements (Mn Co, Al, W, Sn, B, C and S) on biodegradability and in vitro biocompatibility of pure iron. Acta Biomater 7:1407–1420
Liu Z, Fan T, Zhang W et al (2005) The synthesis of hierarchical porous iron oxide with wood templates. Microporous Mesoporous Mater 85:82–88
Liu B, Zheng Y, Ruan L (2010) In vitro investigation of Fe30Mn6Si shape memory alloy as potential biodegradable metallic material. Mater Lett 65:540–543
Long J, Laughlin DE, McHenry ME (2008) Structural and soft magnetic properties of a new Fe-Zr soft magnetic nanocrystalline alloy. J Appl Phys 103:07E708
Melican M, Zimmerman M, Dhillon M et al (2001) Three-dimensional printing and porous metallic surfaces: a new orthopedic application. J Biomed Mater Res 55:194–202
Moravej M, Mantovani D (2011) Biodegradable metals for cardiovascular stent application: interests and new opportunities. Int J Mol Sci 12:4250–4270
Moravej M, Prima F, Fiset M, Mantovani D et al (2010a) Electroformed iron as new biomaterial for degradable stents: development process and structure-properties relationship. Acta Biomater 6:1726–1735
Moravej M, Purnama A, Fiset M et al (2010b) Electroformed pure iron as a new biomaterial for degradable stents: in vitro degradation and preliminary cell viability studies. Acta Biomater 6:1843–1851
Moravej M, Amira S, Prima F et al (2011) Effect of electrodeposition current density on the microstructure and the degradation of electroformed iron for degradable stents. Mater Sci Eng B 176:1812–1822
Moszner F, Sologubenko AS, Schinhammer M et al (2011) Precipitation hardening of biodegradable Fe–Mn–Pd alloys. Acta Mater 59:981–991
Mouzou E, Paternoster C, TolloueiR et al (2014) A comparative study of the degradation of pure Fe and Fe-20Mn-1.2C alloy in modified Hanks' solution for biodegradable cardiovascular device. In: Abstract book of the 6th symposium on biodegradable metals, Maratea, Italy, 24–29 Aug 2014

Mueller PP, May T, Perz A et al (2006) Control of smooth muscle cell proliferation by ferrous iron. Biomaterials 27:2193–2200
Murakami T, Ohara K, Narushima T et al (2007) Development of a new method for manufacturing iron foam using gases generated by reduction of iron oxide. Mater Trans 48:2937–2944
Nasution AK, Murni NS, Sing NB et al (2015) Partially degradable friction-welded pure iron–stainless steel 316L bone pin. J Biomed Mater Res Part B 103B:31–38
Neacsu P, Ion RN, Mitran V et al (2015) State of the art and recent patents on Mg-based biodegradable bone implants. Recent Pat Regenerative Med 4(3):168–188
Nie FL, Zheng YF, Wei SC et al (2010) In vitro corrosion, cytotoxicity and hemocompatibility of bulk nanocrystalline pure iron. Biomed Mater 5:1843–1851
Niendorf T, Brenne F, Hoyer P et al (2015) Processing of new materials by additive manufacturing iron-based alloys containing silver for biomedical applications. Metall Mater Trans A 46:2829–2833
Niinomi M, Nakai M, Hieda J (2012) Development of new metallic alloys for biomedical applications. Acta Biomater 8:3888–3903
Obayi CS, Tolouei R, Paternoster C et al (2015) Influence of cross-rolling on the micro-texture and biodegradation of pure iron as biodegradable material for medical implants. Acta Biomater 17:68–77
Orinak A, Orinakova R, Kralova ZO et al (2014) Sintered metallic foams for biodegradable bone replacement materials. J Porous Mater 21:131–140
Orinakova R, Orinak A, Kupkova M et al (2015) Study of electrochemical deposition and degradation of hydroxyapatite coated iron biomaterials. Int J Electrochem Sci 10:659–670
Peatman B (2015) Biotech funding update. http://cirtecmed.com/biotech-funding-update/
Peck M, Dusserre N, McAllister TN et al (2011) Tissue engineering by self-assembly. Mater Today 14:218–224
Pepperhoff W, Acet M (2001) Constitution and magnetism of iron and its alloys. Springer, Berlin
Persaud-Sharma D, McGoron A (2012) Biodegradable magnesium alloys: a review of material development and applications. J Biomim Biomater Tissue Eng 12:25–39
Peuster M, Wohlsein P, Brugmann M et al (2001) A novel approach to temporary stenting: degradable cardiovascular stents produced from corrodible metal-results 6–18 months after implantation into New Zealand white rabbits. Heart 86:563–569
Peuster M, Hesse C, Schloo T et al (2006) Long-term biocompatibility of a corrodible peripheral iron stent in the porcine descending aorta. Biomaterials 27:4955–4962
Pierson D, Edick J, Tauscher A et al (2012) A simplified in vivo approach for evaluating the bioabsorbable behavior of candidate stent materials. J Biomed Mater Res Part B 100B:58–67
Purnama A, Hermawan H, Couet J et al (2010) Assessing the biocompatibility of degradable metallic materials: state-of-the-art and focus on the potential of genetic regulation. Acta Biomater 6:1800–1807
Purnama A, Hermawan H, Champetier S et al (2013) Gene expression profile of mouse fibroblasts exposed to a biodegradable iron alloy for stents. Acta Biomater 9:8746–8753
Quadbeck P, Hauser R, Kümmel K et al (2010) Iron based cellular metals for degradable synthetic bone replacement. In: Proceedings of powder metallurgy world congress & exhibition. PM2010, Florence, Italy 10–14 Oct 2010, vol 4. pp 95–102
Quadbeck P, Kümmel K, Hauser R et al (2011) Structural and material design of open-cell powder metallurgical foams. Adv Eng Mater 13:1024–1030
Quadbeck P, Redlich C, Göhler H et al (2014) Methodical screening of corrosion mechanisms of iron alloys for the manipulation of degradation rates. In: Abstract book of the 6th symposium on biodegradable metals, Maratea, Italy, 24–29 Aug 2014
Rabinkin A (1979) On magnetic contributions to $\gamma \rightarrow \varepsilon$ phase transformations in Fe-Mn alloys. Calphad 3:77–84
Ratner BD (2004) Biomaterials tutorial. An introduction to biomaterials. http://www.uweb.engr.washington.edu/research/tutorials/introbiomat.html

Reindl A, Borowsky R, Hein SB et al (2014) Degradation behavior of novel Fe/ß-TCP composites produced by powder injection molding for cortical bone replacement. J Mater Sci 49:8234–8243

Russo T, D'Amora U, Gloria A et al (2013) Systematic analysis of injectable materials and 3D rapid prototyped magnetic scaffolds: from CNS applications to soft and hard tissue repair/regeneration. Procedia Eng 59:233–239

Ryan G, Pandit A, Apatsidis DP (2006) Fabrication methods of porous metals for use in orthopaedic applications. Biomaterials 27:2651–2670

Ryan GE, Pandit AS, Apatsidis DP (2008) Porous titanium scaffolds fabricated using a rapid prototyping and powder metallurgy technique. Biomaterials 29:3625–3635

Sanchez AHM, Luthringer BJC, Feyerabend F et al (2015) Mg and Mg alloys: how comparable are in vitro and in vivo corrosion rates? a review. Acta Biomaterialia 13(2015):16–31

Schaffer JE, Nauman EA, Stanciu LA (2012) Cold-drawn bioabsorbable ferrous and ferrous composite wires: an evaluation of mechanical strength and fatigue durability. Metall Mater Trans B 43B:984–994

Schinhammer M, Hänzi AC, Löffler JF, Uggowitzer P (2010) Design strategy for biodegradable Fe-based alloys for medical applications. Acta Biomater 6:1705–1713

Schinhammer M, Gerber I, Hänzi AC et al (2012) Recrystallization behavior, microstructure evolution and mechanical properties of biodegradable Fe–Mn–C(–Pd) TWIP alloys. Acta Mater 60:2746–2756

Schinhammer M, Steiger P, Moszner F et al (2013a) Degradation performance of biodegradable Fe-Mn-C(-Pd) alloys. Mater Sci Eng C 33:1882–1893

Schinhammer M, Gerber I, Hänzi AC et al (2013b) On the cytocompatibility of biodegradable Fe-based alloys. Mater Sci Eng C 33:782–789

Schomig A, Kastrati A, Mudra H, Blasini R, Schuhlen H, Klauss V, Richardt G, Neumann FJ (1994) Four-year experience with Palmaz-Schatz stenting in coronary angioplasty complicated by dissection with threatened or present vessel closure. Circulation 90:2716–2724

Serruys PW, Kutryk MJ, Ong AT (2006) Coronary-artery stents. N Engl J Med 354:483–495

Sing NB, Mostavan A, Hamzah E et al (2015) Degradation behavior of biodegradable Fe35Mn alloy stents. J Biomed Mater Res Part B 103B:572–577

Stephani G, Andersen O, Quadbeck P et al (2010) Cellular metals for functional applications—an overview. In: Proceedings of powder metallurgy world congress & exhibition. PM2010, Florence, Italy 10–14 Oct 2010, vol 4. pp 95–102

Sua X, Tang NY, Toguri JM (2001) Thermodynamic evaluation of the Fe–Zn system. J Alloy Compd 325:129–136

Swaminathan R (2003) Magnesium metabolism and its disorders. Clin Biochem Rev 24(2):47–66

Tampieri A, D'Alessandro T, Sandri M et al (2012) Intrinsic magnetism and hyperthermia in bioactive Fe-doped hydroxyapatite. Acta Biomater 8:843–851

Tan L, Yu X, Wan P et al (2013) Biodegradable materials for bone repairs: a review. J Mater Sci Technol 29(6):503–513

Trinidad J, Marco I, Arruebarrena G et al (2014) Processing of magnesium porous structures by infiltration casting for biomedical applications. Adv Eng Mater 16(2):241–247

Ulum MF, Arafat A, Noviana D et al (2014a) In vitro and in vivo degradation evaluation of novel iron-bioceramic composites for bone implant applications. Mater Sci Eng C 36:336–344

Ulum MF, Nasution AK, Yusop AH et al (2014b) Evidences of in vivo bioactivity of Fe-bioceramic composites for temporary bone implants. J Biomed Mater Res Part B Appl Biomater 00B. doi:10.1002/jbm.b.33315

Ulum MF, Murni NS, Noviana D et al (2014c) Peri-implant assessment of Fe-HA composite for temporary bone implants. Eur Cells Mater 28(3):81

Waksman R, Pakala R, Baffour R et al (2008) Short-term effects of biocorrodible iron stents in porcine coronary arteries. J Interv Cardiol 21:15–20

Waksman R, Erbel R, Di Mario C et al (2009) Early- and long-term intravascular ultrasound and angiographic findings after bioabsorbable magnesium stent implantation in human coronary arteries. JACC: Cardiovasc Interv 2(4):312–320

Walker J, Shadanbaz S, Woodfield TBF et al (2014) Magnesium biomaterials for orthopedic application: a review from a biological perspective. J Biomed Mater Res Part B 102B:1316–1331

Wang X, Dong LH, Ma XL, Zheng YF (2013) Microstructure, mechanical property and corrosion behaviors of interpenetrating C/Mg-Zn-Mn composite fabricated by suction casting. Mater Sci Eng C 33:618–625

Wegener B, Sievers B, Utzschneider S et al (2011) Microstructure, cytotoxicity and corrosion of powder-metallurgical iron alloys for biodegradable bone replacement materials. Mater Sci Eng B 176:1789–1796

Willbold E, Gu X, Albert D et al (2015) Effect of the addition of low rare earth elements (lanthanum, neodymium, cerium) on the biodegradation and biocompatibility of magnesium. Acta Biomater 11:554–562

Witte F, Hort N, Vogt C et al (2008) Degradable biomaterials based on magnesium corrosion. Curr Opin Solid State Mater Sci 12:63–72

Wu CZ, Chen SC, Shih YH et al (2011) Development of the novel ferrous-based stainless steel for biomedical applications, Part I: high-temperature microstructure, mechanical properties and damping behavior. J Mech Behav Biomed Mater 4:1548–1553

Wu J, Lu X, Tan L et al (2013) Effect of hydrion evolution by polylactic-co-glycolic acid coating on degradation rate of pure iron. J Biomed Mater Res Part B 101B:1222–1232

Yabuuchi K, Kasada R, Kimura A (2013) Effect of Mn addition on one-dimensional migration of dislocation loops in body-centered cubic Fe. Acta Mater 61:6517–6523

Yang R, Zhao DL, Wang YM et al (2001) Effects of Cr, Mn on the cohesion of the γ-iron grain boundary. Acta Mater 49:1079–1085

Yusop AH, Bakir AA, Shaharom NA et al (2012) Porous biodegradable metals for hard tissue scaffolds: a review. Int J Biomater 2012:1–10

Yusop AHM, Daud NM, Nur H et al (2015) Controlling the degradation kinetics of porous iron by poly(lactic-co-glycolic acid) infiltration for use as temporary medical implants. Sci Rep 5:11194. doi:10.1038/srep11194

Zberg B, Uggowitzer PJ, Löffler JF (2009) MgZnCa glasses without clinically observable hydrogen evolution for biodegradable implants. Nat Mater 8(11):887–891

Zhang YS, Zhu XM, Zhong SH (2004) Effect of alloying elements on the electrochemical polarization behavior and passive film of Fe–Mn base alloys in various aqueous solutions. Corros Sci 46:853–876

Zhang EL, Chen HY, Shen F et al (2010) Biocorrosion properties and blood and cell compatibility of pure iron as a biodegradable biomaterial. J Mater Sci Mater Med 21:2151–2163

Zhen Z, Xi TF, Zheng YF (2013) A review on in vitro corrosion performance test of biodegradable metallic materials. Trans Nonferrous Met Soc China 23:2283–2293

Zheng YF, Gu XN, Witte F (2014) Biodegradable metals. Mater Sci Eng R Rep 77:1–34

Zhu S, Huang N, Xu L et al (2009) Biocompatibility of Fe–O films synthesized by plasma immersion ion implantation and deposition. Surf Coat Technol 203:1523–1529

Zivic F, Babic M, Grujovic N et al (2012) Effect of vacuum-treatment on deformation properties of PMMA bone cement. J Mech Behav Biomed Mater 5:129–138

Zivic F, Babic M, Grujovic N et al (2013) Influence of loose PMMA bone cement particles on the corrosion assisted wear of the orthopaedic AISI 316LVM stainless steel during reciprocating sliding. Wear 300:65–77

Porous Metals in Orthopedics

Karel Lietaert, Ruben Wauthle and Jan Schrooten

Abstract This chapter aims to bring the reader some knowledge about porous metals and their use in orthopedics in particular. The first section highlights the importance of porous metals. This section is followed by an overview of the different production processes used today. These are divided in two groups: additive and non-additive manufacturing processes. From the first group, selective laser melting and electron beam melting are treated in detail. From the second group, the production processes for Tritanium® and Trabecular Metal™ are explained. The third section gives an overview of the equations which govern the mechanical properties of porous metals. The importance and possibilities of finite element modelling are also considered in this chapter. Hereafter the standards available for testing of porous metals in medicine are described. In the fifth section the most important materials for (porous) orthopedic implants are reviewed. Although biodegradable porous metals are shortly touched in this section, the emphasis is on the bio-inert materials as these comprise the majority of porous implants used today. The sixth section concludes this chapter and points out some practical aspects which need to be considered in the design and production of a porous orthopedic implant.

Keywords Porous metal · Orthopedics · Implant · Scaffold

K. Lietaert (✉)
3D Systems, Grauwmeer 14, 3001 Leuven, Belgium
e-mail: karel.lietaert@3dsystems.com

K. Lietaert
Department of Materials Engineering, KU Leuven,
Kasteelpark Arenberg 44, 3001 Leuven, Belgium

R. Wauthle
FMI Instrumed, De Brauwweg 17, 3125 AE Schiedam,
The Netherlands

J. Schrooten
Antleron, Gaston Geenslaan 1, 3001 Leuven, Belgium

F. Zivic et al. (eds.), *Biomaterials in Clinical Practice*,
https://doi.org/10.1007/978-3-319-68025-5_10

1 Introduction

Today, the number of applications using porous metal implants is increasing at a very high pace. Figure 1 illustrates this increased interest in porous metals by the number of publications found on Pubmed between 1995 and 2013 using the search strings [metals] and [porosity]. Between 2003 and 2013, the number of publications on porous metals has been multiplied by a factor of 10.

This increased interest in porous metal implants is no surprise, given the increased number to total hip replacements, recently called "The operation of the century" (Learmonth et al. 2007). While total hip arthroplasty has become a routine treatment for hip osteoarthritis and as the number of surgical interventions increased from the seventies on, the number of necessary revision operations has also increased.

Revisions are usually necessary in cases of mechanical loosening, infection and instability or dislocation (Bozic et al. 2009). The reason of these failures is often because of polyethylene wear and periprosthetic osteolysis, and since the introduction of metal-on-metal bearings, also because of metallosis (Sundfeldt et al. 2006). When these effects cause large bone defects that cannot be regenerated by the human body, there is a high chance of an aseptic loosening of the implant.

During revision surgery, the surgeon will reconstruct and fill the bone defect with new structures on which the actual revision implant will be attached. These new structures can be autografts, polymethylmethacrylate (PMMA, bone cement) or allografts. Until today, structural bone and compacted grafts are still the gold standard to create a mechanical stable reconstruction in the case of large bone defects. These type of bone grafts have an unmatched performance of withstanding postoperative mechanical loads (Brubaker et al. 2007; Villanueva et al. 2008).

The increased demand for this type of allograft bone in combination with its limited availability, have pushed surgeons towards using artificial bone substitute

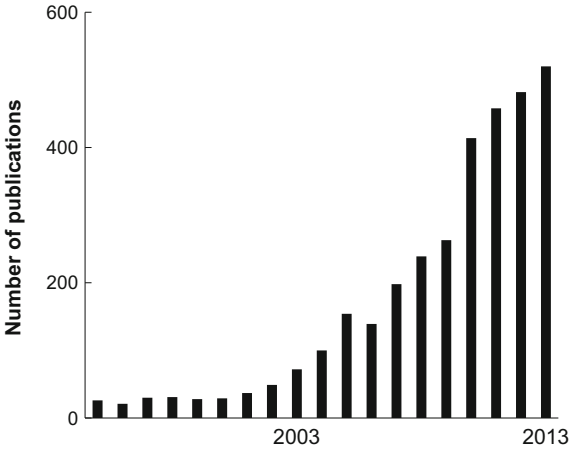

Fig. 1 Number of resulting publications on Pubmed using the search strings [metals] and [porosity]

materials. The requirements for these substitute materials are: (1) the ability to provide initial fixation and (2) the guarantee for long term mechanical stability for surrounding implants.

Porous metals have shown to fulfill these requirements by allowing for bone ingrowth and avoiding stress shielding by reducing the stiffness of the solid metal. On top of that it still provides sufficient strength to be used as bone substitute in load bearing implant applications. The first commercially available porous implants only had a porous coating made out of cobalt-chrome. With the introduction of surgical grade 5 Ti-6Al-4 V, the majority of the porous implants was made out of this material, which is until today the most used material for load bearing implants (Learmonth et al. 2007). Another material that is currently used in porous form, is tantalum (Ta).

This chapter will give a comprehensive overview of the current state of the art of porous metals used as implant materials. In that context, it is intended to be used as a reference for selection of the right porous material, design and production process.

Firstly, this chapter will discuss the most common ways of manufacturing porous metals, with an emphasis on additive manufacturing or 3D printing technologies which currently are available on an industrial scale.

Secondly, this relatively new type of materials needs specific considerations in terms of mechanical testing and validation. This will be the topic of the second and third section in which the mechanical properties and available standards will be discussed. The choice of the material itself will be the next topic that has a significant influence on these mechanical properties, but also on the biological performance. The different materials that are currently available to be used as a porous biomaterial will be listed in this next section.

To conclude, the final section will elaborate on the newly created range of applications made possible by porous metals. This section will also summarize the most influencing factors that should be considered when designing a porous biomaterial.

2 Production

Many different production processes for porous metals exist. Porous metals with closed porosity are of little interest in orthopedics as these do not allow bone ingrowth. Therefore, only production of open porous metals is considered here. The interested reader is referred to (Goodall and Mortensen 2014) for a complete overview. Applications in other medical fields, for example stents in cardiovascular applications, can also be classified as porous metals. However, the term ‘porous metals’ in biomedical engineering is usually limited to orthopedic applications. This section conforms to this convention in order to limit the subjects covered and allow an in-depth analysis of some concepts.

Production processes can be divided in two groups: Additive Manufacturing (AM) and non-additive or traditional manufacturing. An important difference

between these groups is the degree of control over the mesostructure they offer. The mesostructure of a porous material is defined as the structure associated with the porosity and the pores (e.g. pore size, shape and interconnectivity). The length scale of the mesostructure is smaller than the part dimensions (macrostructure) but larger than the dimensions governing material properties (microstructure) (Goodall and Mortensen 2014). The possibility to change the mesostructure of porous metals is what makes them more difficult but at the same time more interesting to work with than non-porous metals.

AM production processess are defined by ASTM as 'a process of joining materials to make objects from 3D model data, usually layer upon layer, as opposed to subtractive manufacturing methodologies' (ASTM 2012). These technologies have been developed in the last two decades. They allow a precise control of the mesostructure of porous materials by precise placement of the struts. This means that porous metals with a regular structure, i.e. a repetition of a certain unit cell in 3D, can be produced with this technology. These production processes also enable the production of patient-specific implants and functionally graded structures (e.g. variation of porosity throughout the implant) (Rotaru et al. 2015; Hazlehurst et al. 2014). These are some of the reasons for the growing application of AM technology in production of (porous) orthopedic implants.

Production processes in the non-AM group have been available longer than AM technology and include for example casting, sintering, foaming and chemical vapour deposition (e.g. Trabecular Metal™, Zimmer, explained below). The different processes enable a different level of control of the mesostructure but it is in general lower than for AM processes. Porosity and pore size can usually be controlled to be in a certain range. Some production processes can guarantee 100% open or closed porosity, whereas others always lead to a mixture of both. The shape of the pores (equivalent to a unit cell in AM) is more difficult to control and here non-AM processes are at a disadvantage compared to AM processes (Campoli et al. 2013). Despite these limitations, non-AM processes have their own advantages. Their lower cost, broader material range and the possibility to produce smaller pore sizes are only some examples. Many of these production processes have been used for decades already but are developed further or used for new materials nowadays.

In the group of metal AM technologies, Selective Laser Melting (SLM) and Electron Beam Melting (EBM) are the dominant production processes and will be covered here (Frazier 2014). Figure 2a, b show a schematic representation of SLM and EBM, respectively. Both SLM and EBM are powder bed based processes and start with the deposition of one powder layer on a solid build plate. The thickness of this powder layer is in the range of tens of microns. After layer deposition, the energy source selectively melts the powder (only where needed, based on the CAD file of the product). By partly remelting the previous layer every time a layer is scanned, a connection between different layers is formed. After scanning one layer, the build platform is lowered by exactly one layer thickness. Thereafter, a new powder layer is deposited and the process repeats.

SLM and EBM machines have a lot in common but there are also important differences. In SLM, the energy source is a laser beam. In the present generation of SLM machines, a fiber laser is used and the power output can vary between 100 W

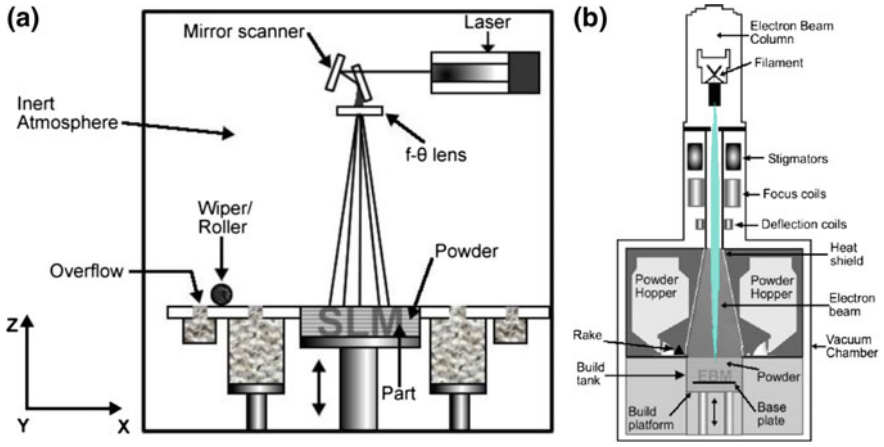

Fig. 2 **a** Schematic of the SLM process (Sidambe 2014). **b** Schematic of the EBM process (Sidambe 2014). These images are distributed under the Creative Commons Attribution License by their original creators. More information can be found on: https://creativecommons.org/licenses/by/4.0/

and 1 kW. Machines with more than one laser are available. These can scan different regions of the build platform and thus increase the build rate [up to 105 cc/h (SLM Solutions 2015)]. An inert gas atmosphere fills the SLM process chamber during production in order to prevent oxidation of the powders. This technology is available under different commercial names: LaserCusing (Concept Laser), Selective Laser Melting (SLM Solutions), Direct Metal Laser Sintering (EOS), Direct Metal Printing (3D Systems) etc. EBM machines use an electron beam as power source. These machines are commercialized by only one manufacturer: Arcam AB (controlled by General Electric since 2016). The electron beam provides up to 3 kW of power (Arcam AB 2015). The EBM process takes place in a vacuum chamber because the presence of gas molecules would lead to scattering of the electron beam and thus disturb the process (Hiemenz 2007). As stated above, both SLM and EBM enable a high degree of control of the porous metal's mesostructure. Figure 3a, b show some examples.

The group of non-AM processes has mostly been used to produce coatings on non-porous implants. However, some important clinical 'stand-alone' porous metallic products are manufactured with these processes as well. Examples of these are Regenerex® (Biomet), Biofoam® (Wright Medical Technology), Gription® (Depuy) and Trabecular Metal™ (TM, Zimmer) (Levine 2008). As an example, the production process for a porous coating (Tritanium®, Stryker) and one'stand-alone' porous structure (TM, Zimmer) are explained here.

The production of Tritanium® starts with a polyurethane foam. The mesostructure of this foam is important for the properties of the final metal product. Via low-temperature arc vapor deposition, commercial purity Ti (cpTi) is deposited on the struts of the polyurethane foam. The coated polyurethane foam is placed on

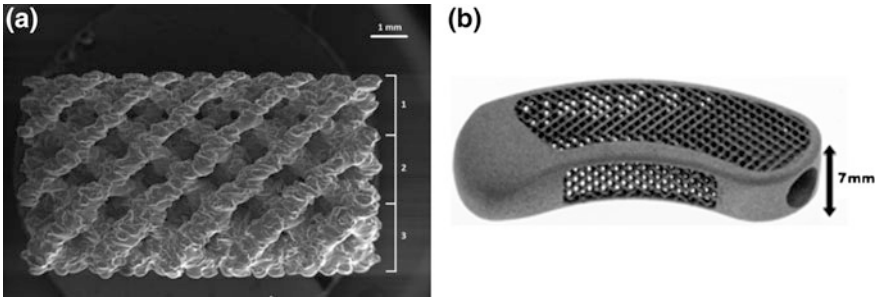

Fig. 3 **a** Porous Ti6Al4V EBM sample (van Grunsven et al. 2014). This image is distributed under the Creative Commons Attribution License by its original creators. More information can be found on: https://creativecommons.org/licenses/by/4.0/. **b** Spinal Ti6Al4V implant with porous structure for bone ingrowth produced by SLM (property of 3D Systems, LayerWise NV, Belgium)

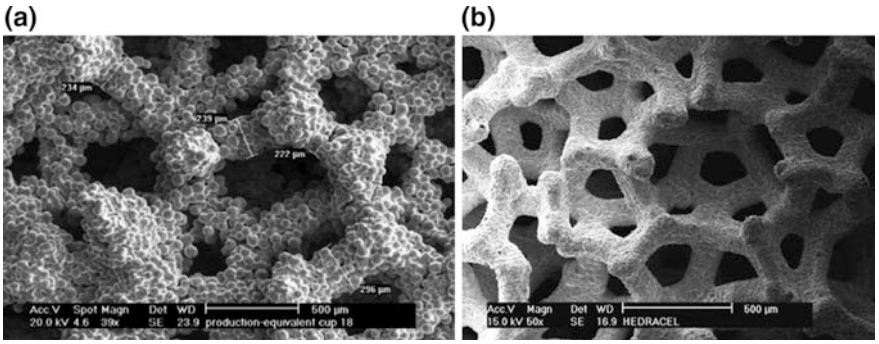

Fig. 4 **a** Tritanium® surface with indication of strut size (Muth et al. 2012). **b** Porous Ta (Muth et al. 2012). These images are distributed under the Creative Commons Attribution License by their original creators. More information can be found on: https://creativecommons.org/licenses/by/4.0/

the substrate where the final Tritanium® coating should adhere to, the whole is placed in a vacuum furnace and goes through a sintering cycle. During this cycle, the polyurethane is burnt out and the connection between different cpTi particles on one hand and the coating and the substrate on the other hand, is formed. Next, a polymeric binder is applied to the implant and a new sintering cycle is performed. The binder improves the connection between the cpTi particles and is volatilized in the sintering cycle. After the sintering cycle, the density of the cpTi struts and the connection between the coating and the substrate have improved. Depending on the requirements the implant should satisfy, more coating and sintering steps can be applied. Machining of the implant after coating is also possible. Figure 4a) shows a Scanning Electron Microscopy image of a Tritanium® coating with indication of the strut size (Muth et al. 2012).

The production of TM was invented and patented by Ultramet and later applied by Implex (now Zimmer) for orthopedic applications (Lefebvre 2013; Kaplan 2000). The process also uses a polyurethane foam as starting material. This foam is impregnated with a carbonaceous liquid and subjected to a thermal cycle in order to cure and crosslink the liquid and eventually react to form vitreous carbon (Stankiewicz 2000). This carbon foam is placed in a reaction chamber and Ta is deposited on its surface by chemical vapor deposition. The struts gain strength and stiffness by the formation of a Ta layer on their surface. The mesostructure of TM can be controlled by changing the polyurethane foam, the vitreous carbon production process and the Ta deposition time (Kaplan 2000). The resulting material is typically 75-85% porous and consists of 1 wt% of vitreous carbon and 99 wt% of Ta (Zardiackas et al. 2001). Figure 4b shows the mesostructure of TM.

3 Mechanical Properties

Bone is a porous structure with mechanical properties that vary widely depending on age, sex, physical activity, disease etc. Cortical bone has a strength between 52 and 219 MPa and a stiffness between 7.1 and 27.6 GPa. Trabecular bone has much lower mechanical properties: a strength between 1.6 and 3.9 MPa and stiffness between 0.1 and 10.4 GPa (Alvarez and Nakajima 2009). Bone constantly goes through a remodeling cycle and adapts itself to the environment. Wolff's law describes the response of bone to mechanical stimulus: regions that experience a high load strengthen while a lack of load leads to bone resorption. In addition to the possibility of bone ingrowth, this is the main reason to incorporate porosity in an orthopedic implant. The distribution of load between the implant and the surrounding bone is governed by their elastic modulus. A stiffer implant carries a larger share of the total load. Given an elastic modulus of around 110 GPa for Ti alloys, 240 GPa for CoCr and 185 GPa for Ta, a significant modulus mismatch ($E_{implant} \gg E_{bone}$) is to be expected for non-porous implants (Chen and Thouas 2015; Thijs et al. 2013). This can lead to bone resorption around the implant and ultimately implant loosening. The incorporation of porosity in metal implants grants an additional level of control of the mechanical properties and leads to a better match between implant and bone.

The most general laws describing the mechanical properties of open porous metals (compression) were described by Gibson and Ashby (G&A) (Gibson and Ashby 1999):

$$\frac{E^*}{E_s} = C_1 \left(\frac{\rho^*}{\rho_s}\right)^n \tag{1}$$

$$\frac{\sigma^*_{pl}}{\sigma_{ys}} = C_2 \left(\frac{\rho^*}{\rho_s}\right)^m \tag{2}$$

With $C_1 = 1$, $n = 2$, $C_2 = 0{,}3$ and $m = 3/2$. The properties of the porous metal are denoted by the superscript * and the properties of the strut material by the subscript s. E = elastic modulus, ρ = density, σ_{ys} = yield strength and σ_{pl} = plastic collapse strength.

Equations (1) and (2) have been determined based on the application of engineering beam theory on a cubic unit cell with elastic-ideally plastic struts with a square cross-section. These assumptions restrict the applicability of the equations. Experimentally observed values are mostly in the expected order of magnitude although the constant C and exponent n or m are generally different from G&A's values. Many other analytical models for the mechanical properties of porous metals exist but the basic Eqns. (1) and (2) remain widely used (Goodall and Mortensen 2014).

In order to overcome the limitations of analytical models, Finite Element Modeling (FEM) of the mechanical properties of porous metals has also been undertaken (Boccaccio et al. 2011; Lacroix et al. 2009). The combination of FEM and AM can be a very powerful approach as these manufacturing technologies allow the production of samples with exactly the same geometry as the CAD model used for FEM. A comparison of the output of FEM and experimental results from these AM based porous metals can lead to an optimized FEM model and thus a better prediction of the mechanical properties of porous implants (Campoli et al. 2013). An extension of this approach is the design and production of porous metals with a gradient in porosity. These lead to an improved match between the implant and the expected biomechanical load (Wieding et al. 2014; Razi et al. 2012).

Scaffold geometry has much more influence on bone regeneration than only via the mechanical properties of the scaffold. As recently reviewed by A. Zadpoor, different features of a scaffold can be optimized in order to improve bone regeneration (Zadpoor 2015). The influence of pore size has been recognized for some time already, as well as the need for interconnected porosity (Karageorgiou and Kaplan 2005). More recently, it has been shown that also scaffold curvature controls the response of bone forming cells: the tissue growth process is accelerated on surfaces with a higher curvature and favors concave over convex surfaces (Knychala et al. 2013; Bidan et al. 2012; Bidan et al. 2013a, b; Rumpler et al. 2008; Gamsjager et al. 2013; Ripamonti and Roden 2010; Ripamonti et al. 2012). It has also been shown that the pore shape of a scaffold influences the inflammatory response of cells in an in vitro environment (Almeida et al. 2014). However, it is unclear which geometrical feature is responsible for this effect. An FEM toolbox which allows modeling of mechanical as well as other properties can be used to design new porous metal architectures (mesostructure) with optimized properties. These can satisfy the often conflicting requirements better than present porous metal architectures (Giannitelli et al. 2014).

4 Medical Device Testing for Porous Metals

Only a few years ago the first ISO standard was published for mechanical testing of cellular metals (ISO 2011), regardless of the material or manufacturing method. Also, new ASTM standards have been established for solid Ti6Al4V processed using AM. These specify the static mechanical properties (ASTM 2014), but no standards yet exist that specify evaluation methods or minimum requirements to what additively manufactured porous implants have to comply.

The broad range of influencing factors definitely complicates standardization, but the more the mechanical behavior of these porous metals is known, the more it helps to set rules and regulations. A relatively fast and easy way to assess and investigate the quality or behavior of porous structures used for implants is by doing compression tests. However, destructive testing of all possible variations is rather time consuming and costly.

In order to reduce the amount of experiments, finite element and analytical models have been developed that accurately can predict the mechanical properties of cellular structures made by AM (Campoli et al. 2013; Smith et al. 2013; Ahmadi et al. 2014), but still some amount of experimental data is necessary to 'calibrate' or validate these models. Also, these models cannot be used currently to evaluate actual processing characteristics or post-treatments. Nevertheless, these models are considered as potentially very valuable tools for porous implant performance simulations.

For a complete understanding of the mechanical behavior of porous metals, Fig. 5 shows a typical stress-strain curve of a porous Ti6Al4 V and CP Ti structure under compression. Porous CP Ti deforms continuously without fracture, while Ti-6Al-4V ELI shows signs of a local fracture, after reaching a first maximum

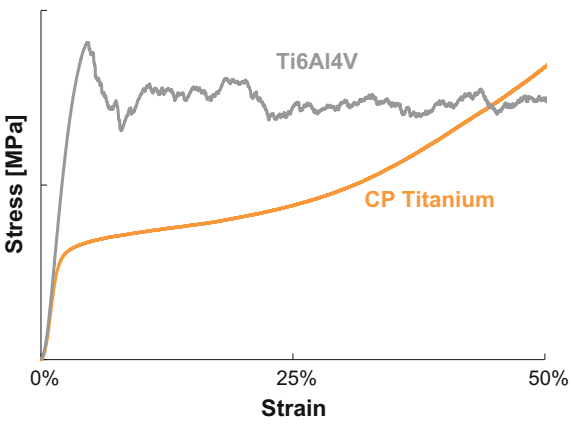

Fig. 5 Typical stress-strain curves under a compressive load for a material with a local maximum (e.g. Ti6Al4V) and for a material with continuous deformation (e.g. Tantalum, CP Ti). Picture created with data from (Wauthle 2014)

compression point. The architecture of the porous construct holds the structure together, while it continues to deform until all the struts fail. This compressive failure behavior continues until a plateau is reached and full compression occurs.

For metallic plasma sprayed coatings, however, an FDA guidance document exists that specifies required information on microstructure and mechanical properties. Today, this guidance is sometimes used for evaluating additively manufactured implants, but the FDA is currently also working on a guidance document for additive manufacturing of medical devices (FDA 2016).

In the end, it is still the medical device specific standards for testing that remain applicable when porous biomaterials are used as (part of) an implant. For intervertebral body fusion devices for example, the standard ASTM F2077 is available.

5 Materials

Metals used for biomedical applications can be divided into two groups: bio-inert and biodegradable. The most important bio-inert metals are stainless steels, Ti alloys, NiTi, Ta and CoCr. These metals have been used in clinical practice for several decades in both porous and non-porous form. Biodegradable metals have been studied intensively recently, with a focus on Mg alloys and Fe alloys. The interested reader is referred to (Chen and Thouas 2015) and (Helsen and Missirlis 2010) for a more complete overview of the different metallic biomaterials and their properties (non-porous).

Stainless steels are very important materials in industrial applications and have non-surprisingly made the transition from industrial to biomedical applications. The most basic biomedical stainless steel is AISI 316L. This material is based on AISI 302 stainless steel but has an improved corrosion resistance due to the addition of 2.0–3.0% Mo, an increase of the Ni content to 12.0–15.0% and a decrease of the C content below 0.030%. Despite these modifications, localized corrosion and stress corrosion cracking are not prevented entirely. However, the material is still widely used due to its much lower cost than for example Ti alloys and CoCr. The corrosion of 316L is especially problematic due to its high Ni content, which can be toxic when released in the human body. In order to overcome this limitation, Ni-free stainless steels have been developed. Nitrogen is the most promising element to replace Ni in stainless steels (Sumita et al. 2004). Research efforts concentrate on the Fe–Cr–Mn–Mo–N system. It has been shown that alloys from this system can reach higher strength and improved corrosion resistance compared to 316L. In combination with new surface modification processes for stainless steels, this research track could lead to a renewed interest in stainless steels for biomedical applications (Talha et al. 2013). These nickel-free stainless steels have also been produced in porous form and can be engineered to have mechanical properties close to those of human bone (Alvarez et al. 2008).

Pure Ti and Ti alloys are extensively used in orthopedics today due to their high strength, relatively low elastic modulus, corrosion resistance and biocompatibility.

Based on the dominant crystal structure, different kinds of titanium alloys can be distinguished: α, α + β and β. Titanium exhibits a hexagonal close-packed crystal structure (α) at room temperature and a body centered cubic crystal structure (β) above 1155 K. Depending on the alloying elements added to Ti and the thermal history of the material, the β phase can be stabilized to a greater or lesser extent. This leads to a different crystal structure and different mechanical properties of the material. The extensive possibilities to control Ti alloy chemistry, crystal structure and microstructure have led to a variety of alloys with different mechanical properties in orthopedics today, see Table 1 (more information in Geetha et al. 2009).

The success of porous Ti and its alloys for orthopedic applications has led to the development of a whole range of production processes (Li et al. 2014). Most commercially available products are based on a non-AM production process. Examples include Tritanium® (Stryker, Cp Ti), Biofoam® (Wright Medical Technology, Cp Ti), Regenerex® (Biomet, Ti alloy), Gription® (Depuy, Cp Ti) and Stiktite™ (Smith and Nephew, Cp Ti) (Levine 2008; Levine and Fabi 2010; Smith & Nephew 2015; Muth et al. 2012). However, as both the metal AM market and the share of medical devices in this market are growing strongly, more and more AM based Ti implants will be used in the future (Wohlers 2013; Roland Berger 2013).

Ta is used mostly in porous form and in rather small implants due to its high elastic modulus, high density and high price (Wauthle et al. 2015b). It is commercially available only from Zimmer in the TM product line (production process explained above) and is used in hip, knee, spinal and other orthopedic applications (Issack 2013; Dunbar et al. 2001; Sinclair et al. 2012; Frigg et al. 2010). Over the years, the material has proven to be non-toxic, corrosion-resistant and osteoconductive but does not outperform Ti-6Al-4V (Jafari et al. 2010). Recently AM of porous Ta for biomedical applications has been reported (SLM) (Wauthle et al. 2015b). This evolution could lead to a wider application of porous Ta in orthopedics in the near future.

Table 1 Mechanical properties of pure Ti and some important Ti alloys

Alloy	Yield strength (MPa)	Stiffness (GPa)	Type	References
CpTi, grade 1	170	115	α	ASTM (2013e, F67), Davis & Associates (2003)
Ti-6Al-4V ELI	760–795	110	α + β	ASTM (2013a, F136, 2013d, F3001), Davis & Associates (2003)
Ti-6Al-7Nb	900–1050	105	α + β	ASTM (2011), Davis & Associates (2003)
Ti-13Nb-13Zr	973–1037	79–84	β	ASTM (2013b, F1713), Davis & Associates (2003)
Ti-12Mo-6Zr-2Fe	1060–1100	74–85	β	ASTM (2013c, F1813), Davis & Associates (2003)

Recently, additive manufacturing of porous tantalum-titanium alloys was reported. Researchers were able to make these alloys with a non-powder bed based additive manufacturing system (Laser Powder Deposition, LPD). This technology allows mixing and deposition of elemental powders to make alloys. This makes LPD more versatile and flexible than SLM and EBM in this aspect as these technologies mostly use pre-alloyed powders. However, the importance of LPD in the production of porous metals for orthopedic applications is very limited compared to SLM and EBM. The cell growth on the porous tantalum-titanium alloys was shown to increase with Ta content. In addition, the relatively easy control of the alloy composition allows control of the elastic modulus. This might lead to the production of porous metallic implants which show the biological performance of pure Ta without costing as much or having as high an elastic modulus as pure Ta (Fuerst et al. 2015).

NiTi (48–52 wt% Ni) is used in orthopedics today due to its relatively low elastic modulus, biocompatibility, corrosion resistance and two other remarkable properties: the Shape Memory Effect (SME) and PseudoElasticity (PE). The SME allows the material to be permanently deformed but recover its initial shape upon heating. PE can only occur in a specific temperature range and allows the material to recover large strains upon removal of the load, without thermal activation (Jani et al. 2014). These effects are used in different medical fields: orthopedic, orthodontic, vascular and neurosurgical applications exist (Petrini and Migliavacca 2011). So far, porous NiTi production has been based on powder metallurgy only. Both AM and non-AM production processes have been used (Speirs et al. 2013; Bansiddhi et al. 2008). Porous NiTi has been commercially available for spinal fusion since 2002 (Actipore™, Biorthex) (Bansiddhi et al. 2008).

CoCr is used in total joint replacements because of its high corrosion, wear and fatigue resistance. These properties are strongly influenced by the production process used to manufacture the implant (e.g. casting vs. forging) (Chen and Thouas 2015). Non-AM production processes are limited to porous coatings with a porosity of around 30–50%, no production of ‘standalone’ porous CoCr structures with these processes has been reported so far (Levine and Fabi 2010). These coatings on non-porous implants improve implant fixation by bone ingrowth and have been highly successful in hip surgery (Babis and Mavrogenis 2013). Recently, AM of CoCr has been reported by both SLM and EBM (Hazlehurst et al. 2013, Mater Des) (Kircher et al. 2009). Open porous structures have been studied and opportunities for functionally graded hip stems with limited stress shielding are under development (Hazlehurst 2013, Mater Des) (Hazlehurst 2013, Med Hypotheses).

Ceramics and polymers dominate the degradable biomaterials category today but both material classes have their limitations. Pure ceramics are often too brittle for convenient use and pure polymers have insufficient strength for most orthopedic applications. In addition, sterilization of these polymers is not as easy as for other material classes (Eglin and Alini 2008). This reduces the ease of handling and thus restricts their use. Moreover, the degradation mechanism of most of the biodegradable polymers is based on hydrolysis (e.g. poly lactic acid based

materials) and leads to acidification of the local environment (Doppalapudi et al. 2014). This is a complex process, making it difficult to predict the degradation rate of a device in a particular application (Wuisman and Smit 2006). Intensive research on this subject is ongoing and some promising approaches under development (e.g. polymer-ceramic composites) (Straley et al. 2010; Woodruff et al. 2012; Doppalapudi et al. 2014). However, no optimal solution has been found yet, especially for load-bearing applications (Ambrose et al. 2015). In order to overcome the limitations of ceramics and polymers for certain orthopedic applications, research efforts into biodegradable metals have expanded considerably the last few years (Hermawan 2012).

Most of the research on biodegradable metals has focused on Mg alloys so far. This has resulted in the near-commercialization of some Mg based products. The Chinese magnesium alloy producer Eontec plans to start clinical trials for its biodegradable Mg product in 2015. It leads a large Chinese Research and Development consortium named 'Strategic Alliance for Technology Innovation of the Medical Magnesium Alloy Industry' and has contacts with the German company AAP Implantate, also involved in biodegradable Mg research (PR Newswire 2015). Other companies are already closer to approval of their product: clinical trials for a Mg-based biodegradable stent (Drug Eluting Absorbable Metal Scaffold, Biotronik) are ongoing and a pilot study on a compression screw (Magnezix®, Syntellix) has shown promising results (Haude et al. 2013; Windhagen et al. 2013).

The high degradation rate of most biomedical Mg alloys prevents a real breakthrough of this material for now, especially when used in open porous form (Zheng et al. 2014; Lietaert et al. 2013). The high degradation rate has two important effects. First, a high degradation rate leads to an untimely loss of mechanical loading capacity. Second, fast degradation can lead to the accumulation of degradation products (e.g. H_2 gas) in the surrounding tissue (Kaya et al. 2007). Many attempts to reduce the degradation rate by alloying have been undertaken. These include alloying Mg with Al, Ca, Li, Mn, Zn, Zr, Sr, rare earth elements and combination of these (Ding et al. 2014). All these elements influence the degradation rate but also the mechanical properties and the biocompatibility of the resulting alloy. Despite these attempts, no satisfactory solution has been found so far. Research into new production processes for Mg and its alloys is ongoing and might overcome the current limitations. For example, SLM of Mg on a lab-scale has been reported and could lead to new microstructures and thus an adapted degradation rate (Ng et al. 2010; 2011a, b; Zhang et al. 2012; Gieseke et al. 2013; Wei et al. 2014). Other options to reduce the degradation rate exist as well, for example the application of a coating (Hornberger et al. 2012). Maybe a combination of different measures to control the degradation rate will result in a breakthrough of Mg alloys in medicine in the future.

Fe-based materials are under development as an alternative to Mg alloys. Cardiovascular applications have received most of the research efforts so far with a recent animal study on nitrided iron stents as a provisional endpoint (Feng et al. 2013). Research into orthopedic applications of porous Fe alloys is ongoing (Orinakova et al. 2013). Here also, the development of AM production processes

might lead to new possibilities (Song et al. 2014). Zn-based materials and Bulk Metallic Glasses are also being researched but are still further from clinical practice (Gong et al. 2015; Kaur et al. 2014).

6 Applications and Conclusions

Metal additive manufacturing is here to stay and will definitely change the future of implant manufacturing. One of the greatest advantages is the almost unlimited design freedom that allows to create regular open porous structures that can be used as functional implants.

Porous metal implants have been of interest for many years now because they avoid stress-shielding effects by a lower stiffness, but still provide sufficient mechanical strength. On top of that, they ensure a good initial fixation by the high coefficient of friction and a long-term stability by the ability of bone ingrowth into the open porosity.

Figures 6 and 7 show the traditional material selection charts for the strength and the Young's modulus versus the density but now updated with experimental results

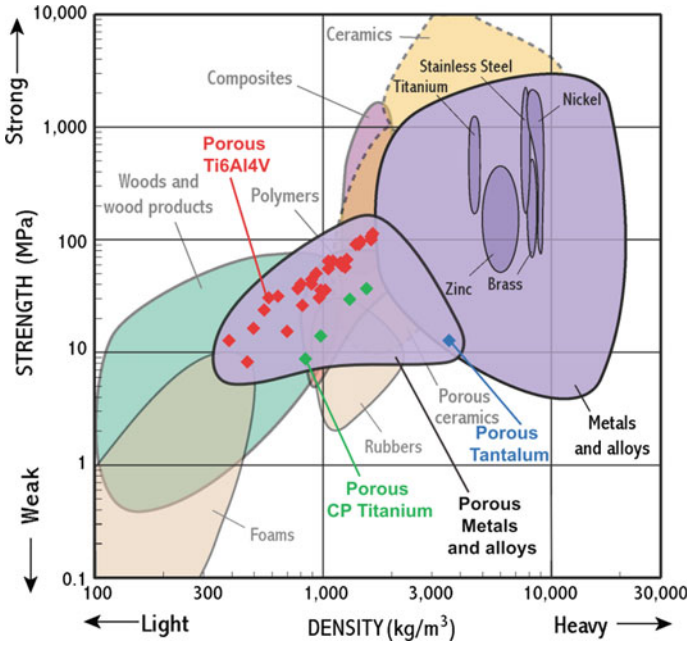

Fig. 6 Material selection chart for the combination of strength and density. All reported results in this dissertation for the yield strength of porous metallic implants are displayed as *red* (porous Ti6Al4V), *green* (CP Titanium) and *blue* (Tantalum) *diamond markers*. Chart obtained and reprinted with permission from (Wauthle 2014)

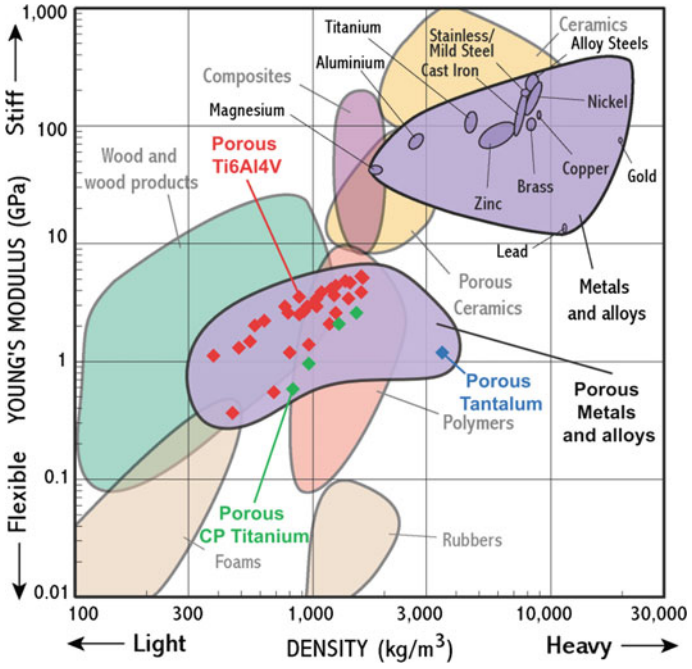

Fig. 7 Material selection chart for the combination of Young's modulus and density. All reported results in this dissertation for the stiffness of porous metallic implants are displayed as *red* (porous Ti6Al4V), *green* (CP Titanium) and *blue* (Tantalum) *diamond markers*. Chart obtained and reprinted with permission from (Wauthle 2014)

of porous titanium and tantalum reported previously (Wauthle 2014). It is clear from these figures that the application range of these metals has been extended by new regions that have been defined by these porous metals. For the strength, this new region ranges from the traditional foams to the solid metals fully overlapping the polymer application range (Fig. 6). The new stiffness values start from the foams and partly overlap with the polymers, but are still an order of magnitude lower compared to the solid metals (Fig. 7).

These updated material selection graphs can be useful tools in selecting the right material and density for a certain implant application. But regardless of the mechanical design requirements, there are a lot of other conditions that should be considered while choosing the right porous metal for implants:

The porous implant design

It all starts with designing a porous implant. Additive manufacturing techniques allow for almost full design freedom, but changing the porous implant architecture in combination with a certain material, will affect the mechanical properties and bone regeneration performance.

Increasing the **structure relative density** of porous implants increases the static mechanical properties like the yield strength, maximum strength and stiffness by a more than linear relationship. The fatigue strength also increases with an increasing structure relative density, and this is linearly related to the static mechanical properties.

The load that porous implants have to withstand has in general multiple directions and therefore it is suggested to use isotropic unit cell designs like the diamond or rhombic dodecahedron, although they have slightly lower strength.

The selected **implant material** influences both the mechanical and biological performance. For statically loaded applications, porous Ti6Al4 V is still the material of choice, but since both tantalum and pure titanium have a purely ductile deformation behavior, these metals exhibit an excellent fatigue behavior. Other biodegradable metals like Mg and Fe are still under development.

The characteristics of the manufacturing process

Every manufacturing technique has its limitations and proper knowledge about the characteristics of the manufacturing process allows to manufacture porous implants with reproducible and uniform mechanical properties.

Regardless of the structure relative density, the unit cell design, the material and the build orientation, additive manufacturing is able to manufacture porous implants with high **reproducibility** of the mechanical properties. In most cases, the standard deviation is less than 5% of the mean value. Horizontal struts should be avoided during additive manufacturing. Improper selection of the **build orientation** can result in inferior mechanical properties (Wauthle et al. 2015a).

Post-processing operations

Once a porous implant is manufactured, many post-processing operations can be applied in order to change or optimize the mechanical or bone regeneration properties. **Heat treatments** change the microstructure and the corresponding mechanical properties of porous metallic implants. If certain conditions are met, bone will grow into porous implants made out of a biocompatible metal. **Bio-functionalizing surface treatments or growth factors** can speed up the process of bone regeneration and implant fixation.

Production cost

Eventually, at some point the material and manufacturing cost needs to be taken into account when considering serial manufacturing of porous metallic implants. Titanium and titanium alloys are relatively **cheap materials** and are easy to (post-) process. Tantalum, on the other hand, is up to 20 times more expensive for the same volume and is difficult to post-machine. Therefore, the use of tantalum for porous implants will be mostly limited to small sized applications.

Additive manufacturing techniques are often associated with being a slow and costly way of manufacturing, but recent developments show that these technologies can be successfully used in an economic way to produce porous metals (Wauthle 2014)

Acknowledgements Karel Lietaert would like to acknowledge the support of the agency for Innovation by Science and Technology (IWT) of the Flemish government through Baekeland mandate 'IWT140257'.

References

Ahmadi SM, Campoli G, Amin Yavari S et al (2014) Mechanical behavior of regular open-cell porous biomaterials made of diamond lattice unit cells. J Mech Behav Biomed Mater 34C:106–115

Almeida CR, Serra T, Oliveira MI et al (2014) Impact of 3-D printed PLA-and chitosan-based scaffolds on human monocyte/macrophage responses: unraveling the effect of 3-D structures on inflammation. Acta Biomater 10:613–622

Alvarez K, Sato K, Hyun SK et al (2008) Fabrication and properties of Lotus-type porous nickel-free stainless steel for biomedical applications. Mater Sci Eng, C 28:44–50

Alvarez K, Nakajima H (2009) Metallic scaffolds for bone regeneration. Mater 2:790–832

Ambrose CG, Hartline BE, Clanton TO et al (2015) Polymers in orthopaedic surgery. In: Puoci F (ed) Advanced polymers in medicine, 1st edn. Springer International Publishing Switzerland, Cham, pp p129–p145

Arcam AB (2015) Arcam A2X—Setting the standard for additive manufacturing. http://www.arcam.com/wp-content/uploads/arcam-a2x.pdf. Accessed 18 Feb 2015

ASTM (2011) F1295-11: Standard specification for wrought titanium-6aluminium-7niobium alloy for surgical implant applications

ASTM (2012) F2792-12a: standard practice for reporting data for test specimens prepared by additive manufacturing

ASTM (2013) F136-13: standard specification for wrought titanium-6aluminium-4vanadium eli (extra low interstitial) alloy for surgical implant applications

ASTM (2013) F1713: standard specification for wrought titanium-13niobium-13zirconium alloy for surgical implant applications

ASTM (2013) F1813-13: standard specification for wrought titanium-12molybdenum-6zirconium-2iron alloy for surgical implant

ASTM (2013) F3001-13: standard specification for additive manufacturing titanium-6aluminium-4vanadium eli (extra low interstitial) with powder bed fusion

ASTM (2013) F67-13: standard specification for unalloyed titanium, for surgical implant applications

ASTM (2014) F2924: standard specification for additive manufacturing titanium-6 aluminum-4 vanadium with powder bed fusion

Babis GC, Mavrogenis AF (2013) Cobalt-chrome porous-coated implant-bone interface in total joint arthroplasty. In: Karachalios T (ed) Bone-implant interface in orthopedic surgery, 1st edn. Springer, London, pp p55–p65

Bansiddhi A, Sargeant TD, Stupp SI et al (2008) Porous NiTi for bone implants: a review. Acta Biomater 4:773–782

Bidan CM, Kommareddy KP, Rumpler M et al (2012) How linear tension converts to curvature: geometric control of bone tissue growth. PLoS One 7

Bidan CM, Kommareddy KP, Rumpler M et al (2013a) Geometry as a factor for tissue growth: towards shape optimization of tissue engineering scaffolds. Adv Healthc Mater 2:186–194

Bidan CM, Wang GM, Dunlop JW (2013b) A three-dimensional model for tissue deposition on complex surfaces. Comput Method Biomechanic Biomed Eng 16:1056–1070

Boccaccio A, Ballini A, Pappalettere D et al (2011) Finite element method (FEM), mechanobiology, and biomimetic scaffolds in bone tissue engineering. Int J Biol Sci 26:112–132

Bozic KJ, Kurtz SM, Lau E et al (2009) The epidemiology of revision total hip arthroplasty in the United States. J Bone Joint Surg Am 91:128–133

Brubaker SM, Brown TE, Manaswi A et al (2007) Treatment options and allograft use in revision total hip arthroplasty: the acetabulum. J Arthrop 22:52–56
Campoli G, Borleffs MS, Amin Yavari S et al (2013) Mechanical properties of open-cell metallic biomaterials manufactured using additive manufacturing. Mater Des 49:957–965
Chen Q, Thouas GA (2015) Metallic implant biomaterials. Mater Sci Eng, R 87:1–57
Davis & Associates (2003) Metallic materials. In: Davis JR (ed) Handbook of materials for medical devices, 1st edn. ASM International, Materials Park OH, pp 21–50
Ding Y, Wen C, Hodgson P et al (2014) Effects of alloying elements on the corrosion behavior and biocompatibility of biodegradable magnesium alloys: a review. J Mater Chem B 2:1912–1933
Doppalapudi S, Jain A, Khan W et al (2014) Biodegradable polymers—an overview. Polym Advan Technol 25:427–435
Dunbar MJ, Wilson DAJ, Hennigar AW et al (2001) J Bone Joint Surg Am 91:1578–1586
Eglin D, Alini M (2008) Degradable polymeric materials for osteosynthesis: tutorial. Eur Cell Mater 16:81–90
FDA (2016) 3D printing of medical devices. http://www.fda.gov/MedicalDevices/ProductsandMedicalProcedures/3DPrintingofMedicalDevices/default.htm. Accessed 29/8/2016
Feng Q, Zhang D, Xin C et al (2013) Characterization and in vivo evaluation of a bio-corrodible nitride iron stent. J Mater Sci—Mater Med 24:713–724
Frazier WE (2014) Metal additive manufacturing: a review. J Mater Eng Perf 23:1917–1928
Frigg A, Dougall H, Boyd S et al (2010) Can porous tantalum be used to achieve ankle and subtalar arthrodesis? A pilot study. Clin Orthop Relat R 468:209–216
Fuerst J, Medlin D, Carter M et al (2015) LASER additive manufacturing of titanium-tantalum alloy structured interfaces for modular orthopedic devices. JOM 64:775–780
ISO (2011) 13314: Mechanical testing of metals—ductility testing—compression test for porous and cellular metals
Gamsjager E, Bidan C, Fischer F et al (2013) Modelling the role of surface stress on the kinetics of tissue growth in confined geometries. Acta Biomater 9:5531–5543
Geetha M, Singh AJ, Asokamani R et al (2009) Ti based biomaterials, the ultimate choice for orthopaedic implants—a review. Prog Mater Sci 54:397–425
Giannitelli SM, Accoto D, Trombetta M et al (2014) Current trends in the design of scaffolds for computer-aided tissue engineering. Acta Biomater 10:580–594
Gibson LJ, Ashby MF (1999) Cellular solids—structure and properties. Cambridge University Press, Cambridge
Gieseke M, Noelke C, Kaierle S et al (2013) Selective laser melting of magnesium and magnesium alloys. Paper presented at the magnesium technology conference, San Antonio TX, 3–7 March 2013
Gong H, Wang K, Strich R et al (2015) In vitro biodegradation behavior, mechanical properties, and cytotoxicity of biodegradable Zn-Mg alloy. J Biomed Mater Res B 103:1632–1640
Goodall R, Mortensen A (2014) Porous Metals. In: Laughlin D, Hono K (eds) Physical metallurgy, 5th edn. Elsevier, Amsterdam, pp p2399–p2596
Haude M, Erbel R, Erne P et al (2013) Safety and performance of the drug-eluting absorbable metal scaffold (DREAMS) in patients with de-novo coronary lesions: 12 months results of the prospective, multicenter, first-in-man BIOSOLVE-I trial. Lancet 381:836–844
Hazlehurst KB, Wang CJ, Stanford M (2013a) The potential of a cobalt chrome molybdenum femoral stem with functionally graded orthotropic structures manufactured using Laser Melting technologies. Med Hypotheses 81:1096–1099
Hazlehurst KB, Wang CJ, Stanford M (2013b) Evaluation of the stiffness characteristics of square pore CoCrMo cellular structures manufactured using laser melting technology for potential orthopedic applications. Mater Des 51:949–955
Hazlehurst KB, Wang CJ, Standford M (2014) An investigation into the flexural characteristics of functionally graded cobalt chrome femoral stems manufactured using selective laser melting. Mater Des 60:177–183
Helsen JA, Missirlis Y (2010) Biomaterials—a tantalus experience. Springer, Heidelberg

Hermawan H (2012) Biodegradable metals—from concept to applications. Springer, Heidelberg
Hiemenz J (2007) Electron beam melting. Adv Mater Process March 2007:45–46
Hornberger H, Virtanen S, Boccaccini AR (2012) Biomedical coatings on magnesium alloys—a review. Acta Biomater 8:2442–2455
Issack PS (2013) Use of porous tantalum for acetabular reconstruction in revision hip arthroplasty. J Bone Joint Surg Am 95:1981–1987
Jafari SM, Bender B, Coyle C et al (2010) Do tantalum and titanium cups show similar results in revision hip arthroplasty? Clin Orthop Relat R 468:459–465
Jani JM, Leary M, Subic A et al (2014) A review of shape memory alloy research, applications and opportunities. Mater Des 56:1078–1113
Kaplan RB (2000) Open cell tantalum structures for cancellous bone implants and cell and tissue receptors. EP 0560279 B1
Karageorgiou V, Kaplan D (2005) Porosity of 3D biomaterial scaffolds and osteogenesis. Biomater 26:5474–5491
Kaur G, Pandey OP, Singh K et al (2014) A review of bioactive glasses: their structure, properties, fabrication and apatite formation. J Biomed Mater Res A 102:254–274
Kaya RA, Cavusoglu H, Tanik C et al (2007) The effects of magnesium particles in posterolateral spinal fusion: an experimental in vivo study in a sheep model. J Neurosurg Spine 6:141–149
Kircher RS, Christensen AM, Wurth KW (2009) Electron beam melted (EBM) Co-Cr-Mo alloy for orthopaedic implant applications. Paper presented at the Solid Freeform Fabrication Symposium, University of Texas at Austin, Austin TX, 3–5 August 2009
Knychala J, Bouropoulos N, Catt C et al (2013) Pore geometry regulates early stage human bone marrow cell tissue formation and organization. Ann Biomed Eng 41:917–930
Lacroix D, Planell JA, Prendergast PJ (2009) Computer-aided design and finite-element modelling of biomaterial scaffolds for bone tissue engineering. Philos Trans A 373:1993–2009
Learmonth ID, Young C, Rorabeck C (2007) The operation of the century: total hip replacement. Lancet 370:1508–1519
Lefebvre LP (2013) Porous metals and metallic foams in orthopedic applications. In: Dukhan N (ed) Metal foams: fundamentals and applications, 1st edn. DEStech Publications, Lancaster, pp p317–p362
Levine B (2008) A new era in porous metals: applications in orthopaedics. Adv Eng Mater 10:788–792
Levine BR, Fabi DW (2010) Porous metals in orthopedic applications—a review. Materialwiss Werkst 41:1002–1010
Li Y, Yang C, Zhao H et al (2014) New developments of Ti-based alloys for biomedical applications. Mater 7:1709–1800
Lietaert K, Weber L, Van Humbeeck J et al (2013) Open cellular magnesium alloys for biodegradable orthopaedic implants. J Magnes Alloys 1:303–311
Muth J, Poggie M, Kulesha G et al (2012) Novel highly porous metal technology in artificial hip and knee replacement: processing methodologies and clinical applications. JOM 65:318–324
Ng CC, Savalani MM, Man HC et al (2010) Layer manufacturing of magnesium and its alloy structures for future applications. Virtual Phys Prototyping 5:13–19
Ng CC, Savalani MM, Lau ML et al (2011a) Microstructure and mechanical properties of selective laser melted magnesium. Appl Surf Sci 257:7447–7454
Ng CC, Savalani M, Man HC (2011b) Fabrication of magnesium using selective laser melting technique. Rapid Prototyping J 17:479–490
Orinakova R, Orinak A, Buckova LM et al (2013) Iron based degradable foam structures for potential orthopedic applications. Int J Electrochem Sci 8:12451–12465
Petrini L, Migliavacca F (2011) Biomedical applications of shape memory alloys. J Metall. doi:10.1155/2011/501483
PR Newswire (2015) Chinese magnesium alloy manufacturer Eontec expects to have its medical magnesium alloy available for clinical trial in 2015. www.prnewswire.com/news-releases/chinese-magnesium-alloy-manufacturer-eontec-expects-to-have-its-medical-magnesium-alloy-available-for-clinical-trial-in-2015-300002124.html. Accessed 21 Apr 2015

Razi H, Checa S, Schaser K-D et al (2012) Shaping scaffold structures in rapid manufacturing implants: a modeling approach toward mechano-biologically optimized configurations for large bone defect. J Biomed Mater Res B 100:1736–1745
Ripamonti U, Roden L (2010) Biomimetics for the induction of bone formation. Expert Rev Biomed Devices 7:469–479
Ripamonti U, Roden L, Renton L (2012) Osteoinductive hydroxyapatite-coated titanium implants. Biomater 33:3813–3823
Roland Berger (2013) Additive manufacturing—a game changer for the manufacturing industry? http://www.rolandberger.com/media/pdf/Roland_Berger_Additive_Manufacturing_20131129.pdf. Accessed 18 Feb 2015
Rotaru H, Schumacher R, Kim S-G et al (2015) Selective laser melted titanium implants: a new technique for the reconstruction of extensive zygomatic complex defects. Maxillofac Plast Reconstr Surg. doi:10.1186/s40902-015-0001-9
Rumpler M, Woesz A, Dunlop JW et al (2008) The effect of geometry on three-dimensional tissue growth. J R Soc Interface 5:1173–1180
Sidambe AT (2014) Biocompatibility of advanced manufactured titanium implants—a review. Mater 7:8168–8188
Sinclair S, Konz G, Dawson J et al (2012) Host bone response to polyetheretherketone versus porous tantalum implants for cervical fusion in a goat model. Spine 37:571–580
SLM Solutions (2015) SLM 500 HL Laser beam melting system. http://stage.slm-solutions.com/download.php?f=9004e24eca5e8bc0fa296f27daf32523. Accessed 18 Feb 2015
Smith M, Guan Z, Cantwell WJ (2013) Finite element modelling of the compressive response of lattice structures manufactured using the selective laser melting technique. Int J Mech Sci 67:28–41
Smith & Nephew (2015) SMF stem. http://www.smith-nephew.com/global/assets/pdf/smf_stem_st.pdf. Accessed 18 Feb 2015
Speirs M, Kruth J-P, Van Humbeeck J et al (2013) The effect of SLM parameters on geometrical characteristic of open porous NiTi scaffolds. Paper presented at the VRAP Advanced Research in Virtual and Rapid Prototyping conference, Leiria, 1–5 Oct 2013
Song B, Dong S, Deng S et al (2014) Microstructure and tensile properties of iron parts fabricated by selective laser melting. Opt Laser Technol 56:451–460
Stankiewicz P (2000) Method for producing controlled aspect ratio reticulated carbon foam and the resultant foam. US 6103149 A
Straley KS, Foo CW, Heilshorn SC (2010) Biomaterial design strategies for the treatment of spinal cord injuries. J Neurotraum 27:1–19
Sumita M, Hanawa T, Teoh SW (2004) Development of nitrogen-containing nickel-free austenitic steels for metallic biomaterials—review. Mater Sci Eng, C 24:753–760
Sundfeldt M, Carlsson LV, Johansson CB et al (2006) Aseptic loosening, not only a question of wear: a review of different theories. Acta Orthop 77:177–197
Talha M, Behera CK, Sinha OP (2013) A review on nickel-free nitrogen containing austenitic stainless steels for biomedical applications. Mater Sci Eng, C 33:3563–3575
Thijs L, Montero Sistiaga ML, Wauthle R et al (2013) Strong morphological and crystallographic texture and resulting yield strength anisotropy in selective laser melted tantalum. Acta Materer 61:4657–4668
van Grunsven W, Hernandez-Nava E, Reilly GC et al (2014) Fabrication and mechanical characterization of titanium lattices with graded porosity. Metals 4:401–409
Villanueva M, Rios-Luna A, Pereiro De Lamo J et al (2008) A review of the treatment of pelvic discontinuity. HSS J 4:128–137
Wauthle R (2014) Industrialization of selective laser melting for the production of porous titanium and tantalum implants. Dissertation, KU Leuven
Wauthle R, Vrancken B, Beynaerts B et al (2015a) Effects of build orientation and heat treatment on the microstructure and mechanical properties of selective laser melted Ti6Al4V lattice structures. Addit Manuf 5:77–84

Wauthle R, van der Stok J, Amin Yavari S et al (2015b) Additively manufactured porous tantalum implants. Acta Biomater 14:217–225

Wei K, Gao M, Wang Z et al (2014) Effect of energy input on formability, microstructure and mechanical properties of selective laser melted AZ91D magnesium alloy. Mater Sci Eng, A 611:212–222

Wieding J, Wolf A, Bader R (2014) Numerical optimization of open-porous bone scaffold structures to match the elastic properties of human cortical bone. J Mech Behav Biomed Mater 37:56–68

Windhagen H, Radtke K, Weizbauer A et al (2013) Biodegradable magnesium-based screw clinically equivalent to titanium screw in hallux valgus surgery: short term results of the first prospective, randomized, controlled clinical pilot study. Biomed Eng OnLine 12

Wohlers T (2013) Wohlers report 2013. Wohlers Associates, Fort Collins CO

Woodruff MA, Lange C, Reichert J et al (2012) Bone tissue engineering: from bench to bedside. Mater Today 15:430–435

Wuisman PI, Smit TH (2006) Bioresorbable polymers: heading for a new generation of spinal cages. Eur Spine J 15:133–148

Zadpoor AA (2015) Bone tissue regeneration: the role of scaffold geometry. Biomater Sci 3:231–245

Zardiackas LD, Parsell DE, Dillon LD (2001) Structure, metallurgy, and mechanical properties of a porous tantalum foam. J Biomed Mater Res 58:180–187

Zhang B, Liao H, Coddet C (2012) Effects of processing parameters on properties of selective laser melting Mg-9%Al powder mixture. Mater Des 23:753–758

Zheng YF, Gu XN, Witte F (2014) Biodegradable metals. Mater Sci Eng, R 77:1–34

Properties and Behavior of Shape Memory Alloys in the Scope of Biomedical and Engineering Applications

Vladimir Dunić, Radovan Slavković and Elzbieta A. Pieczyska

Abstract Shape memory alloys (SMA) are widely and frequently applied in cases when it is useful to employ their advantages through specific behavior (pseudoelasticity or shape memory effect) in various conditions. Effects of shape memory and pseudoelasticity can be employed in innovative ways as actuating or sensing elements in many nowadays applications. There are various alloying elements which can form a SMA such as Ni, Ti, Cr, Cu, etc., but the most frequently used and known alloy is NiTi. By addition of other alloying elements the properties of the SMA can be changed to fit demands of the consumers. The investigation of such materials is very important for successful application, so the researchers investigate procedures and algorithms for comparison of experimental and numerical results to provide the best performance of SMA devices. Strong thermomechanical coupling is observed during the SMA loading, so SMA are known as highly thermosensitive materials what can be used as advantage, but also it can be a problem during the alloy production process. The strong thermomechanical coupling and the related high thermosensitivity increase the need for simulation of complex thermomechanical response in realistic problems. The complex stress states and deformation range impose the requirements for accurate analysis of large strain problems. Application of SMA started several decades ago with an engineering application in pipe couplings, while today one of the most commonly known are biomedical applications (i.e. cardiovascular stents and orthodontic braces). The main reasons for wide range of biomedical applications of NiTi alloys are the specific behavior,

V. Dunić (✉) · R. Slavković
Faculty of Engineering, University of Kragujevac, Sestre Janjić 6,
Kragujevac, Serbia
e-mail: dunic@kg.ac.rs

R. Slavković
e-mail: radovan@kg.ac.rs

E.A. Pieczyska
Institute of Fundamental Technological Research, Polish Academy of Sciences,
Pawińskiego 5B, Warszawa, Poland
e-mail: epiecz@ippt.pan.pl

F. Zivic et al. (eds.), *Biomaterials in Clinical Practice*,
https://doi.org/10.1007/978-3-319-68025-5_11

good biocompatibility and good fatigue performance what is important factor under the high cyclic external loading.

Keywords SMA · Properties · Modeling · Application

1 Introduction

During the last several decades shape memory alloys (SMA) have become fascinating materials for researchers and engineers, but also for many satisfied customers of devices made of such materials (Otsuka and Wayman 1998). There are many advantages provided by SMA, but the most important one is the possibility to use the advanced properties and behavior effects in industrial, technical and biomedical applications where various engineering solutions are adapted (Duering et al. 1990). Hence, it is of high importance to understand the mechanism of SMA phenomenological effects and to identify material properties as important factors which influence the SMA behavior.

Environment and surrounding conditions can influence various states of the material, which depend on the crystal lattice so the possible effects could be different for the alloy with the same concentration of the alloying elements. For example, depending on material temperature of the SMA, during the exploitation of the same alloy, expected behavior of the alloy can be different. That makes the SMA very sensitive to the temperature change, but also offers multifunctionality. The high thermal sensitivity may be used as advantage by employing the effects of shape memory and pseudoelasticity in a proper manner, if the material properties are well known (Otsuka and Wayman 1998; Duering et al. 1990), but at the same time, during the production process, the thermal sensitivity is recognized as undesired property.

Experimental investigation gives a lot of details about the SMA behavior, but a correct numerical analysis is always useful because the results can predict the exploitation problems and possible damage of the material what is important for reliability of construction. Furthermore, the SMA behavior is caused by complex thermomechanical state what makes research more challenging. During the last few decades, many researchers all around the world have been trying to improve the established procedures for experimental and numerical investigation of SMA towards more reliable data necessary for correct prediction of the material behavior. This paper aims to summarize these results. The SMA properties, behavior in various conditions and their application in scope of the available research results and investigation approaches are described.

The structure of this work is organized to present current state of the research in following form:

Firstly, introduction is given in a form of comprehensive description of SMA properties and phenomenological behavior effects shown in diagrams and figures. The thermomechanical behavior in various loading conditions is analyzed as

important factors which influence SMA behavior. As an extension, current mathematical investigation of SMA behavior is presented in a review form of the existing constitutive models and modeling approaches. A special case of thermomechanical experimental research and constitutive models capable to catch the SMA phenomena are discussed. The review of previous works has defined the demands and directions of potential research.

In the second part, the overview of SMA application with the emphasis on biomedical devices is presented. The application is divided into biomedical and technical sections. As highly biocompatible materials, SMA are used in many medical fields but also the technical application is highly important in a form of actuators and sensors, and as reliable materials are widely used in important engineering solutions.

At the end, the presented information are summarized and the final remarks are given. Current challenges are described and further directions for the research are introduced.

2 Shape Memory Alloy Properties: Experimental Investigation and Modeling

Shape memory alloys belong to a specific group of multifunctional or smart materials (Lagoudas 2010) due to very advanced characteristics which manifest useful effects in various engineering solutions. The SMA effects are described as a capability of the material to recover the shape and geometry under specific conditions (stress state, temperature field, magnetic field, electric field etc.). The maximal inelastic deformations of SMA recorded during the exploitation depend on the alloy composition and can reach nearly 10% of strain (Lagoudas 2010). These effects offer capabilities of sensing (conversion of mechanical signal into non-mechanical) and actuation (conversion of non-mechanical signal into mechanical). Possibility to use those effects and properties classifies such materials to a special subgroup of active or responsive materials (Lagoudas 2010).

The SMA are metallic alloys composed of elements such as Ni, Ti, Cu, Co, Cr, etc. (Table 1). One of the first research steps in investigation of metallic materials was related to steel. During the investigation of steel phases and steel microstructure, several phases can be noticed, such as austenite and martensite. The martensite phase got the name in honor of German metallurgist Adolf Martens (1850–1914), who investigated phase change in steel (Otsuka and Wayman 1998; Grabe 2007). Various kinds of transformations are possible in metallic materials, but one of the most interesting is martensitic transformation. The martensitic transformation is defined as the solid phase transformation without diffusion of atoms (Jovanović et al. 2003; Grabe 2007). The new phase is formed by moving of atoms from the nodes of old to new lattice, but the relative distance is smaller than distance between the atoms (Jovanović et al. 2003). The transformation is based on homogeneous slip

Table 1 Alloys with shape memory effects

Primary elements	Other elements	Effects	Comment
NiTi-	-Cu, -Nb	SME, two way SME, pseudoelasticity	Resistance to corrosion, biocompatible
NiTi-	-Pd, -Pt, -Hf, -Zr	High temperature SMA	Trans. strain ≈3%
Cu-	-Zn, -Al (-Ni, -Be, -Mn, -Nb)	SME, pseudoelasticity	Electrical and thermal conductivity
Fe-	-NiCoTi, -MnSi, -Pd, -Pt	SME	Trans. strain ≈2.5–4.5%
CoNi-	-Al, -Ga	SME, pseudoelasticity	Brittle nature, magnetic properties
Ni-	-MnGa, -FeGa, -MnAl	Magnetic SME, pseudoelasticity	Magnetic properties

of the neighbouring planes and the corresponding changes in the distance between the planes (Jovanović et al. 2003). The name of that shearing process is twinning which can be noticed at the material surface as embossment (Jovanović et al. 2003). The martensite transformation in steels was observed as irreversible. Buehler et al. (1963) investigated the reversibility of the phase transformation in NiTi alloy and its influence on the mechanical properties. They have found that the main factors which control the phase transformation are "alloy composition, temperature and mode of plastic deformation" (Buehler et al. 1963). The research was conducted at the Naval Ordnance Laboratory (NOL), so the NiTi alloy got the name NiTiNOL in that honor. A few years later, Buehler and Wiley were awarded a patent for the development of the NiTi alloy series (Barbarino et al. 2014).

The research on SMA properties presented in (Otsuka and Wayman 1998; Duering et al. 1990; Lagoudas 2010; Buehler et al. 1963; Barbarino et al. 2014; Wang et al. 2012) can be summarized as follows:

- NiTi alloy contains 49–57% nickel and the ideal composition of NiTiNOL can only vary between 38 and 50% titanium by weight,
- very small increase of the Ni content in alloys can reduce transformation temperatures and increase yield stress significantly,
- the alloying elements such as Co or Fe added to NiTi causes decrease of transformation temperatures,
- High Temperature SMA based on Ti and Pd, Pt, Au, Zr, Hf are characterised by transformation temperatures above 100 °C,
- alloying element Cu makes stress hysteresis much narrower, while Nb makes it much wider.

The parameters of the alloy phases are important factors for the SMA behavior (Fig. 1). The ratio between the phases can be controlled by various external factors

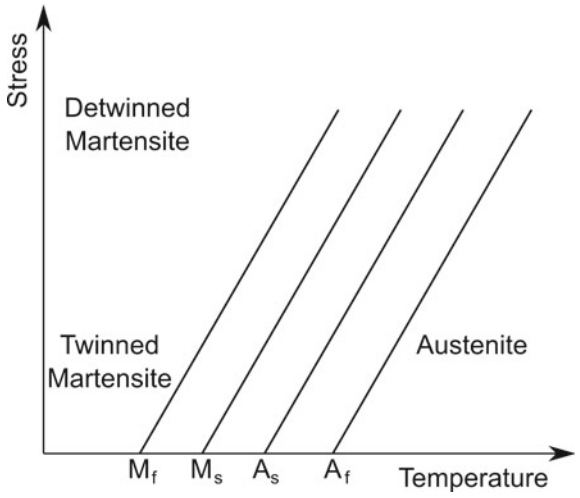

Fig. 1 Scheme of stress-temperature phase diagram for SMA: M_s-martensite start, M_f-martensite finish, A_s-austenite start, A_f-austenite finish (Lagoudas 2010)

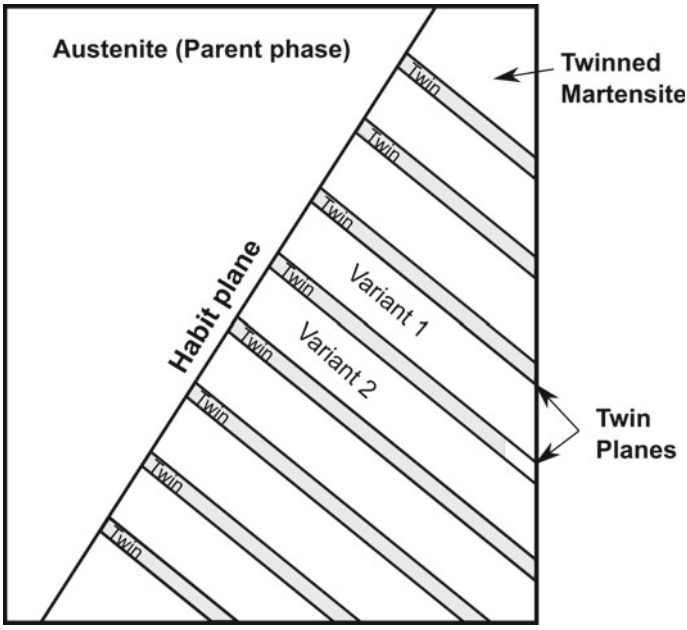

Fig. 2 Scheme of interface between the austenite and martensite phases in SMA (Lagoudas 2010; Otsuka and Ren 2005)

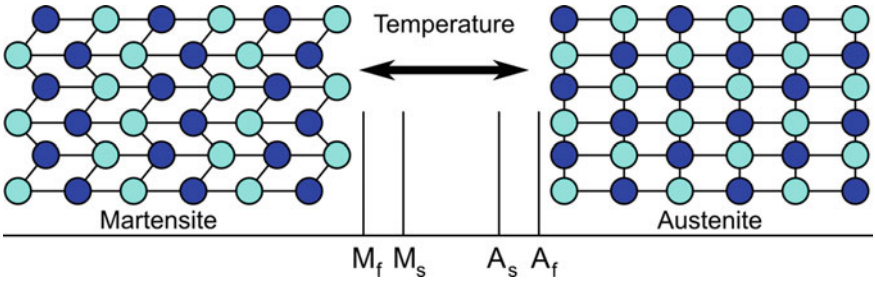

Fig. 3 Scheme of temperature-induced phase transformation of SMA (Lagoudas 2010)

such as: stress, temperature, concentration, magnetic field, etc. The SMA can be observed in two phases with different crystal lattice: austenite (A) and martensite (M). The austenite is a phase which appears at high temperatures, while the martensite is available at low temperatures. The physical and mechanical properties depend on these two phases. The austenitic structure is harder with higher Young's modulus, while the martensitic structure is softer and more elastic (it can be easily deformed by application of force) (Jani et al. 2014). As it was already described for steels, the martensitic transformation between the phases occurs by shear lattice distortion. The orientation direction of each crystal is called a variant (see Fig. 2).

The martensitic variants can be organized as a twinned (combination of martensitic variants) and a detwinned martensite (a specific variant is dominant) (Lagoudas 2010).

As SMA are very thermosensitive materials, the crystal lattice can be transformed by a temperature change (Fig. 3). The cooling of the material below some limiting temperature is responsible for the forward martensitic transformation. The transformation includes changes of the crystal lattice from austenite to twinned martensite. The reverse martensitic transformation from martensite to austenite is caused by heating of the material above some temperature limit. These limits are, so called, start and finish temperatures. The accurate determination of these limits is of great importance for the martensitic transformation process. Usually, the martensite and austenite temperature limits are denoted by M and A and start and finish points are defined by indices "s" and "f". During both directions of the transformation, two limit temperatures can be determined—one when the transformation is initiated and the other when it is completed (martensitic start M_s and finish M_f and austenitic start A_s and finish A_f temperature, respectively).

A mechanical loading can also change the crystal lattice. If the load is applied at the low temperature (twinned martensite), some variants can be reoriented and detwinned what causes change of the material shape (Fig. 4). By heating above the austenitic finish temperature A_f reverse phase transformation occurs and the crystal lattice transforms from the detwinned martensite to the austenite (Fig. 4). After cooling below martensitic finish temperature M_f the twinned martensite is formed again. This effect is known as shape memory effect (SME) (see Fig. 5). If the material temperature is above the austenitic finish temperature A_f, the loading

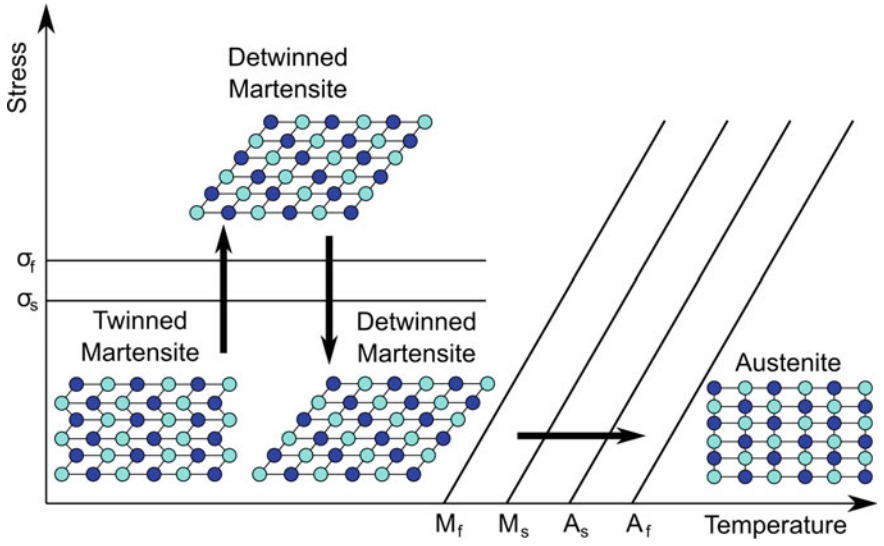

Fig. 4 Schematic of the shape memory effect of SMA (Lagoudas 2010)

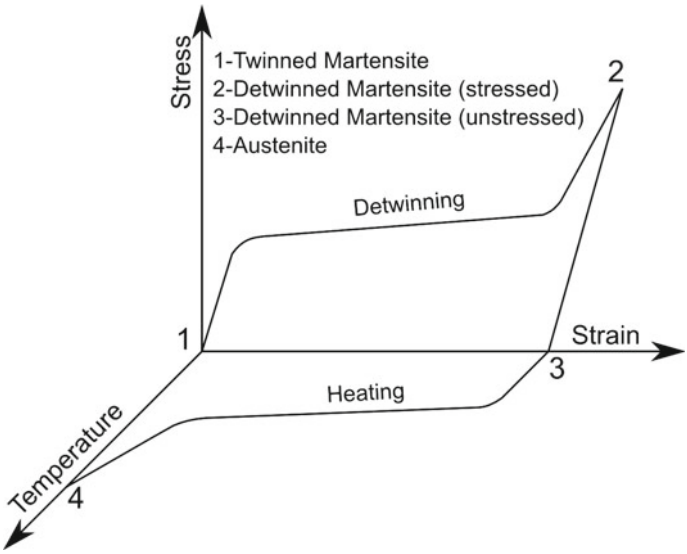

Fig. 5 Stress–strain-temperature curves of SME (Lagoudas 2010)

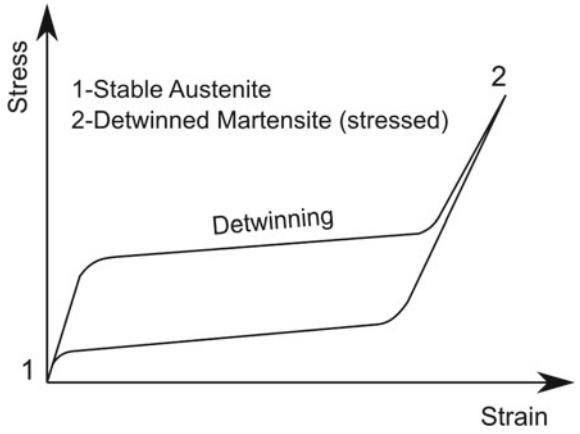

Fig. 6 Stress–strain curve of pseudoelasticity

process induces the transformation to detwinned martensite from the stable austenite, which exists at that temperature. After unloading, the crystal lattice structure is returned to the austenitic phase (Fig. 7). This effect is known as pseudoelasticity (Otsuka and Wayman 1998; Duering et al. 1990; Lagoudas2010) (see Fig. 6).

The crystal structure of austenite is cubic crystal $B2$, while martensite can have different structures what depends on alloying elements. In NiTi alloys, martensitic phase has monoclinic $B19'$ structure. Direct transformation $B2 \rightarrow B19'$ does not happen, because, there is martensitic R-phase ($B2 \rightarrow R \rightarrow B19'$) (Fig. 8). For

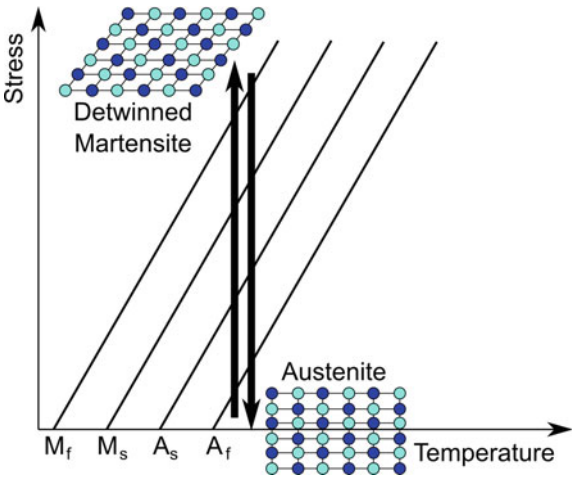

Fig. 7 Scheme of pseudoelastic loading path of SMA (Lagoudas 2010)

example, by addition of Cu or Pd the martensite can form orthorhombic *B*19 structure or *R*-phase (Lagoudas 2010; Grabe 2007).

As it was already stated, the martensitic transformation occurs by moving of atoms (lattice shearing) along habit plane or lattice invariant plane which forms interface between the martensite and austenite (Lagoudas 2010; Panico and Brinson 2007). There are two lattice invariant shear mechanisms: slip and twinning. In SMA, twinning is the most common mechanism. The details are presented in Fig. 2.

Also, as it was observed in Shaw and Kyriakides (1995), Hallai and Kyriakides (2013), the forward and reverse martensitic transformation did not occur homogeneously in the specimens. The transformation occurs by nucleation and propagation of fronts due to exothermic nature for transformation from austenite to martensite and endothermic nature for transformation from martensite to austenite. Those fronts are developing in form of bands similar to those observed in mild steel "Lüders bands". Pieczyska et al. recorded by infrared camera two directions of the transformation bands accompanying pseudoelastic TiNi SMA deformation (Pieczyska et al. 2006, 2013; Pieczyska 2008, 2012). The temperature difference between the band and the other material (Fig. 10) has been investigated by Pieczyska et al. (2014). The experimental results of TiNi SMA subjected to tension presented in Pieczyska et al. (2013) were completed by numerical modeling and published by Dunić et al. (2014).

Since the A_f temperature of the SMA equals 293 K, the material is superelastic at room temperature (above 293 K), so after the unloading the specimen almost recovers its initial length, structure and properties. Moreover, its stress–strain curve manifests large hysteresis loop: the process of stress-induced martensite forward transformation (SIMT) is exothermic whereas the reverse one-endothermic. Use of the fast (538 Hz) and sensitive (0.02 K) infrared camera allowed to obtain the temperature distribution on the SMA specimen during the loading and

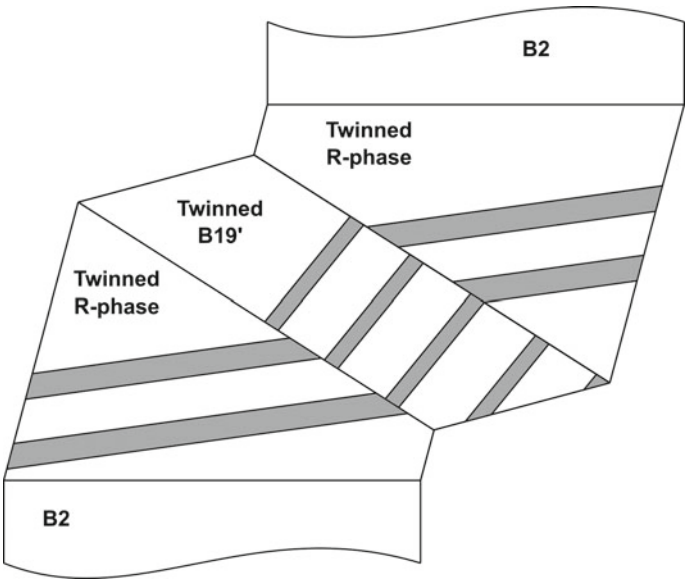

Fig. 8 Scheme of the transformation B2 → R-phase → B19′ (Zhang and Sehitoglu 2004)

transformation processes, calculation of the temperature changes with high accuracy. In the final part of the SMA loading a decrease of the average specimen temperature revealed the saturation stage of the forward transformation (Pieczyska et al. 2013).

The thermal response determined by measurements performed with a high-performance infrared system indicates that the initial macroscopically homogeneous transformation initiates at the same stress level (400 MPa) for all stress and strain rates applied. The stress of nucleation of the localized martensitic transformation depends on the strain rate. The higher the strain rate, the higher the specimen temperature. Thus higher stress and more dynamic run of the developing transformation is observed, which is accompanied by the formation of numerous fine transformation bands. At the stage of the advanced martensitic forward and reverse transformation, a new generation of narrower needle-like transformation bands can be observed, in particular noticed at higher strain rates. The fine bands appear to nucleate at regular distances from the primarily developed wider bands and evolve in a perpendicular direction. For both stress- and strain-controlled approaches, the nucleation of the localized martensitic forward transformation takes place either in the weakest area of the sample grip or in any other area, whereas the reverse transformation always initiates in the central part of the specimen. We can consider the process of the reverse transformation to be more uniform in comparison to the forward transformation since the bands observed latter are less uniformly distributed on the specimen surface (Fig. 9).

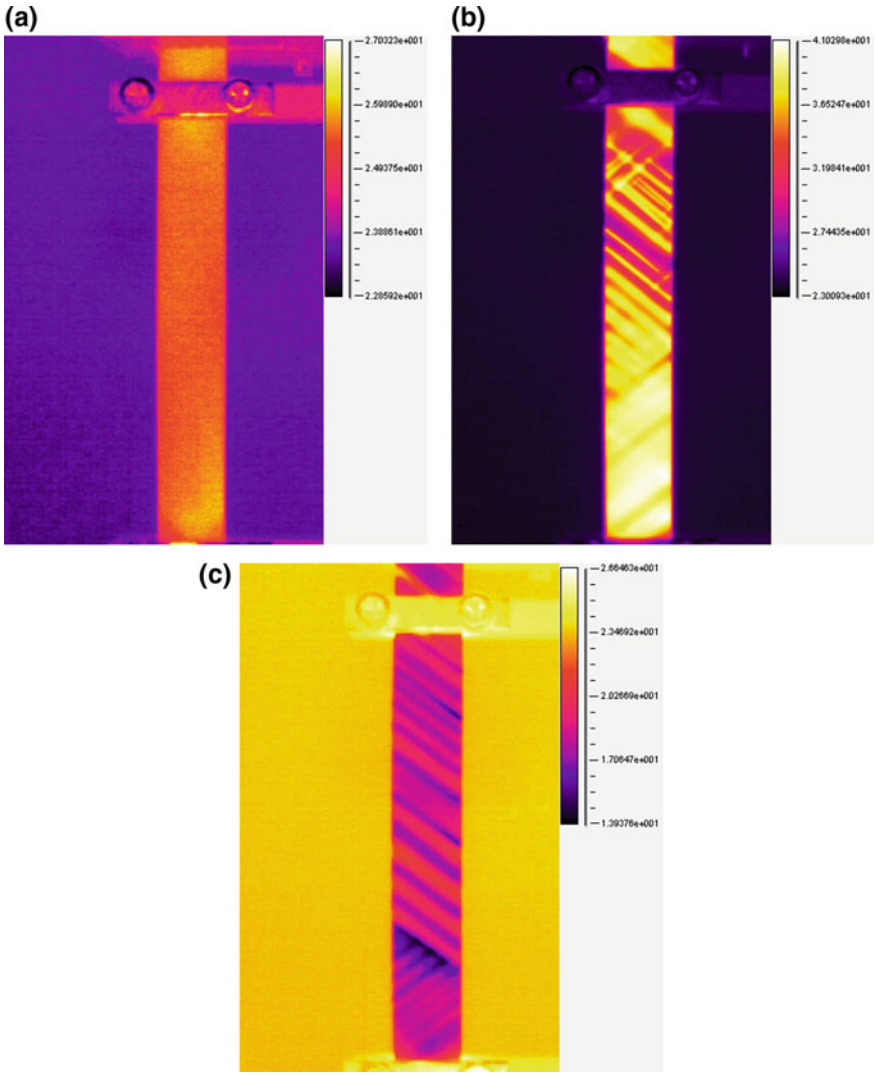

Fig. 9 Infrared imaging observed by fast and sensitive infrared camera for TiNi SMA during tension at high strain rate. *Loading* **a** exothermic uniform transformation, **b** two directions of transformation bands of higher temperature; *Unloading* **c** two directions of transformation bands of lower temperature from the other part of the SMA specimen

Taking into account stress–strain curves and their related temperature changes obtained due to the fast and sensitive infrared system, three separate stages can be distinguished during the martensitic forward phase transformation (see Fig. 11). At the beginning, the first stage of loading process (I) is characterized by low transformation rate and almost elastic behavior (in numerical analysis is purely elastic,

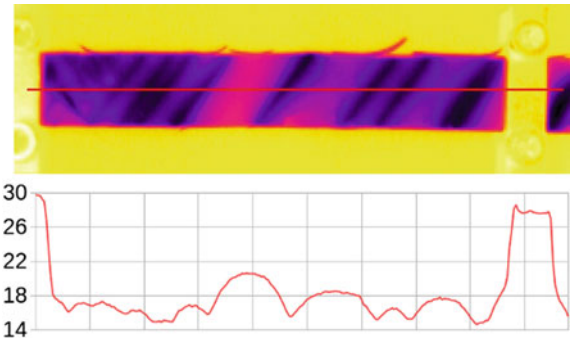

Fig. 10 Temperature distribution on the specimen surface and temperature profile along the specimen length at the end of localised martensitic transformation in TiNi subjected to tension (Pieczyska et al. 2014)

while in the experimental investigation, there are some nucleation of the martensitic transformation) (Dunić et al. 2014). In the second stage (II), onset of the very intense localised transformation is observed, followed by strong increase of the temperature. When the martensitic transformation is almost completed; the third stage (III) is observed as saturation phase. The temperature decreases because the heat outflow to surroundings is higher than the production of heat (Pieczyska et al. 2013).

The non-uniform character of the stress-induced transformation was also observed in ferromagnetic shape memory alloys, e.g. NiFeGaCo single crystals presented by Pieczyska (2015).

Comprehensive research on mechanical properties of shape memory materials (alloys, polymers and composites) subjected to various loading modes is presented by Tobushi et al. (2013). The book embraces results obtained for SMA subjected to tension, compression, simple shear, torsion and cycling loading. In the case of simple shear and torsion the loading process is more complex, but the deformation is much more homogeneous and the specimen temperature distribution is almost uniform.

2.1 SMA Constitutive Modeling Approaches

In general, constitutive modeling depends on various requirements, but the opposing two are the simplicity of the model and the level of details captured by numerical analysis. The users of material models need simple and robust model with few material constants capable to consider the highest possible level of simulated details. Researchers offered several approaches depending on the scale of investigation. Three major groups of the SMA constitutive models can be distinguished (Lagoudas et al. 2012; Arghavani et al. 2010b) as: micromechanics-based models, micro-macro and macro (phenomenological) models (see Fig. 12).

The micromechanical or micro-models are appropriate for investigation of SMA microstructure at the micro level (nucleation, interface motion, twinning, etc.).

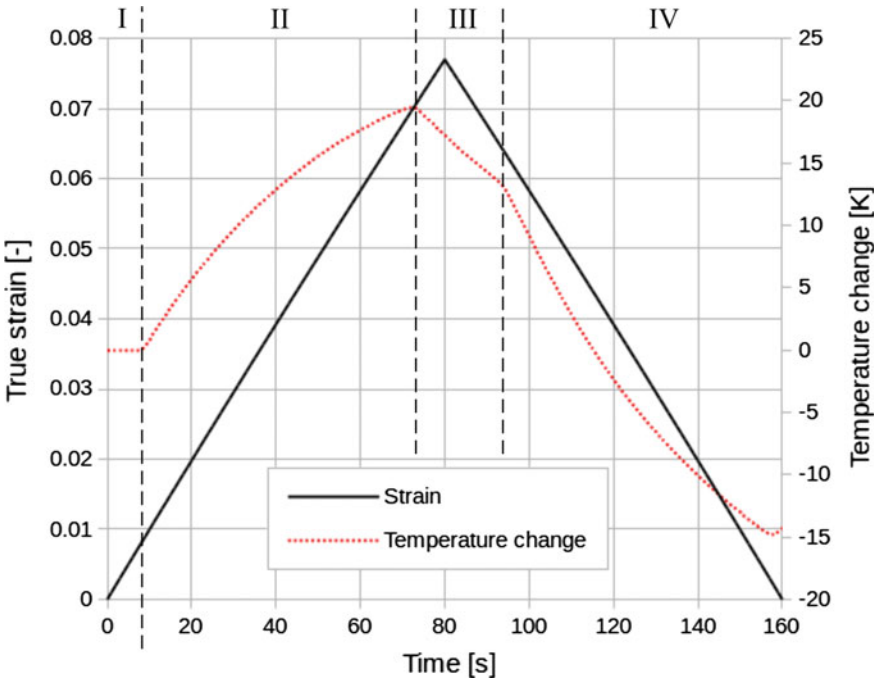

Fig. 11 Three different stages of martensitic transformation (uniaxial tension test controlled by strain rate $10^{-3}\,s^{-1}$) (Pieczyska et al. 2014)

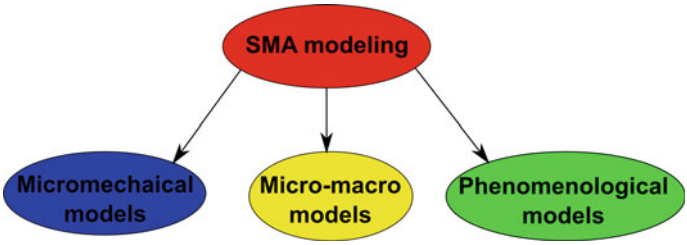

Fig. 12 Three major groups of the SMA constitutive models

Regions of martensite are modeled as separate zones what causes existence of a large number of internal variables. That makes difficulties in engineering application, but the fundamental phenomena are clearly visible and understandable.

The phenomenological or macro-models consider the behavior of materials at the macro-scale. Such constitutive models are based on the data obtained during the experimental investigation. The constitutive relations employ the continuum thermodynamics with internal variables for successful simulation. For SMA, the

martensitic volume fraction is usually used as an internal variable. Such material models are more suitable for implementation and application because of simplicity and quick computations, but the microscopic details cannot be taken into account.

The micro-macro models have been developed as a combination of the micro- and macro- models. Based on modeling of single crystal with a homogenization, it is possible to predict the behavior of the material at macro-scale. The thermodynamic laws are applied to estimate martensitic transformation. The micro-structure behavior is used to describe interaction energy due to the martensitic transformation. This is an advantage but some difficulties exist due to a large number of internal variables.

The phenomenological SMA models can be divided into two groups (Arghavani 2010): models (a) with and (b) without internal variables (see Fig. 13). The models without internal variables consider phase transformation without the variables which define phase mixture. Such models are described by strain, stress, temperature and entropy. Two kinds of such models are recognized: polynomial potential and hysteresis model (Arghavani 2010). On the other hand, the models with internal variables depend on variable which can describe internal structure of SMA. Additionally, the constitutive relations depend on a set of mechanical (stress or strain) and thermal (temperature or entropy) variables.

Many researchers (Table 2) are working on development of SMA constitutive models. The most popular topics are certainly: hardening during the transformation, asymmetric response in tension and compression, modeling of martensite detwinning, two-way SME, the effect of reorientation, the accumulation of plastic strains during the cyclic loading, the influence of thermomechanical coupling, behavior under fatigue loading, sublooping, etc. (Lagoudas 2010).

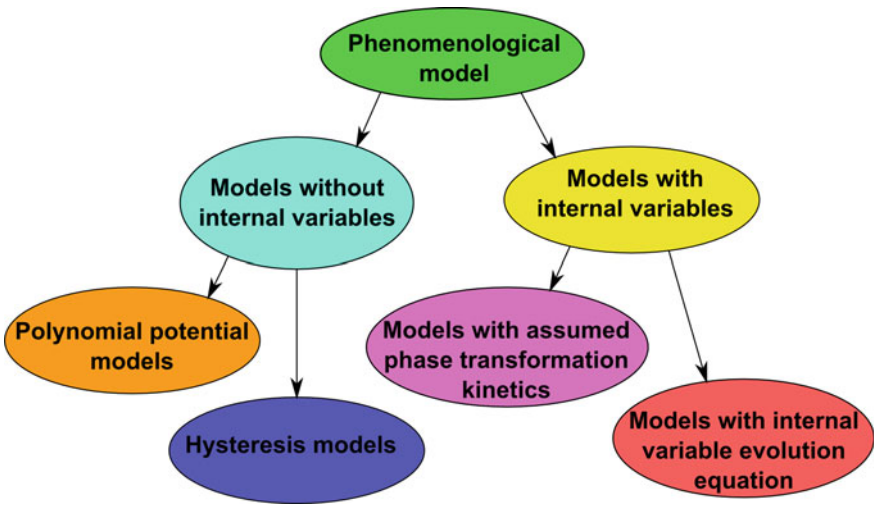

Fig. 13 Phenomenological SMA models

Table 2 Research groups with focus on material models with internal state variable

Country	Principal researcher	Affiliation
Brazil	M. Savi, A. Paiva	Instituto Militar de Engenharia, Rio de Janeiro
France	C. Lexcellent (C. Bouvet, A. Vivet)	Franche-Comte University
France	Mumni, W. Zaki	Ecole Polytechnique
Germany	S. Resse	Technical university Braunschweig
Germany	O. Bruhns	Ruhr-University, Bochum
Germany	D. Helm	University of Kassel
Italy	F. Aurrichio	University of Pavia
Poland	B. Raniecki	IPPT, PAN
Serbia	R. Slavković, V. Dunić	University of Kragujevac
Singapore	P. Thamburaja	National University of Singapore
USA	D. Lagoudas	Texas A&M University
USA	C. Brinson	Northwestern University

The complex geometries (biomedical stents and industrial applications of SMA) motivated development of 3D phenomenological models, although the 1D models are still interesting for application (i.e. simulation of SMA wires behavior). One of the first was presented by Liang and Rogers (1992). It was thermomechanical based on micro- and macro- mechanics and one internal variable: the martensitic volume fraction. As the benchmark example, a torsion of the SMA rod was used. Raniecki and Lexcellent (1994) proposed a model capable to simulate complex stress states. The model was based on observation of uniaxial stress states. A combination of thermodynamic laws and a relation between the second invariant of stress and strain deviators was used for derivation of the model. A free energy function for pseudoelasticity models was presented with ideal pseudoelastic flow, with isotropic linear and nonlinear transformation hardening. As the extension of this work, Leclercq and Lexcellent (1996) increased number of internal variables to simulate SMA behavior. They used two internal parameters: "the volume fraction of self-accommodating (pure thermal effect) and oriented (stress induced) product phase". During the same year, Boyd and Lagoudas (1996) presented the thermodynamical constitutive model for monolithic SMA. They used a free energy function and a dissipation potential to model pseudoelasticity and shape memory effect. They considered three cases based on the number of internal state variables. Raniecki and Lexcellent (1998) continued their research proposing the thermodynamic theory for pseudo-elastic behavior of SMA which takes into account tension-compression asymmetry. During the same year, Souza et al. (1998) proposed 3D phenomenological model to describe the mechanical behavior of polycrystalline solids under stress loading. A transformation strain tensor was introduced to take into consideration stress induced martensitic transformation. Qidwai and Lagoudas (2000a, b) derived "constitutive relations in stress-temperature space using Lagrangian formulation". They investigated various

transformation functions with idea to propose the most proper one. A numerical implementation of SMA thermomechanical constitutive model was given using closest point projection and the convex cutting plane return mapping algorithm which was already used in plasticity. Auricchio (2001) presented efficient and robust algorithm for 3D SMA model for large strains intended for analysis of SMA-based devices. During the same year, Thamburaja and Anand (2001) investigated super-elastic behavior of SMA in tension-torsion. That was a polycrystalline model, where each element was a crystal with the orientation, texture etc. The macroscopic responses were calculated as average over the entire volume. Also, Lexcellent et al. (2002) done research under biaxial proportional loading experimentally on a CuZnAl and CuAlBe alloys to define initial phase transformation surface. Auricchio and Petrini (2002, 2004a, b) continued research to capture asymmetric behavior of SMA and thermomechanical coupling effect. In paper published in 2002 they considered 3D model proposed by Souza et al. (1998) and suggested improvements needed for development and implementation of algorithm into FEM framework. In 2004 they presented model which can take into account thermomechanical coupling in order to simulate such problems. Between those two papers, Helm and Haupt (2003) developed the phenomenological model able to capture multiaxial loading behavior of SMA with the one- and two-way SME, pseudo-elastic and pseudo-plastic behavior. The model is based on a free energy function and evolution equations for internal variables. Popov and Lagoudas (2007) introduced polycrystalline 3D SMA model based on modified phase diagram. The model uses three internal variables to predict the martensitic transformation and detwinning what makes it suitable for numerical analysis of complex thermomechanical loading problems. Panico and Brinson (2007) proposed a macroscopic phenomenological model able to capture effects of multiaxial and non-proportional loading alongside an evolution of twinned and detwinned martensite. The inelastic strain is split into two parts: derived from creation of detwinned martensite and reorientation of previously existing martensite variants. Zaki and Moumni (2007) used two internal variables: the martensite volume fraction and martensite orientation strain tensor to take into account self-accommodation, orientation and reorientation of martensite with one-way SME and pseudoelasticity. Also, they presented a procedure for material parameters identification in order to compare the numerical and experimental results. Reese and Christ (2008) presented a new phenomenological constitutive model extended to large strain problems. The reason for this was increasing requirement to simulate NiTi stents. A year later Christ and Reese (2009) proposed a new thermomechanically coupled material model for SMA. The relations are presented for the large strain case. A multiplicative decompositions of the deformation gradient was used. The thermomechanical coupling was realized in a monolithic approach. Thamburaja (2010) presented the thermomechanically coupled polycrystalline SMA constitutive model for large strain problems. The model was capable to simulate behavior of SMA under multiaxial loading conditions. Arghavani et al. (2010a) introduced a phenomenological constitutive model for SMA based on irreversible thermodynamics and internal variables: the amount of martensite and the direction of variants. Using

these variables, multiaxial non-proportional loadings can be captured more accurately. Later Arghavani et al. (2010c) extended the Panico and Brinson (2007) small strain model to solve finite strain problems by using a multiplicative decomposition of deformation gradient and an additive decomposition of inelastic strain rate tensor into transformation and reorientation parts. During the same year, Hartl et al. (2010) considered "the generation and evolution of irrecoverable viscoplastic strains in the SMA material". There are situations when such strains appear when they are subjected to high temperatures. They proposed a constitutive model which can take into account that behavior. Lagoudas et al. (2012) published work about the thermomechanical SMA constitutive model. The improvements with respect to Boyd and Lagoudas (1996) are the smooth transition and dependence of thermodynamic force on applied stress magnitude. Recently there were few ideas concerning small strain constitutive models reformulation to be able to solve large strain problems (Teeriaho 2013; Stupkiewicz and Petryk 2013). Stupkiewicz and Petryk (2013) have recently presented a model of pseudoelasticity in SMA and a methodology for extension of the model from the small-strain to finite-deformation regime. They have employed the multiplicative decomposition of the deformation gradient and exponential mapping of the logarithmic transformation strain. Also, Teeriaho (2013) suggested the similar idea for the theory presented in (Lagoudas 2010). He used the Eulerian rate type formulation with an additive decomposition of the stretching tensor. Finally, Dunić et al. (2014) investigated influence of loading rate controlled by stress and strain on SMA behavior. The specimens are investigated experimentally at various strain rates. The numerical analysis was done by partitioned coupling of finite element programs for structural and heat analysis. Good quantitative and qualitative results were obtained what verified high thermal sensitivity of SMA and necessity of thermomechanical coupling for accurate simulation.

2.2 *Loading Rate Influence on SMA Behavior*

A special review will be presented for the influence of loading rate on the SMA behavior. As it was observed in Pieczyska (2008, 2012), Pieczyska et al. 2013), the behavior of SMA is different for various loading rates. The stress–strain response hardens and the hysteresis loop becomes wider for the higher strain rates. In order to simulate such behavior, Mirzaeifar et al. (2011) used an explicit finite difference scheme to investigate the response of SMA in tension, taking into account the effect of generated latent heat accompanying the transformation. They considered several case studies with different specimen geometry, loading and unloading rates, as well as boundary conditions. Morin et al. (2011) examined the strain rate dependence of the SMA mechanical pseudoelastic response by using the FEM and studied influences of the strain rate and the environment conditions. Grandi et al. (2012) performed a number of numerical tests, which investigated the SMA mechanical behaviour in various conditions. Yang and Dui (2013) also examined TiNi alloys

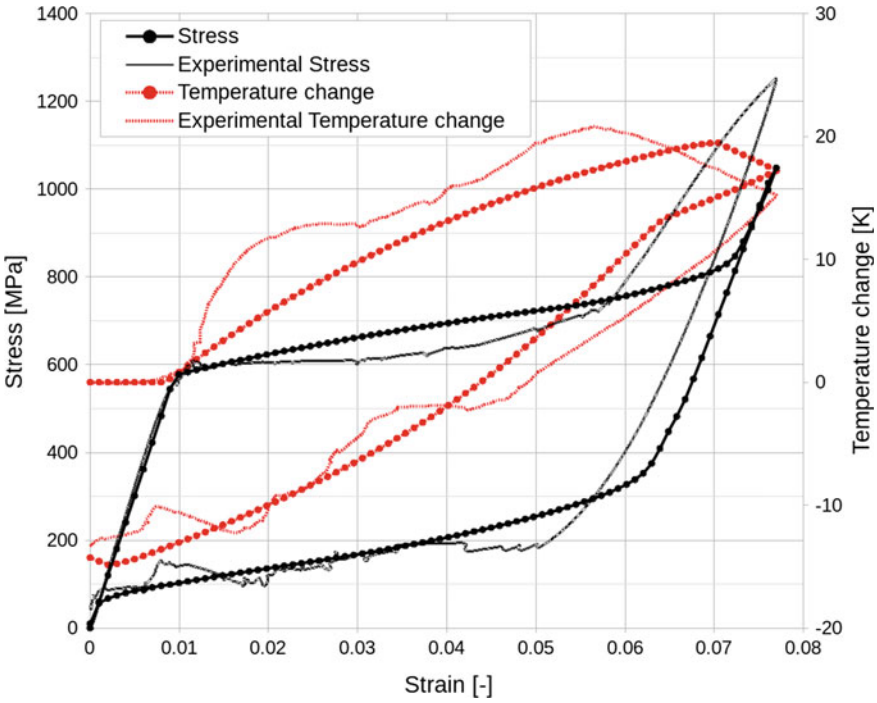

Fig. 14 Stress–strain and temperature change-strain dependence for the strain rate $10^{-3}\,s^{-1}$ (Pieczyska et al. 2013; Dunić et al. 2014)

under tensile loading. They focused on the strain localization and propagation phenomena. Among others, the rate-dependent stress–strain hysteresis was discussed by taking into account the specimen temperature changes. Three kinds of boundaries at the testing specimen ends were discussed. TiNi SMA was experimentally analyzed under tension for various stress and strain rates by Pieczyska et al. (2013). The nucleation and development of stress-induced martensitic transformation were investigated based on the temperature distribution on the specimen surface, measured by a fast and sensitive infrared camera. Details about stress–strain dependences were analyzed with respect to the loading manner. Creation of numerous fine transformation bands was observed at different stages of the martensitic forward and reverse transformation. The obtained effects, related to the transformation, were discussed depending on the loading conditions.

Dunić et al. (2014) investigated comparison of experimental data to the numerical simulation results. The comparison have been done for SMA tension tests under different loading rates. It was shown that the results are reproduced quantitatively and qualitatively by the numerical FEM model, which verifies the accuracy of the proposed investigation method. As it can be noticed in Fig. 14, the forward martensitic transformation has the exothermic nature (temperature increases), while the reverse transformation is endothermic (temperature decreases).

Because of the thermoelastic effect and strong influence of thermomechanical coupling, temperature of the examined specimen even decreases below the beginning temperature.

3 Applications of SMA

A possibility to convert thermal energy in mechanical work, reliability, biocompatibility and multifunctionality of the SMA, make them good candidates for engineering solutions. SMA are promising for aerospace, aircraft, medical, transportation, naval and oil industry. SMA are also applied in daily used devices as i.e. in coffee makers, rice cookers, air-conditioners, headphones, flexible eyeglasses, etc., but recently increasing applications are in various kind of biomedical devices.

Although the NiTi is the most expensive and more difficult to produce, it is still the most popular and the most commonly studied SMA alloy, because of the best properties: strong pseudoelasticity and SME, higher stability in cyclic application, high strength, ductility and fatigue properties, electrical sensitivity, resistance to corrosion and the most important for biomedical application—good biocompatibility. However, presence of Ni is questionable, especially some medical authorities, because of possible Ni release, which has been proved to cause toxic, carcinogenic, and immune-sensitizing effects (Auricchio et al. 2015a). But, after many investigations, it was found that NiTi alloys are very corrosion resistant and that fear is unreasonable, because Ti oxidized more rapidly than Ni, protecting the surface by TiO_2 film acting as barrier to Ni release (Auricchio et al. 2015a). If the exploitation conditions are extreme, like in a human body, spacial surface modification techniques are used as additional protection (Auricchio et al. 2015a).

By addition of various alloying elements to NiTi (Cu, Co, Fe, Nb, Mo), a set of SMA with improved hysteresis, corrosion resistance, transformation temperatures, fatigue behavior is provided (Arghavani 2010).

Various SMA behaviors can be classified in two groups: primary and secondary effects. Some of those effects can be used for application of SMA. The primary effects are (Arghavani 2010):

- Shape Memory Effect,
- Pseudoelasticity.

The secondary effects can be also relevant in some practical application:

- Tension-compression asymmetry,
- Generation of recovery stresses,
- High damping capacity i.e. ability to dissipate vibration energy of structures subjected to dynamic loading.

Additionally, Magnetic Shape Memory Alloys (MSMA), also recognized as ferromagnetic SMA, are known as popular multifunctional materials which has

ability to produce reversible strains of up to 10% under a magnetic field. Some of the best known are NiMnX alloys, where X=Fe, Ga, In, Sn, Sb (Pieczyska 2015; Pieczyska et al. 2011; Haldar et al. 2014). Looking at the microstructure, MSMA have a high-symmetry cubic structure in the high-temperature phase and a low-symmetry tetragonal structure composed of martensitic variants in the low-temperature phase (Pieczyska et al. 2011). The strains induced by magnetic field are caused by reorientation of the martensitic variants, phase transformation or a combination (Haldar et al. 2014). The advantage of MSMA is rapid control of magnetic field (50–100 times higher frequency of acting comparing to classic SMA), but accompanying disadvantage is small strokes of the response. The application of such materials is wide in smart structures, actuators and sensors (Lagoudas 2010).

3.1 Medical Application

The most commonly found commercial biomedical applications of SMA are performed by using the pseudoelasticity effect. Biocompatibility after the surface treatment and its good properties give unique advantage for biomedical use (orthodontic, cardiovascular, orthopedic, surgical instruments etc.) (Arghavani 2010).

3.1.1 Orthodontic Application

The first application of NiTi in medical purpose, since 1970s (Auricchio et al. 2015a), is in orthodontic arch wires production (Fig. 15). They have been used as more effective solution for the teeth alignment purpose. The main advantage in comparison to steel arch wires is ability to operate in pseudoelastic stage where stress changes can be neglected for large strain increment. That allows small force which can move the teeth during the longer period without additional adjustment. Due to almost constant temperature in the mouth, it is possible to provide constant force for large strains. Various kinds of SMA can be produced to allow optimal force for different needs (Lagoudas 2010; Arghavani 2010). Application of SMA, allows readjustment of the wires only a few times a year instead of every 3–4 weeks for stainless steel wires (Auricchio et al. 2015a).

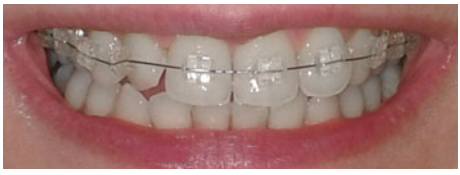

Fig. 15 Orthodontic applications of SMA: nitinol brace used for alignment purposes in dental practice

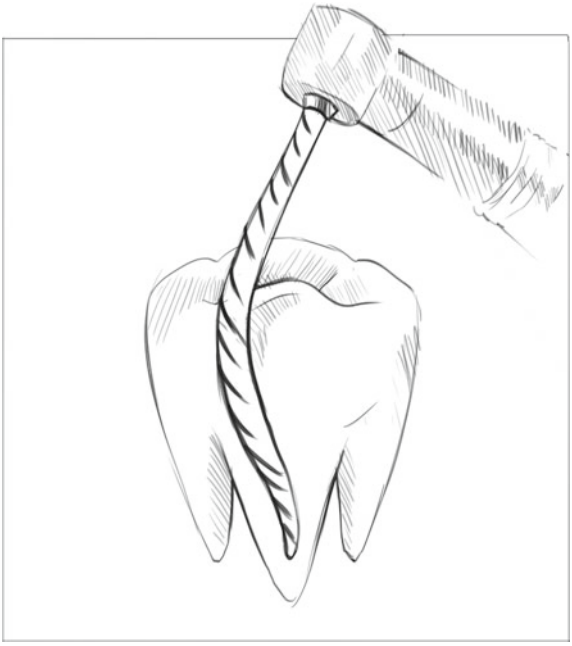

Fig. 16 Orthodontic applications of SMA: scheme of NiTi drill used for root canal surgery (Lagoudas 2010)

Beside this, there are other orthodontic applications of SMA such as NiTi drills used for root canal surgery procedures (Fig. 16) and for periodontal implants (Auricchio et al. 2015a) (Fig. 17).

3.1.2 Orthopedic Application

To obtain an effective connection between fractured bone segments, it is important to provide stable fixing and proper compression between the bone parts. The fixation device is used to strengthen broken bones and to keep the accurate alignment during the healing. The device need to be biocompatible, minimally invasive and it should provide an appropriate compression. SMA staples, fixations, implants, correction nails etc. provide all these requirements in a very efficient way (Auricchio et al. 2015a).

3.1.3 Cardiovascular Application

Cardiovascular application of SMA is of great importance due to development of noninvasive surgery and increasing number of cardiovascular problems

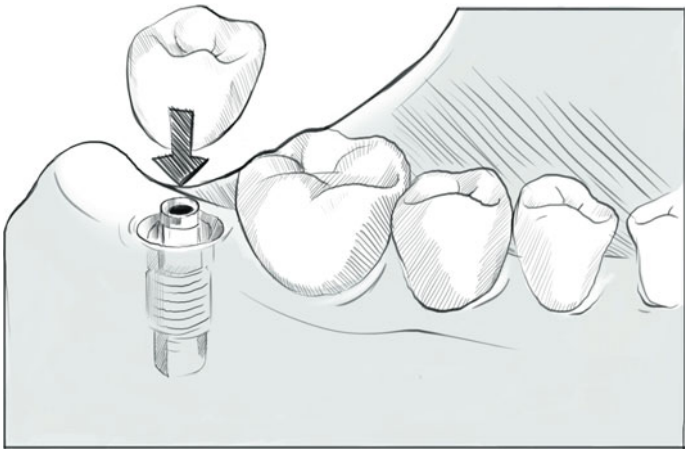

Fig. 17 Periodontal SMA implant (Auricchio et al. 2015a)

(atherosclerosis, hypertension, coronary heart disease, heart stroke) with high death rate (Auricchio et al. 2015b). The cardiovascular devices can be divided in three possible groups: (1) catheters and guidewires; (2) embolic filters; and (3) stents (Auricchio et al. 2015b). The most widely known cardiovascular application is the self-expanding NiTi stent. It is used to support the circumference of tubular passages. When the stents are made of stainless steel, often they do not fit well or the vessel can be damaged after the implantation. On the other hand NiTi stent is self-expandable, so after the implantation the temperature exceeds A_f and the stent expands to its original larger dimensions. The force is not large because it works in pseudoelastic stage, so the walls of the vessel are slowly moved (Arghavani 2010).

The most important property of the stent is its fatigue life which is influenced by the pulsating of blood and by life activities. In fact, stent can experience up to 40 million loading-unloading cycles each year, what makes the fatigue lifetime a major design criterion (Auricchio et al. 2015a).

3.1.4 Other Medical Applications

Among those presented popular applications, SMA can be also used in (Auricchio et al. 2015a):

- General surgery—devices used for surgical interventions need to be flexible and able to apply constant forces over a large deformation range [laparoscopic surgery devices, foot staple used in foot surgery (Fig. 18) (Christ and Reese 2009)],
- Colorectal surgery—expansion devices, sutureless anastomosis (ColonRing) (Auricchio et al. 2015a),
- Otolaryngology—stapes prosthesis in human ear,

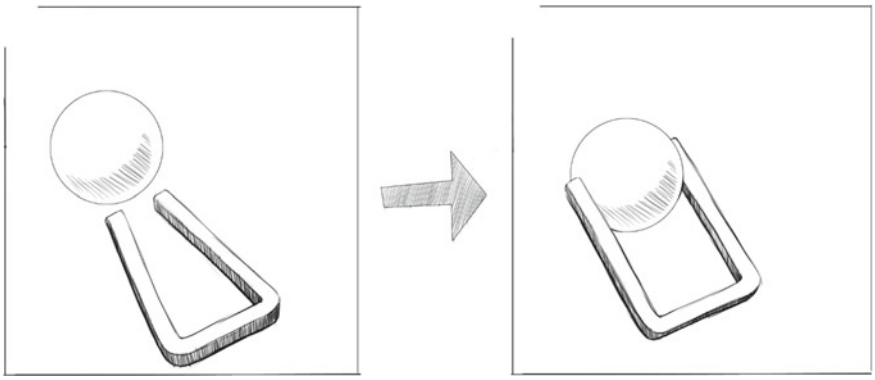

Fig. 18 Staple used for bone fixation after the foot surgery (Christ and Reese 2009)

- Neurosurgery—stents, coils, guidewires,
- Ophthalmology—flexible eyeglasses frame,
- Urology—urethral stents and prostatic stents,
- Gynecology—implant for birthcontrol, devices for breast tumor location,
- Physiotherapy—to activate atrophied muscles using the gloves with TiNi wires.

For example, the foot staple can be used in foot surgery to fix bone segments after the shortening of bones. The bone is cut into the segments and the remaining bone segments need to be fixed to help them grow together (Christ and Reese 2009). The function of the staple is shown in Fig. 18. As it can be observed, the initial sample is cooled down below the martensite finish temperature M_f, then, it is opened mechanically into the desired position (Christ and Reese 2009). Then the staple is heated above the austenite finish temperature A_f. It will recover the original shape if no obstacles are placed between the staples legs (Christ and Reese 2009). Inserting the bone between the legs leads to clamping between the staple and the bone (Christ and Reese 2009).

3.2 Other Technical Applications

Beside the popular medical applications, SMA has become interesting for use in many other areas. The number of commercial applications is growing each year, with the largest application represented by actuators and motors (Menna et al. 2015). The market of SMA has annual growth rate of 12.8% in period 2011–2016 (Menna et al. 2015).

One of the first technical applications of SMA was a pipe couplings (Helm 2007). The advantage of such connector is high durability, easy installation, lightweight design, and the capability to connect various materials (Helm 2007). The coupling principle is shown in Fig. 19: the connectors are produced in the

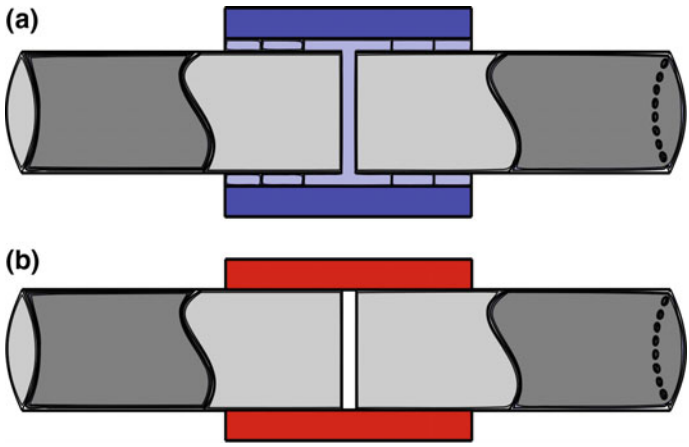

Fig. 19 Scheme of SMA connectors for pipe couplings (Aerofit 2015)

austenite phase and the connector inner size is smaller than the devices which need to be coupled (Helm 2007). The connectors are cooled to a temperature below austenite start to allow inducing of the martensitic transformation by mechanical loading. After unloading, the residual inelastic deformations exists (Helm 2007). The assembling can be done (Fig. 19) by heating of the coupling device above the austenite finish temperature what causes a strong connection (Helm 2007).

Also, as important field of interest, SMA application has been extended to control of civil structures (Song et al. 2006). This application should improve response of civil structures (buildings) to external disturbances and unexpected loading (earthquakes) towards structural safety (Song et al. 2006). The main desired functional properties are actuation, sensing, energy dissipation, self accommodation, structure healing etc. (Menna et al. 2015). Such improvements are necessary extend the structure lifetime and serviceability and the control during the earthquakes. As it was stated by Song et al. (2006), the control of civil structures can be active, passive and semi-active in a form of actuators, passive energy dissipaters and dampers for civil structure control.

4 Conclusions

Materials with advanced characteristics which can be used for technical and medical application attracts attention. Nowadays, with advent of many alloys with shape memory characteristics, researchers and engineers have become motivated to take attention on experimental and numerical investigation of the SMA. Many national and international projects have topics which consider various investigation approaches with the special focus on demands set by industry. Although, there are

various kinds of SMA, one of the most popular is NiTi alloy because of very good mechanical properties and in general high biocompatibility. Of course, NiTi alloys are also one of the most expensive one, but reliable behavior is a key factor which is always important for engineering solutions.

The presented overview gives good base for further investigation of SMA. The details about the characteristics, phenomenological effects and properties are summarized to provide comprehensive knowledge to the reader. Current state of the experiment and modeling research in world has been prepared to present what has been already done and what are the challenges. Efficient and accurate simulations of SMA behavior are fascinating and very useful for many scientific and industrial problems. Also, the high thermal sensitivity of SMA and its influence on the behavior was stressed to explain that taking into account thermomechanical coupling is necessary for correct experimental and numerical investigation of SMA. That is specially important for loading of the SMA at high strain rates when the material exhibits phase transformation which influences change of the temperature.

Various application possibilities are available in literature, but in this work an overview of the most interesting and the most popular solutions is given. Biomedical application is of course the most popular because, it saves the human life and the research is strongly supported. But also, technical application in reliable solutions (aerospace, transportation or civil engineering) is of great importance and the investigation results can help engineers to use SMA in more efficient way.

One of the most recent research challenges in experimental investigation is cyclic loading of SMA because of the change of material characteristic. But also, the numerical simulation of such problems is one of the tasks which should present the applicability of the presented implementation and to define necessary improvements. Also, special case of the subloop cyclic loading is necessary to be examined as real demand in structure exploitation. As extension, the investigation of SMA stents in the fatigue environment is realistic objective, so the procedures for such experimental and numerical investigation have to be established. A special group of SMA with the magnetic properties has been recognized as useful and applicable. So, it is necessary to extend investigation of the coupling to thermo-magneto-mechanical level and to provide possibility to solve such multi-physics problems.

As a special demand for biomedical practice, modeling of stents should be observed. A good example of minimal invasive surgery is implantation of stents to reopen cardiovascular vessels. More than one million of stents are implanted in the world annually. Beside the cardiovascular stents, there are other kind of stents which can be used to help people with the minimal surgery activities. Because of that, modeling of stents has become one of the special demands.

Acknowledgements The research has been carried out with support of the Ministry of Education, Science and Technological Development, Serbia under Grant No. TR32036 and No. III41007, the National Science Center, Poland under Grant No. 2014/13/B/ST8/04280 and No. 2014/15/B/ST8/04368 and KMM-VIN Research Fellowship (1.08-13.09, 2013) for stay of Vladimir Dunić at the IPPT, PAN.

References

Aerofit I (2015) Shape memory alloy (SMA), fluid fitting system, product handbook and engineering data. URL http://www.aerofit.com/images/aerofit/pdfs/sma/catalog/SMA-catalog_book-11-08.pdf

Arghavani J (2010) Thermo-mechanical behavior of shape memory alloys under multiaxial loadings: constitutive modeling and numerical implementation at small and finite strains. PhD thesis, Sharif University of Technology, Tehran, Iran

Arghavani J, Auricchio F, Naghdabadi R, Reali A, Sohrabpour S (2010a) A 3–D phenomenological constitutive model for shape memory alloys under multiaxial loadings. Int J Plasticity 26(7):976–991. doi:10.1016/j.ijplas.2009.12.003

Arghavani J, Auricchio F, Naghdabadi R, Reali A, Sohrabpour S (2010b) A 3D finite strain phenomenological constitutive model for shape memory alloys considering martensite reorientation. Continuum Mech Therm 22(5):345–362. doi:10.1007/s00161-010-0155-8, URL 10.1007/s00161-010-0155-8

Arghavani J, Auricchio F, Naghdabadi R, Reali A, Sohrabpour S (2010c) A 3D finite strain phenomenological constitutive model for shape memory alloys considering martensite reorientation. Continuum Mech Therm 22(5):345–362. doi:10.1007/s00161-010-0155-8

Auricchio F (2001) A robust integration-algorithm for a finite-strain shape memory alloy superelastic model. Int J Plasticity 17(7):971–990. doi:10.1016/S0749-6419(00)00050-4

Auricchio F, Petrini L (2002) Improvements and algorithmical considerations on a recent three-dimensional model describing stress-induced solid phase transformations. Int J Numer Meth Eng 55(11):1255–1284. doi:10.1002/nme.619

Auricchio F, Petrini L (2004a) A three-dimensional model describing stress-temperature induced solid phase transformations: thermomechanical coupling and hybrid composite applications. Int J Numer Meth Eng 61(5):716–737. doi:10.1002/nme.1087

Auricchio F, Petrini L (2004b) A three-dimensional model describing stress-temperature induced solid phase transformations: solution algorithm and boundary value problems. Int J Numer Meth Eng 61(6):807–836. doi:10.1002/nme.1086

Auricchio F, Boatti E, Conti M (2015a) Chapter 11—SMA biomedical applications. In: Lecce L, Concilio A (eds) Shape memory alloy engineering. Butterworth-Heinemann, Boston, pp 307–341. doi: 10.1016/B978-0-08-099920-3.00011-5

Auricchio F, Boatti E, Conti M (2015b) Chapter 12—SMA cardiovascular applications and computer-based design. In: Concilio A, Lecce L (eds) Shape memory alloy engineering. Butterworth-Heinemann, Boston, pp 343–367. doi:10.1016/B978-0-08-099920-3.00012-7

Barbarino S, Saavedra Flores E, Ajaj R, Dayyani I, Friswell M (2014) A review on shape memory alloys with applications to morphing aircraft. Smart Mater Struct 23(6):063001. doi:10.1088/0964-1726/23/6/063001

Boyd J, Lagoudas D (1996) A thermodynamical constitutive model for shape memory materials. Part I. The monolithic shape memory alloy. Int J Plasticity 12(6):805–842. doi:10.1016/S0749-6419(96)00030-7

Buehler W, Gilfrich J, Wiley R (1963) Effect of low-temperature phase changes on the mechanical properties of alloys near composition TiNi. J Appl Phys 34(5):1475–1477

Christ D, Reese S (2009) A finite element model for shape memory alloys considering thermomechanical couplings at large strains. Int J Solids Struct 46(20):3694–3709. doi:10.1016/j.ijsolstr.2009.06.017

Duering T, Melton K, Stockel D, Wayman C (eds) (1990) Engineering aspects of shape memory alloys. Butterworth-Heinemann, London

Dunić V, Pieczyska E, Tobushi H, Staszczak M, Slavković R (2014) Experimental and numerical thermo-mechanical analysis of shape memory alloy subjected to tension with various stress and strain rates. Smart Mater Struct 23(5):055026. doi: 10.1088/0964-1726/23/5/055026

Grabe C (2007) Experimental testing and parameter identification on the multidimensional material behavior of shape memory alloys. PhD thesis, Institut für Mechanik, Ruhr-Universität Bochum, Germany

Grandi D, Maraldi M, Molari L (2012) A macroscale phase-field model for shape memory alloys with non-isothermal effects: Influence of strain rate and environmental conditions on the mechanical response. Acta Mater 60(1):179–191. doi:10.1016/j.actamat.2011.09.040

Haldar K, Lagoudas DC, Karaman I (2014) Magnetic field-induced martensitic phase transformation in magnetic shape memory alloys: modeling and experiments. J Mech Phys Solids 69:33–66. doi:10.1016/j.jmps.2014.04.011

Hallai J, Kyriakides S (2013) Underlying material response for Lüders-like instabilities. Int J Plasticity 47:1–12. doi:10.1016/j.ijplas.2012.12.002

Hartl D, Chatzigeorgiou G, Lagoudas D (2010) Three-dimensional modeling and numerical analysis of rate-dependent irrecoverable deformation in shape memory alloys. Int J Plasticity 26(10):1485–1507. doi:10.1016/j.ijplas.2010.01.002

Helm D (2007) Numerical simulation of martensitic phase transitions in shape memory alloys using an improved integration algorithm. Int J Numer Meth Eng 69(10):1997–2035. doi:10.1002/nme.1822

Helm D, Haupt P (2003) Shape memory behaviour: modelling within continuum thermomechanics. Int J Solids Struct 40(4):827–849. doi:10.1016/S0020-7683(02)00621-2

Jani JM, Leary M, Subic A, Gibson MA (2014) A review of shape memory alloy research, applications and opportunities. Mater Design 56:1078–1113. doi:10.1016/j.matdes.2013.11.084

Jovanović M, Lazić V, Adamović D, Ratković N (2003) Mašinski materijali. Univerzitet u Kragujevcu, Mašinski fakultet u Kragujevcu

Lagoudas D (2010) Shape memory alloys: modeling and engineering applications. Springer, Berlin

Lagoudas D, Hartl D, Chemisky Y, Machado L, Popov P (2012) Constitutive model for the numerical analysis of phase transformation in polycrystalline shape memory alloys. Int J Plasticity 32–33:155–183. doi:10.1016/j.ijplas.2011.10.009

Leclercq S, Lexcellent C (1996) A general macroscopic description of the thermomechanical behavior of shape memory alloys. J Mech Phys Solids 44(6):953–980. doi:10.1016/0022-5096(96)00013-0

Lexcellent C, Vivet A, Bouvet C, Calloch S, Blanc P (2002) Experimental and numerical determinations of the initial surface of phase transformation under biaxial loading in some polycrystalline shape-memory alloys. J Mech Phys Solids 50(12):2717–2735. doi:10.1016/S0022-5096(02)00007-8

Liang C, Rogers C (1992) A multi-dimensional constitutive model for shape memory alloys. J Eng Math 26(3):429–443. doi:10.1007/BF00042744

Menna C, Auricchio F, Asprone D (2015) Chapter 13—Applications of shape memory alloys in structural engineering. In: Concilio LL (ed) Shape memory alloy engineering. Butterworth-Heinemann, Boston, pp 369–403. doi:10.1016/B978-0-08-099920-3.00013-9

Mirzaeifar R, DesRoches R, Yavari A (2011) Analysis of the rate–dependent coupled thermo-mechanical response of shape memory alloy bars and wires in tension. Continuum Mech Thermodyn 23(4):363–385. doi:10.1007/s00161-011-0187-8

Morin C, Moumni Z, Zaki W (2011) A constitutive model for shape memory alloys accounting for thermomechanical coupling. Int J Plasticity 27(5):748–767. doi:10.1016/j.ijplas.2010.09.005

Otsuka K, Ren X (2005) Physical metallurgy of Ti–Ni–based shape memory alloys. Prog Mater Sci 50(5):511–678. doi:10.1016/j.pmatsci.2004.10.001

Otsuka K, Wayman C (eds) (1998) Shape memory materials. Cambridge University Press, Cambridge

Panico M, Brinson L (2007) A three-dimensional phenomenological model for martensite reorientation in shape memory alloys. J Mech Phys Solids 55(11):2491–2511. doi:10.1016/j.jmps.2007.03.010

Pieczyska E (2008) Analiza doświadczalna właściwości termomechanicznych stopów TiNi oraz poliuretanu z pamiecia ksztaltu (Experimental analysis of thermomechanical properties of TiNi shape memory alloys and shape memory polyurethane). Prace IPPT-IFTR Reports, Institute of Fundamental Technologica Research of the Polish Academy of Sciences, in Polish, graphs in English, Habilitation thesis

Pieczyska E (2012) Experimental investigation of stress-induced martensite transformation activity in shape memory alloy. Report grant No NN501 2208 37, Institute of Fundamental Technological Research of the Polish Academy of Sciences

Pieczyska E (2015) Mechanical behavior and infrared imaging of ferromagnetic NiFeGaCo SMA single crystal subjected to subsequent compression cycles. Meccanica 50(2):585–590. doi:10.1007/s11012-013-9868-7

Pieczyska E, Gadaj S, Nowacki W, Tobushi H (2006) Phase–transformation fronts evolution for stress- and strain-controlled tension tests in TiNi shape memory alloy. Exp Mech 46(4):531–542. doi:10.1007/s11340-006-8351-y

Pieczyska E, Dutkiewicz J, Masdeu F, Luckner J, Maciak R (2011) Investigation of thermomechanical properties of ferromagnetic NiFeGa shape memory alloy subjected to pseudoelastic compression test. Arch Metall Mater 56(2):401–408. doi:10.2478/v10172-011-0043-7

Pieczyska E, Tobushi H, Kulasinski K (2013) Development of transformation bands in TiNi SMA for various stress and strain rates studied by a fast and sensitive infrared camera. Smart Mater Struct 22(3):035007. doi:10.1088/0964-1726/22/3/035007

Pieczyska E, Staszczak M, Dunić V, Slavković R, Tobushi H, Takeda K (2014) Development of stress-induced martensitic transformation in TiNi shape memory alloy. J Mater Eng Perform 23(7):2505–2514. doi:10.1007/s11665-014-0959-y

Popov P, Lagoudas D (2007) A 3-D constitutive model for shape memory alloys incorporating pseudoelasticity and detwinning of self-accommodated martensite. Int J Plasticity 23(10–11):1679–1720. doi:10.1016/j.ijplas.2007.03.011 (in honor of Professor Dusan Krajcinovic)

Qidwai M, Lagoudas D (2000a) Numerical implementation of a shape memory alloy thermomechanical constitutive model using return mapping algorithms. Int J Numer Meth Eng 47(6):1123–1168

Qidwai M, Lagoudas D (2000b) On thermomechanics and transformation surfaces of polycrystalline NiTi shape memory alloy material. Int J Plasticity 16(10–11):1309–1343. doi:10.1016/S0749-6419(00)00012-7

Raniecki B, Lexcellent C (1994) RL-models of pseudoelasticity and their specification for some shape memory solids. Eur J Mech A Solid 13(1):21–50

Raniecki B, Lexcellent C (1998) Thermodynamics of isotropic pseudoelasticity in shape memory alloys. Eur J Mech A Solid 17(2):185–205. doi:10.1016/S0997-7538(98)80082-X

Reese S, Christ D (2008) Finite deformation pseudo-elasticity of shape memory alloys—constitutive modelling and finite element implementation. Int J Plasticity 24(3):455–482. doi:10.1016/j.ijplas.2007.05.005

Shaw J, Kyriakides S (1995) Thermomechanical aspects of NiTi. J Mech Phys Solids 43(8):1243–1281. doi:10.1016/0022-5096(95)00024-D

Song G, Ma N, Li HN (2006) Applications of shape memory alloys in civil structures. Eng Struct 28(9):1266–1274. doi:10.1016/j.engstruct.2005.12.010

Souza A, Mamiya E, Zouain N (1998) Three-dimensional model for solids undergoing stress-induced phase transformations. Eur J Mech A Solid 17(5):789–806. doi:10.1016/S0997-7538(98)80005-3

Stupkiewicz S, Petryk H (2013) A robust model of pseudoelasticity in shape memory alloys. Int J Numer Meth Eng 93(7):747–769. doi:10.1002/nme.4405

Teeriaho JP (2013) An extension of a shape memory alloy model for large deformations based on an exactly integrable Eulerian rate formulation with changing elastic properties. Int J Plasticity 43:153–176. doi:10.1016/j.ijplas.2012.11.009

Thamburaja P (2010) A finite-deformation-based phenomenological theory for shape-memory alloys. Int J Plasticity 26(8):1195–1219. doi:10.1016/j.ijplas.2009.12.004 (special Issue In Honor of Lallit Anand)

Thamburaja P, Anand L (2001) Polycrystalline shape-memory materials: effect of crystallographic texture. J Mech Phys Solids 49(4):709–737. doi:10.1016/S0022-5096(00)00061-2

Tobushi H, Matsui R, Takeda K, Pieczyska E (2013) Mechanical properties of shape memory materials. Materials science and technologies, mechanical engineering theory and applications. NOVA Publishers, New York

Wang M, Jiang M, Liao G, Guo S, Zhao X (2012) Martensitic transformation involved mechanical behaviors and wide hysteresis of NiTiNb shape memory alloys. Prog Nat Sci Mater Int 22 (2):130–138. doi:10.1016/j.pnsc.2012.03.010

Yang S, Dui G (2013) Temperature analysis of one-dimensional NiTi shape memory alloys under different loading rates and boundary conditions. Int J Solids Struct 50(20–21):3254–3265. doi:10.1016/j.ijsolstr.2013.05.026

Zaki W, Moumni Z (2007) A three–dimensional model of the thermomechanical behavior of shape memory alloys. J Mech Phys Solids 55(11):2455–2490. doi:10.1016/j.jmps.2007.03.012

Zhang X, Sehitoglu H (2004) Crystallography of the B2 → R → B19′ phase transformations in NiTi. Mater Sci Eng A 374(1–2):292–302. doi: 10.1016/j.msea.2004.03.013

Bioactive Biomaterials: Potential for Application in Bone Regenerative Medicine

Jelena Najdanović, Jelena Rajković and Stevo Najman

Abstract Critical-sized bone defects can be repaired by using bone tissue engineering (BTE) procedures which rely on the combined use of cells, scaffolds and biologically active molecules. Based on their bioreactivity, biomaterials can be bioinert or bioactive. Bioinert biomaterials cause fibrous capsule formation upon implantation which favors the appearance of micromovements in the implant-tissue interface so the prosthesis fails. Bioactive biomaterials elicit a specific biological response thus avoiding fibrous layer formation and are able to interact with the biological environment. Bioactive biomaterials can be natural (bovine bone mineral matrix, hyaluronic acid, collagen, gelatin, fibrin, agarose, alginate, chitosan, silk) or synthetic (ceramics, metals, polymers, hydrogels and composites). Ceramics (bioactive glasses, glass–ceramics, calcium phosphates ceramics and cements) are most frequently used among these biomaterials due to similarity with the bone mineral phase. Another advantage from the use of ceramics is the presence of biologically active hydroxycarbonate apatite layer formed on the surface of these biomaterials, which represents the bonding interface with the tissues. Bioactive biomaterials have wide application as medical devices and in drug delivery systems. Since cells cannot survive without an adequate blood supply, future directions in bioactive biomaterials applications lies in the construction of bioactive and biodegradable 3D scaffolds that have osteogenic and angiogenic features. A possible alternative to improve osteogenic and angiogenic potential of the applied biomaterials is to incorporate bioactive biomolecules (e.g. growth factors) into the scaffold. One of the future perspectives in this area is the construction of smart biomaterials that respond to their environment in predetermined way regarding the protein release, thus allowing release initiated by microenvironmental conditions.

J. Najdanović · S. Najman (✉)
Department for Cell and Tissue Engineering and Institute
of Biology and Human Genetics, Faculty of Medicine, University of Niš,
Bul. Zorana Đinđića 81, 18000 Niš, Serbia
e-mail: stevo.najman@gmail.com

J. Rajković
Department of Biology and Ecology, Faculty of Sciences and Mathematics,
University of Niš, Višegradska 33, 18000 Niš, Serbia

F. Zivic et al. (eds.), *Biomaterials in Clinical Practice*,
https://doi.org/10.1007/978-3-319-68025-5_12

Keywords Bioactive biomaterials · Osteoinduction · Osteoconduction · Natural bone substitute · Ceramics · Implantation

1 Introduction to Bioactive Biomaterials in Medicine

Bone remodeling process occurs through whole life. A bone, highly vascularized and dynamic tissue, has high regenerative capacity which means that majority of the fractures can be healed spontaneously. Nevertheless, when critical-sized defects or nonunions occur, surgical interventions are inevitable (Stevens 2008). Critical-sized defects are wounds within a bone that are of such size that cannot heal spontaneously, or in which pathologic process detain regeneration (Allo et al. 2012).

Large bone defects can be reconstructed by using a gold standard in bone regenerative medicine—autografts (Schroeder and Mosheiff 2011). Autografts are osteoinductive and osteoconductive and have numerous osteogenic cells and adequate blood supply that altogether support graft viability (Schroeder and Mosheiff 2011). To avoid autologous bone harvest procedure, which represents health risks for the patient, alternative is the use of allografts (Bishop and Pelzer 2007). However, allografts lack vascular network (Griffith et al. 2005), osteoinductive growth factors as well as osteogenic cells (Cornejo et al. 2012). The other possibility for regeneration of large bone defects are bone tissue engineering (BTE) procedures which rely on the combined use of cells, scaffolds and biologically active molecules (Healy and Guldberd 2007; O'Keefe and Mao 2011; Najdanović et al. 2016). During bone tissue regeneration, the host cells respond to an osteogenic signal, while three-dimensional (3D) scaffold supports the growth of responsive host cells and allow the formation of extracellular matrix (ECM) and a vascularized host bed (Burg et al. 2000).

Biomaterials for BTE must be able to promote differentiation of progenitor cells into osteoblasts (osteoinductive), support bone growth encourage the ingrowth of the surrounding bone (osteoconductive), and to integrate into existing bone (osseointegration) (Stevens 2008). Any biomaterial applied in BTE must be bioresorbable and replaced with newly regenerated biological tissue in the body (Langer and Vacanti 1993).

The term "osseointegration" was first mentioned in 1965 by Brånemark in order to describe the successful fixation of implant into bone tissue (Brånemark et al. 2001). During osseointegration, osteoblast precursors accumulate, bone matrix forms and biomineral formation can eventually occur. The response of bone to an osseointegrated implant is similar to the response that occurs during bone fracture healing and includes the formation of blood clot upon implantation (Davies 2003). A blood clot is a peculiar scaffold for blood cells and, at the same time, a source of biological signals and differentiation factors inductive for the osteogenic process

(Puleo and Nanci 1999). Osteogenic transcription factors regulate osteogenic differentiation of mesenchymal stem cells (MSCs) and regulate expression of the following genes: osteocalcin, osteopontin, bone sialoprotein, alkaline phosphatase and collagen type-I (ALP) (Long 2011). Several days after the implantation, osteoblasts secrete a bone matrix directly onto the implant surface that subsequently develops into immature (woven) bone (Davies 2003). At the end, immature bone is being replaced with the mature bone at the implant site, thus providing biological (mechanical) stability of the implant.

1.1 Implant-Tissue Interactions

Interactions between the implant and tissue can be extracellular and intracellular. Extracellular interaction is dependent on biomaterial's surface features. Adsorption of non-collagenous proteins and collagen at biomaterials' surface are influenced by surface nanometer scale porosity, biomaterial surface topographic configurations and negatively charged signals. Protein adsorption depends on various features. Interactions between osteoblast receptors and the corresponding protein ligands on the surface contribute to the cellular adhesion. Also, the adsorbed proteins on the implant surface, e.g. bone growth factors and activated enzymes, have a direct influence on the cell differentiation and proliferation. For example, osteoblast proliferation is favored over fibroblast proliferation on the surface of bioactive ceramics (Seitz et al. 1982).

Intracellular interaction is caused by the release of soluble agents from the biomaterial surface. Keeting and his team reported that soluble silicon released from the glass surface was a potent mitogen for human osteoblast-like cells, and that it also increased DNA synthesis and enhanced alkaline phosphatase activity and osteocalcin release (Keeting et al. 1992). It has been shown that osteoblasts' proliferation is more rapid on bioactive glass substrates compared to synthetic HA (Vrouwenvelder et al. 1993).

2 Classification of Biomaterials in Medicine

Reactivity of the biomaterial with the native tissues is of key importance for the construction of the implants (Vallet-Regi and Ruiz-Hernandez 2011). In the past, biomaterials for BTE were constructed to be "bioinert", while biomaterials today are mostly designed to be "bioactive" which refers to ability to interact with the cells and biological molecules and regenerate bone tissue (Langer and Vacanti 1993; Hench and Polak 2002).

2.1 Bioinert Biomaterials

Bioinert biomaterials are used in order to reduce the immune reaction and the reaction to foreign body as much as possible (Hench 1980). After implantation of a bioinert biomaterial, fibrous capsule surrounds the material as an answer to the foreign body (Castner and Ratner 2002). Subsequently, a formed capsule favors the appearance of micromovements in the implant-tissue interface. As a consequence, the prosthesis fails and it must be replaced (Salinas et al. 2013).

To overcome such problems, two approaches have been developed: biological fixation and bioactive fixation (Cao and Hench 1996). Biological fixation represents the construction of materials with rough surfaces and pores larger than 100 μm which allow tissue ingrowth and angiogenesis. During bioactive fixation, intimate biomaterial-bone apposition is established which has a mechanically strong bond as a consequence (Salinas et al. 2013).

In earlier experimental and clinical applications, bioinert biomaterials were thought to be superior over bioactive ones because these biomaterials generate a minimal tissue response. Nevertheless, survivability of bioinert implants decrease in long-term periods (>10 years) so the development of bioactive biomaterials became more attractive in tissue engineering (Hench 1998a).

2.2 Bioactive Biomaterials

The term “bioactivity” relates to all interactions and effects that materials exert on cells thus activating responses or leading to specific cell behaviors (Navarro et al. 2008). Bioactive biomaterials are created in such way that elicit a specific biological response and avoid fibrous layer formation. These biomaterials have interaction with the biological environment thus enhancing the biological response as well as the tissue/surface bonding (Navarro et al. 2008). Bioactive biomaterials provide an environment that is consistent with bone growth. This enables development of mineralizing interface which is a natural bond junction between living and non-living biomaterials (Cao end Hench 1996).

Mineralization and binding between the bone tissue and the implant are one of the most important approaches for increasing bioactivity during the repair (Navarro et al. 2008). Also, mechanical properties of the bioactive biomaterial are important. The structure of bone determines its mechanical properties while mechanical load determines bone structure during repair. Therefore, the perfect bioactive biomaterial should enhance newly formed bone formation which has mechanical properties similar to the normal host bone site (Hench 1998b).

Amongst the crucial factors in the design of bioactive biomaterials are the pore size and interconnection of pores (Davis et al. 2005). Large interconnected pores promote colonization of biomaterials (Karande et al. 2004), but if the pores are extremely large, the consequence is impaired vascularization because endothelial

cells cannot bridge the pores larger than a cell diameter (Salem et al. 2002). Integrity of the material is also affected by the size of pores so the cellular effects should be in balance with the mechanical properties of applied biomaterial (Karande et al. 2004). When the pores are smaller than 100 nm, diffusion of nutrients and factors are affected, which lead to the failure of implanted grafts and poor survival of implanted cells (Zimmermann et al. 2004). Pore length and numbers has an influence on the diffusion of nutrients and factors in the polymers (Botchwey et al. 2003). Very small pores in hydrogels constructed from self-assembling peptides support adhesion of endothelial cells and formation of capillary network as well as rapid cell migration (Narmoneva et al. 2005).

Bioactive materials are osteoconductive since they provide the surfaces adequate to support the adhesion and proliferation of osteoblasts (Hench and West 1996). Among them, there are also osteoinductive materials which, besides facilitating bone growth, have a role in conducting bone formation (Hench and West 1996). While osteoconduction is an extracellular response, osteoinduction is an intracellular response induced by the release of large amounts of Si (IV) and Ca^{2+} ions which stimulate the genes response in order to produce the bone formation (Salinas et al. 2013).

Based on the type of effect exerted on bone tissue, bioactive biomaterials divide into two classes—Class A and Class B. The bioactive glasses that enhance bone proliferation and differentiation of progenitors (osteoproduction) due to reactivity at a cellular level in the body has a Class A bioactivity. In contrast to that, Class B bioactive biomaterials, such as synthetic HA, lead only to bone growth along the implant surface—osteoconduction (Hench and West 1996). It has been shown that bone proliferation in vivo is enhanced in the presence of bioactive glasses with the same or even greater growth rate compared to an autogeneous bone applied for same defect (Hench and West 1996). As a consequence of the enhanced osteogenic behavior, production of biological growth factors is also enhanced and therefore, cell proliferation and the formation of newly organized tissues are stimulated (Hench 1998a).

Class A bioactive materials are able to form a biologically active hydroxycarbonate apatite (HCA) layer on their surfaces in vivo within a few minutes to a few hours (Cao and Hench 1996; Hench and West 1996), while well-crystallized HCA layer onto Class B bioactive materials need more than one week to be formed (Hench and West 1996). Sol–gel chemistry can be used to synthesize HCA coatings on various types of substrates which are formed probably by the mechanism of heterogeneous nucleation of HCA crystals within the nanometer-sized pores that create supersaturated Ca–P solutions (Pereira and Hench 1996).

It is thought that the biomaterials which will enhance tissue regeneration should have higher molecular control of interfacial reactions than the one in Class A bioactive biomaterials. The molecular control comprises the release control of the elements and chemical compounds which activate the genes important for mitosis and cell differentiation. Resorption of bioactive materials is also important and it is

controlled at molecular level by the metabolic processes of the tissue which is being replaced. The genetic activation of the enzymes and growth factors synthesis and the ability to adsorb and desorb biologically active molecules without losing the conformation and biological function are also important. Sol–gel processing provides the chemical control of a biomaterial's dissolution rate and surface chemical binding sites (Hench 1998a).

Class A bioactive biomaterials can form a biologically active, hydrated silica-gel layer on their surfaces a few minutes after exposure to the body fluids either in vivo or in vitro. This hydrated silica-gel layer is highly porous three-dimensional network which is totally interpenetrated with pore liquid (Hench 1998a). Pore-liquid networks can be enriched by incorporation of various organic and biological molecules (Avnir et al. 1997). A spectrum of differing volume fraction and size distributions of porosities can be accomplished in films (Brinker et al. 1995) and porous matrices (Hench and Orefice 1997) by changing the production conditions.

3 Bioactive Biomaterials in Bone Regenerative Medicine

The clinical survivability of the biomaterials such as bioactive glasses, ceramics, glass-ceramics, and composites is higher than in the case of bioinert biomaterials (Cao and Hench 1996; Hench and West 1996). Among the successful clinical applications of bioactive biomaterials are bioactive synthetic hydroxyapatite coatings and filling of bone defects (Ratner et al. 2004), bioactive glass middle-ear prostheses, endosseous alveolar ridge maintenance implants (Cao and Hench 1996) and bioactive A/W glass-ceramic in iliac crest donor site repair and replacement of vertebrae (Cao and Hench 1996).

Hydroxyapatite, in bulk and granular forms, was used as bone spacers and fillers (Shores and Holmes 1993). Glass-ceramic A–W, due to its high mechanical strength and good bone-bonding ability, has been used as artificial vertebrae, intervertebral discs, and iliac crests in dense bulk form (Yamamuro 1993).

The success was made in the application of BG particulate in the 6-mm defect in a rabbit femur by Oonishi et al. (1997). New trabecular bone was formed within one week, while after three weeks regenerated trabecular bone formed around the bioactive glass particles throughout the defect and bonded the particles together. Synthetic HA particulate did not succeed to fill the same defect even after twelve weeks of the surgical procedure. In this later case, the bridges between bone ends did not grow in thickness and only a small amount of bone were found between HA particles (Oonishi et al. 1997).

Wheeler et al. demonstrated that the accelerated bone formation was accompanied by resorption of the gel glass particles in 3 months. Active mineralization occurred throughout the grafted bone defects, with osteoblasts lining the new bone, formed around the gel-glass particulates. All grafted defects had significantly more bone within the area than the unfilled controls (Wheeler and Stokes 1997).

Wheeler and his associates (Wheeler et al. 1998) examined bone regeneration in cancellous skeletal defects of rabbits distal femur augmented with USB (90–710-μm particle size) or OV (300–355-μm particle size) bioactive glass particles and compared it with normal cancellous bone. Statistically higher bone quantity was found in the defect filled with USB and NORM than in the defect with OV ($p < 0.05$) at both observation points (4 and 12 weeks). This can be explained by the larger mean particle size of the OV than the USB particles combined with more numerous particles within the USB-grafted defects. Greater particles number in combination with the smaller particle size caused greater surface area of bioactive glass in the USB-filled defects, which further provided more sites for osteoblast adhesion and osseous formation than in the defects filled with OV.

Bioactive calcium phosphates and silica-based glasses are suitable for small bone defects filling (Yuan et al. 2010) where the bone regeneration kinetics is preferable over mechanical properties (Salinas and Vallet-Regı 2013). Due to their fragility and low resistance to fatigue, these types of bioactive biomaterials are inappropriate choice for large bone defects repair.

Bioactive biomaterials that have application in bone regenerative medicine could be classified as natural and synthetic bone substitutes (Fig. 1). Nanomaterials belong to a special class of bioactive biomaterials that comprises both natural and synthetic biomaterials (Fig. 1).

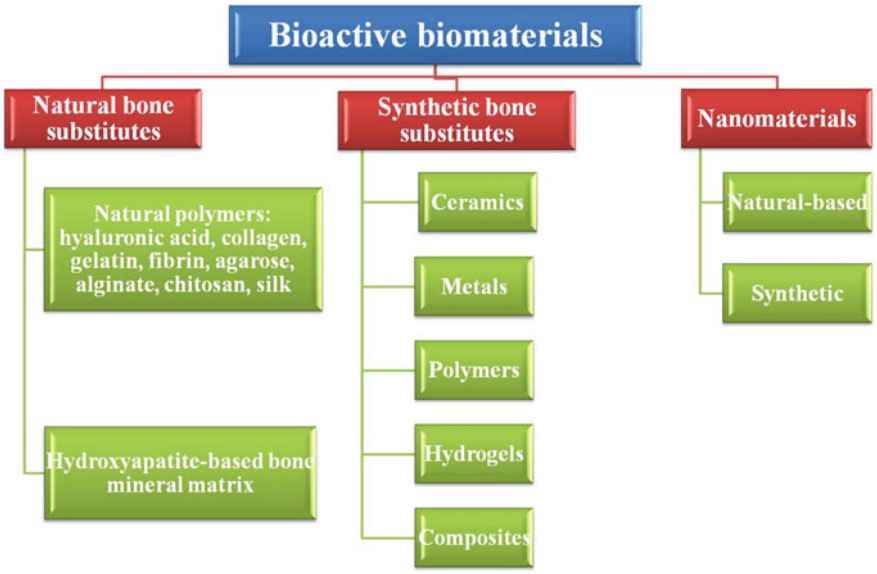

Fig. 1 Types of bioactive biomaterials that have application in bone regenerative medicine

3.1 *Natural Bone Substitutes*

In our laboratory, we are dealing with bone biology and bone regeneration in animal models. For this purpose, various biomaterials as bone substitutes and scaffolds for cells, growth factors and drugs are exploited. Commercial, hydroxyapatite-based bone mineral matrix (BMM) Bio-Oss® (Geistlich-Pharma, Wolhusen, Switzerland) combined with platelet-rich plasma (PRP) as a source of growth factors and adipose-derived stem cells (ADSCs) in vitro induced towards endothelial cells (ECs) were used to provide "biological triad" principle in subcutaneous implants (Fig. 2). Such combination caused increased vascularization in bioengineered implants and more pronounced osteogenic process (Najdanović et al. 2015). Also, in vitro osteoinduced ADSCs delivered with PRP on BMM as a carrier (Fig. 2) induced formation of osteocalcin-positive callus-like tissue in ectopic implants and intensive resorption of BMM granules (Cvetković et al. 2015).

In a simulated intraoperative procedure, we have shown that subcutaneous implants composed of BMM as a carrier, PRP and freshly isolated adipose derived stromal vascular fraction cells, rapidly triggered osteogenic process and had excellent osteogenic capacity (Najman et al. 2016). The same BMM combined with blood diluted with inflammatory macrophages has shown a favorable effect on the process of angiogenesis and synthesis of an organic fraction of bone matrix

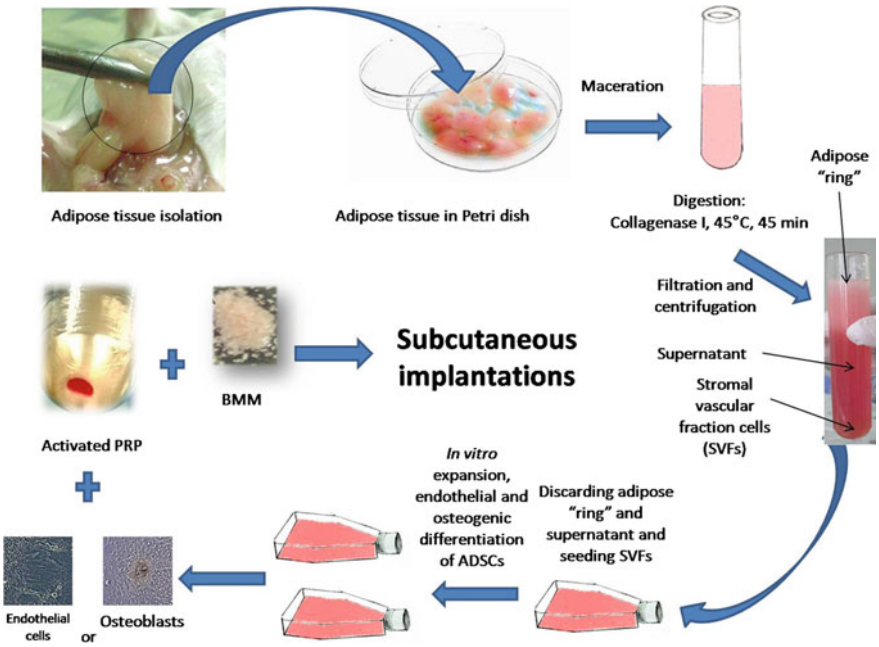

Fig. 2 Preparation of subcutaneous bioengineered implants according to the triad model with cells, scaffold and regulatory signals

(Živković et al. 2015). Bio-Oss granules supplemented with PRP have also served as carriers for different forms of vitamin D which is utilized in the regeneration of osteoporotic bone (Fig. 3). Cholecalciferol and alfacalcidol, locally applied with this bioactive carrier/scaffold in the area of femoral defect, decrease the resorption of Bio-Oss particles, delay early bone regeneration and induce the formation of new healthy bone tissue in the case of alfacalcidol or high amount of the well mineralized bone tissue in the case of cholecalciferol (Rajković et al. 2015).

An important bioactive effect in various tissues, including bone and cartilage, has been shown by using some natural polymers: hyaluronic acid, collagen, gelatin, fibrin, agarose, alginate, chitosan, silk.

Hyaluronic acid has been applied for surgical adhesions, knee pain (Furth et al. 2007), cartilage regeneration (Jazayeri et al. 2017).

Although collagen is mostly used in soft tissue regeneration (Furth et al. 2007), it has been found that collagen-based osteochondral grafts have consistently integrated layer structure and good porosity as well as mechanical properties (Levingstone et al. 2014).

Main use of gelatin is cartilage tissue regeneration, while fibrin is a potential scaffold for stem cell cultures which could be further used in bone and cartilage tissue engineering (Jazayeri et al. 2017).

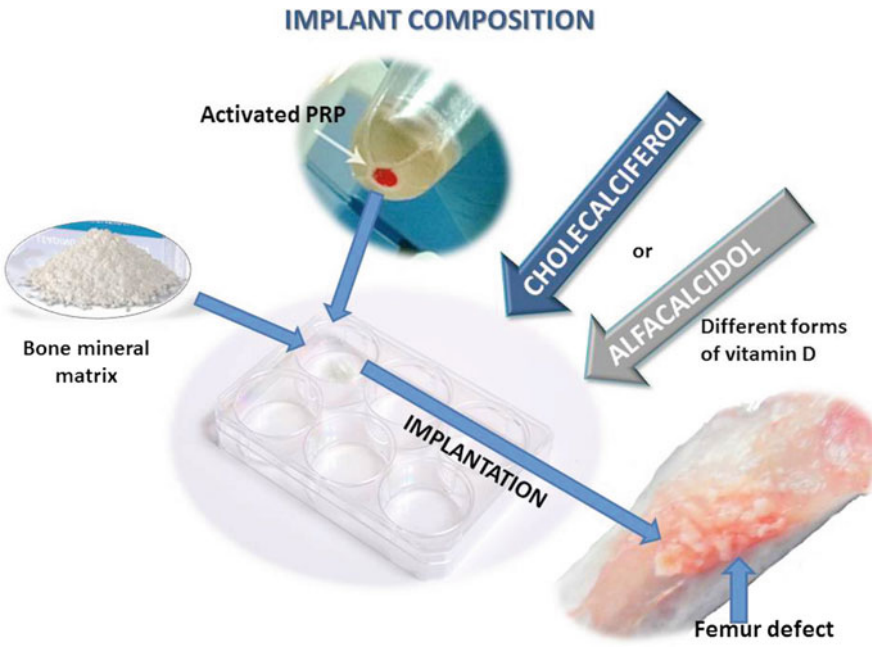

Fig. 3 Preparing of orthotopic implants of BMM granules supplemented with PRP as carriers for different forms of vitamin D in the regeneration of osteoporotic bone

It has been shown that agarose scaffolds increase stem cells' differentiation into chondocytes (Awad et al. 2004). These scaffolds are the versatile ones for the application in bone tissue engineering (Jazayeri et al. 2017).

Alginate can be used in the form of hydrogels that bears cell-adhesion ligands (Langer and Tirrell 2004). These biomaterials have been applied as scaffolds for cell encapsulation and transplantation, which brought good results regarding engineering such bone tissue that can grow out of modest numbers of implanted cells (Alsberg et al. 2002) and in drug delivery (Tonnesen and Karlsen 2002).

Chitosan-based injectable materials and its derivatives could be applied as osteogenic bone substitutes (Shi et al. 2006). Ge and his associates found that combinations of chemically modificated hyaluronic acid and also chitin-chitosan-HA biomaterial promoted neovascularization, had osteoinductive effects and rapidly degraded in vivo (Ge et al. 2004). The other advantage of chitosan application in bone regenerative medicine is the ability to induce recruitment and attachment of osteogenic cells (Kim et al. 2002). It was also found that scaffolds composed of chitosan/alginate/hydroxyapatite, which was the carrier for recombinant BMP-2 and mesenchymal stem cells, had excellent effect on formation of new bone that resulted in almost completed repair of critical sized bone defects in rats 12 weeks after implantations (He et al. 2014).

Due to its biocompatibility and slow degradation rate (Hege and Schiller 2015), silk is good candidate for application in bone regenerative medicine. In spite of that, silk lacks osteoinductivity, so the addition of osteoinductive factors to silk is necessary (Huang et al. 2014). Huang and associates examined the effect of osteoinductive-nanoscaled silk/HA composite scaffolds and found that the addition of hydroxyapatite to silk enhanced biocompatibility and mechanical strength of the scaffolds (Huang et al. 2014).

One of the most attractive directions in bone regenerative medicine is the use of bioinspired biomaterials. Construction of such biomaterials is based on mimicking natural biological design in order to construct synthetic biomaterials (Green et al. 2016). For example, this mechanism has been applied for the construction of boundary between bone replacements and natural bone in a rat calvarial defect. The boundary was made out of glue substrate that was secreted by *Phragmatopoma californica*, a sandcastle worm (Winslow et al. 2010). The glue was moderately resorbed and replaced by new lamellar bone.

3.2 Synthetic Bone Substitutes

3.2.1 Ceramics

Ceramic materials, which include bioactive glasses (BGs), glass–ceramics, calcium phosphates ceramics (CaPs) and cements (Navarro et al. 2008), are mostly used as bone defect fillers (Vogel et al. 2001). These biomaterials are similar to the bone mineral phase and have structural and surface features which enable binding to the

bone without forming an interface that consists of fibrous connective tissue (Schepers et al. 1991).

Simultaneously with the implantation procedure, time-dependent kinetic modification of the ceramics surface begins. Hydroxycarbonate apatite (HCA) layer developed at the biomaterial surface is bioactive and represents the bonding interface with tissues due to its similarity with the mineral bone phase (Hench 1998b). Bioactive glasses applied in BTE are able to induce bone tissue growth processes—enzyme activity (Aksay and Weiner 1998), revascularization (Keshaw et al. 2005) as well as osteoblast differentiation from mesenchymal stem cells and osteoblast adhesion (Lu et al. 2005; Schepers et al. 1991).

During the early implantation period, apatite layer formation on the ceramic surface precede bone matrix integration into apatite (Kokubo 1990). This apatite layer contains nano-crystals of carbonate-ion-containing apatite with structure and crystallinity similar to the one in bone mineral phase (Kokubo 1990). Osteoblasts that proliferate on the apatite form a biological apatite/collagen extracellular matrix (Loty et al. 2000), thus enabling direct contact between surface of the apatite layer and surrounding bone (Kokubo et al. 2003).

Immersion of bioactive biomaterials into a simulated body fluid (SBF), an aqueous solution with mostly the same ingredients as human extracellular fluid, is another approach applied to achieve a bone-like apatite layer formation. SBF is cell-free and protein-free, so the apatite layer is formed due to the chemical reaction between bioactive ceramics and the surrounding fluid. Thanks to such features of SBF, new types of biomaterials that are bioactive have been designed—glass-ceramics, organic–inorganic hybrids, coatings as well as bioresorbable ceramics (Ohtsuki et al. 2009).

Some of the most frequently used ceramics in medicine are: Bioglasss in the Na_2O–CaO–SiO_2–P_2O_5 system (Hench et al. 1971), hydroxyapatite (HA) ($Ca_{10}(PO_4)_6(OH)_2$ (Jarcho et al. 1977), β-tricalcium phosphate (TCP) ($Ca_3(PO_4)_2$ (Rejda et al. 1977), HA/TCP bi-phase ceramic (Daculsi et al. 1990), glass ceramic A–W containing crystalline oxyfluoroapatite ($Ca_{10}(PO_4)_6$(O, F2)) and β-wollastonite (CaO × SiO_2) in an MgO–CaO–SiO_2 glassy matrix (Kokubo et al. 1982).

In 1971, Hench and associates made the first bioactive glass Bioglass® by the conventional melt-derived process (Hench et al. 1971). Nowadays, it exists in the particulate form of following commercial products: Perioglas® (periodontal bone filler), Novabone® (orthopedic bone filler), Novamin (additive for toothpaste), but its disadvantage is that it cannot be made into a scaffold because it crystallizes on sintering and forms a glass-ceramic. A Sol–gel derived glass is a procedure for production of scaffolds from bioactive glasses. It is developed as an alternative to the traditional melt processing in order to ensure an interconnected nanoporous structure through the whole glass (Jones 2009). Nanoporosity influence cell response, especially osteoblast response (Biggs et al. 2007). Nevertheless, the greatest advantage of bioglass prepared by sol–gel method is the introduced foaming step that creates porous scaffolds with interconnected macropore networks.

45S5 Bioglasst (USB) is an effective graft material for the use in oral and maxillofacial bone surgery (Oguntebi et al. 1993), mostly because of its bioactivity based on the following composition −45% SiO_2, 24.5% CaO, 24.5% Na_2O, and 6% P_2O_5. Such composition of USB stimulates apatite gel layer formation on the surface of the particles, which attracts osteoprogenitor cells and osteoblasts, thus stimulating formation of bone (Hench et al. 1991). USB has a wide range of particle size (from 90 to 710 mm) which was shown as an optimal feature for bone tissue regeneration of critical-sized calvaria defects (Bergman and Litkowski 1995). Numerous studies have proved the potential of 45S5 bioactive glass for skeletal applications (Piotrowski et al. 1975).

Bioactive gel-glasses are advantageous over bioactive glasses, such as 45S5 Bioglasst (BG), for several reasons. Among these reasons is the absence of Na_2O in the Bioactive gel-glasses structure, which ensures that there is no rapid increase in interfacial pH following the surface reactions. Also, a large surface silanols-rich area can be obtained in situ in the gel-glasses by controlling the ultrastructure processing, aging, and stabilization treatments. Therefore, bioactive gel-glasses can nucleate a biologically active HCA layer within minutes more rapidly than bioactive melt glasses with much lower contents of silica. Thanks to sol–gel processing, bioactive compositions can obtain wide range of silica content and variable levels of CaO and P_2O_5 (Pereira et al. 1994).

Bioactive glasses can also be designed to deliver ions which activate complex gene transduction pathways and thus enhance cell differentiation and osteogenesis (Hench and Polak 2002; Tsigkou et al. 2007). Crystalline HA can be used for the adjustment of resorption rate of bioactive glasses and bioceramics. Other calcium phosphates possess a greater capacity to be resorbed but their strength for sustaining load is lower (Oonishi et al. 1995).

Biologically relevant levels of soluble ions of Si, Ca, P, and Na can be released by bioactive glass surfaces. These ions further promote intra- and extra-cellular responses (Xynos et al. 2001). Bioactive glasses based on borate support cell proliferation and differentiation in vitro (Fu et al. 2010a; Marion et al. 2005) as well as the tissue infiltration in vivo (Fu et al. 2010b), while bioactive glasses which have Cu, Zn or S as components favors bone growth (Fu et al. 2010a; Wang et al. 2011; Zheng et al. 2012).

3.2.2 Metals

Since none of the orthopedic metallic biomaterials is bioactive by itself, there are two methods to make them bioactive: coating implants' surface with a bioactive ceramic and chemical modification of the biomaterials' surface. The second procedure is used in order to accomplish deposition of a bioactive ceramic in vivo or to promote adhesion of cells and proteins and other interactions between tissue and biomaterial (Navarro et al. 2008).

Some metals may become bioactive due to ceramic component formed on their surfaces by chemical etching process. For example, as a result of the chemical

reaction of TiO_2 with NaOH, a sodium hydrogen titanate gel layer is formed. Subsequently, the thermal treatment produces amorphous sodium titanate which displays a bioactive response (Salinas and Vallet-Regı 2013).

Osseointegration of an implant can be improved by coating the implants with inorganic and organic components that are similar to the ones in physiological extracellular bone matrix (ECM) (de Jonge et al. 2005). These depositions of bioactive biomaterials enable direct implant–bone bonding and enhance implant osseointegration due to the accelerated speed and amount of new bone formed at the interface (de Jonge et al. 2005). Described cell-biomaterial interactions are mediated by integrins which also probably cooperate with osteogenic factors that accumulate on the implant surface thus regulating proliferation and differentiation of osteoblasts (Siebers et al. 2005). The coating which had the successful application in BTE are nano-CaP/collagen and CaP/ALP composite coating onto titanium surfaces (de Jonge et al. 2009), growth factors loaded on collagen or CaP-coated implants (Li et al. 2010) and DNA-based coating onto titanium implants using the layer-by-layer (LbL) deposition technique (Schouten et al. 2010).

3.2.3 Polymers

Polymers can be either biological or synthetic. Biological polymers contain inherent biological informations that are necessary for induction of chemotactic responses as well as cell attachment. The alterative for biological polymers are synthetic ones which can be produced into various three-dimensional scaffolds with different porosities and surface characteristics (Stevens 2008).

Biological polymers physodic (P2) and 3-hydroxy physodic acid (P3), that are main compounds of methanol extracts (ME) isolated from the lichen *Hypogymnia physodes*, induced a significant decrease in the HeLa cells viability and proliferation in vitro (Stojanović et al. 2014). Obtained data are interesting for further investigation of biological activity of these biopolymers. It has been shown that lichen derivates have pro-apoptotic effects on tissues around bone implants which might be a mechanism for protection from cancer development in different tissues (Odabasoglu et al. 2012). This could be a possible future direction for examination of physodic (P2), 3-hydroxy physodic acid (P3) and ME of the *H. physodes* as bioactive agents in BTE.

Synthetic hydroxyapatite (sHA, $Ca_{10}(PO_4)_6(OH)_2$) is one of the most applied materials for bone defect reparation due to its similarity to the bone mineral, as well as its bioactivity and osteoconductivity (LeGeros 2002). Various commercial porous forms of sHA are in use (e.g. ApaPore® (Apatech Ltd., Elstree, UK)), but their resorption rate is low so they can be only used for bone augmentation (mechanical support of diseased bone), and not for regeneration. Silicon or carbonate substituted apatites can be used for increasing their resorption rate which is still slow (Jones 2009).

Functional groups and binding sites at the polymers surface influence their bioactivity. In order to achieve bioactivity, polymer surface can be modified usually by physisorption of proteins and peptides on the surface, dipcoating and amino- and carboxyl-directed immobilization of biomolecules (Ma et al. 2002) or biochemically in order to induce mineralization with HA layers (Kato et al. 1996).

3.2.4 Hydrogels

In order to supply three-dimensional cellular microenvironment with high content of water, hydrogels can be obtained by using minimally invasive techniques and gelled in situ by photocrosslinking or ionically (Stevens 2008). Due to viscoelasticity, hydrogels could be applicable in regeneration of cartilage (Stevens et al. 2004) and bone (Lutolf et al. 2003). Our team have shown that although 2-hydroxyethyl methacrylate, poly(alkylene glycol) (meth)acrylates and itaconic acid are able to swell in phosphate buffer, physical integrity and soft and rubbery consistency of these biomaterials are maintained even when swelling experiments were performed for a long time after reaching the equilibrium state (Takić-Miladinov et al. 2016). Also, the tested hydrogels induce genotoxic effects, which intensity depend on chemical composition, extract concentration and degree of crosslinking of these hydrogels.

3.2.5 Composites

Inorganic-organic composites "mimic" the composite nature of the native bone regarding to combined toughness of a polymer phase and compressive strength of an inorganic phase. Nanosized inorganic component are probably more bioactive than the micro-sized components (Stevens 2008). Since cell's transmembrane integrin receptors bind biologically active peptide motifs, e.g. arginine-glycine-aspartic acid (RGD), implementation of such motifs is among most applied methods for enhancing functionality of these biomaterials (Bökel and Brown 2002). Optimization of biodegradability of the applied biomaterial with the one specific for remodeling and regeneration of native bone tissue can be achieved with proteolytically degradable peptide motifs that are recognized by cell-secreted matrix metalloproteases (Lutolf et al. 2003).

Biodegradable polymers can be combined with bioactive inorganic materials in order to construct nanocomposites and organic-inorganic (O/I) hybrids (Allo et al. 2012). Better cell attachment and responses could be achieved by modification of the surface of nanocomposites or O/I hybrids via changing functional groups present at the surface of these biomaterials. As a consequence, vascularization is successful and mineralization occurs in the scaffolds. The limitation of porous 3D nanocomposites and O/I hybrids scaffolds are unknown long-term in vivo behavior regarding angiogenic stimulus, degradation and ion release kinetics (Allo et al. 2012).

3.3 Nanomaterials

Nanomaterials represent a special type of biomaterials that can be found in nature but also can be synthetic (Adlakha-Hutcheon et al. 2009). Nanomaterial-based scaffolds have significant application both in tissue engineering and in drug delivery. Due to biodegradability, these biomaterials support cell growth and infiltration in a manner that natural replacement with new biological tissue occurs, which is of significance in bone regenerative medine (Marchesan and Prato 2013). Since smart nanodevices target site of the certain disease, an external signal induce controlled release of multiple agents, which is powerful mechanism for drug delivery. Graphene-based nanomaterials are applicable in bone tissue engineering (Shin et al. 2016). For example, the beneficial effect of graphene-based biomaterials on enhancement of adherence, proliferation, and differentiation of osteogenic cells was estimated (Shi et al. 2012; Venkatesan et al. 2014). In addition, graphene can be used to replace the effect of BMP-2 as an inductive factor for cell differentiation (Nayak et al. 2011) or in order to boost osteoconductivity via stimulation of osteogenic cells differentiation and biomineralization process (Kim et al. 2011).

4 Bioactive Biomaterials in Dentistry

Bioactive biomaterials play a key role in dentistry where they are used for a dental treatment, in the therapy of the pulp and root canal as well as in dental surgery (Goldberg and Smith 2004; Mauth et al. 2007; Grotra and Subbarao 2012). They are essential in restoring impaired teeth and jaw bone structure. A wide range of biomaterials is used in dentistry including inorganic salt, polymers, ceramics, metals and composites. Bioceramics and bioglasses have a wide spread application in dentistry and medicine because they interact with and induce regeneration of the surrounded tissue which is important for successful regeneration.

Biocompatible white powder, which consists of ceramics particles, can be used in root canal repair due to the ability to stimulate cementogenesis and form a hermetic seal in the root canal (Sharma et al. 2013). Portland cement or Mineral trioxide aggregate (MTA) is a type of the bioactive material, composed of calcium and silicate, which maintains pulp and periodontal tissue vitality (Roberts et al. 2008) and has characteristic of apatite formation.

Calcium phosphates are good choice for both craniofacial and dental applications (Thein-Han et al. 2012). Likewise, hydroxyapatite was applied for the production of HA-based (n-HA/polyamide (PA)) biomaterials by using CAD/CAM technology and implanted into a fracture of mandibular condyle. The results of the treatment showed that patients gained a jaw contour that had proper temporomandibular joint activity (Li et al. 2011).

Bioglass and Bioglass-type glasses particulates were used with success in periodontal bone repair (Wilson et al. 1993). Bioactive glass BaG 45S5 is very

reliable at the sites of tooth extraction for the tooth roots treatment and maintaining a solid ridge for dentures (Jazayeri et al. 2017). Biosilicate is a bioactive glass-ceramic used for open dentinal tubules of a vital tooth. These bioactive glass-ceramic induce HCA (hydroxyl carbonate apatite) deposition in open dentinal tubules thus offering a new opportunity for treating dentine hypersensitivity (Tirapelli et al. 2010).

For maxillofacial and craniofacial surgery, synthetic bone materials and freeze-dried bone are in use, while β-Tricalciumphosphate (β-TCP) and histoacryl are good filling materials for the bone defects treatments (Sharma et al. 2013).

Poly (lactid) acid/hydroxyapatite (PLLA/HA) is a polymer matrix composite material that has been successfully used as anosteochondral construct for mandible bone regeneration (Schek et al. 2005) and Ceramic Matrix Composites are used in order to increase mechanical strength of the construct to resist load-bearing applications, chiefly in the jaw compression (Friedman et al. 1991). For the necessary step in oral and maxillofacial surgery—guided tissue regeneration, polymers including tissue-derived collagen (Karfeld-Sulzer and Weber 2012; Wang and Carroll 2001) and synthetic polyesters (Karfeld-Sulzer and Weber 2012; Gentile et al. 2011) are frequently used.

Dentin extracellular matrix proteins (ECMPs) and Dentonin (peptide) are amongst the most promising biomolecules for application in pulp repair and regeneration (Goldberg et al. 2006). ECMPs can stimulate proliferation and differentiation of dental pulp stem cell and their migration to sites of injury, while Dentonin activates reparative mineralization of the cornal pulp and root canal lumen.

Emdogain, a biomaterial composed of porcine proteins, can be applied in periodontal regeneration after gum disease and injuries.

Among the metals, most frequently used biodegradable metals (BMs) are Mg-based BMs due to efficacy in maxillofacial bone defects treatment (Li et al. 2014).

In the field of prosthetics, due to low cytotoxicity, silicone oral tissue conditioners are suitable for daily dental practice (Krunić et al. 2011).

5 Bioactive Biomaterials in Drug Delivery Systems

The application of biomaterials as carriers for sustained and controlled drug delivery has become a very popular approach in the treatment of different diseases. By using drug delivery systems, target sites in the body can obtain an effective concentration of drug avoiding the side effects of systemic treatment.

In the case of impaired bone regeneration associated with bone metabolic disorders, local delivery of anti-osteoporotic drugs and anabolic agents (e.g. growth factors) using bone substitutes causes more rapid bone “answer” to the treatment and provide a better osseointegration of implants (Kyllönen et al. 2015).

Besides the good choice of anabolic drug, an adequate selection of delivery system is essential. In order to be used as systems for the drug delivery, biomaterial should be synthesized as a biocompatible and should provide long and gradual drug release. Most of the biomaterials used in tissue engineering are biodegradable and this feature is particularly important for local drug releasement.

Different synthetic and natural polymers, bioceramics and biocomposites that are widely used as scaffolds for tissue engineering may serve as carriers for drug delivery. After the incorporation or absorption, obtained bioactive implants release drugs in their surroundings affecting the bone regeneration and osseointegration.

Biomaterials based on calcium and phosphates are often used for bone regeneration as a bone substitutes and, therefore, represent good candidates as bioactive local drug delivery carriers. Because of the similarity with an inorganic bone phase, these biomaterials exhibit osteoconductive properties and may be resorbed by osteoclasts thus enabling sustained drug release (Kyllönen et al. 2015; Verron et al. 2010). CaPs based biomaterials are available in the form of powders, granules, ceramic, cement and coatings.

The potential ways for the local drug delivery in bone disorders involve implants coating, the application of injectable forms of bone cements and gels and, in the cases of large bone defects, application of bioactive scaffolds for tissue regeneration (Kyllönen et al. 2015).

Calcium phosphate cements (CPC) are suitable carriers for the local drug delivery due to their osteoconductivity, good protein absorbability and gradual release of different agents (Guo et al. 2005; van de Watering et al. 2012; Wu et al. 2012; Ginebra et al. 2006). During the system designing, a chosen drug or growth factor may be incorporated into the solid or liquid phase of the cement or first incorporated in the microparticles that can be inserted into the delivery system. Using cements in combination with growth factors showed a favorable impact on bone regeneration, especially in osteoporotic conditions (Blom et al. 2001; van de Watering et al. 2012).

Disadvantage of this system is a need for enough space in the bone fracture area, in order to deliver required amount of the chosen drug (Kyllönen et al. 2015). Also, CPCs are slowly biodegradable in vivo and suffer of the lack of porosity which may be improved with various modifications (Xu et al. 2004).

Utilization of bone cement as a carrier for antimicrobial drugs is particularly recommended against infection associated with implant application (Neut et al. 2005).

Heat produced during the polymerization and postpolymerization treatments in cold-polymerized PMMA (Kostić et al. 2011), a non-biodegradable acrylic cements which is commonly used for implant fixation in orthopedics and dental surgery, restrict the range of drugs to deliver but they found to be very effective in delivering antibiotics (Minelli and Benini 2007).

Implant coatings is strategy of particular importance for metallic inert materials that are often used for hard tissue repair (Goodman et al. 2013). Drug insertion in coatings represents a good strategy in bone fracture healing due to the capability of

the delivered agents to influence on implant osseointegration. Metal implants can be coated with the suitable drug directly, but the better results in the treating of bone fractures can be achieved by absorption or incorporation of the drug onto the CaP materials which can be used as coatings around the implant (Liu et al. 2007). Hydroxyapatite coatings can be the way to deliver growth factors, DNA or various bioactive molecules (Sachse et al. 2005; Yu et al. 2012; Goodman et al. 2013). This approach enabled gradual releasement of the applied drug and enhanced osseointegration of the implant in experimental animals. Using anti-osteoporotic drugs as components of the coatings may improve bone microarchitecture around the titanium implant in osteoporotic rat tibiae (Pyo et al. 2014). The lack of this strategy is the possibility of the drug releasement only in near vicinity of the implant and the general resistance of the coating (Kyllönen et al. 2015).

A wide range of synthetic and natural polymers, ceramics and metals are available in the forms of micro- and nano-particles which represent very important systems for the delivery and sustained release of various agents for the treatment of a broad spectrum of diseases (Chau et al. 2008).

Particulated forms of biomaterials may adsorb or encapsulate drugs and deliver them to the place of releasement. Particles can be used alone, combined within cements, hydrogels and scaffolds or even form a coatings on implants. In any of these cases, the selected drug is being physically or chemically incorporated in/onto the particles and thus protected from degradation until its release begins in the target tissue. Different scaffolds with incorporated drug-loaded particles found to be more effective in enhancing osteogenesis in comparison with the scaffold alone with adsorbed BMP-2 (Wei et al. 2007). Controlled drug releasement depends on particle size, material properties, their degradability and formulation of delivery systems (Kim and Pack 2006). Pharmacokinetics of the applied drug is of a key importance for the selection of suitable system for their delivery.

Biodegradable polymer microparticles are the most common particulated biomaterial that has been used for controlled drug delivery due to biocompatibility and degradation mechanisms (Makadia and Siegel 2011). In bone therapy, PLGA based particles in combination with growth factors showed to stimulate osteogenic cell differentiation (Kirby et al. 2011).

Ca- and P-based particles have advantage over the other materials in bone regeneration, because of the similarity with the inorganic bone composition and high osteoconductivity as well as biocompatibility and bioactivity. Hydroxyapatite particles have a high affinity for proteins and other bioactive molecules and can be used with high efficiency to load and deliver drugs such as bisphosphonates (BP), growth factors etc. which are used in osteoporotic bone therapies (Lee et al. 2011). Combination with bioresorbable polymers such as PLGA, provide better systems for drug delivery because of slow PLGA degradation under physiological conditions. Sustained release of BP from PLGA/hydroxyapatite composite or from hydroxyaptite microsphere, reduces local osteoclastic activities (Boanini et al. 2008; Seshima et al. 2006).

HA/PLGA or HA alone nanoparticles that have been used as bioactive systems for vitamin D delivery have also showed to improve regeneration of osteoporotic bone (Ignjatović et al. 2013)

In addition to bone therapy, nanostructures are attractive biomaterials for other biomedical application because of their small sizes and an ability to deliver drugs inside target cells. They represent an effective approach in tumor therapy due to the possibility of targeting tumor cells, and avoiding side effects of conventional chemotherapy. Cell-specific targeting can be achieved by active mechanism, by applying functionalized NPs, or passive mechanisms, which refers to the effect of enhanced permeability and retention effect (EPR) (Acharya and Sahoo 2011; Steichen et al. 2013). Different nanostructures, such are liposomes, dendrimers, polymers, silicon or carbon materials, magnetic and gold nanoparticles, can serve as carriers for local drug delivery (De Jong and Borm 2008; Wilczewska et al. 2012). PLGA particles are widely in use as drug delivery systems due to low toxicity, biodegradability, biocompatibility and possibility for controlled and constant release of carried agents (Bala et al. 2004; Sadat et al. 2014). So far, they have been used for delivery of anti-cancer therapy, immunomodulatory agents, anti-hypertensive drugs and hormones. Carbon nanomaterials are widely examined as chemotherapy, carriers for genes and proteins, designed for potential applications in the cancer treatment (Liu et al. 2008, 2011). We have demonstrated that carbon nanotubes functionalized with a Toll-like receptor 7 agonist have immunomodulatory effects on human dendritic cells which can be applied in therapies (Čolić et al. 2014).

In cancer diagnostic and therapy, gold nanoparticles (GNPs) are also found as perspective carriers and agents for drug delivery because of their specific physical and chemical properties (Huang et al. 2007). Beside their tunable size and shape which enable controlled plasmon resonance for photo thermal therapeutic treatments by conversion of near-infrared light into thermal energy, they are biocompatible, not toxic and capable for drug delivery due to small dimensions and large surface area for functionalization with drugs, genes and biomolecules (Han et al. 2007). In our study, we investigated the effect of differently sized GNPs on functions of immune, dendritic, cells and found that 10 nm-sized GNPs have more powerful inhibitory effects on antitumor functions as well as maturation of DCs, in comparison with larger 50 nm-sized GNPs (Tomić et al. 2014).

Biomaterials used in medicine as medical devices are associated with risk of microbial infection. Bacteria growth made biofilms on their surfaces that are resistant to antibiotics and host immunity and may cause implant failure.

The approach of biomaterial coating with antimicrobial agents such as antimicrobial polymers, antibiotics, plant extracts etc. was found to be effective in obtaining therapeutically bioactive materials for the infection prevention. Plant extracts have shown great success in combating the various strains of bacteria. *Staphylococcus aureus* is the most frequent causer of biofilm formation on the material surfaces and therefore the coatings which prevent its colonization and

biofilm growth are favorable. In addition to the biomaterials testing, we are dealing with antimicrobial, antioxidant and cytotoxic effects of different plant extracts often used in Ethnomedicine. *Inula helenium* and *Carlinae radix* essential oils showed significant antimicrobial effect against *Staphylococcus aureus* (Stojanović-Radić et al. 2012a, b). The potential use of these plant extracts as coatings on biomaterials, in order to prevent infection, is subjected to our further research.

6 Future Directions and Perspectives

Biomaterials from the so-called "third-generation" were constructed in the way so that, at the molecular level, are able to trigger specific cellular responses (Hench and Polak 2002) and to integrate the biodegradability and bioactivity concepts. Also, these biomaterials must be able to promote specific cellular actions and performances. The bioactivation of the biomaterials' surface induced with biomolecules guide and stimulate cell migration, adhesion, proliferation as well as differentiation towards the certain cell line (Navarro et al. 2008).

Injectable cement composite mixed with living cells was obtained by involving undifferentiated bone marrow stromal cells into a hydrogel containing CaP particles. This kind of biomaterials are well vascularized and integrated into the host tissue upon implantation which has been shown on the mouse model (Trojani et al. 2006).

Development of bioactive and biodegradable 3D scaffolds with osteogenic and angiogenic potential is a major challenge, because cells cannot survive without an adequate blood supply. A possible alternative to improve osteogenic and angiogenic potential of the materials is incorporation of the active biomolecules such as growth factors into the scaffold (Allo et al. 2012).

Since shape, architecture and mechanical support are not enough for providing long-lasting structure for developing scaffold (Furth et al. 2007), designing of the smart biomaterials became one of the most important future directions in construction of bioactive materials (Davis et al. 2005). Smart biomaterials actively participate in functional tissue development (Furth et al. 2007). These biomaterials respond to their environment in previously determined manner which includes protein release. Consequently, delayed release as well as release stimulated by microenvironmental factors is possible (Anderson et al. 2004). Since microenvironmental factors have the influence on progenitor and stem cells differentiation, modification of bioactive injectable materials by using peptide-like nanofibers may be one of the key solutions in future cell therapies (Davis et al. 2005).

Acknowledgements This work was supported by the Ministry of Education, Science and Technological Development of the Republic of Serbia [grant number III 41017].

References

Acharya S, Sahoo SK (2011) PLGA nanoparticles containing various anticancer agents and tumour delivery by EPR effect. Adv Drug Deliv Rev 63(3):170–183

Aksay IA, Weiner S (1998) Biomaterials-is this really a field of research? Curr Opin Solid State Mater Sci 3(3):219–220

Allo BA, Costa DO, Dixon SJ et al (2012) Bioactive and biodegradable nanocomposites and hybrid biomaterials for bone regeneration. J Funct Biomater 3(2):432–463

Alsberg E, Anderson KW, Albeiruti A et al (2002) Engineering growing tissues. Proc Natl Acad Sci USA 99:12025–12030

Anderson DG, Burdick JA, Langer R (2004) Materials science. Smart biomaterials. Science 305 (5692):1923–1924

Avnir D, Klein LC, Levy D et al (1997) Organo-silica Sol–gel materials. In: Apeloig Y, Rappoport Z (eds) The chemistry of organosilicon compounds—part 2. Wiley& Sons, Chichester

Awad HA, Wickham MQ, Leddy HA et al (2004) Chondrogenic differentiation of adipose-derived adult stem cells in agarose, alginate, and gelatin scaffolds. Biomaterials 25(16):3211–3222

Bala I, Hariharan S, Kumar MR (2004) PLGA nanoparticles in drug delivery: the state of the art. Crit Rev Ther Drug Carrier Syst 21(5):387–422

Bergman S, Litkowski L (1995) Bone in-fill of non-healing calvarial defects using particulate bioglass and autogenous bone. In: Wilson J, Hench LL, Greenspan D (eds) Bioceramics. Elsevier Science, Tarrytown, New York, pp 17–21

Biggs MJ, Richards RG, Gadegaard N et al (2007) The effects of nanoscale pits on primary human osteoblast adhesion formation and cellular spreading. J Mater Sci Mater Med 18(2):399–404

Bishop AT, Pelzer M (2007) Vascularized bone allotransplantation: current state and implications for future reconstructive surgery. Orthop Clin North Am 38(1):109–122

Blom EJ, Klein-Nulend J, Yin L et al (2001) Transforming growth factor-β1 incorporated in calcium phosphate cement stimulates osteotransductivity in rat calvarial bone defects. Clin Oral Implants Res 12(6):609–616

Boanini E, Torricelli P, Gazzano M et al (2008) Alendronate–hydroxyapatite nanocomposites and their interaction with osteoclasts and osteoblast-like cells. Biomaterials 29(7):790–796

Bökel C, Brown NH (2002) Integrins in development: moving on, responding to, and sticking to the extracellular matrix. Dev Cell 3(3):311–321

Botchwey EA, Dupree MA, Pollack SR et al (2003) Tissue engineered bone: measurement of nutrient transport in threedimensional matrices. J Biomed Mater Res A 67(1):357–367

Brånemark R, Brånemark PI, Rydevik B et al (2001) Osseointegration in skeletal reconstruction and rehabilitation: a review. J Rehabil Res Dev 38(2):175–181

Brinker CJ, Raman NK, Logan MN et al (1995) Structure-property relationships in thin films and membranes. J Sol–Gel Sci Technol 4(2):117–135

Burg KJ, Porter S, Kellam JF (2000) Biomaterial developments for bone tissue engineering. Biomaterials 21(23):2347–2359

Cao W, Hench LL (1996) Bioactive Materials. Ceram Int 22:493–507

Castner DG, Ratner BD (2002) Biomedical surface science: foundations to frontiers. Surf Sci 500 (1):28–60

Chau D, Agashi K, Shakesheff K (2008) Microparticles as tissue engineering scaffolds: manufacture, modification and manipulation. Mater Sci Technol 24(9):1031–1044

Cornejo A, Sahar DE, Stephenson SM et al (2012) Effect of adipose tissue-derived osteogenic and endothelial cells on bone allograft osteogenesis and vascularization in critical-sized calvarial defects. Tissue Eng Part A 18(15–16):1552–1561

Cvetković VJ, Najdanović JG, Vukelić-Nikolić MĐ et al (2015) Osteogenic potential of in vitro osteoinduced adipose-derived mesenchymal stem cells combined with platelet-rich plasma in ectopic model. Int Orthop 39(11):2173–2180

Čolić M, Džopalić T, Tomić S et al (2014) Immunomodulatory effects of carbon nanotubes functionalized with a toll-like receptor 7 agonist on human dendritic cells. Carbon 67:273–287
Daculsi G, LeGeros RZ, Heughebaert M et al (1990) Formation of carbonateapatite crystals after implantation of calciumphosphate ceramics. Calcif Tissue Int 46(1):20–27
Davies JE (2003) Understanding peri-implant endosseous healing. J Dent Educ 67(8):932–949
Davis ME, Hsieh PCH, Grodzinsky AJ et al (2005) Custom design of the cardiac microenvironment with biomaterials. Circ Res 97(1):8–15
De Jong WH, Borm PJ (2008) Drug delivery and nanoparticles: applications and hazards. Int J Nanomed 3(2):133–149
De Jonge LT, van den Beucken JJ, Leeuwenburgh SC et al (2009) In vitro responses to electrosprayed alkaline phosphatase/calcium phosphate composite coatings. Acta Biomater 5 (7):2773–2782
Friedman CD, Costantino PD, Jones K et al (1991) Hydroxyapatite cement. II. Obliteration and reconstruction of the cat frontal sinus. Arch Otolaryngol Head Neck Surg 117(4):385–389
Fu Q, Rahaman MN, Bal BS et al (2010a) Silicate, borosilicate, and borate bioactive glass scaffolds with controllable degradation rate for bone tissue engineering applications. II. In vitro and in vivo biological evaluation. J Biomed Mater Res A 95(1):172–179
Fu Q, Rahaman MN, Fu H et al (2010b) Silicate, borosilicate, and borate bioactive glass scaffolds with controllable degradation rate for bone tissue engineering applications. I. Preparation and in vitro degradation. J Biomed Mater Res A 95(1):164–171
Furth ME, Atala A, Van Dyke ME (2007) Smart biomaterials design for tissue engineering and regenerative medicine. Biomaterials 28(34):5068–5073
Ge Z, Baguenard S, Lim LY et al (2004) Hydroxyapatitechitin materials as potential tissue engineered bone substitutes. Biomaterials 25:1049
Gentile P, Chiono V, Tonda-Turo C et al (2011) Polymeric membranes for guided bone regeneration. Biotechnol J 6(10):1187–1197
Ginebra MP, Traykova T, Planell J (2006) Calcium phosphate cements as bone drug delivery systems: a review. J Controlled Release 113(2):102–110
Goldberg M, Smith AJ (2004) Cells and extracellular matrices of dentin and pulp: a biological basis for repair and tissue engineering. Crit Rev Oral Biol Med 15(1):13–27
Goldberg M, Lacerda-Pinheiro S, Jegat N et al (2006) The impact of bioactive molecules to stimulate tooth repair and regeneration as part of restorative dentistry. Dent Clin North Am 50 (2):277–298
Goodman SB, Yao Z, Keeney M et al (2013) The future of biologic coatings for orthopaedic implants. Biomaterials 34(13):3174–3183
Green DW, Ben-Nissan B, Yoon K-S et al (2016) Bioinspired materials for regenerative medicine: going beyond the human archetypes. J Mater Chem B 4(14):2396–2406
Griffith CK, Miller C, Sainson RC et al (2005) Diffusion limits of an in vitro thick prevascularized tissue. Tissue Eng 11(1–2):257–266
Grotra D, Subbarao CV (2012) Bioactive materials used in endodontics. Rec Res Sci Tech 4 (6):25–27
Guo D, Xu K, Zhao X et al (2005) Development of a strontium-containing hydroxyapatite bone cement. Biomaterials 26(19):4073–4083
Han G, Ghosh P, Rotello VM (2007) Multi-functional gold nanoparticles for drug delivery. Adv Exp Med Biol 620:48–56
He X, Liu Y, Yuan X et al (2014) Enhanced healing of rat calvarial defects with MSCs loaded on BMP-2 releasing chitosan/alginate/hydroxyapatite scaffolds. PLoS ONE 9:e104061. doi:10.1371/journal.pone.0104061
Healy KE, Guldberg RE (2007) Bone tissue engineering. J Musculoskelet Neuronal Interact 7 (4):328–330
Hege CS, Schiller SM (2015) New bioinspired materials for regenerative medicine. Curr Mol Bio Rep 1(2):77–86
Hench LL (1980) Biomaterials. Science 208(4446):826–831

Hench LL (1998a) Bioactive materials: the potential for tissue regeneration. J Biomed Mater Res 41(4):511–518
Hench LL (1998b) Bioceramics. J Am Ceram Soc 81(7):1705–1728
Hench LL, Orefice R (1997) Sol–gel technology. In: Kirk-Othmer encyclopedia of chemical technology, 4th edn, vol 22. Wiley, New York, p 497
Hench LL, Polak JM (2002) Third-generation biomedical materials. Science 295(5557):1014–1107
Hench LL, West JK (1996) Biological applications of bioactive glasses. Life Chem Rep 13:187–241
Hench LL, Splinter RJ, Allen WC et al (1971) Bonding mechanisms at the interface of ceramic prosthetic materials. J Biomed Mater Res 5(6):117–141
Hench LL, Andersson OH, LaTorre GP (1991) The kinetics of bioactive ceramics part III: surface reactions for bioactive glasses compared with an inactive glass. Bioceramics 4:156–162
Huang X, Bai S, Lu Q et al (2014) Osteoinductive-nanoscaled silk/HA composite scaffolds for bone tissue engineering application. J Biomed Mater Res B Appl Biomater 103(7):1–13
Huang X, Jain PK, El-Sayed IH et al (2007) Gold nanoparticles: interesting optical properties and recent applications in cancer diagnostics and therapy. Nanomedicine (Lond) 2(5):681–693
Ignjatović N, Uskoković V, Ajduković Z et al (2013) Multifunctional hydroxyapatite and poly (D, L-lactide-co-glycolide) nanoparticles for the local delivery of cholecalciferol. Mater Sci Eng C Mater Biol Appl 33(2):943–950
Jarcho M, Kay JL, Gumaer RH et al (1977) Tissue, cellular and subcellular events at bone–ceramic hydroxyapatite interface. J Bioeng 1(2):79–92
Jazayeri HE, Tahriri M, Razavi M et al (2017) A current overview of materials and strategies for potential use in maxillofacial tissue regeneration. Mater Sci Eng C Mater Biol Appl 70(Pt 1):913–929
Jones JR (2009) New trends in bioactive scaffolds: the importance of nanostructure. J Eur Ceram Soc 29(7):1275–1281
Karande TS, Ong JL, Agrawal CM (2004) Diffusion in musculoskeletal tissue engineering scaffolds: design issues related to porosity, permeability, architecture, and nutrient mixing. Ann Biomed Eng 32(12):1728–1743
Karfeld-Sulzer LS, Weber FE (2012) Biomaterial development for oral and maxillofacial bone regeneration. J Korean Assoc Oral Maxillofac Surg 38(5):264–270
Kato K, Eika Y, Ikada Y (1996) Deposition of hydroxiapatite thin layer onto a polymer surface carrying grafted phosphate polymer chains. J Biomed Mater Res 32(4):687–691
Keeting PE, Oursler MJ, Wiegand KE et al (1992) Zeolite A increases proliferation, differentiation, and transforming growth factor beta production in normal adult human osteoblast-like cells in vitro. J Bone Mineral Res 7(11):1281–1289
Keshaw H, Forbes A, Day RM (2005) Release of angiogenic growth factors from cells encapsulated in alginate beads with bioactive glass. Biomaterials 26(19):4171–4179
Kim IS, Park JW, Kwon IC et al (2002) Role of BMP, betaig-h3, and chitosan in early bony consolidation in distraction osteogenesis in a dog model. Plast Reconstr Surg 109:1966
Kim KK, Pack DW (2006) Microspheres for drug delivery. In: Ferrari M, Lee AP, Lee LJ (eds) BioMEMS and Biomed Nanotechnol. Springer, New York, pp 19–50
Kim S, Ku SH, Lim SY et al (2011) Graphene–biomineral hybridmaterials. Adv Mater 23 (17):2009–2014
Kirby GT, White LJ, Rahman CV et al (2011) PLGA-based microparticles for the sustained release of BMP-2. Polymers 3(1):571–586
Kostic M, Krunic N, Nikolic L et al (2011) Influence of residual monomer reduction on acrylic denture base resins quality. Hemijska industrija 65(2):171–177
Kokubo T (1990) Surface chemistry of bioactive glass-ceramics. J Non-Cryst Solids 120(1–3):138–151
Kokubo T, Shigematsu M, Nagashima Y et al (1982) Apatite- and wollastonite-containing glass-ceramics for prosthetic application. Bull Inst Chem Res Kyoto Univ 60(3–4):260–268

Kokubo T, Kim HM, Kawashita M (2003) Novel bioactive materials with different mechanical properties. Biomaterials 24(13):2161–2175
Krunić N, Lj Nikolić, Kostić M et al (2011) In vitro examination of oral tissue conditioners potential toxicity. Chem Ind 65(6):697–706
Kyllönen L, D'Este M, Alini M et al (2015) Local drug delivery for enhancing fracture healing in osteoporotic bone. Acta Biomater 11:412–434
Langer R, Tirrell DA (2004) Designing materials for biology and medicine. Nature 428:487–492
Langer R, Vacanti JP (1993) Tissue engineering. Science 260(5110):920–926
Lee JH, Ko IH, Jeon SH et al (2011) Localized drugs delivery hydroxyapatite microspheres for osteoporosis therapy. In: Proceedings of SPIE, biosens nanomed IV: 8099 of 80990K, San Diego, Calif, USA
LeGeros RZ (2002) Properties of osteoconductive biomaterials: calcium phosphates. Clin Orthopaed Related Res 395:81–98
Levingstone TJ, Matsiko A, Dickson GR et al (2014) biomimetic multi-layered collagen-based scaffold for osteochondral repair. Acta Biomater 10(5):1996–2004
Li H, Zheng Y, Qin L (2014) Progress of biodegradable metals. Prog Nat Sci Mater Int 24(5):414–422
Li J, Hsu Y, Luo E et al (2011) Computer-aided design and manufacturing and rapid prototyped nanoscale hydroxyapatite/polyamide (n-HA/PA) construction for condylar defect caused by mandibular angle ostectomy. Aesthet Plast Surg 35(4):636–640
Li M, Liu X, Ge B (2010) Calcium phosphate cement with BMP-2-loaded gelatin microspheres enhances bone healing in osteoporosis: a pilot study. Clin Orthop Relat Res 468(7):1978–1985
Liu Y, Enggist L, Kuffer AF et al (2007) The influence of BMP-2 and its mode of delivery on the osteoconductivity of implant surfaces during the early phase of osseointegration. Biomaterials 28(16):2677–2686
Liu Z, Chen K, Davis C et al (2008) Drug delivery with carbon nanotubes for in vivo cancer treatment. Cancer Res 68(16):6652–6660
Liu Z, Robinson JT, Tabakman SM et al (2011) Carbon materials for drug delivery & cancer therapy. Mater Today 14(7–8):316–323
Long F (2011) Building strong bones: molecular regulation of the osteoblast lineage. Nat Rev Mol Cell Biol 13(1):27–38
Loty C, Sautier JM, Boulekbache H et al (2000) In vitro bone formation on a bonelike apatite layer prepared by a biomimetic process on a bioactive glass-ceramic. J Biomed Mater Res 49 (4):423–434
Lu HH, Tang A, Oh SC et al (2005) Compositional effects on the formation of a calcium phosphate layer and the response of osteoblast-like cells on polymer-bioactive glass composites. Biomaterials 26(32):6323–6334
Lutolf MP, Weber FE, Schmoekel HG et al (2003) Repair of bone defects using synthetic mimetics of collagenous extracellular matrices. Nat Biotechnol 21(5):513–518
Ma Z, Gao C, Gong Y et al (2002) Immobilization of natural macromolecules on poly-L-lactic acid membrane surface in order to improve its cytocompatibility. J Biomed Mater Res 63 (6):838–847
Makadia HK, Siegel SJ (2011) Poly lactic-co-glycolic acid (PLGA) as biodegradable controlled drug delivery carrier. Polymers (Basel) 3(3):1377–1397
Marchesan S, Prato M (2013) Nanomaterials for (Nano)medicine. ACS Med Chem Lett 4(2):147–149
Marion NW, Liang W, Reilly GC et al (2005) Borate glass supports the in vitro osteogenic differentiation of human mesenchymal stem cells. Mech Adv Mater Struct 12(3):239–246
Mauth C, Huwig A, Graf-Hausner U et al (2007) Restorative applications for dental pulp therapy. In: Ashammakhi N, Reis RL, Chiellini (eds) Topics in tissue engineering, vol 3, pp 1–30
Minelli EB, Benini A (2007) PMMA as drug delivery system and in vivo release from spacers. In: Romano C, Crosby L, Hofmann G, Meani E (eds) Infection and local treatment in orthopedic surgery. Springer, New York, pp 79–91

Najdanović JG, Cvetković VJ, Stojanović S et al (2015) The influence of adipose-derived stem cells induced into endothelial cells on ectopic vasculogenesis and osteogenesis. Cell Mol Bioeng 8(4):577–590

Najdanović JG, Cvetković VJ, Stojanović S et al (2016) Effects of bone tissue engineering triad components on vascularization process: comparative gene expression and histological evaluation in an ectopic bone-forming model. Biotechnol Biotechnol Equip 30(6):1122–1131

Najman SJ, Cvetković VJ, Najdanović JG et al (2016) Ectopic osteogenic capacity of freshly isolated adipose-derived stromal vascular fraction cells supported with platelet-rich plasma: a simulation of intraoperative procedure. J Craniomaxillofac Surg 44(10):1750–1760

Narmoneva DA, Oni O, Sieminski AL et al (2005) Self-assembling short oligopeptides and the promotion of angiogenesis. Biomaterials 26(23):4837–4846

Navarro M, Michiardi A, Castaño O et al (2008) Biomaterials in orthopaedics. J R Soc Interface 5 (27):1137–1158

Nayak TR, Andersen H, Makam VS et al (2011) Graphene for controlled and accelerated osteogenic differentiation of human mesenchymal stem cells. ACS Nano 5(6):4670–4678

Neut D, Hendriks JG, van Horn JR et al (2005) Pseudomonas aeruginosa biofilm formation and slime excretion on antibiotic-loaded bone cement. Acta Orthop 76(1):109–114

Odabasoglu F, Yildirim OS, Aygun H et al (2012) Diffractaic acid, a novel proapoptotic agent, induces with olive oil both apoptosis and antioxidative systems in Ti-implanted rabbits. Eur J Pharmacol 674(2–3):171–178

Oguntebi B, Clark A, Wilson J (1993) Pulp capping with bioglass and autologous demineralized dentin in miniature swine. J Dent Res 72(2):484–489

Ohtsuki C, Kamitakahara M, Miyazaki T (2009) Bioactive ceramic-based materials with designed reactivity for bone tissue regeneration. J R Soc Interface 6(Suppl 3):S349–S360

O'Keefe RJ, Mao J (2011) Bone tissue engineering and regeneration: from discovery to the clinicean overview. Tissue Eng Part B Rev 17(6):389–392

Oonishi H, Kushitani S, Iwaki H (1995) Comparative bone formation in several kinds of bioceramic granules. In: Wilson J, Hench LL, Greenspan D (eds) Eighth international symposium on ceramics in medicine. Elsevier Science Ltd, Tokyo, pp 137–144

Oonishi H, Kushitani S, Yasukawa E et al (1997) Particulate bioglass compared with hydroxyapatite as a bone g raft substitute. J Clin Orthop Rel Res 334:316–325

Pereira MM, Hench LL (1996) Mechanisms of hydroxyapatite formation on porous gel-silica matrices. J Sol–Gel Sci Technol 7(1):59–64

Pereira MM, Clark AE, Hench LL (1994) Calcium phosphate formation on sol–gel derived bioactive glasses in vitro. J Biomed Mater Res 28(6):693–698

Piotrowski G, Hench LL, Allen WC et al (1975) Mechanical studies of the bone bioglass interfacial bond. J Biomed Mater Res 9(4):47–61

Puleo DA, Nanci A (1999) Understanding and controlling the bone–implant interface. Biomaterials 20(23–24):2311–2321

Pyo SW, Kim YM, Kim CS et al (2014) Bone formation on biomimetic calcium phosphate-coated and zoledronate-immobilized titanium implants in osteoporotic rat tibiae. Int J Oral Maxillofac Implants 29(2):478–484

Rajković J, Stojanović S, Đorđević L et al (2015) Locally applied cholecalciferol and alfacalcidol act differently on healing of femur defects filled with bone mineral matrix and platelet-rich plasma in ovariectomized rats. Biotechnol Biotechnol Equip 29(5):963–969

Ratner BD, Hoffman AS, Schoen FJ et al (2004) Biomaterials science: an introduction to materials in medicine, 2nd edn. Academic Press, New York

Rejda BV, Peelen JGJ, de Groot K (1977) Tricalcium phosphate as a bone substitute. J Bioeng 1 (2):93–97

Roberts HW, Toth JM, Berzins DW et al (2008) Mineral trioxide aggregate material use in endodontic treatment: a review of the literature. Dent Mater 24(2):149–164

Sachse A, Wagner A, Keller M et al (2005) Osteointegration of hydroxyapatite-titanium implants coated with nonglycosylated recombinant human bone morphogenetic protein-2(BMP-2) in aged sheep. Bone 37(5):699–710

Sadat Tabatabaei Mirakabad F, Nejati-Koshki K, Akbarzadeh A et al (2014) PLGA-based nanoparticles as cancer drug delivery systems. Asian Pac J Cancer Prev 15(2):517–535
Salem AK, Stevens R, Pearson RG et al (2002) Interactions of 3T3 fibroblasts and endothelial cells with defined pore features. J Biomed Mater Res 61(2):212–217
Salinas AJ, Vallet-Regı M (2013) Bioactive ceramics: from bone grafts to tissue engineering. RSC Advances 3(28):1116–1131
Salinas AJ, Esbrit P, Vallet-Regí M (2013) A tissue engineering approach based on the use of bioceramics for bone repair. Biomater Sci 1(1):40–51
Schek RM, Taboas JM, Hollister SJ et al (2005) Tissue engineering osteochondral implants for temporomandibular joint repair. Orthod Craniofacial Res 8(4):313–319
Schepers E, de Clercq M, Ducheyne P et al (1991) Bioactive glass particulate material as a filler for bone lesions. J Oral Rehabil 18(5):439–452
Schouten C, van den Beucken JJ, Meijer GJ et al (2010) In vivo bioactivity of DNA-based coatings: an experimental study in rats. J Biomed Mater Res A 92(3):931–941
Schroeder JE, Mosheiff R (2011) Tissue engineering approaches for bone repair: concepts and evidence. Injury 42(5):609–613
Seitz TL, Noonan KD, Hench LL et al (1982) Effect of fibronectin on the adhesion of an established cell line to a surface reactive biomaterial. J Biomed Mater Res 16(3):195–207
Seshima H, Yoshinari M, Takemoto S et al (2006) Control of bisphosphonate release using hydroxyapatite granules. J Biomed Mater Res B Appl Biomater 78(2):215–221
Sharma M, Murray PE, Sharma D (2013) Modern approaches to use bioactive materials and molecules in medical and dental treatments. Int J Curr Microbiol App Sci 2(11):429–439
Shi C, Zhu Y, Ran X et al (2006) Therapeutic potential of chitosan and its derivatives in regenerative medicine. J Surg Res 133(2):185–192
Shi X, Chang H, Chen S et al (2012) Regulating cellular behavior on few-layer reduced graphene oxide films with well-controlled reduction states. Adv Funct Mater 22(4):751–759
Shin SR, Li YC, Jang HL et al (2016) Graphene-based materials for tissue engineering. Adv Drug Deliv Rev 105(Pt B):255–274
Shores EC, Holmes RE (1993) Porous hydroxyapatite. In: Hench LL, Wilson J (eds) An introduction to bioceramics. World Scientific, Singapore, pp 181–198
Siebers M, Ter Brugge P, Walboomers X et al (2005) Integrins as linker proteins between osteoblasts and bone replacing materials. A critical review. Biomaterials 26(2):137–146
Steichen SD, Caldorera-Moore M, Peppas NA (2013) A review of current nanoparticle and targeting moieties for the delivery of cancer therapeutics. Eur J Pharm Sci 48(3):416–427
Stevens MM (2008) Biomaterials for bone tissue engineering. Mater Today 11(5):18–25
Stevens MM, Qanadilo HF, Langer R et al (2004) A rapid-curing alginate gel system: utility in periosteum-derived cartilage tissue engineering. Biomaterials 25(5):887–894
Stojanović IŽ, Najman S, Jovanović O et al (2014) Effects of depsidones from *Hypogymnia physodes* on HeLa cells viability and growth. Folia Biol (Praha) 60(2):89–94
Stojanović-Radić Z, Čomić L, Radulović N et al (2012a) Antistaphylococcal activity of *Inula helenium* L. root essential oil: eudesmane sesquiterpene lactones induce cell membrane damage. Eur J Clin Microbiol Infect Dis 31(6):1015–1025
Stojanović-Radić Z, Čomić L, Radulović N et al (2012b) Commercial Carlinae radix herbal drug: Botanical identity, chemical composition and antimicrobial properties. Pharmaceutical biology 50(8):933–940
Takić-Miladinov D, Tomić S, Stojanović S et al (2016) Synthesis, swelling properties and evaluation of genotoxicity of hydrogels based on (Meth)acrylates and Itaconic Acid. Mat Res 19(5):1070–1079
Thein-Han W, Liu J, Xu HH (2012) Calciumphosphate cement with biofunctional agents and stem cell seeding for dental and craniofacial bone repair. Dent Mater 28(10):1059–1070
Tirapelli C, Panzeri H, Soares RG et al (2010) A novel bioactive glass-ceramic for treating dentin hypersensitivity. Braz Oral Res 24(4):381–387

Tomić S, Đokić J, Vasilijić S et al (2014) Size-dependent effects of gold nanoparticles uptake on maturation and antitumor functions of human dendritic cells in vitro. PLoS ONE 9(5):e96584. doi:10.1371/journal.pone.0096584

Tonnesen HH, Karlsen J (2002) Alginate in drug delivery systems. Drug Dev Ind Pharm 28 (6):621–630

Trojani C, Boukhechba F, Scimeca JC et al (2006) Ectopic bone formation using an injectable biphasic calcium phosphate/Si-HPMC hydrogel composite loaded with undifferentiated bone marrow stromal cells. Biomaterials 27(17):3256–3264

Tsigkou O, Hench LL, Boccaccini AR et al (2007) Enhanced differentiation and mineralization of human fetal osteoblasts on PDLLA containing Bioglass® composite films in the absence of osteogenic supplements. J Biomed Mater Res A 80(4):837–852

Vallet-Regi M, Ruiz-Hernandez E (2011) Bioceramics: from bone regeneration to cancer nanomedicine. Adv Mater 23(44):5177–5218

van de Watering FC, Molkenboer-Kuenen JD, Boerman OC et al (2012) Differential loading methods for BMP-2 within injectable calcium phosphate cement. J Control Release 164 (3):283–290

Venkatesan J, Pallela R, Kim S-K (2014) Applications of carbon nanomaterials in bone tissue engineering. J Biomed Nanotechnol 10(10):3105–3123

Verron E, Khairoun I, Guicheux J et al (2010) Calcium phosphate biomaterials as bone drug delivery systems: a review. Drug Discov Today 15(13–14):547–552

Vogel M, Voigt C, Gross U et al (2001) In vivo comparison of bioactive glass particles in rabbits. Biomaterials 22(4):357–362

Vrouwenvelder CA, Groot CG, de Groot KJ (1993) Histological and biochemical evaluation of osteoblasts cultured on bioactive glass, hydroxylapatite, titanium alloy, and stainless steel. J Biomed Mater Res 27(4):465–475

Wang H-L, Carroll WJ (2001) Guided bone regeneration using bone grafts and collagen membranes. Quintessence Int 32(7):504–515

Wang XP, Li X, Ito A et al (2011) Synthesis and characterization of hierarchically macroporous and mesoporous CaO–MO–SiO(2)–P(2)O(5) (M = Mg, Zn, Sr) bioactive glass scaffolds. Acta Biomater 7(10):3638–3644

Wei G, Jin Q, Giannobile WV et al (2007) The enhancement of osteogenesis by nano-fibrous scaffolds incorporating rhBMP-7 nanospheres. Biomaterials 28(12):2087–2096

Wheeler DL, Stokes KE (1997) In vivo evaluation of sol–gel bioglasst: part I: histological findings. In: Transactions of the 23rd annual meeting of the society for biomaterials, New Orleans, LA

Wheeler DL, Stokes KE, Hoellrich RG et al (1998) Effect of bioactive glass particle size on osseous regeneration of cancellous defects. J Biomed Mater Res 41(4):527–533

Wilczewska AZ, Niemirowicz K, Markiewicz KH et al (2012) Nanoparticles as drug delivery systems. Pharmacol Rep 64(5):1020–1037

Wilson J, Yli-Urpo A, Risto-Pekka H (1993) Bioactive glasses: clinical applications. In: Hench LL, Wilson J (eds) An introduction to bioceramics. World Scientific, Singapore, pp 63–74

Winslow BD, Shao H, Stewart RJ et al (2010) Biocompatibility of adhesive complex coacervates modeled after the Sandcastle glue of *P. californica* for craniofacial reconstruction. Biomaterials 31(36):9373–9381

Wu CC, Wang CC, Lu DH et al (2012) Calcium phosphate cement delivering zoledronate decreases bone turnover rate and restores bone architecture in ovariectomized rats. Biomed Mater 7(3):035009

Xu HH, Takagi S, Quinn JB et al (2004) Fast-setting calcium phosphate scaffolds with tailored macropore formation rates for bone regeneration. J Biomed Mater Res A 68(4):725–734

Xynos ID, Edgar AJ, Buttery LDK et al (2001) Gene-expression profiling of human osteoblasts following treatment with the ionic products of BioglassW 45S5 dissolution. J Biomed Mater Res 55(2):151–157

Yamamuro T (1993) A/W glass-ceramic: clinical applications. In: Hench LL, Wilson J (eds) An introduction to bioceramics. World Scientific, Singapore, pp 89–104

Yu X, Wang L, Jiang X et al (2012) Biomimetic CaP coating incorporated with parathyroid hormone improves the osseointegration of titanium implant. J Mater Sci Mater Med 23 (9):2177–2186

Yuan H, Fernandes H, Habibovic P et al (2010) Osteoinductive ceramics as a synthetic alternative to autologous bone grafting. Proc Natl Acad Sci USA 107(31):13614–13619

Zheng K, Yang SB, Wang JJ et al (2012) Characteristics and biocompatibility of Na(2)O–K(2)O–CaO–MgO–SrO–B(2)O(3)–P(2)O(5) borophosphate glass fibers. J Non-Cryst Solids 358 (2):387–391

Zimmermann WH, Melnychenko I, Eschenhagen T (2004) Engineered heart tissue for regeneration of diseased hearts. Biomaterials 25(9):1639–1647

Živković J, Najman S, Vukelić M et al (2015) Osteogenic effect of inflammatory macrophages loaded onto mineral bone substitute in subcutaneous implants. Arch Biol Sci 67(1):173–186

Bioactive Coatings

Kwang Leong Choy, Matthias Schnabelrauch and Ralf Wyrwa

Abstract From traditional approaches of employing bulk materials to the new generation of bioactive coated implants, the design of such medical tools is being directed towards the implementation bioactive compounds to allow the direct bonding of living tissues and osteoconduction. However, the development of an optimal bioactive implant for tissue regeneration has not been achieved. The research for novel materials is hindered by the biocompatibility and bioactivity of the compound as well as their mechanical properties. To improve the bioactivity of the implants, the increase of surface area of the implant as well as the use of resorbable compounds is being studied with promising results. Among all different materials and composite employed, the common materials include calcium phosphates and resorbable bioglasses inspired in natural scaffold composition of bones and teeth. In some cases, this material is being used as a coating and combined with further treatments and functional coatings which may reinforce its bioresponsive properties, and in some cases, it can provide additional properties such as antimicrobial activity. In addition, a specific class of bioactive coatings based on biodegradable polymers has also been developed. These coatings temporally aim at accelerating wound healing and forming new tissue at the material-tissue interface around implanted devices or protecting those implants against biomaterial-associated infections. Bioactive, degradable coatings can be generated both from natural and synthetic polymers. Common strategies, reviewed here, are based on natural polymers like proteins, polysaccharides, or glycosaminoglycanes to improve their bioactivity either by chemical functionalization of the biopolymer itself (e.g. introduction of bioactive groups) or by immobilization of bioactive components (e.g. cell adhesion peptides). Degradable or at least water-soluble

K.L. Choy (✉)
UCL Institute for Materials Discovery, University College of London,
Roberts Building Malet Place, London WC1E 7JE, UK
e-mail: k.choy@ucl.ac.uk

M. Schnabelrauch · R. Wyrwa
Department of Biomaterials, INNOVENT e. V, Pruessingstrasse 27b, 07745 Jena, Germany

F. Zivic et al. (eds.), *Biomaterials in Clinical Practice*,
https://doi.org/10.1007/978-3-319-68025-5_13

synthetic polymers as polylactones or polyethylene glycols have been used for long time to create carrier materials for bioactive agents. As exemplary illustrated, those polymers are also used creating either substrate-adhering nanofilms or hydrogel-based thick coatings with high bioactivity to stimulate cell adhesion or avoid microbial adhesion. This chapter aims to summarize all recent approaches in the development of various bioactive coating materials, as well as the coating techniques and further treatment, functionalization and surface modification.

Keywords Bioactive coatings · Calcium phosphates · Bioglass · Biodegradable polymers · Osteoconduction

1 Introduction

During the last decades numerous implant devices based on various classes of materials for a wide range of clinical applications have been developed to improve patients' life. In the past, the selection of a specific implant material was often made on the basis of its bulk properties, especially its mechanical parameters, and in terms of the biological behaviour. More or less inert materials have been preferred to prevent strong foreign body reactions and implant rejection. In fact, the proper integration of an artificial implant into the surrounding tissue is a key clinical outcome of a successful implantation procedure. As a consequence, all processes initiated by the implant insertion at the host tissue-material interface must occur without inducing adverse reactions like chronic inflammatory response, the formation of undesired fibrous tissue, or the occurrence of implant-related infections. In this view the concept of bioinert implant materials has been successful for many years and is valid for many implants still today. Nevertheless, along with our advanced knowledge of the complex biological reactions at the tissue-material interface and driven by increasing clinical demands and patient expectations, this concept began to shift in the middle of the 1990s toward the development of bioactive implant surfaces to elicit a specific biological response at the material interface. Following this new strategy, micro-structured implants and implants with porous surface structures have been developed, achieving a more stable interlocking between the implant and the surrounding tissue. Thus, the concept of bioactive implant fixation was established resulting in an improved primary fixation of many bone implants and often also in an increased implant lifetime. A key feature of this concept consists in the use of approved and mostly bioinert implant materials with suitable bulk properties for the chosen clinical application combined with a specific surface design and/or surface coating enabling the implant to actively interact in a desired way with the biological environment. This interaction can vary with the implant function and its location in the body. In the case of bone implants an increase in bioactivity is mainly directed to a rapid adhesion and anchorage of bone cells (osteoblasts) to the implant surface to promote mineralization and tight binding of newly formed bone tissue to the implant.

Several approaches have been considered to render originally inert implants bioactive. An already mentioned strategy represents the micro- or nano-structuring of implant surfaces which can be performed by common processes like ablation, etching or blasting. Another versatile approach which has gained growing importance during the last decades is the development of bioactive and optionally degradable coatings.

Bioactive coatings are coatings that have the capability of direct bonding to living tissues, such as soft tissue and bone, forming a strong chemical bond. Osteoconduction on biologically active ceramics is attributed to the formation of bioactive bone-like apatite. The apatite originates from the chemical interaction of the ceramics with the surrounding body fluids. Therefore, the design and development of advanced bioactive and/or biodegradable materials is highly dependent on the control of their chemical reactivity in and with body fluids. However, the current common bioactive coatings based on ceramics and bioglass have yet to show suitability for all required clinical applications. Therefore, the development of novel designs of bioactive materials is necessary. Emerging bioactive coatings, for example those based on bioactive composite coating, polymer-based bioactive and degradable coatings as well as antimicrobial coatings receiving increasing attentions and being exploited for biomedical applications. Novel biologically active materials designed based on chemical reactivity in body fluids are here reviewed.

Coatings offer unique possibilities to control the surface properties of an implant by a variety of features including surface structure, porosity and roughness, chemical composition, hydrophilicity-hydrophobicity balance, the presence of functional groups, the degradation behaviour and last but not least the incorporation of drugs or other bioactive molecules.

Among known bioactive materials, calcium phosphates and resorbable bioglasses have already found widespread applications as coatings for orthopaedic and dental implants. Whereas calcium phosphates closely resemble the composition of the mineral phase of bone displaying osteoconductive, and in some cases also osteoinductive properties, bioglasses are able to form silicate-rich layers promoting deposition of hydroxyapatite and thereby rapid osseointegration.

Bioactive coatings based on natural polymers like collagen or gelatine have also been used to improve cell acceptance of various implants for many years. An overview on common biopolymers and their chemically modified derivatives used as implant coatings and the obtained biological effects, especially in terms of improved implant integration by stimulating cell activity but also protection of implants against microbial infection, will be provided. Special attention will be paid to new advanced coating concepts like the incorporation of peptide sequences derived from high molecular weight proteins to trigger cell adhesion on implant surfaces or the approach to generate macromolecular assemblies by combining different bio-macromolecule mimicking the natural extracellular matrix and its unique biological functions. Finally, new developments in the field of synthetic polymers designed to show specific biological effects like promotion of cell adhesion or antimicrobial activity are highlighted.

Bioactive coatings have been applied onto various substrates for biomedical applications. These include Ti-alloy, stainless steel, magnesium alloy, bioactive ceramics and polymer composites. Ti-alloy (e.g. Ti-6Al-4V) has been proven to be suitable for load bearing implants such as hip implants (Hench 1991; Geetha et al. 2009). However, it has poor biological activity and weak interface bonding between Ti implant and tissue because of "stress shielding" caused by the mismatch of Young's modulus (Liu et al. 2004).

Stainless steel substrates is an economical alternative for orthopaedic implants (Garcia et al. 2004) to reduce costs in public health services. On the other hand, phosphate coated magnesium alloy implants have shown excellent biological responses, together with outstanding mechanical properties and degradability in the physiological elements, and have been therefore, extensively studied. (Song 2007; Hornberger et al. 2012). However, corrosion of magnesium alloys would occur in human body fluid or blood plasma even though with the presence of phosphate coating.

Bioactive ceramics and bioglass have been used in bone repairing (Liu and Miao 2004) and different applications (Galliano et al. 1998) as they could elicit a specific biological in vivo response at the interface and attach to the tissues.

However, the application of many materials for medical implants is often hindered due to their stiffness, which is generally to be higher than human cortical bone. Composite theory states that, when the stiffness of a ceramic or metallic implant is higher than the bone, there is, according to the load sharing principle (Hull and Clyne 1996), a possibility of bone resorbtion due to a reduced mechanical environment, (Park and Lakes 2007). This is following the "Wolff's Law", i.e., with the imposed changing stress/strain, bone would remodel such that the stress or strain is retained within particular levels (Wolff 1892). For example in total hip replacement, bone resorption in the proximal femur has led to a common problem of aseptic loosening of the prosthesis attributed to stress and strain in the femoral cortex due to implantation of the metallic femoral hip replacement (Learmonth 2012). Elastic characteristics of the implant play an important role in allowing the femur to attain a physiologically acceptable stress state. In fact, human hard tissues serve as templates, since they are natural composites, for the development of replacement tissue. In order to address the problem of modulus-mismatch between existing implant materials and bone, and promote good adhesion and bonding between the implant and host tissue, concept of analogue biomaterials has been introduced (Bonfield et al. 1981). Subsequently, a variety of bioactive composite materials has been investigated and developed (Bonfield et al. 1981; Boccaccini et al. 2010a). These composite materials consisting of more than one type of materials (e.g. metallic, ceramic, or polymeric) have been designed as either reinforcement or matrix for biomedical applications.

The non-metallic nature of polymer composite implants would avoid the generation of at least one source of particles or ions formed at metallic implant surfaces (Agins et al. 1988). These polymer composites implants could exhibit isoelastic properties (i.e. similar stiffness to their surrounding host tissues) because of their

non-isotropic properties and versatility in design, such feature is increasingly believed to promote bone in-growth and reduce stress shielding (Huiskes et al. 1992; Williams 2000).

Wang (2003) has reviewed some promising composites for tissue replacement and regeneration, as well as the rationale and strategy of developing these composites and the factors influencing the production and performance of bioactive composites have been discussed to meet various clinical requirements.

2 Processing/Characterisation/Biocompatibility and Bioactivity Properties of Bioactive Coatings

2.1 Hydroxyapatite Coatings

Hydroxyapatite (HA) is a calcium phosphate-based apatite with the chemical formula $[Ca_{10}(PO_4)_6(OH)_2]$, which has similar chemical composition and crystal structure as the apatite in the human teeth and bones, as first identified by DeJong (1926). Thus, HA is a biocompatible material with the desired bioactive and osteoconductive properties (Yamamuro et al. 1990; Corpe et al. 2000). However, synthetic HA was only accepted as a promising biomaterial for use in bone grafts, orthopaedics, and dentistry 40 years ago. The crystallinity between natural hydroxyapatite and synthetic HA coatings has been studied. The crystallinity of the synthetic HA coatings can be controlled to be similar to biological apatites with less crystallinity by controlling the heated treatment of apatite coatings to a temperature between 400 and 600 °C. At higher temperatures (>700 °C), the apatite coatings appeared more crystalline, with a mixture of hydroxyapatite, octacalcium phosphate and magnesium phosphate (Assis de et al. 2005).

However, HA is brittle with low fracture toughness and poor fatigue resistance and higher Young's modulus than human cortical bone. Therefore, the applications are limited to the use in low load or non weight bearing *in-service* conditions, such as bone fillers, ossicular bone replacement under low loads and materials for maxillofacial reconstruction (Yamamuro et al. 1990).

The combination of the high mechanical strength and load bearing of metals (e.g. Ti-6Al-4V and stainless steel 316L) with the osteoconductive properties of calcium phosphates has overcome the physical limitations of HA and enabled hydroxyapatite coatings on bioinert metal implants to be widely used in hard tissue replacement implants and orthopaedic applications such as femoral stem in a hip replacement device. HA coatings deposited onto metallic alloys have demonstrated the ability to simulate bone formation, to improve the implant to bone bonding and enable a more natural osseointegration of the metallic implants with surrounding tissues, as well as minimising the risk associated with the liberation of metallic wear particles or metallic ions from implants (Agins et al. 1988). Hence HA has been developed as biological fixation of load bearing biomedical implants as an alternative to cemented fixation.

Stoichiometrically, HA has a molar ratio of Ca:P of 1.67. According to the American Society for Testing and Materials (ASTM) F1609 (ASTM 2014) and International Organization of Standardization (ISO) 13779-2 (ISO 2000) the properties of HA coatings and their specifications for biomedical implants applications, crystalline HA content lower than 45% and the ratio of Ca:P should be within the range of 1.67–1.76, with the HA coating adhesion from pull out tests of implants greater than 15 MPa. Dumbleton and Manley (2004) have summarised a list of commercially available medical implants as shown in Table 1.

(i) **Coating manufacturing methods**
The deposition methods would affect the coating microstructure and properties. Various coating methods have been explored to deposit HA coatings to increase bioactivity and to improve bonding. These include plasma spraying (De Groot et al. 1987; Berndt et al. 1990; Klein et al. 1991), electrophoretic deposition (Ducheyne et al. 1990), sputtering (Ong et al. 1992), sol–gel (Liu et al. 2002),

Table 1 Properties of commercially available hydroxyapatite coatings (Dumbleton and Manley 2004)

Manufacturer	Hydroxyapatite content (%)	Crystallinity (%)	Thickness (μ)	Porosity (%)	Location of coating
Stryker orthopaedics (Ostenoics)	>90	70	50	Dense	Proximal part of stem
Stryker orthopaedics (Benoist Girard)	>90	>75	60	<10	Proximal part of stem
Joint replacement instrumentation (JRI)			200		Fully coated stem
DePuy, J&J (Landanger)		>50	155 ± 50	<10	Fully coated stem
Biomet		62	55	5	Proximal part of stem
Smith and Nephew			200 ± 50	20	Proximal part of stem
Corin	97	>75	80–120	3–10	Proximal part of stem
Centerpulse (Intermedics)	94	72	55 ± 5	3	Proximal part of stem
Zimmer	70 (and 30% tri-calcium phosphate)		80–130		Proximal part of stem

pulsed laser deposition (Lo et al. 2000) and electron beam evaporation combined with ion beam mixing (Mohseni et al. 2014a). To date, only plasma spraying is being used commercially and approved by the US Food and Drug Administration (FDA). The advantages and limitations of these method have been reviewed and discussed (Zhang 2013; Mohseni et al. 2014a).

Thermal spraying such as plasma spraying is a major coating method used to manufacture HA coatings onto metal implants. It involves the melting of ceramic HA powders in a plasma and the molten powders are subsequently spray deposited onto the surface of medical implants. This is a relatively low cost process with a high deposition rate. The effect of process parameters (e.g. particle size and velocity, oxygen pressure, fuel gas type, and spraying power and distance) on the microstructure and properties of HA coatings has been reviewed (De Groot et al. 1987; Berndt et al. 1990; Klein et al. 1991). Earlier investigations have shown that these coatings can successfully enhance clinical success to as little as a 2% failure rate after 10 years. Pure crystalline HA (with Ca:P = 1.65) has also been deposited with adequate mechanical adhesion (23 MPa) onto non metallic polymer composites (e.g. carbon fiber/polyamide based composite) by plasma spraying that complies with ISO 13779 (Auclair-Daigle et al. 2005a, b). The HA coating also exhibited bioactivity in simulated body fluid which is needed for orthopedic applications.

Despite the capability of plasma sprayed HA coatings to improve bone strength, provide initial osseointegration and their excellent clinical performances, the optimum coating properties required in order to achieve maximum bone response have yet to be realised. This is due to the intrinsic drawbacks of the plasma spraying process. These are attributed to the high temperature melting and/or thermal decomposition during the plasma spraying, which tends to cause variation, non-uniformity and uncontrollability in phases, crystallinity, density and microstructure of HA coatings which would lead to different mechanical properties and behaviours. Typically, partially dehydrated HA is the main constituent in plasma-sprayed HA coatings, together with amorphous CaP and other more soluble phases originating during deposition at high-temperatures, such as tri-calcium phosphate (TCP). The ratio of HA to TCP is crucial for bone regeneration. The crystallinity for plasma-sprayed HA coatings is approximately 65% (Ong et al. 2006). Such high processing temperature may also cause phase transformation, grain growth, and high residual stress in the HA coating and poor controlled stability and reproducibility (Hench 1991). Table 2 shows the thermal effects of HA.

Rapid cooling during plasma sprayed deposition tends to produce amorphous coatings, micro-crack and low porosity. This would lead to poor coating adhesion, limiting the optimum fixation with the implants, interface separation between the coating and the substrate, and the long term durability of the HA coatings. Furthermore, plasma spraying is a line-of-sight coating technique. Difficulties may exist in coating complex 3D implants uniformly and even coatings on porous metal surfaces. Furthermore, this is a relative high deposition process, thus it cannot incorporate growth factors and biologically active agents that stimulate bone healing.

Table 2 Thermal effects of hydroxyapatite (Hench 1991)

Temperature (°C)	Reaction (s)
25–200	Evaporation of absorbed water
200–600	Evaporation of lattice water
600–800	Decarbonation
800–900	Dehydroxylation of HA forming partially or completely dehydroxylated oxyhydroxyapatite
1050–1400	HA decomposes to form β-TCP and tetracalcium phosphate (TTCP)
<1120	β-TCP is stable
1120–1470	β-TCP is converted to α-TCP
1550	Metling temperature of HA
1630	Lemting temperature of TTCP, leaving behind CaO
1730	Melting of TCP

Other deposition techniques have been explored to improve the quality of HA coatings, such as electrophoretic deposition (Ducheyne et al. 1990), pulsed laser deposition (Lo et al. 2000), sputter deposition (Yang et al. 2005), sol–gel (Chai and Ben-Nissan 1999), deposition of apatite coatings from simulated body fluids (Bigi et al. 2002) and Electrostatic spray assisted vapour deposition (Choy 2003; Hou et al. 2007).

The ability of **electrophoretic deposition (EPD)** to form coatings onto complex shapes at low temperatures and at low cost has attracted increasing interests for biomedical applications (Ducheyne et al. 1990; Zhitomirsky and Gal-Or 1997; Wang et al. 2002). During the EPD process, HA powders are deposited from a stable colloidal suspension using a DC electric field (Wang et al. 2002). However, the HA coatings deposited by EPD tend to be porous, which may lead to corrosion and coating spallation due to the penetration of body fluids. The use of post annealing to reduce the coating porosity would lead to coating shrinkage and cracking (Soares et al. 2004). The micron sized grain structure has poor adhesion, fracture toughness and compressive strengths, therefore, this limits the use of EPD HA coatings on metal implants.

Sputtering is also a promising method to produce adherent HA coatings with good bioactivity that could address some of the brittleness of plasma spray deposited HA, that limits its usage in load bearing conditions, whilst exhibiting good bioactivity (Yang et al. 2005; Mohseni et al. 2014a). However, sputtering is also a line-of-sight process and has difficulty to coat the 3D implants uniformly. Other drawbacks of this technique include the use of expensive and sophisticated reactor and vacuum systems and slow deposition rate. Moreover, the sputtering occurs at low deposition temperatures, hence the deposited HA coatings tend to be amorphous and require subsequent annealing to achieve the desired crystallinity. Otherwise, the low crystallinity would accelerate the dissolution of the film in the body.

Other vacuum deposition techniques such as ion beam assisted deposition (IBAD) have also been explored. This method combines ion beam bombardment and physical vapour deposition, which enable the deposition at low temperature and the close interaction between the coating materials and the substrate at the atomic scale, creating an intermixed zone at the interface of the substrate and the coating that results in adherence, high reproducibility and reliable HA coatings (Cui and Luo 1999; Hamdi and Ide-Ektessabi 2003). However, IBAD is also a direct-line-of-sight deposition process and has similar difficulties in coating the 3D implants uniformly. Furthermore, the HA coatings would tend to crack after heat treatment, likely due to the thermal expansion mismatch between the coating and the substrate which could reduce the coating adhesion (Choi et al. 1998).

Pulsed laser deposition (PLD) involves the use of high power laser energy to vaporize the bulk coating material from a target, which subsequently condense onto a substrate. The process would be repeated to achieve the required coating thickness. Although PLD allows the deposition of thin and adherent stoichiometric HA onto titanium substrate surface (Lo et al. 2000), this is a direct-line-of-sight deposition process and would have similar difficulties in uniformly coating 3D implants. Furthermore, it also has a limited deposition zone.

Sol–gel method tends to use alkoxide based precursors. This method involves the formulation of a homogeneous solution containing all of the component metals in the correct stoichiometry. Therefore, the control of chemical homogeneity and stoichiometry of the synthesised materials at molecular level is made possible. This method has been used to synthesise HA powder and coatings (e.g. via dipping or spin-coating). Nanocrystalline thin film hydroxyapatite coatings have been produced via the sol-gel route where the sol precursor can be applied to the substrate by dipping or spray coating. Coating thickness varied between 70 and 1000 nm depending on the number of applied layers. However, the sol–gel produced HA coatings tend to require subsequent heat treatment at high temperatures (e.g. 1000 °C) (Chai and Ben-Nissan 1999) and these processes would need to be repeated to achieve the desired thickness which is time consuming and laborious. Furthermore, the removal of solvent and organic residues of sol-gel coating during heat treatment tends to lead to a weak structural integrity.

Apatite coating from simulated body fluids. The bioactivity of hydroxyapatite-coating with the ductility of metallic implants have been used in load-bearing parts, however, they exhibit high elastic modulus and no biodegradability. Whereas, living bone is a composite consisting of 70 weight% inorganic component, hydroxyapatite, and 30 weight% organic component, collagen (Park and Lakes 2007). The organic component acts as a template for the structure of inorganic component and control its deposition to form finely constructed organic–inorganic hybrids of life via biomineralization (Mann 2001). The unique composition and structure of natural bone not only would give high strength and fracture toughness, but also deformability and low elastic modulus.

However, the hydroxyapatite fabricated by plasma-spray technique (as described in earlier section) is different from bone apatite in the point of composition and

structure, where bone apatite exhibited a broad X-ray diffraction pattern due to its low crystallinity and small crystallite size (20–40 nm) (Kamitakahara et al. 2007).

Kamitakahara et al. (2007) reviewed the development of bone-like apatite coating on substrates for bone reconstruction using solutions mimicking body fluid which shows high affinity against bone tissue. The **biomimetic approach** consists of soaking metal implants in simulated body fluids at a physiologic temperature and pH. Apatite coatings have successfully been formed by the immersion of chemically pre-treated substrates such as glasses, metals, and polymers in metastable simulated body fluids (SBF) (Kim et al. 2011; Rezwan et al. 2006). The advantages of such approach include: (a) a low-temperature process, therefore, applicable to any heat-sensitive substrate including polymers; (b) ability to form bone-like apatite crystals having high bioactivity and good resorption characteristics; (c) uniformly deposited onto complex and/or implant geometries; and (d) capable of incorporating stimulating factors for bone-growth. This low temperature process allows bone-like apatite coating to be applied on the surfaces of biodegradable polymers which can be used as scaffolds for bone reconstruction (Chau et al. 2004) or as an adsorbent of organic substances (Kawai et al. 2006) during the biomineralization process.

Although SBF mimics the inorganic composition, pH and temperature of human blood plasma, it is unknown whether these conditions are optimal for a coating process. Other drawbacks include processing times from 7 to 14 days requiring daily resupply of SBFs and the need to maintain supersaturation for crystal growth, which requires constant pH. Moreover, local precipitation or formation of heterogeneous coatings due to the low solubility of HA and limited operational range of concentrations for the metastable phase could result from the low solubility of HA and the limited concentration range for the metastable phase. This operation is extremely difficult and might lead to local precipitation or uneven coatings. Such an intricate and long process can hardly be applicable in the coated prostheses industry (Habibovic et al. 2002).

New and promising coating methods are continuously being developed in order to deposit HA with optimal coating properties. One of these methods is **Electrostatic spray assisted vapor deposition (ESAVD)** (Choy 2003), which is a novel and cost-effective technique that has been used to deposit adherent HA coatings in a single step onto Ti-alloy substrates. Pure and well-crystallized HA coatings with well controlled structure and stoichiometry at molecular level have been successfully deposited at 500 °C using the single-step ESAVD method from a sol solution consisting of phosphorus hydroxyl-alkoxide, alkoxy-nitrate, and some remaining calcium nitrate (see Fig. 1). A detailed overview of this deposition technique for the synthesis and deposition of nanostructured oxide materials has been reported by Hou et al. (2007). The in vitro study indicated that the deposited HA coatings were sufficiently stable to maintain their structural integrity in SBF. After 14-day immersion in SBF, the surface of the coating was completely covered by a biomineral particulate layer (particle size less than 100 nm) consisting of biologically active bone-like carbonate-containing apatite. The layer resulted from

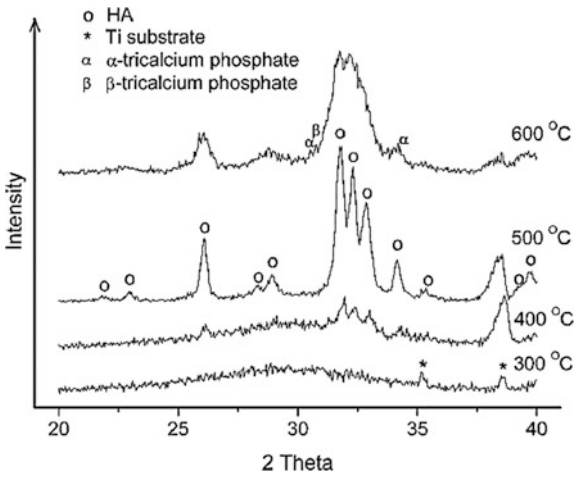

Fig. 1 XRD of HA coatings deposited at different deposition temperatures (Hou et al. 2007)

the chemical reaction of the ceramic surface with surrounding body fluid leading to the precipitation of the ions from SBF solution as shown in Fig. 2. Thus, the HA coatings deposited by ESAVD method showed osteoconduction.

(ii) **Coating adhesion**

The adhesion and bond strength of HA coating to the metal implant, as well as the similarity of the HA coating composition and biocompatibility with the bone, is crucial in order to make use of the load-bearing ability of the metal alloy implant. Any detachment or coating spalling from the implant in the human body would have adverse effects due to the detached particles (Wang et al. 1996). Figure 3 shows the comparison of adhesion strength values of HA coatings on Ti-6Al-4V deposited using various techniques.

From Fig. 3, HA coating produced by sputtering has the best adhesion to Ti-6Al-4V substrate. However, due to the drawbacks of HA coatings as described earlier, sputtering is yet to be used widely at a commercial scale for the manufacturing of HA onto medical implants. In general the adhesion of HA onto

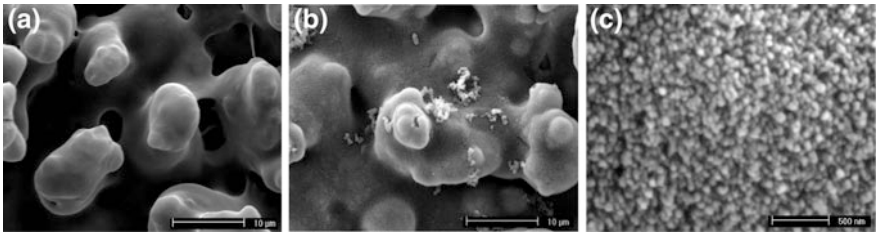

Fig. 2 Surface morphology of the as-deposited and soaked HA coatings. **a** As-deposited HA coating; **b** after 14-day immersion in SBF; **c** a higher magnification of **b** (Hou et al. 2007)

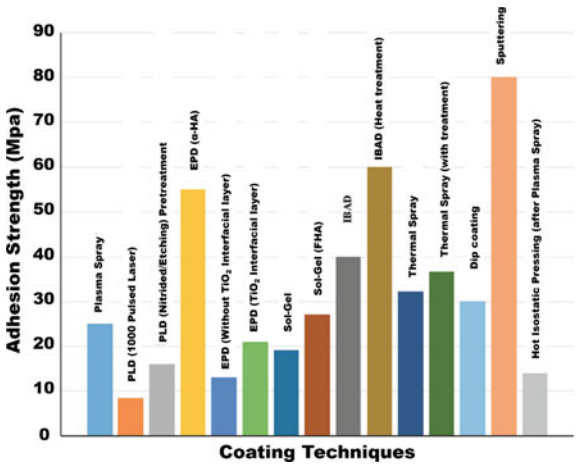

Fig. 3 Quantitative comparison of different coating techniques (Mohseni et al. 2014b)

substrates is rather weak susceptible to fatigue failure. Hence the adhesion of HA coatings needs to be improved for load bearing implants.

(iii) **Improvement of coating adhesion**

The low coating adhesion has hindered the wide use of HA coated implants. The improvement of the bonding between the ceramic HA coating and the metallic implant is important irrespective of the coating manufacturing methods. In fact, there is an increasing demand for durable and reliable load bearing medical implants, such as hip and knee replacement, going as far as to exceed the lifetime of the patient. HA coated implants experience loss of the biomaterial fixation after the implants have been in the human body for a long time. The failure noted by orthopaedists and dentists tend to occur at the HAP-titanium interface and through dissolution of the coating itself (Geesink et al. 1987). Revision surgeries are needed to re-secure or insert new coated implant. Thus, the interfacial control and improvement between the implant and natural tissue is crucial. Hence surface modification and texturing have been explored to enhance osseointegration as summarised below.

(a) Pretreatment and post treatment

The work by Riedel, for example, has indicated the importance of surface topography on the effect of mesenchymal stem cell and osteoblast response to titanium surface. Polished pre-treated Ti surface outperformed those prepared from the as-received condition. Similarly argon etching, especially with the optimal etching energy of 700 eV, also demonstrated positive impact on the cellular interaction of the as-received substrates. Such improvement may be due to the hierarchical texturization of the etching imparted on the surface of the substrates (Riedel 2010). Furthermore, post-anneal etched surface outperformed the annealed hydroxyapatite (deposited by sputtering) surface.

Other surface treatment such as laser surface nitriding and subsequent etching of the substrate has also shown to be an effective pre-treatment method for improving the adhesion strength of HA coated onto Ti-6Al-4V (Man et al. 2009).

In addition, the substrate cleaning method also influences the HA coating adhesion. HA coatings adhered better to ultrasonically cleaned substrates than to high pressure air cleaned substrates tested according to ASTM C-633 (Hsiung et al. 2012). Furthermore, the same authors also found that a combination of ultrasonic cleaning and cryogenic treatments can effectively improve the HA adhesion and coating properties.

(b) Interfacial layer
The deposition of interfacial layer such as TiO_2 (Blind et al. 2005) and TiN (Kummer and Jaffe 1992; Blind et al. 2005) prior to the deposition of HA have been developed to improve the bonding and adhesion of HA to Ti-alloy substrates. Compositionally graded coating has also been explored to improve the adhesion of HA to Ti-alloy substrates (Park and Condrate 1999).

(c) Double-layered porous structures
Bioactive coatings with double porous structure in micro and macro scales as reported in the literature (Raines et al. 2010; Gittens et al. 2011), for example, could be adapted here as one of the combined approaches to improve the coating adhesion of HA to metal implants. Such structures exploit the benefits of micropores (0.05–10 μm in size) in promoting osteoblast attachment and proliferation on Ti implant. Whilst, the macropores (50–400 μm in size) on implant surface could provide mechanical locking to improve the fixation strength between implant and tissue after implantation (Bobyn et al. 1980; Zhou et al. 2014).

(d) Functionalisation of HA
Bosco et al. (Bosco et al. 2015) reported the functionalization of hydroxyapatite nanocrystals with anti-osteoporotic drug (e.g. alendronate) as bioactive components for bone implant coatings to decrease osteoclastic activity to address the unbalance between osteoclasts and osteoblasts in patients, especially with bone metabolic disease. The functionalization assists the coated implants to regain load-bearing functions (i.e. mastication or gait cycle) owing to a locally improved bone quality and help towards a more successful bone implant

(e) Other surface modification
Current medical implants have no signalling interaction at the tissue-implant interface, thus reducing the ultimate efficacy of these devices by forcing biology to treat it as a foreign entity. This limitation needs to be addressed in order to realise the full potential and extend the lifetime of the next generation of devices. Meyers and Grinstaff (2012) have reviewed the used of biomimetic approach to modify the device surface, and explored its effectiveness in communicating with the surrounding cells and proteins. Both the covalent and adsorptive strategies for device modification and their advantages and disadvantages have been reviewed. A biomimetic approach that combines non-fouling and bioactive surfaces seems to be promising in this field. Results

suggested that natural ECM components might replace other strategies to afford non-fouling enzymatically degradable surfaces, or loosely bound through non covalent methodologies which might allow the cells to remodel up and integration with device surface, and synthetic coatings. However, several questions remain, including the appropriate ratios of "non-fouling" and "signalling" components and the performance of the bioactive coatings in in vivo and in vitro studies.

Although stringent antiseptic operative procedures, infection rates (0.5–3.0%) of total joint hip arthroplasties still occur during in primary total hip arthroplasty (Antti-Poika et al. 1990; Nasser 1992; Hendriks et al. 2004). This could lead to significant medical costs, increase in morbidity and decrease in patient satisfaction (Nasser 1992). Various surface modification methods have been explored to incorporate antibacterial property to biomaterials in order to minimise infections in implants. These include incorporating chitosan nanoparticles with antimicrobial agents (Schmidmaier et al. 2006), surface functionalization via attaching polycationic group (Cen et al. 2004), coating of silver ions (Ewald et al. 2006) and antibiotic (e.g. minocycline/rifampin) (Bosetti et al. 2002). The increase in antibiotic resistance has becoming a major medical concern, whereas silver is a promising antibacterial material. A recent approach includes the creation of a multifunctional surface by co-depositing the osteoconductive HA with antibacterial Ag (Bosetti et al. 2002). In this case, the in vitro cytotoxicity was observed between HA and Ag-HA surfaces, and anti-bacteria properties of Ag–HA increased.

(iv) **Other bioactive ceramic coatings**
HA coated implants experience loss of the biomaterial fixation after long-term insertion in the human body. This failure tends to occur at the HAP-titanium interface, with dissolution of the coating itself as described by orthopaedists and dentists (Geesink et al. 1987). Alternative bioactive coating based on calcium titanate (CT) coating has been explored as this is chemically stable and the dissolution of the coating layer in a living body can be prevented (Ohtsu et al. 2004). It has been demonstrated by Ohtsu et al. (2007) that a crystallized CT coating (ca. 50 nm thick) on titanium can activate osteogenesis in hard tissues in rat. Moreover, CT reacts actively with titanium, therefore, it is expected the bonding strength at the coating-substrate interface could be improved.

2.2 Bioglass Coatings

Bioglass formulations are glasses to which living bone tissue can be bonded. Conventional glass contains at least 65% silicon oxide which is useful to provide resistance to humidity, however, silicon oxide is biologically inactive. The work on bioglass was initiated by Hench et al. in the late 1960s (Hench et al. 1971). Hench

el al. developed the first bioactive glass based on Na_2O–CaO–SiO_2–P_2O_5 system, demonstrating that glasses consisting of 40–45% of silicon oxide, 20–25% of sodium oxide, and 20–25% of calcium oxide are bioactive (Hench et al. 1971).

Hench et al. have investigated the role of glass and the physical, chemical, and biological aspects of the bone-bond formation with the surrounding tissue (Hench and Clark 1982). Dycheyne (1985) has reviewed structural, mechanical and biological properties of bioreactive glasses, covering: (a) the relationship between the composition and bonding and its influence on the bone bonding mechanism and the rate of bond formation; (b) mechanical properties of these bioglasses, where various degrees of success could be achieved for the use of bioglass in highly stressed applications; and (c) the effect of loading on the glass properties and their bonding characteristics. The author has also established the influence of a critical set of parameters based on the failure analysis of bioactive glasses. Interface of various glasses and glass ceramics in a bony implantation bed has been reviewed by Gross and Strunz (1985).

Most of the bioactive glasses contain a relatively large amount of SiO_2. Calcium phosphate glass-ceramics without silica, (x)CaO–(90−x)P_2O_5–(y)Na_2O–(10−y) TiO_2 (x = 45–60, y = 0–10) have been reported by Kasuga et al., and the glass composition of (x = 60 and y = 7) has been explored as a coating on Ti-29Nb-13Ta-4.6Zr alloy by glazing method, i.e. placing the glass powder on the β-Ti alloy substrate and heating at 800 °C in air. The glass layer reacted with the oxide layer formed on the alloy to form strongly bonded phosphate reaction layer with tensile bond strength 20–25 MPa and in vitro bioactivity tests showed that the glass-ceramic coating is bioactive (Kasuga et al. 2003). Like bioceramic HA, bioactive glass has high chemical stability, ability to form strong bonds with metallic substrates, can help to increase the corrosion resistance of the substrate and it is also a biocompatible material. Furthermore, bioactive glass has a higher dissolution rate and higher bioactivity than hydroxyapatite (Xiao and Liu 2006). Moreover the composition of the bioactive glass coating can be tailored to have close thermal expansion coefficient match between the coating and the substrate (Peddi et al. 2008). Additionally, bioactive glass coatings can induce the formation of a thin layer of inorganic component of human bone of hydroxycarbonate apatite (HCA) when placed in biological environment of the body (Hench 1998). Bioactive glasses have been explored for biomedical applications (Vallet-Regí et al. 2003; Balamurugan et al. 2006).

CaO–SiO_2–P_2O_5 containing bioactive glasses tend to bond directly to soft and hard tissues, for a range of different compositions. These compositions have also been shown, through in vivo tests, to not produce a toxic response, neither local nor global, nor inflammation and foreign-body immune system responses (Sepulveda et al. 2002). It has recently been shown that the cellular response of osteoblasts to bioactive glass is genetically controlled (Hench and Polak 2002).

The key difference between HAP and bioglass is that the bioactivity of glass can be tailored and controlled by varying its chemical composition to be close to the bone. It has been shown (Lopez-Sastre et al. 1998a) that bioglass has better physical and chemical characteristics for spraying at high temperature and would produce

bioglass coatings with larger pore size, higher porosity and larger contact area with bones than HA coatings. However, the comparative study performed by Lopez-Sastre et al. (1998a) showed that HAP coating gave a stronger and earlier fixation to the bone than bioglass. The failure of the bioglass coating tends to occur at the interface between bone and coating. The mechanical tests of bioglass indicated that the shearing force was between four and ten times greater for HAP. With bioglass there was retarded maturation and newly-formed coatings were poorly mineralised. HA coated implants have better integration than those coated with bioglass (GSB formula) which could be due to the presence of an excessive amount of aluminium oxide in bioglass. In addition, HA also demonstrated intense new bone formation with highly mineralised osseous trabeculae near the interface, whereas bioactive glass coatings a showed macrophage reaction with small amounts of new bone. Moreover, bioactive glass coatings were observed to be brittle, which would eventually lead to fractures on the interface that would cause the failure of the implants (Takeshita et al. 1996; Zhang et al. 2001).

In addition, like HA, the drawbacks of bioactive glass include poor mechanical properties, such as low tensile strength, fracture toughness, fatigue resistance and elastic modulus (Rawlings 1993). Therefore, bioactive glasses are mainly used in low or non-load bearing situations or compressive load situations in solid or powder form to make use of their bioactivity, for examples, bone restoration and augmentation, middle ear repair, vertebral and iliac crest replacements (Cao and Hench 1996). In addition, bioactive glass is being investigated as promising coating for prosthetic metallic implants in order to improve the osseointegration of the medical implants, and protect the metallic implants against corrosion from the body fluids and the tissue (Jones 1996).

Sol–gel is the common method used for the synthesis of bioactive glass. It not only has a lower synthesis temperature as compared to traditional melt processed bioactive glass but also achieves higher bioactivity and biodegradability (Fathi and Doostmohammadi 2009b). The bioactive range of bioactivity in the system $CaO–SiO_2–P_2O_5$ is larger for sol–gel bulk materials than for correspondent glasses obtained by melting (Gallardo et al. 2001). The high surface area of the sol–gel derived nanoporous structure helps to improve the rate of HCA layer formation and the bonding with host tissue (Chen et al. 2010).

Bioactive glass coatings can be deposited using the coating techniques describe in Sect. 3.2.1(i). Garcia et al. have shown that coating of bioactive glass on biomedical grade stainless steel exhibited better corrosion resistance and bioactivity as compared to the uncoated substrates (Garcia et al. 2004). Different techniques have been used to deposit bioactive glasses onto implants. These include plasma spraying (Lopez-Sastre et al. 1998b; Arifin et al. 2014), sol–gel (Kokubo et al. 2003; Liu and Miao 2004; Fathi and Doostmohammadi 2009a), electrophoretic deposition (EPD) (Boccaccini et al. 2007; Moskalewicz et al. 2013; Pishbin et al. 2014), and sputtering techniques (Saino et al. 2009; Stan et al. 2009). The strengths and limitation of each of these processing techniques have been reviewed and presented earlier under Sect. 3.2.1(i).

Bioglass coatings deposited by plasma spray tend to have a weak glass/metal interface which together with rapid dissolution in body fluids when implanted would cause coating failure (Hench and Wilson 1993). Other techniques, such as enamelling, have also failed because the glass crystallized significantly, resulting in lack of adhesion to the substrate (Pazo et al. 1998).

New generation of bioactive glasses with various compositions are being developed and may hold promise as reviewed by Jones (2013). Solgi et al. (2015) have developed bioactive SiO_2–CaO–P_2O_5–SrO quaternary glass by incorporating a small amount of strontium (5 mol%). This bioactive glass can stimulate bone cell production of alkaline phosphatase bioactivity and it is a biocompatible material. Strontium is a bone-seeking agent, and could benefit patients suffering from osteoporosis as it can suppress osteoclast activity (Hoppe et al. 2014). Such strontium containing bioactive glass could also be produced in the form of coatings (Gorustovich et al. 2009).

Functionalisation in general, the body tends to respond to a foreign object (e.g. medical implant) by coating readily with plasma proteins (Latour 2005). Living cells, when in contact with the material surface, interact with the molecular structure of the adsorbed protein layer which could lead to conformational changes that influence the protein stability and protein–surface interaction (Roach et al. 2005). It is essential to minimise structural changes in proteins and to increase implant efficacy through surface modifications. Grafting of the surface by appropriate chemical bonding is one of the approaches to minimize structural changes in proteins, without weakening their effectiveness (Verné et al. 2009). Magyari et al. (2015) investigated the in vitro bioactivity of the surface modified bioactive glasses of SiO_2–CaO–P_2O_5 by functionalization with aminopropyl-triethoxysilane and/or by fibrinogen in order to understand the influence of the proteins on the apatite-like layer growth and the blood compatibility of these materials. They have found that the fibrinogen adsorbed on the glass surfaces induces a growing of the apatite-like layer and good blood compatibility of the materials after fibrinogen and bovine serum albumin adsorption.

Bioactive glass ceramic coatings based on (Bioverit®I) have been applied on Al_2O_3 in order to improve the osseointegration of Al_2O_3 ceramics for total hip and knee arthroplasty. The 35 μm thick coating consisted of 30.5% SiO_2, 11.4% P_2O_5, 15.9% Al_2O_3, 14% CaO, 14.8% MgO, 5.8% K_2O, 2.3% Na_2O and 4.9% F^- (weight %) and was fabricated by a sintering process at 1000–1300 °C. The coating exhibited advantage under load-bearing conditions with higher interfacial shear strength and formation of mineralised bone directly in contact with the implant. On the other hand, the uncoated Al_2O_3 was found to bind to the bone through a thick connective tissue layer, which results in low interfacial shear strength (Ignatius et al. 2005). Despite this promising result, further investigations still need to be conducted on the stability of the coating after longer implantation periods and under more critical loading conditions

2.3 Polymer-Based Bioactive and Degradable Coatings

2.3.1 Natural Polymer Derived Coatings

Numerous natural and synthetic polymers have been explored as coatings for surface modification of different biomaterials. Among the natural polymers especially peptides and proteins, but also various polysaccharides and glycosaminoglycans, have been widely used to improve the cell acceptance of a selected implant material.

Immediately after incorporation of a foreign material into the body, extracellular matrix (ECM) proteins like fibronectin and vitronectin are non-specifically adsorbed on the material surface. Cells indirectly interact with the material surface via the adsorbed proteins controlled by cell membrane receptors, so called integrins. Integrins bind to specific domains of adsorbed proteins of which the arginine-glycine-aspartic acid (RGD) tripeptide is the most prominent. Because the availability and accessibility of these specific domains of adsorbed proteins are influenced by the material surface properties, the latter ones also strongly influence the adhesion and further behaviour of cells (Vasitaa et al. 2008).

Several approaches have been explored for the immobilization of proteins like collagen (Geissler et al. 2000; Morra et al. 2009) gelatine (Marois et al. 1995; Liu et al. 2008; Vanderleyden et al. 2014), fibronectin (Cornelissen et al. 2013) and laminin (Oyane et al. 2005; Bougas et al. 2012) onto implant surfaces. Most of these studies report an accelerated tissue healing and an increase in new tissue formation. For bone implants it was stated that the adhesion of mesenchymal stem cells on selected extracellular matrix proteins promotes their differentiation along the osteogenic pathway (Salasznyk et al. 2004). In addition, in many studies, an enhanced osteointegration of implants was observed in different animal models (Morra et al. 2003; Schliephake et al. 2005). Although an extensive literature has been published, especially on collagen coating there are still some mechanistic aspects on the biological activity not yet fully understood. Among these open points (Morra et al. 2009) are:

(i) the role of supramolecular arrangement of collagen ("monomeric" versus "fibrillar");
(ii) collagen surface chemistry (specifically the role of chemical crosslinking and of covalent attachment to the surface versus simple adsorption);
(iii) optimal collagen surface density; and
(iv) characterization of the collagen coated surfaces.

Covering of biomaterial surfaces with high-molecular weight proteins is often connected with specific problems including immune reactions, denaturation processes caused by substrate surfaces or the procedures of surface immobilization, or also loss of bioactivity during sterilization. A promising approach to engineer the material-tissue biointerface consists in the attachment of short bioadhesive ligands specifically binding to cellular receptors. Currently, the most prominent ligand for

integrins, major extracellular matrix receptors, is the already mentioned RGD motif (Ruoslahti and Engvall 1980). The process of integrin-mediated cell adhesion comprises a complex cascade of various overlapping events including cell attachment, cell spreading, organisation of actin cycloskeleton, and formation of focal adhesions (Lebaron and Athanasiou 2000; Hersel et al. 2003).

Normally, stable linkage of adhesion peptides is necessary because the ligands have to withstand both contractile forces of the cells during formation of focal adhesion (Katz et al. 2000) and manual forces resulting from the incorporation of the ligand-containing implants during surgery. In the last years various strategies have been reported to attach RGD or similar peptides either directly to the biomaterial surface by covalent linking via a spacer or via incorporation into a polymeric coating. A variety of functional groups including hydroxyl, carboxyl, amino or thiol functions are principally suitable for the covalent RGD peptide attachment to the spacer or the substrate coating. Special efforts have been undertaken to stimulate cell adhesion on metallic bone and dental implants to achieve rapid ingrowth of those implants into the surrounding tissue. Conventional techniques like plasma or chemical vapour deposition have been used to pre-activate the metallic surfaces for the subsequent coating process.

A family of different RGD motifs (e.g. RGD, RGDS, GRGD, YRGDS, YRGDG, YGRGD, GRGDSP, GRGDSG, GRGDSY, GRGDSPK, CGRGDSY, GCGYGRGDSPG, RGDSPASSKP G_4RGDASSK, CGGNGEPRGDTYRAY) containing further amino acids in the sequence functioning as spacers, binding units for selective coupling and marker groups simplifying the detection of the peptide on the surface have been developed. Cyclic RGD-derived peptide structures with a high integrin affinity have been introduced by Kessler (Aumailley et al. 1991) (Fig. 4).

Besides the RGD sequence, other cell adhesion motifs have been identified which can address other integrins, secondary binding sites of integrins or other cell

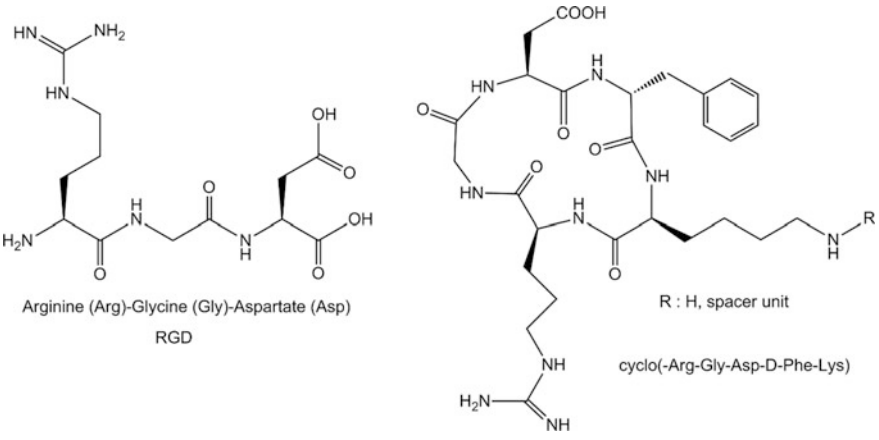

Fig. 4 Linear (*left*) und cyclic RGD (*right*) sequence containing cell adhesion motif

receptors, mainly the proteoglycans receptor or the 67-kDa laminin receptor (for an overview see Hersel et al. 2003). A triple-helical, collagen-mimetic GFOGER peptide, selectively promoting β2β1 integrin binding was recently used as bioadhesive coating (Reyes et al. 2007).

Direct immobilization of the RGD motif on titanium, hydroxyapatite or glass surfaces can be performed using conventional silane chemistry as exemplarily shown in Fig. 5 (Olbrich et al. 1996; Porte-Durrieu et al. 2004).

Alternative synthetic routes to attach the RGD peptide to titanium surfaces represent the use of 11-carboxyundecylphosphonic acid (Gawalt et al. 2003) or carboxy-terminated oligo(ethylene glycol)-alkane phosphate as adhesion promoters (Gnauck et al. 2007). In analogy to the silane chemistry also amino-functionalized titanate linkers have been used to link RGD via a dextran layer onto titanium (Dubs et al. 2009).

Cyclic RDG peptides have been bound to titanium surface via specific anchor groups, e.g. phosphonate (Auernheimer et al. 2005) or thiol groups (Elmengaard et al. 2005) introduced into the peptide molecules directly during peptide synthesis.

A variety of natural and synthetic polymers were equipped with RGD-derived peptides using mainly covalent linkages via amide bond formation. For this purpose an activated polymeric carboxyl group was reacted with the nucleophilic N-terminus of the peptide. Common peptide coupling reagent like 1-ethyl-3-(3-dimethylaminopropyl)-carbodiimide (EDC) can be used to activate the carboxylic group. Preparing the N-hydroxysuccinimide active ester of the polymer in the first step, the peptide coupling can also be performed in water. Amino groups of polymers can be transformed into carboxyl groups (e.g. by succinic anhydride) prior to attaching the RGD peptide as described above. Similarly, polymeric hydroxyl groups can be pre-activated (e.g. with N,N′-disuccinimidyl carbonate or p-nitrophenyl chlorocarbonate) prior to peptide coupling or the peptide can be coupled to the polymer hydroxyl function using a diisocyanate. Polymers with

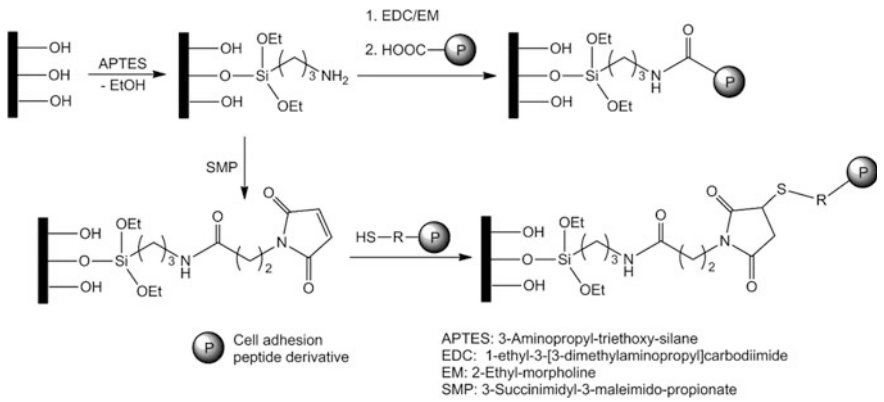

Fig. 5 Direct binding of cell adhesion peptides onto titanium surfaces via different silanization routes

introduced thiol groups can be linked to cysteine-containing RGD sequences by formation of a disulfide bonding. More recent approaches also use chemoselective ligation to form stable bonds without the need of activating agent and without interfering with other functional groups. A more detailed overview of those reactions is given by Hersel et al. (2003).

It seems to be obvious that the RGD peptide has to stand out from the artificial surface to reach the binding site of the integrin. It is assumed that peptides that extend out 11–46 Å from the surface can reach the majority of receptors (Hersel et al. 2003).

The many years of encouraging results of in vitro cell adhesion and proliferation on RGD functionalized biomaterials have led to numerous in vivo studies. In these studies to confirm the biological activity and evaluate the clinical applicability more variable results have been obtained. It has been seen that in many cases the effectiveness of RGD-based coatings was not as high as promised by the in vitro results. Nevertheless, positive results were achieved for example in bone regeneration. In vivo studies with RGD coated titanium bone implants using different animal models have shown a better bone on-growth combined with a reduction in fibrous tissue anchorage, and an improved mechanical fixation of the implant within the surrounding tissue as compared to the uncoated implant samples (Elmengaard et al. 2005; Schliephake et al. 2005; Shannon et al. 2008).

Polysaccharides are polyfunctional biomacromolecules of innate biocompatibility. Whereas some members of this class like cellulose or chitin are more or less stable in the human body others, including dextran or chitosan, PDLA are degraded over time. Polysaccharides offer a diverse set of physicochemical properties based on their sources, monosaccharides, composition and molecular weight. Due to their polyfunctional character there exists a wide range of physical and chemical modifications of native polysaccharides able to meet technological needs (Shelke et al. 2014). Among commercially available polysaccharides chitosan has found considerable interest to develop bioactive coatings for biomaterials.

Chitosan obtained by deacetylation of the parent polysaccharide chitin is a linear copolymer of β-(1–4) linked 2-acetamido-2-deoxy-β-d-glucopyranose and 2-amino-2-deoxy-β-d-glycopyranose. The molecular weight is in the range between 50 and 100 kDa and common products contain 10–30% of remaining N-acetyl residues. Chitosan is normally insoluble in aqueous solutions at a pH above 7, but is readily soluble in dilute acids at pH < 5. As a cationic polymer chitosan is able to interact with negatively charged molecules rendering it a promising candidate in drug delivery systems and gene therapy (Dash et al. 2011; Anitha et al. 2014). Apart from that, chitosan exhibits enhanced wound healing, osteoconductive, and antimicrobial properties (Bumgardner et al. 2003). It was recently shown that the physical adsorption of chitosan on titanium implant surfaces of different roughness improve the surface wettability without modifying the surface roughness. These results suggest that polyelectrolyte surface modification on Ti surfaces could enhance bone formation and increase osseointegration in dental and orthopedic implants (Park et al. 2011). In an in vivo study chitosan-coated pins were implanted in the tibia of adult male New Zealand white rabbits and histologically evaluated for

healing and bone formation. After 12 weeks minimal inflammatory response and a typical healing sequence of fibrous, woven bone formation, followed by development of lamellar bone, were observed for the chitosan-coated pins (Bumgardner et al. 2007). Polyelectrolyte multilayer structures containing chitosan have been developed as functional coatings and intensively tested in vitro. The formation of multilayers on titanium film surfaces was performed using a layer-by-layer (LBL) self-assembly technique, based on the polyelectrolyte-mediated electrostatic adsorption of chitosan and gelatine. Cell proliferation and cell viability of osteoblasts on those films as well as on control samples exhibited higher values for multilayer-modified titanium films in vitro (Cai et al. 2005). A rat tibia model with bilateral placement of titanium alloy implants was employed to analyse the bone response to those polyelectrolyte multilayer chitosan/gelatine and chitosan/hyaluronan surfaces in vivo. The results showed that the chitosan/gelatine and chitosan/hyaluronan coatings have a positive effect on mechanical implant anchorage in normal bone (Zankovych et al. 2013).

Since the antimicrobial activity of chitosan is rather low, considerable efforts have been undertaken to synthesize more potent antimicrobially active chitosans usable as coatings for biomaterial surfaces. A common approach to increase the antimicrobial activity of chitosan is the improvement of the water solubility and the positive charge density within the molecule. This results in the synthesis of numerous derivatives (Fig. 6) like N-1-carboxymethyl-2-(4-methyl-piperazinyl)-substituted chitosan (Masson et al. 2008), 6-Amino-6-deoxychitosan (Yang et al. 2012) or O-quaternary ammonium N-acyl thiourea chitosan (Li et al. 2015).

In a recent study structure–activity relationships in terms of the antimicrobial activity and human cell toxicity of different N-alkyl quaternary chitosan derivatives were systematically investigated (Sahariah et al 2015). N-alkyl and N,N-dialkyl chitosan derivatives with ethyl, butyl, and hexyl chains were synthesized and

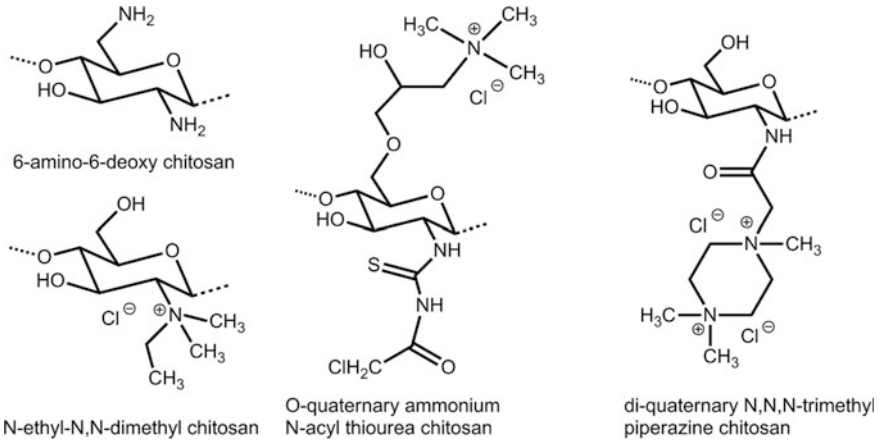

Fig. 6 Selected antimicrobially active chitosan derivatives with a higher antimicrobial activity compared to unmodified chitosan

subsequently quaternized to provide the corresponding N,N,N-methy-dialkyl as well as N,N,N-dimethy-alkyl chitosan derivatives. The well-defined derivatives were tested for antibacterial activity against Gram positive (*S. aureus, E. faecalis*) and Gram negative (*E. coli, P. aeruginosa*) bacteria. A correlation with the length of the alkyl chain was found, but the order was dependent on the bacterial strain. With a few exceptions a descending order in antimicrobial activity with increasing hydrophobicity was detected. The most active compound was N, N-dimethyl-N-ethyl chitosan. Toxicity against human red blood cells and human epithelial Caco-2 cells was found to be proportional to the length of the alkyl chain. Shortening the alkyl chain length resulted in lowering of the hemolytic activity and also of the cytoxicity against epithelial cells of the chitosan derivatives. On determining the selectivity toward bacterial cells over human red blood cells which is expressed by the ratio HC50 (50% hemolysis)/MIC (minimal inhibition concentration), again the N,N-dimethyl-N-ethyl chitosan exhibited the highest values. Also the N,N,N-trimethyl chitosan was found to possess a promising selectivity. Overall, highly selective compounds, which were significantly more active against bacteria than human cells could be obtained (Sahariah et al. 2015).

In addition to various proteins further macromolecular constituents like glycosaminoglycans (GAGs) and more complex proteoglycans are present in the ECM. GAGs are complex negatively charged unbranched heteropolysaccharides composed of disaccharide repeating units (for structures see Fig. 7).

In contrast to proteins, GAGs may be less immunogenic and less sensitive to denaturation processes. Due to their anticoagulation properties, heparin coatings have been investigated for years in haemodialysis systems, coronary stents and other blood-contacting medical devices (Kim and Jacobs 1996; van der Giessen et al. 1998; Wendel and Ziemer 1999). In addition, it is known, that both the high-sulfated GAGs heparan sulfate and heparin are able to interact not only with ECM components (collagen, fibronectin) but also with growth factors to sequester the latter ones in their active conformation and protect them against proteolytic attacks. Various growth factors containing heparin-based coatings have been developed to improve the efficiency of the highly active but also very sensitive protein molecules. Among growth factors used in this approach are basic fibroblast growth factor (bFGF) (Wissing et al. 2000), recombinant human bone morphogenic protein (BMP-2) (Kodama et al. 2008), and vascular endothelial growth factor (VEGF) (Wang et al. 2013).

In contrast to the concept of immobilization of a single biologically active macromolecule onto the biomaterial surface, a relatively new and innovative approach consists in the in vitro building of an artificial ECM (aECM) mimicking the microenvironment of the native ECM in its ability to guide morphogenesis in tissue repair and engineering (Bierbaum et al. 2012). In many native ECMs collagen fibrils are the basic constituent. As a consequence, most often collagen, especially collagen type I, is used to generate aECM in combination with typical components of the ECM like glycopeptides, glycosaminoglycans or proteoglycans. Depending on the tissue target and the purpose, aECM with a broad compositional

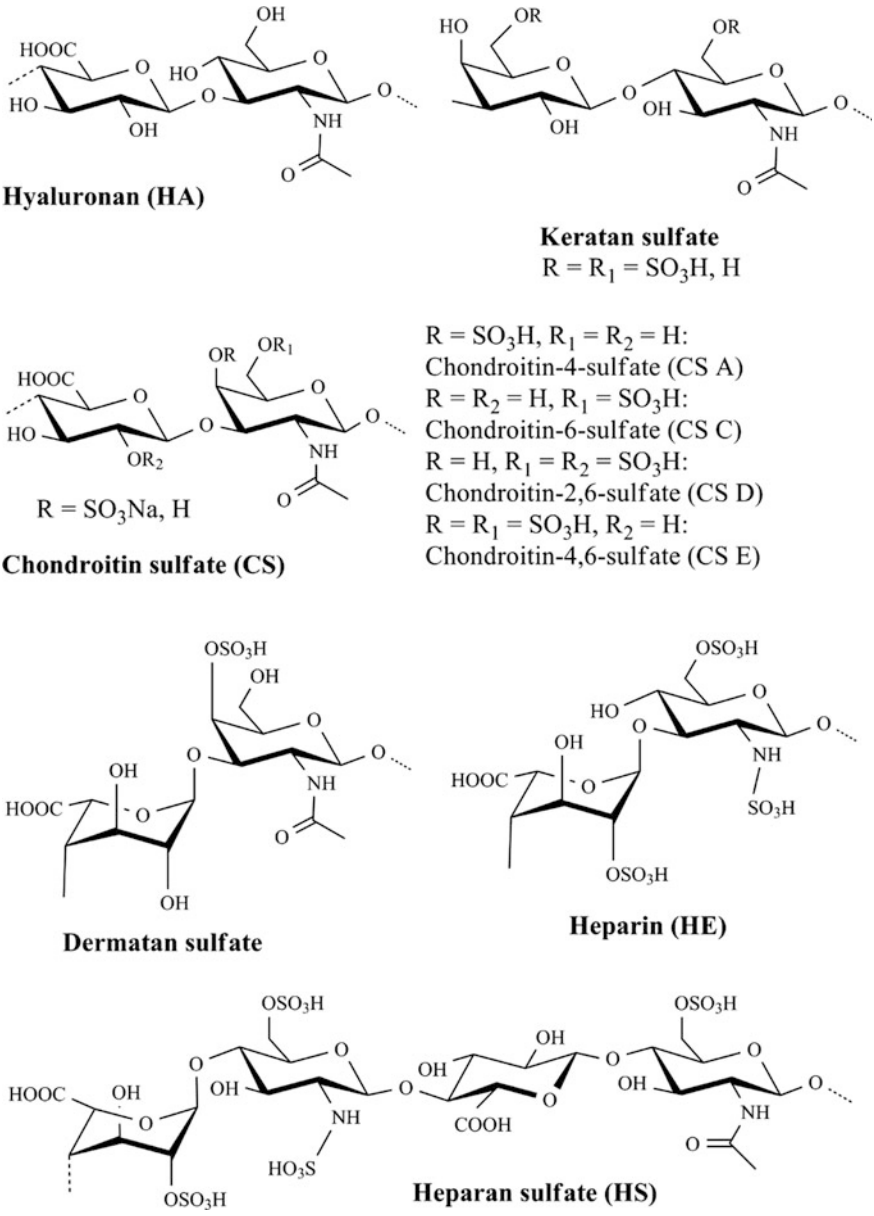

Fig. 7 Repeating units of natural glycosaminoglycans (GAGs)

and structural variety is available to tune the cell- and tissue-relevant environmental properties including mechanical stability, bioadhesive character, proteolytic susceptibility, and growth factor binding capacity.

Collagen-based aECM can be built using either suspensions of insoluble collagen fibers, or solutions of collagen monomers which then are allowed to form fibrils in vitro (Bierbaum et al. 2012). Both the resulting constructs can then be used in similar ways to coat biomaterial surfaces by simple physical adsorption or covalent immobilization.

Various multi-component aECMs have been reported in the literature containing collagen type I as basic structural element in combination with other collagens (type III (Bierbaum et al. 2003) or type V (Birk 2001)), and other proteins (fibronectin (Bierbaum et al. 2003), laminin (Tate et al. 2009)). While proteoglycans can only be included in collagen-based aECM to a limited degree due to inhibition of the fibril formation, the incorporation of GAGs is possible and results in aECM with interesting properties, especially with regard to growth factor interactions. The GAG-collagen interaction is unspecific and is mainly driven by electrostatic interactions between the negatively charged carboxylate and sulphate groups of the GAGs and positively charged amino acids of the related protein. Furthermore, many mediator proteins (growth factors, interleukins, further chemokines) interacting in vivo with GAGs are of basic nature or have basic amino acids or at least a sequence of basic amino acids. Having this in mind, collagen/GAG-based aECMs represent a promising future tool to modulate growth factor accumulation and release. Hence, aECMs comprising collagen and different sulfated GAGs have been intensively studied during the last decade. The incorporation of heparin into collagen matrices has an impact on the release of VEGF and stimulates angiogenesis (Wolf-Brandstetter et al. 2006). Matrices containing collagen type II and chondroitin sulfate have been shown to increase proliferation of chondrocytes and endothelial cells (Cao and Xu 2008) in vitro. Hyaluronan, the only non-sulfated GAG, does not interact with growth factors and has only a minor effect on cells if included into collagen matrices. This is changed if hyaluronan is chemically sulfated leading to derivatives with degrees of substitution (DS) in a range between 1.0 and 3.0 (the DS values is the average number of introduced substituents per disaccharide repeating unit, i.e. in the case of hyaluronan the DS can range between 0 and 4) (Hintze et al. 2009). It could be demonstrated by biophysical and immunological methods that matrices with sulphated hyaluronans exhibit a stronger binding strength to BMP-2 and TGF-β1 than chondroitin sulfate-containing matrices at a comparable DS of the GAGs (Hintze et al. 2012, 2014). In a further study poly(lactide-co-glycolide) scaffolds were coated with collagen matrices containing either chrondoitin sulfate or hyaluronan sulfate, and the effect of these coatings on the prolifertation and osteogenic differentiation of human mesenchymal stem cells was investigated in vitro. Whereas only minor differences were found in cell proliferation, osteogenic differentiation, determined by alkaline phosphatase activity and mineral deposition, was strongly enhanced compared to uncoated samples (Wojak-Cwik et al. 2013). Recently, the new sulfated GAG/collagen aECMs have been tested in a mini-pig model as coatings for dental implants to reveal their potential for improving healing processes in vivo. The coated implants supported peri-implant bone formation within a healing period of 8 weeks and showed an increased bone volume density compared to uncoated implants (Korn et al. 2014).

2.3.2 Bioactive and Degradable Coatings Based on Synthetic Polymers

In the literature there exists a variety of coating materials derived from synthetic organic polymers. Unlike many natural macromolecules only very few of them are known to directly promote cell adhesion, proliferation, and differentiation. One example of a cell adhesion stimulating synthetic polymer is the plasma polymerized polyallylamine (PPAAm) network. The surface coating is performed under vaccum in a microwave plasma reactor in the presence of allylamine monomer (Finke et al. 2007). Different substrates including metals used for bone and dental implants, ceramics and even polymers can be used. As a result of titanium, a thin, homogeneous, highly cross-linked polymeric film is deposited on the substrate. This film is resistant to hydrolysis and delamination and sufficiently equipped with free amino groups. The incubation of human osteoblastic MG-63 cells onto PPAAm-coated titanium discs demonstrated enhanced osteoblastic focal contact formation as vinculin, paxillin and phosphorylated focal adhesion kinase, concerning actin cytoskeleton development. Interestingly, these cell responses on PPAAm are similar to collagen-bonded surfaces (Finke et al. 2007). Comparable results were also obtained depositing the PPAAm coating onto electrospun poly(L-lactide-co-DL-lactide, PLDLL) fiber meshes (Schnabelrauch et al. 2014).

The PPAAm coating did not affect the fragile microstructure of the fibre mesh preserving the advantageous structural properties of these materials with regard to their use in tissue engineering.

In vitro cell experiments using human gingiva epithelial cells, human uroepithelial cells, and MG-63 cells confirmed an improved cell spreading on PPAAm surfaces already after 0.5 h of incubation (Fig. 8). First in vivo data on the biocompatibility of PPAAm-modified polylactide meshes demonstrated that the coating has no influence on the local inflammatory reaction.

Synthetic biodegradable polymers including polyesters (polylactides, polyglycolides, poly(-lactide-co-DL-lactic acid and polyphosphazenes) are normally of hydrophobic nature and lack innate specific cell adhesion and proliferation activity. Coatings derived from these polymers are currently used mainly in controlled drug delivery for local therapies (Malafaya et al. 2005; Seyednejad et al. 2011) and also for growth factor release systems (Schmidmaier et al. 2001), as well as vaccine applications (Andrianov et al. 2009; Ulery et al. 2011).

Poly(lactic acid) has suitable biodegradation behaviour and high mechanical stability (Garlotta 2001) and it tends to be used in the form of thin films for biomedical applications, including tissue engineering and drug delivery therapies (Tsuji and Ikarashi 2004; Garric et al. 2005). A rapid aerosol assisted deposition process has been developed for the preparation of biodegradable poly(D,L-lactic acid) (PDLLA) films with well controlled surface morphology and thickness (Hou et al. 2008). It involves the generation of polymer fine aerosol droplets which are directed towards a heated substrate, with rapid evaporation of solvent, and subsequently deposits a polymer film onto the substrate.

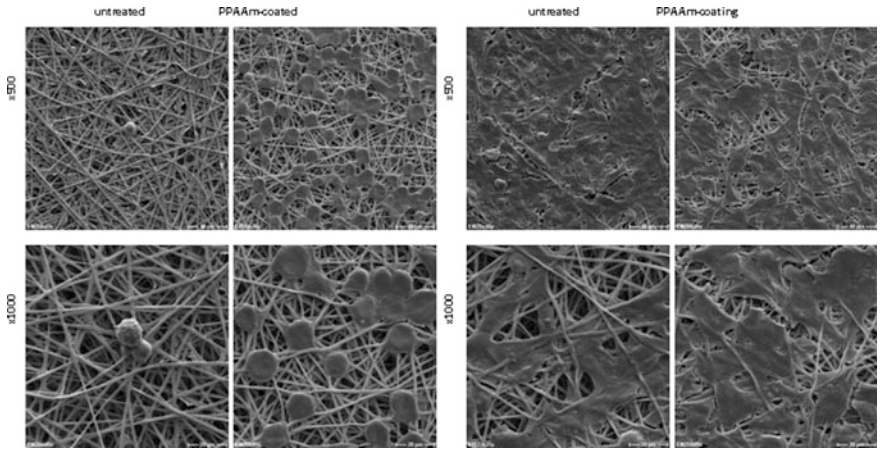

Fig. 8 Scanning electron microscopical images showing spreading of Ca9-22 human gingival epithelial cells on untreated and PPAAm-coated PLDLL fiber meshes after 0.5 and 24 h (scale bar = 40 μm (*upper row*) and 20 μm (*lower row*)) (reproduced from Schnabelrauch et al. 2014)

Additionally, polymer coatings are under investigation to increase the corrosion resistance and to control the degradation behaviour e.g. of magnesium and Mg alloy implants (Hornberger et al. 2012; Smith and Lamprou 2014).

The control of interfacial interactions between a biomaterial and its biological environment is a key feature for the design of biomaterial and biosensor surfaces. Resistance to nonspecific protein or cell interactions is a particularly relevant issue in microfluidic, diagnostic, and implantable devices ranging from small-diameter vascular grafts to biochips in medical diagnostics. Despite considerable research efforts, surface coating that completely eliminate protein adsorption onto a medical device over a long time has not been achieved. Nevertheless a variety of coatings have been identified to substantially reduce protein adsorption. Polyethylene glycol (PEG) has great potential to create non-fouling and represents the standard for comparison with newly developed non-fouling materials. A combination of the water retaining mechanism of the polymer chain and its resistance to compression to its extended coil conformation is regarded as the most probably factor in prevention of PEG surfaces protein adsorption (Bridges and Garcia 2008). As a current drawback to the use of PEG, its lack of versatile grafting techniques to stably link PEG molecules to biomaterial surfaces remains the most prominent. To solve this problem several new robust grafting techniques for PEG on metal surfaces have been developed using e.g. potent phosphonate (Zoulalian et al. 2006), phosphate (Gnauck et al. 2007) or dopamine (Dalsin et al. 2005) linker (see Fig. 9). Other hydrophilic polymers such as poly(2-oxazoline)s (Konradi et al. 2008), poly (glycerols) (Calderon et al. 2010) phosphorylcholine-derived degradable polymers (Nederberg et al. 2004) are also potential candidates to resist protein adsorption. Interestingly, PEG and poly(2-oxazoline)s which are supposed to be non-degradable until now have been found in a recent study to undergo oxidative

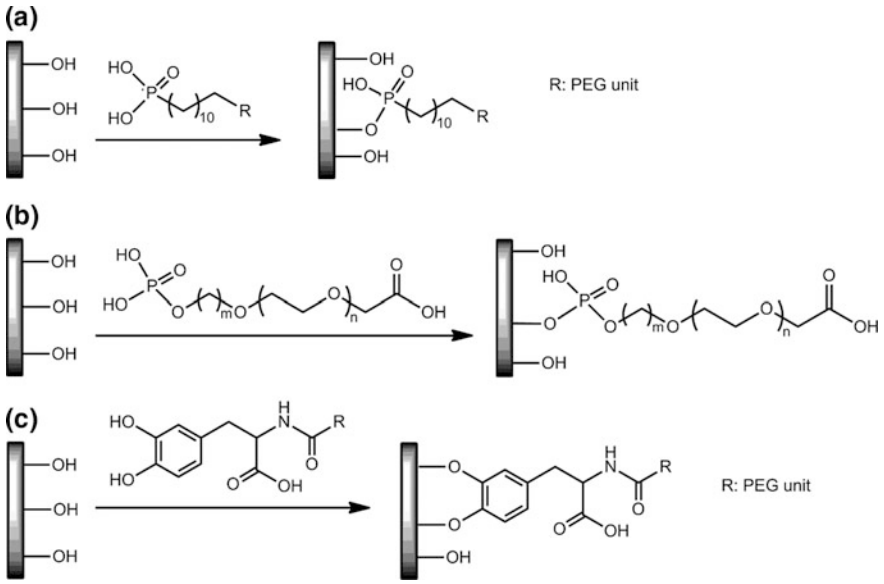

Fig. 9 Immobilization of functionalized PEG structures to titanium surface via **a** phosphonate, **b** phosphate, and **c** dopamine linker

degradation under biologically relevant conditions (Ulbricht et al. 2014). Under the influence of reactive oxygen species a time and concentration dependent degradation of both polymers occurs suggesting that a mid- and long-term biodegradation in vivo appears feasible.

PEGs and other hydrophilic polymers are often applied as molecularly thin self-assembled monolayers (SAMs) on planar surfaces on inorganic substrates. In an aqueous cell-containing medium the stability of those layers are limited. Polymer brushes which are more mechanically robust than SAMs can be generated on non-planar surfaces including colloidal suspensions. Those polymeric coatings can be prepared by surface-initiated polymerizations allowing control over functionality, grafting density, and thickness of the brushes.

Extensive research efforts have focused on hydrogel-based implant coatings of different thicknesses (Hofmann 2002). Hydrogels offer many advantages over traditional surface modification strategies, including nanoscale dimensions with complex architectures, the formation of viscoelastic network structures, the possibility to tune the mechanical strength, swellability, and biodegradability of the hydrogel, the incorporation of multiple chemical functionalities and bioactive molecules, and the ability to deposit onto a variety of material substrates (Bridges and Garcia 2008). Due to the limited biodegradability of many known antimicrobially active synthetic polymers, currently natural polymers derived, for example, from chitosan are often used as hydrogel forming substances. There is an ongoing need to both develop new antimicrobial active and biodegradable hydrogel precursors.

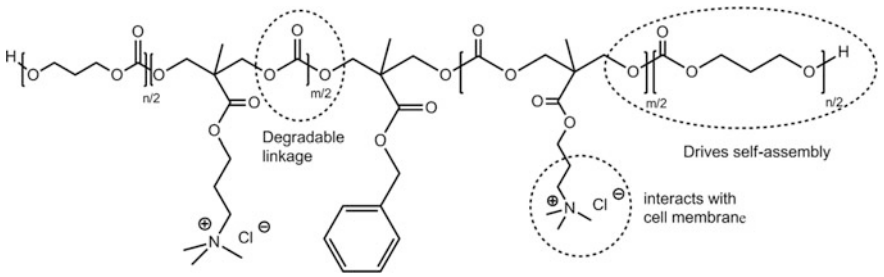

Fig. 10 Cationic, amphiphilic, and biodegradable polycarbonate with antimicrobial activity against Gram-positive bacteria

Most antimicrobial polymers have been designed to kill pathogens via a membrane disruption mechanism. That requires macromolecules with a sufficient cationic charge to promote adhesion to the cellular membrane of the microbe. In addition, the polymer should contain a hydrophobic moiety that will attach onto or integrate into the cellular membrane for lysing the membrane. Hydrophilic/hydrophobic balance (amphiphilicity) of an antimicrobial polymer is particularly important because it significantly impacts how the polymer interacts with cellular membranes (Engler et al. 2013). There exist different approaches to control amphiphilicity. In a recent work, cationic biodegradable polycarbonates have been prepared by metal-free organocatalytic ring-opening polymerization of functional cyclic carbonates (Fig. 10; Nederberg et al. 2011).

Nanoparticles of these polymers are able to disrupt microbial membranes selectively and efficiently thus inhibiting the growth of Gram-positive bacteria, methicillin-resistant *Staphylococcus aureus* (MRSA) and fungi, without inducing significant haemolysis over a wide range of concentrations.

2.4 Bioactive Composite Coatings

Although metallic orthopaedic implants are widely used and there is a strong bonding between the bioactive coating (such as HA) and the bone structure, limitations have been identified. For instance, it has been recognized that there could be an issue with the mechanical stability of the interface between the coating and the metallic substrate during surgical operation, after implantation for a prolonged period and/or post-surgery infections, which have caused the failure of the implants. Various strategies have been explored to address such limitations and one of them is to explore the use of bioactive composite coatings.

Bioactive composites have been shown to successfully overcome the brittleness usually attributed to HA and bioglass coatings, while retaining bioactivity, and also to potentially be used to confer additional properties to the coatings (Simchi et al. 2011; Mehdipour and Afshar 2012; Venkateswarlu et al. 2012; Gopi et al. 2013;

Pishbin et al. 2013; Cordero-Arias et al. 2015). The combination of bioactive glass/ceramic structure with an appropriate biopolymer to form a biocomposite coating has been shown to be able to transform the brittle HA and bioactive glass coating structure into a compliant and soft composite structure (Chen et al. 2006; Kim et al. 2011), while retaining their bioactivity and enable the incorporation of additional functional properties such as corrosion resistance, antibacterial property and release of biomolecules and drugs (Chen et al. 2006; Rezwan et al. 2006; Simchi et al. 2011; Mehdipour and Afshar 2012; Venkateswarlu et al. 2012; Gopi et al. 2013; Pishbin et al. 2013; Cordero-arias et al. 2015), and removing the need to densify glass ceramics at high temperatures. Various bioactive composite coatings have been investigated and some examples are being highlighted here. These bioactive composite coatings have been deposited onto metallic substrates by various processing techniques. These include sol–gel, thermal spray, laser spinning, plasma spray, electrophoretic and electrochemical deposition (Zheng et al. 2000; Jun et al. 2010a; Boccaccini et al. 2010b; Mehdipour and Afshar 2012; Gopi et al. 2013; Pishbin et al. 2013; Cordero-Arias et al. 2014; Pishbin et al. 2014).

Glasses, 6P57 and 6P68, with thermal expansion coefficients that matched Ti-6Al-4V were prepared and used to coat Ti-6Al-4V. Crack free bioactive composite coatings consisting of 20% of hydroxyapatite (HA) and/or Bioglass (BG) particles (45 μm) in silicate glass coatings were fabricated by enamelling technique on Ti-6Al-4V substrates. HA and/or BG particles were incorporated into these coatings to increase bioactivity of the silicate coatings while maintaining good adhesion to the substrate. There was no apparent reaction at the glass/HA interface at the temperatures 800–840 °C, whereas the BG particles softened and some infiltration of the glass coating occurred during heat treatment. The effectiveness of BG incorporation would depend on the softening temperature of the glass coating, with higher softening temperatures leading to increased degradation of the BG, whereas this was not the case for HA (Gomez-Vega et al. 2000).

Bioactive glass (SiO_2–CaO–P_2O_5–MgO)/chitosan composite coating was deposited on a 316L stainless steel substrate via electrophoretic deposition from a mixed ethanol-water suspension containing ceramic glass particles and chitosan with the aim to improve corrosion resistance and osseointegration. The water to ethanol ratio of 30% was found to yield a high deposition rate and a uniform, smooth and crack-free coating (7 μm thick) and the current density of the bioactive composite coating tested in artificial saliva was decreased by 52% and corrosion potential shifted toward more noble values as compared to the uncoated samples (Mehdipour and Afshar 2012).

Functionally graded composite coatings are also being considered to enhance interfacial bonding between dissimilar solids in order to minimise thermal stresses, suppress the onset of plastic yielding and to arrest any cracks. HA powder was mixed with titanium oxide (TiO_2) in different weight percentages and spray deposited to produce functionally graded bioactive coatings on Ti-6Al-4V metal substrate. The first layer consisting of TiO_2 particulate coatings was sintered at 900 °C for a few minutes followed by subsequent layers of HA–TiO_2 composites of different weight ratios (75% TiO_2 and 25% HA, 50% TiO_2 and 50% HA, 25% TiO_2

and 75% HA, and 100% HA) were performed in sequence and these layers were sintered again at 900 °C for a few minutes in order to obtain good adhesion between layers. The hardness and Young modulus values of HA–TiO_2–Ti functionally graded coating were 15.1 and 0.405 GPa, respectively (Roop Kumar and Wang 2002).

Gopi et al. (2013) reported the use of electrodeposition to deposit carbon nanotubes (CNTs) reinforced hydroxyapatite composite coatings on titanium to exploit the capability of CNTs imparting strength and toughness to brittle hydroxyapatite (HAP). The CNTs/HA composites exhibited efficient corrosion protection of titanium substrate in SBF solution and the enhancement of cell viability of the CNTs-HAP composite coating on titanium.

Multifunctional composite chitosan/Bioglass coatings loaded with gentamicin antibiotic was developed as a potential suitable approach to improve the surface properties of metallic implants by providing both bioactive and anti-bacterial properties for orthopaedic implants. The biocomposite coatings formed bonelike apatite upon immersion in SBF, confirming their bioactivity. The coating released 40% of its gentamicin payload within 5 days of burst release followed by a sustained drug delivery over a period of 8 weeks. It seems the release kinetics could inhibit bacterial growth for the first 2 days and support cellular proliferation for up to 10 days. However, further works are still needed to establish the interfacial bonding of these coatings to the metallic substrate and the optimum gentamicin loading that would provide minimum inhibitory concentration against bacteria as well as supporting cellular attachment and proliferation (Pishbin et al. 2014).

Alternative polymer for bioactive coating is alginate (Cheong and Zhitomirsky 2008) which is a natural polysaccharide. Alginate has been studied for different applications, e.g. biosensors, drug delivery systems and tissue engineering (Joshi et al. 2011; Lee and Mooney 2012). This polymer has a potential binding effect with proteins, growth factors and bone forming cells, and has been explored by Cordero-Arias et al. (Cordero-Arias et al. 2014) to develop nanostructured TiO_2 particles in alginate and TiO_2-bioactive glass/alginate composite coatings on stainless steel coatings for bone contacting materials by electrodeposition from ethanol/water suspensions. Titania has shown to be biocompatible (Nie et al. 2000; Navarro et al. 2008; Bai et al. 2011) and exhibit antibacterial properties (Cui et al. 2005), and enhance implant integration with host tissue when used in bone tissue replacement applications (Navarro et al. 2008). Bioglass particles improved the mechanical properties of the coatings by increasing the adhesion to the substrate and also accelerates the formation of hydroxyapatite after immersion of the coatings in simulated body fluid and the coated substrates shown improved electrochemical behaviour and confirmed the corrosion protection function of the coatings (Cordero-Arias et al. 2014). ZnO/alginate and ZnO-bioactive glass/alginate composite coatings also exhibiting antimicrobial properties and provide corrosion protection (Cordero-arias et al. 2015).

Other composite coating based on a silica xerogel/chitosan (30%) hybrid has been developed as a novel surface treatment for metallic implants. Silica xerogel presents a great bioactivity, with a good chemical bonding to the surrounding

tissues, especially bone (Radin et al. 2005; Avnir et al. 2006) while chitosan (>30%) is a biocompatible, non-toxic and biodegradable natural polymer (Bumgardner et al. 2003). Both compounds are excellent candidates for the development of hybrid coating materials on metallic substrates at room temperature, overcoming the cracking problem of the silica xerogel onto Ti-based implants (Jun et al. 2010b).

Osteoblastic cells cultured on the hybrid coatings were more viable than those on a pure chitosan coating and the alkaline phosphate activity of the cells was significantly higher on the hybrid coatings than on a pure chitosan coating (Jun et al. 2010a). These promising results indicated the potential of silica xerogel/chitosan hybrids as a potentially useful at room temperature processed bioactive coating materials on titanium-based medical implants.

Biologically active molecules can be incorporated using the biomimetic approach during the formation of bone-like apatite layer in SBF. Biocomposite coating based on laminine–apatite has been developed from a metastable calcium phosphate solution containing laminine to give cell-adhesive properties (Uchida et al. 2004). In addition, enzymes and proteins (Leonor et al. 2002) can also be incorporated in the apatite layer during formation in a solution mimicking body fluid (i.e. simulated body fluid) at low synthetic temperature conditions.

Electroactive biocomposite coatings. Liao et al. (2014) have explored conducting polymer as an intelligent electrical implant surface and a bone-mimetic electrophysiological micro-medium as well as citric acid, a small biomolecule found in natural bone, to develop nano-architectured conducting polymer on bone implants via a green fabrication approach in order to improving bioactivity of conducting polypyrrole coating on bone implants (Wallace and Spinks 2007; Liao et al. 2014). In the green approach, citric acid was used to facilitate the template-free electrochemical polymerization for the construction of 1D nano-architectured PPy (NAPPy) on biomedical titanium in PBS. Enhanced bioactivity has been demonstrated in implants modified by 1D NAPPy/citrate from the in vitro biomineralization investigation in simulated body fluid and biological activities (e.g. adhesion, spreading, proliferation and osteogenic differentiation) of osteoblasts. This showed that 1D NAPPy/citrate could be used as a more bionic implant surface and the citrate-assisted green approach could potentially be extended to the construction of other CPs and 1D nano-structures of electroactive materials that are stable, biocompatible, exhibit biomolecule affinity suitable for potential biomedical applications as reviewed by Liao et al. such as biological sensing (Travas-Sejdic et al. 2014), switching biointerface (Liao et al. 2014), neural probes (Abidian et al. 2010), drug delivery (Abidian et al. 2006) and tissue engineering (Balint et al. 2014).

Despite various bioactive composites have been investigated, only a few bioactive composites have been used clinically (Hench 1998). For example, PE/0.4-HA composite has been used as an implant for reconstruction of the orbital floor. The widely use of bioactive coatings is still limited until their long term in vivo performance has been established.

2.5 Antimicrobial Coatings

Microorganisms are omnipresent and represent a crucial factor in the whole living cycle and virtually anywhere human come into contact with them. However, in different areas of life and technical fields, strong hygienic conditions and sterile procedures are absolute requirements of a modern society. The elimination or extensive reduction of microbes is important for example in food industries, the manufacture of packaging materials, textiles for clothing, air conditioning and ventilation systems as well as in kitchens and sanitary facilities. Particularly, an antimicrobial feature with a high degree of efficiency is essential for general healthcare applications in hospital environments and for medical devices to eliminate pathogenic germs like bacteria and fungi. These microbes compromise the health of the patients especially with immune deficiencies and they might enhance the risk for nosocomial infections leading to serious medical conditions which could cause death in worst case scenarios.

Because of different requirements regarding antimicrobial effects, in recent years, a variety of sophisticated strategies were developed to kill or inhibit the growth of microorganisms. However, the effective removal or combat of microbes is still a scientific challenge especially in view of the worldwide increase of multi-resistant bacteria. The chosen method among those in the antimicrobial arsenal strongly depends on the specific application and sources of microbial contamination.

Particularly for the continued fight of infectious diseases in hospitals the strategy of antimicrobial coating of everyday objects, and especially of medical devices, with novel materials using new technological approaches has been proposed and tested. Thereby coatings based on antibiotics including antimicrobial peptides, antiseptics, antibodies, inorganic components like antimicrobial metal ions, fluorinated compounds, hydrogels, polyelectrolyte multilayers, antibacterial polymers as well as nitrogen monoxide releasing materials and nanostructured surfaces could prevent the adhesion and adsorption of microbes or kill them (Lichter et al. 2009; Wang and Zreiqat 2010; Arora et al. 2013; Gallo et al. 2014). A variety of such coatings are already in use or they are part of clinical studies.

Well known is the application of antibiotics like ciprofloxacin, vancomycin, oxacillin, tobramycin, gentamicin, or rifampicin which are incorporated in polymer matrices to function as a controlled antibiotic release system (McMillan et al. 2011; Brooks 2013). Also film forming antibiotic formulations like gentamicin palmitate can be used for antibacterial coatings showing a suitable retarded drug release (Kittinger et al. 2011; Fölsch et al. 2015).

For the metal ions incorporation approach e.g. of Ag, Cu, or Zn into antibacterial inorganic or organic coatings various methods are applied using chemical and physical processes like sol–gel chemistry, ion beam implantation, or the use of plasma. Metal ions will be released from the surface as the antimicrobial agent whereby the source could be pure metal, colloids, metal or oxide nanoparticles as well as coordinative bound metal ions (Knetsch and Koole 2011; Jaiswal et al. 2012; Gallo et al. 2014).

A relatively new group of coating materials include hydrogels, anti-adhesive polymers and super-hydrophobic surfaces (Ng et al. 2014). These materials exhibit a new mode of action preventing microbial adhesion and adsorption without the risk of drug resistance development. For instance, hydrogels based on natural or synthetic polymers exhibit three-dimensional networks with a very high degree of water content leading to the intrinsic antimicrobial as well as antifouling properties (Ng et al. 2014).

A further promising approach to generate antimicrobial surfaces is the use of polymers with antimicrobial properties (Arora et al. 2013). Thereby the mechanism of action is based on contact killing without releasing antimicrobial substances. It is well known that immobilized quaternary ammonium or phosphonium moieties containing at least one long alkyl chain penetrate and destroy bacterial cell membranes (Xue et al. 2015). Due to these properties permanent antibacterial coatings exhibiting high efficacy even against multi-resistant pathogenic germs without antibiotic resistance threats could be generated.

Over the last decades nitrogen monoxide (NO) also came in focus to develop new NO releasing coating materials due to its strong antibacterial effect (Nablo et al. 2005). It has been demonstrated that the hydrophobic NO penetrates bacterial cell membranes and is able to destroy plated colonies of bacteria. Moreover, NO in low concentrations is an essential mediator of numerous mammalian biological processes and exhibit e.g. an important factor in wound healing (Chen 2005). Consequently a NO releasing coating combines antibacterial with increased wound healing effects (Kim et al. 2015).

3 Future Trends

From the review of the development of bioactive ceramic coatings, despite materialist biocompatible characteristics, it is clear that the adhesion strength of these to medical implants would need to be improved and optimised further in order to increase the durability and long term reliability for load bearing biomedical devices. The mechanical properties of HA components would need to be optimised, ideally offering a Young's modulus less than 20 GPa and improved mechanical strength, both in compression and tension (Auclair-Daigle et al. 2005a, b). This can be achieved with a combination of approaches. These include: (i) the continuous development of coating technology that can deposit uniform, reproducible and adherence bioactive coatings onto implants with well controlled structure (e.g. phase stability, crystallinity, thickness, porosity) and composition at nanoscale level; (ii) use of nanotechnology and biomimetic approach; (iii) to develop interlayer and/or composition graded layer; (iv) pre-surface and post-surface treatment to improve the interface control and properties; (v) surface functionalization; and (vi) use of bioactive composites.

Most of the bioactive coatings have been developed for orthopedic applications. Others applications areas in cardiology, neurology, and ophthalmology are

underexplored. For examples, coatings that could improve small vascular graft integration while preventing occlusion could have a significant clinical impact, and replacing drug-eluting stent with the use of pro-healing stent that integrates appropriately with both endothelial cells and smooth muscle while preventing platelet and leukocyte adhesion (Meyers and Grinstaff 2011).

In order to achieve long term reliable bioactive coated implants and biomedical devices, in-depth integrated studies on the structure, material surface chemistry, molecular biology, biochemistry, protein absorption, biomimetic, genetic engineering, tissue engineering, surface engineering, nanoscience and technology are needed in order to design, discover and engineer robust, bioactive, biochemical and biomechanical compatible coatings with well controlled structure and composition that are not only be able to replace tissues but also to regenerate them.

Acknowledgements The authors would like to acknowledge the EU funded 543898-TEMPUS-1-2013-1-ES-TEMPUS-JPHES project which has facilitated our collaboration in producing this book chapter as well as Antonio Rafa Ruiz Gonzalez and Dr. Joao Restivo for proof reading this book chapter.

References

Abidian MR, Corey JM, Kipke DR, Martin DC (2010) Conducting-polymer nanotubes improve electrical properties, mechanical adhesion, neural attachment, and neurite outgrowth of neural electrodes. Small 6:421–429

Abidian MR, Kim D-H, Martin DC (2006) Conducting-polymer nanotubes for controlled drug release. Adv Mater 18:405

Agins HJ, Alcock NW, Bansal M, Salvati EA, Wilson PD, Pellicci PM, Bullough PG (1988) Metallic wear in failed titanium-alloy total hip replacements. A histological and quantitative analysis. J Bone Jt Surg 170:347–356

Andrianov AK, DeCollibus DP, Gillis HA, Henry HK, Marin A, Prausnitz MR, Babiuk LA, Townsend H, Mutwiri G (2009) Poly[di(carboxylatophenoxy)phosphazene] is a potent adjuvant for intradermal immunization. Proc Natl Acad Sci 106:18936–18941

Anitha A, Sowmya S, Sudheesh Kumar PT, Deepthi S, Chennazhi KP, Ehrlich H, Tsurkan M, Jayakumar R (2014) Chitin and chitosan in selected biomedical applications. Progr Polym Sci 39:1644–1667

Antti-Poika I, Josefsson G, Konttinen Y, Lidgren L, Santavirta S, Sanzén L (1990) Hip arthroplasty infection: current concepts. Acta Orthop 61:163–169

Arifin A, Sulong AB, Muhamad N, Syarif J, Ramli MI (2014) Material processing of hydroxyapatite and titanium alloy (HA/Ti) composite as implant materials using powder metallurgy: a review. Mater Des 55:165–175. doi:10.1016/j.matdes.2013.09.045

Arora S, Yadav V, Kumar P, Gupta R, Kumar D (2013) Polymer based antimicrobial coatings as potential biomaterial: a review. Int J Pharm Sci Rev Res 23:279–290

Assis de CM, Vercik de LCO, Santos dos ML, Fook MVL, Guastaldi AC (2005) Comparison of crystallinity between natural hydroxyapatite and synthetic cp-Ti/HA coatings. Mater Res 8:207–211

ASTM (2014) ASTM F1609. Standard Specification for Calcium Phosphate Coatings for Implantable Materials

Auclair-Daigle C, Bureau MN, Legoux J, Yahia L (2005a) Bioactive hydroxyapatite coatings on polymer composites for orthopedic implants. J Biomed Mater Res, Part A 73:398–408

Auclair-Daigle C, Bureau MN, Legoux JG, Yahia L (2005b) Bioactive hydroxyapatite coatings on polymer composites for orthopedic implants. J Biomed Mater Res—Part A 73:398–408. doi:10.1002/jbm.a.30284

Auernheimer J, Zukowski D, Dahmen C, Kantlehner M, Enderle A, Goodman SL, Kessler H (2005) Titanium implant materials with improved biocompatibility through coating with phosphonate-anchored cyclic RGD peptides. Chem BioChem 6:2034–2040

Aumailley M, Gurrath M, Mueller G, Calvete J, Timpl R, Kessler H (1991) Arg-Gly-Asp constrained within cyclic pentapeptides. Strong and selective inhibitors of cell adhesion to vitronectin and laminin fragment P1. FEBS Lett 291:50–54

Avnir D, Coradin T, Lev O, Livage J (2006) Recent bio-applications of sol–gel materials. J Mater Chem 16:1013–1030

Bai Y, Park IS, Lee SJ, Bae TS, Duncan W, Swain M, Lee MH (2011) One-step approach for hydroxyapatite-incorporated TiO_2 coating on titanium via a combined technique of micro-arc oxidation and electrophoretic deposition. Appl Surf Sci 257:7010–7018

Balamurugan A, Sockalingum G, Michel J, Fauré J, Banchet V, Wortham L, Bouthors S, Laurent-Maquin D, Balossier G (2006) Synthesis and characterisation of sol gel derived bioactive glass for biomedical applications. Mater Lett 60:3752–3757

Balint R, Cassidy NJ, Cartmell SH (2014) Conductive polymers: towards a smart biomaterial for tissue engineering. Acta Biomater 10:2341–2353

Berndt CC, Haddadt GN, Farmer AJD, Gross KA (1990) Thermal spraying for bloceramlc applications. Mater Forum 161–173

Bierbaum S, Beutner R, Hanke T, Scharnweber D, Hempel U, Worch H (2003) Modification of Ti-6Al-4V surfaces using collagen I, III, and fibronectin. I. Biochemical and morphological characteristics of the adsorbed matrix. J Biomed Mater Res 67A:421–430

Bierbaum S, Douglas T, Hanke T, Scharnweber D, Tippelt S, Monsees TK, Funk RH, Worch H (2006) Collageneous matrix coatings on titanium implants modified with decorin and chondroitin sulfate: characterization and influence on osteoblastic cells. J Biomed Mater Res 77A:551–562

Bierbaum S, Hintze V, Scharnweber (2012) Functionalization of Biomaterials surfaces using artificial extracellular matrizes. Biomatter 2(3):1–10

Bigi A, Boanini E, Panzavolta S, Roveri N, Rubini K (2002) Bonelike apatite growth on hydroxyapatite–gelatin sponges from simulated body fluid. J Biomed Mater Res 59:709–715

Birk DE (2001) Type V collagen: heterotypic type I/V collagen interaction in the regulation of fibril assembly. Micron 32:223–237

Bougas K, Stenport VF, Currie F, Wennerberg A (2012) Laminin coating promotes calcium phosphate precipitation on titanium discs in vitro. J Oral Maxillofac Res 2:e5. doi:10.5037/jomr.2011.2405

Blind O, Klein LH, Dailey B, Jordan L (2005) Characterization of hydroxyapatite films obtained by pulsed-laser deposition on Ti and Ti-6AL-4V substrates. Dent Mater 21:1017–1024

Bobyn JD, Pilliar RM, Cameron HU, Weatherly GC (1980) The optimum pore size for the fixation of porous-surfaced metal implants by the ingrowth of bone. Clin Orthop Relat Res 150:263–270

Boccaccini AR, Chicatun F, Cho J, Bretcanu O, Roether JA, Novak S, Chen Q (2007) Carbon nanotube coatings on bioglass-based tissue engineering scaffolds. Adv Funct Mater 17:2815–2822. doi:10.1002/adfm.200600887

Boccaccini AR, Erol M, Stark WJ, Mohn D, Hong Z, Mano JF (2010a) Polymer/bioactive glass nanocomposites for biomedical applications: a review. Compos Sci Technol 70:1764–1776

Boccaccini AR, Erol M, Stark WJ, Mohn D, Hong Z, Mano JF (2010b) Polymer/bioactive glass nanocomposites for biomedical applications: a review. Compos Sci Technol 70:1764–1776. doi:10.1016/j.compscitech.2010.06.002

Bonfield W, Grynpas MD, Tully AE, Bowman J, Abram J (1981) Hydroxyapatite reinforced polyethylene—a mechanically compatible implant material for bone replacement. Biomaterials 2:185–186

Bosco R, Iafisco M, Tampieri A, Jansen JA, Leeuwenburgh SCG, van den Beucken JJJP (2015) Hydroxyapatite nanocrystals functionalized with alendronate as bioactive components for bone implant coatings to decrease osteoclastic activity. Appl Surf Sci 328:516–524

Bosetti M, Masse A, Tobin E, Cannas M (2002) Silver coated materials for external fixation devices: in vitro biocompatibility and genotoxicity. Biomaterials 23:887–892

Bridges AW, García AJ (2008) Anti-inflammatory polymeric coatings for implantable biomaterials and devices. J Diabetes Sci Technol 2:984–994

Brooks BD (2013) Comparisons of release of several antibiotics from antimicrobial polymer-coated allograft bone void filler. Int J Biomed Mater Res 1:21. doi:10.11648/j.ijbmr.20130102.11

Bumgardner JD, Wiser R, Gerard PD, Bergin P, Chestnutt B, Marin M, Ramsey V, Elder SH, Gilbert JA (2003) Chitosan: potential use as a bioactive coating for orthopaedic and craniofacial/dental implants. J Biomater Sci Polym Ed 14:423–438. doi:10.1163/156856203766652048

Bumgardner JD, Chesnutt BM, Yuan Y, Yang Y, Appleford M, Oh S, McLaughlin R, Elder SH, Ong JL (2007) The integration of chitosan-coated titanium in bone: an in vivo study in rabbits. Implant Dent 16:66–79

Cao W, Hench LL (1996) Bioactive materials. Ceram Int 22:493–507. doi:10.1016/0272-8842(95)00126-3

Cao H, Xu SY (2008) EDC/NHS-crosslinked type II collagen-chondroitin sulfate scaffold: characterization and in vitro evaluation. J Mater Sci Mater Med 19:567–575

Cai K, Rechtenbach A, Hao J, Bossert J, Jandt KD (2005) Polysaccharide-protein surface modification of titanium via a layer-by-layer technique: characterization and cell behaviour aspects. Biomaterials 26:5960–5971

Cen L, Neoh KG, Kang ET (2004) Antibacterial activity of cloth functionalized with N-alkylated poly(4-vinylpyridine). J Biomed Mater Res, Part A 71:70–80

Chai CS, Ben-Nissan B (1999) Bioactive nanocrystalline sol-gel hydroxyapatite coatings. J Mater Sci Mater Med 10:465–469. doi:10.1023/A:1008992807888

Chen AF (2005) Nitric oxide: a newly discovered function on wound healing. Acta Pharmacol Sin 26:259–264

Chen QZ, Blaker JJ, Boccaccini AR (2006) Bioactive and mechanically strong Bioglass®-poly(D, L-lactic acid) composite coatings on surgical sutures. J Biomed Mater Res Part B Appl Biomater 76:354–363

Chen Q-Z, Li Y, Jin L-Y, Quinn JMW, Komesaroff PA (2010) A new sol–gel process for producing Na_2O-containing bioactive glass ceramics. Acta Biomater 6:4143–4153

Cheong M, Zhitomirsky I (2008) Electrodeposition of alginic acid and composite films. Colloids Surf A Physicochem Eng Asp 328:73–78

Choi J, Kong Y, Kim H, Lee I (1998) Reinforcement of hydroxyapatite bioceramic by addition of Ni_3Al and Al_2O_3. J Am Ceram Soc 81:1743–1748

Choy K (2003) Chemical vapour deposition of coatings. Prog Mater Sci 48:57–170. doi:10.1016/S0079-6425(01)00009-3

Cordero-Arias L, Cabanas-Polo S, Gilabert J, Goudouri OM, Sanchez E, Virtanen S, Boccaccini AR (2014) Electrophoretic deposition of nanostructured TiO_2/alginate and TiO_2—bioactive glass/alginate composite coatings on stainless steel. Adv Appl Ceram 113:42–49. doi:10.1179/1743676113Y.0000000096

Cordero-arias L, Cabanas-polo S, Goudouri OM, Misra SK, Gilabert J, Valsami-jones E, Sanchez E (2015) Electrophoretic deposition of ZnO/alginate and ZnO-bioactive glass/alginate composite coatings for antimicrobial applications. Mater Sci Eng, C 55:137–144. doi:10.1016/j.msec.2015.05.034

Corpe RS, Young TR, Steflik DE, Whitehead RY, Wilson MD, Jaramillo C (2000) Correlative experimental animal and human clinical retrieval evaluations of hydroxyapatite (HA)-coated and non-coated implants in orthopaedics and dentistry

Cornelissen CG, Dietrich M, Gromann K, Frese J, Krueger S, Sachweh JS, Jockenhoevel S (2013) Fibronectin coating of oxygenator membranes enhances endothelial cell attachment. Biomed Eng Online 12:7. doi:10.1186/1475-925x-12-7v

Cui C, Liu H, Li Y, Sun J, Wang R, Liu S, Greer AL (2005) Fabrication and biocompatibility of nano-TiO_2/titanium alloys biomaterials. Mater Lett 59:3144–3148

Cui FZ, Luo ZS (1999) Biomaterials modification by ion-beam processing. Surf Coatings Technol 112:278–285

Dalsin JL, Lijun Lin L, Tosatti S, Janos Vörös J, Textor M, Messersmith PB (2005) Protein resistance of titanium oxide surfaces modified by biologically inspired mPEG-DOPA. Langmuir 21:640–646

Dash M, Chiellini F, Ottenbrite RM, Chiellini E (2011) Chitosan—a versatile semi-synthetic polymer in biomedical applications. Progr Polym Sci 36:981–1014

De Groot K, Geesink R, Klein C, Serekian P (1987) Plasma sprayed coatings of hydroxylapatite. J Biomed Mater Res 21:1375–1381

De Jong WF (1926) La substance minerale dans les os. Recl des Trav Chim des Pays-Bas 45:445–448

Dubs M, Weisser J, Linke R, Pfuch A, Imhof D, Schnabelrauch M (2009) Dextran-based coating system for the immobilization of cell adhesion promoting molecules on titanium surfaces. Mat-wiss Werkstofftech 40:853–860

Ducheyne P (1985) Bioglass coatings and bioglass composites as implant materials. J Biomed Mater Res 19:273–291

Ducheyne P, Radin S, Heughebaert M, Heughebaert JC (1990) Calcium phosphate ceramic coatings on porous titanium: effect of structure and composition on electrophoretic deposition, vacuum sintering and in vitro dissolution. Biomaterials 11:244–254

Dumbleton J, Manley MT (2004) Hydroxyapatite-coated prostheses in total hip and knee arthroplasty. J Bone Jt Surg 86:2526–2540

Elmengaard B, Bechtold JE, Søballe K (2005) In vivo effects of RGD-coated titanium implants inserted in two bone-gap models. J Biomed Mater Res 75A:249–255

Engler AC, Tan JPK, Ong ZY, Coady DJ, Ng VWL, Yang YY, Hedrick JL (2013) Antimicrobial polycarbonates: investigating the impact of balancing charge and hydrophobicity using a same-centered polymer approach. Biomacromol 14:4331–4339

Ewald A, Glückermann SK, Thull R, Gbureck U (2006) Antimicrobial titanium/silver PVD coatings on titanium. Biomed Eng Online 5:22

Fathi MH, Doostmohammadi A (2009a) Bioactive glass nanopowder and bioglass coating for biocompatibility improvement of metallic implant. J Mater Process Technol 209:1385–1391. doi:10.1016/j.jmatprotec.2008.03.051

Fathi MH, Doostmohammadi A (2009b) Bioactive glass nanopowder and bioglass coating for biocompatibility improvement of metallic implant. J Mater Process Technol 209:1385–1391

Finke B, Luethen F, Schroeder K, Mueller PD, Bergemann C, Frant M, Ohl A, Nebe BJ (2007) The effect of positively charged plasma polymerization on initial osteoblastic focal adhesion on titanium surfaces. Biomaterials 28:4521–4534

Fölsch C, Federmann M, Kuehn KD, Kittinger C, Kogler S, Zarfel G, Kerwat M, Braun S, Fuchs-Winkelmann S, Paletta JRJ (2015) Coating with a novel gentamicinpalmitate formulation prevents implant-associated osteomyelitis induced by methicillin-susceptible Staphylococcus aureus in a rat model. Int Orthop 39:981–988

Gallardo J, Galliano P, Duran A (2001) Bioactive and protective sol-gel coatings on metals for orthopaedic prostheses. J Sol-Gel Sci Technol 21:65–74

Galliano P, De Damborenea JJ, Pascual MJ, Duran A (1998) Sol-gel coatings on 316L steel for clinical applications. J Sol–Gel Sci Technol 13:723–727

Gallo J, Holinka M, Moucha CS (2014) Antibacterial surface treatment for orthopaedic implants. Int J Mol Sci 15:13849–13880

Garcia C, Cere S, Duran A (2004) Bioactive coatings prepared by sol–gel on stainless steel 316L. J Non Cryst Solids 348:218–224

Garlotta D (2001) A literature review of poly(lactic acid). J Polym Environ 9:63–84

Garric X, Molès J, Garreau H, Guilhou J, Vert M (2005) Human skin cell cultures onto PLA50 (PDLLA) bioresorbable polymers: influence of chemical and morphological surface modifications. J Biomed Mater Res, Part A 72:180–189

Gawalt ES, Avaltroni MJ, Danahy MP, Silverman BM, Hanson EL, Midwood KS, Schwarzbauer JE, Schwartz J (2003) Bonding organics to Ti alloys: facilitating human osteoblast attachment and spreading on surgical implant materials. Langmuir 19:200–204

Geesink RGT, de Groot K, Klein CPAT (1987) Chemical implant fixation using hydroxyl-apatite coatings: the development of a human total hip prosthesis for chemical fixation to bone using hydroxyl-apatite coatings on titanium substrates. Clin Orthop Relat Res 225:147–170

Geetha M, Singh AK, Asokamani R, Gogia AK (2009) Ti based biomaterials, the ultimate choice for orthopaedic implants–a review. Prog Mater Sci 54:397–425

Geissler U, Hempel U, Wolf C, Scharnweber D, Worch H, Wenzel K (2000) Collagen type I-coating of Ti-6Al-4V promotes adhesion of osteoblasts. J Biomed Mater Res 51:752–760

Gittens RA, McLachlan T, Olivares-Navarrete R, Cai Y, Berner S, Tannenbaum R, Schwartz Z, Sandhage KH, Boyan BD (2011) The effects of combined micron-/submicron-scale surface roughness and nanoscale features on cell proliferation and differentiation. Biomaterials 32:3395–3403

Gnauck M, Jaehne E, Blaettler T, Tosatti S, Textor M, Adler H-PJ (2007) Carboxy-terminated oligo(ethylene glycol)-alkane phosphate: Synthesis and self-assembly on titanium oxide surfaces. Langmuir 23:377–381

Gomez-Vega JM, Saiz E, Tomsia AP, Marshall GW, Marshall SJ (2000) Bioactive glass coatings with hydroxyapatite and Bioglass particles on Ti-based implants. Process Biomater 21:105–111. doi:10.1016/S0142-9612(99)00131-3

Gopi D, Shinyjoy E, Sekar M, Surendiran M, Kavitha L, Sampath Kumar TS (2013) Development of carbon nanotubes reinforced hydroxyapatite composite coatings on titanium by electrodeposition method. Corros Sci 73:321–330. doi:10.1016/j.corsci.2013.04.021

Gorustovich AA, Roether JA, Boccaccini AR (2009) Effect of bioactive glasses on angiogenesis: a review of in vitro and in vivo evidences. Tissue Eng Part B Rev 16:199–207

Gross U, Strunz V (1985) The interface of various glasses and glass ceramics with a bony implantation bed. J Biomed Mater Res 19:251–271

Habibovic P, Barrere F, Blitterswijk CA, Groot K, Layrolle P (2002) Biomimetic hydroxyapatite coating on metal implants. J Am Ceram Soc 85:517–522

Hamdi M, Ide-Ektessabi A (2003) Preparation of hydroxyapatite layer by ion beam assisted simultaneous vapor deposition. Surf coatings Technol 163:362–367

Hersel U, Dahmen C, Kessler H (2003) RGD modified polymers: biomaterials for stimulated cell adhesion and beyond. Biomaterials 24:4385–4415

Hench LL (1991) Bioceramics: from concept to clinic. J Am Ceram Soc 74:1487–1510

Hench LL (1998) Bioceramics. J Am Ceram Soc 81:1705–1728. doi:10.1111/j.1151-2916.1998.tb02540.x

Hench LL, Clark AE (1982) Adhesion to bone. Biocompat Orthop Implant 2:129–170

Hench LL, Polak JM (2002) Third-generation biomedical materials. Science (80–) 295:1014–1017

Hench LL, Splinter RJ, Allen WC, Greenlee TK (1971) Bonding mechanisms at the interface of ceramic prosthetic materials. J Biomed Mater Res 5:117–141

Hench LL, Wilson J (1993) An introduction to bioceramics. World Scientific

Hendriks JGE, Van Horn JR, Van Der Mei HC, Busscher HJ (2004) Backgrounds of antibiotic-loaded bone cement and prosthesis-related infection. Biomaterials 25:545–556

Hintze V, Moeller S, Schnabelrauch M, Bierbaum S, Viola M, Worch H, Scharnweber D (2009) Modification of hyaluronan influence the interaction with human bone morphogenetic protein-4(hBMP-4). Biomacromolecules 10:3290–3297

Hintze V, Miron A, Moeller S, Schnabelrauch M, Wiesmann H-P, Worch H, Scharnweber D (2012) Sulfated hyaluronan and chondroitin sulfate interact differently with human transforming growth factor-β1 (TGF-β1). Acta Biomater 8:2144–2152

Hintze V, Samsonov SA, Anselmi M, Moeller S, Becher J, Schnabelrauch M, Scharnweber D, Pisabarro MT (2014) Sulfated glycosaminoglycans exploit the conformational plasticity of bone morphogenetic protein-2 (BMP-2) and alter the interaction profile with its receptor. Biomacromol 15:3083–3092

Hoffman AS (2002) Hydrogels for biomedical applications. Adv Drug Deliv Rev 54:3–12

Hoppe A, Sarker B, Detsch R, Hild N, Mohn D, Stark WJ, Boccaccini AR (2014) In vitro reactivity of Sr-containing bioactive glass (type 1393) nanoparticles. J Non Cryst Solids 387:41–46

Hornberger H, Virtanen S, Boccaccini AR (2012) Biomedical coatings on magnesium alloys—a review. Acta Biomater 8:2442–2455. doi:10.1016/j.actbio.2012.04.012

Hou X, Choy K, Leach SE (2007) Processing and in vitro behavior of hydroxyapatite coatings prepared by electrostatic spray assisted vapor deposition method. J Biomed Mater Res, Part A 83:683–691

Hou X, Choy K-L, Yan J (2008) Deposition of biodegradable poly(d, l-lactic acid) films using aerosol-assisted method. Surf Coatings Technol 202:5175–5179

Hsiung J, Kung H, Chen H, Chang KY (2012) Applications of thermal spray coating in artificial knee joints

Huiskes R, Weinans H, Van Rietbergen B (1992) The relationship between stress shielding and bone resorption around total hip stems and the effects of flexible materials. Clin Orthop Relat Res 274:124–134

Hull D, Clyne TW (1996) An introduction to composite materials. Cambridge university press

Ignatius A, Peraus M, Schorlemmer S, Augat P, Burger W, Leyen S, Claes L (2005) Osseointegration of alumina with a bioactive coating under load-bearing and unloaded conditions. Biomaterials 26:2325–2332. doi:10.1016/j.biomaterials.2004.07.029

ISO (2000) ISO 13779–2. Implants for surgery—hydroxyapatite—part 2: Coatings of hydroxyapatite

Jaiswal S, McHale P, Duffy B (2012) Preparation and rapid analysis of antibacterial silver, copper and zinc doped sol–gel surfaces. Colloids Surfaces B Biointerfaces 94:170–176

Jones DA (1996) Principles and prevention of corrosion. Prentice Hall

Jones JR (2013) Review of bioactive glass: from Hench to hybrids. Acta Biomater 9:4457–4486

Joshi A, Solanki S, Chaudhari R, Bahadur D, Aslam M, Srivastava R (2011) Multifunctional alginate microspheres for biosensing, drug delivery and magnetic resonance imaging. Acta Biomater 7:3955–3963

Jun SH, Lee EJ, Yook SW, Kim HE, Kim HW, Koh YH (2010a) A bioactive coating of a silica xerogel/chitosan hybrid on titanium by a room temperature sol–gel process. Acta Biomater 6:302–307. doi:10.1016/j.actbio.2009.06.024

Jun S-H, Lee E-J, Yook S-W, Kim H-E, Kim H-W, Koh Y-H (2010b) A bioactive coating of a silica xerogel/chitosan hybrid on titanium by a room temperature sol–gel process. Acta Biomater 6:302–307

Kamitakahara M, Ohtsuki C, Miyazaki T (2007) Coating of bone-like apatite for development of bioactive materials for bone reconstruction. Biomed Mater 2:R17–R23. doi:10.1088/1748-6041/2/4/R01

Katz BZ, Zamir E, Bershadsky A, Kam Z, Yamada KM, Geiger B (2000) Physical state of the extracellular matrix regulates the structure and molecular composition of cell-matrix adhesions. Mol Biol Cell 11:1047–1060

Kasuga T, Nogami M, Niinomi M (2003) Calcium Phosphate Glass-Ceramics for Bioactive Coating on a β-Titanium Alloy. Adv Eng Mater 5:498–501

Kawai T, Ohtsuki C, Kamitakahara M, Tanihara M, Miyazaki T, Sakaguchi Y, Konagaya S (2006) Removal of formaldehyde by hydroxyapatite layer biomimetically deposited on polyamide film. Environ Sci Technol 40:4281–4285

Kim J, Won J, Shin US, Kim H (2011) Improvement of bioactive glass nanofiber by a capillary-driven infiltration coating with degradable polymers. J Am Ceram Soc 94:2812–2815

Kim JO, Noh J-K, Thapa RK, Hasan N, Choi M, Kim JH, Lee J-H, Ku SK, Yoo J-W (2015) Nitric oxide-releasing chitosan film for enhanced antibacterial and in vivo wound-healing efficacy. Int J Biol Macromol 79:217–225

Kim SW, Jacobs H (1996) Design of nonthrombogenic polymer surfaces for blood-contacting medical devices. Blood Purif 14:357–372

Kittinger C, Marth E, Windhager R, Weinberg AM, Zarfel G, Baumert R, Felisch S, Kuehn K-D (2011) Antimicrobial activity of gentamicin palmitate against high concentrations of Staphylococcus aureus. J Mater Sci Mater Med 22:1447–1453

Klein CPAT, Patka PV, Van der Lubbe HBM, Wolke JGC, De Groot K (1991) Plasma-sprayed coatings of tetracalciumphosphate, hydroxyl-apatite, and α-TCP on titanium alloy: an interface study. J Biomed Mater Res 25:53–65

Knetsch MLW, Koole LH (2011) New strategies in the development of antimicrobial coatings: the example of increasing usage of silver and silver nanoparticles. Polymers (Basel) 3:340–366

Kodama T, Goto T, Miyazaki T, Takahashi T (2008) Bone formation on apatite-coated titanium incorporated with bone morphogenetic protein and heparin. Int J Oral Maxillofac Implants 23:1013–1019

Kokubo T, Kim HM, Kawashita M (2003) Novel bioactive materials with different mechanical properties. Biomaterials 24:2161–2175. doi:10.1016/S0142-9612(03)00044-9

Konradi R, Pidhatika B, Mühlebach A, Textor M (2008) Poly-2-methyl-2-oxazoline: a peptide-like polymer for protein-repellent surfaces. Langmuir 24:613–616

Korn P, Schulz MC, Hintze V, Range U, Mai R, Eckelt U, Schnabelrauch M, Moeller S, Becher J, Scharnweber D, Stadlinger B (2014) Chondroitin sulfate and sulfated hyaluronan-containing coatings of titanium implants influence peri-implant bone formation in a minipig model. J Biomed Mater Res 102A:2334–2344

Kummer FJ, Jaffe WL (1992) Stability of a cyclically loaded hydroxyapatite coating: effect of substrate material, surface preparation, and testing environment. J Appl Biomater 3:211–215

Latour RA (2005) Biomaterials: protein-surface interactions. Encycl Biomater Biomed Eng 28:1–15

Lebaron RG, Athanasiou KA (2000) Extracellular matrix cell adhesion peptides: functional application in orthopaedic materials. Tissue Eng 6:85–103

Learmonth ID (2012) Interfaces in total hip arthroplasty. Springer Science and Business Media

Lee KY, Mooney DJ (2012) Alginate: properties and biomedical applications. Prog Polym Sci 37:106–126

Leonor IB, Azevedo HS, Alves CM, Reis RL (2002) Effecs of the incorporation of proteins and active enzymes on biomimetic calcium-phosphate coatings. In: Key engineering materials. Transaction Technology of Publication, pp 97–100

Li Z, Yang F, Yang R (2015) Synthesis and characterization of chitosan derivatives with dual-antibacterial functional groups. Int J Biol Macromol 75:378–387

Liao J, Zhu Y, Yin Z, Tan G, Ning C, Mao C (2014) Tuning nano-architectures and improving bioactivity of conducting polypyrrole coating on bone implants by incorporating bone-borne small molecules. J Mater Chem B 2:7872–7876. doi:10.1039/C4TB01053A

Lichter JA, Van Vliet KJ, Rubner MF (2009) Design of antibacterial surfaces and interfaces: polyelectrolyte multilayers as a multifunctional platform. Macromolecules 42:8573–8586

Liu B, Lin P, Shen Y, Dong Y (2008) Porous bioceramics reinforced by coating gelatine. J Mater Sci Mater Med 19:1203–1207

Liu D-M, Yang Q, Troczynski T (2002) Sol–gel hydroxyapatite coatings on stainless steel substrates. Biomaterials 23:691–698. doi:10.1016/S0142-9612(01)00157-0

Liu J, Miao X (2004) Sol–gel derived bioglass as a coating material for porous alumina scaffolds. Ceram Int 30:1781–1785. doi:10.1016/j.ceramint.2003.12.120

Liu X, Chu PK, Ding C (2004) Surface modification of titanium, titanium alloys, and related materials for biomedical applications. Mater Sci Eng R Reports 47:49–121. doi:10.1016/j.mser.2004.11.001

Lo WJ, Grant DM, Ball MD, Welsh BS, Howdle SM, Antonov EN, Bagratashvili VN, Popov VK (2000) Physical, chemical, and biological characterization of pulsed laser deposited and plasma sputtered hydroxyapatite thin films on titanium alloy. J Biomed Mater Res 50:536–545

Lopez-Sastre A, Gonzalo-Orden JM, Altónaga JAR, Altónaga JR, Orden MA (1998a) Coating titanium implants with bioglass and with hydroxyapatite. Int Orthop 22:380–383

Lopez-Sastre S, Gonzalo-Orden JM, Altónaga JA, Altónaga JR, Orden MA (1998b) Coating titanium implants with bioglass and with hydroxyapatite. A comparative study in sheep. Int Orthop 22:380–383

Magyari K, Baia L, Vulpoi A, Simon S, Popescu O, Simon V (2015) Bioactivity evolution of the surface functionalized bioactive glasses. J Biomed Mater Res Part B Appl Biomater 103:261–272

Malafaya PB, Silva GA, Reis RL (2005) Strategies for delivering bone and cartilage regenerating factors. In: Reis RL, San Roman J (eds) Biodegradable systems in tissue engineering and regenerative medicine. CRC Press, Baton Rouge, pp 253–280

Man HC, Chiu KY, Cheng FT, Wong KH (2009) Adhesion study of pulsed laser deposited hydroxyapatite coating on laser surface nitrided titanium. Thin Solid Films 517:5496–5501

Mann S (2001) Biomineralization: principles and concepts in bioinorganic materials chemistry. Oxford University Press

Marois Y, Chakfe N, Deng X, Marois M, How T, King MW, Guidoin R (1995) Carbodiimide cross-linked gelatin: a new coating for porous polyester arterial prostheses. Biomaterials 16:1131–1139

Másson M, Holappa J, Hjálmarsdóttir M, Rúnarsson ÖV, Nevalainen T, Järvinen T (2008) Antimicrobial activity of piperazine derivatives of chitosan. Carbohydr Polym 74:566–571

McMillan DJ, Lutton C, Rosenzweig N, Sriprakash KS, Goss B, Stemberger M, Schuetz MA, Steck R (2011) Prevention of Staphylococcus aureus biofilm formation on metallic surgical implants via controlled release of gentamicin. J Biomed Sci Eng 4:535

Mehdipour M, Afshar A (2012) A study of the electrophoretic deposition of bioactive glass-chitosan composite coating. Ceram Int 38:471–476. doi:10.1016/j.ceramint.2011.07.029

Meyers SR, Grinstaff MW (2011) Biocompatible and bioactive surface modifications for prolonged in vivo efficacy. Chem Rev 112:1615–1632

Meyers SR, Grinstaff MW (2012) Biocompatible and bioactive surface modifications for prolonged in vivo efficacy. Chem Rev 112:1615–1632. doi:10.1021/cr2000916

Mohseni E, Zalnezhad E, Bushroa AR (2014a) Comparative investigation on the adhesion of hydroxyapatite coating on Ti-6Al-4V implant: a review paper. Int J Adhes Adhes 48:238–257. doi:10.1016/j.ijadhadh.2013.09.030

Mohseni E, Zalnezhad E, Bushroa AR (2014b) Comparative investigation on the adhesion of hydroxyapatite coating on Ti-6Al-4V implant: a review paper. Int J Adhes Adhes 48:238–257

Morra M, Cassinelli C, Cascardo G, Cahalan P, Cahalan L, Fini M, Giardino R (2003) Surface engineering of titanium by collagen immobilization. Surface characterization and in vitro and in vivo studies. Biomaterials 24:4639–4654

Morra M, Cassinelli C, Cascardo G, Bollati D (2009) Collagen I-coated titanium surfaces for bone implantation. In: Puleo DA, Bizios R (eds) Biological interactions on material surfaces. Springer, Dordrecht, pp 373–396

Moskalewicz T, Seuss S, Boccaccini AR (2013) Microstructure and properties of composite polyetheretherketone/Bioglass® coatings deposited on Ti-6Al-7Nb alloy for medical applications. Appl Surf Sci 273:62–67. doi:10.1016/j.apsusc.2013.01.174

Nablo BJ, Rothrock AR, Schoenfisch MH (2005) Nitric oxide-releasing sol–gels as antibacterial coatings for orthopedic implants. Biomaterials 26:917–924

Nasser S (1992) Prevention and treatment of sepsis in total hip replacement surgery. Orthop Clin North Am 23:265–277

Navarro M, Michiardi A, Castaño O, Planell JA (2008) Biomaterials in orthopaedics. J R Soc Interface 5:1137–1158

Ng VWL, Chan JMW, Sardon H, Ono RJ, García JM, Yang YY, Hedrick JL (2014) Antimicrobial hydrogels: a new weapon in the arsenal against multidrug-resistant infections. Adv Drug Deliv Rev 78:46–62

Nederberg F, Bowden T, Nilsson B, Hong J, Hilborn J (2004) Phosphoryl choline introduces dual activity in biomimetic ionomers. J Am Chem 126:15350–15351

Nederberg F, Zhang Y, Tan JPK, Xu K, Wang H, Yang C, Gao S, Guo XD, Fukushima K, Li L, Hedrick JL, Yang YY (2011) Biodegradable nanostructures with selective lysis of microbial membranes. Nature Chem 3:409–414

Nie X, Leyland A, Matthews A (2000) Deposition of layered bioceramic hydroxyapatite/TiO_2 coatings on titanium alloys using a hybrid technique of micro-arc oxidation and electrophoresis. Surf Coatings Technol 125:407–414

Ohtsu N, Sato K, Saito K, Hanawa T, Asami K (2004) Evaluation of degradability of $CaTiO_3$ thin films in simulated body fluids. Mater Trans 45:1778–1781

Ohtsu N, Sato K, Yanagawa A, Saito K, Imai Y, Kohgo T, Yokoyama A, Asami K, Hanawa T (2007) $CaTiO_3$ coating on titanium for biomaterial application—optimum thickness and tissue response. J Biomed Mater Res, Part A 82:304–315

Olbrich KC, Andersen TT, Blumenstock FA, Bizios R (1996) Surfaces modified with covalently-immobilized adhesive peptides affect fibroblast population motility. Biomaterials 8:759–764

Ong JL, Appleford M, Oh S, Yang Y, Chen W-H, Bumgardner JD, Haggard WO (2006) The characterization and development of bioactive hydroxyapatite coatings. JOM 58:67–69

Ong JL, Lucas LC, Lacefield WR, Rigney ED (1992) Structure, solubility and bond strength of thin calcium phosphate coatings produced by ion beam sputter deposition. Biomaterials 13:249–254

Chou YF, Mari C, Thomas R, Quarto N, Contag CH, Wu B, Longaker MT, Adipose-derived adult stromal cells heal critical-size mouse calvarial defects. Nat Biotechnol 22:560

Oyane A, Uchida M, Ito A (2005) Laminin-apatite composite coating to enhance cell adhesion to ethylene-vinyl alcohol copolymer. J Med Mater Res A 72:168–174. 2012. Biomaterials 33 (30):7386–7393. doi:10.1016/j.biomaterials.2012.06.066

Park E, Condrate RA (1999) Graded coating of hydroxyapatite and titanium by atmospheric plasma spraying. Mater Lett 40:228–234

Park J, Lakes RS (2007) Biomaterials: an introduction. Springer Science and Business Media

Park JH, Schwartz Z, Olivares-Navarrete R, Boyan BD, Tannenbaum R (2011) Enhancement of surface wettability via the modification of microtextured titanium implant surfaces with polyelectrolytes. Langmuir 27:5976–5985

Pazo A, Saiz E, Tomsia AP (1998) Silicate glass coatings on Ti-based implants. Acta Mater 46:2551–2558

Peddi L, Brow RK, Brown RF (2008) Bioactive borate glass coatings for titanium alloys. J Mater Sci Mater Med 19:3145–3152

Pishbin F, Mouriño V, Flor S, Kreppel S, Salih V, Ryan MP, Boccaccini AR (2014) Electrophoretic deposition of gentamicin-loaded bioactive glass/chitosan composite coatings for orthopaedic implants. ACS Appl Mater Interfaces 6:8796–8806. doi:10.1021/am5014166

Pishbin F, Mouriño V, Gilchrist JB, McComb DW, Kreppel S, Salih V, Ryan MP, Boccaccini AR (2013) Single-step electrochemical deposition of antimicrobial orthopaedic coatings based on a bioactive glass/chitosan/nano-silver composite system. Acta Biomater 9:7469–7479. doi:10.1016/j.actbio.2013.03.006

Porte-Durrieu MC, Guillemot F, Pallu S, Labrugere C, Brouillaud B, Bareille R, Amedee J, Barthe N, Dard M, Baquey (2004) Cyclo-(DfKRG) peptide grafting onto Ti-6Al-4V: physical characterization and interest towards human osteoprogenitor cells adhesion. Biomaterials 25:4837–4846

Radin S, El-Bassyouni G, Vresilovic EJ, Schepers E, Ducheyne P (2005) In vivo tissue response to resorbable silica xerogels as controlled-release materials. Biomaterials 26:1043–1052

Raines AL, Olivares-Navarrete R, Wieland M, Cochran DL, Schwartz Z, Boyan BD (2010) Regulation of angiogenesis during osseointegration by titanium surface microstructure and energy. Biomaterials 31:4909–4917

Rawlings RD (1993) Bioactive glasses and glass-ceramics. Clin Mater 14:155–179

Reyes CD, Petrie TA, Burns KL, Schwartz Z, Garcia AJ (2007) Biomolecular surface coating to enhance orthopaedic tissue healing and integration. Biomaterials 28:3228–3235

Rezwan K, Chen QZ, Blaker JJ, Boccaccini AR (2006) Biodegradable and bioactive porous polymer/inorganic composite scaffolds for bone tissue engineering. Biomaterials 27:3413–3431

Riedel NA (2010) Sputter deposited hydroxyapatite thin films to enhance osseointegration

Roach P, Farrar D, Perry CC (2005) Interpretation of protein adsorption: surface-induced conformational changes. J Am Chem Soc 127:8168–8173

Roop Kumar R, Wang M (2002) Functionally graded bioactive coatings of hydroxyapatite/titanium oxide composite system. Mater Lett 55:133–137. doi:10.1016/S0167-577X(01)00635-8

Ruoslahti E, Engvall E (1980) Complexing of fibronectin glycosaminoglycans and collagen. Biochim Biophys Acta 631:350–358

Sahariah P, Benediktssdottir BE, Hjalmarsdottir MA, Sigurjonsson OE, Sørensen KK, Thygesen MB, Jensen KJ, Masson M (2015) Impact of chain length on antibacterial activity and hemocompatibility of quaternary N-alkyl and N, N-dialkyl chitosan derivatives. Biomacromol 16:1449–1460

Saino E, Maliardi V, Quartarone E, Fassina L, Benedetti L, De Angelis MGC, Mustarelli P, Facchini A, Visai L (2009) In vitro enhancement of SAOS-2 cell calcified matrix deposition onto radio frequency magnetron sputtered bioglass-coated titanium scaffolds. Tissue Eng Part A 16:995–1008

Salasznyk RM, Williams WA, Boskey A, Batorsky A, Plopper GE (2004) Adhesion to vitronectin and collagen I promotes osteogenic differentiation of human mesenchymal stem cells. J Biomed Biotechnol 2004:24–34

Schliephake H, Scharnweber D, Dard M, Sewing A, Aref A, Roessler S (2005) Functionalization of dental implant surfaces using adhesion molecules. J Biomed Mater Res B Appl Biomater 73:88–96

Schmidmaier G, Lucke M, Wildemann B, Haas NP, Raschke M (2006) Prophylaxis and treatment of implant-related infections by antibiotic-coated implants: a review. Injury 37:S105–S112

Schmidmaier G, Wildemann B, Stemberger A, Haas NP, Raschke M (2001) Biodegradable poly (D, L-lactide) coating of implants for continuous release of growth factors. J Biomed Mater Res 58:449–455

Schnabelrauch M, Wyrwa R, Rebl H, Bergemann C, Finke B, Schlosser M, Walschus U, Lucke S, Weltmann K-D, Nebe JB (2014) Surface-coated polylactide fiber meshes as tissue engineering matrices with enhanced cell integration properties. Int J Polym Sci, article ID 439784

Sepulveda P, Jones JR, Hench LL (2002) Bioactive sol-gel foams for tissue repair. J Biomed Mater Res 59:340–348

Seyednejad H, Ghassemi AH, van Nostrum CF, Vermonden T, Hennink WE (2011) Functional aliphatic polyesters for biomedical and pharmaceutical applications. J Controlled Rel 152:168–176

Simchi A, Tamjid E, Pishbin F, Boccaccini AR (2011) Recent progress in inorganic and composite coatings with bactericidal capability for orthopaedic applications. Nanomedicine nanotechnology. Biol Med 7:22–39. doi:10.1016/j.nano.2010.10.005

Smith JR, Lamprou DA (2014) Polymer coatings for biomedical applications: a review. Trans IMF 92:9–19

Shannon FJ, Cottrell JM, Deng X-H, Crowder KN, Doty SB, Avaltroni MJ, Warren RF, Wright TM, Schwartz J (2008) A novel surface treatment for porous metallic implants that improves the rate of bony ongrowth. J Biomed Mater Res 86A:857–864

Shelke NB, James R, Cato T. Laurencin CT, Kumbar SG (2014) Polysaccharide biomaterials for drug delivery and regenerative engineering. Polym Adv Technol 25:448–460

Soares GA, de Sena LÁ, Rossi AM, Pinto M, Muller CA, de Almeida Soares GD (2004) Effect of electrophoretic apatite coating on osseointegration of titanium dental implants. In: Key engineering materials. Transaction Technology of Publication, pp 729–732

Solgi S, Khakbiz M, Shahrezaee M, Zamanian A, Tahriri M, Keshtkari S, Raz M, Khoshroo K, Moghadas S, Rajabnejad A (2015) Synthesis, characterization and in vitro biological evaluation of sol–gel derived Sr-containing nano bioactive glass. Silicon 1–8

Song G (2007) Control of biodegradation of biocompatable magnesium alloys. Corros Sci 49:1696–1701

Stan GE, Morosanu CO, Marcov DA, Pasuk I, Miculescu F, Reumont G (2009) Effect of annealing upon the structure and adhesion properties of sputtered bio-glass/titanium coatings. Appl Surf Sci 255:9132–9138

Takeshita F, Ayukawa Y, Iyama S, Suetsugu T, Kido MA (1996) A histologic evaluation of retrieved hydroxyapatite-coated blade-form implants using scanning electron, light, and confocal laser scanning microscopies. J Periodontol 67:1034–1040

Tate CC, Shear DA, Tate MC, Archer DR, Stein DG, LaPlaca MC (2009) Laminin and fibronectin scaffolds enhance neural stem cell transplantation into the injured brain. J Tissue Eng Regen Med 3:208–217

Travas-Sejdic J, Aydemir N, Kannan B, Williams DE, Malmström J (2014) Intrinsically conducting polymer nanowires for biosensing. J Mater Chem B 2:4593–4609

Tsuji H, Ikarashi K (2004) In vitro hydrolysis of poly(l-lactide) crystalline residues as extended-chain crystallites. Part I: long-term hydrolysis in phosphate-buffered solution at 37 °C. Biomaterials 25:5449–5455

Uchida M, Oyane A, Kim H, Kokubo T, Ito A (2004) Biomimetic coating of laminin-apatite composite on titanium metal and its excellent cell-adhesive properties. Adv Mater 16:1071–1074

Ulbricht J, Jordan R, Luxenhofer R (2014) On the biodegradability of polyethylene glycol, polypeptoids and poly(2-oxazoline)s. Biomaterials 35:4848–4861

Ulery BD, Nair LS, Laurencin CT (2011) Biomedical applications of biodegradable polymers. J Polym Sci, Part B: Polym Phys 49:832–864

Vallet-Regí M, Ragel C, Salinas AJ (2003) Glasses with medical applications. Eur J Inorg Chem 2003:1029–1042

Van der Giessen WJ, van Beusekorn HM, Eijgelshoven MH, Morel MA, Serruys PW (1998) Heparin-coating of coronary stents. Semin Interv Cardiol 3:173–176

Vanderleyden E, Van Bael S, Chai YS, Kruth JP, Schrooten J, Dubruel P (2014) Gelatin functionalized porous titanium alloy implants for orthopaedic applications. Mater Sci Eng C Mater Biol Appl 42:396–404

Vasitaa R, Shanmugama K, Kattia DS (2008) Improved biomaterials for tissue engineering. Curr Topics Med Chem 8:341–353

Venkateswarlu K, Rameshbabu N, Chandra Bose A, Muthupandi V, Subramanian S, Mubarakali D, Thajuddin N (2012) Fabrication of corrosion resistant, bioactive and antibacterial silver substituted hydroxyapatite/titania composite coating on Cp Ti. Ceram Int 38:731–740. doi:10.1016/j.ceramint.2011.07.065

Verné E, Vitale-Brovarone C, Bui E, Bianchi CL, Boccaccini AR (2009) Surface functionalization of bioactive glasses. J Biomed Mater Res, Part A 90:981–992

Wallace G, Spinks G (2007) Conducting polymers–bridging the bionic interface. Soft Matter 3:665–671

Wang C, Ma J, Cheng W, Zhang R (2002) Thick hydroxyapatite coatings by electrophoretic deposition. Mater Lett 57:99–105

Wang G, Zreiqat H (2010) Functional coatings or films for hard-tissue applications. Materials (Basel) 3:3994–4050

Wang HG, Yin TY, Ge SP, Zhang Q, Dong QL, Lei DX, Sun DM, Wang GX (2013) Biofunctionalization of titanium surface with multilayer films modified by heparin-VEGF-fibronectin complex to improve endothelial cell proliferation and blood compatibility. J Biomed Mater Res A 101:413–420

Wang M (2003) Developing bioactive composite materials for tissue replacement. Biomaterials 24:2133–2151
Wang S, Lacefield WR, Lemons JE (1996) Interfacial shear strength and histology of plasma sprayed and sintered hydroxyapatite implants in vivo. Biomaterials 17:1965–1970
Wendel HP, Ziemer G (1999) Coating techniques to improve the hemocompatibility of artificial devices used for extracorporeal circulation. Eur J Cardiothorac Surg 16:342–350
Williams D (2000) Perspective on the contributions of biomaterials and tissue-engineering to bone repair, reconstruction, and regeneration. In: Davies JE (ed) Bone engineering, pp 577–584
Wissink MJ, Beernink R, Poot AA, Engbers GH, Beugeling T, van Aken WG, Feijen J (2000) Improved endothelialization of vascular grafts by local release of growth factor from heparinized collagen matrices. J Control Release 64:103–114
Wojak-Cwik IM, Hintze V, Schnabelrauch M, Moeller S, Dobrzynski P, Pamula E, Scharnweber D (2013) Poly(L-lactide-co-glycolide)scaffolds coated with collagen and glycosaminoglycans: impact on proliferation and osteogenic differentiation of human mesenchymal stem cells. J Biomed Mater Res 101A:3109–3122
Wolf-Brandstetter C, Lode A, Hanke T, Scharnweber D, Worch H (2006) Influence of modified extracellular matrices on Ti-6Al-4V implants on binding and release of VEGF. J Biomed Mater Res 79A:882–894
Wolff J (1892) Das Gesetz der Transformation der Knochen. Berlin A. Hirchwild (trans. Maquet P, Furlong R (1986). The Law of Bone Remodelling)
Xiao XF, Liu RF (2006) Effect of suspension stability on electrophoretic deposition of hydroxyapatite coatings. Mater Lett 60:2627–2632
Xue Y, Xiao H, Zhang Y (2015) Antimicrobial polymeric materials with quaternary ammonium and phosphonium salts. Int J Mol Sci 16:3626–3655
Yamamuro T, Hench LL, Wilson J (1990) CRC handbook of bioactive ceramics: bioactive glasses and glass-ceramics. In Calcium Phosphate and Hydroxylapatite ceramics, vol 2. CRC press
Yang J, Cai Y, Hu Y, Li D, Du Y (2012) Preparation, characterization and antimicrobial activity of 6-amino-6-deoxychitosan. Carbohydr Polym 87:202–209
Yang Y, Kim K-H, Ong JL (2005) A review on calcium phosphate coatings produced using a sputtering process–an alternative to plasma spraying. Biomaterials 26:327–337. doi:10.1016/j.biomaterials.2004.02.029
Zankovych S, Diefenbeck M, Bossert J, Mückley T, Schrader C, Schmidt J, Schubert H, Bischoff S, Faucon M, Finger U, Jandt KD (2013) The effect of polyelectrolyte multilayer coated titanium alloy surfaces on implant anchorage in rats. Acta Biomater 9:4926–4934
Zhang C, Leng Y, Chen J (2001) In vitro mechanical integrity of hydroxyapatite coatings on Ti-6Al-4V implants under shear loading. J Biomed Mater Res 56:342–350
Zhang S (2013) Hydroxyapatite coatings for biomedical applications. CRC Press
Zheng X, Huang M, Ding C (2000) Bond strength of plasma-sprayed hydroxyapatite/Ti composite coatings. Biomaterials 21:841–849
Zhitomirsky I, Gal-Or L (1997) Electrophoretic deposition of hydroxyapatite. J Mater Sci Mater Med 8:213–219
Zhou R, Wei D, Feng W, Cheng S, Yang H, Li B, Wang Y, Jia D, Zhou Y (2014) Bioactive coating with hierarchical double porous structure on titanium surface formed by two-step microarc oxidation treatment. Surf Coatings Technol 252:148–156
Zoulalian V, Monge S, Zürcher S, Textor M, Robin JJ, Tosatti S (2006) Functionalization of titanium oxide surfaces by means of poly(alkyl-phosphonates). J Phys Chem B 110:25603–25605

Nanometals in Cancer Diagnosis and Therapy

Sonia Prado-López, Noelia González-Ballesteros and M. Carmen Rodríguez-Argüelles

Abstract Cancer is not a static disease that can be easily monitored and treated. It is a dynamic, time-dependent and environment-dependent pathology in which all molecular and cellular interactions are constantly reshaped in response to environmental stimuli. None of the current treatment approaches, which include the combination of tumour removal by surgery, chemotherapy or radiation, are exempt of problems. Surgical removal has been the cornerstone of treatment for most types of cancer but it is limited to accessible tumours. Chemotherapy and radiation, which are used to eradicate the remaining cancer cells after tumour reduction, produce toxicity problems and can cause damage to the healthy tissues to different degrees. Against this backdrop, nanomedicine, with a variety of non-metallic and metallic nanomaterials, has emerged as a promising option in the fight against cancer. Here, we review some metallic nanomaterials and their applications in cancer nanotheragnosis. In particular, we focus on the latest studies carried out over the last five years related to gold, silver and iron nanomaterials' use in Cancer Imaging, Drug Delivery, Gene Therapy and Thermotherapy.

Keywords Nanometals · Cancer · Gene therapy · Cancer imaging · Photothermal therapy

S. Prado-López (✉)
Department of Genetics, Biochemistry and Immunology,
University of Vigo, 36310 Vigo, Spain
e-mail: soniapradolopez@uvigo.es

S. Prado-López
Centro de Investigaciones Biomedicas, CINBIO, University of Vigo,
36310 Vigo, Spain

N. González-Ballesteros · M. Carmen Rodríguez-Argüelles
Department of Inorganic Chemistry, University of Vigo, 36310 Vigo, Spain

F. Zivic et al. (eds.), *Biomaterials in Clinical Practice*,
https://doi.org/10.1007/978-3-319-68025-5_14

1 Introduction

Metals have been used to treat different diseases since ancient times. Chinese and Indian cultures as well as the Greeks, Romans and Arabs used to use metal compounds to treat and avoid different illnesses centuries ago. For instance, gold was used in the preparation of tonics by Chinese, Arabic and Indian cultures in the fourth and fifth century B.C. and in the Middle Ages to treat various mental diseases, syphilis, leprosy, ulcer, epilepsy and diarrhoea (Dykman and Khlebtsov 2012). Subsequently, metal compounds were also used to treat arthritic, tuberculosis and inflammatory processes (Bhattacharyya et al. 2011). In addition to gold, other metallic compounds such as zinc, copper, arsenic, mercury, gallium, palladium and ruthenium have been used in therapy and diagnostics (Arrowsmith et al. 2012; Hordyjewska et al. 2014; Medici et al. 2015; Sakurai et al. 2008).

But what really highlighted metals as potentially relevant agents in medicine was the discovery of cisplatin. Rosenberg et al. (1965) discovered this compound by chance, whilst studying the effect of electric fields in *Escherichia coli* cultures. In these experiments a difference of potential was applied between two electrodes of platinum in the presence of ammonium chloride. They observed that the bacteria grew, but did not divide. To try to explain this discovery the culture medium was analysed finding platinum(II) and platinum(IV) complexes. The ability of these complexes to inhibit cell division without killing the bacteria suggested that tumour cells' proliferation could be reduced. Further investigations in vivo, in the murine sarcoma 180 model, revealed the complex with the highest inhibitory activity, the *cis*-$[PtCl_2(NH_3)_2]$ also known as cisplatin (Rosenberg et al. 1970). Ten years after its discovery, cisplatin obtained the FDA's approval for the treatment of testicular and bladder cancers. Subsequently, cisplatin became an important drug in the treatment of lung, ovarian, head and neck and gastric cancers. Cisplatin exerts its anticancer effects by interacting with DNA. Its ability to crosslink with the purine bases produces alterations in the mechanisms of DNA reparation, which can subsequently induce apoptosis in the cancer cells (Dasari and Tchounwou 2014). Since its discovery, other platinum compounds like carboplatin and oxaliplatin (Pinato et al. 2014) as well as other metals have been developed (Medici et al. 2015) with the aim of enhancing the therapeutic index and overcoming cisplatin's resistance and toxicity.

The other turning point in the development of metal cancer therapies was the advent of nanotechnology. From 1980 onwards, a great revolution in nanotechnology began due to new methods of synthesis and the improved techniques for nanomaterials' characterization. But what is considered as nanotechnology? The term nanotechnology refers to a multidisciplinary field of research that combines chemistry, physics, biology, engineering, medicine and pharmacology (Cai et al. 2008). Applications of nanotechnology to medicine and physiology imply materials and devices designed to interact at cellular and molecular scales (nanoscale). Due to their chemical, electrical, optical and magnetic properties, metal nanomaterials are receiving increased attention for cancer nanotheragnosis (Schleich et al. 2015).

2 Gold Nanomaterials

Nowadays Gold Nanomaterials are used in many different biomedical applications. Due to their properties the most often used in cancer therapy and diagnosis are Gold nanoparticles (AuNPs), Gold nanoshells (AuNShs), Gold Nanorods (AuNRs) and Gold Nanocages (AuNCs) (Muddineti et al. 2015).

Gold nanoparticles have recently been at the forefront of nanomedicine because of their unique physico-chemical properties (Cao-Milan and Liz-Marzán 2014; Dykman and Khlebtsov 2012). Firstly, they are inert and non toxic due to the low reactivity of the golden core, which makes them good candidates for drug and gene delivery applications (Ghosh et al. 2008). Secondly, the unique optical properties conferred by their localized Surface Plasmon Resonance (SPR), make them suitable candidates for cancer detection and therapy (Dykman and Khlebtsov 2012; Jin 2012). Furthermore, they can be easily functionalized with different moieties like antibodies, proteins, peptides and nucleic acids to specifically target different kinds of cells and/or with biocompatible polymers (Fig. 1). It has been reported that polymers like polyethylene glycol (PEG) facilitate their stability and prolong their circulation time in vivo, which improves their gene and drug delivery applications (Conde et al. 2014). The cited AuNPs' properties are influenced by the chemical composition of the particle as well as the size, shape and surface/colloidal properties. The development of methods for the synthesis of AuNPs with controlled size, shape, solubility and stability in a reproducible manner has become a priority for biomedical applications.

In general, the synthetic procedures to obtain AuNPs are based on the chemical reduction of gold(I) and gold(III) salts, in an aqueous or organic solution in the presence of a surface stabilizer. These methods are the most widely employed, since they are very simple and offer a great control over the AuNPs' structure. A well known standard procedure for AuNPs' synthesis is the Turkevich method (Turkevich et al. 1951). This aqueous approach garners almost spherical particles with a tuneable size distribution, and was improved by Frens (1973). Nowadays, we know that by using different reductants and stabilizing agents it is possible to obtain AuNSs with a

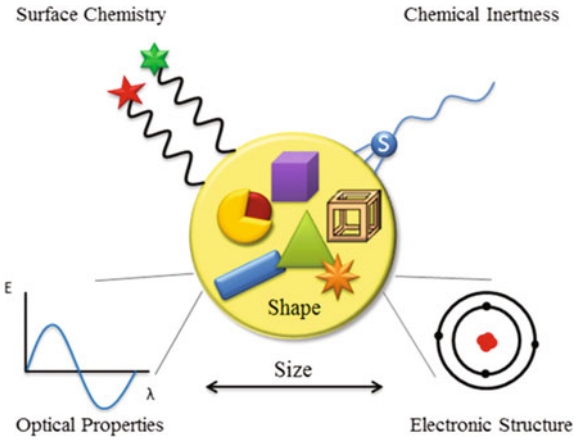

Fig. 1 Schematic representation of AuNPs' physico-chemical properties

wide range of diameters and narrow size distribution. For example, Brust et al. (1995) obtained AuNPs in a size range between 2 and 10 nm by using $NaBH_4$ as reductant and organothiol as stabilizer. Meanwhile, Murphy et al. obtained nanoparticles ranging from 10 to 50 nm by using a seed growth method, the employed reductant agent was ascorbic acid and hexadecyltrimethylammonium bromide (CTAB) was the stabilizer (Jana et al. 2001). Through this use of a seed growth method bigger nanoparticles of between 50 and 200 nm were synthesized, when the reduction agent was hydroquinone and the stabilizer was citrate (Perrault and Chan 2009). Recently, the cited seed growth method has been widely employed in AuNPs' synthesis, since it allows the fine-tuning of nanoparticles' size and shape in a very precise manner (Liu et al. 2012).

Different methods have been put forward to obtain the AuNShs. Naomi Halas' research group described the first method for AuNShs' synthesis (Averitt et al. 1997) consisted of a one-step process in which an Au_2S dielectric core is surrounded by a gold shell. In the latter study the size range of the AuNShs is from 520 to 900 nm. Another common method for AuNShs implies the synthesis of these particles starting from a silica core (Stöber et al. 1968). The gold coating of the silica core can be made in an aqueous solution using a seed growth method (Oldenburg et al. 1999). This method produces a very wide range of AuNShs' sizes. Nowadays, AuNShs have emerged as highly effective theragnostic agents for different pathologies such as cancer. By tuning the composition and dimensions of the core covert, we can play with the SPR to match a wide range of wavelengths, and hence they become interesting tools for cancer imaging and photothermal therapeutic medical applications (Li and Chen 2015).

Another kind of gold nanomaterials are the AuNRs. These are generally smaller than their counterparts AuNShs. A broad range of procedures for obtaining nanorods have been described in the literature, including the electrochemical, seed growth method, aluminium template, photochemical reduction, lithography and seedless methods (Ng et al. 2013). Like AuNShs, the AuNRs can be adjusted to the NIR region by manipulating their aspect length/width ratio, making them ideal tools for cancer imaging and photothermal therapy among other applications (Alkilany et al. 2012). However, the major issue for the application of AuNRs in photothermal therapy is their instability under intense laser light. Such instability can derivate in a conversion into AuNP and therefore in a loss of the longitudinal NIR resonance, resulting in a limitation for their application in vivo (Kennedy et al. 2011).

Finally, AuNCs are relatively new nanostructures consistent in gold nanocubes with controllable pores on their surface. Their synthetic route involves a galvanic replacement reaction between silver nanocubes and $HAuCl_4$ in aqueous solution. Adjusting the molar ratio of silver and gold, the dimensions, the wall thickness and the porous size can be changed (Sun et al. 2002). As a result the SPR peak of AuNCs could be continuously tuned from 425 to 1030 nm for their use in a great diversity of applications such as biosensing, bioimaging and drug delivery (Jiang and Pinchuk 2015).

3 Silver Nanomaterials (AgNMs)

Silver nanomaterials have been widely studied due to their interesting properties, such as their broad-spectrum antimicrobial activity. This fact has promoted the use of silver nanoparticles (AgNPs) in different biomedical products including catheters, antiseptic sprays and bandages. AgNMs have gained greater prominence due to their promising role as anticancer agents (Wei et al. 2015). More recently, AgNPs have been the object of an extensive study due to their remarkable optical properties, slightly superior to those found in gold. In this context, the engineering of their plasmonic properties can facilitate numerous applications in the field of cancer. The SPR properties can be tuned by varying their sizes and shapes. Nevertheless, they are less stable than AuNPs (Jiang and Pinchuk 2015).

The AgNPs' synthesis procedures can be divided into chemical, physical and biological. Among the chemical methods we can find reduction, combustion, precipitation, hydrolysis and polymerization. However, the most often used is the reduction method. The cited procedure implies the reduction of silver nitrate in an aqueous solution through the use of a reducing agent, like sodium borohydride, sodium citrate or ascorbic acid. A capping agent is often added to the nanoparticles to promote their stability, avoid their aggregation and facilitate their biocompatibility.

Physical methods for AgNPs' synthesis include techniques like laser, radio frequency inductive heat, plasma, physical vapour condensation, arc-discharge and direct current magnetron sputtering. The principal advantages over the chemical methods are the absence of toxic chemicals and the ability to gain particles with a more homogenous size distribution, which is relevant for their biological applications. The main disadvantage is the amount of energy required for their synthesis (Umer et al. 2012; Wei et al. 2015). In the biological approach the toxic reagents are removed, and non-toxic molecules produced by living organisms like bacteria, fungi, yeast and plants are used: chitosan, for example (Rodríguez-Argüelles et al. 2011). However, further work is required in order to obtain AgNPs with anticancer properties.

4 Magnetic Nanoparticles (MagNPs)

Due to their interesting properties MagNPs have become a promising agent in biomedical applications such as cell tracing, tissue imaging and drug/gene delivery. Characteristics like particle size, stability and other physicochemical properties are relevant elements in their in vivo applications. Different studies suggest that size distribution from 10 to 100 nm are optimal for many of the cited applications, since they have a high circulation time, low toxic threshold and high values of magnetization (Singh et al. 2014). It is important to highlight, however, that in other reports a high degree of instability has also been associated with particles less than 20 nm. Another important aspect to consider is the instability of the bare metallic nanoparticles. These particles are chemically active and easily oxidized, which results in their magnetism being lost (Lu et al. 2007). In order to overcome this

problem the MagNPs are stabilized by different methods. The most common approach involves the use of surfactants, polymers and inorganic compounds as coating agents. The cited strategies also reduce the nanoparticles' aggregation and improve their biocompatibility (Laurent et al. 2008).

The MagNPs can be classified into three broad groups: metals, alloys and oxides. Within the metallic group the most relevant materials are iron, nickel, cobalt and manganese. As part of this group, iron oxides have attracted great interest due to their reduced toxicity when compared to other metal oxides (Conde et al. 2014).

To date, numerous methods for MagNPs' synthesis have been developed. Regarding iron oxide nanoparticles, both Fe_3O_4 and γ-Fe_2O_3, the co-precipitation technique is probably the simplest and most efficient method. The Fe_3O_4 nanoparticles are synthesized from an aqueous Fe^{2+}/Fe^{3+} salt solution by the addition of a base under inert conditions. The γ-Fe_2O_3 particles can be obtained from the Fe_3O_4 nanoparticles solely by oxidation. Recently, a range of methods like thermal decomposition, microemulsion, hydrothermal synthesis, sol-gel reactions, electrochemical and vapor/aerosol have been employed to obtain not only iron, but also other types of MagNPs (Laurent et al. 2008; Lu et al. 2007).

5 Nanomaterials Characterization

Before any nanomaterial is used for medical applications, it must be thoroughly characterized. As a result, physicochemical and biological procedures are required. It is known that properties such as size and surface chemistry determine their behaviour in biological systems (Conde et al. 2014). In this respect, there are a wide variety of techniques to study the morphology and the surface of nanoparticles (Hall et al. 2007). For example, UV-Vis spectroscopy provides information about shape and size based on the particle SPR band. Dynamic light scattering (DLS) analyses the average hydrodynamic size and size distribution of the particles in solution. A more precise morphology characterization is carried out by transmission electron microscopy (TEM) and/or scanning electron microscopy (SEM) (Fig. 2). Moreover, the nanoparticle crystallographic structure and composition can be determined combining high-resolution transmission electron microscopy (HRTEM) and dispersive X-ray spectroscopy (EDX). Furthermore, the use of X-ray photoelectron spectroscopy (XPS) provides information regarding atomic composition and chemical state of the surface atoms within the nanoparticle. In order to characterize the functional groups of the nanoparticle surface the Fourier transform infrared (FTIR) spectroscopy is used (Sergeev and Klabunde 2013).

Before making the jump from the bench to the bedside table, features like sterility, pyrogenicity, toxicity, absorption, distribution, metabolism and mechanism of excretion need to be assessed. The cited characterization includes both in vitro and in vivo studies. In particular, sterility and absence of pyrogenicity are essential characteristics for clinical applications. Because of this, the *Limulus amebocyte* lysate (LAL) and the rabbit pyrogen assays are often used to investigate the

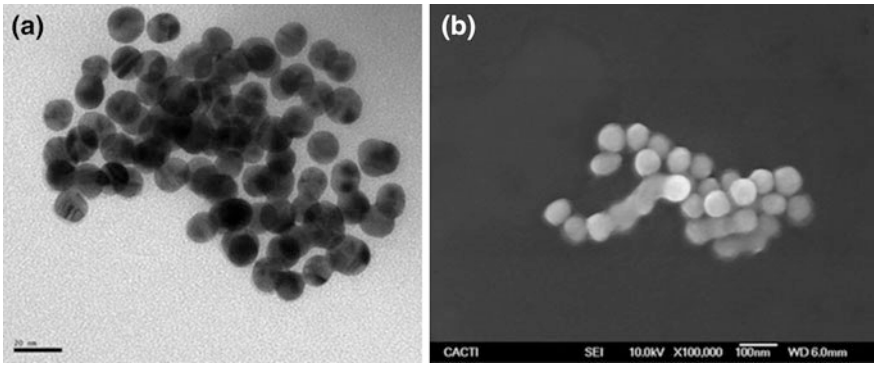

Fig. 2 Representative TEM (**a**) and SEM (**b**) images of AuNPs. The present snapshots are part of a current project conducted by our group

presence of NPs with endotoxin contamination (Hall et al. 2007). Other important points are toxicity and biocompatibility, for these aspects both in vitro and in vivo models are required for their evaluation. For example, the effect of NPs in cell viability and in the immunology system is initially assessed by the use of cell-based assays. However, to improve the safety and efficiency of NPs in vivo assays are required. Animals like zebra fish are regularly used as in vivo for the toxicity screening model. A comprehensive overview of the methods used for the viability assessment, together with the NPs' immunological interactions, is reported in the literature. Besides toxicity and biocompatibility, information about NPs' absorption, distribution, metabolism and excretion (ADME) are essential for their clinical applications. Techniques like electron microscopy (EM) can provide information about the distribution of certain types of nanoparticles into cells and tissues, which gives indications as to their state of aggregation and tissue penetration capacities but not about their functional status (Hall et al. 2007). Despite the latter, many researchers claim that NPs' characterization is still very poor, and that new procedures and protocols are needed in order to detect all the NPs' potential hazards (De Jong and Borm 2008).

6 Nanometals in Cancer Imaging

Early detection of cancer is crucial for successful treatment of the disease. However, detection, diagnosis and follow-up rely on techniques such as radiographs, ultrasound, computed tomography (CT), and magnetic resonance imaging (MRI). The main weakness of these techniques is that they only detect the cancer once it has become a physical entity, and is formed by millions or even billions of cells. Another drawback is the fact that they merely provide information about tumour size and extension, ignoring any tumour heterogeneity. Cancer is a genetic disease arising from the unregulated clonal expansion of cells that have mutated by chance at some

key genes, known as cancer genes. Cancer cells multiply much faster than tumour growth, implying that selection for space and resources of cancer cells is strong (Greaves and Maley 2012; Klein 2009). We now know that cancer is an evolutionary process mainly driven by continuous Darwinian natural selection of the fittest clones (Cairns 1975; Nowell 1976). Because of this, it is not surprising that most human cancers show high levels of intratumour heterogeneity at both phenotype and genotype levels (Kreso et al. 2013; Marusyk and Polyak 2010; Michor and Polyak 2010; Swanton 2012). This has important implications not only for diagnosis and treatment, but also for progression (Merlo et al. 2010). Due to these factors there is a need for more specific techniques that allow the reporting and characterization of the genetic changes involved in the oncogenic process in individual cases.

In this context, and with the purpose of overcoming the shortcomings of the conventional anatomical imaging methods, the molecular imaging methods arise. These new methods refer to "the development of molecular probes for the visualization of the cellular function, characterization and the measurement of molecular processes in living organisms at the cellular and molecular level without perturbing them" (Weissleder 2006). The molecular imaging methods will allow clinicians not only to see the tumour location and extension, but the expression and activity of specific molecules related with cancer origin, progression and response to therapy.

At present, a variety of nanomaterial types are being investigated to explore their potential in molecular imaging for biomedical applications, among them are gold and silver nanomaterials, quantum dots (QDs), iron oxide nanoparticles and dendrimers (Nune et al. 2009). However, some of them, like the QDs, despite their properties as fluorescence labelling agents for biological cells, present significant cytotoxicity problems, which is a pitfall in their potential clinical applications (Bradburne et al. 2013). Nevertheless, metal nanomaterials due to their physicochemical properties arise as ideal candidates for cancer labelling and imaging. The tumour targeting capacity through their functionalization with different ligands represents a significant improvement over the classic contrast median employed in cancer theragnosis. Numerous studies have shown that nanometals can be bound to different ligands like peptides, antibodies, proteins and small molecules offering a great potential for cancer diagnosis and treatment (Wang and Thanou 2010).

So far, AuNPs have been utilized as a contrast-enhancing agent for optical, CT, Raman, X-ray, diffusion reflection and photo acoustic imaging applications. They exhibit a potent X-ray absorption capacity, relatively short-term toxicity, high absorption coefficient and physical density. These qualities make them a good option for exploring cancer, rather than the typical based contrast agents consisting of iodinated molecules that also possess longer circulation times and worse CT contras capacities (Mieszawska et al. 2013).

Lately, novel X-ray CT imaging methods for tumour targeting based on AuNPs have started to be developed. The methods are based on AuNPs that selectively target tumour specific antigens which improves contrast in X-ray CT images. Related to this, Popovtzer et al. describe a new platform for in vivo CT molecular imaging, based on a new class of immuno-targeted gold nanomaterials that selectively target tumour specific antigens (Popovtzer et al. 2008). The authors applied this technique

to the early detection of Squamous cell carcinoma (SCC) which represents more than 90% of all head and neck cancers. In these experiments, they synthesized AuNRs and conjugated them with UM-A9 antibodies, which connect specifically to SCC head and neck cancer. Later they studied their feasibility to effectively induce contrast enhancement in CT imaging. All the experiments were done in vitro by the use of the human cancer cell lines (UM-SCC-1) and (UM-SCC-5) together with samples of fibrosarcoma (UM-FS-1) and melanoma (UM-Mel-1) employed as negative control, since this cell line does not express the A9 antigen. As a result, they demonstrated that AuNRs were attached to the cancer cells with high density, yielding a distinguishable CT attenuation number, that makes the targeted cells detectable in sufficient concentration. A recent study from the same group (Reuveni et al. 2011) has shown that an undetectable tumour by the classic anatomical computed tomography becomes clearly visible by the use of anti-epidermal growth factor receptor conjugated gold nanoparticles for tumour imaging detection in vivo. In the same way, Hainfeld et al. show that AuNPs can enhance the visibility of millimetre sized human breast tumours in mice and that active tumour targeting (with anti-Her2 antibodies) is more efficient than passive targeting (Hainfeld et al. 2011). Surface modified AuNPs in combination with X-ray imaging has also been employed for the hepatocellular carcinoma early diagnosis (Rand et al. 2011).

Another candidate for cancer imaging is silver; the scientific rationale underlying the selection of AgNPs to induce apoptosis in mammalian cells has been highlighted by many studies (Austin et al. 2011; Yin et al. 2013). However, in comparison with other nanometals, the published studies make very little reference to their potential as cell imaging enhancers. In this respect, a recent work by Li et al. investigated the potential of multifunctional aptamer silver conjugates as theragnostic agents in cancer. The authors employed the human acute lymphoblastic leukemia (ALL) cell line, CCRF-CEM, together with the human Burkitt's lymphoma cell line, Ramos, as an in vitro model. The experiment's outcome reveals that aptamer-silver conjugates can target and induce apoptosis on the cancer cell lines. Moreover, the synthesized multifunctional probes Ag-Sgc8-FAM also produce fluorescence-enhanced imaging to monitor the apoptotic process. This opens a new road for the use of aptamer-silver conjugates as a highly specific and sensitive way for targeted cancer therapy and imaging (Li et al. 2015a).

Magnetic nanoparticles are also employed as imaging contrast agents in diagnosis and tracing, not only in cancer but also in a range of different pathologies. To date a few MagNPs formulations like Feridex IV®, Endorem®, Lumiren®, Combidex® and Resovist® have been employed as MRI contrast agents (Singh et al. 2014). MRI is a non-invasive imaging technology that produces three-dimensional detailed anatomical images by using a strong magnetic field and pulses of radio waves to make images of structures inside the body (Waters and Wickline 2008; Weissleder 2006). Clear advantages of MRI over X-ray CT are the absence of ionizing radiation, which can cause detrimental effects on the patient health, as well as the improved contrast capacities between soft tissues. Moreover, as AuNPs, the MagNPs can be coated and conjugated with tumor targeting ligands (Li et al. 2013b, 2015b; Wadajkar et al. 2013), which improves their tumor targeting

capacities, reducing toxicities and provides a barrier from Reticuloendothelial Clearance System (RES) producing longer circulation times. The increase in the circulation times contributes to an improvement in the imaging time window and the tumour spatial resolution.

7 Nanometals in Drug Delivery

One of the greatest challenges in cancer treatment is the establishment of effective Drug Delivery Systems (DDS) that allows the dispensation of chemotherapeutic agents with high levels of effectiveness and low toxicity. Lately, different kinds of nanomaterials are arising as promising tools for drug delivery due to their particular characteristics. Firstly, their small size allows the potential for crossing different biological barriers within the body, which facilitates their delivery even to the most inaccessible places. Secondly, nanomaterials can be created and modified to target specific cells as well as to load and deliver drugs on them. Drugs can be entrapped, dissolved, absorbed, attached and encapsulated. Meanwhile, once in the target place drugs can be delivered using different approaches like ligand-receptor dependent and independent interactions (De Jong and Borm 2008). All the above mentioned allow reduction in dose of the required drug and a reduction in the occurrence of adverse effects, thus leading to an improvement of safety and therapeutic efficacy. In this scenario, metallic nanomaterials arise as versatile agents that can be used in a wide variety of biomedical applications, including drug delivery for cancer treatment. For example, AuNPs, due to their stability, functional flexibility, tunable monolayers and low toxicity are good candidates for drug delivery via multiple strategies. AuNPs can be conjugated with drugs via physical absorption, covalent or ionic bonding (Pissuwan et al. 2011). After their synthesis AuNPs are normally subjected to surface modification by polymers. This surface modification increases the NPs' stability, biocompatibility, facilitates their functionalization and avoids their aggregation, so reducing the risk of embolism (Muddineti et al. 2015).

All these factors are being exploited to target and treat cancer tissues, as illustrated in a recent study carried out by Battacharya et al. (Patra et al. 2010). The authors used multifunctional AuNPs as a potential therapeutic approach for ovarian cancer. The AuNPs conjugated with thiolated polyethylene glycol (HS-PEG), cisplatin, and folic acid displayed a toxic effect on the ovarian cancer cell lines. In the same way, Setua et al. employed multifunctional nanostructures comprising an AuNP surface functionalized with anticancer drug cisplatin (AuNP–cisplatin) to treat glioblastoma multiforme (GBM). The treatment is based on the use of cisplatin, combined with radiotherapy. After cellular uptake, the compound exerts its effect by inducing crosslinking in the DNA which finally results in cell apoptosis (Setua et al. 2014). Moreover, the complementary radiation therapy resulted in an enhanced synergy between cisplatin and radiotherapy mediated cytotoxicity, and photo/auger electron mediated radiosensitisation which resulted in the complete tumour ablation.

Furthermore, AgNPs have been employed alone, or in combination with gold, magnetic iron oxide nanoparticles and graphene oxide (GO) as effective drug carriers in cancer therapy. The drug release from NPs can be caused by different mechanisms like temperature, magnetic field, light source and pH (Li et al. 2015c). An example of the drug carrier properties of AgNPs is a study conducted recently by Chen et al. in which they developed multifunctional nanocarriers based on Fe_3O_4@C@Ag with a diameter of 200 nm. For their synthesis, AgNP were deposited onto the surface of Fe_3O_4@C in dimethyl formamide (DMF) solution by reducing $AgNO_3$ by glucose. Then the drug doxorubicin (DOX) was bound to the nanostructure through the interaction between the carboxyl group of Fe_3O_4@C@Ag nanoparticles and hydroxyl group of DOX. Once obtained, the hybrid nanoparticles were employed to test their suitability as therapy and imaging agents in cancer. With the latter purpose two cancer cell lines were employed: 1- Hela, from cervix carcinoma and 2- MCF-7, from breast cancer. After the NPs' delivery, the cell cultures were subjected to irradiation by NIR, which resulted in the presence of strong fluorescence in the cell nucleus due to the presence of DOX (Chen et al. 2013). Moreover, most cells were in the state of apoptosis as a result of the drug action. In the same way, Shi et al. developed a GO@Ag-DOX-NGR nanocomposite that showed excellent therapeutic efficacy, tumor-targeting efficiency, NIR laser-controlled drug releasing function and X-ray imaging ability in vitro (MCF-7 line) and in vivo in a xenograft tumor mouse model (Shi et al. 2014), demonstrating that there is a great potential of GO@Ag-DOX-NGR for cancer diagnosis and therapy. For the synthesis the authors employed chemical deposition of AgNPs onto GO through a hydrothermal reaction. It has been reported that GO has a very promising potential in drug delivery. Later DOX was linked to GO@Ag via ester bonds. A highlight was that the achieved drug loading efficiency was very high. After drug loading, the next step was to construct active tumour targeting capacity, as well as stability in physiological solutions. With the cited aim GO@Ag-DOX was functionalized by DSPE-PEG2000-NGR. The resulting GO@Ag-DOX-NGR exhibits high stability in various physiological solutions including saline, serum and cell media. Moreover, results showed that the AgNPs were a fundamental element together with the NIR laser in the DOX release control.

MagNPs are other nanometallic particles which have been used as an effective approach for drug site-specific delivery in cancer and other pathologies since 1963 (Meyers et al. 1963). Due to their properties, MagNPs can be targeted to the tumour places by specific ligands (Li et al. 2013a). Once in the tumour the drug can be unloaded by the action of an external magnetic agent. An important aspect is that in absence of any coating these NPs tend to agglomerate, forming large clusters. This reduces their effectiveness, increases toxicity and also the risk of vascular accidents. To overcome these problems a range of compounds have been proposed and used to coat MagNPs (Andrade et al. 2011). It has been shown that coating avoids the aggregation ability as well as providing better conditions for biofunctionalization. However, it can affect the magnetic properties. It has also been reported that variations in shape and size also have a strong impact on the magnetic properties (Gubin 2009; Krishnan 2010). Therefore, the use of these NPs in drug delivery in

the clinic requires a thorough nanoconstruct design. The first clinical cancer therapy trial in humans, using magnetic microspheres, took place in 1996. In this study, Lübbe et al. treated advanced solid tumours in 14 patients (Lübbe et al. 1996). They were able to develop a magnetic fluid to which the drug, 4-epidoxorubicin, was chemically bound. Techniques like magnetic resonance tomography and histology revealed the presence of magnetic particles in half of the patients. Relevant organ toxicity was not detected but epidoxorubicin associated toxicity appeared at doses greater than 50 mg/m^2. The optimization of these carriers has continued to this day and several reports have shown enhanced tumour targeting and drug delivery. A good number of reports describe improved MagNPs-drug constructs for cancer therapy (Corem-Salkmon et al. 2011; Li et al. 2013a; Rudzka et al. 2013). Another example of the tumour therapy advances are the MagNPs formulas for brain tumours (Chertok et al. 2011).

8 Nanometals in Gene Therapy

Recently, gene therapy has arisen as a promising treatment in destroying cancer cells. This therapeutic approach implies the modification or correction of abnormal genes by the administration of a genetic material (DNA, RNA or oligonucleotides) with the aim of tumour eradication by the activation of tumour genes that produce suppressor, cytotoxic or apoptotic proteins. This kind of therapy is carried out by using viral and non viral vectors to transport the foreign genetic material that otherwise could not reach the nucleus of the target cell without degradation. The optimal vehicle for the genetic material must be able to stay in the blood system for a long time avoiding uptake by the macrophages. Further, once in the target cell it should be able to arrive at the nucleus, sorting both liposomal and nuclease degradation. Non viral vectors are more suitable for this purpose than their viral counterparts which present low DNA carrying capacity, irregular cytotoxicity and triggering of strong immune responses, among other disadvantages (Pissuwan et al. 2011). In this scenario, some metal nanoparticles like gold and iron oxide together with other non viral factors like cationic polymers, liposomas and surfactants are very suitable gene delivery vehicles in cancer therapy (Rosi et al. 2006). In this section we will focus on the first two (gold and iron oxide nanoparticles) and their capacities as gene delivery agents in cancer. Due to their demonstrated stability and enhanced binding properties, AuNP based nanocarriers are being studied for the treatment of different types of cancers that include brain, breast and prostate, among others (Ekin et al. 2014). In this regard, Qing Du et al. report a new drug delivery system for the target therapy of neuroblastoma cancer (Du et al. 2014). This system is obtained by functionalizing the surface of AuNPs with DNA that contains cellular prion protein (PrPC) aptamers and the drug of interest DOX. PrPC is one of the membrane proteins that is expressed on the neuroblastoma cells and has an aptamer that can bind with the 23–90 epitope. To evaluate the efficiency of the designed complex the authors employed two cellular lines, A549 and SK-N-SH

from lung and neuroblastoma cancer. The lung line was employed as a control since it did not express PrPC on its surface. Study results demonstrated that the AuNP-DNA-DOX complex could be successfully utilised to release DOX in the target SK-N-SH cells with a remarkable effect on cell viability, while the control cells remain unaffected. This approach will allow improvements in the drug release in the tumor sites reducing the regular required doses of the drug and hence decreasing the drug toxicity. Cleavage of mRNA by siRNA has attracted much attention in cancer therapy lately. The most delicate step is delivery; siRNA cannot be directly injected in the circulatory system since they will be rapidly degraded by the RNA nucleases or removed by renal clearance due to their small size. So, how can we overcome this problem? Several studies show that encapsulation of siRNA into a delivery system to protect them from enzymatic degradation and increase their size to avoid renal clearance (Lee et al. 2013). In a recent interesting study, carried out by Kim et al. the authors employed a nanostructure as vehicles for siRNA delivery in cervix cancer in vitro (Kim et al. 2014). In the latter work the authors developed a size-regulated nanostructure consistent in 20 kDa siRNA-loaded to uPIC-AuNP which results in a 38 nm construct. The cellular delivery efficiency was investigated in the cervical cancer cell line (Hela) by use of a luciferase assay showing sequence specific gene silencing without toxicity. Moreover, blood circulation time and gene silencing effect was studied in a subcutaneous tumor model after intravenous injection of the uPIC-AuNP constructs resulting in appreciable increases in the blood circulation times compared to bare AuNPs and uPICs. As others did before them, the authors attribute this effect to the PEG outlayer that will protect the nanostructure from possible detrimental interactions in the circulatory system. Finally, they probed efficient accumulation of siRNA and specific gene silencing in the tumour tissue after systemic delivery, showing the strong potential of uPIC-AuNP for solid tumour treatment. In the same way, Ekin et al. used AuNPs as microRNA nanocarriers in breast and prostate cancer (Ekin et al. 2014). In this study the authors employed the human cancer cell lines PC3 (prostate cancer) and MCF-7 (breast cancer) to evaluate the delivery efficiency of miRNAs by AuNPs. For this, small size AuNPs (13 nm) were modified with thiolated RNAs and then the miR-145 was hybridized to the RNAs that were chemically attached to the AuNP. The short RNA molecule, miR-145, is a well-known tumour suppressor that is down-regulated in prostate and breast tumours. To explore the feasibility of engineered AuNPs as nanocarrier platforms for delivery of miRNAs to the prostate/breast cancer cells, both PC3 and MCF-7 cells were transfected with pre-miR-145. Subsequently, the authors checked for the presence of mature miR-145 molecules and their stability by miRNA qRT-PCR. The cited analysis reveals that miR-145 molecules are produced in an effective way in the transfected cell lines compared with the untransfected group. The effect of temperature in the transfection efficiency was also evaluated revealing that a maintained temperature of 72 °C resulted in a more efficient delivery of miR-145 molecules to cells.

Other metallic nanoparticles such as superparamagnetic iron oxide nanoparticles (SPIONs) are also being studied as candidates for nucleic acids delivery in cancer.

There are a raft of approaches for nucleic acids targeting and delivery, one of which is the magnetofection. This method, coined by Plank et al. 2000 refers to a nucleic acid delivery under the influence of a magnetic field (Plank et al. 2000). The nucleic acids are associated to magnetic nanoparticles that release the load under a magnetic stimulus. An interesting review that compiles the last 10 years in the magnetofection was published in 2011 by Plank et al. (2011). Among the variety of magnetic nanoparticles, SPIONs are currently being studied as an important vehicle to conjugate nucleic acids and other therapeutic agents for different cancer treatment strategies (Prijic et al. 2012). Some conducted studies reveal that a very important subject in magnetofection is the SPION synthesis procedure. The physicochemical properties of these magnetic nanoparticles are affected by the shape, size, magnetic core composition and surface properties (Wahajuddin and Arora 2012). For this reason, in order to improve the use of magnetofection in cancer, SPION synthesis fine-tuning has become a relevant step. In this respect, Prosen et al. conducted an extensive study to investigate the effect of different variables in the steps of SPION synthesis on the physicochemical properties and magnetofection efficacy in a murine melanoma cell line (B16F1) (Prosen et al. 2013). They concluded that the magnetofection efficacy is significantly affected by pH. To obtain a pronounced gene expression the cited parameter should be in an alkaline range. The potential of SPION as a promising cancer gene therapy agent by magnetofection has already been demonstrated (Mulens et al. 2013; Prijic et al. 2012). Moreover, the new technologies in synthesis together with the constant development of new coating polymers make SPIONs a highly attractive option for cancer diagnosis and therapy. Nevertheless, further systematic studies about their elimination outline in the human body are required to apply them to a clinical setting in a safe way.

9 Metalnanomaterials in Photothermal Therapy

The first attempt of thermal therapy in cancer was four decades ago when therapeutic lasers started to be used to treat pancreatic tumours, brain tumours and liver metastases (Brunetaud et al. 1995). Since then, thermal therapy has attracted a great deal of interest in the battle against cancer. This has led to the development of a novel class of anticancer particles that include several types of nanomaterials like AuNPs, AgNPs, SPIONs, paramagnetic copper-nickel alloy NPs, magnetic cationic liposomes and nanoshells (Sakamoto et al. 2010).

The use of metal nanomaterials (MNPs) allows selective ablation and a reduction in the exposure time to the irradiation source. To treat the tumour the MNPs are administrated to the patient and allowed to localize the tumour by diffusion or by a tumour recognition molecule attached to the surface. This is followed by cellular internalization and by the exposition of a remote excitation source. The most commonly used are: (1) radiowaves (Gannon et al. 2008), (2) nearinfrared (NIR) laser light (Hirsch et al. 2003) or (3) an alternating magnetic field (Johannsen et al. 2005) (Fig. 3). During this process the photons will be strongly absorbed or

scattered at specific resonant wavelengths and the absorbed light is converted into heat, which generates thermal cytotoxicity in the cancer cells, when tissues are heated above the hyperthermia temperature (42 °C) (Cobley et al. 2010). A marked increase in the local temperature is associated with proteins' denaturation which can lead to cytoskeleton collapse. Meanwhile, moderate hyperthermia can be employed as an adjuvant in combination with chemotherapy as it acts as a cancer cell sensitizer by increasing membrane permeability (Huff et al. 2007).

Thermotherapy can be employed to treat cancer alone or in combination with other approaches like surgery, chemotherapy, radiation, gene therapy and immunotherapy (Alphandéry 2014). In this context gold nanomaterials like AuNShs, AuNRs, AuNCs and AuNPs are being successfully employed by thermotherapy to treat solid tumours in vitro and in vivo in animal models (Huang and El-Sayed 2010; Tiwari et al. 2015). Hirsch et al. (2003) were the first to apply thermal ablative therapy with AuNShs. In the in vitro study the authors incubated human breast epithelial carcinoma cells (SK-BR-3) with AuNShs, previously stabilized alongside PEG. Followed by NIR laser light activation at 820 nm, 35 W/cm^2 for 7 min to induce cell damage. Cells were then studied for cell viability, membrane permeability/damage and nanoshell binding. This showed that the AuNShs therapy produced either both irreversible loss of the membrane integrity or cell death. The effect was confined to the laser/nanoshell treatment area. Exposure of the cells to AuNShs or NIR separately did not affect cell viability or membrane

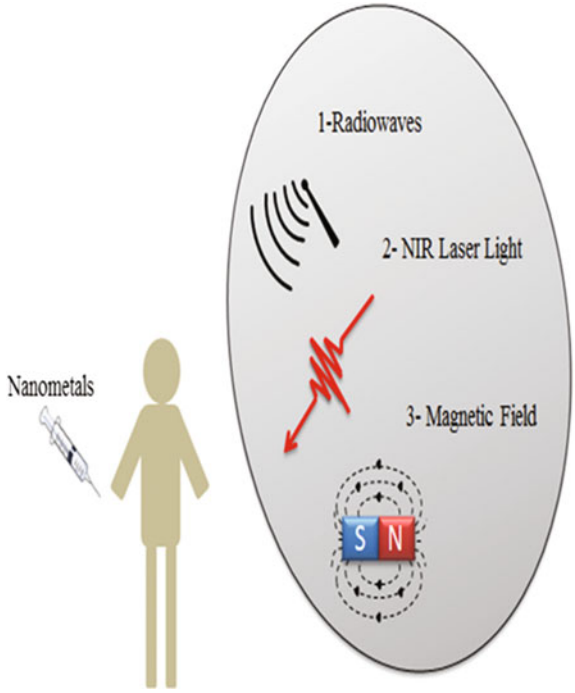

Fig. 3 Schematic illustration of the different excitation sources employed to generate metal-nanoparticle mediated hyperthermia in tumor cells

integrity. Similar results were obtained in vivo in female non obese diabetic CB17-Prkdc SCID7J mice after transmissible venereal tumour (TVT) tumour inoculation. Analysis reveals that AuNShs treated tumours present successful cell destruction confined to the tumour area. Histology also confirmed the presence of AuNSs over a large volume within the tumour. In the same line AuNRs have proved to be excellent candidates for image guided therapies based on pinpoint hyperthermia due to their cell-specific targeting and their optical resonance properties (Huff et al. 2007). AuNRs have also been extensively studied for cancer theragnosis, and at present are being implicated in new diagnosis and therapeutic approaches based on their properties (Peralta et al. 2015; Zhang et al. 2015).

Like gold, MagNPs like iron oxide nanoparticles have been studied and employed for hyperthermia based therapy in cancer for the last three decades (Kumar and Mohammad 2011). Tumour cell death is induced by magnetic hyperthermia in different ways: the activation of necrosis, apoptosis, autophagy and/or through immune system stimulation. This second way has been attracting a great deal of attention lately. For instance, Kobayashi et al. published a recent review about "antitumor immunity by magnetic nanoparticle-mediated hyperthermia" (Kobayashi et al. 2014). Some in vivo studies, cited in this review, suggest that the activation of the immune system by the hyperthermia generated with MagNPs can induce the regression of the primary tumours as well as the metastatic masses that have never been exposed to heat. Numerous clinical trials employing magnetic hyperthermia in the treatment of different kinds of cancers are being implemented due to the promising results obtained both in vitro and in vivo (Luo et al. 2014; Zhao et al. 2013).

The suitability as photothermal agents of other nanometals like silver have begun to be explored to treat different kinds of cancer. One of the first studies to tackle this subject was conducted by Boca et al. The authors studied the hyperthermia activity of synthesized chitosan-coated silver nanotriangles (CS-AgNTs) against a line of human non-small lung cancer (NCI-H460). The CS-AgNTs increases the biocompatibility, prevents AgNTs' aggregation and reduces the cytotoxicity, meanwhile the triangular shape is essential for NIR application (Boca et al. 2011).

In the hyperthermia experiments PEG capped gold nanorods (PEG-AuNRs) are used as positive control and for activity comparison between gold and silver nanomaterials. The cells were incubated with the AuNRs and subjected to laser excitation at 800 nm for 10 min. A control sample without AuNRs was also included in the experiment, whereupon cell viability was assed by microscopy after propidium iodide (PI) staining. The results clearly show that CS-AgNPs exhibit higher hyperthermia activity than PEG-AuNRs while no deleterious effects were present in the control sample. Moreover, the conduced cellular uptake assays reveal that incubation times of more than one hour result in a significant increase in the CS-AgNPs' uptake by cancer cells when compared with the PEG-AuNRs' uptake. Authors believe this effect could be due to chitosan's high affinity to proteins present in the cellular environment, a characteristic which is absent in the PEG. Additionally, to assess the possible toxic effect of the metallic nanoparticles in the

healthy tissue that surrounds tumours, CS-AgNPs and PEG-AuNRs were added to healthy human embryonic kidney cells (HEK) in vitro. The results revealed that CS-AgNPs exhibit a low toxicity, and 95% of HEK cells are viable after 24 h of contact with the metal nanomaterial. Meanwhile, it presents a deleterious effect on the cancer cells in similar conditions.

Thompson et al. (2014) have also demonstrated the efficiency of CS stabilized silver nanoparticles as photothermal agents in the treatment of common ductal carcinoma and triple negative breast cancer. In this research, a novel aspect is the determination of the ideal concentration of CS-AgNPs to induce irreversible cell damage by hyperthermia. The authors established that infrared radiation (either 0.79 or 2.94 W/cm^2) applied for 60 s to cell cultures with 100 or 250 μg/mL of AgNPs led to a 90% decrease in cell viability. The level of energy employed and the time of exposure is much lower in comparison with Boca et al. whose findings needed to expose the cultures to 54 W/cm^2 for 10 min to achieve the same viability effect. It is important to highlight that the concentration of nanoparticles employed by Boca et al. was much lower. Moreover, Thompson et al. as others had done before, confirmed that cancer cells have a differential response to AgNPs, as their proliferation capacities are affected by the treatment contrary to what happens to non-tumorigenic cells. In conclusion, CS-AgNP is a novel class of nanoparticles to explore in vitro and in vivo as phototherapeutic agents against cancer.

10 Conclusions and Future Perspectives

The development of nanotechnology has created a wealth of applications in the biomedical field, particularly in cancer. During recent decades, multidisciplinary groups have tested the NMs' capacities as optimal tools in cancer therapy and diagnostics. All scientific data hitherto gained strongly suggests that NMs, due to their unique physicochemical properties, hold the key in the fight against cancer. Their utility in cancer detection and tracing, together with their therapeutic capacities through drug and/or gene delivery and photo-thermal therapy, has been reported in the present review. Despite all the promising results several issues need to be addressed before making the jump to the clinic. Among the main challenges are the standardization of manufacture and the NMs' characterization procedures. The impact on human health also needs further study. Therefore, new or improved methods to assess the sterility, toxicity and ADME need to be developed by scientists and government regulatory agencies.

Acknowledgements SPL is supported by the European Research Council (grant ERC-2013-CoG- no 617457-PHYLOCANCER).

References

Alkilany AM, Thompson LB, Boulos SP et al (2012) Gold nanorods: their potential for photothermal therapeutics and drug delivery, tempered by the complexity of their biological interactions. Adv Drug Deliv Rev 64(2):190–199

Alphandéry E (2014) Perspectives of breast cancer thermotherapies. J Cancer 5(6):472–479

Andrade A, Ferreira R, Fabris J et al (2011) Coating nanomagnetic particles for biomedical applications. In: Fazel R (ed) Biomedical engineering: frontiers and challenges. InTech, Rijeka, Croatia, pp 157–176

Arrowsmith RL, Pascu SI, Smugowski H (2012) New developments in the biomedical chemistry of metal complexes: from small molecules to nanotheranostic design. Organomet Chem 38:1–35

Austin LA, Kang B, Yen CW et al (2011) Plasmonic imaging of human oral cancer cell communities during programmed cell death by nuclear-targeting silver nanoparticles. J Am Chem Soc 133:17594–17597

Averitt RD, Sarkar D, Halas NJ (1997) Plasmon resonance shifts of Au-coated Au_2S nanoshells: Insight into multipotent nanoparticle growth. Phys Rev Lett 78(22):4217–4220

Bhattacharyya S, Kudgus RA, Bhattacharya R et al (2011) Inorganic nanoparticles in cancer therapy. Pharm Res 28(2):237–259

Boca SC, Potara M, Gabuden AM et al (2011) Chitosan-coated triangular silver nanoparticles as a novel class of biocompatible, highly effective photothermal transducers for in vitro cancer cell therapy. Cancer Lett 311(2):131–140

Bradburne CE, Delehanty JB, Boeneman-Gemmill K et al (2013) Cytotoxicity of quantum dots used for in vitro cellular labeling: role of QD surface ligand, delivery modality, cell type, and direct comparison to organic fluorophores. Bioconjugate Chem 24(9):1570–1583

Brunetaud JM, Mordon S, Maunoury V et al (1995) Non-PDT uses of lasers in oncology. Lasers Med Sci 10:3–8

Brust M, Fink J, Bethell D et al (1995) Synthesis and reactions of functionalized gold nanoparticles. J Chem Soc Chem Commun 16:1655–1656

Cai W, Gao T, Hong H et al (2008) Applications of gold nanoparticles in cancer nanotechnology. Nanotechnol Sci Appl 1:17–32

Cairns J (1975) Mutation selection and the natural history of cancer. Nature 255:197–200

Cao-Milan R, Liz-Marzán LM (2014) Gold nanoparticle conjugates: Recent advances toward clinical applications. Expert Opin Drug Deliv 11(5):741–752

Chen J, Guo Z, Wang HB et al (2013) Multifunctional Fe_3O_4@C@Ag hybrid nanoparticles as dual modal imaging probes and near-infrared light-responsive drug delivery platform. Biomaterials 34:571–581

Chertok B, David AE, Yang VC (2011) Brain tumor targeting of magnetic nanoparticles for potential drug delivery: effect of administration route and magnetic field topography. J Control Release 155(3):393–399

Cobley CM, Au L, Chen J et al (2010) Targeting gold nanocages to cancer cells for photothermal destruction and drug delivery. Expert Opin Drug Deliv 7(5):577–587

Conde J, Dias JT, Grazú V et al (2014) Revisiting 30 years of biofunctionalization and surface chemistry of inorganic nanoparticles for nanomedicine. Front Chem 2:48

Corem-Salkmon E, Ram Z, Daniels D et al (2011) Convection-enhanced delivery of methotrexate-loaded maghemite nanoparticles. Int J Nanomedicine 6:1595–1602

Dasari S, Tchounwou PB (2014) Cisplatin in cancer therapy: molecular mechanisms of action. Eur J Pharmacol 740:364–378

De Jong WH, Borm PJA (2008) Drug delivery and nanoparticles: applications and hazards. Int J Nanomedicine 3(2):133–149

Du YQ, Yang XX, Li WL et al (2014) A cancer-targeted drug delivery system developed with gold nanoparticle mediated DNA-doxorubicin conjugates. RSC Adv 4:34830–34835

Dykman L, Khlebtsov N (2012) Gold nanoparticles in biomedical applications: recent advances and perspectives. Chem Soc Rev 41:2256–2282
Ekin A, Karatas OF, Culha M et al (2014) Designing a gold nanoparticle-based nanocarrier for microRNA transfection into the prostate and breast cancer cells. J Gene Med 16:331–335
Frens G (1973) Controllated nucleation for the regulation of the particle size in monodisperse gold suspension. Nat Phys Sci 241:20–21
Gannon CJ, Patra CR, Bhattacharya R et al (2008) Intracellular gold nanoparticles enhance non-invasive radiofrequency thermal destruction of human gastrointestinal cancer cells. J Nanobiotechnol 6:2
Ghosh P, Han G, Mrinmoy D et al (2008) Gold nanoparticles in delivery applications. Adv Drug Deliv Rev 60(11):1307–1315
Greaves M, Maley CC (2012) Clonal evolution in cancer. Nature 481:306–313
Gubin SP (2009) Magnetic nanoparticles. Wiley-VCH Verlag GmbH and Co, KGaA, Weinheim
Hainfeld JF, O'Connor MJ, Dilmanian FA et al (2011) Micro-CT enables microlocalisation and quantification of Her2-targeted gold nanoparticles within tumour regions. Br J Radiol 84:526–533
Hall JB, Dobrovolskaia MA, Patri AK et al (2007) Characterization of nanoparticles for therapeutics. Nanomedicine 2(6):789–803
Hirsch LR, Stafford RJ, Bankson JA et al (2003) Nanoshell-mediated near-infrared thermal therapy of tumors under magnetic resonance guidance. Proc Natl Acad Sci U S A 100(23): 13549–13554
Hordyjewska A, Popiolek Å, Kocot J (2014) The many "faces" of copper in medicine and treatment. Biometals 27(4):611–621
Huang X, El-Sayed M (2010) Gold nanoparticles: optical properties and implementations in cancer diagnosis and photothermal therapy. J Adv Res 1(1):13–28
Huff TB, Tong L, Zhao Y et al (2007) Hyperthermic effects of gold nanorods on tumor cells. Nanomedicine 2(1):125–132
Jana NR, Gearheart L, Murphy CJ (2001) Seeding growth for size control of 5–40 nm diameter gold nanoparticles. Langmuir 17(37):6782–6786
Jiang K, Pinchuk AO (2015) Noble metal nanomaterials: synthetic routes, fundamental properties, and promising applications. Solid State Phys. doi:10.1016/bs.ssp.2015.02.001
Jin Y (2012) Engineering plasmonic gold nanostructures and metamaterials for biosensing and nanomedicine. Adv Mater 24(38):5153–5165
Johannsen M, Gneveckow U, Eckelt L et al (2005) Clinical hyperthermia of prostate cancer using magnetic nanoparticles: presentation of a new interstitial technique. Int J Hyperth 21(7):637–647
Kennedy LC, Bickford LR, Lewinski N et al (2011) A new era for cancer treatment: gold-nanoparticle-mediated thermal therapies. Small 7(2):169–183
Kim HJ, Takemoto H, Yi Y et al (2014) Precise engineering of siRNA delivery vehicles to tumors using polyion complexes and gold nanoparticles. ACS Nano 8(9):8979–8991
Klein CA (2009) Parallel progression of primary tumours and metastases. Nat Rev Cancer 9 (4):302–312
Kobayashi T, Kakimi K, Nakayama E et al (2014) Antitumor immunity by magnetic nanoparticle-mediated hyperthermia. Nanomedicine 9(11):1715–1726
Kreso A, O'Brien CA, van Galen P et al (2013) Variable clonal repopulation dynamics influence chemotherapy response in colorectal cancer. Science 339:543–548
Krishnan KM (2010) Biomedical nanomagnetics: a spin through possibilities in imaging diagnostics, and therapy. IEEE Trans Magn 46(7):2523–2558
Kumar CSSR, Mohammad F (2011) Magnetic nanomaterials for hyperthermia-based therapy and controlled drug delivery. Adv Drug Deliv Rev 63(9):789–808
Laurent S, Forge D, Port M et al (2008) Magnetic iron oxide nanoparticles: synthesis, stabilization, vectorization, physicochemical characterizations, and biological applications. Chem Rev 108:2064–2110

Lee JM, Yoon TJ, Cho YS (2013) Recent developments in nanoparticle-based siRNA delivery for cancer therapy. Biomed Res Int 2013:1–10

Li D, Zhang YT, Yu M et al (2013a) Cancer therapy and fluorescence imaging using the active release of doxorubicin from MSPs/ni-LDH folate targeting nanoparticles. Biomaterials 34 (32):7913–7922

Li H, Hu H, Zhao Y et al (2015a) Multifunctional aptamer-silver conjugates as theragnostic agents for specific cancer cell therapy and fluorescence-enhanced cell imaging. Anal Chem 87:3736–3745

Li H, Yan K, Shang Y et al (2015b) Folate-bovine serum albumin functionalized polymeric micelles loaded with superparamagnetic iron oxide nanoparticles for tumor targeting and magnetic resonance imaging. Acta Biomater 15:117–126

Li J, Zheng L, Cai H et al (2013b) Polyethyleneimine-mediated synthesis of folic acid targeted iron oxide nanoparticles for in vivo tumor MR imaging. Biomaterials 34(33):8382–8392

Li J, Wang Y, Liang R et al (2015c) Recent advances in targeted nanoparticles drug delivery to melanoma. Nanomedicine Nanotechnol Biol Med 11:769–794

Li W, Chen X (2015) Gold nanoparticles for photoacoustic imaging. Nanomedicine 10(2): 299–320

Liu X, Xu H, Xia H et al (2012) Rapid seeded growth of monodisperse, quasi-spherical, citrate-stabilized gold nanoparticles via H_2O_2 reduction. Langmuir 28:13720–13726

Lu AH, Salabas EL, Schüth F (2007) Magnetic nanoparticles: synthesis, protection, functionalization, and application. Angew Chem Int Ed 46(8):1222–1244

Lübbe AS, Bergemann C, Riess H et al (1996) Clinical experiences with magnetic drug targeting a phase I study with 4′-epidoxorubicin in 14 patients with advanced solid tumors. Cancer Res 56:4686–4693

Luo S, Wang LF, Ding WJ et al (2014) Clinical trials of magnetic induction hyperthermia for treatment of tumours. OA Cancer 2(1):2

Marusyk A, Polyak K (2010) Tumor heterogeneity: causes and consequences. Biochim Biophys Acta 1805:105–117

Medici S, Peana M, Nurchi VM et al (2015) Noble metals in medicine: latest advances. Coord Chem Rev 284:329–350

Merlo LMF, Shah NA, Li X et al (2010) A comprehensive survey of clonal diversity measures in Barrett's esophagus as biomarkers of progression to esophageal adenocarcinoma. Cancer Prev Res 3(11):1388–1397

Meyers PH, Cronic F, Nice CMJ (1963) Experimental approach in the use and magnetic control of metallic iron particles in the lymphatic and vascular system of dogs as a contrast and isotopic agent. Am J Roentgenol Radium Ther Nucl Med 90:1068–1077

Michor F, Polyak K (2010) The origins and implications of intratumor heterogeneity. Cancer Prev Res (Phila) 3(11):1361–1364

Mieszawska AJ, Mulder WJM, Fayad ZA et al (2013) Multifunctional gold nanoparticles for diagnosis and therapy of disease. Mol Pharm 10(3):831–847

Muddineti OS, Ghosh B, Biswas S (2015) Current trends in using polymer coated gold nanoparticles for cancer therapy. Int J Pharm 484:252–267

Mulens V, Morales MP, Barber DF (2013) Development of magnetic nanoparticles for cancer gene therapy: a comprehensive review. ISRN Nanomaterials 2013:1–14

Ng VWK, Berti R, Lesage F et al (2013) Gold: a versatile tool for in vivo imaging. J Mater Chem B 1:9–25

Nowell PC (1976) The clonal evolution of tumor cell populations. Science 194:23–28

Nune SK, Gunda P, Thallapally PK et al (2009) Nanoparticles for biomedical imaging. Expert Opin Drug Deliv 6(11):1175–1194

Oldenburg SJ, Jackson JB, Westcott SL et al (1999) Infrared extinction properties of gold nanoshells. Appl Phys Lett 75:2897–2899

Patra CR, Bhattacharya R, Mukherjee P (2010) Fabrication and functional characterization of goldnanoconjugates for potential application in ovarian cancer. J Mater Chem 20(3):547–554

Peralta DV, Heidari Z, Dash S et al (2015) Hybrid paclitaxel and gold nanorod-loaded human serum albumin nanoparticles for simultaneous chemotherapeutic and photothermal therapy on 4T1 breast cancer cells. ACS Appl Mater Interfaces 7:7101–7111

Perrault SD, Chan WCW (2009) Synthesis and surface modification of highly monodispersed, spherical gold nanoparticles of 50–200 nm. J Am Chem Soc 131:17042–17043

Pinato O, Musetti C, Sissi C (2014) Pt-based drugs: the spotlight will be on proteins. Metallomics 6:380–395

Pissuwan D, Niidome T, Cortie MB (2011) The forthcoming applications of gold nanoparticles in drug and gene delivery systems. J Control Release 149(1):65–71

Plank C, Zelphati O, Mykhaylyk O (2011) Magnetically enhanced nucleic acid delivery. ten years of magnetofection-progress and prospects. Adv Drug Deliv Rev 63:1300–1331

Plank C, Scherer F, Schillinger U et al (2000) Magnetofection: enhancement and localization of gene delivery with magnetic particles under influence of a magnetic fields. J Gene Med 2(5) Suppl:S24

Popovtzer R, Agrawal A, Kotov NA et al (2008) Targeted gold nanoparticles enable molecular CT imaging of cancer. Nano Lett 8(12):4593–4596

Prijic S, Prosen L, Cemazar M et al (2012) Surface modified magnetic nanoparticles for immuno-gene therapy of murine mammary adenocarcinoma. Biomaterials 33:4379–4391

Prosen L, Prijic S, Music B et al (2013) Magnetofection: a reproducible method for gene delivery to melanoma cells. BioMed Res Int 2013:1–11

Rand D, Ortiz V, Liu Y et al (2011) Nanomaterials for X-ray imaging: gold nanoparticle enhancement of X-ray scatter imaging of hepatocellular carcinoma. Nano Lett 11:2678–2683

Reuveni T, Motiei M, Romman Z et al (2011) Targeted gold nanoparticles enable molecular CT imaging of cancer: an in vivo study. Int J Nanomedicine 6:2859–2864

Rodríguez-Argüelles MC, Sieiro C, Cao R et al (2011) Chitosan and silver nanoparticles as pudding with raisins with antimicrobial properties. J Colloid Interface Sci 364:80–84

Rosemberg B, VanCamp L, Krigas T (1965) Inhibition of cell division in *Escherichia coli* by electrolysis products from a platinum electrode. Nature 205:698–699

Rosenberg B, VanCamp L (1970) The successful regression of large solid sarcoma 180 tumors by platinum compounds. Cancer Res 30(6):1799–1802

Rosi NL, Giljohann DA, Thaxton CS et al (2006) Oligonucleotide-modified gold nanoparticles for intracellular gene regulation. Science 312(5776):1027–1030

Rudzka K, Viota JL, Muñoz-Gamez JA et al (2013) Nanoengineering of doxorubicin delivery systems with functionalized maghemite nanoparticles. Colloids Surf B 111:88–96

Sakamoto JH, van de Ven AL, Godin B et al (2010) Enabling individualized therapy through nanotechnology. Pharmacol Res 62(2):57–89

Sakurai H, Yoshikawa Y, Yasui H (2008) Current state for the development of metallopharmaceutics and anti-diabetic metal complexes. Chem Soc Rev 37:2383–2392

Schleich N, Danhier F, Preat V (2015) Iron oxide-loaded nanotheranostics: major obstacles to in vivo studies and clinical translation. J Controlled Release 198:35–54

Sergeev GB, Klabunde KJ (2013) Experimental techniques. Nanochemistry, 2nd edn. Elsevier, Oxford, pp 75–85

Setua S, Ouberai M, Piccirillo SG et al (2014) Cisplatin-tethered gold nanospheres for multimodal chemo-radiotherapy of glioblastoma. Nanoscale 6:10865–10873

Shi J, Wang L, Zhang J et al (2014) A tumor-targeting near-infrared laser-triggered drug delivery system based on GO@Ag nanoparticles for chemo-photothermal therapy and X-ray imaging. Biomaterials 35:5847–5861

Singh D, McMillan JM, Kabanov AV et al (2014) Bench-to-bedside translation of magnetic nanoparticles. Nanomedicine 9(4):501–516

Stöber W, Fink A, Bohn E (1968) Controlled growth of monodisperse silica spheres in the micron size range. J Colloid Interface Sci 26:62–69

Sun Y, Mayers BT, Xia Y (2002) Template-engaged replacement reaction: a one-step approach to the large-scale synthesis of metal nanostructures with hollow interiors. Nano Lett 2(5):481–485

Swanton C (2012) Intratumor heterogeneity: evolution through space and time. Cancer Res 72 (19):4875–4882

Thompson EA, Graham E, MacNeill CM et al (2014) Differential response of MCF7, MDA-MB-231, and MCF 10A cells to hyperthermia, silver nanoparticles and silver nanoparticle-induced photothermal therapy. Int J Hyperth 30(5):312–323

Tiwari PM, Bawage SS, Singh SR (2015) Gold nanoparticles and their applications in photomedicine, diagnosis and therapy. In: Hamblin MR, Avci HP (eds) Applications of nanoscience in photomedicine. Elsevier, United Kingdom, pp 249–266

Turkevich J, Stevenson PC, Hillier J (1951) A study of the nucleation and growth processes in the synthesis of colloidal gold. Discuss Faraday Soc 11:55–75

Umer A, Naveed S, Ramzan N et al (2012) Selection of a suitable method for the synthesis of copper nanoparticles. Nano Brief Rep Rev 7(5):1–18

Wadajkar AS, Menon JU, Tsai YS et al (2013) Prostate cancer-specific thermo-responsive polymer coated iron oxide nanoparticles. Biomaterials 34:3618–3625

Wahajuddin SA (2012) Superparamagnetic iron oxide nanoparticles: magnetic nanoplatforms as drug carriers. Int J Nanomedicine 7:3445–3471

Wang M, Thanou M (2010) Targeting nanoparticles to cancer. Pharmacol Res 62(2):90–99

Waters EA, Wickline SA (2008) Contrast agents for MRI. Basic Res Cardiol 103(2):114–121

Wei L, Lu J, Xu H et al (2015) Silver nanoparticles: synthesis, properties and therapeutic applications. Drug Discov Today 20(5):595–601

Weissleder R (2006) Molecular imaging in cancer. Science 312(5777):1168–1171

Yin N, Liu Q, Liu J et al (2013) Silver nanoparticle exposure attenuates the viability of rat cerebellum granule cells through apoptosis coupled to oxidative stress. Small 9:1831–1841

Zhang Z, Liu C, Bai J et al (2015) Silver nanoparticle gated, mesoporous silica coated gold nanorods (AuNR@MS@AgNPs): Low premature release and multifunctional cancer theranostic platform. ACS Appl Mater Interfaces 7:6211–6219

Zhao L, Kim TH, Ahn JC et al (2013) Highly efficient “theranostics” system based on surface-modified gold nanocarriers for imaging and photodynamic therapy of cancer. J Mater Chem B 1(42):5806–5817

Part II
Biomaterial Properties and Characterization

Chemical Bulk Properties of Biomaterials

Matthias Schnabelrauch

Abstract Biomaterials are made from different classes of known materials including metals and alloys, ceramics, glasses, as well as natural and synthetic polymers. This great variety of materials is a result of the different application profiles, biomaterials normally have to fulfil in the body. The basis for the specific properties of a distinct biomaterial is its composition and structure at an atomic and molecular level determining the chemical nature and finally the behaviour of these materials in a living organism. In this chapter it is aimed to introduce the fundamental concepts describing the atomic bondings and the corresponding molecular structures of the main classes of material. Main correlations between these molecular structures of materials and their resulting chemical behaviour will be discussed to better understand and predict the properties of those materials with regard to their use in contact with the living matter.

Keywords Biomaterials · Molecular structure · Chemistry · Reactivity

1 Introduction

A wide variety of different biomaterials belonging to the major classes of materials, namely metals, ceramics, and polymers is used in medicine for implants, prostheses, catheters, stents, wound dressings, heart valves, bone cements, intraocular lenses and other medical products.

Today, it is common knowledge that the bulk and the surface properties of a medical material used in or at the human body strongly influence the dynamic interactions at the tissue-material interface and in doing so they often decide success or failure of this material.

M. Schnabelrauch (✉)
Biomaterials Department, INNOVENT e. V, Pruessingstrasse 27B,
07745 Jena, Germany
e-mail: ms@innovent-jena.de

F. Zivic et al. (eds.), *Biomaterials in Clinical Practice*,
https://doi.org/10.1007/978-3-319-68025-5_15

Both the bulk and the surface properties of biomaterials are determined by their structure (Dee et al. 2002). At the atomic level materials are characterized by different types of strong (primary) interatomic bonds: covalent, ionic and metallic. In addition to these three strong bonds there are several weak (secondary) bonds that significantly influence the properties of materials, especially natural and synthetic polymers. Among these weak bonds are hydrogen bonds, van der Waals bonding, or hydrophobic interactions (Cooke 2004).

The properties of materials are related to the nature of their atomic bonding. Because the majority of biomaterials are solids, the three-dimensional arrangement of atoms or ions in a solid is one of the most important structural features of a defined material. Often atoms or ions are arranged in an orderly repeated pattern in three dimensions which is then called a crystal structure. Crystal structures allow atoms to be closely packed, i.e. they have the maximum possible number of near, contacting neighbours, maximizing the number of strong bonds and at the same time minimizing the energy of the aggregate. As a consequence biomaterials, possessing a high level of crystallinity normally have quite different properties compared to an amorphous material characterized by a non-regular three-dimensional assignment of atoms. However not only the physical bulk properties of a biomaterial including density, hardness, melting or boiling temperature, solubility, electrical conductivity or strength, but also the chemical characteristics like reactivity, electronegativity, biodegradability, corrosion resistance, acidity/basicity are determined by the atomic structure of the specific material. Especially the susceptibility to chemical degradation which can be desired or undesired dependant on the specific medical application is an important feature of biomaterials.

In contrast to the bulk of a material its surface is inevitably different regarding chemical reactivity. Because each surface is the termination of the three-dimensional structure of a material, atoms on one side of the surface lacks near neighbour atoms altering the electronic nature of these atoms. As a consequence surface atoms possess higher reactivity compared to atoms in the bulk. In their attempt to reduce free energy, surface atoms tend to bind to any available reactive molecule to reach a more favourable energy state. When a biomaterial is incorporated into the body it will be surrounded by an aggressive multi-component, aqueous medium containing a variety of active species like ions, proteins, enzymes, and other biomolecules with reactive functional groups. This will result in a complex system of chemical interactions at the material-tissue interface determining the biocompatibility of the introduced material and its proper functioning into the body. The study of the chemical interactions at the material-tissue interface therefore is a key element to develop implant materials with high biological acceptance and a high level of functionality.

Based on their principal atomic and molecular structures, in this chapter, the chemical behaviour of the different classes of biomaterials will be discussed with particular reference to the conditions to which they are exposed in the human body.

2 The Role of Water in the Interaction Between Biomaterials and the Living Matter

Water is the predominant chemical component in the human body and in other living organisms. It accounts about 70% of the weight of all cells and most reactions in a cell takes place in aqueous media (Vogler 2004). In a water molecule two hydrogen atoms are covalently linked to a single oxygen atom. The electronegative oxygen attracts electrons much more strongly than hydrogen resulting in a net positive charge on the hydrogen atoms and a net negative charge on the oxygen atom (Fig. 1). Due to the charge on each of these atoms the water molecule has a net dipole moment. When a water molecule with its positively charged region (i.e. its two hydrogen atoms) comes into the vicinity of the negatively charged part of another water molecule, the electrostatic attraction may lead to a weak interaction called hydrogen bonding. Hydrogen bondings in water are much weaker than covalent ones and quite transient in nature persisting only for a very short time. But each water molecule can form hydrogen bondings with two neighbouring water molecules via its two hydrogen atoms resulting in the formation of a three-dimensional (3D) network. To illustrate this property the concept of Lewis acidity and basicity, common in general chemistry might be a helpful tool (Vogler 2004). A Lewis acid is a molecule that can accept electrons or more generally electron density from a donor molecule. In contrast a Lewis base is an electron density donor. Water is an amphoteric molecule in which hydrogen atoms act as a Lewis acid accepting electron density from the unshared electron pairs on the oxygen, the Lewis base of a neighbouring water molecule. In this concept water forms a 3D network through Lewis acid-base self-association reactions.

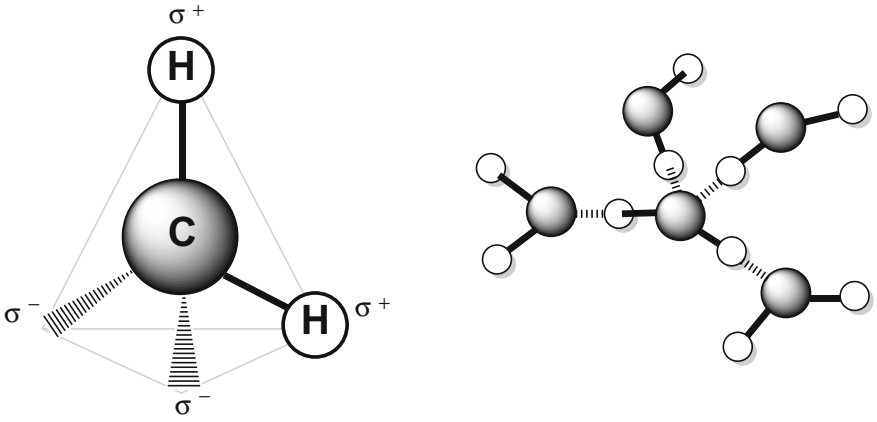

Fig. 1 Molecule structure of water (*left*) and formation of hydrogen bond network derived from five water molecules (*right*)

A very important chemical outcome of this propensity to self-associate and form 3D networks is the specific behaviour of water as a solvent for ions containing positive or negative charges and for polar compounds like alcohols, sugars, DNA, RNA, and most proteins. Ionic or polar compounds are surrounded ("hydrated") by water molecules which are of relatively small size (~3 Å). The partially negative dipole ends of the water are attracted to positively charged components of the solute, and vice versa for the positive dipole ends (Vogler 2004; Alberts et al. 2002).

In contrast to those hydrophilic substances, hydrophobic compounds like hydrocarbons that are largely non-polar can not be solved by water. Nonpolar substances tend to aggregate in aqueous solution and exclude water molecules. This hydrophobic effect is fundamental to the organization of lipids into bilayers, a key structural element of life. In addition, this effect drives protein folding which is important in biomaterials because it is involved in the reaction of proteins at material surfaces like denaturation at material surfaces.

At surfaces water shows different interaction behaviour. On certain surfaces commonly termed hydrophilic, water spreads and on other hydrophobically called surfaces water beads up. Using the Lewis acid-base concept hydrophilic surfaces can be distinguished from hydrophobic ones by the presence of Lewis acid or base functionalities able to interact with water molecules by competition for hydrogen bonds and disruption of the bulk water structure (Fig. 2).

The response of cells to a biomaterial is a key factor in the determination of the success of biomedical implants. It has been assumed that this biological response occurs by interactions with material that resides in the same thin surface region that affects water wettability within a material thickness dimension of not more than a few nanometers (Vogler 2004). It is further believed that cells do not directly interact with the material surface itself but with proteins bound to the surface of the

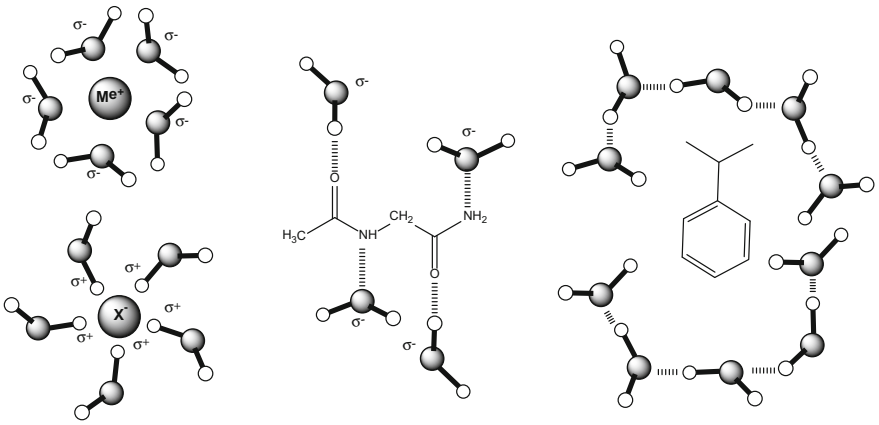

Fig. 2 Behaviour of charged molecules (*left*), polar, non-charged substances (*middle*), and hydrophobic compounds (*right*) in aqueous medium

implant material. This process of protein adsorption takes place almost immediately upon the material comes into contact with blood. Consequently, cells, once arriving the surface do not see the biomaterial surface but instead the protein coating on the biomaterial. The nature and ability of deposited proteins to interact with cells in a specific way dictates the initial cellular and subsequent host responses. It is strongly assumed that wetting of the material surface plays an import role in the interaction processes of proteins and cells with the hydrated interface, maybe through or by displacing of the so-called vicinal water layer that is more or less bound to the surface depending on the strength of the original water-surface interaction (Vogler 2004).

In addition to the unique role of water as solvent and wetting agent for biomaterial surfaces, it can also directly act as chemical agent attacking biodegradable material structures. Most of the synthetic designed-to degrade polymeric materials like polylactides, and their copolymers are subjected to cleavage of hydrolytically sensitive bonds. The small water molecules are able to diffuse into polymeric structures and dependent on the ratio of hydrolytic degradation rate and rate of diffusion a surface erosion process occurs solely on the material surface or a more or less homogeneous bulk erosion process takes place. Due to its Lewis acid-base characteristics, as mentioned above, water containing catalytic substances present in the body fluid (e.g. acid or enzymes) are able to cleave polar linkages like e.g. ester bonds in polymers. In the case of polylactides, lactic acid is formed which is a natural product of muscular contraction in animals.

Overall water is an active participant in biological systems and its special mediating role in many biochemical processes and even chemical reactions must be considered to study the complex interactions between biomaterials and the surrounding tissue.

3 Chemical Properties of Different Classes of Biomaterials

Biomaterials currently used for biomedical applications include metals and alloys, ceramics, and polymers. As described above the chemical properties, and as a consequence, the application potential of these materials is governed by their atomic and molecular structures. In the following part basic structural aspects of the three major biomaterial classes will be reviewed in relation to their specific chemical properties.

3.1 Metals and Alloys

Three different groups of metallic materials dominate the medical field of applications: stainless steel, cobalt-chromium-molybdenium and cobalt-nickel alloys,

and pure titanium and titanium alloys (Table 1). To a minor extent also gold alloys, platinum group metals and tantalum are used (Park and Kim 2003; Pilliar 2009).

Metals are characterized by metallic interatomic bondings. At atomic level metals consist of a positively charged ion core with valence shell electrons forming a cloud of loosely electrons around the metal ions. They are built up of repeating unit cells with a specific number of atoms in specific positions maximizing the numbers of nearest-neighbor atomic contacts. Among the various known unit cells found in crystalline lattice structures, metals and alloys used as biomaterials often form either face-centered cubic, body-centered cubic or hexagonal close-packed unit cells (Fig. 3; Cigada et al. 2002). The close positioning of neighbouring atoms and the shared electron cloud result in the fact that the metallic bonds are non-directional and electron movement within metals is much easier than in materials with ionic or covalent bondings.

These specific features of the metallic bond determine the common properties of this biomaterial class especially the high mechanical strength of many metals, its plastic deformation ability as well as the high thermal and electric conductivity. Despite these favourable properties pure metals are often too soft, brittle or tend to corrode rapidly. To overcome these drawbacks metals are commonly used as alloys as it is the case of 316L stainless steel, cobalt-chromium-molybdenum alloy, and titanium alloys. Alloys are formed by two or more different metals or also non-metallic elements (e.g. carbon, hydrogen) and conventionally manufactured by melting the components together.

Table 1 Chemical compositions of selected alloys used as implant materials (Brunski 2004)

Elements	Stainless Steel	Co-Cr-Mo	Pure Titanium	Ti-6Al-4 V
	316L	F75 (Vitallium)	Cp-Ti, grade 4	
Fe	60–65	Max. 0.75	Max. 0.5	Max. 0.25
Cr	17.00–20.00	27.0–30.0		
Ni	12.00–14.00	Max. 2.5		
Mo	2.00–3.00	5.0–7.0		
Mn	Max. 2.0	Max. 1.0		
Co		58.9–69.5		
Ti			Balance	88.9–90.8
Al				5.5–6.5
V				3.5–4.5
Cu	Max. 0.5			
Si	Max. 0.75	Max. 1.0		
C	Max. 0.03	Max. 0.35	Max. 0.10	Max. 0.08
N	Max. 0.1		Max. 0.05	Max. 0.05
P	Max. 0.025			
S	Max. 0.01			
O			Max. 0.40	Max. 0.13
H			Max. 0.0125–0.015	Max. 0.0125

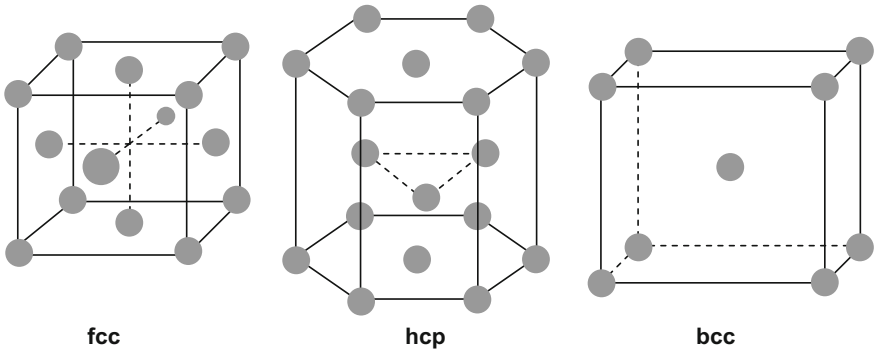

Fig. 3 Common crystal structures of metals: face-centered cubic (fcc), hexagonal close-packed (hcp), and body-centered (bcc)

In contrast to the above mentioned ideal crystal structures, real metal crystals contain lattice defects like vacancies, dislocations or grain boundaries spread throughout the structure. The presence of such defects strongly influences the physical and chemical properties of the metallic material.

The immersion of a metal or metal alloy in physiological environments can lead to corrosion, an electrochemical process resulting in the degradation of the metallic material (Pourbaix 1984; Virtanen 2008; Angelini et al. 2002). Corrosion degradation of implants not only means loss of mass, mechanical stability, and functionality but equally important the release of corrosion products into the living tissue and the flow of a corrosion current causing very often cytotoxic or allergic reactions to the cells surrounding the implant but also to cells at remote locations of the body after transport of corrosion by-products to distant sites inside the body.

Corrosion occurs when electrochemical reactions take place on a metallic surface in the human body fluid acting as a complex electrolyte. Two reactions occur, the anodic oxidation (1) which yields metallic cations, and the cathodic reaction in which the electrons generated in (1) are consumed. The exact cathodic reaction depends on the nature of the electrolyte.

$$\mathrm{Me_{(s)}} \longrightarrow \mathrm{Me^{2+}_{(aq)}} + 2\mathrm{e^-} \tag{1}$$

$$2\mathrm{H^+_{(aq)}} + 2\mathrm{e^-} \longrightarrow \mathrm{H_{2(g)}} \tag{2}$$

$$\mathrm{O_{2(g)}} + 4\mathrm{H^+_{(aq)}} + 4\mathrm{e^-} \longrightarrow 2\mathrm{H_2O_{(g)}} \tag{3}$$

$$\mathrm{O_{2(g)}} + 2\mathrm{H_2O_{(aq)}} + 4\mathrm{e^-} \longrightarrow 4\mathrm{OH^-_{(aq)}} \tag{4}$$

The most important reactions are hydrogen reduction (2) and the reduction of dissolved oxygen under acidic conditions (3) and in neutral or basic solution (4).

As a basic principle the rate of anodic oxidation reaction must be equal the rat of the cathodic reduction reaction (Williams and Williams 2004). Examining corrosion from a thermodynamic point of view it has to be considered that when a metal comes into contact with the solution there will be a net dissolution of metal ions since the Gibbs free energy ΔG for the dissolution reaction is less than for the reverse reaction. This leaves the metal with a net negative charge thus making it more difficult for the cations to leave the surface and increasing the ΔG for the dissolution reaction. There will come a point when the ΔG for the dissolution reaction will equal the ΔG for the reverse reaction. At this point a dynamic equilibrium is reached and a potential difference will be set up across the charged double layer surrounding the metal. This potential difference is a characteristic parameter of a metal and can be measured under standard conditions against a standard hydrogen electrode to obtain the standard electrode potential for this metal. The list of standard hydrogen electrode potentials (Table 2), called the electrochemical series, is a general guide for the reactivity of metallic materials in aqueous media.

Metals at the top of the list are the noble, relatively non-reactive ones whereas at the bottom of the list are the most reactive metals.

Thus in theory corrosion can be predicted from standard electrode potentials. However, irrespective of the standard electrode potentials, the corrosion resistance of many metals is strongly influenced by their ability to become passivated. For this reason various metals and alloys with negative standard electrode potential like titanium and cobalt-chromium alloys can be used as surgical implants in medicine.

Table 2 The electrochemical series: Standard electrode potential for reduction reactions of hydrated ions of selected metals (Marek 2009)

Metal	Reaction	Potential (V)
Gold	$Au^{3+} + 3\ e^- \leftrightarrow Au$	1.498
Platinum	$Pt^{2+} + 2\ e^- \leftrightarrow Pt$	1.188
Palladium	$Pd^{2+} + 2\ e^- \leftrightarrow Pd$	0.987
Silver	$Ag^{+} + e^- \leftrightarrow Ag$	0.799
Mercury	$Hg^{2+} + 2\ e^- \leftrightarrow Hg$	0.788
Copper	$Cu^{2+} + 2\ e^- \leftrightarrow Cu$	0.337
Hydrogen	$2\ H^{+} + e^- \leftrightarrow H_2$	0.0
Tin	$Sn^{2+} + 2\ e^- \leftrightarrow Sn$	−0.136
Molybdenum	$Mo^{3+} + 3\ e^- \leftrightarrow Mo$	−0.200
Nickel	$Ni^{2+} + 2\ e^- \leftrightarrow Ni$	−0.250
Cobalt	$Co^{2+} + 2\ e^- \leftrightarrow Co$	−0.277
Iron	$Fe^{2+} + 2\ e^- \leftrightarrow Fe$	−0.440
Chromium	$Cr^{3+} + 3\ e^- \leftrightarrow Cr$	−0.744
Tantalum	$Ta^{5+} + 5\ e^- \leftrightarrow Ta$	−0.810
Zirconium	$Zr^{4+} + 4\ e^- \leftrightarrow Zr$	−1.539
Titanium	$Ti^{2+} + 2\ e^- \leftrightarrow Ti$	−1.630
Magnesium	$Mg^{2+} + 2\ e^- \leftrightarrow Mg$	−2.360
Calcium	$Ca^{2+} + 2\ e^- \leftrightarrow Ca$	−2.870

Because of their high reactivity these metals or alloys are able to react with oxygen in ambient air forming an insoluble, thin and very stable oxide or hydroxide layer on the implant metals protecting the underlying metal. The formed oxides or hydroxides are of ceramic nature which means that they are electrical insulators reducing or completely preventing the electrochemical reaction. The stability of the oxide or hydroxide layer therefore determines the overall corrosion resistance.

Currently metals or alloys are clinically applied as permanent implants like endoprostheses, dental implants, cardiovascular stents or pacemaker cases. In all of these cases corrosion or other types of degradation are undesired reactions jeopardizes the success of the implant. Considerable research is therefore directed to the development of corrosion-resistant metallic implant materials. However in some cases implants are only temporary needed in the human body for example to support tissue regeneration or to release a drug from a suitable carrier. The controlled and complete degradation of those materials after fulfilling their function is advantageously because no surgical removal of the implant is needed and no foreign material, which often is a source of adverse reactions, remains in the body.

Biodegradable materials known from polymers, bioglasses or different calcium phosphates are already clinically applied as sutures, osteosynthesis materials, bone substitutes and other types of implants. In recent years also metals or metal alloys including magnesium, iron or zinc have been intensively studied to act as biodegradable implants (Niinomi et al. 2012; Witte et al. 2008; Chen et al. 2014). Among these metals, up to now only magnesium and its alloys have found remarkable attention aiming to combine the biodegradation ability with the favorable mechanical properties of metals in an implant material usable also in load-bearing implants.

As expected from the position of magnesium in the electrochemical series conventional as-cast magnesium material readily reacts with water forming magnesium hydroxide and hydrogen gas according to the following overall reaction (5):

$$\mathrm{Mg_{(s)} + 2H_2O_{(aq)} \rightleftharpoons Mg(OH)_{2(s)} + H_{2(g)}} \tag{5}$$

Magnesium hydroxide is able to act as a corrosion protective layer in water but it loses this function with an increasing chloride ion concentration in the medium due to conversion into highly soluble magnesium chloride. The uncontrolled release of larger amounts of hydrogen is a major concern to use magnesium and its alloys in clinical applications.

During the last decade various strategies have been proposed to overcome this problem by a continuous adjustment and control of the degradation rate of magnesium and magnesium alloys. Among these approaches is the fabrication of ultra-pure magnesium, the design of magnesium alloys using alloying elements inducing a specific microstructure, especially grain refinement, and the development of inorganic or organic (polymeric) coatings for magnesium implants (Hornberger et al. 2012; Reifenath et al. 2011).

3.2 Ceramics and Bioactive Glasses

Ceramics and glasses are materials composed of metallic and nonmetallic elements held together by ionic and/or covalent bonds (Park 2008; Turner 2009). Ceramics, in which ionic bonds dominate, combine a metal with positive charge and a nonmetal with anionic charge. Often the anions form a regular three-dimensional lattice providing interstitial sites into which the cations fit resulting in the perfect coordination. The arrangement of cations and anions in the crystal unit cell must meet the ionic radius ratio requirements and ensure the proper charge balance. As an example, in alumina the oxygen ions (O^{2-}) form a close packed hexagonal unit cell in which the octahedral sites are occupied to two thirds by aluminium ions (Al^{3+}, Fig. 4, left). In contrast zirconia, another important bioceramic, forms a face centered cubic unit cell of zirconium (Zr^{4+}) in which the oxygen ions (O^{2-}) occupy the tetrahedral sites (Fig. 4, right) (Turner 2009). In both arrangements a regular pattern with densely packed ions is ensured resulting in a strong ionic bonding throughout the structure. In ceramics with predominantly covalent bonding adjacent atoms share electrons resulting in a fixed number of strong directional bonds throughout the structure. Often those ceramics are characterized by the formation of extended chains, sheets, or three-dimensional networks.

Some ceramics if melted do not develop a crystal structure upon cooling. The individual atoms have nearly the ideal number of nearest neighbors but an orderly repeating arrangement is not maintained throughout the structure. Such compounds are called glasses. Glass-ceramics are glasses that can be transformed in a two-step process including a devitrification into a fine-grained polycrystalline material.

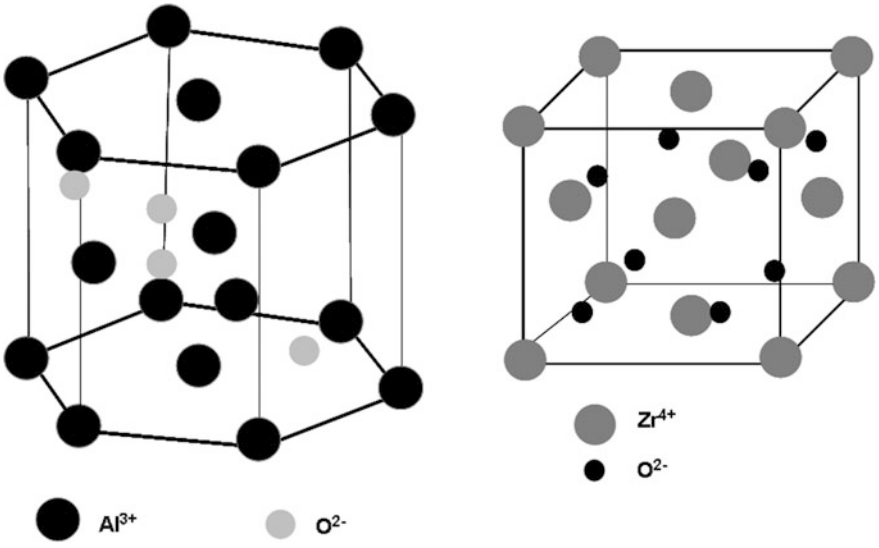

Fig. 4 Hexagonal alumina (*left*) and cubic zirconia (*right*)

Based on the mentioned structural variety of ceramics, glasses, and glass-ceramics it becomes obvious that these materials strongly differ in their chemical behavior including biodegradation and surface reactivity.

The mechanism and rate of degradation of ceramics and glasses depend on their particular chemical composition and structure. Whereas the clinically used oxide ceramics alumina and zirconia are regarded to be bioinert materials exhibiting virtually no degradation, calcium phosphates and various bioglasses are well known biodegradable materials with graded degradation rates.

Both alumina and zirconia have considerable advantage over other materials, especially metals, due to their inertness resulting in a high biocompatibility and non-sensitization of tissue (Turner 2009; Chevalier 2006). Their excellent in vivo wear and friction properties make them suitable for artificial joint surfaces. Although both ceramics have a high compression strength, they are relatively brittle and tend to fracture under tension.

Most alumina used for implant fabrication is either polycrystalline highly dense material of high purity (>99.5%) or artificially grown single crystal material (Park 2008). In the polycrystalline material, key factors determining the mechanical properties are the grain size, grain size distribution, and porosity. Alumina is thermodynamically stable up to temperature of 2000 °C.

The chemistry of zirconia is more complex than the alumina ones. Zirconia can exist in three different phases depending on the temperature and environment. The monoclinic phase transforms to a tetragonal structure at 900–1220 °C and from this tetragonal structure to a cubic phase at 2370 °C. There is a 3–5% volume increase associated with the tetragonal to mono-clinic transformation (Park 2008). As a result cooling down pure zirconia from its sintering temperature can lead to cracking. Therefore orthopaedic-grade zirconia contains small quantities of stabilizing agents (5 wt% Y_2O_3, 2 wt% HfO_2, and 0.5 wt% Al_2O_3) which are added for stabilization. More than 95% of the zirconia is in the metastabile tetragonal phase whereas the remainder is either cubic or monoclinic zirconia (Park 2008). The grain size is kept below 0.5 μm to ensure the tetragonal phase remains stable under physiological conditions (Park 2008). During the last decades in a promising approach the combination of both alumina and zirconia in composite ceramics was investigated resulting in the so called alumina toughened zirconia (ATZ) or zirconia toughened alumina (ZTA) dispersion ceramics (Piconi et al. 2003; Gadow and Kern 2010). These materials show improved mechanical properties, especially a higher fracture toughness and reliability (De Aza et al. 2002; Kelly and Denry 2008).

Bioactive ceramics which are so called due to their active interplay with tissues are mainly calcium phosphates, a complex class of chemical compounds with its most prominent members, hydroxyapatite and tricalcium phosphate. Calcium phosphates have a behavior which depends directly on its chemical composition and structure. Hydroxyapatite being similar to the mineral phase of bone and teeth crystallizes into hexagonal rhombic prisms (Fig. 5). It comprises a framework of PO_4^{3-} tetraeders with a central P^{5+} ion and O^{2-} ions at the four corners. In a similar manner the $(OH)^-$ groups are ionically bonded.

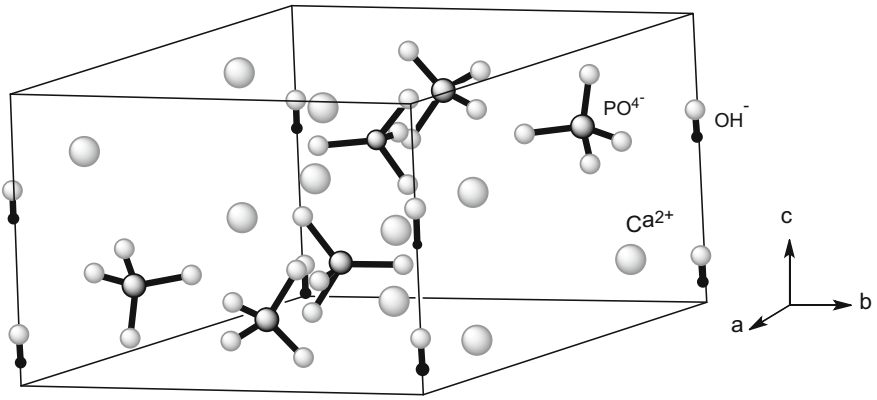

Fig. 5 Unit cell of hydroxyapatite (Ren et al. 2010)

Hydroxyapatite can be synthesized by different procedures from various Ca- and P-containing starting chemicals as well as biogenic sources. An overview about important synthesis methods is given in Table 3.

The route and conditions of the synthesis of hydroxyapatite is greatly influencing its physical and chemical characteristics, especially the rate of resorption. The quality of the obtained hydroxyapatite is commonly represented by values assumed by the theoretical stoichiometric Ca/P ratio of 1.67. There is a tendency in the hydroxyapatite structure that ions in the lattice are substituted by other foreign ions. For example hydroxyl or phosphate ions can be easily substituted by carbonate, hydroxyl or by flouride ions, phosphate ions by silicate ions and calcium ions can be substituted by magnesium ions (Hench and Best 2004).

Hydroxyapatite is insoluble in an alkaline solution but soluble in acidic solutions. In distilled water hydroxyapatite is only slightly soluble but the solubility is increased by the addition of electrolytes. The solubility of sintered hydroxypatite is very low. Hydroxyapatite is highly biocompatible which seems to be a result of a direct chemical bonding to proteins, lipids and other organic compounds present in hard tissue.

Besides hydroxyapatite, there are various other calcium phosphates differing in their chemical composition, structure and their characteristic properties. Table 4 gives an overview on these calcium phosphates used in medical applications.

Among these compounds especially tricalcium phosphate (TCP) in its monoclinic α- and rhombohedral β-polymorphs are widely used as bone substitutes in orthopaedics and dentistry. (Carrodeguas and De Aza 2011; Liu and Lun 2012; Dorozhkin 2011). Due to the structural differences of the both polymorphs, α- and β-TCP differ in their chemical properties. α-TCP has slightly higher water solubility than β-TCP. This was also observed in in vivo-studies. Furthermore it was found in

Table 3 Important synthesis procedures for hydroxyapatite (HA) (Park 2008; Krajewski and Ravaglioli 2002; Sadat-Shojai et al. 2013)

Procedure	Starting materials	Synthesis conditions	Properties of HA
Solid-state reaction	$Ca_3(PO_4)_2$ + $CaCO_3$ $Ca_2P_2O_7$ + $CaCO_3$	900–1300 °C	Ca/P = 1.67, large grain size, irregular forms
Wet chemical method	$Ca(NO_3)_2$ + $(NH_4)_2HPO_4$ $Ca(OH)_2$ + H_3PO_4	r. t. to 100 °C, pH = 7–10	Ca/P < 1.67, fine irregular crystals, low crystallinity
Emulsion method	$Ca(NO_3)_2$ + H_3PO_4 H_2O/cyclohexan, PEG-nonylphenol	pH = 7, r. t.—80 °C	Usually non-stoichiometric, small size (nano, narrow distribution)
Hydrothermal method	Wet chemically prepared HA, other calcium phosphates	100–200 °C (1–2 MPa), 300–600 °C (1–2 kbar)	Ca/P = 1.67, fine single crystals or large crystals, often needle-like morphology
Sol-gel preparation	Gel + Ca^{2+} PO_4^{3-}, e.g. $Ca(OC_2H_5)_2$ + P $(OC_2H_5)_3$	r. t.—60 °C, pH = 7–10	Other calcium phosphates as impurities
Molten salt synthesis	$(NH_4)_2HPO_4$ + $Ca(NO_3)_2$ K_2SO_4, KCl, KBr, $CaCl_2$	1080–1200 °C	Ca/P ~ 1.67, Large crystals
Mechano-chemical preparation	$CaHPO_4$ + CaO ($CaCO_3$)	High-energy mechanical activation	Usually non-stoichiometric CaP ratio, small crystals, diverse morphology
Synthesis from biogenic sources	Biowaste (bovine bones, fish-scales, egg shells), coral, sea shell	Various processes (calcination, hydro-thermal process)	Ca/P ~ 1.67, diverse morphology, high degree of crystallinity

Table 4 Calcium phosphates used in biomedical applications and their properties (Dorozhkin 2012)

Ca/P ratio	Compound	Formula	Solubility		pH stability
			$-\log K_s$	g/l	
0.5	Monocalcium phosphate monohydrate	$Ca(H_2PO_4)_2 \cdot H_2O$	1.14	~18	0.0–2.0
0.5	Monocalcium phosphate anhydrous	$Ca(H_2PO_4)_2$	1.14	~17	[a]
1.0	Dicalcium phosphate dihydrate (brushite)	$CaHPO_4 \cdot 2H_2O$	6.59	~0.088	2.0–6.0
1.0	Dicalcium phosphate anhydrous (monetite)	$CaHPO_4$	6.90	~0.048	[a]
1.33	Octacalcium phosphate	$Ca_8(HPO_4)_2(PO_4)4 \cdot 5H_2O$	96.6	~0.0081	5.5–7.0
1.5	α-Tricalcium phosphate	$\alpha\text{-}Ca_3(PO_4)_2$	25.5	~0.0025	[b]
1.5	β-Tricalcium phosphate	$\beta\text{-}Ca_3(PO_4)_2$	28.9	~0.0005	[b]
1.2–2.2	Amorphous calcium phosphate	$Ca_xH_y(PO4)_z \cdot nH_2O$; n = 3–4.5, 15–20% H_2O	25–33[c]	[c]	5–12[d]
1.5–1.67	Calcium-deficinent hydroxyapatite	$Ca_{10-x}(HPO_4)_x(PO_4)_{6x}(OH)_{2-x}$	~85	~0.0094	6.5–9.5
1.67	Hydroxyapatite	$Ca_{10}(PO_4)_6(OH)_2$	116.8	~0.0003	9.5–12
2.0	Tetracalcium phosphate	$Ca_4(PO_4)_2O$	38–44	~0.0007	[b]

[a]Stable above temperatures of 100 °C; [b]This compound cannot be precipitated from aqueous solution; [c]Cannot be measured precisely; [d]Always metastable

some studies that during the in vivo-resorption of α-TCP hydroxyapatite is formed. Because the rates of degradation of calcium phosphates increase with decreasing Ca/P ratio, tricalcium phosphate with a Ca/P ratio of 1.5 is more rapidly resorbed compared to hydroxyapatite.

In principle the rate of biodegradation (resorption) of the different calcium phosphates which is a major application-related characteristic of these materials is affecting by different factors:

- Chemical parameters (Ca/P ratio, atomic and ionic substitution, impurities)
- Physical characteristics (state of compaction, grain microstructure, porosity, crystallite size, surface area)
- Physicochemical dissolution, which depends on the solubility product of the specific calcium phosphate and local pH of the environment
- Biological factors (cell type surrounding the implant, phagocytosis, age, sex, hormone levels).

About 30 years ago it was first discovered that certain compositions of glass and glass-ceramics are able to bond to bone (Hench 1988). Later it was observed that some glass compositions even bond to soft tissue (Wilson et al. 1981).

Further research has shown that proper specification of the glass composition results in control over the rate of this bonding. Investigating a wide range of glass compositions it has been found that the bone bonding response can vary with the constituents (Jones 2013). In principle, bioglass is composed of SiO_2, Na_2O, CaO and P_2O_5 in different proportions (Hench and Best 2004). In contrast to traditional soda-lime glass, silica is present in the glass composition in less than 60 mol% and the glass contains relatively high amounts of sodium and calcium, and a high Ca/P ratio which promotes the formation of apatite crystals whereas silica and calcium can act as crystallization nuclei. The well-known bioglass 45S5 has 45 wt% SiO_2, both 24.5 wt% Na_2O, and CaO, and 6 wt% P_2O_5 resulting in a Ca/P ratio in the order of 5:1. Various other compositional changes have been studied. Importantly the content of alumina must be below 3 wt% to avoid inhibition of the bone bonding. Further examples of glasses and glass-ceramics developed during the last years and their compositions are given in Table 5.

In the aqueous environment of the human body bioactive glass undergo a rapid surface reaction leading to the bonding to the tissue (Hench and Best 2004). In some cases mineralizing bone can be detected at the interface already after one week. This high level of activity is facilitated by the free exchange of ions between the glass and the surrounding body fluid. Dissolution of ions into the aqueous medium is assumed to be the first step of the reaction (Hench and Best 2004). Due to the structural differences between conventional and bioactive glasses with their more open silicate network, bioactive glasses, coming in contact with aqueous solutions (e.g. body fluids), start to dissolve and release ions (Hench 1991). It is assumed that in the case of the 45S5 bioglass, soluble silicate species are released due to a progressive hydrolysis of the glass network (Brauer 2015). The release of calcium and phosphate ions under physiological conditions soon leads to super-saturation and deposition of an amorphous $CaO–P_2O_5$-rich layer. Further incorporation of other ions like carbonate, hydroxide, and flouride results in the formation of an amorphous apatite-like layer structurally similar to hydroxyapatite. The adsorption of organic bioactive substances (proteins, glycosaminoglycans) and the adhesion of cells further promote bonding to bone.

Table 5 Selected compositions of bioactive glasses and glass ceramics (in wt%) (Hench and Best 2004; Hench 1999; Vogel and Höland 1987; Gerhardt and Boccaccini 2010)

Component	45S5 Bioglass	Ceravital bioactive	A−W GC	Bioverit III
SiO_2	45	40–50	34.2	
P_2O_5	6	10–15	16.3	45–55
CaO	24.5	30–35	44.9	13–19
Na_2O	24.5	5–10		11–18
CaF2			0.5	
MgO			4.6	
Al_2O_3				6–18
Structure	Glass	Glass ceramic	Glass ceramic	Invert glass

3.3 Polymers

The wide variety of polymers used for medical applications includes natural biopolymers, especially proteins, polysaccharides, glycosaminoglycans, polynucleotides, and natural rubber as well as synthetic polymers like polyalkenes, polyesters, polyethers, polycarbonates, polyamides, polyurethanes, poly (ether-ether-ketone)s, polysulfones, and silicones.

Polymers are large macromolecules generated by the combination of a large number of low molecular weight molecules so called monomers. These monomers contain one or more reactive functional sites to react with other monomers forming the polymer in a chemical or enzymatic polymerization reaction. Most polymers are characterized by a high molecular weight often ranging from 10^4–10^7 g mol^{-1}. It has to be noted that the molecular weight of a defined polymer is not a unique value like it is for small molecules (Parisi et al. 2015). Polymerization reactions normally result in a mixture of single macromolecules differing in the number of incorporated monomeric units, i.e. a polymer with an average molecular weight and a distinct molecular weight distribution is obtained. Two statistically useful definitions of molecular weight are the number-average molecular weight M_n and the weight-average molecular weight M_w where N_i is the number of moles of the species i and M_i is the molecular weight of this species i. The ratio M_w/M_n is the polydispersity index PI which is a measure for the breadth of the molecular weight distribution.

$$M_n = \frac{\Sigma N_i M_i}{\Sigma N_i} \tag{6}$$

$$M_w = \frac{\Sigma N_i M_i^2}{\Sigma N_i M_i} \tag{7}$$

Atoms in polymers are predominantly connected by covalent bonds. These bonds are formed if one or more pairs of valence electrons are shared between two atoms again leading to stable electronic shells. In contrast to ionic bonding where electrons were donated from one atom to another, in a covalent bonding the formed electron pairs belong to both atoms allowing each atom to attain the equivalent of a full outer shell with a stable electronic configuration. Covalent bonds are affected by the electronegativity of the connected atoms. Two atoms with equal electronegativity will make nonpolar covalent bonds such as C–C. Different electronegativities between the connecting atoms create a polar covalent bond such as with for example C–N. Covalent bonding includes many kinds of interactions like σ-bonding in polymers or π-bonding in many monomers or conjugated polymers (see Fig. 6). σ-bonds can rotate almost freely around the bond axis whereas in the C=C π-bond, possessing a smaller bond length compared to a C–C single bond, this rotability is lost.

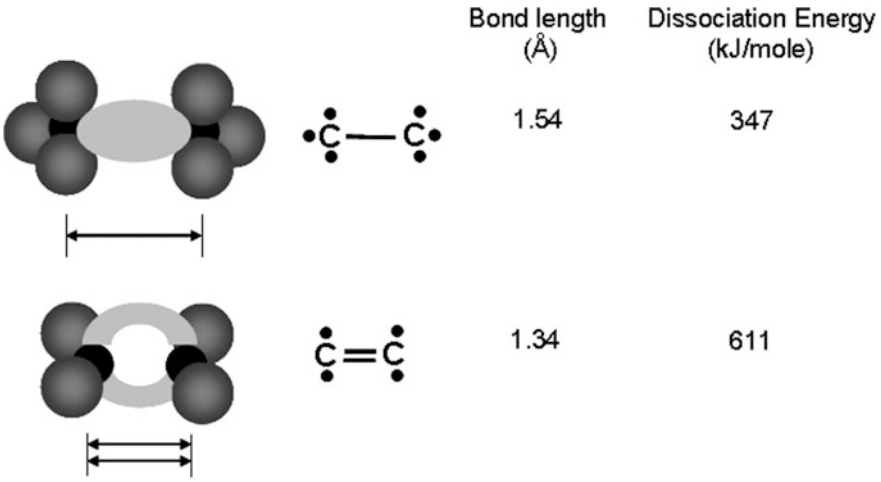

Fig. 6 Covalent bonding of carbon-carbon bonds based on an electron cloud model (Krueger 2004; Billmeyer 1984)

Unless the macromolecules are cross-linked they interact with one another by hydrogen and van der Waals bonds as well as by entanglement. Due to the covalent nature of bonding and with the exception of conductive polymers, electrons in polymers are localized and therefore they are poor thermal and electric conductors.

There are several ways to classify polymers depending on their source (*natural polymers* occurring in plants and animals, *semi-synthetic polymers* derived by chemical modification of natural polymers, and "man made" *synthetic polymers*) but also on different structural parameters:

- Type of monomer (*homopolymers* (1), see Fig. 7) containing only a single type of monomer, *copolymers* (2) or *terpolymers* (3) prepared from two or more monomers and further distinguishable according to the arrangement of the repeating units in the chain as *alternating copolymers* (2a), *block copolymers* (2b), *graft copolymers* (2c), and *random copolymers* (2d)
- Chain structure (*linear polymers* (4) containing long straight chains, *branched polymers* (5) having linear side chains of different lengths along the main chain, *crosslinked polymers* (6) which are three-dimensional networks consisting of long linear chains connected to each other with multifunctional units).
- Tacticity (*isotactic polymers* (7) with the pendant group arranged on the same side of the polymeric backbone, *syndiotactic polymers* (8), containing an alternative arrangement of the pendant groups, and *atactic polymers* (9) in which the pendant groups are arranged randomly).
- Molecular forces (*elastomers* characterized by weak attraction forces between polymeric chains resulting in amorphous materials with high degree of elasticity, *thermoplastics* characterized by intermediate intermolecular forces

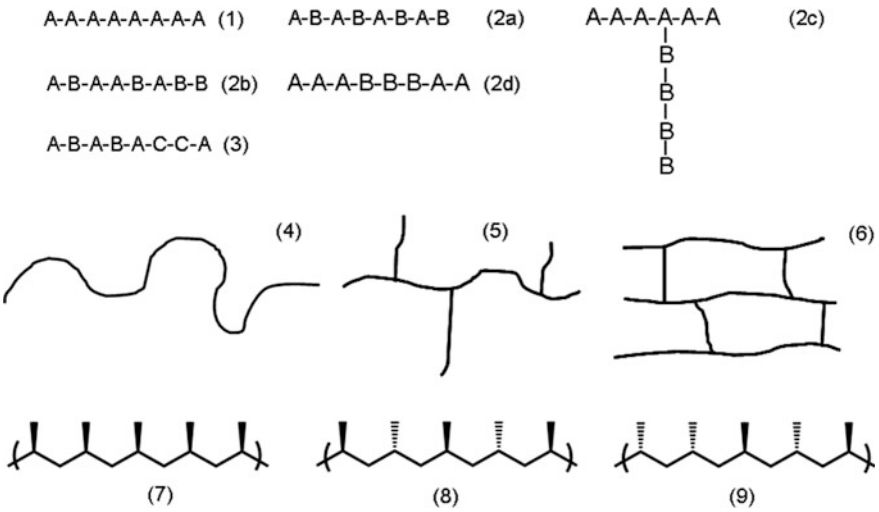

Fig. 7 Classification of polymers with regard to structural parameters (see corresponding numbers in the text above for explanation of the various structures)

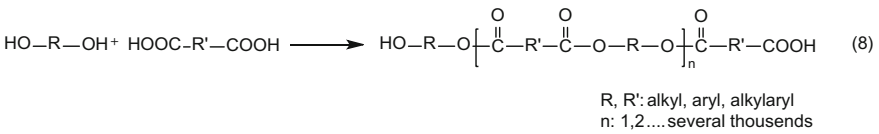

Fig. 8 Synthesis of a polyester as a typical example of a step-crowth polymerzation

between molecules resulting in thermally processible materials, *thermosets* which can not be melted due to crosslinking during heating).

- Molecular weight (*oligomers* characterized by a molecular weight ranging between 500 and 5000 g mol^{-1}, *high molecular weight polymers* having a molecular weight in the range of 10^4–10^6 g mol^{-1}.

Dependent on the above mentioned structural features polymers can form highly ordered, crystalline, semi-crystalline or amorphous structures. Often both crystalline and amorphous regions can be found in one polymer.

Synthetic polymers are synthesized mainly by two polymerization mechanisms, *step-growth polymerization* and *chain polymerization*. In step-growth polymerization reactions reactive monomers containing functional units including carboxylic, hydroxylic or amino groups bond together through an extension of chemical condensation reactions eliminating low molecular weight side products like water or alcohol (Fig. 8) (Cooper et al. 2004).

The formed step-growth polymers (for examples see Fig. 9) can be degraded to their starting monomers upon the addition of the eliminated small molecules.

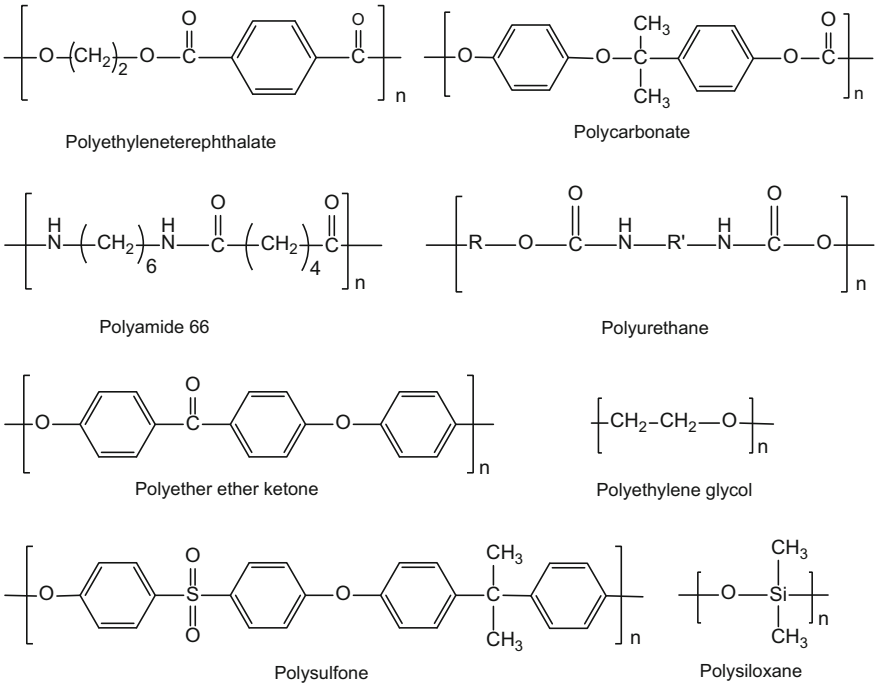

Fig. 9 Polymers synthesized by step-crowth polymerization reactions

Polyesters (e.g. poly(ethylene-terephthalate), polylactides), polyamides or polyurethanes are typical step-growth polymers.

In contrast, chain polymerization involves the linking of unsaturated monomers by the opening of a double bond (Fig. 10). Three main types of chain polymerization, namely free radical polymerization, ionic (cationic and anionic) polymerization and coordination polymerization are known. In general the chain polymerization reaction requires an initiator step (9) able to generate the first active unit and start the chain growth. In the following propagation reaction (10) the monomers are added to the reactive sites onto the growing polymeric chain consisting of an all-carbon backbone of single bonds. The last step is the termination reaction (11), in which the reactive end-site is deactivated.

Well known polymers like polyethylene, polystyrene and polymethylmethacrylate are produced following a chain polymerization mechanism (Fig. 11). The two types of polymerization reactions differ from each other by several points including the rate at which the size of polymer molecules increases, the time required for high monomer conversion, the reaction mechanism, the presence of an active center and a termination reaction (Parisi et al. 2015).

The properties of polymers are strongly influenced by their composition, structure of the chains and side groups, and the molecular weight. Due to their long chains polymers do not crystallize completely but many polymers form

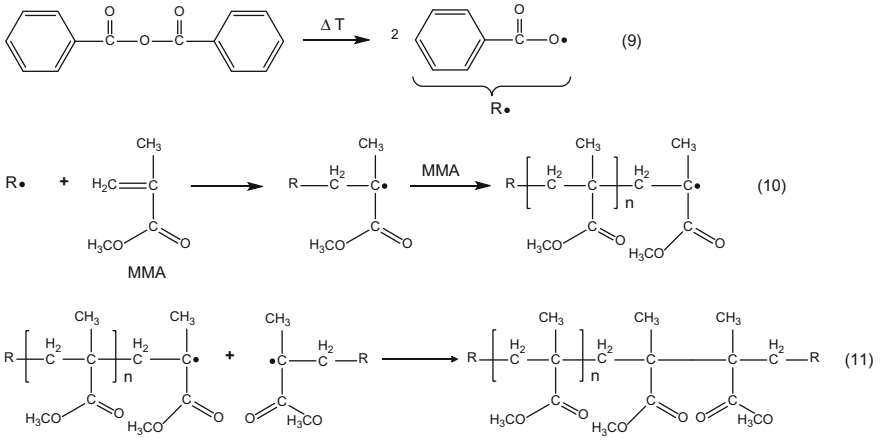

Fig. 10 Reaction mechanism of the radical polymerization of methylmethacrylate as an example for a chain polymerization

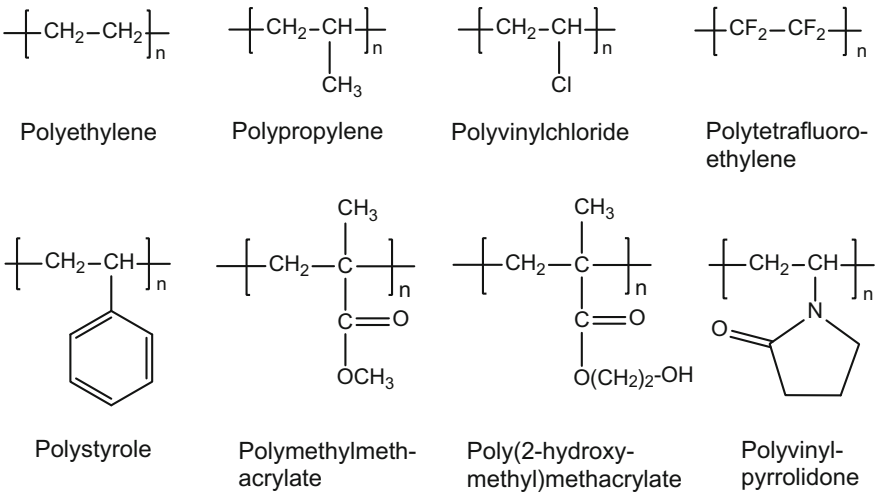

Fig. 11 Polymers synthesized by chain polymerization

semicrystalline structures represented by disordered (amorphous) and ordered crystalline regions. Increasing the molecular weight leads to longer and less mobile polymer chains which results in a more rigid material. It is also important that the polymer chains are equal in length since if there are short chains they will act as plasticizer. Changing the chemical composition of the backbone and the side chain will also change the polymer properties. Substituting the backbone carbon in a –C–C– chain by oxygen will decrease the melting and glass transition temperature

since the chain becomes more flexible (Lee et al. 2003). In the same manner, increasing the size of a side chain in linear polymers will decrease the cristallinity and as a result lowering the melting temperature. Concerning their chemical properties polymers widely differ from each other. With regard to biomaterial applications a key parameter is their behavior in physiological media.

Commonly, polymers do not undergo any chemical changes in vivo and are not degraded to a notable extent during a longer period of time are called bioinert. These polymers are characterized by specific structural elements like a –C–C–, –C–O–C–, or also a –Si–O–Si– backbone. Polymers containing more polar units in their backbone like polyamides, polyurethanes or polyesters can also be made durable against degradation if they contain longer aliphatic or aromatic structure elements within their backbone or if they are cross-linked. Examples of those materials are polyamide 6.6, poly(ethylene-terephthalate) or cross-linked polysiloxane elastomers. Many of these polymers are hydrophobic in nature like polypropylene, polytetrafluoroethylene, polyether-ether-ketones, but also hydrophilic polymeric materials including polyethylene glycols, polyvinylpyrrolidone or poly(2-hydroxyethyl methacrylate) are widely inert to cells and non-degradable materials.

Unlike bioinert polymers there are polymeric materials actively interact with components of the living organism and stimulate specific cellular reactions. Among these materials the most prominent ones are natural polymers, e.g. proteins (Srichana and Domb 2009; Yannas 2004) like collagen, albumin, fibrinogen and elastin as well as polysaccharides (Dräger et al. 2011; Kaplan 1989) and the glycosaminoglycans heparin, heparan sulfate, chondroitin sulfate or even the non-sulfated hyaluronan (Volpi 2006; Schnabelrauch et al. 2013) (Fig. 12) (Table 6).

Collagen, although a structural protein in mammals without chemically reactive side chains, has numerous functions in cell adhesion and regulation. Heparin a high-sulfated glycosaminoglycan has been used as potent anticoagulant for many

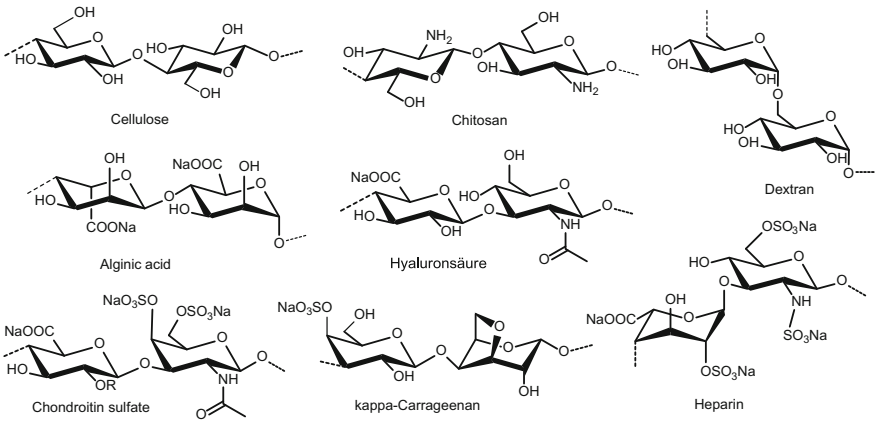

Fig. 12 Selected polysaccharides and glycosaminoglycans used as biomaterials

Table 6 Structural features and chemical properties of proteins used as biomaterials

Protein	Structure	Chemical properties
Collagen (Silver and Garg 1997; Khan et al. 2011)	Protein family comprising of 3 helically arranged polypeptide strains each having a general sequence of –Gly-X-Y- (X fre-quently proline, and Y often hydroxy-proline); e.g. collagen I: 33% glycine, 25% proline and hydroxyproline, MW of native collagen >100,000 g/mol	Triple-helical collagen exists only in acidic solution (film and sponge formation) and is not water-soluble at neutral pH; degradable in the body; stabilization by crosslinking (e.g. glutaraldehyde)
Gelatin (Keenan 1997)	Derivative of collagen, single-strand macromolecule formed by breaking the triple helix-structure of collagen by acidic or alkaline hydrolysis	Water-soluble over wide pH range; thermoreversible sol-gel transitions; chemical crosslinking to tune in vivo-degradation
Albumin (Doppalapudi et al. 2015; Sewald and Jakubke 2002)	Family of globular proteins (most common: serum albumin), non-glycosylated, low molecular mass (~66 kDa), rich on glutamic and asparaginic acid (20–25%) as well as leucine and isoleucine (up to 16%), and cysteine (disulfide bridges)	Easily crystallizable, water-soluble, isoelectric point ~4.6, ampholytic (able to reversibly bind anions and cations), high binding capacity for Ca-, K-, Na-ions, fatty acids, and drugs
Fibrinogen (Weisel and Cederholm-Williams 1997)	Large, complex glycoprotein (MW: 340 kDa) consisting of 3 pairs of non-identical, homologous peptide chains crosslinked by disulfide bonds and 2 pairs of N-linked oligosaccharides	Conversion to insoluble, cross-linked fibrin by action of thrombin (blood clot formation, fibrin adhesives)
Elastin (Gagner et al. 2014)	Fiber protein (molecular weight ~72 kDa) composed of 3-dimensional fiber network of hydrophobic and hydrophilic domains; high contents of glycine, alanine, valine, and proline; in extensively crosslinked, hydrophilic domains high lysine content	Rubber-like, elastic behaviour through block structure and crosslinking which is performed by lysine-derived crosslinker (desmosine) using the copper-depending enzyme lysyloxidase

years in medicine (Gray et al. 2012). Semisynthetic or synthetic polymers containing specific functionalities may also have biological activity. Besides polyanionic polymers (e.g. pentosan polysulfate), some polycationic polymers have been shown to be bioactive. Some polymers carrying quaternary ammonium groups are active against a number of bacteria or fungi, enhance cellular antigen uptake, and exhibit antitumor activities (Kenawy et al. 2007). Polyethyleneimine, a synthetic cationic polymer has been mostly studied as non-viral vector (Godbey et al. 1999).

The major mechanism of these activities based on the attraction and leakage of the negatively charged outer cell surface.

Due to hydrophilic nature of most natural polymers and their polyfunctional character, these materials are predestinated to form hydrogels, an unique class of materials able to adsorb large quantities of water. Hydrogels are crosslinked polymer networks that offer moderate to high physical, chemical, and mechanical stability in the swollen state. They mimic the natural state of many soft tissues in the human body (Omidian and Park 2010). The structure of hydrogels and their properties can be designed for specific applications by selecting suitable starting materials and processing techniques. Furthermore various hydrogels are able to respond to little changes in the environment by altering their properties making hydrogels valuable materials in many biomedical applications. Several natural polymers form hydrogels just by changing physical parameters (e.g. gelatin can be gelled by cooling an aqueous gelatin solution below 35 °C) or by adding physically or chemically crosslinkable substances (formation of alginate gels by addition of calcium salts). Other biopolymers need to be chemically modified by the introduction of crosslinking functionalities including methacrylate, aldehyde, isocyanate, epoxide or thiol groups (Van Vlierberghe et al. 2011).

Biodegradable Polymers denotes polymers which, by means of a chemical or enzymatic hydrolysis in the body undergo conversion to water soluble degradation products.

Depending on the polymer structure three different routes to form degraded water-soluble products are known (Fig. 13). The polymer can have degradable side chains that are hydrolyzed in the body providing residual polymers with hydoxyl, carboxyl or other hydrating groups making the polymer water soluble and excretable from the body. A further route consists in the cross-linking of a water soluble polymer with a hydrolysable cross-linking unit. When placed in the body, hydrolysis of the cross-linking unit results in the formation of the water soluble polymer which can also be excreted. However, in most cases the hydrolysable unit

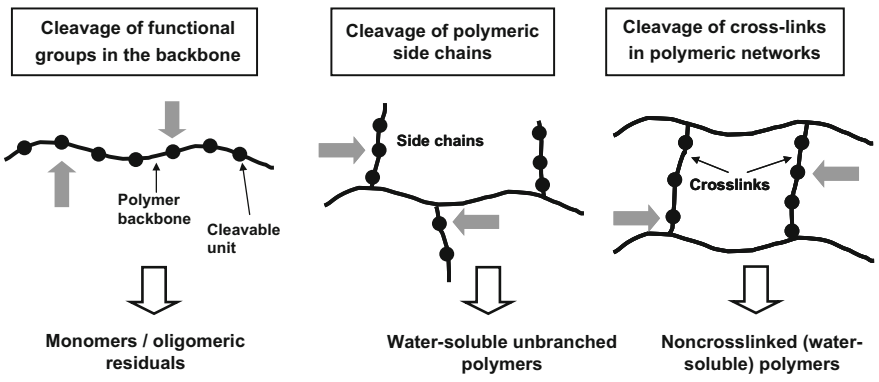

Fig. 13 Degradation routes for biodegradabe polymers

is directly incorporated in the backbone of the polymer chain. When such polymers are placed in the body, the polymer chain is slowly hydrolyzed to form with progressing time ever shorter polymer fragments which at a distinct point of time become water soluble to be excreted or metabolized from the body.

The main material-related factors that determine the overall rate of the degradation process are the chemical stability of the hydrolytically susceptible groups in the polymer backbone, the hydrophilic/hydrophobic character of the repeating unit, the morphology of the polymer including porosity, the initial molecular weight and molecular weight distribution, the device fabrication process, the presence of catalysts and additives, and the geometry of the device implanted in the body. In addition there are several media-related factors influencing the degradation rate including pH, temperature, the presence and concentration of solutes, salts, enzymes, and microbes and the occurrence of stress or strain.

The chemical composition of the polymer chain, i.e. the type of hydrolytically susceptible unit is probably the key parameter determining the rate of degradation. A survey of common hydrolytic bonds appearing in polymer backbones is given in Fig. 14. For example anhydrides tend to hydrolyze faster than ester bonds that in turn hydrolyze faster than urethane or amide bonds. Thus the degradation of the corresponding polymers is in the order: polyanhydrides > polyesters > polyurethanes, polyamides. Based on this knowledge of hydrolytic susceptibility of the polymer backbone structure, it is possible to make predictions about the degradation rate of a given polymer.

Another important parameter affecting polymer backbone degradation is the morphology of the polymer. Polymers can be classified as either amorphous or semi-crystalline. In the crystalline state the polymeric chains are densely packed resisting the penetration of water. Consequently, backbone hydrolysis tends to occur in the amorphous regions of a semi-crystalline polymer and at the surface of the crystalline domains. Among polylactones, poly(L-lactide) and polyglycolide are typical semi-crsystalline polymers whereas poly(D,L-lactide) is amorphous (Tsuji 2010). This is the reason that poly(L-lactide) and poly(D,L-lactide) having an identical chemical composition differ remarkably in their degradation rate and the amorphous poly(D,L-lactide) normally degrades much faster.

During the course of hydrolytic degradation low molecular weight water-soluble oligomers are formed by cleavage of polymer chains and released in the media resulting in a polymer weight loss. Two different basic mechanisms, surface erosion and bulk erosion are known to describe the polymer material degradation (Goepferich 1997) (Fig. 15). Surface erosion takes place when the hydrolytic degradation rate is much higher than the diffusion rate of water within the polymer. The hydrolytic degradation then occurs solely on the polymer surface.

In contrast, bulk erosion takes place when the hydrolytic degradation rate of the polymer is much lower than the diffusion of water within the polymer. As a consequence hydrolytic degradation occurs nearly homogeneously, irrespectively of the depth from the material surface. This might be an open problem because in the final stage of degradation a crash of the whole polymer structure resulting in the release of many polymeric fragments may occur.

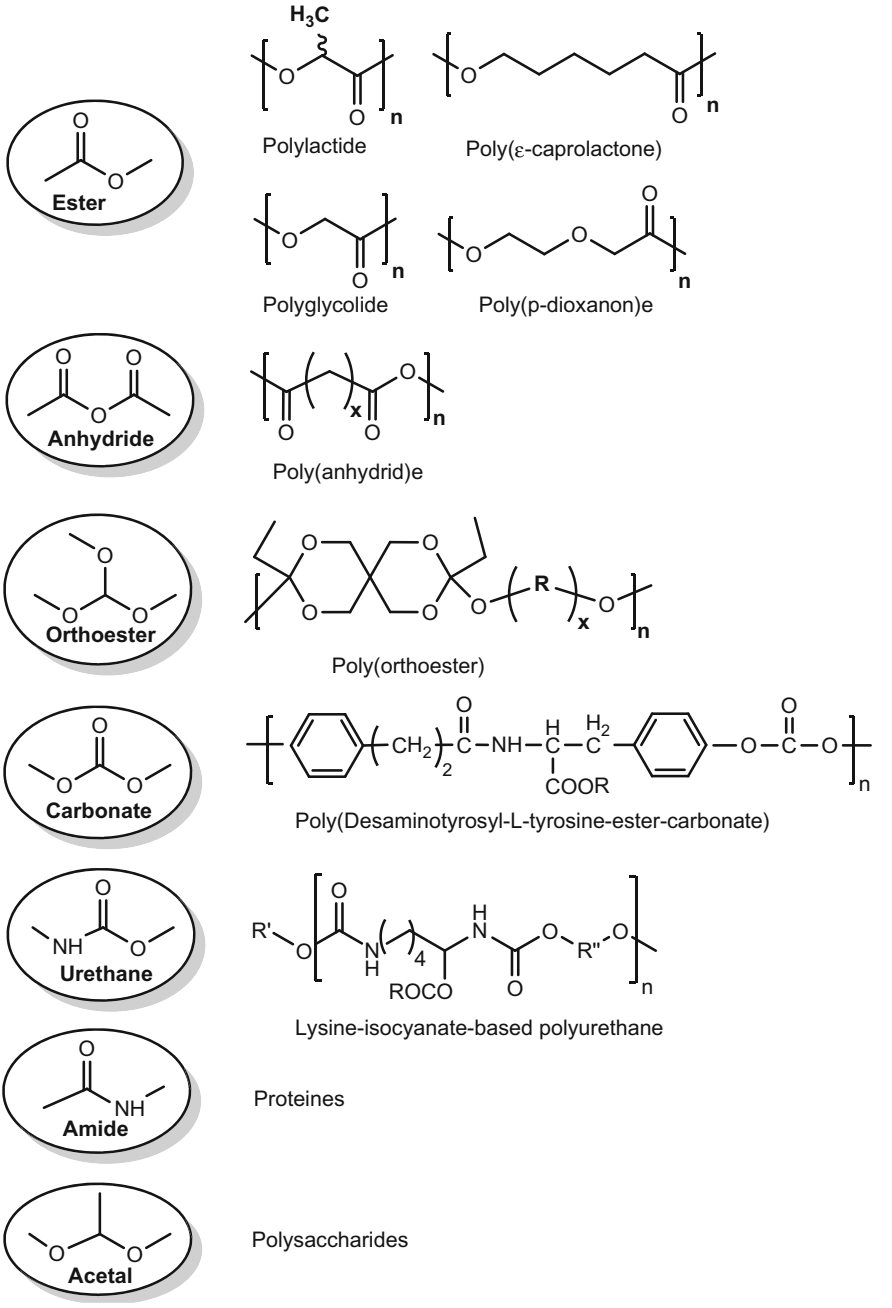

Fig. 14 Different types of hydrolysis-sensitive bonds and examples of biodegradable polymers with those bonds

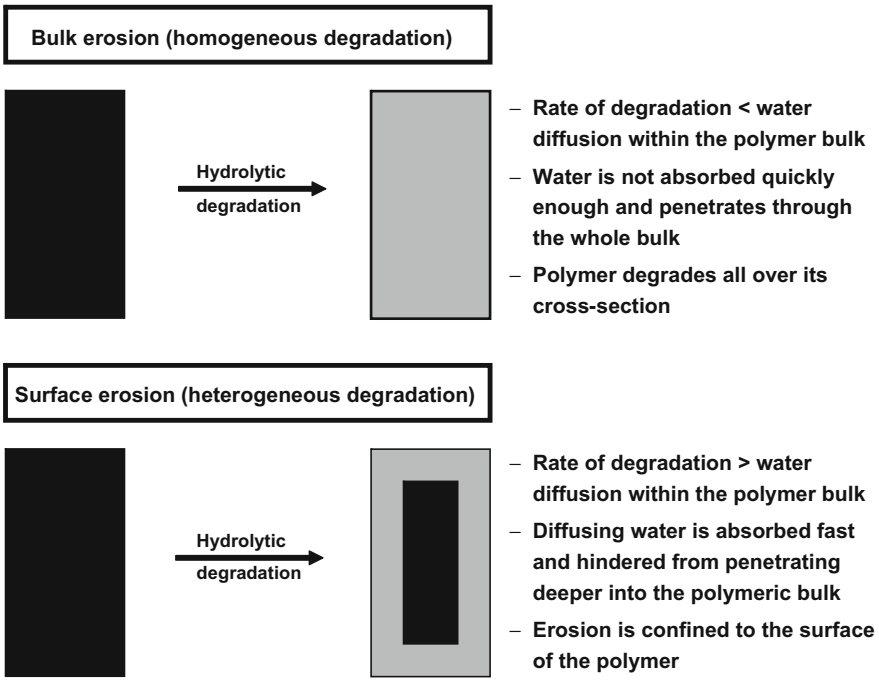

Fig. 15 Bulk and surface erosion of degradable polymers

4 Concluding Remarks

Today a great variety of biomaterials is known differing in their atomic and molecular structure providing a wide range of chemical properties. In the past times the major goal of biomaterial research and development was to provide materials with specific physical properties like mechanical strength, abrasion and fatigue resistance, temperature and medium long-term stability behave more or less inert to the tissue of the living matter. From a chemical point of view it was the intention to create materials that do not react with their environment or if they do to protect these materials by suitable protecting layers. Although this is still a matter of research, in our days a paradigm change occurs and concepts to develop biomaterials interacting with cells and tissues of the living organism in an active way have found growing attraction. Future biomaterial concepts will focus on intervention strategies to actively stimulate chemical and biological processes at the material-tissue interface with the aim to enhance materials and biological performance of implants such as an enhanced lifetime or real integration of the implant. This will render the chemistry of biomaterials without any doubts a much more complex process and a real challenge to generate new materials and material combinations. Besides the bulk chemistry of these future materials the chemistry of biomaterial surfaces will play a decisive role for the success of these materials.

References

Alberts B, Johnson A, Lewis J, Raff M, Roberts K, Walters P (2002) Molecular biology of the cell. Garland Science, New York

Angelini E, Caputo A, Zucchi F (2002) Degradation processes on metallic surfaces. In: Barbucci R (ed) Integrated biomaterials science. Kluwer Academic/Plenum Press, New York, pp 297–324

FW Billmeyer Jr (1984) Textbook of polymer science. Wiley, New York

Brauer DS (2015) Bioactive glasses—structure and properties. Angew Chem Int Ed 54:4160–4181

Brunski JB (2004) Metals. In: Ratner BD, Hoffman AS, Schoen FJ, Lemons JE (eds) An introduction to materials in medicine. Elsevier, San Diego, pp 137–153

Carrodeguas RG, De Aza S (2011) α-Tricalcium phosphate: synthesis, properties and biomedical applications. Acta Biomaterialia 3536–3546

Cigada, A Chiesa R, Pinasco MR, Hisatsune K (2002) Metallic materials. In: Barbucci R (ed) Integrated biomaterials science, Kluwer Academic/Plenum Press, New York, pp 257–296

Chen Y, Xu Z, Smith C, Sankar J (2014) Recent advances on the development of magnesium alloys for biodegradable implants. Acta biomaterialia 10(11):4561–4573

Chevalier J (2006) What future for zirconia as a biomaterial? Biomaterials 27:535–543

Cooke FW (2004) Bulk properties of materials. In: Ratner BD, Hoffman AS, Schoen FJ, Lemons JE (eds) An introduction to materials in medicine. Elsevier, San Diego, pp 23–32

Cooper SL, Visser SA, Hergenrother RW, Lamba NMK (2004) Polymers. In: Ratner BD, Hoffman AS, Schoen FJ, Lemons JE (eds) An introduction to materials in medicine. Elsevier, San Diego, pp 67–79

De Aza AH, Chevalier J, Fantozzi G, Schehl M, Torrecillas R (2002) Crack growth resistance of alumina, zirconia and zirconia toughened alumina ceramics for joint prostheses. Biomaterials 23:937–945

Dee KC, Puleo DA, Bizios R (2002) An introduction to biomaterial interactions. Wiley-Lyss, Hoboken

Dorozhkin SV (2011) Biocomposites and hybrid biomaterials based on calcium orthophosphates. Biomatter 2011, 1, 1–53

Gerhardt L-C, Boccaccini AR (2010) Bioactive glass and glass-ceramic scaffolds for bone tissue engineering. Materials 3:3867–3910

Doppalapudi S, Katiyar S, Domb AJ, Khan W (2015) Biodegradable natural polymers. In: Puoci F (ed) Advanced polymers in medicine. Springer, Cham, pp 32–66

Dorozhkin SV (2012) Biphasic, triphasic and multiphasic calcium orthophosphates. Acta Biomater 8:963–977

Dräger G, Krause A, Möller L, Dumitriu S (2011) Carbohydrates. In: Lendlein A, Sisson A (eds) Handbook of biodegradable polymers. Wiley-VCH, Weinheim, pp 155–193

Gadow R, Kern F (2010) Novel zirconia–alumina nanocomposites combining high strength and toughness. Adv Eng Mater 12:1220–1223

Gagner JE, Kim W, Chaikof EL (2014) Designing protein-based biomaterials for medical applications. Acta Biomater 10:1542–1557

Godbey WT, Wu KK, Mikos AG (1999) Poly(ethylenimine) and its role in gene delivery. J Controlled Release 60:149–160

Göpferich A (1997) Mechanisms of polymer degradation and elimination. In: Domb AJ, Kost J, Wiseman DM (eds) Handbook of biodegradable polymers. OPA, Amsterdam, pp 451–471

Gray E, Hogwood J, Mulloy B (2012) The anticoagulant and antuthrombotic mechanisms of heparin. In: Lever R, Mulloy B, Page CP (eds) Heparin-a century of progress. Handbook of experimental pharmacology, vol 207. Springer, Berlin, pp 43–61

Hench LL (1988) Bioactive ceramics. Ann N Y Acad Sci 523:54–71

Hench LL (1991) Bioceramics: from concept to clinic. J Am Ceram Soc 74:1487–1510

Hench LL (1999) Bioactive glasses and glass-ceramics. Mat Sci Forum 293:27–64

Hench LL, Best S (2004) Ceramics, glasses, and glass-ceramics. In: Ratner BD, Hoffman AS, Schoen FJ, Lemons JE (eds) An introduction to materials in medicine. Elsevier, San Diego, pp 153–170
Hornberger H, Virtanen S, Boccaccini AR (2012) Biomedical coatings on magnesium alloys—a review. Acta Biomater 8:2442–2455
Jones JR (2013) Review of bioactive glass: from Hench to hybrids. Acta Biomaterials 9:4457–4486
Kaplan DL (1989) Introduction to biopolymers from renewable resources. In: Kaplan DL (ed) biopolymers from renewable resources. Springer, Berlin, pp 1–29
Keenan TR (1997) Gelatin. In: Domb AJ, Kost J, Wiseman DM (eds) Handbook of biodegradable polymers. OPA, Amsterdam, pp 307–317
Kelly JR, Denry I (2008) Stabilized zirconia as a structural ceramic: an overview. Dent Mater 24:289–298
Kenawy E-R, Worley SD, Broughton R (2007) The chemistry and applications of antimicrobial polymers: a state-of-the-art review. Biomacromol 8:1359–1384
Khan W, Yadav D, Domb AJ, Kumar N (2011) Collagen. In: Domb AJ, Kumar N, Ezra A (eds) Biodegradable polymers in clinical use and clinical development. Wiley, Hoboken, pp 61–89
Krajewski A, Ravaglioli A (2002) Bioceramics and biological glasses. In: Barbucci R (ed) Integrated biomaterials science. Kluwer Academic/Plenum Press, New York, pp 189–254
Krueger O (2004) Kunststoffe. In: Bargel H-J, Schulze G (eds) Werkstoffkunde. Springer, Berlin, pp 304–335
Lee HB, Khang G, Lee JH (2003) Polymeric biomaterials. In: Park JB, Bronzino JD (eds) Biomaterials: principles and applications. CRS Press, Boca Raton, pp 55–77
Liu B, Lun DX (2012) Current application of β-tricalcium phosphate composites in orthopaedics. Orthopaedic Surg 4:139–144
Marek M (2009) Metal corrosion. In: Narayan R (ed) Biomedical materials. Springer, New York, pp 155–181
Niinomi M, Nakai M, Hieda J (2012) Development of new metallic alloys for biomedical applications. Acta Biomater 8:3888–3903
Omidian H, Park K (2010) Introduction to hydrogels. In: Ottenbrite RM (ed) Biomedical applications of hydrogels handbook. Springer, New York, pp 1–16
Parisi OI, Curcio M, Puoci F (2015) Polymer chemistry and synthetic polymers. In: Puoci F (ed) Advanced polymers in medicine. Springer, Cham, pp 1–31
Park J (2008) Bioceramics: Properties, characterizations, and applications. Springer, New York
Park JB, Kim YK (2003) Metallic biomaterials. In: Park JB, Bronzino JD (eds) Biomaterials: principles and applications. CRC Press, Boca Raton, pp 1–20
Piconi C, Maccauro G, Muratori F, Brach Del Prever E (2003) Alumina and zirconia ceramics in joint replacements. J Appl Biomat Biomech 1:19–32
Pilliar RM (2009) Metallic biomaterials. In: Narayan R (ed) Biomedical materials. Springer, New York, pp 41–81
Pourbaix M (1984) Electrochemical corrosion of metallic biomaterials. Biomaterials 5:122–134
Reifenrath J, Bormann D, Meyer-Lindenberg A (2011) Magnesium alloys as promising degradable implant materials in orthopaedic research. In: Czerwinski F (ed) Magnesium alloys—corrosion and surface treatments. InTech, Rijeka, pp 93–108
Ren F, Leng Y, Xin R, Ge X (2010) Synthesis, characterization and ab initio simulation of magnesium-substituted hydroxyapatite. Acta Biomater 6:2787–2796
Sadat-Shojai M, Khorasani M-T, Dinpanah-Khoshdargi E, Jamshidi A (2013) Synthesis methods for nanosized hydroxyapatite with diverse structures. Acta Biomater 9:7591–7621
Schnabelrauch M, Scharnweber D, Schiller J (2013) Sulfated glycosaminoglycans as promising artificial extracellular matrix components to improve the regeneration of tissues. Curr Med Chem 20:2501–2523
Sewald N, Jakubke H-D (2002) Peptides: Chemistry and biology. Wiley-VCH, Weinheim

Silver FH, Garg AT (1997) Collagen: characterization, processing and medical applications. In: Domb AJ, Kost J, Wiseman DM (eds) Handbook of biodegradable polymers. OPA, Amsterdam, pp 319–346
Srichana T, Domb AJ (2009) Polymeric biomaterials. In: Narayan R (ed) Biomedical materials. Springer, New York, pp 83–119
Tsuji H (2010) Hydrolytic degradation. In: Auras R, Lim L-T, Tsuji H (eds) Poly(lactic acid): synthesis, structures, properties, processing, and applications. Wiley, Hoboken, pp 345–381
Turner IG (2009) Ceramics and glasses. In: Narayan R (ed) Biomedical materials. Springer, New York, pp 3–39
Van Vlierberghe S, Dubruel P, Schacht E (2011) Biopolymer-based hydrogels as scaffolds for tissue engineering applications: a review. Biomacromol 12:1387–1408
Virtanen S (2008) Corrosion of biomedical implant materials. Corrosion of biomedical implant materials 26:147–171
Vogel W, Höland W (1987) The development of bioglass ceramics for medical applications. Angew Chem Int Ed 26:527–544
Vogler EA (2004) Role of water in biomaterials. In: Ratner BD, Hoffman AS, Schoen FJ, Lemons JE (eds) An introduction to materials in medicine. Elsevier, San Diego, pp 59–65
Volpi N (2006) Therapeutic applications of glycosaminoglycans. Curr Med Chem 13:1799–1810
Weisel JW, Cederholm-Williams SA (1997) Fibrinogen and fibrin: characterization, processing and medical applications. In: Domb AJ, Kost J, Wiseman DM (eds) Handbook of biodegradable polymers. OPA, Amsterdam, pp 347–365
Williams DF, Williams RL (2004) Degradative effects of the biological environment on metals and ceramics. In: Ratner BD, Hoffman AS, Schoen FJ, Lemons JE (eds) An introduction to materials in medicine. Elsevier, San Diego, pp 430–439
Wilson J, Pigott GH, Schoen FJ, Hench LL (1981) Toxicology and biocompatibility of bioglasses. J Biomed Mater Res 15:805–817
Witte F, Hort N, Vogt C, Cohen S, Kainer KU, Willumeit R, Feyerabend F (2008) Degradable biomaterials based on magnesium corrosion. Curr Opin Solid State Mater Sci 12:63–72
Yannas IV (2004) Natural materials. In: Ratner BD, Hoffman AS, Schoen FJ, Lemons JE (eds) An introduction to materials in medicine. Elsevier, San Diego, pp 127–137

Assessment of Metallic Alloys Biocompatibility

Carme Nogués, Andreu Blanquer, Lleonard Barrios and Elena Ibañez

Abstract Metallic alloys have been widely used for orthopedic implants since the beginning of the last century. Compared to ceramics and polymers, metallic alloys present excellent mechanical properties and biocompatibility. In this chapter, we review the different in vitro assays currently used to test the biocompatibility of new materials designed to be used in orthopedics: cell adhesion, proliferation and differentiation, mineralization of the extracellular matrix and detection of inflammatory response. In addition, the known causes of alloy toxicity, namely ion release due to material corrosion and characteristics of the material surface (wettability, charge, or topography), are also discussed.

Keywords Metallic alloys · Biocompatibility · In vitro assays · Ti-based alloys

1 Introduction

Metallic alloys present excellent mechanical properties compared to other biomaterials like ceramics and polymers. The extremely high toleration to tensile stress is one of the reasons to be widely used in structural material for skeleton reconstructions. The most commonly used for surgical implants are 316L stainless steel, cobalt-chromium alloys, and titanium and its alloys (Hermawan et al. 2011). The main differences among them lie in their mechanical properties, corrosion resistance and biocompatibility. Stainless steel materials, one of the most frequently used biomaterials in clinical applications, present moderate mechanical properties but good corrosion resistance and they are extensively used for fracture repairs. On the other hand, cobalt-chromium-molybdenum are strong, hard biocompatible materials with good wear and corrosion resistance and are usually used for joint replacements (hip joints) or fracture repairs because they can hold a long service. Finally, pure

C. Nogués (✉) · A. Blanquer · L. Barrios · E. Ibañez
Departament de Biologia Cellular, Fisiologia i Immunologia,
Universitat Autònoma de Barcelona, E-08193 Bellaterra, Spain
e-mail: carme.nogues@uab.cat

F. Zivic et al. (eds.), *Biomaterials in Clinical Practice*,
https://doi.org/10.1007/978-3-319-68025-5_16

titanium or titanium alloys have excellent mechanical properties, excellent corrosion resistance and excellent biocompatibility, for these reasons these materials are used for bone repair and replacement (Gepreel and Niinomi 2013).

An increase use of titanium and its alloys as biomaterials has been observed during these last decades. These alloys have attractive properties such as a lower elasticity modulus (also known as Young's modulus), superior biocompatibility and better corrosion resistance when compared with more conventional stainless steel and cobalt-based alloys. The applications of titanium and its alloys are extensive, from hard tissue replacements in artificial bones, joints, and dental implants to cardiovascular implants such as prosthetic heart valves, protective cases in pacemakers, artificial hearts, and circulatory devices. More recently, a new alloy, the shapememory nickel–titanium (NITINOL) alloy has begun to be used in dental restoration (Hermawan et al. 2011) and intravascular devices, such as stents and occlusion coils (Liu et al. 2004).

Titanium-based alloys have a modulus of elasticity (from 55 to 110 GPa) that approaches the elasticity modulus of the natural bone (30 GPa). In comparison, 316L stainless steel and chromium-cobalt alloys have a much higher modulus of elasticity (210 and 240 GPa, respectively). One of the causes of prosthesis failure through loosening or implant fracture is the difference between the elasticity of the implant material and that of the natural bone. Because of this, one of the goals when designing new alloys is to obtain materials with high strength but an elasticity modulus closer to that of the bone (Geetha et al. 2009).

In the last years, several new metallic alloys have been developed to improve their mechanical properties and biocompatibility. Some of these alloys contain elements which have been classified as toxic because they can cause toxicity, carcinogenicity or metal sensitivity (reviewed in Biesiekierski et al. 2012). Thus, the number of in vivo and in vitro experiments to evaluate the biocompatibility of these new materials has increased during the last 50 years (Hermawan et al. 2011). It is very important to characterize in deep all new materials in terms of biocompatibility, that is, of the interaction between a biomaterial and the human body, and this interaction can only be assessed in in vivo studies using animal models (Pearce et al. 2007). But, before conducting in vivo studies, in vitro analyses are necessary to obtain the essential information about the cytotoxicity of the material, the capacity of cells to adhere and to proliferate and, later on, to differentiate onto the material. In vitro studies can also analyze any unwanted inflammatory response triggered by the new material.

More recently, a large number of metallic alloys made of nontoxic and allergy-free elements have been synthesized (Hermawan et al. 2011). The goal is to synthesize new metallic alloys with low elasticity modulus and free from non-biocompatible elements (e.g., Al, V, Ni, or Co). Longevity has increased during the last years and therefore biomedical implants must be designed to guarantee a long lifetime of the implant after being inserted into the human body (Hynowska et al. 2013). In addition to the properties already mentioned, metallic implants are expected be non-magnetic and with the optimum density to allow their detection in clinical examination techniques such as magnetic resonance imaging or X-ray analysis (Hermawan et al. 2011).

The current challenge is to develop new materials not only with improved mechanical properties but, at the same time, materials that can modify the behavior of the cells (Hofmann and Garcia-Fuentes 2011).

2 In Vitro Assays to Evaluate Material Biocompatibility

Implant materials can trigger undesirable effects on the body when implanted. Some of these negative effects can be detected in in vitro systems whereas others are more difficult to determine because they would appear only after long-term contact between the alloy and the tissue. Animal models allow the evaluation of materials in different situations and in different tissue qualities (e.g. normal healthy or osteopenic bone) and ages (Pearce et al. 2007). However, the use of animal models should be limited to advanced studies (principles of animal reduction), once the cytocompatibility of a material has been demonstrated in in vitro cell cultures in which cell viability, proliferation, adhesion, morphology, immunogenicity and differentiation are routinely analyzed.

2.1 Cell Model Selection

The selection of the appropriate cell model is essential to analyze the interaction between cells and materials. There are different types of cell models: primary cell cultures, finite, immortalized and tumor derived cell lines. To test materials designed for orthopedic implants, osteoblast cells would be the most appropriate.

It has been described that there are noticeable differences regarding bone composition of different species (Aerssens et al. 1998) and significant differences in terms of viability or protein synthesis in cell cultures from different origins (interspecies differences) (Torricelli et al. 2003). Using human cells, interspecies differences are avoided (Czekanska et al. 2012). The inconvenience is that only primary cell cultures or tumor cell lines from humans are available. Tumor cell lines have the advantage of rapid proliferation, unlimited number of cells and reproducibility. Their disadvantages is that they not behave as normal cells, for instance, contact inhibition is disrupted in malignant cell lines, but not in immortalized ones. Alternatively, primary cell cultures present the advantage of a more close behavior to the in vivo cells and thus, the results obtained are more relevant for clinical applications, but with the disadvantages of cell isolation, cell culture establishment, maintenance and replacement when cell line decays (they are finite cell lines) (Bakker and Klein-Nulend 2003). In addition, differences among age (young vs. adult) or physical condition (normal vs. osteopenic bone) of the donor could result in inconsistent results.

The cell lines most currently used for biocompatibility studies are mouse preosteoblast MC3T3 (immortalized cell line that can differentiate to mature osteoblast), human osteosarcoma Saos-2 or MG-63 (tumor cell lines) (Kartsogiannis and Ng 2004; Czekanska et al. 2012).

We have been working with two different cell lines, the mouse preosteoblast MC3T3 cell line and the human osteosarcoma Saos2 for testing different alloys (González et al. 2012; Pellicer et al. 2013; Blanquer et al. 2014; Hynowska et al. 2013, 2014; Blanquer et al. unpublished results), and we have compared the behavior of both cell lines in terms of viability, morphology, cell adhesion and differentiation in the $Ti_{40}Cu_{38}Zr_{10}Pd_{12}$ alloy with no differences between both cell lines.

2.2 *Cell Viability and Proliferation*

The first parameter to analyze, when testing the biocompatibility of a new alloy, is whether the alloy is toxic in in vitro cell cultures. This can be quantified by measuring the activity of cellular enzymes. Live cells contain enzymes capable of reducing different products. When the reduced product is colored or emits fluorescence, the enzyme activity can be quantified because the signal obtained is proportional to the number of live cells (Mosmann 1983). Generally, two different approaches can be used: colorimetric assays (e.g. MTT assay) from cell lysates or fluorescent signal (live/dead kits) from whole cells. In the first case, cells must be destroyed to obtain the colored product and the solution obtained is quantified in a colorimetric readout. In the second case, live cells emit fluorescence (usually green) that can be visualized under a fluorescence microscope; to distinguish live cells from dead cells, propidium iodide or any other counterstain that will only penetrate into cells with a damaged membrane (dead cells) is added (Fig. 1).

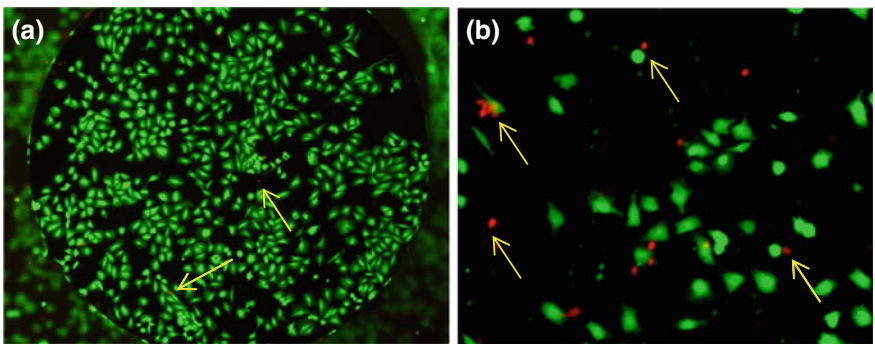

Fig. 1 Cell viability studies. **a** Saos2 cells growing on top a metallic alloy disk ($Ti_{45}Zr_{15}Pd_{30}Si_5Nb_5$) (objective 4×). **b** MC3T3-E1 cells growing on top a metallic alloy disk (Ti–6Al–4V) (objective 20×). Cultures were processed with the live/dead viability/cytotoxicity kit for mammalian cells (Invitrogen). Live cells have esterase activity and thus are green whereas dead cells are *red* (*yellow arrows*) because they have the plasma membrane damaged and propidium iodide can cross the cell membrane

Materials can be cytotoxic because they kill the cells, usually detectable at 24 h, or because they slow down or even block cell proliferation. Proliferation can be evaluated using the same methods mentioned above; the inconvenience is that for each time-point to evaluate, different cell cultures will be needed because either cells will be lysed or cells will die because of the toxicity of the kits used. Another approach is the use of Alamar blue®, a non-toxic cell permeable compound which emits fluorescence when reduced. Fluorescence can be quantified directly without cell lysis and the same culture can be re-evaluated over-time.

The causes for cytotoxicity would be discussed later in detail, but it could originate either from the material released ions to the cell culture medium, or from the material surface itself. Thus, it is important to conduct direct and indirect analyses to distinguish between these two possibilities. In direct analyses cells are seeded on top of the alloy whereas in indirect studies cells are grown in the vicinity of the alloy or in cell culture media that has been in contact with the alloy.

2.3 Adhesion and Morphology

Cell adhesion between cells or between cells and the extracellular matrix (ECM) is essential for embryogenesis, maintenance of tissue integrity, wound healing, immune response, and biomaterial tissue integration. Cell-matrix adhesions such as focal contacts are protein complexes that connect the cell cytoskeleton (actin fibers) with the ECM proteins (fibronectin, collagen, laminin or vitronectin) through transmembrane proteins called integrins (membrane receptors), which allows cells to exert contractile forces on the substratum. The interactions between ECM proteins and their specific membrane receptors induce, in addition, signal transduction processes, which consequently influences cell growth and differentiation (Pellegrin and Mellor 2007).

Cells are often cultured in medium supplemented with serum which contains a wide variety of proteins, including fibronectin that is necessary to form the focal contacts. Serum proteins are usually adsorbed to the surface of the implant material allowing cell adhesion (Bačáková et al. 2004; Bacakova et al. 2011). However, not all surfaces allow the adsorption of serum proteins (explained in more detail in Sect. 3.2). When these proteins are not present on the surface of the alloy, cells cannot attach and finally die due to a phenomenon called anoikis (Grossmann et al. 2001). Thus, in this case, the material may be toxic not because of its composition but because of the characteristics of its surface. There are different techniques to conveniently modify a material surface to allow cell colonization and osteogenic cell differentiation, if necessary (Jayaraman et al. 2004; Vandrovcová and Bačáková 2011; Zareidoost et al. 2012).

Adhesion in culture cells is usually evaluated by immunofluorescence. Typically, actin filaments are labeled to analyze the distribution of stress fibers where vinculin, talin or paxillin (intracellular proteins of focal contacts) are labeled to localize the focal contacts. These proteins allow to evaluate the extent of the

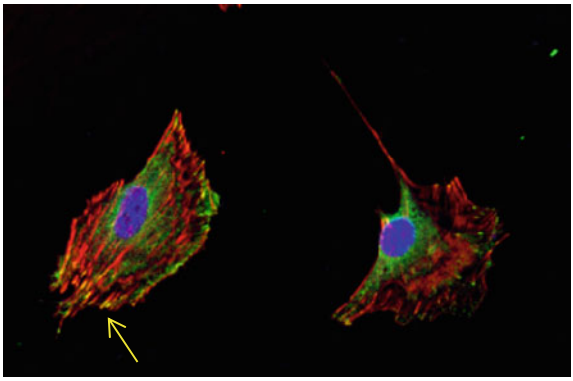

Fig. 2 Cell adhesion. MC3T3-E1 preosteoblast cells growing on top a metallic alloy ($Ti_{40}Zr_{10}Cu_{33}Pd_{12}Nb_5$). Actin stress fibers (*red*) are distributed along the cell forming parallel bundles that end in focal contacts (*orange*), where vinculin (*green*) colocalizes with actin (*yellow arrow*) (objective 60×)

contacts between the cell and the surface material (Fig. 2). It has been described that the extent of a focal adhesion depends on the force applied by actin stress fibers on the substrate. In smooth materials, the distribution of ECM proteins is homogenous and cells can spread forming large parallel stress fibers. By contrast, on rough surfaces, where the distribution of the ECM proteins is related to the morphology of the material, stress fibers are distributed along the direction of the force exerted by the cytoskeleton in contact with the ECM proteins (Passeri et al. 2010). In these surfaces, cells adopt a more irregular shape.

Osteoblast adhesion can also be characterized by the analysis of integrin gene expression. Different patterns of integrin expression have an important effect on cell adhesion, cell migration and cell differentiation, playing an important role in signal transduction (Akiyama 1996; Keselowsky et al. 2004; Yang et al. 2013).

Cell morphology is another indicator of cell healthiness when in contact with implant materials. Morphology can be evaluated using scanning electron microscope which also allows assessing cell adhesion and the interaction between cells and the surface of the alloy (Fig. 3). Healthy cells are usually well spread, with a polygonal shape (Vandrovcová and Bačáková 2011; Blanquer et al. 2014). The nucleus and one or more nucleoli are generally visible.

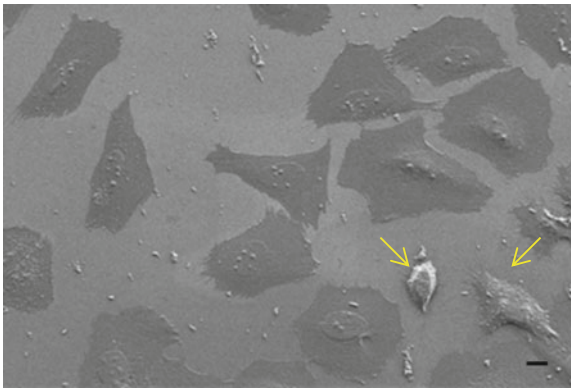

Fig. 3 Cell morphology. Saos2 osteosarcoma cells adhered onto $Ti_{40}Zr_{10}Cu_{38}Pd_{12}$ bulk metallic glass. The majority of the cells are well-spread with a polygonal shape and flat appearance, although some are not entirely attached (*yellow arrows*). *Bar* represents 10 μm

In normal cell culture, a few cells not entirely attached to the surface are usually observed among a majority of well spread cells. But, when the percentage of rounded, not spread cells or cells with membrane protrusions characteristic of apoptotic cells is high, this is an indicator that the surface of the material is not appropriate for cell growing.

2.4 Osteoblast Differentiation

In the case of bone repair, implant materials should allow osteogenic differentiation. This can be assessed by cell cultures where preosteoblast or osteosarcoma cells should be capable to differentiate in vitro in the presence of the metallic alloy when cultured with specific culture medium (supplemented with dexamethasone, ascorbic acid and β-glycerophosphate). Natural bone is a tissue in constant remodelling, i.e., osteoblasts mature (osteogenic differentiation) and calcify the ECM (bone growth) while osteoclast destroy matured osteoblasts (bone resorption) (Kartsogiannis and Ng 2004). Osteoblast differentiation is accomplished in three different phases. The first one is cell proliferation, and during this phase expression of procollagen I, TGF-β, and fibronectin can be detected. The second one is characterized by the secretion of collagen I and the maximal activity of alkaline phosphatase (ALP) enzyme. Finally, the third phase is the mineralization of the ECM, when an accumulation of calcium phosphate and the expression of different extracellular matrix proteins such as osteocalcin (OCN), bone sialoprotein (BSP) and osteopontin (OPN) occurs (Lian and Stein 1995; Popp et al. 2011).

Calcium deposits formed in the ECM are an indicator of successful in vitro osteoblast differentiation and can be specifically stained using Alizarin Red S, an organic compound that allows evaluating calcium-rich deposits (Fig. 4). Mineralization can be detected as early as 7 days or 14 days in Saos-2 or MC3T3 cell cultures, respectively. Calcium deposits appear as dispersed small red spots that increase in size and in color intensity up to 35 days when cells are cultured in differentiation medium (Lian and Stein 1995).

ALP content can be quantified by ALP activity analysis (using p-nitrophenyl phosphate as a substrate) and related to total protein content by reading their absorbance (Bakker and Klein-Nulend 2003). Synthesis of ALP is detectable at 4–5 days after cell seeding and the total amount increases during approximately 4 weeks (Popp et al. 2011), and from then it begins to decrease (Lian and Stein 1995).

Finally, expression of different markers of osteogenesis can be quantified by reverse transcription and real-time PCR (RT-PCR). There is no a consensus in the number of genes to analyze, neither in which the genes to analyze. OCN is the gene most frequently analyzed but others genes such as OPN, Cbfa1 (an osteoblast-specific transcription factor), type I collagen, ALP, BSP, etc. have also been analyzed by different authors (Popp et al. 2011; Saldaña et al. 2011; Liskova et al. 2015). The expression of these genes is detectable from about 2–3 weeks after cell seeding up to 4–5 weeks in culture (Popp et al. 2011).

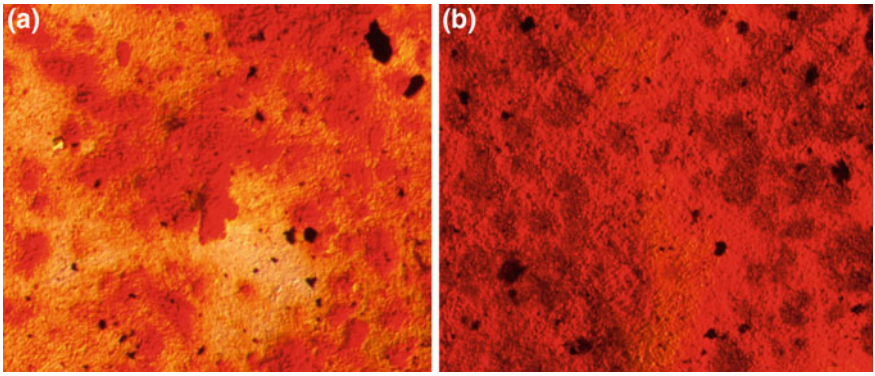

Fig. 4 Osteoblast differentiation. Extracellular matrix mineralization of MC3T3 cells, in the presence of $Ti_{40}Zr_{10}Cu_{38}Pd_{12}$ bulk metallic glass, detected by Alizarin red S. An increase in the number of nodules and the intensity of calcium staining is observed at 21 days (**b**) compared with 14 days (**a**)

The product of some of these genes can also be detected by immunofluorescence. Type I collagen, OCN and other protein markers of osteoblast differentiation can be labeled with specific antibodies and the intensity of the fluorescent signal quantified using specific software (Novotna et al. 2013; Liskova et al. 2015).

2.5 Inflammatory Response

It is well known that the implantation of a prosthetic material can produce tissue damage and inflammation. Usually, the problem is not the material itself, but its corrosion and consequent ion release or wear debris from the material surface, which can trigger inflammation and could end in implant loosening (Pizzoferrato et al. 2002). It has been shown that in patients with loose implants, the tissue surrounding the implant presented high levels of cytokines known to stimulate bone resorption, such as interleukin-1β (IL-1β), interleukin-6 (IL-6) or tumor necrosis factor-α (TNF-α) (Vallés et al. 2006). In addition, in vivo and in vitro experiments indicate that particulate debris is phagocytosed by macrophages, stimulating the secretion of inflammatory cytokines (Ingham and Fisher 2005). It has been proposed that metal implant debris can activate the inflammasome pathway in macrophages, e.g. soluble $CoCl_2$, $CrCl_3$, $MoCl_5$, and $NiCl_2$ ions and cobalt alloy particles induced NADPH/ROS-, active caspase-1-, Nalp3-, and IL-1 β secretion in human macrophages (Caicedo et al. 2009).

Different assays have been use to analyze whether a material can stimulate the secretion of inflammatory cytokines from differentiated macrophages. The simplest experiment is to incubate the material in presence of macrophages and quantify the cytokine secretion by Elisa technique (Neacsu et al. 2015), BioplexMultiplexSystem

(Ullm et al. 2014) or by flow cytometry using a cytometric bead array (Blanquer et al. 2014). Some authors analyze cytokine release in cocultures of macrophages and osteoblast (Horowitz and Gonzales 1996), instead of using monocultures.

We quantified the inflammatory cytokines release from human macrophages in the presence of $Ti_{40}Cu_{38}Zr_{10}Pd_{12}$ alloy. We measured the cytokines release from macrophages after 24 h in the presence of the alloy, when the concentration of copper ions released from the alloy into the culture medium was 32 μg/L (nearly three times the initial concentration). Results showed that the presence of the alloy did not activate the secretion of TNFα, IL-6 or IL-1β (Blanquer et al. 2014).

3 Principal Causes of Toxicity

Toxicity could be due either to the amount of ions released from the implant (corrosion) or to the surface of the material.

Corrosion is the result of the interaction of the metallic alloy with environmental conditions (i.e., pH, chloride ion concentration, temperature, etc.), mechanical factors (i.e., pre-existing cracks, surface abrasion, and film adhesion), electrochemical effects (i.e., applied potential, galvanic effects, pitting, or crevices), and cell concentration around implants. There are several types of corrosion: fretting, pitting and fatigue. Fretting is related to corrosion damage at a small area of contact and it is usually activated by friction. Pitting is due to galvanic corrosion that leads to the creation of small holes in the metal. Finally, fatigue is the apparition of small cracks due to the forces or deformations applied to the material (reviewed in Gepreel and Niinomi 2013).

All metallic alloys currently used in orthopaedic implants (stainless steel alloy, Co-Cr base alloy or Ti-based alloy) are subjected to corrosion when they are in contact with the body for long-term periods (Liu et al. 2004; Gepreel and Niinomi 2013). The release of metallic ions can cause a decrease in cell proliferation or cell death, depending on the concentration of the ions (Yamamoto et al. 1998) and also allergies (Bordignon et al. 2008). They can also induce DNA damaging, mutation or cancer (reviewed in Biesiekierski et al. 2012).

On the other hand, the surface of the material is of great importance because it can modify the adhesion and spreading of the cells. The interaction of the cells with the material occurs at the surface of the material, thus topography (including roughness and morphology of the material), surface chemistry (presence or absence of chemical groups) and surface energy (wettability of the material) can either strengthen or prevent the cell adhesion. When a material does not allow cell adhesion, this material is considered not biocompatible, not necessarily of its composition but because cells can not adhere to it and, as mentioned before, they die.

3.1 Corrosion

Several groups have conducted studies about the cytotoxicity of different elements or ions in culture cells (Yamamoto et al. 1998; Yamazaki et al. 2006; Bordignon et al. 2008; Contreras et al. 2010; Biesiekierski et al. 2012). It is difficult to compare the results obtained by these authors because, first, they have used different cell lines, and second, the element under study was pure in some cases (Yamazaki et al. 2006), in salt compounds in others (Yamamoto et al. 1998; Biesiekierski et al. 2012).

Biesiekierski et al. (2012) published an extensive review on the biocompatibility, carcinogenicity, genotoxicity, mutagenicity, cytotoxicity, allergenicity and the proneness to corrosion of 27 transition metals, where Cobalt and Nickel were among the most toxic elements. All authors agree with the allergenic effect of Nickel (Bordignon et al. 2008; Faurschou et al. 2011), but for Yamamoto et al. (1998) who tested 43 metal salts, Nickel is not the highest toxic element, but Cadmium, Indium, Vanadium and Beryllium are, in a decreasing order. Besides, Aluminum is known to have adverse effects on neurons when it accumulates in the brain and has been reported to play a role in the process of neurodegeneration (El-Rahman 2003). Palladium has been shown to induce inflammation of gingival tissues in individuals exposed to dental material (Faurschou et al. 2011). On the contrary, Zinc, Calcium and Magnesium are rather harmless elements and it appears that the MgZnCa alloy is one of the most promising candidates for bone implants (Zberg et al. 2009).

Copper, for example, is an element considered toxic by most authors (Yamamoto et al. 1998; Yamazaki et al. 2006; Contreras et al. 2010; Biesiekierski et al. 2012), but our group has demonstrated that when alloyed to titanium, zirconium and palladium ($Ti_{40}Cu_{38}Zr_{10}Pd_{12}$), copper is not cytotoxic (Blanquer et al. 2014). Titanium and Zirconium are considered biocompatible (Biesiekierski et al. 2012), but Palladium has been considered cytotoxic (Biesiekierski et al. 2012), non-cytotoxic (Yamazaki et al. 2006) or inductor of immune reactions (Bordignon et al. 2008) depending of the study conducted. We analyzed the amount of copper ions released (the corrosion of the alloy) and their potential toxic effects and our conclusions were that copper released did not increase cell death up to 21 days in culture, neither the secretion of inflammatory cytokines when the alloy was incubated with macrophages. Neither did the presence of Palladium in the alloy (Blanquer et al. 2014). In the same way, Yamazaki et al. (2012) demonstrated that the cytotoxicity of copper could be neutralized when this element is alloyed with 10% of gold.

Therefore, some elements that are known to be toxic in different systems can behave different when alloyed with other elements. Indeed, TiAlV, the most used metallic alloy for implants during this last decade, is composed of two elements, Titanium and Vanadium, considered toxic by several authors (Yamamoto et al. 1998; Biesiekierski et al. 2012).

3.2 Surface

Topography, surface chemistry or surface energy of a biomaterial plays an important role in osteoblast adhesion. As aforementioned, cell adhesion is mediated through ECM molecules. To allow cell adhesion these molecules must be adsorbed on the biomaterial surface in an appropriate amount and a particular spatial conformation to facilitate the contact of cell adhesion receptors (integrins). The adsorption of proteins is influenced by the physical and chemical properties of the material surface (Bačáková et al. 2004). Materials can adsorb adhesion-promoting (fibronectin) and adhesion-inhibiting proteins (serum albumin) onto their surface, and the efficiency of cell adhesion and growth is dependent on the balance between these two types of proteins (Wei et al. 2009).

One of the properties that influenced protein adsorption is wettability of the material surface, which can be assessed by measuring the contact angle of a water droplet onto the material surface. Low contact angles (usually, <90°) are related with hydrophilic surfaces, whereas high contact angles (>90°) are associated with hydrophobic ones. If the material is too hydrophobic proteins are adsorbed in a denatured and rigid state that is inappropriate for binding cells because the specific recognition sites are less accessible to cell adhesion receptors (Bacakova et al. 2011).

Anchorage-dependent cells adhere better to hydrophilic surfaces because in these surfaces proteins are adsorbed in an appropriate geometrical conformation that allows cell receptors to recognize the adhesion-mediating ECM molecules. Once cells are adhered, they spread and adopt a flat shape before proliferating, because cells cannot divide without previous adhesion (Bacakova et al. 2011).

Controversial studies have been published about hydrophilicity/hydrophobicity; it is clear that cells prefer hydrophilic surfaces over hydrophobic ones, but which is the optimal grade of hydrophilicity is still under discussion. It seems that initial osteoblast attachment increases with an increase in surface hydrophilicity (contact angle of 0°) but, after 3 h of incubation, the total number of cells attached to different hydrophilic surfaces, with contact angles from 0° to 80°, did not differ (Wei et al. 2009). However, when the surface is highly hydrophilic, cells adhere and extend forming very large adhesion areas and differentiate instead of proliferating (Bacakova et al. 2011). On the other hand, it has also been reported that MG-63 cells growing on oxygen-terminated nanocrystalline diamond surfaces (contact angle 20°–35°) tend to spontaneously detach from the material after 5–7 days in culture (Grausova et al. 2008). Finally, contact angles of 106° significantly reduce the number of attached cells after 3 h in culture (Wei et al. 2009), as highly hydrophobic surfaces impede cell adhesion, inducing cell death. Our group tested a magnesium based alloy containing Palladium or not ($Mg_{72}Zn_{23}Ca_5$ vs. $Mg_{70}Zn_{23}Ca_5Pd_2$).The contact angle was 86.7° in absence and 104° in presence of Palladium. In the first one, adhesion was poor, with no spread cells at 8 h of culture, but in the presence of Palladium the number of attached cells was very low at 4 h of culture and inexistent at 8 h (Pellicer et al. 2013).

Hydrophilicity is highly related to surface chemistry. There are different mechanical, chemical or physical methods to modify the surface of metallic alloys to improve cell adhesion and bioactivity, but also wear and corrosion resistance (reviewed in Liu et al. 2004). Depending on the surface modification, adhesion-mediating ECM molecules can be adsorbed in a spatial orientation that would promote or inhibit access to the cell receptors. The spatial orientation is indeed more important than the absolute number of molecules absorbed. Positively charged surface are better for cell adhesion because adhesion molecules are negatively charged and thus are preferentially adsorbed (Bacakova et al. 2011; Minagar et al. 2013). But it has also been reported that negatively charged surfaces support better adhesion and differentiation of chondrocytes than neutral or positively hydrogel scaffolds (reviewed in Chang and Wang 2011).

In any case, surface modification does not only referred to modification of the surface charge or the hydrophilicity, but also to the biochemical modification by means of surface-immobilized peptides, proteins, or growth factors (Liu et al. 2004; Bacakova et al. 2011). In addition, most of the mechanical, chemical or physical modifications induce changes in the topography of the materials.

Topography is related to surface roughness and morphology, and it has been described that topography influences osteoblastic proliferation, differentiation and ECM protein expression (Li et al. 2014; Bacakova et al. 2011; Vandrovcová and Bačáková 2011; Zareidoost et al. 2012). Several articles have been published regarding surface roughness. Depending on the roughness amplitude value (Ra), that is, the average peak-to-valley height, roughness has been classified as macroroughness (from several mm to 100 μm), microroughness (from 100 to 1 μm), submicroroughness (from 1 to 100 nm), and nanoroughness (<100 nm). Thus Ra values can range from several millimeters (eye visible) to less than 100 nm (Bacakova et al. 2011).

Roughness usually does not interfere with cell adhesion when the Ra value is higher than the cell dimension or much smaller than it. When higher, cells can spread between the roughnesses, and when smaller, at nanoscale roughness, cells can adhere on the surface. The in-between roughness restrict cell adhesion and spreading because, probably, cells are stressed by the deformation imposed to their cytoskeleton by the surface features of the material (Anselme and Bigerelle 2014). Roughness and surface morphology can be modulated by different mechanical, chemical or physical techniques.

There is a large number of different modifications and a large number of different surface morphologies, thus it is difficult to conclude which surface is better because topography is the result of different parameters, alloy composition, chemistry surface, etc. In general authors agree that nanoroughness is better than microroughness for cell adhesion, growth, and differentiation, although it has also been described that microscale roughness can support osteogenic cell differentiation, even if the initial cell adhesion and proliferation, is not ideal (reviewed in Vandrovcová and Bačáková 2011; Deng et al. 2014).

4 Conclusions and Future Directions

In summary, before a material is used for implant fabrication, all aforementioned issues must be taken into account, that is, the material should not be cytotoxic, should allow proliferation and differentiation, and should not induce an immunological response.

The current challenge is to develop smart materials with improved mechanical properties but, at the same time, able to interact with cells or stimulate a cellular response.

Acknowledgements This study was supported by the Generalitat de Catalunya (2014SGR-524) and the MAT2014-57960-C3-3-R projects from the Spanish Ministerio de Economía y Competitividad (MINECO). A.B was supported by a predoctoral grant from the Universitat Autònoma de Barcelona, Spain.

Bibliography

Aerssens J et al (1998) Interspecies differences in bone composition, density, and quality: potential implications for in vivo bone research. Endocrinology 139(2):663–670

Akiyama S (1996) Integrins in cell adhesion and signaling. Hum Cell 9(3):181–186

Anselme K, Bigerelle M (2014) On the relation between surface roughness of metallic substrates and adhesion of human primary bone cells. Scanning 36:11–20

Bačáková L et al (2004) Cell adhesion on artificial materials for tissue engineering. Physiol Res 53:S35–S45

Bacakova L et al (2011) Modulation of cell adhesion, proliferation and differentiation on materials designed for body implants. Biotechnol Adv 29(6):739–767

Bakker A, Klein-Nulend J (2003) Osteoblast isolation from murine calvariae and long bones. In: Helfrich M, Ralston S (eds) Bone research protocols. Methods in molecular medicine. Humana Press Inc., Totowa, pp 19–28

Biesiekierski A et al (2012) A new look at biomedical Ti-based shape memory alloys. Acta Biomater 8(5):1661–1669

Blanquer A et al (2014) In vitro biocompatibility assessment of Ti40Cu38Zr10Pd12 bulk metallic glass. J Mater Sci Mater Med 25:163–172

Bordignon V et al (2008) Nickel, palladium and rhodium induced IFN-gamma and IL-10 production as assessed by in vitro ELISpot-analysis in contact dermatitis patients. BMC Immunol 9:19

Caicedo MS et al (2009) Soluble and particulate Co-Cr-Mo alloy implant metals activate the inflammasome danger signaling pathway in human macrophages: a novel mechanism for implant debris reactivity. J Orthop Res 27(July):847–854

Chang H, Wang Y (2011) Cell responses to surface and architecture of tissue engineering scaffolds. In: Eberli D (ed) Regenerative medicine and tissue engineering—cells and biomaterials. InTech, pp 569–588

Contreras RG et al (2010) Type of cell death induced by various metal cations in cultured human gingival fibroblasts. In vivo (Athens, Greece) 24:507–512

Czekanska EM et al (2012) In search of an osteoblast cell model for in vitro research. Eur Cells Mater 24:1–17

Deng Z et al (2014) Surface characteristics of and in vitro behavior of osteoblast-like cells on titanium with nanotopography prepared by high-energy shot peening. Int J Nanomed 9:5565–5573

El-Rahman SSA (2003) Neuropathology of aluminum toxicity in rats (glutamate and GABA impairment). Pharmacol Res 47:189–194

Faurschou A et al (2011) Metal allergen of the 21st century—a review on exposure, epidemiology and clinical manifestations of palladium allergy. Contact Dermat 64:185–195

Geetha M et al (2009) Ti based biomaterials, the ultimate choice for orthopaedic implants—a review. Prog Mater Sci 54:397–425

Gepreel MA-H, Niinomi M (2013) Biocompatibility of Ti-alloys for long-term implantation. J Mech Behav Biomed Mater 20:407–415

González S et al (2012) Improved mechanical performance and delayed corrosion phenomena in biodegradable Mg-Zn-Ca alloys through Pd-alloying. J Mech Behav Biomed Mater 6:53–62

Grausova L et al (2008) Bone and vascular endothelial cells in cultures on nanocrystalline diamond films. Diam Relat Mater 17:1405–1409

Grossmann J et al (2001) Apoptotic signaling during initiation of detachment-induced apoptosis ("anoikis") of primary human intestinal epithelial cells. Cell Growth Differ Mol Biol J Am Assoc Cancer Res 12(March):147–155

Hermawan H, Ramdan D, Djuansjah JRP (2011) Metals for biomedical applications. In: Fazel R (ed) Biomedical engineering—from theory to applications. InTech Europe, Rijeka, Croatia, pp 411–430

Hofmann S, Garcia-Fuentes M (2011) Bioactive scaffolds for the controlled formation of complex skeletal tissues. In: Eberli D (ed) Regenerative medicine and tissue engineering—cells and biomaterials. InTech, Rijeka, Croatia, pp 393–432

Horowitz SM, Gonzales JB (1996) Inflammatory response to implant particulates in a macrophage/osteoblast coculture model. Calcif Tissue Int 59:392–396

Hynowska A et al (2014) Nanostructured Ti-Zr-Pd-Si- (Nb) bulk metallic composites: novel biocompatible materials with superior mechanical strength and elastic recovery. J Biomed Mater Res B Appl Biomater 1–11 (online)

Hynowska A et al (2013) Novel Ti-Zr-Hf-Fe nanostructured alloy for biomedical applications. Materials 6:4930–4945

Ingham E, Fisher J (2005) The role of macrophages in osteolysis of total joint replacement. Biomaterials 26:1271–1286

Jayaraman M et al (2004) Influence of titanium surfaces on attachment of osteoblast-like cells in vitro. Biomaterials 25:625–631

Kartsogiannis V, Ng KW (2004) Cell lines and primary cell cultures in the study of bone cell biology. Mol Cell Endocrinol 228:79–102

Keselowsky BG, Collard DM, García AJ (2004) Surface chemistry modulates focal adhesion composition and signaling through changes in integrin binding. Biomaterials 25:5947–5954

Li M et al (2014) Study of biocompatibility of medical grade high nitrogen nickel-free austenitic stainless steel in vitro. Mater Sci Eng C 43:641–648

Lian JB, Stein GS (1995) Development of the osteoblast phenotype: molecular mechanisms mediating osteoblast growth and differentiation. Iowa Orthop J 15:118–140

Liskova J et al (2015) Osteogenic cell differentiation on H-terminated and O-terminated nanocrystalline diamond films. Int J Nanomed 10:1–16

Liu X, Chu PK, Ding C (2004) Surface modification of titanium, titanium alloys, and related materials for biomedical applications. Mater Sci Eng R Rep 47(2004):49–121

Minagar S et al (2013) Cell response of anodized nanotubes on titanium and titanium alloys. J Biomed Mater Res A 101(9):2726–2739

Mosmann T (1983) Rapid colorimetric assay for cellular growth and survival: application to proliferation and cytotoxicity assays. J Immunol Methods 65:55–63

Neacsu P et al (2015) In vitro performance assessment of new beta Ti–Mo–Nb alloy compositions. Mater Sci Eng C 47:105–113

Novotna K et al (2013) Adhesion and growth of vascular smooth muscle cells on nanostructured and biofunctionalized polyethylene. Materials 6:1632–1655
Passeri G et al (2010) Adhesion pattern and growth of primary human osteoblastic cells on five commercially available titanium surfaces. Clin Oral Implant Res 21:756–765
Pearce AI et al (2007) Animal models for implant biomaterial research in bone: a review. Eur Cells Mater 13:1–10
Pellegrin S, Mellor H (2007) Actin stress fibres. J Cell Sci 120:3491–3499
Pellicer E et al (2013) On the biodegradability, mechanical behavior, and cytocompatibility of amorphous Mg72 Zn23 Ca5 and crystalline Mg70 Zn23 Ca5 Pd2 alloys as temporary implant materials. J Biomed Mater Res A 101:502–517
Pizzoferrato A et al (2002) Inflammatory response to metals and ceramics. In: Barbucci R (ed) Integrated biomaterial science. Kluwer Academic/Plenum Publishers, New York, pp 735–791
Popp J et al (2011) In vitro evaluation of osteoblastic differentiation on amorphous calcium phosphate-decorated poly(lactic-co-glycolic acid) scaffolds. J Tissue Eng Regen Med 5:780–789
Saldaña L et al (2011) In search of representative models of human bone-forming cells for cytocompatibility studies. Acta Biomater 7:4210–4221
Torricelli P et al (2003) Comparative interspecies investigation on osteoblast cultures: data on cell viability and synthetic activity. Biomed Pharmacother 57:57–62
Ullm S et al (2014) Biocompatibility and inflammatory response in vitro and in vivo to gelatin-based biomaterials with tailorable elastic properties. Biomaterials 35:9755–9766
Vallés G et al (2006) Differential inflammatory macrophage response to rutile and titanium particles. Biomaterials 27:5199–5211
Vandrovcová M, Bačáková L (2011) Adhesion, growth and differentiation of osteoblasts on surface-modified materials developed for bone implants. Physiol Res 60:403–417
Wei J et al (2009) Influence of surface wettability on competitive protein adsorption and initial attachment of osteoblasts. Biomed Mater (Bristol, England) 4:045002
Yamamoto A, Honma R, Sumita M (1998) Cytotoxicity evaluation of 43 metal salts using murine fibroblasts and osteoblastic cells. J Biomed Mater Res 39(February):331–340
Yamazaki T et al (2006) Biological impact of contact with metals on cells. In Vivo 20:605–612
Yamazaki T et al (2012) Protection against copper-induced cytotoxicity by inclusion of gold. In Vivo 26:651–656
Yang D et al (2013) The molecular mechanism of mediation of adsorbed serum proteins to endothelial cells adhesion and growth on biomaterials. Biomaterials 34(23):5747–5758
Zareidoost A et al (2012) The relationship of surface roughness and cell response of chemical surface modification of titanium. J Mater Sci Mater Med 23:1479–1488
Zberg B, Uggowitzer PJ, Löffler JF (2009) MgZnCa glasses without clinically observable hydrogen evolution for biodegradable implants. Nat Mater 8(11):887–891

Determining the Biological Properties of Biomaterials In Vivo

Perica J. Vasiljević, Jelena Živković, Marija Vukelić-Nikolić and Stevo Najman

Abstract Biocompatibility, bioinertness and biofunctionality are prerequisites was that certain materials could be used in implantation. In vivo studies of biomaterials involves the assessing of overall biocompatibility of the newly synthesized biomaterials. In contact with organism, biomaterials represent foreign bodies and organism can react in various desirable and undesirable ways. As response to biomaterials, two types of hypersensitivity reactions are common, type I and type IV. Materials that are routinely used in dentistry can give rise to hypersensitivity reactions in both sensitised patients and members of the dental team. Hypersensitivity reactions to the endovascular prostheses are among the infrequent and unpredictable reactions that may lead to local or systemic complications. After implantation biomaterials initiate a host response which begins with blood-biomaterial interactions and provisional matrix formation and continues with acute/chronic inflammation, granulation tissue emergence, foreign body reaction, development of fibrous capsule and possible fibrosis. Macrophages are cells that regulate the host response to implanted biomaterial at several levels. Evaluation of the effect of the implant includes a large number of biological parameters e.g. thickness and vascularization of fibrous capsule, the number and size of inflammatory cells, cell infiltration in implant, degenerative and necrotic changes in the surrounding tissues, cell apoptosis, proliferation and differentiation, endothelialization, biodegradation, the thrombus formation, calcification. Effects of biomaterial at the site of implantation depend on its size, shape, surface and physicochemical characteristics. Ideal result of implantation would be complete restoration of normal tissue architecture and function after healing of injuries.

P.J. Vasiljević
Department of Biology and Ecology, Faculty of Science and Mathematics, University of Niš, Višegradska 33, Niš, Serbia

J. Živković · M. Vukelić-Nikolić · S. Najman (✉)
Department of Biology and Human Genetics, Faculty of Medicine, University of Niš, Blvd. Zoran Đinđić 81, 18000 Niš, Serbia
e-mail: stevo.najman@gmail.com

F. Zivic et al. (eds.), *Biomaterials in Clinical Practice*,
https://doi.org/10.1007/978-3-319-68025-5_17

Keywords Biocompatibility · Biomaterials · Hypersensitivity reactions · Implantation · Inflammation · In vivo

1 Introduction

The development of new biomaterials is a lengthy process that includes structural analysis, optimization, testing of biocompatibility and eventually clinical trials.

Tissue damage occurring under different circumstances (trauma, fractures, infections, tumors and the like). Balanced activity of cells the body most damaged part can independently repaired. However, with the emergence of major damage, it is necessary to support the biological potential for reparation for example in a large loss of bone tissue. The resulting damage in regenerative medicine reimbursed graft and implants example. Only in the US are carried out annually over one million compensation and repair of bone tissue (Olivier et al. 2004).

Autotransplantation represents the gold standard for compensation of damage despite many shortcomings. The biggest disadvantage of the autotransplantation is the most commonly a small number of places in the body where it is possible to take material for autotransplantation as its small amount. Alternative autotransplantation including allogeneic and xenogeneic transplant. The possibility of using allogeneic and xenogeneic transplant is limited in terms of histocompatibility and immune tolerance. Some natural [e.g. a natural source of hydroxyapatite to regenerate bone tissue are coral genus Porites (Yaszemski et al. 1996)] or artificial materials can be used as a substitute for the missing tissue. They are so far used in slightly less than 10% of cases resulting compensation (Olivier et al. 2004).

Because of many limitations in using autotransplants and allotransplants, bone tissue engineering (BTE) techniques are becoming nowadays an important alternative for bone defects repair (Li et al. 2014). In bone tissue engineering biodegradable porous scaffolds which mimic 3D structure of natural bone have been imposed as good functional solution. Their characteristics is that they can be mechanical support instead of the missing bone skeleton. Besides, their porosity allows cell growth, cell functions and behavior required for tissue regeneration, as well as vascularization as an important condition for new bone formation. Due to biodegradation ability scaffolds create a space that will be filled with new bone, and thus BTE construct replaced by natural tissue. (Hutmacher 2000). In addition to the above aforementioned properties, scaffolds which by their geometry imitate natural bone extracellular matrix (ECM), i.e. microenvironment for bone cells growth and activity, are tested (Hutmacher et al. 2007; Douglas et al. 2009).

Implantation represents the incorporation of materials into the body. The materials used for this purpose are different as, for example, metals (titanium and its alloys, cobalt–chromium–molybdenum alloy), ceramics (gypsum, hydroxyapatite, alumina, tricalcium phosphate, carbon), glass, polymers (Teflon, silastik, Ivalon). Biocompatibility, bioinertness and biofunctionality are prerequisites was that certain materials could be used in implantation.

The material is biocompatible if it is directly connected with the tissue in which it is installed and contributes to tissue reparation on site. Bioinertness of the material implies its non-toxicity on the body, as well as the exclusion of genotoxicity and the transformation of normal cells into cancer cells. Biofunctionality is reflected in the fact that the fabric retains the normal functions of the installation materials (Ignjatović et al. 2001; Najman et al. 2003, 2004; Vasiljevic et al. 2009, 2013; Jokanović et al. 2016a).

Having in mind that inorganic component of bone is mostly composed of hydroxyapatite, ceramic biomaterials, tricalcium phosphates (TCF) and hydroxyapatites (HAP) have attracted significant attention of researchers. (Ghanaati et al. 2013; Jokanović et al. 2006, 2016a, b). That is the reason why they have a great advantage in biocompatibility compared to other biomaterials. On the other side, their biofunctionality is weaker than in other biomaterials, due to high brittleness they possess. For this reason, ceramic biomaterials cannot be used to repair bone tissue when there is an interruption of continuity of bone (Ignjatović et al. 2001; Najman et al. 2003, 2004; Vasiljevic et al. 2009). There are many attempts to overcome embrittlement, as the main problem in the application of ceramic biomaterials. Disadvantages of ceramics can be at least partly corrected by using polymers such as poly-L-lactide, poly-lactide-co-glycolide, etc. (Durucan and Brown 2000; Ignjatović et al. 2001; Najman et al. 2003, 2004; Vasiljevic et al. 2009, 2013; Mitić et al. 2014). It is shown that composite scaffolds constructed of calcium phosphate and poly (lactide-co-glycolide) (PLGA) have better mechanical properties, such as compressive strength, rather than scaffold without PLGA (Durucan and Brown 2000; Kang et al. 2011). Many studies have shown that PLGA polymer can favorably influence activity of cells essential for the formation and maintenance of bone tissue (Li et al. 2006; Bose et al. 2012).

Polymer component improves mechanical characteristics of composite and contributes to biological characteristics important for expression of specific cell properties during bone growth. On these principles hydroxyapatite composite scaffolds of calcium hydroxyapatite (CHA) and PLGA have been developed, so that PLGA is present as a thin layer on CHA scaffold. CHA is often used in bone tissue engineering because it has good mechanical properties, can be obtained as material of high purity, has good properties for processing and adjustable rate of degradation, all of which is important for adjustment to the healing rate of damaged bone (Agrawal and Ray 2001; Ngiam et al. 2009). The role of PLGA layer is multiple, because it can improve mechanical properties, and to be hydrophobic biological surface of scaffold essential for the various cell activities, such as adhesion, migration, release of metabolites, etc. (Thomas et al. 2014). Porous calcium hydroxyapatite scaffolds covered with PLGA has been showed significant biological advantages over standard bone substitute Geistlich Bio-oss® in in vivo studies of biofunctionality (Jokanović et al. 2016a). Thus, the composite biomaterials of calcium hydroxyapatite and PLGA can fulfill requirements necessary for good bone substitute with good mechanical properties, porosity, biodegradability, topological features, and with the ultimate goal to be osteoconductive and osteoinductive (Jokanović et al. 2016b).

New technologies in the development of potential biomaterial take into account the microenvironment necessary for cell differentiation because there are attempts at integration of active molecules, growth factors and drugs in the tissue matrix (Ripamonti 1993; Ignjatović et al. 2001; Najman et al. 2003, 2004; Vasiljevic et al. 2009, 2013; Mitić et al. 2014).

Examination of biocompatibility includes the evaluation of effects of physiologic environment on material and material on the environment. Evaluation of biocompatibility of biomaterials is possible through two aspects. The first aspect involves in vivo studies for assessing the overall biocompatibility of the newly synthesized biomaterials. In these cases primarily takes into account the physical and chemical characteristics of biomaterials its potential toxicity, biodegradability, the reaction between the tissue and biomaterials, toxicity genotoxicity and mutagenicity degradation products of biomaterials, etc. These tests primarily indicate possible directions of development in the synthesis of new materials that are used in medicine. Another aspect of biocompatibility includes testing the final product i.e. biomaterials to be used clinically to.

The core issue is such a new biomaterial behaves in the treatment of tissue deficits, and what is its biocompatibility and integrativity the tissue microenvironment and whether it supports the development of normal cells (Ohgushi et al. 1989; Ripamonti 1993; Najman et al. 2003, 2004; Vasiljevic et al. 2009, 2013). Today it is used for this purpose in vivo and in vitro experimental approaches which include a series of standardized experimental techniques (Council of Europe 1999; ISO 10993; National Institute of Health 1977).

2 Hypersensitivity Reactions to Biomaterials

In contact with organism, biomaterials represent foreign bodies and organism, in their presence, can react with them in various desirable and undesirable ways. Excessive and inappropriate immune responses to the presence of an antigen are called hypersensitivity or hypersensitivity reactions. Depending on the generated effectors molecules and mechanisms of their action to date have clearly defined four types of hypersensitivity reactions, while the fifth type is still subject of speculations (Rajan 2003).

Classification of hypersensitivity reactions according to Gell and Coombs (Gell and Coombs 1963):

Type I—IgE mediated hypersensitivity
Type II—cytotoxic—IgG/IgM mediated
Type III—immune complex mediated—IgG/IgM immune complex
Type IV—delayed hypersensitivity or cell mediated hypersensitivity.

Whether or not, in what way and to what extent the host will respond to the presence of biomaterials depends on the composition of the applied biomaterials, on

the site of application but largely depends on the physiological characteristics of the host organism. As response to biomaterials, only two types of hypersensitivity reactions are common, type I and type IV.

2.1 Type I of Hypersensitivity Reactions

This type of allergic reaction occurs immediately (within several minutes) after contact between allergens and IgE antibodies, which are already created in the body and which are present on the surface of mast cells and basophilic leukocytes. The reaction between antibodies and antigens results in the release of vasoactive amines, including histamine and adenosine, which causes the symptoms and signs of an allergic reaction of type I. The symptoms experienced by the patient can be very different depending on whether the allergen is injected, inhaled, or orally taken, and depending also on the dose of the allergen (Janeway et al. 2001). Immediate hypersensitivity reactions have diverse clinical and pathologic features, all of which are attributable to mediators produced by mast cells in different amounts and in different tissues. The manifestations of some common immediate hypersensitivity reactions are allergic rhinitis, sinusitis (increased mucus secretion; inflammation of upper airways, sinuses), food allergies (increased peristalsis due to contraction of intestinal muscles), bronchial asthma (bronchial hyperresponsiveness caused by smooth muscle contraction; inflammation and tissue injury caused by late phase reaction) and the most severe form anaphylaxis (fall in blood pressure caused by vascular dilation and airway obstruction due to laryngeal edema). Immediate hypersensitivity may be manifested in many other ways, as in development of skin lesions such as urticaria and eczema (Abbas and Lichtman 2010).

Reports of biomaterials evoking the IgE response are rare, although IgE reactions to some components of biomaterials encountered in other applications, such as nickel and chromium salts in occupational respiratory contact, are known and responses to silicone are controversial (Ratner et al. 1997).

Hypersensitivity type I diagnostic tests

If type I allergy is suspected, it can be diagnosed by a skin test prick (SPT). SPT involves intradermal inoculation of the allergen and provides evidence for sensitization to specific antigen. Results of this test can help in confirmation of the diagnosis of a suspected type I allergy. The main advantage of SPT as compared to an in vitro measurement of specific IgE antibodies is that the test can be interpreted within 15–20 min after the reagent is applied to the skin. Red, papular, and/or vesicular reactions of the skin may appear in positive test conditions. It is minimally invasive, inexpensive, results are immediately available and when carried out by trained health professionals, reproducible. The in vitro measurement of specific IgE antibodies (Pumhirun et al. 2000) is an important complementary tool to diagnose type I allergy, especially in subjects who cannot undergo SPT. For example, SPT is

not recommended in patients who have extensive eczema, dermographism, urticaria, or who are taking antihistamines or other medications which interfere with the proper interpretation of the test results. In vitro test methods may be less sensitive (Hill et al. 2004; Chung et al. 2010) and/or less specific (Ten et al. 1995; Van der Zee et al. 1988) than SPT depending on the method utilized and the allergens employed. Furthermore, in subjects with very high total serum IgE antibodies, low levels of specific IgE antibodies of doubtful clinical relevance are often detected. Moreover, SPT provides immediate information versus in vitro test results which may not be available for days or weeks. Thus, SPT has greater flexibility and is usually less costly (Heinzerling et al. 2013).

2.2 *Type IV of Hypersensitivity Reactions*

Type IV hypersensitivities are referred to as delayed type hypersensitivities because a reaction can typically take 12 or more hours to develop after contact with specific antigen (Brostoff et al. 1991). Reaction occurs after antigenic activation of a large number of TH cells (mainly TH1 subtype), in previously sensitized person, which then recruit other cells to the site of exposure. Sensitization develops only in some people after exposure to some certain antigens which can be inserted into the body in everyday life through food, water, skin, respiratory tract or different preventive, diagnostic and therapeutic procedures.

In evolution of type IV of hypersensitivity several phases were described: recognition and sensitization to antigen, TH lymphocyte activation and effector phase. The effector phase of a delayed-type hypersensitivity response is initiated by contact of sensitized T-cells with an antigen. In this phase, T-cells, which are antigen-activated, are characterized as TDTH cells and, in conjunction with activated antigen presenting cells (APCs), can secrete a variety of cytokines that recruit and activate macrophages, monocytes, neutrophils, and other inflammatory cells (Hallab et al. 2001). The main characteristics of type IV hypersensitivity reactions are localized inflammatory response which occurs after a period of latency after exposition to antigen to which person is sensitized. At the site of inflammation dominate presence of cells of which are the most numerous macrophages.

Type IV of hypersensitivity reaction is usually manifested in the skin in different clinical pattern.

In the last years, there were publications which can throw a new light on these complicated mechanisms leading to the development of the type IV of allergy, especially to drugs, nickel and other haptens and also can explain the differentiation of clinical pattern in respective patients. The skin symptoms in type IV of hypersensitivity are triggered by activation of specific T-cell CD4+ and CD8+. Immunohistochemical and functional analysis of reactive T-cell has shown that the delayed hypersensitivity reaction depends on the secreted cytokines. For the better understanding of these inflammatory cascades deleted type IV of hypersensitivity reactions have been re-classified into four main subtypes (Czarnobilska et al. 2007).

Clinically delayed hypersensitivity eruptions are often an overlap of cytokine pathways, with one preferential reaction dominating the final picture. Type IVa and IVc play a role in the mechanism of contact dermatitis, however type IV b in chronic asthma, chronic allergic rhinitis and maculo-papular exanthema with eosinophilia, type IV c in bullous reactions (i.e. Stevens-Johnsons Syndrome or toxic epidermal necrolysis), so type IV d in pustular exanthema reactions (i.g. AGEP—Acute Generalized Exanthematous Pustule, Behcet disease). This different clinical pattern of allergic disease mainly including drug allergy to nickel and other haptens as well as chronic asthma and allergic rhinitis may be explained by above mechanisms (Czarnobilska et al. 2007).

Hypersensitivity type IV diagnostic tests

For verification of type IV hypersensitivity reactions there are two common methods: (1) cutaneous patch testing and (2) lymphocyte transformation tests (Primeau and Adkinson 2001).

Cutaneous patch testing is considered as gold standard for in vivo evaluation of delayed hypersensitivity reactions (Schalock et al. 2012). It is commonly used for diagnostic purposes in people who already suspected hypersensitivity to the applied biomaterial, but also as preventive measures or determining predisposition to hypersensitivity reactions to different types of biomaterials. This procedure is not complicated, but it carries a certain discomfort for the patient. Also, although very small, there is a risk that the procedure itself, cause sensitization of the patient to the antigen used in the test. A patch test is always carried using some of the already defined batteries of antigens. Procedure of performing this assay consists of the introduction of the antigen in the vehicle such as petrolatum and the exposure of the skin (48–96 h) with the help of fixation bandage.

After exposition time, the reactions are graded on a scale from 1 (mild or absent response) to 4 (severe rash with small, possibly encrusted, weeping blisters) (Hallab et al. 2001). Practical advantages of cutaneous patch testing include ease of performance, rapidity of results, the scope of evaluation, and widespread availability (Granchi et al. 2006; Thyssen et al. 2011) These findings can be viewed as support for the argument that preoperative patch testing potentially prevents significant morbidity (Schalock et al. 2012). Its preoperative use should strongly be considered in patients with a history of metal allergies and its postoperative use in patients presenting with either suspected metal hypersensitivity or implant failure in the absence of infection (Schalock et al. 2012; Granchi et al. 2012).

Lymphocytes transformation testing (LTT) can be used as an alternative method to determine metal sensitivity in a patient. It has been suggested for use when patch testing provides questionable results. This in vitro test measures the proliferation of lymphocytes from a patient's peripheral blood in the presence and absence of a potential allergen (Schalock et al. 2012; Granchi et al. 2012).

An enhanced version of the lymphocyte transformation test, called memory lymphocyte immuno-stimulation assay (MELISA®), is available for healthcare practitioners and can assist in the detection of Type IV hypersensitivities, as

previously described (Valentine-Thon et al. 2006; Stejskal et al. 1996). In summary, a standard number of lymphocytes, with the exclusion of monocytes, are isolated from whole blood specimens for cell culture. The lymphocytes are cultured for 5 days then transferred to new plates containing known antigens, which are then pulsed for 4 h with methyl-^{3}H thymidine to quantify cell proliferation. A negative control is also obtained via lymphocytes from the same patient, which is not added to antigens. After culture, the lymphocytes are harvested onto filter paper and dried. The radioactivity present on the filter paper is measured in a liquid scintillation counter. A stimulation index (SI) is calculated by dividing the counts per minute (cpm) in the test well to the average cpm in the negative control wells (Valentine-Thon et al. 2007; Valentine-Thon and Schiwara 2003; Stejskal et al. 1996). A positive reaction, indicating Type IV hypersensitivity, is defined as a SI greater than 3 and an equivocal reaction is a SI between 2 and 3. A SI less than 2 is considered negative. Clinically, MELISA® has been proven to be an effective tool for the determination of sensitivities to various metals (Valentine-Thon and Schiwara 2003).

In vitro leukocyte migration inhibition testing involves the measurement of mixed-population leukocyte migration activity. Leukocytes in culture actively migrate in a random fashion, but they can be attracted preferentially to chemoattractants, such as those released by Staphylococcus and other bacteria. However, in the presence of a sensitizing antigen, they migrate more slowly, losing the ability to recognize chemoattractants, and are said to be migration-inhibited. Contemporary migration-testing techniques quantify the migration of lymphocyte populations in vitro through, under, or along media such as agarose layers, agarose droplets, capillary tube walls, membrane filters, and collagen gels (Hallab et al. 2000). Over the long term, migration testing alone (as well as any single assay) may be an inadequate detector of delayed type hypersensitivity (Repo et al. 1980).

2.3 Hypersensitivity to Orthopedic Materials

Orthopedic implants can be made of a variety of metallic, plastic, and/or ceramic elements. The metal components of knee prostheses are most commonly stainless steel, followed by cobalt-chromium molybdenum (CoCrMo) alloys, nickel, titanium, beryllium, vanadium, and tantalum (Basko-Plluska et al. 2011; Hallab and Jacobs 2009). Exposure to metal ions can occur in a number of ways. Routine metal exposure in humans occurs through skin contact with jewelry, cell phones, clothing fasteners, and leather and through occupational exposure, dental filings, and medical implants (Thyssen and Menné 2010). Individuals are further exposed to trace metals through smoking and in cosmetics, food, and drinking water (Ashraf 2012; Teow et al. 2011; Borchers et al. 2010).

Sensitization to metal is known to occur independently of the mechanism of exposure (Basko-Plluska et al. 2011). As previously mentioned, metal-ion exposure produces an adaptive immune response wherein macrophage activation leads to development of a delayed-type hypersensitivity reaction (Cadosch et al. 2009; Hallab et al. 2008; Thomas et al. 2000). Pathophysiological mechanism of hypersensitivity evolution to metals is not fully understood. It is believed that the metals in contact with body fluids corrode and set free metal ions which are processed by the immune system. These ions, although not sensitizers, form complexes with native proteins and act as allergens causing hypersensitivity reactions. Cutaneous reactions above the implanted device are primarily T cell-mediated type IV delayed-type reactions. Reported reactions at the site of the metal implant include type IV reactions but are probably complex in nature. Peri-implant reactions seem to be Th1-dominant (Schalock et al. 2012). Metals known as sensitizers (haptenic moieties in antigens) are beryllium, nickel, cobalt, and chromium; in addition, occasional responses to tantalum, titanium and vanadium have been reported (Hallab 2001). Nickel, cobalt, and chromium are the three most common metals that elicit both cutaneous and extracutaneous allergic reactions from chronic internal exposure, but almost all metals present in biomaterials can induce hypersensitivity reactions.

Hypersensitivity reactions to metallic joint implants can present in several ways and may result in localized or systemic allergic dermatitis, sometimes painful, and sometimes as exudative lesions in the periprosthetic region, loss of joint function, implant failure, and patient dissatisfaction (Thyssen and Menné 2010).

In patients with implants containing metal, the clinician should consider metal hypersensitivity when dermatologic allergic symptoms are reported. Furthermore, metal hypersensitivity should be considered in patients with joint implants when they have arthralgia, when periprosthetic radiolucent lines appear, or when aseptic implant loosening is observed (Willert et al. 2005).

In addition to the hypersensitivity of the metal components of the implants, in literature it is described hypersensitivity to the polymer components of the implants. The study of Gil-Albarova et al. (1992) demonstrated that lymphocyte-mediated immune response is activated in patients with aseptic loosening of cemented total hip prostheses. The most significant alterations were the high immune reactivity induced by the monomer of PMMA measured by the LTT, and the increase in total T lymphocytes (CD2 cluster), especially those displaying the interleukin-2 receptor (CD25) which is an early marker for lymphocyte activation. Although they did not perform immunological studies at the cement-bone interface membrane, the increase in total T lymphocytes, especially those displaying the interleukin-2 receptor, suggests the occurrence of a type IV immunological hypersensitivity reaction at that level (cell-mediated response or contact sensitivity). The high rate of lymphoblast transformation produced by PMMA indicates that only this substance, and not the bone cement stabilizers, acts as the allergen.

2.4 Hypersensitivity to Dental Materials

Materials that are routinely used in dentistry can give rise to hypersensitivity reactions in both sensitised patients and members of the dental team. The materials used in odontology includes antiseptics, metals, alloys, porcelains, impression materials, local anesthetics, cements, latex gloves, rubber dams, acrylates, adhesives, mouth washes, and others (Gawkrodger 2005; Khamaysi et al. 2006; Lygre 2002; Mallo-Pérez and Díaz-Donado 2003) Kanerva et al. (1995) identified more than 130 possible allergens derived from materials for use in odontology. In a study by Khamaysi et al. (2006) in patients with oral symptoms, who had undergone dental treatment, the common allergens detected included gold sodium thiosulfate (14.0%), nickel sulfate (13.2%), mercury (9.9%), palladium chloride (7.4%), cobalt chloride (5.0%), and 2-hydroxyethyl methacrylate (5.8%). In another study by Goon et al. (2006) the most common allergens in this group were the (meth) acrylate monomers and elemental mercury. Artificial and natural teeth, metallic dental implants, as well as restorative materials within the mouth interact continually with physiological fluids. They are subject to larger temperature and pH variations than most other parts of the body. Corrosion, the graded degradation of materials by electrochemical attack, is of concern particularly when dental implants are placed in the hostile electrolytic environment provided by the human mouth. Allergic reactions may occur from the presence of ions produced from the corrosion of implants. Typical allergic symptoms and diagnoses were Pustulosis palmaris et plantaris, lichen planus, stomatitis and contact dermatitis which implies that reactions to these materials appeared not only in the mucosa of the oral cavity, but also on the skin of entire body (Gawkrodger 2005; Hamano et al. 1998; Yanagi et al. 2005).

2.5 Endovascular Devices

As endovascular devices coronary stents, perforated foramen occluders, pacemakers and implantable cardioverter defibrillators are frequently used. Hypersensitivity reactions to the biomaterials used in endovascular prostheses are among the infrequent and unpredictable reactions that may lead to local or systemic complications following cardiovascular therapeutic interventions (Honari et al. 2008). A spectrum of responses, varying from benign reactions to excessive inflammation and systemic hypersensitivity reactions are reported and should be considered relative to the context of their application (Nebeker et al. 2006; Fukahara et al. 2003; Dasika et al. 2003).

3 Effects of Biomaterials to Implantation

Implantation to assess the impact biomaterial on the structure and function of tissues. Evaluation of the effect of the implant includes primarily microscopic evaluating. Microscopic evaluation includes monitoring a large number of biological parameters e.g. thickness and vascularization of fibrous capsule, the number and size of inflammatory cells, cell infiltration in implant, degenerative and necrotic changes in the surrounding tissues, apoptosis, cell proliferation and differentiation, endothelialization, biodegradation, the formation of thrombus, calcification (Ignjatović et al. 2001; Najman et al. 2003, 2004; Vasiljevic et al. 2009, 2013; Ignjatović et al. 2013). As experimental models used for implantation mice, rats, rabbits, guinea pigs, dogs, sheep, goats, pigs or other animals. The implantation site are the subcutaneous tissue, muscle, bone or intraperitoneal. Evaluation of results is done in the short term at 2, 4, 6, 8, 12 weeks or long term several months.

Local effects of biomaterials at the site of implantation

After implantation, which represents a kind of tissue injury, biomaterials initiate a host response which begins with blood-biomaterial interactions and provisional matrix formation and continues with acute/chronic inflammation, granulation tissue emergence, foreign body reaction, development of fibrous capsule and possible fibrosis (Anderson et al. 2008). All aforementioned events are interrelated and are partially overlapped. The course of these processes depends on the characteristics of implanted biomaterial, but likewise final fate of this same biomaterial depends on intensity of particularized host tissue reactions.

3.1 Injury

Implantation of biomaterial represents an injury per se because it leads to tissue damage. At the very beginning of host response to tissue injury, predominantly blood and vasculature are involved (Anderson 2008). Cells, growth factors, cytokines and chemokines from blood affect initiation of inflammatory response whose direction and intensity are extremely important for proper healing of injuries (Shapiro 2008). Bleeding and coagulation at the site of implantation are starting events of healing cascade that further follows the order Inflammation-Repair-Remodeling. How will host tissue respond to injury depends on its degree and is in correlation with blood-biomaterial interactions, formation of provisional matrix and inflammatory response. Further, extent of granulation tissue formation, foreign body reaction and fibrosis/fibrous capsule development in implants depends on the aforementioned factors. All of these processes are, in the case of biocompatible biomaterials, ending within 2–3 weeks after implantation (Anderson 1988, 1993).

3.2 Blood-Biomaterial Interactions

After implantation, biomaterial comes in contact with blood which coagulates (Yu et al. 2014; Shiu et al. 2014). Blood plasma, among others, is consisted of approximately three hundred distinct proteins, whereby many of them are involved directly in wound healing process (Powanda and Moyer 1981; Anderson and Anderson 2002). Immediately after implantation, adsorption of proteins from blood and interstitial fluids to the biomaterial surface occurs (Franz et al. 2011). This is also confirmed by the results of our investigations which are showing that after one-week incubation of biomaterial in simulated body fluid (Kokubo 1996) weakly soluble precipitates can be noticed on surface of biomaterial (Vukelić et al. 2011, 2012). Since layer of adsorbed proteins has influence on coagulation, complement system, platelets and finally immune cells, blood-biomaterial surface interactions have a great impact on host inflammatory response to implanted biomaterial (Anderson 2008; Franz et al. 2011; Yu et al. 2014). Blood is a rich source of different cytokines and growth factors, whereby many of them have proangiogenic properties. This fact is very important from aspect of injury healing, because vascularization and angiogenesis are key events that maintain tissue structure and repair process (Najdanović et al. 2015). It is probably that proangiogenic factors from blood affect various cell types involved in vascularization and angiogenesis. So, implants made of nanomaterial NP-CP/DLPLG mixed with full blood and bone marrow cells are better vascularized in regard to implants made of nanomaterial and blood only, 8 weeks after subcutaneous implantation (Janićijević et al. 2008). Blood plasma in combination with biomaterial can be very useful in the field of tissue regeneration as well, according to our previously findings (Ajduković et al. 2005). Our recent results from experiments with subcutaneously implanted biomaterial mixed with blood plasma and adipose-derived stem cells indicated that this concept can be suitable for increasing vascularization (Najdanović et al. 2015).

Textured biomaterial surfaces, in contrast to smooth surfaces, promote coagulation by interrupting the blood flow at the blood-biomaterial interface. It is also known that protein adsorption occurs more on hydrophobic than hydrophilic surfaces (Wilson et al. 2005). Chemical composition of absorbed proteins does not remain constant and successively replacement of adsorbed proteins which happened during time is termed the Vroman effect. It occurs mostly on negatively charged hydrophilic surfaces (Turbill et al. 1996). Deposition of blood proteins on a biomaterial surfaces represent an introduction into provisional matrix formation (Anderson 2008).

3.3 Provisional Matrix Formation

Provisional matrix, constituted mainly of fibrin and fibronectin, arises as a consequence of vascularized tissue injury during biomaterial implantation. It serves as

matrix for cell adhesion but also stimulates them to proliferate, differentiate and synthesize new extracellular matrix components (Anderson and Patel 2013). Fibrin forms the basis of provisional matrix, but beside fibrin, secretory products of complement system, activated platelets, inflammatory and endothelial cells also contribute to provisional matrix structure. Over and above, biomaterial surfaces spontaneously adsorb fibrinogen, precursor of fibrin (Hu et al. 2001). As a component of provisional matrix, fibrin network initiate recruitment of inflammatory cells and fibroblasts. Beside fibrinogen/fibrin, fibronectin and vitronectin have also been described to attach to biomaterial surfaces (Asch and Podack 1990; Gawaz et al. 1997; Lee et al. 2006). Phagocytes are attracted by adsorbed fibrinogen/fibrin, initiating an inflammatory response which occurs physiologically after clot formation (Jennewein et al. 2011). Further, fibronectin and vitronectin regulate inflammatory response to biomaterials by promoting macrophage fusion to foreign body giant cells on biomaterial surfaces. Activated platelets from formed blood clot attract fibroblast through platelet factor 4 (PF4), platelet-derived growth factor (PDGF) and transforming growth factor-beta (TGF-β) release (Riches 1988; Wahl et al. 1989). Thrombin from blood clot, also acts as a chemoattractant for neutrophils, monocytes and lymphocytes by affecting regeneration of damaged tissue (Bar-Shavit et al. 1983; Bizios et al. 1986). So generally, the provisional matrix is composed of adhesive proteins as well as released platelet granule components which besides the above mentioned factors include also thrombospondin, transforming growth factor-alpha (TGF-α) and platelet derived endothelial cell growth factor (PD-ECGF). In this way, fibrin network provides favorable substrate for cell adhesion and migration. Depending on the biomaterial environment at the site of implantation, adherent proteins may promote chronic inflammation or wound healing process (Anderson 2008; Franz et al. 2011).

Attracted phagocytes degrade fibrin network over time, which at the beginning promotes inflammation (Szaba and Smiley 2002) and later fibrin network is gradually being replaced by immature connective tissue which contains immature fibroblasts (cells that are often referred to as mesenchymal stem cells) with the ability to differentiate into various cell types (Alberts et al. 2002). Existence of immature connective tissue in the implant site is of the great importance to the process of reparation and regeneration in general.

3.4 Inflammation

Inflammatory process involves a series of interrelated events that participate in tissue healing and tissue reconstitution at the site of implantation. Its intensity and time duration depend very much on the size, shape and physicochemical characteristics of biomaterial. Inflammatory process is also influenced by extent of injury during implantation procedure and type of injured tissue. At the beginning of host inflammatory reaction, neutrophils followed by monocytes and macrophages are the

most prevalent cell types (Anderson 2001). Inflammatory response triggered by implanted biomaterials can be acute and chronic.

Typical feature of acute inflammatory response, which lasts from minutes to days, is migration of neutrophils and eosinophils to the site of implantation, mast cell degranulation with histamine release and adsorption of fibrinogen to biomaterial surface (Tang et al. 1998; Zdolsek et al. 2007). The major role of neutrophils and subsequently macrophages is to phagocyte microorganisms and foreign materials, and the extent of degradation depends on the properties of biomaterial itself (Anderson 2001). For instance, extended resorption by phagocytes can be a consequence of biomaterials hardness (Najman et al. 2004). Histamine released from mast cells is critical to the recruitment of phagocytes to implanted biomaterials (Tang et al. 1998). Adsorbed and partially denatured proteins, predominantly fibrin/fibrinogen are considered to be ones which determine stream of the acute inflammatory response (Tang and Eaton 1993; Anderson 2001). These proteins induce and modulate leukocyte migration and inflammatory reaction (Jennewein et al. 2011).

Chronic inflammation also begins with recruitment of neutrophils, but in contrast to acute inflammation it is histologically heterogeneous and may cause implant failure. It is predominantly characterized by the presence of macrophages, monocytes, lymphocytes and fibroblasts which become numerous 1–2 weeks after injury and diminish at 6 weeks. Proliferation of blood vessels and development of connective tissue are also characteristics of acute inflammatory response. Surgical wounding per se is enough to attract neutrophils, and presence of biomaterial increases macrophage migration to the site of implantation (Robitaille et al. 2005). Macrophage represents the most important cell type in chronic inflammation. These cells produce the great number of biologically active factors which can affect all aspects of tissue reparation and regeneration after injury (Anderson 2001). It is believed that macrophages and their products are key factors in controlling wound healing and fibrosis (Anderson and McNally 2011). Prolonged chronic inflammation is often cause of impaired wound healing around implanted biomaterial (Dee et al. 2003), and intense inflammatory response usually leads to implant failure. However, the inflammatory response is the first in a series of reactions that lead to normal tissue healing, and in the last few years there has been increasing evidence that controlled inflammation may have beneficial effect on reparative and regenerative processes. Results from our study, among others, showed that inclusion of thioglycollate-elicited peritoneal macrophages in structure of implants composed of mineral bone substitute may support osteogenic process (Živković et al. 2015).

3.5 Granulation Tissue

With regards to biomaterials with good biocompatibility, inflammatory response usually lasts no longer than 2 weeks. Resolution of acute and chronic inflammatory responses is followed by granulation tissue formation that results from proliferation

of fibroblasts and vascular endothelial cells, and is identified by the presence of macrophages, infiltrated fibroblasts and blood vessels. This tissue was named "granulation" according to its granulated look and presence of numerous capillaries (Nowak and Olejek 2004). Formation of granulation tissue after inflammatory response represent hallmark of tissue healing.

Thanks to numerous blood vessels, different cells, cytokines, chemokines and growth factors are coming to the site of biomaterial implantation. Fibroblasts from granulation tissue proliferate and synthesize collagen, elastin, proteoglycans, glycosaminoglycans and other noncollagenous proteins (Lin et al. 1997; Olczyk et al. 2014). Granulation tissue is being subsequently remodeled approximately 7–10 days after injury. This process results in the formation of mature connective tissue (Häkkinen et al. 2012).

One should make a distinction between the terms granulation tissue and granuloma, accumulations of modified macrophages called epithelioid cells. Granuloma is a consequence of chronic inflammation, while granulation tissue is a normal occurrence during tissue healing. A few cell layers usually separate granulation tissue from the implanted biomaterial (Anderson and Patel 2013). Fibroblasts that granulation tissue contains allow contraction and wound closure.

As noted, granulation tissue formation goes along with normal tissue healing process. However, in the case of large tissue injury, abundant granulation tissue forms in an attempt to fill defect, leading frequently to fibrosis or scar formation (Lin et al. 1997; Anderson 2001).

3.6 The Foreign Body Reaction

Macrophages that have attached to foreign biomaterial over time, have a strong ability of phagocytosis and secrete proinflammatory cytokines, Reactive Oxygen Species (ROS) and degradative enzymes. These cells can resorb particles up to a size of 5 μm. In the case of larger particle size, macrophages fuse into foreign body giant cells (Franz et al. 2011). Foreign body reaction involves macrophages, foreign body giant cells and components of previously formed granulation tissue. The normal foreign body reaction can be seen often when biomaterials are implanted, but prolonged reaction can inhibit healing process (Anderson 1988).

There are two morphologically different types of foreign body giant cells, refer as the Langhans type and the foreign body type. The first cell type formation is stimulated by Interferon- γ (IFN-γ). These cells are characterized by round shape appearance and presence up to approximately 20 nuclei. Nuclei are located in peripheral cell region and are arranged in a circular form. The second cell type formation is stimulated by Interleukin-4 (IL-4) or IL-13. These cells have an irregular shape and randomly arranged numerous nuclei (more than 20) (Fais et al. 1994; DeFife et al. 1997; Anderson 2000; Kaji et al. 2000).

During the foreign body reaction, reorganization of previously formed extracellular matrix occurs. Family of enzymes called matrix metalloproteinases

(MMPs) participate in this process, degrading almost every extracellular matrix component (Luttikhuizen et al. 2006). MMPs are secreted by macrophages, while new extracellular matrix components are secreted by fibroblasts. Extracellular matrix represents a rich milieu of different cytokines, chemokines and growth factors which are released by remodeling process. Further fate of cells and processes in the tissue at the site of biomaterial implantation depends very much on the features of these released factors.

Foreign body reaction is greatly determined by the form and surface topography of implanted biomaterial. Porous materials, particulate or microspheres are characterized by significant foreign body giant cell reaction, in contrast to the smooth-surface biomaterials (Anderson 2013).

3.7 Fibrous Capsule Development and Fibrosis

Degradable biomaterials will be resorbed through chronic foreign body reaction. The final outcome of foreign body reaction in the case of non-degradable materials is formation of fibrous capsule around the implant (Luttikhuizen et al. 2006).

Ideal result of implantation would be complete restoration of normal tissue architecture and function after healing of injuries. However, formation of fibrous capsule (usually 50–200 μm in thickness) is generally the final step in the reaction of host tissue to biomaterial (Morais et al. 2010; Anderson and McNally 2011). The reason for this is that organism recognizes the implanted biomaterial as foreign body that should be isolated. This is best accomplished by forming a thin capsule that can be tolerated around the implants, because it prevents prolonged interaction between implanted biomaterial and the host tissue (Konttinen et al. 2005; Nuss and Rechenberg 2008). Fibrous capsule is built primarily of collagen III, produced by fibroblasts that originate from granulation tissue. Presence of thick connective capsule around implants may indicate a strong inflammatory response (El-Warrak et al. 2004a, b). Fibrous encapsulation and fibrosis may result in rejection of the implanted biomaterial (Anderson 2008).

Although inflammatory phase caused by biomaterial implantation is usually followed with fibrosis, these two events are not necessarily mutually proportional (Jones 2008). It could be said that the extent of fibrosis depends primarily on types of different factors found at the site of implantation, which influence inflammatory response. Among the most significant factors that influence the extent of inflammation and fibrosis are IL-1, TNF-α and TGF-β. Overexpression of IL-1β can be the cause of strong inflammatory response that can evolve into a prolonged inflammation which leads to tissue damage and fibrosis. TNF-α overexpression leads to inflammation whose consequence is weak fibrosis. Unlike these, overexpression of TGF-β is cause of mild inflammatory response but strong and progressive chronic fibrosis (Jones 2008).

Macrophages are able to secrete all mentioned cytokines, as well as many other factors and therefore are often referred as key regulators of fibrosis. Thanks to these

secretory factors macrophages recruit fibroblasts, other inflammatory cell types as well as additional macrophages to the site of tissue damage due to the implantation procedure. Ingestion of apoptotic and dead cells in general increases macrophage TGF-β secretion, in this case directing them towards profibrotic manner. On the other hand, macrophages can also promote resolution of fibrosis through clearing of fibroblasts, other type of cells and cellular debris, thereby eliminating profibrotic stimuli (Wynn and Barron 2010).

For many years fibrosis was thought to be a progressive and irreversible process, but it is not necessarily the case. In this regard, ongoing inflammation can reverse fibrosis by virtue of macrophages collagenases that enable degradation of extracellular matrix. Bearing in mind both profibrotic and antifibrotic activity of macrophages, management of the functional state of these cells could be a tool to control fibrosis (Wynn and Barron 2010).

4 Conclusion

Implantation of biomaterial is followed by series of dynamic and interrelated processes as a consequence of local reaction of organism, considering that surrounding tissue is injured and comes into contact with a foreign body. Effects of biomaterial at the site of implantation depend on its size, shape, surface and physicochemical characteristics. Macrophages are cells that regulate the host response to implanted biomaterial at several levels. It is therefore logical that, in future, researching should be focused on these cells in order to improve biomaterials' acceptance which could be useful in tissue engineering and regenerative medicine.

Acknowledgements The printing of this article is financed by EU project 543898-TEMPUS-1-2013-1-ES-TEMPUS-JPHES. Part of the scientific study are supported by Ministry of Education, Science and Technological Development, Serbia, as part of project No. III 41017.

References

Abbas AK, Lichtman AHH (2010) Basic immunology updated edition: functions and disorders of the immune system. Elsevier Health Sciences

Agrawal CM, Ray RB (2001) Biodegradable polymeric scaffolds for musculoskeletal tissue engineering. J Biomed Mater Res 55(2):141–150

Ajduković Z, Najman S, Lj Đorđević et al (2005) Repair of bone tissue affected by osteoporosis with hydroxyapatite-poly-L-lactide (HAp-PLLA) with and without blood plasma. J Biomater Appl 20(2):179–190

Alberts B, Johnson A, Lewis J et al (2002) Molecular biology of the cell, 4th edn. Garland Science, New York. Available via http://www.ncbi.nlm.nih.gov/books/NBK26889/

Anderson J (1988) Inflammatory response to biomaterials. ASAIO Trans 34(2):101–107

Anderson J (1993) Mechanisms of inflammation and infection with implanted devices. Cardiovasc Pathol 2(Suppl. 1):33S–41S
Anderson J (2000) Multinucleated giant cells. Curr Opin Hematol 7(1):40–47
Anderson J (2001) Biological responses to materials. Annu Rev Mater Res 31:81–110
Anderson J (2008) Biocompatibility and bioresponse to biomaterials. In: Atala A, Lanza R, Thomson J, Nerem R (eds) Principles of regenerative medicine, 1st edn. Elsevier Academic Press, Burlington, pp 704–723
Anderson J (2013) Inflammation, wound healing and the foreign-body response. In: Ratner B, Hoffman A, Schoen F, Lemons J (eds) Biomaterials science: an introduction to materials in medicine, 3rd edn. Elsevier Academic Press, Waltham, pp 503–512
Anderson NL, Anderson NG (2002) The human plasma proteome: history, character, and diagnostic prospects. Mol Cell Proteomics 1(11):845–867
Anderson J, McNally A (2011) Biocompatibility of implants: lymphocyte/macrophage interactions. Semin Immunopathol 33(3):221–233
Anderson J, Patel J (2013) Biomaterial-dependent characteristics of the foreign body response and *S. epidermidis* biofilm interactions. In: Moriarty F, Zaat S, Busscher H (eds) Biomaterials associated infection: immunological aspects and antimicrobial strategies. Springer Science + Business Media, New York, pp 119–150
Anderson J, Rodriguez A, Chang D (2008) Foreign body reaction to biomaterials. Semin Immunol 20(2):86–100
Asch E, Podack E (1990) Vitronectin binds to activated human platelets and plays a role in platelet aggregation. J Clin Invest 85(5):1372–1378
Ashraf MW (2012) Levels of heavy metals in popular cigarette brands and exposure to these metals via smoking. Sci World J. doi:10.1100/2012/729430
Bar-Shavit R, Kahn A, Fenton J 2nd et al (1983) Chemotactic response of monocytes to thrombin. J Cell Biol 96(1):282–285
Basko-Plluska JL, Thyssen JP, Schalock PC (2011) Cutaneous and systemic hypersensitivity reactions to metallic implants. Dermatitis 22(2):65–79
Bizios R, Lai L, Fenton J 2nd et al (1986) Thrombin-induced chemotaxis and aggregation of neutrophils. J Cell Physiol 128(3):485–490
Borchers A, Teuber SS, Keen CL et al (2010) Food safety. Clin Rev Allerg Immunol 39(2):95–141
Bose S, Roy M, Bandyopadhyay A (2012) Recent advances in bone tissue engineering scaffolds. Trends Biotechnol 30:547–564
Brostoff J, Scadding GK, Male D et al (1991) Introduction to immune responses. In: Brostoff J, Scadding GK, Male D, Roitt IM (eds) Clinical immunology. Gower Medical Publishing, New York
Cadosch D, Chan E, Gautschi OP et al (2009) Metal is not inert: role of metal ions released by biocorrosion in aseptic loosening—current concepts. J Biomed Mater Res A 91(4):1252–1262
Chung BY, Kim HO, Park CW et al (2010) Diagnostic usefulness of the serum-specific IgE, the skin prick test and the atopy patch test compared with that of the oral food challenge test. Ann Dermatol 22(4):404–411
Council of Europe (1999) Guide to the preparation, use and quality assurance of blood components, 5th edn. Council of Europe Publishing, Strasbourg
Czarnobilska E, Obtułowicz K, Wsołek K (2007) Type IV of hypersensitivity and its subtypes. Przegl Lek 64(7–8):506–508
Dasika UK, Kanter KR, Vincent R (2003) Nickel allergy to the percutaneous patent foramen ovale occluder and subsequent systemic nickel allergy. J Thorac Cardiovasc Surg 126(6):2112
Dee K, Puleo D, Bizios R (2003) An introduction to tissue-biomaterial interactions. Wiley, Hoboken, pp 127–147
DeFife K, Jenney C, McNally A et al (1997) Interleukin-13 induces human monocyte/macrophage fusion and macrophage mannose receptor expression. J Immunol 158(7):3385–3390
Douglas T, Pamula E, Hauk D et al (2009) Porous polymer/hydroxyapatite scaffolds: characterization and biocompatibility investigations. J Mater Sci Mater Med 20(9):1909–1915

Durucan C, Brown PW (2000) Calcium-deficient hydroxyapatite-PLGA composites: mechanical and microstructural investigation. J Biomed Mater Res 51:726–734

El-Warrak A, Olmstead M, Apelt D (2004a) An animal model for interface tissue formation in cemented hip replacements. Vet Surg 33(5):495–504

El-Warrak A, Olmstead M, Schneider R et al (2004b) An experimental animal model of aseptic loosening of hip prostheses in sheep to study early biochemical changes at the interface membrane. BMC Musculoskelet Disord 5:7

Fais S, Burgio VL, Silvestri M et al (1994) Multinucleated giant cells generation induced by interferon-gamma. Changes in the expression and distribution of the intercellular adhesion molecule-1 during macrophages fusion and multinucleated giant cell formation. Lab Invest 71 (5):737–744

Franz S, Rammelt S, Scharnweber D et al (2011) Immune responses to implants—a review of the implications for the design of immunomodulatory biomaterials. Biomaterials 32(28):6692–6709

Fukahara K, Minami K, Reiss N et al (2003) Systemic allergic reaction to the percutaneous patent foramen ovale occluder. J Thorac Cardiovasc Surg 125(1):213–214

Gawaz M, Neumann F, Dickfeld T et al (1997) Vitronectin receptor ($\alpha_v\beta_3$) mediates platelet adhesion to the luminal aspect of endothelial cells. Implications for reperfusion in acute myocardial infarction. Circulation 96:1809–1818

Gawkrodger DJ (2005) Investigation of reactions to dental materials. Br J Dermatol 153(3):479–485

Gell PGH, Coombs RRA (1963) The classification of allergic reactions underlying disease. In: Coombs RRA, Gell PGH (eds) Clinical aspects of immunology. Blackwell Science, Philadelphia

Ghanaati S, Barbeck M, Willershausen I et al (2013) Nanocrystalline hydroxyapatite bone substitute leads to sufficient bone tissue formation already after 3 months: histological and histomorphometrical analysis 3 and 6 months following human sinus cavity augmentation. Clin Implant Dent Relat Res 15:883–892

Gil-Albarova J, Lacleriga A, Barrios C et al (1992) Lymphocyte response to polymethyl-methacrylate in loose total hip prostheses. J Bone Joint Surg Br 74(6):825–830

Goon AT, Isaksson M, Zimerson E et al (2006) Contact allergy to (meth) acrylates in the dental series in southern Sweden: simultaneous positive patch test reaction patterns and possible screening allergens. Contact Dermat 55(4):219–226

Granchi D, Cenni E, Trisolino G et al (2006) Sensitivity to implant materials in patients undergoing total hip replacement. J Biomed Mater Res B 77(2):257–264

Granchi D, Cenni E, Giunti A et al (2012) Metal hypersensitivity testing in patients undergoing joint replacement a systematic review. J Bone Joint Surg Br 94(8):1126–1134

Häkkinen L, Larjava H, Koivisto L (2012) Granulation tissue formation and remodeling. Endod Topics 24(1):94–129

Hallab N (2001) Metal sensitivity in patients with orthopedic implants. Jcr-J Clin Rheumatol 7 (4):215–218

Hallab NJ, Jacobs JJ (2009) Biologic effects of implant debris. Bull NYU Hosp Jt Dis 67(2):182

Hallab N, Jacobs JJ, Black J (2000) Hypersensitivity to metallic biomaterials: a review of leukocyte migration inhibition assays. Biomaterials 21(13):1301–1314

Hallab N, Merritt K, Jacobs JJ (2001) Metal sensitivity in patients with orthopaedic implants. J Bone Joint Surg Am 83(3):428–437

Hallab NJ, Caicedo M, Finnegan A et al (2008) Th1 type lymphocyte reactivity to metals in patients with total hip arthroplasty. J Orthop Surg Res 3(1):6

Hamano H, Uoshima K, Miao WP et al (1998) Investigation of metal allergy to constituent elements of intraoral restoration materials. Kokubyo Gakkai zasshi. J Stomatol Soc Jpn 65 (1):93–99

Heinzerling L, Mari A, Bergmann KC et al (2013) The skin prick test-European standards. Clin Transl Allergy 3(1):3

Hill DJ, Heine RG, Hosking CS (2004) The diagnostic value of skin prick testing in children with food allergy. Pediat Allergy Immnol-Uk 15(5):435–441
Honari G, Ellis SG, Wilkoff BL et al (2008) Hypersensitivity reactions associated with endovascular devices. Contact Dermat 59(1):7–22
Hu W, Eaton J, Ugarova T et al (2001) Molecular basis of biomaterial-mediated foreign body reactions. Blood 98(4):1231–1238
Hutmacher DW (2000) Scaffolds in tissue engineering bone and cartilage. Biomaterials 21:2529–2543
Hutmacher DW, Schantz JT, Lam CX et al (2007) State of the art and future directions of scaffold-based bone engineering from a biomaterials perspective. J Tissue Eng Regen Med 1 (4):245–260
Ignjatovic N, Savic V, Najman S et al (2001) A study of HAp/PLLA composite as a substitute for bone powder, using FT-IR spectroscopy. Biomaterials 22:571–575
Ignjatovic NL, Ajdukovic ZR, Savic VP et al (2013) Nanoparticles of cobalt-substituted hydroxyapatite in regeneration of mandibular osteoporotic bones. J Mater Sci-Mater Med 24 (2):343–354
ISO 10993: Biological evaluation of medical devices
Janeway CA Jr, Travers P, Walport M et al (2001) Immunobiology: the immune system in health and disease, 5th edn. Garland Science, New York
Janićijević J, Najman S, Ignjatović N et al (2008) Nanomaterial NP-CP/DLPLG as potentional tissue graft in osteoreparation in combination with bone marrow cells on subcutaneous implantation model. Hem Ind 62(3):205–210
Jennewein C, Tran N, Paulus P et al (2011) Novel aspects of fibrin(ogen) fragments during inflammation. Mol Med 17(5–6):568–573
Jokanović V, Izvonar D, Dramićanin MD et al (2006) Hydrothermal synthesis and nanostructure of carbonated calcium hydroxyapatite. J Mater Sci Mater Med 17:539–546
Jokanović V, Čolović B, Marković D et al (2016a) Extraordinary biological properties of a new calcium hydroxyapatite/poly(lactide-co-glycolide)-based scaffold confirmed by in vivo investigation. Biomed Tech (Berl). doi:10.1515/bmt-2015-0164
Jokanović V, Čolović B, Marković D et al (2016b) In vivo investigation of ALBO-OS scaffold based on hydroxyapatite and PLGA. J Nanomater. doi:10.1155/2016/3948768
Jones K (2008) Effects of biomaterial-induced inflammation on fibrosis and rejection. Semin Immunol 20(2):130–136
Kaji Y, Ikeda K, Ikeda T et al (2000) IL-4, but not vitamin D(3), induces monoblastic cell line UG3 to differentiate into multinucleated giant cells on osteoclast lineage. J Cell Physiol 182 (2):214–221
Kanerva L, Estlander T, Jolanki R (1995) Dental problems. In: Guind JD (ed) Practical contact dermatitis. Mc Graw-Hill, New York, pp 397–432
Kang Y, Scully A, Young DA et al (2011) Enhanced mechanical performance and biological evaluation of a PLGA coated ®-TCP composite scaffold for load-bearing applications. Eur Polym J 47:1569–1577
Khamaysi Z, Bergman R, Weltfriend S (2006) Positive patch test reactions to allergens of the dental series and the relation to the clinical presentations. Contact Dermat 55(4):216–218
Kokubo T (1996) Formation of biologically active bone-like apatite on metals and polymers by a biomimetic process. Thermochim Acta 280–281:479–490
Konttinen Y, Zhao D, Beklen A et al (2005) The microenvironment around total hip replacement prostheses. Clin Orthop Relat Res 430:28–38
Lee M, Ducheyne P, Lynch L et al (2006) Effect of biomaterial surface properties on fibronectin-α 5 β 1 integrin interaction and cellular attachment. Biomaterials 27(9):1907–1916
Li C, Vepari C, Jin HJ et al (2006) Electrospun silk-BMP-2 scaffolds for bone tissue engineering. Biomaterials 27:3115–3124
Li JJ, Kaplan DL, Zreiqat H (2014) Scaffold-based regeneration of skeletal tissues to meet clinical challenges. J Mater Chem B 2:7272–7306

Lin P, Hirko M, von Fraunhofer J et al (1997) Wound healing and inflammatory response to biomaterials. In: Chu J, von Fraunhofer A, Greisler P (eds) Wound closure biomaterials and devices. CRC Press LLC, Florida, pp 7–19

Luttikhuizen D, Harmsen M, Van Luyn M (2006) Cellular and molecular dynamics in the foreign body reaction. Tissue Eng 12(7):1955–1970

Lygre H (2002) Prosthodontic biomaterials and adverse reactions: a critical review of the clinical and research literature. Acta Odontol Scand 60(1):1–9

Mallo-Pérez L, Díaz-Donado C (2003) Intraoral contact allergy to materials used in dental practice. A critical review. Medicina oral: organo oficial de la Sociedad Espanola de Medicina Oral y de la Academia Iberoamericana de Patologia y Medicina Bucal 8(5):334–347

Mitić ŽJ, Najman SJ, Cakić MD et al (2014) Spectroscopic characterization of bone tissue of experimental animals after glucocorticoid treatment and recovery period. J Mol Struct 1074:315–320

Morais J, Papadimitrakopoulos F, Burgess D (2010) Biomaterials/tissue interactions: possible solutions to overcome foreign body response. AAPS J 12(2):188–196

Najdanović J, Cvetković V, Stojanović S et al (2015) The influence of adipose-derived stem cells induced into endothelial cells on ectopic vasculogenesis and osteogenesis. Cell Mol Bioeng 8 (4):577–590

Najman S, Đorđević LJ, Savic V et al (2003) Changes of HAp/PLLA biocompozites and tissue reaction after subcutaneous implantation. Facta Univ Ser Med Biol 10(3):131–134

Najman S, Savić V, Lj Đorđević et al (2004) Biological evaluation of hydroxyapatite/ poly-L-lactide (HAp/PLLA) composite biomaterials with poly-L-lactide of different molecular weights intraperitoneally implanted into mice. Bio-Med Mater Eng 14(1):61–70

National Institute of Health (1977) Evaluation of hemodialyzers and dialysis membranes. Hemolysis-Rabbit Blood, DHEW Publication 77–1294, Bethesda, MD

Nebeker JR, Virmani R, Bennett CL et al (2006) Hypersensitivity cases associated with drug-eluting coronary stents: a review of available cases from the Research on Adverse Drug Events and Reports (RADAR) project. J Am Coll Cardiol 47(1):175–181

Ngiam M, Liao S, Patil AJ et al (2009) The fabrication of nano-hydroxyapatite on PLGA and PLGA/collagen nanofibrous composite scaffolds and their effects in osteoblastic behaviour for bone tissue engineering. Bone 45:4–16

Nowak G, Olejek A (2004) Biological and molecular aspects of wound healing. Prakt Gyn 12:2–30

Nuss K, von Rechenberg B (2008) Biocompatibility issues with modern implants in bone—a review for clinical. Open Orthop J 2:66–78

Ohgushi H, Goldberg VM, Caplan AI (1989) Repair of bone defects with marrow cells and porous ceramic. Experiments in rats. Acta Orthop Scand 60(3):334–339

Olczyk P, Mencner Ł, Komosinska-Vassev K (2014) The role of the extracellular matrix components in cutaneous wound healing. BioMed Res Int. Article ID 747584, 8 p

Olivier V, Faucheux N, Hardouin P (2004) Biomaterial challenges and approaches to stem cell use in bone reconstructive surgery. Drug Discov Today 9(18):803–811

Powanda MC, Moyer ED (1981) Plasma proteins and wound healing. Surg Gynecol Obstet 153 (5):749–755

Primeau MN, Adkinson NF Jr (2001) Recent advances in the diagnosis of drug allergy. Curr Opin Allergy Clin Immunol 1(4):337–341

Pumhirun P, Jane-Trakoonroj S, Wasuwat P (2000) Comparison of in vitro assay for specific IgE and skin prick test with intradermal test in patients with allergic rhinitis. Asian Pac J Allergy 18 (3):157–160

Rajan TV (2003) The Gell-Coombs classification of hypersensitivity reactions: a re-interpretation. Trends Immunol 24(7):376–379

Ratner BD, Hoffman AS, Schoen FJ et al (1997) Biomaterials science: an introduction to materials in medicine. Elsevier Academic Press, San Diego

Repo H, Kostiala AA, Kosunen TU (1980) Cellular hypersensitivity to tuberculin in BCG-revaccinated persons studied by skin reactivity, leucocyte migration inhibition and lymphocyte proliferation. Clin Exp Immunol 39(2):442–448

Riches D (1988) Macrophage involvement in wound repair, remodeling, and fibrosis. In: Clark R, Henson P (eds) The molecular and cellular biology of wound repair. Plenum Press, New York, pp 213–239

Ripamonti U (1993) Delivery systems for bone morphogenetic proteins. A summary of experimental studies in primate models. Ann Chir Gynaecol Suppl 207:13–24

Robitaille R, Dusseault J, Henley N et al (2005) Inflammatory response to peritoneal implantation of alginate-poly-l-lysine microcapsules. Biomaterials 26(19):4119–4127

Schalock PC, Menné T, Johansen JD et al (2012) Hypersensitivity reactions to metallic implants–diagnostic algorithm and suggested patch test series for clinical use. Contact Dermat 66(1):4–19

Shapiro F (2008) Bone development and its relation to fracture repair. The role of mesenchymal osteoblasts and surface osteoblasts. Eur Cell Mater 15:53–76

Shiu H, Goss B, Lutton C et al (2014) Formation of blood clot on biomaterial implants influences bone healing. Tissue Eng B Rev 20(6):697–712

Stejskal VD, Forsbeck M, Cederbrant KE et al (1996) Mercury-specific lymphocytes: an indication of mercury allergy in man. J Clin Immunol 16(1):31–40

Szaba FM, Smiley ST (2002) Roles for thrombin and fibrin (ogen) in cytokine/chemokine production and macrophage adhesion in vivo. Blood 99(3):1053–1059

Tang L, Eaton JW (1993) Fibrin (ogen) mediates acute inflammatory responses to biomaterials. J Exp Med 178(6):2147–2156

Tang L, Jennings TA, Eaton JW (1998) Mast cells mediate acute inflammatory responses to implanted biomaterials. Proc Natl Acad Sci U S A 95(15):8841–8846

Ten RM, Klein JS, Frigas E (1995) Allergy skin testing. Mayo Clin Proc 70(8):783–784

Teow Y, Asharani PV, Hande MP et al (2011) Health impact and safety of engineered nanomaterials. Chem Commun 47(25):7025–7038

Thomas P, Summer B, Sander CA et al (2000) Intolerance of osteosynthesis material: evidence of dichromate contact allergy with concomitant oligoclonal T-cell infiltrate and TH1-type cytokine expression in the peri-implantar tissue. Allergy 55(10):969–972

Thomas M, Arora A, Katti DS (2014) Surface hydrophilicity of PLGA fibers governs in vitro mineralization and osteogenic differentiation. Mater Sci Eng C 45:320–332

Thyssen JP, Menné T (2010) Metal allergys—a review on exposures, penetration, genetics, prevalence, and clinical implications. Chem Res Toxicol 23(2):309–318

Thyssen JP, Menné T, Schalock PC et al (2011) Pragmatic approach to the clinical work-up of patients with putative allergic disease to metallic orthopaedic implants before and after surgery. Br J Dermatol 164(3):473–478

Turbill P, Beugeling T, Poot A (1996) Proteins involved in the Vroman effect during exposure of human blood plasma to glass and polyethylene. Biomaterials 17(13):1279–1287

Valentine-Thon E, Ilsemann Sandkamp M (2007) A novel lymphocyte transformation test (LTT-MELISA®) for Lyme borreliosis. Diagn Microbiol Infect Dis 57(1):27–34

Valentine-Thon E, Schiwara HW (2003) Validity of MELISA® for metal sensitivity testing. Neuroendocrinol Lett 24(1/2):57–64

Valentine-Thon E, Muller K, Guzzi G et al (2006) LTT-MELISA (R) is clinically relevant for detecting and monitoring metal sensitivity. Neuroendocrinol Lett 27(1):17–24

Van der Zee JS, De Groot H, Van Swieten P et al (1988) Discrepancies between the skin test and IgE antibody assays: study of histamine release, complement activation in vitro, and occurrence of allergen-specific IgG. J Allergy Clin Immunol 82(2):270–281

Vasiljevic P, Najman S, Lj Djordjevic et al (2009) Ectopic osteogenesis and hematopoiesis after implantantion of bone marrow cells seeded on Hap/PLLA scaffold. Hemijska Industrija 63 (4):301–307

Vasiljevic P, Najman S, Vukelic M et al (2013) Potential of HAp composite scaffolds and bone marrow stem cells in bone repair. In: Spasic M (ed) Proceedings the 3rd conference of the

serbian biochemical society, titled “Roots and Branches of Biochemistry”, University of Belgrade
Vukelić M, Mitić Ž, Miljković M et al (2011) Interaction of biomaterials containing calcium hydroxyapatite/poly-l-lactide with the simulated body fluid. Acta Med Median 50(4):35–39
Vukelić M, Mitić Ž, Miljkovic M et al (2012) Apatite formation on nanomaterial calcium phosphate/poly-DL-lactide-co-glycolide in simulated body fluid. J Appl Biomater Funct Mater 10(1):43–48
Wahl SM, Wong H, McCartney-Francis N (1989) Role of growth factors in inflammation and repair. J Cell Biochem 40(2):193–199
Willert HG, Buchhorn GH, Fayyazi A et al (2005) Metal-on-metal bearings and hypersensitivity in patients with artificial hip joints. J Bone Joint Surg Am 87(1):28–36
Wilson C, Clegg R, Leavesley D et al (2005) Mediation of biomaterial-cell interactions by adsorbed proteins: a review. Tissue Eng 11(1–2):1–18
Wynn TA, Barron L (2010) Macrophages: master regulators of inflammation and fibrosis. Semin Liver Dis 30(3):245–257
Yanagi T, Shimizu T, Abe R et al. (2005) Zinc dental fillings and palmoplantar pustulosis. Lancet 366(9490):1050
Yaszemski MJ, Payn RG, Hayes WC et al (1996) Evolution of bone transplantation: molecular, cellular and tissue strategies to engineer human bone. Biomaterials 17(2):175–185
Yu K, Mei Y, Hadjesfandiari N et al (2014) Engineering biomaterials surfaces to modulate the host response. Colloids Surf B Biointerfaces 124:69–79
Zdolsek J, Eaton J, Tang L (2007) Histamine release and fibrinogen adsorption mediate acute inflammatory responses to biomaterial implants in humans. J Transl Med 5:31
Živković J, Najman S, Vukelić M et al (2015) Osteogenic effect of inflammatory macrophages loaded onto mineral bone substitute in subcutaneous implants. Arch Biol Sci 67(1):173–186

Genotoxicity and Mutagenicity Testing of Biomaterials

Vladimir J. Cvetković, Dijana Takić Miladinov and Sanja Stojanović

Abstract Rapid progress in biomedical fields and development of new technologies in bioengineering and tissue engineering, such as 3D bioprinting technologies, lead us to extensive and rapid designing of new biomaterials and medical devices (MDs). The main feature that newly engineered biomaterials must possess, in order to be applied in clinical practice, is to be biocompatible. Besides toxicity testing, genotoxicity and mutagenicity assays are very important in assessment of biocompatibility. Genotoxicity/mutagenicity is a feature that can completely disable the use of some biomaterial and MDs in biomedical and clinical applications especially if material is intended for long term use. Mutagens are agents that can cause heritable changes in DNA and their capacity to cause mutations is defined as mutagenicity. Genotoxicity is a wider term which, besides mutagenicity, refers to the property of an agent to cause various damages to DNA and other disturbances which can affect genes function. In this chapter, we gave an overview of in vitro and in vivo assays that are mostly used in biocompatibility assessment with a focus on the most promising assays for evaluations of genotoxicity and mutagenicity of biomaterials.

Keywords Genotoxicity · Mutagenicity · Biocompatibility · Biomaterials · In vitro · In vivo

V.J. Cvetković · D. Takić Miladinov
Department of Biology and Ecology, Faculty of Sciences and Mathematics, University of Niš, Višegradska 33, 18000 Niš, Serbia

S. Stojanović (✉)
Department for Cell and Tissue Engineering and Department of Biology and Human Genetics, Faculty of Medicine, University of Niš, Blvd. Dr Zoran Đinđić 81, 18000 Niš, Serbia
e-mail: s.sanja88@gmail.com

F. Zivic et al. (eds.), *Biomaterials in Clinical Practice*,
https://doi.org/10.1007/978-3-319-68025-5_18

1 Introduction

The remarkable progress achieved in areas such as cell biology, tissue engineering, biotechnology, regenerative medicine and bioengineering, has resulted in rapid development of new biomaterials and medical devices (MDs). Development of 3D bioprinting technologies employed different biomaterials from which different scaffolds, artificial tissues and even organs are made. By using these technologies, various products intended for medical use have been made such as contact lenses (Maldonado-Codina and Efron 2003), artificial skin (Young et al. 1998) and organs (Prokop 2001), heart valves (Black and Drury 1994) and scaffolds for bone (Cetin et al. 2011; Costa et al. 2007) and cartilage (Keeney et al. 2011) tissue engineering. Biomaterials used in bioengineering are mostly based on hydroxyapatite or different forms of calcium phosphate, when used for preparing scaffolds in bone tissue engineering (BTE), and different natural or synthetic polymers used in soft tissue engineering. In many cases the combination of those two kinds of biomaterials is used. Nanomaterials are nowadays very popular due to their characteristics and have wide variety of applications in biomedical fields, pharmaceutical and clinical application (Salata 2004).

In order to be applied in clinical practice, biomaterials have to undergo pre-clinical testing that includes both in vitro and in vivo testing using different experimental models. The most important requirements that those materials have to meet are to be biocompatible and to support normal functioning of cells and tissues. Biocompatibility is essential property of materials intended for use in biomedical applications and refers to the property of material to be compatible with living tissue or organism, does not exhibit any harmful effects and to support normal functioning of tissues and organism. Biocompatibility reflects a set of complex characteristics that cannot be completely evaluated by a single test or method and requires a battery of tests to evaluate different types of possible harmful effects: cytotoxicity, genotoxicity, mutagenicity, hemocompatibility, systemic toxicity, irritation, sensitization and pyrogenicity (Morais et al. 2010). The first step in biocompatibility assessment is cytotoxicity testing. This property is examined for each new biomaterial and if material is not cytotoxic, other properties are tested.

Mutagenicity represents a capacity of chemical, physical or biological agents to cause damages to DNA that can lead to mutations. Mutations are permanent changes in DNA which in most cases can cause changes in phenotype of affected cells and might result in development of cancer (Eastmond et al. 2009). When mutations occur in genes that control proliferation and cell division, it can influence gene expression in the way which is not normal (Parry and Parry 2012) and may result in cancerogenesis. Genotoxicity is a property of chemical, physical or biological agent to interact with and cause any damages to DNA itself or DNA regulating components and those agents are called genotoxins. Thus, the genotoxicity is a wider term and it is not tightly associated with mutagenicity (Eastmond et al. 2009).

There is a growing concern in connection with possible genotoxic effects of MDs and biomaterials intended for biomedical applications. Many of engineered nanomaterials were found to cause genotoxic effects which could disable their application, so detailed testing is necessary after their synthesis (Singh et al. 2009). Genotoxicity can limit or completely preclude the use of materials in clinical practice so it is very important to evaluate potential genotoxicity of any material intended for long term exposure or implantation. In general, the need for genotoxicity testing of materials is based on its categorization, depending on the type of body contact and contact duration. According to ISO standards, surface devices with permanent contact as well as implant devices with prolonged exposure or permanent contact, require genotoxicity testing (Carraway and Ghosh 2006).

In BTE, biomaterials are often examined alone or in combination with regulatory molecules and cells. Different models for in vivo testing of biomaterials are used such as subcutaneous implantation (Barbeck et al. 2015) or bone defect models (Rajković et al. 2015; Mitić et al. 2014) in small and large animals (Cvetković et al. 2013). We combined freshly isolated adipose-derived mesenchymal stem cells (ADSCs) and platelet rich plasma (PRP) with bone mineral substitute material (Najman et al. 2016), ADSCs induced into endothelial cells and osteoblasts and PRP with bone mineral substitute material (Najdanović et al. 2015, 2016; Cvetković et al. 2015a), and examined their osteogenic capacity and effects on vascularization in ectopic bone forming model in mice. We have also examined the ectopic osteogenic potential of macrophages combined with blood and loaded onto bone mineral substitute material (Živković et al. 2015) and the influence of blood addition to phycogenic bone substitute on vascularization and subcutaneous tissue reaction (Barbeck et al. 2015). Since biomaterials are the main components of implants applied in BTE, and are mainly used in combination with cells and regulatory factors, they must be highly biocompatible without any toxic effects. Therefore, evaluation of genotoxicity and mutagenicity, along with toxicity tests is necessary in biocompatibility assessments of biomaterials.

There are a wide variety of well-established test methods for detection of genotoxic effects of chemicals and materials. These methods can be conducted in non-mammalian (bacteria and yeast) and mammalian (primary cell cultures or permanent cell lines) in vitro systems and different in vivo systems (Carraway and Ghosh 2006). There is no single in vitro test capable to detect all types of genotoxic effects, so it is often necessary to conduct a battery of two or more different tests. In the past two decades over 300 methods have been developed for detection of mutagenic activity (Parry and Parry 2012).

Strategy for mutagenicity and genotoxicity testing should include three major steps: (1) Consideration prior to testing; (2) In vitro testing and (3) In vivo testing, respectively (Eastmond et al. 2009). According to ISO 10993-3, in vivo assays are required only in the case when positive results of in vitro assays indicate a need for further testing.

Prior genotoxicity testing, solubility and stability of testing agents need to be considered (Eastmond et al. 2009). Frequently, substances tested for biological activities have to be dissolved in some type of solvent (Mitrović et al. 2011, 2014;

Stojanović et al. 2013). Appropriate organic, non-organic, polar and non-polar solvents and solutions by their nature could be very toxic. Also, some very acidic or alkaline solutions used in everyday dental clinical practice exert toxic effects (Kostić et al. 2012a) such as inflammatory tissue reaction to the application site (Kostić et al. 2014). Some of them also could be genotoxic. Therefore, safe, non-toxic and non-genotoxic concentrations of solvents should be used in genotoxicity evaluations what implies pre-testing of particular solvent if there are no data about that (Cvetković et al. 2015b). Newer versions of ISO 10993-3 suggest that selection of appropriate sample preparation prior to genotoxicity testing is crucial. They recommend the following methods for sample preparation: dissolution or suspension of the test agent in an adequate solvent and simulated-use extraction and extraction in two or more solvents to determine the solvent with the highest extraction residue of the tested agent. The selection of appropriate method depends on the chemical and physicochemical composition of the test compound. Biomaterials intended for BTE are usually tested in vitro by employing two different approaches, direct or indirect contact. In direct contact studies biomaterials are incubated directly with cells in culture in different time periods after which different cell characteristics can be monitored (Kostić et al. 2012b; Remya et al. 2014). In indirect contact studies cells are incubated with extracts of biomaterials usually prepared by extraction of materials in cell culture media (Stojanović et al. 2016; Takić Miladinov et al. 2016; Vuković et al. 2016) and this approach is employed for assessment of potential extractable components of biomaterials and MDs that are released in a media.

Newly engineered biomaterials could exert toxic properties under certain conditions, thus evaluation of the toxicity of selected material before genotoxicity and mutagenicity testing is very important. Usually, it does not mean that if some agent is not toxic will not be genotoxic or/and mutagenic and vice versa. It is also very important to exclude any toxic effects that can mask genotoxic effect and give false positive results. Only non-toxic concentrations or doses of tested agent for particular model organism should be used for genotoxicity and mutagenicity assays. Depending on the experimental model, in vitro or in vivo toxicity testing should be performed in order to established LC_{50} (Lethal Concentration which kills 50% of test organism's population), LOEC (Lowest Observed Effect Concentration) and NOEC (No Observed Effect Concentration) values prior to further evaluations (Cvetković et al. 2015b). Therefore, toxicity testing of selected agent very often precedes its genotoxicity evaluation (Rajab et al. 2004; Jantová et al. 2008). Since in vitro testing approach is the first step when new compound or biomaterial is tested we usually perform in vitro cytotoxicity and proliferation assays with different cell lines according to potential application of tested compound (Vuković et al. 2016; Savić et al. 2015; Damnjanovic et al. 2014, 2015, Ilić et al. 2015; Mitrović et al. 2011). For biomaterials intended for BTE, very important property is to support proliferation and adhesion of cells to the biomaterials' particles. We have examined the effect of synthesized nanomaterial based on calcium phosphate/poly-(DL-lactide-co-glycolide) on proliferation and adherence of epithelial cells (Najdanović et al. 2017). Some other models for toxicity evaluation could also be

used before genotoxicity/mutagenicity examination. We have also performed studies on evaluation of toxic influence of certain environmental heavy metals on lichens in their natural habitat (Mitrović et al. 2012a, b; Stamenković et al. 2013).

When choosing an appropriate mutagenicity and genotoxicity assay, few parameters should be considered such as: sensitivity, reproducibility, time of performance, simplicity, costs and ability to interpolate the obtained results into humans. Also, very important parameter is whether the biomaterial or MDs is intended for short or long term use and whether it gets in touch with blood or is only for topical application.

Genotoxicity of biomaterials can be defined as ability of biomaterial, medical device or their extracts to induce gene mutations, chromosomal aberrations and other effects on DNA. According to these effects, classification of genotoxicity tests has been made.

According to FDA guidance for industry and food and drug administration staff entitled "Use of International Standard ISO 10993-1, Biological evaluation of medical devices—Part 1: Evaluation and testing within a risk management process", in vitro genotoxicity test batteries are recommended for detection of genotoxic agents since no single test method is capable of detecting all types of genotoxic effects. These test batteries include at least two or three different test procedures, such as bacterial reverse mutation test (Ames test, OECD 471), in vitro mammalian cell tests for chromosomal damage (OECD 473 and OECD 487) and mammalian cell mutation assays (OECD 490) (Kirkland et al. 2005; Kim et al. 2013).

Regarding in vitro mammalian genotoxicity assay, a choice of one of the following is recommended by ISO standards 10993-1 and 10993-3:

- The mouse lymphoma gene mutation assay [OECD 490 (2015) "Guidelines for the Testing of Chemicals—In Vitro Mammalian Cell Gene Mutation Test"], which is preferred since it detects the broadest set of genotoxic mechanisms associated with mutagenic and carcinogenic activity;
- An in vitro chromosomal aberration (CA) assay [OECD 473 (2014) "Guidelines for the Testing of Chemicals—In Vitro Mammalian Chromosome Aberration Test"]; or
- An in vitro micronucleus assay [OECD 487 (2014) "Guidelines for the Testing of Chemicals—In Vitro Mammalian Cell Micronucleus Test"].

According to ISO 10993-3 standard, if the results of performed in vitro tests are negative then further genotoxicity testing in animals is not required but if positive genotoxic or mutagenic effect of tested biomaterial is obtained in examined in vitro system, further in vivo testing should be performed.

When in vivo assay is needed, it is recommended by ISO 10993-1 and ISO 10993-3 standards to choose one of the following:

- Bone marrow micronucleus (MN) Assay in rodents [OECD 474 (2014) "Guidelines for the Testing of Chemicals—Mammalian Erythrocyte Micronucleus Test"]; or

- Bone marrow chromosomal aberration (CA) assay [OECD 475 (2014) "Guidelines for the Testing of Chemicals—Mammalian Bone Marrow Chromosome Aberration Test"]; or
- Peripheral blood (Mammalian erythrocyte) micronucleus assay [OECD 474 (2014)].

This chapter provides an overview of the most used genotoxicity/mutagenicity assays in biocompatibility assessment of biomaterials with regard to basic principles, some examples and obtained results.

2 In Vitro Genotoxicity/Mutagenicity Testing

2.1 Gene Mutation Assays

2.1.1 Ames Test

Ames test is a bacterial reverse gene mutation test used for detection of both mutagenicity and genotoxicity (Ames et al. 1973). It is performed with different engineered strains of *Salmonella typhimurium* and *Escherichia coli* and designed to detect all possible single base pair changes as well as frameshift mutations [OECD 471 (1997) "Guidelines for Testing of Chemicals—Bacterial Reverse Mutation Test"]. The test is based on the ability of tested compound to revert point mutations in genes responsible for biosynthesis of histidine or tryptophan while restoring the ability of those bacteria to generate these amino acids. Mutations affecting a small portion of the DNA molecule, including frameshift and base-pair substitutions referred to as point mutations. Usually, S9 active rat liver microsomes are added into a portion of the test organisms to simulate whole-animal exposure. Due to its simplicity and cost effectiveness, this test is widely used for mutagenicity and genotoxicity testing of different compounds as well as biomaterials and is essential part of recommended battery assays for such testing. For some biomaterials and MDs that are intended for long term use it is very important to examine whether they are capable to induce mutations since mutagenic activity can lead to cancerogenesis. The main disadvantage of Ames test is that obtained results could not indicate the activity of tested material in some other more complex systems. It is often the case that some agent does not show a genotoxic/mutagenic effect in Ames test but exerts genotoxic potential in mammalian systems (Doak et al. 2012).

It is proposed that nanomaterials could be successfully assessed by Ames test (Huang et al. 2010). On the other hand, some studies showed that Ames test does not appear to be suitable for the assessment of nanoparticles such as silver nanoparticles (Ag-NPs) (Li et al. 2012; Kim et al. 2013).

Ames test is widely used for testing of dental materials. Recently, Ames test was used for genotoxicity assessment of dental materials such as silver amalgam (Hassan et al. 2013) and dental porcelain (Noushad et al. 2009) and none of them

did not show genotoxic effect in this assay. However, some dental cement materials were examined by this test and it is indicated that they may have possible mutagenic activities (Kaplan et al. 2004). Four endodontic sealer materials and some of their chemical constituents were examined for mutagenicity by Ames test in *Salmonella*/microsome model (Ørstavik and Hongslo 1985). Some of the examined materials were negative in this test, but some of them induced mutations in specific *Salmonella typhimurium* strains. Authors of this study also showed that there is a difference in the mutagenic activity of examined materials when rat liver microsomes were added (Ørstavik and Hongslo 1985). Six commercially available orthodontic direct-bonding resin systems, that are frequently used to attach orthodontic brackets to tooth enamel, were tested as aqueous and DMSO extracts on *Salmonella typhimurium* strains by this test. Components of some tested extracts were found to yield positive test results and exert mutagenic activity (Cross et al. 1983). The mutagenic activity of the root canal sealing cement, AH Plus, was tested by Ames tests. Material, powdered or freshly mixed, was eluted in DMSO and physiological saline, and it is shown that two different compounds of AH Plus were biologically active in DMSO eluates and caused mutagenic and toxic effects in *S. typhimurium* strains TA100 and TA98 (Schweikl et al. 1998). The potential mutagenicity of new generation of bonding agents was examined by employing in vitro gene mutation assay. Eight different components of three dentine bonding systems (Scotchbond Multi Purpose, Prisma Universal Bond 3 and C&B Metabond) were tested by Ames test using four different *Salmonella typhimurium* strains (TA97a, TA98, TA100 and TA102). The results of this study showed that mutagenic activity of tested dental materials varied depending on the type of the eluate. Also, different mutagenic activity was obtained with different strains of *Salmonella typhimurium* (Schweikl et al. 1996). Polyalkylimide hydrogel (Bio-Alcamid™), intended for soft tissue augmentation, was examined by Ames test and did not show mutagenic effects (Ramires et al. 2005). The genocompatibility of the saline solution extract of porous titanium–nickel (PTN) was evaluated by *Salmonella typhimurium* and *Escherichia coli* reverse mutation assay either with or without S9 activation. Based on the results obtained in this study, porous titanium–nickel extracts were found to be non-mutagenic for *Salmonella* and *E. coli* strains (Assad et al. 2002). Finally, one of the most frequently used bone replacement material—hydroxiapatite (HA) was recently evaluated by this test (Hassan and Swaminathan 2011). Obtained results indicates that synthesized value added HA (HA with added zirconia) was considered to have no reverse mutagenic potential.

2.1.2 The Mouse Lymphoma Assay

The mouse lymphoma assay (OECD 490) is useful in vitro method for detecting gene mutations in mammalian cells. In this assay, L5178Y mouse lymphoma cells,

which are heterozygous at the thymidine kinase locus (Tk) on chromosome 11, are exposed to the test compounds in the presence and absence of exogenous metabolic activation. Since Tk -/- mutants have wild type allele inactivated and are resistant to trifluorothymidine (TFT), only cells that undergo mutation event at Tk locus will form the colonies (Lloyd and Kidd 2012). There are two size classes of mutant colonies and their relative frequency is mutagen dependent (Han et al. 2006). Colony size is an indicator of the mutation type. Large colonies typically correspond to small tk-inactivating mutations (point mutations), while small colonies are often induced by clastogens (Han et al. 2006; Kirkland et al. 2005). The molecular distinction between large and small colony mutants has been made by employing microarray analysis and identifying differences in gene expression pattern between two colony size phenotypes (Han et al. 2006). This assay is very useful in detection base-pair mutations, frameshift mutations, and small deletions.

2.2 Chromosomal Aberration Assays

2.2.1 Chromosomal Aberration Assay

The chromosomal aberration (CA) assay detects large-scale damages of chromosomes, such as structural (fragmentation or intercalation) and numerical (aneuploidy and polyploidy) aberrations (Thompson et al. 2010). This is an in vitro assay commonly carried out by exposing cell cultures to the extracts of tested compounds. After that the cells are treated with colcemid, a compound that blocks mitosis in metaphase. The chromosomes are then stained and analyzed under microscope. The sensitivity of the assay is largely influenced by staining technique. Giemsa is conventional staining method which enables large rearrangements and numerical aberrations to be detected. FISH-staining technique increases the sensitivity of an assay, allowing each chromosome to be differentially stained. The most commonly used cells in this assay are Chinese hamster ovary (CHO) cells. The test system is evaluated in the presence and absence of exogenous metabolic activation.

The genocompatibility of the saline solution extract of porous titanium–nickel (PTN) was evaluated by CA assay. Extracts of porous titanium–nickel were found not to be genotoxic for CHO cells in vitro by this assay either when tested with or without an exogenous metabolic activation system (Assad et al. 2002).

Hydrogels are widely used in soft tissue engineering as wound dressing. Among synthetic components used as monomers for preparation of hydrogels, 2-hydroxyethyl methacrylate (HEMA) is mostly used and examined. Genotoxic potential of 2-hydroxyethyl methacrylate (HEMA) monomer was evaluated by CA assay in human peripheral blood lymphocytes and significant dose-dependent increase in the frequency of chromosomal aberrations was demonstrated in all tested concentrations (Ginzkey et al. 2015).

2.2.2 In Vitro Micronucleus Test

The in vitro micronucleus test (IVMNT) is an alternative to the chromosomal aberration assay for the detection of chromosomal mutations (Schweikl and Schmalz 2000). The IVMNT detects genotoxic damage in the form of micronuclei in the cytoplasm of interphase cells. During cell division, if the chromosomes are broken or the mitotic apparatus of the cell is damaged, chromosome fragments could be incorporated in secondary nuclei instead of into the main nucleus. Secondary nuclei are much smaller than the main nucleus and are referred to as micronuclei. Micronuclei may be the result of aneugenic (whole chromosome) or clastogenic (chromosome breakage) damage (Doherty 2012). In recent years, the IVMNT has become an attractive tool for genotoxicity testing because of its capacity to detect not only clastogenic (chromosome loss) and aneugenic (chromosome breakage) events but also some epigenetic effects and enables those effects to be measured reliably. Also, its simplicity of scoring, accuracy, wide applicability in different cell types, amenability to automation and low costs, made this test to become a first choice in examining genotoxicity in mammalian systems.

Cell cultures are exposed to the test substances both with and without metabolic activation. After exposure to a test substance, cytochalasin B is added for blocking cytokinesis in cell cultures that are grown for a period sufficient to allow chromosomal damage to cause the formation of micronuclei in binucleated or multinucleated interphase cells. Cells are then harvested, stained and analyzed microscopically for the presence of micronuclei. Cells can be stained with classical Giemsa staining technique or with different DNA binding fluorescent dyes. Micronuclei are scored in those cells that complete nuclear division following exposure to the test compound.

The MN assay in its current basic form (with cytochalasin B addition) may reveal following indicators of genotoxicity and cytotoxicity: chromosome breakage, chromosome loss, chromosome rearrangement (nucleoplasmic bridges), gene amplification (nuclear buds), cell division inhibition, necrosis and apoptosis (Fenech 2008).

The OECD guideline 487 for the IVMNT refers to the data supporting the validity of MN test using various rodent cell lines (CHO, V79, CHL and L5178Y). Besides these commercial permanent cell lines, isolated primary cell cultures (e.g. peripheral blood lymphocytes) are also widely used. The major advantage of peripheral blood lymphocytes is that they are primary cells, easy to culture in suspension, can be easily isolated from the human blood and large number of cells could be obtained (Kirsch-Volders et al. 2011). A novel in vitro human reconstructed skin micronucleus (RSMN) assay that measures micronuclei induced in dividing basal cell keratinocytes of the 3D human skin model has recently been developed (Kirsch-Volders et al. 2011).

Extracts of several different dental composite materials were evaluated in V79 fibroblasts by micronucleus test (Schweikl et al. 2005). Different concentrations and

exposure time were conducted that resulted in different responses of V79 fibroblasts. The final conclusion was that some commercial composite materials frequently used in dentistry had mutagenic components which induce higher frequency of micronuclei in V79 fibroblasts. The authors suggested that these components in composite dental materials should be replaced by more biocompatible substances (Schweikl et al. 2005).

Micronucleus assay was used in many genotoxicity assessments of different types of nanomaterials such as aluminium oxide, carbon, cobalt, iron oxide, silicon, silver as well as titanium dioxide (Gonzalez et al. 2011). Some data suggest that for evaluation of the genotoxicity of some nanoparticles such as AgNPs, the in vitro micronucleus assay is more appropriate than the Ames test (Li et al. 2012). Thus, micronucleus assay is good candidate for genotoxicity assessment of nanomaterials.

In vitro micronucleus assay is frequently used for genotoxicity assessment of dental materials. The epoxy resin-based root canal filling material AH Plus, the compounds paste A and paste B were tested for induction of micronuclei in V79 cells. Authors provided the evidence for the induction of chromosomal mutations by freshly mixed AH Plus under examined experimental conditions (Schweikl and Schmalz 2000).

Micronucleus test was used to evaluate chromosomal damage of amorphous silica particles in human pulmonary epithelial cells (A549) and murine macrophages (RAW 264.7). The potential effect of amorphous silica at chromosomal level was detected, but increase in the frequency of micronucleated cells that was observed in A549 cells treated with all doses and particle types, was not statistically significant. One type of examined silica particles to which RAW 264.7 cells were exposed, showed a statistically significant increase in MN frequency at the three highest examined doses. Authors of this study concluded that induced cytotoxic and genotoxic effects was in different extents according to the cell type and particle structure (Guidi et al. 2013).

Genotoxic potential of 2-hydroxyethyl methacrylate (HEMA) monomer, that are used as a component of hydrogels, was evaluated by IVMNT in human peripheral blood lymphocytes and it has been shown that genotoxic effect of 1 mM of HEMA was measurable in the comet assay, but not in the micronucleus test (Ginzkey et al. 2015). This observation could indicate that micronucleus assay is not so sensitive and for low detection levels of genotoxicity, some other tests should also be used. Two other studies, performed with HEMA by employing the same assay with V79 Chinese hamster lung fibroblasts show dose dependent genotoxic effect of HEMA (Lee et al. 2006; Schweikl et al. 2007).

Micronucleus assay has an advantage compared to the other genotoxicity assays because it can be automated. Authors of the latest study (Di Bucchianico et al. 2017) examined genotoxicity potential through micronucleus evaluation of TiO_2 nanoparticles by using flow cytometer.

2.3 *Other DNA Effects*

2.3.1 Sister Chromatid Exchange (SCE) Assay

The sister chromatid exchange (SCE) assay is used to evaluate changes in DNA that may occur due to the genotoxicity of examined material. During DNA replication, two sister chromatids break and rejoin with one another and physically exchange regions of the parental strands (Wilson and Thompson 2007). These breaks, and subsequent exchange, are induced by mutagens that form DNA adducts or that interfere with DNA replication. In this assay, mammalian cells, with and without an exogenous metabolic activation, are exposed to the test material in vitro. Shortly before fixation, some spindle inhibitor, like colcemid, is added to the cells to block and accumulate cells in (pro)metaphase of the second division. Cells are then harvested and preparations of chromosomes are made. Sister chromatids are differentially stained by using different staining systems in order to distinguish them and then examined microscopically to see if segments of DNA have been reciprocated or exchanged between the sister chromatids. Evidence of such exchanges appears as striations or a banding effect along chromatids. Usually, bromodeoxyuridine (BrdU) is added in culture medium for two cell cycles, which incorporates into newly synthesized DNA. Chromatids in which only one strand of DNA incorporates BrdU show a normal dark staining, whereas those with two substituted strands stain less darkly. The sister chromatid exchange (SCE) assay is usually performed on human peripheral blood lymphocytes, stimulated to divide by some nonspecific antigen like phytohaemagglutinin (Gibbs et al. 1982). Indication of genotoxic effect is the increase in the number of SCEs observed in examined cells (test cultures) compared to untreated cultures.

Polyalkylimide hydrogel (Bio-Alcamid™) intended for soft tissue augmentation was examined by SCE assay and did not alter the number of sister chromatid exchanges per cell in CHO-K1 cell cultures (Ramires et al. 2005).

2.3.2 Single Cell Gel Electrophoresis Assay (Comet Assay)

The single cell gel electrophoresis assay (SCGE) or most commonly called “comet” assay was established by Ostling and Johanson in 1984. This test is not included in ISO standard battery tests for genotoxicity evaluation but is increasingly used to examine genotoxicity of different biomaterials intended for application in biomedical fields. It is used for analyzing and quantifying DNA damage in individual cells (Liao et al. 2009; Tice et al. 2000). This method is suitable for both in vivo and in vitro testing and quantification of DNA damage in every eukaryotic cell (Azqueta and Collins 2013). This assay could be used for monitoring DNA damage, DNA repair mechanism as well as assessing the oxidative status of the cells (Azqueta and Collins 2013). By using DNA gel electrophoresis and

fluorescence microscopy, the migration of DNA fragments from individual agarose-embedded cells can be visualized (Olive and Banáth 2006).

After the treatment of cells with tested material is finished, cells are harvested. Second step is embedding the cells in the low-melting point agarose gel in order to prevent denaturation of the proteins in the examined cells. Further, lysis buffer is applied and then incubation of embedded cells in alkaline buffer follows. These steps are necessary prior to electrophoresis in order to unwind and release DNA from cells and therefore single-stranded DNA (ssDNA) is obtained. Lower temperatures are recommended for performing the reaction in order to provide increased reproducibility (Liao et al. 2009). Neutralization step which follows electrophoresis is crucial for renaturation of DNA in the "heads" of the comet but in the "tails" DNA still remained at ssDNA level. Interpretation of the results could be accomplished in a few ways but so called "tail moment" is seemed to be favored nowadays (Liao et al. 2009). The "tail moment" refers to a measurement of DNA migration in the gel by the following calculation: amount of the DNA in the "tail" × "tail" length (Olive et al. 1990a). Also, percentage of DNA in tail is also commonly used parameter.

Comet refers to the image of cell's nuclei, obtained after procedure, which forms comet-like shape. The head of the comet contains undamaged supercoiled DNA while "tail" represents unwind and broken fragments of DNA. Migrating distance of negatively charged DNA molecules towards the anode through the gel in electrophoresis depends on the size of the DNA fragments. This fact was used to determine whether nuclear DNA is more or less damaged under the influence of tested agents. Quantity of DNA liberated from the nucleus (head of the comet) during electrophoresis depends on the genotoxic potential of tested agent (Liao et al. 2009).

If the tested agent is more genotoxic, more breaks would be induced in DNA molecule and more fragments will be formed. Higher number of fragments with lighter molecular weight will result in further migrations in the gel and longer tail will be formed. Visualization of these events in the gel after electrophoresis is enabled by addition of different dyes that can bind to DNA and can be detected by fluorescence microscopy method (Olive and Banáth 2006). Most commonly used dyes for these purposes are ethidium bromide and propidium iodide (Liao et al. 2009) but some other newer fluorescent dyes may also be used.

This method has been improved and nowadays is suitable for detection of DNA damage caused by double and single strand breaks, alkali labile sites, DNA crosslinking with DNA or protein and oxidative base damage. A few modifications of the comet assay are still in use (Singh et al. 1988; Olive et al. 1990b; Collins et al. 1993) but alkaline modification (pH > 13) by Singh et al. (1988) is estimated as the most superior in sensitivity and number of DNA lesions (Liao et al. 2009).

The advantages of Comet assay, compared with other genotoxicity tests, include the following: high sensitivity for detecting low levels of both single and double stranded breaks in damaged DNA, high efficiency and cost-effectiveness,

time-saving, small number of cells needed per sample, flexibility and simple application (Collins et al. 1997, 2008). These advantages have caused its widespread implementation (Liao et al. 2009; Azqueta and Collins 2013).

Comet assay is useful in many areas like genotoxicity testing, human biomonitoring and ecogenotoxicology (Azqueta and Collins 2013). One of the earliest studies using comet assay for genotoxicity evaluation of biomaterials intended for medical purposes was demonstrated by Chauvel-Lebret et al. (2001). They showed the capacity of this assay for genotoxicity evaluation of biomaterials and set foundation for further analysis. Comet assay has been shown as one of the most sensitive methods available for detecting strand breaks.

Comet assay has been proposed as suitable technique for evaluation of genotoxicity of hydrogels intended for cardiac (Thankam and Muthu 2013) and wound healing (Kirf et al. 2010) applications or as drug-delivery systems (Babić et al. 2016).

Recently, we engineered and examined intelligent acrylate based hydrogels with incorporated copper intended for use in wound management (Vuković et al. 2016). Three series of hydrogels, based on 2-hydroxyethyl acrylate (HEA) and itaconic acid (IA), unloaded, with incorporated copper (II) ions and reduced copper were examined on L929 mouse fibroblasts. For evaluation of cytotoxicity prior to genotoxicity testing, we performed MTT assay (Vuković et al. 2016). We have performed Comet assay to assess the genotoxic potential of hydrogels' extracts (unpublished results). By employing Comet assay, we examined the genotoxicity potential of 2-hydroxyethyl methacrylate (HEMA) based hydrogels: PHEMA homopolymer and two terpolymers of HEMA, itaconic acid (IA) and two poly (alkylene glycol) (meth)acrylates (PAGM): poly(ethylene glycol)$_6$ acrylate (P (HEMA/IA/PAGM1)) and poly(propylene glycol)$_5$ methacrylate (P (HEMA/IA/PAGM2)) synthesized by gamma-irradiated radical polymerization (Takić Miladinov et al. 2016). The results of the Comet assay showed that extracts of all tested hydrogels are capable to induce certain genotoxic effects. We showed that genotoxic potential depends on chemical composition, extract concentration as well as on the degree of crosslinking of examined hydrogels (Takić Miladinov et al. 2016). HEMA is commonly used monomer for preparation of acrylate-based hydrogels and is examined by comet assay in different studies on different cell models. Genotoxic effect of HEMA was shown in a dose dependent manner by Comet assay in V79 Chinese hamster lung fibroblasts, in concentrations 1–18 mM (Lee et al. 2006). Increased DNA damage in a dose-dependent manner was observed when HEMA was examined on A549 lung-tumour cells and human peripheral blood lymphocytes in concentrations 0–10 mM (Pawlowska et al. 2010). In the study by Ginzkey et al. genotoxic effect was measurable in the Comet assay at 1 mM of HEMA when examined in human peripheral blood lymphocytes (Ginzkey et al. 2015). Increased DNA "tail" in a dose dependent manner was observed in human gingival fibroblasts by Comet assay at concentrations 1–10 mM of HEMA (Szczepanska et al. 2012). Hydrogel N-vinyl-2-pyrrolidone/acrylic acid (NVP-AA) was examined in HepG2 cells by Comet assay (concentration range

0.25–25 mg/ml) and it is shown that NVP-AA induces a four to six-fold increase in DNA breaks (Devine et al. 2006). Other study performed with the same hydrogel in HepG2 and HaCaT cells showed that this hydrogel is genocompatible (Kirf et al. 2010). Genotoxic potential of alginate-polypropylene fumarate/2-hydroxyethyl methacrylate (ALPF-HEM) was examined in L929 fibroblasts and it is shown that this hydrogel is genocompatible under examined conditions (Thankam and Muthu 2014). The superporous hydrogel containing poly(acrylic acid-co-acrylamide)/O-carboxymethyl chitosan (O-CMC) interpenetrating polymer networks (SPH-IPN), that has been developed as an oral delivery vehicle for protein drugs, was subject to cytotoxicity and genotoxicity testing. In vitro genotoxicity testing in RBL-2H3 and Caco-2 cell lines was monitored for apoptosis and DNA strand breakage by performing Comet assay. It is shown that SPH-IPN did not induce cell apoptosis or DNA breakage in examined cell lines (Yin et al. 2009). Genotoxic potential of resin–based dental restorative materials and substances released from those materials are commonly tested for genotoxicity by Comet assay (Bakopoulou et al. 2009). Genotoxicity of TiO_2 nanoparticles was assessed by mini-gel comet assay (Di Bucchianico et al. 2017) and authors of this study concluded that mini-gel comet assay can be successfully used to efficiently study the genotoxic properties of nanoparticles. Amorphous silica particles were tested on human pulmonary epithelial cells (A549) and murine macrophages (RAW 264.7) to evaluate their cytotoxic and genotoxic effects (Guidi et al. 2013). This study demonstrated that the exposure to amorphous silica particles induces cytotoxic and genotoxic effects to different extents according to cell type and particle structure. A549 cells were remarkably resistant in terms of DNA effects in the Comet assay while RAW 264.7 cells were prone to amorphous silica, exhibiting a generalized increase in DNA strand breaks and chromosomal alteration (Guidi et al. 2013).

Hydroxyapatite, as one of the commonly used bone substitute material, was evaluated on L929 fibroblast cells in vitro by employing MTT test for cytotoxicity and Comet assay for genotoxicity evaluation. This study showed that hydroxyapatite has very low cytotoxic and genotoxic potential (Rajab et al. 2004). A few modifications of hydroxyapatite, fluorapatite and fluor-hydroxyapatite, as well as pure hydroxyapatite were evaluated by Comet assay in V79 cells in vitro. Eluates of tested materials were prepared in series of concentrations from 1 to the 100% and added to the cell culture medium. Conclusion was that DNA brakes were induced by increasing concentrations of eluates of biomaterials in this order hydroxyapatite < fluor-hydroxyapatite < fluorapatite, but compared to the positive control none of them were genotoxic (Jantová et al. 2008). These data indicate good biocompatibility properties of hydroxyapatite and its modifications as bone substitute materials.

Also, the new generation of biomaterials based on bioactive glasses for treatments of bone defects was tested for genotoxicity by Comet assay (Tavakoli et al. 2012). This evaluation was conducted in vitro, particularly in gingival fibroblast cells. Material elution was prepared in concentrations from 1 mg/ml up to the 5 mg/ml. It was concluded that concentrations less than 4 mg/ml have no genotoxic

activity but it is recommended that further biocompatibility examination should be conducted (Tavakoli et al. 2012).

These examples clearly showed that comet assay could be successfully applied in evaluation of genotoxicity of different biomaterials.

3 In Vivo Genotoxicity/Mutagenicity Testing

When tested material is proved to be genotoxic in vitro, the next step is evaluation of its genotoxic potential in animal models in vivo and potentially in humans (Eastmond et al. 2009; Parry and Parry 2012). Various in vivo genotoxicity test systems have been developed in different model organisms (Stamenković-Radak and Anđelković 2016). In vivo genotoxicity assays can be conducted in somatic and/or germ cells. Compared with in vitro genotoxicity assays, in vivo genotoxicity assays have been used to verify the results of in vitro assays and definitely provide biological significance for certain organs or cell types.

Micronucleus test can be performed in cells obtained from peripheral blood or bone marrow of rodents that were previously treated with tested agent or even in humans who might be exposed to some genotoxic agent in their environment. Mouse bone marrow micronucleus test detects damages to the chromosomes or the mitotic apparatus of immature red blood cells found in bone marrow. Unlike main nucleus, micronuclei is not extruded when erythroblasts develop into polychromatic erythrocytes (PCEs), thus an increase in the number of micronucleated PCEs in animals treated with the test agent is an indication for genotoxic effect. The MNs can be initiated by segregation error and lagging acentric chromosome fragment. The in vivo MN assay has been established by OECD test guidelines and many studies (Kang et al. 2013).

Comet assay could also be performed for detecting potential genotoxicity of tested agents in vivo. DNA strand breaks, as markers of genotoxicity, can be detected by Comet assay in vivo (Kang et al. 2013).

Combination of the in vivo Comet and MN assay has been proposed as useful methodology for evaluating genetic damage, and it has been used in the assessment of potential carcinogenicity by complementarily presenting two distinct endpoints of the in vivo genotoxicity individual test (Kang et al. 2013).

In vivo genotoxic potential of aluminium oxide nanomaterials, in different single doses, was examined in peripheral blood cells of Wistar rats using both the comet and micronucleus test. The genotoxicity end points evaluated in this study were the frequency of micronuclei (MN) and the percentage of tail DNA (% Tail DNA) migration. Results of this study suggested that Al(2)O(3) nanomaterials were able to cause size- and dose-dependent genotoxicity in vivo compared to Al(2)O(3)-bulk and control groups (Balasubramanyam et al. 2009). The superporous hydrogel containing poly(acrylic acid-co-acrylamide)/O-carboxymethyl chitosan (O-CMC) interpenetrating polymer networks (SPH-IPN) had been developed as an oral delivery vehicle for protein drugs and was subjected to cytotoxicity and

genotoxicity testing. Micronucleus studies in mouse bone marrow were conducted for in vivo genotoxicity evaluation and it was shown that SPH-IPN superporous hydrogel did not increase micronucleus incidence in mouse bone marrow (Yin et al. 2009). Enhancement of DNA migration was observed when HEMA was tested in human peripheral blood lymphocytes and human samples of salivary glands by Comet assay (Kleinsasser et al. 2004, 2006). In vivo determination of genotoxicity induced by orthodontic appliances was performed by micronucleus and comet assays in buccal cells of healthy patients who underwent orthodontic treatment (fixed appliances) with stainless steel alloy as basic composition (Westphalen et al. 2008). Genotoxic potential of these kinds of dental materials is the consequence of the release of metals like nickel, chromium and iron. In this study the micronucleus assay was shown to be more sensitive than the comet assay (Westphalen et al. 2008).

Drosophila melanogaster is one of the widest and most used eukaryotic model organisms in numerous areas of biology. There are data in evolutionary biology, ecology, genetics, toxicology, development, systematic, behavior, physiology, neurobiology as well as molecular biology about this model organism (Powell 1997). Recently, we have used *Drosophila* as model for different in vivo toxicology studies (Žabar et al. 2013; Mihajilov-Krstev et al. 2014; Cvetković et al. 2015b; Jovanović et al. 2016). *Drosophila* is a good alternative model organism for in vivo testing instead of small rodents because of its short generation period, high number of progeny and it is more economical for maintaining (Lee et al. 1983). In addition, *Drosophila* has similar cell organization to mammals as well as some metabolic pathways but also has ability to activate promutagens (Stamenković-Radak and Anđelković 2016) what is very important for interpretation of the results. In addition, assays for genotoxicity testing in *Drosophila* are more applicable to humans than the bacterial assays (Stamenković-Radak and Anđelković 2016). *Drosophila* is more affordable model organism and good substitution for experimental mammals (Vales et al. 2013) because there is no need for ethics committee approval for conduction of the experiment like that is the case with experimental mammals.

3.1 Genotoxicity Testing in Drosophila

Among the others, a few in vivo genotoxicity and mutagenicity assays in *Drosophila* draws attention of many researches. Two of them are assays for detection mutations in somatic cells, wing-spot somatic mutation and recombination test (SMART) and white-ivory eye spot test. Another one is assay for assessment of mutagenicity in germ cells and it is known as sex-linked recessive lethal test (SLRL). According to Graf and Würgler (1996) genotoxicity assays in somatic models have few advantages over assays in germ cell models. The analyzed markers in somatic models are reliable and easier for scoring. Also, greater number of cells per individual can be analyzed in somatic models and those tests could be

performed in only one generation (Graf and Würgler 1996). If tested agent is proved to be mutagenic in somatic cells then it could be considered as possible mutagen for germ cells as well (Eastmond et al. 2009).

It was concluded that sensitivity of the white-ivory eye spot test significantly differs from wing-spot test what suggests that those assays detect different genotoxic events (Graf and Würgler 1996) and therefore it is assumed that wing-spot test is more reliable. In addition, Ferreiro et al. (1997) concluded that white-ivory test should not be used in general screening because it is less reliable and more difficult for detection of positive effects of tested agents compared with wing-spot test (Ferreiro et al. 1997). For that reason, here we will focus on the wing-spot and sex-linked recessive lethal assays in *D. melanogaster*.

3.1.1 Wing-Spot Somatic Mutation and Recombination Test in *D. melanogaster*

The wing-spot somatic mutation and recombination test (SMART) in *D. melanogaster* is one of the somatic mutation and recombination test which was proposed by Graf et al. in 1984. This method allows the detection of different genetic alterations in somatic cells in vivo such as structural aberrations and recombination and it is simple, low-cost, very reliable test and rapid for performing (Graf et al. 1984).

Two *D. melanogaster* strains are used in wing-spot SMART. The *mwh* strain has recessive mutation that in homozygous expresses multiple hairs per wing cell. The flare (*flr*) strain has recessive mutation that results in unusual shapeless wing hairs compared to wild-type strains which normally exhibit one hair per wing cell (Graf et al. 1984)

In wing-spot SMART, 3-day-old offspring larvae from *mwh* male and *flr* female parental generation represent in vivo model which could be exposed to acute or chronic treatment in this assay (Patenkovic et al. 2009). For optimal results, fifty to one hundred larvae are recommended to treat per series (Graf et al. 1984). Genetic alteration in treated trans-heterozygous larvae can occur in mitosis of progenitor cells from which the wings will evolve, what will change their genotype and finally cause the expression of *mwh* and *flr* phenotype. Changed descendant cells would express *mwh* and/or *flr* hairs phenotype on the wing and formed groups, areas of so-called "spots" on the wing. The size and number of the spots depends on the frequency of the mutation event and the influence of exposure time to the mutagenic agent (Graf et al. 1984).

At the end of experiment the adults are hatched from treated larvae and wings can be easily collected from each individual and permanent preparation of the wings follows. After the wing is mounted on microscopic slide, the "spots" can be examined at 400× magnification (Graf et al. 1984; Patenkovic et al. 2009). Finally, frequencies of the "spots" occurred in the group which were treated with some agent, can be compared with the results obtained from untreated control group where spots might occur spontaneously (Graf et al. 1984). Also, larvae treated with

well-known mutagen (for example methyl methane-sulphonate—MMS) could be included as positive control in experiment (Stamenković-Radak et al. 2005; Patenkovic et al. 2009).

SMART wing-spot test in *D. melanogaster* allows not only evaluation for detecting genotoxic and mutagenic agents but also allows evaluation of antigenotoxic and antimutagenic properties of selected agents. Well-known mutagenic substance can be mixed with potential antimutagenic agent and put into feeding medium for larvae. Also, larvae could be firstly treated with mutagenic agent and after that could be exposed to the potential antimutagenic agent (Patenkovic et al. 2009). If tested agent has the ability to suppress the activity of mutagenic agent, analysis of spots at wing blade would reveal reduced frequency of the mutated spots (Patenkovic et al. 2009). There are hundreds of agents tested by SMART wing-spot test on genotoxicity and mutagenicity but according to our knowledge there is no data on testing of biomaterials such as bone substitute biomaterial by employing this test. Nevertheless, some nanomaterials and commercial materials which are used in dentistry are tested and we will present some of these results.

Arossi and co-workers published interesting results on genotoxicity of nine aqueous extracts of commercially used dental composite resins obtained using SMART wing-spot test on *D. melanogaster* (Arossi et al. 2010). Only one of nine tested aqueous extracts increased the frequency of mutant spot while the other eight extracts did not show significant influence on occurrence of the spots in flies (Arossi et al. 2010). According to author's explanation the material, which increased the frequency of mutant spot in flies, mainly consisted of organic component while inorganic component was less presented (Arossi et al. 2010), so that could be the reason for exerting mutagenic effect. The same group of authors conducted similar research with two dental bonding agents (Arossi et al. 2009). In this research they had found differences in genotoxic potential between two materials but both of them induced genotoxic events. Those were one of the first evaluations of materials used in dentistry which indicated that further investigations on genotoxic properties of those materials are required because of its application directly on living tissues what caries a potential risk to humans.

So far, nanomaterials are most often evaluated using SMART wing-spot test in *D. melanogaster* (Vales et al. 2013; de Andrade et al. 2014; Demir et al. 2013). For example, cobalt nanoparticles as well as ionic form of cobalt chloride were showed to be genotoxic as they are applied to *D. melanogaster* third instar larvae (Vales et al. 2013). According to the authors of this study, genotoxic potential of examined nanoparticles could be referred mostly to oxidative damage caused by tested nanoparticles (Vales et al. 2013).

On the other hand, there are some nanomaterials which showed no significant genotoxic activity in *Drosophila* wing-spot test (de Andrade et al. 2014). High purity of tested multi-walled carbon nanotubes, without the presence of residual contaminating metals, was indicated by authors as one of the reasons for such results (de Andrade et al. 2014). Another example is genotoxic evaluation of titanium, zirconium and aluminium nanoparticles which also showed that tested

materials were not able to induce genotoxic effects in wing-spot test (Demir et al. 2013).

These examples confirm that SMART wing-spot test in *D. melanogaster* have a great potential for different genotoxicity evaluation of materials which are intended for use in humans. However, there are some limitations in genotoxicity testing which imply treatment of *D. melanogaster* larvae. Larvae are started to feed since they have hatched until they transformed into pupae, so the tested agent should be embed into feeding media. Since the larvae are small in size, especially at the moment immediately after hatching, they can ingest only small particles from feeding media. Therefore, biomaterials for treatment should be embedded in feeding media in the form of dilution or extract like Arossi et al. have demonstrated (Arossi et al. 2010). This is not easy to achieve with most of the biomaterials and whenever it is not possible, then material should be pulverized prior treatment in the fine powder form with particle size that larvae can ingest through feeding media, preferably in the form of nanoparticles. It is well-known that some bone substitute materials are in the form of nanomaterials and considering that fact, it is useful to know that this assay could be used for genotoxicity assessment of nanomaterials. In addition, we have demonstrated that *D. melanogaster* larvae could be successfully treated with materials which are in the form of nanoparticles (Jovanović et al. 2016). Thus, it could be expected that SMART wing-spot test in *D. melanogaster* assay will be used for genotoxicity evaluation of various bone substitute biomaterials intended for application in clinical practice.

3.1.2 Sex-Linked Recessive Lethal Test in *D. melanogaster*

The sex-linked recessive lethal (SLRL) test is a short-term in vivo assay which is the widest and one of the mostly used genotoxicity test that involves *Drosophila* as a model (Lee et al. 1983; Stamenković-Radak et al. 2005; Stanić et al. 2009, 2011; Stamenković-Radak and Anđelković 2016). SLRL test can detect mutations of nearly 800 genes which are located on X chromosome what represents about 20% of *D. melanogaster* genome (Abrahamson et al. 1980; Lee et al. 1983). Particularly, this test is used for evaluation of the frequency of minor deletions and gene mutations or aberrations that have a recessive lethal effect in germ cells of the male flies (Würgler, 1980; Lee et al. 1983). SLRL assay provides opportunity to detect various mutations in one single experiment and therefore it could provide information on potential in vivo activity of tested agents (Würgler 1980).

The SLRL test was previously described in details (Lee et al. 1983) but here this test will be presented in brief. For this assay two strains of *D. melanogaster* are used, flies with normal wild-type phenotype (e.g. Oregon-R or Canton-S) and *Basc* strain (Lee et al. 1983; Stamenković-Radak et al. 2005; Stanić et al. 2011). *Basc* strain has three gene marker mutations located on X chromosome for eye shape (narrow eye shape), eye color (light apricot eye color) that is expressed in

hemizygous (in males) and homozygous (in females) condition, and third mutation represents reduced thoracic bristles whose genes are located on X chromosome (Lee et al. 1983; Stanić et al. 2011).

The assay starts by treating the wild-type adult male flies with potential genotoxic agent. Then crossing of the treated males with virgin *Basc* females follows in order to obtain F1 progeny generation. After the adults of F1 is intercrossed, part of the male progeny of F2 generation could inherit recessive lethal mutation on X chromosome which originates from treated parental male flies what finally results in missing the wild-type phenotypic class of the male progeny in F2 generation (Lee et al. 1983). The males are hemizygous for genes on X chromosome and that is the reason why they could not survive early development stage if they inherited this lethal recessive mutation on X chromosome. If tested agent caused lethal recessive mutation then only live hatched males of F2 generation will be those that inherit *Basc* X chromosome and therefore express *Basc* phenotypic class (Lee et al. 1983). Thus the results can be easily scored and calculated according to the eye shape and color of the hatched male flies in F2 generation (Lee et al. 1983; Stanić et al. 2009). For this assay, negative (water or solvent) control and positive (well-known mutagen, for example MMS) is required for interpretation of the final results and comparison with the results obtained for tested agent (Stamenković-Radak et al. 2005).

The SLRL assay also provides the possibility to evaluate genotoxic effect on different stadiums of male germ cell lines (spermatozoa, spermatids and spermatocytes) by forming three successive broods of treated wild-type males with virgin *Basc* females, every 2–3 days (Lee et al. 1983). Therefore, the offspring that is obtained from these successive broods could give information on the influence of tested agent at different developmental stages of germ cells in treated wild-type male flies.

According to our knowledge there are no data about genotoxicity evaluations of biomaterials or bone substitutes biomaterials intended for use in BTE and clinical practice. In our opinion, the underlying problem is the way of treatment of the adult flies with biomaterials. Because the flies are fed with liquid component of the feeding media it is harder to treat adult flies than the larvae. Adult flies in SLRL can be treated by applying liquid extract or dilution of biomaterial what might be possible with some materials. Also, biomaterials which are in the form of nanoparticles could be suspended in some liquid (e.g. water) which might be ingested by adult flies. Nevertheless, SLRL assay in *Drosophila* showed excellent sensitivity and represents suitable assay for evaluation of mutagenicity and antimutagenicity of selected agents in germ cells as it was demonstrated by some studies (Lee et al. 1983; Stamenković-Radak et al. 2005; Stanić et al. 2009, 2011; Stamenković-Radak and Anđelković 2016). Because of its great properties, it could be expected that SLRL assay in *D. melanogaster* will be used in the near future for genotoxicity evaluation of biomaterials.

4 Conclusion

According to an overview of in vitro and in vivo genotoxicity/mutagenicity assay given in this chapter we can conclude that for obtaining the best results and wide image of the biocompatibility of biomaterials and MDs intended for use in biomedical and clinical applications, combination of different genotoxicity/mutagenicity assays should be used. Due to different end points and sensitivity of currently available genotoxicity and mutagenicity assays, it is recommended to combine at least two or even three different in vitro tests and if they are positive or give different results, at least one in vivo test should be performed. Tests performed in mammalian cells and model organisms are desirable and recommended. The most commonly used in vitro assays are Ames test and micronucleus (MN) test. Comet assay has been increasingly used nowadays for testing large numbers of different biomaterials because of its numerous advantages, and we would recommend it as valuable genotoxicity assay for biocompatibility assessment. Regarding in vivo assays, genotoxicity and mutagenicity testing in *Drosophila* is very promising due to the numerous advantages. There are many available protocols for testing in *Drosophila* and guidelines for interpretation of the obtained results described in details thus allowing not only specialized researches to perform these assays. In order to completely evaluate the biocompatibility of some biomaterial or medical device intended for application in biomedical fields, besides cytotoxicity assessment that is the first required step, we recommend the genotoxicity/mutagenicity testing as mandatory, especially when some new biomaterial is engineered.

Acknowledgements The printing of this work is financed by EU project 543898-TEMPUS-1-2013-1-ES-TEMPUS-JPHES. Part of the scientific work is supported by Ministry of Education, Science and Technological Development, Serbia, Grant No. III 41017.

References

Abrahamson S, Würgler FE, DeJongh C, Meyer HU (1980) How many loci on the X-chromosome of *Drosophila melanogaster* can mutate to recessive lethals? Environ Mutagen 2(4):447–453

Ames BN, Lee FD, Durston WE (1973) An improved bacterial test system for the detection and classification of mutagens and carcinogens. Proc Natl Acad Sci USA 70(3):782–786

Arossi G, Dihl R, Lehmann M, Cunha K, Reguly M, de Andrade HH (2009) *In vivo* genotoxicity of dental bonding agents. Mutagenesis 24(2):169–172

Arossi GA, Dihl RR, Lehmann M, Reguly ML, De Andrade HHR (2010) Genetic toxicology of dental composite resin extracts in somatic cells *in vivo*. Basic Clin Pharmacol 107(1):625–629

Assad M, Chernyshov A, Leroux MA, Rivard CH (2002) A new porous titanium-nickel alloy: part 1. cytotoxicity and genotoxicity evaluation. Biomed Mater Eng 12(3):225–237

Azqueta A, Collins AR (2013) The essential comet assay: a comprehensive guide to measuring DNA damage and repair. Arch Toxicol 87(6):949–968

Babić MM, Božić BĐ, Božić BĐ, Filipović JM, Uščumlić GS, Tomić SLj (2016) Evaluation of novel antiproliferative controlled drug delivery system based on poly(2-hydroxypropyl acrylate/itaconic acid) hydrogels and nickel complex with Oxaprozin. Mater Lett 163:214–217

Bakopoulou A, Papadopoulos T, Garefis P (2009) Molecular toxicology of substances released from resin-based dental restorative materials. Int J Mol Sci 10(9):3861–3899

Balasubramanyam A, Sailaja N, Mahboob M, Rahman MF, Hussain SM, Grover P (2009) *In vivo* genotoxicity assessment of aluminium oxide nanomaterials in rat peripheral blood cells using the comet assay and micronucleus test. Mutagenesis 24(3):245–251

Barbeck M, Najman S, Stojanović S, Mitić Ž, Živković JM, Choukroun J, Kovačević P, Sader R, Kirkpatrick CJ, Ghanaati S (2015) Addition of blood to a phycogenic bone substitute leads to an increased *in vivo* vascularization. Biomed Mater 10(5):055007

Black MM, Drury PJ (1994) Mechanical and other problems of artificial valves. Curr Top Pathol 86:127–159

Carraway J, Ghosh C (2006) The challenge to global acceptance of part 3 of ISO 10993. Med Device Technol 17:16–18

Cetin D, Kahraman AS, Gumusderelioglu M (2011) Novel scaffolds based on poly(2 hydroxyethyl methacrylate) superporous hydrogels for bone tissue engineering. J Biomat Sci Polym E 22 (9):1157–1178

Chauvel-Lebret DJ, Auroy P, Tricot-Doleux S, Bonnaure-Mallet M (2001) Evaluation of the capacity of the SCGE assay to assess the genotoxicity of biomaterials. Biomaterials 22 (13):1795–1801

Collins AR, Duthie SJ, Dobson VL (1993) Direct enzymic detection of endogenous oxidative base damage in human lymphocyte DNA. Carcinogenesis 14(9):1733–1735

Collins AR, Dobson VL, Dusinská M, Kennedy G, Stětina R (1997) The comet assay: what can it really tell us? Mutat Res 375(2):183–193

Collins AR, Oscoz AA, Brunborg G, Gajvão I, Giovannelli L, Kruszewski M, Smith CC, Stětina R (2008) The comet assay: topical issues. Mutagenesis 23(3):143–151

Costa VC, Costa HS, Vasconcelos WL, Pereira MM, Oréfice RL, Mansur HS (2007) Preparation of hybrid biomaterials for bone tissue engineering. Mater Res 10(1):21–26

Cross NG, Taylor RF, Nunez LJ (1983) "Single-step" orthodontic bonding systems: possible mutagenic potential. Am J Orthod 84(4):344–350

Cvetkovic V, Najman S, Rajkovic J, Zabar AL, Vasiljevic P, Djordjevic LB, Trajanovic M (2013) A comparison of the microarchitecture of lower limb long bones between some animal models and humans: a review. Vet Med-Czech 58(7):339–351

Cvetković VJ, Najdanović JG, Vukelić-Nikolić MĐ, Stojanović S, Najman SJ (2015a) Osteogenic potential of *in vitro* osteo-induced adipose-derived mesenchymal stem cells combined with platelet-rich plasma in an ectopic model. Int Orthop 39(11):2173–2180

Cvetković V, Mitrović T, Jovanović B, Stamenković S, Todorović M, Đorđević M, Radulović N (2015b) Toxicity of dimethyl sulfoxide against *Drosophila melanogaster*. Biologica Nyssana 6 (2):91–95

Damnjanovic I, Kocic G, Najman S, Stojanovic S, Stojanovic D, Veljkovic A, Conic I, Langerholc T, Pesic S (2014) Chemopreventive potential of alpha lipoic acid in the treatment of culture of colon and cervix cancer cell lines. Bratisl Lek Listy 115(10):611–616

Damnjanovic I, Najman S, Stojanovic S, Stojanovic D, Veljkovic A, Kocic H, Langerholc T, Damnjanovic Z, Pesic S (2015) Crosstalk between possible cytostatic and antiinflammatory potential of ketoprofen in the treatment of culture of colon and cervix cancer cell lines. Bratisl Lek Listy 116(4):227–232

de Andrade LR, Sandin Brito A, de Souza Melero AMG, Zanin H, José Ceragioli H, Baranauskas V, Silva Cunha K, Pierre Irazusta S (2014) Absence of mutagenic and recombinagenic activity of multi-walled carbon nanotubes in the *Drosophila* wing-spot test and *Allium cepa* test. Ecotox Environ Safe 99:92–97

Demir E, Turna F, Vales G, Kaya B, Creus A, Marcos R (2013) *In vivo* genotoxicity assessment of titanium, zirconium and aluminium nanoparticles, and their microparticulated forms. Drosophila. Chemosphere 93(10):2304–2310

Devine DM, Devery SM, Lyons JG, Geever LM, Kennedy JE, Higginbotham CL (2006) Multifunctional polyvinylpyrrolidinone-polyacrylic acid copolymer hydrogels for biomedical applications. Int J Pharm 326(1–2):50–59

Di Bucchianico S, Cappellini F, Le Bihanic F, Zhang Y, Dreij K, Karlsson HL (2017) Genotoxicity of TiO_2 nanoparticles assessed by mini-gel comet assay and micronucleus scoring with flow cytometry. Mutagenesis 32(1):127–137

Doak SH, Manshian B, Jenkins GJ, Singh N (2012) *In vitro* genotoxicity testing strategy for nanomaterials and the adaptation of current OECD guidelines. Mutat Res 745(1–2):104–111

Doherty AT (2012) The *in vitro* micronucleus assay. Methods Mol Biol 817:121–141

Eastmond DA, Hartwig A, Anderson D, Anwar WA, Cimino MC, Dobrev I, Douglas GR, Nohmi T, Phillips DH, Vickers C (2009) Mutagenicity testing for chemical risk assessment: update of the WHO/IPCS harmonized scheme. Mutagenesis 24(4):341–349

Fenech M (2008) The micronucleus assay determination of chromosomal level DNA damage. Methods Mol Biol 410:185–216

Ferreiro JA, Consuegra S, Sierra LM, Comendador MA (1997) Is the white-ivory assay of *Drosophila melanogaster* a useful tool in genetic toxicology? Environ Mol Mutagen 29 (4):406–417

Food and Drug Administration (FDA) Use of international standard ISO 10993-1, "Biological evaluation of medical devices—part 1: evaluation and testing within a risk management process". Guidance for Industry and Food and Drug Administration Staff. Available online: http://www.fda.gov/downloads/medicaldevices/deviceregulationandguidance/guidancedocuments/ucm348890.pdf Accessed on 10 July 2015

Gibbs JH, Potts RC, Brown RA, Robertson AJ, Beck JS (1982) Mechanisms of phytohaemagglutinin (PHA) stimulation of normal human lymphocytes: 'trigger' 'push' or both? Cell Tissue Kinet 15(2):131–137

Ginzkey C, Zinnitsch S, Steussloff G, Koehler C, Hackenberg S, Hagen R, Kleinsasser NH, Froelich K (2015) Assessment of HEMA and TEGDMA induced DNA damage by multiple genotoxicological endpoints in human lymphocytes. Dent Mater 31(8):865–876

Gonzalez L, Sanderson B, Kirsch-Volders M (2011) Adaptations of the *in vitro* MN assay for the genotoxicity assessment of nanomaterials. Mutagenesis 26(1):185–191

Graf U, Würgler FE (1996) The somatic white-ivory eye spot test does not detect the same spectrum of genotoxic events as the wing somatic mutation and recombination test in *Drosophila melanogaster*. Environ Mol Mutagen 27(3):219–226

Graf U, Würgler F, Katz A, Frei H, Juon H, Hall C, Kale P (1984) Somatic mutation and recombination test in *Drosophila melanogaster*. Environ Mol Mutagen 6(2):153–188

Guidi P, Nigro M, Bernardeschi M, Scarcelli V, Lucchesi P, Onida B, Mortera R, Frenzilli G (2013) Genotoxicity of amorphous silica particles with different structure and dimension in human and murine cell lines. Mutagenesis 28(2):171–180

Han T, Wang J, Tong W, Moore MM, Fuscoe JC, Chen T (2006) Microarray analysis distinguishes differential gene expression patterns from large and small colony thymidine kinase mutants of L5178Y mouse lymphoma cells. BMC Bioinform 7(Suppl 2):S9

Hassan A, Swaminathan D (2011) An *in vitro* study to evaluate the genotoxicity of value added hydroxyapatite as a bone replacement material. Sains Malays 40(2):163–171

Hassan A, Daud MHM, Ariffin Z, Alam MK (2013) An *in vitro* study of genotoxicity of silver amalgam. Int Med J 20(4):409–412

Huang Y, Gao H, Gou M, Ye H, Liu Y, Gao Y, Peng F, Qian Z, Cen X, Zhao Y (2010) Acute toxicity and genotoxicity studies on poly (ε-caprolactone)-poly (ethylene glycol)-poly (ε-caprolactone) nanomaterials. Mutat Res-Gen Tox En 696(2):101–106

Ilić DP, Stojanović S, Najman S, Nikolić VD, LjP Stanojević, Tačić A, LjB Nikolić (2015) Biological evaluation of synthesized allicin and its transformation products obtained by microwaves in methanol: antioxidant activity and effect on cell growth. Biotechnol Biotechnol Equip 29(1):189–194

Jantová S, Theiszová M, Letašiová S, Birošová L, Palou T (2008) *In vitro* effects of fluor-hydroxyapatite, fluorapatite and hydroxyapatite on colony formation, DNA damage and mutagenicity. Mutat Res-Gen Tox En 652(2):139–144

Jovanović B, Cvetković V, Mitrović T (2016) Effects of human food grade titanium dioxide nanoparticle dietary exposure on *Drosophila melanogaster* survival, fecundity, pupation and expression of antioxidant genes. Chemosphere 144:43–49

Kang SH, Kwon JY, Lee JK, Seo YR (2013) Recent advances in *in vivo* genotoxicity testing: prediction of carcinogenic potential using comet and micronucleus assay in animal models. J Cancer Prev 18(4):277–288

Kaplan Ç, Diril N, Şahin S, Cehreli MC (2004) Mutagenic potentials of dental cements as detected by the *Salmonella*/microsome test. Biomaterials 25(18):4019–4027

Keeney M, Lai JH, Yang F (2011) Recent progress in cartilage tissue engineering. Curr Opin Biotechnol 22(5):734–740

Kim HR, Park YJ, Shin DY, Oh SM, Chung KH (2013) Appropriate *in vitro* methods for genotoxicity testing of silver nanoparticles. Environ Health Toxicol 28:e2013003

Kirf D, Higginbotham CL, Rowan NJ, Devery SM (2010) Cyto- and genotoxicological assessment and functional characterization of N-vinyl-2-pyrrolidone-acrylic acid-based copolymeric hydrogels with potential for future use in wound healing applications. Biomed Mater 5 (3):35002

Kirkland D, Aardema M, Henderson L, Müller L (2005) Evaluation of the ability of a battery of three *in vitro* genotoxicity tests to discriminate rodent carcinogens and non-carcinogens I. sensitivity, specificity and relative predictivity. Mutat Res 584(1–2):1–256

Kirsch-Volders M, Decordier I, Elhajouji A, Plas G, Aardema MJ, Fenech M (2011) *In vitro* genotoxicity testing using the micronucleus assay in cell lines, human lymphocytes and 3D human skin models. Mutagenesis 26(1):177–184

Kleinsasser NH, Wallner BC, Harréus UA, Kleinjung T, Folwaczny M, Hickel R, Kehe K, Reichl FX (2004) Genotoxicity and cytotoxicity of dental materials in human lymphocytes as assessed by the single cell microgel electrophoresis (comet) assay. J Dent 32(3):229–234

Kleinsasser NH, Schmid K, Sassen AW, Harréus UA, Staudenmaier R, Folwaczny M, Glas J, Reichl FX (2006) Cytotoxic and genotoxic effects of resin monomers in human salivary gland tissue and lymphocytes as assessed by the single cell microgel electrophoresis (comet) assay. Biomaterials 27(9):1762–1770

Kostić I, Najman S, Kostić M, Stojanović S (2012a) Comparative review of gingival retraction agents. Acta Medica Medianae 51(1):81–84

Kostić M, Najman S, Najdanović J, Krunić N, Kostić I (2012b) Application of direct contact test in evaluation of cytotoxicity of acrylic denture base resins. Acta Medica Medianae 51(1):66–72

Kostić I, Mihailović D, Najman S, Stojanović S, Kostić M (2014) The rabbit gingival tissue response to retraction liquids and tetrahydrozoline. Vojnosanit Pregl 71(1):46–51

Lee W, Abrahamson S, Valencia R, Von Halle E, Würgler F, Zimmering S (1983) The sex-linked recessive lethal test for mutagenesis in Drosophila melanogaster: a report of the US Environmental Protection Agency Gene-Tox Program. Mutat Res 123(2):183–279

Lee DH, Lim BS, Lee YK, Ahn SJ, Yang HC (2006) Involvement of oxidative stress in mutagenicity and apoptosis caused by dental resin monomers in cell cultures. Dent Mater 22 (12):1086–1092

Li Y, Chen DH, Yan J, Chen Y, Mittelstaedt RA, Zhang Y, Biris AS, Heflich RH, Chen T (2012) Genotoxicity of silver nanoparticles evaluated using the Ames test and *in vitro* micronucleus assay. Mutat Res 745(1–2):4–10

Liao W, McNutt MA, Zhu WG (2009) The comet assay: a sensitive method for detecting DNA damage in individual cells. Methods 48(1):46–53

Lloyd M, Kidd D (2012) The mouse lymphoma assay. Methods Mol Biol 817:35–54

Maldonado-Codina C, Efron N (2003) Hydrogel lenses—materials and manufacture: a review. Optom Pract 4:101–115

Mihajilov-Krstev T, Jovanović B, Jović J, Ilić B, Miladinović D, Matejić J, Rajković J, Đorđević L, Cvetković V, Zlatković B (2014) Antimicrobial, antioxidative, and insect repellent effects of Artemisia absinthium essential oil. Planta Med 80(18):1698–1705

Mitić Ž, Najman S, Cakić M, Ajduković Z, Ignjatović N, Nikolić R, Nikolić G, Stojanović ST, Vukelić M, Trajanović M (2014) Spectroscopic characterization of bone tissue of experimental animals after glucocorticoid treatment and recovery period. J Mol Struct 1074:315–320

Mitrović T, Stamenković S, Cvetković V, Tošić S, Stanković M, Radojević I, Stefanović O, Čomić L, Đačić D, Ćurčić M (2011) Antioxidant, antimicrobial and antiproliferative activities of five lichen species. Int J Mol Sci 12(8):5428–5448

Mitrović T, Stamenković S, Cvetković V, Đekić T, Baošić R, Mutić J, Anđelković T, Bojić A (2012a) Bioindication of heavy metal pollution in the area of Southeastern Serbia by using epiphytic lichen *Flavoparmelia caperata* (L.) Hale. Biologica Nyssana 3(2):53–56

Mitrović T, Stamenković S, Cvetković V, Nikolić M, Baošić R, Mutić J, Anđelković T, Bojić A (2012b) Epiphytic lichen *Flavoparmelia caperata* as a sentinel for trace metal pollution. J Serb Chem Soc 77(9):1301–1310

Mitrović T, Stamenković S, Cvetković V, Radulović N, Mladenović M, Stanković M, Topuzović M, Radojević I, Stefanović O, Vasić S (2014) *Platismatia glauca* and *Pseudevernia furfuracea* lichens as sources of antioxidant, antimicrobial and antibiofilm agents. EXCLI J 13:938–953

Morais JM, Papadimitrakopoulos F, Burgess DJ (2010) Biomaterials/tissue interactions: possible solutions to overcome foreign body response. AAPS J 12(2):188–196

Najdanović JG, Cvetković VJ, Stojanović S, Vukelić-Nikolić MĐ, Stanisavljević MN, Živković JM, Najman SJ (2015) The influence of adipose-derived stem cells induced into endothelial cells on ectopic vasculogenesis and osteogenesis. Cell Mol Bioeng 8(4):577–590

Najdanović JG, Cvetković VJ, Stojanović S, Vukelić-Nikolić MĐ, Čakić-Milošević MM, Živković JM, Najman SJ (2016) Effects of bone tissue engineering triad components on vascularization process: comparative gene expression and histological evaluation in an ectopic bone-forming model. Biotechnol Biotec Eq 30(6):1122–1131

Najdanović JG, Najman SJ, Stojanović S, Živković JM, Ignjatović N, Uskoković D, Trajanović M (2017) The influence of nanomaterial calcium phosphate/poly-(dl-lactide-co-glycolide) on proliferation and adherence of HeLa cells. In: Lee B et al (eds) Proceedings of the IV advanced ceramics and applications conference. Atlantis Press, pp 387–400

Najman S, Cvetković V, Najdanović J, Stojanović S, Vukelić-Nikolić M, Vučković I, Petrović D (2016) Ectopic osteogenic capacity of freshly isolated adipose-derived stromal vascular fraction cells supported with platelet-rich plasma: a simulation of intraoperative procedure. J Cranio Maxill Surg 44(10):1750–1760

Noushad M, Kannan TP, Husein A, Abdullah H, Ismail AR (2009) Genotoxicity evaluation of locally produced dental porcelain—an *in vitro* study using the Ames and Comet assays. Toxicol In Vitro 23(6):1145–1150

Olive PL, Banáth JP (2006) The comet assay: a method to measure DNA damage in individual cells. Nat Protoc 1(1):23–29

Olive PL, Banáth JP, Durand RE (1990a) Heterogeneity in radiation-induced DNA damage and repair in tumor and normal cells measured using the "comet" assay. Radia Res 122(1):86–94

Olive PL, Banáth JP, Durand RE (1990b) Detection of etoposide resistance by measuring DNA damage in individual Chinese hamster cells. Jnci-J Natl Cancer I 82(9):779–783

Ørstavik D, Hongslo JK (1985) Mutagenicity of endodontic sealers. Biomaterials 6(2):129–132

Ostling O, Johanson K (1984) Microelectrophoretic study of radiation-induced DNA damages in individual mammalian cells. Biochem Bioph Res Com 123(1):291–298

Parry JM, Parry EM (eds) (2012) Genetic toxicology: principles and methods. Methods in molecular biology, vol 817. Humana Press, Springer, New York. http://dx.doi.org/10.1007/978-1-61779-421-6

Patenkovic A, Stamenkovic-Radak M, Banjanac T, Andjelkovic M (2009) Antimutagenic effect of sage tea in the wing spot test of *Drosophila melanogaster*. Food Chem Toxicol 47(1):180–183

Pawlowska E, Poplawski T, Ksiazek D, Szczepanska J, Blasiak J (2010) Genotoxicity and cytotoxicity of 2-hydroxyethyl methacrylate. Mutat Res 696(2):122–129

Powell JR (1997) Progress and prospects in evolutionary biology: the drosophila model. Oxford University Press Inc, New York

Prokop A (2001) Bioartificial organs in the twenty-first century: nanobiological devices. Ann NY Acad Sci 944:472–490

Rajab NF, Yaakob TA, Ong BY, Hamid M, Ali AM, Annuar BO, Inayat-Hussain SH (2004) DNA damage evaluation of hydroxyapatite on fibroblast cell L929 using the single cell gel electrophoresis assay. Med J Malays 59(Suppl B):170–171

Rajković J, Stojanović S, Lj Đorđević, Cvetković T, Najman S (2015) Locally applied cholecalciferol and alfacalcidol act differently on healing of femur defects filled with bone mineral matrix and platelet-rich plasma in ovariectomized rats. Biotechnol Biotec Eq 29 (5):963–969

Ramires PA, Miccoli MA, Panzarini E, Dini L, Protopapa C (2005) *In vitro* and *in vivo* biocompatibility evaluation of a polyalkylimide hydrogel for soft tissue augmentation. J Biomed Mater Res B Appl Biomater 72(2):230–238

Remya NS, Syama S, Gayathri V, Varma HK, Mohanan PV (2014) An *in vitro* study on the interaction of hydroxyapatite nanoparticles and bone marrow mesenchymal stem cells for assessing the toxicological behavior. Colloids Surf B 117:389–397

Salata O (2004) Applications of nanoparticles in biology and medicine. J Nanobiotechnol 2(1):3

Savić V, Nikolić V, Arsić I, Lj Stanojević, Najman S, Stojanović S, Mladenović-Ranisavljević I (2015) Comparative study of the biological activity of allantoin and aqueous extract of the comfrey root. Phytother Res 29(8):1117–1122

Schweikl H, Schmalz G (2000) The induction of micronuclei in V79 cells by the root canal filling material AH plus. Biomaterials 21(9):939–944

Schweikl H, Schmalz G, Göttke C (1996) Mutagenic activity of various dentine bonding agents. Biomaterials 17(14):1451–1456

Schweikl H, Schmalz G, Federlin M (1998) Mutagenicity of the root canal sealer AHPlus in the Ames test. Clin Oral Investig 2(3):125–129

Schweikl H, Hiller KA, Bolay C, Kreissl M, Kreismann W, Nusser A, Steinhauser S, Wieczorek J, Vasold R, Schmalz G (2005) Cytotoxic and mutagenic effects of dental composite materials. Biomaterials 26(14):1713–1719

Schweikl H, Hartmann A, Hiller KA, Spagnuolo G, Bolay C, Brockhoff G, Schmalz G (2007) Inhibition of TEGDMA and HEMA-induced genotoxicity and cell cycle arrest by N-acetylcysteine. Dent Mater 23(6):688–695

Singh NP, McCoy MT, Tice RR, Schneider EL (1988) A simple technique for quantitation of low levels of DNA damage in individual cells. Exp Cell Res 175(1):184–191

Singh N, Manshian B, Jenkins GJ, Griffiths SM, Williams PM, Maffeis TG, Wright CJ, Doak SH (2009) NanoGenotoxicology: the DNA damaging potential of engineered nanomaterials. Biomaterials 30(23–24):3891–3914

Stamenković S, Mitrović TL, Cvetković V, Krstić N, Baošić RM, Marković MS, Nikolić N, Marković VL, Cvijan M (2013) Biological indication of heavy metal pollution in the areas of Donje Vlase and Cerje (Southeastern Serbia) using epiphytic lichens. Arch Biol Sci 65(1):151–159

Stamenković-Radak M, Andjelković M (2016) Studying genotoxic and antimutagenic effects of plant extracts in *Drosophila* test systems. Botanica Serbica 40(1):21–28

Stamenković-Radak MM, Savić T, Vićentić M, Anđelković M (2005) Antigenotoxic effects of royal jelly in the sex linked recessive lethal test with *Drosophila melanogaster*. Acta veterinaria 55(4):301–306

Stanić S, Matić S, Solujić S, Milošević T (2009) Genotoxicity testing of the methanol extract of the plant *Cotinus coggygria* and gallic acid on *Drosophila melanogaster*. Arch Biol Sci 61:261–266

Stanić S, Matić S, Đelić G, Mihailović M, Bogojević D, Solujić S (2011) Study of genotoxicity and antigenotoxicity of the Cotinus coggygria Scop. methanol extract by *Drosophila melanogaster* sex-linked recessive lethal test. Genetika 47(7):874–878

Stojanović I, Radulović N, Cvetković V, Mitrović T, Stamenković S (2013) Antimicrobial activity of methanol extracts of four Parmeliaceae lichen species. Facta universitatis-series: Phys Chem Technol 11(1):45–53

Stojanović S, Mitić Ž, Miljković M, Rajković J, Trajanović M, Najman S (2016) SEM-EDX analysis of Bio-oss® granules after incubation in cell culture medium. In: Lee WE et al (eds) Proceedings of the III advanced ceramics and applications conference, chapter 18. Atlantis Press and the author(s), pp 259–264

Szczepanska J, Poplawski T, Synowiec E, Pawlowska E, Chojnacki CJ, Chojnacki J, Blasiak J (2012) 2-hydroxylethyl methacrylate (HEMA), a tooth restoration component, exerts its genotoxic effects in human gingival fibroblasts trough methacrylic acid, an immediate product of its degradation. Mol Biol Rep 39(2):1561–1574

Takić Miladinov D, Tomić SLJ, Stojanović S, Najdanović J, Filipović J, Trajanović M, Najman S (2016) Synthesis, swelling properties and evaluation of genotoxicity of hydrogels based on (meth)acrylates and itaconic acid. Mater Res 19(5):1070–1079

Tavakoli M, Bateni E, Rismanchian M, Fathi M, Doostmohammadi A, Rabiei A, Sadeghi H, Etebari M, Mirian M (2012) Genotoxicity effects of nano bioactive glass and novabone bioglass on gingival fibroblasts using single cell gel electrophoresis (comet assay): an *in vitro* study. Dent Res J (Isfahan) 9(3):314–320

Thankam FG, Muthu J (2013) Reactive oxygen species-control and management using amphiphilic biosynthetic hydrogels for cardiac applications. Adv Biosci Biotechnol 4:1134–1146

Thankam FG, Muthu J (2014) Infiltration and sustenance of viability of cells by amphiphilic biosynthetic biodegradable hydrogels. J Mater Sci Mater Med 25(8):1953–1965

Thompson SL, Bakhoum SF, Compton DA (2010) Mechanisms of chromosomal instability. Curr Biol 20(6):R285–R295

Tice RR, Agurell E, Anderson D, Burlinson B, Hartmann A, Kobayashi H, Miyamae Y, Rojas E, Ryu JC, Sasaki YF (2000) Single cell gel/comet assay: guidelines for *in vitro* and *in vivo* genetic toxicology testing. Environ Mol Mutagen 35(3):206–221

Vales G, Demir E, Kaya B, Creus A, Marcos R (2013) Genotoxicity of cobalt nanoparticles and ions in *Drosophila*. Nanotoxicology 7(4):462–468

Vuković JS, Babić MM, Antić KM, Filipović JM, Stojanović ST, Najman SJ, Tomić SLJ (2016) *In vitro* cytotoxicity assessment of intelligent acrylate based hydrogels with incorporated copper in wound management. Mater Chem Phys 175:158–163

Westphalen GH, Menezes LM, Prá D, Garcia GG, Schmitt VM, Henriques JA, Medina-Silva R (2008) *In vivo* determination of genotoxicity induced by metals from orthodontic appliances using micronucleus and comet assays. Genet Mol Res 7(4):1259–1266

Wilson DM 3rd, Thompson LH (2007) Molecular mechanisms of sister-chromatid exchange. Mutat Res 616:11–23

Würgler FE (1980) Mutagenicity testing with *Drosophila*. Arch Toxicol 46(1–2):77–87

Yin L, Zhao X, Cui L, Ding J, He M, Tang C, Yin C (2009) Cytotoxicity and genotoxicity of superporous hydrogel containing interpenetrating polymer networks. Food Chem Toxicol 47 (6):1139–1145

Young CD, Wu JR, Tsou TL (1998) Fabrication and characteristics of polyHEMA artificial skin with improved tensile properties. J Membrane Sci 146(1):83–93

Žabar A, Cvetković V, Rajković J, Jović J, Vasiljević P, Mitrović T (2013) Larvicidal activity and *in vitro* effects of green tea (*Camellia sinensis* L.) water infusion. Biologica Nyssana 4(1–2):75–79

Živković JM, Najman S, Vukelić M, Stojanović S, Aleksić M, Stanisavljević M, Najdanović J (2015) Osteogenic effect of inflammatory macrophages loaded onto mineral bone substitute in subcutaneous implants. Arch Biol Sci 67(1):173–186

Histopathological Analysis of Bone Tissue Reaction on Implanted Biomaterials

Dragan Mihailović and Zorica Ajduković

Abstract In implantology, several techniques such as light and polarizing microscopy and histomorphometry are available for evaluation of the bone reactions. Descriptive histology and histomorphometry are the two main types of histological methods. At the microscopic level, bone consists of two forms: woven (an immature disorganized form of bone) and lamellar. During replacement of biomaterial, the remodeling of woven bone is first. Lamellar bone actively replaces woven bone over time and is found in a several structural and functional units with greater organization. Bone remodeling is characterized by the spatial and temporal coupling of bone formation by osteoblasts and bone resorption by osteoclasts. Histomorphometry can be very valuable in measuring the changes in the tissues that surround an implant. The parameters used in the evaluation procedure must be as simple as possible. However, analysis requires considerable expertise and remains time-consuming, despite the reduction in variables. To overcome the limitations presented by the 2D histological section reconstruction from serial sections is an option.

Keywords Bone · Biomaterials · Implant · Histomorphometry

1 Introduction to Bone Biology

Bone and cartilage are highly specialized connective tissues that are engineered by nature to perform a variety of specialized tasks. Bone is a porous viscoelastic anisotropic composite material with three types of constituents; water, a variety of organic constituents (protein and cellular), and an inorganic mineral phase. Cellular

D. Mihailović (✉)
Centre of Pathology, Medical Faculty,
Bulevar dr Zorana Djindjića 81, 18000 Niš, Serbia
e-mail: mihapat@junis.ni.ac.rs

Z. Ajduković
Medical Faculty, Bulevar dr Zorana Djindjića 81, 18000 Niš, Serbia

F. Zivic et al. (eds.), *Biomaterials in Clinical Practice*,
https://doi.org/10.1007/978-3-319-68025-5_19

constituents, matrix, and mineral phase are approximately 8, 25 and 67% of the bone mass, respectively. Bone is a complex calcified, living, biological composite with many different cell types—osteoblasts, osteocytes, quiescent bone lining cells, osteoclasts, and mononuclear resorptive cells (osteomacs or reversal cells) (Pettit et al. 2008; Rauner et al. 2012; Walsh et al. 2003). Osteoblasts are derived from local osteoprogenitor cells that are pluripotent. They are considered osteocytes as soon as they are surrounded by a mineralized matrix or lacunae. Osteocytes are regularly dispersed within the osteon with the long axes of the cells parallel to the lamellae. The osteocytes are located in lacunae that are interconnected by canaliculi (Steiniche and Hauge 2003) and act as mechanosensors in the bone tissue (Paic et al. 2009). Osteoblasts are fully differentiated cells that synthesize membrane-associated alkaline phosphatase and regulate the deposition of the bone matrix molecules, including type I collagen and a variety of non-collagenous proteins. Osteoblast-secreted products including monocyte chemoattractant protein-1 (MCP-1) and the osteoclast differentiating factor receptor activator of NF-kB ligand (RANKL) and its decoy receptor osteoprotegerin (OPG) are critically involved in regulating osteoclastogenesis. RANKL is essential for the formation and fusion of multinucleated cells. Osteoclasts are multinucleated giant cells responsible for resorbing the mineralized bone matrix (Rauner et al. 2012; Walsh et al. 2003).

The two major types of bone tissue are cortical (or compact) bone, which resides primarily in the diaphyses, and cancellous (spongy or trabecular) bone present at the metaphyses and epiphyses (Walsh et al. 2003; Steiniche and Hauge 2003). At the microscopic level, the bone consists of two forms: woven and lamellar. Woven bone, an immature disorganized form of bone, with collagen fibers arranged randomly in a meshwork pattern, is found during embryonic development, in metaphyseal regions during growth, in fracture repair, in tumors and some metabolic bone diseases. The woven bone is characterized by a non-uniform collagen distribution and a random distribution of cells, which imparts a more isotropic behavior. In the lamellar bone, the collagen fibers are arranged in parallel sheets and bundles, and the orientation of collagen fibers alternates between successive lamellae. The lamellar bone actively replaces the woven bone over time and is found in a several structural and functional units with greater organization. In contrast to the woven bone, lamellar bone shows the greatest resistance to load when the forces are directed in a parallel fashion to the longitudinal axis of the collagen fibers (Walsh et al. 2003; Steiniche and Hauge 2003). A lamellar unit is composed of five sublayers made up of mineralized collagen fibers oriented in complex rotated plywood-like structure (Weiner et al. 1999).

The secondary cancellous osteons have the same basic construction as the secondary cortical osteons, but with a different shape. The osteons resemble broad bands, which are made up of parallel lamellae, bounded on one side by the bone marrow and on the other side by an irregular cement line. As in the cortical bone, the interstitial bone is found between the secondary osteons, representing remnants of the previous generations of secondary cancellous osteons (Steiniche and Hauge 2003).

The cornerstone of cortical as well as cancellous bone is the osteon (Steiniche and Hauge 2003). The osteon (or Haversian system) is a characteristic feature of Haversian bone, with a central channel containing blood vessels, lining cells, and nerves. Haversian bone represents the most complex form of cortical bone, and is often referred to as the secondary bone (Walsh et al. 2003). The primary osteon is formed during the initial generation of the bone. Approximately two-thirds of cortical volume is formed by the secondary osteons. The remainder is made up of the interstitial bone, which represents the remnants of previous generations of secondary osteons, and a continuous layer of a few lamellae at the surfaces, termed the subperiosteal and subendosteal circumferential lamellae. The 3D architecture of a secondary cortical osteon is that of branching cylindrical columns. The Haversian canals are connected to one another, and communicate with the periosteum and with the marrow cavity via transverse and oblique channels known as the Volkmann's canals. The blood vessels of the Volkmann's canals are often larger than those of the Haversian canals. The secondary cortical osteons are usually oriented in the long axis of tubular bone. Cement lines, a region of reduced mineralization containing sulfated mucosubstances, are present at the boundaries of an osteon and represent the limit of a structural remodeling between the osteoblast and the osteoclast (Walsh et al. 2003).

The fundamental constituents of bone are the cells and the mineralized extracellular matrix (ECM). Only 10–20% of the bone matrix mass is water. Sixty-seven percent of the bone dry weight is made up of inorganic mineral salts (mainly hydroxyapatite), 30–40% is collagen, and the remainder (about 5%) is non-collagenous protein (NCP) and carbohydrates (Steiniche and Hauge 2003). Extracellular matrix (ECM) of the bone is the structural organic phase of the bone composed primarily of type I collagen (90%) with a variety of non-collagenous proteins (NCPs), glycoproteins, and proteoglycans in relatively small proportions (Walsh et al. 2003). Differences between type I collagen in cortical and cancellous bone were revealed. Cortical bone was found to contain a higher amount of hydroxylysine residues, and in trabecular bone glycosylation of hydroxylysine was found to be higher and pyridinium crosslink concentration to be lower (Suarez et al. 1996). The architecture of the bone collagen was disturbed in the estrogen-deficient state, and increasing dietary levels of calcium resulted in an improvement in the fibril packing as compared to controls (Tzaphlidou and Kafantari 2000). NCPs (osteocalcin, osteopontin and bone sialoprotein) represent a regulatory mechanism by which the extracellular matrix (ECM) influences cell dynamics and remodeling. Bone sialoprotein and osteopontin were found to co-distribute and accumulate in the cement lines and spaces among mineralized collagen fibers (Ingram et al. 1993; Rauner et al. 2012).

The mineral phase of bone is a calcium-deficient, carbonate-containing, poorly crystalline analog of the naturally occurring calcium phosphate mineral species known as hydroxyapatite ($[3Ca_3(PO_4)_2](OH)_2$) (Rauner et al. 2012). Bone mineral crystals were periodically (approximately 67 nm repeat distance) arranged along the fibrils and their location appeared to correspond to collagen hole and overlap zones (Landis et al. 1996).

Ossification occurs either intramembranously (flat bones, e.g. calvariae, and irregular bones) or endochondrally (long bones, vertebral column, and pelvis). Endochondral bone formation is initiated in the middle of the shaft at the primary ossification center (Rauner et al. 2012). The growth plates are characterized by the orderly proliferation and maturation of chondrocytes in longitudinal columns, forming stratified zones of reserve, proliferative, maturing, and hypertrophic cartilage (Poole et al. 1991). Hypertrophic chondrocytes secrete large amounts of a specialized extracellular matrix rich in collagen type X and alkaline phosphatase, which becomes calcified. After the calcification of the collagenous matrix, hypertrophic chondrocytes start producing matrix metalloproteinase 13, which is crucial for the subsequent degradation of the cartilage matrix, and undergo apoptosis (Stickens et al. 2004). After the osteoblast precursor cells have migrated to the surface of the remnant cartilage spicules, they differentiate into fully mature osteoblasts and deposit a predominantly type I collagen containing extracellular matrix (osteoid), which subsequently becomes mineralized into the mature bone matrix. The ossification continues towards the ends of the bones, where the further elongation of long bones occurs in the growth plates of the metaphysis. Finally, the trabecular bone in the diaphysis is broken down by osteoclasts to open up the medullary cavity (Rauner et al. 2012). The same process applies to the secondary ossification center, located in the epiphysis, except that the trabecular bone is retained (Alini et al. 1996).

1.1 Bone Growth, Modeling and Remodeling

Three basic mechanisms are involved in the development and turnover of the bone: longitudinal growth, modeling, and remodeling. Longitudinal growth ceases with closure of the growth plates at the end of the growing period (Steiniche and Hauge 2003). The purpose of remodeling is to adjust the skeleton to changes in mechanical demands, to prevent accumulation of fatigue damage, to repair micro fractures, to ensure the viability of the osteocytes, and to allow the skeleton to participate in the calcium homeostasis. Remodeling is the process by which the skeleton is continuously renewed. Bone remodeling is characterized by the spatial and temporal coupling of bone formation by osteoblasts and bone resorption by osteoclasts (Rodan and Martin 1981), while these processes are locally separated in modeling (Frost 1990). In the bone, four different surfaces or envelopes can be identified—the periosteal (periost), Haversian canal (intracortical), endocortical (endosteal), and the trabecular surface(s). Cancellous bone remodeling activity is 5–10 times greater than in the cortical bone. The remodeling process turns a bone over by localized osteoclastic resorption followed by osteoblastic formation, (i.e., the coupled process of bone remodeling) (Steiniche and Hauge 2003). Bone remodeling occurs as a sequence of events performed by a committed team of cells called the bone multicellular unit (BMU) (Hattner et al. 1965). After activation, osteoclasts start to erode and resorb bone. Osteoclasts create an isolated acidic microenvironment in

order to dissolve the inorganic matrix and degrade the organic matrix with specific enzymes (Teitelbaum 2000). As bone resorption subsides and a resorption pit with a demineralized collagen matrix remains, osteoclasts disappear and mononuclear cells of undetermined lineage remove the collagen remnants and prepare the surface for bone formation. This phase is called reversal. There is a debate about whether the reversal cell is of hematopoietic or mesenchymal origin. Recent evidence suggests that this cell type may be a resident macrophage of the bone termed osteomacs (Pettit et al. 2008). These cells are positive for the macrophage markers F4/80+ and CD68, but negative for the osteoclast marker tartrate-resistant acid phosphatase (TRAP), and are found throughout the periosteum and endosteum. When a certain resorption depth is reached, the osteoclasts are apparently replaced by mononuclear cells that complete the resorption. Following completion of resorption, preosteoblasts invade the area, differentiate into osteoblasts, and begin bone matrix formation (Steiniche and Hauge 2003). After the osteoid maturation time (Parfitt et al. 1987), the bone matrix is subsequently mineralized into a lamellar bone. In normal individuals, the remodeling space is 6–8% of the skeletal volume or 5–25% of the bone surface (Parfitt 1983, 1994). The frequency with which a given site on the bone surface undergoes remodeling is known as the activation frequency (Parfitt et al. 1987). In the cancellous bone of the iliac crest, the sequence of events is recapitulated every second year (an activation frequency of 0.50 per year) in normal young adults (Steiniche 1995). While the process of bone resorption is usually accomplished within 2–3 weeks, the new synthesis of bone requires around 2–3 months (Rauner et al. 2012).

Bone balance is the difference between the amount of bone resorbed and reformed during the remodeling cycle. The bone balance may differ between the different bone envelopes, and is influenced by many local and systemic factors. The bone balance must in general be positive at the periosteal surface (increased bone diameter with age), zero or slightly negative at the surface of the Haversian canals and negative at the endocortical surface (increased diameter of bone marrow cavity with age) and cancellous surface (decrease in the trabecular width with age) (Steiniche and Hauge 2003).

The remodeling process may cause bone to be lost irreversibly by two different mechanisms: (1) by perforations leading to disintegration of the trabecular network and (2) by a negative bone balance at the remodeling site, leading to a thinning of the trabeculae (Steiniche and Hauge 2003). In vivo evidence indicates that osteocyte apoptosis precedes osteoclast formation as osteocyte apoptosis occurs within three days of immobilization and is followed within two weeks by osteoclastogenesis (Aguirre et al. 2006).

1.2 Biomaterials

The biomaterials for hard-tissue implantation must possess certain specific properties. The required properties can be classified roughly under the headings of

biocompatibility, implant construction, and biomechanics (Jansen 2003; Ajduković et al. 2005; Ignjatović et al. 2013). Biocompatibility deals with the interfacial reactions between biomaterials and tissue. Implant construction deals with the engineering of the implant as well as its mechanical properties, such as hardness and strength. Biomechanics is concerned with the mechanical-dynamic properties of an implant and surrounding tissues. For the safe application of implants, they must be evaluated for all these properties (Jansen 2003).

At the end of the experimental period and after retrieval of the specimens, several techniques such as light and polarizing microscopy and histomorphometry are available to evaluate the bone reaction. During replacement of biomaterial, the remodeling woven bone is created first (Walsh et al. 2003).

At the interface between bone and implant the inflammatory cells, mainly lymphocytes, can be seen (Fig. 1) and their absence is the main indicator of biocompatibility (Fig. 2).

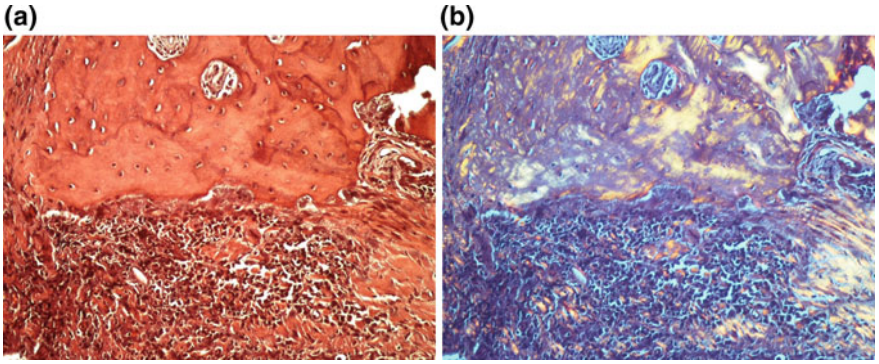

Fig. 1 Inflammatory reaction at the interface between biomaterial and bone. Hematoxylin and eosin (HE) (**a**) and polarized light (**b**), objective ×20

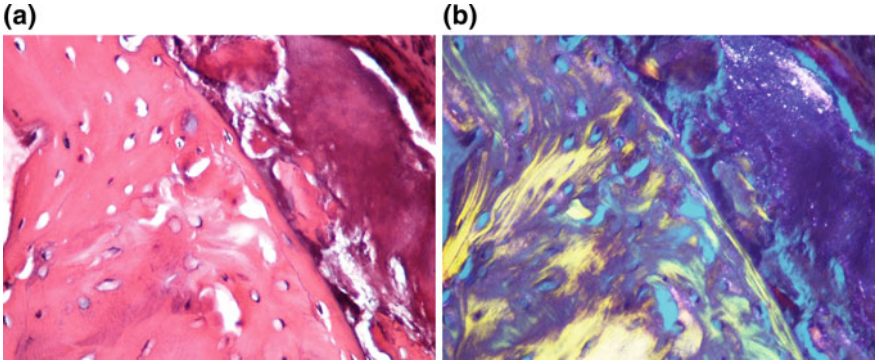

Fig. 2 Replacement of biomaterial without inflammation. HE (**a**) and polarized light (**b**), objective ×40

2 Histomorphometry

It is well known that histotechnology and morphometry are the major methodologies in bone and cartilage related research. Unlike routine histological or pathological laboratories, a laboratory for bone-tissue processing has unique characteristics, such as more demanding fixation, the challenging process of decalcification, media infiltration and embedding, and the need for heavy-duty microtomes. In decalcifying bone specimens, the goal is to achieve sufficient decalcification to allow the successful sectioning but to avoid over-decalcification so that cellular details remain intact. Hematoxylin and eosin (HE) staining remains the basic and most common procedure for most tissues. It can be used for both decalcified and undecalcified specimens. Both Goldner's Masson trichrome stain and the von Kossa stain allow differentiation of the osteoid from the mineralized bone matrix (An and Gruber 2003).

Descriptive histology is used to provide a general evaluation of the tissue of interest, including the morphology, structure, and arrangement of cells, matrix, implant, or tissue-implant interface. Histomorphometry is a methodology for quantitatively analyzing (i) length (perimeter or boundary) (Mijović et al. 1999), such as the surface perimeter of an implant, distance between points, such as the clearance at the implant-tissue interface or the distance between the central lines of two trabeculae, (ii) area (Obradović et al. 2012, 2013; Igić et al. 2012; Petrović et al. 2013), such as trabecular bone area or repair tissue area, (iii) volume (Mihailović et al. 1999a, b, 2003), (iv) optical density, and (v) the number of components of interest, such as trabecular number, vessel number, or cell number. These parameters can be estimated based on two-dimensional (2D) images. Despite its limitations, 2D histomorphometric analysis remains a common and useful method for analyzing the structural changes in the bone tissue.

In the histomorphometric analysis of the implant-bone interface, the useful parameters are: (i) bone apposition (or ongrowth), which is the fractional linear extent of the bone apposed to implant surface divided by the total surface perimeter of the implant (i.e., the surface potentially available for apposition) and (ii) bone ingrowth, which represents the amount of ingrown bone per unit of available surface area, porous space and ingrowth depth (An and Gruber 2003).

The following areas are of interest for the quantitative evaluation of hard-tissue implants: (1) The implant, the histological appearance of an implant can provide information about the stability or degradation behavior of a material, (2) The surrounding tissue, the zone of remodeled bone or soft-tissue capsule surrounding the implant is considered to be the inflammatory and healing reaction in response to the surgical trauma and the continued presence of the implant, (3) The interface, the nature of this tissue is determined by the chemical, physical, and biologic properties of the biomaterial, and (4) The interstitial tissue, this is the tissue that has grown into the pores of a porous implant (Jansen 2003). For bone implants, the optimal situation arises when there is direct bone-to-implant contact.

In general, the following parameters are of major interest in evaluating the bone response close to the implant surface: (1) Percentage of bone contact, i.e. the percentage of implant length at which there is direct bone-to-implant contact, without intervening tissue; these measurements are performed along the total length of the implant, (2) Bone density (areal density), the percentage of bone fill in predetermined areas around the implant (Jansen 2003), (3) Node: terminus ratio, a measure of trabecular interconnection, despite the fact that the majority of so-called termini are artifacts of the plane of sectioning and the mathematical basis is viewed by stereologists as insubstantial, (4) Trabecular pattern factor, where a highly connected structure presents mainly concave surfaces in a section, and a poorly connected structure presents convex surfaces, (5) Marrow space star volume, indicates the mean volume of marrow space that can be seen unobstructed in all directions from a random point within it, and is derived from the distance cubed between the point and its intercepting radius with the bone surface, and (6) Fractal analysis, an index of the complexity of a structure (Aaron and Shore 2003).

To overcome the limitations presented by the 2D histological section 3D reconstruction from serial sections by appropriate software is an option. This is time-consuming, since the spacing between consecutive sections should be between one-third and one-tenth of the length of the feature of interest, i.e. 15–50 μm distant in the case of trabeculae 150 μm long. The main difficulty is image alignment (Yanuka et al. 1984).

3 Conclusions

Bone substitute biomaterials acceptance begins with the formation and remodeling of the woven bone tissue. Lamellar bone actively replaces woven bone over time. Simple method for evaluating woven and lamellar bone on hematoxylin and eosin stained sections is polarizing microscopy. Histomorphometry and 3D modeling after serial sections reconstruction can be very valuable in measuring the changes in the tissues that surround an implant.

Acknowledgements Part of the scientific works are supported by Ministry of Education, Science and Technological Development, Serbia, project No. III41017.

References

Aaron JA, Shore PA (2003) Bone histomorphometry: concepts and common techniques. In: An YH, Martin KL (eds) Handbook of histology methods for bone and cartilage. Humana Press, Totowa, pp 331–352

Aguirre JI, Plotkin LI, Stewart SA et al (2006) Osteocyte apoptosis is induced by weightlessness in mice and precedes osteoclast recruitment and bone loss. J Bone Miner Res 21:605–615

Ajduković Z, Najman S, Dordević LJ et al (2005) Repair of bone tissue affected by osteoporosis with hydroxyapatite-poly-L-lactide (HAp-PLLA) with and without blood plasma. J Biomater Appl 20(2):179–190

Alini M, Marriott A, Chen T et al (1996) A novel angiogenic molecule produced at the time of chondrocyte hypertrophy during endochondral bone formation. Dev Biol 176:124–132

An YH, Gruber HE (2003) Introduction to experimental bone and cartilage histology. In: An YH, Martin KL (eds) Handbook of histology methods for bone and cartilage. Humana Press, Totowa, pp 3–31

Frost HM (1990) Skeletal structural adaptations to mechanical usage (SATMU): 2. Redefining Wolff's law: the remodeling problem. Anat Rec 226:414–422

Hattner R, Epker BN, Frost HM (1965) Suggested sequential mode of control of changes in cell behaviour in adult bone remodelling. Nature 206:489–490

Igic M, Mihailovic D, Kesic L et al (2012) Cytomorphometric and clinical investigation of the gingiva before and after low-level laser therapy of gingivitis in children. Lasers Med Sci 27 (4):843–848. doi:10.1007/s10103-011-0993-z

Ignjatović N, Ajduković Z, Savić V et al (2013) Nanoparticles of cobalt-substituted hydroxyapatite in regeneration of mandibular osteoporotic bones. J Mater Sci Mater Med 24(2):343–354. doi:10.1007/s10856-012-4793-1

Ingram RT, Clarke BL, Fisher LW et al (1993) Distribution of noncollagenous proteins in the matrix of adult human bone: evidence of anatomic and functional heterogeneity. J Bone Miner Res 8:1019–1029

Jansen JA (2003) Histological analysis of bone-implant interface. In: An YH, Martin KL (eds) Handbook of histology methods for bone and cartilage. Humana Press, Totowa, pp 353–360

Landis WJ, Hodgens KJ, Arena J et al (1996) Structural relations between collagen and mineral in bone as determined by high voltage electron microscopic tomography. Microsc Res Tech 33:192–202

Mihailović D, Dordević B, Mihailović V (1999a) Nuclear volume in type I gastric intestinal metaplasia. Anal Quant Cytol Histol 21(2):143–144

Mihailović D, Nikolić J, Bjelaković BB, Stanković BN, Bjelaković G (1999b) Morphometric and biochemical characteristics of short-term effects of ethanol on rat cardiac muscle. Exp Toxicol Pathol 51(6):545–547

Mihailovic D, Tasic-Dimov D, Mijovic Z et al (2003) Nuclear volume and total optical density in Down syndrome. Anal Quant Cytol Histol 2003 25(5):293–296

Mijović Z, Kutlesić C, Mihailović D et al (1999) Roundness of epithelial nuclei in bronchial mucosa. Anal Quant Cytol Histol 21(5):458–460

Obradović R, Kesić L, Mihailović D et al (2013) Low-level lasers as an adjunct in periodontal therapy in patients with diabetes mellitus. Lasers Med Sci 28(1):19–24. doi:10.1007/s10103-012-1058-7

Obradović R, Kesić L, Mihailović D et al (2012) Low-level lasers as an adjunct in periodontal therapy in patients with diabetes mellitus. Diabetes Technol Ther 14(9):799–803. doi:10.1089/dia.2012.0027

Paic F, Igwe JC, Nori R et al (2009) Identification of differentially expressed genes between osteoblasts and osteocytes. Bone 45:682–692

Parfitt AM (1983) Bone histomorphometry: techniques and interpretation. In: Recker RR (ed) The physiologic and clinical significance of bone histomorphometric data. CRC Press Inc, Boca Raton, pp 143–224

Parfitt AM, Drezner MK, Glorieux FH et al (1987) Bone histomorphometry: standardization of nomenclature, symbols, and units. Reports of the ASBMR histomorphometry nomenclature committee. J Bone Miner Res 2:595–610

Parfitt AM (1994) Osteonal and hemi-osteonal remodeling: the spatial and temporal framework for signal traffic in adult human bone. J Cell Biochem 55:273–286

Petrovic M, Kesic L, Obradovic R et al (2013) Comparative analysis of smoking influence on periodontal tissue in subjects with periodontal disease. Mater Sociomed 25(3):196–198. doi:10.5455/msm.2013.25.196-198

Pettit AR, Chang MK, Hume DA et al (2008) Osteal macrophages: a new twist on coupling during bone dynamics. Bone 43:976–982

Poole CA, Glant TT, Schofield TR (1991) Chondrons from articular cartilage. (IV). Immunolocalization of proteoglycan epitopes in isolated canine tibial chondrons. J Histochem Cytochem 39:1175–1187

Rauner M, Stein N, Hofbauer LC (2012) Basics of Bone Biology. In: Pietschmann P (ed) Principles of Osteoimmunology. Springer, Wien-New York, pp 1–26

Rodan GA, Martin TJ (1981) Role of osteoblasts in hormonal control of bone resorption—a hypothesis. Calcif Tissue Int 33:349–351

Steiniche T (1995) Bone histomorphometry in the pathophysiological evaluation of primary and secondary osteoporosis and various treatment modalities. APMIS 51:1–44

Steiniche T, Hauge EM (2003) Normal structure and function of bone. In: An YH, Martin KL (eds) Handbook of histology methods for bone and cartilage. Humana Pres, Totowa, pp 59–72

Stickens D, Behonick DJ, Ortega N et al (2004) Altered endochondral bone development in matrix metalloproteinase 13-deficient mice. Development 131:5883–5895

Suarez KN, Romanello M, Bettica P et al (1996) Collagen type I of rat cortical and trabecular bone differs in the extent of posttranslational modifications. Calcif Tissue Int 58:65–69

Teitelbaum SL (2000) Bone resorption by osteoclasts. Science 289:1504–1508

Tzaphlidou M, Kafantari H (2000) Influence of nutritional factors on bone collagen fibrils in ovariectomized rats. Bone 27:635–638

Walsh WR, Walton M, Bruce W et al (2003) Cell structure and biology of bone and cartilage. In: An YH, Martin KL (eds) Handbook of histology methods for bone and cartilage. Humana Press, Totowa, pp 35–58

Weiner S, Traub W, Wagner HD (1999) Lamellar bone: structure-function relations. J Struct Biol 126:241–255

Yanuka M, Dullien FAL, Elrick DE (1984) Serial sectioning and digitization of porous media for two and three dimensional analysis and reconstruction. J Microsc 135:159–168

Imaging in Clinical and Preclinical Practice

Sladjana Petrović and Nikola Korunović

Abstract Over the years, medical imaging has become an inherent part of modern medicine and biomedical engineering. Various imaging methods, which provide the detailed insight into human body interior, are widely used in clinical and preclinical practice. They enable the accurate diagnosis of complex pathological states, planning and performing of challenging surgical operations, tissue engineering, design of medical devices and much more. The area of medical imaging is very complex, as it is comprised of different imaging modalities and it keeps expanding due to rapid development of modern technologies. An overview of most important imaging techniques, containing references that describe various applications of each of the methods, is given first. More detail is given on the following methods: radiography, computed tomography (CT), ultrasound imaging, magnetic resonance imaging (MRI), mammography and positron emission tomography (PET). Two detailed examples accompany the overview, which are related to monitoring of osteogenesis in large animals using CT and application of imaging techniques in diagnosis and management of osteoporosis.

Keywords Medical imaging · Radiography · Computed tomography (CT) · Magnetic resonance imaging (MRI) · Ultrasound imaging

1 Introduction

Medical imaging involves the use of various methods in order to assess the anatomy or to diagnose and monitor various pathological conditions. Those technologies are able to produce the images of normal and pathological structures in the

S. Petrović (✉)
Faculty of Medicine, University of Niš, Blvd. dr Zoran Djindjić 81, 18000 Niš, Serbia
e-mail: sladjana-petrovic@hotmail.com

N. Korunović
Faculty of Mechanical Engineering,
University of Niš, A. Medvedeva 14, 18000 Niš, Serbia

F. Zivic et al. (eds.), *Biomaterials in Clinical Practice*,
https://doi.org/10.1007/978-3-319-68025-5_20

human body. Medical imaging using different technologies makes possible the exploration of the human body. Each of the imaging methods generates different information related to the pathological condition in question, such as traumas, congenital anomalies, neoplasms, or about the response to treatment in the studied or treated area of the body. The development of relevant technologies has enabled rapid development of medical imaging. In the diagnosis of pathological conditions with different imaging modalities, accuracy and reliability of imaging depends on the use of appropriate radiological diagnostic criteria as well (Petrovic et al. 2013).

In bioengineering and use of biomaterials, imaging has also got an important place. There too, imaging methods have gone through rapid development, again mainly due to technological advancements. Tissue engineering is also an area of possible use in the reconstruction of damaged tissues and organs. Autologous tissue reconstructions are also possible for some defects. Tissue engineering enables various tissue and organ replacement procedures, since autologous transplantation is not always possible.

Damaged skin and perimandibular soft tissue could be the result of radionecrosis and can be reconstructed using supraclavicular islet fasciocutaneous flap (Petrovic et al. 2011b). Breast reconstruction after mastectomy is possible using the extended latissimus dorsi flap and silicone implants (Visnjic et al. 2011). Large burn defects are also a serious medical problem that can be solved using the banana peel pericranial flap (Velickov et al. 2014). Autologous tissue cannot be always used to repair or replace individual organs; that is why bioengineering represents a promising approach, since it enables cultivation of new cells and tissues required for in vivo implantation to replace the cartilage, muscle, bone, and cardiac tissue and blood vessels. Bioengineering, using natural or synthetic scaffolds together with cells in appropriate conditions provides new tissue growth necessary to replace individual organs or organ parts (Langer and Vacanti 1993; Atala 2004; Lee et al. 2008). Restoration of alveolar bone defects has been made possible using the biphasic calcium phosphate/poly-DL-lactide-co glycolide composite (Petrovic et al. 2011a).

Imaging methods are also necessary in establishing the properties and function of biomaterials, especially in the assessment of reaction of adjacent normal tissue to the applied biomaterial at the implant site. In this assessment, advanced 2D imaging methods have a prominent role, almost identical to histological evaluation (Boskey and Pleshko Camacho 2007; Campbell and Kim 2007; Huebsch and Mooney 2007).

Various imaging methods have been employed in the evaluation of biomaterials in clinical and preclinical practice, but three-dimensional (3D) techniques are considered a gold standard in the fields of tissue engineering and regenerative medicine. Different imaging methods have been used in bioengineering: magnetic resonance imaging (MRI), ultrasound (US), radiography, computed tomography (CT), mammography, and positron emission tomography (PET). Each one of them has its own unique properties and functions by different physical principles.

2 Medical Imaging Techniques

2.1 Radiography

Radiography is the method of medical imaging that uses X-rays, i.e. electromagnetic radiation, to visualize internal structures of the human body. A portion of X-rays are absorbed in their passage through the examined part of the body, and the unabsorbed portion of X-rays reach the registering detectors and create a radiological image to be subsequently analyzed. The recording may occur on film or via electronic means. The detector can then provide a superimposed 2D representation of all the object's internal structures.

Radiography does not play any major role in the preclinical use of biomaterials. However, it is very important in clinical practice in the evaluation of biomaterials.

Radiography is an irreplaceable tool in the visualization of skeletal structures, both hips and knees (Fig. 1), especially in arthroplasty and osteosynthetic material implantation (Fig. 2).

Radiography is the most valuable method in the detection of complications, such as pseudoarthrosis, dislocation, periprosthetic fractures (Golubovic et al. 2014), cement extrusion or osteomyelitis. In traumatology, one of the most serious injuries is crush injury of the leg as the consequence of mechanical pressure. External bone fixation is successfully used in such cases to prevent joint movements. In the control and follow-up after repositioning radiography is required, as well as for the assessment of osteoreparation (Golubovic et al. 2014). Missile injuries of the knee joint are among the most complicated injuries of the bone-joint system. These induce large-scale destruction of the bone and other tissues of the knee joint (Golubovic et al. 2013). Evaluation of bone destruction of the knee joint caused by a shrapnel bomb and by a bullet from the gun is possible with X-ray examination (Golubovic et al. 2013).

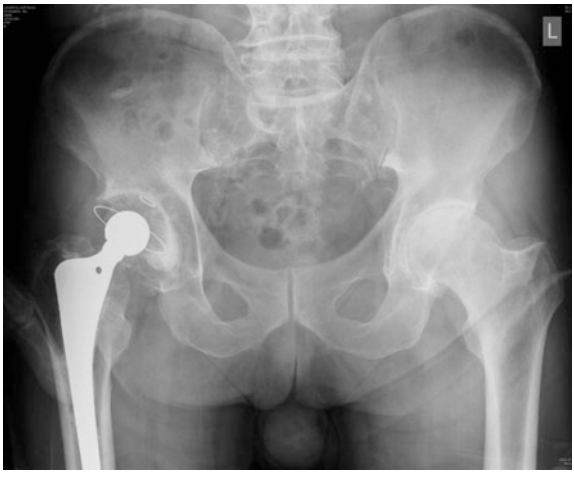

Fig. 1 Anteroposterior radiography of right hip arthroplasty

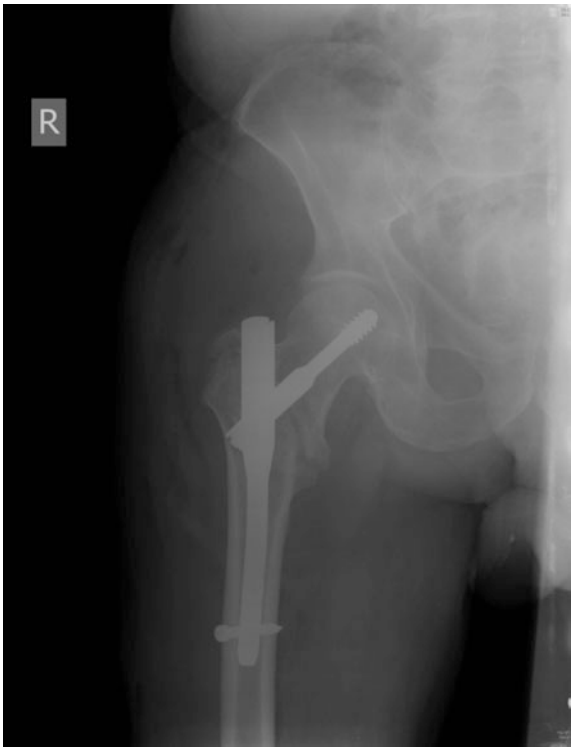

Fig. 2 Anteroposterior radiography of the right hip joint after transtrochanteric fracture osteosintesis

For different kinds of biomaterials used in various pathological conditions and traumas of the head, neck and spine, radiography is the first exploration method. These biomaterials involve various medical tools and implants, such as: cochlear implants, brain stem implants, cerebellar electrodes, aneurysm clips, coils, ear prostheses, ocular prostheses, dental implants, cervical spine plates, thoracic and lumbar spine fixation devices, vertebroplasty, artificial intervertebral disks, skeletal stimulators, nasogastric tubes, central venous catheter (Hunter et al. 2004b). The most important role of radiography in this setting is to demonstrate the presence, localization, and validity of these implants and devices and to identify possible complications.

The method of choice in the evaluation of cardiac implants and medical devices is chest radiography. These implants include pacemakers (Fig. 3), stents, artificial prosthetic valves, and artificial hearts. Chest radiography is necessary in cardiac patients with implants in the follow-up and evaluation of the position, integrity and possible implant-related complications (Hunter et al. 2004a).

Abdominal and pelvic radiography are used in bioengineering for the demonstration of abdominal and pelvic implants and medical devices. These implants include genitourinary and intestinal devices, postoperative implants and various other devices (Hunter and Taljanovic 2005). Genitourinary devices, such as ureteral

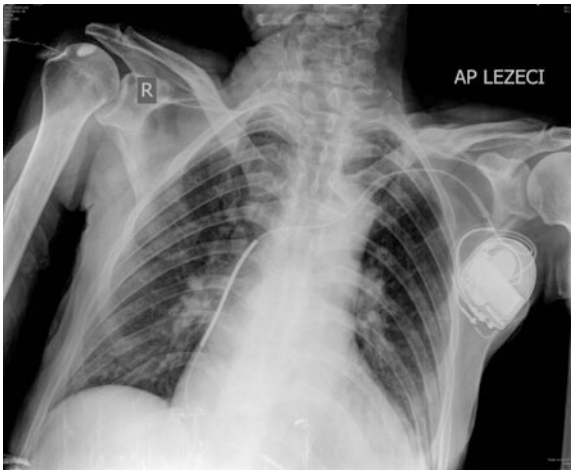

Fig. 3 Anteroposterior chest radiography in a patient with pace-maker

stent in the double pigtail configuration, urethral and bladder neck stents and artificial urinary sphincters, bladder and nephrostomy catheters, clips, intrauterine spirals and pessaries can be demonstrated on abdominal and pelvic radiography. Moreover, biliary catheters and stents, vascular stents and grafts (Fig. 4), inferior vena cava filters can be recognized too. Intestinal devices are Miller-Abbott and nasogastric tubes and gastrostomy and gastrojejunostomy tubes as well. Geniturinary devices are double pigtail ureteral stents, urethral and bladder neck stents, artificial urinary sphincters and bladder catheters.

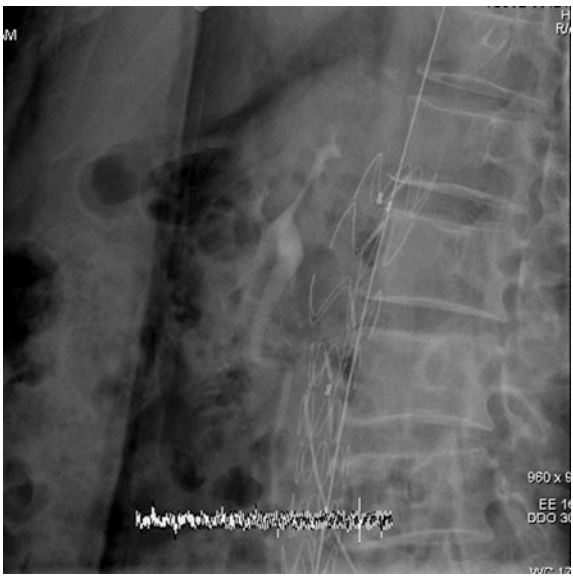

Fig. 4 Latero-lateral abdominal radiography of a patient with expandable stent graft for endovascular aneurysm repair (*EVAR*)

Abdominal and pelvic radiography is able to demonstrate all metal and plastic implants and devices, and can also demonstrate their abnormal position, missing device part(s), as well as the complications that deserve treatment.

2.2 Mammography

Mammography is an X-ray imaging method for breast exploration. It is used for the exploration of both benign and malignant pathological conditions, above all in the detection of breast cancer. It is a ionizing radiation-based method. Biomaterials used in primary breast reconstruction and esthetic interventions are breast implants. Diagnostic imaging methods involve mammography, echosonography and MRI, and are used to detect complications after breast implant surgery, such as implant rupture (Everson et al. 1994), as well as other complications. Mammography is also a useful method in the detection of breast cancer in patients with breast implants (Brinton and Brown 1997).

2.3 Computed Tomography (CT)

Computed tomography (CT) is one of the methods of medical imaging with a broad range of applications in the diagnosis of many pathological conditions (Pan et al. 2008). It is based on ionizing radiation and tomographic image reconstruction. It is a technology that makes use of ionizing radiation to create virtual tomographic images, i.e. virtual slices of the examined anatomical region, and make possible exploration of the interior of the human body. By way of digital geometry, after the creation of a large number of two-dimensional images around a single axis of rotation (Herman 2009), three-dimensional images are generated.

The development of multislice/multidetector CT scanning (MSCT/MDCT) has contributed to an improved spatial and temporal resolution and the technique has enabled quick scanning of a large body volume in a short period of halted breathing. Multiplanar and three-dimensional reconstruction enable better diagnosis, better spatial orientation, better tumor delineation in all three planes, and improved accuracy in the detection of malignant lymph nodes (Petrovic et al. 2013).

MDCT and MRI are the most common methods used for simultaneous diagnosis of primary tumors and metastatic lymph nodes (Petrovic et al. 2011d, 2013). Collet-Sicard syndrome involves some clinical symptoms and can be an atypical presentation of neck fibrosarcoma, where MDCT examination has a crucial role (Petrovic et al. 2011c). MDCT is the method of choice in the diagnosis and staging of laryngeal squamous cell carcinoma, since it allows better assessment of the spread of the primary tumor at the level of larynx and detection of malignant lymph nodes in the neck (Stankovic et al. 2012). MDCT has also an important role in some emergency conditions, such as massive retroperitoneal hemorrhage in case of

bilateral giant angiomyolipomas (Petrovic et al. 2014b). MDCT scanning with thin sections is superior in demonstrating the extent of bone destruction, such as scull base destruction in case of giant glomus jugulare paraganglioma (Petrovic et al. 2010).

Bone erosion can also be detected with MDCT in case of alternaria-associated fungus ball of the orbit, nose and paranasal sinuses (Pesic et al. 2015).

MDCT is a useful technique in the diagnosis of some hereditary diseases, such as CADASIL, visualized in the form of bilateral, supratentorial confluent zones of low attenuation affecting the white matter around the ventricles and present subcortically as well. These changes can be seen in the temporal lobe parenchyma too, in the external capsulas, and the basal ganglia and pons (Stojanov et al. 2014).

CT is a useful tool in preclinical and clinical examination of biomaterials. Moreover, CT is excellent for bone imaging. CT is a 3D visualization method, which can provide a detailed insight into the bone structure or microstructure if high resolution devices are used (Korunovic et al. 2014). Examination of biomaterials in preclinical practice can be performed in vitro and in vivo. Preclinical in vivo imaging is the visualization of living animals for research purposes (Anzivino and Mansi 2012). There are two animal models for in vivo evaluation. Small-animal models involve experimental animals such as mice and rats. In basic research mice and rats are the animals most commonly used. These small animals are easy and relatively cheap to breed. In these studies larger animals are used as well, such as rabbits, dogs, sheep, monkeys, and guinea pigs, but these are generally more demanding and more expensive to breed (Szpalski et al. 2010).

Micro computed tomography (micro-CT) plays an important role in preclinical examination of small animals. The development of this imaging method has improved the quality of exploration of small animals in experimental studies, with higher resolution tomograms that can be obtained. Before the development of micro-CT, experimental studies on small animals were done using clinical CT, that could not produce image resolutions appropriate for small animal exploration (Kerr and Byzova 2012). The most important area of use of micro-CT is the examination of the skeletal system, especially of the newly formed bone during experimental studies (Appel et al. 2013).

The possibility of generation of three-dimensional images of bone and other tissue types is important for qualitative and quantitative analysis in experimental studies. Micro-CT enables visualization of internal structure of various scaffold types, measurement of their porosity, pore size, interactions with the adjacent tissues and other properties (Alberich-Bayarri et al. 2009; Ho and Hutmacher 2006). Follow-up in different time intervals allows the establishment of the degree and distribution of mineralization of newly formed bone tissue (Cartmell et al. 2004).

CT imaging with 3D reconstruction is the most useful tool for the creation of virtual geometrical bone models. These models are used for various purposes, such as preoperative planning, implant design, or bone strength predictions (Vitkovic et al. 2012, 2013; Korunovic et al. 2014). Stress–strain status of bones and implants, and thus their strength and durability, may be predicted using the finite element method—FEM (Trajanovic et al. 2010; Stojkovic et al. 2013; Korunovic

et al. 2010; Vulovic et al. 2011), which relies on the accurate modeling of bone geometry and material properties. CT is the method which can be useful in bone material elasticity measurements, correlating CT bone density with material elasticity settings, such as the Young's modulus (Korunovic et al. 2013).

2.4 Magnetic Resonance Imaging (MRI)

Magnetic resonance imaging (MRI) is a method widely used in medical imaging for the exploration of normal morphology of the human body, as well as in different pathological conditions. This method is an important diagnostic tool used for diagnostic purposes to evaluate the disease spread, presence of metastatic deposits, and for post therapeutic disease control.

MRI uses a strong magnetic field (several times stronger than the Earth's magnetic field) as well as radiofrequency waves for the creation of tomograms. Strong magnets in MRI scanners induce polarization of the hydrogen proton in a molecule of water in human tissues. For the creation of high resolution MRI tomograms, gradient magnetic fields pulse sequences of radio frequency waves are used to enable spatial distribution of proton-emitted signals (Naumova et al. 2014). MR is used for morphological, molecular, and functional imaging. MRI is a radiological method with excellent resolution in the differentiation of soft tissues and its advantage lies in the absence of ionizing radiation (Petrovic et al. 2013). MRI also plays an important role in the evaluation of head and neck tumors, such as head and neck paragangliomas (Petrovic et al. 2011e).

There are certain contraindications for MRI scanning, such as the presence of ferromagnetic implants (pacemakers, cochlear implants, ferromagnetic foreign bodies, as well as other biomedical implants made of ferromagnetic materials—hip and knee prostheses, etc.). If present within strong magnetic fields, these materials can induce injuries and such objects can be displaced as well (Shellock 1987).

The application of new contrast agents in MRI diagnosis, such as supramagnetic contrast agents, as well as advanced MRI techniques, can increase the sensitivity of MRI (Jocic et al. 2013). Advanced MRI techniques, **diffusion weighted imaging (DWI)** and apparent diffusion coefficient (ADC) have an important place in the diagnosis of brain tumors, but ADC is not reliable in the differentiation of meningioma subtypes (Ignjatovic et al. 2014).

Several experiments on animal models have demonstrated the safety and efficacy of porous bioactive titanium metal as a synthetic bone under load-bearing conditions (Fujibayashi et al. 2011). An experimental study of a canine model has demonstrated a good connectivity potential of the porous titanium implants. It has been shown that bioactive titanium implants possess both osteoconductive and osteoinductive qualities, and therefore there is no need to add any osteogenic materials (Fujibayashi et al. 2004; Takemoto et al. 2006) (Fig. 5).

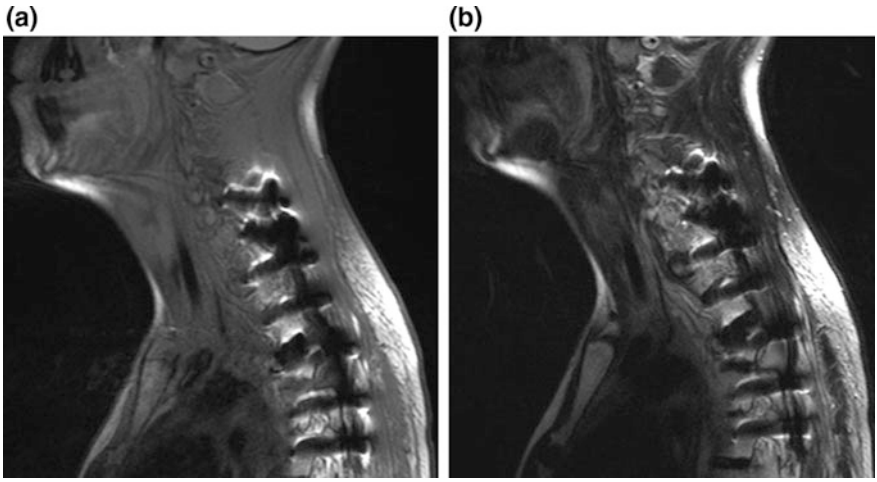

Fig. 5 T1w (**a**) and T2w (**b**) TSE sagittal MR tomograms of the cervical and thoracic spine in a patient with titanium metal fixation devices

MRI has an excellent contrast resolution to distinguish between normal and pathological tissues (Mayer-Kuckuk and Boskey 2006). Due to its exceptional ability to differentiate between soft tissue structures, MRI is a very useful tool for volumetry, i.e. quantification of certain tissues, which is often required in tissue engineering and regenerative medicine (Appel et al. 2013). Thanks to its excellent contrast resolution, MRI is also useful in the differentiation of newly created bone and fatty tissue, as well as residual scaffolds used in regenerative medicine (Potter et al. 2006).

MRI is an excellent method for soft tissue exploration, but with a limited role in bone tissue examinations, regardless of the fact that it can detect some bone tissue changes. MRI is not an appropriate tool for bone tissue analyses (Jiang et al. 2000).

Radiography and micro-CT are the imaging methods with possible use in bone tissue exploration, but these are not the methods of choice to evaluate early bone tissue development, when conventional MRI and new ultra short TE methods (under development) should be used (Tyler et al. 2007).

Micro-MRI, similar to micro-CT machines, have got micrometer spatial resolution. With these machines, excellent spatial resolution and strong magnetic field are the principal advantage. With MRI, numerous phenomena occurring in the developing tissues can be quantitatively assessed. Tissue development can be monitored with MRI from both the initial growth of cell cultures or scaffolds in vitro, and later during implantation in vivo. Implant acceptance by the surrounding tissues can be monitored with MRI in vivo, as well as tissue interactions and structural functional changes (Xu et al. 2008).

2.5 Ultrasound Imaging (Sonography)

Ultrasound imaging (sonography) is a non-invasive exploration method that does not use X-rays and is able to generate real-time images. In an ultrasound transducer, high frequency acoustic waves are created by way of the piezoelectric effect and are directed to reach a specific focusing depth (Appel et al. 2013). The transducer serves as both an emitter and receiver of acoustic waves, and an ultrasound image is produced as the result of wave reflection at the interface of tissues with different acoustic impedances (properties). The ultrasound contrast is the result of differences in acoustic reflectivity, and image generation depends on the time required for an acoustic wave to echo back, and on the strength of the received signal. Ultrasound is widely used in clinical practice to diagnose the diseases affecting parenchymatous organs and blood vessels. It is also used to diagnose the diseases of the neck and parotid glands, such as Rosai-Dorfman disease. This benign condition has been originally described as a bilateral cervical lymphadenopathy and should not be misdiagnosed as neoplastic disease (Petrovic et al. 2014a).

Ultrasound is not widely used to track transplanted cells since high resolution imaging requires the use of high frequencies with shallow penetration (Naumova et al. 2014). A potential area of use of ultrasonography in the field of biomaterials and bioengineering lies in the exploration of newly created cartilage in vitro (Fite et al. 2011; Kreitz et al. 2011; Rice et al. 2009; Sun et al. 2011), fatty tissue (Tsuji et al. 2013), and in damaged cardiac muscle regeneration (Kawamura et al. 2012). Ultrasound elastography is used in in vitro follow-up of polymer scaffolds and their degradation in vivo (Kim et al. 2008; Yu et al. 2013). Color and power Doppler and use of ultrasound contrast media have a role in the exploration of vascular grafts in vitro and in vivo (Hibino et al. 2012; Matsumura et al. 2013; Quint et al. 2012), and contrast media have a role in the evaluation of small vessels in engineered tissues (Dayton and Rychak 2007).

2.6 Multimodality Imaging

Multimodality imaging is a combination of F18-fluorodeoxyglucose positron emission tomography—PET with CT or MRI, i.e. it combines a functional method such as PET with morphological methods such as CT or MRI. This type of imaging, also known as hybrid imaging PET/CT and PET/MRI, has got a wide range of possible applications, but it is used most in oncology. PET alone could not offer satisfactory information about morphology, and hybrid imaging was thus expected to generate both metabolism-related and morphology-related data (Jocic et al. 2013).

In a single examination session, both functional and morphological information can be obtained (Beyer et al. 2002). This multimodality imaging approach has

found its place in clinical radiology for early detection of malignant diseases (Osman et al. 2003), coronary blood vessel diseases (Elhendy et al. 2002) and other pathologies.

The methods of nuclear imaging are widely used in bioengineering in a range of settings (Hendee et al. 2008). Special hybrid MR–PET scanners have been devised for the examination of small animals in tissue engineering (Pancrazio et al. 2007). The principal drawbacks of these hybrid scanners are their lesser availability and high examination costs (Jocic et al. 2013).

3 Sample Applications of Imaging Techniques

3.1 Monitoring of Osteogenesis in Large Animals Using CT

As explained in Sect. 2.3, one of the two animal models for in vivo evaluation of biomaterials based on CT is the large animal model. Larger animals can be examined using multidetector CT (MDCT) (Fig. 6).

The dynamics of osteogenesis inside a defect can be monitored in living animals by MSCT scanners, which represents an advantage over other micro-CT techniques that require sacrificing of animals. On the other hand, the advantage of using MDCT includes multiple scanning of animals and monitoring of the same graft during the experiment (Vuckovic 2013). This technique offers the benefits similar to those described for MCTA techniques (microfocus computerized tomography analysis) (Min et al. 2008). In immunodeficient animals such as athymic mice, the method has produced adequate filling-up of bone defects (Muraglia et al. 1998; Bruder et al. 1998), and the same has been reported for immunocompetent animals such as dogs and sheep (Kon et al. 2000; Arinzeh et al. 2003).

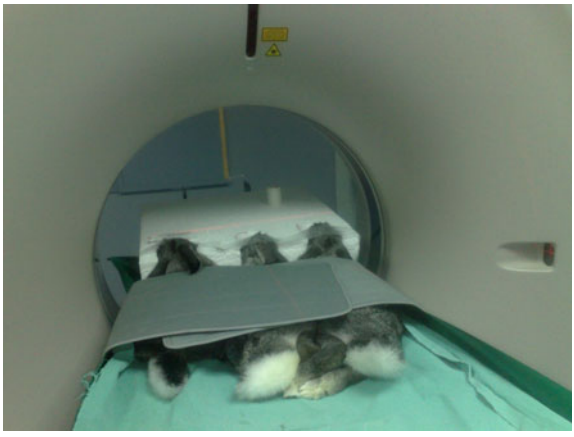

Fig. 6 MDCT examination of experimental animals—rabbits

In order to examine osteogenesis by means of various biomaterials and mesenchymal stem cells in the rabbit calvary, five bone defects were made (labeled as D1–D5 and arranged according to the scheme presented Fig. 7). Two of the defects were located in the parietal bone on both sides of the midline, and the fifth was located in the frontal bone at the level of the median line. The defects were made with a 4 mm diameter steel burr with the reverse-conical profile, using a physiodispenser at the speed of 800 revs/min. All the bone defects were round, 8 mm in diameter, and 2 mm deep. Prior to their filling, the defects were rinsed with sterile saline. After the defect filling, a periosteum reposition was performed, with the flap returned into its place and sutured using individual stitches (Vuckovic 2013).

The scanning of rabbits was performed on a MDCT machine with 64 rows of detectors after 1, 3, and 6 weeks. In the analysis of generated tomograms, 3D VR (Volume Rendering 3 Dimension) and multiplanar reconstruction MPR of the bone structures of rabbit head were used. On VR 3D reconstruction of the bone structure of rabbit head a week after defect filling-up, five artificially made defects filled with various biomaterials were observed (Fig. 8). The defect analysis involved exploration of their appearance, depth and density measurements. On MPR reconstruction, it was necessary to analyze each defect, to determine the presence of newly formed bone and measure its density.

The defect marked with a green arrow indicates the presence of newly formed bone structure, the ventral contour of which is partly in the tabullae externae plane and partly protrudes, and the greatest thickness of newly formed bone is in the center of the defect. A yellow arrow marks the defect with new bone structure of a lower density compared to the defect previously described, the ventral contour of

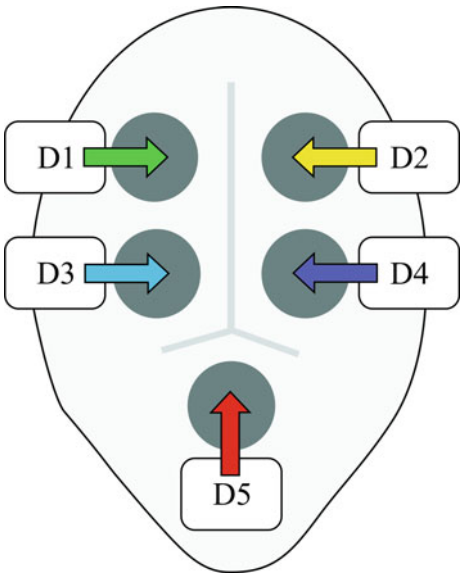

Fig. 7 Schematic order of defect formation in the rabbit calvary

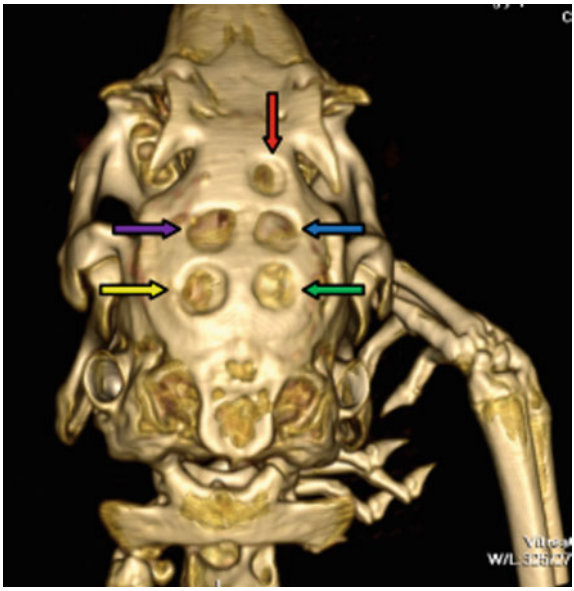

Fig. 8 VR 3D reconstruction of rabbit head with five calvary bone defects filled with different biomaterials one week after implantation

which is located below the level of healthy bone. A red arrow indicates the deepest control defect with spontaneous regeneration.

On MPR reconstruction of the bone structures of rabbit calvary in the sagittal section (Fig. 9) at the level of three artificially formed defects, on the right side to the medio-sagittal line, the defect with the newly formed bone structure marked with a green arrow is observed, the ventral contour of which is largely in the plane of the surface of the surrounding healthy bone and partly protrudes. The defect marked with a blue arrow shows discrete densities of calcium in the dorsal part, while in the control defect marked with a red arrow the structures of calcium density are not detected.

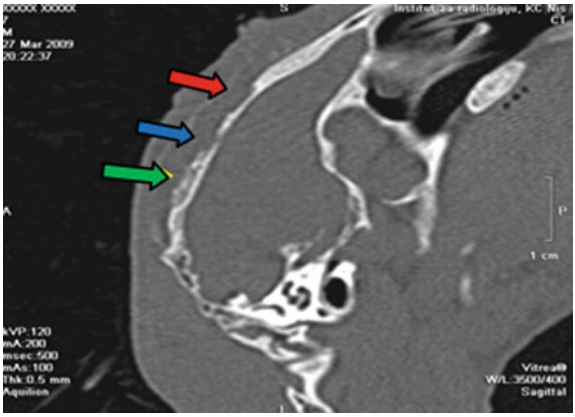

Fig. 9 Sagittal tomogram of rabbit calvary bone defects filled with different biomaterials one week after implantation: *green arrow* shows a newly formed bone structure, *blue arrow* shows discrete densities of calcium, *red arrow* marks the control defect where calcium density is not detected

On MPR reconstruction of the bone structures of rabbit calvary in the coronal section (Fig. 10) at the level of two artificially formed defects, the defect marked with a green arrow shows the presence of newly formed structure, the ventral contour of which is partly in the tabullae externae plane and partly is outside, while in the defect marked with a yellow arrow calcium densities are hardly observed.

On sagittal reconstruction of the rabbit calvary (Fig. 11) at the site of two artificially formed defects on the left side of mediosagittal line, discrete structures of calcium density, i.e. the signs of initial osteoreparation, are observed.

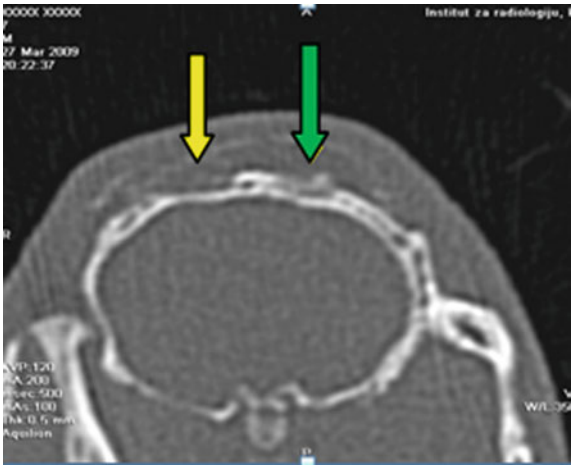

Fig. 10 Coronal tomogram of rabbit calvary bone defects filled with different biomaterials one week after implantation: *yellow arrow* shows hardly observed calcium densities, *green arrow* shows the presence of newly formed bone

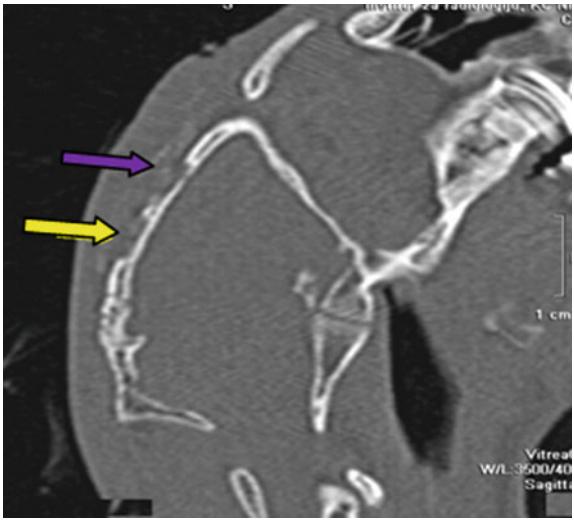

Fig. 11 Sagittal tomogram of rabbit calvary bone defects filled with different biomaterials one week after implantation: *arrows* demonstrate two artificially formed defects with discrete structures of calcium density —initial osteoreparation

On VR 3D reconstruction of bone structures of the rabbit head three weeks after defect filling-up the sites of five artificially formed defects are visualized (Fig. 12), where the defect marked with a green arrow shows the signs of significant osteoreparation. The defect marked with a yellow arrow also shows the signs of significant osteoreparation.

On sagittal reconstruction of the rabbit calvary after three months (Fig. 13) at the level of three artificially formed defects on the right side of mediosagittal line, the defect marked with a green arrow almost completely regenerated, filled with newly formed bone structure so that its ventral contour was located in the tabula eksterna plane. The defect marked with a blue arrow was characterized by the presence of newly formed low density bone structure compared to the defect previously described. In the control defect marked with a red arrow, there was a hardly observable structure of calcium density in the dorsal part and rostral edge, which was the sign of initial osteoreparation. In comparison to the tomogram made a week after the defects had been filled up (Fig. 9), the signs of osteoreparation progression were here visible.

On sagittal reconstruction at the level of two artificially formed defects on the left side to the medio-sagittal line (Fig. 14), a newly formed bone of ventral contour and at the level of tabula externa was observed in the defect marked with a yellow arrow, while in the defect marked with a purple arrow osteoreparation was weaker

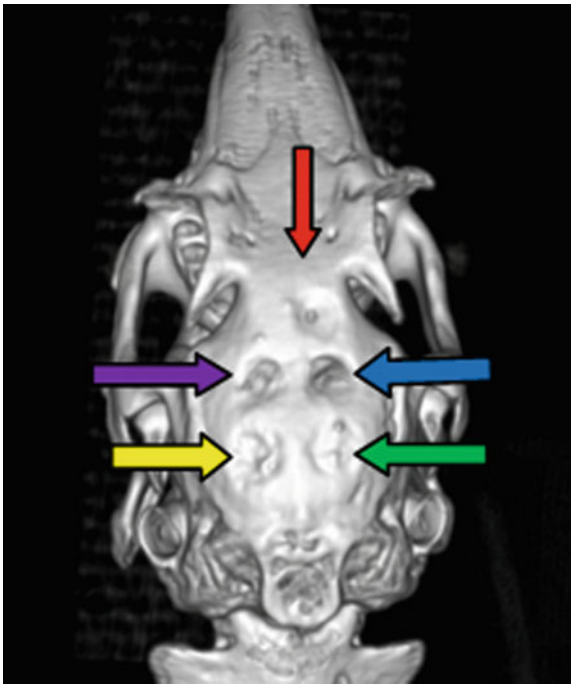

Fig. 12 VR 3D reconstruction of the rabbit head with five calvary bone defects filled with different biomaterials tree weeks after implantation

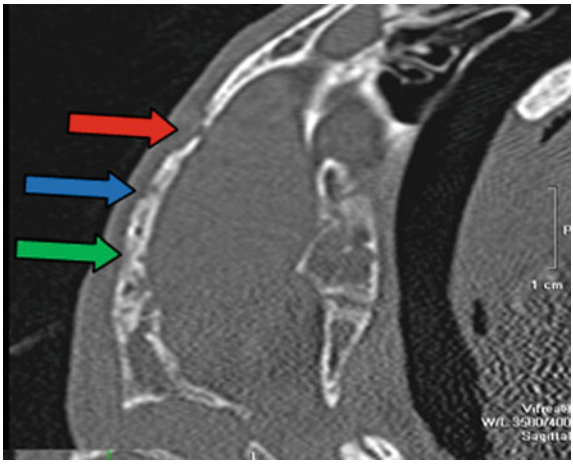

Fig. 13 Sagittal tomogram of rabbit calvary bone defects filled with different biomaterials three week after implantation: *green arrow* demonstrates almost completely regenerated defect with newly formed bone; *blue arrow* shows the presence of a newly formed bone structure, that is not a filled-up defect; *red arrow* shows a hardly observed structure of calcium density—initial osteoreparation

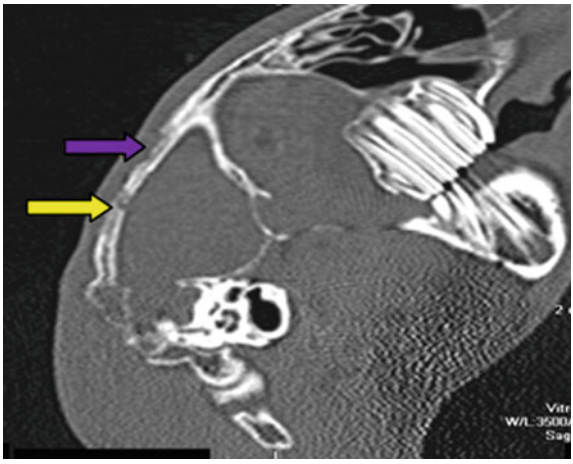

Fig. 14 Sagittal tomogram of the rabbit calvary bone defects filled with different biomaterials three week after implantation: *yellow arrow* demonstrates newly formed bone, with ventral contour at the level of the surrounding healthy bone; *purple arrow* shows weaker osteoreparation, where the ventral contour is below the plane of the surrounding healthy bone

and its ventral contour was below the plane of the surrounding healthy bone. The comparison with the tomogram made one week after the defect had been filled up (Fig. 11) showed significant progression of osteoreparation.

Six weeks after defect filling, on VR 3D reconstruction of the bone structure of rabbit head, three of five artificially formed defects were observed (Fig. 15). The defect marked with a green arrow regenerated completely, so that it could be hardly noticed. It was entirely filled with newly formed bone, and ventral surface and densities matched the surrounding healthy bone. The defect marked with a blue arrow had similar characteristics and was hardly noticed on VR reconstruction, while other defects were of lower densities, with ventral contours below the surrounding healthy bone.

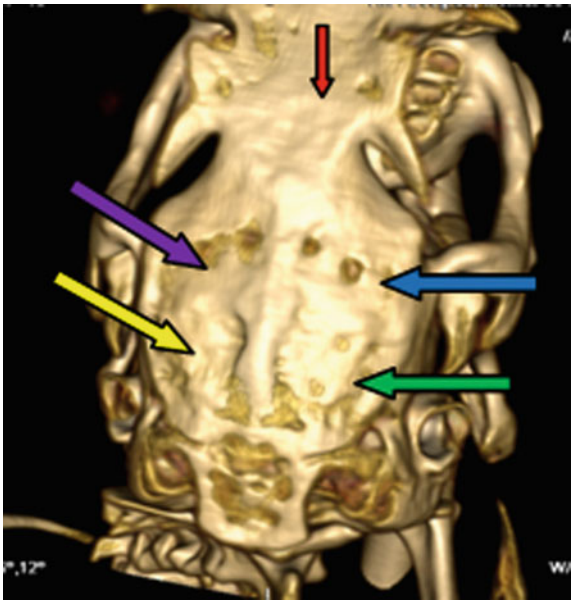

Fig. 15 VR 3D reconstruction of rabbit head with five calvary bone defects filled with different biomaterial six weeks after implantation

Without any stimulation of regeneration, spontaneous regeneration takes place at the defect margins and the new bone expands filling up the defect (Fig. 13). This experiment showed that bone growth could occur inside the defect without any contact with the original bone (Fig. 8) (Vuckovic 2013).

By comparing the density of newly formed bone in the process of regeneration and reparation of calvary bone of rabbits on the sites of formed defects completed with different biomaterials different pattern of these processes was observed.

An incomplete defect in which spontaneous regeneration occurred was used as a general control. In the first two observed periods (first and third week), bone density was unchanged and was 6–8% of healthy bone density. Six weeks after the formation of defects, bone density reached about 70% of intact bone density. It was obvious that in the period from third to sixth week spontaneous regeneration significantly accelerated, in contrast to stimulated osteoreparation, where the reparation processes began significantly earlier (Vuckovic 2013).

MDCT may be used for the monitoring of osteoreparation using scaffold-type biomaterials (Figs. 16, 17 and 18), where it was also necessary to monitor the scaffold appearance and density of newly formed bone.

MDCT may be used for the monitoring of osteoreparation of bone defects supported by biomaterials in small experimental animals such as rats (Fig. 19), as well as the degree of reparation of bone defects after scarification of experimental animals (Fig. 20).

MDCT plays a very important role in the exploration of biomaterials in clinical practice. It is used in the diagnosis of diseases and conditions requiring the use of implants. In the case of tibial pilon fracture, MSCT is required in the surgical

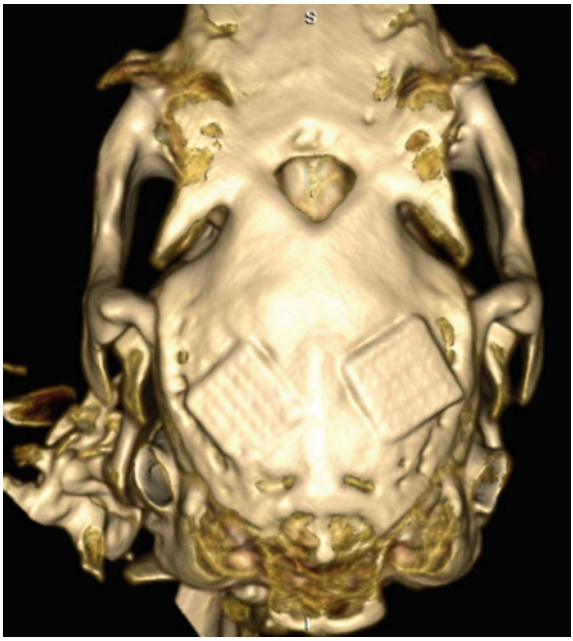

Fig. 16 VR 3D reconstruction of rabbit head with two implanted scaffolds and a control calvary defect

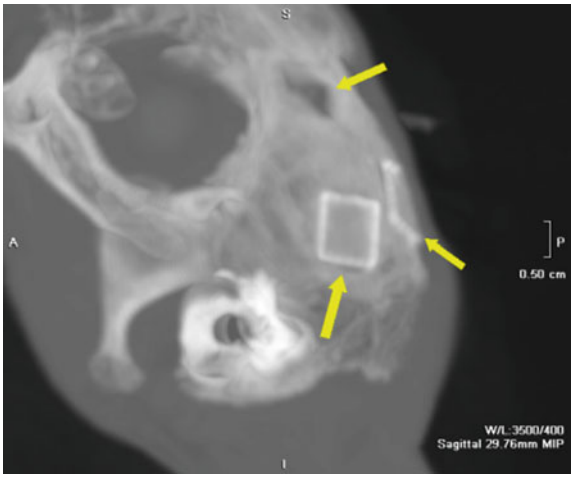

Fig. 17 MIP reconstruction of rabbit head with two implanted scaffolds and a control defect

procedure planning (Vuckovic 2013). MDCT is used in the surveillance for potential complications and evaluation of implant functionality. Implant evaluation is necessary in numerous instances. Figure 21 shows an expandable stent graft for endovascular aneurysm repair (or endovascular aortic repair) (EVAR), with the control MDCT examination performed to evaluate the stent graft flow.

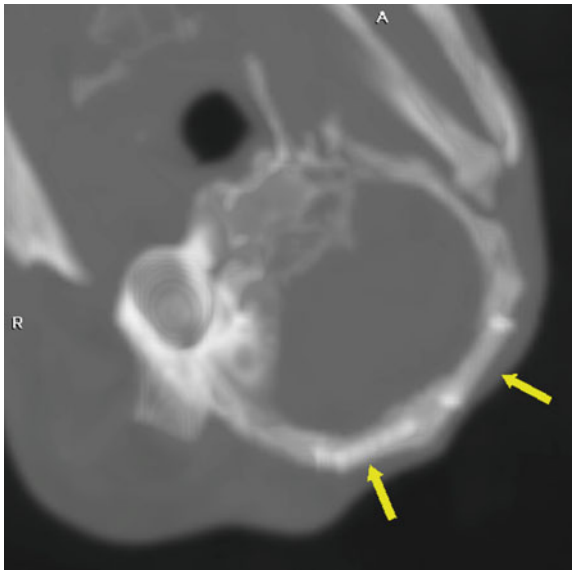

Fig. 18 Coronal tomogram of rabbit head with implanted scaffolds

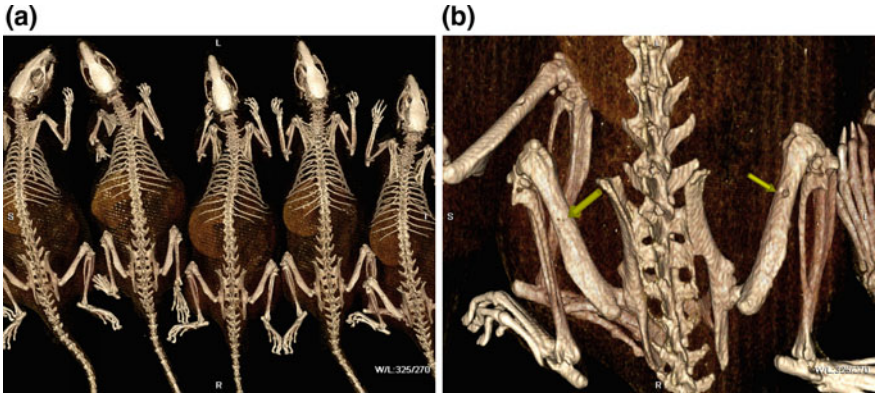

Fig. 19 VR 3D reconstruction of scanned rats (**a**) and femoral bone defects (**b**)

Ionization irradiation is an example of the negative effect of CT use in clinical practice. Moreover, metallic implants may produce some conspicuous CT image artifacts (Haramati et al. 1994). Most extensive CT artifacts are produced by the presence of stainless steel implants, while titanium implants produce the least conspicuous artifacts (Barrett and Keat 2004). Figures 22, 23, 24 and 25 show different types of metal implants as well as the reconstructive techniques that enable their visualization avoiding artifact-generation. Figure 22 shows a metal hip endoprosthesis with the presence of artifacts. Figure 23 also shows a hip

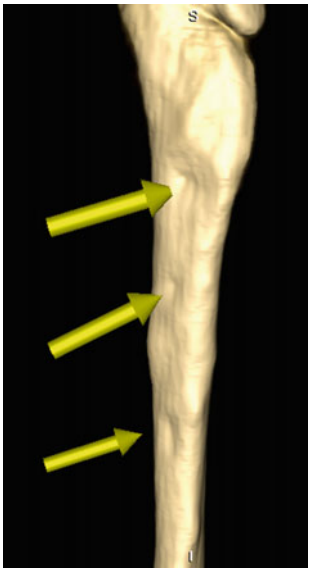

Fig. 20 VR 3D reconstruction of rabbit tibia with three artificial bone defects

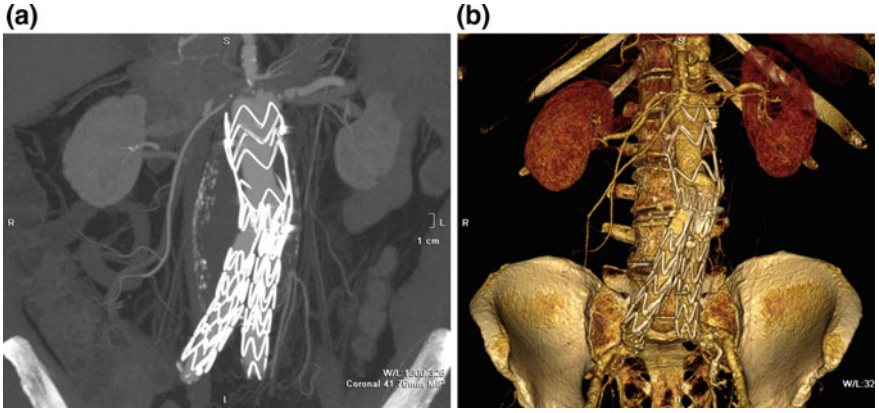

Fig. 21 MIP (**a**) and VR 3D (**b**) reconstruction of expandable stent graft for endovascular aneurysm repair (or endovascular aortic repair) (*EVAR*)

endoprosthesis with artifacts and a right side nephrostomy catheter. Figure 24 shows metal implants used to stabilize the cervical part of the vertebral column. Figure 25 shows a reconstruction for the evaluation of dental restoration and implants.

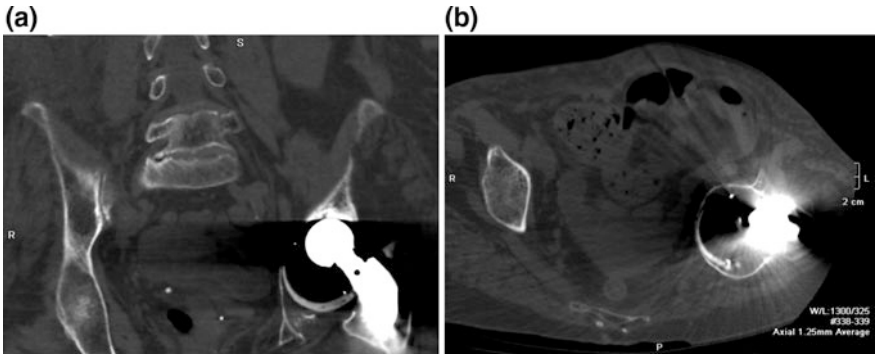

Fig. 22 Coronal (**a**) and axial (**b**) MDCT tomogram—left hip joint arthroplasty with metal endoprosthesis artifacts

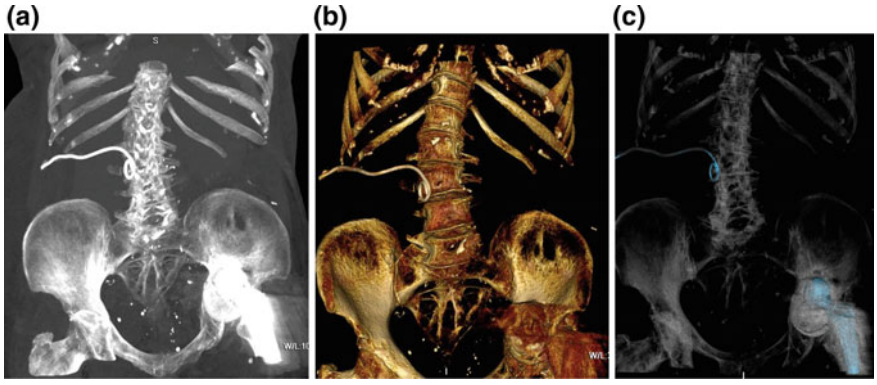

Fig. 23 MDCT VR reconstruction (**a–c**)—left hip joint endoprosthesis artifacts and right nephrostomy catheter

3.2 Imaging Techniques in Diagnosis and Management of Osteoporosis

Diagnosis and management of osteoporosis represent the fields in which a large variety of medical imaging techniques have been used. This chapter describes the most important of those, highlighting their advantages and disadvantages related to aforementioned purpose.

Osteoporosis is defined as a skeletal disease, which is the cause of low bone mass and deterioration of bone tissue on micro level. Osteoporotic bone is fragile and susceptible to fracture (Adams 2009). Screening and treatment of osteoporosis aims at prevention of bone fracture (Griffith and Genant 2008). After invention of CT it was soon recognized as an efficient method for diagnostic activities related to osteoporosis (Adams 2009). However, other methods like Dual-energy X-ray

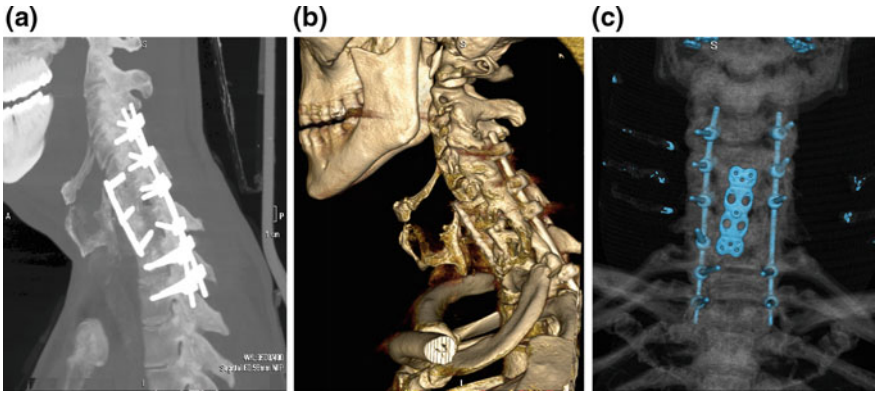

Fig. 24 MDCT MIP (**a**) and VR (**b**, **c**) reconstructions of cervical spine after stabilization by metal fixation devices

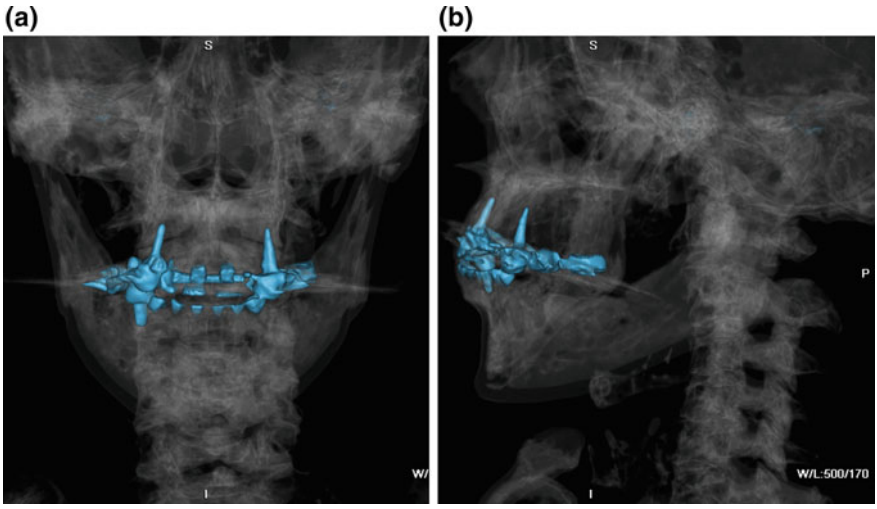

Fig. 25 MDCT VR (**a**, **b**) reconstruction of the jaw in a patient with metal dental implants and bridges

absorptiometry (DXA) became widely adopted in daily medical practice as they are faster, cheaper and simpler to use and also result in smaller radiation dose for a patient (Yates et al. 1995).

It is considered that bone mineral density (BMD) represents the best measure for diagnosis of osteoporosis, as well as for fracture risk assessment (Kanis 2002). BMD represents the amount of bone mineral content per unit volume (or per unit area in DXA) and it is usually measured at the hip and lumbar spine (Kanis et al. 2008). Lower BMD values in these areas indicate a greater possibility of bone

fracture. However, a significant overlap of BMD values in patients with or without fractures has been reported, as well as large differences in bone strength obtained by in vitro mechanical testing of specimens extracted from patients with similar BMD findings. This indicates that the knowledge on macroscopic and microscopic bone structure can be the source of additional information that may be used in prediction of bone strength and drug treatment response monitoring (Genant et al. 2008; Griffith and Genant 2008). In vivo, this insight can only be gained by CT or MRI based techniques.

3.2.1 Dual-Energy X-ray Absorptiometry (DXA)

The basis of DXA method is the difference in the absorption of two different energy levels photon beams by bone tissue and soft tissue. It is a non-invasive technique for BMD measurement and fracture risk assessment that is most widely used. DXA produces a two-dimensional image. BMD is defined as the ratio of bone mineral content at the scanned site and the area of the scanned zone (the real BMD is expressed in grams per square centimeter). This measure is different from real volumetric BMD, expressed in grams per cubic centimeter (Cosman et al. 2013; Celenk and Celenk 2012), which can be obtained using quantitative computed tomography (QCT). The results obtained by DXA (Fig. 26) are expressed relative to the mean bone density of young healthy individuals, 20–40 years old (T-score), or in relation to the value of a healthy group of the same age (Z score).

DXA is based on the use of low-energy X rays, whose absorption is sensitive to the content of calcium, which is the main component of bone (Kanis et al. 2008). The mentioned principle can also represent a disadvantage of this technique. One such example is osteomalacia, which represents aortic calcification at the spine or hip in older people. The presence of osteomalacia may cause the appearance of false-negative results that camouflage the clinical picture. Therefore, the method mostly concentrates on femoral neck area, where no factors exist that could hinder the assessment of density (Denic 2006; Kanis 2002; Celenk and Celenk 2012).

3.2.2 Quantitative Ultrasound Densitometry (QUS)

Quantitative ultrasound densitometry (QUS) is a method that is less reliable and less sensitive than DXA, but more economical and less harmful (producing less ultrasonic radiation). It is an indirect method for measuring BMD, as density evaluation is based on the speed of sound (SOS) and broadband ultrasound attenuation (BUA) at peripheral sites, such as heel and patella (Cosman et al. 2013; Adams 1998). QUS provides information on bone tissue, both structural and qualitative, but unlike DXA it does not indicate the content of calcium (Savino et al. 2013). QUS is considered a safe method as the subjects are not exposed to ionizing radiation. If QUS is used, patients can be monitored more frequently. Predictions of hip and spine osteoporotic fractures by QUS are very good, but it cannot be used for

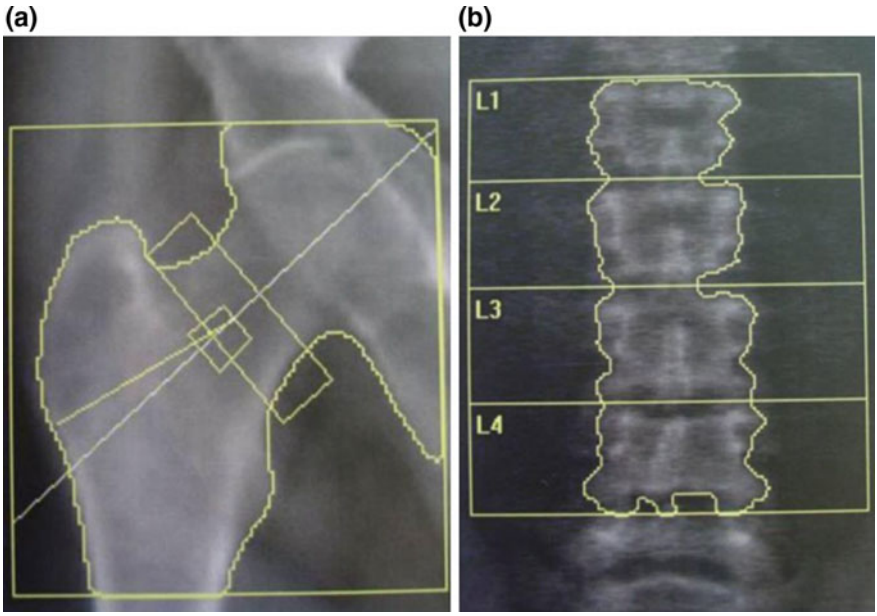

Fig. 26 Bone mineral density measurement using DXA in the area of femoral neck (**a**) and the lumbar spine (**b**) (By Dr Caroline LEBRETON, CHU Raymond Poincaré, Garches, France. [CC BY 2.0 (http://creativecommons.org/licenses/by/2.0)], via Wikimedia Commons)

monitoring of the response to therapy, as BMD changes on the heel do not occur as fast as on the hip or spine (Njeh et al. 1997). Another drawback of this method is the absence of standardization, which refers to the variation of parameters and body areas being tested (Laugier 2008).

3.2.3 Single Energy X-ray Absorptiometry (SXA)

By means of SXA, which is not as commonly used as DXA, BMD is measured at wrist or heel. SXA represents a less accurate method than DXA, as a single energy X-ray beam is used for evaluation of BMD. Because single energy X-ray beam is used, the arm must be placed in the water to measure the correct absorption of rays by soft tissue (Celenk and Celenk 2012; Kanis 2002). The picture obtained by SXA is two-dimensional as well as DXA picture (Adams 1998). The principles behind SXA are the same as those on which Single photon absorptiometry (SPA) is based, except that it uses X-rays instead of gamma rays. Thus there is no need for isotopes (Kanis 2002; Jelic et al. 2008).

3.2.4 Peripheral Dual Energy X-ray Absorptiometry (pDXA)

pDXA is in fact DXA method adapted to the periphery of the skeleton. It measures bone density at the wrist, heel, or finger (Celenk and Celenk 2012). pDXA also uses very low doses of radiation and, compared to DXA, yields faster results. pDXA is portable, as smaller instruments are used. It costs less and also produces a lower radiation dose, as it is performed farther from sensitive organs. Some of the pDXA devices may be used for prediction of osteoporotic fractures, but less efficiently than standard DXA. This is not a method for clinical use in the osteoporosis diagnosis and is not effective for monitoring the effects of the treatments (Hans et al. 2008).

3.2.5 Radiographic Absorptiometry (RA)

With the development of computer aided image processing, RA emerged as one of the methods for the diagnosis of osteoporosis that is in terms of accuracy comparable with DXA and SXA (Yates et al. 1995). Using RA, BMD from radiographs is measured. This technique is a fast and inexpensive and it can rapidly measure bone loss. Bone measurements are usually performed on the hand and heel (Celenk and Celenk 2012; Yang et al. 1994). This method uses an X-ray in the fingers and the aluminum wedge to calculate bone density (Cosman et al. 1991).

3.2.6 Quantitative Computed Tomography (QCT)

QCT represents a technique for BMD measurement based on CT. It is usually coupled with a calibration standard for translation of Hounsfield units (HU) to BMD units. The Hounsfield unit (HU) scale represents a linear transformation of the original scale used for measurement of linear attenuation coefficient, According to HU scale, radiodensity of distilled water at standard pressure and temperature (STP) equals zero Hounsfield units (HU). Radiodensity of air at STP is equal to −1000 HU. An etalon (phantom) is positioned under the patient during the scanning process (Kalender et al. 1995). It contains several inserts of known BMD, equivalent to BMD of various bone tissue types. In the beginning, QCT technique was performed using older axial CT scanners and involved creation of single 8–10 mm axial section images at the center of three lumbar vertebrae, L1–L3, or a series of thinner axial sections through L1–L2 (Bauer et al. 2010; Genant et al. 2008). With introduction of multi-slice spiral scanners, a full 3D image in resolution of 0.5 mm could be created (Fig. 27), which enabled separate measuring of BMD in cortical and trabecular tissue as well as measuring of macro-structural parameters.

3D QCT is often related to as volumetric QCT—vQCT (Genant et al. 2008; Griffith and Genant 2008). When vQCT is used, a more accurate separation of cortical and trabecular tissue is possible. One of the advantages that follow from this fact is separate consideration of BMD in trabecular tissue, which is metabolically more active and may serve as an early indicator of treatment success (Genant

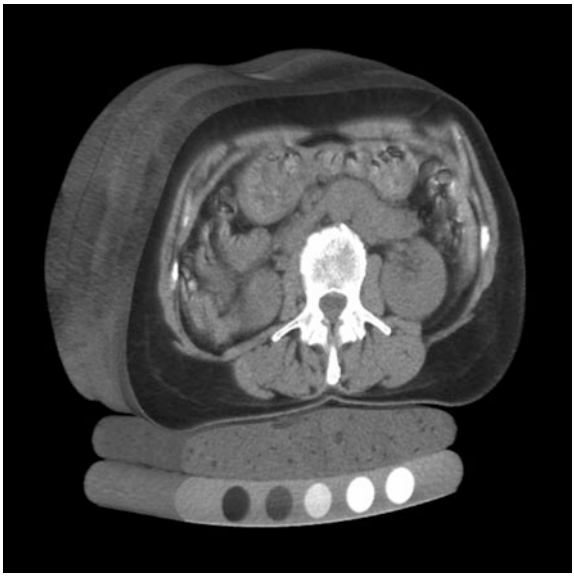

Fig. 27 3D volumetric QCT image of vertebrae (By MindwaysCT Software (MindwaysCT QCT Pro brochure) [CC BY-SA 3.0 (http://creativecommons.org/licenses/by-sa/3.0)], via Wikimedia Commons)

et al. 2008). As compared to QCT or DXA, vQCT also enables more precise measurement of macro-structural bone parameters, such as cross-sectional areas at femur neck or greater trochanter (Fig. 28). This is especially noticeable in the hip region, as proximal femur geometry is much more complicated than vertebral body geometry (Genant et al. 2008). Thickness of cortical bone may be measured from vQCT images, but owing to its low resolution (approximately 0.5 mm) results are not very accurate for cortical thickness bellow 1.5–2 mm. Even quantification of trabecular structure using statistical parameters is reported when vQCT is used. Anyway, the obtained results are highly dependent on image processing procedure applied and are their mutual variation is considerable (Griffith and Genant 2008).

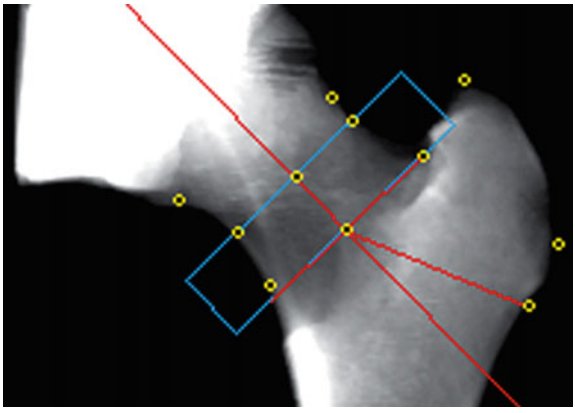

Fig. 28 Identification of area for calculation of macro-structural parameters on proximal femur using specialized software (By MindwaysCT Software (MindwaysCT QCT Pro brochure) [CC BY-SA 3.0 (http://creativecommons.org/licenses/by-sa/3.0)], via Wikimedia Commons)

In summary, the advantages of QCT over non-CT methods are independence of bone size, separate BMD measurement at cortical and trabecular bone, extraction of a larger number of macro-structural parameters with greater precision, rapid data acquisition, relatively small radiation dose comparing to typical CT examination (equivalent to mammogram) and possibility of opportunistic scanning without introduction of the additional radiation dose. It also enables measurement of BMD with scoliosis patients, more accurate predictions with arthritic patients that are obese, have degenerative spine disease, aortic calcification or osteophytes. On the other hand, its limitations are relatively high radiation dose comparing to DXA and similar techniques, limited accessibility of general purpose CT scanners, relative lack of commercial analysis packages for QCT, dependence of results accuracy on staff skill level, fewer reference data for results evaluation and non-applicability of World health organization (WHO) BMD standards related to DXA.

3.2.7 Peripheral QCT (pQCT) and High Resolution Peripheral QCT (HR-pQCT)

In vivo application of QCT is limited by radiation dose a patient can normally sustain. If full-body CT scanners are used, resolution has to be kept above 0.5 mm to avoid overexposure.

Peripheral QCT (pQCT) scanners, which are used to create QCT images at distal radius or tibia, were developed in order to make CT scanning cheaper and more available (Griffith and Genant 2008). BMD measurements obtained using pQCT are not as reliable for prediction of osteoporosis as the ones obtained at hip or spine.

On the other side, high resolution pQCT (HR-pQCT) scanners that became available in recent years, enable creation of peripheral scans with pixel size around 0.1×0.1 mm. Such resolution is sufficient for approximate determination of texture and structure of trabecular network (Genant et al. 2008), which is characterized by trabecular size close to 0.1 mm and trabecular space of 0.2–2 mm. Textural or statistical descriptors are used for this purpose instead of direct measurement of structural parameters, for which the resolution is not high enough (Genant et al. 2008). The overall radiation dose is not very large, as scanning volume is relatively small.

3.2.8 Micro-CT (μCT)

Term μCT relates to CT techniques with resolution of 1–100 μm and is not applicable in vivo for diagnosis and management of osteoporosis. Nevertheless, it can efficiently replace standard techniques for histomorphometric analysis of thin sections, which are generally very tedious (Genant et al. 2008). One of the most popular osteoporosis related research areas is the use of μCT scanners in human

iliac crest biopsies, for investigation of trabecular bone structure (Genant et al. 2008; Borah et al. 2001; Lespessailles et al. 2006; Brandi 2009; Gao et al. 2012).

On commercial μCT scanners, special software is often preinstalled that features 3D analysis of bone microstructure or structural analysis of bone samples subjected to a defined load using finite element method (Borah et al. 2001).

Micro-CT techniques are also widely used in osteoporosis related research performed in vivo on small laboratory animals, such as mice and rats (Genant et al. 2008). Even in this case, the resolution of micro-CT scanners gives the insight into bone microstructure and enables efficient monitoring of animals' reaction to various drug treatments, which may later bi correlated to management of osteoporosis.

3.2.9 Magnetic Resonance Imaging (MRI)

MRI may also be used for BMD measurement and evaluation of microstructure of trabecular bone. Measuring areas are the spine, hip, or total body. Similar to CT based techniques 3D images of relevant areas are obtained in noninvasive manner. The main advantage of MRI is that it is a radiation-free technique (Celenk and Celenk 2012). On the other side, CT techniques are more available, quicker, easier to use and more economically viable.

Unlike QCT, MRI has the potential to be used for volumetric BMD calculations without losing soft tissue signals. Nevertheless, BMD quantification using MRI is more challenging, mainly due to the low proton signals in mineral. Several MRI techniques enhancing the phosphorus signals have been developed for BMD calculations. Examples include solid state P31 nuclear magnetic resonance projection MRI and ultra-short echo MRI (Ho et al. 2013). Subpixel enhancement of non-uniform tissue (SPENT) represents a new MRI technique, able to provide information based on the subvoxel structural uniformity of a sample. Data obtained using this technique has lately also been related to BMD (Yiannakas et al. 2009).

High-resolution magnetic resonance imaging (MRμI) typically enables non-destructive analysis of 1 cm^3 sub-volumes of the whole bone with spatial resolution in the 50–100 mm range (Borah et al. 2001). Most in vivo studies have been undertaken at the peripheral skeleton as the distal radius, distal tibia and the calcaneus. When trabecular bone is imaged in vivo using MRI, one must be aware that trabecular bone itself is not visualized. Rather, a trabecula is present as a signal void that is surrounded by high-intensity bone marrow (Bauer and Link 2008). Thus, the measurements obtained by MRI are mutually comparable only if the same technique of acquisition has been used.

MRI is often applied in ex vivo analysis of specimens obtained by bone biopsy. In this way, the extensive information about trabecular architecture can be obtained as well as and its relationship to biomechanical strength range (Borah et al. 2001).

4 Concluding Remarks

An overview of most important medical imaging techniques, containing examples and references describing their use in medicine and biomedical engineering, was presented. Some of the most important medical imaging modalities include radiography, ultrasound imaging, mammography, computed tomography (CT), magnetic resonance imaging (MRI) and positron emission tomography (PET).

All the presented methods have their advantages as well as drawbacks. Radiography still represents the first choice in many applications, especially when bone tissue, implants or other medical devices present in human body are visualized. It is simple and fast and produces a relatively small dose of ionizing radiation. Nevertheless, the information obtained by radiography is limited. 3D space is projected to 2D image where overlapping of organs makes image less readable. Also, the measuring of distances depends on the direction in which the image was taken. CT based techniques corrects the main shortcoming of radiography as they enable a full 3D insight into human or animal body. Their application is very versatile but, unfortunately, related to a large radiation dose. Thus, the use of CT techniques and related image density must be justified by patient's health condition. CT can produce medical images of great resolution, but the associated radiation dose makes such images unusable for clinical practice. The exception is peripheral quantitative computed tomography (pQCT) that is used for diagnosis of osteoporosis at distal radius or tibia. Greatest resolution is achieved with micro-CT devices, which are only used in vitro or in animal experimentation. MRI also produces 3D images and its main advantage is the absence of ionizing radiation. It is very suitable for soft tissues but cannot directly visualize bone tissue. It is also considerably slower than CT, which makes its application more expensive. The most important contraindication of MRI is the presence of ferromagnetic objects in the imaging field. Ultrasound imaging is also radiation-free, but their application is limited and highly dependent on the skill of specialist using the certain technique.

The importance of medical imaging and the benefits it brings may be summarized as follows:

- The images of normal and pathological structures inside the human body, obtained using various imaging methods, contain invaluable information about the area of the body being studied or treated, related to possible disease, injury, or the response of medical treatment.
- Medical imaging has an important role in the field of biomaterial and bioengineering. This research field has expanded due to rapid development of modern technologies.
- Various imaging techniques are used in clinical and preclinical practice for evaluation of biomaterials. Among those, three-dimensional (3D) imaging represents the most important tool in the field of tissue engineering and regenerative medicine research.

Acknowledgements The research study is part of project III41017 Virtual human osteoarticular system and its application in preclinical and clinical practice, funded by the Ministry of Education and Science of Republic of Serbia, for the period of 2011–2017.

References

Adams J (1998) Single-and dual-energy: X-ray absorptiometry. In: Bone densitometry and osteoporosis. Springer, Berlin, pp 305–334

Adams J (2009) Quantitative computed tomography. Eur J Radiol 71(3):415–424

Alberich-Bayarri A, Moratal D, Ivirico JLE et al (2009) Microcomputed tomography and microfinite element modeling for evaluating polymer scaffolds architecture and their mechanical properties. J Biomed Mater Res B Appl Biomater 91B(1):191–202

Anzivino A, Mansi L (2012) Fabian Kiessling, Bernd J. Pichler (eds): small animal imaging. Basics and practical guide. Eur J Nucl Med Mol Imaging 39(5):915–916

Appel AA, Anastasio MA, Larson JC et al (2013) Imaging challenges in biomaterials and tissue engineering. Biomaterials 34(28):6615–6630

Arinzeh TL, Peter SJ, Archambault MP et al (2003) Allogeneic mesenchymal stem cells regenerate bone in a critical-sized canine segmental defect. J Bone Jt Surg Am 85-a(10):1927–1935

Atala A (2004) Tissue engineering and regenerative medicine: concepts for clinical application. Rejuvenation Res 7(1):15–31

Barrett JF, Keat N (2004) Artifacts in CT: recognition and avoidance. RadioGraphics 24(6): 1679–1691

Bauer JS, Link TM (2008) Advances in osteoporosis imaging. Eur J Radiol 71(3):440–449

Bauer JS, Virmani S, Mueller DK (2010) Quantitative CT to assess bone mineral density as a diagnostic tool for osteoporosis and related fractures. MedicaMundi 54(2):31–37

Beyer T, Townsend DW, Blodgett TM (2002) Dual-modality PET/CT tomography for clinical oncology. Q J Nucl Med Mol Imaging 46(1):24–34

Borah B, Gross GJ, Dufresne TE et al (2001) Three-dimensional microimaging (MRμI and μCT), finite element modeling, and rapid prototyping provide unique insights into bone architecture in osteoporosis. Anat Record 265(2):101–110

Boskey A, Pleshko Camacho N (2007) FT-IR imaging of native and tissue-engineered bone and cartilage. Biomaterials 28(15):2465–2478

Brandi ML (2009) Microarchitecture, the key to bone quality. Rheumatology 48(suppl 4):iv3–iv8

Brinton LA, Brown SL (1997) Breast implants and cancer. J Natl Cancer Inst 89(18):1341–1349

Bruder SP, Kurth AA, Shea M et al (1998) Bone regeneration by implantation of purified, culture-expanded human mesenchymal stem cells. J Orthop Res 16(2):155–162

Campbell CT, Kim G (2007) SPR microscopy and its applications to high-throughput analyses of biomolecular binding events and their kinetics. Biomaterials 28(15):2380–2392

Cartmell S, Huynh K, Lin A et al (2004) Quantitative microcomputed tomography analysis of mineralization within three-dimensional scaffolds in vitro. J Biomed Mater Res A 69(1): 97–104

Celenk C, Celenk P (2012) Bone density measurement using computed tomography. Computed tomography—clinical applications, 1st edn. InTech, Croatia, pp 123–136

Cosman F, Herrington B, Himmelstein S et al (1991) Radiographic absorptiometry: a simple method for determination of bone mass. Osteoporos Int 2(1):34–38

Cosman F, de Beur S, LeBoff M et al (2013) Clinician's guide to prevention and treatment of osteoporosis. Osteoporosis Int 1–23

Dayton PA, Rychak JJ (2007) Molecular ultrasound imaging using microbubble contrast agents. Front Biosci 12:5124–5142

Denic A (2006) Practical approach to diagnostics of osteoporosis-the effect of hypothyroidism and L-thyroxine therapy on bone metabolic activity. Medicinski glasnik. Specialist hospital for thyroid gland disorders and metabolism disorders. Zlatibor 11(20):23–30 (in serbian)

Elhendy A, Bax JJ, Poldermans D (2002) Dobutamine stress myocardial perfusion imaging in coronary artery disease. J Nucl Med 43(12):1634–1646

Everson LI, Parantainen H, Detlie T et al (1994) Diagnosis of breast implant rupture: imaging findings and relative efficacies of imaging techniques. Am J Roentgenol 163(1):57–60

Fite BZ, Decaris M, Sun Y et al (2011) Noninvasive multimodal evaluation of bioengineered cartilage constructs combining time-resolved fluorescence and ultrasound imaging. Tissue Eng C Methods 17(4):495–504

Fujibayashi S, Neo M, Kim H-M et al (2004) Osteoinduction of porous bioactive titanium metal. Biomaterials 25(3):443–450

Fujibayashi S, Takemoto M, Neo M et al (2011) A novel synthetic material for spinal fusion: a prospective clinical trial of porous bioactive titanium metal for lumbar interbody fusion. Eur Spine J 20(9):1486–1495

Gao Z, Hong W, Xu Y (2012) Trabecular bone micro-CT images analysis for osteoporosis diagnosis. J Comput Inf Syst 8(24):10341–10347

Genant H, Engelke K, Prevrhal S (2008) Advanced CT bone imaging in osteoporosis. Rheumatology 47(suppl 4):iv9–iv16

Golubovic Z, Popovic Z, Milenkovic S et al (2013) Missile injury of the knee joint. Acta Facultatis Medicae Naissensis 30(4):225–231

Golubovic I, Stanojlovic M, Ristic B et al (2014) Pseudoarthrosis of tibia after open fracture and external skeletal fascia performed by intramedular fixation. Paper presented at the Book of abstracts of IV Congress of Association of orthopaedic traumatologists with international participation, Belgrade, 2–4 Oct

Griffith JF, Genant HK (2008) Bone mass and architecture determination: state of the art. Best Pract Res Clin Endocrinol Metab 22(5):737–764

Hans DB, Shepherd JA, Schwartz EN et al (2008) Peripheral dual-energy X-ray absorptiometry in the management of osteoporosis: the 2007 ISCD official positions. J Clin Densitom 11(1): 188–206

Haramati N, Staron RB, Mazel-Sperling K et al (1994) CT scans through metal scanning technique versus hardware composition. Comput Med Imaging Graph 18(6):429–434

Hendee WR, Cleary K, Ehman RL et al (2008) Bioengineering and imaging research opportunities workshop V: a summary on imaging and characterizing structure and function in native and engineered tissues. Cytom A 73A(9):779–784

Herman GT (2009) Fundamentals of computerized tomography: image reconstruction from projections. Springer Publishing Company, Incorporated

Hibino N, Duncan DR, Nalbandian A et al (2012) Evaluation of the use of an induced pluripotent stem cell sheet for the construction of tissue-engineered vascular grafts. J Thorac Cardiovasc Surg 143(3):696–703

Ho ST, Hutmacher DW (2006) A comparison of micro CT with other techniques used in the characterization of scaffolds. Biomaterials 27(8):1362–1376

Ho K-Y, Hu HH, Keyak JH et al (2013) Measuring bone mineral density with fat–water MRI: comparison with computed tomography. J Magn Reson Imaging 37(1):237–242

Huebsch ND, Mooney DJ (2007) Fluorescent resonance energy transfer: a tool for probing molecular cell-biomaterial interactions in three dimensions. Biomaterials 28(15):2424–2437

Hunter TB, Taljanovic MS (2005) Medical devices of the abdomen and pelvis. RadioGraphics 25(2):503–523

Hunter TB, Taljanovic MS, Tsau PH et al (2004a) Medical devices of the chest. RadioGraphics 24(6):1725–1746

Hunter TB, Yoshino MT, Dzioba RB et al (2004b) Medical devices of the head, neck, and spine. RadioGraphics 24(1):257–285

Ignjatovic J, Stojanov D, Stojanovic N et al (2014) ADC is not reliable in determinating subtypes of meningiomas. Central Eur J Med 9(6):773–777

Jelic D, Stefanovic D, Petronijevic M, Andjel-Jelic M (2008) Why is double absorptiometry of X-rays gold standard in diagnostics of osteoporosis. Vojnosanit Pregl 65(12):919–922 (in serbian)

Jiang Y, Zhao J, White D et al (2000) Micro CT and micro MR imaging of 3D architecture of animal skeleton. J Musculoskelet Neuronal Interact 1(1):45–51

Jocic M, Petrovic S, Stojanov D (2013) Advanced diagnostic techniques of metastatic lymph nodes. Acta Medica Median 52(4):53–57

Kalender WA, Felsenberg D, Genant HK et al (1995) The European spine phantom—a tool for standardization and quality control in spinal bone mineral measurements by DXA and QCT. Eur J Radiol 20(2):83–92

Kanis J (2002) Diagnosis of osteoporosis and assessment of fracture risk. Lancet 359(9321): 1929–1936

Kanis J, Burlet N, Cooper C et al (2008) European guidance for the diagnosis and management of osteoporosis in postmenopausal women. Osteoporos Int 19(4):399–428

Kawamura M, Miyagawa S, Miki K et al (2012) Feasibility, safety, and therapeutic efficacy of human induced pluripotent stem cell-derived cardiomyocyte sheets in a porcine ischemic cardiomyopathy model. Circulation 126(11 suppl 1):S29–S37

Kerr BA, Byzova TV (2012) MicroCT: an essential tool in bone metastasis research. In: Saba DL (ed) Computed tomography—clinical applications. INTECH Open Access Publisher

Kim K, Jeong CG, Hollister SJ (2008) Non-invasive monitoring of tissue scaffold degradation using ultrasound elasticity imaging. Acta Biomater 4(4):783–790

Kon E, Muraglia A, Corsi A et al (2000) Autologous bone marrow stromal cells loaded onto porous hydroxyapatite ceramic accelerate bone repair in critical-size defects of sheep long bones. J Biomed Mater Res 49(3):328–337

Korunovic N, Trajanovic M, Mitkovic M et al (2010) From CT scan to FEA model of human femur. IMK-14-Istraživanje i razvoj 16(2):45–48

Korunovic N, Trajanovic M, Stevanovic D et al (2013) Material characterization issues in FEA of long bones. In: Papadrakakis M, Kojic M, Tuncer I (eds) SEECCM III 3rd South-East European conference on computational mechanics—an ECCOMAS and IACM special interest conference, Kos Island, Greece, 12–14 June 2013

Korunovic N, Rajkovic J, Petrovic S et al (2014) Application of computed tomography in diagnostics and management of osteoporosis. In: Trajanovic M, Stankovic M (eds) 6th ICT international conference, 14–16 Oct 2014. Regional Chamber of Commerce—Niš, Serbia, Nis

Kreitz S, Dohmen G, Hasken S et al (2011) Nondestructive method to evaluate the collagen content of fibrin-based tissue engineered structures via ultrasound. Tissue Eng C Methods 17 (10):1021–1026

Langer R, Vacanti JP (1993) Tissue engineering. Science (New York, NY) 260(5110):920–926

Laugier P (2008) Instrumentation for in vivo ultrasonic characterization of bone strength. Ultrason Ferroelectr Frequency Control IEEE Trans Ultrason Ferroelectr Frequency Control J Impact Factor Inf 55(6):1179–1196

Lee SJ, Van Dyke M, Atala A et al (2008) Host cell mobilization for in situ tissue regeneration. Rejuvenation Res 11(4):747–756

Lespessailles E, Chappard C, Bonnet N et al (2006) Imaging techniques for evaluating bone microarchitecture. Joint Bone Spine 73(3):254–261

Matsumura G, Isayama N, Matsuda S et al (2013) Long-term results of cell-free biodegradable scaffolds for in situ tissue engineering of pulmonary artery in a canine model. Biomaterials 34 (27):6422–6428

Mayer-Kuckuk P, Boskey AL (2006) Molecular imaging promotes progress in orthopedic research. Bone 39(5):965–977

Min S, Sato S, Saito M et al (2008) Micro–computerized tomography analysis: dynamics of bone augmentation within a titanium cap in rabbit calvarium. Oral Surg Oral Med Oral Pathol Oral Radiol Endod 106(6):892–895

Muraglia A, Martin I, Cancedda R et al (1998) A nude mouse model for human bone formation in unloaded conditions. Bone 22(5, Supplement 1):131S–134S

Naumova AV, Modo M, Moore A et al (2014) Clinical imaging in regenerative medicine. Nat Biotechnol 32(8):804–818
Njeh C, Boivin C, Langton C (1997) The role of ultrasound in the assessment of osteoporosis: a review. Osteoporos Int 7(1):7–22
Osman MM, Cohade C, Nakamoto Y et al (2003) Clinically significant inaccurate localization of lesions with PET/CT: frequency in 300 patients. J Nucl Med 44(2):240–243
Pan X, Siewerdsen J, La Riviere PJ, Kalender WA (2008) Anniversary paper. Development of X-ray computed tomography: the role of medical physics and AAPM from the 1970s to present. Med Phys 35(8):3728–3739
Pancrazio JJ, Wang F, Kelley CA (2007) Enabling tools for tissue engineering. Biosens Bioelectron 22(12):2803–2811
Pesic Z, Otasevic S, Mihailovic D et al (2015) Alternaria-associated fungus ball of orbit nose and paranasal sinuses: case report of a rare clinical entity. Mycopathologia 1–5
Petrovic S, Petrovic D, Bojanovic A (2010) Giant glomus jugulare with internal jugular vein involvement—case report. HealthMED 4(4):1075–1079 (supplement 1)
Petrovic D, Ajdukovic Z, Petrovic S et al (2011a) Semiquantitative radiological and clinical assessment of the restoration of alveolar bone defects treated with biphasic calcium phosphate/poly-dl-lactide-co glycolide composite. HealthMED 5(6):2105–2114
Petrovic D, Visnjic M, Vuckovic I et al (2011b) Reconstruction of the skin and perimandibular soft tissue after osteoradionecrosis using the supraclavicular islet fasciocutaneous flap. HealthMED 5(1):223–229
Petrovic S, Grozdanovic D, Kovacevic P et al (2011c) Collet Sicard syndrome as atypical presentation of neck fibrosarcoma: a case report. Bosn J Basic Med Sci 11(2):137–140
Petrovic S, Petrovic D, Stojanov D et al (2011d) Classification of neck Lymphadenopathies using multidetectors computerized tomography. HealthMED 5(1):63–72
Petrovic S, Petrovic D, Ristic S et al (2011e) The systematic review of head and neck paragangliomas: clinical presentation, classification, multimodalities imaging findings, differential diagnosis and treatment outcomes. HealthMED 5(4):907–916
Petrovic S, Jocic M, Stojanov D (2013) Application of imaging methods in the diagnostics of malignant neck lymph nodes. Acta Med Median 52(2):45–50
Petrovic D, Mihailovic D, Petrovic S et al (2014a) Asymptomatic flow of Rosai-Dorfman disease. Vojnosanit Pregl 71(8):780–783
Petrovic S, Tasic A, Mihailovic D et al (2014b) Bilateral giant angiomyolipomas revealed after massive retroperitoneal hemorrhage—a case report. Vojnosanitetski Pregled Mil Med Pharm Rev 71(4):408–412
Potter K, Sweet DE, Anderson P et al (2006) Non-destructive studies of tissue-engineered phalanges by magnetic resonance microscopy and X-ray microtomography. Bone 38(3): 350–358
Quint C, Arief M, Muto A et al (2012) Allogeneic human tissue-engineered blood vessel. J Vasc Surg 55(3):790–798
Rice MA, Waters KR, Anseth KS (2009) Ultrasound monitoring of cartilaginous matrix evolution in degradable PEG hydrogels. Acta Biomater 5(1):152–161
Savino F, Viola S, Benetti S et al (2013) Quantitative ultrasound applied to metacarpal bone in infants. PeerJ 1:e141
Shellock FG (1987) Biological effects of MRI: a clean safety record so far. Diagn Imaging 9: 96–101
Stankovic M, Milisavljevic D, Stojanov D et al (2012) Influential factors, complications and survival rate of primary and salvage total laryngectomy for advanced laryngeal cancer. Coll Antropol 36(Suppl 2):7–12
Stojanov D, Grozdanovic D, Petrovic S et al (2014) De novo mutation in the NOTCH3 gene causing CADASIL. Bosn J Basic Med Sci 14(1):48–50
Stojkovic M, Korunovic N, Trajanovic M et al (2013) Design study of anatomically shaped lattice scaffolds for the bone tissue recovery. In: Papadrakakis M, Kojic M, Tuncer I

(eds) SEECCM III 3rd South-East European conference on computational mechanics—an ECCOMAS and IACM special interest conference, Kos Island, Greece, 12–14 June 2013
Sun Y, Responte D, Xie H et al (2011) Nondestructive evaluation of tissue engineered articular cartilage using time-resolved fluorescence spectroscopy and ultrasound backscatter microscopy. Tissue Eng C Methods 18(3):215–226
Szpalski C, Barr J, Wetterau M et al (2010) Cranial bone defects: current and future strategies. Neurosurg Focus 29(6):E8
Takemoto M, Fujibayashi S, Neo M et al (2006) Osteoinductive porous titanium implants: effect of sodium removal by dilute HCl treatment. Biomaterials 27(13):2682–2691
Trajanovic M, Korunovic N, Milovanovic J et al (2010) Application of computer models of Mitkovic selfdynabizable internal fixator in rehabilitation of femur traumas. Facta Univ Ser Mech Eng 8(1):27–38
Tsuji W, Inamoto T, Ito R et al (2013) Simple and longstanding adipose tissue engineering in rabbits. Int J Artif Organs 16(1):110–114
Tyler DJ, Robson MD, Henkelman RM et al (2007) Magnetic resonance imaging with ultrashort TE (UTE) PULSE sequences: technical considerations. J Magn Reson Imaging 25(2):279–289
Velickov A, Kovacevic P, Petrovic D et al (2014) Second look procedure for large burn defect by banana peel pericranial flap based on one artery. Srp Arh Celok Lek 142(3–4):219–222
Visnjic M, Kovacevic P, Paunkovic L et al (2011) Breast reconstruction with extended Latissimus dorsi flap and silicone implant. HealthMED 5(5):1232–1239
Vitkovic N, Milovanovic J, Trajanovic M et al (2012) Different approaches for the creation of femur anatomical axis and femur shaft geometrical models. Strojarstvo J Theory Appl Mech Eng 54(3):247–255
Vitkovic N, Milovanovic J, Korunovic N et al (2013) Software system for creation of human femur customized polygonal models. Comput Sci Inf Syst 10(3):1473–1497
Vuckovic I (2013) Regenerative potential of fat tissue in reconstruction of bone defects on experimental model of rabbit calvary. PhD thesis, Medical Faculty University of Nis Serbia
Vulovic S, Korunovic N, Trajanovic M et al (2011) Finite element analysis of CT based femur model using finite element program PAK. J Serb Soc Comput Mech 5(2):160–166
Xu H, Othman SF, Magin RL (2008) Monitoring tissue engineering using magnetic resonance imaging. J Biosci Bioeng 106(6):515–527
Yang S-O, Hagiwara S, Engelke K et al (1994) Radiographic absorptiometry for bone mineral measurement of the phalanges: precision and accuracy study. Radiology 192(3):857–859
Yates AJ, Ross PD, Lydick E et al (1995) Radiographic absorptiometry in the diagnosis of osteoporosis. Am J Med 98(2):41S–47S
Yiannakas MC, Carmichael DW, Farquharson MJ et al (2009) Subpixel enhancement of nonuniform tissue (SPENT): a novel MRI technique for quantifying BMD. J Bone Miner Res 24(2):324–333
Yu J, Takanari K, Hong Y, Lee K-W et al (2013) Non-invasive characterization of polyurethane-based tissue constructs in a rat abdominal repair model using high frequency ultrasound elasticity imaging. Biomaterials 34(11):2701–2709

Selected Instrumental Methods for Physicochemical and Spectroscopic Characterization of Different Biomaterials

Žarko Mitić

Abstract Different physicochemical and spectroscopic instrumental methods are of great importance in determination of surface characteristics, spatial structure, composition and structure of different biomaterials and highlighting the differences between biomaterials. This review paper summarized the most common instrumental methods and techniques [Scanning electron microscopy (SEM), Transmission electron microscopy (TEM), Energy dispersive X-ray (EDX) spectroscopy, Fourier transform infrared (IR) spectroscopy, Matrix-assisted laser desorption-ionization time of flight mass spectrometry (MALDI-TOF MS), Atomic absorption spectrometry (AAS) and Inductively coupled plasma-atomic emission spectrometry (ICP-AES)], that can be used for physicochemical and spectroscopic characterization of different biomaterials that are widely used in medicine, dentistry and pharmacy.

Keywords SEM · TEM · EDX · FTIR · MALDI-TOF MS · AAS/ICP-AES

1 Physico-chemical and Spectroscopic Characterization

1.1 Scanning Electron Microscopy (SEM)

Scanning electron microscopy is one of the most applied instrumental methods in the characterization of different biomaterials (Merrett et al. 2002). SEM devices operate at magnifications from 10× to more than 300,000×. These devices are able to provide accurate information of the chemical composition of biomaterials near on its surface. The principle in the typical SEM experiment is in the strike of the generated and focused fine electron beam of about 5 nm diameter. The electron energies (E) are ranging from 100 to 50,000 eV. When the electrons strike to the

Ž. Mitić (✉)
Faculty of Medicine, University of Niš,
Bul. dr Zorana Đinđića 81, 18000 Niš, Serbia
e-mail: zak_chem2001@yahoo.com

F. Zivic et al. (eds.), *Biomaterials in Clinical Practice*,
https://doi.org/10.1007/978-3-319-68025-5_21

test surface and penetrate through it, the emission of electrons and photons from biomaterials occurs and they are collected and detected. Because of the interaction of the primary high-energy electrons with the material, there is inelastic and elastic scattering (Balac et al. 2010).

Considering that, SEM devices can generate different images depending on whether secondary electrons ("backscattered electrons") are detected. These electrons represent a part of the elastically scattered electrons, which are returned to the primary material from the surface. The probability of this phenomenon enables a contrast between regions of different composition of analyzed biomaterials. In the primary interaction of electrons with biomaterials, the emission of electrons from the electron shells of atoms can be detected. In this manner, the precise information about the morphology of biomaterials is obtained (Eliades and Brantley 2001).

The authors (Ignjatović et al. 1999a, b, 2001a, b, c), have studied the effects of hot pressing parameters on the designing of structures and properties of the hydroxyapatite/poly-L-lactide (HA/PLLA) biocomposite blocks. Interdependences of temperature (T), pressure (P) and time (t) of hot pressing and density (d), compressive strength and elasticity modules were defined. Microstructures of the fracture surfaces were observed by SEM technique. In the studies (Ignjatović et al. 2001a, b, c), the microstructure of HA/PLLA composite biomaterial surface was analyzed by SEM before and after implantation. This study revealed bioresorption of the PLLA polymer phase and generation of collagen (Coll) protein bars at the sites of implanted bioresorbable PLLA. Jovanović et al. (2008) analyzed biodegradable microspheres, made of poly-D,L-lactide (PDLLA), by using SEM to characterize the particles. In the study by Sörensen et al. (2013), authors investigated the ability of bioceramics to release the highly effective bisphosphonate zoledronic acid (BP-ZOL) using a number of instrumental methods, including SEM. The results created the base for further development of drug-delivery systems with controlled drug loading and prolonged release.

SEM can also be used to study the surface properties of materials that are used in orthopedics, such as femoral heads and hip prosthesis. This type of examination is very important for monitoring the changes of surface of such materials that occur under the influence of mechanical forces. Chevaliera et al. (2011) investigated the microstructure of Al–Zr nanocomposites, recently developed as alternative bearing materials for femoral hip in orthopedics, by using SEM. They examined surface characteristics during wear, crack resistance and ageing behavior of newly developed femoral heads and compared them to other ceramics that are used nowadays in orthopedics. Affatato et al. (2012) investigated the wear performance of vitamin E-stabilized crosslinked acetabular cups based on polyethylene (PE) in comparison with those of conventional standard and crosslinked PE-acetabular cups, by using SEM. These materials are very important and have enormous application in orthopedics and because of that it is very important to examine their wear characteristics.

The field-emission scanning electron microscopy (FE-SEM) is the technique that uses the phenomenon of field electron emission. The obtained image is based on the difference in work function of the various crystallographic planes on the surface of

biomaterials. This technique was used to characterize the morphology and surface properties of ketoprofen-loaded nanoparticles (KET-NP) (Vučen et al. 2013). The nanoparticulate carriers composed of HA/poly (D,L-lactide-co-glycolic acid (PLGA) were analyzed by using SEM in order to determine their morphology (Ignjatović et al. 2013).

1.2 Transmission Electron Microscopy (TEM)

Transmission electron microscopy is one of the most significant variations of electron microscopy techniques. The advantage of this method is an extremely large magnification range, from 50× to 10^6×. The images of biomaterials obtained on TEM microscope have the electron diffraction data. In the classical TEM experiment, accelerated electrons are directed to the thin sample of material, whose thickness is less than 200 nm. There are different modes of electrons scattering in the material, so there are two types of information that can be obtained. The diffraction image of material is formed by elastic and inelastic scattering. The inhomogeneities in the material, like grain boundaries, dislocations, defects and presence of other phases, produce local spatial variations in the intensity of the transmitted electron beam. An extremely small effective wavelength (λ) of the electron is responsible for large magnification of TEM, so it is possible to achieve very high resolution with high voltage devices (Eliades and Brantley 2001). Vukomanović et al. (2010) used TEM to characterize the samples of nanosized, plate-like HA and to analyze the influence of the ultrasound on their growth mechanism. In the study (Masanori et al. 2003), mechanisms responsible for degradation of resin-dentin bonds were understood by using transmission electron microscopic methods. TEM examination revealed the presence of micro morphological alterations in the collagen-fibrils (resin elution and alteration of the Coll-fibrils), after 1 year of water storage, seem to be responsible for bond degradation leading to the bond strength reduction.

1.3 Energy Dispersive X-Ray (EDX) Spectroscopy

Energy dispersive X-ray (EDX) spectroscopy uses X-ray spectrum (λ from 1 to 20 nm) that is emitted by a strong pattern, bombed with focused beam of electrons to produce a localized semi-quantitative chemical analysis of the sample. Theoretically all the elements from "Be" to "U" can be detected by EDX, although not all instruments are equipped for "light" elements. The basis is the radiation of patterns with high energy electrons and observation of emitted X-rays, which are characteristic of the individual elements. In this way, chemical analysis of the sample can be performed, or if it is in scanning mode chemical topography of the surface layers can be obtained, to the depth of penetration of the electrons

(Stojanovic et al. 2016). This technique became especially important when it began to be used in electron microscopes, either TEM or SEM. Considering the fact that the microscope may receive an electron beam whose diameter is less than 2 nm, nanometer area and volumes can be chemically analyzed. Two techniques, EDX and WDX, are used. The energy of emitted X-rays is measured by EDX, and the wavelength is measured by Wavelength Dispersive X-ray Spectroscopy (WDX). Both methods (EDX and WDX), have many advantages and disadvantages. For example, EDX is more frequently used method because it provides relatively quick analysis and the entire energy spectrum is measured in "one step". In the case of WDX technique, the whole range of wavelengths has to be scanned (Eliades and Brantley 2001).

In the study (Ajduković et al. 2007), EDX technique was used for characterization of composite biomaterial based on biphasic calcium phosphate (BCP) and poly-(D,L-lactide-co-glycolide) (DLPLG). Powdered polymer DLPLG was homogenized at appropriate ratio with addition of BCP into the suspension and then all samples were characterized by using EDX among other techniques. Because the morphology of HA/PLLA composite biomaterial is very sensitive, Ignjatović et al. (1999a, b) analyzed its surface microstructure by SEM coupled with an EDX detector system. In the study by Farzadi et al. (2014), the effect of Mg incorporation in the stoichiometric HA powders was examined. The effect of Mg incorporation on HA structure was studied on lattice constants, as well as the degree of crystallinity and the crystal size. Although XRD patterns suggested smaller crystallite size, such a result was still consistent with TEM results. TEM results showed that the change in size was not significant in Mg-doped HA in comparison to HA. XRD analysis confirmed that substitution of Ca with Mg in apatite lattice resulted in a change in lattice parameters. It has been shown that the Mg, C, and O elements are evenly distributed, by using SEM-EDX analysis.

1.4 Vibrational Spectroscopy

Vibrational spectroscopy is a technique that represents one of the most important spectroscopic methods for biomaterial characterization. This method is based on the comparative calculation and measuring of the characteristics of vibrational transitions (their energy, intensity, polarization) in mutual complementary spectra of the scattering and absorption of infrared (IR) light by the molecules in free or condensed (solid or liquid) form (Mitić et al. 2017). It is applicable to the biomolecular structure, but also to the molecular condensed state. Since diffraction methods have limited relevance in crystalline and non-crystalline form, vibrational spectroscopy techniques are of particular significance. Vibrational spectroscopic methods, Infrared (IR) spectroscopy and Raman spectroscopy (RS), are widely used for the characterization of calcium phosphates (CPs). CPs are present either as natural biological minerals (teeth, bone and ectopic calcifications) or as biomaterials (biocomposites, bioceramics, coatings) (Dorozhkin 2011).

Calcium phosphate (CP) based biomaterials, especially apatites, are complex structures affording many ion substitutions and vacancies, which may be poorly crystallized. Examination of these biomaterials by diffraction techniques does not always give information on fine structural details such as the presence and location of CO_3^{2-}, HPO_4^{2-} or OH^- groups. FTIR and Raman spectroscopy bring, in addition to structural characterization, very valuable information and may be used for a quantitative determination of a very limited amount of material. They may also yield information on the orientation of molecular species and crystals. In addition, vibrational microscopic techniques can also be used for investigations on biological tissues or materials, and they allow a rather accurate mapping of specific mineral characteristics (Ben-Nissan 2014).

1.4.1 Infrared (IR) Spectroscopy

Infrared (IR) spectroscopy is one of the vibrational spectroscopy methods. Devices that register the IR spectra in the mid-IR region (wavelength from 2.5 to 25 μm or wavenumber from 4000 to 400 cm^{-1}) are most commonly used. The variations of structurally characteristic groups and vibration bonds can be systematically monitored by Fourier transform infrared (FTIR) spectroscopy (Mitić et al. 2017). This is one of the methods that can provide an indirect evaluation of the synthesized calcium phosphate materials from TCP up to HA and bioceramics obtained from these materials (Dorozhkin 2009, 2013, 2015).

In chemical analysis of CP products, FTIR spectroscopy has numerous advantages. Among others, FTIR represents a very sensitive technique for determining phase composition, and also, a comparatively quick and easy everyday approach. The spectra of synthesized and commercial CP products can be analyzed. Considering that, the summary of IR spectrum tables for the characteristic absorption bands for CP chemical groups is created. FTIR method is more sensitive than XRD method, especially in determining the presence of new phases. The CP can be characterized by using FTIR and considering three spectrum parameters: location of absorption maximum, peak width, and absorption maximum of OH vibrations (Theophanides 2012). The presence of the characteristic absorption bands in the IR spectra, which represent atomic groups in the biomolecules, is important for rapid identification of characteristic molecular components of their primary and secondary structure (Eliades and Brantley 2001; Balac et al. 2010).

FTIR spectroscopy can provide molecular structure information about different composite biomaterials were used as bone substitutes and mineralized and non-mineralized connective tissues (Boskey and Camacho 2007; Vukelić et al. 2012; Mitić et al. 2014; Mendelsohn and Diem 2006; Ignjatović et al. 2014). IR spectroscopy coupled with FTIR microspectroscopic imaging has been widely applied to the analyses of different tissues (in health and disease). Spatially resolved FTIR data has provided insights into molecular changes that occur in diseases of different connective or collagen-based tissues, including osteoporosis, osteopetrosis, osteogenesis imperfecta and pathologic calcifications (Boskey and Camacho

2007; Mendelsohn and Diem 2006). FTIR spectroscopy imaging is a powerful tool for studying biomolecules and biological samples (Mitić et al. 2011, 2014). FTIR microspectroscopic imaging has significant advantages compared with many other imaging methods for the characterization of biomaterials, so the application of FTIR microspectroscopic imaging has been presented in a number of publications (Vukelić et al. 2012; Mitić et al. 2014; Mendelsohn and Diem 2006; Boskey and Camacho 2007).

In the studies (Ignjatović and Uskoković 2004a, b; Ajduković et al. 2005) authors have studied HA/PLLA bioresorbable-polymer composite biomaterials that can be used for the bone tissue reconstruction. HA/PLLA blocks were implanted intraperitoneally into the mice and after explantation blocks were studied by using FTIR spectroscopy. The HA/PLLA composite biomaterial before implantation was characterized by FTIR spectroscopy, according to absorption bands that arisen from HA and PLLA. The spectrum obtained 12 weeks after implantation of HA/PLLA composite biomaterial was characterized by the presence of earlier considered absorption bands of the HA/PLLA composite. A wide IR band at approx. 3420 cm^{-1} is dominant in this part of the IR spectrum and corresponds to the collagen IR spectrum with a wide absorption band with maximum at approx. 3420 cm^{-1}. In the study by Ignjatović and Uskoković (2004a, b), characteristic absorption bands were registered and defined by FTIR spectroscopy, so the formation of new functional groups and chemical compounds during the bone healing process by using biocomposite HA/PLLA was confirmed. Mitić et al. (2014) were confirmed, by using FTIR spectroscopy, that bone tissue composition was changed after glucocorticoid (GC) treatment used for induction of osteoporosis process. The influence of GCs on the composition of the mandible in experimental animals has been shown by already present IR bands and the appearance of new IR bands in the region of 3500–1300 cm^{-1}. Marković et al. (2011) have studied biological hydroxyapatite (BHA), extracted from human mandible bone, and carbonated hydroxyapatite (CHA), synthesized by the chemical precipitation method, by using FTIR and Raman spectroscopy. The FTIR and Raman spectroscopic studies showed that carbonate ions substitute both phosphate and hydroxyl ions in the crystal structure of BHA as well as in CHA, indicating that both of them are mixed AB-type of CHA. In the studies (Ignjatović et al. 2000, 2001a, b, c), chemically synthesized HA/PLLA composite biomaterial was analyzed by FTIR spectroscopy. The intensity decrease of IR absorption band at approx. 1760 cm^{-1} (C = O group from PLLA) indicates the resorption of used PLLA.

Adsorption of drugs on apatite surfaces, such as biomaterials based on CP, can be used to enhance a therapeutic activity. FTIR and Raman spectroscopy has been extensively used for understanding the interactions of biomolecule ionic end groups with apatite surfaces. For example, bisphosphonate (BP) adsorption on apatite in vitro or, potentially in vivo, was studied by using surface-enhanced Raman spectroscopy (SERS). Bisphosphonates molecules were utilized as successful antiresorptive agents. They have a high affinity for apatite surfaces and prevent mineral dissolution and bone resorption by inhibiting the activity of osteoclasts (Cukrowski et al. 2007; Pascaud et al. 2013). In the study by Affatato et al. (2012),

possible chemical changes across the section of the vitamin E-stabilized crosslinked acetabular cups based on PE in comparison with conventional standard and crosslinked PE-acetabular cups were investigated during wear by using FTIR spectroscopy.

The IR spectra observed for well-crystallized stoichiometric CPs, like apatite, correspond to the theoretical prediction although some anomalies can be noted. The IR spectra of tricalcium phosphates (TCP) and tetracalcium phosphates (TTCP) are particularly complex, and all predicted IR bands cannot be distinguished and identified due to superimposition (Ben-Nissan 2014).

There are several differences between the IR spectra of different CP phases, so their identification and, to some extent, their quantification are allowed. In the IR spectra of HA and related compounds, overtone and combination bands are the most frequently observed as a group of weak intensity bands. These IR bands are sometimes misinterpreted, but overtone and combination bands of protonated molecules are also used in near infrared (NIR) characterization of CPs. There are very broad and dissymmetric bands observed in the IR spectra of the amorphous CP. So, it can be concluded that there are several components (Ben-Nissan 2014).

Barbeck et al. (2015) have been investigated the effects of the addition of blood to the Algipore® on the severity of in vivo tissue reaction. FTIR spectroscopy was used for the chemical composition analysis of the bone substitute. The FTIR analysis data showed that the Algipore® material is mainly composed of HA with some carbonate content. The subcutaneous implantation model was then applied for up to 30 days to analyze the tissue reactions by using immunohistochemical, histochemical and histomorphometrical methods.

1.5 Matrix-Assisted Laser Desorption-Ionization Time of Flight Mass Spectrometry (MALDI-TOF MS)

Mass spectrometry (MS) is an instrumental method has been extensively used in chemistry and biochemistry for identification of organic compounds. The MS method allows detection of compounds by separating ions by their unique mass (i.e. mass to charge m/*e* ratios) using a mass spectrometer (Williams and Fleming 2007; Silverstein et al. 2005; Mitić et al. 2017). The MS method is based on the fact that every compound has a unique fragmentation pattern i.e. mass spectrum. The sample is ionized and the different sample ions are separated based on their differing masses and relative abundance. A typical mass spectrometer is comprised of these components: ion source, mass analyzer, detector and signal processor (Herbert and Johnstone 2003; Mitić et al. 2017). Matrix-assisted laser desorption-ionization time of flight mass spectrometry (MALDI-TOF MS) has become an important tool in the analysis of different biomolecules and polymers (Hendrick 2004; Montaudo and Lattimer 2002). The MALDI technique, which is based on UV absorbing matrix, is a soft ionization technique. Biomolecules and synthetic polymers have low

volatility and low thermal stability, which has limited the use of MS as instrumental method for characterization. These problems have been reduced through the development of MALDI-TOF MS, which allows the mass determination of biomolecules by ionization and vaporization without degradation.

The principle of this method is that focused laser beam is used, either in UV or IR region, which can "evaporate" the components of the solid phase. The resulting ions are injected into the tube, accelerated and ultimately detected. Their time of flight (TOF) is proportional to their mass. MALDI-TOF technique is well suited for the analysis of different polymers (synthetic or natural), macromolecules (e.g., proteins, polysaccharides, polynucleotides), as well as for the monitoring of therapeutic concentration of the drug.

De Miguel et al. (2014) analyzed HA, by using MALDI-TOF MS in order to yields a deeper understanding of bone targeted carriers. In the study by Bhandari et al. (2012), sCT-PEG-BP conjugates were synthesized and then characterized by MALDI-TOF MS. It has been shown that BP-mediated targeting of PEGylated sCT to the bone represents a new class of targeted antiresorptive compounds that has not previously been attempted. Vukomanović et al. (2011), used MALDI-TOF MS/ultra-performance liquid chromatography (UpLC) for characterization of the PLGA/HA core-shell nanostructures which are used as a carrier for antibiotic clindamycin. This method was also used to determine the amount of clindamycin released from the PLGA/HA after predetermined periods of time.

1.6 Atomic Absorption Spectrometry (AAS) and Inductively Coupled Plasma-Atomic Emission Spectrometry (ICP-AES)

AAS and ICP-AES are the most commonly instrumental techniques that have been used for elemental analysis. These techniques have a large variety of applications, thanks to their high specificity, multi-element capability and good detection limits. All kinds of dissolved samples can be analyzed (Rouessac and Rouessac 1994).

Atomic Absorption Spectrometry (AAS) is an instrumental technique that measures quantities of chemical elements present in the samples. The chemical element of interest, absorb a certain amount of radiation, in the form of light photons. Absorbed energy is measured by this method. The sample is then excited, and the corresponding spectrum of the chemical element is obtained. Absorbance (A) is directly proportional to the concentration of analyte absorbed for the existing set of conditions (Pungor 1995). With ordinary monochromators (filters or prisms) it is very difficult to accomplish the determination of the specific element of interest when it is present with other elements. Detection limits could be severely compromised, so the selection of the monochromator is crucial to obtain a linear calibration curve. A very important part of an Atomic absorption spectrometer is the

monochromator, because of the thousands of generated lines that needs to be separated. A diffraction grating as monochromator has commonly used in AAS spectrometers.

In the ICP-AES analysis, a plasma source is used to dissociate the sample into its constituent elements (atoms or ions). After exciting the constituents to a higher energy level, the specific elements emit light. An optical spectrometer separates this light in the characteristic wavelengths, so an emission spectrum is presented like a plot of the radiation intensity (y-axis) versus the wavelength (x-axis). There are many different transitions that are possible between the various excited states that imply complicated emission spectrum. This technique provides a quantitative analysis of the original sample (Farrukh 2012).

In the study by Thamaraiselvi et al. (2006), biomimetic HA was synthesized using calcium nitrate dihydrate and ammonium hydrogen phosphate dissolved in synthetic body fluid (SBF). Biomimetic HA resembles human bone in composition and structure. For the chemical analysis of Na and Mg in sintered powders, AAS technique was used. The presence of Mg and Na in the sintered sample showed that synthesized HA was biomimic in nature. In the study by Joschek et al. (2000), the properties of porous HA ceramics made of natural bone were investigated by ICP-optical atom emissions spectroscopy (OES) and flame atomic absorption spectroscopy (AAS), among the other techniques. The investigation of its chemical composition revealed small amounts of other inorganic compounds. ICP-OES and AAS results showed that there were trace amounts of Al, Fe, Mg, K, Si, Na, V and Zn, but it probably contains carbonated apatite also. Yoshidal et al. (2001) used AAS and ICP-AES to propose a concept that explains why carboxylic acids either adhere to or decalcify HA. ICP-AES was performed to determine the amounts of Ca and P extracted from HA plates by all acids and from HA powder. AAS was used to measure the dissolution rate of the calcium salts in their own respective acid solutions and water. Mitić et al. (2014) were examined the influence of GCs on the composition of the mandible in tested animals after recovery and healing phase by different instrumental methods, including AAS and ICP-AES. The increase of Ca, Mg and P content, determined by AAS and ICP-AES, and mineral part of bones was statistically significant in recovery and treatment phase that included calcitonin and thymus extract.

Acknowledgements The printing of this work is financed by EU project 543898-TEMPUS-1-2013-1-ES-TEMPUS-JPHES. Parts of the scientific works are supported by Ministry of Education, Science and Technological Development, Serbia, Project No. 41017.

References

Affatato S, Bracco P, Costa L, Villa T, Quaglini V, Ton A (2012) In vitro wear performance of standard, crosslinked, and vitamin-E-blended UHMWPE. J Biomed Mater Res A 100:554–560

Ajduković Z, Najman S, Lj Đorđević, Savić V, Mihailović D, Petrović D, Uskoković D (2005) Repair of bone tissue affected by osteoporosis with hydroxyapatite-poly-L-lactide (HAp-PLLA) with and without blood plasma. J Biomater Appl 20:179–190

Ajduković Z, Ignjatović N, Petrović D, Uskoković D (2007) Substitution of osteoporotic alveolar bone by biphasic calcium phosphate/poly-d, l-lactide-co-glycolide biomaterials. J Biomater Appl 21:317–328

Balać I, Bugarski B, Ćosić I, Dramićanin M, Đorđević D, Filipović N, Ignjatović N et al (2010) Biomaterijali. Institut tehničkih nauka SANU, Srbija

Barbeck M, Najman S, Stojanović S, Mitić Ž, Živković JM, Choukroun J, Kovačević P, Sader R, Kirkpatrick CJ, Ghanaati S (2015) Addition of blood to a phycogenic bone substitute leads to increased *in vivo* vascularization. Biomed Mater 10:055007

Ben-Nissan B (2014) Advances in calcium phosphate biomaterials. Chem Forensic Sci 8:246–284

Boskey A, Camacho NP (2007) FT-IR imaging of native and tissue-engineered bone and cartilage. Biomaterials 28:2465–2478

Chevaliera J, Taddeib P, Gremillarda L, Devillea S, Fantozzia G, Bartoloméc JF, Pecharromanc C, Moyac JS, Diazd LA, Torrecillasd R, Affatato S (2011) Reliability assessment in advanced nanocomposite materials for orthopedic applications. J Mech Behav Biomed Mater 4:303–314

Cukrowski I, Popovic L, Barnard W, Paul SO, van Roovyen PH, Liles DC (2007) Modeling and spectroscopic studies of bisphosphonates-bone interactions. The Raman, NMR and crystallographic investigations of Ca-HEDP complexes. Bone 41:668–678

De Miguel L, Noiray M, Surpateanu G, Iorga BI, Ponchel G (2014) Poly (γ-benzyl-L-glutamate)-PEG-alendronate multivalent nanoparticles for bone targeting. Int J Pharmaceut 460:73–82

Dorozhkin SV (2009) Calcium orthophosphate-based biocomposites and hybridbiomaterials. J Mater Sci 44:2343–2387

Dorozhkin SV (2011) Calcium orthophosphates occurrence, properties, biomineralization, pathological calcification and biomimetic applications. Biomatter 1(2):121–164

Dorozhkin SV (2013) Detailed history of calcium orthophosphates from 1770s till 1950. Mat Sci Eng C 33:3085–3110

Dorozhkin SV (2015) Calcium orthophosphate deposits: preparation, properties and biomedical applications. Mat Sci Eng C 55:272–326

Eliades G, Brantley WA (2001) Instrumental techniques for study of orthodontic materials. In: Brantley WA, Eliades T (eds) Orthodontic materials: scientific and clinical aspects. Thieme Verlag, Stuttgart D, pp 50–75

Farrukh MA (2012) Atomic absorption spectroscopy. InTech, Rijeka HR

Farzadi A, Bakhshi F, Solati-Hashjin M, Asadi-Eydivand M, Azuanabu Osman N (2014) Magnesium incorporated hydroxyapatite: synthesis and structural properties characterization. Ceram Int 40:6021–6029

Hari Bhandari K, Newa M, Chapman J, Doschak MR (2012) Synthesis, characterization and evaluation of bone targeting salmon calcitonin analogs in normal and osteoporotic rats. J Control Release 158:44–52

Hendrick N (2004) Introduction to Matrix-Assisted Laser Desorption/Ionisation Time-of-Flight Mass Spectrometry (MALDI TOF MS). Department King's College, London UK

Herbert CG, Johnstone RAW (2003) Mass spectrometry basics. CRC Press LLC, Florida USA

Ignjatović N, Uskoković D (2004a) Molecular spectroscopy analysis of the substitution of bone tissue by HAp/PLLA composite biomaterial. Spectroscopy 18:553–565

Ignjatović N, Uskoković D (2004b) Synthesis and application of hydroxyapatite/polylactide composite biomaterial. Appl Surf Sci 238:314–319

Ignjatovic N, Plavsic M, Miljkovic M, Zivkovic LJ, Uskokovic D (1999a) Microstructural characteristic of Ca-hydroxyapatite/poly-L-lactide based composites. J Microsc 196:243–248

Ignjatović N, Tomić S, Dakić M, Miljković M, Plavšić M, Uskoković D (1999b) Synthesis and properties of hydroxyapatite/poly-L-lactide composite biomaterials. Biomaterials 20:809–816

Ignjatović N, Plavšić M, Najman S, Savić V, Uskoković D (2000) Analysis of in vivo substitution of bone tissue by HAp/PLLA composite biomaterial with PLLA of different molecular weights using FTIR spectroscopy. Mater Sci Forum 352:143–150

Ignjatović N, Delijić K, Vukčević M, Uskoković D (2001a) Microstructure and mechanical properties of hot-pressed hidroxyapatite/poly-L-Lactide biomaterials. Key Eng Mater 192–195:737–740

Ignjatović N, Savić V, Najman S, Plavšić M, Uskoković D (2001b) A study of HA/PLLA composite as a substitute for bone powder, using FT-IR spectroscopy. Biomaterials 22: 571–575

Ignjatović N, Delijić K, Vukcević M, Uskoković D (2001c) The designing of properties of hydroxyapatite/poly-L-lactide composite biomaterials by hot pressing. Z Metallkd 92:145–149

Ignjatović N, Uskoković V, Ajduković Z, Uskoković D (2013) Multifunctional hydroxyapatite and poly (d, l-lactide-co-glycolide) nanoparticles for the local delivery of cholecalciferol. Mat Sci Eng C 33:943–950

Ignjatović N, Vranješ Djurić S, Mitić Ž, Janković D, Uskoković D (2014) Investigating an organ-targeting platform based on hydroxyapatite nanoparticles using a novel in situ method of radioactive ^{125}Iodine labeling. Mater Sci Eng, C 43:439–446

Joschek S, Nies B, Krotz R, Göpferich A (2000) Chemical and physicochemical characterization of porous hydroxyapatite ceramics made of natural bone. Biomaterials 16:1645–1658

Jovanović I, Jordović B, Petković M, Ignjatović N, Uskoković D (2008) Preparation of smallest microparticles of poly-L-lactide by modified precipitation method: influence of the process parameters. Microsc Res Techniq 71:86–92

Marković S, Veselinović L, Lukić MJ, Karanović L, Bračko I, Ignjatović N, Uskoković D (2011) Synthetical bone-like and biological hydroxyapatites: a comparative study of crystal structure and morphology. Biomed Mater 6:045005

Masanori H, Hiroki O, Hidehiko S, Masayuki K, Haruhisa O (2003) In vitro degradation of resin-dentin bonds analyzed by microtensile bond test, scanning and transmission electron microscopy. Biomaterials 24:3795–3803

Mendelsohn R, Diem M (2006) Vibrational microscopic imaging: towards molecular pathology. BBA Biomembr 1758:813–974

Merrett K, Cornelius RM, McClung WG, Unsworth LD, Sheardown H (2002) Surface analysis methods for characterizing polymeric biomater. J Biomat Sci Polym E 13:593–621

Mitić Ž, Stolić A, Stojanović S, Najman S, Ignjatović N, Nikolić G, Trajanović M (2017) Instrumental methods and techniques for structural and physicochemical characterization of biomaterials and bone tissue: a review. Mat Sci Eng C 79:930–949

Mitić Ž, Cakić M, Nikolić GM, Nikolić R, Nikolić GS, Pavlović R, Santaniello E (2011) Synthesis, physicochemical and spectroscopic characterization of copper(II)-polysaccharide pullulan complexes by UV-Vis, ATR-FTIR, and EPR. Carbohydr Res 346:434–441

Mitić Ž, Najman S, Cakić M, Ajduković Z, Ignjatović N, Nikolić R, Nikolić G, Stojanović S, Vukelić M, Trajanović M (2014) Spectroscopic characterization of bone tissue of experimental animals after glucocorticoid treatment and recovery period. J Mol Struct 1074:315–320

Montaudo G, Lattimer R (2002) Mass spectrometry of polymers. CRC Press LLC, Florida USA

Pascaud P, Gras P, Coppel Y, Rey C, Sarda S (2013) Interaction between a bisphosphonate, tiludronate, and biomimetic nanocrystalline apatites. Langmuir 29:2224–2232

Pungor E (1995) A practical guide to Instrumental analysis. CRC Press LLC, Florida USA

Rouessac F, Rouessac A (1994) Chemical analysis, modern instrumentation methods and techniques. Wiley, NY USA

Silverstein R, Webster F, Kiemle D (2005) Spectrometric identification of organic compounds, 7th edn. Wiley, NY USA

Sörensen TC, Arnoldi J, Procter P, Robioneck B, Steckel H (2013) Bone substitute materials delivering zoledronic acid: physicochemical characterization, drug load, and release properties. J Biomater Appl 27:727–738

Stojanović S, Mitić Ž, Miljković M, Rajković J, Trajanović M, Najman S (2016) SEM-EDX analysis of BIO-OSS® granules after incubation in cell culture medium. In: Lee WE, Gadow R, Mitic V, Obradovic N (eds) Proceedings of the III Advanced Ceramics and Applications Conference. Atlantis Press/Springer-Verlag Publishing, Chapter 18, pp 259–264

Thamaraiselvi TV, Prabakaran K, Rajeswari S (2006) Synthesis of hydroxyapatite that mimic bone minerology. Trends Biomater Artif Organs 19:81–83

Theophanides T (2012) Infrared Spectroscopy. Mater Sci. Eng Technol 6:135–160

Vučen SR, Vuleta G, Crean AM, Moore AC, Ignjatović N, Uskoković D (2013) Improved percutaneous delivery of ketoprofen using combined application of nanocarriers and silicon microneedles. J Pharm Pharmacol 65:1451–1462

Vukelić MĐ, Mitić ŽJ, Miljković MS, Živković JM, Ignjatović NL, Uskoković DP, Živanov-Čurlis JŽ, Vasiljević PJ, Najman SJ (2012) Apatite formation on nanomaterial calcium phosphate/poly-DL-lactide-co-glycolide in simulated body fluid. J Appl Biomater Function Mater 10:43–48

Vukomanović M, Mitrić M, Škapin SD, Žagar E, Plavec J, Ignjatović N, Uskoković D (2010) Influence of ultrasonic processing on the macromolecular properties of poly (d, l-lactide-co-glycolide) alone and in its biocomposite with hydroxyapatite. Ultrason Sonochem 17:902–908

Vukomanović M, Škapin SD, Poljanšek I, Žagar E, Kralj B, Ignjatović N, Uskoković D (2011) Poly(d, l-lactide-co-glycolide)/hydroxyapatite core-shell nanosphere. Part 2: Simultaneous release of a drug and a prodrug clindamycin and clindamycin phosphate. Colloid Surface B 82:414–421

Williams D, Fleming I (2007) Spectroscopic methods in organic chemistry, 4th edn. McGraw-Hill, London UK

Yoshidal Y, Van Meerbeek B, Nakayama Y, Yoshioka M, Snauwaert J, Abe Y, Lambr P (2001) Adhesion to and decalcification of hydroxyapatite by carboxylic acids. J Dent Res 80:1565–1569

An Overview of In Vitro Mechanical and Structural Characterization of Hip Prosthesis Components

S. Abdel Jaber and Saverio Affatato

Abstract Total Hip Replacement nowadays represents an established surgical technique that helps patients to restore a proper joint function and relieve them from pain. Research, laboratory results and improvement in the industrial testing of total hip replacement components brought important knowledge in the preclinical validation of prostheses. The preclinical validation of hip joint prostheses is a critical step for further development of new implant designs act to reduce the possibility of catastrophic failures and revision surgery. The objective of a preclinical test is to determine the wear rate and its dependence on the test conditions. In the field of wear analysis computational modelling may have the potential to help product design in minimizing wear. Best practice suggested is to enhance the data collection derived from physical wear testing through numerical modelling.

Keywords Hip prosthesis · Mechanical characterization · International guidelines · Wear testing

1 Introduction

Total Hip Replacement (THR) nowadays represents an established surgical technique that helps patients to restore a proper joint function and relieve them from pain. Hospital data analysis and orthopaedic registers give important information on the magnitude of this matter. Over 600.000 hip procedures are performed annually in Europe, while this number rises to 1.4 million in the worldwide panorama (Affatato 2012; Devine 2011; Eingartner 2007). Research, laboratory results and improvement in the industrial testing of THR components brought important knowledge in the preclinical validation of prostheses. The preclinical validation of hip joint prostheses is a critical step for further development of new implant designs

S. Abdel Jaber · S. Affatato (✉)
Medical Technology Laboratory, Rizzoli Orthopaedic Institute,
Via di Barbiano 1/10, 40136 Bologna, Italy
e-mail: affatato@tecno.ior.it

F. Zivic et al. (eds.), *Biomaterials in Clinical Practice*,
https://doi.org/10.1007/978-3-319-68025-5_22

act to reduce the possibility of catastrophic failures and revision surgery. This chapter has the purpose to shed light on the various approaches used during mechanical and in vitro testing of THR components, with particular insight to the various components of hip joint replacement into play.

2 From History to Modern Concepts of Total Hip Replacement

2.1 Hip Joint Anatomy

The human hip joint is an articulation formed between the coxal bone and the femur (Fig. 1).

It is also known as a ball-in-socket joint: the acetabulum constitutes the socket in with the hemispherical femoral hear is inserted. The hemispheric inner cavity called acetabulum is covered by a cartilage layer, except for the central region where the *ligamentum teres* grows. As counterpart the femoral head is covered by cartilage with except for the *fovea captis* i.e. the ligamentum teres insert. This particular ligament provides a strong connection between femoral head and acetabulum. The cartilage layers allow to distribute and reduce the compressive loads the articulation is subjected to during movement activity. The proximal epiphysis includes femoral head and neck and both greater and lesser trochanter. The whole acetabulum—femoral head and neck articulation is surrounded by the *articular capsule* that with the help of three ligaments (*iliofemoral, ischiofemoral and pubofemoral*) and the muscles ensures stability to the joint. In addition the inner core of the capsule is covered by the synovial membrane, necessary for the production of synovial fluid that provides the low friction condition between the counter-faces of acetabulum and femoral head (Thompson 2002; Gray et al. 1995; Traina et al. 2012).

2.2 Hip Joint Kinematics

The hip may be considered a three degrees of freedom joint, allowing three movement directions: flexion/extension, abduction/adduction and intra-extra rotation (Fig. 2).

Flexion is considered the movement that brings the thigh up towards the abdomen: normally the range of flexion goes from 0° (totally extended leg) to 130°. Extension is the movement in the opposite direction, with a range from 0 to 30. Abduction ranges between 0° and 45°, and is the movement that brings the leg

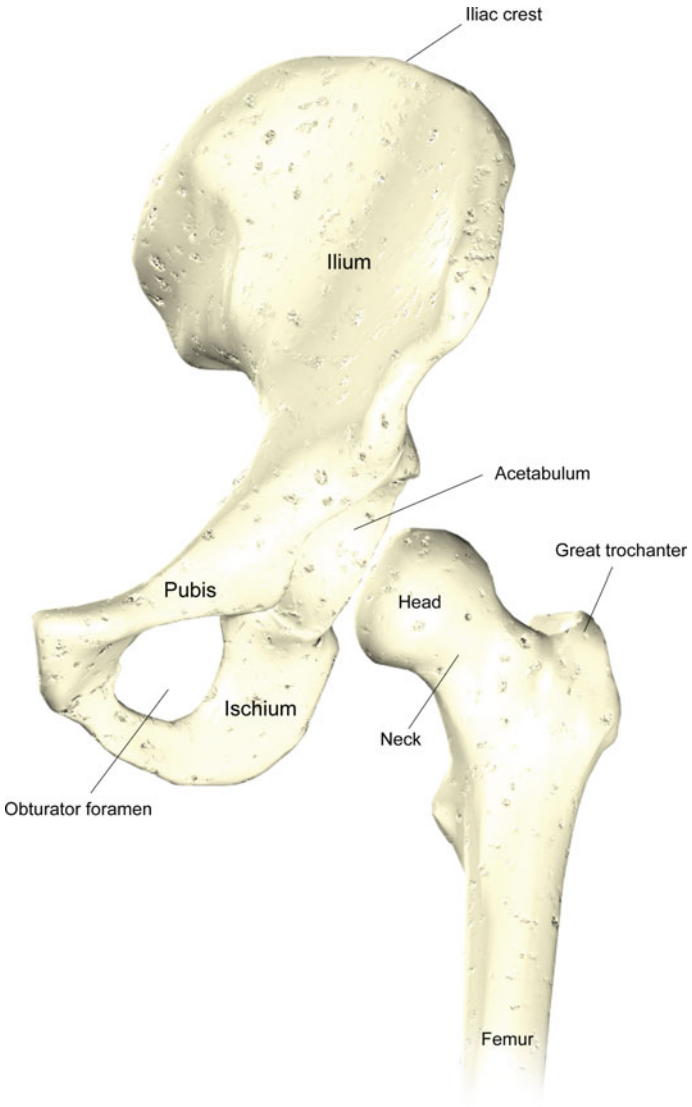

Fig. 1 Hip joint anatomy

away from each other. The opposite movement, adduction ranges from 0° to 30°. Hip joint allows also extra rotation for a maximum of 40° and intra rotation for 30°. The specific movement turns inward and outward the hip joint (Gray et al. 1995; Traina et al. 2012).

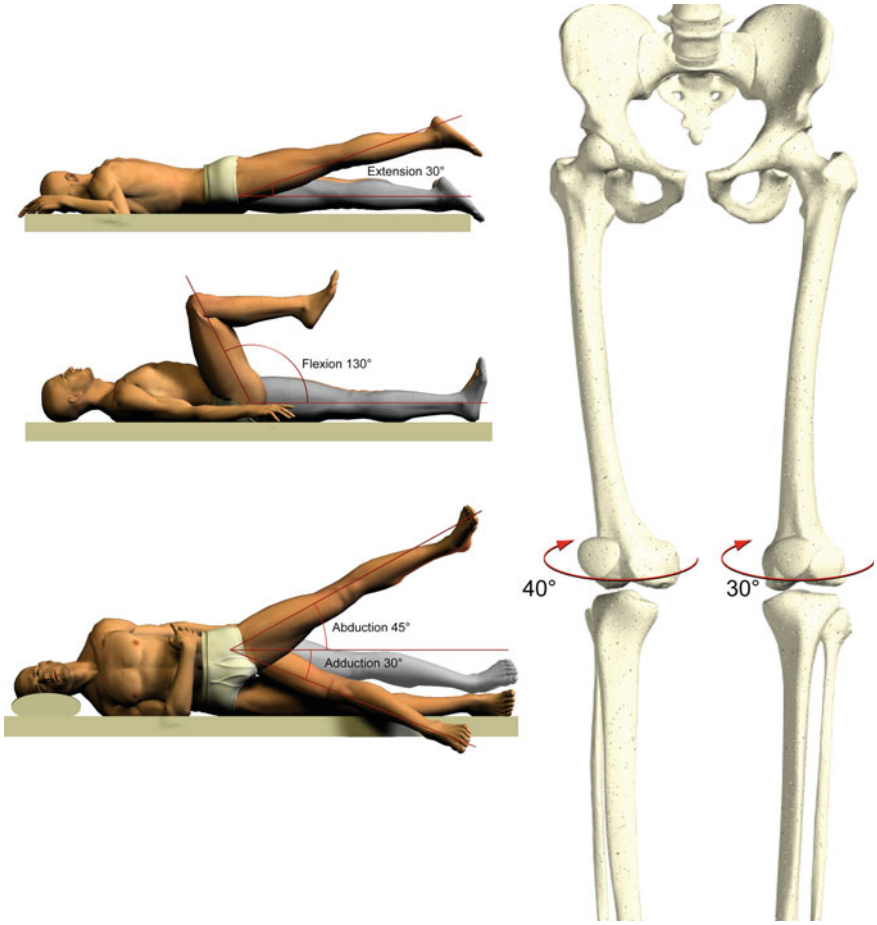

Fig. 2 Hip joint kinematics

3 Hip Joint Biomechanics

The hip joint allows withstanding the body weight and the dynamic loading through the various range of activities during life. The hip has a centre of rotation at the centre of the femoral head. The distribution of the body weight occurs through the body's centre of gravity (it moves distally and away from the supporting leg during a single leg stance allowing to the body weight to work as a lever arm (extending from the centre of gravity to the hip centre of rotation) (Delp et al. 1994; Canale and Beaty 2007; Traina et al. 2012). Abductor muscles help to counterbalance the body weight in order to avoid pelvic tilt of the supporting leg. Since the abductor muscle force lever arm [distance between the great trochanter and the centre of rotation

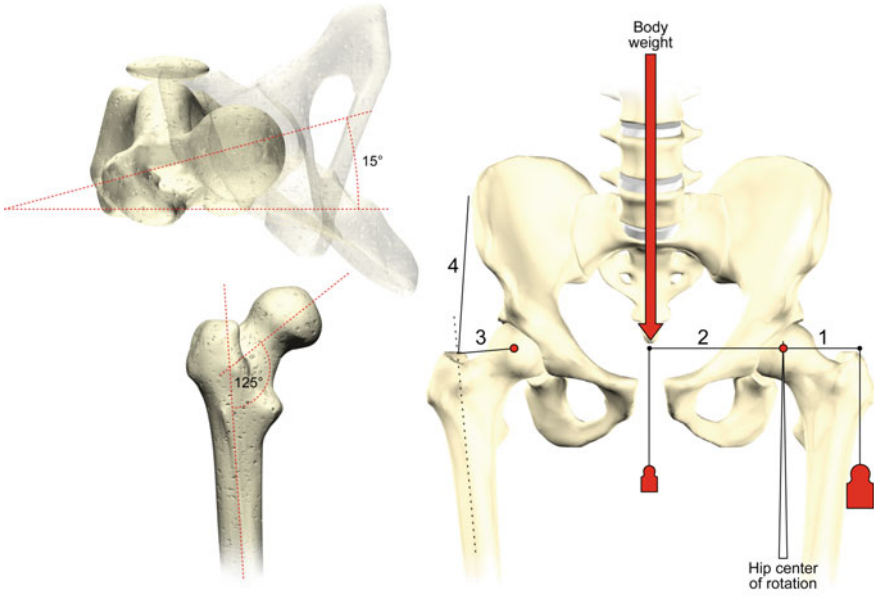

Fig. 3 Hip joint biomechanics. In particular, in the picture numbers *1* and *2* represent the force applied by the body weight, number *3* represent the offset, and the number *4* represent the abductor force

(COR) of the hip] is three times smaller than the body weight lever arm (body centre of mass- COR of hip distance), the hip joint must carry a load that is three times greater than the body weight during stance phase (Vasavada et al. 1994; Traina et al. 2009). This ratio increases when the subjects accomplish more demanding activities like running or jumping (Canale and Beaty 2007). The abductor muscle lever arm depends on the femoral offset, which directly depends on the femoral neck length and orientation (Fig. 3).

Neck-shaft angle is usually around 125°. If the value is greater, this forms a condition of a valgus angle; on the contrary the angle is defined *varus*. Femoral offset is influenced by the aforementioned conditions. By a fixed femur neck length, an increase in the neck shaft angle reduces the femoral offset and vice versa. Another important value is the ante-version angle, around 15° (Kapandji 1998), which is the angle between the long axis of the neck femur and a line tangent to the posterior femoral condyles (Argenson et al. 2007). Increased value of ante-version angle corresponds to reduce femoral off-set, thus a reduction of the abductor muscle force lever arm. Several pathologies may induce variations in the activity and forces exerted by abductor muscles, because of a reduction of the femoral offset angle, inducing then pelvic tilting and consequently limping (Noble et al. 2003; Argenson et al. 2007; Kapandji 1998; Traina et al. 2012).

4 History of Hip Joint Replacement

Hip Joint replacement is nowadays composed by a stem, a neck that shows a morse taper at its end that allows the press-fit union with the femoral head. Stems may have various shapes, surface coatings, orientations, dimensions depending on the application they were built for (cemented, cementless, short/long stemmed, etc.), that must ease particular physiological and anatomical aspects of the single patient. In addition to this variety, wider range of geometrical anatomical parameters is covered by modular necks in those prostheses where stem and neck are two different parts. The femoral head is metallic or ceramic while it's counterface, the acetabular liner that fits in the metallic acetabular component, has several material options, going from polymers (UHMWPE) to metals to ceramics.

Gluck tried first attempts of hip replacement in Germany in 1890, who used ivory to replace a femoral head. Various materials where used trying to divide the joint surfaces in order to avoid further degeneration of the joint. In the 1927 short stemmed prostheses made of ivory and featuring hemispherical head were proposed: these where later improved with metal reinforcement by the Judet brothers in the 1940s, involving acrylic materials and steel in a further improvement. This short stemmed version saw many failures, which brought to the long stem concept, in order to better ease the stresses through the femoral shaft (Knight et al. 2011; Gomez and Morcuende 2005; Learmonth et al. 2007). Sir John Charnley in the 1960s developed the first hip implant; it was a combination of a monoblock stainless steel stem (fixed with acrylic cement) and with a femoral head of 22.2 mm of diameter coupled with a Teflon (PTFE) acetabular cup (Rieker 2003). To solve inflammatory reactions in the joints and due to wear particles travelling via blood after first attempts using Teflon bearings, Sir Charnley adopted HDPE, and later ultra-high-molecular-weight polyethylene (UHMWPE).

In the 70s Co-Cr-Mo alloys replaced the first generation metal-on-metal coupling, due to better short term results (Pramanik et al. 2005). Ceramic-on-ceramic (COC) bearing hip prostheses was a solution when aseptic loosening and osteolysis emerged as a major problem in metal-on-polyethylene contact. Currently new materials, surface textures, and geometries are being researched. The materials that are most commonly used are titanium alloys, stainless steel, special high-strength alloys, composite materials, ceramics and UHMWPE (Ratner 2004) (Fig. 4).

The materials used need to satisfy important requirements for the use in the human body. In particular, they must have biocompatibility, high strength, high resistance to mechanical and chemical wear and fatigue resistance.

Since hip joint implant failure and revision surgery still constitute an open issue in the clinical panorama, component fatigue testing is performed before clinical use to validate the safety of the total joint replacements against fatigue failure. Both fatigue test prediction and tribological wear tests of various biomaterials are important steps in the development process of new implant designs. This process can aid the design of fatigue resistant components and to obtain quality control and further knowledge on wear mechanisms in joint prostheses.

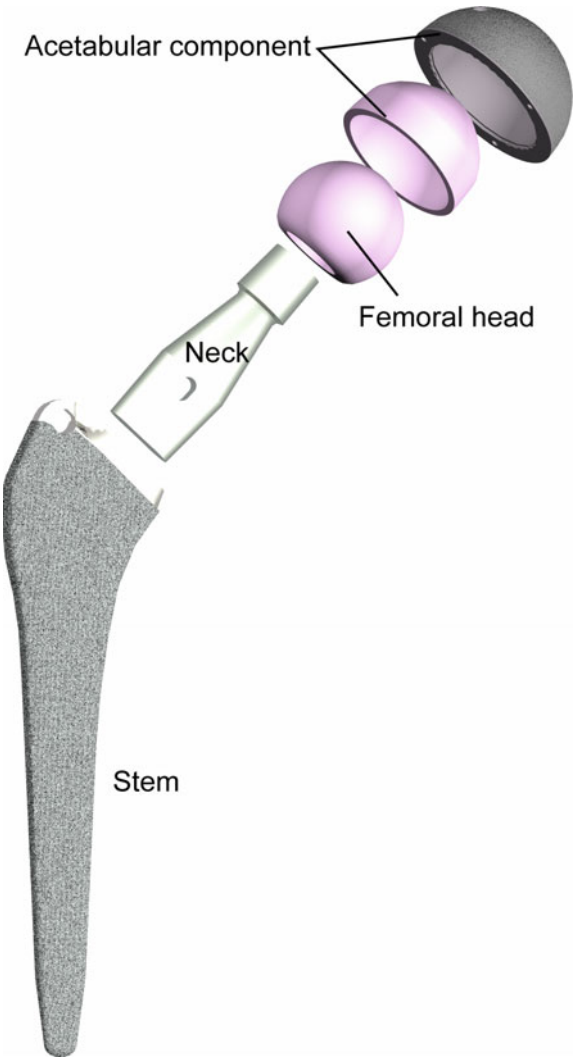

Fig. 4 Modern modular total hip joint replacement

5 Fatigue Testing

A test method for determining the endurance properties of stemmed femoral components of total hip joint prostheses is suggested by the international guidelines ISO 7206. These recommendations used under specified laboratory conditions, define the environments of testing such as the parameters and the requirements for the endurance limit of stemmed femoral components tested in accordance with this document. The value of the endurance limit test forces and the corresponding number of load cycles are specified. In particular:

- ISO 7206–1 Implants for surgery—Partial and total hip joint prostheses—Part 1: Classification and designation of dimensions. Provides a means of classification and standardizes the designation of dimensions for partial and total hip joint prostheses.
- ISO 7206–4 Implants for surgery—Partial and total hip joint prostheses—Part 4: Determination of endurance properties of stemmed femoral components.
- ISO 7206–6 Implants for surgery—Partial and total hip joint prostheses—Part 6: Determination of endurance properties of head and neck region of stemmed femoral components.
- ISO 7206–8 Implants for surgery—Partial and total hip joint prostheses—Part 8: Endurance performance of stemmed femoral components with application of torsion.
- ISO 7206–10 Implants for surgery—Partial and total hip-joint prostheses—Part 10: Determination of resistance to static load of modular femoral heads.

6 Femoral Stem Analysis

The ISO 7206-4 describes laboratory test method implemented for the determination of the endurance properties of stemmed femoral components of THR and partial hip joint replacement. This international standard disposes a set of conditions of testing and values of endurance limit forces and corresponding number of load cycles in order to keep into consideration the most important parameters that affect the hip stem component, aiming to reduce the complexity of the matter and to simplify the reproducibility of the setup. The load levels required as well as the minimum number of cycles without fracture of the implant are described by ISO 7206-8.

The fatigue test according to ISO 7206-4 simulates the dynamic loading of a hip stem during gait verifying the endurance properties of the complete femoral component under loading conditions that include a torsional component (Fig. 5).

Among the possible orientations of the load, the ISO 7206-4 determines that the application of the load has to be applied at 10° adduction and 9° in flexion. These test conditions in addition to the height level of the specimen embedding definition, are intended to represent the clinical situation where the prosthesis has become loosened proximally in the femur. Proximal loosening of the stem is presumed to simulate worst case conditions and are consistent with the clinical observations of stem failures (Baleani et al. 1999; Mollan et al. 1984; Ploeg et al. 1999; Røkkum et al. 1995; Wroblewski 1979; Ploeg et al. 2009).

6.1 Femur Neck and Head Analysis

ISO 7206-6 describes test methods for determining the endurance properties under specified laboratory conditions of the head and neck region of stemmed femoral

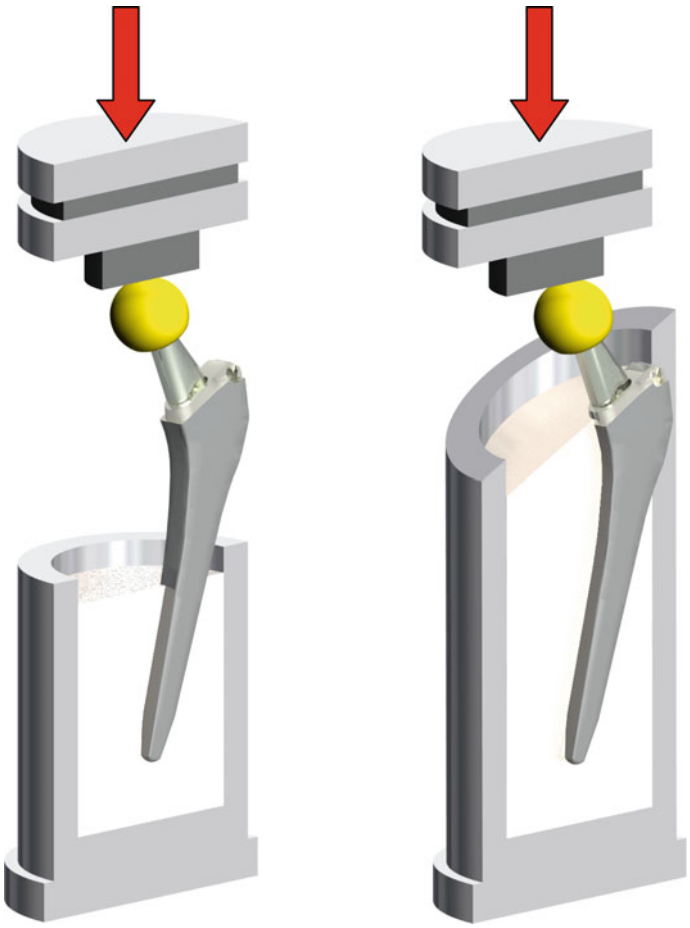

Fig. 5 ISO 7206 fatigue testing

components, in a well-ingrown stem condition, for booth modular and non-modular designs for various materials. This test allows analysing the neck region of the stem from the mechanical point of view, permitting also to draw conclusions concerning the fretting properties of modular fittings in this region. The test conditions in this part of ISO 7206 are intended to represent a correctly and firmly fixed prosthesis. Therefore, it should be noted that the tests in this part of ISO 7206 might not be representative of the most unfavourable clinical conditions. The ISO 7206-10 is followed for the femoral heads of partial or total hip-joint replacements of modular making (i.e. a head/neck conical taper connection). It defines methods of determining the load required, under specified laboratory conditions, to cause failure of the head (disassembly or fracture) under static axial loads. It applies to components made of metallic and non-metallic materials.

7 Standards for Wear Testing of THR

7.1 Wear and Total Hip Replacement

The objective of wear evaluation is to determine the wear rate and its dependence on the test conditions. Several factors affecting wear must be kept into consideration: load, range of motion, lubricant, etc. The biomaterials used in THR play an undoubted role in wear reduction and increase the length of prosthesis.

The prevalence of primary and revision total hip and knee arthroplasty increased steadily between 1990 and 2002. The need to solve or reduce wear problems is of primary importance. Tribology research leads to greater implant efficiency, better performance, fewer breakdowns, and significant savings. The purpose of research in tribology is, reasonably, the minimization and elimination of losses resulting from friction and wear at all levels of technology where the rubbing of surfaces is involved. There is no doubt that the biomaterials used play an important role, and as consequence in vitro tests for such materials are of great importance. Wear tests are conducted on materials and designs used in prosthetic hip implants to obtain quality control and acquire further knowledge about the tribological processes in joint prostheses. Considering that all new materials have to be tested before clinical trials, wear tests on new and improved materials play an important role in the pre-clinical validation phase. These machines can also be used as research tools allowing experiments to be conducted in a controlled environment, where variables such as surface roughness and scratching could change and the effects measured. Typically, these apparatus are called simulators, and, while there is no absolute definition of a joint simulator, its description as a mechanical rig used to test a joint replacement, under conditions approximating those occurring in the human body, is acceptable (Affatato et al. 2008). Simulator tests, moreover, can be used to conduct accelerated protocols that replicate/simulate particularly extreme conditions, thus establishing the limits of performance for the material (Affatato et al. 2016a, b, c; Affatato et al. 2012). In other words, a hip joint wear simulator (a schematic picture is shown in Fig. 6) is any device, which re-produces the wear phenomenon in a simplified manner (Affatato et al. 2008). In order to accomplish this, a hip joint wear simulator will typically apply a set of motions and loads and a lubricant that, in combination, create tribological conditions comparable, but not necessarily identical, to those occurring in vivo (Dowson 1998).

7.2 International Guidelines

Artificial joints are medical devices and in order to receive the CE mark or approved by the FDA before they can be marketed in the Europe or in the United States respectively, they must be analysed according to the international standard ISO 14971(ISO-14971, 2007).

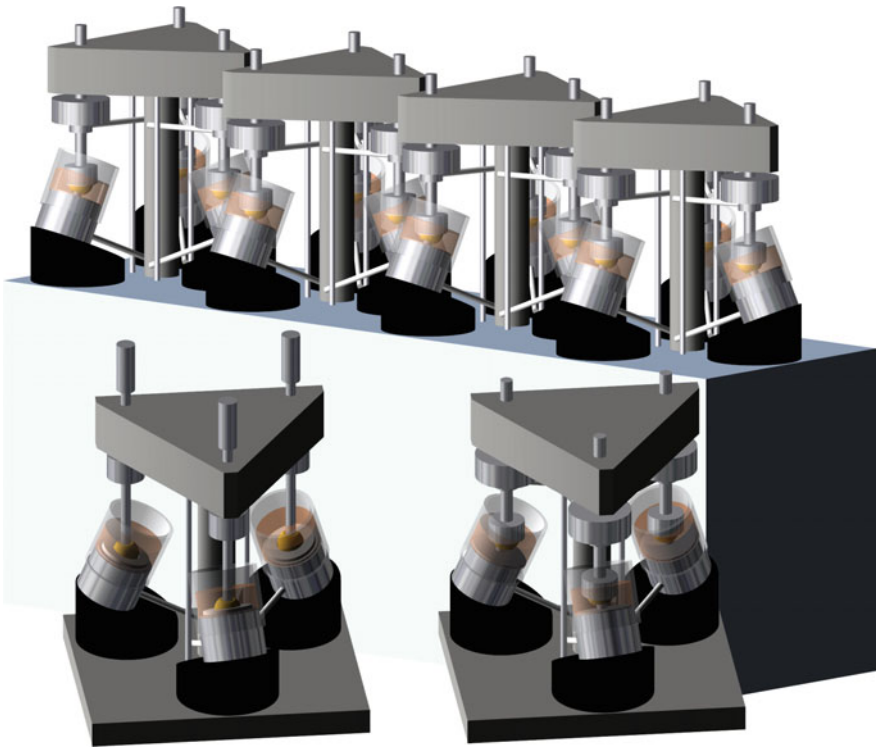

Fig. 6 Hip simulator in anatomical and up-side down configurations

Specific recommendations about to approach the methods of wear assessment and the applied kinematics are detailed by the ISO guidelines since 2000. In particular, these guidelines identify three degrees of freedom (abduction/adduction, inward/outward rotation, and flexion/extension) and axial load obtained from gait analysis. The aim of this normative is to specify the kinematics between the articular components relatively to the relative angular movements, the pattern of the applied force, frequency and duration of testing, sample configuration and test environment. In particular:

- ISO 14242–1 Implants for surgery—Wear of total hip-joint prostheses—Part 1: Loading and displacement parameters for wear-testing machines and corresponding environmental conditions for test.
- ISO 14242–2 Implants for surgery—Wear of total hip joint prostheses—Part 2: Methods of measurement.
- ISO 14242–3 Implants for surgery—Wear of total hip joint prostheses—Part 3: Loading and displacement parameters for orbital bearing type wear testing machines and corresponding environmental conditions for test.

In particular, the ISO 14242 parts 1 and 2 suggest performing a hip wear test using an axial load having a double peak profile with a peak intensity of 3000 N. Moreover, the flexion/extension angular movement is a simple sinusoid between 25° and −18°, while the abduction/adduction is a sinusoid between 7° and –4°, and the inward/outward rotation work in a range between 2° and −10°.

Many studies take into account different load profiles for their laboratory tests to investigate substantial differences in final results. The first simulations were characterized by sinusoidal load profiles, with variable peak loads, even if the real forces between the ball and the cup were known. A broad debate, however, is still open about weather simplistic load profiles can reproduce physiological wear patterns and weight loss, thus reducing mechanical sophistication and managing competences. A lot is known about UHMWPE, the problems associated to THR wear, its mechanical properties, and wear response, but modest information is available on in vivo loads and kinematics responsible for the wear of the insert. Therefore, the scientist are focussing their attention in that so-called "*patient's daily activities*" (Abdel Jaber et al. 2014; 2015a, b; Battaglia et al. 2014). In these new approaches of simulation is recreated a *worst-case scenario* for testing, as well as for implant design. Measurements providing activity-specific loading would help to suggest guidelines for test conditions in order to evaluate implant fixation and polyethylene wear (Abdel-Jaber et al. 2016).

8 Numerical Analysis on THR

A novel method for preclinical testing is computational modelling through Finite Element numerical models. Over the last two decades this mathematical and computational technique has been widely developed also in the analysis of medical devices and human bone and tissues. Regulations in this field do not yet exist, and the findings that this numerical model affords are usually used for experimental data validation or corroboration and for foresee paths in which the experimental analysis might find a development for improvement. Researchers use numerical modelling during preclinical validation studies also because of the economic impact that experimental analysis represents and sometimes for the impossibility to create certain in vitro studies.

Failure prediction of orthopaedic implants is a very articulated matter due to the several parameters involved into play. Complex geometries and loading patterns into play, various material properties of biological tissues in an environment that is constantly adapting to the boundary conditions that an implant determines once implanted (Viceconti et al. 2009; Arunajadai et al. 2004; Affatato 2012). The concern with whether a model and its results are "correct" is of great importance for developers and users as well as for people affected by decisions based on such models. Model validation is usually defined to mean "substantiation that a computerized model within its domain of applicability possesses a satisfactory range of

accuracy consistent with the intended application of the model" (Schlesinger et al. 1979). If we translate this aspect into a hip prosthesis we obtain an extension of risk analysis or, in agreement with Viceconti et al. "a systematic approach for the preclinical validation of joint prostheses" (Viceconti et al. 2009). Usually, such scenario is associated with the identification of a failure mode or a combination of failure modes. In this way, each failure mode is associated with its driving biomechanical parameters (either numerical or experimental). Once the risk analysis is completed, the information can be used in structured preclinical validation protocols to support the design of new devices (Martelli et al. 2011). Bone biomechanics have been extensively investigated in the past both with in vitro experiments and numerical models. Both experiments and numerical models experience limitations relative to their accuracy and their respective fields of application. In in vitro experiments, the use of numerical models should improve the most relevant loading configurations among a number of motor tasks that cannot be replicated in vitro. Acceptable simplifications might be identified and a variety of different conditions (material properties, interface, etc.) that would require enormous experimental effort for the in vitro simulation, could be explored speedily (Cristofolini et al. 2010).

In the field of wear analysis computational modelling may have the potential to help product design in minimizing wear. To this matter are associated various limitations which must be kept in consideration, since a huge number of variables are into play and there are still many unknown aspects in wear and tribology of total joint replacements. Best practice suggested is to enhance the data collection derived from physical wear testing through numerical modelling (Strickland and Taylor 2014).

Acknowledgements The author's whish to thank Luigi Lena (Rizzoli Orthopaedic Institute) for his help for drawing these original figures.

References

Abdel Jaber S et al (2014) In vitro effects on mobile polyethylene insert under highly demanding daily activities: stair climbing. Int Orthop

Abdel Jaber S et al (2015a) In vitro effects on mobile polyethylene insert under highly demanding daily activities: stair climbing. Int Orthop 39(7):1433–1440

Abdel-Jaber S et al (2015b) Wear simulation of total knee prostheses using load and kinematics waveforms from stair climbing. J Biomech 48(14):3830–3836

Abdel-Jaber S et al (2016) A new protocol for wear testing of total knee prostheses from real joint kinematic data: towards a scenario of realistic simulations of daily living activities. J Biomech

Affatato S (2012) Testing of Artificial hip joints. Encycl Tribol

Affatato S et al (2008) Tribology and total hip joint replacement: current concepts in mechanical simulation. Med Eng Phys 30(10):1305–1317

Affatato S et al (2012) In vitro wear performance of standard, crosslinked, and vitamin-E-blended UHMWPE. J Biomed Mater Res, Part A 100(3):554–560

Affatato S, Salvatore J et al (2016a) Does cyclic stress and accelerated ageing influence the wear behavior of highly crosslinked polyethylene? J Mech Behav Biomed Mater 59:418–429
Affatato S, De Mattia JS et al (2016b) Wear performance of neat and vitamin E blended highly cross-linked PE under severe conditions: the combined effect of accelerated ageing and third body particles during wear test. J Mech Behav Biomed Mater 64:240–252
Affatato S, Freccero N, Taddei P (2016c) The biomaterials challenge: a comparison of polyethylene wear using a hip joint simulator. J Mech Behav Biomed Mater 53:40–48
Arunajadai SG et al (2004) Failure mode identification through clustering analysis. Qual Reliab Eng Int 511–526
Argenson J-NA et al (2007) Anatomy of the dysplastic hip and consequences for total hip arthroplasty. Clin Orthop Relat Res 465:40–45
Baleani M, Cristofolini L, Viceconti M (1999) Endurance testing of hip prostheses: a comparison between the load fixed in ISO 7206 standard and the physiological loads. Clin Biomech 14:339–345
Battaglia S et al (2014) A new protocol from real joint motion data for wear simulation in total knee arthroplasty: stair climbing. Med Eng Phys 36:1605–1610
Canale ST, Beaty JH (2007) Campbell's operative orthopaedics, 11th edn. Mosby Elsevier, Philadelphia
Cristofolini L et al (2010) Mechanical testing of bones: the positive synergy of finite-element models and in vitro experiments. Philos Trans Series A Math Phys Eng Sci 368:2725–2763
Delp SL, Komattu AV, Wixson RL (1994) Superior displacement of the hip in total joint replacement: effects of prosthetic neck length, neck-stem angle, and anteversion angle on the moment-generating capacity of the muscles. J Orthop Res 12(6):860–870
Devine J (2011) Developing PEEK polymer as a bearing material for implants. In Medical device and diagnostic industry
Dowson D (1998) History of tribology, 2nd edn. p 2017
Eingartner C (2007) Current trends in total hip arthroplasty. Ortopedia Traumatologia Rehabilitacja 1(16):8–14
Gomez PF, Morcuende JA (2005) Early attempts at hip arthroplasty–1700s to 1950s. Lowa Orthop J 25:25–29
Gray H, Williams PL, Bannister LH (1995) Gray's anatomy: the anatomical basis of medicine and surgery, 38th edn. Churcill Livingstone, New York
Kapandji IA (1998) The physiology of joints. Volume 2: lower Limb, 5th edn. Churchill Livingstone, New York
Knight SR, Aujla R, Biswas SP (2011) Total hip arthroplasty—over 100 years of operative history. Orthop Rev 3(e16)
Learmonth ID, Young C, Rorabeck C (2007) The operation of the century: total hip replacement. Lancet 370(9597):1508–1519
Martelli S et al (2011) Extensive risk analysis of mechanical failure for an epiphyseal hip prothesis: a combined numerical-experimental approach. Proc Inst Mech Eng Part H J Eng Med 225:126–140
Mollan RA et al (1984) Failure of the femoral component in the Howse total hip arthroplasty. Clin Orthop Relat Res 142–147
Noble PC et al (2003) Three-dimensional shape of the dysplastic femur: implications for THR. Clin Orthop Relat Res 27–40
Ploeg HL et al (1999) Fatigue strength testing of hip stems with statistical analysis. Bio-Med Mater Eng 9:243–263
Ploeg HL, Bürgi M, Wyss UP (2009) Hip stem fatigue test prediction. Int J Fatigue 31:894–905
Pramanik S, Argawal AK, Rai KN (2005) Chronology of total hip joint replacement and materials development. Trends Biomater Artif Organs 19(1):15–26
Ratner BD (2004) Biomaterials science: an introduction to materials in medicine, 2nd edn. Academic press, Elsevier
Rieker CB (2003) Tribology in total hip arthroplasty—historical development and future trends. Centerpulse Orthopaedics Ltd

Røkkum M et al (1995) Stem fracture with the Exeter prosthesis. 3 of 27 hips followed for 10 years. Acta Orthop Scand 66:435–439

Schlesinger S et al (1979) Terminology for model credibility. SIMULATION 32:103–104

Strickland M, Taylor M (2014) Joint wear simulation. In: Jin Z (ed) Computational modelling of biomechanics and biotribology in the muscoloskeletal system: Biomaterials and tissues, Woodhead Publishing, Cambridge, pp 39–76

Thompson JC (2002) Netter's Concise Atlas of Orthopaedic Anatomy, 1st edn. Saunders Elsevier, Philadelphia

Traina F et al (2009) Sex diffenrences in hip morphology: is stem modularity effective for total hip replacement? J Bone Joint Surg Am 91(6):121–128

Traina F, De Fine M, Affatato S (2012) Anatomy of the hip and suitable prostheses. In: Affatato S. (ed) Wear of orthopaedic implants and artificial joints, Woodhead Publishing, Cambridge, pp 93–114

Vasavada AN et al (1994) Compensating for changes in muscle length in total hip arthroplasty. Effects on the moment generating capacity of the muscles. Clin Orthop Relat Res 302:121–133

Viceconti M et al (2009) Pre-clinical validation of joint prostheses: a systematic approach. J Mech Behav Biomed Mater 2(1):120–127

Wroblewski BM (1979) The mechanism of fracture of the femoral prosthesis in total hip replacement. Int Orthop 3:137–139

Characterization of Mechanical Properties of Metal Biomaterials

Milija Kraišnik, Aleksija Đurić and Miroslav Milutinović

Abstract Of all the biomaterials which are used today for the production of implants, instruments and devices in different medical applications, metal materials take a dominant position. The superiority in relation to other biomaterials is mostly the consequence of extraordinary mechanical properties, which especially occur under the influence of high external loads. Because of that, the use of metal biomaterials is focused on the production of implants and elements for the fixation of broken limbs and the replacement of parts of damaged bones and/or joints. There is a significant application of metal biomaterials in the area of stomatology as well. The paper emphasizes the significance of mechanical characterization of metal biomaterials. In that, there is a presentation of a great number of standard procedures which are applied for the determining of mechanical properties and identification of microstructural defects. At the end, for three groups of metal materials (stainless steels, Co–Cr alloys and Titanium and its alloys), the concrete values are presented for some mechanical properties which may have a decisive influence to application opportunities. The paper presents a contribution to the discussion of mechanical characterization problems, what is directly related to the selection of metal biomaterials for different medical applications, especially at surgical and orthopaedic interventions.

Keywords Metal biomaterials · Mechanical properties · Characterization methods

1 Introduction

Biomaterials are a special group of engineering materials intended for the production of components which are in interaction with biological systems (Agrawal et al. 2014). Because of their extraordinary properties, they have been found a wide

M. Kraišnik (✉) · A. Đurić · M. Milutinović
University of East Sarajevo, Faculty of Mechanical Engineering,
Vuka Karadžića 30, 71123 East Sarajevo, Bosnia and Herzegovina
e-mail: milijakraisnik@yahoo.com

F. Zivic et al. (eds.), *Biomaterials in Clinical Practice*,
https://doi.org/10.1007/978-3-319-68025-5_23

application in different areas, primarily in medicine and stomatology. In the general case, biomaterials are divided into metal, polymer, ceramic and composite materials (Davis 2003; Park and Kim 2003). Particular or combined, the named types of materials are dominantly used today for making of implants and medical instruments and devices (Siraparapu et al. 2014).

Metal biomaterials are classic representatives of biomaterials and for sure have been in use for the longest period of time in various surgical disciplines. Chronologically observed, the first efforts of applying metal components for medical purposes were related to the implants for bone fracture fixation (Lane 1895). Then, in 1922, in the USA, the first operation of replacing the damaged hip joint with the artificial one was performed (Reynolds and Tansey 2007). Later on, the medical applications of metal biomaterials have been developing significantly, so that today, besides their initial purpose, they have some other very significant clinical uses at cardiovascular operations, replacement and reparation of hard tissues (knee, shoulder, hip, tooth etc.), making of different orthopaedic and teeth prosthetic devices or surgical instruments etc.

For a certain metal material to be used for biomedical purposes, it must be biocompatible with the surrounding tissues and nontoxic. If the given requirements are not met, the materials cannot be used regardless of its superior design from the engineering aspect. Also, metal biomaterials must have a high corrosion resistance which does not allow the development of corrosion when they are in touch with live tissues, as well as an extraordinary electrical and thermal conductivity. Besides that, depending on purpose, there are also specific requirements which metal biomaterials must meet, such as the mechanical continuity with the surrounding tissue, low value of elasticity module or high wear resistance at the contact places (i.e. artificial joints). In that, the commercial aspect of their production must not be neglected as well.

A significant criterion in the selection of metal biomaterials for specific surgical requirements is the discussion of chemical composition, microstructure or physical properties, such as density, thermal conductivity, thermal propagation etc. (Hermawan et al. 2011). However, from the engineering approach, it is also very important that the selected biomaterial may accomplish the requirements of external load. This ability of a material, which is under a direct influence of mechanical characteristics, is called bifunctionality and is related to the possibility of performing a required function in a very difficult environment, such as a human body (Gotman 1997). Some information that can contribute to an adequate selection of biomaterials have been disclosed in Tanikić et al. (2012), thus for example: during a day human bones are loaded with the strain of about 4 MPa, while in particular body parts (i.e. tendons and ligaments) short strengths can be generated with the size of 40–80 MPa, a healthy hip is exposed to an average load which can be even up to 3 times bigger than the human weight, while at a jump it must be able to amortize instantly a significantly high load (extremely up to 10 times bigger that the weight). If it is taken into account that during different daily activities of a human there are multiple cyclic repetition of loads (it is estimated that one joint of a hand

finger is annually exposed to 10^6 of cycles) (Tanikić et al. 2012), it is clear that the adequate selection of biomaterials must be approached very studiously.

The previously stated indicators undoubtedly indicate to the fact that during the exploitation metal biomaterials are exposed to the activity of static, dynamic and impact loads, due to which the development and accumulation of various microstructural damages occur (Teoh 2000). Actually, in a greater number of implants and medical devices, the mechanical behaviour of metal biomaterials can be of crucial importance for their application opportunities (Roeder 2013; Agrawal et al. 2014). Because of that, it is of essential importance to put efforts into an accurate identification of mechanical properties of metal biomaterials. The first step on the path towards the reaching of the named goal is the knowing of standard procedures for mechanical characterization and identification of microstructural defects.

2 Methods for Characterization of Mechanical Properties

Mechanical properties are quantified parameters which enable the analysis of behaviour of metal biomatters under the activity of different external loads and exploitation conditions. Depending on the permeability, way and the duration of the load activity, as well as on the temperature on which the testings are performed, there is a great number of standard procedures for determining mechanical properties. Pursuant to the speed of load change, testings can be static, dynamic and impact. Static testings are characterized by a calm or slow increase of load, not faster than 10 MPa/s. Actually, in the named testing circumstances, the load changes have a quasistatic character. At dynamic testings, there are fast, and in some cases instantaneous (impact) load changes, both in terms of intensity and direction of activity. The direction and course of the load activity are extremely important factors in mechanical characterization of biomaterials. Due to that, during the static testings biomaterials can be tested on: tensioning, pressure, bending, torsion, shearing, buckling, etc. (Fig. 1).

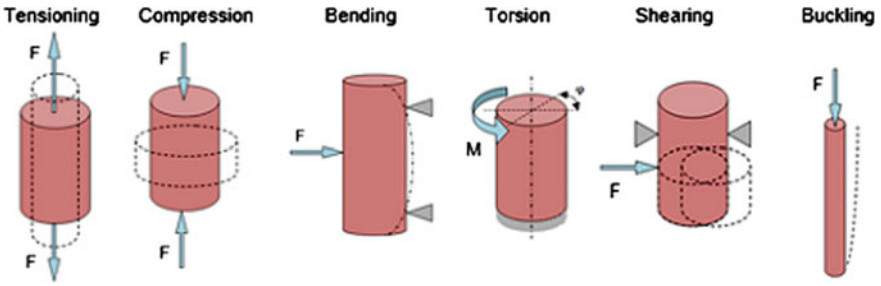

Fig. 1 Typical loads

Temperature is also a significant factor of the behaviour of a material under the activity of external loads. Because of that, mechanical testings are realized in different thermal conditions—room, increased or decreased temperature. To perform a complete characterization, it is necessary to observe the results of mechanical testings in the function of the testing duration (i.e. time) as well, because the experience has shown that the same biomaterial acts differently under the activity of a short-term load in relation to a long-term load.

Generally, all the methods for the determination of mechanical characteristics of metal biomaterials are divided into destructive and non-destructive methods. The division is done depending on the degree of damaging the microstructure of samples after the testing.

2.1 Mechanical Destructive Testings

By applying the destructive testings, there is a significant violation of microstructural integrity of a material, what often results in fracture. Although they are of older date, they are still the fundamental approach in determining mechanical characteristics. This chapter will present a few standard methods which are used for determining the resistance of biomaterials under the influence of external loads. The methods are used identically for the characterization of other metal materials as well, and also, with minor modifications, for other materials (i.e. polymers, wood, paper etc.).

2.1.1 Tensile Testing

Tensile testing is the most important and most often used method of characterization of mechanical properties of biomaterials. For the testings, the most often used materials are the ones with round, square and rectangular cross-section, but other shapes can be used as well. The testings are realized on special testing machines, in such a way that the biomaterial samples are getting loaded with external tension load up to the complete destruction. During the testing, the value of generated stress is determined depending on the deformation of the length of the sample (Fig. 2).

On the basis of the stress-strain curve (σ-ε), the most significant properties of resistance of metal biomaterials are determined: upper yield strength—R_{eH}, lower yield strength—R_{eL} and tensile strength—R_M. For a more complete characterization, elastic limit—σ_e, proportional limit—σ_p, and Young's modulus of elasticity-E are determined as well.

Yield Strength is the strength at which great plastic deformations start in biometals, with a small increase of external load. Due to that, yield strength can also be defined as a limit strain which marks the transition of elastic area into plastic area of material behaviour. Numerical values of yield strength present the quotient of

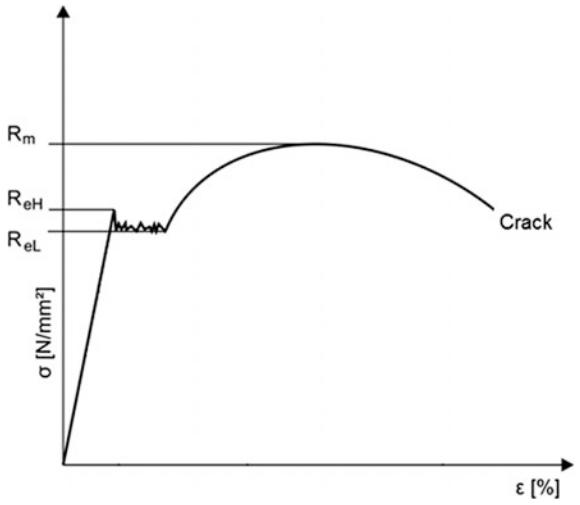

Fig. 2 Stress-strain curve

force $F_{eH/L}$ at which the plastic deformation starts, and the initial surface of the cross-section of the tested sample S_0:

$$R_{eH/L} = \frac{F_{eH/L}}{S_0} \tag{1}$$

In some biometals, the transition from the elastic area into plastic happens gradually, so that the yield strength cannot be determined from the diagram (σ-ε). In such cases, ***technical (conventional)*** **yield strength** is determined, presenting the strength at which plastic deformations of 0.2% occur in the material:

$$R_{e0.2} = \frac{F_{e0.2}}{S_0} \tag{2}$$

Ultimate Tensile Strength is a maximal resistance by which a biometal can be loaded in such a way that a fracture does not occur. It is determined on the basis of the following formula:

$$R_M = \frac{F_{MAX}}{S_0} \tag{3}$$

Tensile strength is an extremely important mechanical characteristic of all biometals, because it enables the prediction of their behaviour and allow a direct estimation of other mechanical characteristics.

Elastic Limit is a maximal tension which does not cause plastic deformations in a biometal. Because of the difficulties related to accurate determining, it is often defined as a tension which causes minor plastic deformations in biometal, from 0.005 or 0.01%. During the exploitation, it must be ensured that the strengths in an

implant do not go beyond the elastic limit values. However, it must be taken into account that the final forms of implants are most often obtained by a plastic deformation process, where operating strengths are significantly bigger than the elastic limit. Due to that, the elasticity limit has a significant role in the selection of biometals, especially for orthopaedic and dental implants.

Proportional limit is the biggest tension in a biometal which allows the linear dependence between the tension and deformations. A precise determining of the proportional relationship violation is related to the accurate identification of stress and strain during the testing.

Young's Modulus of Elasticity is the basic characteristic of every biometal and it presents the measure of rigidity or resistance to deformation. In the area of proportionality ($\sigma < \sigma_p$) it presents the slope of the curve $\sigma = f(\varepsilon)$ and is defined by the relation between the tension and unit elongation:

$$E = \frac{\sigma}{\varepsilon}, \tag{4}$$

which presents Hooke's law.

Module of elasticity is closely related to the energy of interatomic forces in a material, what is directly related to the melting temperature. The binding forces and module of elasticity are bigger in metal biomaterials with a bigger melting temperature. Besides that, the module of elasticity values also depend on microstructural condition and are mostly bigger than the human tissue, what may affect the healing quality and period of a patient.

Besides the resistance properties, for a mechanical characterization of biomaterials, deformation properties are also used: elongation (unit elongation ε and elongation with breaks A), and the contraction with breaks of the cross-section and tested sample Z.

Elongation is the most important property of deformation. Unit elongation is determined on the basis of the formula (5) and presents the relation of the current elongation (ΔL) and the undeformed referent length of the sample (L_0):

$$\varepsilon = \frac{L \quad L_0}{L_0} = \frac{\Delta L}{L_0} \tag{5}$$

Elongation with breaks is mostly used for the characterization of metal biomaterials, which presents the unit elongation at the moment when the sample is broken:

$$A = \frac{L_f \quad L_0}{L_0} \tag{6}$$

Reduction of area is the narrowing of the cross-section at the place when the sample fractured. It is determined pursuant to the model (7), where S_0 is the initial surface of the cross-section, and S is the cross-section surface at the place where the sample is broken:

$$Z = \frac{S_0 \quad S}{S_0} \tag{7}$$

Deformation properties are significant not only for the behaviour description of metal biomaterials under the activity of external loads, but can also be indirectly used for a preliminary quality assessment. The existence of porosity, inclusions or other forms which violate the integrity of the microstructure may be the cause of smaller values of the elongation with breaks and the reduction of area in relation to the values obtained by testing of materials which do not contain errors. Also, at the analysis of testing results it must be taken into account that the deformation properties do not depend exclusively on the material properties, but also on the testing conditions.

Deformation properties affect the correct selection of a biomaterial, because it is important for the implant constructors that the material capable of minor deformation before the fracture is used, if a too big mechanical load occurs after the installation. On the other hand, it is also important that the material possesses certain plastic properties so that it can be produced in a simpler and more economic manner by some of deformation processes.

2.1.2 Compression Testing

Compression testing is used on metal biomaterials which are exposed to the activity of external pressure load during use. It is mostly the case with orthopaedic and dental implants. Also, the results of compression testing are used for technological purposes, i.e. for the estimation of the possibility of deformation of biometals during the implant production. The testing procedure is very similar to the tensile testing, only the course of the load activity is opposite.

The pressure testing starts with positioning of, mostly cylindrical, sample in the testing machine workspace. Compression is realized by means of two parallel surfaces of the tool, which are perpendicular to the direction of the external load activity. Graphical interpretation of the testing results is the stress-strain curve $\sigma = f(\varepsilon)$, on the basis of which the material resistance properties and deformation properties can be determined. It is the fact that the change of external load activity course, in relation to the tensile testing, leads to the decrease of the height of the sample, but it does not exclude the application of identical equations for the material behaviour characterization.

Characteristic mechanical properties determined by compression testing of metal biomaterials are:

Yield strength presents the strength generated by the compression force at the moment when more significant plastic deformations occur. It is defined with the relation:

$$R_{cH} = \frac{F_{cH}}{S_0} \tag{8}$$

Compression Strength is the maximal strength by which a metal biomaterial is loaded during the testing. It is determined at the moment of macroscopic destruction of the material (cracks or fractures) and is defined by the relation:

$$R_{CM} = \frac{F_{CMAX}}{S_0} \tag{9}$$

The elastic and proportional limit are rarely determined by compression tests.

So, generally, to describe the behaviour of metal biomaterials under the influence of compression loads identical indicators of hardness are used as in tensile tests. However, the compression hardness can be determined only in brittle materials. Plastic materials behave differently during compression, because they can be significantly deformed without any cracks or fractures. That is why at their testing, analogous to the yield strength at tensile testing, the strength is determined which, in the material, causes a permanent decrease of the tested sample height by 0.2% in relation to the initial value:

$$R_{c0.2} = \frac{F_{c0.2}}{S_0} \tag{10}$$

For a quantitative description of deformation properties at compression tests the following indicators are used, defined at the moment of fracture or significant macroscopic damages of the sample—shortening—ΔH (11), unit shortening—ε_c (12) and spreading—Z_c (13):

$$\Delta H = H_0 - H \tag{11}$$

$$\varepsilon_c = \frac{H_0 - H}{H_0} = \frac{\Delta H}{H_0} \tag{12}$$

$$Z_c = \frac{S - S_0}{S_0} \tag{13}$$

2.1.3 Bending Testing

Due to the extreme brittleness of ceramic and some composite biomaterials, bending tests are not capable of describing their behaviour in the loaded state adequately. The basic problem is the presence of surface microcracks, which cause the concentration of tension and significantly influence the wrong estimation of hardness. In some cases, only the positioning of a material sample in the testing

machine may cause a fracture. Because of that, for a more complete characterization of mechanical properties of the named biomaterials bending testing results are often used.

Due to the fact that metal biomaterials are more or less plastic, bending test results do not have an especially high potential for the characterization of their mechanical properties. However, for the purpose of a more complete overview of the methods for determining the mechanical properties of metal biomaterials, the bending test in three points will be described in the part which follows (Fig. 3).

The testing is performed in such a way that a sample of the tested material is placed on two cylindrical supports. The force acts in the middle of the distance between the supports. Testing is performed until the appearance of cracks at the external surface of the sample or until the final fracture. The distribution of loads in the sample is uneven. The highest tensions are generated in the surface layers of the material, compression ones on the side where the force acts and the tensile ones on the opposite side.

Flexural Strength is the basic property of resistance and presents a maximal strength by which a biomaterial is loaded during the bending. It is determined as the relation between the maximal bending moment and the resistance moment which presents the geometrical characteristic of the cross-section of the sample (14):

$$R_{fM} = \frac{M_{f\,max}}{W} \tag{14}$$

Maximal bending moment is calculated by the formula (15), and in that L is the distance between the supports, and $F_{f\ max}$ is the highest force which loads the sample during the bending.

$$M_{f\,max} = \frac{F_{f\,max}}{2} \quad \frac{L}{2} = \frac{F_{f\,max}}{4} \quad L \tag{15}$$

If a sample with a round cross-section is used for testing, with the diameter *D*, the bending strength is determined as follows (16)

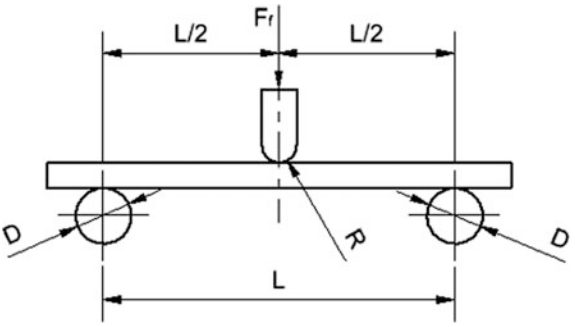

Fig. 3 Three point bending test

$$R_{fM} = \frac{8F_{f\,max}}{D^3} \frac{L}{\pi} \tag{16}$$

Bending strength can be determined only in metal biomaterials which fracture during testing. In plastic biometals, to describe the resistance properties, the value of strength is used which is generated at the moment when the bending moment causes plastic deformations of the sample of 0.2%:

$$R_{f0.2} = \frac{M_{f0.2}}{W} \tag{17}$$

Deflection-f is the basic property of biomaterials deformation and it presents the size of movement of force attack point in any moment of bending. The highest value of deflection is established in the moment when the sample fractures and is called the ***deflection at fracture—f_f.***

As a quantitative indicator of the flexibility of a biomaterial, ***unit deflection*** is used (18):

$$\varphi = \frac{f}{L} \tag{18}$$

A characteristic unit which connects the resistance properties and deformation properties is called rigidity—K_c (19):

$$K_C = \frac{R_{fM}}{f_f} \frac{D}{30} \tag{19}$$

Often, the ***bending factor—K_s*** is used as an additional indicator of resistance properties of a material (20):

$$K_s = \frac{R_{fM}}{R_M} \tag{20}$$

2.1.4 Hardness Testing

Although the scientific-professional public may deny the existence of a unique definition of hardness, it seems as the easiest thing to state that the hardness presents the resistance a material offers to the indentation of the other, harder body, with accurately defined shape, dimensions and indentation force, into its microstructure (Chandler 1999). In the absence of other sources, the hardness testing results are often used for the purpose of preliminary estimation of other mechanical properties (i.e. tensile strength).

Determination of hardness is based on different approaches, and due to that it can be quantified in different ways. For metal biomaterials, the approaches are used

requiring the measurement of the indenter indentation depth at the standard value of indentation force, or the measurement of elastic rebound of the indenter from the surface of the tested sample. On the basis of the way the force acts, all hardness testings can be divided into static and dynamic.

Brinell procedure of hardness determination is presented to the public for the first time in 1900. Although a lot of time has passed, due to its simplicity and accuracy of results, today it presents a standard method for the quantification of metal materials hardness.

Testing methodology is based on the activity of a spherical indenter to the surface of the tested sample.

Measure of hardness (HB) is the medium tension which the indenter generates per the area of the imprint:

$$HB = \frac{F}{D\pi h} = \frac{2F}{D\pi\left(D - \sqrt{D^2 - d^2}\right)} \approx \frac{0.102 \quad 2F}{D\pi\left(D - \sqrt{D^2 - d^2}\right)} \left[\mathrm{N/mm^2}\right] \qquad (21)$$

Due to the imperfection of the imprint form, the arithmetic mean of two diametrically opposed diameters is used (Fig. 4).

Depending on the type of testing material, a hardened steel pellet is used as the indenter, or the hard metal pellet with the diameter D = 10; 5; 2,5; 2 and 1 mm. The selection of the indenter diameter should provide the standard relation d/D = 0.25–0.5. The imprint depth must be smaller than 1/8 of the tested sample depth. Indentation force (F) depends on the diameter of the indenter and the type of material. To provide similar testing conditions, hardness determination for a concrete material should be realized at a constant relation $F/D^2 = k$. In this way, it is

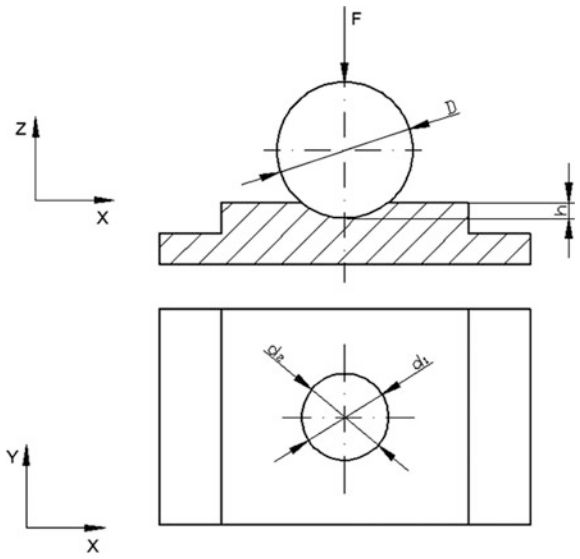

Fig. 4 Brinell hardness testing

possible to compare the results obtained at different values of indentation force and the radius of the indenters. Also, the indentation time is a significant factor for the obtained results. For the validity of testing, the duration length of loading the sample with maximal force is the most important factor. The values of this interval depend on the type of material.

Denotation of hardness depends on the material used for the making of the indenter. (HBS—steel or HBV—hard metal). Besides that, the denotation may also contain the numerical values related to the testing conditions.

Vickers procedure of hardness determination was developed in 1924, as the alternative to Brinell method. The driving force for its development was the idea to use a four-sided diamond pyramid, with a square basis and the angle of 136° between the adjacent sides as an indenter, instead of a pellet. It further enabled the forming of similar imprints in the tested material, regardless of the size of indentation force.

The realization of Vickers test is often more simple in relation to other methods, because the needed calculations for the quantification of hardness are independent of the indenter size and indentation force. Because of that, it can be used for testing of all metal biomaterials with minimal damaging of the surface. A special advantage is the fact that with the help of this method the hardness of very thin layers and microstructural constituents can be determined (Fig. 5).

The measure of hardness in Vickers method is identical as in Brinell test and presents the quotient of indentation force (F) and area of the imprint (S) in the tested sample (22):

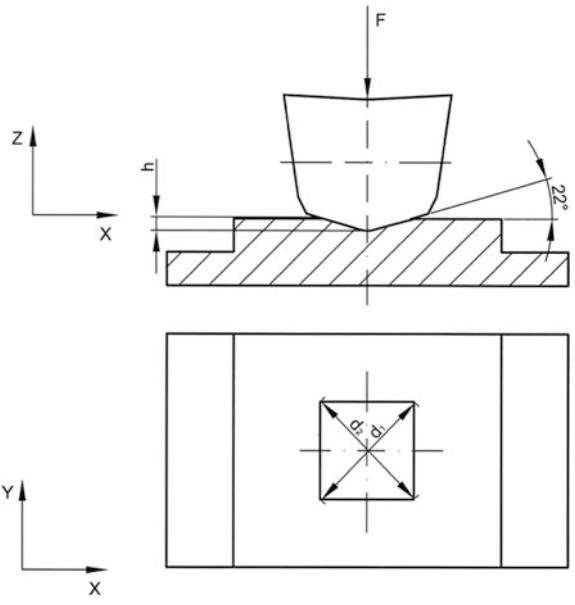

Fig. 5 Vickers hardness testing

$$HV = \frac{F}{S} = \frac{F}{\frac{d^2}{2\ \sin(136^0/2)}} \approx 0.1891 \frac{F}{d^2} \left[\mathrm{N/mm^2}\right] \tag{22}$$

The mean value of the imprint diagonals is used for calculations. Generally, the values of the indentation force can be arbitrary, but it is still common that for steel biomaterials the forces of 300 N are used, while for other biomaterials smaller values are used. The indentation time is shorter for harder materials.

The denotation of hardness determined by Vickers procedure, besides the symbol HV, should also contain the data related to the force and time of indentation.

Hardness testing method based on Rockwell was developed in the USA and patented in 1919, (Low 2001). It is, actually, the family of a great number of procedures which differ among themselves in terms of shapes and dimensions of indenters and the indentation force. As a difference from Brinell and Vickers method, the measure of hardness in Rockwell's terms is the depth of indentation, whose calculation value presents the difference between the depths of imprints made by the activity of two different indentation forces. The indentation depth value is then converted into the units from Rockwell's scale.

Depending on the type of tested material, the following indenters are used in Rockwell procedure: the hardness of soft and medium-hard materials is determined by the assistance of hardened steel pellets, whose diameters are 1/16″ or 1/8″, while for hard materials a diamond cone is used, with the angle of 120° and the tip curvature radius of 0.2 mm. The total indentation forces are also different and in the range from 150 N at the determination of surface layers hardness to 1500 N for the identification of macrohardness. Due to the stated, a great number of tests have been developed in which Rockwell's hardness determination approach was incorporated. However, the widest practical application appears in HRB and HRC tests, which use the pellet with the diameter of 1/16″, or the cone, respectively. In HRB procedure, the total indentation force is 1000 N, and in HRC procedure this value is 1500 N.

The hardness testing by Rockwell's procedure, regardless of the shape of the indenter, is realised in three phases (Fig. 6).

At the beginning of the testing, the indenter is loaded with the preloading force F_0, what eliminates the influence of surface unevenness, corrosion or impurities to the testing results. The indentation depth at this phase is h_1. In the second phase, the indenter is additionally loaded with the force F_1 and then an imprint is formed in the tested sample with the depth h_2, under the influence of the total load ($F = F_0 + F_1$). The duration period of the total load depends on the type of tested material and is generally shorter if a material is harder. At the end, the sample is unloaded from the activity of the force F_1, and due to that the elimination of elastic deformations occurs, and the indentation depth is decreased to the final value h_3.

If the indentation depth h_3 would be directly converted into the units of Rockwell's scale, with nominal value of 0.002 mm, bigger values of hardness for softer materials would be obtained and vice versa. To avoid the named illogicalities,

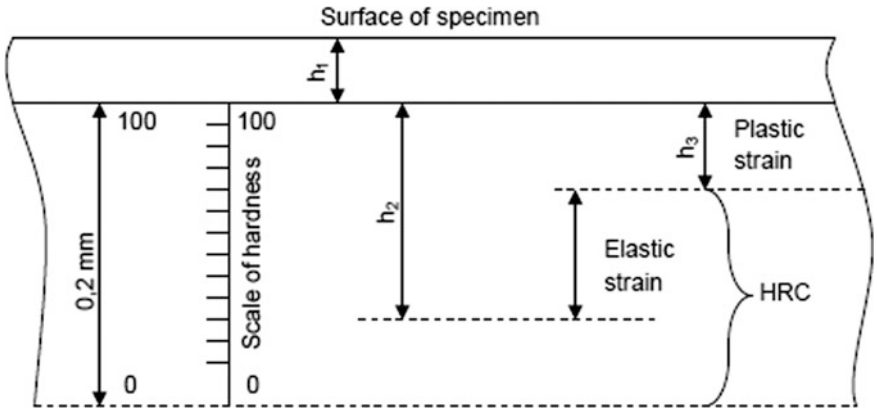

Fig. 6 Rockwel hardness testing

the final indentation depth h_3 is subtracted from a certain constant. For HRB procedure, the constant is 130, and for HRC it is 100, Numerical values of hardness are dimensionless units and are defined by the following formulae:

$$HRB = 130 - \frac{h_3}{0.002} \tag{23}$$

$$HRC = 100 - \frac{h_3}{0.002} \tag{24}$$

The basic advantage of Rockwell procedure is the simplicity and speed of realization, because additional calculations are not required. Its imperfection is the fact that a dissipation of results may occur in some cases.

2.1.5 Fatigue Testing

Testings have shown that under the activity of dynamic loads a gradual damaging of materials occur, what is known as fatigue in engineering practice. Periodical changes of strength accelerate the accumulation of critical level of microstructure damaging, in such a way that the fracture of material will happen much before than it would be the case under static loads. Material fatigue is closely related to errors in the microstructure of metal biomaterials, especially to dislocations. The explanation of the material fatigue phenomenology is based on the appearance of sliding lines, i.e. the plastic deformations in the area of maximal tensions. Due to the stockpiling of dislocations, the plastically deformed zones get stronger and become the place of microcavities nucleation at long-term dynamic loads. Further periodical changes of strength simulate the growth of microdamaging, accelerate their connection and finally, at the identified number of cycles, lead to the fracture of the material.

The moment when a material fractures under the influence of changeable load depends on the size of tension, the type of load and the number of cyclic repetitions. In general case, changeable load may be direct and alternating (Fig. 7).

At the material fatigue testing, samples can be loaded by straining, pressure, bending, twisting or combined dynamic load. However, the most often used tests are the ones based on alternating activity of straining-pressure load and the load due to rotating bending. Pursuant to (Teoh 2000), all the tests for estimation of fatigue fracture of a biomaterial can be categorized in the following way:

- the approach which is based on establishing the dependence between the dynamic load and the number of cycles until the appearence of fracture of the sample,
- the approach based on fracture mechanics theory;
- the approach based on the simulation of physiological multi-axial loads.

The first two approaches can be used for characterization of metal biomaterials fatigue. The testing results have a strong influence to the preliminary selection of materials for implants which will be exposed to cyclic-changeable loads during exploitation. A characteristic example is the selection of materials for orthopaedic implants. The third approach is relatively expensive, because it requires a simulation of physiological systems.

Due to the fact that the material fatigue tests which are based on fracture mechanics theory are often used for testing of brittle ceramic implants or composite implants for dental applications, in the continuation of the text a test will be described which enables the establishing of relations between the dynamic tensions and number of cycles until the appearance of macroscopic damages on metal biomaterials.

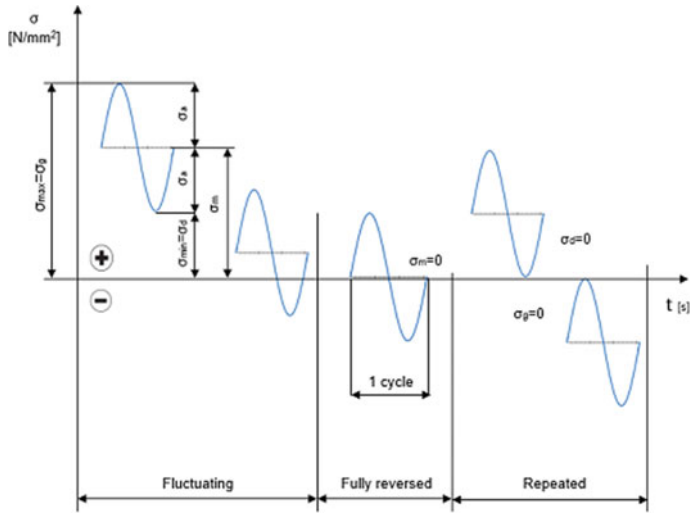

Fig. 7 Variable stresses under cyclic load

A set of test tubes is used for testing. The tubes have a standard shape and dimensions, and are gradually loaded with different amplitude changes of strength, maintaining a constant value of medium strength. The testing is realised until the appearance of fracture or visible cracks on the test tube. In the beginning, the amplitudes are bigger, and later they get smaller, until they reach the strength value which allows an endless cyclic repetition without damaging the test tube. The results of the series of testings are presented graphically in the dynamic endurance diagram (S)—the number of cyclic changes until the fracture (N). By connecting the points which correspond to the probability of destruction of the material of 50%, Wöhler fatigue curve is obtained for a certain medium strength (Fig. 8).

The mechanical characteristic which is used for quantification of resistance of the material under the activity of cyclic-changeable loads is called **dynamic strength** σ_D. That is the biggest strength which a material can endure indefinitely long at a given cyclic load, without a fracture. In graphical sense, dynamic strength is the strength which corresponds to the part of the Wöhler curve which T asymptotically gets close to the value defined by the expression (25):

$$\sigma_D = \sigma_{sr} + \sigma_a \tag{25}$$

The dynamic strength value is influenced by a great number of factors: chemical composition, errors in material, microstructural condition, thermal treatment, quality of previous processing etc. However, the type of tension, character of cyclic changes and medium strength size have the strongest influence. Because of that, for a complete characterization of behaviour of a material under the activity of cyclic-changeable loads the diagrams are used which enable a clear presentation of the dependence of dynamic strength on the medium strength at a direct and

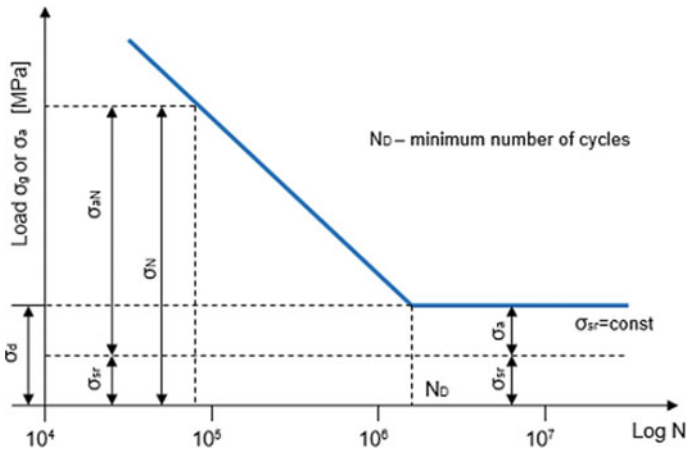

Fig. 8 Wöhler fatigue curve

alternating load, for different types of tension. In that sense, Smith's and Haj's diagram have the biggest practical importance.

2.1.6 Toughness Testing

Toughness testing belongs to the standard procedure of the characterization of mechanical properties of metal biomaterials. The testing is realised by the impact activity of the force, and the results serve to describe the resistance of materials to a brittle fracture. There are many methods for the quantification of toughness, which differ in terms of shape and dimensions of the material sample and impact body, and also in terms of the type of load. While Izod test is used in the USA, Europe typically uses the test based on the impact activity of Charpy pendulum (Fig. 9).

Pursuant to **Charpy impact test,** the toughness of a material, or its impact hardness at bending, is the work used on deformation and fracture of the tested material sample, reduced to the unit of cross-section. The fracture must be realized with one impact, under the speed of pendulum from 5 to 5.5 m/s. For the testing, the samples with standard dimensions are used most often, with "V" or "U" shape of the notch. There is a tendency that the samples with V" notch are used more.

Toughness testing is realized in such a way that a sample is centred between the supports, where notch is at the side opposite to the place of contact with the pendulum. The pendulum is allowed to fall freely from the height h_1, and it

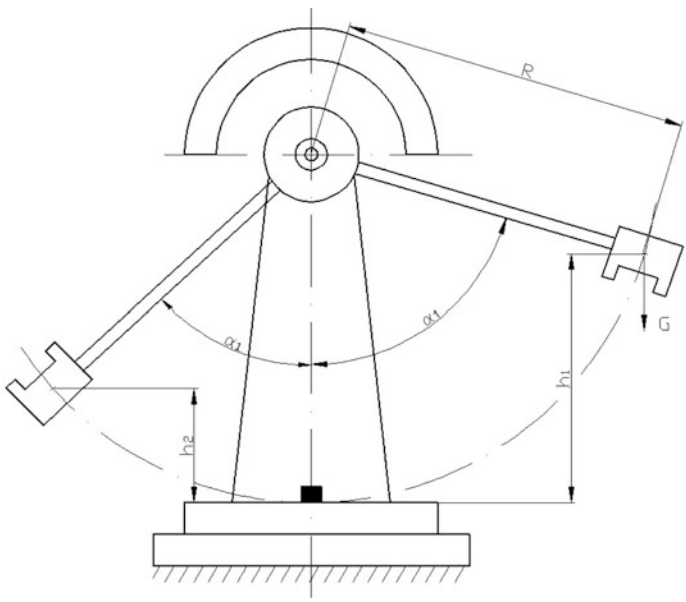

Fig. 9 Charpy impact test

corresponds to the angle α_1. After the fracture of the sample, the pendulum rotates for the angle α_2, i.e. it stops at the height h_2.

The difference of potential energy of the initial position in relation to the final position of the pendulum presents a work used for the deformation and fracture of the sample, i.e. impact toughness.

$$KV(KU) = W_1 - W_2 = mgR(\cos\alpha_2 - \cos\alpha_1)\,[\mathrm{J}] \tag{26}$$

For precise measurements the results will have to be corrected due to the loss of energy because of friction in the kinematic couple and air resistance.

The size of toughness is significantly affected by the testing temperature. With the increase of temperature, the oscillation of atoms around their equilibrium positions increases, and that affects the increase of toughness. On the other hand, tests have shown that many metal biomaterials, especially those which crystallize per BCC lattice have a critical temperature, below which the effect of toughness decrease is very present. In metal biomaterials which crystallize per FCC lattice this phenomenon is less expressed.

The tensile testing results can be used for the determination of toughness, because the surface below the curve σ-ε presents the amount of absorbed energy per material volume unit. Because of that, metal biomaterials which have a high tensile strength and plasticity have a good toughness at the same time.

2.2 Non-destructive Testing

Non-destructive testing methods are mostly highly sophisticated and enable (without any destruction) the identification of errors in the microstructure of metal biomaterials which may occur in the production process or later, by subsequent mechanical processing. Besides that, non-destructive testing methods are used intensively for the control of implants before surgical interventions, and some are applied for a continuous monitoring of the condition after the installation.

In general case, the presence of errors in microstructure is intolerable, because they violate the homogeneity of biomaterials, decrease the cross-section and act as the sources of strength concentration, what affects the mechanical properties, i.e. bearing capacity, reliability and safety of the installed implant. Due to the fact that the principal goal of the application of non-destructive methods is the identification of microstructural defects, these testings are often called defectoscopic testings.

In the defectoscopy, there is a great number of methods based on certain physical phenomena. Description of methods, which are most often used for the identification and characterization of different defects in metal biomaterials, will be given in the continuation of the text.

2.2.1 Ultrasonic Testing

Testing by ultrasonic waves is one of the most favourable non-destructive testing methods. Ultrasonic devices are so improved that ultrasonic testings are now considered as standard defectoscopic testings. Besides the identification of location and size of different internal defects, the application of ultrasound enables the realization of other testings as well, such as the measurement of the material thickness or the intensity of residual strengths. The ultrasonic testings make possible the discovery of defects at the depth of 8–10 m, whose dimensions are even up to 10^{-6} mm. Most of ultrasonic defectoscopy devices uses the waves with the frequency of 0.5–5 MHz.

The methodology of ultrasound testing is based on the spreading of a high frequency mechanic-acoustic wave in a homogeneous environment without significant losses. At the passing of ultrasonic waves from one acoustic environment to the other, there is a partial reflection from the boundary of the environments and a significant diffraction. This phenomenon is used for identification of microstructural defects of metal biomaterials.

In modern defectoscopy, many methods are used, but the most applied ones are the Pulse echo method, Through transmission method and Resonance method.

Pulse echo method is based on the reflection of ultrasonic waves. If there are no errors in a material, the ultrasonic wave will reflect from the boundary surface of the material, and on the basis of the accepted signal it is possible to determine the time needed for response, i.e. the thickness of the subject. On the contrary, when the ultrasonic wave finds an error in material on its way, the response time is shorter. It is clear that the time differences of the response enable the locating of the error in the material. Besides that, on the basis of the reflection wave signal size it is possible to determine the size of the effect as well. The flaw of the pulse echo method is the lack of possibility to identify defects in narrow zones of direct contact of the ultrasonic probe with the tested material.

The application of the through transmission method is based on the effect of ultrasonic wave energy absorption at the passing through the microstructure of the tested material. The energy decrease at the receiver is also present when there are no defects in the material. However, if the ultrasonic wave reaches the defect, the energy decrease intensity is more expressed and is directly proportional to its size. Only bigger errors can be located by this method.

Resonance method is based on the principle of undamped oscillations. It is mostly used for the control of material thickness and the identification of defects at which the access is possible only from one side of the material.

2.2.2 Radiographic Testing

At the testing with radiographic methods, the tested material is ventilated by electromagnetic waves. Regarding the fact that the waves have a small wavelength and high frequency, they are capable of penetrating through hard materials.

Basically, radiographic methods are based on the fact that different materials have a different radiation absorption coefficient. Because of that, during the ventilation of the material, waves lose their intensity, so that the output wave always has a smaller intensity than the input one. The difference in radiation intensity depends on the wavelength, density and thickness of a material. The information on the existence of errors or inhomogeneity of the material are obtained by means of radiographic films—photographic method or by observation on a fluorescent screen—visual method. For the identification of microstructural defects, the radiographic method based on the ionization of gases and the appearance of photo-electrons which are detected in the ionization chamber can be used as well. However, the photographic method has the greatest application in industrial defectoscopy.

For the testing with radiographic methods, roentgen rays (X-rays) and γ -rays are used. In the first case, Rtg generator is used as the radiation source, and the testing method is called roentgenography. The radiographic testing which uses a radioactive isotope as the radiation source is called gammagraphy. The isotopes Ir_{192}, Co_{60}, Ga_{75}, Ta_{170} are most often used as the sources of γ radiation. The selection of the isotope depends on the thickness of sample and the type of material. Due to the fact that γ-rays have a greater power of ventilation, because of a smaller wavelength in relation to X-rays, gammagraphy is used to test the samples with bigger dimensions. However, the possibility of modifying the radiation source in accordance with different needs, thus affecting the speed and accuracy of testing, presents the basic advantage of roentgenography in relation to gammagraphy.

The testing principle is similar for both tests and schematically shown in Fig. 10.

The waves emitted from the radiation source ventilate the tested material. When they come to the radiographic film, placed on the opposite side of the sample, a photo effect occurs due to the ionization. If there is an error in the material, the effect of dimming the film will be expressed more. That is the consequence of a smaller radiation absorption in the material.

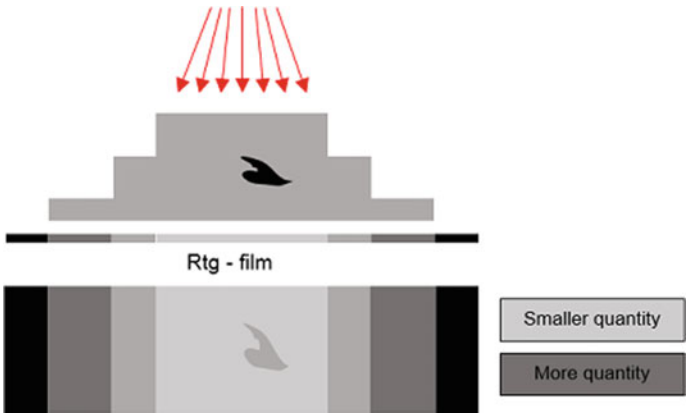

Fig. 10 Schematic presentation of radiographic testing

2.2.3 Magnetic Particle Testing

Magnetic particle testing is primarily used for the detection of surface discontinuities of ferromagnetic materials. However, the method can also be used for the location of defects which are immediately below the surface layer of the tested material.

Depending on the object under test, a variety of techniques can be used (Burke et al. 2013), as well as the various instruments for the detection of magnetic fields (Motukisi 2012). One application of this method relates to the testing of welded joints (Baldev et al. 2000), then the pressure vessel (Wahed et al. 2013) and other welded structures. Test method with magnetic particles, in addition to testing of welded joints, is widely used in the automotive industry; e.g., test shafts (Vetterlein 2008), and other machine parts. Also, use of this method is present in the aviation industry in terms of inspection steel components (Burke et al. 2013). In addition to selection method for the identification of surface defects, a very important role have human factors too (Lux et al. 2007), which can lead to erroneous results. Nowadays, in order to improve the tests, there are a variety of numerical methods which simulates the movement of magnetic particles in a generated magnetic field (Sand et al. 2016; Lindner et al. 2013).

To be able to realize magnetic testings, it is necessary to generate a magnetic field of sufficient magnitude in the sample. The essence of the testing is based on the phenomenon of magnetic field dissipation above the place of the defect. In homogeneous materials with no defects, magnetic force lines are straight lines. Otherwise, a turning or dissipation of magnetic field occurs at the places of defect. The intensity of dissipation depends on the dimensions and distance of the defect from the surface of the sample, and also on the position of the defect in relation to magnetic force lines. The greatest accuracy is achieved when the defect is perpendicular to the direction of the magnetic field (Fig. 11a). In the case that the defect is of parallel orientation, the identification is not possible (Fig. 11b). Because

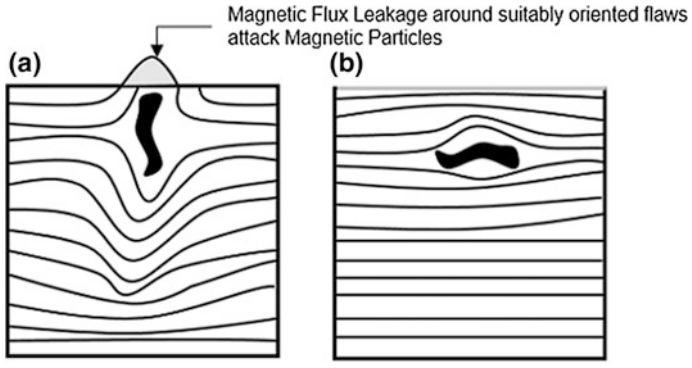

Fig. 11 Visualization of microstructural defect with the assistance of magnetic particles

of that, practical testings are always performed in two direction which are mutually perpendicular.

Because of the fact that magnetic force lines are invisible, ferromagnetic powder (Fe_3O_4 or Fe_2O_3) is used for the identification of defects. When they are in a magnetic field, the powder particles are oriented in the direction of the force lines. However, at the places of discontinuity, due to the turning of particles, their grouping occurs, what is a visual indicator of the existence of a defect. For easier identification of defects, ferromagnetic particles are often coloured. The colour is selected depending on the intensity of contrast in relation to the tested material. The shape and dimensions of particles can significantly influence the testing quality. The experience has shown that it is the best thing to use the ferromagnetic particles with the ratio of length and radius between one and two. For the increase of testing sensitivity, and of more mobile and uniform distribution on relatively large testing zones, magnetic particles are used in suspension with water or oil. In this way, in the conditions of high colour contrast, it is possible to notice very precisely the long and narrow discontinuities of the tested material surface.

Testing by magnetic particles is simple for realization. Defects are identified at the tested material surface and reflected really, regardless of dimensions and shape. The basic flaw of this method is the inability to determine the depth of defect.

2.2.4 Liquid Penetrant Testing

Liquid penetrant testing is one of the oldest methods for non-destructive material testing. Its realization is very simple, and the results are confidential. Liquid penetrant tests serve exclusively for the identification of surface defects of nonporous materials, such as cracks, pores etc.

The method is based on the activity of capillary forces, i.e. on the ability of certain liquids to penetrate into very narrow cracks, and then to be absorbed by means of other liquid, so called developer.

A schematic presentation of the liquid penetrant testing, realized in a few steps, is given in Fig. 12. The initial testing phase requires the cleaning of the sample surface. Then the penetrant liquid is inflicted, which, due to the capillary effect fulfils the space of surface discontinuities. After some time, the surplus of the

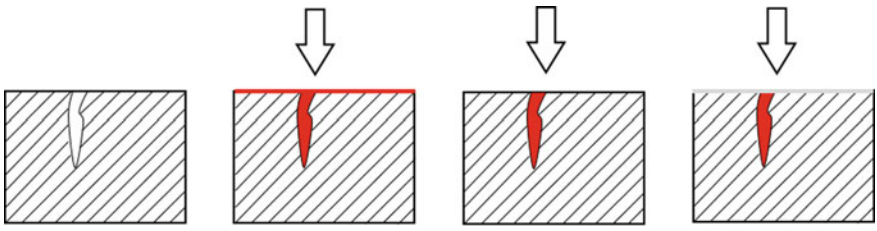

Fig. 12 Schematic presentation of liquid penetrant testing

penetrant is removed by a water jet, and the tested surface is treated with the developer. Because of much bigger capillary effect of the developer in relation to the crack, the penetrant is extracted to the testing surface. In that, it leaves a trace which can be noticed easily, indicating the location and dimensions of surface discontinuities.

The indication of a crack on the tested surface is much bigger than its real size, so that it is possible to identify very narrow discontinuities by penetrant tests, with the width of even 0.001 mm. The identification of surface defects is also made easier due to the expressive contrast of the penetrant trace in relation to the tested surface. Besides the coloured penetrants, fluorescent penetrants can be used as well, visible under ultraviolet light. The possibility of testing all types of metal materials and high sensitivity to minor surface discontinuities are the basic advantages of the penetrant testing.

3 Application Potential and Mechanical Properties of Some Metal Biomaterials

Most metal materials are not acceptable for biomedical applications. At the moment, there is an opinion that adequate materials are only the ones based on iron, cobalt, nickel, titanium, tantalum, zirconium and precious metals. However, the production of zirconium is too expensive, and inadequate mechanical properties of tantalum and precious metals do not allow any more serious application in the field of implant production, especially in orthopedy. Today alloys are dominantly used for the making of metal implants, which, unlike pure biometals, enable a better combination of mechanical properties and greater resistance to corrosion. An exception is the pure titanium, which, due to its extraordinary mechanical properties and excellent biocompatibility, has a high potential for various medical applications, with the focus on orthopaedy and stomatology. The research and practical results by now imply that the greatest opportunities for implants making are offered by stainless steels, Co–Cr alloys, pure titanium and its alloys (Davis 2003; Hermawan et al. 2011). The titanium alloys with β-structure have a particularly high application potential. That is the consequence of the fact that β-alloys of titanium have the lowest elastic modulus of all metal materials used for biomedical applications (Mohammed et al. 2014).

The fatigue cracks are very often appearance in the metal implants. This is a consequence of the cyclic load impact. However, in a physiological environment, exploitation conditions are further deteriorated, due to the complex reactions between fatigue and corrosion. It generally stimulates the development of micro-structural damage. Various actions that can lead to mitigation of mentioned effects were considered in the paper (Antunes and Lopes de Oliveira 2012). Aspects of the development of new metal alloys for biomedical applications are disclosed in detail in the study (Niinomi et al. 2012).

Table 1 Application of metals as implants used in human body (Patel and Gohil 2012)

Types of Materials	Applications
Stainless steel	Joint replacements (hip, knee), bone plate for fracture fixation, dental implant for tooth fixation, heart valve, spinal instruments, surgical instruments, screws, dental root implant, pacer, fracture plates, hip nails, shoulder prosthesis
Cobalt-chromium alloy	Bone plate for fracture fixation, screws, dental root implant, pacer, and suture, dentistry, orthopaedic prosthesis, mini plates, surgical tools, bone and joint replacements (hip, knee), dental implants
Titanium and its Alloys	Cochlear replacement, bone and joint replacements (hip, knee), dental implants for tooth fixation, screws, suture, parts for orthodontic surgery, bone fixation devices like nails, screws and plates, artificial heart valves and surgical instruments, heart pacemakers, artificial heart valves

All metal materials for implants are nonmagnetic and with high density. That is significant for them to be compatible with the techniques used for magnetic resonance and to be recorded with X-rays. Also, metal materials are exposed to different loads during exploitation, what in a general engineering approach implies a good combination of hardness and toughness. Still, a concrete application of metal biomaterials for implant making depends exclusively on specific medical requirements. Thus, for example, the materials for making of stents must be plastic enough to expand stenotic blood vessels, but also rigid enough to maintain the dilatation. High toughness, elasticity, rigidity, hardness and fatigue fracture resistance are the essential mechanical properties which characterize the metal implants in orthopaedy. Dental applications imply the use of hard and rigid materials. For better results, the alloys with shape memory effect are used.

Generally, metal biomaterials are used almost exclusively for making of bearing implants (Patel and Gohil 2012). Characteristic examples are artificial hip implants, dental implants (crowns and bridges), knee prosthesis, stents, hernia meshes or fracture fixation elements such as wires, needles, screws, nuts, plates etc. (Hiromoto 2008). Some of the application opportunities of metal biomaterials are shown in Table 1.

Pursuant to the previous consideration, it is clear that mechanical properties must be clearly identified and carefully analysed at the selection of metal biomaterials for specific surgical applications. Because of that, the continuation of the text gives an overview of mechanical properties of more often use metal biomaterials.

3.1 Stainless Steels

The notion of stainless steels implies a great group of steels characterized by a corrosion resistance in a wide spectrum of corrosion aggressive environments.

Chrome presents the basic alloying element. Due to the other advantages as well, such as high hardness, good plasticity and workability, low production costs etc., stainless steels have become very often used biomaterials for orthopaedic implants making. The first implant which was successfully used in surgical interventions in 1920s was also made of stainless steel.

Of all commercial stainless steels, only austenitic ones are used as biomaterials—AISI 316, 316L, 316LVM, 316Ti and precipitation hardened AISI 630 (17-4 PH) steels, primarily for making of artificial joints and fractured bones fixators. Still, in the practice by now, AISI 316L (ASTM F138 i F139) steel (Malekani et al. 2012) has had the greatest number of biomedical applications. With the aim to increase biocompatibility, a new generation of stainless steels has been developed in recent years, not containing nickel due to its toxicity and allergic effect to a patient's organism (Hermawan et al. 2011; Malekani et al. 2012). The plasticity of stainless steel is bigger than in the pure titanium which crystalizes in hexagonal crystal lattice. Because of that, the shaping of stainless steel implants is easier and simpler. However, the lower resistance to fatigue fracture and corrosion, in relation to titanium, limit the application of stainless steels for the production of modern joint implants (Li 2007). Typical mechanical characteristics of stainless steels used for implant production are given in Table 2.

In addition to the above data, in the literature can be found and other data related to mechanical properties of stainless steels (Table 3).

The high possibilities of the stainless steel application in medicine have been reduced due to negative effects that have been generally associated with the percentage of nickel, what depends on the type of steel (Yang and Ren 2010).

Table 2 Mechanical characteristics of some stainless steels for biomechanical applications (Brunski 1996, 2004)

Material	Condition	Young's modulus [GPa]	Tensile strength [MPa]	Yield strength (0.2% offset) [MPa]	Fatigue endurance limit strength (at 10^7 cycles, R = −1) [MPa]
F55 F56 F138 F139	Annealed	190	586	331	241–276
	30% cold-worked	190	930	792	310–448
	Cold forged	190	1351	1213	820
F745	Annealed	190	483	221	221–280
AISI 630-17-4 PH	Heat to 551 °C	197	1215	1135	–

Table 3 The literature overview of the mechanical properties of stainless steel

Material	Study	Yield strength [MPa]	Tensile strength [MPa]	Fatigue strength (10^7 cycles) [MPa]	Young's modulus [GPa]
Stainless steels AISI 316	Poitout (2016)	170–790	480–1000	180–550	–
Stainless steel 316L	Chen and Thouas (2015)	–	540–1000	–	200
316L SS, annealed plate (ASTM 2003) Fe, 16–18.5 Cr, 10–14 Ni, 2–3 Mo	ASTM (2003)	190	490	–	193
F55, F138 annealed	Silver (1994)	170–205	480–515	–	–
F55, F138 cold-worked		310–690	655–860	–	–
F55, F56, F138, F139, annealed	Ratner et al. (2013)	331	586	241–276	190
F745, annealed		221	483	221–280	190
316L annealed	Totten (2004)	170–210	480–645	190–230	–
316 L cold worked		310–1160	655–1265	530–700	–

3.2 *Co–Cr Alloys*

The research of Co–Cr alloys for biomedical applications started at the beginning of the previous century. In that period, the first cobalt-based alloy Co–Cr–Mo was patented, known as Vitallium denture, the purpose of which was the production of dental implants. Further development has enabled the application extension, so that today Co–Cr alloys are very often used metal biomaterials. Significantly greater wear resistance and high corrosion resistance in body liquids in relation to stainless steels and titanium alloys presents the basic of superiority of Co–Cr alloys. Because of that, they are most often used for making of implants with high contact load, i.e. artificial hip or knee, especially the prosthesis head, but they can also be used at other anatomic locations. On the other hand, Co–Cr alloys belong to the group of metal biomaterials with lower plastic properties, and that aggravates the production of implants with bigger dimensions. In relation to titanium alloys, they have a worse biocompatibility and high elastic modulus (Li 2007).

In general case, the classification of Co–Cr alloys implies two characteristic groups: the first of them are CoCrMo alloys (27–30% Cr, 5–7% Mo, 2.5% Ni), used for many years in stomatology, and the other is CoNiCrMo alloys (19-21% Cr, 33–37% Ni and 9–11% Mo), primarily intended for the production of orthopaedic implants. Pursuant to ASTM, four Co–Cr alloys are recommended for surgical applications: one casted alloy—Co–Cr–Mo (F75) and three forged alloys—Co–Cr–W-Ni (F90), Co–Ni–Cr–Mo (F562), Co–Ni–Cr–Mo–W-Fe (F563) (Park and Kim

Table 4 Mechanical properties of Co–Cr alloys (Park and Kim 2003)

Material	Condition	Young's modulus [GPa]	Tensile strength [MPa]	Yield strength (0.2% offset) [MPa]	Elongation ε [%]	Fatigue endurance limit strength (at 10^7 cycles, R = −1) [MPa]
CoCrMo (F75)	Cast/annealed	210	655–889	448–517	>8	207–310
	Powder metallurgy/ Hot isotactic pressing	253	1277	841	–	725–950
CoCrWNi (F90)	Wrought	210	860	310	10	Not available
	44% cold worked	210	1606	1896	–	586
CoNiCrMo (F562)	Hot forged	232	1206	965–1000	–	500
	Cold-worked and aged	232	1795	1500–1585	8	689–793 (axial tension R = 0.05, 30 Hz)

2003). However, the former practice has shown that only Co–Cr–Mo and Co–Ni–Cr–Mo alloys have been used intensively for implant production.

In Table 4 the values of some mechanical characteristics for typical biomedical Co–Cr alloys are given.

Based on the literature data, Co–Cr alloys may –ve the characteristics that are specified in Table 5.

3.3 Titanium and Titanium Alloys

Commercially pure titanium (CP titanium) is one of the rare materials which naturally correspond to demands for biomedical applications and has been used successfully for the production of implants and medical devices since 1950 (Zhou et al. 2007). The first concrete medical application was related to the production of plates and screws for bone fractures curing. Because of its extraordinary biomechanical characteristics, it has soon become an unavoidable material in bioengineering. Characterization of the properties of pure titanium for biomedical applications is exposed in study (Gałuszka et al. 2017). In relation to other biometals, titanium and titanium alloys have a better specific hardness, low elasticity modulus and especially expressed biocompatibility. The corrosion resistance is also high because of the formation of a very thin oxide film. However, titanium and its alloys have lower

Table 5 The literature overview of the mechanical properties of Co–Cr alloy

Material	Study	Yield strength [MPa]	Tensile strength [MPa]	Elongation ε [%]	Young's modulus [Gpa]	Fatigue endurance limit strength (at 10^7 cycles, R = −1) [MPa]
F75	Jevremovic et al. (2012)	672–724	1363–1472	1.76–4.26	–	–
F75, ascast/annealed	Ratner et al. (2013)	448–517	665–889	–	210	207–310
F799 hot forged		896–1200	1389-–1586	–	210	600–896
F90 annealed		448–648	951–1200	–	210	–
F562 hot forged		965–1000	1206	–	232	500
F75	Petrovic et al. (2012)	776–769	1171–1188	5-7	–	–
F75 as-cast	Totten (2004)	430–490	716–890	5–8	–	300
F90 annealed		350–650	862–1220	37–60	–	345
F90 cold worked		1180–1610	1350–1900	10–22	–	490–587
F562 annealed		300	800	40	–	340
F562 cold worked		650–1413	1000–1827	10–20	–	435–555

shaping abilities, worse tribological characteristics and smaller wear resistance, what is the consequence of relatively low hardness.

Pure titanium has two crystal modifications. By 882.5 °C a hexagonal densely packed crystal lattice (α-titanium) is present, and later a volume-centred cubic lattice occurs (ß-titanium). On the basis of this criterion, the classification of titanium alloys in α, α + ß and ß alloys has been performed. It seems that the two-phase α + ß alloy Ti-6Al-4 V has the widest biomedical application. With the aim to increase toughness, ELI Ti6Al4 V has been developed, with a very small amount of oxygen, nitrogen, carbon and iron interstitials. Pure titanium has a better corrosion resistance than its alloys, but α-alloys have a greater stability at increased temperatures than ß-alloys, and in that their hardness and shaping abilities are lower. On the other hand, ß-alloys have a very low elasticity modulus, what provides a smaller rigidity of implants, i.e. contributes to smaller loading of bones. The suspicions that a long-term use of implants containing vanadium and aluminium nay cause health complications initiated the development of the other generation of biomedical titanium alloys.

Commercially pure titanium is mostly used for making of dental implants, but it can also be successfully used in orthopaedy, as well as for surgical instruments

Table 6 Mechanical properties of titanium and titanium-based biomedical alloys (Brunski 2004, Geetha et al. 2009)

Material	Microstructure	Young's modulus [GPa]	Tensile strength [MPa]	Yield strength [MPa]	Elongation ε [%]
CP Ti	α	105	785	692	15–24
TiAl6V4	α + β	110	960–970	850–900	6–10
TiAl6Nb7	α + β	105	1024	921	8–15
TiAl5Fe2,5	Metastable β	110	1033	914	15
TiNb13Zr13	Metastable β	79	1030	900	10–16
TiNb35Ta5Zr7	Metastable β	55	590	530	–
TiMo15Zr5Al3	Metastable β	82	812	771	18–25

making. Titanium alloys have a wider medical application. Generally, the low elasticity modulus, including also the very beneficial combination of other mechanical properties, categorize titanium and its alloys into a group of materials which are extraordinarily adequate for the production of implants with wide application possibilities.

Mechanical characteristics of commercially pure titanium and titanium-based biomedical alloys are shown in Table 6.

4 Conclusion

Adequate selection of metal biomaterials for different medical applications, among the other, must be based on an approach which enables the compatibility of mechanical properties of materials with the conditions in which they will be used. It further implies that mechanical properties of biomaterials must be good enough to enable the medical implants, devices and instruments to perform the desired function under the activity of external loads. Also, mechanical properties must be taken into account at the discussing of selection of technical procedure for the production of biomedical components.

Generally, mechanical properties of metal biomaterials are the most significant bearers of information from the aspect of estimating the biofunctionality of medical components and adequate selection of technical procedure for their production.

References

Agrawal CM, Ong JL, Appleford MR, Mani G (2014) Basic properties of materials. In: Introduction to biomaterials: basic theory with engineering applications. Cambridge University Press, Cambridge, pp 19–47

Antunes RA, Lopes de Oliveira MC (2012) Corrosion fatigue of biomedical metallic alloys: mechanisms and mitigation. Acta Biomater 8:937–962

ASTM (2003) ASTM F 138: standard specification for Wrought 18chromium-14nickel-2.5molybdenum stainless steel bar and wire for surgical implants (UNS S31673), West Conshohocken, ASTM International

Baldev R, Subramanian V, Jayakumar T (2000) Non-destructive testing of welds. Narosa Publishing House, New Delhi

Brunski JB (1996) Metals. In: Ratner BD, Hoffman AS, Shoen FJ, Lemons JE (eds) Biomaterials science: an introduction to materials in medicine. Academic Press, San Diego, pp 37–50

Brunski JB (2004) Metals. In: Ratner BD, Hoffman AS, Shoen FJ, Lemons JE (eds) Biomaterials science: an introduction to materials in medicine, 2nd edn. Academic Press, pp 137–153

Burke S, Ditchburn R (2013) Review of literature on probability of detection for magnetic particle nondestructive testing, Maritime Platforms Division, Defence Science and Technology Organisation (DSTO)

Chandler H (ed) (1999) Introduction to hardness testing. In: Hardness testing, 2nd edn. ASM International, pp 1–13

Chen Q, Thouas G (2015) Metallic implant biomaterials. Mater Sci Eng 87:1–57

Davis JR (ed) (2003) Overview of biomaterials and their use in medical devices. In: Handbook of materials for medical devices. ASM International, pp 1–11

Gałuszka G, Madej M, Ozimina D, Kasińska J, R. Gałuszka R (2017) The characterisation of pure titanium for biomedical applications. Metalurgija 56(1–2):191–194

Geetha M, Singh AK, Asokamani R, Gogia AK (2009) Ti based biomaterials, the ultimate choice for orthopaedic implants—a review. Progr Mater Sci 54(3):397–425

Gotman I (1997) Characteristics of metals used in implants. J Endourol 11(6):383–389

Hermawan H, Ramdan D, Djuansjah JRP (2011) Metals for biomedical applications. In: Faze Rezai RF (ed) Biomedical engineering—from theory to applications. InTech, Rijeka, pp 411–430

Hiromoto S (2008) Corrosion of metallic biomaterials in cell culture environments. Electrochem Soc Inter 17(2):41–44

Jevremovic D, Puskar T, Kosec B, Vukelic Đ, Budak I, Aleksandrovic S, Egbeer D, Williams R (2012) The analysis of the mechanical properties of F75 Co–Cr alloy for use in selective laser melting (SLM) manufacturing of removable partial dentures (RPD). Metalurgija 171–174

Lane WA (1895) Some remarks on the treatment of fractures. BMJ 1:861–863

Li JP (2007) Porous titanium for biomedical applications: development; characterization and biological evaluation. PhD thesis, University of Twente

Lindner J, Menzel K, Nirschl H (2013) Simulation of magnetic suspensions for HGMS using CFD, FEM and DEM modeling. Comput Chem Eng 54:111–121

Low S (2001) Rockwell hardness measurement of metallic materials. National Institute of Standards and Technology, Washington

Luk B, Luk A, Chan H (2007) Human factors and ergonomics in dye penetrant and magnetic particles nondestructive inspection methods. Eng Lett 15(1):EL15125

Malekani J, Schmutz B, Gu Y, Schuetz M, Yarlagadda P (2012) Orthopedic bone plates: evolution in structure, implementation technique and biomaterial. Int J Eng Technol 1(1):135–140

Mohammed MT, Khan ZA, Siddiquee AN (2014) Beta titanium alloys: the lowest elastic modulus for biomedical applications: a review. Int J Chem Nucl Metall Mater Eng 8(8):772–777

Motukisi E (2012) Magnetic particle inspection: characterisation of the magnetic field for various magnetization techniques. In: 18th world conference on non destructive testing, Durban, South Africa, pp 16–20

Niinomi M, Nakai M, Hieda J (2012) Development of new metallic alloys for biomedical applications. Acta Biomater 8:3888–3903

Park JB, Kim YK (2003) Metallic Biomaterials. In: Park JB, Bronzino JD (eds) Biomaterials: principles and applications. CRC Press, Boca Raton, pp 1–20

Patel NR, Gohil PP (2012) A review on biomaterials: scope, applications & human anatomy significance. Int J Emerg Technol Adv Eng 2(4):91–101

Petrovic V, Vicente Haro J, Ramón BJ, Portolés L (2012) Additive manufacturing solutions for improved medical implants. Biomedicine 147–180

Poitout D (2016) Biomechanics and biomaterial in orthopaedics, 2nd edn. Springer, Berlin. doi:10.1007/978-1-84882-664-9

Ratner B, Hoffman A, Schoen F, Lemons J (2013) Biomaterials science: an introduction to materials in medicine. Elsevier, Amsterdam

Reynolds LA, Tansey EM (eds) (2007) Early development of total hip replacement. First published by the Welcome Trust Centre for the History of Medicine at UCL

Roeder R (2013) Mechanical characterization of biomaterials. In: Bandyopadhyay A, Bose S (eds) Characterization of biomaterials. Elsevier, Amsterdam, pp 49–104

Sand A, Stener J, Toivakka M, Carlson J, Pålsson B (2016) A Stokesian dynamics approach for simulation of magnetic particle suspensions. Miner Eng 90:70–76

Silver F (1994) Biomaterials, medical devices and tissue engineering: an Integrated approach. Springer, Berlin. doi:10.1007/978-94-011-0735-8

Siraparapu YD, Bassa S, Sanasi PD (2014) A review on recent applications of biomaterials. Int J Sci Res. ISSN (Online) 2319-7064:70-75

Tanikić D, Manić M, Đenadić, D, Ranđelović S, Milovanović J, Đekić P (2012) Metals and alloys in function of biomaterials. Mil Tech Courier LX(2):202–215 (in Serbian)

Teoh SH (2000) Fatigue of biomaterials: a review. Int J Fatigue 22:825–837

Totten G, Liang H (eds) (2004) Mechanical tribology: materials, characterization, and applications. Marcel Dekker

Vetterlein T (2008) Application of magnetic particle inspection in the field of the automotive industry. In: 17th world conference on nondestructive testing, Shanghai, China, pp 25–28

Wahed M, Farhan M (2013) an investigationof non destructive testing of pressure vessel. Int J Emerg Technol Adv Eng 3–1:243–248

Yang K, Ren Y (2010) Nickel-free austenitic stainless steels for medical applications. In: Science and technology of advanced materials, pp 1–13. doi:10.1088/1468-6996/11/1/014105

Zhou YL, Niinomi M, Akahori T, Nakai M, Fukui H (2007) Comparison of various properties between titanium-tantalum alloy and pure titanium for biomedical applications. Mater Trans 48 (3):380–384

Manufacturability of Biomaterials

Saša Ranđelović

Abstract The increasing use of biomaterials in different areas of modern medicine raises the question of applicable technologies for their processing, as well as the ability to operate and control the parameters of such processes. The manufacturability of biomaterials primarily proceeds determined by their origins, mechanical properties, chemical composition, microstructure, the applicability of various technological and thermomechanical processes, dimensions and the purpose of a finished part. All these analyses require application of the most advanced production methods in order to obtain a safe and reliable element that will replace the natural biological functions of humans. When it is considered that all of these complex functions and requirements need to be fully met, or at least to as great an extent as possible, merely in the initial reviewing process, the manufacturability of biomaterials can appear to be the most crucial mechanical property to be imposed.

Keywords Manufacturability · Materials · Stress · Deformation · Technology

1 Introduction

A biomaterial is any metallic, ceramic or polymeric material that is used to replace or restore function to a body tissue and that is continuously or intermittently in a contact with bodily fluids. Biomaterials can be derived either from nature or they can be synthesized in the laboratory using an assortment of chemical approaches, utilizing metallic components, polymers, ceramics or composite materials (Ratner et al. 1996). Some applications of synthetic and natural materials in medicine can be classified according to the place where they are implanted, and to the role they play in a human organism: the skeletal system (joint replacements, bone defects, artificial tendons and ligaments, dental implants), the cardiovascular system (blood

S. Ranđelović (✉)
Faculty of Mechanical Engineering, University of Niš,
A. Medvedeva 14, 18000 Niš, Serbia
e-mail: sassa@masfak.ni.ac.rs

F. Zivic et al. (eds.), *Biomaterials in Clinical Practice*,
https://doi.org/10.1007/978-3-319-68025-5_24

vessel prostheses, heart valves), organs (artificial hearts, skin repair), etc. For each of these groups, the proper materials and their modifications have already been selected (titanium, Ti-Al-V alloy, stainless steel, polyethylene, polymethyl acrylate, Teflon, dacron, silicone rubber, polyurethane, etc.) that are most suitable for the required natural functions and anatomical forms.

Applied production technologies and process parameters are defined according to the final requirements that need to be fulfilled (Bakerjian 1992). First of all, questions arise as to the following: the part level of dimensions, chemical and biological environmental body conditions, the predicted time of use and exploitation, the required level of accuracy, and the quantity and number of needed products (Helsen and Breme 1998). All of these directly affect the market price of products.

2 Manufacturability of Metallic Biomaterials

When molten metals are cooled into a solid state, the atoms rearrange themselves into a crystal structure. There are three basic crystal structures for most metals: body-centered cubic, face-centered cubic, and hexagonal close-packed. Every structure has different properties and shows distinct behavior when subjected to loading in the application (Lange 1985).

Each body and its interior structure, under the effects of external forces, passes through the zone of elastic deformations, or, under high loads, enters the zone of permanent or plastic deformations. After the action is terminated, in the first zone, the elastic deformation forces disappear, while in the plastic zone, they permanently deform the body, i.e., its internal grain structure. The grain structure itself is not ideal, i.e., various irregularities of various shapes and sizes may be observed in it through a microscope, which serves to explain numerous phenomena of the physical behavior of metals. Those irregularities can occur in the form of interstitial atoms, impurities, dislocations, grain boundaries, and pores.

Dislocation is a defect that could explain the discrepancy between the actual strength of metals and the theoretical calculations based on molecular dynamics (Fig. 1).

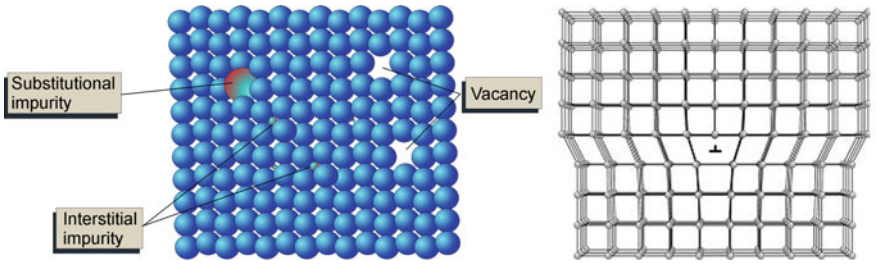

Fig. 1 Internal dislocation models of metals

The ideal atomic structure of a metal, without irregularities such as excessive atoms and flaws, results in the highest possible deformation force, i.e., the highest internal stress. Such a structure results in very low manufacturability in the processes of the plastic deformation of metals (Hull and Bacon 2009). An increase in the number of flaws, up to a certain number in a unit of volume, leads to reduction of the internal stresses required to effect a plastic or permanent deformation of the metal. Also, their excessive number causes an increase in internal stresses, requiring a higher deformation force to deform metal. In the first case, there is an almost ideal atomic structure without disruption of the links between atoms, while in the second case, the number of disruptions and disturbances in the structure is so high that any dislocation movement is very difficult, since they prevent one another from progressing. The ideal manufacturability of a metal, using plastic deformation procedures, requires an optimum number of dislocations per volume unit of the chosen metal (Dieter et al. 2003).

After the invention of the electron microscope, many scientists directly observed the existence of dislocations or imperfections of microstructures. Since then, a dislocation theory has evolved that explains many of the physical and mechanical phenomena in metals (Hull and Bacon 2009). Another important type of defect, on the upper level dimensions, is the grain boundary. The mechanical properties of metals are significantly influenced by the size and shape of their grain. At ambient temperatures, metals with large grain size generally have low strength and hardness, and are also low in ductility. Since grain boundaries hinder the movement of dislocations, they also influence the strain hardening process to increase the strength and ductility of metals (Krausz and Krausz 1996).

Pure metals have relatively limited properties, however, these properties can be enhanced by alloying the metals. Most of the metals used in engineering applications and production technology are in the form of their alloy. Numerous alloys consist of two or more solid phases in the form of either solid solutions or intermetallic compounds that depend on the alloying composition and temperature (Drozda et al. 1992). A phase is defined as a homogenous portion in a material that has its own physical and chemical characteristics and properties (Ashby and Jones 2011). Every pure metal is considered to be a phase, as is every solid solution and intermetallic compound. Alloying a metal with finely dispersed particles as a second-phase is one of the most important methods for strengthening alloys and enhancing their properties. The second-phase particles present as obstacles to the movement of dislocations, thus increasing the overall strength and hardness of the alloys (Steck et al. 2001).

In the metal forming process, “manufacturability” commonly refers to the ease with which a material can be shaped by plastic flow without the onset of external or internal fractures. This general term includes all other terms like forgeability, rollability, extrudability and formability of bulk and sheet metal working. Under laboratory conditions, the well-known mechanical tests that are used to measure this parameter are tensile testing, compression testing, torsion testing and cupping tests (Lee et al. 2011).

All available information and research on metal-working clearly shows that manufacturability is influenced not only by the microstructure of the material, the applied temperature, the strain rate and the strain, but also the state of the stress in the deformation zone (Bhadeshia and Honeycombe 2006). It is now generally understood that manufacturability consists of two independent parts: the state of stress manufacturability and the intrinsic manufacturability. The parameters and production methods that directly influence these two parts are further discussed below.

2.1 State of Stress Manufacturability

The state of stress manufacturability depends upon the geometry of the deformation zone in which the workpiece is subjected to a state of three-dimensional stress.

Every process of plastic deformation of metals causes a certain state of stress in the deformation zone where shape and dimensions are transformed. Depending on the method of shaping and the geometry of the tool, a certain state of stress and deformation occurs, which does not depend on the material itself. The state of stress manufacturability is therefore specific to a metal-working process. In the most general state, it is the spatial (three-dimensional) state of stress that causes various deformation states in certain parts of the volume for the duration of the process (Steck et al. 2001). Total deformation and susceptibility of a material to deformation or manufacturability are different in individual methods. The choice and design of a proper geometry of tools and their contact surfaces for the desired geometry of a finished workpiece directly cause the plastic flow of metal. In the tool itself, for a proper method, that geometry can be transitional roundings and gradients in the tool (forging), die angle and length of contact at the exit (extrusion), profile, rounding and angle of the rollers (rolling technology), die round and contact surface of the blank holder (deep drawing technology), but also the quality of the contact surfaces of tools and materials. Contemporary software solutions for the modeling of tools and simulation of processes allow technology designers to vary the above-mentioned tool parameters at an early phase, and to monitor their effects on the virtual model. After obtaining the true and optimal results, with satisfactory stress and deformation states, the production process of the designed element can start in earnest, with a very small risk of error. The state of stress manufacturability is therefore specific to a metal-working process (Lange 1985).

The total stress at the specified point of a deformable volume is a variable that is determined to be the quotient of the differential increase in force and the unit area element when it tends towards zero:

$$\vec{t}^{(n)} = \lim_{\Delta A \to 0} \frac{\Delta \vec{F}}{\Delta A} = \frac{d\vec{F}}{dA} \tag{1}$$

whose value depends on the normal direction of the selected plane. If the above-mentioned total stress vector in the selected point is decomposed into two normal directions, the normal and tangential components of the stress are obtained:

$$\vec{t^{(n)}} = \vec{\sigma}_n + \vec{\tau}_n \quad \text{or} \quad t^2 = \sigma^2 + \tau^2 \tag{2}$$

Since the stress state at a point depends on the position of the selected plane, or its normal, the total stress by Cauchy is a scalar product:

$$\vec{t^{(n)}} = \vec{n} \cdot T_\sigma \tag{3}$$

where the stress state at the point of the solid—body defined by the stress tensor with nine components is

$$T_\sigma = \begin{bmatrix} \sigma_x & \tau_{xy} & \tau_{xz} \\ \tau_{yx} & \sigma_y & \tau_{yz} \\ \tau_{zx} & \tau_{zy} & \sigma_z \end{bmatrix} \tag{4}$$

According to the law of the conjugate of shear stress, the stress state is defined by six independent components of the stress tensor (Lange 1985).

The stress tensor in the selected point can be decomposed into a spherical stress tensor (T_σ^s) and stress deviator (D_σ):

$$T_\sigma = T_\sigma^s + D_\sigma = \begin{bmatrix} \sigma & & \\ & \sigma & \\ & & \sigma \end{bmatrix} + \begin{bmatrix} \sigma_x - \sigma & \tau_{xy} & \tau_{xz} \\ \tau_{yx} & \sigma_y - \sigma & \tau_{yz} \\ \tau_{zx} & \tau_{zy} & \sigma_z - \sigma \end{bmatrix} \tag{5}$$

where is σ-the mean normal stress.

A change in the shape and dimensions of the body can produce only deviatoric stress, while spherical stress tensor products only change the volume of the body. The matrix display shows that shape change is not possible without the presence of shear stress, as confirmed by the real conditions of plastic deformation.

Medium normal stress or normal hydrostatic pressure is defined by the following relation:

$$\sigma = \frac{\sigma_x + \sigma_y + \sigma_z}{3} = \frac{\sigma_1 + \sigma_2 + \sigma_3}{3} = p \tag{6}$$

where:

σ_1 , σ_2 , σ_3 is the main principal stress.

Principal normal stresses act in three perpendicular planes called the main planes (principal planes), in which the tangential stresses are zero (Lange 1985).

The main tangential stresses (principal shear stresses) act in plane pairs at an angle of ±45° in relation to the main planes, and they are determined using the relations:

$$\tau_{12} = \pm\frac{\sigma_1 - \sigma_2}{2}; \quad \tau_{23} = \pm\frac{\sigma_2 - \sigma_3}{2}; \quad \tau_{31} = \pm\frac{\sigma_3 - \sigma_1}{2}; \tag{7}$$

Three of these terms are shear components that actually cause the plastic flow (there can be no plastic deformation or dislocation movement without a shear stress), and the other three components are diagonal components that are hydrostatic in nature. The hydrostatic components actually decide the state of stress manufacturability, since if these are tensile, any weak interface in the material, such as at a non-metallic inclusion, will generate internal fractures. In order to achieve the state of stress manufacturability, the hydrostatic components should be essentially compressive in nature. The occurrence of tensile stress in any form significantly reduces the achieved level of deformation and very quickly leads to the appearance of perturbation structure and fracture (Lange 1985).

Effective normal stress (effective, equivalent stress) is a positive scalar value, the equivalent effect of all components of a stress tensor:

$$\sigma_e = \frac{1}{\sqrt{2}}\sqrt{(\sigma_1 - \sigma_2)^2 + (\sigma_2 - \sigma_3)^2 + (\sigma_3 - \sigma_1)^2} \tag{8}$$

and the effective tangential stress:

$$\tau_e = \frac{\sigma_e}{\sqrt{3}} \tag{9}$$

The ratio of mean normal stress and effective stress produces the workability, or manufacturability, parameter β:

$$\beta = 3\frac{\sigma}{\sigma_e} \tag{10}$$

It is observable in the figure that the β parameter has considerably higher absolute values in the zone where the material is upsetting, i.e., when compressive stresses are dominant (extrusion technology, rolling, forging), than it does in the zone in which the tensile stresses are dominant (wire drawing). If there is failure of the material, the manufacturability parameter β and boundary effective deformation define a point above the boundary curve, while if there is no destruction, the state of stress is defined in the zone below the curve with appropriate values β and $\varphi_{\text{e.g.}}$ (Fig. 2).

The issue of boundary deformability of sheet metal in comparison with the volume deformation represents a somewhat simpler analysis, because it is a two-dimensional state of stress (Fig. 3). Primarily, it largely depends on which sheet metal deformation process is considered (deep drawing, bending, stretching,

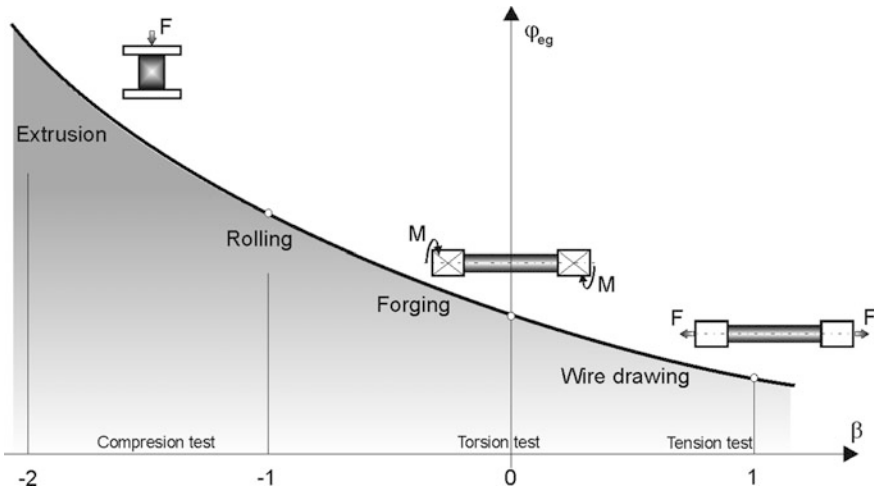

Fig. 2 Curve of manufacturability in bulk plastic deformations

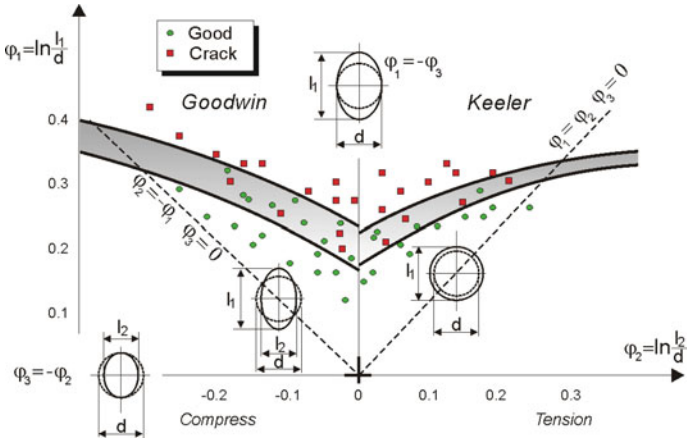

Fig. 3 Curve of manufacturability in sheet metal forming

diameter reduction), as well as on the fact that it cannot be defined with only one parameter (Emmens 2011). It should be noted that the boundary curve, according to Keeler–Goodwin, is situated somewhere inside the grey area, and that there are always exceptions and irregularities that will unequivocally indicate the extent of the mentioned zones.

All the points in the diagram lying below the curve represent deformation states in which the structure in the metal is without cracks, while the points lying on the curve and above it represent states of deformation in which deformability of the material has been fully exhausted (Banabic et al. 2000).

A network of measuring cells in the form of circles is applied to the undeformed surface of the sheet metal, which, due to the plastic deformation, can have a positive deformation in the direction of the main axis, while in the normal direction, along the width, the deformation can be negative (Fig. 3). The points below the zone of the boundary curve represent the cases in which there is no destruction (green), while the points above the curve (red) represent those in which there is destruction.

In practical calculations, the typical degree of deformation, with a positive sign, is elected as an indicator strain state. Absolute deformation (elongation) represents the appropriate dimensions before and after the deformation process (Fig. 4):

$$\Delta x = x_0 - x_1 \quad \Delta y = y_0 - y_1 \quad \Delta z = z_0 - z_1 \tag{11}$$

Also, it is possible to define the notion of nominal strain, for example:

$$\varepsilon_x = \int_{x_0}^{x_1} \frac{\Delta x}{x_0} = \frac{x_1 - x_0}{x_0} \quad \varepsilon_z = \frac{\Delta z}{z_0} = \frac{z_0 - z_1}{z_0} \tag{12}$$

The relative changes in cross-section or reduction in area:

$$\psi = \frac{\Delta A}{A_0} = \frac{A_0 - A_1}{A_0} \tag{13}$$

The relation between stress and strain in the area of elasticity, or a deformation corresponding to a stress, or by Hook's law in the x direction:

$$\varepsilon_x = \frac{1}{E}\left[\sigma_x - \mu_p\left(\sigma_y + \sigma_z\right)\right] \tag{14}$$

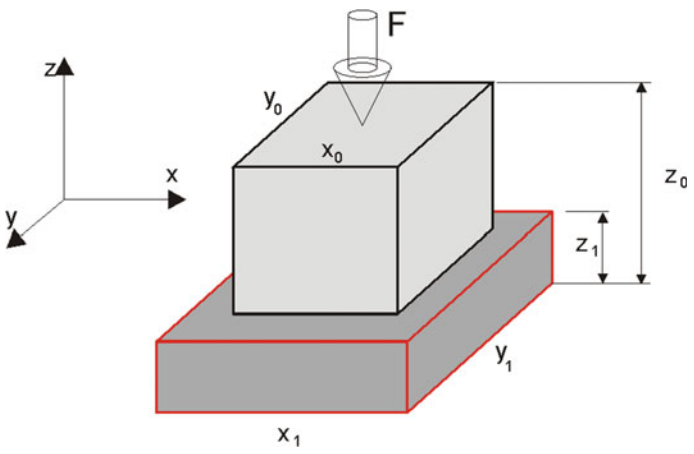

Fig. 4 Ideal deformation model

or tangential deformation in the xy plane:

$$\gamma_{xy} = \frac{\tau_{xy}}{G} \tag{15}$$

where E is Young's elasticity modulus, G is the shear modulus, and μ_p is Poisson's ratio (Smalmman and Bishop 1999).

The modulus of elasticity and shear modulus are internal characteristics of the selected materials, which are directly proportional in relation to the interatomic forces and their distance and inversely proportional to the distance between atoms in an equilibrium state, a fact that does not depend on the process of its production. The mathematical relationship between these parameters is given by:

$$G = \frac{E}{2(1+\mu_p)} \tag{16}$$

In the field in which plastic stress and strain relation, or constitutive equation, are not unique, a stress state corresponds to only one strain state, but the opposite is not true, that is, the conditions of a strain may produce different stress states (Callister and Rethwisch 2014).

During the process of plastic deformation continuum, the entire volume is not exposed to plastic deformation at just any moment, but rather takes place only in the zone of immediate effect tools. The mechanical stress and strain scheme show a stress and strain state in the zone of plastic deformation.

The volume stress and strain state are represented by three arrows, the plane stress and strain state by two arrows, and the linear stress state by one arrow (Fig. 5).

The total stress in the process of plastic deformation consists of plastic deformation stress and the stress of contact friction (Boisse et al. 2003). The law of lower resistance may be defined by the following formulation: if there a possibility of the movement of dots in deformable bodies by different trajectories and different directions, every point will move in the direction of lower resistance (Lange 1985).

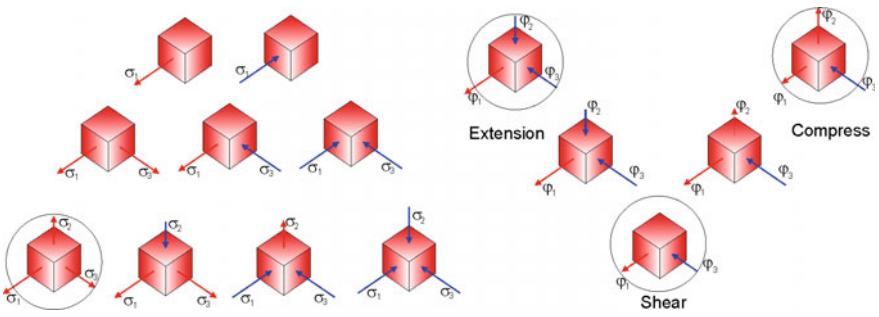

Fig. 5 The stress strain state illustrated by the mechanical scheme

It is very important to determine the trajectories of the points with the lowest resistance inside of the body so as to monitor them while observing practical problems. This complex continuum mechanics problem is solved based on experience and virtual modeling through finite element methods of the simulation of material flow in the metal-forming process.

In accordance with this law, the "principle of the shortest normal" is formulated: movement of any point of deformable bodies in the plane normal to the external surface (Fig. 6).

In the process of upsetting the prism, with the rectangular cross-section a × b, under real conditions (friction coefficient $\neq 0$), material will flow mainly in two directions, until it reaches the point on the line equidistant from the sides so that the lines of the section flow (neutral line) will remain unchanged.

At higher degrees of deformation, a cross-section degenerates to an approximate elliptical in order to get a circular cross-section at a very low height (Fig. 7a). Under ideal conditions, the afore-mentioned deformation (compression) principle is not completely filled, because the material tends to keep its initial shape (Fig. 7b).

The total deformation of metals and their alloys represents the sum of elastic and plastic deformations. The elastic deformation disappears after relaxation of the deformation forces. Given that the density of the material in the deformation process does not change, the law of mass or volume conservation can be defined in the following words: the volume of deformable bodies before deformation is equal to the volume of the bodies after deformation.

However, if the elastic and plastic deformations are of approximately the same order of magnitude, then it is called elastic - plastic deformation. The presence of elastic deformation results in a negligible change in the shape and dimensions of the body.

The previous facts may be most simply explained through the prism upsetting (Fig. 4), from the law of conservation of volume as follows:

$$V_0 = z_0 y_0 x_0 = z_1 y_1 x_1 = V_1 = const. \tag{17}$$

From the above, the relation is obtained:

$$\frac{z}{z_0}\frac{y_1}{y_0}\frac{x_1}{x_0} = 1 \quad \text{i.e.} \quad \ell n\frac{z_1}{z_0} + \ell n\frac{y_1}{y_0} + \ell n\frac{x_1}{x_0} = 0 \quad \text{i.e.} \quad \varphi_z + \varphi_y + \varphi_x = 0 \tag{18}$$

where φ_x is the logarithmic degree of deformation.

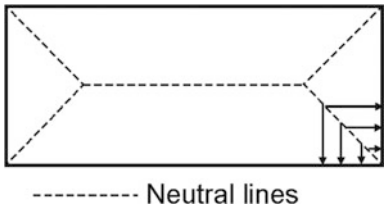

Fig. 6 Principle of the shortest normal illustration

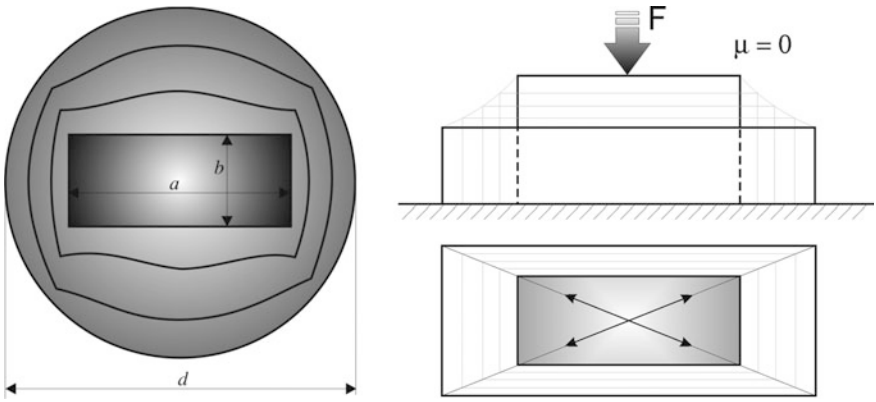

Fig. 7 The rectangular cross-section deformation at upsetting

From the last relations, we can draw the following conclusions:

- at plastic deformation, the algebraic summation of the logarithmic degree of deformation in three mutually perpendicular directions is equal to zero.
- all three levels of deformation do not have the same sign;
- the deformation process cannot be realized in one direction only (uniaxial deformation does not exist).

The velocity that forms is the speed of a moving part of the tool (v), while the strain rate ($\dot{\varphi}$) represents a change in the degree of deformation per unit of time or the speed of movement dislocation of the structure within the continuum:

$$\dot{\varphi} = d\varphi/dt \tag{19}$$

According to this definition, at continual stretching or upsetting of the cylindrical tube at a constant rate of deformation (v), the following strain rate is obtained:

$$\dot{\varphi} = \frac{d\phi}{dt} = \frac{d\ell/\ell}{dt} = \frac{1}{\ell}\frac{d\ell}{dt} = \frac{v}{\ell} \tag{20}$$

$$\dot{\varphi} = \frac{d\dot{\varphi}}{dt} = \frac{dh/h}{dt} = \frac{1}{h}\frac{dh}{dt} = \frac{v}{h} \tag{21}$$

where l and h are the dimensions of the current samples. By definition, the strain rate is a very complex physical value in the design process of plastic deformation.

The volume conservation law directly implies that the sum of the total strain in the three normal areas is:

$$\dot{\varphi}_z + \dot{\varphi}_y + \dot{\varphi}_x = 0 \tag{22}$$

One of the fundamental laws of the cold metal-forming process is work hardening (Fig. 8), which is reflected in the following:

- an increase in the stress values,
- lower plasticity values.

The plasticity properties during the metal-forming process, at successive operations, can be completely exhausted, so that further processing is not possible without causing cracks and destruction of the workpiece. It is therefore necessary to carry out a heat treatment after a certain number of operations in order to restore the plastic properties of the metal. The hardening effects of the cold forming process are very prominent, while in the hot deformation process, they are negligible (Lange 1985).

2.2 *Intrinsic Manufacturability*

This part of manufacturability is decided by the constitutive behavior of the material and is sensitive to the processing history (chemical composition, initial microstructure, thermo-mechanical treatment or heat treatment), the deformation temperature, the applied strain rate and the strain. This response is embedded implicitly in the flow stress variation with temperature, strain rate and strain and is

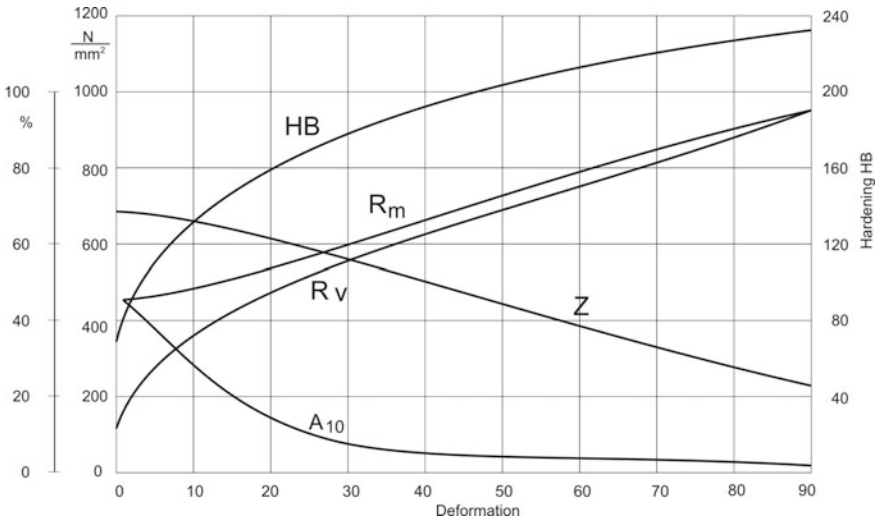

Fig. 8 The mechanical parameters of work hardening for a lower carbon stell

represented mathematically as a constitutive equation. However, the explicit response of the material in terms of a change in its microstructure can be studied in detail using suitable material models.

The plastic deformation of an element means that there are no disruptions of the metal structure, such as the onset of micro-cracks, local uncontrolled flow of a part of the grain structure, etc. It is a direct consequence of the volume conservation law, which indicates its nonchangeability during the deformation process. In order to prevent it from happening during and after the process of plastic deformation, various thermal procedures that reduce internal stresses (recrystallization) or use of more suitable materials that can be deformed at a higher degree of deformation without developing micro-cracks (superplastic materials) will do the trick. Both examples indicate an enhanced intrinsic manufacturability that dominates over the state of stress manufacturability, since if the mechanism of deformation causes microstructural damage, the state of stress control may reduce its intensity but cannot eliminate it completely. In technological terms, the intrinsic manufacturability offers multiple possibilities for solving the problems that occur in the deformation process itself.

It is advisable therefore to select the optimum intrinsic manufacturability parameters first and then design the best upper and lower die possible to obtain the required shape. This consideration of process design ensures success in every case. In orthopedic surgery, the biomaterials used are generally based on stainless steels, superalloys based on cobalt and chromium (Co-Cr), titanium and its alloys and, more recently and very rarely, composite materials.

2.2.1 Manufacturability of Stainless Steel

There are many ferrous-based alloys that are commercially identified as stainless steel. Only austenitic and precipitation reinforced steels are used in orthopedic surgery as a biomaterial. Non-alloyed iron, carbon steels and other alloyed steels cannot be used in orthopedic surgery for the manufacture of implants, since they are subject to corrosion in aggressive solutions containing oxygen (Ashby 2005).

Austenitic stainless steels are ranked first in terms of the number of varieties and total industrial production. They are corrosion consistent within a number of more or less aggressive environments. Their minimum yield strength at room temperature is about 210 N/mm^2 and they are not subject to thermal strengthening. They retain good properties at very low temperatures. The maximum application temperature is about 760 °C, up to which there is no decrease in mechanical strength and resistance to oxidation. They can be considerably strengthened with a cold metal-forming process (Randjelovic et al. 2012a, b). They are used in conditions in which good resistance to atmospheric corrosion and corrosion at elevated temperatures is desired. They have good weldability.

The alloying elements that ensure the formation of an austenitic microstructure are nickel, copper and oxygen. The total mass share of alloying elements generally exceeds 8%.

Although carbon is not an alloyed element, it too is contained in the austenitic microstructure in order to increase creep resistance. Oxygen is also influential, since it increases strength at both ambient and low temperatures. Due to their high proportion of alloying elements, austenitic steels are more expensive than martensitic and ferritic stainless steels with mid-range and lower chromium content. However, their good properties, especially their good deformability at elongation and weldability, justify the price difference.

The presence of chromium in stainless steels leads to the formation of a self-regenerative oxide layer that is resistant to perforation and has a high degree of electrical resistance, thus providing protection against corrosion to the fullest extent. Nickel, as an alloying element, increases corrosion resistance and provides better manufacturability of steel, especially forgeability. Molybdenum provides higher resistance to pitting, and magnesium and silicon influence improved manufacturability. Carbon must be strictly controlled, because its presence is undesirable; carbon content must not exceed 0.03%, since the alloying elements build carbides that are unfavorable (especially chromium carbide). Attaching chromium creates zones with reduced corrosion resistance, and as carbides are usually separated by grain boundaries of crystals, it promotes intergranular corrosion, as well as irregularities in the conditions of the micro crystal lattice, with a consequent deterioration of mechanical properties.

Contact corrosion can occur in implants made of stainless steel. If the two parts of the implant are fitted to one another, for example, by a plate-screw, the gap between them has a lower concentration of oxygen than in neighboring areas, and thereby forms a so-called oxygen concentration cell with a stress that is capable of overcoming the passive nature of the protective layer of cobalt oxide that forms on the surface of the alloy, allowing the occurrence of localized corrosion and its progression (Yan et al. 2007).

Fatigue failure is possible in all these materials, if they are exposed to alternately variable loads, which is to be expected, especially for the femoral component of the hip joint. Fatigue failure starts with small cracks resulting from some defect in the crystal lattice or mechanical error processing, cracks that steadily increase with each cycle of changes in the load or stress states, until they reach a critical size value, and fractures occur. In order to avoid the presence of any inclusions, which can lead to errors in the crystal lattice or the occurrence of initial cracks, stainless steel AISI 316LVM is melted in a vacuum.

Using stainless steel, through methods of cold and hot plastic deformation, the real parts of the joint prostheses (total hip, knee, shoulder and elbow), parts for fracture fixation, such as plates, screws, and external fixators, and parts for fixation of the spine are created. The necessary holes for attachment of the implant are obtained through profile milling methods in the case of irregular holes, or drilling if the holes are regular (Fig. 9). Irregular holes allow for small displacements and settings when embedding the implants, depending on the specific conditions of the surgical procedure for the selected patient.

Fig. 9 Orthopedic implants made of stainless steel

2.2.2 Manufacturability of Cobalt and Its Alloys

Cobalt superalloys are used because pure metals cannot fulfill all of the requirements for the production of high quality implants. Responding alloying elements are added to improve mechanical properties and increase strength, corrosion resistance, ductility, and so on.

Research and development of cobalt-based superalloys dates back to the early twentieth century, when the first patent - based superalloy, cobalt Co-Cr-Mo, which was intended for use in dentistry (Bonfield and Tanner 1997), was invented. Furthermore, its development and modification created superalloys suitable for forging and casting in the production of implants with complicated configurations. Initially, this material was known under the commercial name of BS21 and was produced in the form of granules, the smelting being performed in indirect arc furnaces (Vincent 1990).

For the production of biomedical parts with complicated configurations, using conditions and methods developed for dentistry, casting has been developed, and when it comes to implants, casting is done in a vacuum. Alloys of Co-Cr-Mo (ASTM F-175) are suitable for casting when the same level leads to a powder, thus achieving maximum occupation of the crystal lattice without microporosity, obtaining a homogeneous fine-grained structure with high mechanical properties and a high isostatic pressure process (Doni et al. 2013).

2.2.3 Manufacturability of Titanium and Its Alloys

Titanium is an extremely reactive element that resides in the earth's crust as a stable oxide, which only confirms the fact that the metal version of titanium and oxygen are not easily separated. For this reason, titanium has only been in commercial use in the United States from the end of the fourth decade of the last century. Although titanium began to be used for medical purposes much later than other biocompatible metallic materials, its use for medical purposes was soon improved significantly owing to its favorable properties, such as a relatively high specific strength, low elasticity modulus, high biocompatibility and an extremely low level of toxicity, although it also exhibited worse tribological properties, especially when compared to stainless steel and Co-Cr alloys. Thanks to the quick reaction of titanium with

oxygen at room temperature, a very stable, passivating oxide film forms on the surface of titanium (Long and Rack 1998).

Commercially pure titanium, which is popularly marked as CP titanium, is characterized by an α single phase microstructure. CP titanium can contain very low amounts of iron, nitrogen and oxygen, while the total content of other elements is mandatorily lower than 0.7%. Because of slight, but strictly defined, differences in composition, CP titanium is produced in four basic compositions, which are numbered from 1 to 4. The higher the number, the higher the value of the tensile strength that characterizes these compositions. Compared to the titanium alloys, pure titanium is characterized by an increased resistance to corrosion, while the α titanium alloys have a higher resistance to elevated temperatures and better weldability than the β alloys.

Commercially pure titanium is used primarily in dentistry, for dental implants, although it is also used in orthopedics in the form of wire mesh, which serves as a porous sintered coating on the surface of artificial joints made of titanium alloys (Frosch and Stürmer 2006).

Titanium and titanium alloys, in particular, alloys of the α and β types, such as Ti-6Al-4V, are considered to be the most attractive biocompatible metallic materials, due to their excellent combination of mechanical properties, corrosion resistance and biocompatibility.

However, the value of the modulus of elasticity is still significantly higher than the modulus of elasticity of human bones. In addition, research conducted over the past decade has shown that vanadium is extremely toxic, and for this reason, the development of new alloys that contain elements that would not be toxic to the human body is being worked on intensively.

In addition, in the development of new biocompatible titanium alloys, it is very important to achieve a lower modulus of elasticity close to that of bone tissue.

The basic idea in the development of new alloys for medical applications is the use of vanadium, aluminum, niobium, tantalum and zirconium as replacements, in order to avoid the negative characteristics of the widely used Ti-6Al-4V alloy, since it was shown that the toxicity of the above-mentioned elements is extremely low (Agrawal 1998).

The alloy Ti-13Nb-13Zr, developed in the USA, has shown exceptional properties. This is a β type titanium alloy and is characterized by low values of modulus of elasticity and strength, which are significantly improved compared to the commercial Ti-6Al-4V alloy, making it extremely interesting for applications in biomedical engineering.

The relatively low hardness of the alloys, however, affects their poor wear resistance, and thus these alloys cannot be used to create joint surfaces without additional surface treatment, such as ion implementation (Calin et al. 2014).

2.3 *Forgeability of Biomaterials*

Many of the previously mentioned alloys can be processed by hot or cold forging and drawing technology. Most often, it is all about forging performed in closed tools at elevated temperatures where the necessary redundant material ensures accuracy in terms of the forging geometry and dimensions of the set. The upper and lower tools are made of high quality steel that can suffer shock loading at elevated temperatures. They consist of a mold cavity corresponding to the shape of the finished work (negative) and extra space for storing excess material in the final stage of forging (ASM 1998). These two spaces are connected by a transitional bridge through which flows surplus material or flash.

The dimensions of the tools and the quality of the machined surfaces directly determine the accuracy of the finished parts. Excess material after the forging process eliminates additional deformation procedures (deburring) or cutting. If the geometrical requirements are less complex, the part can be fully enclosed in forging tools, so-called net shape working processes, which require neither excess material nor additional treatment of the finished work (Randjelovic et al. 2012a, b). Forging technology produces a homogenous, fine grain crystal structure without the use of microporosity, resulting in improved mechanical properties (Lange 1985). Continuity of the flow lines and the continuous transfer of loads without the occurrence of stress concentration are also provided (Fig. 10).

The molds (negatives) are made of hardened steel blocks, after which they are installed into a forging press. The front material (often in the form of pieces of an axle or strip) is heated in an oven until just below the liquid limit of this material (the point at which it becomes malleable). If the piece achieves the right temperature, it will be placed onto the lower mold (ASM 1998). Then, the top mold is closed with deformation force, one or more times. By this manipulation, the malleable material is beaten into the final shape. After forging, the product is taken out of the molds and placed inside a press in order to remove excess material, which is fitted with grinding blades (Fig. 11).

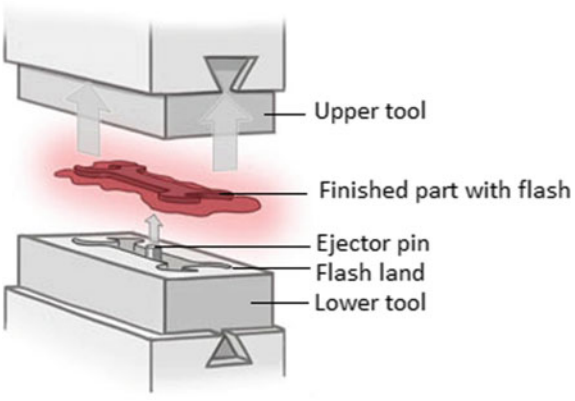

Fig. 10 Forging process illustration

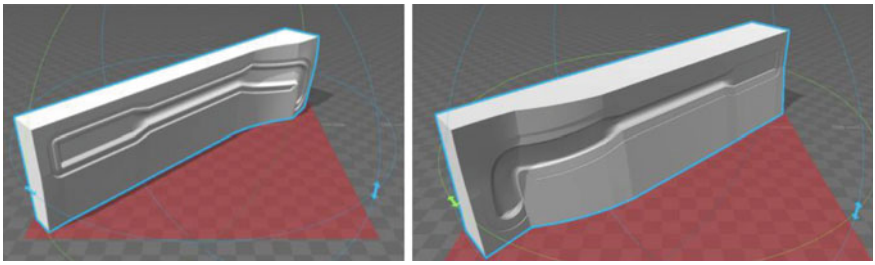

Fig. 11 Upper and lower tools for forging technology

2.4 Castingability of Biomaterials

Metal casting technology represents a procedure mastered by humans many centuries ago. However, contemporary casting technologies, especially in bioengineering, unite the traditional knowledge with new structural designs, a choice of suitable materials, the rapid construction of tools, and software simulation of the casting process. Lost waxing or investment casting represents one of the dominant processes in the production of metal-based orthopedic aids. This technology is very suitable for both small and large orthopedic implants that successfully replace the functions of biological organs in the human body (Fig. 12). Metals and their alloys (stainless steel alloys, brass, aluminium, carbon steel, etc.) exhibit extremely worthy manufacturability properties during casting, and thus implementation of this technology meets both the medical and the technological requirements.

In technological terms, it consists of several phases that directly determine the entire procedure and manufacturability of the mentioned materials. Firstly, the wax pattern is made through investment of the liquid in the designed individual or grapelike mold cavities (treelike), which are integrated with the runner system. The technology of low pressure injection is the most frequently used so that the remotest reaches of the volume will be filled in (Randjelovic et al. 2015). The aim of this stage is to make the dimensions of the cavities identical to the given dimensions and shape of the finished workpiece (Zhixia and Masakazu 2011). The obtained result is a spatial shell, which has to be coated with some slurry or ceramic material that will very soon form a coating layer over a more or less irregular spatial form on a common assembly. The hardened formed structure is thus prepared for wax

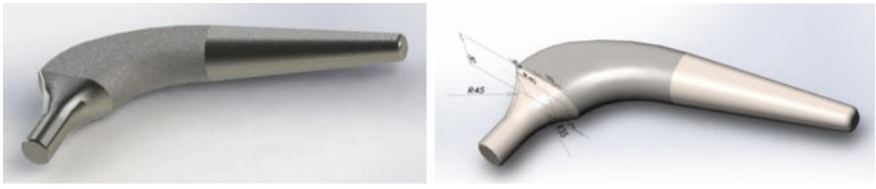

Fig. 12 Biomedical implants with dimensions produced by investment casting

removal, using high temperatures and melting, which will result in a hollow structure ready for casting. The molten metal is poured into the structure through the sprue and runner system; after the metal has hardened, the brittle slurry shell around the casting is removed using mechanical impacts, which produces one or several finished products on the designed assembly (Fig. 13).

The process of generation of the ceramic shell can be divided into the primary (interior contact surface with the metal) and the secondary (outer ceramic layer). The primary process of ceramic shell casting represents the bonding of several layers of ceramic powder over the previously-made wax mold, which comprises:

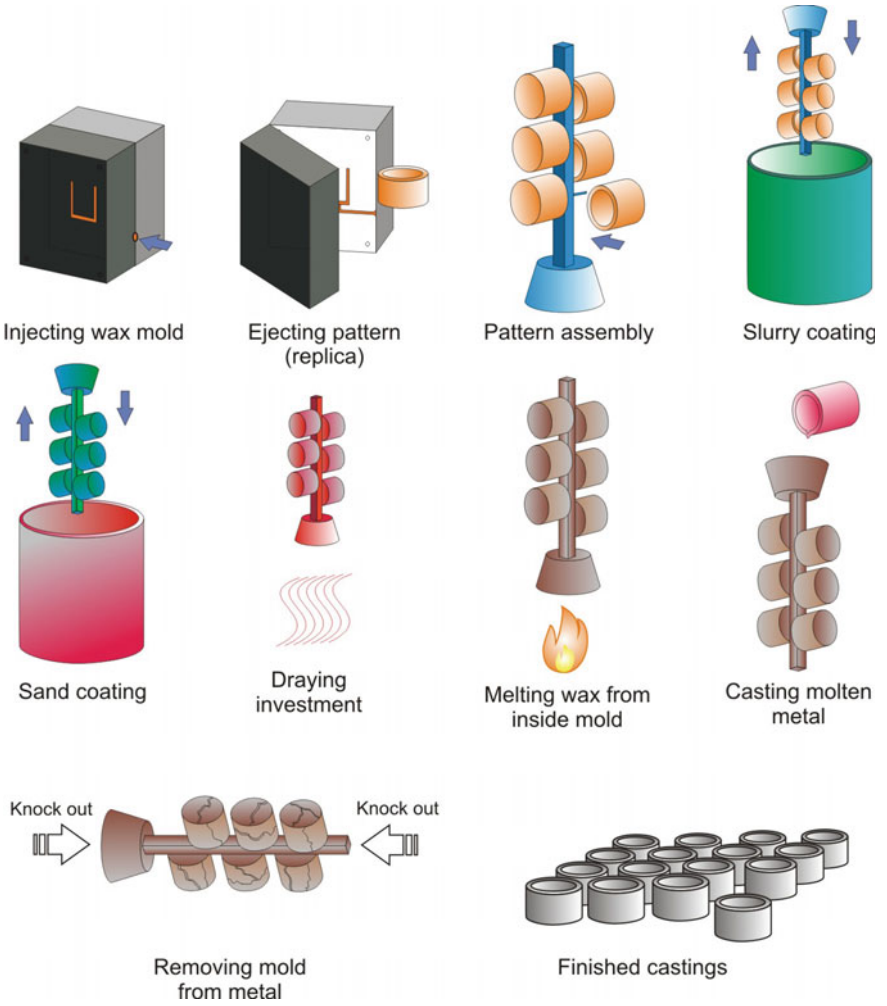

Fig. 13 Lost waxing or investment casting process

- washing of the external surface of the wax pattern in order to remove residual impurities,
- chemical treatment of the external surface of the wax pattern in order to improve hydrophilic properties,
- application of a coating of fine grainy ceramic suspension based on the Co-Cr alloy,
- application of a coating of up to ten layers of matrix made of coarse ceramic particles, up to several millimeters thick.
- application of a coating of finish made of fine ceramic particles.

Each of these layers contains a silicon binder for the establishment of strong bonds between the power articles. The secondary process of coating of ceramic particles comprises dipping the primary ceramic shell into the suspension of fine ceramic particles in the form of dust and the binder, drying it between applications of individual layers.

When the ceramic mold is finished, the wax inside is melted in order to provide a hollow mold for casting molten metal. The wax is melted in an autoclave under a high pressure of 8–10 bars at a temperature of 440–450 °C, depending on the size and volume of the mold cavity (Ratner et al. 1996).

The problems that may arise during removal of the wax are the onset of cracks in the ceramic mold due to uncontrolled wax expansion or incomplete draining of the wax from the ceramic mold. For molten metal casting, the ceramic mold obtained is prepared in two ways. It is first fired at a temperature slightly above that for metal casting, and left to cool gradually until the casting begins, or alternately, it is not allowed to cool prior to the metal casting process. The casting regime largely depends on the chosen metal and the characteristics and properties of the ceramics themselves. The limiting factors during the wax heating process are the onset of cracks and failure of the ceramic molds. In cases in which there is residual wax inside the ceramic mold and the flammable air is not sufficiently oxidized, incomplete combustion of the residual wax will cause air to be trapped inside the structure of the finished product. If impurities in the form of dust and free particles from ceramic powder are observed, this is also indicative that the casting will not have a satisfactory quality.

Investment casting is most frequently used for production of complex spatial forms for which other procedures would require more time and would increase the processing cost. As for biomaterials, one primarily has in mind orthopedic applications (femoral stems, hip prosthesis, knee joint components, etc.) and dentistry (dental devices), for which there is a pronounced demand for reconstructive surgery of affected or missing parts of the skeletal system. The most frequent technological flaw is poor filling of the empty space in the created mold, which directly results in bad or low-quality casting.

Investment casting is a very reliable industrial process, which is widely implemented wherever a high quality of castings and components of many varied forms and functions (automotive and aviation industries, etc.) is required.

3 Manufacturability of Porous Materials

Porous materials are used in cementless endoprostheses as a substitute for cement; they are applied to the endoprosthesis in order to enable the bone to grow into the porous structure, and thereby ensure fixation of the prosthesis. There is a variety of such materials, which are constantly under laboratory and clinical investigation. The application of a porous coating to metals, polymers, ceramics and composite materials is being tested. Bone tissue engineering is today considered to be a promising approach to second generation bone substitutes (Hao and Harris 2008). Porous materials are appropriate scaffolds for osteoblast cell cultures. The morphology of porosity influences cell spreading and cell ingrowth in bone substitutes. Macrointerconnections are necessary to promote cell ingrowth, and microporosity seems to influence the hanging adhesion of cells on the material. Porosity has a detrimental influence on mechanical strength, which directly causes the need for the handiness of the device when surgeons have additionally to adapt the machine to the block implants. It has generally been admitted that mechanical strength is not an important parameter for bone substitutes, but material with low mechanical properties will crumble under cyclic loading, and the resulting micromovements should generate fibrous tissue encapsulation. Mechanical strength, macrointerconnections and surface physico-chemical characteristics of bone substitutes are thus of equal importance, and none must be neglected if clinical success is to be guaranteed.

When a prosthesis with porous material is applied, it leads to a significant increase in the active contact area between the bone tissue and the metal, which leads to condition of an increased possibility that metal ions will diffuse into the surrounding tissue (Benson and Boretos 1995).

"Trabecular metal" is a special kind of porous biomaterial whose structure is most similar to that of cancellous (trabecular) bone. The cellular structure of trabecular metal approaches the physical and mechanical properties of bone more than that of any other synthetic material. The unique, highly porous trabecular configuration ensures quick and generous infiltration of bone tissue. The crystal microtexture of trabecular metal is conductive for the direct growth of bone tissue.

Tantalum, of which trabecular metal is made, is marked by strength and corrosion resistance, with excellent biocompatibility, and as such, it has been successfully used in surgery for more than fifty years, including for individual component parts of pacemakers in cardio surgery (Balla et al. 2010).

Magnesium represents a promising biomaterial for bone replacement, because of its excellent characteristics, such as a low ionization energy, satisfactory strength, and good biocompatibility and biodegradability. The open cellular structure of magnesium enables rapid integration with the host bone and provides a space to maintain stable blood flow and tissue ingrowth of the new bone (Bhumbra et al. 1998). Owing to its ability to meet during casting, magnesium makes for a very interesting metal for obtaining a complex anatomical shape. Its deformable features also provide the possibility of permanent plastic deformation by hot forging processes.

4 Manufacturability of Ceramic Materials

The increased interest in biomaterials is related to developments from the middle of the previous century, when new potential for the implementation of ceramics in medicine was discovered. This group includes some very chemically resistant materials, which remain almost unchanged when in contact with a physiological environment, i.e., they retain their physical and chemical properties in a living organism. However, their traditional brittleness, low resistance to fracture and lack of toughness initially presented large technological limitations for bioceramic materials, which were then only an alternative for metallic materials.

New generations of bioceramic materials with significantly increased mechanical properties have considerably contributed to their increased manufacturability and wider application. High chemical stability and high compressive strength, along with outstanding aesthetic quality, paved the way for implementation of these materials, first in dentistry, and later in orthopedics.

The ceramics of metal oxides of α-Al_2O_3, ZrO_2, TiO_2, the fibers of glass carbon and its composites, metals or steels coated with thin films such as TiN, SiC, ZrO_2, BN, B_4C, phlogopite glass-ceramics and feldspar porcelain all belong among the inert biomaterials that are most often used nowadays in prosthetics and orthopedics (Narayan et al. 2015).

Aluminum oxide of high density and strength (99.5% α-Al_2O_3) and zirconium oxide ZrO_2 represent the most important bioinert ceramic materials. They were developed as replacements for metallic alloys and are fitted into the places where high load capacity (hip prosthesis) is required, as well as being used for dental implants, as they exhibit excellent biocompatibility and high resistance to corrosion. The problem that occurs with these materials is the slow but continuous growth of an initial crack, should it occur at any place, which requires frequent replacement and may prove to be very complex.

Monolithic aluminum oxide ceramics (Al_2O_3) have low impact toughness (<5 MPa/m^2), low flexural strength (<600 MPa) and high wear resistance. Tetragonal modification of zirconium oxide ceramics (t-ZrO_2), which is stabilized by yttrium, has a relatively high impact toughness (6–15 MPa/m^2), high flexural strength (1000–1500 MPa), higher thermal ductility and higher wear resistance. The mechanical and tribological properties of monolithic Al_2O_3 ceramics can be improved through the addition of t-ZrO_2.

Depending on the temperature, zirconium oxide occurs in three crystal modifications: above 2370 °C, it assumes a cubic crystal grid, below 1170 °C, it transforms into a monoclinic crystal structure, and in the interval between these two structures, it has a tetragonal crystal structure. The transformation from tetragonal into monoclinic develops rapidly, with an increase in volume of 3–5% that causes large fractures during cooling. This exact phenomenon of transformation of ZrO_2 weakens the mechanical properties of implants, so it is not used in its pure state. In the production of hard sintered elements, it is produced in cubic and tetragonal cubic modification. With the aim of retarding or eliminating crystal transformation,

various admixtures, such as stabilizers, are added (MgO, CaO or Y_2O_3) that preserve high temperature cubic structures even at ambient temperatures. Regarding these crystal structures retained at ambient temperatures, ZrO_2 can be classified as either fully stabilized zirconia or partly stabilized zirconia (Donachie 1998).

The components of prostheses that are made of ceramic materials are the heads and cartridge cementless acetabular cups.

Ceramic materials made from crystals of aluminum oxide, Al_2O_3, are known as "Biolox" 10. Ceramic material made of zirconium oxide crystals is significantly stronger than that based on aluminum oxide, and is known as ZTA ceramic.

Following all of these materials, there emerged bioactive ceramic materials of a second generation that have the ability to fuse with bone tissue (hydroxiapatite) on the contact surface.

Hydroxyapatite is a ceramic material that is used for coating components of the cementless total hip joint, the proximal part of the femoral component and the metal part of the acetabular component. The porous coating of hydroxyapatite overgrows bone tissue, and thus leads to faster and better connected cementless endoprosthesis components.

Thanks to the observed problems, biomaterials have become even more significantly improved, since they do not change the living tissue, but only assist in its recovery.

5 Manufacturability at Laser Technology

The development of new production technologies and processing methods has enabled the production of special medical devices, elements and supplies without which modern medicine would not be conceivable. Such medical elements inevitably require the application of non-conventional methods with completely new working parameters and processing conditions. These technologies are divided into two main groups: technologies that add material and technologies that remove material. Lasers plays a major role among new technologies. They can be used for precision cutting, selective hardening of a product, surface finishing, grinding, microjoining, welding, drilling, wire forming, etc. Their manufacturing accuracy is within the range of 10 μm. CO_2, Nd:YAG and diode lasers are all currently available.

The manufacturability of existing materials with these technologies is something that is being particularly considered for the purpose of meeting the set requirements.

Austenitic stainless steels are used for fabricating vascular stents, as well as electrodes, conducting lead wires and pulse generator housings for cardiac pacing systems (304, 316, 316L alloys). The production of vascular stents presents a particular challenge, since these devices experience extensive change in cross-sectional dimensions during expansion to their 'working' diameter in vivo.

Towards this specific goal, complex designs have been developed that allow for such widespread deformation while keeping local strains in the metal within safe

limits, avoiding the hazard of extensive yielding and cracking. The stents can be formed according to these complex designs by laser-machining fine patterns into thin-walled cylindrical tubes with highly polished surfaces (Bandyopadhyay et al. 2011).

Solid state lasers (Nd:YAG) using flash lamps are the standard beam source for stent cutting. For the cutting of stainless steel, cobalt chromium or nitinol stents, aspect ratios (cutting curve width/ wall thickness) of about 12:1 can be achieved (Gupta et al. 2004). The major drawback of these lasers is the intrinsic formation of a temperature gradient within the laser rod during operation. This causes lensing effects and mechanical stresses in the rod, leading to a disturbed beam shape with a lower beam quality.

The trend towards device miniaturization and tighter tolerances for stents requires smaller cuts and less heat input, and consequently improved beam quality and pulse durations. In recent years, new, promising laser resonator architectures have been developed. In fact, diode-pumped solid-state lasers provide a sharper power distribution, i.e., an improved beam profile quality. Nevertheless, mechanical resonator instability effects can still affect the cutting process. Fiber lasers appear to present the solution to this issue. Housed within a glass fiber OD <0.5 mm, no misalignment can occur; an optimized beam profile is ensured.

Although optimized melt cutting lasers are available, the achievable cutting width for the final product is still limited in terms of cutting depth. Since laser melt cutting is a thermal process, the formation of a heat-affected zone is unavoidable. The enlargement of the cutting width related to the removal of the heat-affected zone leads to a given wall thickness ~ 300 μm to a reduced achievable aspect ratio for the final product of 12:1. In the case of inert gases used for the process (which is preferable for the fine cutting of nitinol), burrs and residual parts remain within the tubing, and the cut structure needs to be removed semi-automatically (Steegmueller et al. 2006). As a result of mechanical impact, a deformation of the part can occur. Also, melt removal through gas stream momentum is strongly restricted to small cutting widths, since an appropriate steam channel cannot be established below ~ 8 μm. The fineness of possible structures is therefore limited.

Ultrashort-pulse lasers offer another way of cutting materials. No melt is produced, as the laser transfers the material directly from the solid to the vapour phase. Therefore, no burrs or slag are produced, leading to an immediately clean surface. Also, due to the very short energy impact, the entirety of the irradiated material is removed through vaporisation, and a heat-affected zone is not formed. The lateral resolution is therefore diffraction-limited, leading to the ultimate miniaturization. However, beam cauterization reduces the possible miniaturization, as the depth of focus leads to an enlargement of the cutting width at the upper and lower slot ends.

6 Conclusion

This overview of biomaterials and their physical characteristics in production operations primarily aims for familiarization with and indication of the possibility of their application in modern medicine. Every engineer's goal is for the design of an implant to be as light as possible, with minimum volume of the workpiece, so that it has sufficient strength in the critical cross-sections, is consistent in different biological environments and transmits the applied load over the maximum lifetime. When a biomaterial is required to meet all these conditions, its production technology, molding technology, stress-strain state and manufacturability under given conditions must be resolved. New technological solutions and manufacturability analyses represent the attempt to make only the best possible replicas of ideal natural, human organs that doctors can use in the best possible way for the benefit of their patients.

Acknowledgements This paper is part of the project "Virtual human osteoarticular system and its application in preclinical and clinical practice", funded by the Ministry of Education and Science of the Republic of Serbia, project No. III41017.

References

Agrawal CM (1998) Reconstructing the human body using biomaterials. JOM 50:31–35. doi:10.1007/s11837-998-0064-5

Ashby MF (2005) Materials selection in mechanical design, 3rd edn. Elsevier, Oxford, p 602

Ashby MF, Jones DRH (2011) Engineering materials, vol 1, Elsevier, p 472

ASM Handbook (1998) Forming and forging, vol 14, p 2014

Bakerjian R (eds) (1992) Tool and manufacturing engineers handbook, design for manufacturability, vol 6, Society of Manufacturing Engineers, p 452

Balla VK, Bodhak S, Bose S, Bandyopadhyay A (2010) Porous tantalum structures for bone implants: Fabrication, mechanical and in vitro biological properties. Acta Biomater 6:3349–3359

Banabic D, Bunge HJ, Poohlandt K, Tekkaya AE (2000) Formability of metallic materials, plastic anisotropy, formability testing, forming limits. Springer, Heidelberg, p 335

Bandyopadhyay A, Balla VK, Mangal R, Susmita B (2011) Laser surface modification of metallic biomaterials. JOM 63:94–99. doi:10.1007/s11837-011-0099-x

Benson JS, Boretos JW (1995) Biomaterials and the future of medical devices. Med Device Diag Ind 17(4):32–37

Bhadeshia HKDH, Honeycombe RWK (2006) Steels, microstructure and properties, 3rd edn. Elsevier, p 357

Bhumbra RS et al (1998) Enhanced bone regeneration and formation around implants. J Biomed Mater Res Appl Biomater 43:162–167

Boisse P, Altan T, Luttervelt K (2003) Friction & flow stress in forming & cutting, p 177

Bonfield W, Tanner KE (1997) Biomaterials a new generation. Mater World, 18–20

Calin M, Helth A, Gutierrez MJJ, Bönisch M, Brackmann V, Giebeler L, Gemming T, Lekka CE, Gebert A, Schnettler R, Eckert J (2014) Elastic softening of β-type Ti–Nb alloys by indium (In) additions. J Mech Behav Biomed Mater 39:162–174

Callister WD, Rethwisch DG (2014) Materials science and engineering: An introduction, 9th edn. Wiley, New York, p 975
Dieter GE, Kuhn HA, Semiatin SL (2003) Handbook of workability and process design, ASM International, p 400
Donachie M (1998) In: Davis JR (eds) Biomaterials, metals handbook desk edition, 2nd edn. ASM International, pp 702–709
Doni Z, Alves AC, Toptan F et al (2013) Dry sliding and tribocorrosion behaviour of hot pressed CoCrMo biomedical alloy as compared with the cast CoCrMo and Ti6Al4V alloys. Mater Des 52:47–57
Drozda T, Bakerjian R, Wick C, Benedeict TJ, Veilleux FR (eds) (1992) Tool and manufacturing engineers handbook, design for manufacturability, vol 6. 4th edn. Society of Manufacturing Engineers, Michigan
Emmens WC (2011) Formability, a review of parameters and processes that control, limit or enhance the formability of sheet metal. Springer briefs in applied sciences and technology, p 112
Frosch KH, Stürmer KM (2006) Metallic biomaterials in skeletal repair. Eur J Trauma 32:149–159. doi:10.1007/s00068-006-6041-1
Gupta V, Johnson AD, Martynov V et al (2004) Nitinol thin film three-dimensional devices: fabrication and applications. In: Proceedings "shape memory and superelastic technologies 2004". ASM International, pp 639–650
Hao L, Harris R (2008) In: Bartolo PJ, Bidanda B (eds) Bio-Materials and prototyping applications in medicine, pp 79–107. doi:10.1007/978-0-387-47683-4_6
Helsen AJ, Breme JH (eds) (1998) Metals as biomaterials, Wiley. p 522
Hull D, Bacon DJ (2009) Introduction to dislocations, 5th edn. Elsevier, Liverpool, p 268
Krausz AS, Krausz K (1996) Unified constitutive laws of plastic deformation, Ottawa, p 463
Lange K (1985) Handbook of metalforming. McGraw-Hill, New York, p 1232
Lee BS, Matsumoto H, Chiba A (2011) Fractures in tensile deformation of biomedical Co-Cr-Mo-N alloys. Mater Lett 65:843–846
Long M, Rack HJ (1998) Titanium alloys in total joint replacement—a materials science perspective. Biomaterials 19:1621–1639
Narayan R, Bose S, Bandyopadhyay A (2015) Biomaterials science: processing, properties and applications V: ceramic transactions. Wiley, New Jersey
Randjelovic S, Misic D, Trajanovic M et al (2012a) Customization of elements for orthopedic external and internal fixation. In: 5th international conference MCP CE. University of Novi Sad, 19–21 Sept 2012
Randjelovic S, Manic M, Trajanovic M et al (2012b) The impact of die angle on tool loading in the process of cold extruding steel. Mater Technol 46(2):149–154
Randjelovic S, Milutinovic M, Nikolic S et al (eds) (2015) Risk assessment in injection molding process. J Technol Plast 40(2):23–33
Ratner BD, Hoffman AS, Schoen FJ, and Lemons JE (1996) Biomaterials science: an introduction to materials in medicine. Academic Press, New York, USA
Smalmman RE, Bishop RJ (1999) Modern physical metallurgy & materials engineering. 6th edn. Butterworth-Heinemann, p 438
Steck E, Ritter R, Peil U, Ziegenbein A (2001) Plasticity of metals: experiments, models, computation, Wiley, p 427
Steegmueller R, Strobel M, Flaxmeier E, Schuessler A (2006) Micro-welding for improved radiopacity of Nitinol stents. In: Proceedings "shape memory and superelastic technologies 2004". ASM International, pp 591–595
Vincent J (1990) Materials technology from nature. Metal Mater 395
Yan Y, Neville A, Dowson D (2007) Tribo-corrosion properties of cobalt-based medical implant alloys in simulated biological environments. Wear 263:1105–1111
Zhixia L, Masakazu K (2011) Current progress in inorganic artificial biomaterials. J Artif Organs 14:163–170. doi:10.1007/s10047-011-0585-5

Computer Modeling of Stent Deployment in the Coronary Artery Coupled with Plaque Progression

Nenad Filipovic, Zarko Milosevic, Igor Saveljic, Dalibor Nikolic and Milos Radovic

Abstract In this chapter a complex problem of stent deployment with plaque formation and progression for specific patient in coronary arteries is described. Stent enables widening of the stenosed part of the blood vessel. We firstly describe state of the art for blood flow in the stented arteries. Blood flow simulation is described by Navier-Stokes and continuity equations. Blood vessel tissue is modeled with nonlinear viscoelastic material properties. The governing finite element equations used in modeling wall tissue deformation with emphasis on implementation of nonlinear constitutive models are described. Continuum based methods for modeling the evolution of plaque is derived. The LDL penetration is defined by the convection-diffusion equation, while the endothelial permeability is shear stress dependent. The Kedem-Katchalsky equations are employed for the coupling of solute dynamics and fluid dynamics at the endothelium while three additional reaction-diffusion partial differential equations are used for modeling the inflammatory process. The recruitment of macrophages is based on the probabilistic functions with cellular automata approach. Detailed software components for stent deployment and blood flow analysis are described. We present examples with rigid and deformable arterial wall with stented and unstented arteries. Effective stress analysis results for stent deployment are shown as well. As it can be noted, areas near the connectors between the stent struts are marked with the highest stress and these parts can undergo plastic deformation. Moreover, wall shear stress is considerably reduced after stent deployment due to the reduction of the narrowing and the opening of the artery.

Keywords Stent deployment · Computer modeling · Plaque formation and development · Stress analysis

N. Filipovic (✉) · Z. Milosevic · I. Saveljic · D. Nikolic · M. Radovic
Faculty of Engineering, University of Kragujevac, 34000 Kragujevac, Serbia
e-mail: fica@kg.ac.rs

F. Zivic et al. (eds.), *Biomaterials in Clinical Practice*,
https://doi.org/10.1007/978-3-319-68025-5_25

1 Introduction

The human vascular system represents a highly complex structure and different treatments and procedures applied on its deformed parts, e.g. stent placement or bypass, are in many cases elaborate and complicated.

Most interventional procedures for percutaneous revascularization require implantation of coronary stents. On the basis of the results of the BElgianNEtherlands STENT (BENESTENT) and the STentREStenosis Study (STRESS) trials coronary stenting was facilitated by excluding anticoagulant therapy after stent implantation (Colombo et al. 1995; Karrillon et al. 1996; Schomig et al. 1996) and became widely accepted.

A number of research studies have reported attempts to evaluate the features of stent design that make a specific stent more or less suitable for a particular type of lesion or anatomy. Colombo et al. (2002) provide a detailed review on that.

In brief, stents can be classified according to their mechanism of expansion (self-expanding or balloon-expandable), their composition (stainless steel, nitinol, tantalum, cobalt-based alloy, active coating, inert coating, or biodegradable) as well as their design (coil, mesh structure, ring, slotted tube, custom design or multi-design). Manufacturers agree that all stents can be implanted in native coronary arteries of adequate size. Some stents are approved for implantation in vein grafts while few stents are specifically designed to be implanted in a particular lesion. There are substantially different characteristics of many currently used stents, such as recoil, strut thickness, degree of foreshortening, metal to artery ratio and degree of radiopacity. The ability of a stent to cover a lesion depends both on the diameter of the crimped stent and on the friction of the delivery system and stent, flaring of the distal struts during interaction with the lesion, flexibility of the stent and of the delivery balloon, and push ability of the delivery system.

Determination of the optimal lumen cross-sectional area without damaging the artery is the main objective of stenting most coronary lesions. Today, reaching a large final lumen diameter represents the safest way of limiting restenosis. Other concerns for stent selection are minimal recoil, appropriate lesion coverage and limited plaque prolapse. A registry report indicating a restenosis rate of 11% and a bimodal distribution of the loss index (Antoniucci et al. 2000) increases the likelihood of increased biocompatibility of the carbon coated stent for individuals allergic to metal components of stainless steel.

Lesions situated on a curve (>90°) or immediately followed by a curve represent significant challenges. Changing the natural conformation of a coronary vessel may have an unfavourable effect on flow dynamics and increase the risk of adverse events during follow-up, as described in Gyongyosi et al. (2000).

Since there is a variety of stents available now, any artery can be implanted with a stent. Furthermore, it seems that stents not only improve the immediate and long-term results of peripheral interventional procedures but also widen their applicability. It is essential to choose the most suitable stent for the lesion and

vessel that will be treated, considering the fact that not all stents are equivalent. While all kinds of stents can be implanted at the iliac level, balloon-expandable stents are still recommended for placement in many situations. However, at the femoro-popliteal level it seems that new self-expandable stents show better results. On the other hand, covered stents make no improvement to results in peripheral occlusive disease and, therefore, should be used in the treatment of arterial rupture, arteriovenous fistulas and aneurysms. The problem that remains is restenosis after stenting.

Based on all available scientific evidence, the choice of stent depends on operator experience, characteristics and location of the lesion, stents available in the catheterization laboratory and the approach applied. Stent implantation is in most cases conducted selectively (Henry et al. 2000). Randomized trials have not yet provided us with the principles of selecting a particular stent for a specific lesion (Rana et al. 2013; Mehta et al. 2013). On the other hand, there are a large number of observational studies that support the views described in this chapter. It can be said that confidence and experience of the operator have a pivotal role in choosing a particular stent for treating a specific lesion, in spite of all theoretic and practical considerations provided so far. Such evidence is supported by the results of a recent study by Sharafuddin et al. (2008).

Compared to balloon angioplasty, the restenosis rate can be reduced to 20–30% by using stents (Fischman et al. 1994). Nowadays, coating stents with antiproliferative drugs seems to work well for patients since the restenosis rate decreases by 85% or more (Morice et al. 2002; Azaouzi et al. 2012). These drugs function by preventing neointimal proliferation. However, the drug can be delivered to the tissue only for a specific period of time: hence, the long-term clinical outcome of such stents is still unknown.

While an implanted stent effectively enables a widening of the stenosed part of the blood vessel, it causes local injury to the vascular endothelium and also affects local haemodynamics in a manner conducive to the growth of new tissue that is termed neointimal hyperplasia (NI) and subsequent restenosis (Newman et al. 1996; Murata et al. 2002; Azaouzia et al. 2013). Recent findings indicate that changes in wall shear stress (WSS) distributions after stent implantation might represent an important factor in the process of restenosis i.e. an excessive growth of new tissue in the stented segment which can block the artery again. The successfulness of the stenting procedure depends on the level of restenosis severity. Neointimal hyperplasia was proven to depend on several factors such as arterial injury, areas of flow-induced low WSS less than 0.5 N/m^2, areas of flow-induced high wall shear stress gradients (WSSG) higher than 200 N/m^3, as well as other patient-specific medical factors such as diabetes mellitus (Murphy and Boyle 2008; DePaola et al. 1992). Non-uniform WSS within an arterial segment also affects the establishment of cell density gradients, gene expression, migration, and proliferation after vascular injury (Balossino et al. 2008).

The evaluation of haemodynamic changes caused by stent implantation is thus important to minimize those negative biological effects and to optimise the stent

design. Besides experimental investigations using particle image velocimetry (Balossino et al. 2008), computational fluid dynamics (CFD) has been used extensively to predict increased areas of low WSS and high WSSG in stented arteries (Murphy and Boyle 2008; Balossino et al. 2008; Gay and Zhang 2009; He et al. 2005; Natarajan and Mokhtarzadeh-Dehghan 2000; LaDisa et al. 2003, 2005, 2006; Seo et al. 2005; Tortoriello and Pedrizzetti 2004; Berry et al. 2000; Rajamohan et al. 2006; Athanasiou et al. 2012).

Compared to experimental and in vivo methods, CFD techniques are more flexible and simpler to use. They can provide detailed information on critical local flow parameter near the stent struts and the arterial wall that are not accessible in biological flows. However, modeling often has its own limitations in the form of simplifications to the real problem.

Many computational studies in the literature dealt with the influence of stent physical parameters on fluid dynamical changes correlated with the restenosis process (Murphy and Boyle 2008; Balossino et al. 2008; He et al. 2005; Natarajan and Mokhtarzadeh-Dehghan 2000; LaDisa et al. 2003; Tortoriello and Pedrizzetti 2004; Berry et al. 2000; LaDisa et al. 2006; Rajamohan et al. 2006). Stent strut spacing and thickness as well as the number of struts were proven to have influence on the distribution of values of low and high shear stress. However, the unrealistic assumption in the computational models that the stented artery is a simple cylindrical, rigid tube or even flat plane is implicit to most of these investigations. In reality, the coronary vasculature within which stents are commonly deployed exhibits a highly complex geometry with extensive curvature. This vessel curvature can have significant effect on the skewness of the velocity profile and the general behaviour of the flow in the stented segment.

Numerous studies were performed with an aim to compare steady-state versus pulsatile flow simulations and investigate the effect of non-Newtonian blood properties on the resulting flow parameters (Balossino et al. 2008; Seo et al. 2005; LaDisa et al. 2006; Rajamohan et al. 2006). In one investigation, the pulsatile flow simulations showed that the flow separation zones in the region between the stent wires also periodically increase and decrease in size. The results also indicated that the character of stent induced flow disturbance in pulsatile flow is highly dynamic. Other analyses showed that although the non-Newtonian properties have a very limited impact on the general characteristics of the flow field, they cause limited reduction in the size of the flow separation zone downstream of the stent (Seo et al. 2005).

In summary, there are strong limitations to the reported investigations of blood flow in stented arteries, mainly with respect to an idealised geometry of artery and stent. To the best of the authors' knowledge, no study so far has reported a universally applicable method to perform a blood flow analysis in a patient-specific artery with widening intervention of the stenosed part of the artery.

2 Methods

2.1 Geometrical Stent Modeling

This section describes the integration of bio-anatomical patient-specific model parts for stent deployment.

A clinical user for a planned stenting intervention must be able to predict the post-interventional artery shape and possible damages to the endothelium as well as the effects of the stenting on the vessel wall, the blood flow characteristics and the biological response. To enable such complex predictions, we developed the Patient Specific 3D Modeller software that consists of the following steps:

- Selection and extraction of the region of interest of the stenosed artery segment including plaque identification;
- Mesh generation of the stent model from CAD data or geometry description;
- Virtual placement and delivery of the stent and the balloon into the selected artery segment;
- Virtual simulation of the physical deployment of the stent;
- Post-processing of a resulting geometry of the stented artery including stent details and output to Blood Flow Analysis.

We developed a method that enables a virtual stenting intervention in a patient-specific, stenosed artery. This highly complex physical problem includes all system components of the stenting procedure, namely, the stenosed artery, the stent and the balloon to inflate the stent.

A virtual positioning in the reconstructed artery is performed before the balloon is gradually inflated, it widens the stent in radial direction which enables the stenosed artery dilation (Fig. 1).

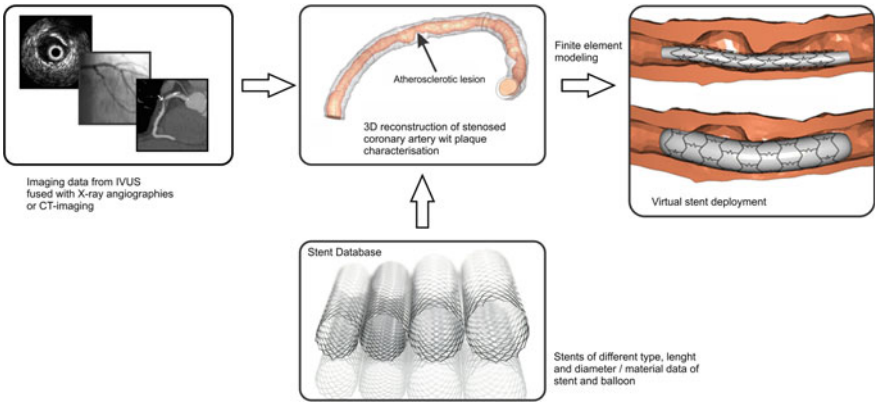

Fig. 1 Procedure for virtual stent deployment

In preparation of the numerical model of the stenosed artery, the plaque region is selected. All elements of the arterial wall forming the stenosis are defined as a new region for which separate material properties can be applied. The basis for the element selection is the plaque identification of the segmentation process. In Fig. 2, a half of the stenosed artery model is shown with the defined plaque region.

The placement and adjustment of the stent and the balloon to artery curvature is realised using the midline of the artery in the region of interest. The construction of the artery midline as an auxiliary geometrical measure takes into consideration that the stent can be fitted into the stenosed region. For that purpose, at three or four characteristic cross sections, along the artery length in the selected region of interest, the midpoints are constructed, which are used for the construction of the midline using a spline function. Bending of the stent according to the midline is

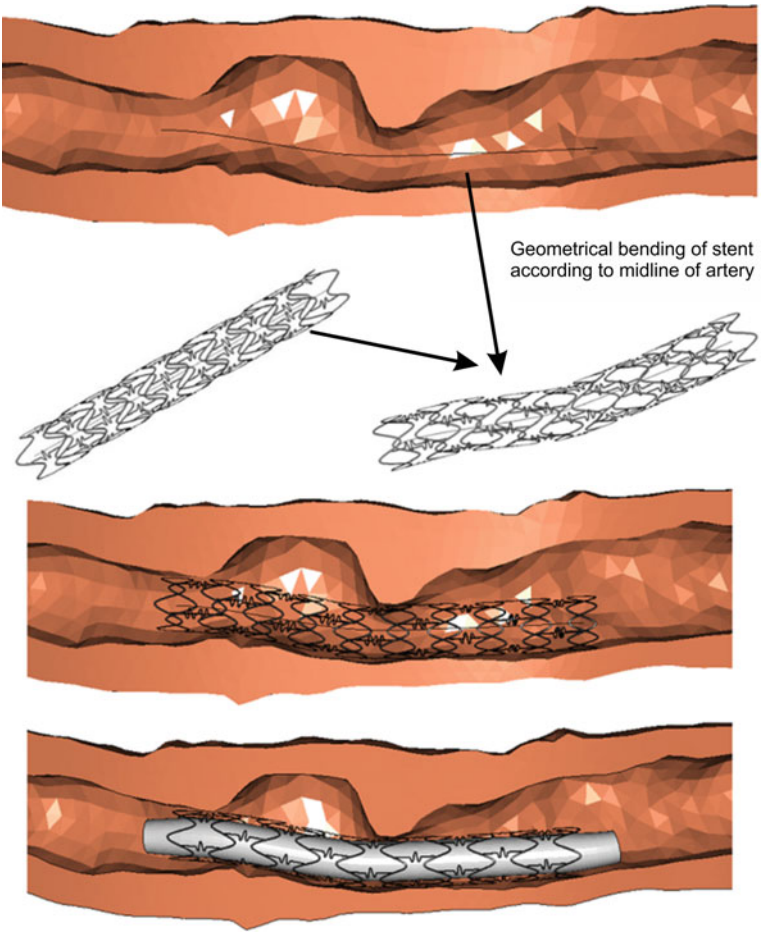

Fig. 2 Bending of the stent and the balloon according to artery curvature

done geometrically. The balloon is built as a covering surface around the midline with a diameter 20% smaller than the stent diameter. Figure 2 shows the region of interest with the midline and fitting of the stent and the balloon.

For post-processing of the virtual stenting intervention, the clinician is not only provided with comprehensible animations and graphical outputs showing the process and the final state of the implanted device, but also with a number of indicators that allow a judgment on the performance of the selected stent and of its interactions with the specific artery. Such indicators include the inflation pressure—lumen area relationship, the final dilation of the artery, stress and strain distributions both for the stent and the artery, and the contact stress between the vessel wall and the stent struts. The clear markers for the assessment of arterial injury sustained during intervention are also provided (Fig. 3).

2.2 Three-Dimensional Simulation of Blood Flow, Mass Transport and Fluid-Structure Interaction

In this section, a continuum based approach for plaque formation and development in 3D was presented with corresponding governing equations and numerical procedures. We simulated the blood flow with the 3D Navier-Stokes and continuity equations:

$$-\mu\nabla^2 u_l + \rho(u_l \cdot \nabla)u_l + \nabla p_l = 0 \tag{1}$$

$$\nabla u_l = 0 \tag{2}$$

where $\boldsymbol{u_l}$ is blood velocity in the lumen, p_l is the pressure, μ is the dynamic viscosity of the blood, and ρ is the blood density.

Blood lumen mass transfer is coupled with the blood flow and modeled by the convection-diffusion equation:

$$\nabla \cdot (-D_l \nabla c_l + c_l u_l) = 0 \tag{3}$$

in the fluid domain, where c_l is the blood lumen solute concentration, and D_l is the lumen solute diffusivity.

Mass transfer in the wall of the artery is coupled with the transmural flow and modeled by the convection-diffusion-reaction equation:

$$\nabla \cdot (-D_w \nabla c_w + k c_w u_w) = r_w c_w \tag{4}$$

in the wall domain, where c_w is the arterial wall solute concentration, D_w is the arterial wall solute diffusivity, K is the solute lag coefficient, and r_w is the consumption rate constant.

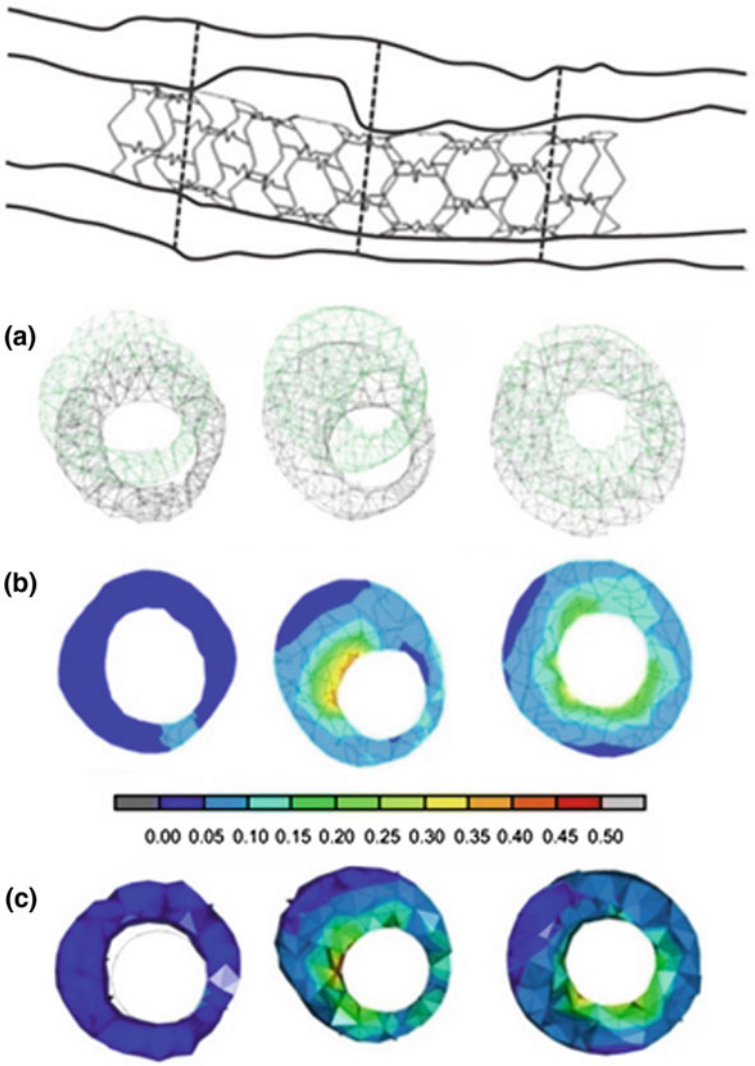

Fig. 3 Results post-processing: **a** vessel dilation, **b** stresses and **c** strains. Units are kPa

LDL transport in lumen of the vessel is coupled with Kedem-Katchalsky equations:

$$J_v = L_p(\Delta p - \sigma_d \Delta \pi) \tag{5}$$

$$J_s = P\Delta c + \left(1 - \sigma_f\right) J_v \bar{c} \tag{6}$$

where L_p is the hydraulic conductivity of the endothelium, Δc is the difference in solute concentration across the endothelium, Δp is the pressure drop across the endothelium, $\Delta\pi$ is the oncotic pressure difference across the endothelium, σ_d is the osmotic reflection coefficient, σ_f is the solvent reflection coefficient, P is the solute endothelial permeability, and $\bar{c}$ is the mean endothelial concentration.

The basic relations for mass transport in the artery. Transport processes in the blood govern the nutrient supply upon which the metabolism of the artery wall is critically dependent. Oxygen transport and LDL transport, two different mass transport processes in large arteries, are described. Blood flow through the arteries is mostly referred to as the motion of a fluid-type continuum, with the wall surfaces treated as impermeable (hard) boundaries. However, the transport of macromolecules (LDL, globulin, albumin) or gases (e.g. O_2, CO_2) is a convection-diffusion physical process with permeable boundaries through which the diffusion occurs. In the further analysis, the assumption is that the blood flow (i.e. a diluted mixture is considered) is not affected by the concentration of the transported matter. Convection-diffusion equation governs the mass transport process:

$$\frac{\partial c}{\partial t} + v_x \frac{\partial c}{\partial x} + v_y \frac{\partial c}{\partial y} + v_z \frac{\partial c}{\partial z} = D\left(\frac{\partial^2 c}{\partial x^2} + \frac{\partial^2 c}{\partial y^2} + \frac{\partial^2 c}{\partial z^2}\right) \tag{7}$$

where c is the macromolecule or gas concentration; v_x, v_y and v_z represent the blood velocity components in the coordinate system x, y, z; and D denotes the diffusion coefficient, assumed constant, of the transported material.

Boundary conditions for LDL transport. LDL is a macromolecule is well known as an atherogenic molecule and it is directly responsible for the process of atherosclerosis. Moreover, tt is known that this macromolecule is able to pass through the endothelium by minimum three different mechanisms: pinocytotic vesicular transport, receptor-mediated endocytosis, and phagocytosis (Goldstein et al. 1979). It has been reported that the permeability coefficient of an intact arterial wall to LDL is of the order of 10^{-8} (cm/s) (Bratzler et al. 1977). The following relation describes the conversion of the mass among the LDL going through a semipermeable wall, proceeding towards the vessel wall by a filtration flow and diffusing back to the mainstream at the vessel wall:

$$c_w v_w - D\frac{\partial c}{\partial n} = K c_w \tag{8}$$

where c_w is the surface concentration of LDL, v_w is the filtration velocity of LDL transport through the wall, n is the coordinate normal to the wall, D is the diffusivity of LDL, and K is the overall mass transfer coefficient of LDL at the vessel wall. A uniform constant concentration C_0 of LDL is applied at the artery tree inlet as classical inlet boundary condition for Eq. (7).

Finite element modeling of diffusion-transport equations

The reason for the domination of the convection terms in the case of blood flow with mass transport is the low diffusion coefficient (Kojic et al. 2008). For the purpose of obtaining a stable numerical solution, special stabilizing techniques need to be applied. Therefore, the streamline upwind/Petrov-Galerkin stabilizing technique (SUPG) (Brooks and Hughes 1982) is implemented within a standard numerical integration scheme. By including the diffusion equations and transforming them into the incremental form, the incremental-iterative form of finite element equations of balance is obtained. The final equations are:

$$\begin{bmatrix} \frac{1}{\Delta t}\mathbf{M}_{\mathbf{v}} + {}^{n+1}\mathbf{K}_{\mathbf{vv}}^{(i-1)} + {}^{n+1}\mathbf{K}_{\boldsymbol{\mu}\mathbf{v}}^{(i-1)} + {}^{n+1}\mathbf{J}_{\mathbf{vv}}^{(i-1)} & {}^{n+1}\mathbf{K}_{\mathbf{vp}}^{(i-1)} & \mathbf{0} \\ \mathbf{K}_{\mathbf{vp}}^{\mathbf{T}} & \mathbf{0} & \mathbf{0} \\ {}^{n+1}\mathbf{K}_{\mathbf{cv}}^{(i-1)} & \mathbf{0} & \frac{1}{\Delta t}\mathbf{M}_{\mathbf{c}} + {}^{n+1}\mathbf{K}_{\mathbf{cc}}^{(i-1)} + {}^{n+1}\mathbf{J}_{\mathbf{cc}}^{(i-1)} \end{bmatrix} \times \begin{Bmatrix} \Delta\mathbf{V}^{(i)} \\ \Delta\mathbf{P}^{(i)} \\ \Delta\mathbf{C}^{(i)} \end{Bmatrix} = \begin{Bmatrix} {}^{n+1}\mathbf{F}_{\mathbf{v}}^{(i-1)} \\ {}^{n+1}\mathbf{F}_{\mathbf{p}}^{(i-1)} \\ {}^{n+1}\mathbf{F}_{c}^{(i-1)} \end{Bmatrix} \tag{9}$$

where the matrices are:

$$\begin{aligned} &(\mathbf{M}_{\mathbf{v}})_{jjKJ} = \int_V \rho N_K N_J dV, && (\mathbf{M}_{\mathbf{c}})_{jjKJ} = \int_V N_K N_J dV \\ &\left({}^{n+1}\mathbf{K}_{\mathbf{cc}}^{(i-1)}\right)_{jjKJ} = \int_V D N_{K,j} N_{J,j} dV && \left({}^{n+1}\mathbf{K}_{\mu v}^{(i-1)}\right)_{jjKJ} = \int_V \mu N_{K,j} N_{J,j} dV \\ &\left({}^{n+1}\mathbf{K}_{\mathbf{cv}}^{(i-1)}\right)_{jjKJ} = \int_V N_K\, {}^{n+1}c_j^{(i-1)} N_J dV && \left({}^{n+1}\mathbf{K}_{vv}^{(i-1)}\right)_{jjKJ} = \int_V \rho N_K\, {}^{n+1}v_j^{(i-1)} N_{J,j} dV \\ &\left({}^{n+1}\mathbf{J}_{\mathbf{cc}}^{(i-1)}\right)_{jjKJ} = \int_V \rho N_K\, {}^{n+1}v_j^{(i-1)} N_{J,j} dV && \left({}^{n+1}\mathbf{K}_{\mathbf{vp}}^{(i-1)}\right)_{jjKJ} = \int_V \rho N_{K,j} \hat{N}_J dV \\ &\left({}^{n+1}\mathbf{J}_{\mathbf{vv}}^{(i-1)}\right)_{jkKJ} = \int_V \rho N_K\, {}^{n+1}v_{j,k} N_J dV \end{aligned} \tag{10}$$

and the vectors are:

$$\begin{aligned} {}^{n+1}\mathbf{F}_c^{(i-1)} &= {}^{n+1}\mathbf{F}_q + {}^{n+1}\mathbf{F}_{sc}^{(i-1)} - \frac{1}{\Delta t}\mathbf{M}_c\left\{{}^{n+1}\mathbf{C}^{(i-1)} - {}^{n}\mathbf{C}\right\} \\ &\quad - {}^{n+1}\mathbf{K}_{\mathbf{cv}}^{(i-1)}\left\{{}^{n+1}\mathbf{V}^{(i-1)}\right\} - {}^{n+1}\mathbf{K}_{cc}^{(i-1)}\left\{{}^{n+1}\mathbf{C}^{(i-1)}\right\} \\ \left({}^{n+1}\mathbf{F}_q\right)_K &= \int_V N_K q^B dV \qquad \mathbf{F}_{\mathbf{sc}}^{(i-1)} = \int_S D N_K \nabla {}^{n+1}\mathbf{c}^{(i-1)} \cdot \mathbf{n} dS \end{aligned} \tag{11}$$

Note that $\hat{N}_J$ are the interpolation functions for pressure (which are taken to be for one order of magnitude lower then the interpolation functions N_I for velocities).

The matrices $\mathbf{M}_{cc}$ and $\mathbf{K}_{cc}$ are the 'mass' and convection matrices; $\mathbf{K}_{cv}$ and $\mathbf{J}_{cc}$ correspond to the convective terms of Eq. (9); and $\mathbf{F}_c$ is the force vector that follows from the convection-diffusion equation in (9) and linearization of the governing equations.

Mesh moving algorithm

In this section, Arbitrary Lagrangian Euler (ALE) formulation is described, which is used for mesh moving algorithm and blood flow simulation. ALE formulation for fluid dynamics and 3D mesh moving algorithm are applied in order to make plaque formation and development algorithm, on one side, and to connect blood flow simulation with bioprocess modeling, on the other side and (Filipovic et al. 2006). The governing equations, which include the Navier-Stokes equations and the continuity equation, can be written in the ALE formulation as (Filipovic et al. 2006):

$$\rho\left[v_i^* + \left(v_j - v_j^m\right)v_{i,j}\right] = -p_{,i} + \mu v_{i,jj} + f_i^B \tag{12}$$

$$v_{i,i} = 0 \tag{13}$$

where v_i and v_i^m denote the velocity components of a generic fluid particle and of the point on the moving mesh occupied by the fluid particle, respectively; ρ is fluid density, p is fluid pressure, μ is dynamic viscosity, and f_i^B are the body force components. The symbol "*" stand for the mesh-referential time derivative, that is, the time derivative at a considered mesh point:

$$()^* = \frac{\partial(\,)}{\partial t}\Big|_{\xi_i = const} \tag{14}$$

and the symbol "$_{,i}$" denotes partial derivative, i.e.:

$$(\,)_{,i} = \frac{\partial(\,)}{\partial x_i} \tag{15}$$

We use x_i and ξ_i as Cartesian coordinates of a generic particle in space and of the corresponding point on the mesh. The repeated index involves summation, from 1 to 3, i.e. j = 1, 2, 3 in Eq. (12), and i = 1, 2, 3 in Eq. (13). For Eq. (12) derivation, we used the following expression for the material derivative (corresponding to a fixed material point) $D(\rho v_i)/Dt$,

$$\frac{D(\rho v_i)}{Dt} = \frac{\partial(\rho v_i)}{\partial t}\Big|_{\xi} + (v_j - v_j^m)\frac{\partial(\rho v_j)}{\partial x_i} \tag{16}$$

The generic point on the mesh, with the mesh-referential derivative and the convective term are presented on the right-hand side.

Then, we apply the conventional Galerkin procedure for space discretization of the fluid domain. The finite element equations for a 3D domain that follow from Eqs. (12) and (13) are:

$$\rho \int_V h_\alpha v_i^* dV + \rho \int_V h_\alpha \left(v_j - v_j^m\right) v_{i,j} dV = -\int_V h_\alpha p_{,i} dV + \int_V \mu h_\alpha v_{i,jj} dV + \int_V h_\alpha f_i^B dV \tag{17}$$

$$\int_V \bar{h}_\beta v_{i,i} dV = 0 \tag{18}$$

where $h_\alpha(r,s,t)$ and $\bar{h}_\beta(r,s,t)$ are the interpolation functions for the velocities and pressure, respectively, as polynomials of the isoparametric coordinates r, s, t (Kojic et al. 2008). The number of nodes of the selected finite element governs the number of interpolation functions. In general, number of interpolation functions h_α and $\bar{h}_\beta$ is different. The integration is performed over the volume V of a finite element. We will further use the transformed Eq. (17) by applying the Gauss theorem:

$$\rho \int_V h_\alpha v_i^* dV + \rho \int_V h_\alpha \left(v_j - v_j^m\right) v_{i,j} dV - \int_V h_{\alpha,i} p dV + \int_V \mu h_{\alpha,j} v_{i,j} dV = \int_S h_\alpha \left[-p n_i + \mu v_{i,j} n_j\right] dS \tag{19}$$

We gradually integrate the system of Eq. (19) over a time period using a time step Δt, which may be constant or varying in the time period. Hence, we need an incremental form of equations corresponding to the time step. The system of Eq. (19) is nonlinear with respect to the velocities and the element volume changes, thus we perform a linearization with respect to time, using the known values at a given time t. The computational algorithm we aim to establish is implicit, thus we want to satisfy the system of Eq. (19) at the end of time step Δt, i.e. at time $t + \Delta t$, where t is the time at the start of the current time step. For a generic quantity F defined at a mesh point, we produce the following approximation (Kojic et al. 2008):

$${}^{t+\Delta t}F|_{{}^t\xi} = {}^tF|_{{}^t\xi} + F^* \Delta t \tag{20}$$

Applying this relation to the left (LHS) and right-hand side (RHS) of Eq. (19), we obtain the following:

$${}^t(LHS) + (LHS)^* \Delta t = {}^{t+\Delta t}(RHS) \tag{21}$$

The following relations are used for calculating the mesh-referential time derivatives:

$$\left(\frac{\partial F}{\partial x_i}\right)^* = \frac{\partial F^*}{\partial x_i} - \left(\frac{\partial v_k^m}{\partial x_i}\right)\frac{\partial F}{\partial x_k} \tag{22}$$

$$(dV)^* = \frac{\partial v_k^m}{\partial x_k} dV \tag{23}$$

The fluid velocities and pressure are also expressed in the incremental form:

$${}^{t+\Delta t}v_i = {}^{t}v_i + \Delta v_i \tag{24}$$

$${}^{t+\Delta t}p = {}^{t}p + \Delta p \tag{25}$$

where Δv_i and Δp are the velocity and pressure increments in time step. The interpolations for the velocities and pressure are adopted as follows:

$$\Delta v_i = h_\alpha \Delta V_i^\alpha \tag{26}$$

$$\Delta p = \bar{h}_\alpha \Delta P^\alpha \tag{27}$$

where ΔV_i^α and ΔP^α are the nodal values increments, and summation over index α is implied.

Using the linearization (21) and the expressions (20), and (22)–(27), from (18) and (19) we obtain the system of ordinary differential equations in the form:

$${}^{t}\mathbf{M}_{(1)}\mathbf{V}^* + {}^{t}\mathbf{K}_{(1)\,vv}\Delta\mathbf{V} + {}^{t}\mathbf{K}_{vp}\Delta\mathbf{P} = {}^{t+\Delta t}\mathbf{F}_{(1)} - {}^{t}\mathbf{F}_{(1)} \tag{28}$$

and

$${}^{t}\mathbf{M}_{(2)}\mathbf{V}^* + {}^{t}\mathbf{K}_{(2)\,vv}\Delta\mathbf{V} = {}^{t+\Delta t}\mathbf{F}_{(2)} - {}^{t}\mathbf{F}_{(2)} \tag{29}$$

The integrals are evaluated over the known volumes and surfaces at the start of a time step. The element matrices are evaluated at time t, and the right-hand side vectors consist of the terms which correspond to start and end of time step. The vectors ${}^{t+\Delta t}\mathbf{F}_{(k)}$, $k = 1, 2$ contain terms with the prescribed values at the end of the time step, as given pressures on the boundary, or velocities of the mesh. On the contrary, the vectors ${}^{t}\mathbf{F}_{(k)}$, $k = 1, 2$ are evaluated with all values at start of the time step. Further we use:

$$\mathbf{V}^* = \Delta\mathbf{V}/\Delta t \tag{30}$$

and

$$\mathbf{P}^{*} = \Delta\mathbf{P}/\Delta t \tag{31}$$

so that the systems of Eqs. (28) and (29) have the unknown increments $\Delta\mathbf{V}$ and $\Delta\mathbf{P}$ only. The solutions of (28) and (29) give the first approximation and we form an iterative scheme of the form Kojic et al. (2008) and Filipovic et al. (2006):

$${}^{t+\Delta t}\hat{\mathbf{K}}^{(i-1)}\Delta\mathbf{U}^{(i)} = {}^{t+\Delta t}\mathbf{F}^{(i-1)} \tag{32}$$

where ${}^{t+\Delta t}\hat{\mathbf{K}}^{(i-1)}$ is the system matrix, ${}^{t+\Delta t}\mathbf{F}^{(i-1)}$ is the unbalanced force vector, and $\Delta\mathbf{U}^{(i)}$ is the vector of nodal variables for the equilibrium iteration "*i*",

$$\left\{\Delta\mathbf{U}^{(i)}\right\} = \begin{Bmatrix} \Delta\mathbf{V}^{(i)} \\ \Delta\mathbf{P}^{(i)} \end{Bmatrix} \tag{33}$$

with

$$\Delta\mathbf{U} = \Delta\mathbf{U}^{(1)} + \Delta\mathbf{U}^{(2)} + \cdots \tag{34}$$

The iteration ceases when a convergence criteria are satisfied, e.g. when $\left\|\Delta\mathbf{U}^{(i)}\right\| \leq \varepsilon_D$ where ε_D is a selected numerical tolerance.

Then, we use the penalty formulation and express the pressure in terms of the velocity components:

$$p = -\lambda v_{i,i} \tag{35}$$

where λ is a large (penalty) number. We use this expression for pressure in Eq. (12) which then contains the velocities only, Eq. (13) is eliminated, and the corresponding terms in the finite element equations change accordingly.

2.3 *Modeling the Deformation of Blood Vessels*

Blood vessel tissue has complex mechanical characteristics. The tissue can be modeled by using various material models, from linear elastic to nonlinear viscoelastic. We here summarize the governing finite element equations used in modeling wall tissue deformation with emphasis on implementation of nonlinear constitutive models.

The finite element equation of balance of linear momentum is derived from the fundamental differential equations of balance of forces acting at an elementary material volume. The inertial forces in this equation are included in dynamic analysis. Then, by applying the principle of virtual work we got:

$$\mathbf{M}\ddot{\mathbf{U}} + \mathbf{B}^{w}\dot{\mathbf{U}} + \mathbf{K}\mathbf{U} = \mathbf{F}^{ext} \tag{36}$$

Here the element matrices are: $\mathbf{M}$ is mass matrix; $\mathbf{B}^{w}$ is the damping matrix, in case when the material has a viscous resistance; $\mathbf{K}$ is the stiffness matrix; and $\mathbf{F}^{ext}$ is the external nodal force vector which includes body and surface forces acting on the element. The dynamic differential equations of motion are obtained using the standard assembling procedure. These differential equations can further be integrated in a way described, with a selected time step size Δt. The nodal displacements ${}^{n+1}\mathbf{U}$ at the end of the time step are finally obtained according to the equation:

$$\hat{\mathbf{K}}_{tissue}\,{}^{n+1}\mathbf{U} = {}^{n+1}\hat{\mathbf{F}} \tag{37}$$

where $\hat{\mathbf{K}}_{tissue}$ is the tissue stiffness matrix and ${}^{n+1}\hat{\mathbf{F}}$ is vector of total forces. Note that this equation is obtained under the assumption that the problem is linear: displacements are small, the viscous resistance is constant, and the material is linear elastic.

In many circumstances of blood flow, the wall displacements can be large, as in case of aneurism or heart: hence, the problem becomes geometrically nonlinear. Also, the tissues of blood vessels have nonlinear constitutive laws, leading to materially-nonlinear FE formulation. Therefore, the approximations adopted to obtain Eq. (37) may not be appropriate. For a nonlinear problem, instead of (37) we have the incremental-iterative equation:

$${}^{n+1}\hat{\mathbf{K}}_{tissue}^{(i-1)}\,\Delta\mathbf{U}^{(i)} = {}^{n+1}\hat{\mathbf{F}}^{(i-1)} - {}^{n+1}\mathbf{F}^{\mathrm{int}(i-1)} \tag{38}$$

where $\Delta\mathbf{U}^{(i)}$ are the nodal displacement increments for the iteration 'i', and the system matrix ${}^{n+1}\hat{\mathbf{K}}_{tissue}^{(i-1)}$, the force vector ${}^{n+1}\hat{\mathbf{F}}^{(i-1)}$ and the vector of internal forces ${}^{n+1}\mathbf{F}^{\mathrm{int}(i-1)}$ correspond to the previous iteration.

We here emphasize the material nonlinearity of blood vessels, which is used in further applications. As presented, the geometrically linear part of the stiffness matrix, $({}^{n+1}\mathbf{K}_L)_{tissue}^{(i-1)}$, and the nodal force vector, ${}^{n+1}\mathbf{F}^{\mathrm{int}(i-1)}$, are defined in equation:

$$\left({}^{n+1}\mathbf{K}_L\right)_{tissue}^{(i-1)} = \int_V \mathbf{B}_L^{T}\,{}^{n+1}\mathbf{C}_{tissue}^{(i-1)}\mathbf{B}_L dV, \quad \left({}^{n+1}\mathbf{F}^{\mathrm{int}}\right)^{(i-1)} = \int_V \mathbf{B}_L^{T}\,{}^{n+1}\boldsymbol{\sigma}^{(i-1)} dV \tag{39}$$

where the consistent tangent constitutive matrix ${}^{n+1}\mathbf{C}_{tissue}^{(i-1)}$ of tissue and the stresses at the end of the time step ${}^{n+1}\boldsymbol{\sigma}^{(i-1)}$ depend on the material model used.

Calculation of the matrix ${}^{n+1}\mathbf{C}_{tissue}^{(i-1)}$ and the stresses ${}^{n+1}\boldsymbol{\sigma}^{(i-1)}$ for the tissue material models are used in further applications. In each of the subsequent sections we will give the basic data about the models used in the analysis.

2.4 Plaque Formation and Progression Modeling—Continuum Approach

Continuum based methods are an efficient way for modeling the evolution of plaque. In our model, LDL concentration is first introduced into the system of partial differential equations as a boundary condition. The model simulates the inflammatory response formed at the initial stages of plaque formation.

Regarding the particle dynamics, the model is based on the involvement of LDL/oxidized LDL, monocytes and macrophages, and foam cells and extra cellular matrix. Reaction-diffusion differential equations are used to model these particle dynamics. The adhesion rate of the molecules depends on the local hemodynamics which is described by solving the Navier-Stokes equations. Intima LDL concentration is a function of the wall shear stress, while the adhesion of monocytes is a function of shear stress and VCAM. Finally, we simulated the arterial wall alterations. We used a finite element solver to solve the system of the equations. The lumen is defined as a 2D domain while the intima is simplified as a 1D model due to its thin geometry. Firstly, we calculated the LDL penetration to the arterial wall and the wall shear stress. Then, the concentration of the various components of the model is calculated in order to simulate the intima fattening in the final step.

The LDL penetration is defined by the convection-diffusion equation, while the endothelial permeability is shear stress dependent. This model yields results about the atherosclerotic plaque formation in initial stages. More specifically, concentration of LDL is calculated on the artery wall and in the next step of the oxidized LDL. Furthermore, monocytes and their modified form (macrophages) are also counted. Solution to the system provides to the user the concentration of foam cells created when a threshold on LDL concentration is reached.

The previous model describes the initial stages of atherosclerosis. However, atherosclerosis is characterized by the proliferation of SMCs. A medical user needs a prediction for the plaque formation which is based on the concentration of SMCs, the necrotic core and the extracellular matrix. In this respect a new approach to count the concentration of SMCs is being developed.

We modelled the inflammatory process by three additional reaction-diffusion partial differential equations (Filipovic et al. 2011):

$$\begin{aligned} &\partial_t O = d_1 \Delta O - k_1 O \cdot M \\ &\partial_t M + div(v_w M) = d_2 \Delta M - k_1 O \cdot M + S/(1+S) \\ &\partial_t S = d_3 \Delta S - \lambda S + k_1 O \cdot M + \gamma (O - O^{thr}) \end{aligned} \tag{40}$$

where O is the oxidized LDL in the wall, M and S are concentrations in the intima of macrophages and cytokines, respectively; d_1, d_2, d_3 are the corresponding diffusion coefficients; λ and γ are degradation and LDL oxidized detection coefficients; and v_w is the inflammatory velocity of plaque growth (Filipovic et al. 2011, 2013; Filipovic 2013).

2.5 *Particle Dynamics Model of Plaque Formation—Cellular Automata*

Atherosclerosis is characterized by the accumulation of lipids, molecules and cells into the arterial wall and by its fattening. Even though continuum based models accurately describe the mass transport and penetration of molecules into the wall, they have the disadvantage of assuming that blood is homogenous and unaffected by its constituents.

Cellular Automata methods assume that a system is discretized into a finite number of cells which can be in a defined state. The model can be described in 2D and in 3D with or without an implemented stent. The recruitment of macrophages is based on probabilistic functions. The macrophages can randomly adhere in multiple sites. The functions depend on the cells already localized on a site as well as to the adjacent ones. Furthermore, the functions are based on experimental data. First, the number of macrophages on the sites is counted. Then, we used the probabilistic functions to calculate the probability for each cell to adhere on the site. Finally, the cells are recruited on the sites based on the calculated probability (Fig. 4). User defines the LDL concentration and the length of the artery and the kind of simulation. At the beginning, a specified number of cells are adhered on the wall, which may be reduced due to the death probability.

Fig. 4 Plaque progression using cellular automata

2.6 Plaque Growth—ODE Model

Apart from lipids and macrophages, the atherosclerotic plaque consists of smooth muscle cells (SMC), collagen and fibrous tissue. The SMCs cover the lipid core and insulate it from the physiological vascular tissue. Various cells in the arterial wall as well as the macrophages express the chemoattractant (PDGF) which is responsible for the proliferation of SMCs. The previously described models did not take any account of these processes. To this end a new model based on differential equations is developed to examine the evolution of the atherosclerotic plaque.

The model simulates the LDL penetration and oxidation, the adhesion, penetration as well as the differentiation of monocytes to macrophages. In the next step, LDL is phagocyted by the macrophages producing PDGF which causes the proliferation of SMCs. Finally, foam cells are created after reaching a threshold of LDL concentration. In the model, the oxidized LDL is considered as a parameter which depends on the blood flow. Foam cells are created when LDL and macrophages are into the intima. Pro-inflammatory events signal the accumulation of chemokines and cytokines. On the other hand, the endothelial cells are modified and monocytes adhere onto it. Various coefficients are involved in the model defining the strength of the inflammatory response or the proliferation of SMCs. The model provides to the user a prediction for plaque formation based on the concentration of lipids, macrophages and foam cells.

A simple ODE model was created in order to model plaque progression for human data. Let Y denote the plaque size, either an area or volume, and let t denote the time, we consider the following equation:

$$\dot{Y}_i(t) = \left(\frac{a \cdot ICAM^i(t_0) + b \cdot LDL^i(t_0) + c \cdot \frac{CHOLESTEROL^i(t_0)}{HDL^i(t_0)} + d}{wss(t)} \right) \cdot I_{Q_i > \theta} \quad (41)$$

where $ICAM^i(t_0)$, $LDL^i(t_0)$, $CHOLESTEROL^i(t_0)$ and $HDL^i(t_0)$ are baseline ICAM, LDL, cholesterol and HDL values for i-th patient. $I_{Q_i > \theta}$ is a step function:

$$I_{Q_i > \theta} = \begin{cases} 1 & if\ Q_i(t) > \theta \\ 0 & if\ Q_i(t) < \theta \end{cases} \quad (42)$$

In Eq. (41), $Q(t)$ is total amount of LDL that has "entered" inside the arterial wall until time t:

$$Q(t) = \int_0^t C_{intima}(t)dt \quad (43)$$

where $C_{intima}(t)$ is the amount of LDL which enters inside the arterial wall at time t:

$$C_{intima}(t) = \xi(wss) \cdot f(HDL) \cdot LDL(t_0) \tag{44}$$

WSS function $\xi(wss)$ and $f(HDL)$ are defined as:

$$\xi(wss) = \frac{\xi}{wss(t)} \tag{45}$$

$$f(HDL) = CHOLESTEROL(t_0)/HDL(t_0) \tag{46}$$

Endothelial permeability to LDL ξ, from Eq. (45), is set to 2×10^{-10} m/s^{-1}.

This ODE model, given in Eq. (41), shows that the plaque progression starts when the amount of LDL which has entered inside the arterial wall (Q) exceeds some threshold (θ). This threshold is set by using step function.

3 Software for Stent Deployment

After the stent deployment, our software system invokes the blood flow module and visualizes the blood flow model after the stent positioning.

Algorithms for meshing and blood flow analysis of the stented artery model will be deployed from the ARTreat software system using input from the previous step (stent deployment). The system will invoke the blood flow analysis system and the user will be able to view the blood flow before and after stenting.

3.1 Component Architecture and Interoperability

The PAKF computational fluid dynamics (CFD) module calculates the blood flow simulation result with pre and post stent deployment geometries, returns structured 3D data grids containing the wall shear stress (WSS), velocity and pressure. In the blood flow analysis module, three components are implemented:

Pre-processing unit: The pre-processing unit uses the reconstructed geometry from textual file, described in the previous chapters, for generating 3D finite element mesh, optimizing and adapting it in the appropriate format for blood flow simulation. User sets different parameters from the GUI and generates the model in accordance with those parameters. The whole model is exported in textual DAT file.

Finite Element Solver: Is the main processing unit created upon PAKF finite element solver software that uses DAT file generated at pre-processing unit for performing blood flow simulation. All simulation results are stored in UNV textual file for every mesh node and element.

Post processing unit: The post processing unit uses the UNV file generated in the previous step to import all data, extract the parameters results in a structured 3D

Grid and, finally, save the data to the IDSS repository for further visualization. UK created a special visualization component in Windows Forms and WPF utilizing OpenGL based technologies. The component is integrated to the IDSS main window and the final user can inspect the results per parameters in 3D by rotating, zooming and or cutting the 3D grid. The same process is used for pre and post stenting use cases and models as well.

Data flows, data structures and file formats

The pre-processing unit exports a textual DAT file. All data related to the finite element mesh are annotated in specific parts of the file, including:

- **Mesh nodes** data for every node in one row: ID of the node, constraints and the x, y and z coordinates.
- **Mesh elements** data for every element are in one row: ID of the element, IDs of nodes that are part of that element and ID of material related for that element.
- **Load data** where initial velocity values: ID of node and velocity value.
- **Time data** organized in two columns: the first represents time and the second velocity value in that moment.
- **Material data** where all material values related to the blood flow simulation are described for each specific methodology, e.g. blood density, viscosity, etc.

Figure 5 describes the process used within Blood Flow Computational Fluid Dynamics Solver.
Input Pre-processor data:

Reconstructed geometry in textual file from the IDSS repositories.

Input parameters, in textual file, related to the finite element model:

- Material parameters;
- Finite element mesh resolution parameters;
- Time function parameters;
- Initial load data parameters.

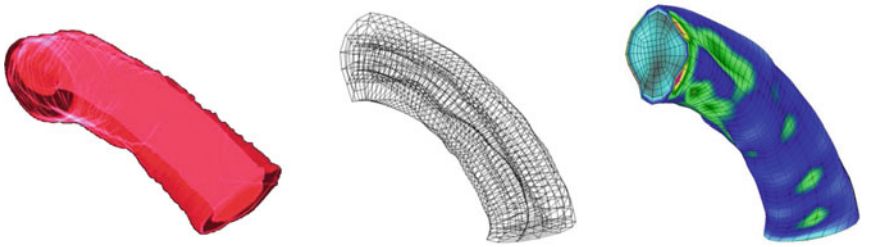

a. Reconstructed geometry *b.Generated finite element mesh* *c. Simulation results*

Fig. 5 Generating finite element model and simulation results

Input solver data:

- DAT textual file that contains data related to the FE model.
- Input postprocessor data.
- UNV textual file that contains simulations results related to the FE mesh entities (Fig. 6).

File with input parameters have to be exported to the location where pre-processor (PREP) executable is with the same filename and with the extension cfg (configuration file). After executing PREP executable cfg file is imported and

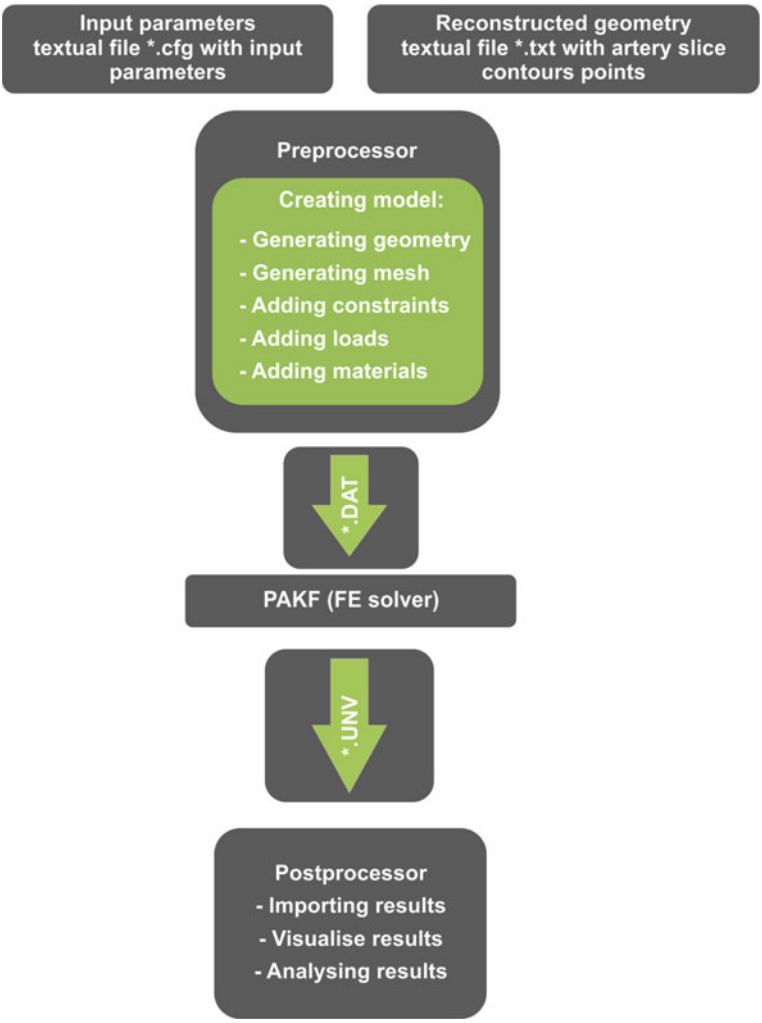

Fig. 6 Software scheme for input/output data

finite element mesh with all necessary parameters is exported in DAT file based on the reconstructed geometry file which is located at path written in file named "Files". DAT file is exported in folded PAK which is on the same location as PREP executable.

The next step is executing solver indirectly via PAK.bat file at PAK folder. After finishing simulation, the solver generates files PAK.UNV and PAK.lst which is solver's control file (Fig. 7).

Geometry preparation and meshing for CFD analysis

After pre-processor imports slice contour points with coordinates of initial geometry, slices are generated and represented via Bezier splines and surfaces (Fig. 8).

Those entities are further used for generating FE structured mesh with brick eight node 3D elements (Fig. 9). Information on the initial loads and constrains on mesh nodes are integrated in order to assure a more realistic simulation.

Use cases and examples

User enters all the necessary values in the GUI for generating the finite element model such as material properties, mesh density factors, time function values, times steps etc.

The next steps are:

- Run calculation.
- Start Solver in the background.
- Waiting for the calculation to finish and export the results to an intermediate directory.

Use the visualization component to import the resulting.UNV file.

Within the GUI the user chooses which parameters will be shown, while they are also able to zoom the model and save screen shots for the areas of interest, as shown in the following picture (Fig. 10).

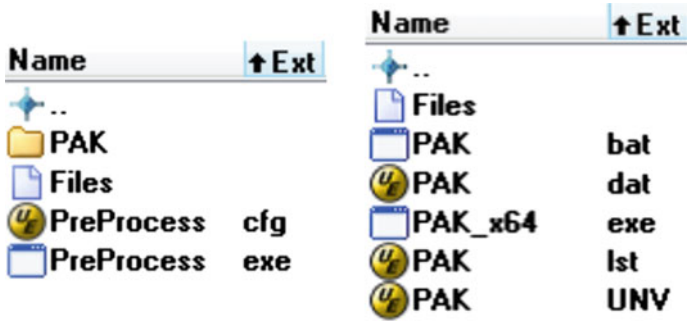

Fig. 7 Folder structure of the pre-processing and post processing components

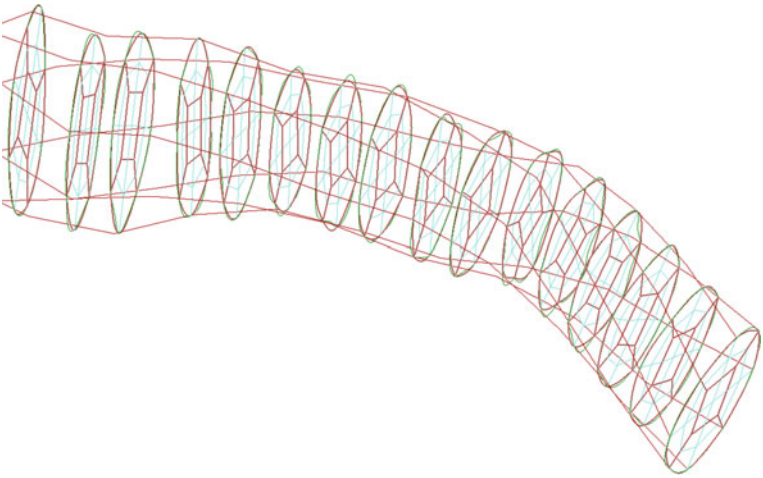

Fig. 8 Initial geometry

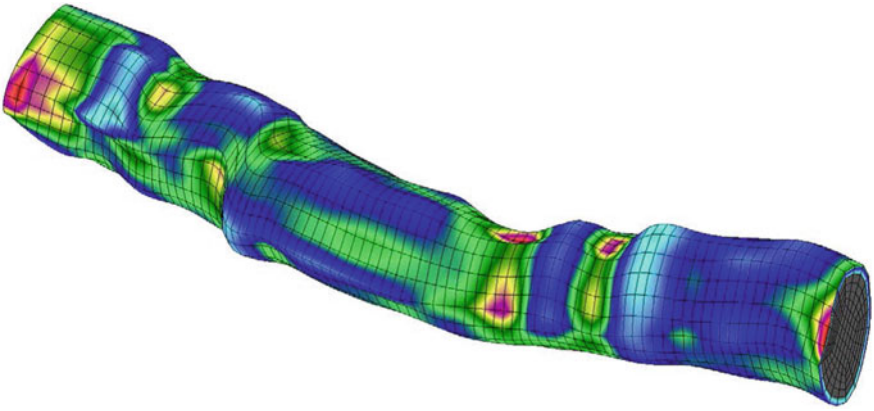

Fig. 9 Structured finite element mesh—shear stress distribution

The user is able to visualize both pre and post stenting blood flow results as depicted in the Fig. 11.

Shear stress distribution for CNR patient #13 for baseline (before stenting) and follow up (after stenting) is shown in Fig. 12. Average shear stress for the ring 1 cm before and 1 cm after stenosis is also calculated.

Shear stress distribution for CNR patient #13 RCA as well as 1 cm before and 1 cm after stenosis is presented in Figs. 13 and 14.

Shear stress distribution for patient with CX coronary artery before and after stenting is shown in Fig. 15.

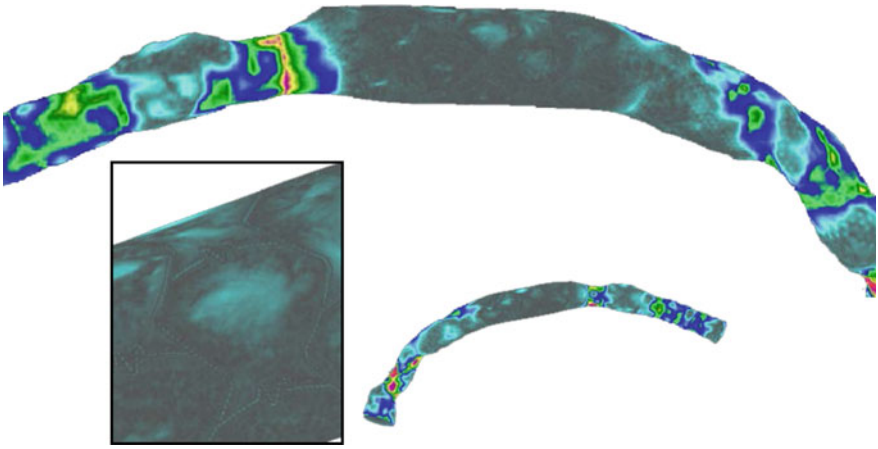

Fig. 10 Shear stress distribution visualization for the artery after stent deployment

Shear stress distribution for patient CX coronary artery with different positions of stent is shown in Fig. 16.

The clinical user is able to save the intermediate processing steps, to recall each step when needed and have a full access, using XML or text based format, to complex parameters of computational analysis and their visualized results.

Stent positioning software module has been designed as an easy to use 3D interactive tool for assisting the clinician's decision on defining the stenosis area and select the most suitable stent for the repository available at the Hospital's CATHLab Clinic. For performance issues it is represented to the clinician as accurate 3D wireframe cylinders which can be positioned in real time in the artery midline. Potentially, the system can support the stent of the same class available in the market.

Stent Deployment module developed uses PAK finite element analysis software. The module has been integrated in the software system through the data layer, the stent deployment module runs off-line. The clinical doctor is generating an "input data folder" for the stent deployment module containing: the patient-specific artery geometry from anatomy reconstruction, the geometry of artery midline, the straight crimped stent model, material data from stent database, the selected stent position and the process parameters for stent deployment. Within the automated stent deployment module: the 3D meshes of artery, stent and balloon are generated, the initial bending of the stent at the defined position within the artery is modelled, the contact, boundary and load conditions are applied and then the solver run is started. The results are stored back in an "output data folder" for visualization and further processing. The user is able to visualise in image format different parameters of the FEA calculation and some comparative measures in a summary report. The resulting stented artery geometry is transferred for further blood flow analysis.

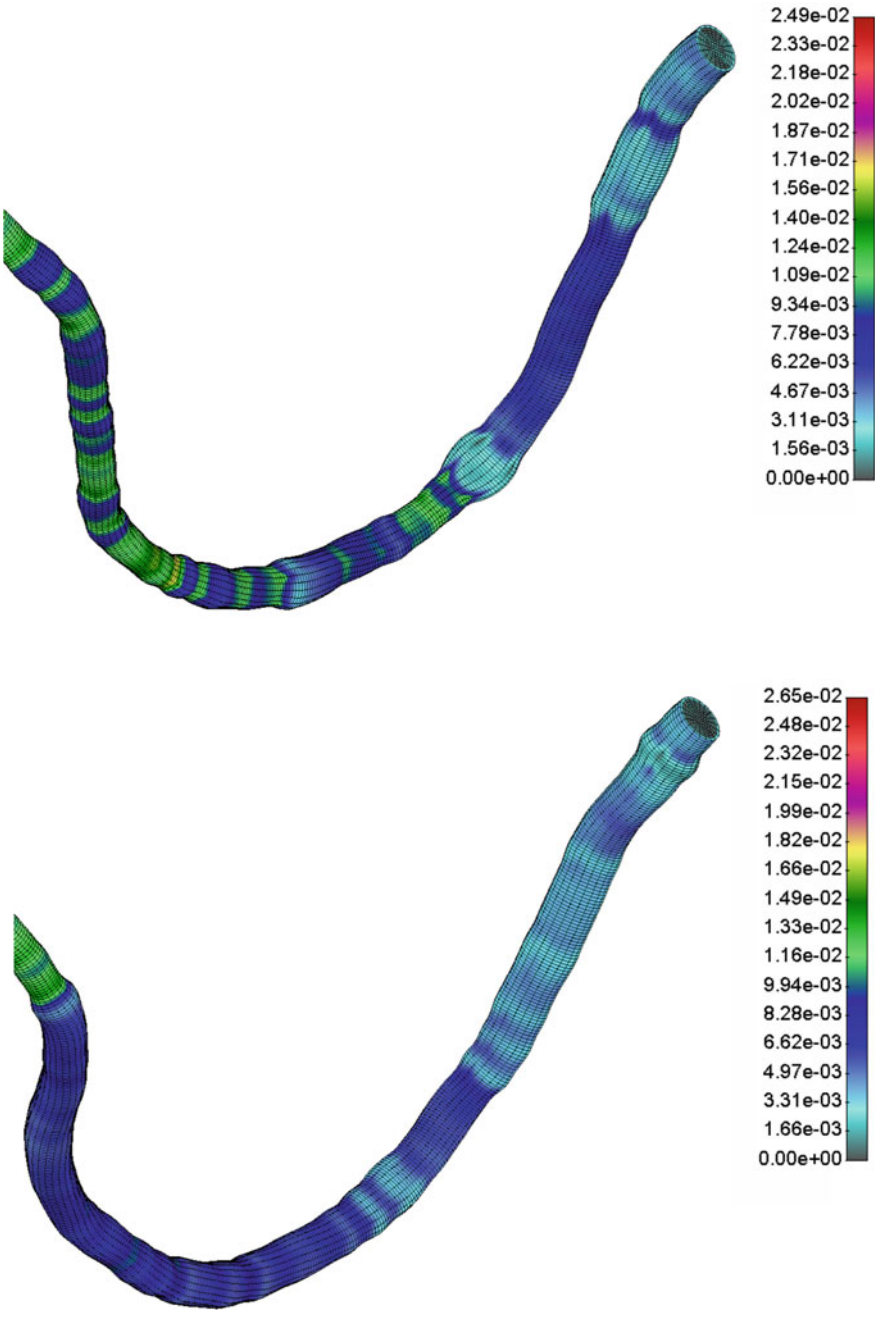

Fig. 11 Wall shear stress distribution. Blood flow analysis in a patient before (*upper panel*) and after (*bottom panel*) stent deployment

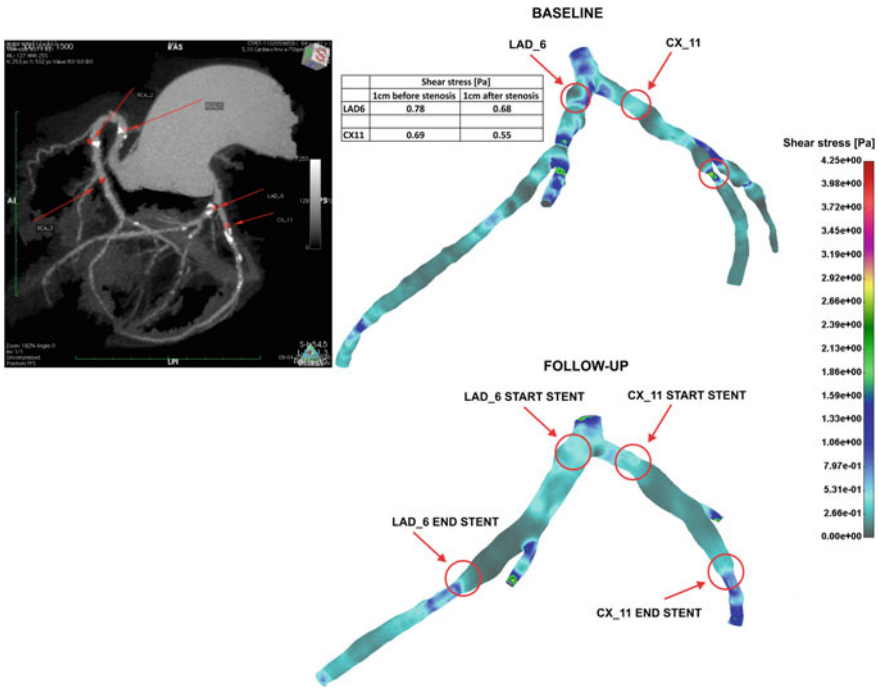

Fig. 12 CNRPatient #13 LAD_6, CX 11, baseline (before stenting), follow-up (after stenting)

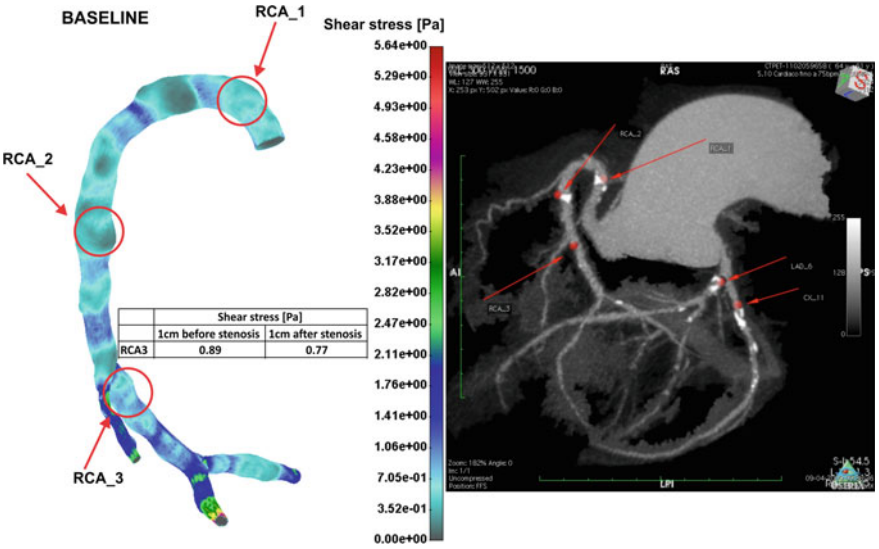

Fig. 13 Patient with right coronary artery, shear stress 1 cm before and 1 cm after stenosis

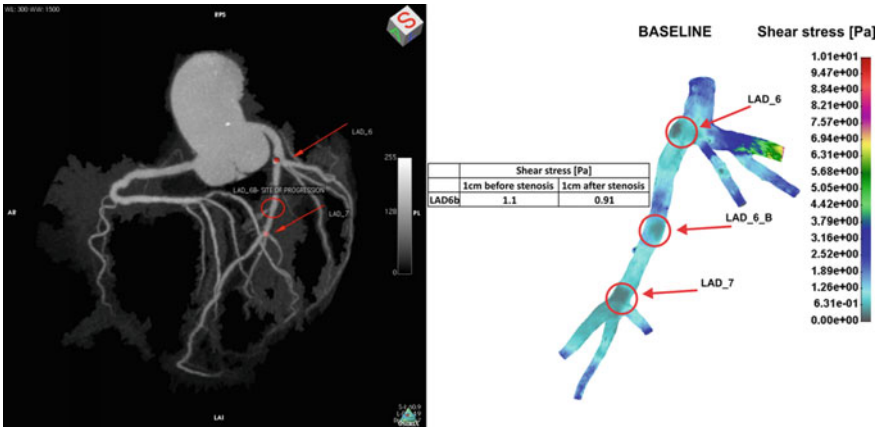

Fig. 14 Patient with LAD coronary artery, shear stress 1 cm before and 1 cm after stenosis

Blood Flow Analysis module is a CFD module implemented using the software PAK, a general purpose computational solver. Module is receiving the pre and post stented geometry of the arterial branch from Geometry Optimization and the Stent Deployment module accordingly. The user is able to set up the Blood Flow Parameters including material, finite element mesh resolution, time function and initial load data parameters. The PAK solver, running in the background, is applying automatically the most suitable FE Model for flow modelling in large blood vessels. The output of the module is stored for further visualization and post-processing steps. User is able to visualise in the 3D interactive module and compare visually the wall shear stress and velocity results to the stenosis area.

4 Numerical Results

4.1 Nitinol Material Model

For the past several years, nitinol as a Shape Memory Alloy (SMA) material has had a number of applications due to its characteristic behavior under thermal and mechanical loads. The shape memory effect, after which it is named, represents the ability of the material to undergo thermally recoverable deformation on the order of 6% or more strain.

We assumed that the wall material is orthotropic nonlinear elastic, and the Fung material model is adopted (Fung et al. 1979). The strain energy function is defined. The material parameters c, a_1, a_2, a_4 are determined using data fitting procedure from Kojic et al. (2008). Material parameters obtained from the fitting procedure are:

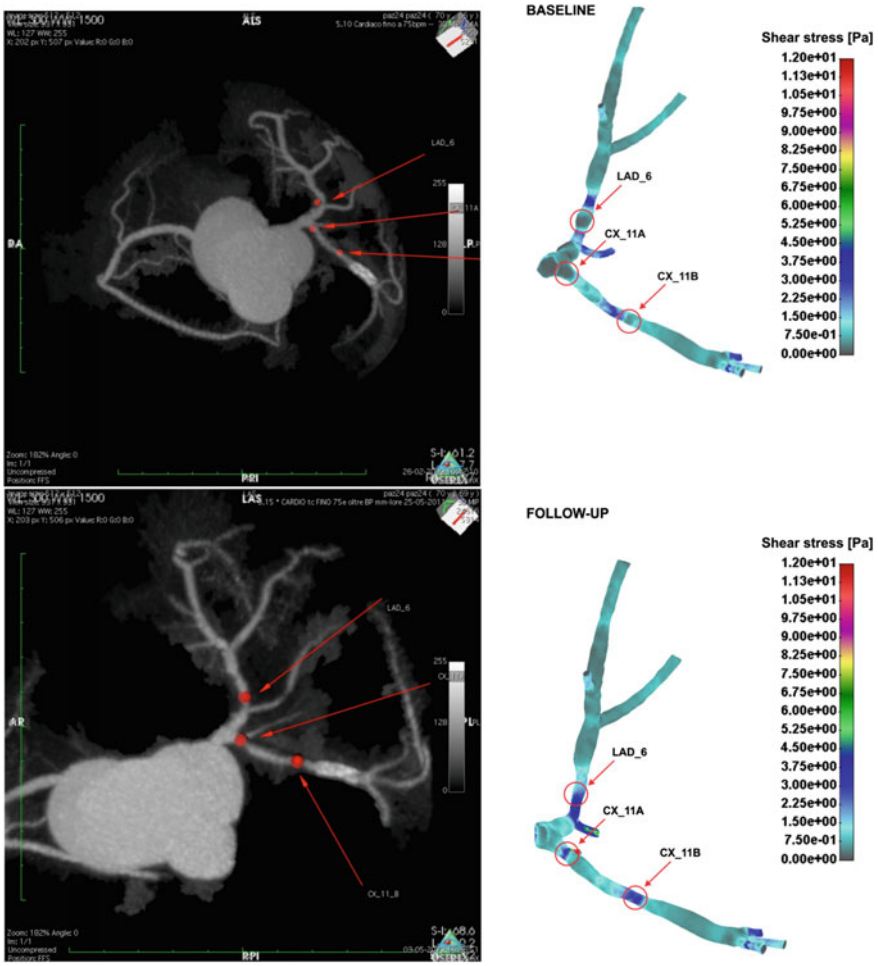

Fig. 15 Patient with CX coronary artery, shear stress distribution 1 cm before and after stenting

$$c = 0.7565\,(\text{MPa}), \quad a_1 = 0.166, \quad a_2 = 0.084, \quad a_4 = 0.045 \tag{47}$$

For the stent material, the alloy of Nitinol is adopted (for the definition of this material. Material parameters characterizing this alloy are (Kojic et al. 2008):

$$\begin{aligned} &E = 60{,}000\,(\text{MPa}) \quad \nu = 0.3 \\ &\sigma_s^{AS} = 520 \quad \sigma_f^{AS} = 750 \quad \sigma_s^{SA} = 550 \quad \sigma_f^{SA} = 200 \\ &\beta^{AS} = 250 \quad \beta^{SA} = 20 \quad \varepsilon_L = 7.5\% \quad C = 0\,(\text{MPa/K}) \end{aligned} \tag{48}$$

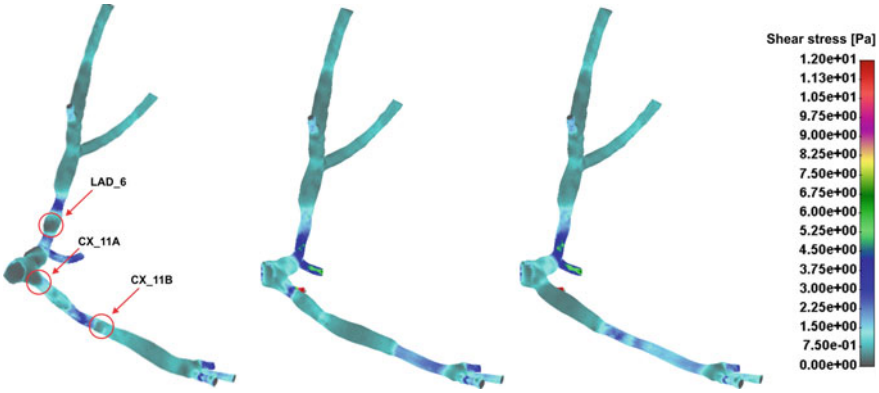

Fig. 16 Shear stress distribution for different positions of the stent for patient with CX coronary artery

where all σ- and β-parameters are in (MPa). Material parameters of blood are: density $\rho = 1.05 \times 10^{-3}\left(\mathrm{g/mm^3}\right)$ and dynamic viscosity $\mu = 3.675 \times 10^{-3}(\mathrm{Pa\,s})$.

4.2 Stress Analysis for Stent Deployment

We implemented numerical analysis of the material behavior using the boundary conditions and loads mentioned above. To examine different loading conditions, we apply hemodynamic flow as well as stent deployment procedure at the arterial wall.

The stent is loaded by an internal uniform radial pressure that linearly varies from zero to 1 MPa. In all the analyses 8-node brick elements are used to avoid locking-problems and due to the artery incompressibility requirement (Kojic et al. 2008). In particular, in the simulations we use up to 232,214 elements and 257,532 nodes, resulting in 666,354 variables. The interaction between the expanding stent and the artery is described as contact between deformable surfaces. As contact conditions, there is finite sliding, no-friction, with the constraint enforced by a Lagrange multiplier method. The stenotic segment of the artery which was examined before and after stent deployment is presented in Figs. 17 and 18.

The effective von Mises stress distribution in the stent is presented in Fig. 19. It can be seen that the highest stresses are detected near the connectors between the stent struts. These parts are subjected to plastic deformation with maximal stress around 180 MPa.

The effective stress distribution in the arterial wall at the two different cross-section locations at the end of stent deployment with maximum deployment pressure is shown in Fig. 20. It can be observed that higher stress exists when wall thickness is reduced during deployment procedure.

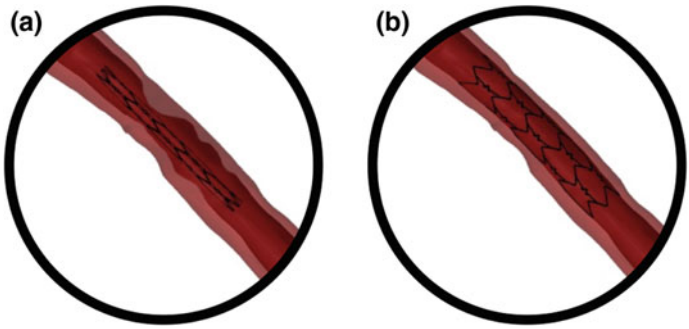

Fig. 17 Stent positioning before **a** and after **b** stent deployment

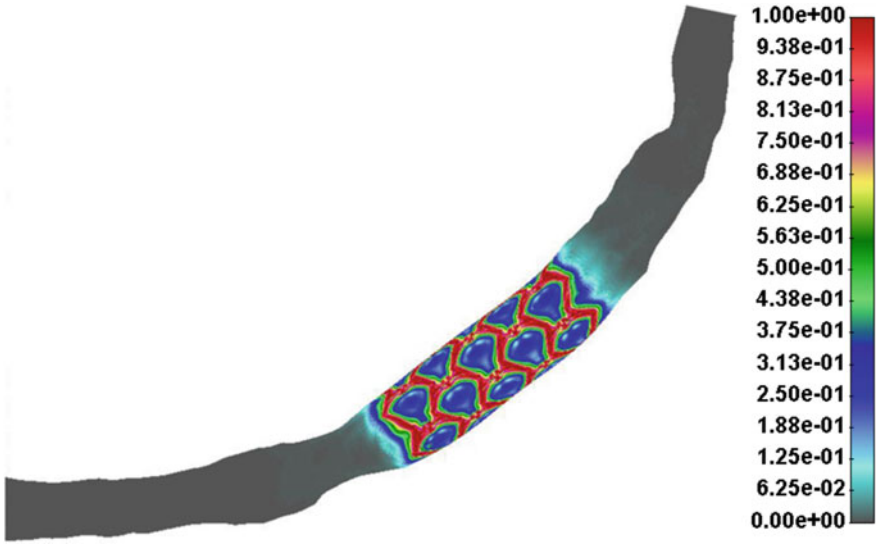

Fig. 18 Effective stress distribution inside the arterial wall after stent deployment. The units are in MPa. Blood flow analysis was performed by finite element method described in the methods section

Effective stress distribution for the inflation pressure 1 kPa for stent deployment in the carotid artery is presented in Fig. 21.

In the clinical study conducted within FP7 ARTreat project (www.artreat.org, www.artreat.kg.ac.rs) we examined plaque position for the coronary artery for baseline and follow-up time. Study for patients have also included stent position. Measurements are done with CT and the results are compared with computer simulation.

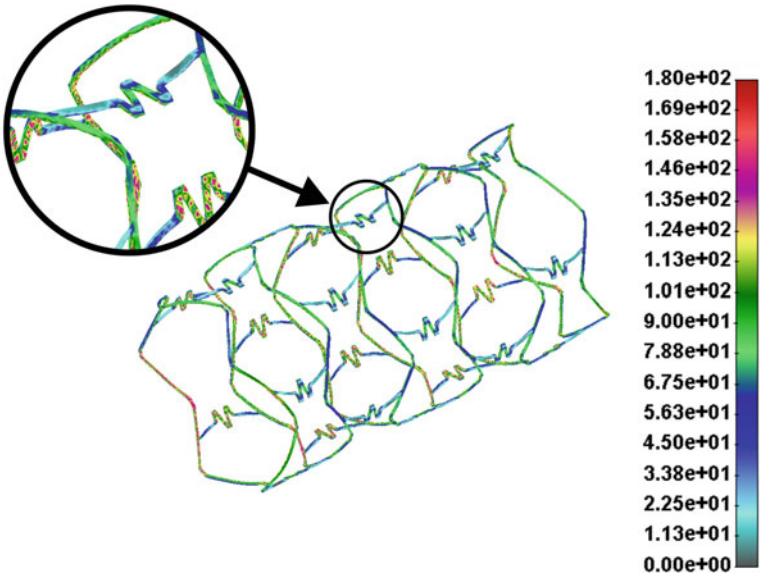

Fig. 19 Effective von Mises stress distribution for inflation pressure of 1 MPa. The units are in MPa

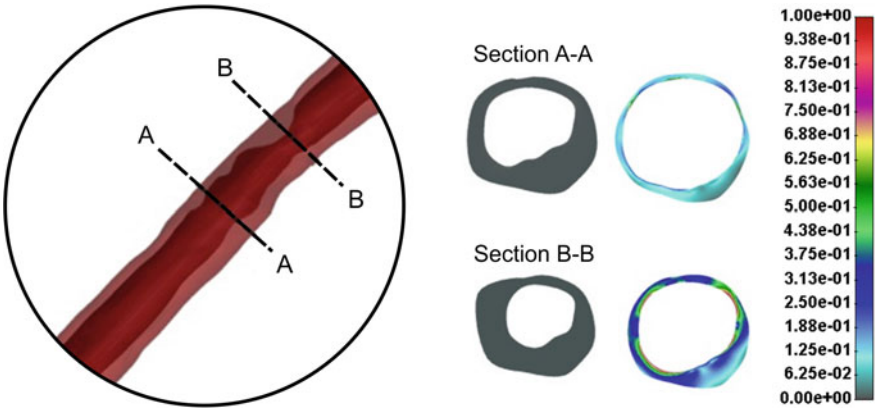

Fig. 20 Effective stress distribution in the two different cross-section locations inside the arterial wall at the end of stent deployment

Plaque position at CX and LAD artery for baseline and follow-up is presented in Fig. 22. Stent position can also be seen from Fig. 22. Shear stress and plaque concentration for this patient is shown in Fig. 23. It can be seen that plaque concentration on the specific cross-section location is matched with CT measurement.

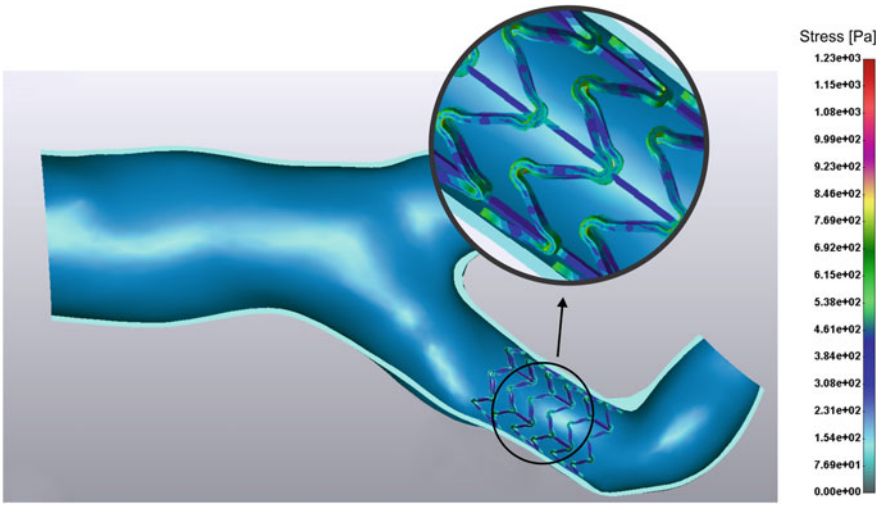

Fig. 21 Stent deployment in the carotid artery. Stress distribution for the inflation pressure 1 kPa

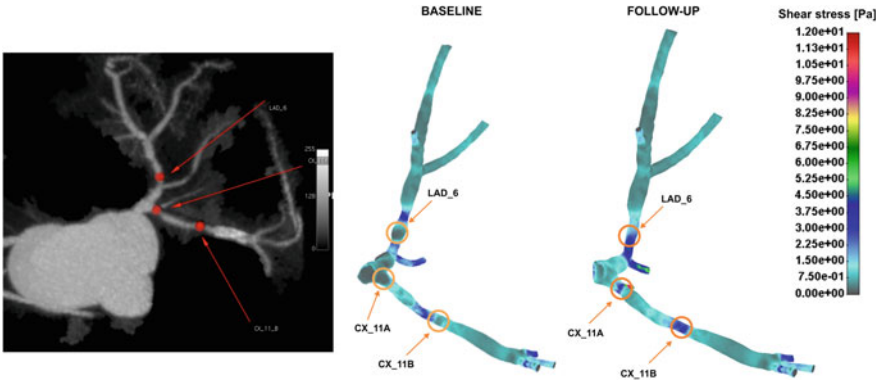

Fig. 22 Baseline and follow-up for plaque position at CX and LAD

5 Discussion and Conclusions

We analyse stent modeling with plaque formation and progression for specific patient in the coronary and carotid arteries. A coupled 3D artery reconstruction from CT and Angiography image modalities, with ability of detection of luminal narrowing is described as well as generation of finite element models and their processing. A number of different patients with significant in stent restenosis for the same time period of the follow–up were analysed. The geometry of the patients for the baseline and follow-up is used with image techniques described in detail. By

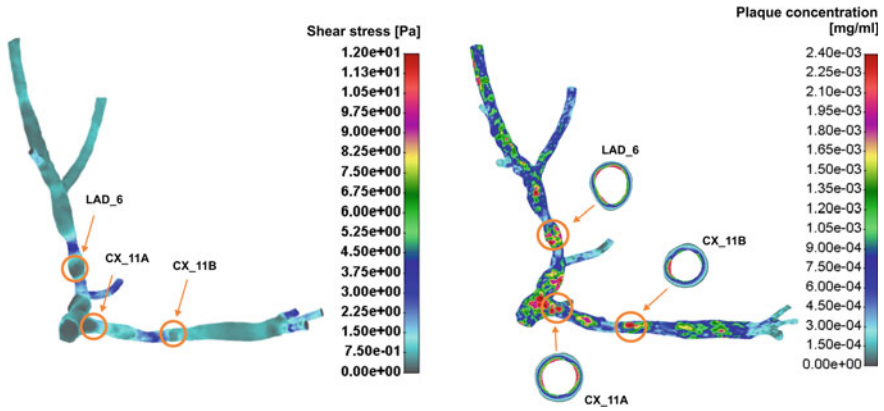

Fig. 23 Shear stress and plaque concentration for patient with stent deployment

applying realistic boundary conditions for each patient, we coupled the flow equations with the transport equation.

Blood flow simulation is described with Navier-Stokes and continuity equation. The governing finite element equations used in modeling wall tissue deformation with emphasis on implementation of nonlinear constitutive models are described. Using the Kedem-Katchalsky equations we performed the coupling of fluid dynamics and solute dynamics at the endothelium. The examples with rigid and deformable arterial wall with stented and unstented arteries are presented.

These methodologies, representing the patient-specific modeling tools, are suitable for use for clinical treatment decisions. Obtained results are very valuable because they make possible to visualize and present spatial distribution of biomechanical quantities which is practically impossible to achieve without modeling. Additional aim of this chapter was to validate our computer simulation model for plaque progression in patients with stented coronary arteries.

Stress distribution of the artery wall and stent during expansion of occluded zones is analyzed. Also, shear stress distribution before and after stent deployment is compared. The process of stent pushing the arterial wall towards the outside allowing the widening of the occluded artery can be observed from the comparison with the preoperative situation. Better understanding of stent deployment procedure and arterial wall response as well as optimal stent design can be obtained using computer simulation.

References

Antoniucci D, Bartorelli A, Valenti R et al (2000) Clinical and angiographic outcome after coronary arterial stenting with the Carbostent. Am J Cardiol 85:821–825

Athanasiou L, Karvelis P, Tsakanikas V, Naka K, Michalis L, Bourantas C, Fotiadis D (2012) A novel semiautomated atherosclerotic plaque characterization method using grayscale intravascular ultrasound images: comparison with virtual histology. IEEE Trans Inf Technol Biomed 16(3):391–400

Azaouzi M, Makradi A, Belouettar S (2012) Deployment of a self-expanding stent inside an artery: A finite element analysis. Mater Des 41:410–420

Azaouzia M, Lebaalb N, Makradia A, Belouettara S (2013) Optimization based simulation of self-expanding Nitinol stent. Mater Des 50:917–928

Balossino R, Gervaso F, Migliavacca F, Dubini G (2008) Effects of different stent designs on local hemodynamics in stented arteries. J Biomech 41:1053–1061

Berry JL, Santamarina A, Moore JE, Roychowdhury S, Routh WD (2000) Experimental and computational flow evaluation of coronary stents. Ann Biomed Eng 28:386–398

Bratzler RL, Chisolm GM, Colton CK, Smith KA, Lees RS (1977) The distribution of labeled low-density lipoproteins across the rabbit thoracic aorta in vivo. Atherosclerosis 28:289–307

Brooks AN, Hughes TJR (1982) Streamline upwind/Petrov-Galerkin formulations for convection dominated flows with particular emphasis on the incompressible Navier-Stokes equations. Comput Methods Appl Mech Eng 32:199–259

Colombo A, Hall P, Nakamura S et al (1995) Intracoronary stenting without anticoagulation accomplished with intravascular ultrasound guidance. Circulation 91:1676–1688

Colombo A, Stankovic G, Moses JW (2002) Selection of coronary stents. J Am Coll Cardiol 40:1021–1033

DePaola N, Gimbrone MAJ, Davies PF, Dewey CF (1992) Vascular endothelium responds to fluid shear stress gradients. Arterioscler Thromb 12:1254–1257

Filipovic N (2013) PAK-Athero, finite element program for plaque formation and development. University of Kragujevac, Serbia

Filipovic N, Mijailovic S, Tsuda A, Kojic M (2006) An implicit algorithm within the arbitrary Lagrangian-Eulerian formulation for solving incompressible fluid flow with large boundary motions. Comput Methods Appl Mech Eng 195:6347–6361

Filipovic N, Rosic M, Tanaskovic I, Milosevic Z, Nikolic D, Zdravkovic N, Peulic A, Fotiadis D, Parodi O (2011) ARTreat project: three-dimensional numerical simulation of plaque formation and development in the arteries. IEEE Trans Inf Technol Biomed PMID:21937352

Filipovic N, Nikolic D, Saveljic I, Djukic T, Adjic O, Kovacevic P, Cemerlic-Adjic N, Velicki L (2013) Computer simulation of thromboexclusion of the complete aorta in the treatment of chronic type B aneurysm. Comput Aided Surg 18(1–2):1–9

Fischman DL, Leon MB, Baim DS, Schatz RA, Savage MP, Penn I, DetreK Veltri L, Ricci D, Nobuyoshi M, Cleman M, Heuser R, Almond D, Teirstein PS, Fish RD, Colo A (1994) A randomized comparison of coronary-stent placement and balloon angioplasty in the treatment of coronary artery disease. N Engl J Med 331:496–501

Fung YC, Fronek K, Patitucci P (1979) Pseudoelasticity of arteries and the choice of its mathematical expression. Am J Physiol 237:620–631

Gay M, Zhang LT (2009) Numerical studies on fluid-structure interactions of stentdeployment and stented arteries. Eng Comput 36:61–72

Goldstein J, Anderson R, Brown M (1979) Coated pits, coated vesicles, and receptor-mediated endocytosis. Nature 279:679–684

Gyongyosi M, Yang P, Khorsand A, Glogar D, The Austrian Wiktor Stent Study Group and European Paragon Stent Investigators (2000) Longitudinal straightening effect of stents is an additional predictor for major adverse cardiac events. J Am Coll Cardiol 35:1580–1589

He Y, Duraiswamy N, Frank AO, Moore JE Jr (2005) Blood flow in stented arteries: a parametric comparison in three-dimensions. J Biomech Eng 22:637–647

Henry M, Klonaris C, Amor M, Henry I, Tzvetanov K (2000) State of the art: which stent for which lesion in peripheral interventions? Tex Heart Inst J 27(2):119–126

Karrillon GJ, Morice MC, Benveniste E et al (1996) Intracoronary stent implantation without ultrasound guidance and with replacement of conventional anticoagulation by antiplatelet therapy: 30-day clinical outcome of the French multicenter registry. Circulation 94:1519–1527

Kojic M, Filipovic N, Stojanovic B, Kojic N (2008) Computer modeling in bioengineering: theoretical background, examples and software. Wiley, Chichester, England

LaDisa JF, Guler I, Olson LE, Hettrick DA, Kersten JR, Warltier DC, Pagel PS (2003) Three-dimensional computational fluid dynamics modeling of alterations in coronary wall shear stress produced by stent implantation. Ann Biomed Eng 31:972–980

LaDisa JF, Olson LE, Guler I, Hettrick DA, Kersten JR, Warltier DC, Pagel PS (2005) Circumferential vascular deformation after stent implantation alters wall shear stress evaluated with time-dependent 3D computational fluid dynamics models. J Appl Physiol 98:947–957

LaDisa JF, Olson LE, Douglas HE, Warltier DC, Kersten JR, Pagel PS (2006) Alterations in regional vascular geometry produced by theoretical stent implantation influence distributions of wall shear stress: analysis of curved artery using 3D computational fluid dynamics models. Biomed Eng Online 16(5):40

Mehta R, Harjai K, Boura J, Tcheng J, Dixon S, Stone G, Grines C (2013) Short-term outcomes of balloon angioplasty versus stent placement for patients undergoing primary percutaneous coronary intervention: Implications for patients requiring early coronary artery bypass surgery. Am Heart J 165(6):1000–1007

Morice MC, Serruys PW, Sousa JE, Fajadet J, Hayashi B, Perin M, Colombo A, Schuler G, Barragan P, Guagliumi G, Molnàr F (2002) A randomized comparison of a Sirolimus-Eluting stent with a standard stent for coronary revascularization. N Engl J Med 349:1315–1323

Murata T, Hiro T, Fujii T, Yasumoto K, Murashige A, Kohno M, Yamada J, Miura T, Matsuzaki M (2002) Impact of the cross-sectional geometry of the post-deployment coronary stent on in-stent neoinimal hyperplasia: an intravascular ultrasound study. Circ J 66:489–493

Murphy J, Boyle F (2008) Assessment of the effects of increasing levels of physiological realism in the computational fluid dynamics analyses of implanted coronary stents. In: 3th annual international IEEE EMBS conference

Natarajan S, Mokhtarzadeh-Dehghan MR (2000) A numerical and experimental study of periodic flow in a model of a corrugated vessel with application to stented arteries. Med Eng Phys 22:555–566

Newman VS, Berry JL, Routh WD, Ferrario CM, Dean RH (1996) Effects of vascular stent surface area and hemodynamics on intimal thickening. J Vasc Interv Radiol 7:387–393

Rajamohan D, Banerjee RK, Back LH, Ibrahim AA, Jog MA (2006) Developing pulsatile flow in a deployed coronary stent. J Biomech Eng 128:347–359

Rana H, Andrews J, Chacko B, Hansen K, Levy P (2013) Mortality in patients with premature lower extremity atherosclerosis. J Vasc Surg 57(1):28–36

Schomig A, Neumann FJ, Kastrati A et al (1996) A randomized comparison of antiplatelet and anticoagulant therapy after the placement of coronary-artery stents. N Engl J Med 334:1084–1089

Seo T, Schachter LG, Barakat AI (2005) Computational study of fluid mechanical disturbance induced by endovascular stents. Ann Biomed Eng 33(4):444–456

Sharafuddin MJ, Hoballah JJ, Kresowik TF, Sharp WJ, Golzarian J, Sun S, Corson JD (2008) Long-term outcome following stent reconstruction of the aortic bifurcation and the role of geometric determinants. Ann Vasc Surg 22(3):346–357 Epub Apr 14

Tortoriello A, Pedrizzetti G (2004) Flow-tissue interaction with compliance mismatch in a model stented artery. J Biomech 37:1–11

Part III
Clinical Applications

Biomaterials in Dentistry—Implantology and Guided Bone Regeneration

Zoran Pesic and Ana Pejcic

Abstract The use of biomaterials and implant therapy in dentistry is becoming a more popular and acceptable procedure for the replacement of both single and multiple teeth. Procedures have evolved for maintaining and regenerating bone to provide an optimal environment for subsequent implant placement. Both guided bone regeneration and implantology have applications in dentistry for increasing the width and height of the alveolar ridge in areas with insufficient alveolar bone in jaws, as well as repairing and maintaining bone defects around the teeth. The application of these techniques involves the use of a wide range of materials, including autogenous bone grafts, allografts, xenografts, alloplasts, bone-promoting factors, resorbable/nonresorbable barrier membranes, and implants used either alone or in a variety of combinations. The methods of guided bone regeneration utilize biological materials or synthetic specimens. Furthermore, insight into the future development of membrane fabrication, as well as platelet-rich fibrin membranes, will strongly influence the development of guided bone regeneration. This article describes a series of six patients treated with guided bone regeneration using bovine bone mineral, a resorbable collagen membrane, a growth factor, platelet-rich plasma, and an implant placed with a minimum follow-up period of eighteen months.

Keywords Guided bone regeneration · Implantology · Bone substitute · Collagen membrane · Implant · Platelet-rich plasma

Z. Pesic (✉)
Maxillofacial Surgery, Faculty of Medicine, University of Nis,
Dr. Z. Djindjica Blvd 81, 18000 Nis, Serbia
e-mail: pesic.z@gmail.com

A. Pejcic
Periodontology and Oral Medicine, Faculty of Medicine, University of Nis,
Dr. Z. Djindjica Blvd 81, 18000 Nis, Serbia

F. Zivic et al. (eds.), *Biomaterials in Clinical Practice*,
https://doi.org/10.1007/978-3-319-68025-5_26

1 Introduction

1.1 The Basic Characteristics of the Bone

The bone is a specialized connective tissue most prominently characterized by its mineralized organic matrix, which impacts the physical properties that allow bone tissue to resist load, to support functional organs such as teeth, and to protect highly sensitive body parts such as the central nervous system. Bone tissue provides mechanical stability to the skeleton, which is needed for load bearing, locomotion, and the protection of internal organs.

A bone consists mainly of two structures: an organic component, such as a matrix that contains collagen, and a mineral component that is predominantly hydroxyapatite (Rho et al. 1997; Yu et al. 2009). In the mineralized organic bone matrix, both living and dead cells are present. Three types of cell are known to play a role in bone homeostasis: osteoblasts, osteocytes, and osteoclasts. Osteoblasts are progenitor cells with large nuclei. Osteocytes arise from osteoblasts, being located in bony lacunae. Osteoclasts are large, multinucleated gain cells, which are located in surface pits of the bone. New bone formation is dependent on the presence of osteoprogenitors, which are undifferentiated mesenchymal cells that can migrate to target sites, proliferate, and differentiate into osteoblasts (Greenstein et al. 2009).

The differentiation of osteoblasts from osteoprogenitor cells is dependent upon the presence and/or release of factors that induce or promote bone growth, among them bone growth factors and proteins, as well as platelet-derived growth factors and fibroblast growth factors (Schilephake 2002; Kaigler et al. 2011; Rao et al. 2013).

Bone metabolism involves resorption of the existing bone by osteoclasts and the subsequent formation of a new bone matrix by osteoblasts. These activities are essential for bone remodeling, regeneration, and repair (de Long et al. 2007).

Bone regeneration and development are processes that are regulated by many growth factors and transcription to coordinate the interaction of cells and matrix as a response to external and internal stimuli (Kneser et al. 2006; Farzad and Mohammadi 2012).

Bone is a dynamic tissue that constantly undergoes remodeling. Bone formation results from a complex cascade of events that involves proliferation and differentiation of primitive mesenchymal cells into the osteoblast cells. The osteoblasts form osteoid, which begins to mineralize after 13 days. Growth factors affect the growth and differentiation of the osteoblast (Luu et al. 2007).

Bone loss and bone damage may occur as a result of genetic conditions, infectious diseases, tumors, or trauma. Additional causes of bone loss or bone damage specific to the oral cavity include severe periodontal disease, tooth loss, and post-extraction atrophy of the jaws.

The regeneration of bone (or the stimulation of bone production) is often required to treat a loss of bone tissue caused by trauma, osteonecrosis, tumors, or disease.

1.1.1 Regenerative Bone Therapy

During the process of regenerating lost or damaged parts of the bone, a damaged tissue regenerates in two ways: (1) Endogenous cells reform the damaged tissues, or (2) Exogenous cells or tissues replace the damaged cells or tissues (Montanari et al. 2013).

Periodontal regeneration is bone regeneration of a lost or injured part of the bone through the process of bone healing or the incorporation of naturally derived or biocompatible synthetic scaffolds, aimed at replacing the missing or damaged osseous tissues (Montanari et al. 2013). There are several modalities of bone regeneration, which include bone grafting, guided bone regeneration, and tissue engineering.

To improve patient-care results, scientists are making great efforts towards the creation of bone substitutes and the development of ways to improve bone healing. However, there is no ideal system for the treatment of bone defects. Autologous bone material is the gold standard for repairing bone defects, as it has osteoinductive properties (Laurencin et al. 2006; Gielkens et al. 2008). This method is associated with an additional invasive intervention that leads to an increased risk of infection and pain during recovery. Autologous material can only replace a certain amount of bone tissue (Sorger et al. 2001). Heterologous transplants bear the risk of infection and rejection of the donor material. The use of platelet-rich preparations may help to fulfill some of these requirements, particularly as an aid to bone regeneration (Anitua 1999; Lee et al. 2010a, b).

1.1.2 Alveolar Bone

The alveolar process is a part of the attachment apparatus for the teeth, with the tooth cementum and periodontal membrane. Bone remodeling occurs in the alveolar process during the growth of the jaw, eruption of the teeth, and tooth replacement. The attachment apparatus distributes and resorbs the pressure forces.

The process's alveolaris develops in conjunction with the development and eruption of the teeth and is gradually resorbed if the teeth are lost. The bone tissue that covers the alveolar process is the bone of the alveolar process, and the bone that covers the alveolus is the alveolar bone proper. On radiographs, the proper alveolar bone, derived from cells of the dental follicle, appears as lamina dura.

The remodeling of the proper alveolar bone commences with the tooth's functional period, as soon as it comes into occlusal contact with its antagonist. The alveolar bone is constantly being remodeled. The cortical bone mass replaced by a new bone and the bone trabeculae are first resorbed and then reformed.

Defects of the alveolar bone occur as a result of trauma, inflammation, recessive surgical intervention such as tumor resection, bone loss after periodontal disease or atrophia after tooth loss. In the posterior maxilla, the phenomenon of pneumatization of the sinus maxillaris increases after tooth loss, which results in a vertically compromised bone level. Thus, bone reconstruction before or simultaneous to implant placement is often necessary (Ten Cate 1994; Caneva et al. 2012; Santos et al. 2013).

1.1.3 Periodontitis

Periodontal disease is characterized by the destruction of periodontal tissues. If left untreated, it will eventually lead to tooth loss. To restore some parts of the tooth-supporting apparatus, regenerative periodontal surgery procedures should be carried out. Periodontal regenerative procedures are used in situations in which the treatment outcome is expected to improve the local gingival architecture, as well as the function and prognosis of periodontitis-involved teeth (Polimeni et al. 2000).

Periodontal regeneration includes regeneration of the cementum, the periodontal ligament, and the alveolar bone. Periodontal regeneration requires specific cell activities of progenitor cells, which must proliferate, migrate into the wound area, and differentiate. Progenitor cells colonizing the periodontal defect should have specific capabilities to form the cementum, bone, and periodontal ligament fibers.

One of the first methods used in the attempt to obtain a new attachment was scaling and root planning combined with soft tissue curettage (Zaugg et al. 2014). Another technique was the elevation of tissue flaps in order to get access to the defect. All granulation tissue in the defect was removed and flaps were sutured to accomplish complete coverage of the defect. In a number of clinical trials, the flap approach was combined with the placement of bone grafts or implants materials into bony defects (Buduneli 2012).

In cases of a lack of adequate alveolar bone, several procedures and materials have been developed to overcome the problem. In dentistry, bone substitution materials were used for socket preservation, periodontal defects, ridge augmentation, defects following shortening of the tooth root and cyst, sinus lifts, and implant dentistry (Scheyer et al. 2012).

For regenerative periodontal therapy, various methods have been developed (barrier membranes, replacement grafts, growth factors and a combination of these procedures) (Kim 2010).

1.2 Guided Bone Regeneration

Periodontal treatment based on the principles of guided tissue regeneration is currently the most advanced of the regenerative methods. This is a procedure that attempts to regenerate the lost periodontal structures. The lost periodontal structures include the alveolar bone, the periodontal ligament, and the cementum. GTR is used in periodontal surgery to stabilize the wound area and exclude the epithelium during wound healing (AAP 1992, 1996).

The mechanisms of guided bone regeneration (GBR) generally follow the same principles as for GTR. Tissues using tissue barriers are commonly referred to as membranes. Tissue barriers and membranes prevent the intrusion of cells from the neighboring, undesired tissues (Retzepi and Donos 2010).

When a periodontal patient is evaluated for a GTR procedure, the radiographs must be evaluated in order to assess the type of bone loss. Patients with a horizontal

type of bone loss are usually not amenable to GTR procedures, whereas patients with vertical or intrabony defects are possible candidates (Dimitriou et al. 2011).

If the intrabony defect is narrow and deep with only one osseous wall, then the combination technique is recommended for the maintenance of the critical space for regeneration. If the intrabony defect is narrow and deep with two or three walls, then the "membrane alone" technique may be considered (Darby 2011).

The barrier membranes and graft materials are the two most commonly used materials for GBR today. GBR involves the use of resorbable or nonresorbable barriers (membranes) to exclude epithelial and connective tissue cells from the root surface during wound healing. This is believed to facilitate the regeneration of lost cementum, periodontal ligament, and alveolar bone (Al-Hamdan et al. 2003; Shue et al. 2012).

Incision is strictly intrasulcular. If needed, only one releasing incision along the lateral tooth width is made. Scaling and root planning remove the granulation tissue. With regard to the defect, an appropriate membrane is selected, which is further trimmed according to the bony defect. The membrane should completely cover the defect and overlap the bone margins by about 2 mm. It is tightly fixed to the neighboring teeth with sling sutures. The flap is coronally advanced after careful dissection of the periosteum at its base. Primary closure of the interdental space and tension-free fixation of the flap over the membrane are carried out by using horizontal and vertical mattress sutures (Needleman et al. 2002; Giannoudis et al. 2012).

1.2.1 Membranes for Guided Bone Regeneration

Specially designed membranes are used to provide and maintain sufficient space for the proliferation of the mesenchymal cells. The membranes are made of materials such as expanded polytetrafluoroethylene (ePTFE), polyglactic acid, polylactic acid, and collagen (Liu and Kerns 2014; Owen et al. 2010).

Tissue barriers are divided into two main groups: non-resorbable and resorbable (Donos et al. 2011). The first generation membranes (nonresorbable) consist of expanded polytetrafluoroethylene (ePTFE, Gore-Tex periodontal material) and are still regarded as the standard for regenerative periodontal therapy by some practitioners. They have to be removed in a second surgical operation after four to six weeks. There is a considerable risk of infection due to bacterial colonization of the membrane. The membrane tends to collapse into the defect. Titanium-reinforced membranes facilitate better space-keeping and may even allow for horizontal bone regeneration (Piatelli et al. 1995).

Resorbable membranes for guided tissue/bone regeneration do not require a "second surgery" for the removal of the membrane. Clinical results obtained with resorbable membranes have been very similar to those achieved with non-resorbable membranes (Coïc et al. 2010).

Bioresorbable materials that may be used for the fabrication of resorbable membranes belong to the groups of natural or synthetic polymers (Taguchi et al. 2005;

de Santana et al. 2010). Natural products are different from synthetic materials. Human collagen, e.g., lyophilized durra mater (allograft) or bovine collagen (xenograft), has certain disadvantages (Kothiwale et al. 2009).

Polyglycolide, polylatide, and copolymers of these aliphatic polyesters have the following characteristics: they are biocompatible, and their special design facilitates the stiffness of the membrane and allows for tissue integration (Cortelini et al. 1996; Meinig 2010).

Guided tissue regeneration is intended to lead to considerable alteration of the local morphology of the periodontal defect. With regards to attachment gain, certain periodontal lesions respond considerably better to guided tissue regeneration than to conventional treatment modalities (Kim et al. 2011a, b). Therefore, the indications are: two- and three-walled, at least 4 mm deep bony pockets; buccal and lingual degree II furcation of mandibular and maxillary molars; bony defects after surgical removal of impacted wisdom teeth, and bony defects after placing implants (Santana et al. 2009; Chen et al. 2013).

1.2.2 Postoperative Care

The patient must be briefed about the delicate wound healing processes. Postoperative care includes: (1) mouth rinses twice daily with a 0.1–0.2% chlorhexidine solution. Tooth brushing must be avoided in the surgically treated area; (2) if necessary, supragingival biofilm at the gingival margin is carefully removed and antibiotics prescribed; (3) if a nonresorbable membrane has been implanted, it is surgically removed after four to six weeks; (4) when using a resorbable membrane, sutures are removed after 7–10 days.

1.2.3 Biomaterials Used for Bone Regeneration

Various graft and implant materials are used and can be grouped into four categories:

1. *Autogenous grafts* (*bone*): Vital osteoblasts are transplanted, and osteogenesis may be expected. There is no risk of transmission of infectious diseases; however, the disadvantage is a second surgical site. These materials may be intraoral and extraoral autogenous bone grafts. The primary sources of bone fill material are intraoral autogenous bone grafts. The main limitation of this technique is the amount of bone available to be used for donation. Extraoral autogenous bone grafts are taken from the iliac crest. This technique has an additional surgical procedure outside the mouth (Keles et al. 2010).
2. *Allogenic grafts*: (e.g., mineralized/demineralized freeze-dried bone allograft). These are substitutes for the autogenous bone that ensure sufficient volume of the graft material. An allogenic graft induces bone and cementum formation through a differentiation factor—bone morphogenetic protein (BMP) (Berner et al. 2012).

3. *Xenograft*: This is porous bovine bone material prepared through protein extraction from a bovine bone, with the ability to enhance bone formation. (Bio-Oss, PerGen P015). Bio-Oss is the most widely applied xenograft material. Bio-Oss is derived from cancellous bone. PepGen P-15 is from the cortical bone (Palachur et al. 2014).
4. *Alloplastic graft* (e.g., tricalcium phosphate, hydroxyapatite, calcium carbonate, bioactive glasses): This is a synthetic bone substitute or inorganic implant material. It may be used as a more or less inert filler for infrabony lesions. Hidroxyapatite is the most popular example of this category (Lynch et al. 1999; Kaushal et al. 2014).

If the intrabony defect is narrow and shallow with two or three walls, then a bone graft alone may be considered, because the defect size is sufficient to accommodate the autogenous bone from the oral cavity If bone grafts such as demineralized freeze-dried bone allografts are used, the predictability of the regenerative techniques caused by their possible release of bone-inducing proteins (known as bone morphogenic proteins), as well as maintenance of the critical space for regeneration, can be helpful.

The inorganic alloplastic graft materials may not be recommended, because studies show encapsulation with little bone fill and periodontal regeneration; thus, they serve as space fillers only (Genco et al. 1990).

Various alloplastic bone substitution materials of different origin and chemical composition have been investigated in recent years (Ereno et al. 2010). Non-resorbable alloplastic materials act as replacement bone, and resorbable materials grow into the bone. In dentistry, xenogeny grafting has been shown to be one of the most effective methods of creating bone, whereas alloplastic graft material constitutes the second most popular form of bone grafting material.

Bone replacement grafts may have various properties:

- **Osteogenesis** is the process during which new bone is formed by osteoblasts contained in the transplanted graft itself.
- **Osteoinduction** is the ability of the bone substitute to transform the mezenchimal cells into the osteoblasts and lead to new bone formation.
- **Osteoconduction** is the process that allows for bone apposition from the stimulation of the existing surrounding bone close to the filling material, which is inert.

For the present time, the autogenic bone is considered the "gold standard" among bone-substitution materials (Nkenke et al. 1994).

1.2.4 Growth Factors

Recently, there has been interest in examining the role played by growth factors in periodontal regeneration. Enamel matrix derivative (EMD) is a product that

contains proteins derived from porcine enamel that have been shown to be important in the development of the supporting tooth apparatus, including the formation of cementum, periodontal ligament, and alveolar bone (Dupont et al. 2012).

Other growth factors that are used for periodontal regeneration are: autologous platelet-rich plasma (PRP) and platelet-derived growth factor-PDGF (Lekovic et al. 2001; Marx 2001; Kazakos et al. 2011).

1.2.5 Biomaterials

Developing engineered tissue is another interesting approach to bone regeneration.

Bone tissue engineering using various cell sources and materials, aimed at solving the problem of the treatment of numerous clinical indications, requires the regeneration of damaged or deficient bone (Kolambkar et al. 2011).

These fall into two broad classes: polymers and ceramics.

1. ***Polymers*** are large organic macromolecules composed of many monomers in a regular pattern.

Natural polymers include modified polysaccharides (chitosan) and polypeptides (collagen, cellulose agarose, and hyaluronan) (Hutmacher et al. 2001). Synthetic polymers (poliglycolic acid, polylactic acid) provide a platform for exhibiting the biomechanical properties of scaffolds in tissue engineering.

Tissue repair and regeneration through tissue engineering is dependent on the use of biodegradable polymer scaffolds, which serve as a carrier matrix for bioactive substances.

2. The available ***ceramic materials*** include calcium phosphate (tricalcium phosphate and hydroxyapatite), calcium sulfate, and bioactive glass.

CaP biomaterials are useful in tissue engineering for the regeneration of hard tissues (Lee et al. 2012a, b). Calcium phosphate biomaterials are similar to bone mineral. They are osteoconductive and osteoinductive and can be effective carriers of bone cell seeds (Wang et al. 2007). An investigation showed the superior regenerative effects observed with HA (Wei and Ma 2004).

Beta-Tricalcium phosphate (β-TCP) was used to repair marginal and periapical periodontal defects, as well as miscellaneous alveolar bony defects (Stavropoulos et al. 2010; Chawla et al. 2011).

Calcium sulfate (CS) acts as a barrier, which makes it ideal for use as an adjunct with other materials (Nilsson et al. 2004).

Bioactive Glass (Bioglass) is suitable for bone regeneration in periodontology and dental implant surgery. Bioactive glass, such as PerioGlas, has the ability to inhibit the down-migration of epithelium. Bioactive glass is a ceramic composed principally of SiO_2 (Subbaiah and Thomas 2011; Varanasi et al. 2011; Sohrabi et al. 2012).

In recent studies, authors reported that chitosan membrane effectively contributed to the formation of new bone and cementum in surgically-created defects in beagle dogs (Yeo et al. 2005; Xu et al. 2012).

Polylactic acid (*PLA*) is a bioabsorbable membrane (Atrisolb). The results showed that the outcome of treatment with membrane may be similar to open flap debridement.

PLGA is another type of synthetic biomaterial used as a barrier in GTR/GBR. It is a combination of PLA and polyglycolic acid (PGA) in various proportions (Kim et al. 2009).

1.3 Implantology

Implantology, a relatively young dentistry discipline that has emerged very quickly, was invented and developed to satisfy esthetic and functional goals of producing new, artificial dentition to replace lost material. Implantology can be defined as inserting native or foreign materials into the body tissues. These inserted tissues can be made of different materials.

Dental implantology uses the alveolar bone and its nearby tissues for embedding the new material. As transplantation includes the transfer and embedding of the living tissue, here materials are inserted into the tissue with active, functional characteristics. The prosthetic replacement of teeth that have been lost requires anchoring in the jawbone. This anchoring is achieved by inserting aloplastic materials into the jawbone. The patient's desire to have a prosthetic device anchored solidly in the alveolar bone has inspired dentists for centuries to solve this problem and fulfill their patient's requirements. However, in the absence of functional stimulation, which is a consequence of tooth extraction, bone loses its form and density, the final result of which is a loss of width and height of the alveolar ridge (Byrne 2014). The rate of this reduction can go up to 22% in the vertical dimension and up to 63% in the horizontal dimension (Tan et al. 2012).

Except in cases when implants are placed into extraction sites immediately, when some bone resorption can be expected, it can be generally concluded that the implant, once placed, saves alveolar bone in its vertical dimension. However, the usefulness of the implant is the chief criterion for the treatment's success (Byrne 2014). With time, this criterion was developed and adjusted. Today, the following criterion is in use (Papaspyridakos et al. 2012): First comes the patient's satisfaction: comfort, function, aesthetics, and general satisfaction. The next criterion is the condition of the periimplant bone: the presence of bone loss, the presence of implant mobility, and the presence of infection and pain. Peri-implant soft tissue criteria consider the degree of healthy probing depth, the absence of suppuration, bleeding on probing, edema, hyperplasia, swelling, and recession. The criteria of prosthetic success include the function and esthetics, as well as the presence of complications.

Many factors have an influence on osseointegration, surveillance, and the stability of the implants and prosthetic devices connected to them. Porter and von Fraunhofer (2005) found that factors like the age of patients, smoking, general health factors, loading condition, length of implant, and oral hygiene have a huge impact on the success of implant therapy. One more factor with very significant influence should be added, and that is the qualitative and quantitative characteristics of bone tissue, considered to be a factor with great influence on implant logical therapy. For centuries, the types of material used in implantology have changed and developed. Materials for implant production must meet certain criteria, such as biocompatibility, mechanical strength and relatively low technical demands for production (Byrne 2014). All these criteria must meet one main criterion, and that is the possibility of the implants osteointegrating.

Osteointegrated implants have a direct attachment of bone tissue to the surface of the implant without a connective tissue barrier in between them, according to the definition by Branemark et al. (1997), which was later modified by numerous authors. For example, Albrektsson and Zarb (1993) said that osseointegration is a process in which rigid asymptomatic fixation is achieved and maintained in between bone and implant. This connection is maintained during the functional loading. Polycrystalline metals and ceramics (Byrne 2014), as materials for implant production, have their advantages and disadvantages. For example, ceramics have high biocompatibility, but are difficult to machine, being brittle. Metals are easier to machine, and they are ductile, elastic and chemically reactive. Metals are usually covered with reactive surface oxide, usually a ceramic layer that interfaces with tissue (Byrne 2014).

If the implants are made of metals whose surfaces are made of very stable oxides, Ti (TiO_2), Al (Al_2O_3), and Ta (Ta_2O_5), they have high biocompatible potential and are suitable for implantation (Byrne 2014). Osseous healing around implants is of great importance for osseointegration, as well as the attachment of a blood clot (Spiekermann 1995). If the gap between implant and bone wall is smaller than 0.2 mm, it can be closed with concentric bony apposition. In another case, the gap will be closed with woven bone, later transformed into a lamellar bone (Spiekermann 1995).

The term ‘primary stability’ is of great importance for every implantologist; it represents the biomechanical interlocking of the implant and the surrounding bone and is in relation to bone density (Gotllow 2008). Stability is better if the bone contains more dense cortical tissue. The term ‘secondary stability’ represents the stability of the implant placed in the bone before the conventional healing period of 15 to 30 weeks. With time, the stability of the implants does not depend on whether they are placed in dense or soft bone, because the stability of the implants placed in a dense bone decreases (Friberg et al. 1991). Davies (2003) found that primitive cells from a blood clot, forced out by firm contact with surface irregularities, migrate so as to interface and transform into the osteoblasts that produce bone on the implant’s surface. This process is called contact osteogenesis. In cases when the surface is smooth, this blood clot between the implant and the bone transforms into bone, a process that is called distant osteogenesis. When the implant’s surface is

rougher, the implant integrates more rapidly, with a greater surface of bone-to-implant contact (Gotllow 2008).

Over time, materials for the production of implants have changed. The beginning of the implant era started with CrCoMo alloys, (Spiekermann 1995), but today, all implant materials can be grouped into metals, ceramics and compound materials. The most widely used material today for implant production is titanium. Coated with titanium dioxide, it displays excellent incorporation into living bone. Besides titanium, tantalum and ceramic implants are also used.

An implant's surface can be different according to the level of roughness. Coating implants with hydroxyapatite has delivered disputable results in the long run (Spiekermann 1995). The roughness of the implant's surface can vary. Low roughness is less than 1μm, moderate is between 1 and 2 μm, and high roughness is over 2 μm. Many investigations today are directed towards modification of the surface of the implant at the nanometer level. Microtopography, nanotopography, and changed surface chemistry are the parameters that cannot be analyzed separately. It is very difficult to analyze in vivo the influence of nanotopograpy of an implant's surface on the implant-bone relation. When analyzed tridimensionally, some implants have this implant-bone connection based on osseointegration. In the case of osseointegration, the combination of bone-to-implant contact is present in terms of bone on-growth and bone ingrowth into a highly porous implant surface (de Arriba et al. 2013; Rosenberg et al. 2010). Typical presenters are implants with trabecular parts.

Trabecular metal material is an 80% porous, tantalum-based biomaterial with a trabecular structure designed for bone on-growth and bone ingrowth (osseoincorporation). This material, as well as this system, has been used in other medical specialties, like orthopedics (Suheil and Boutros 2013) and dental implantology, introduced by the Zimmer Co. in the form of trabecular metal dental implants. Compared to other implant systems, this system has the advantage of ingrowth of osseous tissue into the implant body, which results in greater surface area, better implant-to-bone contact, and better stability. Prosthetic devices have stronger stability and anchoring, which influences patients' quality of life. In the case we presented, a classical titanium implant failed and was discarded. In the same place, a new trabecular metal dental implant was placed to be loaded immediately.

2 Case Reports

2.1 Comparison of Different Methods of Alveolar Bone Regeneration

Periodontal diseases represent a family of heterogenous chronic inflammatory lesions that involve the periodontium, gingiva, and alveolar bone. Periodontal diseases are caused by peridontopathogens, almost Gram-negative bacteria, and the host's immune response to the chronic infection. Infection results in tissue and bone

destruction. To overcome the problem of reduced amount of bone, several procedures and materials have been developed (Burg et al. 2000; Ramseier et al. 2012). The second most popular form of bone grafting material in dentistry is alloplastic graft material. The materials commonly used in all approaches are ceramics, polymers, and composites (Kobayashy et al. 2011).

The main purpose of these case reports was the characterization of a variety of biomaterials and methods that are both commercially available and frequently used for dental application as bone substitutes.

The purpose of this study is to compare a new biomaterial (Bio-Oss) with an already existing treatment principle with regard to their respective abilities to preserve dimensions of the alveolar bone and to promote bone regeneration.

2.1.1 Case Report 1

A 53-year-old male patient came to the Department of Periodontology, Clinic of Dentistry, and Faculty of Medicine in Nis, for the periodontal treatment recommended by his dentist because of the presence of constant discomfort and pain in the upper left lateral incisor (Fig. 1).

He had no relevant medical history and denied engaging in either smoking or the use of alcohol.

Initially, a periodontal examination was performed, including the assessment of plaque index, bleeding on probing, periodontal pocket depth, and clinical attachment loss. The presence of periodontal disease (periodontitis) was established. A detailed examination revealed the presence of periodontal pockets between the upper left lateral incisors. To evaluate the qualitative changes in the gingival soft tissue, the gingival index was then accessed and scored as 2 (moderate inflammation and spontaneous bleeding), as described previously (Löe 1967).

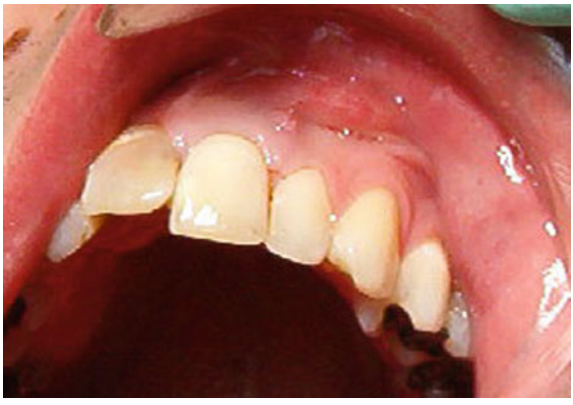

Fig. 1 Redness and swelling in the upper left lateral incisor

The patient had never been treated for periodontitis, and the diagnosis was severe localized chronic periodontitis. The initial treatment plan was nonsurgical basic periodontal therapy to control the disease and reduce chronic periodontitis.

The treatment involved giving oral hygiene instructions, and both supragingival and subgingival scaling, followed by root planning with mini Gracey curettes (Mini Five Gracey Curette, Hu-Friedy, Chicago, IL, USA) and rinsing of the mouth with 0.12% chlorhexidine.

When the basic therapy was done, surgical therapy was indicated. The surgical site was anesthetized by a local administration of 2% lidocaine hydrochloride with 1:200,000 adrenalines. When the mucoperiosteal flap was reflected (Fig. 2), there was a large bone defect in the apical third of the root in the form of fenestration. In consultation with the patient, after complete treatment, removal of the granulation tissue (Fig. 3) and disinfection of the surgical field, a bone substitute was applied (Bio-Oss®—Geistlich Pharma AG, Wolhusen, Switzerland) (Fig. 4). A Bio-Oss xenograft was utilized as the principal grafting material. At the end of the surgery, the flap was repositioned and sutured (Fig. 5). The stitches were removed after 10 days.

The observation period was 18 months and included the estimation of the oral biofilm, gingivitis, probing depth, and clinical attachment loss and bone level, as assessed from standardized radiographs. Both the periodontal probing depth and the clinical attachment loss were reduced.

Tests have shown a highly significant, increasing trend in bone formation associated with Bio-Oss® resorption. Bio-Oss® used alone appears to be a suitable material for periodontal pockets.

These findings indicate that angular bone defects can be successfully treated with biomaterials (Bio-Oss®) in combination with basic therapy. Degradation of the filler material seems to occur particularly during the first six months, but without affecting the clinical parameters, which improved consistently.

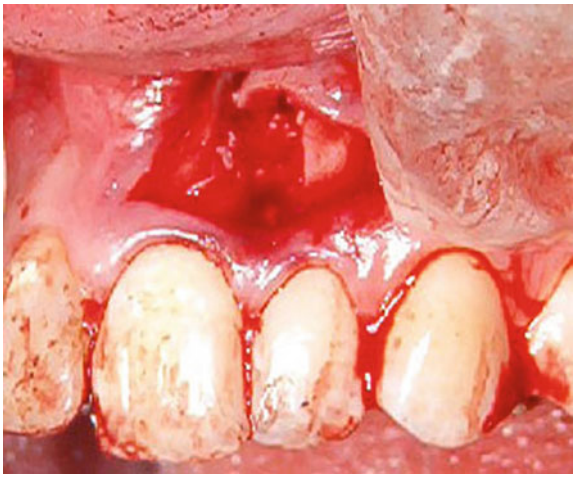

Fig. 2 Fenestration of the alveolar bone

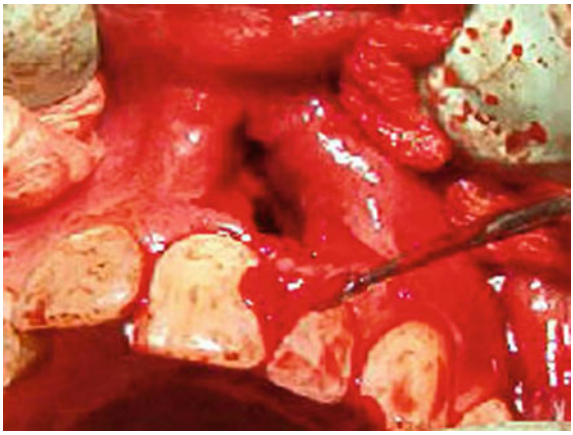

Fig. 3 Granulation tissue

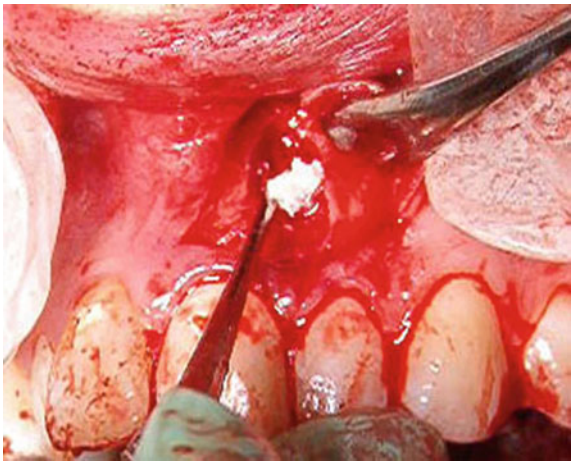

Fig. 4 The application of biomaterials

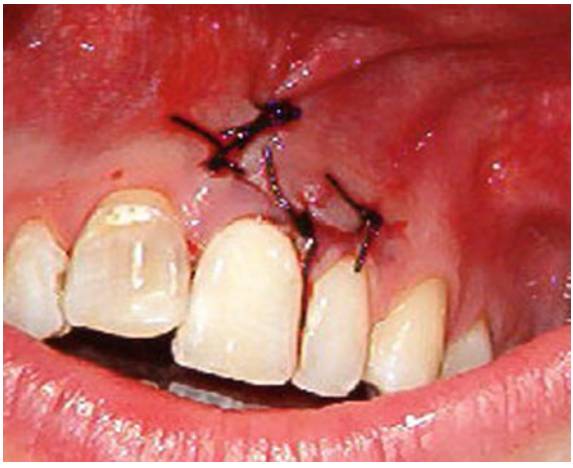

Fig. 5 Sutures of the operative field

2.1.2 Case Report 2

A 25-year-old female patient reported to the Department of Periodontology, Clinic of Dentistry, and Faculty of Medicine in Nis, with a chief complaint of mild pain localized in the upper right first molar for the preceding week, with a recent episode of swelling and pus formation (Fig. 6). The patient also gave a history of similar episodes (3–4 times in the preceding year). She did not give any relevant medical history and reported being in a condition of good general health. There was no history of dental trauma or injurious habits reported by the patient.

On intraoral examination, an interradicular aspect of the upper right first molar revealed a probing pocket depth (PPD) of 10 mm, with a clinical attachment level (CAL) of 11 mm. No mobility was detected in relation to the upper right first molar. Although bleeding on probing and pus exudation was present, there were no signs of swelling. A digital periapical radiograph taken using a long cone technique revealed the presence of an interradicular periodontal pocket on tooth 16 (Fig. 7).

After the initial patient care, oral prophylaxis was performed, and the patient was evaluated for acceptable oral hygiene maintenance. Reevaluation after 4 weeks following the nonsurgical periodontal therapy revealed PPD and CAL as still being 9 and 10 mm, respectively. Flap surgery was indicated.

The area subjected to surgery was anaesthetized by nerve block or infiltration anesthesia, depending upon the surgical site, using a local anesthetic solution of 2% lidocaine hydrochloride with adrenalines. The conventional approach consisting of periodontal access flap surgery was initiated by intracrevicular (sulcular) incisions using number 12 surgical blades on the buccal aspects. The full-thickness (mucoperiosteal) flap was reflected using a periosteal elevator to expose the alveolar bone in the area of the osseous defect (Fig. 8). The osseous defect was debrided off the granulation tissue using hand instruments and ultrasonic instruments, thus exposing the root surface, alveolar bone, and periodontal ligament. After disinfection of the surgical field, the bone defect was filled with a bone substitute

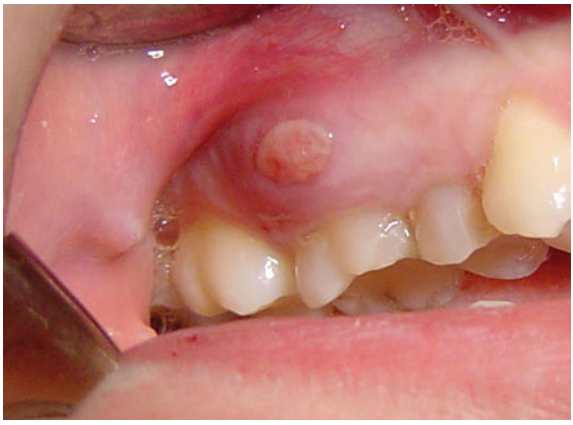

Fig. 6 Periodontal abscesses

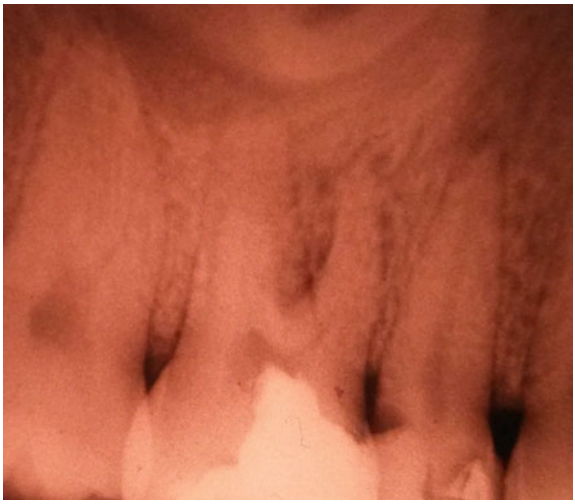

Fig. 7 Interradicular periodontal pocket

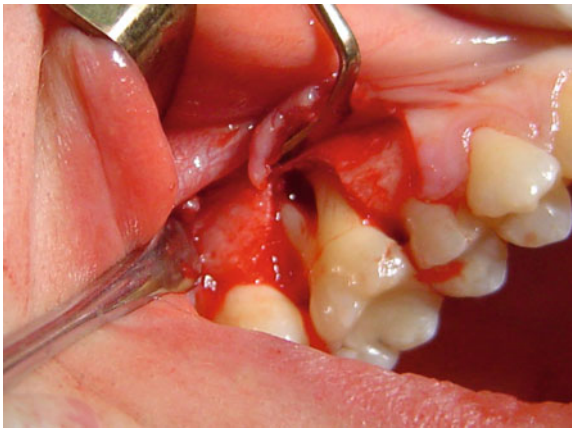

Fig. 8 A large alveolar bone defect on the vestibular site

(Bio-Oss®—Geistlich Pharma AG, Wolhusen, Switzerland) (Fig. 9). The flap was then repaired in its original position and fixed with stitches (Fig. 10). The stitches were removed after 10 days.

Two months after the periodontal therapy, the patient exhibited good plaque control and healthy gingival tissues. On control X-rays, a newly formed interradicular bone could be seen (Fig. 11).

The purpose of this case was to investigate the effect of a porous xenographic bone graft (Bio-Oss®) on the formation of new cementum and new bone in intrabony defects. After 8 weeks, new cementum with inserted collagen fibers was observed on the exposed surfaces. The amount of new bone was significantly greater using the bone graft. The use of Bio-Oss® in combination with the basic therapy may enhance new bone and cementum formation.

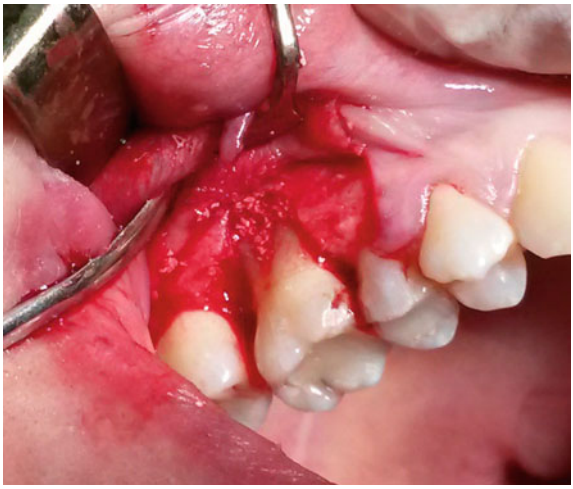

Fig. 9 The defect filled with biomaterial

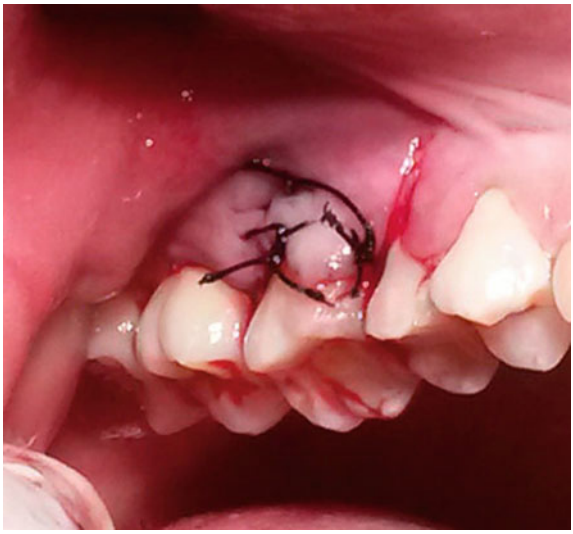

Fig. 10 A flap fixed with stitches

2.1.3 Case Report 3

A 53-year-old male patient, a healthy, never-smoker, came to the Department of Periodontology, Clinic of Dentistry, Faculty of Medicine in Nis, due to the presence of pressure and swelling in the area of the upper right lateral incisor (Fig. 12). The patient reported no use of antibiotics or other medicines in the previous 6-month period.

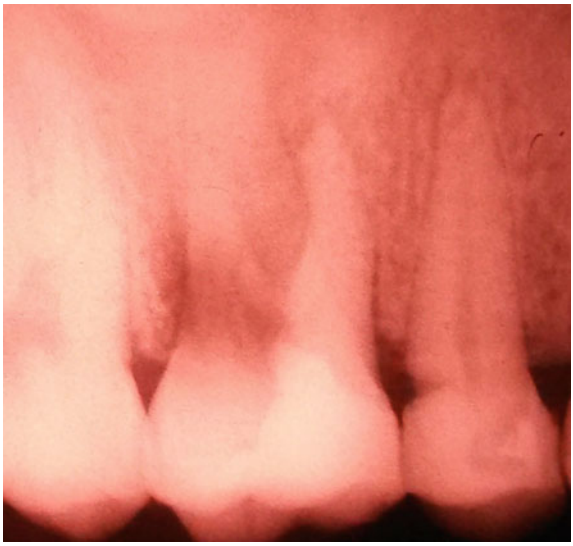

Fig. 11 Newly formed interradicular bone

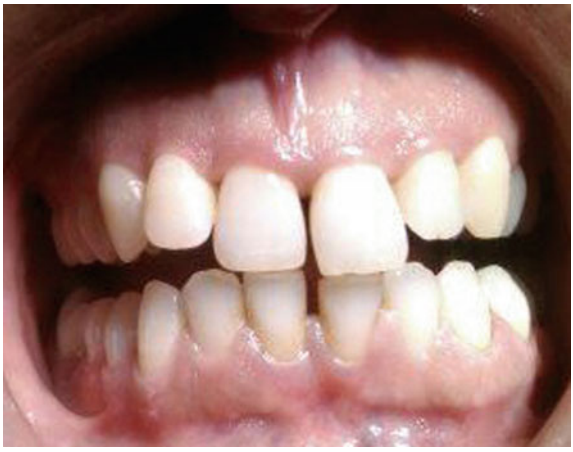

Fig. 12 Swelling in the area of the upper right lateral incisor

After diagnosis of the presence of a periodontal abscess, he had radiography performed on the same region. An X-ray image clearly showed the expansion of the periodontal space and dilution of the bone septum (Fig. 13).

The patient underwent a conservative therapy, which included giving oral hygiene instructions, scaling and root planning aimed at plaque control.

Surgical treatment was performed after the active treatment, when resolution of the inflammation was achieved, which was confirmed by the absence of bleeding on probing and clinical signs of gingival health (color, shape, size, consistency and surface structure). A week after the conservative therapy, surgical therapy was

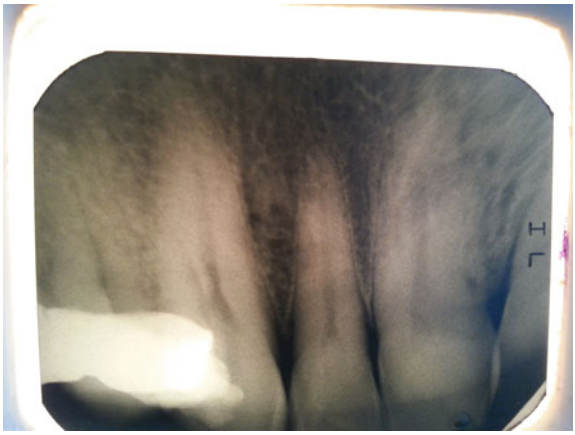

Fig. 13 Expansion of the periodontal space

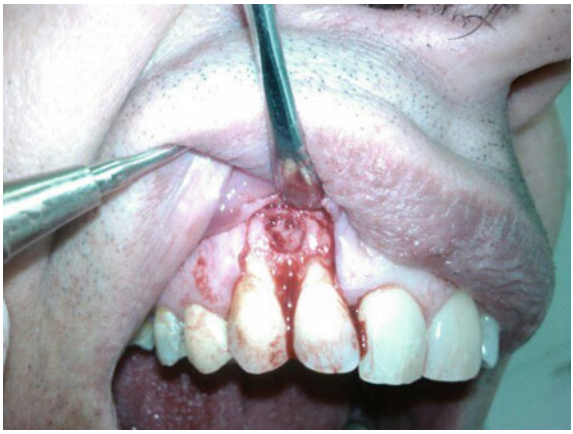

Fig. 14 Fenestration of the alveolar bone

performed. After reflecting the flap in the area of the upper right lateral incisor and canines, a large bone defect, the size of a pea, was observed (Fig. 14). Previously, the patient had agreed that, if there was any indication, the defect could be filled with the bone substitute. After cleaning the bone defect (Fig. 15), the bone substitute (Bio-Oss® Bone Substitute (Geistlich Pharma AG, Wolhusen, Switzerland) was used to fill the defects (Fig. 16). After that, the flap was repaired in its pre-operation position and attached with sutures (Fig. 17). The stitches were removed after 10 days.

In this case, we evaluated the clinical and radiographic response to Bio-Oss when used in combination with conservative therapy for the treatment of an intrabony defect (5–7 mm) around a single-root tooth after reflecting a full-thickness flap. Clinical probing depths and attachment levels were measured before treatment and 18 months later as well.

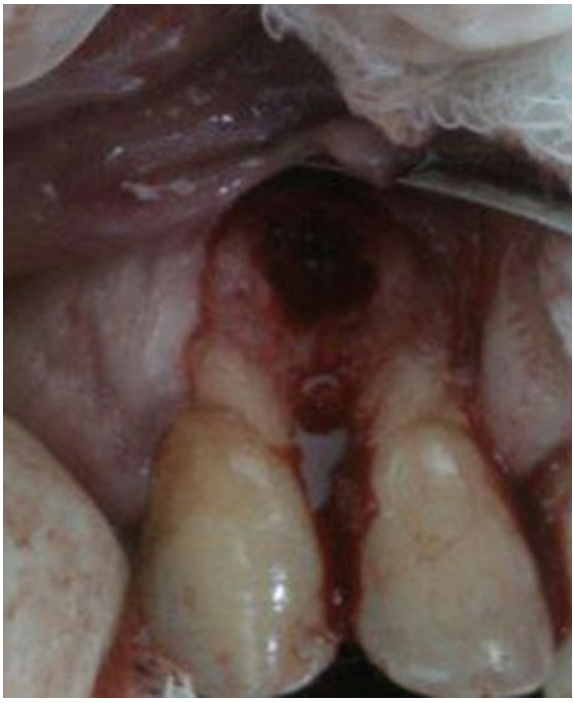

Fig. 15 A cleaned bone defect

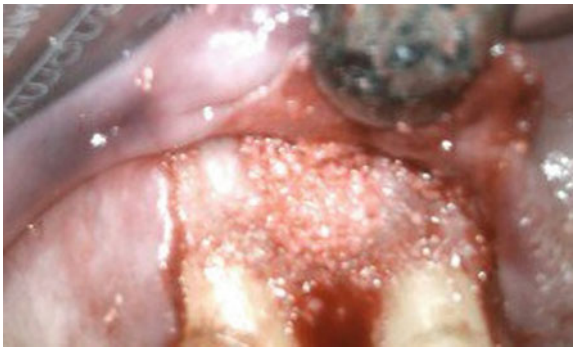

Fig. 16 Bone defect filled with biomaterials

A reduction in pocket depth and a gain in the clinical attachment level were observed (Fig. 18). This case demonstrated that Bio-Oss® has the capacity to induce regeneration of the periodontal attachment apparatus when placed in intra-bony defects (Fig. 19).

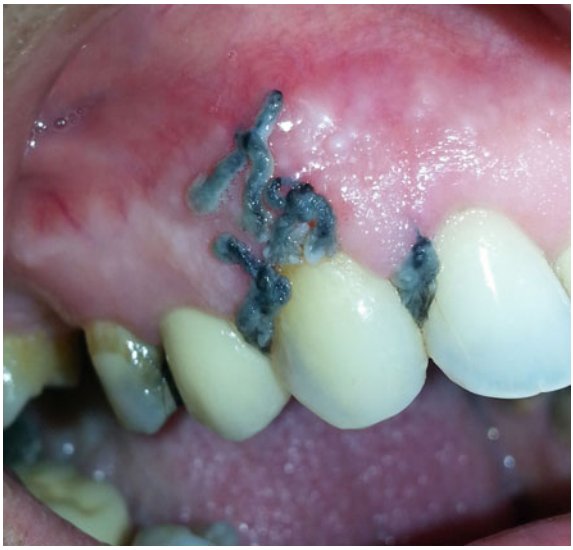

Fig. 17 Stitches on the operative field

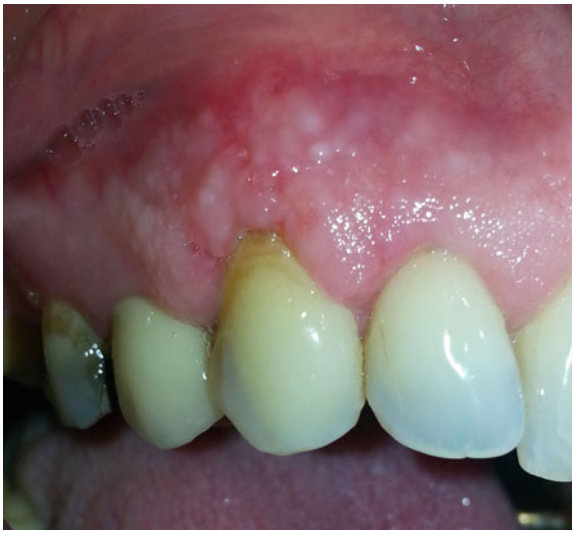

Fig. 18 Clinical condition after 18 months

2.1.4 Case Report 4

A 58-year-old male patient came to the Department of Prosthodontics, Clinic of Dentistry, and Faculty of Medicine in Nis, with a chief complaint of pain and continuous discomfort in the upper left region of the jaw for the previous two months. The patient's medical history was uneventful.

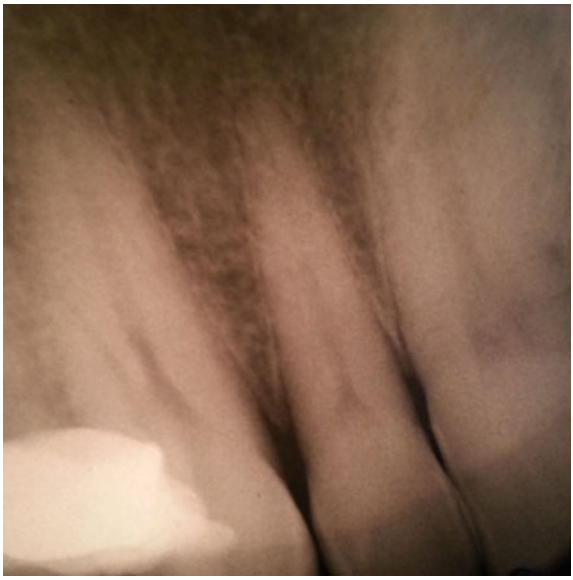

Fig. 19 New formation of the alveolar bone

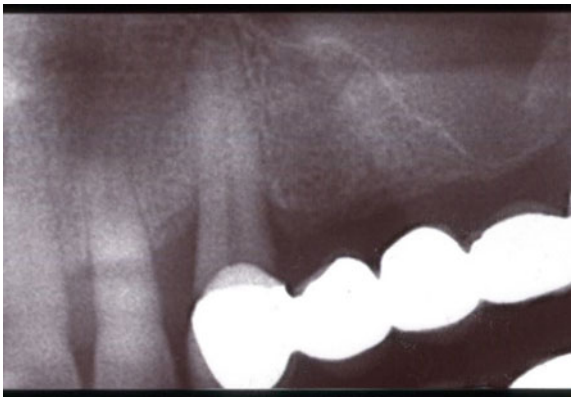

Fig. 20 A deep infrabony bone defect of the upper left canines

At the clinical examination, cracking of the upper left fixed bridge was reported. After removing the bridge, there was a vertical resorption in the upper left canine, otherwise supported to the bridge, which extended to the upper left second molar. The gingiva of the left upper canines showed clear signs of inflammation and an 8 mm probing depth mesially and vestibularly to tooth 23.

The periapical radiograph showed a deep infrabony bone defect of the upper left canine (Fig. 20). Electric pulp testing and thermal pulp testing were carried out to rule out an endo-periodontal lesion. The upper left canine showed a normal response with electric and thermal pulp testing, and hence no endodontic intervention was required. Given the condition of the patient and his desire to have a

fixed bridge re-created, surgical methods of guided bone regeneration were proposed. Therefore, considering the dental history and radiographs, a periodontal surgery was planned.

The initial therapy, consisting in giving oral hygiene instructions, supra- and subgingival scaling, and root planning under local anesthesia, was performed. Two weeks after the initial therapy, surgical therapy was initiated. Prior to surgery at the baseline, clinical measurements, including probing pocket depth (PPD), clinical attachment loss (CAL), and gingival recession (GR), were recorded.

Before the surgical treatment, the patient was advised to rinse his mouth with 0.2% chlorhexidine gluconate solution for 1 min. After administration of local anesthesia, a mucoperiosteal flap was raised. Severe osseous destruction was observed on the mesial surface of 23 (Fig. 21). The tooth had the periodontal attachment remaining on the palatal and distal surfaces. During the surgery, a lack of vestibular alveolar bone was documented, as well as the presence of bareness of the root.

It was explained and proposed to the patient that the proper course was application of a bone substitute and a resorbable membrane, the aim of which was to prevent the formation of new bone. The patient agreed.

After thorough root planning and apical curettage, this large osseous defect on the mesial surface (Fig. 22) was filled with the bone graft (Bio-Oss® Bone Substitute—Geistlich Pharma AG, Wolhusen, Switzerland) and the vestibular defect was covered with a membrane (Bio-Gide® Collagen membrane—Geistlich Pharma AG, Wolhusen, Switzerland (Figs. 23a, b, 24). The lap was repositioned and sutured with 5-0 silk non-resorbable interrupted sutures (Fig. 25).

Antibiotics and analgesics were prescribed for one week. The sutures were removed ten days later. The patient was monitored on a weekly schedule after surgery to ensure good oral hygiene in the surgical area. Supportive periodontal maintenance at 3 months was prescribed to maintain the periodontal health and to

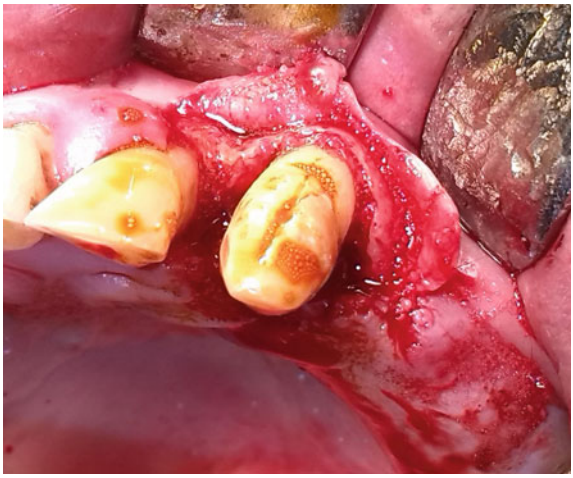

Fig. 21 Severe osseous destruction

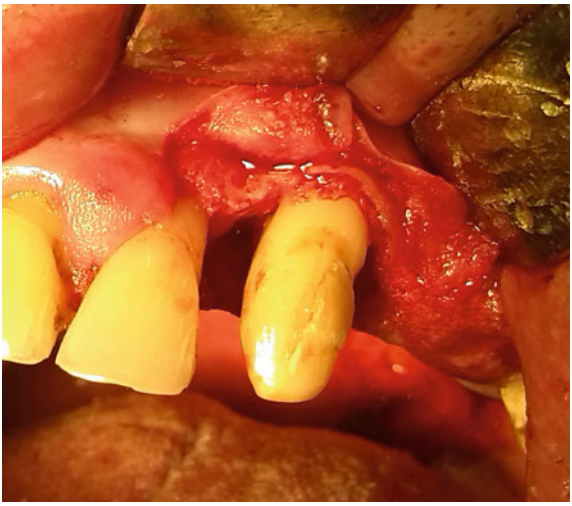

Fig. 22 Mesial and vestibular defect of the bone

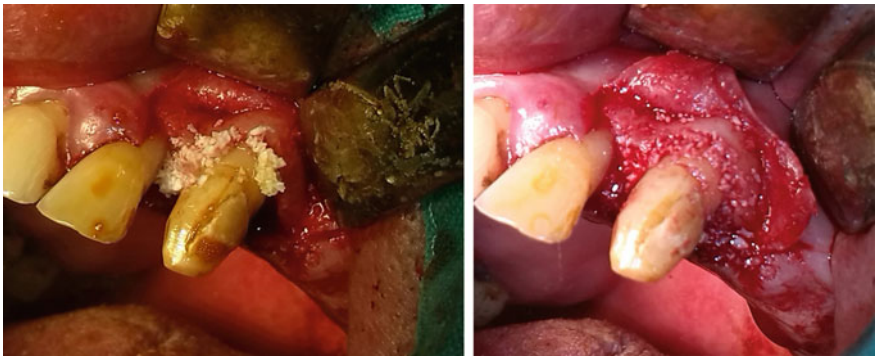

Fig. 23 The application of the biomaterials

re-evaluate this area. At the 18 month follow-up, the tooth was asymptomatic with successful healing, mobility was absent and probing depth was minimal. The radiograph after the 18-month follow-up showed evidence of apparent bone fills with the resolution of the osseous defect (Fig. 26).

This case evaluated the clinical and radiographic response to the composite use of Bio-Oss® porous mineral bone in combination with a Bio-Gide® bilayer collagen membrane to achieve regeneration when treating human periodontal bone defects. Preoperative recordings of the treatment area included radiographs, clinical probing depths, and clinical attachment levels; cementum with inserted collagen fibers and new bone formation on the surface of the graft materials was also observed.

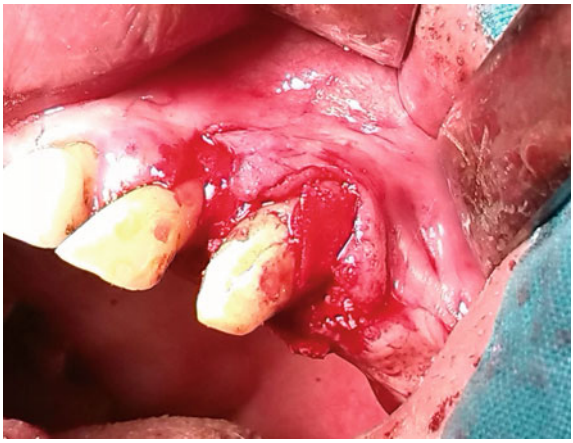

Fig. 24 Vestibular defect covered with a membrane

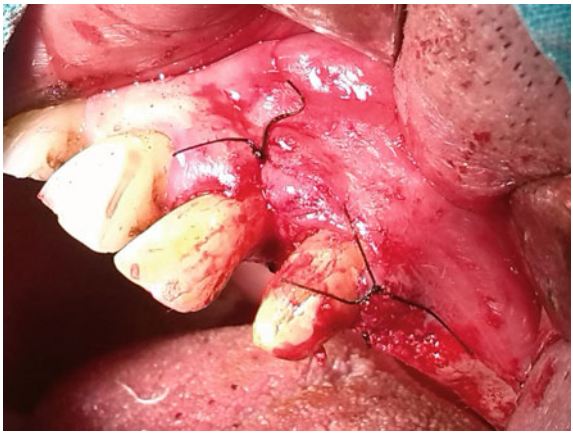

Fig. 25 Interrupted sutures

This case report demonstrated that Bio-Oss® porous bone in combination with the Bio-Gide® collagen membrane has the capacity to stimulate substantial new bone and cementum formation with Sharpey's fiber attachment. The combination of Bio-Oss and guided bone regeneration techniques shows optimal properties for periodontal regeneration.

2.1.5 Case Report 5

A 27-year-old male patient reported to the Department of Periodontology, Clinic of Dentistry, and Faculty of Medicine in Nis, with a chief complaint in the form of occasional edema in the apical region of the upper right incisors for the previous six months. Occasionally, bleeding occurred during brushing of the teeth. The patient

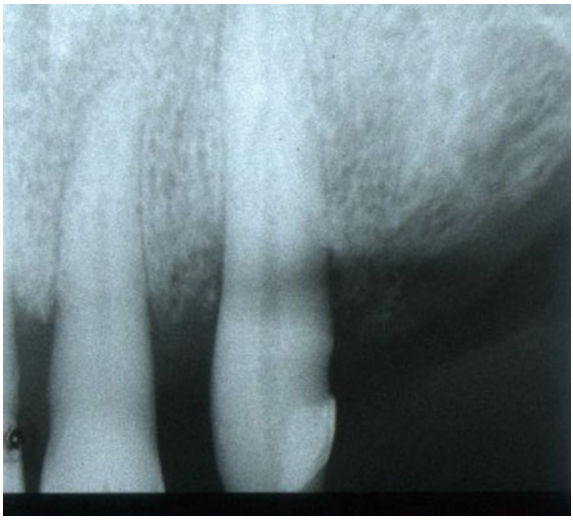

Fig. 26 Resolution of the osseous defect

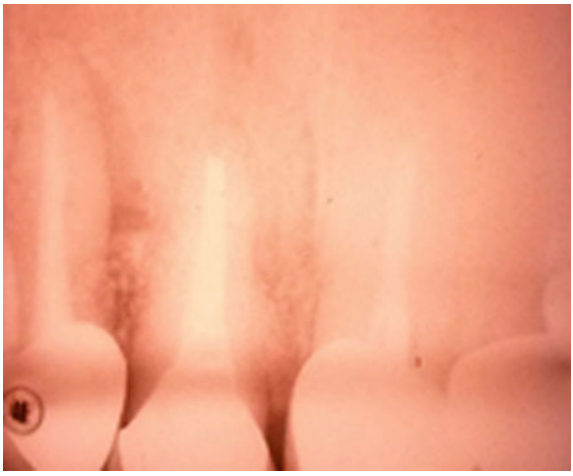

Fig. 27 Thinning of the bone and expansion of the periodontal ligament

also reported that his mother lost all her teeth at an early age due to the mobility of her teeth.

On clinical examination, the oral hygiene status of the patient was found to be moderate gingivitis. The investigations carried out included: (1) routine hematological investigations, which were found to be within the normal ranges; (2) radiography that showed the enlargement of bone beams and a thickening of the periodontal ligament in the apical part of the upper lateral incisor (Fig. 27). The treatment plan consisted of systemic administration of 25 mg of metronidazole three times daily for 7 days. The patient was recalled 1 week after the systemic administration of medication for further therapy. Non-surgical periodontal therapy

was initiated, with a positive response. Even with the maintenance of satisfactory oral hygiene, the inflammation was resolved, but residual edema still existed.

Therefore, surgical intervention was discussed with and recommended to the patient. It was decided that a modified Widman flap would be used with the inclusion of platelet-rich plasma (PRP). The patient agreed to the procedure and signed a written consent form. The region of the upper right lateral incisor was selected for the surgery.

The surgical procedure consisted of:

- Preparation of PRP (Fig. 28): 8 ml of blood were drawn through venipuncture of the antecubital vein. Blood was collected in a sterile tube containing an anticoagulant to avoid platelet activation and degranulation. The first centrifugation used in such situations is called the "hard spin," which allows for blood separation into three layers: the bottom-most RBC layer, the top-most acellular plasma layer, called the PPP, and an intermediate PRP layer called the "buffy coat." A second centrifugation, called the "soft spin", allows the platelets (PRP) to settle at the bottom of the tube with very few RBCs. The acellular plasma, PPP, was found at the top. Most of the PPP was removed with a syringe and discarded, and the remaining PRP was shaken well so as to be ready for use (Fig. 29).
- Open flap debridement: Periodontal flap surgery was done by performing a horizontal incision with the preservation of the interdental papillae, and a full thickness mucoperiosteal flap was reflected on the vestibular side. Thorough debridement and root planning of the exposed root surface were performed with hand instrumentation (Fig. 30).
- Placement of the PRP: The PRP was then carried to the defect and carefully packed into it (Fig. 31). The PRP was properly condensed in the defect to the level of the surrounding bony walls (Fig. 32). The flap was adapted back to its original position and suturing was done using non-resorbable silk thread (Figs. 33 and 34).

Fig. 28 "Soft spin" centrifugation with three layers

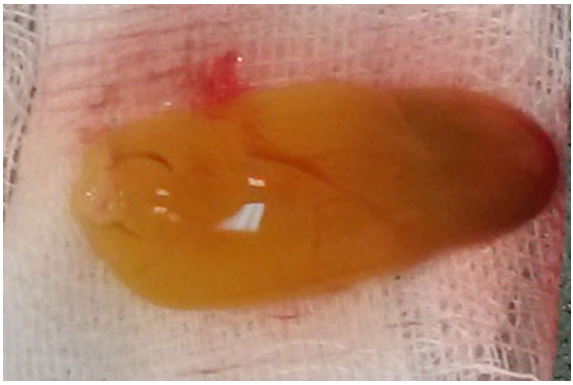

Fig. 29 Prepared platelet-rich plasma

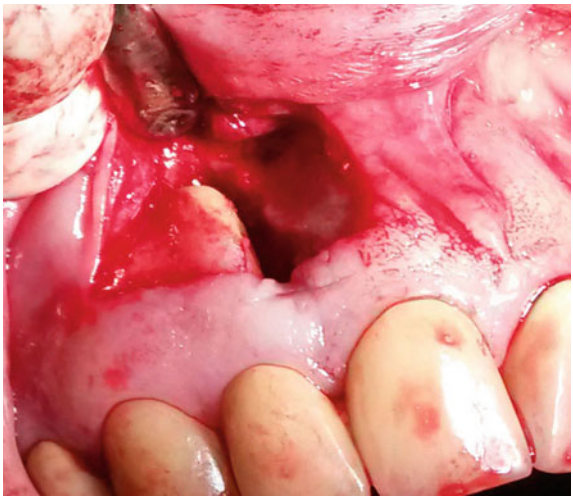

Fig. 30 Bone defect

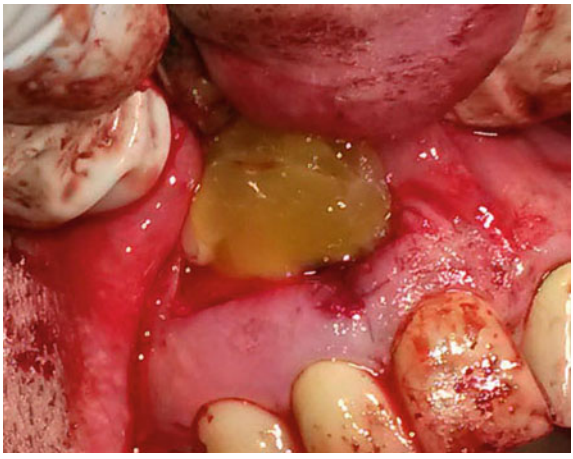

Fig. 31 Placement of the PRP

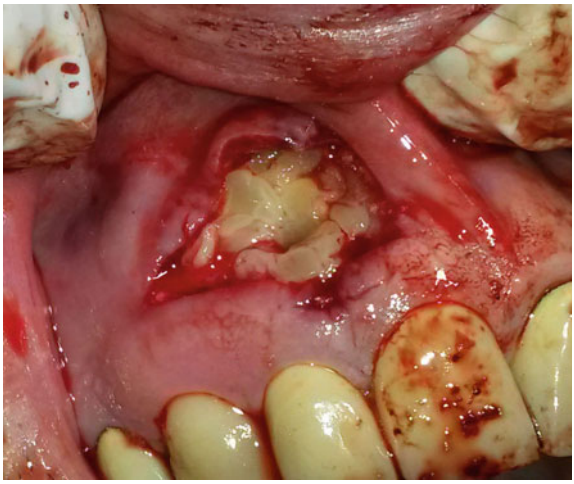

Fig. 32 PRP properly condensed in the defect

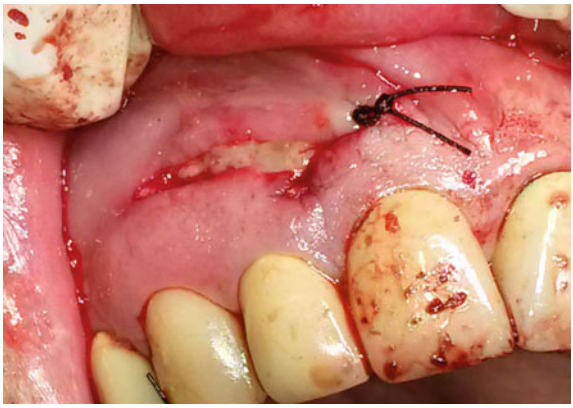

Fig. 33 Readapted flap

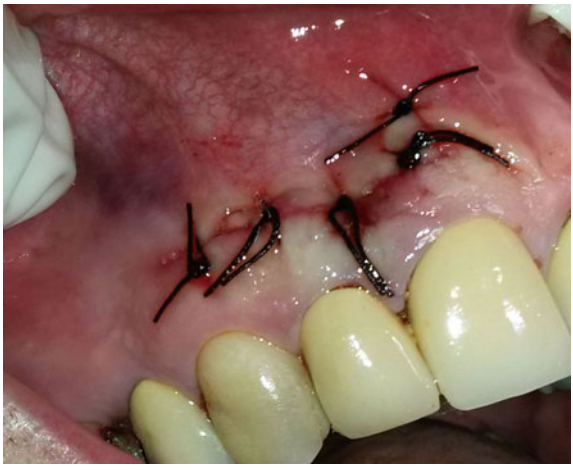

Fig. 34 Sutures on the operating area

The platelet-derived growth factor is the most described growth factor associated with periodontal health. Growth factors are a class of natural biologic mediators that regulate the key cellular events in tissue regeneration, including cell proliferation, chemotaxis, differentiation, and matrix synthesis via binding to specific cell surface receptors. The increase in bone volume was more pronounced after combination with platelet-rich plasma. The use of growth factors to regulate biological events affecting surgical outcomes has recently attracted the attention of researchers, and its use in periodontal regeneration has shown promising results.

2.1.6 Case Report 6: Implantology

As was mentioned before, herein we report a substitution of a failed classical titanium implant in the upper jaw with an implant made of another biomaterial. Today, we realize that titanium is the most popular material for dental implant production, but a new trend has appeared in a tendency to use it only as an alternative or a second chance solution in cases when dental implants made of a biomaterial have failed. There are numerous reasons for the loss of an implant. Two groups of implant failure exist. The first group happens before osseointegration, whereas the second group includes late failures which happen after the osseointegration period, usually arising during and after the prosthetic restorative phase, according to Rosenberg (2010). The rate of implant failure before functional loading is about 2.5% and can result from the influence of several factors. In the early phase, the reason for losing the implant can be infection or tissue trauma. In the later phase, the most common reasons are overloading of the implant and iatrogenic factors. According to Rosenberg, more than one factor is usually responsible for the loss of the implant (2010). The risk of unsuccessful implant therapy is not connected to the type of implant system. In this case study, we describe the failure of an implant placed in the region of tooth 15.

In this patient, progressive periodontal disease was present. As preimplantation preparation, therapy of the present periodontal disease was performed, including application of a bone substitute application and a membrane. After preoperative analysis and measuring, preparation for implant placement was performed in the region of the second premolar on the left side (Fig. 35). The preparation involved drilling, the speed of which was 750 rpm, permanent cooling and rinsing with saline solution. The drill set was new, having been used to place fewer than 5 implants before this one. After drilling, a transcrestal sinus lift procedure was performed. Without damage to the sinus mucosa, the sinus floor was elevated and the space was partially filled with particles of a spongious bone substitute, Bio-Oss. (Bio-Oss—Geistlich Pharma AG). Then, an 11.5, 3.5 mm implant was placed with 25 rpm and a torque of 25 Nm (Fig. 36). The surgical wound was closed in a primary manner (Fig. 37).

The stitches were removed on the seventh day. At the beginning of the third week, after implant placement, pain was present in the operative area. Two days later, the implant was expelled and the site of the expelled implant was simply

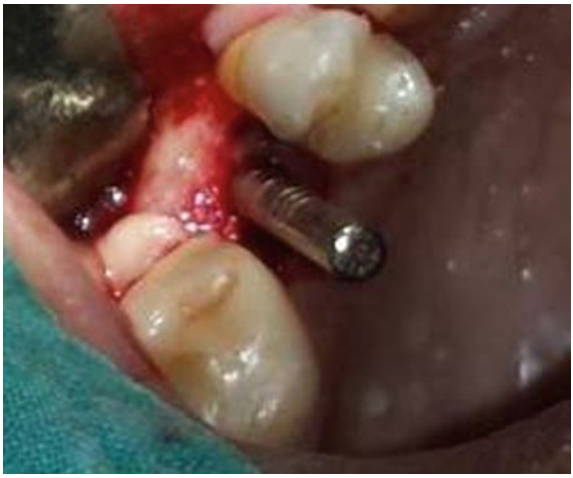

Fig. 35 Preparation for primary implant with parallel indicator

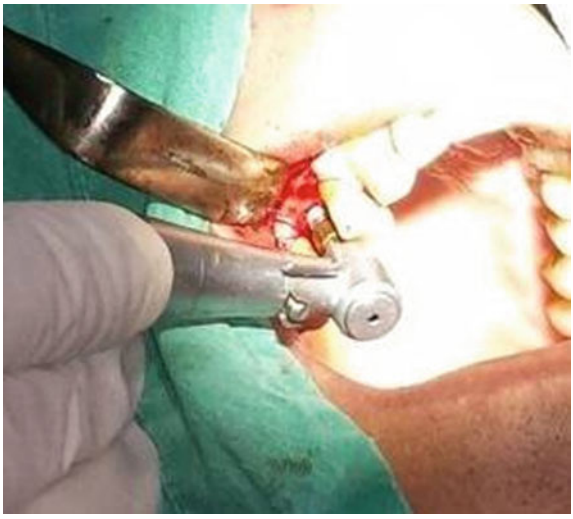

Fig. 36 Insertion of primary implant

curetted, without applying a bone substitute. Six months later, tooth 14 was extracted for endodontic and periodontal reasons. The plan for implant and prosthetic reconstruction included placing a new implant in the region of tooth 15 (Fig. 38). The new implant was placed where the previous one had been expelled (Fig. 39). According to the plan, trabecular metal implant 4.1, 11.5 mm, was to be placed. The same previous sinus lift procedure was performed (Fig. 40). At the same time, another implant, the trabecular metal dental implant (Zimmer) was placed in the region of tooth 17 (Fig. 41). A day later, an immediate, non-occluded crown with an extension was placed on the implant in the region of tooth 17. Later, a provisional prosthetic device was exchanged for a permanent bridge (Fig. 42).

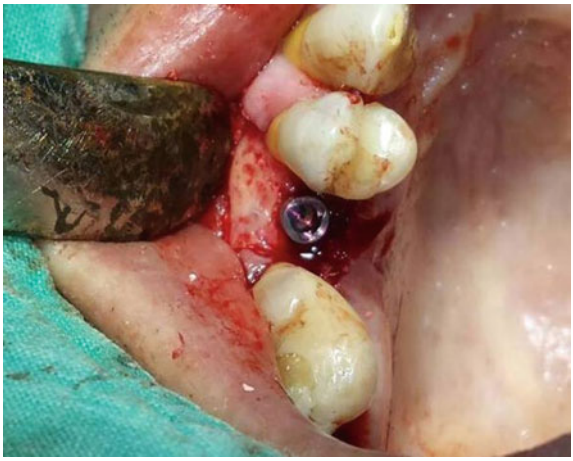

Fig. 37 Primary implant in position

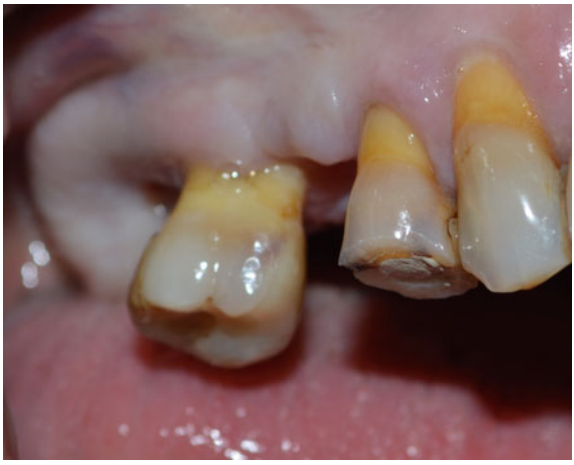

Fig. 38 Six months after implant expulsion

3 Discussion

Many advances have been made over the past few decades in regard to the regeneration of periodontal apparatus. We tested three of the most studied and relevant sources of biomaterial. We showed that all three sources possess an adequate proliferation capacity for potential tissue engineering applications. Tissue repair and regeneration through tissue engineering is dependent on the use of materials that can serve as a carrier matrix for bioactive substances or incorporated cells. The adhesion of cells to bioresorbable materials and the proliferation of cells on these scaffolds are important components for tissue engineering projects and play a fundamental role in regulating cell differentiation, growth, and survival.

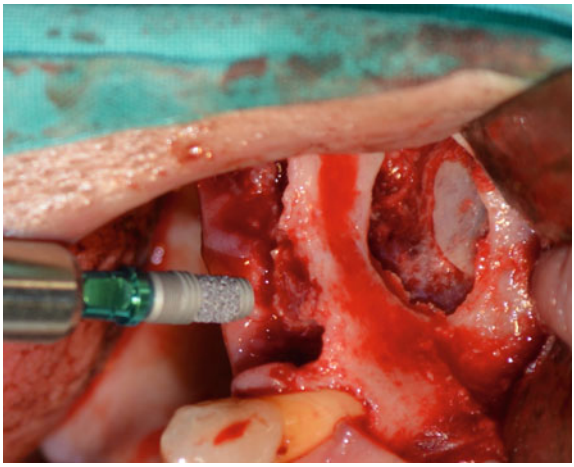

Fig. 39 Placing of a secondary implant

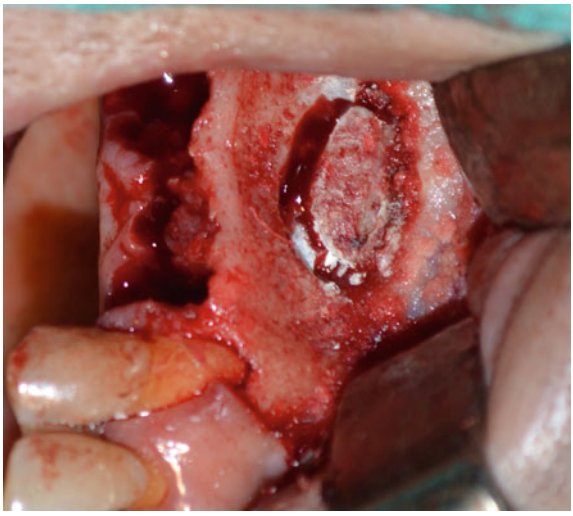

Fig. 40 Sinus lift procedure

More research needs to be focused on in vivo systems to improve the outcome of biomaterial-based delivery systems. Further approaches in this field will rely on a combination of therapies.

The best clinical results were demonstrated by the following materials: bovine bone mineral, fully synthesized homogenous hydroxyapatite and beta tricalcium phosphate, and demineralized and mineralized freeze-dried bone allografts. While this statement is applicable to osteoconductive materials, current research is focused on the application of growth factors—the natural proteins that regulate tissue regeneration.

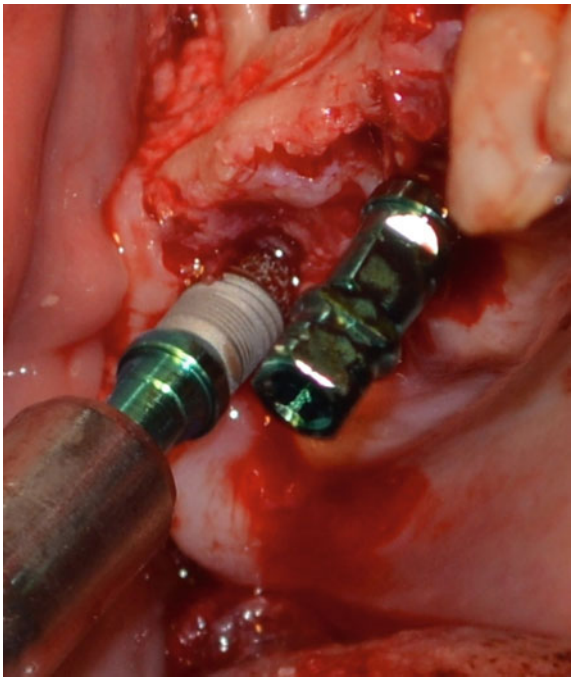

Fig. 41 Placing an implant in the distal position

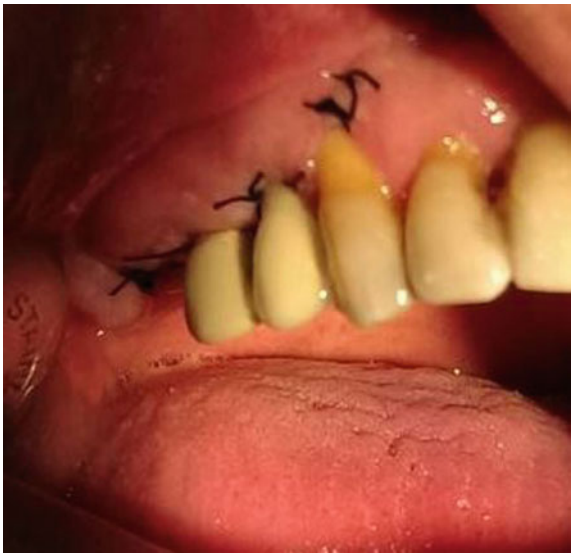

Fig. 42 Temporary crown in place

Several restoring techniques have been developed for regenerating periodontal tissues, including guided tissue regeneration, bone grafting and the use of enamel matrix derivatives. Principles of guided tissue regeneration dictate that one of the

goals of therapy is to modulate the repopulation of the wound with cells derived from the periodontal ligament rather than from the gingival tissues (Lee et al. 2010a, b).

Bioresorbable and non-resorbable membranes can successfully be used for bone regeneration. Bioresorbable membranes generally show better clinical performance compared with non-resorbable membranes and are the barriers of choice wherever possible (Caffesse et al. 1999). Our test results are in agreement with the results of other authors (Lee et al. 2010a, b; Ivic-Kardum 2011; Boerckel et al. 2011; Molina et al. 2013).

The combination of Bio-Oss® and resorbable membranes in the treatment of infrabony defects results in a decreased probing depth and an increased level of attachment with histologically proven periodontal regeneration.

In the first observation period, there was a significantly higher gain of clinical attachment in sites at which material was added compared to the second period. In cases in which biomaterial was implanted, the bone regeneration process was faster and more efficient (Jégoux et al. 2010).

In recent decades, significant progress has been made in periodontal therapy regarding its various aspects. A number of bone grafts have been used in different clinical trials with different degrees of success. Upon analysis of the various clinical reports, it has been seen that the use of many bone graft materials (DFDBA, FDBA, Hydroxyapatite, and Ceramics, etc.) have resulted in significant improvement of clinical parameters. In our study as well, Bio-Oss®, the natural porous mineral bone, resulted in significant improvement of all clinical parameters, with a mean bone fill of 51.01%. Our results are in accordance with other similar studies using Bio-Oss® or other types of bone graft (Mora and Quhayoun 1995; Camelo et al. 1998; Richardson et al. 1999; Bernabé et al. 2012; Baltran et al. 2014).

The results of these studies suggest that Bio-Oss®, alone or with a membrane as a bone graft material, is quite predictable when used as bone fill in infrabony defects.

Since the introduction of dental implants, bone grafting has become an important procedure required for the treatment of patients with limited bone availability. Bone auto graft, alone or together with other bone substitutes, has been the biomaterial of choice for clinicians worldwide. However, different xenogenic, allogenic and synthetic biomaterials have shown promising results in many bone augmentation procedures.

The literature has shown that early bone loss can be significantly reduced through socket grafting (Abshagen et al. 2009; Ahn et al. 2011). The process of socket grafting requires an understanding of wound healing and an appreciation of the biological properties of the products available for the procedure. Various types of bone substitution material have been created that show ossification and new bone formation (Kim et al. 2013a, b).

In the last two decades, implantology has become one of the most well-established and independent disciplines in dentistry. Its sudden elevation was based on the development of materials, implant design and understanding of bone and implant interaction. The goals of implantology are shortening surgical

interventions and decreasing the cost of treatment with satisfying esthetic and functional demands, which should result in better quality of life for patients. The chief material used from the beginning of implantology up until today has been titanium (Spiekermann 1995). However, there are new concepts, such as porous surfaces of implants and trabecular metal. One of the reasons for the wide use of titanium and its high success rate (Ballo 2011) is its bio inert behavior (Ramazanoglu and Oshida 2011).

The characteristics of the implant's surface play a central role in the process of osseointegration (Ramazanoglu and Oshida 2011), because of its ultimate contact with a bone. A greater surface area provides better and stronger anchoring of the implant in the bone. Nowadays, for this reason, implants have surfaces treated on the nanoscale level. There are different technologies for achieving this goal, such as anodic oxidation, acid treatment, alkali treatment, a combination of anodization and chemical etching, hydrogen peroxide treatment, sol-gel treatment, chemical vapor deposition, and a combination of chemical vapor deposition and the sol gel method (Pachauri et al. 2014). The main reason for this treatment is that nanobiomaterials have an increased percentage of atoms and crystal structures, and provide a higher surface area than conventional ones (Ramazanoglu and Oshida 2011).

There are different ways of manipulating an implant's surface on the nano level. The first method is compaction of nanoparticles of titanium dioxide to yield better surfaces of dental implants, whereas the second method is on the molecular level and involves implicit molecular self-assembly. This molecular disposal positions molecules with exposed chain groups, which provides a possibility for cells to adhere and can have osteoinductive potential. The third method is chemical treating, in which, by applying different chemical agents, reactive groups on the metal's surface are exposed. An optical method with the deposition of nanoparticles on the metal's surface is also described. The reason for these treatment procedures is stimulating cell adhesion, cell differentiation, and cell proliferation on implant-bone contact surfaces as well (Mendonça et al. 2008). This reaction occurs on the nanoscale level, but this is not sufficient for achieving robust osseointegration and implant stability (Mendonça et al. 2008). It can be said that nanoscale modifications of the surfaces of titanium dental implants enhance interfacial bone formation measured by bone-to-implant contact (Mendonça et al. 2008), but it cannot be said that these modifications are sufficient for the stable anchoring of implants.

For decades, it has been well known that the greater the implant-bone contact, the better the stability of the implant (Spiekermann 1995). When this opinion was applied in practice, the greatest changes and innovations were in implant design. This characteristic gives the possibility for trabecular implants to have new bone formation in pores early on (two weeks). At the same time, there has been no statistical difference in stability when testing in canine mode compared to test implants (Kim et al. 2013a, b). This characteristic provides the possibility for trabecular implants to be used in immediate restoration.

Today, implant placement in a tooth socket immediately after extraction with the application of non-occluding dental prosthetic devices is a well-known and widely used practice. However, using an implant in the same place where another implant

system was used and lost is challenging, especially in the case of immediate loading with a non-occluding crown. Numerous implant systems with different implant designs and surface types give the possibility today of changing access if any of them fail. In the case of a failed implant that was lost in the most critical period between the second and fourth weeks after placement, the implant was replaced with an implant of different system, design and surface. Basically, the trabecular metal dental implant is a modification of the Tapered Screw-Vent Implant (Zimmer Dental Inc.). The middle part of the implant is made of trabecular metal (Zimmer Dental inc.). Trabecular metal is composed of tantalum over a vitreous carbon substrat. The idea came from other medical specialties, like orthopedics and neurosurgery, in which tantalum has been in use for a long time.

However, tantal has a much higher price compared to titanium, and that is the reason why tantalum and its alloys do not have wider use in dental implant production. A trabecular Metal Implant (Zimmer Dental inc.) has an internal vitreous carbon core (Collins et al. 2014). Because of its higher price, the trabecular metal implant can be perceived as an alternative or secondary solution for positions and cases in which classical implants have failed. Besides a high rate of success in implantology today, there are still situations when, by the action of numerous different factors, implants can be lost. Lack of osseointegration of an implant is a typical cause, as described in this case, but here, the role of an untreated periodontal infection must be kept in mind. The role of periodontal disease in implantology was described in 2010 by Rosenberg, who found much higher rates of implant loss in patients who had periodontitis than in those who did not. This influence on implant success, as well as the influence on other diseases, sheds new light on the influence of periodontitis on general conditions of health (Pejcic et al. 2011a, b, c, d; Pejcic et al. 2012; Pejcic et al. 2014). In the case described, the patient was a heavy smoker, which could influence the success of implantological and periodontal treatment (Pejcic et al. 2012). Different biomaterials provide the possibility of looking for different solutions. In this case, the failed osseointegration of a titanium implant indicates the placing of a tantalum-based implant as an alternative and successful solution. Because of their characteristics which allow for osseoincorporation with wide contact surfaces and good stability, trabecular metal implants (Zimmer Dental inc.) can be immediately loaded, providing opportunities to satisfy esthetic demands.

4 Conclusion

One of the most common problems in dentistry is the regeneration of damaged bone with the aim of repairing or replacing lost or damaged bone tissue by stimulating the natural regenerative process. Various materials and techniques have been used for this purpose. Bone regeneration involves the use of surgical procedures which, by utilizing a mechanical barrier, create a secluded space around the defect to permit bone regeneration without the competition of other tissues.

Periodontal disease, tooth extraction, a long-term use of removable appliances and traumatic injuries typically result in advanced alveolar bone loss that prevents guided bone regeneration and the placement of implants in an optimal prosthetic position. The stability of dental implants is associated with successful osseointegration into the thick jawbone. Due to bone defects, bone regeneration is often needed before an implant can be inserted. Guided bone regeneration is developing very dynamically in dental surgery and implantology. It relies on building up bone in places where it is lacking, utilizing a variety of grafting materials. The use of autogenous platelet-rich plasma allows for the employment of growth factors that blood platelets contain in the formation of new bone tissues. The usage of biomaterials together with platelet-rich plasma allows for the creation of a resorbable carrier for the growth factor (auto-xenogenic graft).

Particularly in the fields of periodontal, reconstructive, and maxillofacial surgery, there is a need for successful methods to restore bone. Fortunately, innovations in surgical techniques, together with advances in the biologic understanding of bone and soft tissue regeneration, have increased the predictability of reconstructing alveolar ridge deformities.

Our clinical projects indicate positive effect therapies for the treatment of bone defects in the case of alveolar bone tissue. The results of our cases overlap with the data reported by other authors who have demonstrated similar improvement in radiographic and clinical parameters. This clinical project confirmed the positive effect therapy of biomaterials for bone regeneration and implantology.

At its foundation, a successful implant restoration case involves a team approach, with detailed communication between the various clinicians, technicians, and the patient. Thanks to the team concept the dental profession has embraced, complications have been minimized and therapeutic horizons have been expanded. Although further research is still needed to make successful implant dentistry and guided bone regeneration a predictable procedure, the environment for success is better than ever.

References

Abshagen K, Schordi I, Gerber T et al (2009) In vivo analysis of biocompatibility and vascularization of the synthetic bone grafting substitute Noo Bone. J Biomed Mater Res A 91 (2):557–566

Ahn JJ, Cho SA, Byrne G et al (2011) New bone formation following sinus membrane elevation without bone grafting: histologic findings in humans. Int J Oral Maxillofac Implants 26(1): 83–90

Albrektsson T, Zarb GA (1993) Current interpretations of the osseointegrated response: clinical significance. Int J Prosthodont 6(2):95–105

Al-Hamdan K, Eber R, Sarment D et al (2003) Guided tissue regeneration-based root coverage: metaanalisis. J Periodontol 74:1529–1533

Anitua E (1999) Plasma rich in growth factors: preliminary results of use in the preparation of future sites for implants. Inter J Oral and Maxillofacial Impl 14(4):529–535

Ballo A (2011) Dental implant surfaces—physicochemical properties, biological performance, and Trends. In: Turkyilmaz I (ed) Implant dentistry—a rapidly evolving practice. In Tech, Rijeka, pp 19–35

Baltran V, Engelke W, Jose Dias F (2014) Oclusive barriers in combination with particulate Bio-Oss graft: a pilot study on rabbit calvaria. Int. J Clin Exp Med 7(7):1714–1720

Bernabé PF, Melo LG, Cintra LT et al (2012) Bone healing in critical-size defects treated with either bone graft, membrane, or a combination of both materials: a histological and histometric study in rat tibiae. Clin Oral Implants Res 23:384–388

Berner A, Boerckel JD, Saifzadeh S et al (2012) Biomimetic tubular nanofiber mesh and platelet rich plasma-mediated delivery of BMP-7 for large bone defect regeneration. Cell Tissue Res 347:603–612

Boerckel JD, Kolambkar YM, Dupont KM et al (2011) Effects of protein dose and delivery system on BMP-mediated bone regeneration. Biomaterials 32:5241–5251

Branemark PI, Hansson B, Adell R et al (1997) Ossteointegrated implants in in the treatment of the edentulous jaw: experience from 10 year period. Almqist–Wiksell, Stockholm

Buduneli N (ed) (2012) Pathogenesis and treatment of periodontitis. InTech, Rijeka

Burg KJ, Porter S, Kellam JF (2000) Biomaterial developments for bone tissue engineering. Biomaterials 21(23):2347–2359

Byrne G (ed) (2014) Fundamentals of implant dentistry. Wiley Blackwell, Hoboken

Caffesse RG, Mota LF, Quinones CR et al (1999) Clinical comparison of resoebable and non-resorbable barriers for guided periodontal tissue regeneration. J Clin Periodontol 24: 747–752

Camelo M, Schenk RK, Rasperini G et al (1998) Clinical, Radiographic and Histologic evaluation of human periodontal defects treated with Bio-Oss and Bio-Guide. Int J Periodont Rest Dent 18:321–331

Caneva M, Botticelli D, Pantani F et al (2012) Deproteinized bovine bone mineral in marginal defects at implants installed immediately into extraction sockets: an experimental study in dogs. Clin Oral Impl Res 23(1):106–112

Chawla K, Lamba AK, Faraz F et al (2011) Evaluation of β-tricalcium phosphate in human infrabony periodontal osseous defects: a clinical study. Quintessence Int 42:291–300

Chen TH, Tu YK, Yen CC et al (2013) A systematic review and meta-analysis of guided tissue regeneration/osseous grafting for the treatment of Class II furcation defects. J Dent Sci 8: 209–224

Coïc M, Placet V, Jacquet E et al (2010) Mechanical properties of collagen membranes used in guided bone regeneration: a comparative study of three models. Rev Stomatol Chir Maxillofac 111:286–290

Collins M, Bassett J, Wen HB et al (2014) Trabecular metal dental implants: overview of design and developmental research. Quntessenza Internazionale 30(2):41–50

Cortelini P, Pini Pratio G, Tonetti M (1996) Periodontal regeneration of human intrabony defects with bioresorbable membranes. A controlled clinical trial. J Periodontol 67:217–223

Darby I (2011) Periodontal materials. Aust Dent J 56(Suppl 1):107–118

Davies JE (2003) Understanding peri-implant endosseous healing. J Dent Educ 67:932–949

de Arriba C, Gracia M, Pingarron M et al (2013) Osseoincorporation of porous tantalum cylinders implanted in human subjects: 12-week interim results. Academy of Osseointegration Annual Meeting, London

de Long WG, Einhorn TA, Koval K et al (2007) Bone grafts and bone grafts substitutes in orthopedic trauma surgery. A critical analysis. J Bone Joint Surg Am 89:649–658

Dimitriou R, Jones E, McGonagle D et al (2011) Bone regeneration: current concepts and future directions. BMC Med 9:66

Donos N, Retzepi M, Wall I et al (2011) In vivo gene expression profile of guided bone regeneration associated with a micro-rough titanium surface. Clin Oral Implants Res 22: 390–398

Dupont KM, Boerckel JD, Stevens HY et al (2012) Synthetic scaffold coating with adeno-associated virus encoding BMP2 to promote endogenous bone repair. Cell Tissue Res 347:575–588

Ereno C, Guimarães SA, Pasetto S et al (2010) Latex use as an occlusive membrane for guided bone regeneration. J Biomed Mater Res A 95:932–939

Farzad M, Mohammadi M (2012) Guided bone regeneration: a literature review. J Oral Health Oral Epidemiol 1(1):3–18

Friberg B, Jemt T, Lekholm U (1991) Early failures in 4,641 consecutively placed Brånemark dental implants: a study from stage 1 surgery to the connection of completed prostheses. Int J Maxillofac Implants 6(2):142–146

Genco R, Goldman H, Coen DW (eds) (1990) Contemporary periodontics. St Louis Mosby, London

Giannoudis PV, Faour O, Goff T et al (2012) Masquelet technique for the treatment of bone defects: tips-tricks and future directions. Injury 42:591–598

Gielkens PF, Schortinghuis J, de Jong JR et al (2008) The influence of barrier membranes on autologous bone grafts. J Dent Res 87:1048–1052

Gotllow A (2008) Influence of implant design and surface properties on osseointegration and implant. In: Jokstad A(ed) Osseointegration and dental implants. Wiley, Hoboken, pp 225–238

Greenstein G, Greenstein B, Cavallaro JD et al (2009) The role of bone decortication in enhancing the results of guided bone regeneration: a literature review. J Periodontol 80:175–189

Hutmacher DW, Goh JC, Teoh SH (2001) An introduction to biodegradable materials for tissue engineering applications. Ann Acad Med Singapore 30(2):183–191

Ivic-Kardum M (2011) Regenerative periodontal therapy using Bio-oss and resorbable membrane. Medix 17(96), abstract

Jégoux F, Goyenvalle E, Cognet R et al (2010) Mandibular segmental defect regenerated with macroporous biphasic calcium phosphate, collagen membrane, and bone marrow graft in dogs. Arch Otolaryngol Head Neck Surg 136:971–978

Kaigler D, Avila G, Wisner-Lynch L et al (2011) Platelet-derived growth factor applications in periodontal and periimplant bone regeneration. Expert Opin Biol Ther 11(3):375–385

Kaushal S, Kapoor A, Singh P et al (2014) Evaluation of OSSIFI® as alloplastic bone graft material in treatment of periodontal infrabony defects. J Clin Diagn Res 8(10):ZC61–ZC65

Kazakos K, Lyras DN, Thomaidis V et al (2011) Application of PRP gel alone or in combination with guided bone regeneration does not enhance bone healing process: an experimental study in rabbits. J Craniomaxillofac Surg 39:49–53

Keles GC, Sumer M, Cetinkaya BO et al (2010) Effect of autogenous cortical bone grafting in conjunction with guided tissue regeneration in the treatment of intraosseous periodontal defects. Eur J Dent 4(4):403–411

Kim YK (2010) Clinical application and classification of bone graft material according to component. J Korean Dent Assoc 48:263–274

Kim EJ, Yoon SJ, Yeo GD et al (2009) Preparation of biodegradable PLA/PLGA membranes with PGA mesh and their application for periodontal guided tissue regeneration. Biomed Mater 4:055001

Kim JH, Kim MK, Park JH et al (2011a) Performance of novel nanofibrous biopolymer membrane for guided bone regeneration within rat mandibular defect. In Vivo 25:589–595

Kim YK, Kim SG, Oh JS et al (2011b) Analysis of the inorganic component of autogenous tooth bone graft material. J Nanosci Nanotechnol 11:7442–7445

Kim DG, Huja SS, Tee BC et al (2013a) Bone ingrowth and initial stability of titanium and porous tantalum dental implants: a pilot canine study. Implant Dent 22(4):399–405

Kim YK, Um IW, Kim KW et al (2013) Tooth-derived bone graft material. J Korean Assoc Oral Maxillofac Surg 39:103–111

Kneser U, Schefer DJ, Polykandroitis E et al (2006) Tissue Engineering of bone: the reconstructive surgeon's point of view. J Cell Mol Med 10(1):7–19

Kobayashy H, Turner AS, Seim HB et al (2011) Evaluation of a silica-containing bone graft substitute in a vertebral defect model. J Biomed Mater Res A 92(2):596–603

Kolambkar YM, Dupont KM, Boerckel JD et al (2011) An alginate-based hybrid system for growth factor delivery in the functional repair of large bone defects. Biomaterials 32:65–74
Kothiwale SV, Anuroopa P, Gajiwala AL (2009) A clinical and radiological evaluation of DFDBA with amniotic membrane versus bovine derived xenograft with amniotic membrane in human periodontal grade II furcation defects. Cell Tissue Bank 10:317–326
Laurencin C, Khan Y, El-Amin SF (2006) Bone graft substitutes. Expert Rev Med Cevices 3: 49–57
Lee CK, Koo KT, Kim TI, Seol YJ, Lee YM, Rhyu IC et al (2010a) Biological effects of a porcine-derived collagen membrane on intrabony defects. J Periodontal Implant Sci 40: 232–238
Lee J, Stavropoulos A, Susin C et al (2010) Periodontal regeneration: focus on growth and differentiation factors. Dent Clin North Am 54(1):93–111
Lee JS, Park WY, Cha JK et al (2012a) Periodontal tissue reaction to customized nano-hydroxyapatite block scaffold in one-wall intrabony defect: a histologic study in dogs. J Periodontal Implant Sci 42:50–58
Lee MJ, Kim BO, Yu SJ (2012b) Clinical evaluation of a biphasic calcium phosphate grafting material in the treatment of human periodontal intrabony defects. J Periodontal Implant Sci 42:127–135
Lekovic V, Camarago PM, Weinlaender M (2001) Combination use of bovine porous bone mineral, enamel matrix proteins, and a bioabsorbable membrane in intrabony periodontal defects in humans. J Periodontal 72:583–589
Liu J, Kerns DG (2014) Mechanisms of guided bone regeneration: a review. Open Dent J 8:56–65
Löe H (1967) The gingival index, the plaque index and the retention index systems. J Periodontol 38(Suppl):610–616
Luu HH, Song WX, Luo X et al (2007) Distinct roles of bone morphogenetic proteins in osteogenic differentiation of mesenchymal stem cells. J Orthop Res 25(5):665–677
Lynch SE, Genco RJ, Marx RE (eds) (1999) Tissue engineering. Application in maxillofacial surgery and periodontics. Quintessence Publishing, Chicago
Marx RE (2001) Platelet-rich plasma (PRP): what is PRP and what is not PRP? Implant Dent 10 (4):225–228
Meinig RP (2010) Clinical use of resorbable polymeric membranes in the treatment of bone defects. Orthop Clin North Am 41:39–47
Mendonça G, Mendonça DB, Aragão FJ et al (2008) Advancing dental implant surface technology–from micron- to nanotopography. Biomaterials 29(28):3822–3835
Molina GO, Tomás de Oliveira M, Buss L et al (2013) Histometric analysis of alveolar bone regeneration with expanded polytetrafluoroethylene (e-PTFE) and latex membranes. Braz J Oral Sci 12(3):184–188
Montanari M, Callea M, Yavuz I et al (2013) A new biological approach to guided bone and tissue regeneration. Case Rep 9. pii: bcr2012008240BMJ
Mora F, Quhayoun JP (1995) Clinical evaluation of natural and porous hydroxylapatite implants in periodontal bone lesions: results of a 1-year follow-up. J Clin Periodontol 22:877–884
Needleman I, Tucker R, Giedrys E et al (2002) A systematic review of guided tissue regeneration for periodontal infrabony defects. J Periodontal Res 37:380–388
Nilsson M, Wang JS, Wielanek L et al (2004) Biodegradation and biocompatability of a calcium sulphate-hydroxyapatite bone substitute. J Bone Joint Surg 86-B:120–125
Nkenke E, Weisbach V, Winckler E et al (1994) Morbidity of harvesting of bone grafts from the iliac crest for preprosthetic augmentation procedures: a prospective study. Int J Oral Maxillofac Syrg 33(2):157–163
Owen GR, Jackson JK, Chehroudi B et al (2010) An in vitro study of plasticized polylactic-co-glycolic acid films as possible guided tissue regeneration membranes: material properties and drug release kinetics. J Biomed Mater Res A 95:857–869
Pachauri P, Bathala LR, Sangur R (2014) Techniques for dental implant nanosurface modifications. J Adv Prosthodont 6(6):498–504

Palachur D, Rao KVP, Murthy KRV et al (2014) A comparative evaluation of bovine-derived xenograft (Bio-Oss Collagen) and type I collagen membrane (Bio-Gide) with bovine-derived xenograft (Bio-Oss Collagen) and fibrin fibronectin sealing system (TISSEEL) in the treatment of intrabony defects: a clinico-radiographic study. J Indian Soc Periodontol 18(3):336–343

Papaspyridakos P, Chen CJ, Singh M et al (2012) Success criteria in implant dentistry: a systematic review. J Dent Res 91(3):242–248

Pejcic A, Lj Kesic, Brkic Z et al (2011a) Effect of periodontal treatment on lipoproteins levels in plasma in patients with periodontitis. South Med J 104(8):547–552

Pejcic A, Lj Kesic, Milasin J (2011b) C-reactive protein as a systemic marker of inflammation in periodontitis. Eur J Clin Microbiol Infect Dis 30(3):407–414

Pejcic A, Kesic LJ, Milasin J et al (2011c) The effects of periodontal therapy on C-reactive protein and periodontal pathogens in periodontitis patients. Acta Stomatologica Croatica 45(1):14–23

Pejcic A, Lj Kesic, Pesic Z et al (2011d) White blood cell count in different stages of chronic periodontitis. Acta Clinica Croatica 50(2):159–167

Pejcic A, Zivkovic V, Bajagic V et al (2012) Histological changes of gingival epithelium in smokers and non-smokers. Cent Euro J Med 7(6):756–760

Pejcic A, Djordjevic V, Kojovic D et al (2014) Effectiveness of periodontal treatment in renal transplant recipients. Med Princ Pract 23(2):149–153

Pejčić A, Kesić Lj, Ilić S et al (2012) Association between chronic periodontitis and serum lipid level. Vojnosanit Pregl 69(9):771–777

Piatelli A, Scarano A, Russo P et al (1995) Evaluation of guided bone regeneration in rabbit tibia using bioresorbable and non-resorbable membranes. Biomaterials 17:791–796

Polimeni G, Xiropaidis A, Wikesjö UME (2006) Biology and principles of periodontal wound healing/regeneration. Periodontol 41:30–47

Porter JA, von Fraunhofer JA (2005) Success or failure of dental implants? A literature review with treatment considerations. Gen Dent 53(6):423–432

Ramazanoglu M, Oshida Y (2011) Osseointegration and bioscience of implant surfaces-current concepts at bone-implant interface, implant dentistry: a rapidly evolving practice. InTech, Rijeka, pp 57–59

Ramseier CA, Rasperini G, Batia S et al (2012) Advanced reconstructive technologies for periodontal tissue repair. Periodontol 2000 59:185–202

Rao SM, Ugale GM, Warad SB (2013) Bone morphogenetic proteins: periodontal regeneration. N Am J Med Sci 5(3):161–168

Retzepi M, Donos N (2010) Guided bone regeneration: biological principle and therapeutic applications. Clin Oral Implants Res 21:567–576

Rho J, Tsui T, Pharr G (1997) Elastic properties of human cortical and trabecular lamellar bone measured by nanoindentation. Biomaterials 18:1325–1330

Richardson CR, Mellonig JT, Burnsvold MA et al (1999) Clinical evaluation of Bio-Oss a bovine derived xenograft for the treatment of periodontal osseous defects in humans. J Clin Periodontol 26:421–428

Rosenberg E, Evian C, Stern K et al (2010) Implant failure: prevalence, risk factors, management, and prevention. In: Froum S (ed) Dental implant complications. Blackwell Publishing, Chichester, pp 110–118

Santana RB, de Mattos CM, Van Dyke T (2009) Efficacy of combined regenerative treatments in human mandibular class II furcation defects. J Periodontol 80:1756e64

Santana RB, de Mattos CM, Francischone CE et al (2010) Superficial topography and porosity of an absorbable barrier membrane impacts soft tissue response in guided bone regeneration. J Periodontol 81:926–933

Santos PL, Gulinelli JL, Telles CS et al (2013) Bone substitutes for peri-implant defects of post-extraction implants. Int J Biomater 2013:136–307

Scheyer ET, Schupbach P, McGuire MK (2012) A histologic and clinical evaluation of ridge preservation following grafting with demineralized bone-matrix, cancellous bone chips, and resorbable extracellular matrix membrane. Int J Periodont Restor Dent 32:543–552

Schilephake H (2002) Bone growth factors in maxillofacial skeletal reconstruction. Inter J Oral Maxillofac surg 31:469–484
Shue L, Yufeng Z, Mony U (2012) Biomaterials for periodontal regeneration: a review of ceramics and polymers. Biomatter 2:271–277
Sohrabi K, Saraiya V, Laage TA et al (2012) An evaluation of bioactive glass in the treatment of periodontal defects: a meta-analysis of randomized controlled clinical trials. J Periodontol 83:453–464
Sorger JL, Hornicek FJ, Zavatta M et al (2001) Allograft fractures revisited. Clin Orthop Relat Res 382:66–74
Spiekermann (ed) (1995) Implantology. Thieme Medical Publishers Inc, New York
Stavropoulos A, Windisch P, Szendröi-Kiss D et al (2010) Clinical and histologic evaluation of granular Beta-tricalcium phosphate for the treatment of human intrabony periodontal defects: a report on five cases. J Periodontol 81:325–334
Subbaiah R, Thomas B (2011) Efficacy of a bioactive alloplast, in the treatment of human periodontal osseous defects-a clinical study. Med Oral Patol Oral Cir Bucal 16:e239–e244
Suheil M, Boutros M (2013) Trabecular Metal™ Implants—from orthopedics to dental implantology. Academy of Osseointegration Annual Meeting, London
Taguchi Y, Amizuka N, Nakadate M et al (2005) A histological evaluation of guided bone regeneration induced by collagenous membrane. Biomaterials 26:6158–6166
Tan WL, Wong TL, Wong MC et al (2012) A systematic review of post-extractional alveolar hard and soft tissue dimensional changes in humans. Clin Oral Implants Res 23(Suppl 5):1–21
Ten Cate AR (ed) (1994) Oral histology. Development, structure, and function, 4th edn. St Lous, Mosby
The American Academy of Periodontology (1992) Glossary of periodontal terms (3rd edn). Chicago
The American Academy of Periodontology (1996) Annals of Periodontology—world workshop in periodontics. Am Acad Periodontol 1:621 (Chicago)
Varanasi VG, Owyoung JB, Saiz E et al (2011) The ionic products of bioactive glass particle dissolution enhance periodontal ligament fibroblast osteocalcin expression and enhance early mineralized tissue development. J Biomed Mater Res A 98:177–184
Wang H, Li Y, Zuo Y et al (2007) Biocompatibility and osteogenesis of biomimetic nano-hydroxyapatite/polyamide composite scaffolds for bone tissue engineering. Biomaterials 28:3338–3348
Wei G, Ma PX (2004) Structure and properties of nano-hydroxyapatite/polymer composite scaffolds for bone tissue engineering. Biomaterials 25:4749–4757
Xu C, Lei C, Meng L et al (2012) Chitosan as a barrier membrane material in periodontal tissue regeneration. J Biomed Mater Res B Appl Biomater 100:1435–1443
Yeo YJ, Jeon DW, Kim CS et al (2005) Effects of chitosan nonwoven membrane on periodontal healing of surgically created one-wall intrabony defects in beagle dogs. J Biomed Mater Res B Appl Biomater 72:86–93
Yu Q, Pan XG, Ji GP et al (2009) The association between lower incisal inclination and morphology of the supporting alveolar bone–a cone-beam CT study. Int J Oral Sci 1:217–223
Zaugg B, Sahrmann P, Roos M et al (2014) Improving scaling and root planning over the past 40 years: a meta-analysis. Dentistry 4:3

Knee Arthroplasties

Aleksandar Radunovic, Zoran Popovic and Maja Vulović

Abstract Total knee arthroplasty is an operating procedure in which the knee is replaced with an artificial joint. This is one of the most common operating procedures in orthopedics today. Performance of these procedures requires knowledge of the anatomical features of the joint, the biomechanical characteristics of the implant, complications that can occur after installing them, and the solutions to those complications, as well as the needs of particular patients with their unique pathological and physiological characteristics. Lengthening of patients' lives, as well as increased requirements in terms of activities, have spurred the development of new concepts regarding endoprosthesis and biomaterials that allow for significantly longer survival of the implant and contribute to a reduction in the number of unwanted reactions. There is a global trend towards an increasing number of knee arthroplasties that follows the trend of an increasing number of complications with the widest range of modalities in which they occur. Both of these trends spurred the development of different implants.

Keywords Hip · Arthroplasty · Biomaterials · Complications · History · Anatomy

A. Radunovic (✉) · Z. Popovic
Clinic for Orthopedic Surgery and Traumatology,
Military Medical Academy, Crnotravska 17, Belgrade, Serbia
e-mail: aradunovic71@gmail.com

Z. Popovic
e-mail: ortopop@gmail.com

M. Vulović
Department of Anatomy, Faculty of Medical Sciences,
University of Kragujevac, Kragujevac, Serbia
e-mail: maja@medf.kg.ac.rs

F. Zivic et al. (eds.), *Biomaterials in Clinical Practice*,
https://doi.org/10.1007/978-3-319-68025-5_27

Knee Arthroplasty
Knee arthroplasty is a surgical procedure in which altered degenerative articular cartilage of the knee joint suffering from some degree of damage is replaced with artificial surfaces. The successful performance of these procedures requires knowledge of anatomic and biomechanical properties of the joint, as well as knowledge of the characteristics of implants and surgical techniques.

1 Anatomy of the Knee Joint

The knee joint connects the thigh bone with the lower leg. This is the largest joint in the human body, very complex and capable of performing movements under high load, but also often exposed to damage. In the upright position, the knee joint carries about 70% of the weight of the body, and when the legs are flexed, about 90%. The movements that take place in this joint are bending (flexion), stretching (extension), and internal and external rotation.

1.1 Bones and Menisci

The upper part of the knee joint is the distal stumps of the femur (extremitas distalis femoris), which consists of a skeletal massif, where two bony prominences, the external and internal condyles of the femur (*condylus lateralis et medialis femoris*), are distinguished. These two bumps are connected to a smooth front fascia that is slightly sunken and makes a joint with the patella (*facies patellaris*) and the tactile rear notch that separates the deep pit (*fossa intercondylaris*).

The lower part of the knee joint is the proximal tibial stumps (*extremitas superioris tibiae*) in which different external and internal bony prominences (*condylus_lateralis et medialis tibiae*) can be seen. On the front, there is a bulge that is the shinbone (*tuberositas tibiae*).

The patella is a small bone of sesamoid spherical shape. On its upper half, the tendon attaches to the four-head femur muscle stretching down the patellar ligament, which attaches to the tibial tuberosity, allowing for a lever mechanism effected with the four-head thigh muscle.

The articular surface of the condyle of the femur is not absolutely regular, yet going from front to back, it draws an arc that is more convex in the rear, namely, the diameter of the curvature at the front part of the articular surface is larger than that of the rear surface of the condyle of the tibia part. The joint condyle surfaces of the tibia are extremely shallow and appear as outer and inner menisci along the peripheral edges of the meniscus (*meniscus medialis et lateralis*).

Menisci are fibrocartilage-like creations of semi-lunar shape that have multiple functions:

(A) increasing congruence in operation of the convex articular surface of the femur and the flat articular tibial surface
(B) increasing stability of the knee joint
(C) playing the role of a shock absorber.

Menisci are triangular in cross-section, with the base facing into the field. The lower surface is flat and the upper concave, thus achieving an increase in knee joint stability. The outer meniscus is more closed than the inner and attaches the front and rear ends of the inner menisci, located in front of and behind the outer attachment. The menisci themselves are on the peripheral edges of the fibrous sheaves attached to the capsule and ligaments, with their front ends connected by a transverse link (Mrvaljević 2006).

1.2 Knee Ligaments

The shape of the articular surfaces does not allow for the necessary stability of the knee joint (as is the case, for example, with the hip), and therefore the knee has a very complex capsule-ligament structure. It permits stability under the load to which the knee is daily exposed.

Cruciate knee ligaments are the strongest knee ligaments that are positioned intraarticularly and extrasynovially, which means that, though in the knee joint, a synovial membrane around them has a true pocket and separates them from the intrasynovial structure in the knee. Their materials, vascularization, and histological structure (composed of fibrocytes) form the condition that the lesions of these ligaments are irreparably natural, and in case of damage to them, the only option for appropriately selected patients is surgical reconstruction. The anterior cruciate ligament (*ligamentum cruciate anterius*, LCA) is proximally attached to the rear of the medial surface of the external femoral condyle and stretches obliquely forward and down, medially and distally merging in front of the intercondylar area of the tibia (*area intercondylaris tibiae anterior*), between the front edges of the meniscus. The anterior cruciate ligament (*ligamentum cruciatum posterius*) is proximally attached to the front of the outer surface of the inner femoral condyle and goes back and down, laterally and distally merging in the posterior intercondylar field of the tibia (*area intercondylaris tibiae posterior*), behind the rear ends of the meniscus. A rupture of the rear cruciate ligament by an identical principle as that of the ACL cannot heal.

The joint capsule is a strong fibrous cuff that wraps up the knee and is further reinforced by front, side and rear ligamental enhancements. The front capsule joints are the patellar ligament and the patellar retinacula, external and internal (*retinaculum patellae laterale et mediale*). The retinacula represent lateral extensions of

the four-head femur muscle that comes in addition to the condyle cups of the shinbone. Their deep transverse fibers connect the femoral condyles with the patella. The retinacula prevent lateral patellar displacements.

The lateral capsular reinforcements are external and internal ligaments (collateral fibular ligament, tibial collateral ligament). The outer bond is stronger, in the form of ribbons separated from the capsule that extend from the outer cusp of the femur (*epicondylus lateralis femoris*) to the fibula head (*caput fibulae*). The inner joint connection is in the form of ribbons grown together with the articular capsule and the base of the inner meniscus, which extends from the inner cusp of the femur (*epicondylus medialis femoris*) to the inside of the body of the tibia.

1.3 Knee Muscles

1.3.1 Extensor Mechanism

The four-headed femoral muscle (*M. quadriceps femoris*) consists of four heads that occupy the front parts of the lateral and medial thigh vines. *M. rectus femoris* makes up the central part of the four-headed muscle, proximally attached to the lower front iliac spike (*spina illiaca anterior inferior*) and its distal attachment, as well as the distal attachments of the other components of *m. quadriceps* making the common tendon that is attached to the patellar base. Fibers of *m. rectus femoris* cross the patella, and nearly all participate in the building of the patellar tendon that connects the patella to the tibial tuberosity (*tuberositas tibiae*).

M. vastus lateralis: the upper attachment is on the outer-rear parts of the proximal and middle parts of the femur. The distal attachment becomes tendinous at about 2–3 cm from the base of the patella, and the fibers are inserted directly into the patella at an angle of about 12–15°.

M. vastus medialis is in the upper part, attached to the intertrochanteric ridge and the internal lip *lineae aspere*; distally, the fibers become aponeurotic within a few millimeters of the patella and at the point at which they are attached to it.

M. vastus intermedius is the smallest of the four components of the four-headed muscle, with proximal attachment to the upper 2/3 of the anterior side of the femur and lower attachment directly to the base of the patella. Its fibers do not exceed the patella and do not participate in construction of the patellar ligament.

The four-headed muscle is the flexor of the thigh at the hip and the extensor of the knee. The direction of the force of the quadriceps is described by the Q-angle, which is the angle of inclination between the line that runs along the center of the patella and the tibial tuberosity and the line connecting the anterior superior iliac spine and the center of the patella. This angle is larger in women (about 16°) than in men (12°) and shows that the natural action of the quadriceps has a tendency towards lateral subluxation of the patella.

1.3.2 The Flexor Mechanism

The two-headed thigh muscle (*m. biceps femoris*), in its proximal part, merges with the lumps at the buttocks (*tuber ischiadicum*) in the pelvis and distal muscle on the fibular head. This muscle is a knee flexor and thigh extensor.

The semitendinosus muscle (*m. semitendinosus*) also merges, proximally to distally, with sitting lumps and attaches to the anteromedial side of the proximal tibia in *pes anserinus*.

The semimembranosus muscle (*m. semimembranosus*) is attached to the proximal and distal sitting lumps on the posteromedial part of the medial condyle of the tibia.

M. sartorius proximally attaches to the front of the anterior extremity of the iliac crest of the pelvis (*spina iliaca anterior superior*), then crosses over the front of the thigh and attaches distally to *pes anserinus*. This is the longest muscle in the body, and its contraction leads to flexion of the hip and knee.

1.4 Vascularization of the Knee

The knee joint is extremely well-vascularized using the upper, middle and lower geniculate arteries (*aa. geniculatae superior, inferior et medius*), a branch of *a. popliteae*.

2 Biomechanics of the Knee

The knee performs movements of flexion and extension around the lateral axis, passing through the femoral bone condyle. When fully flexed, the thigh and lower leg form an angle of 130°, while passively, 150° can be achieved. In full extension, the thigh and lower leg form an angle of 180°.

At full extension, a strong tightening of the lateral knee connections appears, because at that point, the condyles of the femur work alongside its largest diameter. Apart from the lateral connections at full extension, there is a tightened posterior capsule, the anterior cruciate ligament. An especially significant movement is the locking of the knee in extension, leading the anterior cruciate ligament to tighten, and consequently the lower leg to rotate externally by 5°, fixing the knee joint in a stable position.

In flexion, collateral ligaments relax and permit the rotator movements of the knee joint. The relative vulnerability of the knee is caused by its rotatory movements. These movements take place in the horizontal line and around the axis that coincides with the longitudinal axis of the rotator of the lower leg. The amplitude of movement is about half the width of the patella. Rotating movements are not performed in the position of full extension of the knee when the phenomenon of

locking appears, but with gradual flexion, relaxation of the capsule occurs, along with that of the collateral ligaments and cruciate ligaments, and rotational movement becomes both possible and more ample. The inner rotation is always smaller than the outer.

There are two types of rotatory movement of the knee: willing and automatic. Willing rotation can be performed only after 20° of flexion and 20° before the last extension and is only a further increase in the amplitude of automatic, conditioned rotation. Generally, knee movements are synchronized moves of extensions and external rotation of the tibia, as well as flexion with internal rotation of the tibia (Nikolic 2006).

The role of the menisci in knee motion is very important, with one of the most important factors being to transfer load from the femur to the shinbone. The femoral condyles, which are spherical in shape, press the flat tibial condyle; the menisci are inserted between them. The force suffered by the meniscus on the upper surface has its horizontal and vertical components, and on the lower surface, only the vertical one is transmitted. The horizontal component on the upper surface leads to radial expansion of the meniscus, which resists its own inner architecture (especially circumferentially organized collagen fibers) and the peripheral strong meniscus attachments. There are circumferential meniscus tensions that are resisting forces, thus the meniscus is held in balance, and this mechanism's compressive force receives and evenly distributes the articulatory surface, thereby reducing the pressure that this area suffers. The compressed knee load that is transmitted through the meniscus depends on the knee's position, being at least 50% when in traction, and at least 85% at 90° of flexion. Numerous papers show that in knees that underwent surgical removal of part of the meniscus after injury, a significant increase in the loading of articular cartilage and consequent degenerative changes occured.

The next most important role of the meniscus is increasing the congruency (morphological matching) of the joint surface. The knee has very poor congruency (the spherical articular surface of the femur articulates to the flat tibial condyles). The menisci fill the dead space between the articular surfaces and deepen the articular tibial surface. In this way, the stability of the joint is increased.

Ultimately, the menisci, as proprioceptive structures, correspond to the feedback mechanism in determining the sense of joint position.

3 History of Knee Arthroplasty

As early as the end of the 19th century, pioneers in surgery were trying to heal osteoarthritic (OA) knees with interpositional arthroplastics. In this procedure, insertion of a tissue or material between degeneratively changed articular surfaces for the reconstruction of said surface is performed. Various autologous, heterologous tissues and materials are used for this purpose, such as anterior knee bursa, femoral fascia, pork bladder, nylon, and cellophane. All these procedures have shown disappointing results. The 1930s began with the interposition of metal in the

sense of partial arthroplasty of a tibia or making a metal mold for a femur, but these procedures also had very poor results, so such operations were discontinued. Some surgeons are trying resection arthroplasty, which means removal of the articular surfaces of both bones. While removing small amounts of bone, a spontaneous fusion of bones can occur, and when too much bone is removed, instability occurs. These procedures have been performed only in the most severe cases, with consequent bad results.

In the'50s, a hinge type of endoprosthesis was used, the first to show satisfactory results. This type of prosthesis only allowed for movement in the frontal plane, and therefore was technically undemanding in its implantation, because there was no need for strict conservation of the ligaments. By all accounts, this type of prosthesis could not be widely accepted because it could not imitate the complex movements of the knee due to the high degree of loosening. In the early 1970s, there were several attempts at new designs, and concepts from this era can be classified as follows:

3.1 Anatomical Approach

A group of designers studied the possibility of a prosthesis whose implantation preserved both cruciate ligaments, thus allowing the femoral roll-back on the tibia (posterior femoral translation during the progression of flexion). At the end of the '70s, Yamamoto presented the design of a prosthesis consisting of an anatomically-shaped femoral part made of COP alloy (Co, Cr, Ni, Mo, C, and P). The tibial component was one-piece, mildly sunk, made of polyethylene with the central part cut out in order to preserve the cruciate ligaments. Waugh (1973) and Sheed (1974) designed their own types of endoprosthesis, the common factor among all of them being a tibial component in a horseshoe shape, for preservation of the ligamentum cruciatum posterius (LCP).

The 1980s brought significant progress in the field of knee arthroplasty, particularly in regard to surgical techniques and new instruments. Development of new instruments made cartilage thickness resection equal to the thickness of endoprosthetic material that led to the cementless fixation of a prosthesis (up until then, the components had been fixed with cement).

3.2 Functional Approach

Supporters of the functional approach tried to simplify knee kinematics by removing both cruciate ligaments. The first such system originating from this concept was a total condylar prosthesis, developed at the Hospital for Special Surgery in New York by Insall and associates (1976). This prosthesis consisted of two symmetrical condylar surfaces of the femur with increased radius of curvature

of the posterior articular surface made of polyethylene, perfectly congruent in extension and partially congruent in flexion (congruence = matching of articular surfaces). This design has proven to be extremely successful and shows a very high percentage of survival. Two problems crystallized in relation to this design: the first was possible front displacement of the femoral component, especially in flexion, which could lead to dislocation of the front of the tibia or tibial loosening. Another problem manifested in limited flexion of the knee, which, in the largest number of cases, was about 90°. These problems led to further development of the design, with the femoral component setting the transverse bulkhead between the last parts of the femoral condyles and the tibial component in elevation in the middle part, preventing posterior dislocation of the femur in flexion, so as to roll the femur back on the tibia and thus increase flexion. This type of prosthesis is known as the Insall Burstein Posterior Stabilized (IBPS). This is one of the most successful prosthetic designs ever and became the foundation of modern knee arthroplasty. Later, it experienced minor modification by the author, who introduced a tibial component with a lower part made of metal, which put the polyethylene insert on directly so as to reduce polyethylene deformation under the load. This design has seen a lot of variation by different producers. All of them have realization of movement of the knee joint through so-called guided motion, which means that some segments of knee movement, e.g., femoral roll back, take place through mechanical interaction between the femoral and tibial components. Regardless of the outstanding success of the endoprosthesis, complications have arisen involving the patellofemoral joint, leading to further development of the design and an increase of the contact surface of the joint, preventing lateral subluxation of the patella.

3.3 Unicompartmental Knee Arthroplasty

This procedure replaces the articular surface of only one of the femoral condyles and the tibia. The indication for this procedure is a deterioration of the cartilage in one knee compartment, which is usually a consequence of the trauma. Regardless of this, the procedure was first performed in the 1950s, with controversial results (Insall et al. 1976). Further results obtained in the early 1970s were not satisfactory either, but in the next decade, through the introduction of new designs of unicompartmental endoprosthesis, knee scores became better. With the beginning of the first decade of the 21st century, significant improvements in designs and surgical techniques for implantation of unicompartmental endoprostheses appeared, and far more precise instruments for the installation of endoprostheses were constructed, with very good results. Compared to total knee arthroplasty, a unicompartmental (unicondilar) endoprosthesis has the advantages of preservation of the cruciate ligaments, features of nearly physiological range of motion, and significantly less resection of bone, which theoretically means easier revision. The latest

papers show an 85–95% probability of long-term survival of the prosthesis, which is almost identical to that of the total knee endoprosthesis. In conclusion, for the right patients, the procedure may be a good surgical option.

3.4 Patellofemoral Joint

Symptoms related to the patellofemoral joint are cited as one of the most common causes of failed knee arthroplasty (Spitzer and Vince 1995). During the 1980s, many authors found that up to 30% of patients had these problems, which turned this good procedure into a disappointing one and opened up a debate on the need for replacement of the articular surface of the patella and the best way in which to do it. This problem occurred with the development of an endoprosthesis design that had greater flexion, so the designers' aim was to cut the trochlear part of the femoral component in order to provide an adequate jointing of the patella in all stages of movement. Relying on this criterion, a large number of variations in the design of the prosthesis appeared, with various versions of the trochlear groove, which had a positive impact on reducing the incidence of complications of the patella. A significant contribution to reducing these complications was the attention brought to proper rotational positioning of the femoral component (Rand 1994).

There is another point that is still being debated: should we resurface the patellar articular surface and swap it for the artificial one? In the early days of total knee arthroplasty (TKA), there was no patellar resurfacing, until it was noticed that up to 40% of patients complained of anterior knee pain (Schroeder-Boersch et al. 1998). After that, some type of patellar resurfacing was introduced, and there was a decrease in the complications. However, a new spectre of complication arose: patellar fractures, ruptures of patellar ligaments, and polyethylene wear and loosening (Mont et al. 1999).

Nowadays, it is surgeon preference and the details of the specific case that will determine whether or not this method will be performed, with many publications still weighing in on the pros and cons.

4 Materials for Producing Endoprosthesis

A biomaterial is defined as any material that is used to create objects that replicate functions of the body in a safe, reliable, economical and physiologically acceptable way. The types of material that are in use in the practice of orthopedic surgery have changed over time, thanks to new knowledge and a better understanding of previous failures, as well as attempts to imitate bone more naturally, but there are certain criteria that each material must fulfill: biocompatibility, non-toxicity, strength, resistance to wear and corrosion, availability, and economic efficiency. The implants used today in TKA can be divided into three groups: metals, polymers and ceramics.

4.1 Metals

4.1.1 Stainless Steel

Due to its tendency to corrode in the human body and its inadequate resistance to repeated stress for plastic deformation, this metal is not suitable for permanent implants. It is, however, suitable for non-permanent implants, e.g., management of bone fractures.

4.1.2 Cobalt

The alloys of cobalt (Co–Cr–Mo and Co–Cr–Ni) are more resistant to the corrosive processes in the body due to the formation of a resistant chromium oxide surface layer (passivation layer). In addition to good corrosion resistance, with the implant being composed of these alloys, the ability to release ions was observed in vivo. Chromium and nickel are well-known suspected carcinogens, and the same goes for cobalt. Traces of these metals are found not only in the soft tissues around the implant, but also in blood and urine, sometimes at concentrations higher than those that occur during professional exposure to these metals. Due to sporadic fractures, implants made of cobalt alloys were created as superalloys. The special technological procedure code (compression under extremely high pressure) increases the fatigue resistance of these metals. It is extremely difficult to create a porous surface through this process. The production process of a porous surface leads to reduced fatigue resistance, thus it is recommended that the porous layer be avoided in areas of critical load implant. Components made of Co–Cr alloys have a modulus of elasticity about two times higher than that of the titanium implant, and approximately ten times that of the cortical, which contributes to reducing stress on the cement when using this method of implant fixation, but makes it less suitable for the cementless type of fixation. These types of implant of the joint surface must be done by technological process in the articular surface, and therefore the femoral knee endoprosthesis component is, as a rule, made of the above-mentioned alloys. Titanium is solid, but cannot be processed in the articular surface.

4.1.3 Titanium and Its Alloys

The most commonly used titanium alloys are Ti6Al4V, Ti-6Al-7NB and Ti-5AL-2.5Fe. Alloys of titanium have great resistance to corrosion, which makes them bio-inert, a feature they owe to formation of a layer of titanium oxide on the surface, which is a type of ceramic. Lack of this layer can make them porous and friable, and its abrasion leads to the release of particles into the surrounding tissue:

titanium debris was found in the surrounding bone. Although titanium bioimplants are considered highly biocompatibile, the debris particles can cause unwanted tissue response and lead to aseptic implant loosening. As a rule, the tibial component (tibial tray) of TKA is made of titanium, since this part of the endoprosthesis is exposed to extreme loadings. In the previous types of total knee endoprosthesis, this part was made from a steel alloy, but it often ended up fracturing because of the stress and the transfer of powers through the tibial plateau. For this reason, this part of the construct of titanium, and more recently of tantalum alloys, makes these materials unable to meet the load requirements. Neither titanium nor tantalum alloys can be processed in the articular surface, and for this reason, the basic concept of TKA means a tibial polyethylene insert.

There are two types of tissue response to the implant (Mano et al. 2002; Rossi et al. 2008; Migirov et al. 2011). The first type is the tissue responding to the implanted materials or toxicity of the chemicals being discharged while damaging its surface. The second type is non-adherent fibrous capsule formation-fibrosis between the implant and the tissue in its immediate environment. This is a natural response that protects the body from intruding particles. The intention is to fix the implant in the human body, with expectation the bone contact surface of the implant will grow, but this, unfortunately, is not happening regularly. Fibrosis, as a tissue reaction to a foreign body, occurs in almost all implants, consisting of phases very similar to those of wound healing (Kyriakides et al. 2001). The presence of this tissue can lead to micromovements that still generate the creation of debris and the consequent inflammatory cascade reaction to same, which leads to osteolysis.

4.1.4 Tantalum

Twenty years ago, implants made of tantalum appeared. Like earlier, the new technology was applied to total hip arthroplasty (THA) first. Implants made of porous tantalum have so much in common with natural bone trabeculae that they were called trabecular metal. Trabecular has a porosity of 75–85%, allowing for three to four times greater bone ingrowth, compared to the conventional porous-coating (Bobyn et al. 2004). Its elasticity module is similar to that of bones and permits the transfer of the load-minimizing stress-shielding phenomenon. (This phenomenon is related to the reduction of bone density due to the reduction of the normal load of bones, occurring when the implant takes part of the load characteristics onto itself.) It depends on the implant. The phenomenon relies on Wolff's law, relating to the bone in a healthy man, which remodels itself in accordance with the exposed load. Accordingly, the burden on the bone reduces, becoming diluted in some places and outright smaller in others, since no stimulus for the continuous remodeling essential to maintaining bone mass appears.

4.2 Ceramics

The ceramics used in the manufacturing of implants today are comprised mainly of aluminum oxide (Al_2O_3) and zirconium oxide (ZrO_2). Ceramic materials are highly resistant to pressure, but are not resistant to traction or shear, and they are brittle. Their percentage of wear is extremely small (1–3 micrometres/year) and they have excellent lubricative and friction characteristics. The trait that most favors ceramic implants is their biocompatibility, which is much more pronounced than that of metal implants and is now one of the main indications for their use in cases of intolerance to some of the components of metal implants. Their main unfavourable feature is low resistance to fracture, because of the impossibility of plastic deformation of the materials, hence the smallest cracks can lead to catastrophic implant fractures. At the moment, more manufacturers are developing special types of ceramic, with a much higher resistance to pressure and shot, each with its own trade name and a protected composition.

At present, three generations of ceramic implants have been produced. The first generation of implants was used up until year 2000, and its incidence of fragility was as much as 5%. This was a high incidence of complications, regardless of the fact that the first generation of ceramics was not competitive enough with other materials used as inserts in endoprosthesis. The next generation of ceramics was produced in the year 2000, and a serious analysis presented in 2002 by the Scott in San Diego indicated that the brittleness had been reduced to below 1%.

4.3 Polyethylene

Despite designer success in solving the afore-mentioned problems, the 1990s were marked by the observation of almost catastrophic problems with polyethylene. This polymer has a low coefficient of friction (the wear on polyethylene on metal joints is roughly 100–300 micrometres/year), while the combination of ceramic polyethylene has an even smaller percentage of wear. There is also significantly higher risk of fracture, which has been fixed by introducing new generations of ceramics. The process and degree of wear are very unpredictable, and many factors can affect it. The characteristics of polyethylene as a joint surface are significantly improved by creating a highly cross-linked ultra-high molecular weight polyethylene (UHMWPE), with the addition of vitamin E to reduce oxidative damage. UHMWPE is one of the most desirable polymers in the world of orthopedic implants due to its mechanical strength and biocompatibility. Despite these modifications, polyethylene remains one of the main limitations for the long-term success of TKA. Unlike the highly congruent hip joint that functions according to the type of ball and hole geometry, articulation of the knee is complex. In TKA, wear occurs due to a combination of rolling, sliding and rotator movements on a loaded surface, which can lead to its delamination, burrs and fatigue fracture. Shearing

mechanisms are significantly different from those that occur in hip arthroplasty, in which the dominant mechanisms are microadhesion and microabrasion. Shearing is also remarkable at the back side of the tibial component.

Osteolysis associated with polyethylene wear was identified as a significant problem in some designs of TKA. The main causal factor is small debris particles, which stimulate the cellular response to an intruding body, leading to the osteolysis.

The first reports of osteolysis around TKA were related to the existence of bone resorption around cementless tibial implants. Openings on metal components, such as the screws for fixation of tibial components and zones of discontinuity of rusty coating components, were identified as channels for the debris that leads to osteolysis. Later, the researchers recognized the existence of osteolysis in components with fixed cement. It was thought that debris particles find their way to the bone through channels in the cement (Scuderi 2011).

The type and composition of particles of debris have been identified as another key factor in the generation of osteolysis. It is known that the particles of polyethylene, polymethylmethacrylate and metals present in the debris cause a significant inflammatory response (Jacobs et al. 2001). A difference in the macroscopic appearance of particles of debris was found. TKA with debris consisting of flakes larger than the total hip arthroplasty (THA) and tissue response is characterized by the presence of a small number of macrophages (Schmalzreid et al. 1994). Those facts lead to the conclusion that large polyethylene particles produced by delamination and material fatigue do not produce the same cell response as small particles of debris. One of the possible sources of small particle debris in TKA referred to the wear on the interface between the rear surface of the polyethylene tibial insert and the metal component (Wasielewski et al. 1997).

The next factor that influences the degree of wear is the patient, with dependent factors such as age, weight, and level of activity. These factors determine the intensity and type of wear. Advanced age is usually associated with a lower level of activity. And yet, it is the conditions that indicate when performing TKA is appropriate, so it can happen that a patient of a younger age, who undergoes TKA due to, for example, rheumatoid arthritis, gains a lower level of activity due to the nature of the disease itself. Excessive patient weight, which normally contributes to the development of osteoarthritis, may contribute to the reduced activity after knee replacement surgery. In fact, this means that the degree of activity is the most important patient-related factor influencing the load of the artificial joint.

The characteristics of the implants and the properties of the materials of which they are made also influence both wear-resistance and the degree and amount of particular polyethylene debris formation. The technology behind making polyethylene involves connecting the ethylene monomers in the polymer chains to create polyethylene powder. The physical characteristics and molecular polyethylene weight are determined, to a large extent, by the polymerization process, which is affected by the temperature, pressure and chemicals used in these reactions as catalizators. Mistakes in the production process can lead to the formation of cracks in the body components, as well as non-homogeneous distribution of the mixture, which, in some places, appears as weak points that lead to the occurrence

of delamination and fractures after loading of the implant under in vivo conditions (Tanner et al. 1995). The components produced according to rigid standards, with no defects, demonstrated an almost complete absence of delamination after years of in vivo loading. This is why the various technological processes (pressure at elevated temperature, carbon fiber reinforcement fibers) attempting improvement of the mechanical properties of polyethylene did not, unfortunately, achieve any significant success. The process of creating the components themselves may lead to differences in the behavior of implants. Generally, polyethylene inserts are obtained in two ways: mechanics or compression molding.

Components formed mechanically are derived from polyethylene sheets or bars.

In compression molding, the components are made from polyethylene powder in appropriate molds. Components made through compression molding have been found to have a lower degree of shearing (Tanner et al.1995; Won et al. 2000).

The method of sterilization is one of the factors affecting such mechanical properties of polyethylene as the carrying surface. The most typical method of sterilization used over the years has been gamma ray sterilization. This leads to the formation of free radicals, which allows for the occurrence of oxidative processes when the product is kept in an environment rich with oxygen over longer periods of time. The first study that correlated the damage to the implant with oxidative processes was performed by Bohl et al. (1999), who found a percentage of failure of 21% due to the excessive wear of components from ages 8–11. It was found that components sterilized by this method developed a strong tape of oxidized polymer below the surface, which significantly reduced the considerable contribution to its mechanical strength and susceptibility to premature shearing based on the time of insertion of the components (Collier et al. 1996). Following these conclusions, implant manufacturers changed the method of sterilization and began to apply ethylene oxide or gamma irradiation in a non-oxygen environment.

In order to improve the characteristics of polyethylene, manufacturers have started applying the process known as cross-linking (using the high-dose electron irradiation or gamma radiation variable) to achieve higher shearing resistance (McKellop et al. 1999). Considering a significant difference in the biomechanics of the hip and knee, and thus the load of the implant, the modification did not introduce the same uniform improvement in TKA as it did in THA (Muratoglu et al. 2004). Taking into account that these components are implemented in TKA for a relatively short time, their behavior has not been fully explored.

While considering shearing resistance, the thickness of the polyethylene of the implant should be taken into account. It is shown that with polyethylene inserts thinner than 6 mm, the contact stress exponentially increases with decreasing thickness (Bartel et al. 1986). For a long time, it was thought that most of the debris comes from the joint loading surface. The optimal design of the loading surface means the one which reduces the contact load, and thereby increases the resistance to shearing. The effect of the contact surface load depends on the contact surfaces through which the transfer of the load takes place (Bartel et al. 1986). When the loading surface has a small contact surface between the femoral and tibial components, the load distribution takes place over smaller areas, which means a greater

amount of stress per unit area of polyethylene insertion. The contact zone between the femoral component and the polyethylene articular surface is determined by the geometry of these products.

Less congruent components have a smaller contact zone and an increased contact load, and thus, in theory, less desirable characteristics concerning wear. It is considered, however, that the movements of this type of articulation are closer to the actual physiological, because they allow the surrounding soft tissues to significantly affect the movement. Highly congruent articulation maximizes the contact area, and thus the resistance to shearing, but it can reduce the amount of stress suffered by the surrounding soft tissue by taking part of it onto itself, thus leading to increased local stress on the components (Benjamin et al. 2001).

Cruciate retaining (CR) implants are designed with the intention of emulating a more natural physiological knee movement. They allow the surrounding soft tissues and ligaments to guide motion, especially the locking compression plates (LCP). In subsequent papers, a significant percentage of failure of this design was found, due to the shearing of polyethylene, which is explained by a larger contact load directed to the lower contact zone of the flat articular surface (Benjamin et al. 2001; Feng et al. 1994).

Polyethylene inserts with congruent surfaces and a raised front lip have been developed in order to improve anteroposterior stability, thus preventing uncontrolled sliding of the femoral component. Meanwhile, femoral implants have shown good clinical results, including lower incidence of polyethylene shearing compared with less congruent designs (Hirakawa et al. 1996).

The aim of the development of posterior stabilized (PS) design was resolving deformities that could not as yet be solved satisfactorily. PS design involves highly congruent articulation with a polyethylene peg in the middle part of the insert and a metal deflector device that connects the rear portions of the femoral condyles of the implant, with the aim of preventing posterior subluxation of the tibia. This latest design, in spite of certain theoretical considerations about the possible complications, achieved great results in vivo. The main drawback is the subsequent identification of the polyethylene tibial components in the peg as a source of polyethylene debris, as well as fractures of the peg (Puloski et al. 2001). It is still unclear as to whether this fracture occurs as a result of shearing and tearing during the normal functioning of a component or as an abnormal hyperextension of the components, leading to impingement between the peg and deflector on the femoral component.

Mobile bearing implants have been developed in order to enable exceptional conformity between the articular surfaces and knee kinematics, as close as possible to the physiologic one. These implants have a large contact surface. The mobile contact area between their metal and polyethylene tibial components allows for rotation and/or translation of these implants while standing under load. The advantage of those implants over fixed bearing is the possibility of auto-correction of the tibial component, avoiding the posterolateral or posteromedial tibial wear of polyethylene. Besides the excellent clinical results of some of the endoprostheses made according to the principles of this design, there remains a problem of the

occurrence of osteolysis. In this design, the small amount of debris that is created is caught between relatively mobile surfaces and creates additional debris.

Surgical factors: good surgical technique is a prerequisite for successful knee arthroplasty in all aspects, including minimizing wear and consequential osteolysis. The components of an endoprosthesis can be badly positioned in the frontal, sagittal and coronal planes. Inadequate restoration of the mechanical limb axis leads to inadequate distribution of the load on the articular surface and early degradation of the polyethylene. Minor deviations from the neutral mechanical axis lead to accelerated wear that becomes evident only after many years of functioning of the implants. The studies that dealt with this issue found extremely high correlation between wear and positions established by the mechanical shaft (Collier et al., in press). Improper positioning of components in the sagittal plane may lead to asymmetrical wear, especially for a CR component design. With this type of component malposition, knee hyperextension can also arise, leading to posterior component impingement in the PS design. Irregular wear can also occur with the malpositioning of components in the transverse plane (rotational).

At the end of the discussion about wear and osteolysis, the question that remains regards surgical management of these problems. Patients in the early stages of particulate debris and consequent osteolysis are usually non-symptomatic. Osteolytic lesions may be seen on radiographs, but with no other clinical signs, this is of no great importance. In some cases, lesions can be followed radiographically, with minimal progression in the imaging and clinical presentation. In cases of slow progression that are asymptomatic, revision surgery is not necessary. However, most of these changes have progression accompanied by significant symptomatology over time, leading to loosening of the endoprosthesis. The fields of bone resorption can progress to the point of weakening of the bone implant support and lead to peri-prosthetic or prosthetic fractures (Benevenia et al. 1998; Huang et al. 1999).

5 Fixation of Prosthesis Components

The beginnings of component fixation in TKA are linked to the introduction of polymetilmethacrylate (PMMA) in 1902 by a chemist named Otto Rohm. It was soon being used in many fields. In 1936, Kulzer discovered that mixing PMMA powder and liquid monomer resulted in a doughy mass that, by adding benzoyl peroxide and heating it at 100 C, becomes extremely solid. The first clinical use of PMMA was an attempt to close the cranial defects in monkeys in 1938. When chemists discovered a way to cause polymerization in MMA at room temperature by adding tertiary aromatic amines, a bone-like PMMA cement ensued that, with variations in production, is still in use nowadays. The modern packaging of PMMA bone cement consists of a two-component system: a polymer powder made out of PMMA and/or methacrylate copolymer, and also benzoyl peroxide as the initiator of radical polymerization. The powder includes a radio-opacitic agent and,

optionally, antibiotics. In the liquid phase, methyl methacrylate is the main ingredient, although one can sometimes find other methacrylates. At the end, an inhibitor is added that prevents premature polymerization during storage, and in some cement, color is added, too.

Radio-opacity is a desirable property so that the cement may be visible in X-rays. Studies have shown that, when using barium for this purpose, a significantly larger percentage of osteolytic changes appear. Additionally, the barium ion is poorly soluble, but highly toxic. Zirconium dioxide, on the other hand, has a significantly higher grit potential as its negative trait.

Bone cement is used for fixation of artificial joints. It fills the space between the endoprosthesis and the bone or cement-bone, as cement-endoprosthesis interfaces are also very important. The basic roles of cement are component fixation and the transfer of forces between the implant and the bone in both directions. In a case in which the interface loads exceed the load capacity of the cement, possible fractures can appear, due to fatigue.

The cement with antibiotics added is used for the gradual release of said antibiotics in cases in which need for this application is indicated. The surface of the implant is extremely suitable for the development of bacterial colonies, because in this environment, bacteria can much more easily avoid the natural defense of the organism.

The first few published series were followed by disappointing results, yet it was concluded that the cause of the failure was hidden in the design of the endoprosthesis (Insall et al. 1976). After the study was released describing the "cement disease" after cement fixation of the components, development began of design components for TKA, which are fixed in the alternate way. This idea occurred in the late '80s, and the implants manufactured showed good results. Development of the technology led to the creation of a porous metal coating, which allowed for the biological fixation of components of the endoprosthesis. The most popular surfaces at this stage were: metal beads, fiber mesh, and a plasma spray-coated surface (Berger et al. 2001). Each of these surfaces had certain disadvantages. Additional studies have shown that, although these surfaces produced very good results in THA, in TKA, they faced many problems, and most surgeons again turned to fixation with PMMA (Berger et al. 2001; Cloke et al. 2008). Particular authors believe that with good surgical technique and the proper selection of patients (young, active), cementless knee arthroplasty could have an equal share of good results as the cement, with considerably easier revision surgery (Hofmann and Scott 2002; Hofmann et al. 2002). At this moment, fixation of endoprostheses with PMMA is still the gold standard, but the steady development of materials and advances in understanding the causes of the failure of previous designs and technologies are constantly taking place.

6 Designs of Knee Endoprosthesis

Today, the following knee endoprosthesis designs are used (Table 1).

In regard to relation between the insert and the tibial plateua, there are: fixed bearing and mobile bearing endoprostheses.

There are also patients for whom only one compartment of the knee (either medial or lateral) is affected by arthritic changes, so we would perform a replacement of only one femoral and one tibial condyle with a unicondylar endoprosthesis.

6.1 The Following Terms Are Necessary to Understand the Design of a Knee Endoprosthesis

The femoral rollback means posterior translation of the femur during progressive flexion. It enables better function of the quadriceps and greater knee flexion by preventing posterior impingement during the final knee flexion through normal knee flexion controlled by LCA and LCP. Both designs of unconstrained endoprosthesis permit this: with CR preserved, LCP provides the posterior translation of the femur, as with a normal knee. In PS design, the peg on the tibial plateau in contact with the transverse bulkhead at the rear part of the intercondylar femoral component leads to a posterior displacement of the femur.

Constraint means the ability of the endoprosthesis to enable varus-valgus and flexial extensional stability at ligament weakness or bone instability. In the present design, the unconstrained condition of the endoprosthesis cannot enable stability.

Modularity means the ability to upgrade the standard endoprosthesis to compensate for bone loss or stabilizing ligament weakness or absence. The options that allow for this are:

(a) the metal tibial plateau with modular polyethylene inserts; these components are significantly more expensive than polyethylene monoblocks and have the same degree of aseptic loosening
(b) metal augmentations for the management of bone defects
(c) modular femoral and tibial stems.

Advancement of augmentation is available for intraoperative adjustments to an individual knee. The lack represents an increased degree of osteolysis of modular components and increased wear due to micro-movements between the polyethylene insert and the metal tibial component.

Table 1 Designs of knee endoprosthesis

Unconstrained	Constrained
CR-Posterior cruciate retaining	Hinged
PS-Posterior cruciate substituting	Non hinged

6.2 *Cruciate Retaining Design*

A design that has minimally limited movement depends on an intact and sufficient LCP, which provides stability in flexion. Indications for this type of prosthesis are arthritic changes with a minimum loss of bone, soft tissue with minimum laxity and preserved LCP and varus deformity <10° and valgus deformity <15°. The advantage of this type of endoprosthesis is avoidance of posterior impingement between the peg on the tibial plateau and the posterior femoral bulkhead that can occur in PS design and even fracturing of a peg. Implanting this type of prosthesis requires less bone resection (Figs. 1 and 2). Joint proprioception is better for the preservation of LCP. Those who support this design claim that its movements better emulate normal knee kinematics, but this claim has been demonstrated repeatedly and disputed in various studies.

The lack of design represents the possibility of a subsequent rupture of the LCP and consequent instability of the knee, as well as possible rapid wear of the polyethylene for LCP that are too tight.

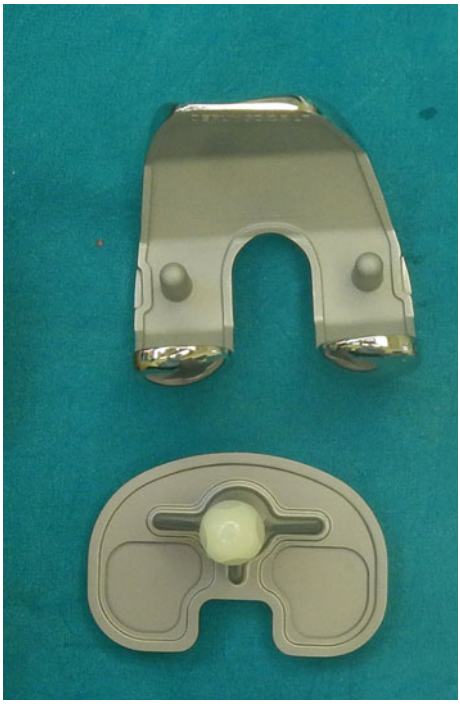

Fig. 1 Femoral and tibial components of a CR type of endoprosthesis

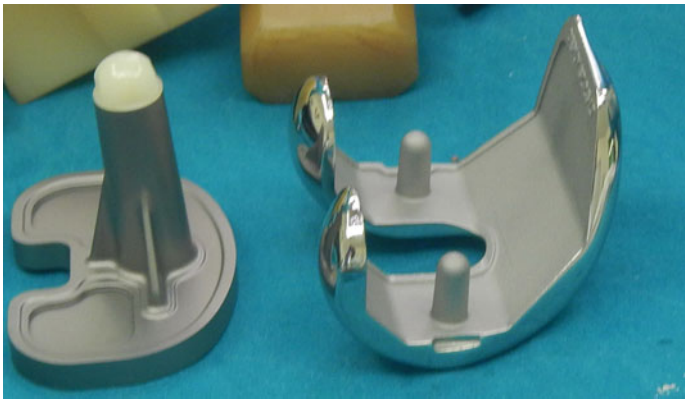

Fig. 2 Femoral and tibial components of a CR type of endoprosthesis

6.3 Posterior Stabilized Design

This design is a bit more "constrained," i.e., it has a minimum of movements that are more limited. Its implantation sacrifices LCP. As previously mentioned, the anteroposterior stability in the absence of LCP allows for the existence of the tibial plateau peg and the bulkhead at the back of the femoral components (Figs. 3 and 4). The polyethylene insert located on the tibia has much deeper articular surfaces. Indications for this type of prosthesis are: weakness of the extensor mechanism (reducing the risk of anterior instability), inflammatory arthritis (which can lead to ruptured LCP), and the absence or weakness of the LCP. The advantages of this design are the fact that it is easier to balance the knee without LCP and easier surgical exposition. The possible disadvantages are the tibial insert peg leaping over the femoral bulkhead in a case of inadequate surgical technique and ligament balance, increased wear of the polyethylene on the tibial peg, more bone resection and more frequent aseptical loosening.

6.4 Constrained Non-hinged Design Features

This is a design in which the movements are limited, with no shaft connecting the femoral and tibial components. A massive stand on the tibial part and a big box femoral component allows for varus-valgus and rotational stability. Indications for this type of prosthesis are: weakness of collateral ligaments and moderate bone deficit. This indication area is also an advantage of this design, and its disadvantages are: significantly larger bone resection of the femur and frequent aseptic loosening.

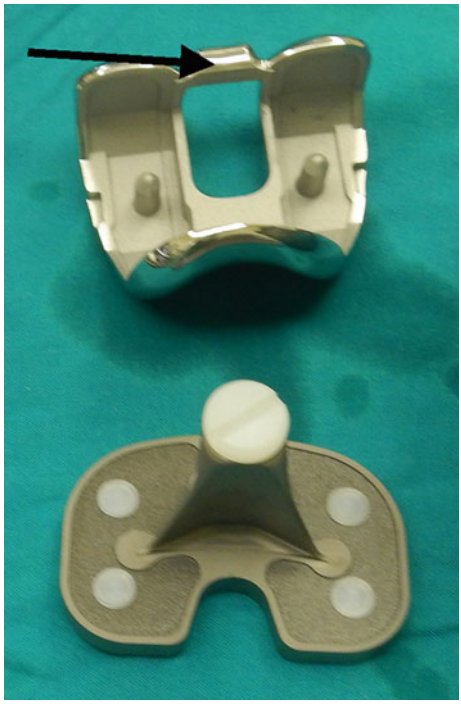

Fig. 3 Femoral and tibial components of a PS type of endoprosthesis. The *arrow marks* the posterior peg

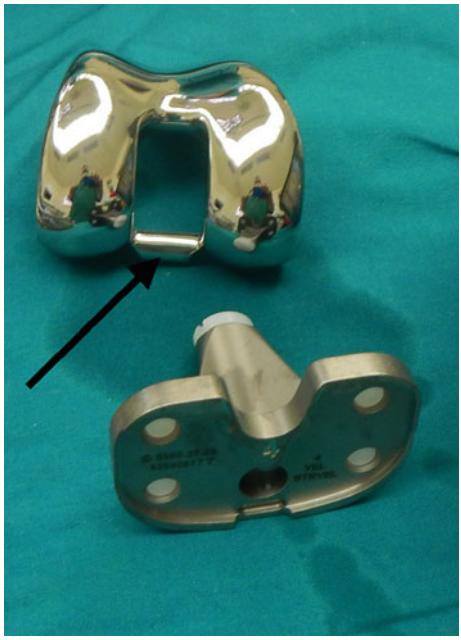

Fig. 4 Femoral and tibial components of a PS type of endoprosthesis. The *arrow marks* the posterior peg

6.5 Constrained Hinged Design

With this type of endo-prosthesis, femoral and tibial components are connected to each other by an axis that allows for rotation (the rotating hinge) (Fig. 5). Indications for this design are a global knee ligament deficit, hyperextension instability (which can be seen after tumor resection), and massive bone deficits (at the neuropathic joints). Their indication area, which makes them a salvage procedure in these states, represents the main advantage, and its principle imperfections are significant bone resection and loosening. It must be noted that the rotator hinge is a significant improvement compared with the earlier classical hinge, the design of which led to high incidences of complication, mostly loosening.

6.6 Mobile and Fixed Bearing Design

This represents a design with minimally limited movements in which the polyethylene insert can rotate on the metal tibial component whose upper surface is highly polished. It is usually implanted in younger, more active patients. As a benefit, there is an increase in the contact area that reduces overload of the polyethylene insert and wear. The disadvantage is a spin-out that occurs due to a loose flexion gap, allowing for rotation of the tibia behind the femur. Consequently, in fixed bearing, we have an insert that is rigidly fixed on the tibial component.

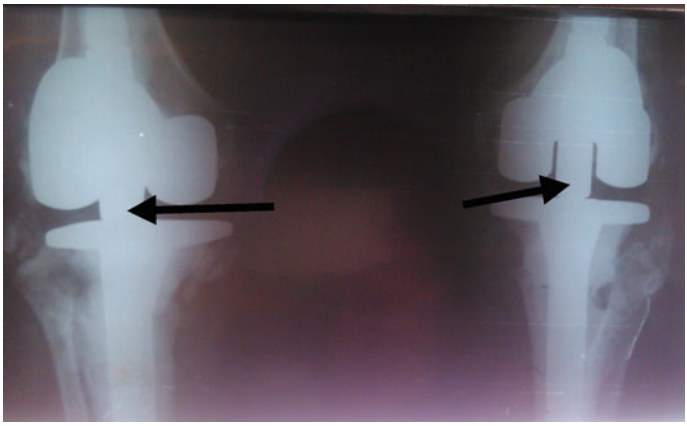

Fig. 5 X-ray of an implanted rotating hinge type of endoprosthesis. The *arrows* show the hinge that provides mediolateral stability

6.7 Unicompartmental Arthroplasty

This is performed by replacing the articular surfaces of only one condyle of the femur and tibia (Fig. 6). The indication is cartilage destruction in only one compartment of the knee. The main advantages are that it spares resection of bone tissue and generally involves less intraoperative trauma, but the disadvantage is a higher percentage of loosening compared to TKA.

6.8 Tumor and Custom-Made Endoprosthesis

This is the endoprosthesis that solves the problem of a large residual bone defect after resection of bone tumors or after a failed primary or revision knee. There are manufacturer-predefined components the combinations of which allow the endoprosthesis to be adapted or custom-made for the individual patient (modularity of prosthesis) based on CT scans and 3D knee reconstructions.

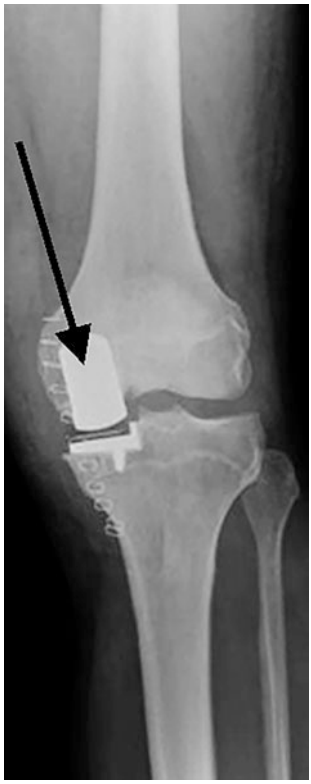

Fig. 6 X-ray of a unicondylar endoprosthesis-AP

7 Preoperative Planning

A good treatment plan is one of the key factors for successful performance of the procedure. Preoperative planning begins with the selection of appropriate candidates for knee arthroplasty. Perceiving the causes of the patient's symptoms, insight into his/her general medical condition, comorbidity, and a detailed physical examination are essential steps, as well as a good evaluation of the patient's expectations and presenting him/her with the possibility of surgery and potential complications.

8 The Indications for Knee Arthroplasty

The primary indications for total knee arthroplasty are knee pain and loss of function. Thus, clinical examination of the patient must begin with an insight into the degree and type of symptoms. There must be a complaint of pain that greatly reduces the quality of life of patients, and that is resistant to conservative treatment. The exclusion of all other possible causes must be established. In a differential diagnosis, the following usually come to mind: coxarthrosis (degeneration of hip articular cartilage) on the same side, diseases of the spine, peripheral vascular disease, meniscal pathology and knee bursitis. It should not be forgotten that the group of patients who recorded the lowest degree of satisfaction after knee arthroplasty was composed of those who experienced mild preoperative discomfort. Thus, all modalities of conservative treatment must be applied prior to surgery.

The most common indications for knee arthroplasty are gonarthrosis, inflammatory arthritis, rheumatoid arthritis, osteochondromatosis, villocondular synovitis, metabolic arthritis, osteonecrosis, gout, pseudogout, post-traumatic arthritis, and intraarticular fractures.

Gonarthrosis is osteoarthritis (OA) of the knee joint. This is a progressive disease that affects not only the cartilage, but also the subchondral bone and the soft tissue of the joint (ligaments and capsule) (Popovic 2004). Although OA is defined as a non-inflammatory disease, the synovitis that occurs can lead to an increased number of immune cells and induction of cytokines and proteases that affects the extracellular matrix of cartilage and further accelerates the progression of osteoarthritis (Sun 2010) (Figs. 7 and 8).

Gonarthrosis has unknown etiology, but is multifunctional, with lots of causal factors. The main predisposing causes for the occurrence of this condition are:

1. Increased body weight. It is considered that a BMI (body mass index) greater than 27 significantly increases the risk of gonarthrosis. Felson and coworkers showed that weight loss of 5 kg reduces the risk of developing knee OA by 50% (Felson et al.1992).
2. Physical activity. Participation in contact sports (especially football and rugby) seriously elevates the risk of knee ligament damage. After frequent training and trauma, leading to frequent micro- and macrotrauma, and after a sporting career,

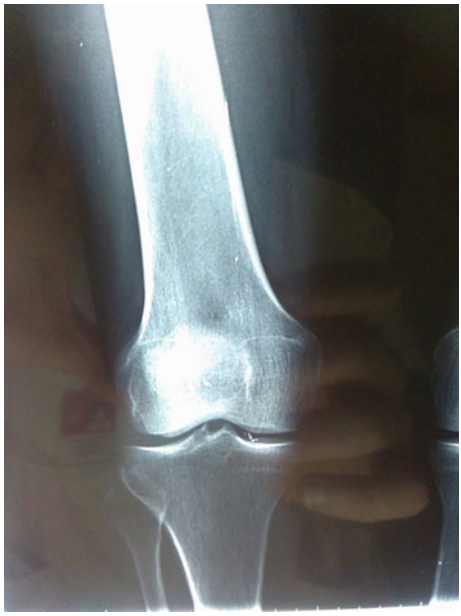

Fig. 7 X-ray of a normal knee-anteroposterior

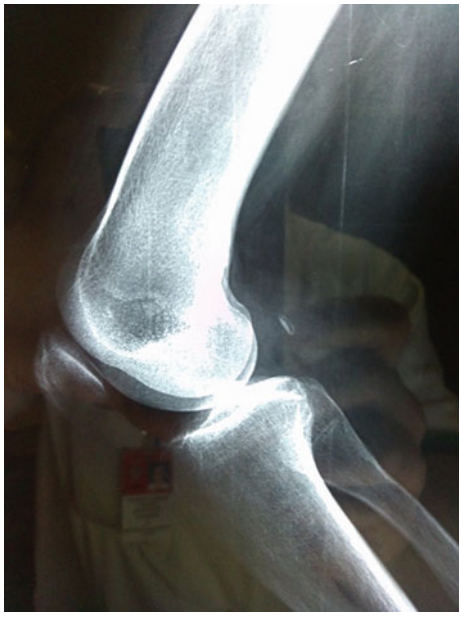

Fig. 8 X-ray of a normal knee-profile

osteoarthrosis can develop. Joint tissue is extremely sensitive to the biomechanical environment and mechanical overload. An excessive and reduced load can cause a catabolic effect (catabolism = degradation). A moderate level of exercise is one of the most important environmental factors in the maintenance of homeostasis and joint cartilage integrity. Mechanic stimulation of articular cartilage in the physiological range generates a biochemical signal that increases anabolism (building) of chondrocytes. Excessive mechanical loads can turn the balance of chondrocytes to catabolism, leading to cartilage degradation. The same effect can occur during reduced mechanical loading (immobilization), leading to thinning and softening of the cartilage, proteoglycan reduction, fibrillation of the cartilage matrix, ulcerations and erosions (Grad et al. 2011).

3. Operative removal of the meniscus (partial or total) and deformities of the knee (varus-valgus) are two other risk factors for developing osteoarthritis of the knee.
4. Older age is a significant factor, due to the cumulative effect of various risk factors and normal biological changes that make the joint less capable of regeneration.
5. Gender also affects the frequency of occurrence, with osteoarthritis in general and that of knees in particular being so much more common in women, as well as having a more serious clinical presentation (Zhang and Jordan 2010).

Radiographically, osteoarthritis is manifested by a narrowing of the joint spaces, the development of osteophytes, and subchondral sclerosis (Figs. 9,10), due to loading of the subchondral bone and development of a cyst formation in it. Over time, loss of the subchondral bone structure that gives elastic support to cartilage arises, which leads to its eventual decay. The clinical symptoms of knee OA are pain and contractures, the outcome of which leads to disorder in the functional ability of the extremities. Radiographic signs do not always correlate with the severity of the symptoms. Although X-ray is still the main tool for the diagnosis of knee OA with a supporting clinical picture, magnetic resonance imaging (MRI) and computerized tomography (CT) are also available for use in less clear cases. Standard projections in which the X-ray is performed are anteroposterior (AP) and profile recording. In special cases, a special radiograph can be applied (Merchants axial view of patellofemoral joint, tunnel view, patella sunrise shot) (Fig. 11).

8.1 Contraindications for TKA

Absolute contraindications for TKA are: knee infection, chronic and acute, absence or dysfunction of the extensor mechanism of the knee, and serious vascular disease of the lower extremity. There are relative contraindications: comorbidity, which does not provide safe anesthesia, inadequate soft tissue envelope, morbid obesity and a history of osteomyelitis in or near the knee joint.

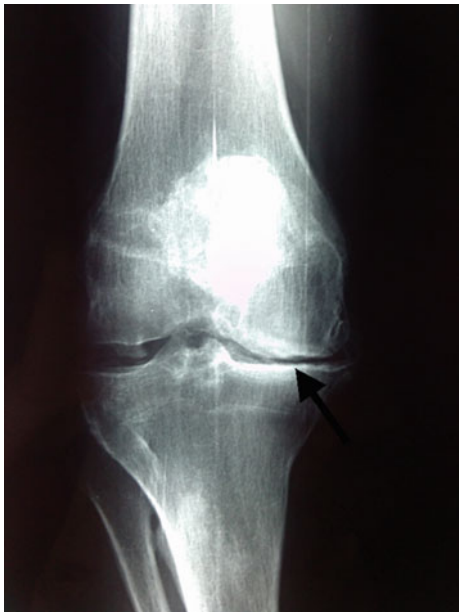

Fig. 9 X-ray of an arthrotic knee-anteroposterior (the *arrow marks* the narrowing of the joint space)

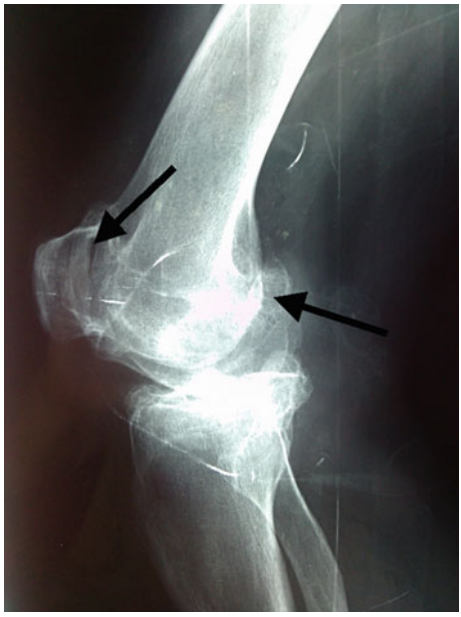

Fig. 10 X-ray of an arthrotic knee-profile (the *arrows* mark irregularities in the joint cartilage and osteophytes)

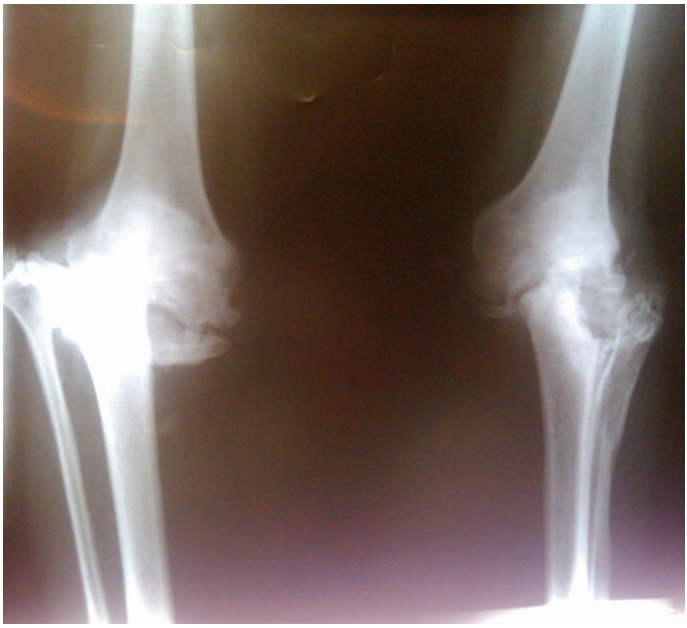

Fig. 11 X-ray of extreme gonarthrosis and subsequent ligament destruction

8.2 Preoperative Templating

Within preoperative planning, preoperative templating is very important. In particular, a preoperative determination of the probable size of the prosthesis by introduction of digital radiography by the surgeon–operator must be achieved. This process takes place with the aid of stencils that draw the prosthesis components on transparent paper suspended over an X-ray recording. With the introduction of the digital X-ray, several manufacturers have developed software that has achieved greater precision. In this way, the surgeon can plan the size of the preoperative bone resection, the size of the components and the steps needed to prepare the operation in advance. Although the intraoperative measures help determine the size of the prosthesis components more precisely, preoperative templating is considered a standard procedure nowadays (Peek et al. 2012).

9 Surgical Technique

Knee arthroplasty is performed under general endotracheal anesthesia, spinal, epidural or regional block anesthesia. The patient is positioned on their back, with the set holding the distal extension that prevents extension of the knee flexed during

the operation. Placement of the Esmarch cuff (tourniquet) is optional and depends on the surgical school and personal preference of the surgeon. In a case in which the tourniquet is positioned, intra- and postoperative bleeding is less likely and results in a cleaner cement box. On the other hand, applying an Esmarch can lead to a higher percentage of complications, such as thromboembolism (Tai et al. 2011), superficial wound infection, hematoma, the occurrence of bullous skin changes (Alcelik et al. 2012), nerve injury (Wilgis 1971), and vascular injury (especially when there are atherosclerotic alterations) (Irvine and Chan 1986). One of the main factors that influences the frequency and severity of the occurrence of complications in the application of an Esmarch is the length of its application (Olivecrona et al. 2013).

The most common surgical approach for arthroplasty of the knee is medial parapatellar arthrotomy (Langenbeck) (Fig. 12). Besides this, other approaches used are: the lateral parapatellar, subvastus approach, U-shaped (Textor), an inverse U-shaped (Putti), H-shaped (Ollier), and the S form (Payr).

By cutting the soft tissue, the distal femoral bone stumps are exposed. Then, the standard anatomical points upon which the positioning of the components of the prosthesis will be oriented in all planes are marked (Fig. 13). By determining the anatomical points, with the help of instruments and tools, cutting of the articular surface begins.

The instrumentation itself can be extra- and intra-medullar. Extra-medullar instrumentation is placed on the outside of the bones and oriented to external markers on the bone until the intramedullary instrumentation is placed in the medullary bone canal (Fig. 14).

Each producer of endoprostheses has its own instruments for implantation, which requires specificity and good training of the surgeons involved (Fig. 15).

After resection of the articular surfaces (Figs. 16, 17, 18 and 19), the adequacy of the same is tested with the trial component (Fig. 20).

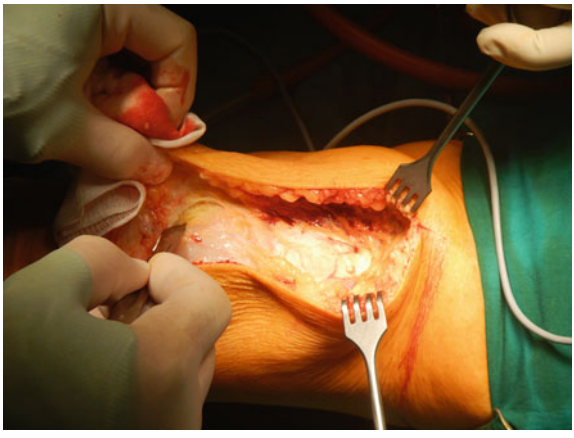

Fig. 12 Surgical approach for total condylar knee arthroplasty

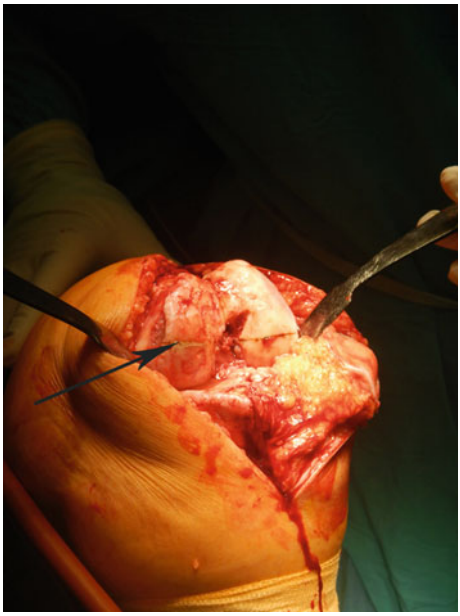

Fig. 13 Exposed articulating surfaces of the femur and tibia. The *arrow* shows the marked biepicondylar line and longitudinal femur axis line

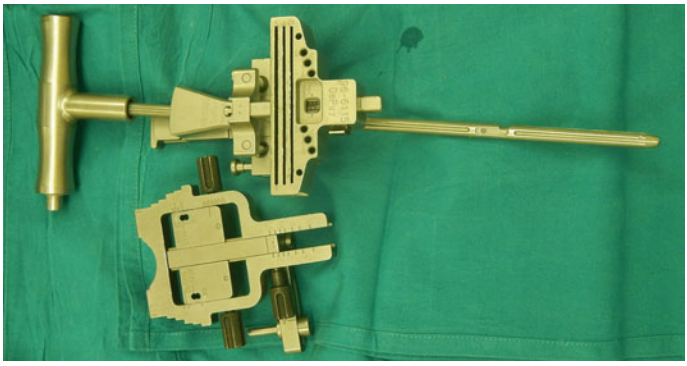

Fig. 14 Intramedullar instrumentation for the femur

After assistance of the instrumentation approach towards the proximal part of the tibia in a similar way, the degree and size of the bone resection depend on the size and type of the deformity, as well as the design of the endoprothesis. Thus, preoperative planning is crucial, since it enables selection of the right design and size of prosthesis and predicts the bone resection of the articular surfaces. After finishing the processing, the articular surface test components are positioned so as to check

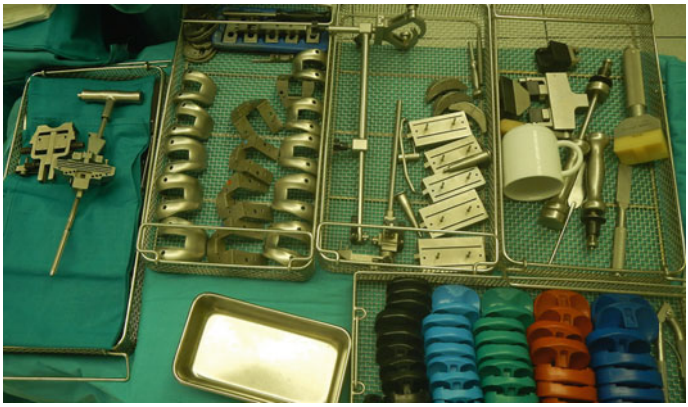

Fig. 15 Some of instruments for implantation of a totalcondylar knee endoprosthesis

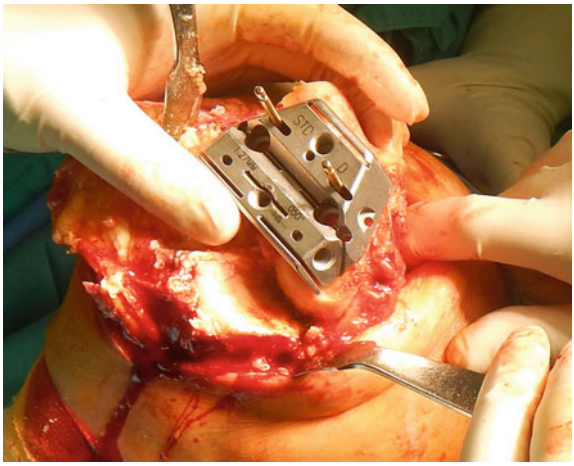

Fig. 16 Femoral cut block positioned

the adequacy of the previous procedures and the various thicknesses of the inserts testing the mobility and stability of the artificial joint. Then, the trial components are removed, and the resected surface is thoroughly rinsed, dried and time-prepared for femoral and tibial cementing. The definitive component is placed and fixed with bone cement with the trial insert positioned between the articular surfaces (Figs. 21, 22 and 23).

The time necessary for the cement to harden depends on several factors: the type of cement mixing, the viscosity of the cement itself, the possible presence of antibiotics, and outdoor temperature. The average time ranges from 10 to 15 min. Then, once again, the optimal c thickness of the insert is tested in terms of knee stability and mobility, and the desired definitive thickness is then set. The next step is hemostasis, and finally, the suturing of the operative wound in layers and bandaging.

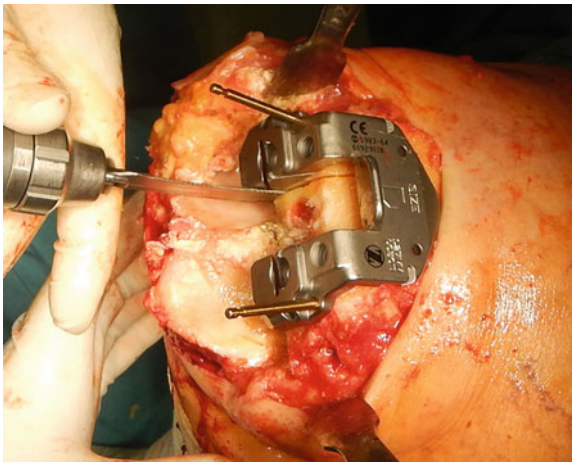

Fig. 17 Femoral notch cut block positioned (PS type of endoprosthesis)

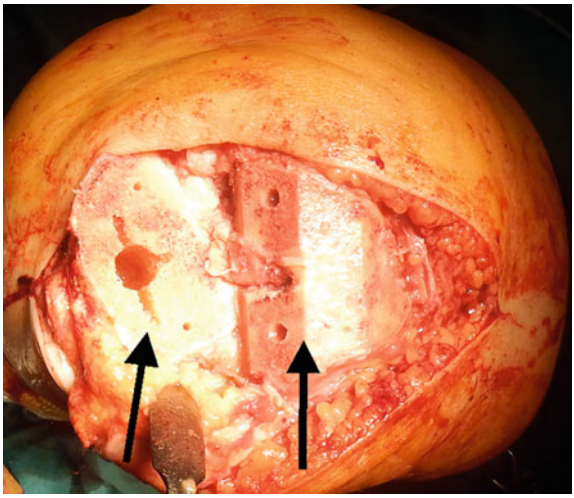

Fig. 18 Resected articulating surfaces of the femur and tibia, marked with *arrows*

Recently, navigation systems for determining the component's position have been developed. The navigational system consists of a sensor that detects the position of the marker in space, while exposing bone epiphyses of the femur and tibia with a special marker instrument, in order to measure the standard anatomical parameters of the bones to meet the demands of the software. Either an assistant or the surgeon her/himself manipulates a touch-screen monitor through the coated sterile cover. By marking the anatomical points requested by the software program, it deals with this information and displays the image based on the knee sensors. Each of the resection blocks wears a sensor, so that at any time, thanks to a real-time picture on the monitor, the adequacy position of the cut-blocks can be

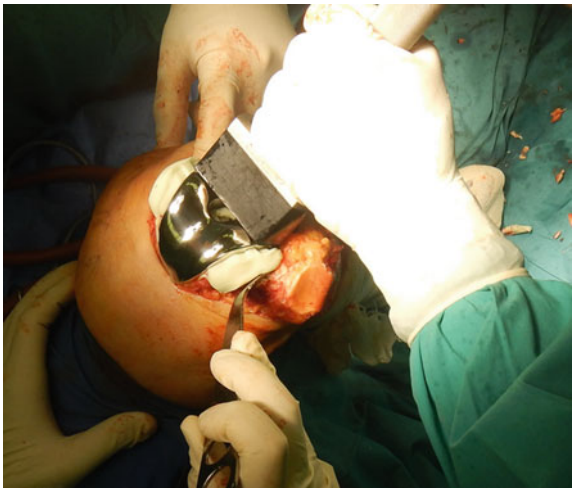

Fig. 19 Implantation of the endoprosthesis components

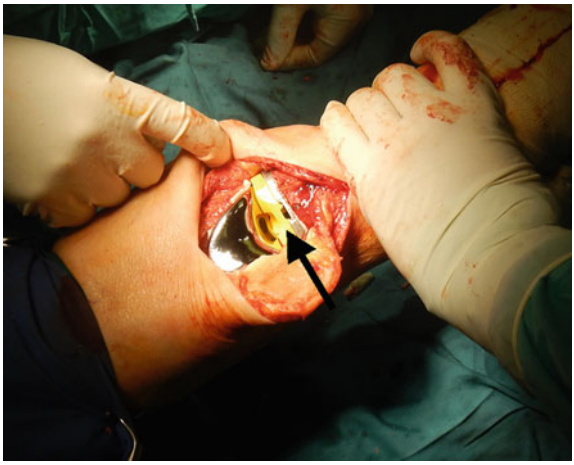

Fig. 20 Endoprosthesis components with trial insert (marked by *arrow*)

controlled. There are constant readouts on the monitor of the values of all parameters of the position of the prosthesis so that the possibility of malposition of the components can be reduced.

10 Complications of Knee Arthroplasty

After implantation of the prosthesis in the knee joint, there is the possibility of complications. The factors specific to implants in the knee joint are relatively poor coverage of the knee joint with soft tissues and the disproportionate size of the

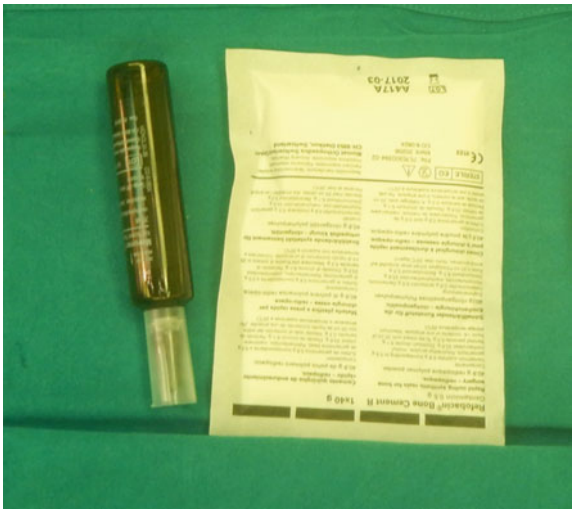

Fig. 21 Bone cement components

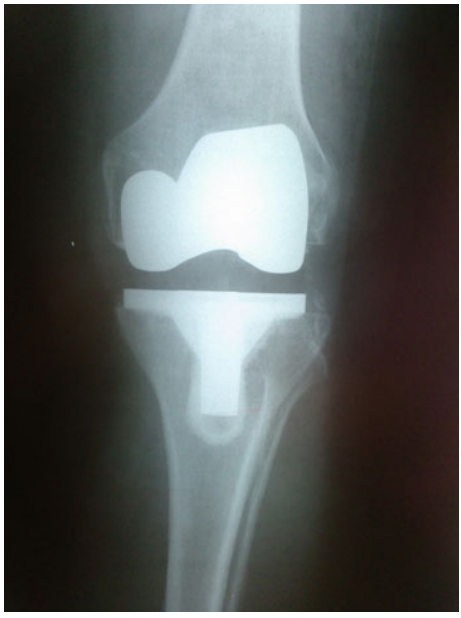

Fig. 22 X-ray of an implanted totalcondylar endoprosthesis anteroposterior

foreign body in relation to the dimensions of the joint. The occurrence of complications is more commonly associated with aging patients (especially common in people older than 65), associated comorbidity, the hospital conditions under which they tend to develop, and the intervention of design prostheses (Katz et al. 2004).

Infections can be superficial and deep. Superficial infections are treated with parenteral antibiotics and surgical methods, such as debridement and drainage.

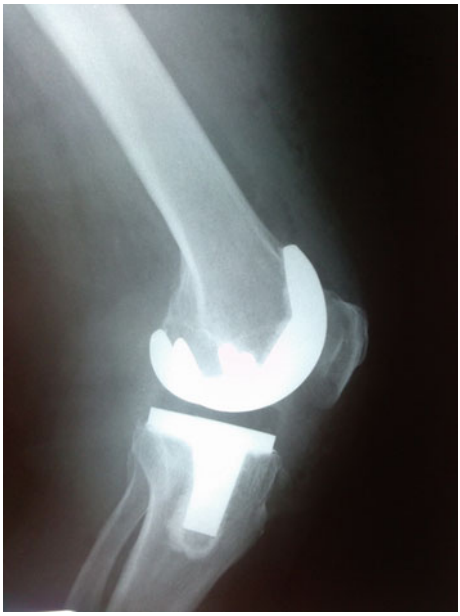

Fig. 23 X-ray of an implanted total condylar endoprosthesis profile

Deep infections are treated with radical surgical treatment and reartroplastics in one or two acts. Other modalities of eradicating infection include arthroscopic debridement, arthrodesis, and amputation in the most severe cases. The incidence of infection has differed according to some publications, ranging from 0.6 to 1.8% (Font-Rodriquez et al. 1997; Cheung et al. 2008), but may go as high as 12% (Blom et al. 2004). A high percentage of infection in this case is associated with the use of hinged prostheses, the presence of rheumatoid arthritis and previous surgical interventions on the knee (Bengtson and Knutson 1991). Mortality due to complications occurred in 0.53% of patients (Cheung et al. 2008).

Periprosthetic fractures represent a severe complication that can be localized to the tibia, fibula and femur, where the most common is a supracondylar fracture (Hajdu et al. 2004). Risk factors for supracondylar femoral fractures are osteopenia, a severe form of osteoporosis, weaker flexion, femoral notching and rheumatoid arthritis. Periprosthetic fractures occur with an incidence of 0.3–2.5%. It is accepted nowadays that surgical treatment is the method of choice for these complications (Culp et al. 1987; Healy et al. 1993; Shinsky et al. 2001). The incidence of fractures of the patella after TKA is 1–2% (Harwin 1998; Lynch et al. 1987; Ortiguera and Berry 2002). Predisposing factorising of lateral release and maltracking will injure the badly positioned implant (Chalidis et al. 2007; Keating et al. 2003). The solution of these complications depends on localization, comminution, preservation of the extensor mechanism, the stability of the implant and bone quality. Modality treatment includes conservative treatment, osteosynthesis and patellectomy.

Septic and aseptic loosening and patellar complications are frequent causes of revision of knee endoprosthesis. The factors that influence the occurrence of these

complications are positioning and shape of the implant components, the existence of knee deformity (valgus) and the condition of the peripatellar structures (retinaculum and collateral ligament) (Nelissen et al. 1992).

One of the most common causes of pain after total knee arthroplasty is instability, in which the pain is caused by abnormal stress on the knee and soft tissue shell. After TKA, instability can occur in flexion, extension, mid-flexion, hyperextension and global instability (Parratte and Pagnano 2008). Instability in the early postoperative period occurs due to inadequate ligamentary balance, iatrogenic injuries of the ligaments, discrepancies in flexion and extensional gaps, or previous neuromuscular pathology. Late instability can occur due to poor positioning of prosthesis components, secondary ligament elongation, polyethylene wear, and loosening of components (Parratte and Pagnano 2008). Treatment of these complications includes procedures for physical rehabilitation, rearthroplasty of a hinged endoprosthesis, and arthrodesis, all depending on the cause and degree of instability (Yoshiya et al. 2001).

Osteolysis and shearing occur as the consequences of debris originating from the articular surfaces or parts of the implant. The mechanical properties of the implant, and thus the process of superficial abrasion, have an impact on the way the implant components are sterilized. Sterilization by gamma irradiation reduces the mechanical properties of the implant by lowering the rate of oxidation of the polyethylene components (Naudie et al. 2007; Cheung et al. 2008).

Nerve damage occurs in 0.9–1.3% of patients. The most common is peroneal nerve damage (Schinsky et al. 2001). Vascular injuries are rare and usually related to lesions on the popliteal arteries. Surgical incision may be complicated by superficial complications such as erythema, infection and skin necrosis. Opinions on the use of drainage for this type of intervention are controversial, because many publications favor greater blood loss in the implementation of drainage (Parker et al. 2004).

Deep vein thrombosis (DVT) and pulmonary embolism are possible serious complications of this intervention. DVT is diagnosed on the basis of clinical, ultrasound examination and venography. For thromboprophylaxis aspirin, low molecular weight heparin and warfarin can be used (Eikelboom et al. 2001).

Stiffness, one of the complications of knee arthroplasty, occurs as a result of inadequate size or incorrect positioning of the implant, infection, inadequate bone resection, elevation of the articular line, ligament imbalance and heterotopic ossification. Its incidence is from 1.3 to 12%.

References

Alcelik I, Pollock RD, Sukeik M (2012) A comparison of outcomes with and without a tourniquet in total knee arthroplasty: a systematic review and meta-analysis of randomized controlled trials. J Arthroplasty 27:331–340

Bartel DL, Bicknell VL, Wright TM (1986) The effect of conformity, thickness, and material on stresses in ultra-high molecular weight components for total joint replacement. J Bone Joint Surg Am 68:1041–1051

Benevenia J, Lee FY, Buechel F, Parsons JR (1998) Pathologic supracondylar fracture due to osteolytic pseudotumor of knee following cementless total knee replacement. J Biomed Mater Res 43:473–477

Bengtson S, Knutson K (1991) The infected knee arthroplasty. A 6-year follow-up of 357 cases. Acta Orthop Scand 62(4):301–311

Benjamin J, Szivek J, Dersam G, Persselin S, Johnson R (2001) Linear and volumetric wear of tibial inserts in posterior cruciate-retaining knee arthroplasties. Clin Orthop Relat Res 392: 131–138

Berger RA, Lyon JH, Jacobs JJ, Barden RM, Berkson EM, Sheinkop MB, Rosenberg AG, Galante JO (2001) Problems with cementless total knee arthroplasty at 11 years followup. Clin Orthop Relat Res 392:196–207

Blom AW, Brown J, Taylor AH, Pattison G, Whitehouse S, Bannister GC (2004) Infection after total knee arthroplasty. J Bone Joint Surg Br 86(5):688–691

Bobyn JD, Poggie RA, Krygier JJ, Lewallen DG, Hanssen AD, Lewis RJ, Unger AS, O'Keefe TJ, Christie MJ, Nasser S, Wood JE, Stulberg SD, Tanzer M (2004) Clinical validation of a structural porous tantalum biomaterial for adult reconstruction. J Bone Joint Surg Am 86 (2):123–129

Bohl JR, Bohl WR, Postak PD, Greenwald AS (1999) The coventry award: The effects of shelf life on clinical outcome for gamma sterilized polyethylene tibial components. Clin Orthop Relat Res 367:28–38

Chalidis BE, Tsiridis E, Tragas AA, Stavrou Z, Giannoudis PV (2007) Management of periprosthetic patellar fractures: a systemic review of literature. Injury 38:714–724

Cheung A, Goh SK, Tang A, Keng TB (2008) Complications of total knee arthroplasty. Current Orthopaedics 22:274–283

Cloke DJ, Khatri M, Pinder IM, McCaskie AW, Lingard EA (2008) 284 press-fit Kinemax total knee arthroplasties followed for 10 years: poor survival of uncemented prostheses. Acta Orthop 79(1):28–33

Collier JP, Sperling DK, Currier JH, Sutula LC, Saum KA, Mayor MB (1996) Impact of gamma sterilization on clinical performance of polyethylene in the knee. J Arthroplasty 11:377–389

Collier MB, Engh CA Jr, Engh G (in press) The correlation between limb alignment and polyethylene wear in retrieved total knee arthroplasties. J Bone Joint Surg Am

Culp RW, Schmidt RG, Hanks G, Mak A, Esterhai JL Jr, Heppenstall RB (1987) Supracondylar fracture of the femur following prosthetic knee arthroplasty. Clin Orthop 222:212–222

Eikelboom JW, Quinlan DJ, Douketis JD (2001) Extended-duration prophylaxis against venous thromboembolism after total hip or knee replacement: a meta-analysis of the randomised trials. Lancet 7 358(9275):9–15

Felson DT, Zhang Y, Anthony JM, Naimark A, Anderson JJ (1992) Weight loss reduces the risk for symptomatic knee osteoarthritis in women. The Framinghan study. Ann Intern Med 116(7):535–539

Feng EL, Stulberg SD, Wixson RL (1994) Progressive subluxation and polyethylene wear in total knee replacements with flat articular surfaces. Clin Orthop Relat Res 299:60–71

Font-Rodriquez DW, Scuderi GR, Insall JN (1997) Survivorship of cemented total knee arthroplasty. Clin Orthop 345:79–86

Grad S, Eglin D, Alini M, Stoddart MJ (2011) Physical stimulation of chondrogenic cells in vitro: a review. Clin Orthop Relat Res 469(10):2764–2772

Hajdu L, Stojković-Jovanović T, Mikulić S, Kević S (2004) Complications after implantation of total knee replacement and treatment options. News Neurol Psychiatr Border Areas 616.728.3-089.28-06

Harwin SF (1998) Patellofemoral complications in symmetrical total knee arthroplasty. J Arthroplast 13:753–762
Healy WL, Silski JM, Incavo SJ (1993) Operative treatment of distal femoral fractures proximal to total knee replacements. J Bone Joint Surg 75-A:27–34
Hirakawa K, Bauer TW, Stulberg BN, Wilde AH, Borden LS (1996) Characterization of debris adjacent to failed knee implants of 3 different designs. Clin Orthop Relat Res 331:151–158
Hofmann AA, Scott DF (2002) Cementless total knee arthroplasty. In: Scuderi GR (eds) Surgical techniques in total knee arthroplasty. Springer, New York, Inc., pp 262–27
Hofmann AA, Heithoff SM, Camargo M (2002) Cementless total knee arthroplasty in patients 50 years or younger. Clin Orthop Relat Res 404:102–107
Huang CH, Yang CY, Cheng CK (1999) Fracture of the femoral component associated with polyethylene wear and osteolysis after total knee arthroplasty. J Arthroplasty 14:375–379
Insall JN, Ranawat CS, Aglietti P, Shine J (1976) A comparison of four models of total knee-replacement prostheses. J Bone Joint Surg Am 58(6):754–765
Irvine GB, Chan RN (1986) Arterial calcification and tourniquets: letter. Lancet 2:1217
Jacobs JJ, Roebuck KA, Archibeck M, Hallab NJ, Glant TT (2001) Osteolysis: basic science. Clin Orthop Relat Res 393:71–77
Katz JN, Barrett J, Mahomed NN, Baron JA, Wright RJ, Losina E (2004) Association between hospital and surgeon procedure volume and the outcomes of total knee replacement. J Bone Joint Surg Am 86(9):1909–1916
Keating EM, Haas G, Meding JB (2003) Patella fracture after post total knee replacements. Clin Orthop 416:93–97
Kyriakides TR, Hartzel T, Huynh G, Bornstein P (2001) Regulation of angiogenesis and matrix remodeling by localized, matrix-mediated antisense gene delivery. Mol Ther 3:842–849
Lynch AF, Rorabeck CH, Bourne RB (1987) Extensor mechanism complications following total knee arthroplasty. J Arthroplasty 2:135–140
Mano T, Ueyama Y, Ishikawa K, Matsumura T, Suzuki K (2002) Initial tissue response to a titanium implant coated with apatite at room temperature using a blast coating method. Biomaterials 23:1931–1936
McKellop H, Shen FW, Lu B, Campbell P, Salovey R (1999) Development of an extremely wear-resistant ultra high molecular weight polyethylene for total hip replacements. J Orthop Res 17:157–167
Migirov L, Kronenberg J, Volkov A (2011) Local tissue response to cochlear implant device housings. Otol Neurotol 32:55–57
Mont MA, Yoon TR, Krackow KA, Hungerford DS (1999) Eliminating patellofemoral complications in total knee arthroplasty: clinical and radiographic results of 121 consecutive cases using the Duracon system. J Arthroplasty 14:46–55
Mrvaljević D (2006) Anatomy of the lower extremity—membrum inferius, 14th edn. Savremena Administracija, Beograd
Muratoglu OK, Bragdon CR, Jasty M, O'Connor DO, Von Knoch RS, Harris WH (2004) Knee-simulator testing of conventional and cross-linked polyethylene tibial inserts. J Arthroplasty 19:887–897
Naudie DD, Ammeen DJ, Engh GA, Rorabeck CH (2007) Wear and osteolysis around total knee arthroplasty. J Am Acad Orthop Surg 15(1):53–64
Nelissen RG, Brand R, Rozing PM (1992) Survivorship analysis in total condylar knee arthroplasty. A statistical review. J Bone Joint Surg 74(3):383–389
Nikolic D (2006) Meniscal and ligaments injures. Belgrade
Olivecrona C, Lapidus LJ, Benson L, Blomfeldt R (2013) Tourniquet time affects postoperative complications after knee arthroplasty. Int Orthop 37(5):827–832. doi:10.1007/s00264-013-1826-4
Ortiguera CJ, Berry DJ (2002) Patellar fracture after total knee arthroplasty. J Bone Joint Surg 84:532–540
Parker MJ, Roberts CP, Hay D (2004) Closed suction drainage for hip and knee arthroplasty. A meta-analysis. J Bone Joint Surg Am 86-A(6):1146e52

Parratte S, Pagnano MW (2008) Instability after total knee arthroplasty. J Bone Joint Surg Am 90(1):184–194
Peek AC, Bloch B, Auld J (2012) How useful is templating for total knee replacement component sizing? Knee 19(4):266–269
Popovic Z (2004) Diseases of the knee. In: Vukašinović Z (eds) Special orthopedics. Institute for Orthopedic Surgery "Banjica", Belgrade
Puloski SK, McCalden RW, Mac-Donald SJ, Rorabeck CH, Bourne RB (2001) Tibial post wear in posterior stabilized total knee arthroplasty: an unrecognized source of polyethylene debris. J Bone Joint Surg Am 83:390–397
Rand JA (1994) Current concepts review. The patellofemoral joint in total knee arthroplasty. J Bone Joint Surg 76-A:612–619
Rossi S, Tirri T, Paldan H, Kuntsi-Vaattovaara H, Tulamo R, Narhi T (2008) Peri-implant tissue response to TiO_2 surface modified implants. Clin Oral Implants Res 19:348–355
Schinsky MF, Macaulay W, Parks ML, Kiernan H, Nercessian OA (2001) Nerve injury after primary total knee arthroplasty. J Arthroplasty 16:1048
Schmalzried TP, Jasty M, Rosenberg A, Harris WH (1994) Polyethylene wear debris and tissue reactions in knee as compared to hip replacement prostheses. J Appl Biomater 5:185–190
Schroeder-Boersch H, Scheller G, Fischer J, Jani L (1998) Advantages of patellar resurfacing in total knee arthroplasty. Two-year results of a prospective randomized study. Arch Orthop Trauma Surg 117:73–78
Scuderi GR (2011) Complications after total knee arthroplasty. How to manage patients with osteolysis. J Bone Joint Surg 93:2127–2135
Spitzer AI, Vince KG (1995) Patellar considerations in total knee replacement. In: Scuderi GR (ed) The Patella. Springer, New York
Sun HB (2010) Mechanical loading, cartilage degradation, and arthritis. Ann N Y Acad Sci 1211 (1/2010):37–50
Tai TW, Lin CJ, Jou IM (2011) Tourniquet use in total knee arthroplasty: a metaanalysis. Knee Surg Sports Traumatol Arthrosc 19:1121–1130
Tanner MG, Whiteside LA, White SE (1995) Effect of polyethylene quality on wear in total knee arthroplasty. Clin Orthop Relat Res 317:83–88
Wasielewski RC, ParksN Williams I, Surprenant H, Collier JP, Engh G (1997) Tibial insert undersurface as a contributing source of polyethylene wear debris. Clin Orthop Relat Res 345:53–59
Wilgis EF (1971) Observations on the effects of tourniquet ischaemia. J Bone Joint Surg 53: 1343–1346
Won CH, Rohatgi S, Kraay MJ, Goldberg VM, Rimnac CM (2000) Effect of resin type and manufacturing method on wear of polyethylene tibial components. Clin Orthop Relat Res 376:161–171
Yoshiya S, Kurosaka M, Kuroda R (2001) Complications of total knee arthroplasty. Progress Clin Med JMAJ 44(5):235–240
Zhang Y, Jordan JM (2010) Epidemiology of osteoarthritis. Clinical Geriatric Medicine 26 (3/2010):355–369

Total Endoprothesis of Hip Joint: Characteristics and Application in Patients in the Central Region of Serbia

Maja Vulović, Branko Ristić, Ivana Živanović-Mačužić, Dejan Jeremić, Neda Ognjanović, Marija Kovačević, Zoran Popovic, Aleksandar Radunović, Zoran Milenkovic, Miloš Milosavljević, Bojan Milosevic and Marko Spasic

Abstract Total hip arthroplasty is a surgical procedure in which the hip joint is replaced with an artificial one. Performance of this procedure requires knowledge of the anatomical features of the joint, the characteristics of the endoprosthesis, and the needs and pathological and physiological characteristics of the patient. This retrospective analysis includes the data contained in 874 medical histories of patients of both sexes implanted with a unilateral total hip endoprosthesis who were treated

M. Vulović (✉) · I. Živanović-Mačužić · D. Jeremić · N. Ognjanović · M. Kovačević
Department of Anatomy, Faculty of Medical Sciences, University of Kragujevac, Svetozara Markovica 69, Kragujevac, Serbia
e-mail: maja@medf.kg.ac.rs

I. Živanović-Mačužić
e-mail: ivanaanatom@yahoo.com

D. Jeremić
e-mail: dejananatom@yahoo.com

N. Ognjanović
e-mail: ognjanovic.neda@yahoo.com

M. Kovačević
e-mail: marijakovacevic.mk@gmail.com

B. Ristić · B. Milosevic · M. Spasic
Department of Surgery, Faculty of Medical Sciences, University of Kragujevac, Svetozara Markovica 69, Kragujevac, Serbia
e-mail: branko.ristic@gmail.com

B. Milosevic
e-mail: drbojanzm@gmail.com

M. Spasic
e-mail: drmspasic@gmail.com

B. Ristić · Z. Milenkovic
Clinic for Orthopedic Surgery and Traumatology, Clinical Center Kragujevac, Zmaj Jovina 30, Kragujevac, Serbia
e-mail: drzmilenkovic@yahoo.com

F. Zivic et al. (eds.), *Biomaterials in Clinical Practice*,
https://doi.org/10.1007/978-3-319-68025-5_28

at the Orthopedic Clinic of the Clinical Center, Kragujevac, from January 1st, 2009 to December 1st, 2014. Analysis of the data revealed that 69.3% of the patients were women. The most common type of implanted prosthesis was the cementless one, and the most frequent indication was degenerative joint damage. Total arthroplasty of the hip joint has become one of the most common interventions in orthopedic surgery. The increasing need for this method of treatment required the development of new biomaterials, as well as new types of prosthesis, which, in the future, will decrease the occurrence of adverse reactions and complications during and after implantation of the prosthesis, as well as extending their useful life.

Keywords Hip prosthesis · Complications · Biomaterials

1 Introduction

Total hip arthroplasty is the operative procedure that replaces the hip joint with an artificial one. It has remained the most commonly performed and successful reconstructive procedure in orthopedic surgery since its introduction more than 40 years ago (Charnley 1972). Application of this procedure requires knowledge of the anatomical features of the joint, the characteristics of the endoprosthesis, and the needs and pathological and physiological characteristics of the patient.

1.1 The Anatomy of the Hip Joint

The hip joint connects the upper end of the femur with the pelvic bone. The articular surfaces of the head of the femur and the patellar pelvic bone (*acetabulum*) are covered with articular cartilage.

Z. Popovic · A. Radunović
Clinic for Orthopedic Surgery and Traumatology, Military Medical Academy, Crnotravska 17, Belgrade, Serbia
e-mail: ortopop@gmail.com

A. Radunović
e-mail: aradunovic71@gmail.com

M. Milosavljević
Clinical Center Kragujevac, Zmaj Jovina 30, Kragujevac, Serbia
e-mail: m.milosavljevic77@gmail.com

B. Milosevic · M. Spasic
General and Thoracic Surgery Department, Clinical Center Kragujevac, Zmaj Jovina 30, Kragujevac, Serbia

The femur, also known as the thigh bone, is the longest bone in the human body. Its upper extremity is joined with the pelvic bone, and its lower end, the distal one, with the tibia and the patella. The upper extremity consists of the head, neck and trochanteric massif (large and small trochanter) (Fig. 1). The body of the femur is long, directed obliquely downward and inward and cylindrical in shape. The lower extremity, more massive than the upper one, consists of two massive bony protuberances: the external and internal condyles.

The head of the femur has the shape of an irregular sphere and represents two-thirds of the full sphere, with an average radius of about 25 mm. It tends to be larger in men than in women. Its size and shape determine the parameters corresponding to the acetabulum. It is covered with articular cartilage and retracts into the acetabulum of the pelvic bone. With the rest of the femoral neck, it is connected and flattened in the sagittal direction and is 35–50 mm long. It carries the fossa, which is used for the ligament of the femoral head that supplies blood to the joint, but has no role in the stability of the joint. The head of the femur is vascularised from three sources: through small blood vessels located inside the connections of the femoral head (*ligamentum teres*), from the blood vessels of the medullary canal,

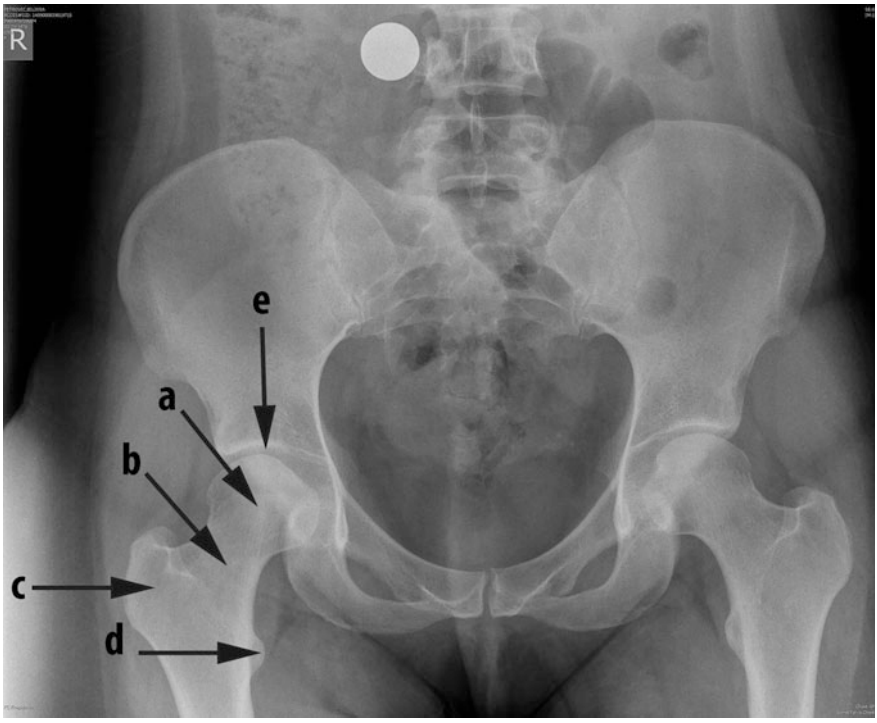

Fig. 1 X-ray of the hip joint. *Arrow a* indicates the head of the femur, *arrow b* indicates the femoral neck, *arrow c* indicates the greater trochanter, *arrow d* indicates the lesser trochanter, and *arrow e* indicates the acetabulum

and from the blood vessels that surround the neck of the femur. The medial circumflex femoral artery plays a particularly important role.

The neck of the femur, together with the axis of the body, forms an angle open inward and downward, called the collo-diaphyseal angle, with an average size of 125° (125°± 5°). The size of this angle changes during the lifespan, so that at birth, it is 150°, while later on, due to bone remodeling, it diminishes to a value of 125°. The neck makes a straight and slight medial rotation, which is called anteversion and is 15°–20°. The collo-diaphyseal angle can be increased, as in coxa valga (values higher than 130°), or decreased, as in coxa vara (values less than 120°). This angle makes it easier to perform reefs in the hip joint and is also usually higher in men than in women. The neck is wider towards the body of the femur than it is towards the head, and between them, it is narrowest, with the two sides. At the front side of the neck, the joint capsule of the hip joint attaches to the intertrochanteric line (Fig. 1).

The bone massif located outside of the neck, where the gluteal muscles are attached, is called the greater trochanter. Beside it, there is the lesser trochanter and the femoral tubercle, which represents the top intertrochanteric line immediately above the upper aspect of the neck. On the outer and distal sides of the greater trochanter is the bony crease where the outer head of a large four-headed thigh muscle, the "vastus lateralis ridge," is attached to the bone. This crease can be partially covered with trochanteric bursa. Good identification of the ridge is very important if osteotomy of the greater trochanter or the greater exposure during the surgical procedure is planned. The lesser trochanter is a small conical protrusion that is separated from the lower part of the rear neck and has two facets: the striated one and smooth one, which aligns with a large adductor of the thigh and the uneven inner side, attaching to m. iliopsoas. It is an excellent marker for orientation during surgery, because its position corresponds to the transcondyllar line of the femur (Mrvaljević 2006).

1.2 Acetabulum

On the outer side of the pelvis, there is a hinge cup, the acetabulum, which is in the form of a recess of semicircular shape about 60 mm in diameter, as shown in Fig. 1 (the arrow e indicates the acetabulum). It is built out of portions of all three pelvic bones in different percentages: the iliac bone makes up two-fifths (40%), the pubic bone one-fifth (20%) and the ischium two-fifths (40%) (Schuenke et al. 2006). These three pieces of bone are connected by three-radial cartilage, whose fusion begins at the age of 14–16 and ends around 23 years (Moore and Dalley 2006). The articular surface of the acetabulum is of semilunar form, within which a piece of cartilage in a horseshoe shape is found. The acetabulum is surrounded by an unequally expressed circumferential edge, the margin of the acetabulum (limbus acetabuli), which consists of three notches, of which the acetabular groove is particularly deep. On the peripheral edge, the labrum acetabuli are fixed; their role

is to deepen the articular surface of the acetabulum and restrict the movement of synovial fluid to the peripheral parts of the hip. The labrum follows the entire circumference of the acetabulum, except in the lower part, in the area of the acetabular groove, where the transverse ligament of the acetabulum is located. It is vascularized by upper and lower gluteal arteries and the obturator artery. The non-articular part of the acetabulum is the fossa acetabuli. It is filled with grease and blood vessels for vascularisation of the hip joint. In the horizontal plane, the acetabulum is oriented at an angle of 45°, and in the sagittal plane, at an angle of 15° (Mrvaljević 2006).

1.3 Articular Capsule

The hip joint (Fig. 1) is a synovial joint, or a diarthrodial, wrapped up in the joint capsule and ligaments, the synovial membrane being filled with synovial fluid (Byrne et al. 2010). The joint capsule is a two-layer structure that surrounds the hip joint and consists of fibrous outer and inner synovial membranes. It is attached to the forward part of the femur, back on the intrertrochanteric line, and on one finger inside of the interchanteric reefs, thus covering the entire head and neck of the femur as well, excluding the outer third of its back. The capsule is reinforced by deep circular and superficial longitudinal fibers. Circular fibers (zona orbicularis or the angular ligament) in the form of a ring rest on the head and neck of the femur, and thus prevent fallout of the femoral head. The longitudinal fibers form three joint links: the iliofemoral ligament, or Bigelow, the schiofemoral ligament and the pubofemoral ligament. The iliofemoral ligament is located on the front side of the capsule and forms a structure in the shape of an inverted Y. The hip joint capsule is strong, but there are weak points located between the iliofemoral and pubofemoral ligaments (anterior point), between the iliofemoral and ischiofemoral ligaments, and between the pubofemoral and ischiofemoral ligaments. Dislocations occur most often under the influence of external forces (Schuenke et al. 2006; Mrvaljević 2006).

1.4 The Muscles of the Hip Joint

The hip joint is covered with 21 muscles on all sides. They enable mobility and simultaneously affect the stability of the joint. On the front and inside, there are lateral fibers of pectineus muscle and m. iliopsoas. Next to them is the long head of the m. quadriceps femoris, while laterally, there are deep fibers of the tractus iliotibialis. Above and outwards, the rectus femoris muscle, together with the gluteus minimus muscle, reflects the head, yet distally and inward, we find part of

the pectineus muscle fibers and the external obturator muscle. In the back, from top to bottom, are: the middle gluteal muscle, the piriformis muscle, the superior gemellus muscle, the internal obturator, the inferior gemellus muscle, the quadratus femoris muscle and the adductor magnus. The key muscle for surgeons in the hip region is the m. piriformis, due to its relation to neurovascular elements, which are arranged along its upper and lower sides. The quadriceps femoris muscle, m. gluteus maximus and m. tensor fasciae latae represent entry into the hip joint. The medium and small gluteal muscles are the main abductor muscles of the hip joint. The strongest flexor of the hip joint is m. iliopsoas, consisting of two muscles: m. psoas major and m. iliacus. M. psoas major attaches to the lowest thoracic vertebra, all five lumbar vertebrae, the intervertebral discs and the transverse processus of all lumbar vertebrae. M. iliacus attaches to the iliac fossa, on the basis of the sacrum and lumbar sciatic ligaments. The joint's muscular body ends in a lesser trochanter and is innervated by the femoral nerve and the lumbar plexus branches. Its effect is assisted by m. sartorius, m. tensor fascia latae and m. rectus femoris.

The main extensor of the hip joint is m. gluteus maximus. It starts from the posterior gluteal line, at the side of the sacrum, the back side of the tailbone and the seat of the sacroiliac ligament, with lower attachment at the gluteal tuberosity, the external branch of the rough trifurcation lines. It belongs to the superficial thigh muscle group and is innervated by n. gluteus inferior. In addition to extensions, it has a role in external rotation.

The main abductors in the hip joint are m. gluteus medius, which belongs to the middle thigh group, and m. gluteus minimus, which is grouped together with the pelvitrochanteric muscles in the deep thigh muscle group. Both muscles have their origin at the middle and anterior gluteal line, and their insertion at the great trochanter. They are innervated by n. gluteus superior. In addition to abduction, they are also the external rotators.

The pelvitrochanteric muscle group consists of 6 muscles: m. piriformis, m. obturatorius internus and externus, m. gemelus superior and inferior, and m. quadratus femoris. All of them have their origins at the pelvic bone, and their lower ends are attached to the great trochanter. They are innervated by plexus sacralis (exept m. obturatoius externus, which is innervated by n. obturatorius as the branch of the plexus lumbalis). They are external thigh rotators (m. piriformis is also an accessory abductor of the thigh).

The muscles of the inner thigh groups include three adductor muscles (m. adductor longus, m. adductor brevis and m. adductor magnus), m. pectineus and m. gracilis. Starting at the upper attachment, they stretch from the pubic bone and ischium to the linea aspera. In their function, all three are adductors of the thigh in the hip joint, but are also flexors and external rotators, too. Their innervation is derived from n. obturatorius, m.pectineus, m. adductor longus and n. femoralis, while m. adductor magnus receives fibers from n. ishiadicusa (Mrvaljević 2006; Onyemaechi et al. 2014).

1.5 Blood Vessels and Nerves of the Hip

The large blood vessels and nerves of the hip joint supply both local structures and the entirety of the lower limbs with blood and innervation. The anterior and posterior parts of the hip receive separate innervation. On the back side, there are the sciatic nerve, the posterior femoral cutaneous nerve, the upper and lower gluteal blood vessels and nerves, and nerves for short rotators of the hip and hip joint. The front structure includes branches of the femoral cutaneous nerve, the obturator nerve, the lateral femoral cutaneous nerve and the great femoral nerve. The front inner side is innervated by the obturator nerve. The deep branch of the femoral artery provides external and internal circular arteries, which, together with the obturator artery, are the main blood vessels of the hip, together with the accompanying veins (Mrvaljević 2006; Onyemaechi et al. 2014).

1.6 Mechanics of the Hip Joint

The hip joint is a sphere-shaped, multi-axis joint that allows for a wide range of movement in multiple planes. In the frontal plane, movements of flexion and extension are performed, in the sagittal plane, movements of adduction and abduction, and in the horizontal plane, movements of external and internal rotation. During flexion, the femoral head rotates forward and backward through the slides in the acetabulum, while extension movements are in the opposite direction. All these movements have some limitations caused by the anatomical structures of the hip joint. Thus, internal rotation is limited by the ischiofemoral ligament tension and outward rotation by the pubofemoral and iliofemoral ligaments. Flexion in the hip joint depends on whether the knee is stretched or flexed. With lower leg flexion, limited contact with the anterior abdominal wall will occur in hope flexion, yet when the lower leg is stretched, the muscle tension of the leg's hamstring becomes limited (Snell 2011; Mrvaljević 2006).

The movement of flexion is carried out by the following muscles: m. iliopsoas, rectus femoris, and the sartorius and adductor muscles. Extension includes the participation of m. gluteus maximus and the abduction: m. gluteus medius and minimus, m. sartorius, m. tensor fascia latae, and m. piriformis. M. adductor longus, brevis and magnus, m. pectineus and m. gracilis allow for the adduction. The pelvitrohanteric muscles and m. gluteus maximus perform external rotation. Internal rotation is performed by m. gluteus medius (anterior fibers), m. gluteus minimus and m. tensor fascia latae.

1.7 Endoprosthesis of the Hip Joint

In cases with subjective and objective indicators of the disruption of normal function of the hip joint that cannot be removed through conservative methods of treatment, a surgical method that involves implantation of an endoprosthesis of the hip joint is applied. The endoprosthesis may be total [total hip replacement (THR)] or partial, depending on whether it replaces the entire hip joint or only parts of it. Partial hip endoprosthesis, as the name suggests, involves replacing only one part of the hip joint. THR replaces the femoral and acetabular joint parts. It is one of the most common surgical interventions around the world (Onyemaechi et al. 2014) and is believed to be performed in more than 800,000 operations per year.

Replacement of the natural hip joint, in general, consists of several stages, which include:

- Luxation of the hip joint, followed by osteotomy in the neck of the femur and the removal of the natural femoral head
- Hip socket creation and installation of an acetabular joint component
- Insertion of the body prosthesis into the medullary canal of the femur bone, with elements that replace the natural neck of the femur
- Placement of an artificial femoral head on the neck of the body prosthesis

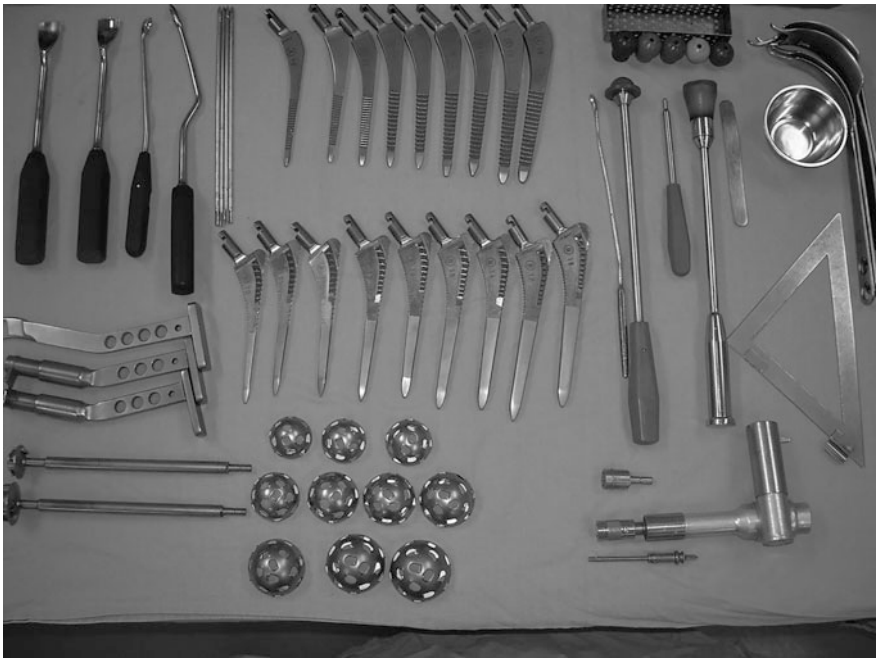

Fig. 2 The instruments used for the installation of an endoprosthesis

- Repositioning of the head endoprosthesis in an artificial acetabulum and connection of elements of the artificial hip joint into one unit (Jun and Choi 2010).

Today, there are a number of different hip endoprostheses (Fig. 2). The type of hip prosthesis that fits with the patient depends on the cause of damage to the hip, preservation of bone mass of the hip joint, hip strain, age of the person, daily activities and comorbidity.

In consultation with the patient, the doctor chooses the best possible solution for each case. According to some authors, a person of lower age may seek to incorporate a hip prosthesis that will preserve bone mass for any revision in the future (usually a cementless prosthesis).

Total hip endoprosthesis can be divided into three groups, according to the indication of installation:

(a) Standard or primary endoprosthesis;
(b) Revision or secondary endoprosthesis;
(c) Special endoprosthesis—tumor.

Standard or primary endoprostheses are used in the treatment of primary and secondary degenerative changes in the hip joint and for the treatment of fractures. Revision prostheses are used in solving the complications that occur after implantation of the primary endoprosthesis. Special, tumor endoprostheses are specifically designed, modular endoprostheses used in reconstructive surgery associated with extensive bone destruction.

According to the method of fixation of the hip replacement, they can be divided into cement, cementless and hybrid endoprostheses.

2 Indications for THR

The most common indication for THR is osteoarthritis of the hip (70%), followed by dysplasia, trauma (Fig. 3), osteonecrosis of the femoral head, systemic connective tissue diseases (such as rheumatoid arthritis, systemic lupus erythematosus, ankylosing spondylitis, etc.), and Paget disease (Lukoschek et al. 1998; Simon et al. 2010; Siopack and Jergesen 1995).

Osteoarthritis, which, according to etiology, can be primary or secondary, is characterized by damage to the articular cartilage. It can affect any joint, but those most commonly affected by this process are the joints of the hands, spine, knees and hips. Diagnosis of the disease is made based on the clinical picture (health history and physical examination) and classical radiography of the hip in two directions to detect narrowing of the joint space, subchondral sclerosis, existence of ostephytes and deformities of the femoral head and acetabulum. The clinical picture is characterized by the presence of symptoms such as pain, stiffness (contractures), occurrence of joint crepitation, and a limited range of movements. The occurrence of osteoarthritis is correlated with the age of the patient. Primary arthrosis rarely

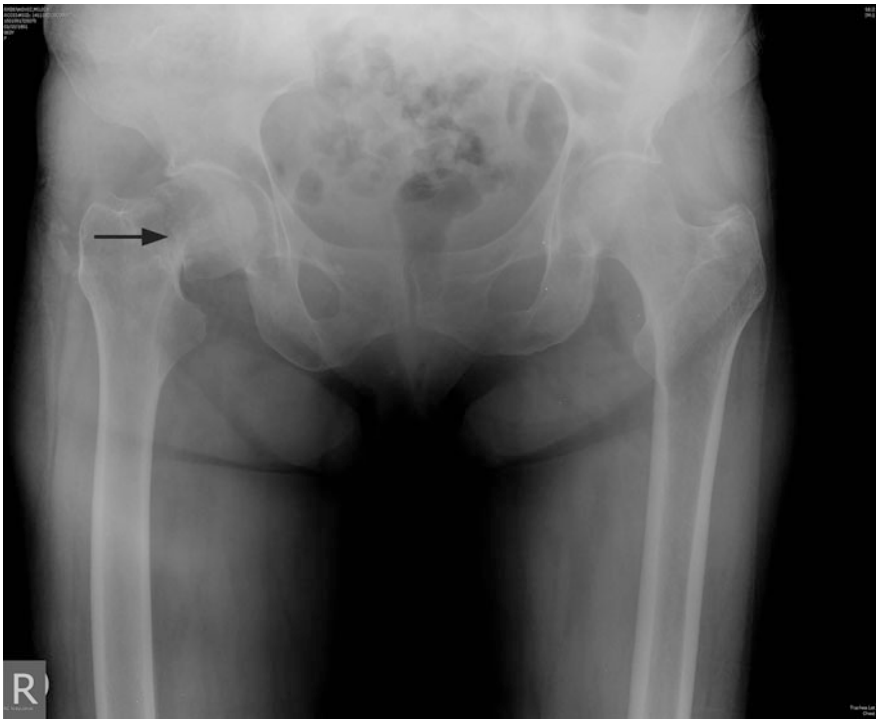

Fig. 3 An X-ray of the hip and pelvis. The *arrow* indicates a fracture of the right hip

occurs in people younger than 40 years of age. It is more frequent in women than in men, and the incidence of this disease increases with age (Østerås et al. 2013; Bierma-Zeinstra et al. 2002; Grotle et al. 2008) (Fig. 4).

All of these conditions are characterized by the presence of pain and movement disorders in the hip joint that do not respond to conservative therapy and limit the normal life and activity of the patient, to the point that arthroplasty is the best method for achieving better functioning of the hip joint and improving quality of life.

The most important symptoms indicating THR as the treatment method of choice are pain and dysfunction of the hip joint, which are followed by radiological indicators of pathological changes in the joint. The mere presence of pain without radiological indicators is not an indication for surgery.

An active infection in the hip area is a contraindication for primary arthroplasty. Factors such as chronic diseases and orthopedic comorbidities may be a relative contraindication for this intervention. A special category of patient consists of young, active people and athletes, who should choose the type of prosthesis fixation carefully, owing to the possible need for revision and so as to better preserve the bone mass.

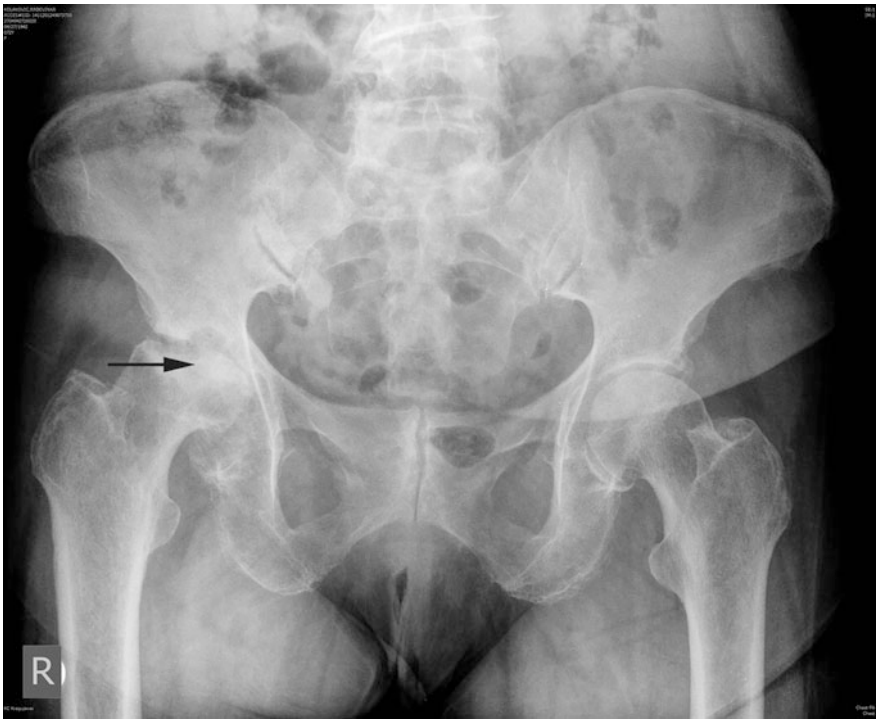

Fig. 4 X-ray of the pelvis and hip joint. The *arrow* indicates the degenerative changes in the head of the right femur caused by osteoarthritis

3 Historical Development of the Hip Joint Prosthesis

The first hip replacement operation, in which a wooden block was inserted between the damaged joint surfaces of the hip joint, was performed in 1840 in New York, by an American surgeon named Carnochan. In later years, other materials were used, such as fascia, used by Lexer in 1908 (Abdulkareem 2013), leather, muscle fiber, submucosa of the pig bladder, used by Bear in 1918, and gold foil, used by Sir Robert Jones (Gomez and Morcuende 2005; Pramanik et al. 2005; Learmonth et al. 2007). In 1880, Oliver used periarticular soft tissue for the lining of the articular surfaces (Santanapipatkul and Udomkiat 2012). The results of the interventions that utilized these materials were painful, and they could not solve the problems of the patients in the long term.

The next decade of the 19th century, in terms of techniques for treatment of diseased hip joints, was marked by replacement of the damaged femoral head. In 1891, Themistocles Gluck, a German surgeon, used an artificial joint made of ivory as a replacement for the diseased hip joint, which led to pioneering steps in hemiarthroplasty, a technique in which a femoral stem is inserted into the femoral

diaphysis (Knight et al. 2011). Fixation was done with nickel-plated screws (Gomez and Morcuende 2005), and then the bone was cemented. Gluck was the first surgeon to use cement for fixation of their dentures (Learmonth et al. 2007). Delbet, in 1919, used rubber as the material for the head of the femur in the treatment of fractures of the femoral neck, while in 1926, Groves used a "wedge" made of ivory as a substitute for the articular surface of the femoral head.

In 1923, Marius Smith-Petersen, a Boston physician, introduced a new technique for hip arthroplasty, using membranes similar to synovia and glass that covered the head of the reshaped femur head, in order to stimulate the regeneration of cartilage on both sides of the glass mold. His technique was improved by introducing new materials, such as Viscaloid (a celluloid derivative, 1925), Pyrex (1933), and Bakelite (1939). In 1938, a cobalt-chromium alloy called Vitallium was introduced. This prosthesis was more durable than the earlier ones, while tissue reaction was minimal. The main disadvantage was reflected in its instability; however, there were some cases described in which the prosthesis functioned satisfactorily for over 20 or even 40 years (Santanapipatkul and Udomkiat 2012). Later, Smith-Petersen and Philip Wiles worked on the development of total hip joint prostheses made of stainless steel (Smith-Petersen 1948; Wiles 1957; Knight et al. 2011). The first implantation of a metal-on-metal total hip prosthesis was performed by Philip Wiles in London in 1938. This prosthesis, made of stainless steel, was not stable enough.

During the period from 1938 to 1946, a couple of Parisian doctors, the Judet brothers, developed the first short stem prosthesis, in the form of a wedge made of poly-methyl-methacrylate (PMMA) with a head shaped like two-thirds of a sphere and a short handle, which was later replaced by similar prostheses made of Vitallium. Its articular surfaces were smooth, but the wrist became loose after implantation, which contributed to the debris created by wear (Pramanik et al. 2005; Smith-Petersen 1948).

In 1939, Frederick Thompson of New York and Austin Moore of South Carolina independently developed a prosthesis that consisted of a metal stem (shank) implanted in the femur, associated with a metal ball coming into the acetabulum. Thompson and Bohlman built a 12 inch-long prosthesis made of Vitallium in 1939 (Pramanik et al. 2005).

In the 1950s, Thompson, Moore and Bohlman, based on the concept originated by the brothers Judet, developed a femoral stem prosthesis with a long handle, which had openings used for biological fixation, and which allowed for the ingrowth of bone tissue (Gomez and Morcuende 2005). The prosthesis was a replacement for the head of the femur, while the acetabulum had not been altered, and was used in the treatment of fractures of the hip joint and arthritis. This prosthesis served as the basis for the development of the McKee-Farrar total hip prosthesis.

In 1950, McKee designed the first metal-on-metal hip joint prosthesis, for which he introduced an acetabular mold made of cobalt-chromium and used screw fixation (Gomez and Morcuende 2005). In later versions of this prosthesis, developed in the 1960s, fixation was achieved using acrylic cement (McKee-Farrar prosthesis) or screws (McKee Ring prosthesis) (Pramanik et al. 2005). The use of acrylic cement

in orthopedic practice was introduced by Sven Kiaer in 1950 (Mahalingam and Reidy 1996). Despite their strong performance, the shortcomings of these prostheses were poor bonding with the thighbone, debris created by wear, loose joints and the consequent pain suffered by the patients. A high percentage of hip joint operation revisions (caused by the development of joint tissue and lower mobility) inspired the development of a mold prosthesis that changed the acetabulum of the affected hip, used in practice in the 1950s by Otto E. Aufranc, Gaenslen (in 1952), McBride (1955) and Urist (1957). The problem was solved by designing a prosthesis that is fixed into the acetabulum (hip socket, arthroplasty). Despite its good results, this technique has not found great application (Pramanik et al. 2005).

The English physician Sir John Charnley is considered the father of modern total hip arthroplasty. Having studied the joints of animals, he introduced, in 1958, the model of the total hip, which changes the femoral head and acetabular articular surface. In his first attempts, Charnley used poly-tetra-fluoro-ethylene (PTFE, Teflon), which encapsulated the acetabulum and the femoral head (Collis 1991). However, the side effect was the development of aseptic necrosis of the femoral head and bone tissue reaction to the material used for the acetabular component (Charnley 1961; Havelin et al. 1995; Bannister 1993). Then, he developed a prosthesis in which the acetabular articular surface was replaced with a Teflon mold, while the head of the femur of small diameter, made of metal, was associated with the handle, fixed with rigid acrylic cement. The drawbacks of this prosthesis were insufficient stability and the formation of debris, which was the cause of a strong inflammatory reaction (Cornell and Ranawat 1986; Collis 1991). In his new model of total hip joint prosthesis, Charnley used poly methyl-methacrylate as cement for fixation. Newer versions of the prosthesis used the high molecular weight polyethylene (HMWPE) as a material for making an acetabular articular surface, whose endurance characteristics were 500–1000 times better in comparison with the Teflon mold (Pramanik et al. 2005).

In the 1970s, Muller further developed Charnley's prosthesis by designing a 32-mm head and a shaped handle that facilitated insertion (Muller 1975). In addition, the McKee-Farrar total arthroplasty technique was applied, which used a cement Co–Cr–Mo prosthesis, while Pierre Boutin, a French orthopedist, performed the first implantation in the 1970s by using a ceramic-on-ceramic type of prosthesis. At the end of the 1970s, non-cement prostheses were being combined with metal-plastic, such as the Endler model, which was discarded due to instability (Kolundzic et al. 2012).

During the 1980s and early 1990s, the main shortcomings of total hip arthroplasty were related to the weakening of the joint and aseptic osteolysis, which led to the design of new ceramic prostheses. The debris that occurs as the result of friction is one of the main problems for the modern techniques of hip replacement. The immune system reacts to particles of polyethylene, which causes a reaction that destroys part of the bone around the implant, leading to osteolysis and making the prosthesis unstable.

Total hip arthroplasty involves the use of a prosthesis consisting of a metal stem or shaft and acetabular cups made of different materials, for example, the contact

surface of the femoral head and the acetabulum. In recent decades, different combinations of material have been in use: metal-to-metal, metal-on-polyethylene, ceramic-on-ceramic (Pramanik et al. 2005).

After the 1990s, prostheses made of ultra-high molecular weight polyethylene (UHMWPE) in combination with a metal or ceramic femoral head were the ones most in use. In recent years, prostheses in which the cups are coated with hydroxyapatite, which has a role in stimulating bone infiltration, have been examined, and coated biocompatible prostheses of porous materials with good mechanical properties similar to bone tissue (Santanapipatkul and Udomkiat 2012) has also seen expanded interest. From the time of implantation of the first total hip prosthesis up until today, the process of intervention, as well as the materials used for prostheses, has been subject to constant change and improvement.

4 The Division of the Total Hip Prosthesis Based on Fixation Method

According to the method of fixation of the hip joint, the endoprosthesis can be a cementless hip endoprosthesis, a cement endoprosthesis or a hybrid endoprosthesis. The important differences between the cement and cementless endoprosthesis are in the method of fixation, their surfaces and their form. Cement endoprostheses are completely smooth, while cementless must be rough, with micro and macro pores on the surface, which later grow into the bone. This does not happen with all of them, since cement prostheses can be made with either a rough surface, a specially textured rough surface or a specially treated surface whose goal is better adhesion of the cement to the surface of the implant.

4.1 Cement Type of Prosthesis

Cement fixation of the implant involves interposition of a biologically inert material such as Polymethylmethacrylate (PMMA) bone cement between the prosthesis and the bone, with the main task of increasing the contact surface between the endoprosthesis and the socket in the bone by about 200 times (Fig. 5). The cement should provide stability between the two contact surfaces: those of the cement and the bone, and those of the implant and the cement. In this way, the entire system can successfully resist biomechanical requirements, and thus reduce the load per unit of the contact surface. The use of cement for fixation of the femoral component of some models of prosthesis has resulted in a duration of 20 years or more.

The poly(methyl methacrylate) (PMMA) bone cement has been used in orthopedic surgery for over 50 years. Based on its chemical composition, it is an ester of methacrylic acid with a polymerized double bond (methyl methacrylate) (MMA). It

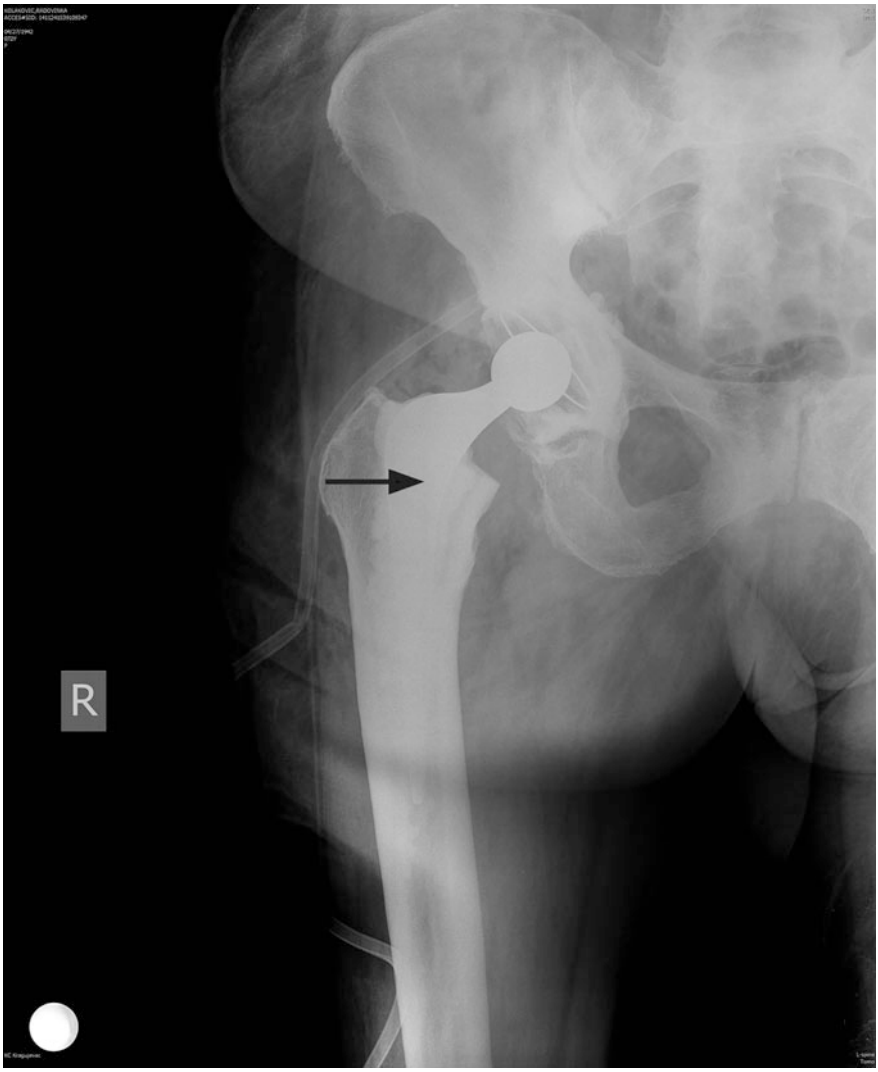

Fig. 5 X-ray of the right hip. The *arrow* indicates the cement type of prosthesis

was synthesized for the first time in 1843, as a saturated ester of ethyl methacrylate. In the 1940s, Röhm and Haas produced several polymer methyl methacrylates. In 1941, Kleinschmidt used this polymer to close a defect in the skull. PMMA was first used in dentistry in 1950, in attempts to make orthopedic prostheses out of this material, but the idea was soon abandoned (Judet and Judet 1950). In the 1960s, Charnley used it in orthopedic surgery as a means to fix an endoprosthesis.

Bone cement is a two-component system consisting of powder and liquid (Lai et al. 2013). The powder consists of particles, beads with a diameter of 40 μm,

composed of MMA copolymers, benzoyl peroxide (BPO as an initiator) and zirconium or barium to provide radiographic visibility. The monomers are liquid (Figs. 6 and 7). The process of polymerization results from mixing the fluid and powder at room temperature (Kuehn et al. 2005), when the monomer is polymerized in the presence of radicals derived from the BPO initiator. This results in a viscous liquid or paste. The process lasts for 2–5 min, depending on the temperature and the cement, and passes through the following four phases:

1. the mixing stage, which lasts 1 min, and which homogenizes the liquid and powder; this process can be performed manually using a spatula and bowls
2. the liquid phase, in which the cement does not turn into a sticky mass
3. the working stage (the important factors are the temperature and the cement), in which the cement is applied (it lasts for approximately 2–4 min)
4. a phase of hardening, when the cement sticks to the contact surface.

Since the polymerization is exothermic, a decrease in the temperature can prolong the process (Jiranek 2005; Deramond et al. 1999). Polymerization causes a reduction in the distance between the monomers, which results in hardening of the cement and a subsequent reduction in its volume, by 6–7%. Since this process is performed manually, air bubbles occur within the bone cement, which significantly affects its porosity (Fig. 8). This may be reduced through centrifugation of the

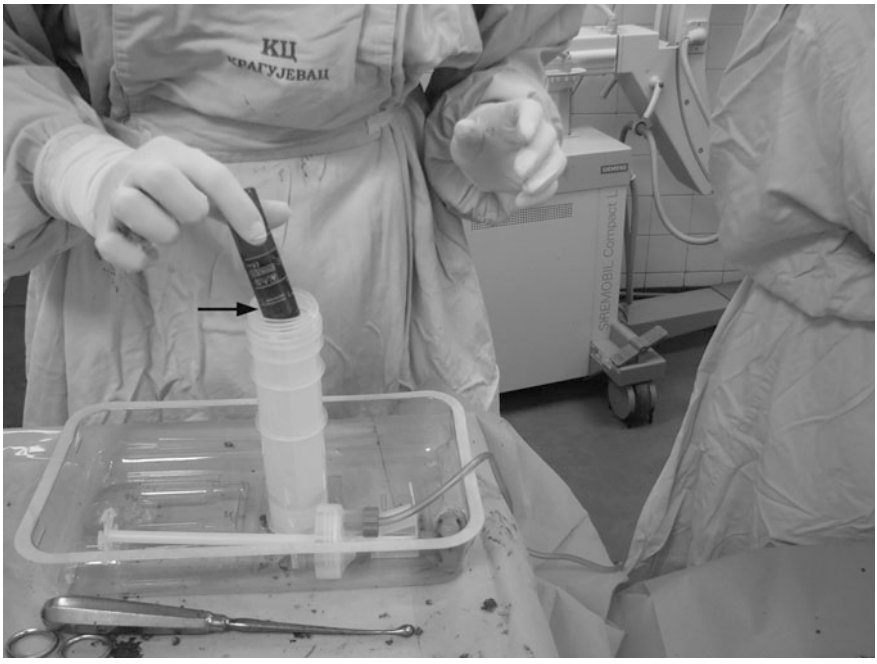

Fig. 6 A method of preparing bone cement. The *arrow* indicates the pouring of the liquid into a container for preparation of the cement

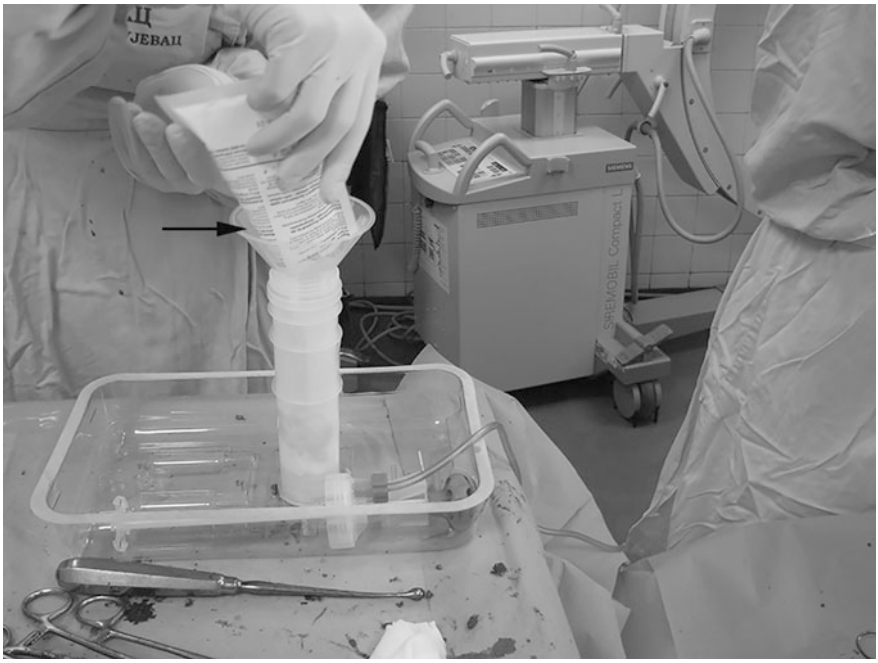

Fig. 7 A method for preparing bone cement. The *arrow* indicates the powder that was poured into a container for the preparation

liquids and powders, as well as the use of a cement gun (James et al. 1992). A better homogenization of the cement material was prepared through stirring and under a vacuum in a variety of ways (Zivic et al. 2012).

Today, multiple brands of bone cement are in use, 15 of them in Norway alone, while some authors describe as many as 67 brands (Kühn 2000). Bone cement is classified into three groups by type of viscosity: low, medium and high viscosity cement (Kühn 2000).

The durability of a femoral stem fixed with cement depends on several factors. Apart from the preparation, sterilization and installation of the cement, the thickness of the layer and the previous preparation of the medullary canal are also very important. A series of experiments showed that a thicker layer of cement has better mechanical characteristics, and that for this purpose, it is necessary to remove the upper layer of spongiotic tissue from the medullary canal. Removal of bone debris and blood from the medullary canal prior to cementation adds strength, increasing bone cement contact and the efficiency of its surface (Figs. 9 and 10). The use of pulsatile lavage of the channel and cement pressurization increases the strength of the interface by up to 185%. Penetration of the bone cement into the spongiotic bone depends on the duration of pressurization and the viscosity of the cement. An additional quality of pressurization is achieved by occlusion of the distal segment of the channel's so-called cement restrictor (plug), and by using the gun for

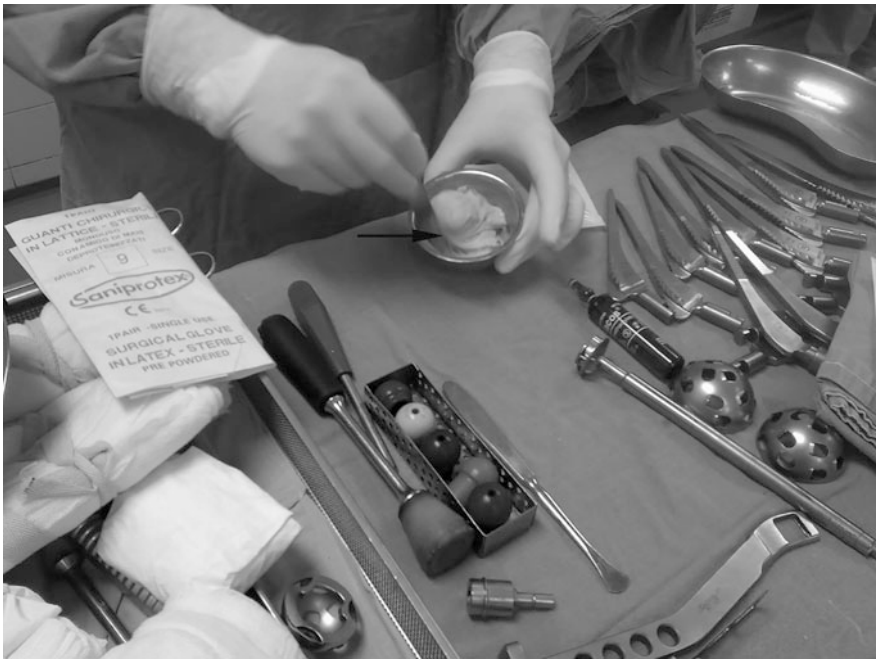

Fig. 8 Manual preparation of cement. The *arrow* indicates the pan for preparation

application (Figs. 11, 12 and 13). Low viscosity cement applied under high pressure to the porous bone surface makes for the strongest interface (Majkowski et al. 1993). In addition to these factors, the geometry of the cement blocks plays an important role. Previous studies have shown that the optimal geometry is irregular, but it uniformly covers the proximal, distal, medial and lateral spaces between the implant and the bone.

An acetabular component fixed by cement should hold the side bumps in cement interdigitation. This means that the cement should be tied to this unevenness, which results in a good mechanical implant–cement connection. This is achieved through the special method of cementing that includes pressurization or increased pressure within the structure of the cement during the polymerization process. By bonding cement, such an interdigitation as the protrusion of cement is transformed into the previously prepared bone perforation. The durability of these components is in direct correlation with the quality of the contact surface of the bone cement. Cemented acetabular components have shown excellent early results, but the problems that occurred, most often after a period of 10 years, were also related to the loss of these components (Smith et al. 1998; Schulte et al. 1993). It was the most common cause of osteolysis along the area of bone-cement surface contact, caused by the reaction of the tissue to particles of debris (Schmalzried et al. 1992).

Acetabular components possess wings or extensors (flanges and spacers) to facilitate proper cementing components (Figs. 14 and 15)

Fig. 9 Preparation of the femoral canal for implantation of the prosthesis

Fixation cement has certain advantages:

1. it increases the total contact area of the implant-bone, optimizing stress distribution
2. it significantly reduces the compressive and shear forces, increasing the fatigue threshold bone
3. it provides quick and strong initial stability of the components
4. the bone-cement-implant system provides an elastic, controlled movement between the cement and the bone, and distributes powers.

The disadvantages of cement fixation are:

1. it requires proper preparation and application of the cement
2. once started, the loosening and deteriorating process of cement blocks cannot be stopped spontaneously
3. mechanical performance in in vitro conditions become significantly reduced in the biological environment
4. loosening of the cement blocks under conditions of physiological stress of the joint often occurs before the end of the expected duration of the implant.
5. prolongs the duration of surgery.

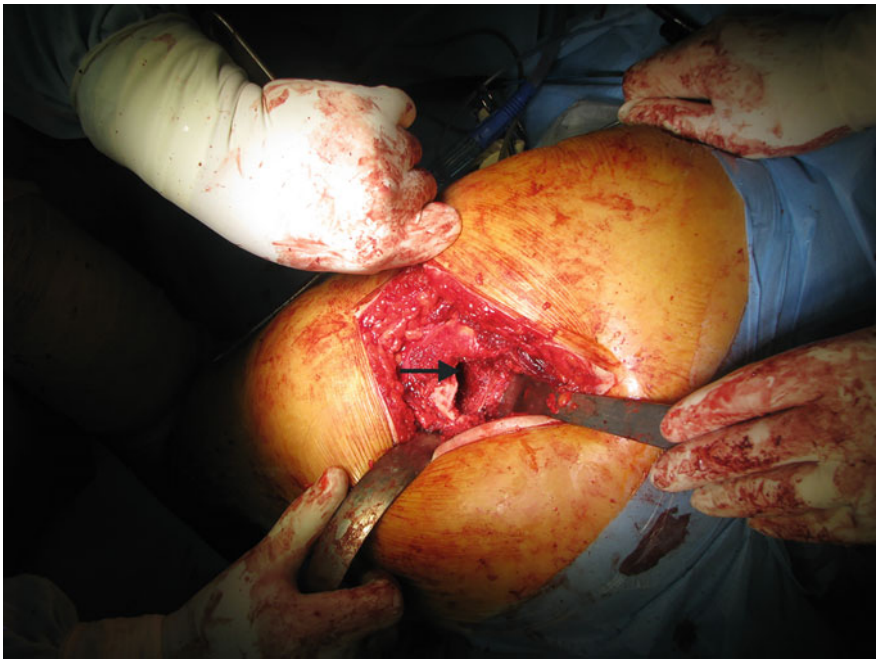

Fig. 10 Prepared femoral canal for implantation prosthesis and cement. The *arrow* indicates the opening of the femoral canal

Sophisticated computerized analyses by finite element analysis have shown the maximum load of the cement blocks on the femoral component in the medial and distal parts.

4.2 Cementless Type of Prosthesis

Therefore, it was observed that with a fixed prosthesis, the cement that was applied according to the first generation of application techniques often led to loosening and a shorter duration of the endoprosthesis, which was thought to be connected to the emergence of "cement disease," and prompted the development of a cementless endoprosthesis (Corten et al. 2011a, b) (Fig. 16).

The problems regarding fixation, pain and osteolysis led to the first generation of cementless femoral stems. Many years of development and improvement of these new generations has significantly reduced these complications.

The design of cementless components is based on the existence of a special texture or surface, or the porosity of the implant itself. It is realized through special technological procedures. The aim of this structure is the incorporation of the

Fig. 11 Application gun for cement, marked with an *arrow*

implant into the process of osteogenesis. To accomplish this, it is necessary to fulfill the following conditions:

1. pore size must be within a certain range
2. intimate contact between the implant and the bone must be established
3. mobility of the implant within the bone should be kept to a minimum.

In 1981, Albrektsson and colleagues described the process of osteointegration, which was created between the implant and the human bone. Subsequent studies in humans and animals have contributed to a better understanding of this process (Albrektsson et al. 1981; Galante et al. 1971; Zweymüller et al. 1988). The osteointegration process depends on several factors: the surface of the implant, the primary fixation, and the implant's mobility. If it comes down to the existence of pores on the implant, their size should be between 50 and 400 μm and the percentage of voids in the coating should be 30–40% (Haddad et al. 1987; Albrektsson et al. 1981). Adequate fixation of the contact between the implant and the bone has an impact on the reduction of micromovements of the femoral stem, the size of which has influence on the manner of osteointegration. If these movements are greater than 150 μm, there is a formation of fibrous tissue, and if it is from 40 to 150 μm, it creates a combination of bone and fibrous tissue. Micromovements less than 20 μm result in the occurrence of bone tissue (Engh et al. 1992; Pilliar et al. 1986; Jasty et al. 1997).

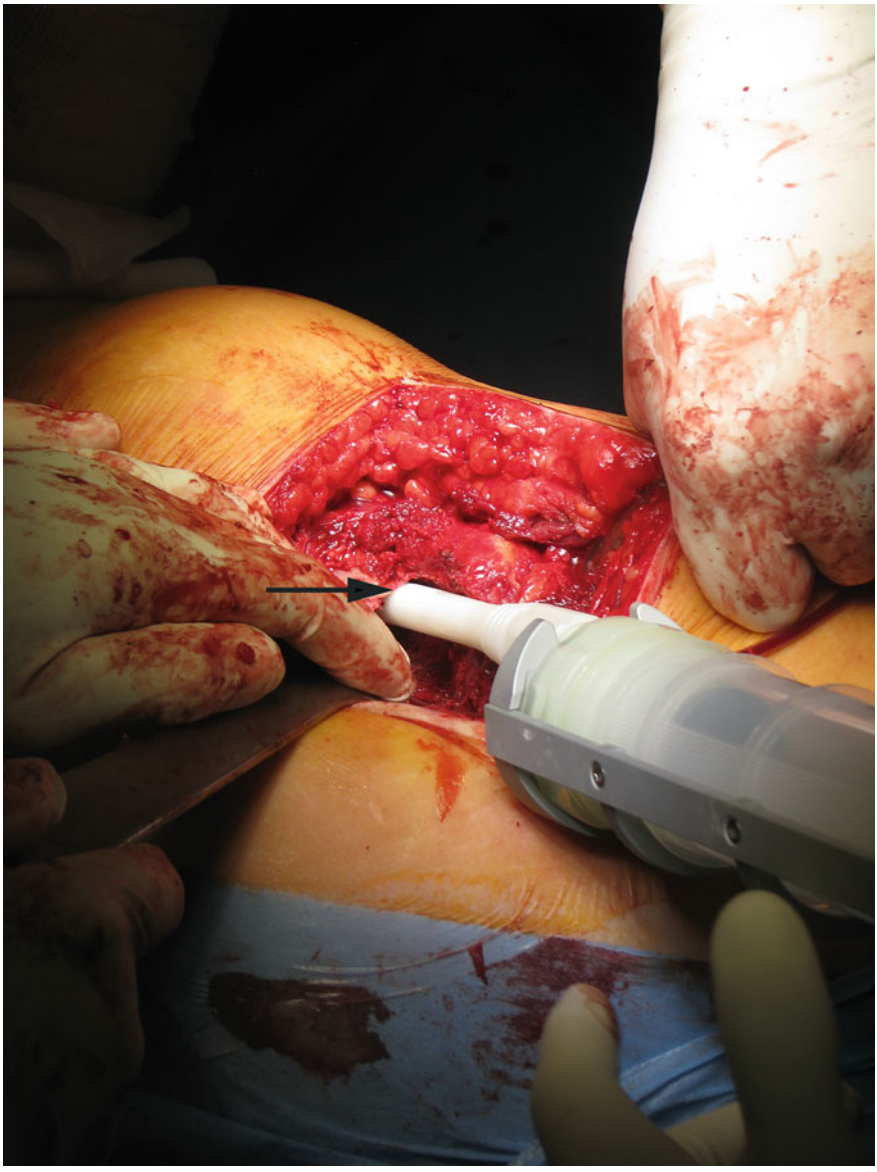

Fig. 12 Insertion of bone cement into the femoral canal using a gun for application (marked with an *arrow*)

For a cementless endoprosthesis, it is very important to provide good primary fixation of the prosthesis in the bone bed, and after a while, this is followed by the secondary fixation of the prosthesis. The cementless femoral component is modelled so that the distal part can wedge itself into the diaphysis of the femur, and thus

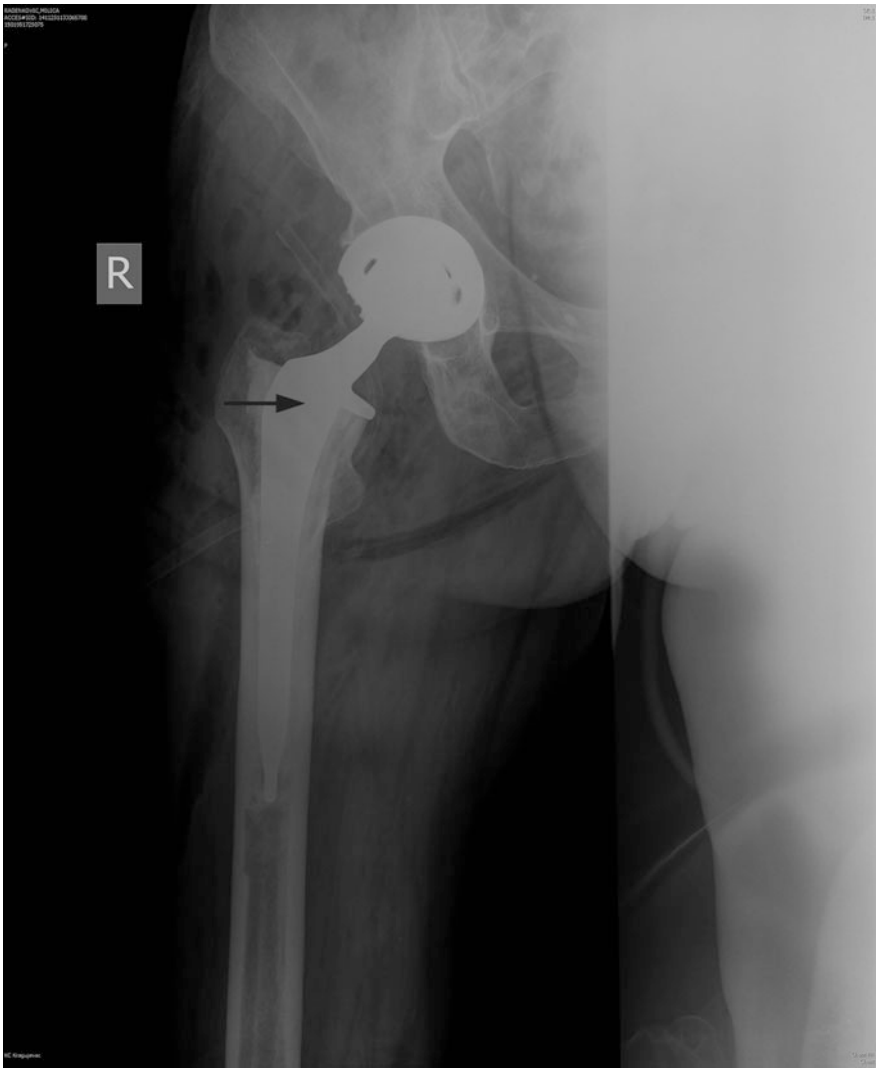

Fig. 13 Cement implanted into the femoral canal. The *arrow* indicates the implanted cement in the canal

become primarily fixed. This method of fixation is called the "press-fit" fixation, and it represents the primary, initial fixation. The goal is to perform the entire fixation process with less damage to the surrounding tissue, which is achieved through better design and improvement of the mechanical properties of the endoprosthesis. Depending on the surface of the femoral bone, ingrowth of stems within the porous surface appears, or ongrowth in case of the rough surface. Ingrowth occurs when the bone grows inside a porous surface. Ongrowth occurs when the

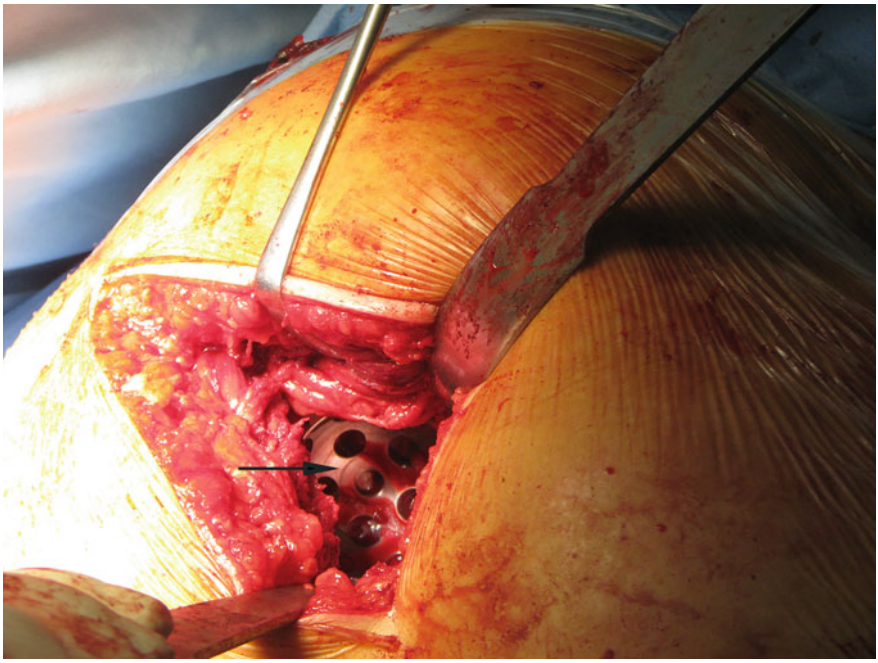

Fig. 14 Implanted acetabular component (marked with an *arrow*)

bone grows onto a roughened surface. Ingrowth surfaces include sintered beads, fiber mesh, and porous metals.

Ongrowth surfaces are created in two ways:

1. sandblasting, which is achieved by bombing the implant with small abrasive particles that produce surface roughness in the range of 5 μm or 3DO
2. spray-plasma, which involves mixing a metal powder with an inert, ionized gas under pressure, creating melted metal that is sprayed onto the implant (Khanuja et al. 2011).

Hydroxyapatite that has osteoconductive properties can be directly applied to the implant in the form of a spray. It is believed that the optimal thickness could be 50 μm (Nakashima et al. 1997; Søballe and Overgaard 1996; Søballe et al. 1993).

Cementless femoral stems are usually made of cobalt-chrome-alloy molybden and titanium aluminum-vanadium alloy, and come in different designs. Design in this case means the geometry of the implant and the place at which the prosthesis is fixed to the bone.

The cement-free acetabular component can be fixed in two ways: either by turning it into the pelvic bone or through the principle of "press-fit" fixation. The use of screws ensures better primary fixation. Different modalities of these components can be applied in relation to whether they contain a porous layer or not. Threaded components with a view to assuring outstanding fixation, and that can be

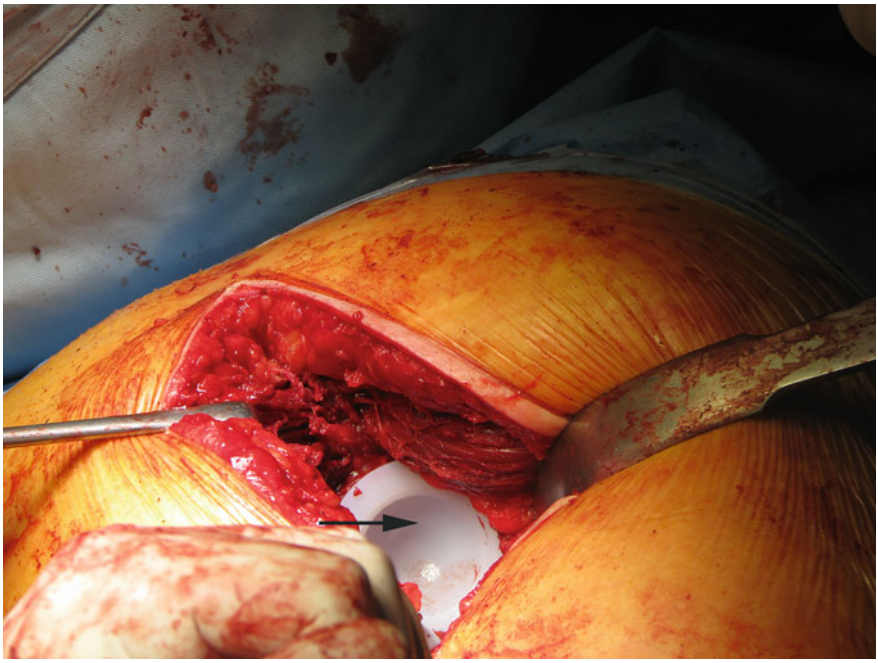

Fig. 15 Implanted acetabular liner (marked with an *arrow*)

used with acetabular bone defects, are currently in use. Unfortunately, their clinical results have shown the complete opposite, with a high percentage of loosening, and after only a short period following delivery of the implantation. Currently, the so-called "press-fit" fixation, with or without screws, is the dominant method of fixation of acetabular components in the pelvic bone.

4.3 Hybrid Type of Prosthesis

A hybrid endoprosthesis (Fig. 17) is a combination of the previous two types of prosthesis: part of the prosthesis has no cement (usually the acetabular component), while the second part uses bone cement (often the femur part) (Fig. 18), (Schmalzried and Harris 1993). The National Institute of Health of the United States endorsed the use of this method of fixation in 1995 because of the excellent long-term results (NIH 1995).

The choice of prosthesis and method of fixation depend on factors that are related to the geometry and morphological characteristics of the femoral canal and the quality of the bone.

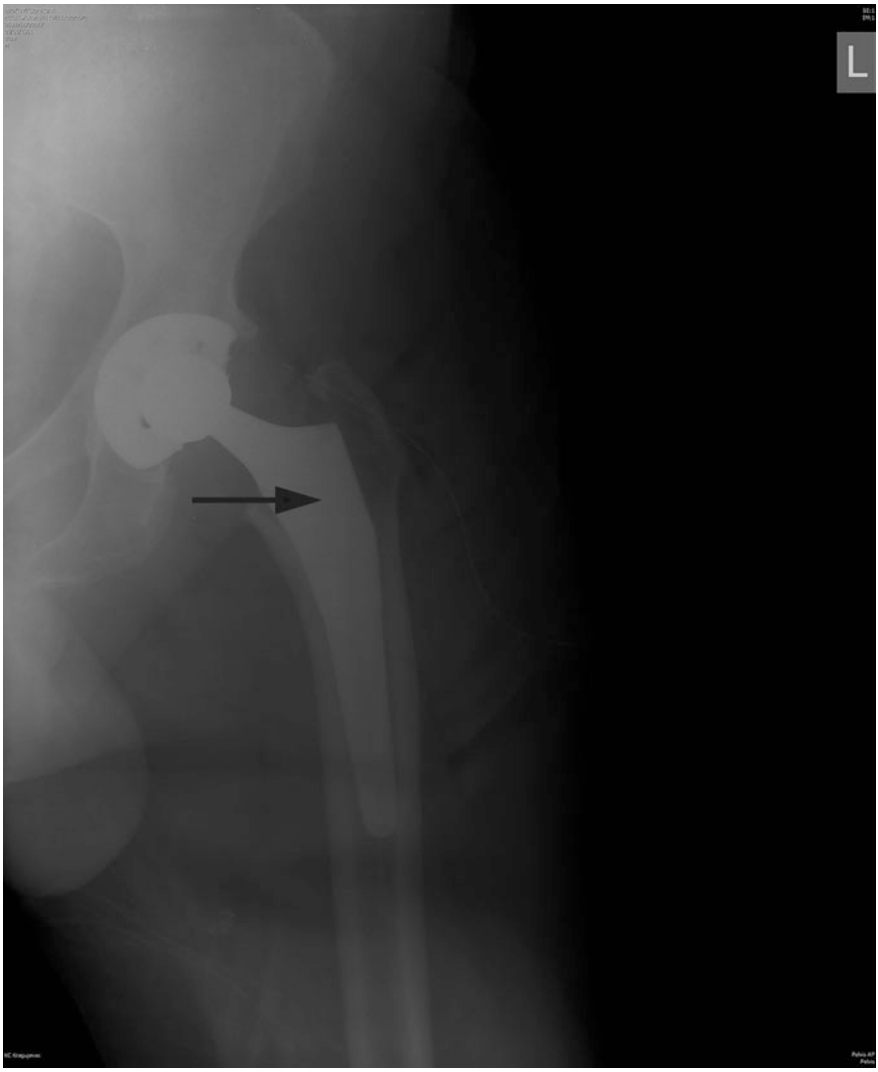

Fig. 16 X-ray of the left hip. The *arrow* indicates the cementless prosthesis

Classification by Dorr includes the division of the femur into three types, based on the morphological characteristics of the bone and on the way in which fixation of the femoral stems is carried out. The Dorr type A bone occurs more frequently in men and younger people. It is characterized by a thick, less porous cortex and a narrow diaphyseal channel and is suitable for cement fixation of the femoral stent.

The Dorr type B, similar to the previous type, is more common in males and is characterized by the highest level cortical porosity. The Dorr type C is usually seen

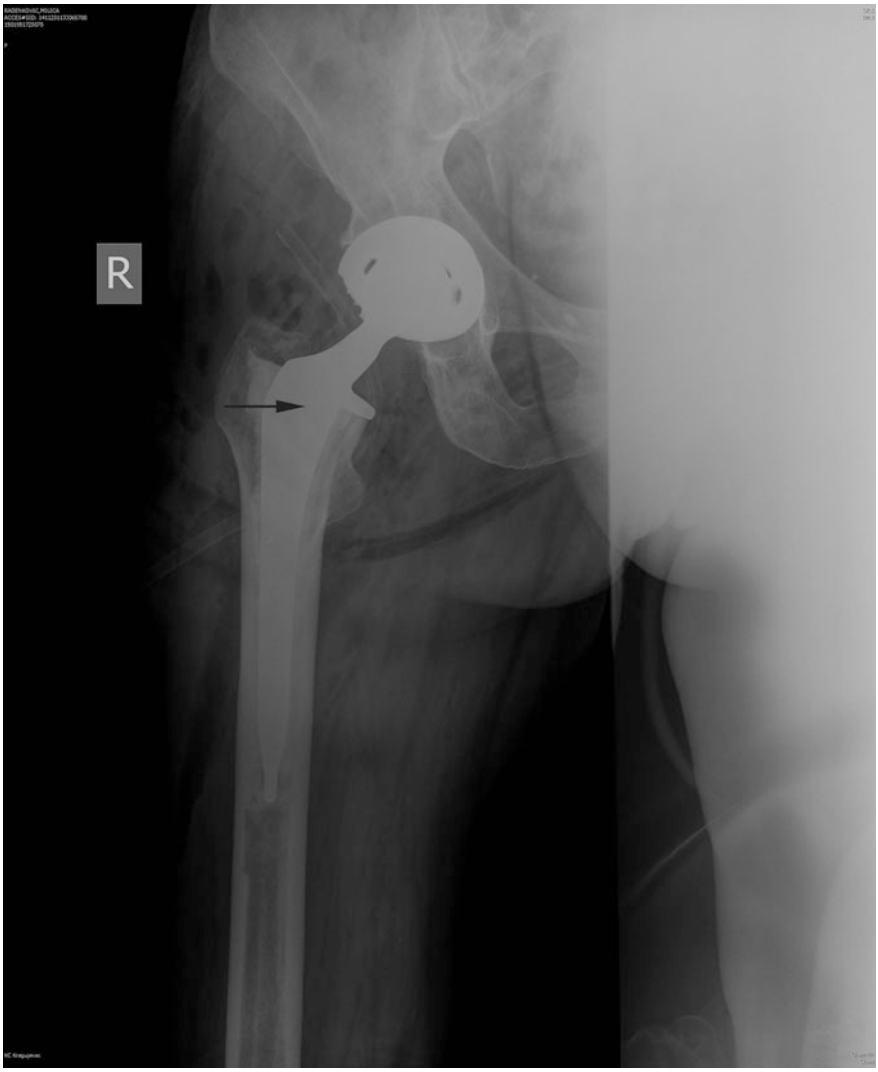

Fig. 17 X-ray of the right hip. The *arrow* indicates the implanted hybrid prosthesis

in older women and in the presence of cortical bone damage, similar to the B type (Dorr et al. 1993). Patients with Dorr B and C types of osteoporotic bones have an altered bone cortex and an expanding intramedullary canal (Zhao and Sun 2013), and are considered good candidates for cement fixation. For patients for whom the femoral canal has a small diameter and the cortical bone is preserved, the use of a cementless stem is recommended (Berry 2001).

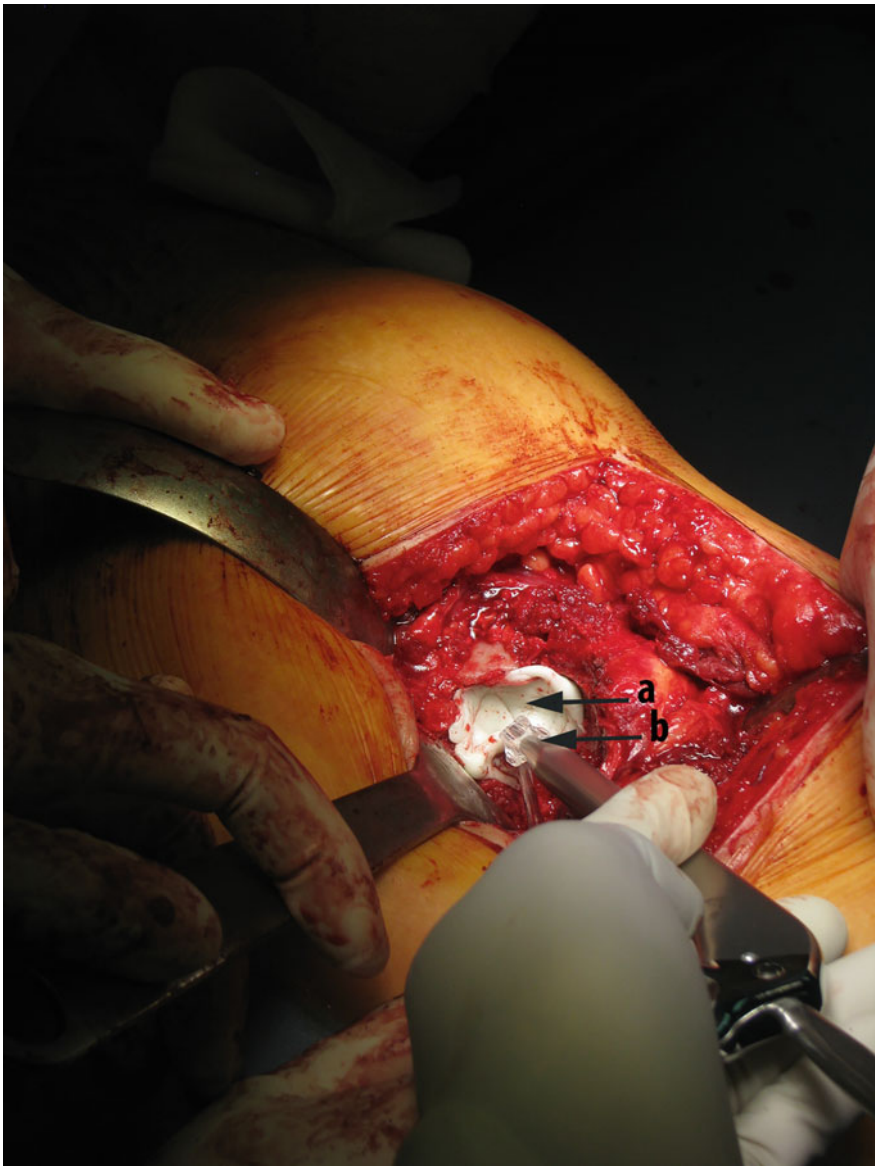

Fig. 18 Implantation of the femoral stem (*arrow b*) in the femoral canal filled with bone cement (*arrow a*)

5 Biomaterial for Building Up the Prosthesis

The materials for hip arthroplasty, as well as the appearance and manner of production of the prostheses, have changed over time, but all of these merchandises must meet the following criteria: biocompatibility, non-toxicity, corrosion resistance, durability, and toughness and low modulus of elasticity. Metals that are used include stainless steel, titanium and its alloys, cobalt superalloys, magnesium and tantalum. The use of components of both ceramic, polymer and composite materials are known as carbon-carbon composites. Cobalt alloys became available in the 1930s. Titanium and its alloys began to be used in the 1980s because of their biocompatibility compared to the other most frequently materials. The titanium alloy Ti-6Al-4V is widely used in almost every endoprosthesis (Zivic et al. 2011).

Synthetic polymers occupy an important place in the design and use of implants. In the beginning, such materials as polyamide and polytetrafluoroethylene (PTFE) with limited physical and chemical properties were used. Through better control of the production process and synthesis, better materials were obtained, such as ultra-high molecular polyethylene (UHMWPE), which is the material of choice for the production of components for endoprostheses today (Hawkins 2005). They are very often used in implants made of poly-L-lactide (PLLA), especially in areas with no great burden.

6 Types of Surgical Approach When Performing THR

THR is a method that includes multiple options for surgical approach to the hip joint, such as the front (anterior), rear (posterior), side (lateral), and medial. It also describes a combined and minimally invasive approach with two incisions (minimally-invasive, two-incision approach).

The front, or femoral, or Smith-Petersen approach is an interneural and intermuscular approach to the hip joint. In 1936, Watson-Jones introduced the anterolateral approach, which was later modified by Charnley (1979), Harris (1967) and Muller (1974).

The lateral approach involves a direct lateral approach and trans-trochanter techniques. The direct lateral was first described by McFarland and Osborne (1954), and later modified by Hardinge (1982). The trans-trochanter technique was introduced by Charnley and Ferreiraade (1964), and later modified by Harris (1973), Glassman et al. (1987) and McLauchlan (1984). Dislocation, which occurs in the anterior and lateral approaches, sees a rise of between 0.5 and 2% (Lindgren et al. 2012; Kwon et al. 2006).

The posterior approach was described by Langeenbeck, and later modified by Koccher, in 1907 (Dawson et al. 1996; Moore 1957; Marcy and Fletcher 1954). Moore's technique is called the "Southern" approach (Fig. 19), and is the one most commonly used (Moore et al. 2006). This surgical technique has previously been

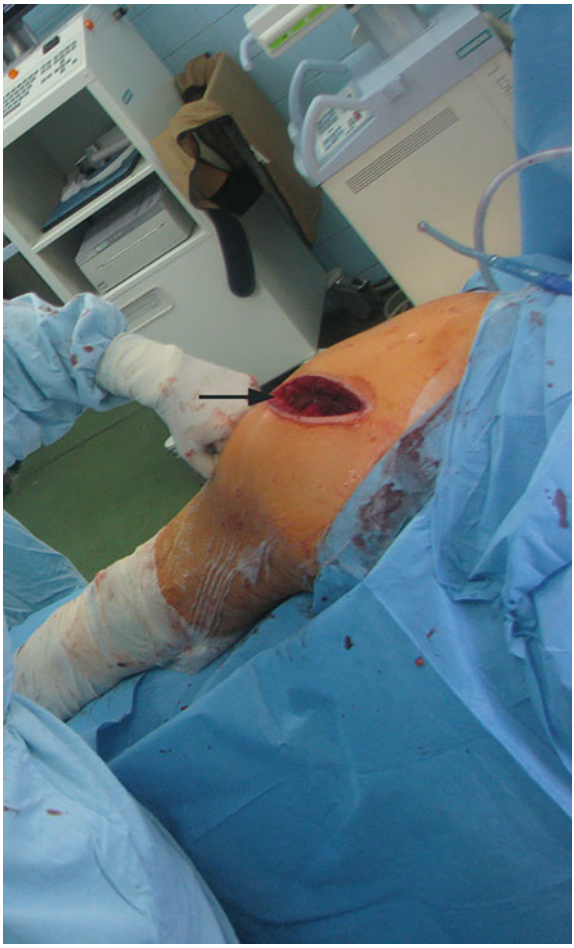

Fig. 19 Rear access to the hip joint during running of THR (incision marked by an *arrow*)

associated with an increased incidence of endoprosthesis dislocation (4.5%), but more recent studies have shown that, with proper posterior soft tissue repair, dislocation occurs in only 0.5% of cases. The advantage of this approach is a lower percentage of nerve injury, and the fact that it is easier to perform. The disadvantage is weaker exposure of the acetabulum (Jolles and Bogoch 2004; Lindgren et al. 2012; Jolles and Bogoch 2006).

The medial approach was introduced by Ludloff in 1908 (Koizumi et al. 1996), and modified by Ferguson in 1973 (Ferguson 1973). In 2001, a minimally invasive approach was introduced with the aim of decreasing traumatization of the soft tissue.

7 Complications of THR

THR is a surgical intervention with certain risks. Complications, grouped according to their time of origin, are: intraoperative, early postoperative and late postoperative. Intraoperative complications include anesthetic and metabolic disorders, neurovascular disorders, problems in the femur and pelvis, and excessive bleeding. Early complications are divided into two groups: general (thrombosis and allergic reactions) and local (hematoma, infection, dislocation of the prosthesis, complications of osteotomy of the greater trochanter and ectopic calcification or periarticular ossification). Late postoperative complications include fractures of the femur with a built-in endoprosthesis, displaced femoral neck fractures, the instability of the endoprosthesis, systemic complications, disease, particles and late infection (Kolundžić and Orlić 2011; Lehil and Bozic 2014).

Ectopic bone formations in the periarticular tissues after arthroplasty of the hip joint can occur in 43% of patients. These are classified into three groups (modified Brooker's classification): Level 0, without visible ossification of the X-ray; Level I, with heterotopic ossification; Level II, with severe heterotopic ossification (Neal et al. 2002; Kocic et al. 2006). Severe heterotopic ossifications have great clinical importance, because they can cause limited mobility of the hip joint and their incidence is 9%. The cause of this complication, or its etiopathogenesis, is not fully understood, but it is believed that soft tissue damaged through surgical intervention and inflammation facilitates the migration of awakened osteoprogenitor cells and allows for new bone formation (Sodemann et al. 1988). Prevention of the occurrence of periarticular bone tissue involves application of early postoperative radiotherapy and the use of non-steroidal anti-inflammatory drugs (NSAIDs), while the use of a low-frequency pulsed electromagnetic field, apart from preventing its occurrence, also reduces the incidence of the most severe forms of these complications (Kocic et al. 2006).

Infections of the implant are one of the most common complications and are present in all branches of orthopedics with an incidence of 0.5–4% (Barnes et al. 2006; Berry 2001). The factors that play a role in the occurrence of infections are numerous. Those pertaining to patients are their age, presence of comorbidities such as diabetes and other chronic diseases, and use of steroids, tobacco, or alcohol. The experience of the surgeon, the type of operating technique, the quality of the debridement of necrotic muscle and impurities of the wounds, flushing, and quality of care after surgery are also important. Features of the biomaterials, relating to their biocompatibility, surface characteristics, and size of the possible "dead space," also influence the occurrence of this complication.

The most common cause of infection is Gram-positive bacteria, the main example among them being *Staphylococcus aureus*, with a frequency of 30%. Among other causes, coagulase-negative *Staphylococci* (22%), Gram-negative bacilli (10%), anaerobes (5%), and *Enterococci* (3%) were also found (Trampuz et al. 2005).

The materials for prostheses are stainless steel, titanium and titanium alloys, all of which have slightly different degrees of adherence and proliferation of fibroblasts on their surface, thus affecting the degree of infection and bacterial growth. Implants made of stainless steel show a higher rate of infection compared to titanium (Melcher et al. 1994; Arens and Hansis 1996; Chang and Merritt 1994; Perren 1991).

Metal cannot cause an infection, but it can influence the development of infection by providing a substrate for the growth of bacteria and by preventing drainage (Solomon et al. 2001).

Besides the differences in their chemical composition, the materials used for endoprotheses are applied in various forms of finishing layer, with regard to their superficial structure, i.e., its roughness. The roughness of biomaterials determines the size of the total area of the implant, which has an impact on many properties; biocompatibility is determined by the host body and the potential infection (Darouiche 2001).

Coarse-textured, protruded surfaces and hydrophobic surfaces provide greater opportunity for bacterial adhesion compared to smooth surfaces.

At a later stage, in the 14 days after surgery, infection can occur through blood circulation. Immediately after placement of the implant, bacteria and proteins from both the plasma and the host cell compete for occupation of the cell surface proteins (Gristina et al. 1988; Gristina 1987). Any necrotic or poorly vascularized tissue or extracellular fluid contained in the space between the implant and the healthy tissue creates a favorable environment for the adherence of bacteria and their growth (Schlegel and Perren 2006).

Adherence of bacteria to the surface of the implant takes place in two phases (Darouiche 2001). In the first phase, the bacteria adhere on the surface by means of exopolysaccharides (EPSs), and are then grouped into multilayer structures of biofilm (Costerton et al. 2005; Harris and Richards 2006).

Biofilm made of bacteria is less susceptible to antibiotics and the immune system of the host (Costerton et al. 2005; Götz 2002), so that the biofilm and the bacteria within it are often the cause of infection around the implant (Trampuz et al. 2003).

In order to achieve less interactivity between biomaterials and bacteria, a lot of effort has been invested into the design and appearance of the surface of implants. One of these procedures involves polishing of the metal surfaces, because it has been shown that a rough surface facilitates bacterial adhesion (Quirynen and Bollen 1995; Harris et al. 2004). Titanium implants whose surface is covered with nitrogen ions, which reduce adhesion of *S. aureus*, *S. epidermidis*, *Streptococcus mutans* and *Pseudomonas aeruginosa*, have shown good results (Harris and Richards 2004; Koerner et al. 2002; Cyster et al. 2003; Groessner-Schreiber et al. 2003). This finishing layer/surface of the implant is suitable for osteosynthesis.

A joint implant with layers repulsive to proteins enables reduced adsorption of said proteins, biofilm development and adhesion of bacteria. This can be achieved in several ways: by coating implants with proteins, such as heparin and albumin, surface modification of the hydrophilic chains, with a phosphoryl choline-modified polymeric barrier or with a layer of polyethylene glycol (PEG) (Nagaoka and

Kawakami 1995; Galliani et al. 1994; Kinnari et al. 2005; Mori et al. 1982; Ruiz et al. 1999). Layers on the surface of the implant containing hydrophilic proteins (e.g., albumin) inhibit the adhesion of *S. aureus* and *S. epidermidis* (Pascual et al. 1986).

A decrease in the adsorption of blood serum, plasma, and proteins such as albumin and fibrinogen, as well as reducing adhesion of *S. aureus*, *S. epidermidis*, *P. aeruginosa*, *Streptococcus mutans*, also affects the existence of PLL-g-PEG (poly-L-lysine-polyethylene glycol) on the surface layer of the implant (Tosatti et al. 2003; Park et al. 1998; Desai et al. 1992).

Infections associated with surgical implants are treated with antibiotics, and the application of systemic antibiotics is associated with side effects, as a consequence of their toxicity and poor penetration to the place where their action is needed (Duran 2000).

Local application of antibiotics has been effective in treating infections, so it was reasonable to coat the osteosynthetic implants made of stainless steel and titanium with a thin polymer film infused an antibiotic. The biocompatible and biodegradable polymers used for this purpose include polylactic-glycolic acid (PLGA) and poly-DL lactide (PDLLA) (Mäkinen et al. 2005; Gollwitzer et al. 2003; Lucke et al. 2003). The idea behind this procedure was a slow local release of antibiotics, along with the decomposition of the polymer sheet. Studies were conducted with gentamicin, ciprofloxacin, and vancomycin, the major threat being development of resistance to antibiotics. In order to avoid this, combinations of antibiotics were not used, and the concentration of released antibiotics was set permanently above the minimum inhibitory concentration.

Besides antibiotics, the use of antiseptics with broad-spectrum antimicrobial activity against Gram-positive and Gram-negative bacteria on the implant's surface, such as chlorhexidine or quaternary ammonium salts, is recommended. Antiseptics have side effects in terms of hypersensitivity of the host tissue and a lethal effect on fibroblasts via the same mechanism that breaks down the cell walls of bacteria, however, they may also cause bacterial resistance (Davies et al. 2005).

Numerous studies were conducted using silver ions as the superficial layer of the implants for osteosynthesis because of their broad-spectrum antibacterial properties (Alt et al. 2004).

While performing a total hip arthroplasty, prophylactic use of antibiotics reduces late postoperative morbidity, but it is also associated with an irrational use of antibiotics, leading to resistance, diarrhea associated with antibiotics, or superinfection with *Clostridium*.

Before conducting the intervention, all patients receive a prophylactic single dose of a second-generation cephalosporin and thromboprophylactic therapy. The operating theaters use drain exhaust systems (Geneva Hip Atrhoplasy Registry 1996/2010).

Despite the existence of numerous studies, clinical trials and review articles, there is still no uniform protocol for the application of an antibiotic prophylaxis regarding both the mode and the length of application, as well as the type of antibiotic that is used.

Some of the literature shows that nerve damage occurs in 3–4% of cases of primary THR and in 7.5% of cases with revision surgery, occurring more frequently in women and cases of long-term, advanced hip dysplasia. The most common damaged nerve is the sciatic nerve (0.7–1%), during the rear surgical approach (Ben-David et al. 2003). Nerve damage is caused by traction, ischemia, compression, extension of the limbs or hematoma formation (Craig et al. 2001; Ince et al. 2007; Picado et al. 2007; Stojkovic Jovanovic et al. 2013). In the anterolateral and direct lateral approaches to the articular hip, there is a possibility of damage to *n. gluteus superior*. During surgical intervention, blood vessels can be damaged (0.2–0.3%). The blood vessels that are most often damaged are the femoral vein and artery and *a. iliaca externa* (Stojkovic Jovanovic et al. 2013; Shoenfeld et al. 1990; Lavernia et al. 2007).

One of the most important complications after arthroplasty of the hip is a dislocation. Its frequency varies from 1 to 10%, but mostly comes in at 2–3% (McCollum and Gray 1990; Lewinnek et al. 1978; Mahoney and Pellicci 2003; Kovacevic et al. 2011). Posterior dislocation has the highest incidence (60–90%) of all locations and occurs at the position of the leg in flexion, adduction and in internal rotation. The position of the legs that makes for front dislocation is an extension, abduction and external rotation (Coventry et al. 1974). This complication is more common in women than in men, and is associated with the method of surgical procedure used in surgery (Woo and Morrey 1982). It occurs most often in the first month after surgery (40–70%), according to some authors, as well as in the third month (Berry 2001), and even sometimes years after surgery. The bibliography mentions dislocation after 5 years of installation with a frequency of 0.5%, mostly due to stretching of the capsule (Fender et al. 1999; Mahoney and Pellicci 2003).

Factors contributing to the emergence of dislocations may pertain to the patient, surgeon, or a combination of both factors. Most often, they include: previous surgery on the hip joint, the type of surgical approach, bone impingement, orientation of the prosthesis components—the optimum inclination being considered to be 40°–50° with 15°–25° anteversion (McCollum and Gray 1990), and the correct choice of prosthesis, especially the size of the femoral head and choice of acetabular liners. The clinical signs and symptoms that suggest luxation are the presence of pain, limb shortening, or a change in the position of the extremities with radiological confirmation of dislocations. Dislocations are resolved by repositioning. The most commonly performed procedure is closed reduction, and if this does not solve the problem, surgical repositioning must be applied. Precautions for reducing the chance of dislocation include a conversation with the patient after surgery and familiarization with the positions that need to be avoided and that could lead to this complication. Particular attention should be paid to the patient's safety while standing up from a chair and getting out of bed.

Thromboembolic disease is a possible complication that occurs after THR installation. In order to prevent or reduce the risk of its occurrence, prophylactic medication is used (warfarin, aspirin, low molecular weight heparin, fondaparinux, melagatran, etc.) (Johanson et al. 2009; Fishmann 2008), as is early mobilization of

the patient immediately after surgery, if possible. Differences in the length of administration, dosage and the combination of these products may occur based on the various centers and regions.

Foreign micro-particle disease is a multifactorial complication characterized by an inflammatory reaction in the vicinity of the components of the hip endoprosthesis, which consequently leads to the demineralization and loss of critical mass of bones with the aseptic loosening of the prosthesis (Kolundzic and Orlic 2008; Hernandez et al. 1994; Garcia-Cimbrelo and Munuera 1992; Schmalzried et al. 1992; Lombardi et al. 1989; Nicolli et al. 2011). Foreign particles such as metal, polyethylene and bone cement are released in the process of friction or abrasion on the contact surfaces between the components of the endoprosthesis and the bone or those between the bone and the bone cement. One of the most common ways to release the particles is friction between the contact surfaces between the metal femoral head tems and the polyethylene acetabular component. Recent studies show that a significantly higher risk for the development of foreign micro-particle disease exists in patients in whom the prosthesis was installed at younger ages (Kolundzic and Orlic 2008), associated, as they are, with higher levels of physical activity. It is noted that the percentage of these complications is higher in patients whose indication for hip replacement was a developmental anomaly, in comparison to other reasons for the operation, as well as after surgical interventions that lasted longer than 90 min or less than 50 min and after those performed by less experienced surgeons. An important role is played by the individual's susceptibility, characterized by a molecular surface for the development of inflammatory reactions, which involve many cellular and humoral mediators of inflammation. There are studies that show the importance of the inclining acetabular angle, which should be $45° \pm 5°$, in the development of these complications. If this angle is not achieved, due to poor biomechanics of the joint and greater friction, it leads to the occurrence of this complication. On the other hand, there are data that indicate the occurrence of this condition even when a satisfactory angle of inclination is achieved (Kolundzic et al. 2005; Kordelle and Starker 2000; Kolunđžić 2002; Småbrekke et al. 2004; Eskelinen et al. 2006). Aseptic loosening occurs in all materials used for endoprosthesis, with the same mediators of inflammation, the largest incidence occurring with cementless prostheses without hydroxyapatite coating (Eskelinen et al. 2005; Maloney et al. 1993). The development of new materials such as highly crosslinked polyethylene (HXLPE), has shown a lower level of wear compared to the older, non-crosslinked polyethylene parts (Berry et al. 1994).

As a complication of THR, a hematoma can occur. There is an increasingly prevalent opinion that patients with hip arthroplasty should not be supplied with a drain for postoperative hematoma due to the risk of infection through the drain. Surgeons have been understandably reluctant to skip this step, fearing infection from a postoperative hematoma, which is in accordance with conventional surgical beliefs. In any case, if surgeons decide not to put in the drain, they should take care that a perfect hemostasis is obtained (Mitkovic et al. 2002).

8 Statistical Data Related to the Application of Endoprostheses of the Hip Joint in the Central Region of Serbia

Data were taken from the medical records of 874 patients of both sexes, treated at the Orthopedic Clinic of the Clinical Center in Kragujevac from January 1st, 2009 to December 1st, 2014. Unilateral total hip endoprosthesis was performed on all patients. The observed parameters were age, sex, fixation of the prosthesis and the cause of the intervention. The youngest patient was 26 and the oldest 89. Data were statistically analyzed through different tests.

In patients with cement-type THR, a femoral stem made out of the stainless steel alloy FeCrNiMnMoNbN was used in multiple sizes, along with a cobalt chrome alloy for the head stems. The stem area was uneven due to the existence of longitudinal channels, whose role was to increase the contact surface anchored in the cement.

In cementless prostheses, the stem was the titanium aluminum alloy Ti6Al4V and the acetabular shell was the head of a cobalt chromium molybdenum alloy with an acetabular polyethylene cap. The femoral stem had highly polished surfaces that facilitated insertion, with a circumferential plasma spray on it that formed the fixation surface of the bone and the implant.

All types of implanted endoprosthesis were produced by renowned manufacturers (guaranteed by ISO certificates and CE standards), made of biologically indifferent materials (alloys TiAlVa4, CoCrMo, UMWPH, ceramics).

The most frequently used approach to the THR was the posterior approach (Onyemaechi et al. 2014; Chechik et al. 2013), together with the lateral one.

In all patients, thromboprophylaxis was conducted by administering low molecular weight heparin over 30 consecutive days. In the evening, after the operation, the first dose of heparin was administered.

There are differences in the recommendations regarding the length of administration, dosage and the combination of these products in various centers and regions (Fishmann 2008).

Antibiotic prophylaxis was conducted using a first-generation cephalosporin half an hour prior to surgical incision by intravenous application of the first dose, and then administration of the next three doses at 24 h-intervals after surgery.

Of the total number of 874 patients, 606 were women and 286 men, as can be seen in Table 1. Percentages show that women made up 69.34% and men 30.66%,

Table 1 The number of male and female patients with THR

Sex	Cases					
	Valid		Missing		Total	
	N	Percent (%)	N	Percent (%)	N	Percent (%)
Female	606	100.0	0	0	606	100.0
Male	268	100.0	0	0	268	100.0

which shows that the THR was performed more frequently in women than in men, possibly explaining the previous research that linked the indications for this intervention and their representation among the sexes. These data were also correlated with the fact that osteoarthritis, as the most common cause of hip endoprosthesis, occurs more frequently in women over 40 years of age (Østerås et al. 2013; Bierma-Zeinstra et al. 2002; Grotle et al. 2008). Studies conducted in England showed a higher percentage of men, while in Canada, there was no difference in representation of the sexes regarding prosthesis insertion (Peterson et al. 2010; Judge et al. 2010).

The analysis of statistical data in female patients showed that the average age of women was 63.46, SD $\pm$ 9.76, and the average age of men was 63.94, SD $\pm$ 9.85, which indicates the same age of patients of both sexes with THA, as shown in Table 2. The youngest female patient was 31 and the oldest was 90. For males, the youngest patient was 26 years old and the oldest was 82 (Table 2).

Extensive statistical studies have shown that there is no statistically significant difference between the variables regarding gender and age of the patients, as shown by the Mann-Whitney test (Table 3), $p = 0.22$, and using the Kolmogorov-Smirnov test for variable age, depending on the age of both sexes, as shown in the distribution of the data deviating from normal $p = 0.05$ for women and men at $p = 0.008$.

When it comes to the choice of the manner of fixation of the prosthesis, there is still no consensus on which method is the best; therefore, in Sweden and Norway, a higher percentage of surgeons use a method of fixation with cement, compared to North America and Australia, where cementless fixation of the prosthesis is preferred (Corten et al. 2011a, b). In 2012, in the United States, 93% of THR were cementless.

The important factors in the selection of the prosthesis and the manner of fixation are the age and sex of the patient at the time of the intervention, which has great significance for the longevity of the implant (Corten et al. 2011a, b).

Comparing the cost of installation of the prostheses, the speed of recovery and the quality of life after surgery, some studies have shown that cement prostheses are the cheapest for installation, while hybrid prostheses provide the best quality of life after the intervention, and thus are the most favorable choice for most patients. Cementless hip prostheses are the most expensive to install, but the most commonly used type of prosthesis in England, Wales, Italy, Australia, Canada and the United States (Pennington et al. 2013).

Of the total number of 606 women, cement prostheses were implanted in 173 female patients (19.8% of the total number of patients of both sexes and 28.5% of women). In men, of the total number of 268, this type of prosthesis was implanted in 75, which makes 8.6% of all patients of both sexes and 28% of all men.

Cementless prostheses were implanted in 309 women (35.4% of all patients and 51% of all women). This type of prosthesis was implanted in 131 men (representing 15% of the total number of patients and 48.9% of men). The hybrid prosthesis was implanted in 124 women (14.2% of all patients and 20.5% of female patients) and 62 men (7.1% of all patients and 23.1% of the total number of men).

Table 2 Age characteristics of men and women with THR

	Sex			Mean	Std. error
Age	Female	Mean		63.4554	0.39655
		95% confidence interval for mean	Lower bound	62.6767	
			Upper bound	64.2342	
		5% Trimmed mean		63.6216	
		Median		63.0000	
		Variance		95.293	
		Std. deviation		9.76182	
		Minimum		31.00	
		Maximum		90.00	
		Range		59.00	
		Interquartile range		13.00	
		Skewness		−0.184	0.099
		Kurtosis		−0.056	0.198
	Male	Mean		63.9403	0.60152
		95% confidence interval for mean	Lower bound	62.7560	
			Upper bound	65.1246	
		5% Trimmed mean		64.4270	
		Median		65.0000	
		Variance		96.970	
		Std. deviation		9.84735	
		Minimum		26.00	
		Maximum		82.00	
		Range		56.00	
		Interquartile range		11.75	
		Skewness		−0.678	0.149
		Kurtosis		0.681	0.297

Table 3 Application of the Mann-Whitney test to show the variable gender and age of the patients

	Age
Mann-Whitney U	76981.000
Wilcoxon W	260902.000
Z	−1.228
Asymp. Sig. (2-tailed)	0.220

Analysis of the data showed that the most common type of cementless prosthesis was implanted in 440 patients, representing 50.3% of the total number of patients treated (this type of prosthesis was implanted in 309 female patients and 131 male

patients), which may be linked to the fact that this type of implant is commonly used in England, Wales, Italy, Australia, Canada and the United States (Pennington et al. 2013). The reason for this distribution can be found in the demographics of the population. The smallest percentage were the hybrid prostheses—21.3% (implanted in 124 female and 62 male patients)

Applying the Chi-Square test, it was demonstrated that there was no connection between the manner of fixation and the sex of the patient, $p = 0.667$, as can be seen in Table 4.

In analysis of the data related to the indications for THR, all factors that have caused this intervention were divided into two groups. The first group was related to trauma or injury, and the second group included all other factors: osteoarthritis of the hip joint, dysplasia, osteonecrosis of the femoral head, and connective tissue diseases (such as rheumatoid arthritis, systemic lupus erythematosus, ankylosing spondylitis and Paget's bone disease). It can be seen in Table 5 that trauma as the cause of THR existed in 21.2% of the total number of patients, i.e., 185 patients (140 women and 45 men). In 78.8% of all patients, the factors resulting in

Table 4 Application of the chi-square test for the assessment of relationship between sex of the patient and fixation method

	Value	Df	Asymp. Sig. (2-sided)
Pearson chi-square	0.809(a)	2	0.667
Likelihood ratio	0.800	2	0.670
Linear-by-Linear Association	0.395	1	0.530
N of valid cases	874		

Table 5 The relationship between causes of THR and the patient's sex

			Cause		1
			Trauma	Other	Total
Sex	Female	Count	140	466	606
		% within sex	23.1	76.9	100.0
		% within cause	75.7	67.6	69.3
		% of total	16.0	53.3	69.3
	Male	Count	45	223	268
		% within sex	16.8	83.2	100.0
		% within cause	24.3	32.4	30.7
		% of total	5.1	25.5	30.7
Total		Count	185	689	874
		% within sex	21.2	78.8	100.0
		Cause	100.0	100.0	100.0
		% of total	21.2	78.8	100.0

Table 6 Application of the chi-square test in order to show variables of the gender of patients and the manner of prosthesis fixation

	Value	Df	Asymp. sig. (2-sided)	Exact sig. (2-sided)	Exact sig. (1-sided)
Pearson chi-square	4.436 (b)	1	0.035		
Continuity correction (a)	4.066	1	0.044		
Likelihood ratio	4.582	1	0.032		
Fisher's exact test				0.039	0.021
Linear-by-Linear Association	4.431	1	0.035		
N of valid cases	874				

indication for this intervention are listed in a group of "other causes of THR" (Table 5). These data indicate that osteoarthritis is the most common cause of THR and that it was present with a frequency of 70% (Østerås et al. 2013; Bierma-Zeinstra et al. 2002; Grotle et al. 2008).

The Chi-Square test indicated a statistically significant difference between the variables of gender and the cause of the prosthesis, $p = 0.039$, i.e., the cause was related to gender. Degenerative disease as the cause of prosthesis was present in 53.3% of women and 25.5% of men, while trauma as the cause was present in 16% of women and 5.1% of men (Table 6). The coefficient of contingency is enclosed.

During the six-year period from 2009 to 2014, the largest number of THR interventions was carried out in 2013, with 193 patients, which represents 22.1% of the total number of patients.

Analysis of the data showed that the lowest number of THR interventions was performed during the fall (18.3%) and the most numerous in spring (30.5%), most frequently on women (186 female patients, which represents 21.3% of patients).

It can be seen that the average age of patients with a cement type prosthesis was 72.53 years, followed by 57.39 years with cementless and 66.39 years with a hybrid (Table 7). The cement type of prosthesis was used in patients with the highest average age, and the cementless type of prosthesis was used in patients with the youngest average age, which is in accordance with the recommendations on the selection and method of fixation of the prosthesis, as well as with age demands and the level of physical activity suitable for the age.

By applying the Kruskal Wallis test, a statistically significant difference was found in the method of fixation of prostheses between the cement and cementless, as well as between the cement and hybrid prostheses. Thus, between the cementless and the hybrid, a high, statistically significant difference appeared, indicating that the cementless type of prosthesis was used more often in younger patients and the cement type in the elderly patients.

Trauma as a cause of hip arthroplasty was found in 185 patients with an average age of 64.5. The oldest patient was 90 years old and the youngest 26. Factors of THR implantation that were classified as "other" causes were represented in 689

Table 7 Relationship between patient age and prosthesis type

Descriptives					
Manner of fixation				Statistic	Std. error
Age	Cement type	Mean		72.5323	0.45597
		95% Confidence	Lower bound	71.6342	
		Interval for mean	Upper bound	73.4303	
		5% Trimmed		73.0063	
		Mean		73.5000	
		Median		51.562	
		Variance		7.18065	
		Std. deviation		36.00	
		Minimum		90.00	
		Maximum		54.00	
		Range		7.00	
		Interquartile range		−1.361	0.155
		Skewness		3.673	0.308
		Kurtosis			
	Cementless type	Mean		57.3909	0.36648
		95% confidence	Lower bound	56.6706	
		Interval for mean	Upper bound	58.1112	
		5% Trimmed		57.5455	
		Mean		58.0000	
		Median		59.095	
		Variance		7.68734	
		Std. deviation		26.00	
		Minimum		86.00	
		Maximum		60.00	
		Range		9.00	
		Interquartile range		−0.341	0.116
		Skewness		1.835	0.232
		Kurtosis			
	Hybrid type	Mean		66.3978	0.44134
		95% confidence	Lower bound	65.5271	
		Interval for mean	Upper bound	67.2686	
		5% Trimmed		66.8100	
		Mean		67.0000	
		Median		36.230	
		Variance		6.01914	
		Std. deviation		39.00	
		Minimum		81.00	
		Maximum		42.00	
		Range		4.00	

(continued)

Table 7 (continued)

Descriptives					
Manner of fixation				Statistic	Std. error
		Interquartile range		−1.800	0.178
		Skewness		6.739	0.355
		Kurtosis			

Table 8 Relationship between the variables of method of fixation and the cause of THR installation

Manner of fixation * cause cross tabulation						
				Cause		Total
				Trauma	Other	
Manner of fixation	Cement type	Count % within % within % of total	Manner of fixation Cause	54 21.8% 29.2% 6.2%	194 78.2% 28.2% 22.2%	248 100.0% 28.4% 28.4%
	Cementless type	Count % within % within % of total	Manner of fixation Cause	85 19.3% 45.9% 9.7%	355 80.7% 51.5% 40.6%	440 100·0% 50.3% 50.3%
	Hybrid type	Count % within % within % of total	Manner of fixation Cause	46 24.7% 24.9% 5.3%	140 75.3% 20.3% 16.0%	186 100.0% 21.3% 21.3%
Total		Count % within % within % of total	Manner of fixation Cause	185 21.2% 100.0% 21.2%	689 78.8% 100.0% 78.8%	874 100.0% 100.0% 100.0%

patients, with an average age of 63.3. The youngest patient was 35 and the oldest one was 85.

The cementless type of prosthesis, which was the most frequently used in our sample of patients, was present in 9.7% of patients with trauma as the cause for

THR implantation and in 40.6% of patients with other indications for this intervention (Table 8).

9 Conclusion

Total arthroplasty of the hip joint is the most common surgical intervention in orthopedics. Performance of this method requires knowledge of several factors, such as: the anatomy of the hip joint, indications and contraindications for THR, possible complications, knowledge of the age characteristics and demands of patients, and proper selection and application of prostheses and their characteristics. Technological progress has led to the development of new biomaterials, as well as new types of prosthesis that will, in the future, affect the reduction or disappearance of adverse reactions and complications of installing the prosthesis, as well as extending their lifespan.

References

Abdulkareem IH (2013) The evolution of total hip arthroplasty (THA). Hard Tissue 2(4):40

Albrektsson T, Brånemark PI, Hansson HA, Lindström J (1981) Osseointegrated titanium implants. Requirements for ensuring a long-lasting, direct bone-to-implant anchorage in man. Acta Orthop Scand 52(2):155–170

Alt V, Bechert T, Steinrücke P, Wagener M, Seidel P, Dingeldein E, Scheddin D, Domann E, Schnettler R (2004) Nanoparticulate silver. A new antimicrobial substance for bone cement. Orthopade 33(8):885–892

Arens S, Hansis M (1996) Titanium implants in accident surgery-when are they necessary? Langenbecks Arch Chir Suppl Kongressbd 113:938–940

Bannister GC (1993) Total Hip Replacement—which type? Curr Orthop 7:165

Barnes AM, Chang W, Morello R, Cabral WA, Weis M, Eyre DR, Leikin S, Makareeva E, Kuznetsova N, Uveges TE, Ashok A, Flor AW, Mulvihill JJ, Wilson PL, Sundaram UT, Lee B, Marini JC (2006) Deficiency of cartilage-associated protein in recessive lethal osteogenesis imperfecta. N Engl J Med 355(26):2757–2764

Ben-David B, Joshi R, Chelly JE (2003) Sciatic nerve palsy after total hip arthroplasty in a patient receiving continuous lumbar plexus block. Anesth Analg 97(4):1180–1182

Berry DJ (2001) Primary total hip arthroplasty. In: Chapman MW (eds) Chapman's orthopaedic surgery, 3rd edn. Lippincott Williams & Wilkins, Philadelphia

Berry DJ, Barnes CL, Scott RD, Cabanela ME, Poss R (1994) Catastrophic failure of the polyethylene liner of uncemented acetabular components. J Bone Joint Surg 76(4):575–578

Bierma-Zeinstra SM, Oster JD, Bernsen RM, Verhaar JA, Ginai AZ, Bohnen AM (2002) Joint space narrowing and relationship with symptoms and signs in adults consulting for hip pain in primary care. J Rheumatol 29(8):1713–1718

Byrne DP, Mulhall KJ, Baker JF (2010) Anatomy & biomechanics of the hip. Open Sports Med J 4:51–57

Chang CC, Merritt K (1994) Infection at the site of implanted materials with and without preadhered bacteria. J Orthop Res 12(4):526–531

Charnley J (1961) Arthroplasty of the hip: a new operation. Lancet 1:1129–1132

Charnley J (1972) The long-term results of low-friction arthroplasty of the hip performed as a primary intervention. J Bone Joint Surg 54(1):61–76
Charnley J (1979) Low friction arthroplasty of the hip: theory and practice. Springer, Berlin
Charnley J, Ferreiraade S (1964) Transplantation of the greater trochanter in arthroplasty of the hip. J Bone Joint Surg Br 46:191–197
Chechik O, Khashan M, Lador R, Salai M, Amar E (2013) Surgical approach and prosthesis fixation in hip arthroplasty world wide. Arch Orthop Trauma Surg 133(111):1595–1600. doi:10.1007/s00402-013-1828-0
Collis DK (1991) Long-term (twelve to eighteen-year) follow up of cemented total hip replacements in patients who were less than fifty years old. J Bone Joint Surg 73:593–597
Cornell CN, Ranawat CS (1986) The impact of modern cement techniques on acetabular fixation in cemented total hip replacement. J Arthroplasty 1(3):197–202
Corten K, Bourne RB, Charron KD, Au K, Rorabeck CH (2011a) Comparison of total hip arthroplasty performed with and without cement: a randomized trial. A concise follow-up, at twenty years, of previous reports. J Bone Joint Surg Am 93(14):1335–1338. doi:10.2106/JBJS.J.00448
Corten K, Bourne RB, Charron KD, Au K, Rorabeck CH (2011b) What works best, a cemented or cementless primary total hip arthroplasty?: minimum 17-year followup of a randomized controlled trial. Clin Orthop Relat Res 469(1):209–217. doi:10.1007/s11999-010-1459-5
Costerton JW, Montanaro L, Arciola CR (2005) Biofilm in implant infections: its production and regulation. Int J Artif Organs 28(11):1062–1068
Coventry MB, Beckenbaugh RD, Nolan DR, Ilstrup DM (1974) 2012 total hip arthroplasties: a study of postoperative course and early complications. J Bone Joint Surg 56(2):273–284
Craig J, Della V, Di Cesara PE (2001–2002) Complications of total hip arthroplasty: neurovascular injury, leg-length discrepancy, and instability. Bull Hosp Joint Dis 60(3–4):134-42
Cyster LA, Parker KG, Parker TL, Grant DM (2003) The effect of surface chemistry and nanotopography of titanium nitride (TiN) films on 3T3-L1 fibroblasts. J Biomed Mater Res A 67(1):138–147
Darouiche RO (2001) Device-associated infections: a macroproblem that starts with microadherence. Clin Infect Dis 33(9):1567–1572
Davies R, Holt N, Nayagam S (2005) The care of pin sites with external fixation. J Bone Joint Surg Br 87(5):716–719
Dawson J, Fitzpatrick R, Murray D, Carr A (1996) Comparison of measures to assess outcomes in total hip replacement surgery. Qual Health Care 5(2):81–88
Deramond H, Wright NT, Belkoff SM (1999) Temperature elevation caused by bone cement polymerization during vertebroplasty. Bone 25:17–21
Desai NP, Hossainy SF, Hubbell JA (1992) Surface-immobilized polyethylene oxide for bacterial repellence. Biomaterials 13(7):417–420
Dorr LD, Faugere MC, Mackel AM, Gruen TA, Bognar B, Malluche HH (1993) Structural and cellular assessment of bone quality of proximal femur. Bone 14(3):231–242
Duran LW (2000) Preventing medical device related infections. Med Device Technol 11(6):14–17
Engh CA, O'Connor D, Jasty M, McGovern TF, Bobyn JD, Harris WH (1992) Quantification of implant micromotion, strain shielding, and bone resorption with porouscoated anatomic medullary locking femoral prostheses. Clin Orthop Relat Res 285:13–29
Eskelinen A, Remes, Helenius I, Pulkkinen P, Nevalainen J, Paavolainen P (2005) Total hip arthroplasty for primary osteoarthritis in young patients in the Finnish Arthroplasty Register. 4661 primary replacements followed for 0–22 years. Acta Orthop 76(1):28–41
Eskelinen A, Paavolainen P, Helenius I, Pulkkinen P, Remes V (2006) Total hip arthroplasty for rheumatoid arthritis in younger patients: 2557 replacements in the finnish arthroplasty register followed for 0–24 years. Acta Orthop 77(6):853–865
Fender D, Harper WM, Gregg PJ (1999) Outcome of charnley total hip replacement across a single health region in England: the results at five years from a regional hip register. J Bone Joint Surg Br 81(4):577–581

Ferguson AB Jr (1973) Primary open reduction of congenital dislocation of the hip using a median adductor approach. J Bone Joint Surg Am 55(4):671–689
Fishmann A (2008) VTE prevention in major orthopedic surgery. Cleve Clin J Med 75(7):471
Galante J, Rostoker W, Lueck R, Ray RD (1971) Sintered fiber metal composites as a basis for attachment of implants to bone. J Bone Joint Surg Am 53(1):101–114
Galliani S, Viot M, Crémieux A, Van der Auwera P (1994) Early adhesion of bacteremic strains of Staphylococcus epidermidis to polystyrene: influence of hydrophobicity, slime production, plasma, albumin, fibrinogen, and fibronectin. J Lab Clin Med 123(5):685–692
Garcia-Cimbrelo E, Munuera L (1992) Early and late loosening of the acetabular cup after low-friction arthroplasty. J Bone Joint Surg (Am) 74:1119–1129
Glassman AH, Engh CA, Bobyn JD (1987) A technique of extensile exposure for total hip arthroplasty. J Arthroplasty 2:11–21
Gollwitzer H, Ibrahim K, Meyer H, Mittelmeier W, Busch R, Stemberger A (2003) Antibacterial poly(D, L-lactic acid) coating of medical implants using a biodegradable drug delivery technology. J Antimicrob Chemother 51(3):585–591
Gomez PF, Morcuende JA (2005) Early attempts at hip arthroplasty 1700s to 1950s. Iowa Orthop J 25:25–29
Götz F (2002) Staphylococcus and biofilms. Mol Microbiol 43(6):1367–1378
Gristina AG (1987) Biomaterial-centered infection: microbial adhesion versus tissue integration. Science 237(4822):1588–1595
Gristina AG, Naylor P, Myrvik Q (1988–1989) Infections from biomaterials and implants: a race for the surface. Med Prog Technol 14(3–4):205–224
Groessner-Schreiber B, Neubert A, Müller WD, Hopp M, Griepentrog M, Lange KP (2003) Fibroblast growth on surface-modified dental implants: an in vitro study. J Biomed Mater Res A 64(4):591–599
Grotle M, Hagen KB, Natvig B, Dahl FA, Kvien TK (2008) Prevalence and burden of osteoarthritis: results from a population survey in Norway. J Rheumato l35:677–684
Haddad RJ Jr, Cook SD, Thomas KA (1987) Biological fixation of porous-coated implants. J Bone Joint Surg Am 69(9):1459–1466
Hardinge K (1982) The direct lateral approach to the hip. J Bone Joint Surg Br 64(1):17–19
Harris LG, Richards RG (2004) *Staphylococcus aureus* adhesion to different treated titanium surfaces. J Mater Sci Mater Med 15(4):311–314
Harris LG, Richards RG (2006) Staphylococci and implant surfaces: a review. Injury 37:3–14
Harris LG, Tosatti S, Wieland M, Textor M, Richards RG (2004) *Staphylococcus aureus* adhesion to titanium oxide surfaces coated with non-functionalized and peptide-functionalized poly (L-lysine)-grafted poly (ethylene glycol) copolymers. Biomaterials 25(18):4135–4148
Harris WH (1967) A new lateral approach to the hip joint. J Bone Joint Surg Am 49(5):891–898
Harris WH (1973) Extensive exposure of the hip joint. Clin Orthop Relat Res 91:58–62
Havelin LI, Vollset SE, Engesaeter LB (1995) Revision for aseptic loosining of uncemented cups in 4325 primary hip prostheses. A report from the Norwegian Arthroplasty Register. Acta Orthop Scand 66(6):494–500
Hawkins ME (2005) Development of polymers for minimally invasive orthopedic implants, in Graduate School of the University of Notre Dame. University of Notre Dame, Notre Dame, p 122
Hernandez JR, Keating EM, Faris PM, Meding JB, Ritter MA (1994) Polyethylene wear in uncemented acetabular components. J Bone Joint Surg 76(2):263–266
Ince A, Kemper M, Waschke J, Hendrich C (2007) Minimally invasive anterolateral approach to the hip: risk to the superior gluteal nerve. Acta Orthop 78(1):86–89
James SP, Jasty M, Davies J, Piehler H, Harris WH (1992) A fractographic investigation of PMMA bone cement focusing on the relationship between porosity reduction and increased fatigue life. Biomed Mater Res 26(5):651–662
Jasty M, Bragdon C, Burke D, O'Connor D, Lowenstein J, Harris WH (1997) In vivo skeletal responses to porous-surfaced implants subjected to small induced motions. J Bone Joint Surg Am 79(5):707–714

Jiranek W (2005) Thermal manipulation of bone cement. Orthopedics 28(8):863–866
Johanson NA, Lachiewicz PF, Lieberman JR, Lotke PA, Parvizi J, Pellegrini V, Stringer TA, Tornetta P 3rd, Haralson RH 3rd, Watters WC 3rd (2009) Prevention of symptomatic pulmonary embolism in patients undergoing total hip or knee arthroplasty. J Am Acad Orthop Surg 17(3):183–196
Jolles BM, Bogoch ER (2004) Surgical approach for total hip arthroplasty: direct lateral or posterior. J Rheumatol 31(9):1790–1796
Jolles BM, Bogoch ER (2006) Posterior versus lateral surgical approach for total hip arthroplasty in adults with osteoarthritis. Cochrane Database Syst Rev 9(3):CD003828
Judet J, Judet R (1950) The use of an artificial femoral head for arthroplasty of the hip joint. Bone Joint Surg Br 32(2):166–173
Judge A, Welton NJ, Sandhu J, Ben-Shlomo Y (2010) Equity in access of total joint replacment of hip and knee in England: cross-sectional study. BMJ 341:c4092. doi:10.1136/bmj.c4092
Jun Y, Choi K (2010) Design of patient-specific hip implants based on the 3D geometry of the human femur. Adv Eng Softw 41(4):537–547
Khanuja HS, Vakil JJ, Goddard MS, Mont MA (2011) Cementless femoral fixation in total hip arthroplasty. J Bone Joint Surg Am 93(5):500–509. doi:10.2106/JBJS.J.00774
Kinnari TJ, Peltonen LI, Kuusela P, Kivilahti J, Könönen M, Jero J (2005) Bacterial adherence to titanium surface coated with human serum albumin. Otol Neurotol 26(3):380–384
Knight SR, Aujla R, Biswas SP (2011) Total hip arthroplasty—over 100 years of operative history. Orthop Rev 3(2):e16. doi:10.4081/or.2011.e16
Kocic M, Lazovic M, Kojovic Z, Mitkovic M, Milenkovic S, Ciric T (2006) Methods of the physical medicine therapy in prevention of heterotopic ossification after total hip arthroplasty. Vojnosanit Pregl 63(9):807–811
Koerner RJ, Butterworth LA, Mayer IV, Dasbach R, Busscher HJ (2002) Bacterial adhesion to titanium-oxy-nitride (TiNOX) coatings with different resistivities: a novel approach for the development of biomaterials. Biomaterials 23(14):2835–2840
Koizumi W, Moriya H, Tsuchiya K, Takeuchi T, Kamegaya M, Akita T (1996) Ludloff's medial approach for open reduction of congenital dislocation of the hip. A 20-year follow-up. J Bone Joint Surg Br 78(6):924–929
Kolundzic R, Sulentic M, Smerdelj M, Orlic D, Trkulja V (2005) Stability of endler cementless polyethylene acetabular cup: long-term follow-up. Croat Med J 46(2):261–267
Kolundzic R, Orlic D (2008) Particle disease-aseptic loosening of the total hip endoprosthesis. Lijec Vjesn 130(1–2):16–20
Kolundžić R, Orlić D (2011) Četrdeset godina ugradnje totalne endoproteze zglobova kuka u Hrvatskoj, u klinici za ortopediju Zagreb ortopedska operacija 20. Stoljeća. Iz hrvatske medicinske prošlosti. Liječ Vjesn 133:343–351
Kolundzic R, Trkulja V, Orlic D (2012) History and factors of survival of total hip arthroplasty. Med Glas Zenica 9(1):136–142
Kolunđžić R (2002) Utjecaj biomehaničkih činitelja na opseg i učestalost polietilenske bolesti kod endoproteza zgloba kuka. University of Zagreb
Kordelle J, Starker M (2000) Migration analysis of cemented Muller polyethylene acetabular cups versus cementfree Zweymuller screw-attached acetabular cups. Z Orthop Ihre Grenzgeb 138 (1):46–51
Kovacevic D, Mariscalco M, Goodwin RC (2011) Injuries about the hip in the adolescent athlete. Sports Med Arthrosc 19(1):64–74. doi:10.1097/JSA.0b013e31820d5534
Kovačević M, Kovačević M, Ristić S, Marić S, Dostić M, Marić R, Marić V, Miletić R, Erić D, Lalović N, Potpara D, Mari H (2011) Luksacija kao komplikacija artroplastike kuka. Biomedicinska istraživanja 2(1):40–44
Kuehn K-D, Ege W, Gopp U (2005) Acrylic bone cements. Composition and properties. Orthop Clin North Am 36(1):17–28
Kühn K-D (2000) Bone cements. Up-to-date comparison of physical and mechanical properties of commercial materials. Springer, Heidelberg

Kwon MS, Kuskowski M, Mulhall KJ, Macaulay W, Brown TE, Saleh KJ (2006) Does surgical approach affect total hip arthroplasty dislocation rates? Clin Orthop Relat Res 447:34–38
Lai PL, Chen LH, Chen WJ, Chu IM (2013) Chemical and physical properties of bone cement for vertebroplasty. Biomed J 36(4):162–167. doi:10.4103/2319-4170.112750
Lavernia CJ, Cook CC, Hernandez RA, Sierra RJ, Rossi MD (2007) Neurovascular injuries in acetabular reconstruction cage surgery: an anatomical study. J Arthroplasty 22(1):124–132
Learmonth ID, Young C, Rorabeck C (2007) The operation of the century: total hip replacement. Lancet 370:1508–1519
Lehil MS, Bozic KJ (2014) Trends in total hip arthroplasty implant utilization in the United States. J Arthroplasty 29(10):1915–1918. doi:10.1016/j.arth.2014.05.017
Lewinnek GE, Lewis JL, Tarr R, Compere CL, Zimmerman JR (1978) Dislocations after total hip replacement atrhroplasties. J Bone Joint Surg 60(2):217–220
Lindgren V, Garellick G, Kärrholm J, Wretenberg P (2012) The type of surgical approach influences the risk of revision in total hip arthroplasty: a study from the Swedish Hip Arthroplasty Register of 90,662 total hipreplacements with 3 different cemented prostheses. Acta Orthop 83(6):559–565
Lombardi AV, Mallory TH, Vaugh BK, Drouliiard P (1989) Aseptic loosening in total hip arthroplasty secondary to osteolysis induced by wear debris from titanium-alloy modular femoral heads. J Bone Joint Surg 71(9):1337–1342
Lucke M, Schmidmaier G, Sadoni S, Wildemann B, Schiller R, Haas NP, Raschke M (2003) Gentamicin coating of metallic implants reduces implant-related osteomyelitis in rats. Bone 32 (5):521–531
Lukoschek M, Simank HG, Brocai DR (1998) Cementless hip prosthesis in inflammatory rheumatic diseases. Orthopade 27(6):392–395
Mahalingam K, Reidy D (1996) Smith-Petersen vitallium mould arthroplasty: a 45-year follow-up. J Bone Joint Surg Br 78(3):496–497
Mahoney CR, Pellicci PM (2003) Complications in primary total hip arthroplasty: avoidance and management of dislocations. Instr Course Lect 52:247–255
Majkowski RS, Miles AW, Bannister GC, Perkins J, Taylor GJ (1993) Bone surface preparation in cemented joint replacement. J Bone Joint Surg Br 75(3):459–463
Mäkinen TJ, Veiranto M, Knuuti J, Jalava J, Törmälä P, Aro HT (2005) Efficacy of bioabsorbable antibiotic containing bone screw in the prevention of biomaterial-related infection due to *Staphylococcus aureus*. Bone 36(2):292–299
Maloney WJ, Peters P, Engh CA, Chandler H (1993) Severe osteolysis of the pelvic in association with acetabular replacement without cement. J Bone Joint Surg Am 75(11):1627–1635
Marcy GH, Fletcher RS (1954) Modification of the posterolateral approach to the hip for insertion of femoral-head prosthesis. J Bone Joint Surg Am 36-A:142–143
McCollum DE, Gray WJ (1990) Dislocation after total hip arthroplasty: causes and prevention. Clin Orthop Rel Res 261:159–170
McLauchlan J (1984) The stracathro approach to the hip. J Bone Joint Surg 66:30–31
Melcher GA, Claudi B, Schlegel U, Perren SM, Printzen G, Munzinger J (1994) Influence of type of medullary nail on the development of local infection. An experimental study of solid and slotted nails in rabbits. J Bone Joint Surg Br 76(6):955–959
Mitkovic M, Mladenovic D, Qolubovic Z, Stanojkovic M, Milenkovic S, Micic L, Karalejic S, Jovanovic V, Ciric T, Stojiljkovic P, Kutlesic K, Kostic L, Mandic M, Andelovic D, Soldatovic G, Aranđelovic S, Ristic S, Milic L, Jevtic R, Velićkovic K, Mitkovic M, Brankovic B (2002) New concept of total hip arthroplasty and the results of biomechanical testing and clinical application. Acta Fac Med Naiss 19(3–4):222–229
Moore AT (1957) The self locking metal hip prosthesis. J Bone Joint Surg Am 39-A(4):811–27
Moore K, Dalley A (2006) Lower Limb. In: Moore K, Dalley A (eds) Clinically oriented anatomy, 5th edn. Lippincott Williams & Wilkins, Baltimor, pp 558–565
Moore KL, Dalley AF, Agur AMR (2006) Clinically oriented anatomy, 5th edn. Lippincott Williams & Wilkins, Philadelphia

Mori Y, Nagaoka S, Takiuchi H, Kikuchi T, Noguchi N, Tanzawa H, Noishiki Y (1982) A new antithrombogenic material with long polyethyleneoxide chains. Trans Am Soc Artif Intern Organs 28:459–463

Mrvaljević D (2006) Anatomija donjeg ekstremiteta - membrum inferius, 14-to izdanje. Savremena administracija, Beograd

Muller ME (1974) Proceedings of the second scientific meeting of the hip society. Total hip replacement without trochanteric osteotomy. C.V. Mosby, St Louis, pp 231–7

Muller ME (1975) Total hip replacement: Planning technique and complications. In: Surgical management of degenerative arthritis of the lower limb. Lea and Febiger, Heidelberg, p 91

Nagaoka S, Kawakami H (1995) Inhibition of bacterial adhesion and biofilm formation by a heparinized hydrophilic polymer. ASAIO J 41(3):365–368

Nakashima Y, Hayashi K, Inadome T, Uenoyama K, Hara T, Kanemaru T, Sugioka Y, Noda I (1997) Hydroxyapatite-coating on titanium arc sprayed titanium implants. J Biomed Mater Res 35(3):287–298

Neal B, Gray H, MacMahon S, Dunn L (2002) Incidence of heterotopic bone formatio after major hip surgery. ANZ J Surg 72(11):808–821

Nicolli A, Chiara F, Bortoletti I, Pasqualato F, Mongillo M, Gambalunga A, Biggi F, Trevisan A (2011) Release of metals from metal-on-metal hip prostheses. G Ital Med Lav Ergon 33:257–259

NIH Consensus Conference: Total Hip Replacement (1995) NIH consensus development panel on total hip replacement. JAMA 273:1950–1956

Onyemaechi N, Anyanwu E, Obikili E, Ekezie J (2014) Anatomical basis for surgical approaches to the hip. Ann Med Health Sci Res 4(4):487–494. doi:10.4103/2141-9248.139278

Østerås N, Risberg MA, Kvien TK, Engebretsen L, Nordsletten L, Bruusgaard D, Schjervheim UB, Haugen IK, Hammer HB, Provan S, Øiestad BE, Semb AG, Rollefstad S, Hagen KB, Uhlig T, Slatkowsky-Christensen B, Kjeken I, Flugsrud G, Grotle M, Sesseng S, Edvardsen H, Natvig B (2013) Hand, hip and knee osteoarthritis in a Norwegian population-based study- the MUST protocol. BMC Musculoskeletal Disord 14:201. doi:10.1186/1471-2474-14-201

Park KD, Kim YS, Han DK, Kim YH, Lee EH, Suh H, Choi KS (1998) Bacterial adhesion on PEG modified polyurethane surfaces. Biomaterials 19(7–9):851–859

Pascual A, Fleer A, Westerdaal NA, Verhoef J (1986) Modulation of adherence of coagulase-negative staphylococci to Teflon catheters in vitro. Eur J Clin Microbiol 5 (5):518–522

Paterson JM, Williams JI, Kreder HJ, Mahomed NN, Gunraj N, Wang X, Laupacis A (2010) Provider volumes and early outcomes of primary total joint replacement in Ontario. Can J Surg 53(3):175–183

Pennington M, Grieve R, Sekhon JS, Gregg P, Black N, van der Meulen JH (2013) Cemented, cementless, and hybrid prostheses for total hip replacement: cost effectiveness analysis. BMJ 346:1026. doi:10.1136/bmj.f1026

Perren SM (1991) The concept of biological plating using the limited contact-dynamic compression plate (LC-DCP). Scientific background, design and application. Injury 22:1–41

Picado GH, Garcia FL, Marques W (2007) Damage to the superior gluteal nerve after direct lateral approach to the hip. Clin Orthop Relat Res 455:209–211

Pilliar RM, Lee JM, Maniatopoulos C (1986) Observations on the effect of movement on bone ingrowth into porous-surfaced implants. Clin Orthop Relat Res 208:108–113

Pramanik S, Agarwal AK, Rai KN (2005) Chronology of total hip joint replacement and materials development. Trends Biomater Artif Organs 19(1):15–26

Quirynen M, Bollen CM (1995) The influence of surface roughness and surface-free energy on supra- and subgingival plaque formation in man. A review of the literature. J Clin Periodontol 22(1):1–14

Ruiz L, Fine E, Vörös J, Makohliso SA, Léonard D, Johnston DS, Textor M, Mathieu HJ (1999) Phosphorylcholine-containing polyurethanes for the control of protein adsorption and cell attachment via photoimmobilized laminin oligopeptides. J Biomater Sci Polym Ed 10(9):931–955

Santanapipatkul P, Udomkiat P (2012) Smith-petersen mould arthroplasty: a 48-year follow-up. Siriraj Med J 64(4):127–128

Schlegel U, Perren SM (2006) Surgical aspects of infection involving osteosynthesis implants: implant design and resistance to local infection. Injury 37:S67–S73

Schmalzried TP, Kwong LM, Jasty M, Sedlacek RC, Haire TC, O'Connor DO, Bragdon CR, Kabo JM, Malcolm AJ, Harris WH (1992) The mechanism of loosening of cemented acetabular components in total hip arthroplasty. Analysis of specimens retrieved at autopsy. Clin Orthop Relat Res 274:60–78

Schmalzried TP, Harris WH (1993) Hybrid total hip replacement. A 6.5-year follow-up study. J Bone Joint Surg Br 75(4):608–615

Schuenke M, Schulte E, Schumacher U (2006) Atlas of anatomy. General anatomy and musculoskeletal system. Thieme Stuttgart, New York

Schulte KR, Callaghan JJ, Kelley SS, Johnston RC (1993) The outcome of Charnley total hip arthroplasty with cement after a minimum twenty-year follow-up. The results of one surgeon. J Bone Joint Surg Am 75(7):961–975

Shoenfeld NA, Stuchin SA, Pearl R, Havenson S (1990) The management of vascular injuries associated with total hip arthroplasty. J Vasc Surg 11(4):549–555

Simon JP, Maes M, Robbens E, Bellemans J (2010) Total hip arthroplasty in inflammatory arthritis in patients under 35 years. A 7 to 19 year follow-up. Hip Int 20(2):163–170

Siopack JS, Jergesen HE (1995) Total hip arthroplasty. West J Med 162(3):243–249

Småbrekke A, Espehaug B, Havelin LI, Furnes O (2004) Operating time and survival of primary total hip replacement. An analysis of 31745 primary cemented and uncemented total hip replacements from local hospitals reported to the Norwegian Arthroplasty Register 1987–2001. Acta Ortop Scand 75(5):524–32

Smith SW, Estok DM 2nd, Harris WH (1998) Total hip arthroplasty with use of second-generation cementing techniques. An eighteen-year-average follow-up study. J Bone Joint Surg 80 (11):1632–1640

Smith-Petersen M (1948) Evolution of mould arthroplasty of the hip joint. J Bone Joint Surg 30 (1):59

Snell RS (2011) Clinical anatomy by regions, 9th edn. Lippincott Williams & Wilkins, Baltimore

Søballe K, Hansen ES, Brockstedt-Rasmussen H, Bünger C (1993) Hydroxyapatite coating converts fibrous tissue to bone around loaded implants. J Bone Joint Surg Br 75(5):270–278

Søballe K, Overgaard S (1996) The current status of hydroxyapatite coating of prostheses. J Bone Joint Surg Br 78:689–691

Sodemann B, Persson PE, Nilsson O (1988) Etiology and treatment of periarticular heterotopic ossification after total hip replacement. Rev Chir Orthop Reparatrice Appar Mot 74:329–330

Solomon L, Warwick D, Nayagam S (2001) Apley's system of orthopaedics and fractures, 8th edn. Arnold, London, p 781

Stojkovic Jovanovic T, Martinov D, Boskovic K (2013) Neurovaskularne lezije nakon ugradnje totalne proteze kuka kod kongenitalne displazije kuka: prikaz slučaja. Med Pregl LXVI 9–10:406–410

Tosatti S, De Paul SM, Askendal A, VandeVondele S, Hubbell JA, Tengvall P, Textor M (2003) Peptide functionalized poly(L-lysine)-g-poly(ethylene glycol) on titanium: resistance to protein adsorption in full heparinized human blood plasma. Biomaterials 24(27):4949–4958

Trampuz A, Osmon DR, Hanssen AD, Steckelberg JM, Patel R (2003) Molecular and antibiofilm approaches to prosthetic joint infection. Clin Orthop Relat Res 414:69–88

Trampuz A, Gilomen A, Fluckiger U (2005) Treatment outcome of infections associated with internal fixation devices: results from a 5-year retrospective study (1999–2003). In 45th ICAAC. American Society for Microbiology, Washington DC, 16–19 Dec 2005

Wiles P (1957) The surgery of the osteo-arthritis hip. Br J Surg 45:488–497

Woo RY, Morrey BF (1982) Dislocations after total hip arthroplasty. J Bone Joint Surg 64 (9):1295–1306

Zhao ZS, Sun JY (2013) Total hip arthroplasty using S-ROM prosthesis in elder patients with type C and B bone. J Orthop 10(2):65–69. doi:10.1016/j.jor.2013.04.006

Zivic F, Babic M, Mitrovic S, Vencl A (2011) Continuous control as alternative route for wear monitoring by measuring penetration depth during linear reciprocating sliding of Ti6Al4V alloy. J Alloy Compd 509(19):5748–5754

Zivic F, Babic M, Grujovic N, Mitrovic S, Favaro G, Caunii M (2012) Effect of vacuum-treatment on deformation properties of PMMA bone cement. J Mech Behav Biomed Mater 5(1):129–138. doi: 10.1016/j.jmbbm.2011.08.015

Zweymüller KA, Lintner FK, Semlitsch MF (1988) Biologic fixation of a press-fit titanium hip joint endoprosthesis. Clin Orthop Relat Res 235:195–206